Scientific and Technical Aerospace Reports

STAR

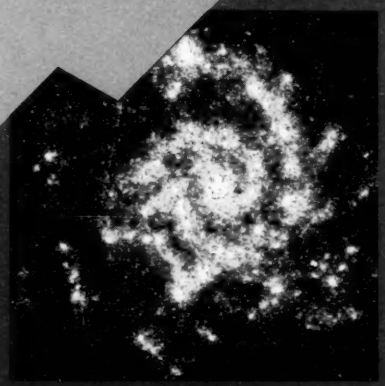

An Abstract Journal

Volume 30, Number 20
October 23, 1992
N92-29228 to N92-30232

Scientific and Technical Aerospace Reports

Scientific and Technical Aerospace Reports (STAR) is an abstract journal that provides comprehensive coverage of worldwide aerospace-related reports. It is a major product of the International Aerospace Database managed by the NASA Scientific and Technical Information (STI) Program. The coverage includes reports on aeronautics, space, and supporting disciplines. *STAR* lists current, publicly available reports entered into the NASA STI Database during the 2-week period preceding publication. A typical citation and abstract appear on page viii. They explain how to read the items that are announced in this journal.

NASA sponsors a companion journal, *International Aerospace Abstracts (IAA)* (*NOVA* for internal NASA use) that lists abstracts of the open literature on aerospace subjects available worldwide. *IAA* is available for sale through the AIAA.

Entries found in *STAR* and *IAA* are available through NASA's online service, RECON, as the International Aerospace Database and through DIALOG as the Aerospace Database.

Information on aerospace and related subjects is gathered by the NASA STI Program through national and international agreements and exchanges and is made available to the NASA community as well as to the public in many forms through various outlets. The section on NASA STI Program Products and Services contains additional information.

For further information please contact:
NASA Center for AeroSpace Information (CASI)
P.O. Box 8757
Baltimore, Maryland 21240-0757
(301) 621-0390

US ISSN 0036-8741

Volume 30 Number 20 / October 23, 1992

TABLE OF CONTENTS

AERONAUTICS For related information see also *Astronautics.*

01 AERONAUTICS (GENERAL) **3399**

02 AERODYNAMICS **3399**
Includes aerodynamics of bodies, combinations, wings, rotors, and control surfaces; and internal flow in ducts and turbomachinery. For related information see also *34 Fluid Mechanics and Heat Transfer.*

03 AIR TRANSPORTATION AND SAFETY **3402**
Includes passenger and cargo air transport operations; and aircraft accidents. For related information see also *16 Space Transportation* and *85 Urban Technology and Transportation.*

04 AIRCRAFT COMMUNICATIONS AND NAVIGATION **3403**
Includes digital and voice communication with aircraft; air navigation systems (satellite and ground based); and air traffic control. For related information see also *17 Space Communications, Spacecraft Communications, Command and Tracking* and *32 Communications and Radar.*

05 AIRCRAFT DESIGN, TESTING AND PERFORMANCE **3404**
Includes aircraft simulation technology. For related information see also *18 Spacecraft Design, Testing and Performance* and *39 Structural Mechanics.* For land transportation vehicles see *85 Urban Technology and Transportation.*

06 AIRCRAFT INSTRUMENTATION **3404**
Includes cockpit and cabin display devices; and flight instruments. For related information see also *19 Space craft Instrumentation* and *35 Instrumentation and Photography.*

07 AIRCRAFT PROPULSION AND POWER **3405**
Includes prime propulsion systems and systems components, e.g., gas turbine engines and compressors; and onboard auxiliary power plants for aircraft. For related information see also *20 Spacecraft Propulsion and Power, 28 Propellants and Fuels,* and *44 Energy Production and Conversion.*

08 AIRCRAFT STABILITY AND CONTROL **3406**
Includes aircraft handling qualities; piloting; flight controls; and autopilots. For related information see also *05 Aircraft Design, Testing and Performance.*

09 RESEARCH AND SUPPORT FACILITIES (AIR) **3406**
Includes airports, hangars and runways; aircraft repair and overhaul facilities; wind tunnels; shock tubes; and aircraft engine test stands. For related information see also *14 Ground Support Systems and Facilities (Space).*

ASTRONAUTICS For related information see also *Aeronautics.*

12 ASTRONAUTICS (GENERAL) **3407**
For extraterrestrial exploration see *91 Lunar and Planetary Exploration.*

13 ASTRODYNAMICS ..... **N.A.**
Includes powered and free-flight trajectories; and orbital and launching dynamics.

14 GROUND SUPPORT SYSTEMS AND FACILITIES (SPACE) ..... **N.A.**
Includes launch complexes, research and production facilities; ground support equipment, e.g., mobile transporters; and simulators. For related information see also *09 Research and Support Facilities (Air).*

15 LAUNCH VEHICLES AND SPACE VEHICLES **3408**
Includes boosters; operating problems of launch/space vehicle systems; and reusable vehicles. For related information see also *20 Spacecraft Propulsion and Power.*

16 SPACE TRANSPORTATION **3408**
Includes passenger and cargo space transportation, e.g., shuttle operations; and space rescue techniques. For related information see also *03 Air Transportation and Safety* and *18 Spacecraft Design, Testing and Performance.* For space suits see *54 Man/System Technology and Life Support.*

17 SPACE COMMUNICATIONS, SPACECRAFT COMMUNICATIONS, COMMAND AND TRACKING . **N.A.**
Includes telemetry; space communications networks; astronavigation and guidance; and radio blackout. For related information see also *04 Aircraft Communications and Navigation* and *32 Communications and Radar.*

N.A.—no abstracts were assigned to this category for this issue.

18 SPACECRAFT DESIGN, TESTING AND PERFORMANCE **3409**
Includes satellites; space platforms; space stations; spacecraft systems and components such as thermal and environmental controls; and attitude controls. For life support systems see *54 Man/System Technology and Life Support.* For related information see also *05 Aircraft Design, Testing and Performance, 39 Structural Mechanics,* and *16 Space Transportation.*

19 SPACECRAFT INSTRUMENTATION **3410**
For related information see also *06 Aircraft Instrumentation* and *35 Instrumentation and Photography.*

20 SPACECRAFT PROPULSION AND POWER **3412**
Includes main propulsion systems and components, e.g., rocket engines; and spacecraft auxiliary power sources. For related information see also *07 Aircraft Propulsion and Power, 28 Propellants and Fuels, 44 Energy Production and Conversion,* and *15 Launch Vehicles and Space Vehicles.*

CHEMISTRY AND MATERIALS

23 CHEMISTRY AND MATERIALS (GENERAL) ..... **N.A.**

24 COMPOSITE MATERIALS **3414**
Includes physical, chemical, and mechanical properties of laminates and other composite materials. For ceramic materials see *27 Nonmetallic Materials.*

25 INORGANIC AND PHYSICAL CHEMISTRY **3416**
Includes chemical analysis, e.g., chromatography; combustion theory; electrochemistry; and photochemistry. For related information see also *77 Thermodynamics and Statistical Physics.*

26 METALLIC MATERIALS **3420**
Includes physical, chemical, and mechanical properties of metals, e.g., corrosion; and metallurgy.

27 NONMETALLIC MATERIALS **3423**
Includes physical, chemical, and mechanical properties of plastics, elastomers, lubricants, polymers, textiles, adhesives, and ceramic materials. For composite materials see *24 Composite Materials.*

28 PROPELLANTS AND FUELS **3427**
Includes rocket propellants, igniters and oxidizers; their storage and handling procedures; and aircraft fuels. For related information see also *07 Aircraft Propulsion and Power, 20 Spacecraft Propulsion and Power,* and *44 Energy Production and Conversion.*

29 MATERIALS PROCESSING **3428**
Includes space-based development of products and processes for commercial application. For biological materials see *55 Space Biology.*

ENGINEERING For related information see also *Physics.*

31 ENGINEERING (GENERAL) **3428**
Includes vacuum technology; control engineering; display engineering; cryogenics; and fire prevention.

32 COMMUNICATIONS AND RADAR **3429**
Includes radar; land and global communications; communications theory; and optical communications. For related information see also *04 Aircraft Communications and Navigation* and *17 Space Communications, Spacecraft Communications, Command and Tracking.* For search and rescue see *03 Air Transportation and Safety,* and *16 Space Transportation.*

33 ELECTRONICS AND ELECTRICAL ENGINEERING **3438**
Includes test equipment and maintainability; components, e.g., tunnel diodes and transistors; microminiaturization; and integrated circuitry. For related information see also *60 Computer Operations and Hardware* and *76 Solid-State Physics.*

34 FLUID MECHANICS AND HEAT TRANSFER **3443**
Includes boundary layers; hydrodynamics; fluidics; mass transfer and ablation cooling. For related information see also *02 Aerodynamics* and *77 Thermodynamics and Statistical Physics.*

35 INSTRUMENTATION AND PHOTOGRAPHY **3456**
Includes remote sensors; measuring instruments and gauges; detectors; cameras and photographic supplies; and holography. For aerial photography see *43 Earth Resources and Remote Sensing.* For related information see also *06 Aircraft Instrumentation* and *19 Spacecraft Instrumentation.*

36 LASERS AND MASERS **3475**
Includes parametric amplifiers. For related information see also *76 Solid-State Physics.*

37 MECHANICAL ENGINEERING **3478**
Includes auxiliary systems (nonpower); machine elements and processes; and mechanical equipment.

38 QUALITY ASSURANCE AND RELIABILITY **3480**
Includes product sampling procedures and techniques; and quality control.

39 STRUCTURAL MECHANICS **3481**
Includes structural element design and weight analysis; fatigue; and thermal stress. For applications see *05 Aircraft Design, Testing and Performance* and *18 Spacecraft Design, Testing and Performance.*

GEOSCIENCES For related information see also *Space Sciences.*

42 GEOSCIENCES (GENERAL) ..... **N.A.**

43 EARTH RESOURCES AND REMOTE SENSING **3488**
Includes remote sensing of earth resources by aircraft and spacecraft; photogrammetry; and aerial photography. For instrumentation see *35 Instrumentation and Photography.*

44 ENERGY PRODUCTION AND CONVERSION **3491**
Includes specific energy conversion systems, e.g., fuel cells; global sources of energy; geophysical conversion; and windpower. For related information see also *07 Aircraft Propulsion and Power, 20 Spacecraft Propulsion and Power,* and *28 Propellants and Fuels.*

45 ENVIRONMENT POLLUTION **3492**
Includes atmospheric, noise, thermal, and water pollution.

46 GEOPHYSICS **3500**
Includes aeronomy; upper and lower atmosphere studies; ionospheric and magnetospheric physics; and geomagnetism. For space radiation see *93 Space Radiation.*

47 METEOROLOGY AND CLIMATOLOGY **3502**
Includes weather forecasting and modification.

48 OCEANOGRAPHY **3504**
Includes biological, dynamic, and physical oceanography; and marine resources. For related information see also *43 Earth Resources and Remote Sensing.*

LIFE SCIENCES

51 LIFE SCIENCES (GENERAL) **3506**

52 AEROSPACE MEDICINE **3509**
Includes physiological factors; biological effects of radiation; and effects of weightlessness on man and animals.

53 BEHAVIORAL SCIENCES **3510**
Includes psychological factors; individual and group behavior; crew training and evaluation; and psychiatric research.

54 MAN/SYSTEM TECHNOLOGY AND LIFE SUPPORT **3512**
Includes human engineering; biotechnology; and space suits and protective clothing. For related information see also *16 Space Transportation.*

55 SPACE BIOLOGY ..... **N.A.**
Includes exobiology; planetary biology; and extraterrestrial life.

MATHEMATICAL AND COMPUTER SCIENCES

59 MATHEMATICAL AND COMPUTER SCIENCES (GENERAL) **3513**

60 COMPUT4R OPERATIONS AND HARDWARE **3513**
Includes hardware for computer graphics, firmware, and data processing. For components see *33 Electronics and Electrical Engineering.*

61 COMPUTER PROGRAMMING AND SOFTWARE **3514**
Includes computer programs, routines, algorithms, and specific applications, e.g., CAD/CAM.

62 COMPUTER SYSTEMS **3524**
Includes computer networks and special application computer systems.

63 CYBERNETICS **3527**
Includes feedback and control theory, artificial intelligence, robotics and expert systems. For related information see also *54 Man/System Technology and Life Support.*

64 NUMERICAL ANALYSIS **3531**
Includes iteration, difference equations, and numerical approximation.

65 STATISTICS AND PROBABILITY **3538**
Includes data sampling and smoothing; Monte Carlo method; and stochastic processes.

66 SYSTEMS ANALYSIS **3541**
Includes mathematical modeling; network analysis; and operations research.

67 THEORETICAL MATHEMATICS ..... **N.A.**
Includes topology and number theory.

PHYSICS For related information see also *Engineering.*

70 PHYSICS (GENERAL) **3542**
For precision time and time interval (PTTI) see *35 Instrumentation and Photography;* for geophysics, astrophysics or solar physics see *46 Geophysics, 90 Astrophysics,* or *92 Solar Physics.*

71 ACOUSTICS **3543**
Includes sound generation, transmission, and attenuation. For noise pollution see *45 Environment Pollution.*

72 ATOMIC AND MOLECULAR PHYSICS **3544**
Includes atomic structure, electron properties, and molecular spectra.

73 NUCLEAR AND HIGH-ENERGY PHYSICS **3549**
Includes elementary and nuclear particles; and reactor theory. For space radiation see *93 Space Radiation.*

74 OPTICS **3550**
Includes light phenomena and optical devices. For lasers see *36 Lasers and Masers.*

75 PLASMA PHYSICS **3553**
Includes magnetohydrodynamics and plasma fusion. For ionospheric plasmas see *46 Geophysics.* For space plasmas see *90 Astrophysics.*

76 SOLID-STATE PHYSICS **3556**
Includes superconductivity. For related information see also *33 Electronics and Electrical Engineering* and *36 Lasers and Masers.*

77 THERMODYNAMICS AND STATISTICAL PHYSICS **3560**
Includes quantum mechanics; theoretical physics; and Bose and Fermi statistics. For related information see also *25 Inorganic and Physical Chemistry* and *34 Fluid Mechanics and Heat Transfer.*

SOCIAL SCIENCES

80 SOCIAL SCIENCES (GENERAL) ..... **N.A.**
Includes educational matters.

81 ADMINISTRATION AND MANAGEMENT **3561**
Includes management planning and research.

82 DOCUMENTATION AND INFORMATION SCIENCE **3561**
Includes information management; information storage and retrieval technology; technical writing; graphic arts; and micrography. For computer documentation see *61 Computer Programming and Software.*

83 ECONOMICS AND COST ANALYSIS ..... **N.A.**
Includes cost effectiveness studies.

84 LAW, POLITICAL SCIENCE AND SPACE POLICY ..... **N.A.**
Includes NASA appropriation hearings; aviation law; space law and policy; international law; international cooperation; and patent policy.

85 URBAN TECHNOLOGY AND TRANSPORTATION **3563**
Includes applications of space technology to urban problems; technology transfer; technology assessment; and surface and mass transportation. For related information see *03 Air Transportation and Safety, 16 Space Transportation,* and *44 Energy Production and Conversion.*

SPACE SCIENCES For related information see also *Geosciences*.

88 SPACE SCIENCES (GENERAL) ..... **N.A.**

89 ASTRONOMY **3564**
Includes radio, gamma-ray, and infrared astronomy; and astrometry.

90 ASTROPHYSICS **3565**
Includes cosmology; celestial mechanics; space plasmas; and interstellar and interplanetary gases and dust. For related information see also *75 Plasma Physics*.

91 LUNAR AND PLANETARY EXPLORATION **3568**
Includes planetology; and manned and unmanned flights. For spacecraft design or space stations see *18 Spacecraft Design, Testing and Performance*.

92 SOLAR PHYSICS **3569**
Includes solar activity, solar flares, solar radiation and sunspots. For related information see *93 Space Radiation*.

93 SPACE RADIATION **3570**
Includes cosmic radiation; and inner and outer earth's radiation belts. For biological effects of radiation see *52 Aerospace Medicine*. For theory see *73 Nuclear and High-Energy Physics*.

GENERAL

Includes aeronautical, astronautical, and space science related histories, biographies, and pertinent reports too broad for categorization; histories or broad overviews of NASA programs.

99 GENERAL **3570**

SUBJECT INDEX **I-1**

PERSONAL AUTHOR INDEX **I-71**

CORPORATE SOURCE INDEX **I-81**

CONTRACT NUMBER INDEX **I-95**

REPORT NUMBER INDEX **I-97**

ACCESSION NUMBER INDEX **I-105**

APPENDIX **A-1**

TYPICAL CITATION AND ABSTRACT

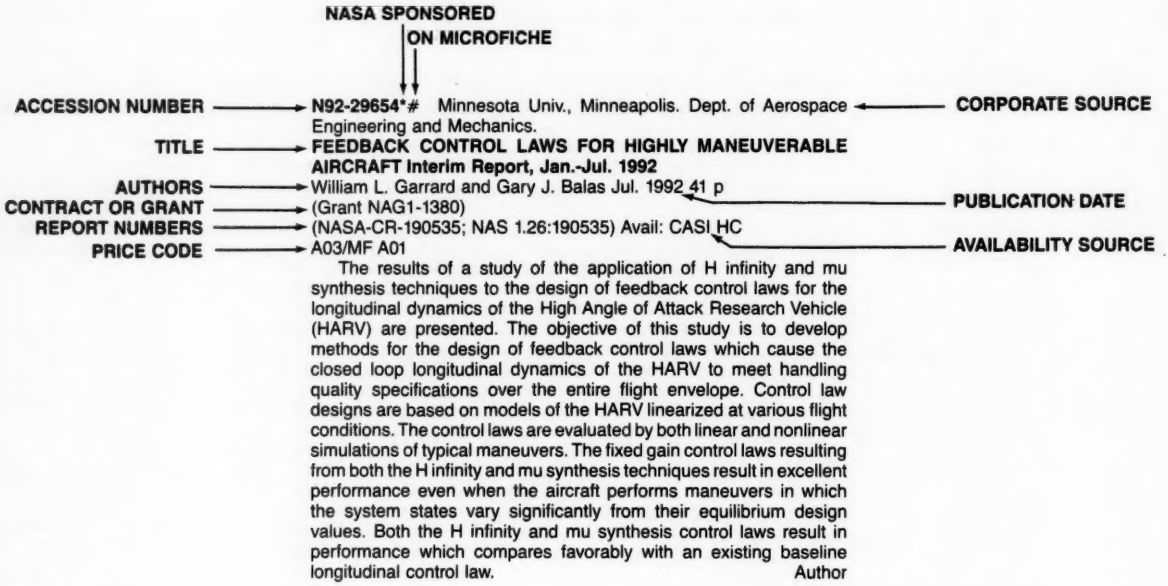
NASA SPONSORED
ON MICROFICHE
ACCESSION NUMBER
N92-29654*# Minnesota Univ., Minneapolis. Dept. of Aerospace Engineering and Mechanics.
CORPORATE SOURCE
TITLE
FEEDBACK CONTROL LAWS FOR HIGHLY MANEUVERABLE AIRCRAFT Interim Report, Jan.-Jul. 1992
AUTHORS
William L. Garrard and Gary J. Balas Jul. 1992 41 p
PUBLICATION DATE
CONTRACT OR GRANT
(Grant NAG1-1380)
REPORT NUMBERS
(NASA-CR-190535; NAS 1.26:190535) Avail: CASI HC
AVAILABILITY SOURCE
PRICE CODE
A03/MF A01
The results of a study of the application of H infinity and mu synthesis techniques to the design of feedback control laws for the longitudinal dynamics of the High Angle of Attack Research Vehicle (HARV) are presented. The objective of this study is to develop methods for the design of feedback control laws which cause the closed loop longitudinal dynamics of the HARV to meet handling quality specifications over the entire flight envelope. Control law designs are based on models of the HARV linearized at various flight conditions. The control laws are evaluated by both linear and nonlinear simulations of typical maneuvers. The fixed gain control laws resulting from both the H infinity and mu synthesis techniques result in excellent performance even when the aircraft performs maneuvers in which the system states vary significantly from their equilibrium design values. Both the H infinity and mu synthesis control laws result in performance which compares favorably with an existing baseline longitudinal control law.
Author

VOLUME 30 NUMBER 20 / OCTOBER 23, 1992

Scientific and Technical Aerospace Reports

A Semimonthly Publication of the National Aeronautics and Space Administration

01 AERONAUTICS (GENERAL)

N92-29874# Messerschmitt-Boelkow-Blohm G.m.b.H., Munich (Germany, F.R.). Helicopter Div.
REPAIR PROCEDURES FOR ADVANCED COMPOSITES FOR HELICOPTERS
Hermann Eschbaumer 1991 25 p Presented at the 17th European Rotorcraft Forum, Berlin, Fed. Republic of Germany, 24-26 Sep. 1991
(MBB-UD-0606-91-PUB; ETN-92-91696) Avail: CASI HC A03/MF A01

Standard repair procedures and the various solutions determined for structural repairs are discussed. Repairs on load introduction areas and extensive damages were rated to require specific repairs and therefore assistance of stress design. Specific repairs are not discussed. Standard repairs applicable for primary and secondary structures are referred to. The differences between 'in house repairs', 'depot and on aircraft repairs', and 'field repairs' are clarified. Suitable nondestructive test techniques for nonstationary inspection are considered and aspects to transfer the required standard repair procedures to maintenance personnel are discussed. ESA

N92-30232# Messerschmitt-Boelkow-Blohm G.m.b.H., Munich (Germany, F.R.). Hubschrauber und Flugzeuge.
ACQUISITION OF AN AEROTHERMODYNAMIC DATA BASE BY MEANS OF A WINGED EXPERIMENTAL REENTRY VEHICLE
E. H. Hirschel, H. Grallert, J. Lafon, and M. Rapuc 19 Aug. 1991 40 p Sponsored in part by ESA
(MBB/FE202/S/PUB/461; ETN-92-91903) Copyright Avail: CASI HC A03/MF A01

A winged aerothermodynamic experimental reentry vehicle is proposed in order to verify and validate the methods of numerical aerothermodynamics as design tool additional to the classical tools, i.e., the wind tunnel. Experimental hypersonic vehicles are reviewed and the aerothermodynamic characteristic of reentry vehicles and the ground simulation problems are considered. The possible configuration and trajectory of a winged experimental vehicle are discussed, together with the required and possible measurements, and the data management and recovery. Use of the obtained data base in the establishment of the methods of numerical aerothermodynamics as additional design tool is outlined. ESA

N92-30122*# Northwest Airlines, Inc., Minneapolis, MN.
CURRENT AND FUTURE DEVELOPMENTS IN CIVIL AIRCRAFT NON-DESTRUCTIVE EVALUATION FROM AN OPERATOR'S POINT OF VIEW
Jeff Register *In* NASA. Langley Research Center, The 1991 International Conference on Aging Aircraft and Structural Airworthiness Jul. 1992 p 279-282 (For primary document see N92-30106 20-39)
Avail: CASI HC A01/MF A04

02 AERODYNAMICS

Includes aerodynamics of bodies, combinations, wings, rotors, and control surfaces; and internal flow in ducts and turbomachinery.

For related information see also *34 Fluid Mechanics and Heat Transfer.*

N92-29329*# Brown Univ., Providence, RI. Div. of Engineering.
PARAMETER IDENTIFICATION FOR NONLINEAR AERODYNAMIC SYSTEMS Semiannual Progress Report No. 5, 23 Oct. 1991 - 23 Apr. 1992
Allan E. Pearson 7 May 1992 34 p
(Grant NAG1-1065)
(NASA-CR-190264; NAS 1.26:190264) Avail: CASI HC A03/MF A01

Continuing work on frequency analysis for transfer function identification is discussed. A new study was initiated into a 'weighted' least squares algorithm within the context of the Fourier modulating function approach. The first phase of applying these techniques to the F-18 flight data is nearing completion, and these results are summarized. Author

N92-29361*# Tennessee Univ., Tullahoma. Space Inst.
DEVELOPMENT OF A MULTIGRID TRANSONIC POTENTIAL FLOW CODE FOR CASCADES Final Technical Report
John Steinhoff 29 Jun. 1992 26 p
(Grant NAG3-398)
(NASA-CR-190480; NAS 1.26:190480) Avail: CASI HC A03/MF A01

Finite-volume methods for discretizing transonic potential flow equations have proven to be very flexible and accurate for both two and three dimensional problems. Since they only use local properties of the mapping, they allow decoupling of the grid generation from the rest of the problem. A very effective method for solving the discretized equations and converging to a solution is the multigrid-ADI technique. It has been successfully applied to airfoil problems where O type, C type and slit mappings have been used. Convergence rates for these cases are more than an order of magnitude faster than with relaxation techniques. In this report, we describe a method to extend the above methods, with the C type mappings, to airfoil cascade problems. Author

N92-29402*# Sverdrup Technology, Inc., Brook Park, OH.
A COMPARISON OF THE CALCULATED AND EXPERIMENTAL OFF-DESIGN PERFORMANCE OF A RADIAL FLOW TURBINE Final Report
Lizet Tirres Jul. 1991 16 p Presented at the 28th Joint Propulsion Conference and Exhibit, Nashville, TN, 6-8 Jul. 1992; sponsored in part by AIAA, SAE, ASME, and ASEE
(Contract NAS3-25266; RTOP 535-05-10)
(NASA-CR-189207; E-7175; NAS 1.26:189207; AIAA Paper 92-3069) Avail: CASI HC A03/MF A01

Off design aerodynamic performance of the solid version of a cooled radial inflow turbine is analyzed. Rotor surface static pressure data and other performance parameters were obtained experimentally. Overall stage performance and turbine blade surface static to inlet total pressure ratios were calculated by using a quasi-three dimensional inviscid code. The off design prediction capability of this code for radial inflow turbines shows accurate

static pressure prediction. Solutions show a difference of 3 to 5 points between the experimentally obtained efficiencies and the calculated values. Author

N92-29445*# National Aeronautics and Space Administration. Langley Research Center, Hampton, VA.
SPATIAL AND TEMPORAL ADAPTIVE PROCEDURES FOR THE UNSTEADY AERODYNAMIC ANALYSIS OF AIRFOILS USING UNSTRUCTURED MESHES M.S. Thesis
John R. Hooker (Purdue Univ., West Lafayette, IN.), John T. Batina, and Marc H. Williams (Purdue Univ., West Lafayette, IN.) Jul. 1992 16 p Presented at the AIAA 10th Applied Aerodynamics Conference, Palo Alto, CA, 22-24 Jun. 1992
(Grant NAG1-372; RTOP 505-63-50-12)
(NASA-TM-107635; NAS 1.15:107635) Avail: CASI HC A03/MF A01

An algorithm which combines spatial and temporal adaption for the time integration of the two dimensional Euler equations on unstructured meshes of triangles is presented. Spatial adaption involves mesh enrichment to add elements in high gradient regions of the flow and mesh coarsening to remove elements where they are no longer needed. Temporal adaption is a time accurate, local time stepping procedure which integrates the flow equations in each cell according to the local numerical stability constraint. The flow solver utilizes a four stage Runge-Kutta time integration scheme with an upwind flux-split spatial discretization. Results obtained using spatial and temporal adaption indicate that highly accurate solutions can be obtained with a significant savings of computing time over global time stepping. Author

N92-29539# Naval Surface Warfare Center, Dahlgren, VA.
SECOND-ORDER SHOCK-EXPANSION THEORY EXTENDED TO INCLUDE REAL GAS EFFECTS Final Report
Frank G. Moore, Michael A. Armistead, Steve H. Rowles, and Fred R. DeJarnette Feb. 1992 177 p
(AD-A247191; NAVSWC-TR-90-683) Avail: CASI HC A09/MF A02

New methods have been developed to compute inviscid surface pressures and temperatures for both perfect and equilibrium chemically reacting flows on both pointed and blunt bodies of revolution. These new methods include an improved Shock-expansion Theory, an improved Modified Newtonian Theory (MNT), and an improved method for angle-of-attack effects. Comparison of these approximate engineering techniques to exact inviscid computations using a full Euler code showed that these new methods gave very good agreement of surface temperature and pressures as well as forces and moments. Incorporation of this new technology into the NAVSWC aeroprediction code will allow the code to be used for engineering estimates of inviscid surface temperature at high Mach numbers. These approximate temperatures can then be used as inputs to perform heat transfer analysis. GRA

N92-29625*# National Aeronautics and Space Administration. Ames Research Center, Moffett Field, CA.
NASA WORKSHOP ON FUTURE DIRECTIONS IN SURFACE MODELING AND GRID GENERATION
W. R. VanDalsem (National Aeronautics and Space Administration. Langley Research Center, Hampton, VA.), R. E. Smith (National Aeronautics and Space Administration. Langley Research Center, Hampton, VA.), Y. K. Choo (National Aeronautics and Space Administration. Lewis Research Center, Cleveland, OH.), L. D. Birckelbaw, and A. A. Vogel Mar. 1992 24 p Workshop held at Moffett Field, CA, 5-7 Dec. 1989
(RTOP 505-59-00)
(NASA-CP-10092; A-92072; NAS 1.55:10092) Avail: CASI HC A03/MF A01

Given here is a summary of the paper sessions and panel discussions of the NASA Workshop on Future Directions in Surface Modeling and Grid Generation held a NASA Ames Research Center, Moffett Field, California, December 5-7, 1989. The purpose was to assess U.S. capabilities in surface modeling and grid generation and take steps to improve the focus and pace of these disciplines within NASA. The organization of the workshop centered around overviews from NASA centers and expert presentations from U.S. corporations and universities. Small discussion groups were held and summarized by group leaders. Brief overviews and a panel discussion by representatives from the DoD were held, and a NASA-only session concluded the meeting. In the NASA Program Planning Session summary there are five recommended steps for NASA to take to improve the development and application of surface modeling and grid generation. Author

N92-29648# Messerschmitt-Boelkow-Blohm G.m.b.H., Munich (Germany, F.R.). Hubschrauber und Flugzeuge.
TECHNOLOGY PROGRAMME: AEROTHERMODYNAMICS AND PROPULSION INTEGRATION. NUMERICAL AND EXPERIMENTAL AEROTHERMODYNAMICS
E. H. Hirschel 26 Aug. 1991 13 p Presented at the Review of the German Hypersonic Research and Technology Programme, Bonn, Fed. Republic of Germany, 16-17 Apr. 1991
(MBB-FE-202-S-PUB-0464-A; ETN-92-91497) Copyright Avail: CASI HC A03/MF A01

Work performed in the fields of 'aerothermodynamic predesign methods (approximate methods)', 'numerical methods of aerothermodynamics' and 'experimental methods of aerothermodynamics' is reviewed. The objective of the work is sketched, major results are listed, examples are given and future efforts are outlined. The examples include applications of predesign methods and numerical methods for the determination of global forces and moments, aerodynamic loads and heat loads (for the latter also a study of the influence of different flow physical model assumptions). From the field of experimental aerothermodynamics, an application of a fluorescence method is given, and the picture of a wind tunnel model is shown in order to demonstrate the complexity of such test articles. At the middle of phase 1 of the technology program, basic aerothermodynamic design tools and methods are available, which will reach the first validation level at the end of phase 1. Large deficiencies in flow physical models (transition laminar-turbulent, turbulence, etc.) were identified and basics oriented and applications oriented work was initiated at universities and research establishments. Thus, work will help the second validation level, which is needed when the development of the Saenger space transportation systems begins. ESA

N92-29649# Messerschmitt-Boelkow-Blohm G.m.b.H., Munich (Germany, F.R.). Unternehmensbereich Flugzeuge.
AEROTHERMODYNAMICS AND PROPULSION INTEGRATION IN THE SAENGER TECHNOLOGY PROGRAMME
E. H. Hirschel 16 Sep. 1991 12 p Previously announced in IAA as A92-17829
(MBB-FE-202-S-PUB-0469-A; AIAA Paper 91-5041;
ETN-92-91499) Copyright Avail: CASI HC A03/MF A01

The objectives of the technology program 'aerothermodynamics and propulsion integration' are defined. An overview of the special aerothermodynamic phenomena which must be regarded in the design of the Saenger lower stage, which presently stands in the center of the technology program, is given. The design tools, which must be provided, the components like the inlet, and the afterbody, which must be designed and tested, and the special problems like forebody optimization, heat load determination, and upper stage separation, which must be treated, are discussed. The general work plan, with the major activities up to the start of the development of the Saenger space transport system is presented, including the development and manufacturing of an experimental vehicle (HYTEX) as a means for the validation of the design tools and methods which are achieved in the technology program, and for the creation of a free flight data base. Examples given include applications of predesign methods and numerical methods for the determination of global forces and moments, aerodynamic loads and heat loads, for the latter also a study of the influence of different flow physical model assumptions. Results from the inlet study, the stage separation study, etc., show the advancement in these areas. ESA

N92-29657*# Texas A&M Univ., College Station. Dept. of Aerospace Engineering.
DETERMINATION OF AERODYNAMIC SENSITIVITY COEFFICIENTS FOR WINGS IN TRANSONIC FLOW
Leland A. Carlson and Hesham M. El-Banna May 1992 6 p
(Grant NAG1-793)
(NASA-CR-190570; NAS 1.26:190570; TAMRF-5802-92-02)
Avail: CASI HC A02/MF A01

The quasianalytical approach is applied to the 3-D full potential equation to compute wing aerodynamic sensitivity coefficients in the transonic regime. Symbolic manipulation is used to reduce the effort associated with obtaining the sensitivity equations, and the large sensitivity system is solved using 'state of the art' routines. The quasianalytical approach is believed to be reasonably accurate and computationally efficient for 3-D problems. Author

N92-29691*# California Polytechnic State Univ., San Luis Obispo. Dept. of Aeronautical Engineering.
COMPUTATION OF THREE-DIMENSIONAL EFFECTS ON TWO DIMENSIONAL WINGS Final Technical Report
Russell M. Cummings Jul. 1992 11 p
(Contract NCC2-536)
(NASA-CR-190576; NAS 1.26:190576) Copyright Avail: CASI HC A03/MF A01

A 2-D numerical investigation was performed to determine the effect of a Gurney flap on a NACA 4412 airfoil. A Gurney flap is a flat plate on the order of 1 to 3 percent of the airfoil chord length, oriented perpendicular to the airfoil chord line and located at the trailing edge of the airfoil. An incompressible Navier Stokes code, INS2D, was used to calculate the flow field about the airfoil. The fully turbulent results were obtained using the Baldwin-Barth one-equation turbulence model. Gurney flap sizes of 0.5, 1, 1.25, 1.5, 2, and 3 percent of the airfoil chord were studied. Computational results were compared with experimental results where possible. The numerical solutions show that the Gurney flap increases airfoil lift coefficient with only a slight increase in drag coefficient. Use of a 1.5 percent chord Gurney flap increases the maximum lift coefficient by approximately 0.3 and decreases the angle of attack for a given lift coefficient by more than 3 degrees. The numerical solutions exhibit detailed flow structures at the trailing edge and provide a possible explanation for the increased aerodynamic performance. Author

N92-29713# Messerschmitt-Boelkow-Blohm G.m.b.H., Munich (Germany, F.R.). Unternehmensbereich Flugzeuge.
HYPERSONIC FLOW PAST RADIATION-COOLED SURFACES
E. H. Hirschel, A. Koc, and S. Riedelbauch (Deutsche Forschungsanstalt fuer Luft- und Raumfahrt, Goettingen, Germany, F.R.) 16 Sep. 1991 10 p Previously announced in IAA as A92-17821
(MBB-FE-202-S-PUB-0468-A; AIAA Paper 91-5031;
ETN-92-91498) Copyright Avail: CASI HC A02/MF A01

Hypersonic vehicles employ surface radiation cooling in order to reduce heat loads. The radiation adiabatic surface temperature is the result of the balance of the heat conduction towards the surface and the heat radiated away from the surface, if no heat transport into the surface occurs. It is shown by means of a local analysis that the radiation adiabatic temperature depends, other than the recovery temperature, on a characteristic boundary layer thickness. The state of the boundary layer (laminar or turbulent) has a much larger influence on the radiation adiabatic temperature than on the recovery temperature. The local analysis explains, for example, why hot spots appear along attachment lines. With the classical wind tunnel simulation techniques the radiation adiabatic temperature cannot be determined. A 'hot experimental technique' is needed if an accurate determination of heatloads in the presence of radiation cooling is desired. It involves a duplication or near duplication of Mach and Reynolds number, total temperature, and a model surface in radiation adiabatic equilibrium. The length scale dependency of the radiation adiabatic temperature then makes a scaling to full size necessary. This is shown to be possible for laminar flow, but not yet for turbulent flow. ESA

N92-29741# Universitaet der Bundeswehr Muenchen, Neubiberg (Germany, F.R.). Fakultaet fuer Luft- und Raumfahrttechnik.
A SEMI EMPIRICAL METHOD FOR THE ANALYTICAL REPRESENTATION OF STATIONARY MEASURED PROFILE COEFFICIENTS FOR APPLICATIONS OF ROTARY WING AERODYNAMICS Ph.D. Thesis [EINE HALBEMPIRISCHE METHODE ZUR ANALYTISCHEN DARSTELLUNG STATIONAAR GEMESSENER PROFILBEIWERTE FUER ANWENDUNGEN DER DREHFLUEGLERAERODYNAMIK]
Manfred Lerch 1990 190 p In GERMAN
(ETN-92-91491) Avail: CASI HC A09/MF A02

The semi empirical process presented is used for the closed representation of aerodynamic coefficients, from the point of view of flow conditions occurring in rotor blades. The aerodynamic coefficients are formulated analytically in the model as a function of the inflow components. Analytical functions are presented on the basis of the superposition principle. They reproduce the various flow conditions by simple theoretical and empirical formulations. The superposition of these functions leads to a qualitatively accurate representation of the aerodynamic coefficients. On the basis of the quaternions transformation, a mechanical auxiliary model was developed for the computation of the motion behavior of helicopter rotors. ESA

N92-29884# National Aerospace Lab., Amsterdam (Netherlands). Fluid Dynamics Div.
EVALUATION OF MEASURED-BOUNDARY-CONDITION METHODS FOR 3D SUBSONIC WALL INTERFERENCE
T. E. Labrujere, T. A. Maarsingh, and J. Smith 31 Mar. 1988 102 p
(NLR-TR-88072-U; ETN-92-91547) Avail: CASI HC A06/MF A02

Measurements of a simple aircraft model on both an appropriately sized and a relatively large, low/speed, solid/wall test section were used to analyze the accuracy and consistency of Measured/Boundary/Condition (MBC) methods. For completeness, the classical method of images, with two different correction procedures, was also analyzed. For the MBC methods, large reductions in the amount of in situ measured boundary data turn out to be possible, while almost retaining the accuracy obtained from abundant boundary data. In addition, high computing efficiency was achieved allowing on line wall interference assessment and correction during a wind tunnel test. The classical assessment methods turns out to be competitive with the MBC methods for the mode and test conditions considered (CL less than or equal to 2, no massive flow separation). Its applicability is limited, like any method requiring a theoretical representation of the mode flow. Some attention was paid to the definition of the reaction of the model to the wall/induced velocity field, i.e., the correction procedure. The analyses suggest that improvements and/or adaptations are desirable. ESA

N92-29889# Universitaet der Bundeswehr Muenchen, Neubiberg (Germany, F.R.). Fakultaet fuer Luft- und Raumfahrttechnik.
PRODUCTION OF PERIODICAL MACH NUMBER VARIATIONS IN HIGH SUBSONIC FLOW IN A BLOW DOWN WIND TUNNEL, AND ITS INFLUENCE ON PROFILE MEASUREMENTS Ph.D. Thesis [ERZEUGUNG PERIODISCHER MACHZAHLAENDERUNGEN IN HOHEN UNTERSCHALL IN EINEM BLOW-DOWN-WINDKANAL UND IHR EINFLUSS AUF DIE PROFILMESSUNGEN]
Robert Spelten 1990 138 p In GERMAN
(ETN-92-91492) Avail: CASI HC A07/MF A02

The properties of unsteady flow in a blow down wind tunnel are described. A follow up system allows the Mach number variations to be correlated from two channel gage lengths. It is determined that transonic profile flows display strong dynamic attenuation phenomena for the transmission of the mass flow stimulation. A process based on the measured Mach number variations was developed, according to which the representative Mach numbers can be theoretically determined for the model. The model developed is to be used for other two and three dimensional models. ESA

N92-29916# National Aerospace Lab., Amsterdam (Netherlands). Fluid Dynamics Div.
A METHOD FOR COMPUTING THE 3-DIMENSIONAL FLOW ABOUT WINGS WITH LEADING-EDGE VORTEX SEPARATION. PART 2: DESCRIPTION OF COMPUTER PROGRAM VORSEP
H. W. M. Hoeijmakers 10 Jan. 1986 282 p
(NLR-TR-86006-U; ETN-92-91546) Avail: CASI HC A13/MF A03

The VORSEP program, which computes the three dimensional flow about wings with leading edge vortex separation, is described. An introduction to the computation method is given. The input required for running the program is detailed. A technical description of VORSEP and its subroutine is given. Common blocks employed in the program are detailed and the auxiliary files used are described. A sample case of the output generated by the program is presented. ESA

N92-30182*# National Aeronautics and Space Administration. Lewis Research Center, Cleveland, OH.
EXPERIMENTAL INVESTIGATION OF THE FLOWFIELD OF AN OSCILLATING AIRFOIL
J. Panda and K. B. M. Q. Zaman Jun. 1992 20 p Presented at the 10th Applied Aerodynamics Conference, Palo Alto, CA, 22-24 Jun. 1992; sponsored by AIAA
(RTOP 505-62-52)
(NASA-TM-105675; E-7046; NAS 1.15:105675; AIAA Paper 92-2622-CP) Avail: CASI HC A03/MF A01

The flowfield of an airfoil oscillated periodically over a wide range of reduced frequencies, 0 less than or = k less than or = 1.6 is studied experimentally at chord Reynolds numbers of R sub c = 22,000 and 44,000. The NACA0012 airfoil is pitched sinusoidally about one quarter chord between angles of attack (alpha) of 5 and 25 degrees. Detailed flow visualization and phase averaged vorticity measurements are carried out for k = 0.2 to document the evolution and the shedding of the dynamic stall vortex (DSV). In addition to the DSV, an intense vortex of opposite sign originates from the trailing edge just when the DSV is shed. After being shed into the wake, the two together take the shape of a large 'mushroom' while being convected away from the airfoil. The unsteady circulation around the airfoil and, therefore, the time varying component of the lift is estimated in a novel way from the shed vorticity flux and is found to be in good agreement with the lift variation reported by others. The delay in the shedding of the DSV with increasing k, as observed by previous researchers, is documented for the full range of k. The DSV, for example, is shed nearly at the maximum alpha of 25 degrees at k = 0.2, but is shed at the minimum alpha of 5 degrees at k = 0.8. At low k, the flowfield appears quasi-steady and the bluff body shedding corresponding to the maximum alpha (25 degrees) dominates the unsteady fluctuations in the wake. Author

03 AIR TRANSPORTATION AND SAFETY

Includes passenger and cargo air transport operations; and aircraft accidents.

For related information see also *16 Space Transportation* and *85 Urban Technology and Transportation.*

N92-29703# National Aerospace Lab., Amsterdam (Netherlands). Flight Div.
ON THE OPTIMIZATION OF WINDSHEAR WARNING AND GUIDANCE SYSTEMS
J. L. Soesman 25 Jun. 1990 31 p Presented at the 17th ICAS Congress Student Session, Stockholm, Sweden, 9-14 Sep. 1990
(NLR-TP-90196-U; ETN-92-91440) Avail: CASI HC A03/MF A01

The results of a survey of several investigations into windshear detection, guidance and modeling is presented. The use of the results to improve future windshear warning and guidance systems and wind models for simulation, to obtain safer operation in windshear conditions, is shown. Some natural causes and simple models of windshear are presented and a theoretical analysis on the effect of windshear on performance and flight safety is made. Optimally guided flight trajectories through windshear that are computed in open loop form, using a point mass model, are compared with simulated closed loop suboptimal trajectories. The effect on survivability of different initial conditions and early warnings by forward looking detection systems are discussed. Experiences with an operational reactive windshear warning system aboard aircraft are reported. Natural causes of the shear, pilot's reactions and their result on the flight safety level are discussed. ESA

N92-30108*# Douglas Aircraft Co., Inc., Long Beach, CA. Airworthiness Assurance Programs.
MAINTAINING THE SAFETY OF AN AGING FLEET OF AIRCRAFT
Amos W. Hoggard *In* NASA. Langley Research Center, The 1991 International Conference on Aging Aircraft and Structural Airworthiness Jul. 1992 p 49-65 (For primary document see N92-30106 20-39)
Avail: CASI HC A03/MF A04

N92-30123*# Airbus Industrie, Blagnac (France).
AGEING AIRPLANE REPAIR ASSESSMENT PROGRAM FOR AIRBUS A300
J. M. Gaillardon, Hans-J. Schmidt, and B. Brandecker *In* NASA. Langley Research Center, The 1991 International Conference on Aging Aircraft and Structural Airworthiness Jul. 1992 p 283-289 (For primary document see N92-30106 20-39)
Avail: CASI HC A02/MF A04

N92-30124*# Federal Express Corp., Memphis, TN. Aircraft Reliability Div.
COMMUNICATION: AN IMPORTANT ELEMENT OF MAINTENANCE AND REPAIR
James S. Tripp *In* NASA. Langley Research Center, The 1991 International Conference on Aging Aircraft and Structural Airworthiness Jul. 1992 p 291-299 (For primary document see N92-30106 20-39)
Avail: CASI HC A02/MF A04

N92-30128*# Federal Aviation Administration, Seattle, WA.
THE FAA AGING AIRPLANE PROGRAM PLAN FOR TRANSPORT AIRCRAFT
Dayton Curtis and Jess Lewis (Federal Aviation Administration, Washington, DC.) *In* NASA. Langley Research Center, The 1991 International Conference on Aging Aircraft and Structural Airworthiness Jul. 1992 p 321-325 (For primary document see N92-30106 20-39)
Avail: CASI HC A01/MF A04

N92-30129*# National Aerospace Lab., Emmeloord (Netherlands).
AGEING AIRCRAFT RESEARCH IN THE NETHERLANDS
J. B. deJonge and G. Bartelds *In* NASA. Langley Research Center, The 1991 International Conference on Aging Aircraft and Structural Airworthiness Jul. 1992 p 327-335 Sponsored in part by FAA and Dept. of Civil Aviation (For primary document see N92-30106 20-39)
Avail: CASI HC A02/MF A04

N92-30130*# Office National d'Etudes et de Recherches Aerospatiales, Paris (France).
SURVEY OF FRENCH ACTIVITIES CONCERNING STRUCTURAL AIRWORTHINESS AND AGING AIRCRAFT
Roger Labourdette *In* NASA. Langley Research Center, The 1991 International Conference on Aging Aircraft and Structural Airworthiness Jul. 1992 p 337-360 (For primary document see N92-30106 20-39)
Avail: CASI HC A03/MF A04

N92-30131*# Department of Transport, Ottawa (Ontario). Airworthiness Branch.
TRANSPORT CANADA AGING AIRCRAFT ACTIVITIES
S. R. Didrikson *In* NASA. Langley Research Center, The 1991 International Conference on Aging Aircraft and Structural Airworthiness Jul. 1992 p 361-365 (For primary document see N92-30106 20-39)
Avail: CASI HC A01/MF A04

N92-30133*# Saab-Scania, Linkoping (Sweden). Aircraft Div.
A MANUFACTURER'S APPROACH TO ENSURE LONG TERM STRUCTURAL INTEGRITY
Hans Ansell, Billy Fredriksson, and Ingvar Holm *In* NASA. Langley Research Center, The 1991 International Conference on Aging Aircraft and Structural Airworthiness Jul. 1992 p 379-405 (For primary document see N92-30106 20-39)
Avail: CASI HC A03/MF A04

04 AIRCRAFT COMMUNICATIONS AND NAVIGATION

Includes digital and voice communication with aircraft; air navigation systems (satellite and ground based); and air traffic control.

For related information see also *17 Space Communications, Spacecraft Communications, Command and Tracking* and *Communications and Radar.*

N92-29440*# Draper (Charles Stark) Lab., Inc., Cambridge, MA.
A SYSTEMS ANALYSIS OF THE IMPACT OF NAVIGATION INSTRUMENTATION ON-BOARD A MARS ROVER, BASED ON A COVARIANCE ANALYSIS OF NAVIGATION PERFORMANCE M.S. Thesis, Massachusetts Inst. of Technology
Douglas Eric Leber (Massachusetts Inst. of Tech., Cambridge.) May 1992 85 p
(Contract NAS9-18426)
(NASA-CR-189868; NAS 1.26:189868; CSDL-T-1126) Copyright Avail: CASI HC A05/MF A01

As part of the Space Exploration Initiative, the exploration of Mars will undoubtedly require the use of rovers, both manned and unmanned. Many mission scenarios have been developed, incorporating rovers which range in size from a few centimeters to ones large enough to carry a manned crew. Whatever the mission, accurate navigation of the rover on the Martian surface will be necessary. This thesis considers the initial rover missions, where minimal in-situ navigation aids will be available on Mars. A covariance analysis of the rover's navigation performance is conducted, assuming minimal on-board instrumentation (gyro compass and speedometer), a single orbiting satellite, and a surface beacon at the landing site. Models of the on-board instruments are varied to correspond to the accuracy of various levels of these instruments currently available. A comparison is made with performance of an on-board IMU. Landing location and satellite orbits are also varied. Author

N92-29605# National Aerospace Lab., Amsterdam (Netherlands). Flight Div.
EUROPEAN STUDIES TO INVESTIGATE THE FEASIBILITY OF USING 1000 FT VERTICAL SEPARATION MINIMA ABOVE FL 290. PART 1: OVERVIEW OF ORGANISATION, TECHNIQUES EMPLOYED, AND CONCLUSIONS
J. M. tenHave, M. E. Cox (Eurocontrol Agency, Brussels, Belgium), and D. A. Forrester (Meterological Office, Bracknell, England) 18 Feb. 1991 27 p Submitted for publication
(NLR-TP-91062-U-Pt-1; ETN-92-91454) Avail: CASI HC A03/MF A01

Primarily in response to airline pressures for fuel economies, International Civil Aviation Organization (ICAO) established a study program to determine the feasibility of having the Vertical Separation Minimum (VSM) used above FK 290 to 1000 ft. The first of a three part article describing a European contribution to this program is presented. The aims and organization of the experimental work are outlined, the choice of methodology available to measure height keeping errors is described, and an indication of the measurement accuracy achieved is given. Overall, the work shows that, whereas it would be feasible to introduce a 1000 ft. VSM in the North Atlantic region, other measures would be necessary before it could be used in continental airspace. Today, in certain areas, the need for a reduced VSM has become even more pressing in order to achieve the gains in airspace capacity necessary to handle rapidly growing volumes of air traffic. ESA

N92-29615# National Aerospace Lab., Amsterdam (Netherlands). Electronics Dept.
APPLICATION OF VME-TECHNOLOGY ON AN AIRBORNE DATA LINK PROCESSOR UNIT
P. J. H. M. Manders 6 Jun. 1988 15 p Presented at the VITA Conference on VME Bus in Research, Zurich, Switzerland, Oct. 1988
(NLR-MP-88040-U; ETN-92-91513) Avail: CASI HC A03/MF A01

The technical concept of a Data Link Processor Unit (DLPU), which is a five slot, VME based, computer system, is described. In civil aircraft the DLPU will interface a secondary surveillance radar mode select transponder with various avionics systems in order to support data link operations. A militarized 68020 processor board will be applied. The interfaces with the transponder and the avionic systems apply a 68000 microprocessor for handling the lower level protocols. Electrically the interfaces with the aircraft systems follow the ARINC specification 429. The requirements for volume, environment, performance and certification are described. The application of the VME bus technology made possible the use of standardized boards and application standardized methods for the multiprocessor communication. ESA

N92-29617# Naval Postgraduate School, Monterey, CA.
PATH TRACKING USING SIMPLE PLANAR CURVES M.S. Thesis
Richard J. Abresch Mar. 1992 103 p
(AD-A248252) Avail: CASI HC A06/MF A02

This thesis presents a method of controlling an autonomous vehicle's motion in a two dimensional environment. Its' purpose is to expand the functionality of a vehicle's motion by complementing a point to point path planning scheme with a path to path scheme. The method introduced in this paper will use the vehicle's position and the desired reference path to calculate the necessary curvature to effect movement onto the desired reference path. The reference path will be a simple planar curve, such as, a circle or line. After successful testing of an operating algorithm, the method shall be incorporated into a robot's software system. This path tracking method will lay the groundwork for a dynamic obstacle avoidance system for a mobile robot. GRA

N92-29906# Naval Postgraduate School, Monterey, CA. Dept. of Computer Science.
INCORPORATION OF GPS/INS INTO SMALL AUTONOMOUS UNDERWATER VEHICLE NAVIGATION M.S. Thesis
James B. McKeon Mar. 1992 60 p
(AD-A248884) Avail: CASI HC A04/MF A01

Navigation of an Autonomous Underwater Vehicle (AUV) is a problem that has not been adequately solved. Although the inclusion of the Global Positioning System (GPS) into AUV navigation has been briefly examined before, this possibility is explored further in this thesis. GPS and Inertial Measurement System (INS) based navigation package offers many advantages for AUV navigation especially for transits and precise object location in shallow water. This thesis provides background information on GPS and INS as they pertain to small AUV employment. Other required components are also examined as they pertain to small AUV employment. The use of the GPS/INS navigation package for AUV transits and precise object location work is presented. Two designs with specified components are developed. A GPS receiver was tested for AUV employment suitability. These test results are presented and analyzed. GRA

05 AIRCRAFT DESIGN, TESTING AND PERFORMANCE

Includes aircraft simulation technology.

For related information see also *18 Spacecraft Design, Testing and Performance* and *39 Structural Mechanics.* For land transportation vehicles see *85 Urban Technology and Transportation.*

N92-29417*# National Aeronautics and Space Administration. Ames Research Center, Moffett Field, CA.
IMPROVING DESIGNER PRODUCTIVITY
Gary C. Hill Feb. 1992 13 p
(RTOP 505-69-50)
(NASA-TM-103929; A-92081; NAS 1.15:103929) Copyright Avail: CASI HC A03/MF A01

Designer and design team productivity improves with skill, experience, and the tools available. The design process involves numerous trials and errors, analyses, refinements, and addition of details. Computerized tools have greatly speeded the analysis, and now new theories and methods, emerging under the label Artificial Intelligence (AI), are being used to automate skill and experience. These tools improve designer productivity by capturing experience, emulating recognized skillful designers, and making the essence of complex programs easier to grasp. This paper outlines the aircraft design process in today's technology and business climate, presenting some of the challenges ahead and some of the promising AI methods for meeting these challenges. Author

N92-29506# Army Aeromedical Research Lab., Fort Rucker, AL.
TEST AND EVALUATION REPORT OF THE IMED VOLUMETRIC INFUSION PUMP MODEL 960A Final Report
James E. Bruckart, Joseph R. Licina, Bill Olding, and Martin Quattlebaum Feb. 1992 67 p
(DA Proj. 3M4-63807-D-836)
(AD-A248538; USAARL-92-18) Avail: CASI HC A04/MF A01

The IMED Volumetric Infusion Pump Model 960A was tested for electromagnetic interference/compatibility in the UH-60A helicopter under the U.S Army Program for Testing and Evaluation of Equipment for Aeromedical Operations. The tests were conducted using current military and industrial standards and procedures for electromagnetic interference/compatibility and human factors. The IMED Volumetric Infusion Pump Model 960A was found to be compatible with the U.S. Army medical evacuation UH-60A Blackhawk. GRA

N92-29511# Washington Univ., Seattle. Dept. of Mechanical Engineering.
TEAR STRAPS IN AIRPLANE FUSELAGE
M. Kosai, A. S. Kobayashi, and M. Ramulu Mar. 1992 15 p
(Contract N00014-89-J-1276)
(AD-A248543; UWA/DME/TR-92/68) Avail: CASI HC A03/MF A01

A procedure based on dynamic fracture mechanics is proposed for assessing the effectiveness of tear straps in a rupturing airplane fuselage weakened by a row of multiple site damage (MSD). A large deformation, elastic-plastic finite element model of the rupturing fuselage with an unsymmetrical crack flap is used to demonstrate the existence of a mixed mode 1 and 2 crack tip deformation and a large axial stress preceding the propagating crack. These numerical results were used to evaluate the dynamic crack curving and crack arrest criteria and hence to assess the possibility of crack curving as the crack approaches a tear strap without the presence of MSD. GRA

N92-29616# National Aerospace Lab., Amsterdam (Netherlands). Flight Div.
RESULTS OF A FLIGHT SIMULATOR EXPERIMENT TO ESTABLISH HANDLING QUALITY GUIDELINES FOR THE DESIGN OF FUTURE TRANSPORT AIRCRAFT
J. A. J. vanEngelen 8 Jul. 1988 18 p Presented at the AIAA Flight Mechanics Conference, Minneapolis, MN, 15-17 Aug. 1988
(NLR-MP-88044-U; GARTEUR-TP-051; ETN-92-91514) Avail: CASI HC A03/MF A01

An experiment on a flight simulator is presented. The main results are discussed and compared with the contemporary handling qualities criteria used to design the flight control system. The experiment was defined and executed in moving base flight simulator. Emphasis of this experiment was put on longitudinal handling qualities. Test pilots evaluated 2 primary and 2 backup systems during a 3 day period in 2 levels of environment disturbances. Fully electrical fly by wire flight control systems stabilize the aircraft and enable the pilot to directly control a predetermined flight parameter. The necessary control surface deflection is determined by an onboard computer. For such advanced aircraft it is imperative to investigate whether existing handling qualities criteria can still be used for the design of primary and backup system, and particularly, whether guidelines are required to cover the change introduced when a failure occurs and the flight control system reverts to a backup system with different characteristics. ESA

N92-29650# Messerschmitt-Boelkow-Blohm G.m.b.H., Munich (Germany, F.R.). Aircraft Div.
CONCURRENT ENGINEERING IN DESIGN OF AIRCRAFT STRUCTURES
J. Krammer, O. Sensburg, J. Vilsmeier, and G. Berchtold 27 Sep. 1991 36 p Presented at the 73rd AGARD Structures and Materials Panel Meeting, San Diego, CA, 7-11 Oct. 1991
(MBB-FE-2-S-PUB-472; ETN-92-91500) Copyright Avail: CASI HC A03/MF A01

The concurrent engineering idea in design of aircraft structures is explained and its meaning is depicted by showing several examples from the design and manufacturing process for new airplanes. Time and cost savings can be achieved if the concurrent engineering philosophies are also applied very early to cover reliability and supportability aspects. ESA

N92-30209*# Old Dominion Univ., Norfolk, VA. Dept. of Mechanical Engineering and Mechanics.
NONLINEAR ANALYSES OF COMPOSITE AEROSPACE STRUCTURES IN SONIC FATIGUE Progress Report, 16 Dec. 1991 - 15 Jun. 1992
Chuh Mei 15 Jun. 1992 13 p
(Grant NAG1-1358)
(NASA-CR-190565; NAS 1.26:190565) Avail: CASI HC A03/MF A01

The primary research effort of this project is the development of analytical methods for the prediction of nonlinear random response of composite aerospace structures subjected to combined acoustic and thermal loads. The progress, accomplishments, and future plans of three random response research topics are discussed, namely acoustics-structure interactions using boundary/finite element methods, nonlinear vibrations of beams and composite plates under harmonic and random excitations, and numerical simulation of the nonlinear response of composite plates under combined thermal and acoustic loading. Author

06 AIRCRAFT INSTRUMENTATION

Includes cockpit and cabin display devices; and flight instruments.

For related information see also *19 Spacecraft Instrumentation* and *35 Instrumentation and Photography.*

N92-29870# Deutsche Forschungsanstalt fuer Luft- und Raumfahrt, Brunswick (Germany, F.R.). Abt. Flaechenflugzeuge.
SENSOR FAULT DETECTION ON BOARD AN AIRCRAFT WITH OBSERVER AND POLYNOMIAL CLASSIFIER Ph.D. Thesis - Technische Univ. [SENSORFEHLERERKENNUNG IN FLUGZEUGEN MIT BEOBACHTER UND POLYNOMKLASSIFIKATOR]
Joerg J. Buchholz Aug. 1991 65 p In GEORGIAN

(DLR-FB-91-34; ISSN-0939-2963; ETN-92-91390) Avail: CASI HC A04/MF A01; DLR, Wissenschaftliches Berichtswesen, Postfach 90 60 58, 5000 Cologne, Fed. Republic of Germany, HC

A sensor fault detection method for the airspeed vector of an aircraft is described. A nonlinear estimator uses a mathematical aircraft motion model and a few measured signals to generate an estimate of the airspeed vector to be monitored. This reference signal and the measurement signal are fed into a learning pattern recognition algorithm, which determined the state of the sensor from the differences between the two signals. In a practical realization, the classifier is parallelized, implemented on a transputer network, and verified using flight test data. ESA

07 AIRCRAFT PROPULSION AND POWER

Includes prime propulsion systems and systems components, e.g., gas turbine engines and compressors; and onboard auxilliary power plants for aircraft.

For related information see also *20 Spacecraft Propulsion and Power, 28 Propellants and Fuels,* and *44 Energy Production and Conversion.*

N92-29425*# National Aeronautics and Space Administration. Hugh L. Dryden Flight Research Facility, Edwards, CA.

EFFECTS OF BLEED AIR EXTRACTION ON THRUST LEVELS ON THE F404-GE-400 TURBOFAN ENGINE

Andrew J. Yuhas (PRC Kentron, Inc., Edwards, CA.) and Ronald J. Ray Jul. 1992 15 p Presented at the 28th AIAA Joint Propulsion Conference, Nashville, TN, 6-8 Jul. 1992

(RTOP 505-68-30)

(NASA-TM-104247; H-1806; NAS 1.15:104247; AIAA Paper 92-3092) Avail: CASI HC A03/MF A01

A ground test was performed to determine the effects of compressor bleed flow extraction on the performance of F404-GE-400 afterburning turbofan engines. The two engines were installed in the F/A-18 High Alpha Research Vehicle at the NASA Dryden Flight Research Facility. A specialized bleed ducting system was installed onto the aircraft to control and measure engine bleed airflow while the aircraft was tied down to a thrust measuring stand. The test was conducted on each engine and at various power settings. The bleed air extraction levels analyzed included flow rates above the manufacturer's maximum specification limit. The measured relationship between thrust and bleed flow extraction was shown to be essentially linear at all power settings with an increase in bleed flow causing a corresponding decrease in thrust. A comparison with the F404-GE-400 steady-state engine simulation showed the estimation to be within +/- 1 percent of measured thrust losses for large increases in bleed flow rate. Author

N92-29427*# DieselDyne Corp., Morrow, OH.

A PRELIMINARY DESIGN AND ANALYSIS OF AN ADVANCED HEAT-REJECTION SYSTEM FOR AN EXTREME ALTITUDE ADVANCED VARIABLE CYCLE DIESEL ENGINE INSTALLED IN A HIGH-ALTITUDE ADVANCED RESEARCH PLATFORM

Richard P. Johnston Jul. 1992 55 p

(Contract NAS2-131313; RTOP 505-69-14)

(NASA-CR-186021; H-1775; NAS 1.26:186021) Avail: CASI HC A04/MF A01

Satellite surveillance in such areas as the Antarctic indicates that from time to time concentration of ozone grows and shrinks. An effort to obtain useful atmospheric data for determining the causes of ozone depletion would require a flight capable of reaching altitudes of at least 100,000 ft and flying subsonically during the sampling portion of the mission. A study of a heat rejection system for an advanced variable cycle diesel (AVCD) engine was conducted. The engine was installed in an extreme altitude, high altitude advanced research platform. Results indicate that the waste heat from an AVCD engine propulsion system can be rejected at the maximum cruise altitude of 120,000 ft. Fifteen performance points, reflecting the behavior of the engine as the vehicle proceeded through the mission, were used to characterize the heat exchanger operation. That portion of the study is described in a appendix titled, 'A Detailed Study of the Heat Rejection System for an Extreme Altitude Atmospheric Sampling Aircraft,' by a consultant, Mr. James Bourne, Lytron, Incorporated. Author

N92-29659*# National Aeronautics and Space Administration. Hugh L. Dryden Flight Research Facility, Edwards, CA.

FLIGHT EVALUATION OF AN EXTENDED ENGINE LIFE MODE ON AN F-15 AIRPLANE

Lawrence P. Myers and Timothy R. Conners Apr. 1992 29 p

(RTOP 533-02-36)

(NASA-TM-104240; H-1764; NAS 1.15:104240) Avail: CASI HC A03/MF A01

An integrated flight and propulsion control system designed to reduce the rate of engine deterioration was developed and evaluated in flight on the NASA Dryden F-15 research aircraft. The extended engine life mode increases engine pressure ratio while reducing engine airflow to lower the turbine temperature at constant thrust. The engine pressure ratio uptrim is modulated in real time based on airplane maneuver requirements, flight conditions, and engine information. The extended engine life mode logic performed well, significantly reducing turbine operating temperature. Reductions in fan turbine inlet temperature of up to 80 F were obtained at intermediate power and up to 170 F at maximum augmented power with no appreciable loss in thrust. A secondary benefit was the considerable reduction in thrust-specific fuel consumption. The success of the extended engine life mode is one example of the advantages gained from integrating aircraft flight and propulsion control systems. Author

N92-29661*# National Aeronautics and Space Administration. Lewis Research Center, Cleveland, OH.

CONTINGENCY POWER FOR A SMALL TURBOSHAFT ENGINE BY USING WATER INJECTION INTO TURBINE COOLING AIR

Thomas J. Biesiadny and Gary A. Klann (Army Aviation Systems Command, Cleveland, OH.) 1992 10 p Prepared for presentation at the 80th Symposium on Heat Transfer and Cooling in Gas Turbines, Antalya, Turkey, 12-16 Oct. 1992; sponsored in part by AGARD Propulsion and Energetics Panel

(RTOP 505-68-32)

(NASA-TM-105680; AVSCOM-TR-92-C-019; E-7058; NAS 1.15:105680) Avail: CASI HC A02/MF A01

Because of one-engine-inoperative (OEI) requirements, together with hot-gas reingestion and hot-day, high-altitude take-off situations, power augmentation for multiengine rotorcraft has always been of critical interest. However, power augmentation by using overtemperature at the turbine inlet will shorten turbine life unless a method of limiting thermal and mechanical stress is found. A possible solution involves allowing the turbine inlet temperature to rise to augment power while injecting water into the turbine cooling air to limit hot-section metal temperatures. An experimental water injection device was installed in an engine and successfully tested. Although concern for unprotected subcomponents in the engine hot section prevented demonstration of the technique's maximum potential, it was still possible to demonstrate increases in power while maintaining nearly constant turbine rotor blade temperature. Author

N92-29927# Universitaet der Bundeswehr Muenchen, Neubiberg (Germany, F.R.). Fakultaet fuer Luft- und Raumfahrttechnik.

EXAMINATION OF THE MAIN ERROR FACTORS WITH REGARDS TO SECONDARY LOSSES IN COMPRESSION AND TURBINE CASCADES BY VARIATIONS OF THE BLADE PICTURE RATIO Ph.D. Thesis [UNTERSUCHUNG DER WESENTLICHEN EINFLUSSFAKTOREN AUF DIE SEKUNDAERVERLUESTE IN VERDICHTER- UND TURBINENGITTERN BEI VARIATION DES SCHAUELSEITENVERHAELTNISSES]

Robert Watzlawick 1991 196 p In GERMAN

(ETN-92-91493) Avail: CASI HC A09/MF A03

Extensive experimental examinations were carried out for determining loss correlations. Three various chord lengths were

considered for compressor and turbine profile, in order to obtain information on the influence of blade picture ratio. It is shown that the reduced secondary loss coefficient with the blade picture ratio is independent of blade height and chord length for compressor and turbine cascades. For turbines, the profile loss coefficient can be used with good approximation as a parameter for secondary loss coefficients, with regard to the strong interaction of profile boundary layer and channel vortex. This parameter is not suitable for compressor correlations. ESA

08 AIRCRAFT STABILITY AND CONTROL

Includes aircraft handling qualities; piloting; flight controls; and autopilots.

For related information see also *05 Aircraft Design, Testing and Performance.*

N92-29449# Ballistic Research Labs., Aberdeen Proving Ground, MD.

THE EFFECT OF YAW CARDS ON THE PITCHING AND YAWING MOTION OF SYMMETRIC PROJECTILES Final Report, Mar. - Aug. 1991

Robert L. McCoy May 1992 46 p

(AD-A250021; BRL-TR-3338) Avail: CASI HC A03/MF A01

This report presents an improved method for analysis of the effect of yaw cards on the determination of the pitching moment coefficient of symmetric missiles. Several comparisons of the present method are made with spark photography range results obtained for the same projectiles, and a proper treatment of yaw-card data is shown to significantly improve the agreement between the two techniques. GRA

N92-29654*# Minnesota Univ., Minneapolis. Dept. of Aerospace Engineering and Mechanics.

FEEDBACK CONTROL LAWS FOR HIGHLY MANEUVERABLE AIRCRAFT Interim Report, Jan. - Jul. 1992

William L. Garrard and Gary J. Balas Jul. 1992 41 p

(Grant NAG1-1380)

(NASA-CR-190535; NAS 1.26:190535) Avail: CASI HC A03/MF A01

The results of a study of the application of H infinity and mu synthesis techniques to the design of feedback control laws for the longitudinal dynamics of the High Angle of Attack Research Vehicle (HARV) are presented. The objective of this study is to develop methods for the design of feedback control laws which cause the closed loop longitudinal dynamics of the HARV to meet handling quality specifications over the entire flight envelope. Control law designs are based on models of the HARV linearized at various flight conditions. The control laws are evaluated by both linear and nonlinear simulations of typical maneuvers. The fixed gain control laws resulting from both the H infinity and mu synthesis techniques result in excellent performance even when the aircraft performs maneuvers in which the system states vary significantly from their equilibrium design values. Both the H infinity and mu synthesis control laws result in performance which compares favorably with an existing baseline longitudinal control law. Author

N92-30025*# National Aeronautics and Space Administration. Langley Research Center, Hampton, VA.

HELICOPTER LOW-SPEED YAW CONTROL Patent Application

John C. Wilson, inventor (to NASA), Henry L. Kelley, inventor (to NASA), and Cynthia A. Crowell, inventor (to NASA) (Army Aerostructures Directorate, Hampton, VA.) 7 Nov. 1991 10 p

(NASA-Case-LAR-14219-1; NAS 1.71:LAR-14219-1; US-Patent-Appl-SN-788908) Avail: CASI HC A02/MF A01

A system for improving yaw control at low speeds consists of one strake placed on the upper portion of the fuselage facing the retreating rotor blade and another strake placed on the lower portion of the fuselage facing the advancing rotor blade. These strakes spoil the airflow on the helicopter tail boom during hover, low speed flight, and right or left sidewards flight so that less side thrust is required from the tail rotor. Author

09 RESEARCH AND SUPPORT FACILITIES (AIR)

Includes airports, hangars and runways; aircraft repair and overhaul facilities; wind tunnels; shock tubes; and aircraft engine test stands.

For related information see also *14 Ground Support Systems and Facilities (Space).*

N92-29352*# North Carolina State Univ., Raleigh.

BUFFET TEST IN THE NATIONAL TRANSONIC FACILITY Final Report

Clarence P. Young, Jr., Dennis W. Hergert, Thomas W. Butler, and Fred M. Herring Jul. 1992 66 p Prepared in cooperation with Boeing Co., Seattle, WA Original contains color illustrations

(Contract NCC1-141; RTOP 505-59-85-01)

(NASA-CR-189595; NAS 1.26:189595) Avail: CASI HC A04/MF A01; 2 functional color pages

A buffet test of a commercial transport model was accomplished in the National Transonic Facility at the NASA Langley Research Center. This aeroelastic test was unprecedented for this wind tunnel and posed a high risk for the facility. Presented here are the test results from a structural dynamics and aeroelastic response point of view. The activities required for the safety analysis and risk assessment are described. The test was conducted in the same manner as a flutter test and employed on-board dynamic instrumentation, real time dynamic data monitoring, and automatic and manual tunnel interlock systems for protecting the model. Author

N92-29505# General Electric Co., Gilbert, AZ. Government Services.

TRANSPORT DELAY MEASUREMENTS: METHODOLOGY AND ANALYSIS FOR THE F-16C COMBAT ENGAGEMENT TRAINER, THE DISPLAY FOR ADVANCED RESEARCH AND TRAINING, AND THE F-16A LIMITED FIELD OF VIEW Final Technical Paper, Mar. 1991 - Jan. 1992

Roger W. Leinenwever and Susanne I. Moran Mar. 1992 30 p

(Contract F33615-88-C-0014)

(AD-A248519; AL-TP-1992-0009) Avail: CASI HC A03/MF A01

Transport delays between the cockpit and visual/sensors in simulation systems can result in significant degradation of flight simulation training. At the Armstrong Laboratory, Aircrew Training Research Division, methodologies for testing visible delays were developed and measurements run on three systems. The tests showed significant transport delays; in some cases, higher than anticipated. Further analysis of the data revealed that the delays were caused by specific hardware and software configurations. Changes in configurations can eliminate the problem entirely, or can decrease transport delays to an acceptable range. GRA

N92-29655*# MCAT Inst., San Jose, CA.

STUDY OF OPTICAL TECHNIQUES FOR THE AMES UNITARY WIND TUNNELS. PART 3: ANGLE OF ATTACK Progress Report

George Lee Jun. 1992 27 p

(Contract NCC2-716)

(NASA-CR-190541; NAS 1.26:190541; MCAT-92-011-Pt-3) Avail: CASI HC A03/MF A01

A review of optical sensors that are capable of accurate angle of attack measurements in wind tunnels was conducted. These include sensors being used or being developed at NASA Ames and Langley Research Centers, Boeing Airplane Company, McDonald Aircraft Company, Arnold Engineering Development Center, National Aerospace Laboratory of the Netherlands, National Research Council of Canada, and the Royal Aircraft Establishment of England. Some commercial sensors that may be applicable to

accurate angle measurements were also reviewed. It was found that the optical sensor systems were based on interferometers, polarized light detector, linear or area photodiode cameras, position sensing photodetectors, and laser scanners. Several of the optical sensors can meet the requirements of the Ames Unitary Plan Wind Tunnel. Two of these, the Boeing interferometer and the Complere lateral effect photodiode sensors are being developed for the Ames Unitary Plan Wind Tunnel. Author

N92-29664*# Vanderbilt Univ., Nashville, TN. Dept. of Physics and Astronomy.
NEUTRALIZER AND SAMPLE CHAMBER FOR THE ATOMIC OXYGEN SIMULATION SYSTEM (AOSS) Final Report, 1 Nov. 1989 - 30 Apr. 1991
Royal G. Albridge, Alan V. Barnes, and Norman H. Tolk 15 May 1992 10 p
(Contract NAS8-37748)
(NASA-CR-184343; NAS 1.26:184343) Avail: CASI HC A02/MF A01

A neutralizer system capable of converting a beam of oxygen ions (O(+) or O2(+)) into a beam of low-energy neutral oxygen atoms (O) was developed. The neutralizer system is to be designed to be compatible with the Atomic Oxygen Simulation System (AOSS) located in the Physical Science Branch of MSFC. The Center for Molecular and Atomic Studies at Surfaces (CMASS) at Vanderbilt University has met these objectives by developing a system that neutralizes the ions through electron transfer during a grazing-incidence reflection of an ion beam from a smooth nickel surface. The purpose is to describe the system, provide schematic representations of the system, and to discuss the use of the system in relation to the AOSS at the Physical Science Branch of MSFC. Author

N92-29709# Anacapa Sciences, Inc., Fort Rucker, AL.
ASSESSMENT OF ARMY AVIATORS' ABILITY TO PERFORM INDIVIDUAL AND COLLECTIVE TASKS IN THE AVIATION NETWORKED SIMULATOR Interim Report, Sep. 1988 - Nov. 1990
Beth W. Smith and Kenneth D. Cross Apr. 1992 92 p
(Contract MDA903-87-C-0523; AF Proj. 3405)
(AD-A250293; ARI-RN-92-32) Avail: CASI HC A05/MF A01

This research evaluates the training effectiveness of the Aviation Networked Simulator (hereafter referred to as AIRNET). The research was designed to (1) assess experienced crewmembers' ability to perform selected individual and collective tasks in AIRNET, and (2) identify the specific design attributes that makes it difficult for crewmembers to perform tasks to standards in AIRNET. Because the research examined only in-simulator performance, inferences about the device's training effectiveness can be drawn only from data indicating that experienced crewmembers cannot perform a task effectively in AIRNET. Specifically, it is assumed that tasks cannot be trained effectively on a device if they cannot be performed adequately on that device. Transfer-of-training studies are required to assess the AIRNET's effectiveness for training tasks that can be performed adequately on the device. The report presents detailed data on the relative effectiveness of crewmembers performing the individual and collective tasks investigated. The report also presents detailed data on crewmember ratings of the adequacy of AIRNET for both performing and training specific tasks and conclusions and recommendations about the need to modify the design of AIRNET components. GRA

N92-30076# Messerschmitt-Boelkow-Blohm G.m.b.H., Munich (Germany, F.R.). Helicopter Div.
EXPERIENCE WITH PILOTED SIMULATION IN THE DEVELOPMENT OF HELICOPTERS
M. Obermayer, K. Kampa, W. Doehnel, and A. Faulkner 1991 12 p Presented at 79th AGARD Flight Mechanics Panel Symposium on Pilot Simulation Effectiveness, Brussels, Belgium, 14-17 Oct. 1991 Previously announced as N92-28528
(MBB-UD-0610-91-PUB; ETN-92-91697) Avail: CASI HC A03/MF A01

Applicability, limitations, acceptance, and effectiveness of helicopter simulation are considered. Some of the key points are the objective and subjective validation of a simulator and the various factors which influence the acceptance by pilots. In this context it is very important to make a tradeoff between simulator sophistication (i.e., cost) and required result (i.e., design input) in the actual phase of development. Other aspects of simulation effectiveness include evaluation and training of critical flight conditions prior to flight tests as well as involving the customer from early concept studies up to full mission simulations, which gives more influence in the design and leads to better identification with product. 'Do's' and 'don'ts' in piloted simulation to achieve maximum simulation effectiveness are presented. ESA

N92-29283*# SRI International Corp., Menlo Park, CA. Geoscience and Engineering Center.
ARCLITE: THE ARCTIC LIDAR TECHNOLOGY FACILITY AT SONDRE STROMFJORD, GREENLAND
J. P. Thayer *In* NASA. Langley Research Center, Sixteenth International Laser Radar Conference, Part 1 Jul. 1992 p 201-203 (For primary document see N92-29228 20-35)
Avail: CASI HC A01/MF A04

N92-29299*# General Electric Co., Philadelphia, PA. Astro Space Div.
GE'S MOBILE, COHERENT DOPPLER LIDAR TEST/EVALUATION FACILITIES
J. T. Sroga, J. W. Scott, S. C. Kiernan, F. J. Weaver, J. E. Trotta, and J. C. Petheram *In* NASA. Langley Research Center, Sixteenth International Laser Radar Conference, Part 1 Jul. 1992 p 265-267 (For primary document see N92-29228 20-35)
Avail: CASI HC A01/MF A04

12 ASTRONAUTICS (GENERAL)

For extraterrestrial exploration see *91 Lunar and Planetary Exploration.*

N92-29879# European Space Agency, Paris (France).
FOURTH MEETING OF THE SPACE AGENCY FORUM ON THE INTERNATIONAL SPACE YEAR (SAFISY-4)
T.-D. Guyenne, ed. Dec. 1991 156 p Meeting held in Moscow, USSR, 16-17 May 1991
(ESA-SP-1141; ISBN-92-9092-140-4; ETN-92-91388) Copyright Avail: CASI HC A08/MF A02; ESA, EPD, ESTEC, Noordwijk, Netherlands, HC

The SAFISY-4 meeting report contains: a report on the SAFISY status, contributions to ISY by SAFISY members, reports of panels of experts, USSR's contribution to ISY, preparation of 1992 events, reports of associations and research groups, and post-1992 collaboration in SAFISY projects. The meeting is aimed at the preparation of the International Space Year, to promote cooperation of a wide circle of specialists and public figures in the interest of in depth studies of the planet Earth. ESA

N92-29929# Naval Postgraduate School, Monterey, CA.
EVALUATING THE MILITARY POTENTIAL OF A DEVELOPING NATION'S SPACE PROGRAM: A CASE STUDY OF BRAZIL M.S. Thesis
Michael J. Collins Sep. 1991 105 p
(AD-A245978) Avail: CASI HC A06/MF A02

This thesis examines how and why a developing nation may use its civilian space program to acquire ballistic missiles. Using a single case study of Brazil, this analysis looks for universal patterns in space program development and for how Third World nations use their civilian space programs for military purposes. This thesis analyzes the relationship between space and missile development, the Missile Technology Control Regime, reasons for building missiles (political, economic, national security, geopolitical, need for technology), Brazilian civil-military relations, and various technologies and space systems. It identifies the critical technologies required for a successful space program; identifies

the critical industries that are missing in Brazil and the technologies that it must import; highlights indicators of military intentions of a civilian space program; and evaluates how the generalizations developed throughout the thesis may be applied to other nations. GRA

N92-30016*# National Aeronautics and Space Administration. Marshall Space Flight Center, Huntsville, AL.
ATLAS 1: ENCOUNTERING PLANET EARTH
Charlotte Shea (Essex Corp., Huntsville, AL.), Tracy McMahan (Essex Corp., Huntsville, AL.), Denise Accardi (Essex Corp., Huntsville, AL.), Michele Tygielski (Essex Corp., Huntsville, AL.), Jeff Mikatarian (Essex Corp., Huntsville, AL.), and Margaret Wiginton, ed. (Essex Corp., Huntsville, AL.) [1984] 62 p LIMITED REPRODUCIBILITY: More than 20% of this document may be affected by color photographs original contains color illustrations
(NASA-TM-107956; NAS 1.15:107956) Avail: CASI HC A04/MF A01; 56 functional color pages

Several NASA science programs examine the dynamic balance of sunlight, atmosphere, water, land, and life that governs Earth's environment. Among these is a series of Space Shuttle-Spacelab missions, named the Atmospheric Laboratory for Applications and Science (ATLAS). During the ATLAS missions, international teams of scientists representing many disciplines combine their expertise to seek answers to complex questions about the atmospheric and solar conditions that sustain life on Earth. The ATLAS program specifically investigates how Earth's middle atmosphere and upper atmospheres and climate are affected by both the Sun and by products of industrial and agricultural activities on Earth H.A.

13 ASTRODYNAMICS

Includes powered and free-flight trajectories; and orbital and launching dynamics.

No abstracts in this category.

14 GROUND SUPPORT SYSTEMS AND FACILITIES (SPACE)

Includes launch complexes, research and production facilities; ground support equipment, e.g., mobile transporters; and simulators.

For related information see also *09 Research and Support Facilities (Air).*

No abstracts in this category.

15 LAUNCH VEHICLES AND SPACE VEHICLES

Includes boosters; operating problems of launch/space vehicle systems; and reusable vehicles.

For related information see also *20 Spacecraft Propulsion and Power.*

N92-29967# Norwegian Defence Research Establishment, Kjeller.
PENGUIN EXTRUDED ALUMINIUM BOX LAUNCHER FOR MARINE APPLICATION [KASSELAUNCHER AV EKSTRUDERT ALUMINIUM FOR FARTOYVERSJON AV PENGUIN]
Johan Andreas Muerer 20 Mar. 1991 113 p In NORWEGIAN (FFI-91/4001; ISSN-0802-2437; ETN-92-91703) Avail: CASI HC A06/MF A02

A new low cost box launcher of extruded aluminum profiles for the Penguin missile is studied. Initial design guidelines are specified and a design proposal is carried out. The design work includes: engineering drawings, identification of critical loads, static and dynamic analysis of critical structural components, and weight and cost estimates. The internal mechanical arrangements of the box launcher are based on the Penguin Mk3 missile with two horizontally placed, ejectable, external booster motors. The box launcher cross section is proposed as a result of the implementation of short span extendable wings in the missile. ESA

N92-29986# Sandia National Labs., Albuquerque, NM.
A NEW HYPERVELOCITY LAUNCHER (HVL) FOR SPACE SCIENCE APPLICATION
L. C. Chhabildas 1991 5 p Presented at the American Institute of Astronautics and Aeronautics (AIAA) Space Programs and Technologies Conference, Huntsville, AL, 24-27 Mar. 1992 (Contract DE-AC04-76DP-00789)
(DE92-010670; SAND-91-1691C; CONF-920373-2) Avail: CASI HC A01/MF A01

Very high driving pressures (tens or hundreds of GPa) are required to accelerate flier plats to hypervelocities. This loading pressure pulse on the fiber plates must be nearly shockless to prevent the plate from melting or vaporizing. This is accomplished by using graded-density impactors referred to as 'pillows'. When this graded-density material is used to impact a flier-plate in a modified two-stage light gas gun, nearly shockless megabar pressures are introduced into the flier plate. The pressure pulses must also be tailored to prevent spallation of the flier-plate. This technique has been used to launch nominally 1-mm-thick aluminum, magnesium, and titanium (gram-size) intact plates to 10.4 km/s, and 0.5-mm-thick aluminum and titanium (half-gram size) intact plates to 12.2 km/s. This is the highest mass-velocity capability attained with laboratory launchers to data, and should open up new regimes of impact physics and lethality studies related to space sciences for laboratory investigations. DOE

N92-30215*# National Aeronautics and Space Administration. Marshall Space Flight Center, Huntsville, AL.
NATIONAL LAUNCH SYSTEM CYCLE 1 LOADS AND MODELS DATA BOOK
F. Bugg, J. Brunty, G. Ernsberger, D. McGhee, L. Gagliano, F. Harrington, D. Meyer, and E. Blades Jun. 1992 568 p
(NASA-TM-103560; NAS 1.15:103560) Avail: CASI HC A24/MF A04

This document contains preliminary cycle 1 loads for the National Launch System (NLS) 1 and 2 vehicles. The loads provided and recommended as design loads represent the maximum load expected during prelaunch and flight regimes, i.e., limit loads, except that propellant tank ullage pressure has not been included. Ullage pressure should be added to the loads book values for cases where the addition results in higher loads. The loads must be multiplied by the appropriate factors of safety to determine the ultimate loads for which the structure must be capable. Author

16 SPACE TRANSPORTATION

Includes passenger and cargo space transportation, e.g., shuttle operations; and space rescue techniques.

For related information see also *03 Air Transportation and Safety* and *18 Spacecraft Design, Testing and Performance.* For space suits see *54 Man/System Technology and Life Support.*

N92-29629# Messerschmitt-Boelkow-Blohm G.m.b.H., Munich (Germany, F.R.). Hubschrauber und Flugzeuge.
SAENGER: THE REFERENCE CONCEPT AND ITS TECHNOLOGICAL REQUIREMENTS - AEROTHERMODYNAMICS
E. H. Hirschel 26 Aug. 1991 16 p Presented at Review of

the German Hypersonic and Technology Programme, Bonn, Fed. Republic of Germany, 16-17 Apr. 1991
(MBB-FE-202-S-PUB-0463-A; ETN-92-91496) Copyright Avail: CASI HC A03/MF A01

The objectives of the technology program 'aerothermodynamics and propulsion integration' are defined. An overview of the special aerothermodynamic phenomena which must be regarded in the design of the Saenger lower stage which presently stands in the center of the technology program is given. The design tools, which must be provided; the components like the inlet, the afterbody, etc., which must be designed and tested; and the special problems like forebody optimization, heat load determination, upper stage integration, etc., which must be treated, are discussed. The general work plan is presented, showing the major activities up to start of the development of the Saenger space transportation system. It includes the development and manufacturing of the experimental vehicle (HYTEXT) as a means for the validation of the design tools and methods which are achieved in the technology program, and for the creation of a freeflight data base. ESA

N92-29680# Messerschmitt-Boelkow-Blohm G.m.b.H., Munich (Germany, F.R.). Hubschrauber und Flugzeuge.
AEROTHERMODYNAMIC CHALLENGES OF THE SAENGER SPACE-TRANSPORTATION SYSTEM
E. H. Hirschel 2 Sep. 1991 13 p Presented at 1st European Symposium on Aerothermodynamics for Space Vehicles, Noordwijk, Netherlands, 28-30 May 1991
(MBB-FE-202-S-PUB-0462-A; ETN-92-91495) Copyright Avail: CASI HC A03/MF A01

The two-stage-to-orbit Saenger space transportation system is the reference concept of the German hypersonics technology program. The technology development concentrates first on the needs of the lower stage. Its requirements on aerothermodynamics and propulsion integration are sketched. The aerothermodynamic design challenge is discussed and the design tools and the design methodology are reviewed. The calibration of both the computational and the experimental methods, as well as the test of vehicle components like the inlet, control surfaces etc., make the Hypersonic Technology Experimental vehicle (HYTEX) mandatory. Contents and workplan of the technology program 'aerothermodynamics and propulsion integration' are laid out. Selected results from the current work are presented. ESA

17 SPACE COMM., SPACECRAFT COMM., COMMAND & TRACKING

Includes telemetry; space communications networks; astronavigation and guidance; and radio blackout.

For related information see also *04 Aircraft Communications and Navigation* and *32 Communications and Radar.*

N92-29365*# Jet Propulsion Lab., California Inst. of Tech., Pasadena.
A DETERMINATION OF THE RADIO-PLANETARY FRAME TIE FROM COMPARISON OF EARTH ORIENTATION PARAMETERS
M. H. Finger and W. M. Folkner *In its* The Telecommunications and Data Acquisition Report 15 May 1992 p 1-21 (For primary document see N92-29364 20-32)
(RTOP 310-10-60-50-00)
Avail: CASI HC A03/MF A04

N92-29368*# Jet Propulsion Lab., California Inst. of Tech., Pasadena.
DEEP-SPACE NAVIGATION WITH DIFFERENCED DATA TYPES. PART 3: AN EXPANDED INFORMATION CONTENT AND SENSITIVITY ANALYSIS
J. A. Estefan and S. W. Thurman *In its* The Telecommunications and Data Acquisition Report 15 May 1992 p 56-73 (For primary document see N92-29364 20-32)
(RTOP 310-10-63-50-00)
Avail: CASI HC A03/MF A04

N92-29369*# Jet Propulsion Lab., California Inst. of Tech., Pasadena.
ORBITER-ORBITER AND ORBITER-LANDER TRACKING USING SAME-BEAM INTERFEROMETRY
W. M. Folkner and J. S. Border *In its* The Telecommunications and Data Acquisition Report 15 May 1992 p 74-86 (For primary document see N92-29364 20-32)
(RTOP 310-10-63-88-01)
Avail: CASI HC A03/MF A04

N92-29370*# Jet Propulsion Lab., California Inst. of Tech., Pasadena.
GEOMETRIC DISTORTION ANALYSIS OF A WIDE-FIELD ASTROGRAPH
W. M. Owen, Jr. and S. B. Shaklan *In its* The Telecommunications and Data Acquisition Report 15 May 1992 p 87-93 (For primary document see N92-29364 20-32)
(RTOP 310-10-63-92-01)
Avail: CASI HC A02/MF A04

N92-29383*# Jet Propulsion Lab., California Inst. of Tech., Pasadena.
DSN ACQUISITION OF MAGELLAN HIGH-RATE TELEMETRY DATA
A. L. Berman and P. A. Au *In its* The Telecommunications and Data Acquisition Report 15 May 1992 p 253-264 (For primary document see N92-29364 20-32)
(RTOP 314-40-22-35-01)
Avail: CASI HC A03/MF A04

18 SPACECRAFT DESIGN, TESTING AND PERFORMANCE

Includes satellites; space platforms; space stations; spacecraft systems and components such as thermal and environmental controls; and attitude controls.

For life support systems see *54 Man/System Technology and Life Support.* For related information see also *05 Aircraft Design, Testing and Performance, 39 Structural Mechanics,* and *16 Space Transportation.*

N92-29422*# Massachusetts Inst. of Tech., Cambridge. Dept. of Aeronautics and Astronautics.
SPACECRAFT DYNAMICS CHARACTERIZATION AND CONTROL SYSTEM FAILURE DETECTION, VOLUME 1 Final Report 9 Feb. 1989 - 8 Feb. 1992
20 Jul. 1992 54 p
(Grant NAG1-968)
(NASA-CR-190517; NAS 1.26:190517) Avail: CASI HC A04/MF A01

The work under this grant has been directed to two aspects of the control of flexible spacecraft: (1) the modeling of deployed or erected structures including nonlinear joint characteristics; and (2) the detection and isolation of failures of the components of control systems for large space structures. The motivation for the first of these research tasks is the fact that very large assemblies in space will have to be built or deployed in situ. A likely scenario is, in fact, a combination of these wherein modules which are folded for transportation into orbit are erected to their final configuration and then jointed with other such erected modules to form the full assembly. Any such erectable modules will have joints. It remains to be seen whether or not joints designed for operational assemblies will have nonlinear properties, but it seems prudent to develop a methodology for dealing with that possibility. The motivation for the second of these research tasks is the fact that we foresee large assemblies in space which will require active control to damp vibrations and/or hold a desired shape. Lightweight structures will be very flexible, with many elastic modes having very low frequencies. In order to control these modes well, the control system will likely require many sensors and many actuators, probably distributed over much of the structure. The combination of a large number of control system components with long

operational periods virtually guarantees that these systems will suffer control system component failures during operation. The control system must be designed to tolerate failures of some sensors and actuators, and still be able to continue to perform its function. Author

N92-29480# Israel Aircraft Industries Ltd., Lod.
OFFEQ-1: PRELIMINARY FLIGHT EVALUATION RESULTS
J. Wittenstein and M. Barlev 1990 12 p
(ITN-92-85126) Avail: CASI HC A03/MF A01

OFFEQ-1, Israel's first satellite, was launched into an orbit with a perigee altitude of 248 km and an apogee attitude of 1170 km at 09:32 UT on 19 Sep. 1988. It was expected to operate successfully for at least one month and to remain in orbit for about three to three and a half months. The satellite was tracked by the ground control station at MBT. The satellite was aloft for nearly four months, and operated successfully for the entire mission, up to loss of signal at the last available communication pass before its final decay. All systems operated successfully during the entire mission. The OFFEQ-1 computer gathered and transmitted data, with more than adequate electrical power. Also the thermal control system provided a very benign environment. The only malfunction occurred in the telemetry memory and the computer successfully reconfigured the telemetry memory to the backup mode. Author (ISA)

N92-29525# Air Force Inst. of Tech., Wright-Patterson AFB, OH. School of Engineering.
AN ANALYSIS OF THE ENDURANCE OF MOBILE SATELLITE COMMAND AND CONTROL SYSTEMS M.S. Thesis
Steven O. Brown Mar. 1992 135 p
(AD-A248084; AFIT/GOR/ENS/92M-03) Avail: CASI HC A07/MF A02

This study investigated the endurance of a single deployed generic mobile space (GMS) command and control (C2) system. Specifically, factors which affect overall system performance were examined. The analysis began with the development of a simulation model for a GMS C2 system. Optimal settings of factor levels were determined by using the model to find peak system endurance and availability. Factors set were field support vehicle (FSV) access, numbers of maintenance personnel, and numbers of spare components available. After optimum values were chosen for these factors, an experimental design was conducted to determine factor effect between maintenance manpower and the component failure and repair rates. It was determined that access to the FSV increases system endurance by 6.1 percent. Increasing maintenance manpower does not significantly affect system availability. Eight components, most in the communications subsystems, were identified for increased spares levels which could increase system endurance by an additional 2.8 percent. Of all factors and combination of factors considered in the experimental design, only the rate of component failures significantly affected system performance. GRA

N92-29810*# National Aeronautics and Space Administration. Goddard Space Flight Center, Greenbelt, MD.
GEOSTATIONARY OPERATIONAL ENVIRONMENTAL STATELLITE(GEOS-N REPORT) Executive Summary
Dec. 1991 43 p
(NASA-TM-107919; NAS 1.15:107919; PB92-147115) Avail: CASI HC A03/MF A01

The Advanced Missions Analysis Office (AMAO) of GSFC has completed a study of the Geostationary Operational Environmental Satellites (GOES-N) series. The feasibility, risks, schedules, and associated costs of advanced space and ground system concepts responsive to National Oceanic and Atmospheric Administration (NOAA) requirements were evaluated. The study is the first step in a multi-phased procurement effort that is expected to result in launch ready hardware in the post 2000 time frame. This represents the latest activity of GSFC in translating meteorological requirements of NOAA into viable space systems in geosynchronous earth orbits (GEO). GOES-N represents application of the latest spacecraft, sensor, and instrument technologies to enhance NOAA meteorological capabilities via remote and in-situ sensing from GEO. The GOES-N series, if successfully developed, could become another significant step in NOAA weather forecasting space systems, meeting increasingly complex emerging national needs for that agency's services. Author

N92-29811*# National Aeronautics and Space Administration. Goddard Space Flight Center, Greenbelt, MD.
GEOSTATIONARY OPERATIONAL ENVIRONMENTAL SATELLITE (GOES-N REPORT). VOLUME 1: TECHNICAL
Dec. 1991 350 p
(NASA-TM-107918; NAS 1.15:107918; PB92-147123) Avail: CASI HC A15/MF A03

The GOES-N study consisted of five distinct tasks including: determining replication costs of GOES I-M and GOES-7 in the GOES-N time frame; defining and evaluating modifications to GOES I-M to improve efficiency or reduce costs; and defining evolutionary changes to the GOES I-M design to satisfy National Weather Service (NWS) 1983 and NOAA 1989 requirements. The categorization and disposition of NOAA requirements is reported in volume 1 section 4. Results of the GOES I-M efficiency/cost improvement modifications study are described in Section 7.1. The system concept options 1, 2, and 3 that generally represent the results of the Task 2, 3A, and 3B studies are summarized in Section 7.2. Another result of the GOES-N study, the determination of which NWS 1983 and NOAA 1989 requirements can be met with the three options, is contained in volume 1 section 7. Conclusions and recommendations are covered in volume 1 section 8. Imager, sounder, control system, space environment monitor, search and rescue, weather facsimile, data collection system, and products/process/communications recommendations were extracted from sections 9, 10, and 11. Section 8 also contains conclusions pertaining to programmatic operational satellite issues (prerequisite development strategies, the direct procurement of instruments by the government, protoflight mission, etc.). Sections 9, 10, and 11 address instrument, control system, image/navigation/registration, and other system design considerations and surveys. These sections are supported by the appendices in volume 2. Author

N92-29812*# National Aeronautics and Space Administration. Goddard Space Flight Center, Greenbelt, MD.
GEOSTATIONARY OPERATIONAL ENVIRONMENTAL SATELLITE (GOES-N REPORT). VOLUME 2: TECHNICAL APPENDIX
Feb. 1992 479 p
(NASA-TM-107920; NAS 1.15:107920; PB92-147131) Avail: CASI HC A21/MF A04

The contents include: operation with inclinations up to 3.5 deg to extend life; earth sensor improvements to reduce noise; sensor configurations studied; momentum management system design; reaction wheel induced dynamic interaction; controller design; spacecraft motion compensation; analog filtering; GFRP servo design - modern control approach; feedforward compensation as applied to GOES-1 sounder; discussion of allocation of navigation, inframe registration and image-to-image error budget overview; and spatial response and cloud smearing study. Author

19 SPACECRAFT INSTRUMENTATION

For related information see also *06 Aircraft Instrumentation* and *35 Instrumentation and Photography.*

N92-30217*# Texas Univ. at Dallas, Richardson.
SUPPORT ACTIVITIES TO MAINTAIN SUMS FLIGHT READINESS Final Technical Report
Willie Wright 19 May 1992 36 p
(Contract NAS1-17399; RTOP 506-48-11-03)
(NASA-CR-189656-Vol-1; NAS 1.26:189656-Vol-1; UTD-23351-961-Vol-1) Avail: CASI HC A03/MF A01

The Shuttle Upper Atmosphere Mass Spectrometer (SUMS),

a component experiment of the NASA Orbital Experiments Program (OEX), was flown aboard the shuttle Columbia (OV102) mounted at the forward end of the nose landing gear well with an atmospheric gas inlet system fitted to the lower fuselage (chin panel) surface. The SUMS was designed to provide atmospheric data in flow regimes inaccessible prior to the development of the Space Transportation System (STS). The experiment mission operation began about one hour prior to shuttle de-orbit entry maneuver and continued until reaching 1.6 torr (about 86 km altitude). The SUMS mass spectrometer consists of the spare unit from the Viking mission to Mars. Bendix Aerospace under contract to NASA LaRC incorporated the Viking mass spectrometer, a microprocessor based logic card, a pressurized instrument case, and the University of Texas at Dallas provided a gas inlet system into a configuration suited to interface with the shuttle Columbia. The SUMS experiment underwent static and dynamic calibration as well as vacuum maintenance before and after STS 40 shuttle flight. The SUMS flew a total of 3 times on the space shuttle Columbia. Between flights the SUMS was maintained in flight ready status. The flight data has been analyzed by the NASA LaRC Aerothermodynamics Branch. Flight data spectrum plots and reports are presented in the Appendices to the Final Technical Report for NAS1-17399. Author

N92-30218*# Texas Univ. at Dallas, Richardson.
SUPPORT ACTIVITIES TO MAINTAIN SUMS FLIGHT READINESS, VOLUME 2. ATTACHMENT A: FLIGHT 61-C REPORT Final Technical Report
Willie Wright May 1992 105 p
(Contract NAS1-17399; RTOP 506-48-11-03)
(NASA-CR-189656-Vol-2; NAS 1.26:189656-Vol-2) Avail: CASI HC A06/MF A02

The Shuttle Upper Atmosphere Mass Spectrometer (SUMS), a component experiment of the NASA Orbital Experiments Program (OEX), was flown aboard the shuttle Columbia (OV102) mounted at the forward end of the nose landing gear well with an atmospheric gas inlet system fitted to the lower fuselage (chin panel) surface. The SUMS was designed to provide atmospheric data in flow regimes inaccessible prior to the development of the Space Transportation system (STS). The experiment mission operation begins about 1 hour to shuttle de-orbit entry maneuver and continues until reaching 1.6 torr (about 86 km altitude). The SUMS flew a total of three missions, 61C, STS-35, and STS-40. Between flights, the SUMS was maintained in flight ready status. The flight data has been analyzed by the NASA LaRC Aerothermodynamics Branch. Flight data spectrum plots and reports are presented in the Appendices to the Final Technical Report for NAS1-17399. This volume is the flight data report for flight 61-C. Author

N92-30219*# Texas Univ. at Dallas, Richardson.
SUPPORT ACTIVITIES TO MAINTAIN SUMS FLIGHT READINESS, VOLUME 3. ATTACHMENT B: FLIGHT STS-35 REPORT, SECTION A Final Technical Report
Willie Wright May 1992 187 p
(Contract NAS1-17399; RTOP 506-48-11-03)
(NASA-CR-189656-Vol-3; NAS 1.26:189656-Vol-3) Avail: CASI HC A09/MF A02

The Shuttle Upper Atmosphere Mass Spectrometer (SUMS), a component experiment of the NASA Orbital Experiments Program (OEX), was flown aboard the shuttle Columbia (OV102) mounted at the forward end of the nose landing gear well with an atmospheric gas inlet system fitted to the lower fuselage (chin panel) surface. The SUMS was designed to provide atmospheric data in flow regimes inaccessible prior to the development of the Space Transportation System (STS). The experiment mission operation begins about 1 hour prior to shuttle de-orbit entry maneuver and continues until reaching 1.6 torr (about 86 km altitude). The SUMS flew a total of three missions, 61C, STS-35, and STS-40. Between flights, the SUMS was maintained in flight ready status. The flight data has been analyzed by the NASA LaRC Aerothermodynamics Branch. Flight data spectrum plots and reports are presented in the Appendices to the Final Technical Report for NAS1-17399. This volume presents flight data for flight STS-35 in graphical format. Author

N92-30220*# Texas Univ. at Dallas, Richardson.
SUPPORT ACTIVITIES TO MAINTAIN SUMS FLIGHT READINESS, VOLUME 4. ATTACHMENT B: FLIGHT STS-35 REPORT, SECTION B Final Technical Report
Willie Wright May 1992 158 p
(Contract NAS1-17399; RTOP 506-48-11-03)
(NASA-CR-189656-Vol-4; NAS 1.26:189656-Vol-4) Avail: CASI HC A08/MF A02

The Shuttle Upper Atmosphere Mass Spectrometer (SUMS), a component experiment of the NASA Orbital Experiments Program (OEX), was flown aboard the shuttle Columbia (OV102) mounted at the forward end of the nose landing gear well with an atmospheric gas inlet system fitted to the lower fuselage (chin panel) surface. The SUMS was designed to provide atmospheric data in flow regimes inaccessible prior to the development of the Space Transportation System (STS). The experiment mission operation begins about 1 hour prior to shuttle de-orbit entry maneuver and continues until reaching 1.6 torr (about 86 km altitude). The SUMS flew a total of three missions, 61C, STS-35, STS-40. Between flights, the SUMS was maintained in flight ready status. The flight data has been analyzed by the NASA LaRC Aerothermodynamics Branch. Flight data spectrum plots and reports are presented in the Appendices to the Final Technical Report for NAS1-17399. This volume present spectra graphs of the reentry of flight STS-35. Author

N92-30221*# Texas Univ. at Dallas, Richardson.
SUPPORT ACTIVITIES TO MAINTAIN SUMS FLIGHT READINESS, VOLUME 5. ATTACHMENT B: FLIGHT STS-35 REPORT, SECTION C Final Technical Report
Willie Wright May 1992 119 p
(Contract NAS1-17399; RTOP 506-48-11-03)
(NASA-CR-189656-Vol-5; NAS 1.26:189656-Vol-5) Avail: CASI HC A06/MF A02

The Shuttle Upper Atmosphere Mass Spectrometer (SUMS), a component experiment of the NASA Orbital Experiments Program (OEX), was flown aboard the shuttle Columbia (OV102) mounted at the forward end of the nose landing gear well with an atmospheric gas inlet system fitted to the lower fuselage (chin panel) surface. The SUMS was designed to provide atmospheric data in flow regimes inaccessible prior to the development of the Space Transportation System (STS). The experiment mission operation begins about 1 hour prior to shuttle de-orbit entry maneuver and continues until reaching 1.6 torr (about 86 km altitude). The SUMS flew a total of three missions, 61C, STS-35, and STS-40. Between flights, the SUMS was maintained in flight ready status. The flight data has been analyzed by the NASA LaRC Aerothermodynamics Branch. Flight data spectrum plots and reports are presented in the Appendices to the Final Technical Report for NAS1-17399. This volume presents spectral graphs of the reentry of flight STS-35. Author

N92-30222*# Texas Univ. at Dallas, Richardson.
SUPPORT ACTIVITIES TO MAINTAIN SUMS FLIGHT READINESS, VOLUME 6. ATTACHMENT B: FLIGHT STS-35 REPORT, SECTION D Final Technical Report
Willie Wright May 1992 113 p
(Contract NAS1-17399; RTOP 506-48-11-03)
(NASA-CR-189656-Vol-6; NAS 1.26:189656-Vol-6) Avail: CASI HC A06/MF A02

The Shuttle Upper Atmosphere Mass Spectrometer (SUMS), a component experiment of the NASA Orbital Experiments Program (OEX), was flown aboard the shuttle Columbia (OV102) mounted at the forward end of the nose landing gear well with an atmospheric gas inlet system fitted to the lower fuselage (chin panel) surface. The SUMS was designed to provide atmospheric data in flow regimes inaccessible prior to the development of the Space Transportation System (STS). The experiment mission operation begins about 1 hour prior to shuttle de-orbit entry

maneuver and continues until reaching 1.6 torr (about 86 km altitude). The SUMS flew a total of three missions, 61C, STS-35, STS-40. Between flights, the SUMS was maintained in flight ready status. The flight data has been analyzed by the NASA LaRC Aerothermodynamics Branch. Flight data spectrum plots and reports are presented in the Appendices to the Final Technical Report for NAS1-17399. This volume presents spectral graphs of the reentry of flight STS-35. Author

N92-30223*# Texas Univ. at Dallas, Richardson.
SUPPORT ACTIVITIES TO MAINTAIN SUMS FLIGHT READINESS, VOLUME 7. ATTACHMENT B: FLIGHT STS-35 REPORT, SECTION E
Willie Wright May 1992 159 p
(Contract NAS1-17399; RTOP 506-48-11-03)
(NASA-CR-189656-Vol-7; NAS 1.26:189656-Vol-7) Avail: CASI HC A08/MF A02

The Shuttle Upper Atmosphere Mass Spectrometer (SUMS), a component experiment of the NASA Orbital Experiments Program (OEX), was flown aboard the shuttle Columbia (OV102) mounted at the forward end of the nose landing gear well with an atmospheric gas inlet system fitted to the lower fuselage (chin panel) surface. The SUMS was designed to provide atmospheric data in flow regimes inaccessible prior to the development of the Space Transportation System (STS). The experiment mission operation begins about 1 hour prior to shuttle de-orbit entry maneuver and continues until reaching 1.6 torr (about 86 km altitude). The SUMS flew a total of three missions, 61C, STS-35, STS-40. Between flights, the SUMS was maintained in flight ready status. The flight data has been analyzed by the NASA LaRC Aerothermodynamics Branch. Flight data spectrum plots and reports are presented in the Appendices to the Final Technical Report for NAS1-17399. This volume presents data from the reentry of flight STS-35 in tabular and graphical format. Author

N92-30224*# Texas Univ. at Dallas, Richardson.
SUPPORT ACTIVITIES TO MAINTAIN SUMS FLIGHT READINESS, VOLUME 8. ATTACHMENT B: FLIGHT STS-35 REPORT, SECTION F Final Technical Report
Willie Wright May 1992 207 p
(Contract NAS1-17399; RTOP 506-48-11-03)
(NASA-CR-189656-Vol-8; NAS 1.26:189656-Vol-8) Avail: CASI HC A10/MF A03

The Shuttle Upper Atmosphere Mass Spectrometer (SUMS), a component experiment of the NASA Orbital Experiments Program (OEX), was flown aboard the shuttle Columbia (OV102) mounted at the forward end of the nose landing gear well with an atmospheric gas inlet system fitted to the lower fuselage (chin panel) surface. The SUMS was designed to provide atmospheric data in flow regimes inaccessible prior to the development of the Space Transportation System (STS). The experiment mission operation begins about 1 hour prior to shuttle de-orbit entry maneuver and continues until reaching 1.6 torr (about 86 km altitude). The SUMS flew a total of three missions, 61C, STS-35, STS-40. Between flights, the SUMS was maintained in flight ready status. The flight data has been analyzed by the NASA LaRC Aerothermodynamics Branch. Flight data spectrum plots and reports are presented in the Appendices to the Final Technical Report for NAS1-17399. This volume presents tabular and graphical spectral data of the reentry of flight STS-35. Author

N92-30225*# Texas Univ. at Dallas, Richardson.
SUPPORT ACTIVITIES TO MAINTAIN SUMS FLIGHT READINESS, VOLUME 9. ATTACHMENT C: FLIGHT STS-40 REPORT. ATTACHMENT D: SUMS SOFTWARE LISTING Final Technical Report
Willie Wright May 1992 129 p
(Contract NAS1-17399; RTOP 506-48-11-03)
(NASA-CR-189656-Vol-9; NAS 1.26:189656-Vol-9) Avail: CASI HC A07/MF A02

The Shuttle Upper Atmosphere Mass Spectrometer (SUMS), a component experiment of the NASA Orbital Experiments Program (OEX), was flown aboard the shuttle Columbia (OV102) mounted at the forward end of the nose landing gear well with an atmospheric gas inlet system fitted to the lower fuselage (chin panel) surface. The SUMS was designed to provide atmospheric data in flow regimes inaccessible prior to the development of the Space Transportation System (STS). The experiment mission operation begins about 1 hour prior to shuttle de-orbit entry maneuver and continues until reaching 1.6 torr (about 86 km altitude). The SUMS flew a total of three missions, 61C, STS-35, STS-40. Between flights, the SUMS was maintained in flight ready status. The flight data has been analyzed by the NASA LaRC Aerothermodynamics Branch. Flight data spectrum plots and reports are presented in the Appendices to the Final Technical Report for NAS1-17399. This volume provides a software listing and graphical data gathered from flight STS-40. Author

20 SPACECRAFT PROPULSION AND POWER

Includes main propulsion systems and components, e.g., rocket engines; and spacecraft auxilliary power sources.

For related information see also *07 Aircraft Propulsion and Power, 28 Propellants and Fuels, 44 Energy Production and Conversion,* and *15 Launch Vehicles and Space Vehicles.*

N92-29343*# National Aeronautics and Space Administration. Lewis Research Center, Cleveland, OH.
APPLIED ANALYTICAL COMBUSTION/EMISSIONS RESEARCH AT THE NASA LEWIS RESEARCH CENTER Progress Report
J. M. Deur (Sverdrup Technology, Inc., Brook Park, OH.), K. P. Kundu, and H. L. Nguyen Jul. 1992 14 p Presented at the 28th Joint Propulsion Conference and Exhibit, Nashville, TN, 6-8 Jul. 1992
(RTOP 537-02-20)
(NASA-TM-105731; E-7135; AIAA Paper 92-3338; NAS 1.15:105731) Avail: CASI HC A03/MF A01; 3 functional color pages

Emissions of pollutants from future commercial transports are a significant concern. As a result, the Lewis Research Center (LeRC) is investigating various low emission combustor technologies. As part of this effort, a combustor analysis code development program was pursued to guide the combustor design process, to identify concepts having the greatest promise, and to optimize them at the lowest cost in the minimum time. Author

N92-29444# Air Force Flight Test Center, Edwards AFB, CA.
FEASIBILITY OF AN ANTIPROTON CATALYZED FISSION FRAGMENT ROCKET M.S. Thesis
David S. Hidinger Mar. 1992 73 p
(AD-A248157; AFIT/GNE/ENP/92M-03) Avail: CASI HC A04/MF A01

The purpose of this project was to investigate the feasibility of an antiproton catalyzed fission fragment rocket (FFR). The FFR is characterized by the extraction of fission fragments from the fuel, and the utilization of their kinetic energy for thrust generation. A significant drawback to previous FFR designs was the required critical nuclear pile as the fission fragment source. The author examined the possibility of replacing the critical pile with a sub-critical pile driven by antiprotons. Recent experiments have revealed that antiprotons stimulate highly energetic fissions in 238U, with a neutron multiplicity of 13.7 neutrons per fissions. This interaction was used as a throttled neutron source. The pile consisted of layers of fissile coated fibers which are designed to allow fission fragments to escape them, where the fragments collide with a fluid. The heated fluid is then ejected from the rocket to provide thrust. The calculations performed indicate that each antiproton injected into the pile can stimulate 8 or more fissions while maintaining a neutron multiplication of less than 0.4. Based on the results, the specific design presented was inadequate. Despite this, the concept of using the antiproton-U interaction as a source of thrust warrants further study. GRA

N92-29448*# Sverdrup Technology, Inc., Brook Park, OH.
THE DEVELOPMENT OF A FIBER OPTIC RAMAN TEMPERATURE MEASUREMENT SYSTEM FOR ROCKET FLOWS Interim Report
Wim A. deGroot Jul. 1992 25 p Presented at the 27th Joint Propulsion Conference and Exhibit, 24-27 Jun. 1991; sponsored by AIAA, SAE, ASME, and ASEE
(Contract NAS3-25266; RTOP 506-42-31)
(NASA-CR-189200; E-7167; NAS 1.26:189200) Copyright Avail: CASI HC A03/MF A01

A fiberoptic Raman diagnostic system for H2/O2 rocket flows is currently under development. This system is designed for measurement of temperature and major species concentration in the combustion chamber and part of the nozzle of a 100 Newton thrust rocket currently undergoing testing. This paper describes a measurement system based on the spontaneous Raman scattering phenomenon. An analysis of the principles behind the technique is given. Software is developed to measure temperature and major species concentrations by comparing theoretical Raman scattering spectra with experimentally obtained spectra. Equipment selection and experimental approach are summarized. This experimental program is part of a program, which is in progress, to evaluate Navier-Stokes based analyses for this class of rocket. Author

N92-29461# Oak Ridge National Lab., TN.
ELECTROSTATIC ION THRUSTER OPTICS CALCULATIONS
J. H Whealton, R. J. Raridon, and D. A. Kirkman (California Univ., Irvine.) 1992 6 p Presented at the 28th Joint Propulsion Conference, Nashville, TN, 6-8 Jul. 1992
(Contract DE-AC05-84OR-21400)
(DE92-006608; CONF-920747-1-Extd-Abst) Avail: CASI HC A02/MF A01

Two- and three-dimensional ion thruster optical calculations including both source and exhaust plasmas are performed. These calculations include both a self-consistent ion source extraction plasma sheath and an explicit computation of the primary ion optics, including sheath and electrode induced aberrations. A study determining the effects of beam space charge, accelerator geometry, and properties of the downstream plasma sheath on the position of the electrostatic potential saddle point near the extractor electrode is made. Results of the electron blocking potential barrier height as a function of electrode thickness and secondary plasma processes are described. DOE

N92-29667*# National Aeronautics and Space Administration. Lewis Research Center, Cleveland, OH.
THE O2 REDUCTION AT THE IFC MODIFIED O2 FUEL CELL ELECTRODE
William L. Fielder, Joseph Singer, Richard S. Baldwin, and Richard E. Johnson (LeTourneau Coll., Longview, TX.) Jul. 1992 13 p
(RTOP 506-41-21)
(NASA-TM-105691; E-7073; NAS 1.15:105691) Avail: CASI HC A03/MF A01

The International Fuel Corporation (IFC) state of the art (SOA) O2 electrode (Au-10 percent Pt electrocatalyst by weight) is currently being used in the alkaline H2-O2 fuel cell in the NASA Space Shuttle. Recently, IFC modified O2 electrode, as a possible replacement for the SOA electrode. In the present study, O2 reduction data were obtained for the modified electrode at temperatures between 23.3 and 91.7 C. BET measurements gave an electrode BET surface area of about 2070 sq. cm/sq. cm of geometric surface area. The Tafel data could be fitted to two straight line regions. The slope for the lower region, designated as the 0.04 V/decade region, was temperature dependent, and the transfer coefficient was about 1.5. The 'apparent' energy of activation for this region was about 19 kcal/mol. An O2 reduction mechanism for this 0.04 region is presented. In the upper region, designated as the 0.08 V/decade region, diffusion may be the controlling process. Tafel data are presented to illustrate the increase in performance with increasing temperature. Author

N92-29903# Air Force Center for Environmental Excellence, Brooks AFB, TX.
FINAL ENVIRONMENTAL IMPACT STATEMENT (EIS) FOR THE SPACE NUCLEAR THERMAL PROPULSION (SNTP) PROGRAM
19 Sep. 1991 332 p
(AD-A248408) Avail: CASI HC A15/MF A03

A program has been proposed to develop the technology and demonstrate the feasibility of a high-temperature particle bed reactor (PBR) propulsion system to be used to power an advanced second stage nuclear rocket engine. The purpose of this Final Environmental Impact Statement (FEIS) is to assess the potential environmental impacts of component development and testing, construction of ground test facilities, and ground testing. Major issues and goals of the program include the achievement and control of predicted nuclear power levels; the development of materials that can withstand the extremely high operating temperatures and hydrogen flow environments; and the reliable control of cryogenic hydrogen and hot gaseous hydrogen propellant. The testing process is designed to minimize radiation exposure to the environment. Environmental impact and mitigation planning are included for the following areas of concern: (1) Population and economy; (2) Land use and infrastructure; (3) Noise; (4) Cultural resources; (5) Safety (non-nuclear); (6) Waste; (7) Topography; (8) Geology; (9) Seismic activity; (10) Water resources; (11) Meteorology/Air quality; (12) Biological resources; (13) Radiological normal operations; (14) Radiological accidents; (15) Soils; and (16) Wildlife habitats. GRA

N92-29904# Air Force Center for Environmental Excellence, Brooks AFB, TX.
FINAL ENVIRONMENTAL IMPACT STATEMENT (EIS) FOR THE SPACE NUCLEAR THERMAL PROPULSION (SNTP) PROGRAM: APPENDICES
19 Sep. 1991 219 p
(AD-A248409) Avail: CASI HC A10/MF A03

Appendix A discusses the methods for calculating both normal and accidental radiation doses and health effects and the methods for calculating the impacts of the normal operations, accident scenarios, and transportation scenarios. Appendix B includes a general description of facility, geography and demography, meteorology, hydrology, geology and seismology, and design criteria. Appendix C discusses the site selection process. Appendix D includes methodology and its effect on archeology, land use, safety, waste management, air quality etc. Appendix E lists environmental compliance requirements. GRA

N92-29913# Illinois Univ., Urbana. Dept. of Electrical Engineering.
TRANSPORT PROCESSES IN BEAMED ENERGY PROPULSION SYSTEMS Final Technical Report, 1 Sep. 1989 - 30 Sep. 1991
Robert A Beddin and Mark J. Mueller Nov. 1991 60 p
(Grant AF-AFOSR-0308-89)
(AD-A247296; UILUENG-91-0511; AAE-91-11; AFOSR-92-0160TR) Avail: CASI HC A04/MF A01

A model of a microwave-induced plasma propulsion system has been developed in one dimension for a transverse electric mode (TE sub 10) of operation in a rectangular waveguide. Available experimental data are compared to the computational results for the case of a planar propagating plasma wave and, using a TE sub 10 mode-shape approximation, for a wave propagating in a waveguide. Temperature profiles, plasma propagation velocities, velocity profiles, and absorbed power histories are obtained for flow of helium from .5 to 1 atmosphere pressure and 500 to 3000 watts input power at a frequency of 2.45 GHz. The computational results show the observed jumping of the plasma towards the microwave source. Peak plasma temperatures range from 8000 to 9000 K over the input power range. For an input power of 1081.7 W, the calculated percentage of power absorbed is approximately 70 percent for the planar case and 40 percent for the waveguide case. Comparisons with experimental data indicate other mechanisms (not involving transient processes), most likely associated with the nonequilibrium

behavior of the plasma, are responsible for the disagreement between the model results and the observed plasma propagation velocities. GRA

N92-30187*# National Aeronautics and Space Administration. Lewis Research Center, Cleveland, OH.
OPTIMIZATION OF ARMORED SPHERICAL TANKS FOR STORAGE ON THE LUNAR SURFACE
D. J. Bents and D. A. Knight 1992 10 p Presented at the 27th Intersociety Energy Conversion Engineering Conference, San Diego, CA, 3-7 Aug. 1992; sponsored in part by SAE, ACS, AIAA, ASME, IEEE, AIChE and ANS
(RTOP 326-81-10)
(NASA-TM-105700; E-7088; NAS 1.15:105700) Avail: CASI HC A02/MF A01

A redundancy strategy for reducing micrometeroid armoring mass is investigated, with application to cryogenic reactant storage for a regenerative fuel cell (RFC) on the lunar surface. In that micrometeoroid environment, the cryogenic fuel must be protected from loss due to tank puncture. The tankage must have a sufficiently high probability of survival over the length of the mission so that the probability of system failure due to tank puncture is low compared to the other mission risk factors. Assuming that a single meteoroid penetration can cause a storage tank to lose its contents, two means are available to raise the probability of surviving micrometeoroid attack to the desired level. One can armor the tanks to a thickness sufficient to reduce probability of penetration of any tank to the desired level or add extra capacity in the form of spare tanks that results in survival of a given number out of the ensemble at the desired level. A combination of these strategies (armoring and redundancy) is investigated. The objective is to find the optimum combination which yields the lowest shielding mass per cubic meter of surviving fuel out of the original ensemble. The investigation found that, for the volumes of fuel associated with multikilowatt class cryo storage RFC's, and the armoring methodology and meteoroid models used, storage should be fragmented into small individual tanks. Larger installations (more fuel) pay less of a shielding penalty than small installations. For the same survival probability over the same time period, larger volumes will require less armoring mass per unit volume protected. Author

23 CHEMISTRY AND MATERIALS (GENERAL)

No abstracts in this category.

24 COMPOSITE MATERIALS

Includes physical, chemical, and mechanical properties of laminates and other composite materials.

For ceramic materials see *27 Nonmetallic Materials.*

N92-29453# Dayton Univ., OH.
CHARACTERIZATION OF FRACTURE IN (0/90)3s SiC/1723 COMPOSITES Interim Report, 27 Aug. 1987 - 17 Sep. 1991
Demirkan Coker and Noel E. Ashbaugh Mar. 1992 68 p
(Contract F33615-87-C-5243)
(AD-A250612; UDR-TR-91-64; WL-TR-91-4119) Avail: CASI HC A04/MF A01

The fracture behavior of 0 DEG/90 DEG sub 3s cross-plied ceramic-matrix composites is evaluated using compact tension specimens. The influence of notch preparation (abrasive water-jet or diamond saw cut) and fatigue precracking is investigated. The extent that a calculated critical stress intensity factor can be used as a fracture toughness parameter is investigated. The stress-intensity factor corresponding to the maximum load, K sub peak, is found to yield consistent values for the precracked specimens. However, this parameter is found to be higher for precracked specimens than for notched specimens. This difference in K sub peak is attributed to fiber bridging of the crack in the precracked specimens. No difference in material behavior is observed between specimens with abrasive water-jet and diamond saw notch extensions. There seems to be no noticeable size effects on K sub peak for precracked specimens, in contrast with the uncracked specimens. GRA

N92-29460# Washington State Univ., Pullman. Dept. of Chemistry.
MNDO STUDY OF BORON-NITROGEN ANALOGUES OF BUCKMINSTERFULLERENE
Xinfu Xia, Daniel A. Jelski, James R. Bowser, and Thomas F. George Mar. 1992 16 p
(Contract N00014-90-J-1193)
(AD-A247777; WSU/DC/92/TR-79) Avail: CASI HC A03/MF A01

An MNDO study of boron-nitrogen analogues of buckminsterfullerene is presented. The relative properties of Carbon-60, Boron carbon, Nitrogen carbon, Boron carbon, Carbon boron nitrogen, and Boron nitrogen are studied. The heats of formation of such 60-atom systems from benzene, naphthalene and their BN analogues are compared. It is found that all these hybrids are approximately as stable as buckminsterfullerene. Surprisingly, it is predicted that Boron nitrogen will be stable and should be relatively simple to synthesize from borazine. GRA

N92-29462# Georgia Inst. of Tech., Atlanta. School of Aerospace Engineering.
COMPRESSIVE RESPONSE OF DEBONDED THICK COMPOSITE SHELLS INCLUDING THE EFFECTS OF TRANSIENT MOISTURE SORPTION Progress Report
George A. Kardomateas Jul. 1991 3 p
(Contract N00014-91-J-1892)
(AD-A250080) Avail: CASI HC A01/MF A01

Two important issues associated with the structural integrity of composite shells are the prediction of the conditions for the loss of stability and the question of accurately assessing the behavior of the structure in the presence of defects. Two other issues included in the project are a study of the growth of internal delaminations and an investigation of the effect of the hydroscopic environment in the context of predicting the combined effects of moisture sorption and external compression with respect to the stress and deformation fields. Author

N92-29556# California Univ., Berkeley. Dept. of Materials Science and Mineral Engineering.
MICROMECHANISMS OF CYCLIC AND ENVIRONMENTALLY-ASSISTED SUBCRITICAL CRACK GROWTH IN CERAMIC-MATRIX COMPOSITES Final Report, 1 Oct. 1988 - 30 Sep. 1991
R. H. Dauskardt and R. O. Ritchie Nov. 1991 113 p
(Contract N00014-89-J-1094)
(AD-A248067; UCB/R/91/N1076) Avail: CASI HC A06/MF A02

The future use of ceramics for advanced structural applications represents an important precursor to potential major improvements in design performance for high temperature, corrosion and wear resistance applications. The limited use of such brittle materials to date has primarily been attributed to their inherently low toughness and lack of defect tolerance. Scientific research in the last decade, however, has resulted in major advances in the toughening of ceramics by such mechanisms as whisker reinforcement, transformation and microcrack toughening. However, very recent work has shown that such toughened ceramics and composites, contrary to conventional wisdom, may become susceptible to cyclic fatigue. The intent of this program was to study and model the physics and fundamental micromechanisms of environmentally-assisted and principally cyclic fatigue crack-growth processes in several classes of ceramic-matrix

composites, chosen to reflect different primary toughening mechanisms. Based on initial studies, the central hypothesis of this work is that the mechanisms of crack-tip shielding, used to enhance fracture toughness, can lead to degradation in crack-growth resistance under cyclic loading. GRA

N92-29593# Ohio State Univ., Columbus. Dept. of Civil Engineering.
A CONSISTENT SHEAR DEFORMABLE THEORY FOR LAMINATED PLATES Final Report, 1 Jul. 1985 - 31 Aug. 1990
Ranbir S. Sandhu, William E. Wolfe, Soon J. Hong, and Harpal S. Chohan Jul. 1991 176 p
(Contract F33615-85-C-3213)
(AD-A250591; WL-TR-91-3021) Avail: CASI HC A09/MF A02

A consistent theory for the interlayer coupling of transverse shear in laminated plates is presented. Starting from a generalization of Reissner's variational principle for elastic orthotropic plates to laminated plates, it is shown that the shear force in any lamina may depend upon the shear deformation of that lamina as well as others. The coupling depends on the material properties, the stacking sequence and the applied surface tractions. Several existing theories of homogeneous as well as laminated plates are seen to arise as specializations/approximations of the general theory. The nature of the constitutive coupling is illustrated by studying a 12-layer graphite-epoxy laminate. The theory is implemented in a finite element computer program and applied to the determination of stresses in cross-ply as well as angle-ply free-edge delamination specimens, and to study the frequencies of vibration of laminated plates. GRA

N92-29594# Ohio State Univ., Columbus. Dept. of Civil Engineering.
VARIATIONAL FORMULATION AND FINITE ELEMENT IMPLEMENTATION OF PAGANO'S THEORY OF LAMINATED PLATES Final Report, Jul. 1985 - Aug. 1990
R. S. Sandh, William E. Wolfe, and Hui-Huang Chyou 12 Jul. 1991 115 p
(Contract F33615-85-C-3213)
(AD-A250592; WL-TR-91-3016) Avail: CASI HC A06/MF A02

Pagano's theory of laminated plates is restated in the form of a set of self-adjoint differential equations. Consistent boundary operators are identified. A general variational principle is stated following standard procedures for linear coupled self adjoint systems of equations. Extensions to relax requirements of differentiability of various field variables are indicated along with specializations to reduce the number of free field variables. One specialization is implemented in a finite element computer program and used to solve several example problems of free-edge delamination specimens. GRA

N92-29645# Pacific Northwest Lab., Richland, WA.
REVIEW OF TEMPERATURE DEPENDENT EFFECTS ON THE OXIDATION PROTECTION OF CARBON/CARBON
E. L. Courtright Oct. 1991 16 p Presented at the Fall Meeting of the Minerals, Metals and Materials Society of AIME and Materials Week of the American Society of Metals, Cincinnati, OH, 20-24 Oct. 1991
(Contract DE-AC06-76RL-01830)
(DE92-012333; PNL-SA-19820; CONF-911003-26) Avail: CASI HC A03/MF A01

There is continued interest in the use of carbon/carbon for a variety of structural applications because of the excellent strength retention exhibited by this composite at high temperatures. However, the principal performance limiting issue, which is oxidation protection, has yet to be solved. Coating development efforts have been extensively pursued and the factors that limit the effectiveness of oxidation protection systems are identified. This paper reviews the temperature dependency of several important criteria such as the limitations imposed by oxygen permeability, and the kinetics of oxidation for candidate coating materials. The influence of active/passive transition, mass loss by evaporation, and thermochemical stability are also included. DOE

N92-29660*# National Aeronautics and Space Administration. Lewis Research Center, Cleveland, OH.
APPROACHES TO POLYMER-DERIVED CMC MATRICES
Frances I. Hurwitz 1992 9 p Presented at the Society for the Advancement of Materials and Process Engineering, Toronto, Ontario, 20-22 Oct. 1992
(RTOP 505-63-40)
(NASA-TM-105754; E-7165; NAS 1.15:105754) Avail: CASI HC A02/MF A01

The use of polymeric precursors to ceramics permits the fabrication of large, complex-shaped ceramic matrix composites (CMC's) at temperatures which do not degrade the fiber. Processing equipment and techniques readily available in the resin matrix composite industry can be adapted for CMC fabrication using this approach. Criteria which influence the choice of candidate precursor polymers, the use of fillers, and the role of fiber architecture and ply layup are discussed. Three polymer systems, polycarbosilanes, polysilazanes, and polysilsesquioxanes, are compared as candidate ceramic matrix precursors. Author

N92-29702# Technische Univ., Delft (Netherlands). Faculty of Aerospace Engineering.
MANUFACTURING OF COMPONENTS OF FIBRE-METAL LAMINATES: AN OVERVIEW
J. Sinke Dec. 1991 33 p
(LR-670; ETN-92-91407) Avail: CASI HC A03/MF A01

To manufacture components of fiber metal laminates the same processes can be used as for conventional materials. In some cases, however, the tools have to be adapted to this laminated material. The workshop properties of fiber metal laminates are good for machining processes (comparable to metal alloys) and are moderate where the forming processes are concerned. The complexity of a component of fiber metal laminates is limited by the use of fibers. The fibers in these laminates limit the failure strain in at least one direction and introduce a considerable anisotropy. Nevertheless, many suitable applications of fiber metal laminates can be manufactured without difficulty. ESA

N92-29723# Naval Surface Warfare Center, Bethesda, MD. Ship Materials Engineering Dept.
EFFECT OF WHISKER ORIENTATION ON THE MECHANICAL PROPERTIES OF SILICON CARBIDE/ALUMINA COMPOSITES Interim Report, Oct. 1990 - Sep. 1991
A. S. Rao 31 Jan. 1992 25 p
(AD-A248737; CDNSWC-SME-92-10) Avail: CASI HC A03/MF A01

Silicon carbide (whisker) and alumina composites were processed with and without concurrent application of an external electric field in order to orient the whiskers in the composites. Both the flexural strength and the fracture toughness of the composites were measured. The results suggest that the application of electric field improves the whisker orientation of the sintered composites. However, the improvement in the mechanical properties of the composites due to the orientation of the dispersed whiskers is not very significant (9-12 percent). Samples processed from flocculated suspensions produce poorly dispersed microstructure. GRA

N92-29795# Los Alamos National Lab., NM.
A PERSPECTIVE ON MoSi2 BASED COMPOSITES
J. J. Petrovic and A. K. Vasudevan (Naval Research Lab., Washington, DC.) 1992 12 p Presented at the Material Research Society Spring Meeting, San Francisco, CA, 27 Apr. - 2 May 1992
(Contract W-7405-eng-36)
(DE92-013434; LA-UR-92-1370; CONF-920402-4) Avail: CASI HC A03/MF A01

MoSi2 based composites represent an important new class of high temperature structural silicides, with significant potential for elevated temperature structural applications in the range of 1200-1600 C in oxidizing and aggressive environments. The properties of MoSi2 which make it an attractive matrix for high temperature composites are described and the development history

of these materials traced. Latest results on elevated temperature creep resistance, low temperature fracture toughness, and composite oxidation behavior are summarized. Important avenues for future MoSi2 based composite development are suggested.
DOE

N92-29875# Messerschmitt-Boelkow-Blohm G.m.b.H., Munich (Germany, F.R.).
STATUS AND PERSPECTIVES OF MODERN COMPOSITE MATERIALS [STAND UND PERSPEKTIVEN MODERNER VERBUNDWERKSTOFFE]
Helmut Kellerer 1991 28 p In GERMAN Presented at the 2nd Symposium Materialforschung, Dresden, Fed. Republic of Germany, 26-29 Aug. 1991
(MBB-Z-0380-91-PUB; ETN-92-91698) Avail: CASI HC A03/MF A01

A classification of composite materials is presented and their properties and manufacturing conditions are reviewed. The following materials are described: glass; carbon; organic and ceramic fibers, such as polyethylene; aramid or boron and silicon carbides; carbon fiber reinforced plastics, such as epoxy composites and thermoplastic resins (PEEK, polysulfides, polyether resins); fiber or particle reinforced aluminum; aluminum boron or carbon composites; fiber reinforced graphites such as carbon-carbon fibers; and piezoceramics. Matrix ductibility, temperature behavior, anisotropy, strength, and production costs of these materials are examined and compared with those of polymers.
ESA

N92-29876# Messerschmitt-Boelkow-Blohm G.m.b.H., Munich (Germany, F.R.).
DEVELOPMENT AND CHARACTERIZATION OF OXIDATION-PROTECTED CFC [ENTWICKLUNG UND CHARAKTERISIERING VON OXIDATIONSGESCHUETZTEM CFC]
Gerd Dietrich and Rolf Meistring 1991 48 p In GERMAN Presented at the 2nd Symposium Materialforschung, Dresden, Fed. Republic of Germany, 26-29 Apr. 1991 Sponsored by BMFT Prepared in cooperation with Schunk Kohlenstofftechnik G.m.b.H., Giessen, Germany, F.R. and Karlsruhe Univ., Germany, F.R.
(MBB-Z-0395-91-PUB; ETN-92-91699) Avail: CASI HC A03/MF A01

Manufacturing process, mechanical and nondestructive characterization, and oxidation protection systems of CFC (Carbon Fiber Composites) are presented. A test apparatus with hot grips was conceived to examine temperature influence in tension, flexibility, and shear strength. Parameter studies for development of oxidation protection layers in CFC were achieved for chemical vapor deposition, silicon liquid impregnation, glazing, and combination of these processes with impregnation of metal organic polymers. It is shown that multilayer coatings, matrix bulk siliconizing, and silica chain glazing allow a long term protection to 1600 C to be obtained.
ESA

N92-30137# Georgia Inst. of Tech., Atlanta. School of Chemical Engineering.
FUNDAMENTAL STUDY OF COMPRESSIVE STRENGTH DEVELOPMENT IN PAN-BASED CARBON FIBERS Final Technical Report, Dec. 1988 - Sep. 1991
A. S. Abhiraman 20 Mar. 1992 82 p
(Grant AF-AFOSR-0193-89)
(AD-A250285; AFOSR-92-0302TR) Avail: CASI HC A05/MF A01

Evolution of mechanical properties in the conversion of two precursor polymeric fibers to carbon fibers has been studied. The focus has been on properties in axial compression of polyacrylonitrile (PAN, a semi rigid polymer) - and polybenzobisthiazole (PBZT, a rigid rod polymer) - based carbon fibers. Mechanical properties of fibers at different extents of progression toward the graphite fiber structure reveal that the evolutions of tensile and compressive properties are not synchronized. Substantial enhancements in both tensile and compressive strengths of carbon fibers occur only with the development of the carbonized morphology with its characteristic basal planes as the fundamental structural units. In addition, the recoil from tension method has been analyzed vis-a-vis axial compressive strength of carbon fibers. Fracture surfaces of specimens from this experiment do not necessarily reveal failure in a simple compression mode, especially including bending. Statistical analysis of the recoil method demonstrates that the fiber failure distribution can be expressed by either a logistic or a Weibull distribution.
GRA

N92-30208*# Virginia Univ., Charlottesville. School of Engineering and Applied Science.
AN APPROXIMATE SOLUTION FOR INTERLAMINAR STRESSES IN LAMINATED COMPOSITES: APPLIED MECHANICS PROGRAM Interim Report
Cheryl A. Rose and Carl T. Herakovich May 1992 192 p
(Grant NAG1-841)
(NASA-CR-190537; NAS 1.26:190537; AM-92-02) Avail: CASI HC A09/MF A02

An approximate solution for interlaminar stresses in finite width, laminated composites subjected to uniform extensional, and bending loads is presented. The solution is based upon the principle of minimum complementary energy and an assumed, statically admissible stress state, derived by considering local material mismatch effects and global equilibrium requirements. The stresses in each layer are approximated by polynomial functions of the thickness coordinate, multiplied by combinations of exponential functions of the in-plane coordinate, expressed in terms of fourteen unknown decay parameters. Imposing the stationary condition of the laminate complementary energy with respect to the unknown variables yields a system of fourteen non-linear algebraic equations for the parameters. Newton's method is implemented to solve this system. Once the parameters are known, the stresses can be easily determined at any point in the laminate. Results are presented for through-thickness and interlaminar stress distributions for angle-ply, cross-ply (symmetric and unsymmetric laminates), and quasi-isotropic laminates subjected to uniform extension and bending. It is shown that the solution compares well with existing finite element solutions and represents an improved approximate solution for interlaminar stresses, primarily at interfaces where global equilibrium is satisfied by the in-plane stresses, but large local mismatch in properties requires the presence of interlaminar stresses.
Author

25 INORGANIC AND PHYSICAL CHEMISTRY

Includes chemical analysis, e.g., chromatography; combustion theory; electrochemistry; and photochemistry.

For related information see also *77 Thermodynamics and Statistical Physics.*.

N92-29355# Morgantown Technology Center, WV.
MODELING DETERMINISTIC CHAOS IN THERMALLY-PULSED COMBUSTION
C. S. Daw (Oak Ridge Associated Universities, Inc., TN.), J. F. Thomas (Oak Ridge Associated Universities, Inc., TN.), and G. A. Richard 1992 14 p Presented at the the Combustion Institute, Central States Spring Meeting on Combustion Fundamentals and Applications, Columbus, OH, 26-28 Apr. 1992
(DE92-011756; DOE/METC-C/92/7013; CONF-9204103-2)
Avail: CASI HC A03/MF A01

Can chaotic behavior occur in combustion systems? In practical combustion systems, mixing processes are governed by turbulent transport, which is itself chaotic in nature. However, in an ideally mixed combustor, the question remains: can chaotic behavior occur? The present paper demonstrates that even neglecting the mixing process, chaotic responses are possible in a 'thermal' pulse combustor. While this result is limited only to thermal pulse combustion, it suggests that chaotic behavior (apart from turbulent mixing) may exist in other practical combustion systems. The

resulting fluctuations in reaction rates, concentrations and temperature may play a role in fluctuating levels of emissions such as NO(sub x). DOE

N92-29423# Wisconsin Univ., Milwaukee. Dept. of Physics.
ZEE STAR ANALYSIS Final Report, Mar. - Sep. 1989
Richard S. Sorbello Dec. 1991 11 p Prepared for Dayton Univ., OH
(Contract F30602-88-D-0028)
(AD-A248342; RL-TR-91-378) Avail: CASI HC A03/MF A01

Forces contributing to the effective valence Z in electromigration have been theoretically studied for the following systems: an impurity in the vicinity of a grain boundary, an impurity in the vicinity of a dislocation, and impurity in a disordered system. The presence of a grain boundary or dislocation was found to change Z and the residual resistivity by an amount on the order of 10 percent to 50 percent. The local transport field in mesoscopic systems was investigated, and the calculations suggest that the scanning tunneling microscope can effectively probe this field. Non-adiabatic recoil effects in the wind force exerted on an impurity were also considered. GRA

N92-29431# Sandia National Labs., Livermore, CA.
STRUCTURE OF A METHANOL/AIR COAXIAL REACTING SPRAY NEAR THE STABILIZATION REGION BY OH FLUORESCENCE IMAGING AND TWO-COMPONENT PHASE-DOPPLER INTERFEROMETRY
P. J. Goix, A. Cessou, D. Stepowski, and C. F. Edwards 1991 18 p Presented at the 24th International Symposium on Combustion, Sydney (Australia), 5-10 Jul. 1992
(Contract DE-AC04-76DR-00789)
(DE92-005328; SAND-91-8714; CONF-920707-1) Avail: CASI HC A03/MF A01

Planar laser-induced fluorescence and two component phase-Doppler interferometry have been used to study the reaction zone structure near the stabilization region of a coaxial methanol/air spray flame. The configuration of the experiment was chosen to simulate the atomizer geometry, surface tension and Weber number of a single coaxial hydrogen/oxygen rocket injector. The measurements are made in a water-cooled, optically-accessible confinement chamber at a pressure of 1 atm. Data are reported for two operating conditions, one yielding a flame length of approximately 1 meter, the other, half that value. Both the Weber number (characterizing the atomization process) and the Reynolds number (characterizing the gas phase mixing process) vary between the two cases, but the data suggest that it is the Weber number which has the dominant effect. In both cases OH imaging shows that the reaction zone is confined to a narrow region, with the OH field being similar in appearance to that of a single-phase turbulent mixing-controlled (diffusion) flame. Size-classified mean velocity vectors derived from the phase-Doppler data show striking differences in the flow pattern for low and high Stokes number droplets. Droplets 10 microns in diameter and below (Stokes number less than 10) appear to follow the recirculating eddies that provide flame stabilization. Increasing the Weber number by a factor of 2.5 decreased the Sauter mean diameter of the spray by as much as one-third, and the arithmetic mean diameter by as much as one-half. We believe that it is this decrease in the spray droplet diameter that is primarily responsible for the very different flame length in the two cases. DOE

N92-29433# Sandia National Labs., Livermore, CA.
A LINEAR EDDY SUB-GRID MODEL FOR TURBULENT REACTING FLOWS: APPLICATION TO HYDROGEN-AIR COMBUSTION
P. A. McMurtry (Utah Univ., Salt Lake City.), S. Menon (Quest Integrated, Inc., Kent, WA.), and A. R. Kerstein 1992 17 p Presented at the 24th International Symposium on Combustion, Sydney (Australia), 5-10 Jul. 1992
(Contract DE-AC04-76DR-00789)
(DE92-006699; SAND-91-8743; CONF-920707-11) Avail: CASI HC A03/MF A01

A new sub-grid mixing model for use in large eddy simulations of turbulent combustion is presented and applied to a hydrogen-air diffusion flame. The sub-grid model is based on Kerstein's linear-eddy model. The model is first used to predict the mixing of a conserved scalar in a turbulent shear flow and predict NO formation in a hydrogen-air diffusion flame using a reduced chemical mechanism involving nine reactive scalars. DOE

N92-29459# Sandia National Labs., Livermore, CA.
HYDROGENATION REACTIONS OF NEUTRAL CARBON CLUSTERS: C(SUB n) (n = 6-75) + D(SUB 2)
T. J. Butenhoff and E. A. Rohlfing 1991 19 p Presented at the 24th International Symposium on Combustion, Sydney (Australia), 5-10 Jul. 1992
(Contract DE-AC04-76DR-00789)
(DE92-005330; SAND-91-8706; CONF-920707-2) Avail: CASI HC A03/MF A01

The hydrogenation reactions of neutral carbon clusters, C(sub n) + D(sub 2), are examined over a wide range of cluster sizes, n = 6-75. Clusters are created by pulsed laser vaporization of graphite and react with D(sub 2) in a pulsed, fast-flow reactor. After supersonic expansion and collimation, the cluster reactants and products are photoionized at 118.2 nm and mass analyzed via high-resolution time-of-flight mass spectrometry. We report reaction propensities that include relative rate as a function of cluster size, the identification of favored reaction products, and the implications of product appearance rates on possible reaction mechanisms. These propensities show strong evidence for the onset of the closed-shell fullerene structures for C(sub 2n) beginning at n = 18. DOE

N92-29514# California Univ., Davis. Dept. of Chemistry.
A STUDY OF THE ADSORPTION OF ACETONITRILE ON A GOLD ELECTRODE FROM AQUEOUS SOLUTIONS USING IN SITU VIBRATIONAL SPECTROSCOPY
Peter W. Faguy, W. R. Fawcett, Guojun Liu, and Artur J. Motheo 24 Apr. 1992 31 p
(Contract N00014-90-J-1235)
(AD-A250191; TR-25) Avail: CASI HC A03/MF A01

The structure of the interphase at the gold/aqueous solution interface with absorbed acetonitrile was studied by subtractively normalized FTIR spectroscopy (SNIFTIRS). Two types of acetonitrile and water molecules were observed in the interphasal region. The first involved chemisorbed molecules in which important vibrational modes are strongly shifted in frequency with respect to that observed in the bulk of the solution. In the case of acetonitrile, adsorption resulted in a C-N stretching band at 2342/cm, and for water, a bending mode at 1688/cm. The second type of molecule in the double layer with a band at 2261/cm in the case of acetonitrile, and at 1628/cm in the case of water was assumed to be hydrogen bonded to chemisorbed water molecules, and thus located further away from the geometrical interface. A band due to perchlorate ion at 1107/cm is attributed to anions attracted into the double layer by the positive charge on the electrode. No evidence was obtained for contact adsorption of this anion. GRA

N92-29551# Oak Ridge National Lab., TN.
ACETATE IN HYDROTHERMAL SOLUTIONS: DECOMPOSITION KINETICS AND METAL COMPLEXATION
J. L. S. Bell, D. A. Palmer, and H. L. Barnes 1992 4 p Presented at the 7th Water-Rock Interaction Conference, Park City, UT, 9-23 Jul. 1992
(Contract DE-AC05-84OR-21400)
(DE92-010542; CONF-920761-5) Avail: CASI HC A01/MF A01

Hydrothermal kinetics experiments indicate that acetate decomposes under achievable hydrothermal conditions dependant upon solution pH and the catalytic and/or oxidizing ability of mineral surfaces present. Surfaces studied thus far include quartz, calcite, pyrite, Ca-montmorillonite, iron-bearing montmorillonite, magnetite, and hematite. Acetate decompositon in hydrothermal brines is expected to affect the ligand concentration, pCO2, and pH buffering capacity of the brine; thus, the kinetics of acetate decomposition have important implications for metal carboxylate speciation.

Potentiometric titrations were used to measure formation constants of acetate complexes with aluminum in NaCl brine to 5 mol/kg and at temperatures to 125 C. DOE

N92-29557# American Chemical Society, Princeton, NJ. Div. of Colloid and Surface Chemistry.
ELECTROCHEMISTRY IN COLLOIDS AND DISPERSIONS. VOLUME 1: ELECTROANALYTICAL METHODS AND APPLICATIONS, ELECTROSYNTHESIS AND ELECTROCATALYSIS, POLYMERS AND LATEXES
4 Feb. 1992 214 p
(Contract N00014-91-J-1616)
(AD-A248335) Avail: CASI HC A10/MF A03

This report summarizes the current status of experimental and theoretical studies which address fundamental and applied aspects of electrochemistry in colloids and dispersions. The range of such microheterogeneous fluids examined includes micellar solutions, microemulsions, emulsions, latexes, and dispersions of solids in liquids. Several broad subtopics are described. These topics include electroanalytical methods and applications, solute distribution, diffusion, and transport, electrosynthesis and electrocatalysis, polymers and latexes, and colloidal metals and semiconductors. GRA

N92-29580# California Inst. of Tech., Pasadena.
SHOCK ENHANCEMENT AND CONTROL OF HYPERSONIC COMBUSTION Annual Technical Report, 1 Apr. 1990 - 30 Mar. 1991
Frank E. Marble 26 Nov. 1991 17 p
(Grant AF-AFOSR-0188-90; AF Proj. 2308)
(AD-A248558; AFOSR-92-0238TR) Avail: CASI HC A03/MF A01

Shock tube studies of shock enhanced mixing of helium into air were reported utilizing the Rayleigh scattering technique. Because of their greater sensitivity in the low concentration range, these measurements were believed to be more accurate than those obtained with laser induced fluorescence. The result indicated that mixing was more rapid and more complete than reported previously. Preliminary work on the consequence of multiple shocks has been promising. Work began on the interaction of shock induced mixing with shear layers in the GALCIT M = 2.5 supersonic wind tunnel. Experiments concerning the details of combustion in large vortices in the Caltech Unsteady Combustion Facility progressed very well using simultaneous measurements of pressure, shadowgraphy, and chemiluminescence. These results reveal a very different ignition mechanism and combustion pattern than had been anticipated. GRA

N92-29595# Pennsylvania State Univ., University Park. Dept. of Materials Science and Engineering.
MODELING OF THE ROLE OF ATOMIC HYDROGEN IN HEAT TRANSFER DURING HOT FILAMENT ASSISTED DEPOSITION OF DIAMOND Interim Report
K. Tankala and T. DebRoy 12 May 1992 30 p
(Contract N00014-92-J-1125)
(AD-A250607; TR-3) Avail: CASI HC A03/MF A01

The temperature and atomic hydrogen concentration profiles in a hot filament type diamond deposition reactor were determined experimentally and theoretically to demonstrate that the reaction of atomic hydrogen on the substrate surface plays an important role in the heating of the substrate. For a given filament temperature, the substrate temperature in helium was significantly lower than that in either pure hydrogen or 1 percent methane-hydrogen atmospheres. The presence of small amounts of methane in hydrogen did not have any significant effect in influencing the shape of the atomic hydrogen concentration profile. In the shape between the filament and the substrate, the concentration field is established mainly due to the diffusive mixing of the atomic hydrogen with the molecular hydrogen and other species in the gas phase. Homogeneous chemical reactions in the gas phase do not significantly affect the atomic hydrogen concentration distribution in this region. GRA

N92-29619# Cornell Univ., Ithaca, NY. Dept. of Chemistry.
LiMoN2: THE FIRST METALLIC LAYERED NITRIDE Technical Report, Dec. 1991 - Nov. 1994
S. H. Elder, Linda H. Doerrer, F. J. DiSalvo, J. B. Parise, and D. Guyomard 2 Apr. 1992 49 p Prepared in cooperation with State Univ., Stony Brook, NY and Bell Communications Research, Redbank, NJ
(Contract N00014-91-J-1269)
(AD-A248446; TR-16) Avail: CASI HC A03/MF A01

We report the first example of a layered ternary lithium nitride in which the lithium can be deintercalated and reintercalated. This ternary nitride, LiMoN2, has been synthesized by the reaction of two different precursors, Li2Mo(N(sup t)Bu)4 and Li2MoO4, with ammonia gas. The structure was refined using a combination of X-ray and neutron powder diffraction data In the space group R3 and the lattice parameters are (A) a = 2.8672(3) and c = 15.813(3) which were obtained from the neutron data. The ideal structure consists of MoN2 layers with Mo in trigonal prismatic holes and Li in octahedral holes between the MoN2 layers. The diffraction studies indicate the presence of cation anti-site defects; the structure is best described as (Li(0.84)Mo(0.16))(sub oct)(Mo(0.84)Li(0.16))(sub tp)N2. LiMoN2 is metallic and Pauliparamagnetic with Chi(sub o) = 0.59 x 10(exp 6) emu g(exp -1). We have employed a variety of different oxidizing agents for the deintercalation of the lithium from LiMoN2 and have been able to deintercalate up to 64 percent of the lithium. This deintercalated species can be reintercalated with n-butyllithium (in hexane) at room temperature. Electrochemical studies show a large hysteresis in charge-discharge cycles. GRA

N92-29719# Pittsburgh Univ., PA. Surface Science Center.
THE ACTIVATION OF CHEMICAL BONDS AT SURFACES Final Technical Report
John T. Yates, Jr. 27 Jan. 1992 10 p
(Contract DAAL03-89-K-0001)
(AD-A248666; ARO-26238.19-CH) Avail: CASI HC A02/MF A01

Studies of the chemisorption, thermal decompositio., and photo decomposition of small molecules on metal and semiconductor oxide surfaces were carried out. In addition, new methods for research in surface science were developed. GRA

N92-29744# National Inst. of Standards and Technology, Gaithersburg, MD.
FINITE-RATE DIFFUSION-CONTROLLED REACTION IN A VORTEX
Ronald R. Rehm, Howard R. Baum, Hai C. Tang, and Daniel W. Lozier Feb. 1992 31 p
(PB92-172006; NISTIR-4768) Avail: CASI HC A03/MF A01

A two-dimensional model of a constant-density diffusion-controlled reaction with finite reaction-rate chemistry occurring between unmixed species initially occupying adjacent half-spaces is formulated and analyzed. The chemical reaction term is taken to be appropriate for an isothermal, bimolecular reaction for simplicity. An axisymmetric viscous vortex field satisfying the Navier-Stokes equations winds up the interface between the species as they diffuse together and react. The diffusion rates for the two species are assumed constant and equal so that mixture fraction or Shvab-Zeldovich variable can be used. The resulting equation for the mixture fraction is linear and can be solved by noting that a Lagrangian coordinate system removes the convection and that the equation permits a global similarity solution. The single nonlinear equation for one species is also analyzed in a Lagrangian coordinate system. Asymptotic and numerical results show the structure of the reaction region and the competing influences of reaction, diffusion, and convection. Author

N92-29901# Colorado Univ., Boulder. Dept. of Chemistry and Biochemistry.
THEORETICAL/EXPERIMENTAL INVESTIGATIONS OF THE STRUCTURE AND DYNAMICS OF HIGHLY ENERGETIC DICATION SPECIES Final Report, 1 Nov. 1988 - 31 Oct. 1991

W. C. Lineberger, Stephen R. Leone, Stephen V. ONeil, Joerg Senekowitsch, and Diane M. Szaflarski 9 Nov. 1991 24 p
(Grant AF-AFOSR-0074-89)
(AD-A247050; AFOSR-92-0153TR) Avail: CASI HC A03/MF A01

Dications possess unusual electronic structures and bonding configurations. They display high energy releases and thus may serve as prototypes for molecular systems which have enormous energy per unit mass. This program combines a parallel experimental and theoretical approach to the study of gaseous molecular dication species. This includes spectroscopy, kinetics and reactions, and high level electronic structure calculations. Broad survey calculations with complete active space self-consistent field (CAS-SCF) wavefunctions have been carried out to characterize many of the hydride, fluoride, and oxide dication species. Highly accurate multireference configuration interaction (MR-CI) wavefunctions have established the electronic structures and stabilities of species such as CF2+, F22+, HS2+, NF2 2+, N2 2+, C2 2+, and PH. Vibrational and rotational constants, tunneling lifetimes, and transition strengths are obtained. Reactive studies have been carried out in a crossed beam arrangement on CO2+, NO2+, and HC with rare gases, and hydrogen. Selective product channels are observed and cross sections obtained. High resolution laser spectroscopy of the 3 pi sub u - 3 pi sub g transition in N2 2+ has been obtained in a coaxial laser/beam apparatus by monitoring the threshold appearance of predissociated fragments. Detailed vibrational and rotational constants are obtained. GRA

N92-29931# American Chemical Society, Princeton, NJ. Div. of Colloid and Surface Chemistry.
ELECTROCHEMISTRY IN COLLOIDS AND DISPERSIONS. VOLUME 2: SOLUTE DISTRIBUTION, DIFFUSION, AND TRANSPORT COLLOIDAL METALS
4 Feb. 1992 230 p
(Contract N00014-91-J-1616)
(AD-A248336) Avail: CASI HC A11/MF A03

This report summarizes the current status of experimental and theoretical studies which address fundamental and applied aspects of electrochemistry in colloids and dispersions. The range of such microheterogeneous fluids examined includes micellar solutions, microemulsions, emulsions, latexes, and dispersions of solids in liquids. Several broad subtopics are described. These topics include electroanalytical methods and applications, solute distribution, diffusion, and transport, electrosynthesis and electrocatalysis, polymers and latexes, and colloidal metals and semiconductors. This report is presented in three volumes, 1, 2, and 3. GRA

N92-29932# American Chemical Society, Princeton, NJ. Div. of Colloid and Surface Chemistry.
ELECTROCHEMISTRY IN COLLOIDS AND DISPERSIONS. VOLUME 3: COLLOIDAL SEMICONDUCTORS
4 Feb. 1992 218 p
(Contract N00014-91-J-1616)
(AD-A248337) Avail: CASI HC A10/MF A03

This report summarizes the current status of experimental and theoretical studies which address fundamental and applied aspects of electrochemistry in colloids and dispersions. The range of such microheterogeneous fluids examined includes micellar solutions, microemulsions, emulsions, latexes, and dispersions of solids in liquids. Several broad subtopics are described. These topics include electroanalytical methods and applications, solute distribution, diffusion, and transport, electrosynthesis and electrocatalysis, polymers and latexes, and colloidal metals and semiconductors. This report is presented in three volumes, 1, 2, and 3. GRA

N92-29941# Massachusetts Inst. of Tech., Cambridge. Dept. of Chemistry.
VIBRATIONAL SPECTRUM AND STRUCTURE OF 1,2-DIMETHYL-1,2-DISILA-CLOSO-DODECABORANE
S. S. Bukalov, L. A. Leites, Lars Wesemann, and Dietmar Seyferth 5 Apr. 1992 12 p
(Contract N00014-91-J-1590)
(AD-A250235; MIT-TR-36) Avail: CASI HC A03/MF A01

The IR spectrum (thin film) of 1,2-dimethyl-1,2-disila-closo-dodecarborane, DMSB, in the region 200 - 3600 cm-1 and its Raman spectrum (solid sample) in the region 5 - 3600 cm-1 are reported. It is concluded that the molecular bonding in DMSB is weaker than that in o-carborane. A Raman band at 399 cm-1 is tentatively assigned to the Si-Si bond. GRA

N92-29943# Sandia Labs., Livermore, CA.
ON TRANSIENT FLAMELETS AND THEIR RELATIONSHIP TO TURBULENT METHANE-AIR JET FLAMES
R. S. Barlow and J. Y. Chen 1991 20 p Presented at the 24th International Symposium on Combustion, Sydney (Australia), 5-10 Jul. 1992
(Contract DE-AC04-76DR-00789)
(DE92-006705; SAND-91-8720; CONF-920707-15) Avail: CASI HC A03/MF A01

Laminar flame calculations are performed to investigate possible physical mechanisms for the apparent 'non-flamelet' behavior that has been measured in turbulent methane-air jet flames. Three factors affecting the structure of methane-air diffusion flames are considered: (1) temporal variation of the scalar dissipation rate, (2) changes in the spatial profile of scalar dissipation, and (3) elimination of differential diffusion by setting all species Lewis numbers to unity. Results indicate that changes in the shape of the scalar dissipation profile and sinusoidal variation of the scalar dissipation have relatively minor effects on species mass fraction profiles. However, significant overshoot of the mass fractions of OH and CO occurs when a flamelet is subjected to a step decrease in scalar dissipation. This overshoot occurs without the flame being first pushed to the brink of extinction, and recovery of the flame to steady-state conditions is relatively slow. Significant changes in species mass fractions also occur when the Lewis numbers are set to unity. DOE

N92-30098*# National Aeronautics and Space Administration. Langley Research Center, Hampton, VA.
CONVERTING A CO2 ATMOSPHERE TO A HIGH-PURITY O2 SUPPLY Patent Application
Ronald A. Outlaw, inventor (to NASA) 29 Jul. 1991 9 p
(NASA-Case-LAR-14398-1; NAS 1.71:LAR-14398-1;
US-Patent-Appl-SN-736985) Avail: CASI HC A02/MF A01

A CO2 atmosphere or any other oxygen bearing gas is converted to a high-purity O2 supply by in-letting a flow of CO2 from the atmosphere into a closed container, which is equipped with a means for creating a glow discharge or other method for dissociation in proximity to a permeable silver membrane kept at a temperature between about 400 and 800 C. A glow discharge is created to dissociate the CO2 to form a partial pressure of atomic and molecular oxygen. The oxygen produced is allowed to absorb, dissolve as atoms, permeate the silver membrane to a vacuum interface in a downstream region thereof, where the atomic oxygen thermally recombines on the surface of the membrane to O2 and desorbs: O + O yields reversibly O2. The desorbed O2 is pumped away from the downstream region to maintain as low a concentration of O2 in the downstream region as possible. The pumped away O2 is then compressed into a storage volume to provide an adequate pressure of oxygen for functional utilization. NASA

N92-30196# Technische Univ., Delft (Netherlands).
ROLE OF POLYELECTROLYTES IN BARIUM SULPHATE PRECIPITATION Ph.D. Thesis
M. C. vanderLeeden 9 Dec. 1991 255 p
(PB92-184761; ISBN-90-9004659-3) Avail: CASI HC A12/MF A03

In the last few decades, the use of additives in precipitation processes to improve process efficiency as well as product performance became a common practice. Additives alter the surface properties of the crystals which leads to changes in nucleation and growth kinetics, and thereby to changes in the shape of the crystals as well as in their agglomeration or dispersion

behavior. The precipitation of barium sulfate from aqueous solutions was selected as a model system for studying the effects of additives both because of its practical advantages and its industrial relevance. Barium sulfate is a notorious problem as an unwanted deposition in the recovery of offshore oil and gas. The treatment of the barium sulfate-scale problem is mainly focused on its prevention by the addition of scale-control additives. The additives selected for the investigation are (poly)phosphonate and polycarboxylate compounds, some of which are commercially available for scale prevention. Author

26 METALLIC MATERIALS

Includes physical, chemical, and mechanical properties of metals, e.g., corrosion; and metallurgy.

N92-29408# Pratt and Whitney Aircraft, West Palm Beach, FL. Government Engines and Space Propulsion.
FATIGUE IN SINGLE CRYSTAL NICKEL SUPERALLOYS Technical Progress Report, 16 Feb. - 15 Mar. 1992
Daniel P. DeLuca and Charles Annis 15 Mar. 1992 10 p
(Contract N00014-91-C-0124)
(AD-A248190; PW/GESP-FR2198-05) Avail: CASI HC A02/MF A01

This program investigates the seemingly unusual behavior of single crystal airfoil materials. The fatigue initiation processes in single crystal (SC) materials are significantly more complicated and involved than fatigue initiation and subsequent behavior of a (single) macrocrack in conventional, isotropic, materials. To understand these differences is the major goal of this project. GRA

N92-29411# Pacific Northwest Lab., Richland, WA.
IRRADIATION EFFECTS ON THE ELECTROCHEMISTRY AND CORROSION RESISTANCE OF STAINLESS STEEL
S. M. Bruemmer, B. W. Arey, C. F. Windisch, Jr., and J. I. Cole (Washington State Univ., Pullman.) Apr. 1992 15 p Presented at the Corrosion 1992 Conference and Exhibition, Nashville, TN, 27 Apr. - 1 May 1992
(Contract DE-AC06-76RL-01830)
(DE92-013504; PNL-SA-20350; CONF-920458-8) Avail: CASI HC A03/MF A01

Nickel-ion irradiation at 500 C is shown to have a strong effect on the surface electrochemistry and intergranular corrosion of stainless steel. Measured current densities in a 1N H2SO4 solution at room temperature are increased at active-passive, passive, and transpassive potentials. Irradiation effects on the current decay behavior and susceptibility to intergranular corrosion were similar for a microcrystalline, fine-grained stainless alloy, and for a very large-grained stainless steel. Radiation-induced segregation at the surface is believed to promote higher currents, whereas segregation at grain boundaries prompts intergranular attack. Analytical electron microscopy measurements reveal silicon enrichment and chromium depletion at internal interfaces in irradiated specimens. Silicon enhances dissolution at transpassive potentials, whereas chromium depletion does the same at active-passive and passive potentials. DOE

N92-29426# Texas Univ., Austin. Dept. of Electrical and Computer Engineering.
MAGNETIC PROPERTIES OF NANO-HETEROGENEOUS AMORPHOUS THIN FILMS Final Report, 1 Jun. 1988 - 31 May 1991
Rodger M. Walser 23 Mar. 1992 15 p
(Contract F49620-87-C-0067)
(AD-A250570; AFOSR-92-0281TR) Avail: CASI HC A03/MF A01

We report continued progress in understanding the nanostructure magnetic property relationships in sputtered, amorphous, thin films. This research has been concentrated on two categories of sputtered magnetic thin films: (1) magnetically soft films, of cobalt-based, binary (cobalt-metalloid) alloys with in-plane anisotropies, and (2) magnetically hard, binary (rare earth metal-transition metal) alloy films with perpendicular anisotropies. Major research results obtained include: (1) development of the first broadband measurement technique and apparatus for determining the complex permeability spectra of magnetic thin films in the 100KHz-200MHz frequency range; (2) processing of magnetically soft amorphous thin films with the highest values of RF permeabilities ever reported in the literature; (3) discovery of a new class of ultrasoft magnetic thin films with coercivities less than 0.1 Oe and completely reversible bias susceptibilities; (4) systematically studied the microstructure, magnetic and magneto-optic properties of Tb-Fe and Gd-Co compositionally modulated films; (4) demonstrated that substrate bias could be used to increase the oxidation resistance and improve the magnetic and magnetooptical properties of sputtered Tb-Fe CMFs; and (5) developed a model of displacement eddy currents to resolve a long standing mystery about the origin of eddy current losses in magnetic recording head laminates. GRA

N92-29436# Pacific Northwest Lab., Richland, WA.
CORROSION RESISTANCE OF STAINLESS STEELS AND HIGH Ni-Cr ALLOYS TO ACID FLUORIDE WASTES
H. D. Smith, D. B. Mackey, K. H. Pool, and E. B. Schwenk (Westinghouse Hanford Co., Richland, WA.) Apr. 1992 9 p Presented at the International High Level Radioactive Waste Management (IHLRWM) Conference: Promoting Understanding Through Education and Communication, Las Vegas, NV, 12-16 Apr. 1992
(Contract DE-AC06-76RL-01830)
(DE92-012338; PNL-SA-20408; CONF-920430-85) Avail: CASI HC A02/MF A01

TRUEX processing of Hanford Site waste will utilize potentially corrosive acid fluoride processing solutions. Appropriate construction materials for such a processing facility need to be identified. Toward this objective, candidate stainless steels and high Ni-Cr alloys have been corrosion tested in simulated acid fluoride process solutions at 333 K. The high Ni-Cr alloys exhibited corrosion rates as low as 0.14 mm/y in a solution with an HF activity of about 1.2 M, much lower than the 19 to 94 mm/y observed for austenitic stainless steels. At a lower HF activity (about 0.008 M), stainless steels display delayed passivation while high Ni-Cr alloys display essentially no reaction. DOE

N92-29483# Pennsylvania Univ., Philadelphia.
QUASI-STATIC INTERGRANULAR CRACKING IN A Cu-Sn ALLOY: AN ANALOG OF STRESS RELIEF CRACKING OF STEELS
E. V. Barrera, M. Menyhard, D. Bika, B. Rothman, and C. J. McMahon, Jr. 1991 10 p Presented at the Fall Meeting of the Minerals, Metals and Materials Society of AIME and Materials Week of the American Society of Metals, Cincinnati, OH, 20-24 Oct. 1991
(Contract DE-FG02-87ER-45290)
(DE92-011646; CONF-911003-25) Avail: CASI HC A02/MF A01

Intergranular cracking in a laboratory-made Cu-8wt percent Sn alloy at 265 to 300 C in vacuum was studied in order to explore the hypothesis that this could serve as an analog to the brittle mode of stress-relief cracking in steels and to test the mechanism proposed earlier to explain that phenomenon. This mechanism involves the stress-induced intergranular penetration along grain boundaries of a surface-adsorbed embrittling element. Sulfur is the active element in this regard in steels, and tin was envisioned as playing the same role in Cu-Sn alloys. Auger spectroscopy was used to confirm earlier reports of the surface activity of tin and to determine the segregation kinetics in the present polycrystals; no other elements were found to segregate to surfaces to any significant degree in the present alloy. Crack growth measurements showed that intergranular cracking occurs in an intermittent manner at an average rate on the order of 0.1 micron/sec over a range of crack length. Crack initiation was found to be remarkably sensitive to the stress intensity, implying the existence of a threshold. The fracture appearance in the regions

of slow crack growth was similar to that observed in steels undergoing stress-relief cracking at 500-600 C. It was concluded that the quasi-static intergranular cracking in the steels and in the Cu-Sn alloy represent two aspects of the same generic phenomenon and that the proposed mechanism of stress-induced intergranular impurity penetration is valid. It is believed that liquid- and solid-metal embrittlement are closely related to the type of intergranular cracking described here. DOE

N92-29547# California Univ., Davis. Materials Science and Engineering Div.
STRENGTHENING MECHANISMS, CREEP AND FATIGUE PROCESSES IN DISPERSION HARDENED NIOBIUM ALLOY Final Report, 1 Feb. 1989 - 31 Jan. 1992
Amiya K. Mukherjee and Jeffery C. Gibeling 20 Apr. 1992 57 p
(Grant AF-AFOSR-0287-89)
(AD-A250282; AFOSR-92-0387TR) Avail: CASI HC A04/MF A01

The creep and fatigue properties of pure Nb and Nb-1 percent Zr alloy were investigated. A model was developed based on the migration of subgrain boundary that can explain the anomalous primary creep transients found in Nb-1 percent Zr alloy, due to coarsening of subgrain structure. TEM investigations confirmed that such subgrain coarsening occurs during primary creep of Nb-1 percent Zr. Baseline low cycle fatigue studies of Nb and Nb-1 percent Zr were completed. Cyclic hardening is observed and there is a microplastic plateau in Nb. The Nb-1 percent Zr is stronger in cyclic deformation than Nb, with little influence of strain rate. The deformation in the alloy at both high and low strain rates is controlled by the interaction between gliding edge dislocation and solute atoms. GRA

N92-29587# Martin Marietta Labs., Baltimore, MD.
A STUDY OF THE INFLUENCE OF ALLOYING ADDITIONS ON THE PASSIVITY OF ALUMINUM Annual Report, 1 Dec. 1990 - 30 Nov. 1991
G. D. Davis, B. J. Rees, B. A. Shaw, and M. Ferry Mar. 1992 57 p
(Contract N00014-85-C-0638)
(AD-A248339; MML-TR-92-13C; MML-TR-91-10C) Avail: CASI HC A04/MF A01

The corrosion behavior of nonequilibrium aluminum tantalum and aluminum tungsten alloys produced by either dynamic compaction or sputter deposition has been evaluated. Dynamical compacted material showed no enhanced passivity as a result of precipitates formed during powder formation. No new precipitates were found that originated during the dynamic compaction process when water was used to reflect the shock wave. Sputter-deposited AlW and AlTa alloys exhibited considerable enhanced resistance to pitting corrosion over a range of pH's extending from pH 9.6 to pH 0. Surface analysis showed that although very little oxidized W is found in the passive film at near-neutral pH's, the passive film at pH3 consists of comparable amounts of oxidized W and Al. A review of the different mechanisms that have been proposed to explain the passivity of this class of alloys suggests that the pitting resistance of Al-W is likely to result from a repassivation of metastable pits due to the stability of oxidized W in low pH environments. GRA

N92-29623# Sandia National Labs., Albuquerque, NM.
METAL VAPOR PLASMA BEHAVIOR DURING VACUUM ARC REMELTING OF ALLOY 718
F. J. Zanner, M. C. Maguire, R. L. Williamson, C. B. Adasczik (Teledyne Allvac Corp., Monroe, NC.), R. R. Roberts (Consarc Corp., Rancocas, NJ.), and R. Strohecker (Strohecker Corp., East Palestine, OH.) 1992 4 p Presented at the 11th International Conference on Vacuum Metallurgy, (France), 11-14 May 1992
(Contract DE-AC04-76DP-00789)
(DE92-011761; SAND-92-0594C; CONF-9205142-1) Avail: CASI HC A01/MF A01

A production vacuum arc remelt (VAR) furnace was modified to enable direct viewing of the metal vapor arc and molten electrode tip during melting of 432 mm dia. alloy 718 electrodes into 508 mm dia. ingots. Diffuse and constricted arcing conditions were characterized using high speed cinematography, standard video format, and monochromatic imaging. Constricted arcing was observed while melting electrodes contaminated with oxide slag of the type used for refractory linings in vacuum induction furnaces. Monochromatic imaging was used to visualize the ion distribution in the arc plasma; these images clearly showed whether the arc operated in a diffuse or constricted model. Diffuse arc melting conditions were very similar to those previously reported in the literature for smaller laboratory sized melts. DOE

N92-29633# Los Alamos National Lab., NM.
OMEGA PHASE FORMATION IN TITANIUM AND TITANIUM ALLOYS
G. T. Gray, III, C. E. Morris, and A. C. Lawson 1992 9 p Presented at the 7th World Conference and Exhibition on Titanium, San Diego, CA, 28 Jun. - 2 Jul. 1991
(Contract W-7405-eng-36)
(DE92-011138; LA-UR-92-887; CONF-920604-2) Avail: CASI HC A02/MF A01

Although the response of titanium alloys to dynamic loading is receiving increased attention in the literature (particularly in the area of shear-band formation), a more limited experimental database exists concerning the detailed structure/property relationships of titanium alloys subjected to shock loading. In this study, preliminary results concerning the influence of alloy chemistry on the property of omega-phase formation and its structure in three titanium alloys are presented. The influence of shock-wave deformation on the phase stability and substructure evolution of high-purity (low-interstitial) titanium, A-70 (3700 ppm oxygen) titanium, and Ti-6Al-4V were probed utilizing real-time velocity interferometry (VISAR) and 'soft' shock-recovery techniques. VISAR wave profiles of shock-loaded high-purity titanium revealed the omega-phase pressure-induced transition to occur at approximately 10.4 GPa. Wave profile measurements on A-70 Ti shocked to pressures up to 35 GPa and Ti-6Al-4V shocked to pressures up to 25 GPa exhibited no evidence of a three-wave structure indicative of a pressure-induced phase transition. Neutron and X-ray diffractometry and TEM analysis confirmed the presence of retained omega-phase in the electrolytic-Ti and the absence of omega-phase in the shock-recovered A-70 Ti and Ti-6Al-4V. Suppression of the alpha-omega phase transition in A-70 Ti, containing a high interstitial oxygen content, is seen to simultaneously correlate with suppression of deformation twinning. Neutron diffraction was used to measure the in-situ bulk lattice constants and volume fraction of the alpha and omega phases in the recovered high-purity titanium samples that were shock loaded. The influence of alloy content on the kinetics of formation/retention of omega-phase and substructure evolution is discussed and contrasted in light of previous literature studies. DOE

N92-29637# Helsinki Univ. of Technology, Otaniemi (Finland). Lab. of Metallurgy.
PROCESS OF FERROCHROMIUM NOW AND IN THE FUTURE
M. Kojo and L. Holappa 1991 52 p
(DE92-506510; TKK-V-C110) Avail: CASI HC A04/MF A01

The most essential objectives in the development of the ferrochromium process are the reduction of energy consumption and improvements in the recovery of chromium. For measuring the activity of chromium oxide in slags, there was developed a measuring system based on an oxygen-ion conductive solid electrolyte. Owing to the high temperature and aggressive nature of the slags, there were difficulties in the measurements for the life of cell and crucible materials. Progress was made by developing the technique, and measurements were carried out for the basic slag system CaO - SiO2 - Cr(sub x)O, as well as for individual 4-component slags. Reproducible results were obtained. DOE

N92-29639# Lawrence Livermore National Lab., CA.
EFFECT OF GRAIN SIZE ON DEFORMATION STABILITY OF COPPER UNDER QUASI-STATIC AND DYNAMIC TENSILE LOADING

D. H. Lassila and W. H. Gourdin 31 Oct. 1991 15 p Presented at the Army Symposium on Solid Mechanics: Synergism of Mechanics, Mathematics and Materials, Plymouth, MA, 4-7 Nov. 1991
(Contract W-7405-eng-48)
(DE92-012677; UCRL-JC-108728; CONF-911195-3) Avail: CASI HC A03/MF A01

The effects of grain size on the deformation stability of copper deformed in tension under quasi-static and dynamic conditions have been studied experimentally and analytically. Oxygen Free Electronic (OFE) copper samples with grain sizes of 15 microns and 120 microns were tested. Results of the tests indicated that an increase in grain size resulted in greater extents of elongation prior to deformation instability and eventual failure under both quasi-static and dynamic loading. We have applied the deformation stability condition of Considere to both a simple power law modified to include a Hall-Petch grain size dependence and the more descriptive mechanical threshold stress (MTS) model. Calculations of the stress-strain behavior in uniaxial tension and the instability strain under quasi-static loading are compared with experiment. Both models predict an increase in the instability strain with increasing grain size, but the power law, included as a heuristic, yields a poor overall fit to both the stress-strain and the instability strains. Under dynamic loading, comparison of the experimental results with analytical predictions were difficult due to inherent inaccuracy in the dynamic stress-strain data. DOE

N92-29647# Napier Coll., Edinburgh (Scotland).
DYNAMIC SOLDER MANAGEMENT Interim Report, Dec. 1991 - Feb. 1992
M. Cummings and G. Lindsay Feb. 1992 13 p
(Contract DAJA45-91-C-0016)
(AD-A250564; R/D-6750-MS-01) Avail: CASI HC A03/MF A01

Results from initial 2D steady-state isothermal simulations of wave soldering of DSM modified PCBs are presented. The effects of small (2mm) obstacles on solder flow paths can be clearly seen. More sophisticated, realistic models are under development and will be reported next quarter. GRA

N92-29651# Kernforschungszentrum G.m.b.H., Karlsruhe (Germany, F.R.). Inst. fuer Material- und Festkoerperforschung.
PROCESSING AND PROPERTIES OF MECHANICALLY ALLOYED SINTERED STEELS WITH HARD INCLUSIONS Thesis - Karlsruhe Univ. [HERSTELLUNG UND EIGENSCHAFTEN MECHANISCH LEGIERTER SINTERSTAEHLE MIT HARTSTOFFEINLAGERUNGEN]
C. Gutsfeld Oct. 1991 130 p In GEORGIAN
(KfK-4909; ISSN-0303-4003; ETN-92-91502) Copyright Avail: CASI HC A07/MF A02

Mechanically alloyed sintered steels with inert hard inclusions are addressed. Their characterization is examined with regard to mechanical properties and sliding wear behavior. Hard materials, NbC, TiC, TiN and Al2O3 are chosen, with volume contents up to 20 percent. It is shown that mechanical alloying of the raw powers is a prerequisite for an extreme fine and homogeneous microstructure. Sintering initiated through phosphorous contents of 0.6 percent is suitable for the consolidation pressureless liquid phase. The mechanical properties can be varied in wide ranges. These materials can complete with powder metallurgy high speed steels with regard to sliding wear behavior. ESA

N92-29674# Laboratoire d'Automatique et d'Analyse des Systemes, Toulouse (France). Groupe Composants et Circuits a Effet du Champ.
A STUDY AND FEASIBILITY OF ULTRA THIN SILICA LAYERS BY RAPID THERMAL PROCESSING Ph.D. Thesis - Inst. National des Sciences Appliquees, Toulouse [ETUDE ET FAISABILITE DE COUCHES DE SILICE ULTRA-MINCES PAR PROCEDE THERMIQUE RAPIDE]
Abdellatif YahiaMessaoud 1991 140 p In FRENCH
(LAAS-91393; ETN-92-91478) Avail: CASI HC A07/MF A02

The kinetics of silicon oxidation by rapid thermal processing in the 1060 to 1240 C range was studied. Care was taken in homogenization, and optimization of the heating and the initial conditions. A special effort was made on the precision of the thickness measurements using ellipsometry and adequate calculations. From the comparison of the experimental thicknesses with simulated ones, using Han and Helms model and comparative temperature evaluation, the real temperature is evaluated with a precision of + or - 5 C. It was concluded that rapid thermal oxidation kinetics does not show any special peculiarity in the 2 to 20 nm range. Electrical measurements in rapid thermal oxidation capacitors were performed. Typically, electrical field breakdown of 15 MV/cm and Qbd equal to 40 C/sq cm were found for oxide thicknesses between 8 and 10 nm. These characteristics compare favorably with the best electrical properties reported in the literature. It is then concluded that rapid thermal oxidation is a very interesting process for the submicron metal-oxide semiconductor technologies. ESA

N92-29706# Ames Lab., IA.
STRUCTURE AND STABILITY OF Al-Cu-Ru FACE-CENTERED ICOSAHEDRAL ALLOYS Ph.D. Thesis
J. E. Shield 25 Feb. 1992 76 p
(Contract W-7405-eng-82)
(DE92-012550; IS-T-1612) Avail: CASI HC A05/MF A01

The phases and microstructures in rapidly solidified Al-Cu-Ru alloys were investigated in this study. A chemically and topologically disordered icosahedral (i) phase grows dendritically from the liquid as the primary solidification product over the entire compositional region studied. The as-solidified i-phase is metastable and transforms to crystalline products at approx. 500 C. The i-phase was not found as a product of the exothermic transformation for any composition, indicating that it is not the low temperature stable phase in the Al-Cu-Ru system. A chemically and topologically ordered i-phase was found to be an equilibrium phase at temperatures above (approx. 670 C and exists over a compositional region of several atomic percent. Once formed, this phase was easily retained at lower temperatures because of kinetic limitations of the transformation to the low temperature crystalline phase. DOE

N92-29803# National Inst. of Standards and Technology, Gaithersburg, MD. Materials Reliability Div.
ALUMINUM-LITHIUM ALLOYS: SURFACE-CRACKED TENSION FRACTURE TESTS AND PHYSICAL AND THERMAL PROPERTIES AT CRYOGENIC TEMPERATURES
P. T. Purtscher, M. Austin, S. Kim, and D. Rule Mar. 1992 72 p Sponsored in part by Astronautics Lab (AFSC), Edwards AFB, CA
(PB92-172477; NISTIR-3986) Avail: CASI HC A04/MF A01

Surface-cracked tension fracture tests were conducted in the T-S orientation at 295, 76, and 4 K on two plate alloys (X2095-T851, plate thickness of 12.7 mm and 2090-T81, plate thickness of 12.7 and 19.1 mm). The cryogenic toughness to room temperature toughness ratio for alloy 2090 is generally higher than that found for alloy X2095. Both alloys have significantly lower tensile properties near the surface of rolled plate than in the center of the plate. The physical properties of seven plate specimens were measured from liquid helium to room temperature. Three variations in chemical composition of alloy X2095, three different samples of alloy 2090, and a single sample of alloy 2219-T87 were included. Thermal expansion between 4 and 320 K were measured on the same seven plate specimens included in the physical properties study. The thermal conductivity of alloy X2095 (4 percent Cu - 1 percent Li) was determined over the temperature range of 4.2 to 300 K using a steady-state apparatus. Author

N92-29807# National Materials Property Data Network, Inc., Columbus, OH.
MARINE STRUCTURAL STEEL TOUGHNESS DATA BANK (ABRIDGED EDITION) Final Report
J. G. Kaufman and M. Prager 1991 337 p
(Contract DTCG23-86-C-20062)
(PB92-163294; SSC-352) Avail: CASI HC A15/MF A03

The Ship Structures Committee has sponsored the development

of a data bank covering the toughness of steels for marine applications. Effort focused on the identification and procurement of sources of data containing quantitative toughness data, and the development from those data of a well-documented computerized data bank available to a wide range of engineers and material scientists. Included were raw data from material suppliers and data from papers and technical reports published by a variety of organizations. The principal focus was on tensile properties, Charpy V notched bar impact values, fracture toughness, nilductility transition temperature (NDTT), and dynamic tear (DT) energies; other toughness parameters were included if available for the same lots of material. The materials include steels identified by the Project Technical Committee representing the sponsoring agencies. About 1000 records representing approximately 10,000 tests of eleven steels are included in this prototype version of the data bank. Standard procedures now exist for efficient addition of data for other alloys and properties. Author

N92-29940# IT Environmental Programs, Inc., Cincinnati, OH.
EVALUATION OF ALUMINUM ION VAPOR DEPOSITION AS A REPLACEMENT FOR CADMIUM ELECTROPLATING AT ANNISTON ARMY DEPOT Final Report, May 1989 - Apr. 1992
R. Ressl and J. Spessard Apr. 1992 128 p
(Contract DAAA15-88-D-0001)
(AD-A250063; REF-JTN-816005; CETHA-TS-CR-91054) Avail: CASI HC A07/MF A02

The U.S. Army Toxic and Hazardous Materials Agency (USATHAMA) conducts research and development projects with the objective of minimizing hazardous waste generation at Army Depots. During one such project, USATHAMA evaluated the feasibility of an Aluminum Ion Vapor Deposition System as an alternative to cadmium electroplating. The test program was conducted at Anniston Army Depot, Anniston, Alabama. IT Environmental Programs, Inc. was USATHAMA's contractor for this program. The Aluminum Ion Vapor Deposition System, referred to herein as an Ivadizer, provides corrosion resistance to metal parts by depositing a thin aluminum film (typically 1 mil or 0.001 inch) on the parts. As a replacement for cadmium electroplating, the Ivadizer has the advantage of generating minimal quantities of hazardous wastes; whereas, cadmium plating generates significant quantities of listed hazardous waste, and cadmium is toxic (and possibly carcinogenic). GRA

N92-30205*# National Aeronautics and Space Administration. Langley Research Center, Hampton, VA.
MECHANICAL PROPERTIES OF COATED TITANIUM BETA-21S AFTER EXPOSURE TO AIR AT 700 AND 800 C
Karl E. Wiedemann (Analytical Services and Materials, Inc., Hampton, VA.), R. Keith Bird, Terryl A. Wallace, and Ronald K. Clark Jun. 1992 12 p Presented at the 7th World Conference on Titanium, San Diego, CA, 29 Jun. - 2 Jul. 1992
(RTOP 506-43-71-01)
(NASA-TM-104220; NAS 1.15:104220) Avail: CASI HC A03/MF A01

Mechanical properties of Beta-21S (Ti-15Mo-3Al-2.7Nb-0.2Si, wt percent) with glass, aluminide, and glass-on-aluminide coatings less than 3-micron thick were studied. Coatings were deposited by sol-gel processing or electron-beam evaporation onto 4.5-mil (113-micron) thick Beta-21S sheet from which, after oxidizing in air at 700 or 800 C, tensile test specimens were machined. Plastic elongation was the most severely degraded of the tensile properties; the glass-on-aluminide coatings were the most effective in preventing degradation. It was found that oxygen trapping by forming oxides in the coating, and reactions between the coatings and the Beta-21S alloy played significant roles. Author

N92-30206*# Virginia Univ., Charlottesville. Dept. of Materials Science and Engineering.
NASA-UVA LIGHT AEROSPACE ALLOY AND STRUCTURES TECHNOLOGY PROGRAM (LA2ST) Progress Report, 1 Jan. - 30 Jun. 1992
Richard P. Gangloff Jul. 1992 499 p
(Grant NAG1-745)
(NASA-CR-190538; NAS 1.26:190538; UVA/528266/MS93/111)
Avail: CASI HC A21/MF A04

The NASA-UVa Light Aerospace Alloy and Structure Technology (LAST) Program continues to maintain a high level of activity, with projects being conducted by graduate students and faculty advisors in the Departments of Materials Science and Engineering, Civil Engineering and Applied Mechanics, and Mechanical and Aerospace Engineering at the University of Virginia. This work is funded by the NASA-Langley Research Center under Grant NAG-1-745. Here, we report on progress achieved between January 1 and June 30, 1992. The objectives of the LA2ST Program is to conduct interdisciplinary graduate student research on the performance of the next generation, light weight aerospace alloys, composites and thermal gradient structures in collaboration with Langley researchers. Technical objectives are established for each research project. We aim to produce relevant data and basic understanding of material mechanical response, corrosion behavior, and microstructure; new monolithic and composite alloys; advanced processing methods; new solid and fluid mechanics analyses; measurement advances; and critically, a pool of educated graduate students for aerospace technologies. The accomplishments presented in this report cover topics including: (1) Mechanical and Environmental Degradation Mechanisms in Advance Light Metals and Composites; (2) Aerospace Materials Science; (3) Mechanics of Materials and Composites for Aerospace Structures; and (4) Thermal Gradient Structures. Author

27 NONMETALLIC MATERIALS

Includes physical, chemical, and mechanical properties of plastics, elastomers, lubricants, polymers, textiles, adhesives, and ceramic materials.

For composite materials see *24 Composite Materials*.

N92-29349# Case Western Reserve Univ., Cleveland, OH. Dept. of Macromolecular Science.
MOLECULAR ENGINEERING OF LIQUID CRYSTALLINE POLYMERS BY LIVING POLYMERIZATION. 19: SYNTHESIS AND CHARACTERIZATION OF POLY 2-(4-BIPHENYLOXY)ETHYL VINYL ETHERBY
Virgil Percec and Myongsoo Lee 27 Mar. 1992 22 p
(Contract N00014-90-J-1828)
(AD-A248285; TR-57) Avail: CASI HC A03/MF A01

The synthesis and living cationic polymerization of 2-(4-biphenyloxy)ethyl vinyl ether (BEVE) are described. Polymers with degrees of polymerization from 3.8 to 22.1 and narrow molecular weight distribution were synthesized and characterized by differential scanning calorometry (DSC) and thermal optical polarized microscopy. When determined from their first DSC heating scans poly(BEVE)s exhibit only a crystalline phase over the entire range of molecular weights. When determined from the second and first cooling scans, poly(BEVE) with a degree of polymerization of 3.8 exhibits an enantiotropic smectic mesophase and a crystallization process on the heating scan, while the polymers with degrees of polymerization from 4.7 to 8.1 exhibit only an enantiotropic smectic mesophase. The polymers with higher degrees of polymerization do not exhibit any mesophase. An explanation for this behavior is provided. GRA

N92-29435# Southern Research Inst., Birmingham, AL.
SYNTHESIS OF A NAPHTHALENE-HYDROXYNAPHTHALENE POLYMER MODEL COMPOUND
2 Oct. 1991 40 p
(Contract DE-AC22-90PC-90038)
(DE92-012264; DOE/PC-90038/T1) Avail: CASI HC A03/MF A01

The objective of this project was the synthesis of one pound of a new naphthalene-hydroxynaphthalene polymer model compound for use in coal combustion studies. Since this compound was an unreported compound, this effort also required the

development of a synthetic route to this compound (including routes to the unique and unreported intermediates leading to its synthesis). DOE

N92-29465# Minnesota Univ., Minneapolis. Dept. of Chemical Engineering and Materials Science.
NONIDEAL FORMATION OF NETWORK POLYMERS Final Report, Jan. 1988 - Jan. 1992
Christopher Macosko and Douglas Miller 20 Mar. 1992 6 p
(Contract N00014-88-K-0366)
(AD-A248072) Avail: CASI HC A02/MF A01

The majority of networks are formed from small monomers, typically with molecular weights less than 500, and often close to 100. In these polymerizations functional groups are close together, and hence may influence one another in a number of ways: groups on the same monomer may not be equally reactive; their reactivity may change as nearest neighbors react; and wasted cycles may form. Conversely network formation may alter the polymerization, for example through phase separation or through a glass transition leading to incomplete conversion. Network formation from small monomers under such non-ideal conditions was the focus of our research, which covered the effects of the following nonidealities: first-shell substitution effect; cyclization instep and chainwise systems; chainwise mechanisms during network formation (free-radical, anionic, and secondary site generation); diffusion; and filler and the interactions of filler with polymer. GRA

N92-29466# Texas Univ., Austin. Dept. of Chemistry.
A NOVEL APPROACH TO SILICON-ON-INSULATOR MATERIALS Final Report
Alan H. Cowley and Richard A. Jones 1991 11 p
(Contract N00014-89-J-1767)
(AD-A248074) Avail: CASI HC A03/MF A01

There is currently a great deal of interest in insulator on semiconductor layer constructions in the electronics community. Calcium fluoride is electronically insulating and lattice matched to both silicon and gallium arsenide, which makes it an ideal insulator for these materials. Also, CaF2 is being used as an insulator with thin films of the high temperature superconducting materials. While there was a great deal of work done in the deposition of CaF2 films by physical techniques, such as molecular beam epitaxy (MBE), this technique is not considered to be viable for large scale production techniques due to the expensive and sophisticated high vacuum equipment involved. Another problem with MBE of CaF2 is that high substrate temperatures (greater than 500 C) seem to be required for good quality films. Due to the differences in thermal expansion between CaF2 and silicon or gallium arsenide, these films tend to crack when cooled to ambient temperature. Therefore, a project was undertaken to see if CaF2 films could be grown by chemical methods. The most useful of these is the Chemical Vapor Deposition (CVD) method, where the material of interest is produced by a chemical reaction on the substrate surface by one or more precursor molecule(s), which are delivered to the substrate in the gas phase. GRA

N92-29479# Los Alamos National Lab., NM.
ELECTRON MICROSCOPY STUDY ON ZIRCONIA AND ALUMINA CERAMIC POWDERS SYNTHESIZED BY MICROWAVE PLASMA PYROLYSIS
K. E. Sickafus, R. Varma, and D. Vollath 1992 10 p Presented at the Material Research Society Spring Meeting, San Francisco, CA, 27 Apr. - 2 May 1992
(Contract W-7405-eng-36)
(DE92-013385; LA-UR-92-1426; CONF-920402-2) Avail: CASI HC A02/MF A01

Morphology, chemistry, and microstructure of zirconia and alumina based ceramic powders synthesized by microwave plasma pyrolysis were studied by transmission electron microscopy. Electron diffraction was used to determine the phases present, while conventional bright field and dark field imaging were used to characterize grain size and density variations. Materials analyzed in this study were either pure zirconia, pure alumina, or a ternary zirconia-yttria-alumina oxide. Solid spheres, hollow spheres, and fragments of hollow spheres were observed. All three modifications of zirconia were observed in the pure zirconia powder. In alumina, the predominant phase was cubic, gamma alumina. In the ternary oxide, most structures exhibited cubic zirconia diffraction patterns. Energy dispersive x-ray spectroscopy revealed chemical inhomogeneities in the ternary oxide powder. DOE

N92-29482# Ames Lab., IA.
ELECTRICAL, OPTICAL, AND MAGNETIC RESONANCE STUDIES OF NOVEL pi-CONJUGATED POLYMERS Ph.D. Thesis
Qing-Xiao Ni 20 Apr. 1992 139 p
(Contract W-7405-eng-82)
(DE92-012548; IS-T-1603) Avail: CASI HC A07/MF A02

Conductivity, optical properties including visible and infrared absorption and photoluminescence, and magnetic resonance properties including electron spin resonance and optically detected magnetic resonance have been studied in polydiethynylsilanes (PDES) and poly(2,5-dibutoxy paraphenylene acetylene) (PDBOPA), which have been recently synthesized. PDES and PDBOPA blend and PDBOPA-based electroluminescent preliminary diodes which were fabricated were also explored. The undoped one-dimensional gap of PDES polymers, which have average molecular weight from approximately 2 x 10(exp 5) to 1 x 10(exp 6), is 2.0 eV in both films and solutions; photoluminescence is barely observed. I2 doping induces a single absorption band at approximately 1.05 eV in solutions and lightly doped films, but another at approximately 0.55 eV in heavily doped films. Both are correlated with strong IR-active vibrations associated with known lines in Raman scattering. DOE

N92-29496# Massachusetts Inst. of Tech., Cambridge. Dept. of Chemistry.
SYNTHESIS AND USEFUL REACTIONS OF ORGANOSILICON POLYMERIC PRECURSORS FOR CERAMICS
Dietmar Seyferth, Carsten Strohmann, Henry J. Tracy, and Jennifer L. Robison 5 Apr. 1992 14 p
(Contract N00014-91-J-1590)
(AD-A248500; TR-34) Avail: CASI HC A03/MF A01

A general discussion of the polymer pyrolysis route to ceramics, what it is, why it is important, and the chemical considerations that are important in its implementation, is followed by some recent examples from research at MIT involving polysilazane and polysilane chemistry. GRA

N92-29508# Case Western Reserve Univ., Cleveland, OH. Dept. of Macromolecular Science.
MOLECULAR ENGINEERING OF SIDE CHAIN LIQUID CRYSTALLINE POLYMERS
Virgil Percec and Dimitris Tomazos 27 Mar. 1992 24 p
(Contract N00014-90-J-1828)
(AD-A248540) Avail: CASI HC A03/MF A01

This chapter discusses the molecular engineering of side chain liquid crystalline polymers mainly by living polymerization reactions. According to thermodynamic schemes, the polymer effect through its molecular weight and backbone flexibility can provide an overall change of entropy of the system. Consequently it can transform virtual mesophases into monotropic and enantiotropic mesophases. The control of molecular weight provided by living cationic polymerization of mesogenic vinyl ethers can be used successfully to tailor-make phase transitions like smectic A (s(sub A)), nematic (n) and re-entrant nematic (n(sub re)) inside chain liquid crystalline polymers and copolymers. Some additional examples of molecular engineering of side chain liquid crystalline polymers containing crown ethers and polypodants and self-assemblying side chain liquid crystalline polymers are presented. GRA

N92-29549# Texas Univ., Austin. Dept. of Chemistry.
SYNTHESIS OF NEW HIGH PERFORMANCE LUBRICANTS AND SOLID LUBRICANTS
R. J. Lagow Mar. 1992 9 p
(Contract DE-FG05-91ER-12119)

(DE92-011940; DOE/ER-12119/1) Avail: CASI HC A02/MF A01

We have started to make a number of classes of new perfluoropolyethers both in the solid lubricant area and liquid lubricant area. We have prepared some chlorofluoroethers for testing as additives for normal petroleum and polyalphaolefin lubricants which are so widely used in the United States. Perfluoropolyethers are not soluble in hydrocarbons. On the other hand, these chlorofluoropolyethers are soluble in substantial amounts in simple hydrocarbons. These are uniquely capable of being additives that flow with the motor oil or the polyalphaolefin. DOE

N92-29566# Case Western Reserve Univ., Cleveland, OH. Dept. of Macromolecular Science.

MOLECULAR ENGINEERING OF LIQUID CRYSTALLINE POLYMERS BY LIVING POLYMERIZATION. 20: SYNTHESIS AND CHARACTERIZATION OF BINARY COPOLYMERS OF 11-(4-CYANO-4'-BIPHENYL) OXY)UNDECANYL VINYL ETHER WITH n-BUTYL VINYL ETHER AND OF 2-(4-CYANO-4'-BIPHENYL) OXY)ETHYL VINYL ETHER WITH n-BUTYL VINYL ETHER

Virgil Percec and Myongsoo Lee 27 Mar. 1992 22 p
(Contract N00014-90-J-1828)
(AD-A248286; TR-58) Avail: CASI HC A03/MF A01

Copolymerization represents the simplest synthetic technique which can be used to tailor make phase transitions of both main chain and side chain liquid crystalline polymers. Indeed, copolymerization was frequently employed to manipulate the phase transitions of side chain liquid crystalline polymers. However, most of the results reported in the literature can be considered only in a qualitative way, since there are only very few cases in which information about both copolymer composition and molecular weight are available. A general classification of side chain liquid crystalline copolymers was recently discussed in a review article. There are two main classes of side chain liquid crystalline copolymers. The first one refers to copolymers containing pairs of structural units with and without mesogenic units. The second class refers to copolymers based on pairs of structural units containing mesogenic units in each structural unit. GRA

N92-29567# Case Western Reserve Univ., Cleveland, OH. Dept. of Macromolecular Science.

MOLECULAR ENGINEERING OF LIQUID CRYSTALLINE POLYMERS BY LIVING POLYMERIZATION. 22: SYNTHESIS AND CHARACTERIZATION OF BINARY COPOLYMERS

Virgil Percec, Myongsoo Lee, and Qiang Zheng 27 Mar. 1992 42 p
(Contract N00014-90-J-1828)
(AD-A248287; TR-60) Avail: CASI HC A03/MF A01

The synthesis and characterization of poly(11-(4-cyano-4'-biphenyl)oxy)undecanyl vinyl ether-co-(2S,3S)-(+)-2-chloro-3-methylpentyl 4'-(8-vinyl(oxyocty(oxy) biphenyl-4-carboxylate)X/Y (poly(6-11)-co-(15-8)X/Y) (where X/Y represents the molar ratio of the two structural units) and poly(2S,3S)-(+)-2-chloro-3-methylpentyl-((4-cyano-4'-biphenyl)oxy) propyl vinyl ether)X/Y (poly(15-8)-co-(6-3))X/Y) with degree of polymerization of about 20 and molecular weight distribution of about 1.1 are described. The mesomorphic behavior of all copolymers determined from both first, second and subsequent differential scanning calorimetric (DSC) scans was discussed as a function of composition. As determined from the second DSC scans, poly(6-11) exhibits enantiotropic smectic A s(sub A) and s(sub X) (unidentified smectic), poly(6-3) enantiotropic nematic mesophases, while poly(15-8) exhibits enantiotropic s(sub A), chiral smectic C and s(sub X) (unidentified smectic) mesophases. Poly(6-11)-co-(15-8)X/Y exhibit a s(sub A) phase over the entire range of compositions. This mesophase displays a continuous dependence of copolymer composition with an upward curvature. Poly(15-8)-co-(6-3)X/Y from 10/0 to 3/7 displays an enantiotropic sA mesophase as their highest phase, while those with X/Y from 2/8 to 1/9 an enantiotropic cholesteric mesophase. GRA

N92-29569# Case Western Reserve Univ., Cleveland, OH. Dept. of Macromolecular Science.

STRUCTURAL REARRANGEMENTS DURING MESOMORPHIC PHASE TRANSITIONS IN POLY(10-((4-CYANO-4' BIPHENYL)OXY)DECANYL VINYL ETHER)

V. Tsukrut, V. Percec, and M. Lee 27 Mar. 1992 28 p
(Contract N00014-90-J-1828)
(AD-A248306; TR-61) Avail: CASI HC A03/MF A01

The side chain liquid crystalline poly 10-((4-cyano-4'-biphenyl)oxydecanyl vinyl ether) exhibits two different smectic phases: at low temperature an ordered smectic E phase with orthorhombic intralayer packing of the mesogenic groups, and at high temperatures a common disordered smectic A phase. In both phases, double-layered longitudinal packing of the macromolecular fragments with a thickness of 6.6-7 nm and overlapping of the slightly tilted mesogenic groups is realized. During the phase transition from the smectic E to the smectic A, a melting of the intralayered packing occurs which leads also to the slight changes of the thickness of the smectic layers as a result of the conformational disordering of the side chains. A smectic A-like structure could be freezed in the glassy state by quick cooling. The development of the ordered smectic E phase as a result of annealing at temperatures higher than Tg is a very slow process since it requires the formation of the ordered intralayered orthorhombic packing of mesogenic groups. GRA

N92-29598# Midwest Research Inst., Golden, CO. National Renewable Energy Lab.

MONOLITHIC AMORPHOUS SILICON MODULES ON CONTINUOUS POLYMER SUBSTRATE

D. P. Grimmer (Iowa Thin Film Technologies, Inc., Ames.) Mar. 1992 113 p
(Contract DE-AC02-83CH-10093)
(DE92-001163; NREL/TP-214-4488) Avail: CASI HC A06/MF A02

This report examines manufacturing monolithic amorphous silicon modules on a continuous polymer substrate. Module production costs can be reduced by increasing module performance, expanding production, and improving and modifying production processes. Material costs can be reduced by developing processes that use a 1-mil polyimide substrate and multilayers of low-cost material for the front encapsulant. Research to speed up a-Si and ZnO deposition rates is needed to improve throughputs. To keep throughput rates compatible with depositions, multibeam fiber optic delivery systems for laser scribing can be used. However, mechanical scribing systems promise even higher throughputs. Tandem cells and production experience can increase device efficiency and stability. Two alternative manufacturing processes are described: (1) wet etching and sheet handling and (2) wet etching and roll-to-roll fabrication. DOE

N92-29643# Los Alamos National Lab., NM.

THE COMPARATIVE EFFECTS OF GAMMA RADIATION AND IN SITU ALPHA PARTICLES ON FIVE STRONG-BASE ANION EXCHANGE RESINS

S. F. Marsh 1991 9 p Presented at the International Conference on Ion Exchange Advances, Cambridge (United Kingdom), 12-17 Jul. 1992
(Contract W-7405-eng-36)
(DE92-000177; LA-UR-91-3097; CONF-920703-1) Avail: CASI HC A02/MF A01

The effects of external gamma radiation and in situ alpha particles were measured on a recently available, macroporous, strong-base polyvinylpyridine resin and on four strong-base polystyrene anion exchange resins. Each resin was irradiated in 7 M nitric acid to 1-10 megaGray of gamma radiation from external Co-60, or to 5-14 megaGray of alpha particles from sorbed Pu-238. Each irradiated resin was measured for changes in dry weight, wet volume, weak-base and strong-base chloride exchange capacities, and exchange capacities for Pu(4) from nitric acid. Alpha-induced resin damage was significantly less than that caused by an equivalent dose of gamma radiation. The polyvinylpyridine

resin offers the greatest resistance to damage from gamma radiation and from alpha particles. DOE

N92-29804# Northwestern Univ., Evanston, IL.
STRUCTURAL BASIS FOR THE MECHANICAL PROPERTIES OF POLYETHYLENES Final Report, Sep. 1984 - Aug. 1990
S. H. Carr and B. Crist Feb. 1991 70 p
(Contract GRI-5084-260-1051)
(PB92-164425; GRI-91/0178) Avail: CASI HC A04/MF A01

The physical properties of polyethylenes used in gas distribution pipes and fittings are largely determined by the nature of the polymer molecules in the resin employed for pipe manufacture. The room temperature toughness of polyethylene in plane strain or brittle fracture conditions and the correlation between this toughness and molecular and/or morphological parameters are investigated. Nonlinear elastic fracture mechanics was applied to small compact tension specimens. J integral fracture toughness of high density polyethylene is 2 kJ/sq m, while that of gas pipe polyethylene is greater than 40 kJ/sq m. Enhanced toughness is based on the resistance of craze fibrils to fracture; coarser fibrils are formed in tough polyethylene. Plastic deformation before crack initiation is confined to planar yield zones. Studies with commercial materials and model blends show that a distribution of differently branched alpha-olefin copolymer chains in the resin gives the greatest toughness. Quantitative thermodynamic analysis of copolymer mixtures shows that these tough systems are not phase separated in the melt state. Author

N92-29831*# National Aeronautics and Space Administration. Marshall Space Flight Center, Huntsville, AL.
BLADDER OPERATED ROBOTIC JOINT Patent Application
Glen A. Robertson, inventor (to NASA) 13 Jul. 1992 11 p
(NASA-Case-MFS-28682-1; NAS 1.71:MFS-28682-1;
US-Patent-Appl-SN-912401) Avail: CASI HC A03/MF A01

This invention is a robotic joint which is operated by inflatable bladders and which can be used in applications where it is desired to move or hold an object. A support block supports an elongated plate to which is pivotally attached a finger. A tension strip passes over a lever attached to the finger and is attached at its ends to the support block on opposite sides of the plate. Bladders positioned between the plate and the tension strip on opposite sides of the plate can be inflated by pumps to pivot the finger, with one of the bladders being inflated while the other is being deflated. NASA

N92-29905# Institute for Defense Analyses, Alexandria, VA.
SURVEY OF RESEARCH INTO ELECTROMAGNETIC AND OTHER WAVE EFFECTS ON MECHANICAL BEHAVIOR AND PROCESSING OF MATERIALS Final Report, May 1989 - Nov. 1991
George Mayer and Benjamin Tao Jan. 1992 94 p
(Contract MDA903-89-C-0003)
(AD-A248614; AD-E501508; IDA-D-1115; IDA/HQ-92-40803)
Avail: CASI HC A05/MF A01

In an effort to assess trends in the general areas of energy effects on materials, a survey was conducted for the period 1960-1990 of the open literature sources with special focus on electromagnetic and other wave phenomena. This survey has not treated nuclear, laser, or photoplastic effects. The statistics and trends in activity have been examined in four main areas: electric fields and currents, ultrasonics, microwaves, and magnetic fields. These energies have been found to affect the structure and mechanical properties of materials, and the changes, some of them substantial, are a main subject of this survey. In addition, beneficial effects, ranging from minor to significant, have been measured during the processing of materials with these energies. It is expected that future understanding and exploitation of these effects will be essential to the widespread development and use of future DoD systems such as electromagnetic guns, toward achieving economics of manufacturing through microwave processing of ceramic armor components and thick-section structural composites, and in other applications. GRA

N92-29908# Sandia National Labs., Albuquerque, NM.
RAMAN FEATURES OF CVD DIAMOND FILMS
M. Alam (New Mexico Inst. of Mining and Technology, Socorro.), D. R. Tallant, and D. E. Peebles 1992 2 p Presented at the 3rd Annual Diamond Technology Workshop, Detroit, MI, 17-18 Mar. 1992
(Contract DE-AC04-76DP-00789)
(DE92-011381; SAND-91-2727C; CONF-9203124-1) Avail: CASI HC A01/MF A01

There is considerable interest in the use of chemically vapor deposited (CVD) polycrystalline diamond films in advanced materials technology. However, most of the potential applications of CVD diamond films require well-controlled properties which depend on the film structure, and in turn, on the conditions under which the films are synthesized. The structure of the vapor-deposited diamond films is frequently characterized by Raman spectroscopy. Despite extensive research, much work still needs to be completed to understand the various features of the Raman spectra and to understand how the processing variables affect the spectral features. This paper examines the Raman spectra of diamond films prepared by a hot-filament-assisted CVD process as a function of substrate processing and deposition parameters. DOE

N92-29953*# National Aeronautics and Space Administration. Langley Research Center, Hampton, VA.
POLYBENZIMIDAZOLES VIA AROMATIC NUCLEOPHILIC DISPLACEMENT Patent Application
John W. Connell, inventor (to NASA) and Paul M. Hergenrother, inventor (to NASA) 31 Oct. 1991 22 p
(NASA-Case-LAR-14643-1; NAS 1.71:LAR-14643-1;
US-Patent-Appl-SN-790730) Avail: CASI HC A03/MF A01

Polybenzimidazoles (PBIs) are heterocyclic macromolecules commonly prepared by the condensation reaction of an aromatic bis(o-diamine) with an aromatic diacid or derivative thereof. These polymers possess high thermal, thermooxidative, and chemical stability; good mechanical properties; and excellent flame resistances, making them high-performance/high-temperature materials which are attractive for use in harsh environments. However, despite these properties, the processing of these polymers is somewhat difficult. In the present invention, several di(hydroxyphenyl) benzimidazole monomers were prepared from the reaction of phenyl 4 hydroxybenzoate with aromatic bis(o-diamine)s. Soluble PBIs were then prepared by the nucleophilic displacement reaction of these di(hydroxyphenyl) benzimidazole monomers with activated aromatic dihalide or dinitro compounds in the presence of an alkali metal base. These polymers had glass transition temperatures (Tgs) of 264-352 C, much lower than their commercial counterparts which exhibited Tgs of 400 C. The lower Tg allows for better compression moldability than other PBIs. These polymers were soluble in cold dimethyl-acetamide (DMAc), as opposed to requiring hot DMAc and pressure to solubilize. The use of the benzimidazole monomers to make PBIs proved to be more economical and easier to process than commercial PBIs. The novelty of this invention lies in the polybenzimidazole polymers. These new compositions of matter exhibited lower TGs and increased solubility which allows for easier processing. NASA

N92-29960# Universiteit Twente, Enschede (Netherlands). Dept. of Computer Science.
AN ONTOLOGY OF CERAMICS
Paul E. vanderVet and Nicolaas Mars, J. I. 16 Dec. 1991 77 p
(Memo-INF-91-85; UT-KBS-91-21; ISSN-0924-3755;
ETN-92-91581) Copyright Avail: CASI HC A05/MF A01

An ontology for the domain of ceramics science is introduced. An ontology is a structured set of concepts in which knowledge about a certain domain is to be expressed. The ontology of ceramics is developed for the Plinius project to function in a system able to acquire knowledge semiautomatically from the title and abstract parts of machine readable document descriptions. A framework for the ontology is discussed. To make the ontology suitable for its intended function in the context of Plinius, details

have been included. The framework is designed following a compositional approach not found in the literature. The advantages of the compositional approach are twofold: conceptual parsimony is achieved, and hierarchies can be specified implicitly. The latter advantage implies that many tangled hierarchies can be handled. The framework is based on a conceptual analysis of the domain, which is extensively discussed. The conceptual foundations have resulted in a framework which is general in the sense that it can be seen how extensions to cover adjacent domains (e.g., metals science, or other chemical applications) are to be realized. Thus, aim of sharable knowledge bases is furthered. ESA

N92-30100*# National Aeronautics and Space Administration. Lyndon B. Johnson Space Center, Houston, TX.
A METHOD FOR MAKING BIOCOMPATIBLE POLYMER ARTICLES USING ATOMIC OXYGEN Patent Application
Steven Koontz, inventor (to NASA) and Glenn Spaulding, inventor (to NASA) 26 Mar. 1992 31 p
(NASA-Case-MSC-21529-1; NAS 1.71:MSC-21529-1; US-Patent-Appl-SN-857901) Avail: CASI HC A03/MF A01

A method for making a biocompatible polymer article using a uniform atomic oxygen treatment is disclosed. The substrate may be subsequently optionally grafted with a compatibilizing compound. Compatibilizing compounds may include proteins, phosphorylcholine groups, platelet adhesion preventing polymers, albumin adhesion promoters, and the like. The compatibilized substrate may also have a living cell layer adhered thereto. The atomic oxygen is preferably produced by a flowing afterglow microwave discharge, wherein the substrate resides in a sidearm out of the plasma. Also disclosed are a vascular prosthesis and other articles made by the biocompatibilizing method of the present invention as well as methods for using such biocompatibilized articles in a cell mass. In addition, various membranes made by the biocompatibilizing method of the present invention are disclosed. Furthermore, methods are disclosed for performing immunodiagnostic testing using the membranes. Also, methods for culturing cells for various purposes using the various membranes are disclosed as well. NASA

N92-30136# Case Western Reserve Univ., Cleveland, OH. Dept. of Macromolecular Science.
MOLECULAR ENGINEERING OF LIQUID CRYSTALLINE POLYMERS
Virgil Percec and Dimitris Tomazos 27 Mar. 1992 218 p
(Contract N00014-90-J-1828)
(AD-A248996; TR-64) Avail: CASI HC A10/MF A03

This chapter reviews the molecular engineering of main chain and side chain liquid crystalline polymers. Several factors influencing the phase transitions of liquid crystalline polymers are critically discussed. These include thermodynamics of phase transitions, isomorphism of liquid crystals, rigidity of rod-like mesogens, and chemical heterogeneity of main chain liquid crystalline copolymers. The use of polyetherification, copolyetherification, living cationic polymerization, and copolymerization in the manipulation of phase transitions of liquid crystalline polymers is extensively discussed. This review also discusses several novel architectures such as liquid crystalline dendrimers and cyclic oligomers, liquid crystalline polymers containing crown ethers and polypodants, electron donor-acceptor complexes of discotic liquid crystalline polymers, as well as, self-assemblying supramolecular liquid crystalline polymers. GRA

28 PROPELLANTS AND FUELS

Includes rocket propellants, igniters, and oxidizers; their storage and handling procedures; and aircraft fuels.

For related information see also *07 Aircraft Propulsion and Power, 20 Spacecraft Propulsion and Power,* and *44 Energy Production and Conversion.*

N92-29330# Georgia Inst. of Tech., Atlanta. School of Aerospace Engineering.
PROGRESS ON COMBUSTION MECHANISMS OF SOLID PROPELLANTS Report, Oct. 1991 - Mar. 1992
E. W. Price and R. K. Sigman 20 Mar. 1992 8 p
(Contract N00014-89-J-1923)
(AD-A248146) Avail: CASI HC A02/MF A01

A brief summary of ongoing research is presented, including sandwich burning studies with new ingredients, and computational modeling of combustion. GRA

N92-29512# Los Alamos National Lab., NM.
STRATEGIES FOR UNDERSTANDING THE DEFLAGRATION-TO-DETONATION TRANSITION
B. W. Asay 1992 18 p Presented at the Fundamental Physics and Chemistry of Combustion, Initiation, and Detonation of Energetic Materials, Los Alamos, NM, 3-6 Mar. 1992
(Contract W-7405-eng-36)
(DE92-013528; LA-UR-92-1343; CONF-9203147-1-Vugraphs)
Avail: CASI HC A03/MF A01

The deflagration-to-detonation (DDT) phenomenon has been studied for many years. However, no comprehensive model of the DDT process is available. It is important to understand the mechanism by which an explosive will detonate when the source of ignition is a weak shock or flame, and is able to predict this response. We have identified several key areas of the DDT problem which need to be understood before any such prediction can be made, and have established a modest program to obtain a more fundamental understanding of the behavior of explosive under the conditions that can lead to DDT. DOE

N92-29669*# National Aeronautics and Space Administration. Lewis Research Center, Cleveland, OH.
PRESSURIZATION OF CRYOGENS: A REVIEW OF CURRENT TECHNOLOGY AND ITS APPLICABILITY TO LOW-GRAVITY CONDITIONS
N. T. VanDresar Jul. 1992 10 p Presented at the 28th Joint Propulsion Conference and Exhibit, Nashville, TN, 6-8 Jul. 1992; sponsored in part by AIAA, SAE, ASME, and ASEE
(RTOP 506-42-73)
(NASA-TM-105746; E-7150; AIAA Paper 92-3061; NAS 1.15:105746) Avail: CASI HC A02/MF A01

A review of technology, history, and current status for pressurized expulsion of cryogenic tankage is presented. Use of tank pressurization to expel cryogenic fluids will continue to be studied for future spacecraft applications over a range of operating conditions in the low-gravity environment. The review examines experimental test results and analytical model development for quiescent and agitated conditions in normal-gravity, followed by a discussion of pressurization and expulsion in low-gravity. Validated, 1-D, finite difference codes exist for the prediction of pressurant mass requirements within the range of quiescent normal-gravity test data. To date, the effects of liquid sloshing have been characterized by tests in normal-gravity, but analytical models capable of predicting pressurant gas requirements remain unavailable. Efforts to develop multidimensional modeling capabilities in both normal and low-gravity have recently occurred. Low-gravity cryogenic fluid transfer experiments are needed to obtain low-gravity pressurized expulsion data. This data is required to guide analytical model development and to verify code performance. Author

N92-29786# Naval Surface Warfare Center, Crane, IN.
MICROCALORIMETRIC STUDY OF THE AGING REACTIONS OF ATOMIZED MAGNESIUM POWDER Interim Report, Oct. 1990 - Sep. 1991

Robert G. Shortridge, Aton Chin, and Bill R. Hubble 20 Feb. 1992 21 p
(AD-A247932; NSWCCR/RDTR-92/0003) Avail: CASI HC A03/MF A01

Magnesium powder is used widely as a fuel in pyrotechnic compositions, e.g., in illuminating flare formulations. Powdered magnesium chemically is a very reactive metal and it is prone to undergo relatively slow surface reactions at room temperature with moist air. In this study, the technique of microcalorimetry has been used to characterize these undesired magnesium degradation reactions. Experiments have been carried out using large magnesium samples to simulate a storage environment and small magnesium samples to simulate the magnesium powder in a pyrotechnic production line environment. Powdered magnesium can react with both water vapor and oxygen found in air with the reaction with water vapor being at least an order of magnitude more rapid. The degradation reactions are relatively slow, e.g., at 70 C and 100 percent relative humidity 1 percent magnesium degradation requires approximately 15 hours reaction time. However, a 1 percent degradation of the powdered magnesium translates into as much as 8 percent decrease in the burn rate of a pyrotechnic composition which incorporates the degraded magnesium. GRA

29 MATERIALS PROCESSING

Includes space-based development of products and processes for commercial applications.

For biological materials see *55 Space Biology*.

N92-29428# Vanderbilt Univ., Nashville, TN. Center for Atomic and Molecular Physics at Surfaces.
SURFACE REACTIONS IN THE SPACE ENVIRONMENT Final Report, 1 Nov. 1989 - 30 Apr. 1991
Royal G. Albridge, Carl S. Ewing, Richard F. Haglund, Jr., Joel B. Tellinghuisen, and Norman H. Tolk May 1992 12 p
(Grant AF-AFOSR-0030-90)
(AD-A250624; AFOSR-92-0424TR) Avail: CASI HC A03/MF A01

The object of this research program is to carry out experimental and theoretical studies of the detailed microscopic mechanisms by which electronic energy is absorbed, transported and dissipated in ionic solids. The ultimate aim of this program is to identify and characterize essential constituent elements of comprehensive models which will quantitatively describe radiation-induced electronic phenomena. The theoretical and experimental aspects of the project have been carried out concurrently and interactively in order to realize the greatest scientific benefit from the collaboration. Throughout this project we have employed (1) experimental techniques already developed to monitor bulk and surface properties before, during, and after electron and photon irradiation and to characterize time and energy-dependent desorption phenomena, and (2) ab initio quantum-theoretical approaches to develop and refine computational models for determining properties of excited electronic states of relevant localized species. This research program bears directly on a broad spectrum of questions germane to the long-term operation of platforms in space, including structural, optical and electronic degradation of materials in the ambient near-earth environment, survivability under and hardening against irradiation from directed-energy weapons, vulnerability in disturbed nuclear atmospheres, and discrimination and sensing techniques based on radiation (glow) signatures. GRA

N92-29470# Oesterreichisches Forschungszentrum Seibersdorf G.m.b.H., Vienna. Hauptabt. Angewandte Physik.
LOGION: THE OPERATION OF LIQUID METAL ION EMITTERS UNDER WEIGHTLESSNESS [LOGION: DER BETRIEB VON FLUESSIGMETALL-IONENEMITTERN UNTER SCHWERELOSIGKEIT]
Friedrich G. Ruedenauer, Willibald Riedler (Graz Univ., Austria), Hans-Michael Fehringer (Graz Univ., Austria), E. Goeschl (Graz Univ., Austria), C. Kropiunig (Graz Univ., Austria), W. Steiger, and K. Torkar (Graz Univ., Austria) Jan. 1992 23 p In GERMAN Sponsored by Bundesministerium fuer Wissenschaft und Forschung
(OEFZS-4616; ETN-92-91506) Copyright Avail: CASI HC A03/MF A01

The Logion experiment consists of a hermetic vacuum system containing a module with two operative integrated single indium ion emitters, and an internal ion collector. The first data files obtained via telemetry from the Mir Space Station, show no significant differences in operating parameters, with respect to ground operation. The results of the experiment are to be used to design an optimal automated control system for similar emitters which will be flown in the Cluster mission for active spacecraft potential control. ESA

N92-30083*# National Aeronautics and Space Administration. Pasadena Office, CA.
SAMPLE POSITIONING IN MICROGRAVITY Patent Application
Govind Sridharan, inventor (to NASA) (Jet Propulsion Lab., California Inst. of Tech., Pasadena.) 1 Nov. 1991 16 p
(Contract NAS7-918)
(NASA-Case-NPO-18448-1-CU; NAS 1.71:NPO-18448-1-CU; US-Patent-Appl-SN-786612) Avail: CASI HC A03/MF A01

Repulsion forces arising from laser beams are provided to produce mild positioning forces on a sample in microgravity vacuum environments. The system of the preferred embodiment positions samples using a plurality of pulsed lasers providing opposing repulsion forces. The lasers are positioned around the periphery of a confinement area and expanded to create a confinement zone. The grouped laser configuration, in coordination with position sensing devices, creates a feedback servo whereby stable position control of a sample within microgravity environment can be achieved. NASA

31 ENGINEERING (GENERAL)

Includes vacuum technology; control engineering; display engineering; cryogenics; and fire prevention.

N92-29335# Corps of Engineers, Huntsville, AL.
GUIDE FOR EVALUATING 12 INCH SUBSTANTIAL DIVIDING WALLS (SDWS) TO PROVIDE PROTECTION FROM REMOTE OPERATION, VOLUME 2 Final Report
Adib R. Farsoun Sep. 1991 67 p
(AD-A250252) Avail: CASI HC A04/MF A01

This report provides installations with procedures to relate Net Explosive Weights (NEWs) to combinations of intervening 12-inch Substantial Dividing Walls (SDWs) to provide protection to personnel from remote operations where an accidental detonation is the hazard. Protection to be Provided is IAW DoD and Army policy: 2.3 psi maximum overpressure exposure and no hazardous fragments. The report consists of two Volumes. Volume 1 is a 'how to' guide for installation use; Volume 2 is the rationale (calculations, etc) behind the Volume 1. Protection from thermal effects from flash fires, deflagrations, etc. is not addressed. GRA

N92-29545# Corps of Engineers, Huntsville, AL.
GUIDE FOR EVALUATING 12 INCH SUBSTANTIAL DIVIDING WALLS (SDWS) TO PROVIDE PROTECTION FROM REMOTE OPERATION, VOLUME 1 Final Report
Adib R. Farsoun Sep. 1991 103 p
(AD-A250251) Avail: CASI HC A06/MF A02

This report provides installations with procedures to relate Net Explosive Weights (NEWs) to combinations of intervening 12-inch Substantial Dividing Walls (SDWs) to provide protection to personnel from remote operations where an accidental detonation is the hazard. Protection to be provided is IAW DoD and Army policy: 2.3 psi maximum overpressure exposure and no hazardous fragments. The report consists of two volumes. Volume 1 is a

'how to' guide for installation use; Volume 2 is the rationale (calculations, etc.) behind Volume 1. Protection from thermal effects from flash fires, deflagrations, etc. is not addressed. GRA

N92-29677*# National Aeronautics and Space Administration. Marshall Space Flight Center, Huntsville, AL.
DEFINITION AND DESIGN OF AN EXPERIMENT TO TEST RASTER SCANNING WITH ROTATING UNBALANCED-MASS DEVICES ON GIMBALED PAYLOADS
W. D. Lightsey, D. C. Alhorn, and M. E. Polites Jun. 1992 19 p
(NASA-TP-3249; M-691; NAS 1.60:3249) Avail: CASI HC A03/MF A01

An experiment designed to test the feasibility of using rotating unbalanced-mass (RUM) devices for line and raster scanning gimbaled payloads, while expending very little power is described. The experiment is configured for ground-based testing, but the scan concept is applicable to ground-based, balloon-borne, and space-based payloads, as well as free-flying spacecraft. The servos used in scanning are defined; the electronic hardware is specified; and a computer simulation model of the system is described. Simulation results are presented that predict system performance and verify the servo designs. Author

32 COMMUNICATIONS AND RADAR

Includes radar; land and global communications; communications theory; and optical communications.

For related information see also *04 Aircraft Communications and Navigation* and *17 Space Communications, Spacecraft Communications, Command and Tracking.* For search and rescue see *03 Air Transportation and Safety,* and *16 Space Transportation.*

N92-29333# Naval Ocean Systems Center, San Diego, CA. Research, Development, Test, and Evaluation Div.
ADAPTIVE SIGNAL PROCESSING AT NOSC
T. R. Albert Mar. 1992 4 p
(AD-A250245) Avail: CASI HC A01/MF A01

Adaptive signal processing work at the Naval Ocean Systems Center (NOSC) dates back to the late 1960s. It began as an IR/IED project by John McCool, who made use of an adaptive algorithm that had been developed by Professor Bernard Widrow of Stanford University. In 1972, a team lead by McCool built the first hardware implementation of the algorithm that could process in real-time at acoustic bandwidths. Early tests with the two units that were built were extremely successful, and attracted much attention. Sponsors from different commands provided funding to develop hardware for submarine, surface ship, airborne, and other systems. In addition, an effort was initiated to analyze performance and behavior of the algorithm. Most of the hardware development and analysis efforts were active through the 1970s, and a few into the 1980s. One of the original programs continues to this date. GRA

N92-29344# Naval Postgraduate School, Monterey, CA.
IMPROVING THE LAMP Mk 3 SH-60B HF COMMUNICATION SYSTEM M.S. Thesis
Frederick C. Adams, Jr. Sep. 1991 64 p
(AD-A245970) Avail: CASI HC A04/MF A01

This thesis examines the over-the-horizon (OTH) communications capability of the SH-60B Seahawk. The LAMPS Mk III communications system incorporated a high frequency (HF) radio in its design to provide reliable two-way voice communications at extended ranges for use during operations that require the helicopter to be below the ship's radio horizons. In addition, the HF radio system is necessary to provide communications with non-LAMPS equipped naval forces and commercial shipping and to provide long-range, sea-air rescue capabilities. Topics addressed with respect to the OTH communications capability of the SH-60B Seahawk are the basis of HF propagation theory, a chronology of events concerning the SH-60B's current HF communication system and an analysis of issues. Author (GRA)

N92-29364*# Jet Propulsion Lab., California Inst. of Tech., Pasadena.
THE TELECOMMUNICATIONS AND DATA ACQUISITION REPORT Progress Report, Jan. - Mar. 1992
Edward C. Posner, ed. 15 May 1992 403 p
(NASA-CR-190460; JPL-TDA-PR-42-109; NAS 1.26:190460)
Avail: CASI HC A18/MF A04

This quarterly publication provides archival reports on developments in programs managed by JPL's Office Telecommunications and Data Acquisition (TDA). In space communications, radio navigation, radio science, and ground-based radio and radar astronomy, it reports on activities of the Deep Space Network (DSN) in planning, in supporting research and technology, in implementation, and in operations. Also included is standards activity at JPL for space data and information systems and reimbursable DSN work performed for other space agencies through NASA. The preceding work is all performed for NASA's Office of Space Operations (OSO). The TDA Office also performs work funded by two other NASA program offices through and with the cooperation of the OSO. These are the Orbital Debris Radar Program and 21st Century Communication Studies. For individual titles, see N92-29365 through N92-29389.

N92-29365*# Jet Propulsion Lab., California Inst. of Tech., Pasadena.
A DETERMINATION OF THE RADIO-PLANETARY FRAME TIE FROM COMPARISON OF EARTH ORIENTATION PARAMETERS **c17**
M. H. Finger and W. M. Folkner *In its* The Telecommunications and Data Acquisition Report 15 May 1992 p 1-21 (For primary document see N92-29364 20-32)
(RTOP 310-10-60-50-00)
Avail: CASI HC A03/MF A04

The orientation of the reference frame of radio source catalogs relative to that of planetary ephemerides, or 'frame tie,' can be a major systematic error source for interplanetary spacecraft orbit determination. This work presents a method of determining the radio-planetary frame tie from a comparison of very long baseline interferometry (VLBI) and lunar laser ranging (LLR) station coordinate and earth orientation parameter estimates. A frame tie result is presented with an accuracy of 25 nrad. Author

N92-29366*# Jet Propulsion Lab., California Inst. of Tech., Pasadena.
OCCULTATION OF A COMPACT RADIO SOURCE BY VENUS **c93**
R. Linfield *In its* The Telecommunications and Data Acquisition Report 15 May 1992 p 22-39 (For primary document see N92-29364 20-32)
(RTOP 310-10-60-60-00)
Avail: CASI HC A03/MF A04

An occultation of the compact radio source P 0507+17 by Venus on 19 Jul. 1988, was observed in Tidbinbilla, Australia at a frequency of 2.3 GHz. The purpose of this observation was to measure the position of Venus in the radio reference frame. When data from both ingress (Venus dayside) and egress (Venus nightside) were used to solve for the position of Venus in ecliptic longitude and latitude, the results were consistent with zero offsets from the nominal values, with an uncertainty of approximately 0.2 arcsec in both coordinates. By using the nightside data alone, a value of -0.026 +/- 0.04 arcsec was obtained for the linear combination delta(lambda) + 0.51delta(beta), where delta(lambda) and delta(beta) were the offsets from their nominal values of the ecliptic longitude and latitude of Venus. Distortion of a vacuum Fresnel fringe pattern by the Venus troposphere, and especially by the Venus ionosphere, was observed. The dayside ionosphere of Venus caused very large distortions; the amplitude of the first Fresnel fringe in the ingress data was eight times larger than was expected for an airless planet. The observed fringe patterns were modeled by using plausible ionospheres (i.e., consistent with

spacecraft measurements of the Venus ionosphere and with solar extreme ultraviolet flux and solar wind pressure measurements at the occultation epoch). However, the range of Venus ionospheric profiles (electron density as a function of altitude) allowed by a priori constraints and by the occultation data was large (e.g., the ionopause height on the dayside was uncertain by a factor of two). This ionospheric uncertainty (particularly on the dayside) translated into a large position uncertainty (0.2 arcsec for the dayside and 0.04 arcsec for the nightside). If it was possible to calibrate the Venus ionosphere by some external means, the accuracy in delta(lambda) and delta(beta) would have been 0.01 arcsec or better. Author

N92-29367*# Jet Propulsion Lab., California Inst. of Tech., Pasadena.

A NANORADIAN DIFFERENTIAL VLBI TRACKING DEMONSTRATION **c93**

R. N. Treuhaft and S. T. Lowe *In its* The Telecommunications and Data Acquisition Report 15 May 1992 p 40-55 (For primary document see N92-29364 20-32)
(RTOP 310-10-60-86-02)
Avail: CASI HC A03/MF A04

The shift due to Jovian gravitational deflection in the apparent angular position of the radio source P 0201+113 was measured with very long baseline interferometry (VLBI) to demonstrate a differential angular tracking technique with nanoradian accuracy. The raypath of the radio source P 0201+113 passed within 1 mrad of Jupiter (approximately 10 Jovian radii) on 21 Mar. 1988. Its angular position was measured 10 times over 4 hours on that date, with a similar measurement set on 2 Apr. 1988, to track the differential angular gravitational deflection of the raypath. According to general relativity, the expected gravitational bend of the raypath averaged over the duration of the March experiment was approximately 1.45 nrad projected onto the two California-Australia baselines over which it was measured. Measurement accuracies on the order of 0.78 nrad were obtained for each of the ten differential measurements. The chi(exp 2) per degree of freedom of the data for the hypothesis of general relativity was 0.6, which suggests that the modeled dominant errors due to system noise and tropospheric fluctuations fully accounted for the scatter in the measured angular deflections. The chi(exp 2) per degree of freedom for the hypothesis of no gravitational deflection by Jupiter was 4.1, which rejects the no-deflection hypothesis with greater than 99.999 percent confidence. The system noise contributed about 0.34 nrad per combined-baseline differential measurement and tropospheric fluctuations contributed about 0.70 nrad. Unmodeled errors were assessed, which could potentially increase the 0.78 nrad error by about 8 percent. The above chi(exp 2) values, which result from the full accounting of errors, suggest that the nanoradian gravitational deflection signature was successfully tracked.
Author

N92-29368*# Jet Propulsion Lab., California Inst. of Tech., Pasadena.

DEEP-SPACE NAVIGATION WITH DIFFERENCED DATA TYPES. PART 3: AN EXPANDED INFORMATION CONTENT AND SENSITIVITY ANALYSIS **c17**

J. A. Estefan and S. W. Thurman *In its* The Telecommunications and Data Acquisition Report 15 May 1992 p 56-73 (For primary document see N92-29364 20-32)
(RTOP 310-10-63-50-00)
Avail: CASI HC A03/MF A04

An approximate six-parameter analytic model for Earth-based differential range measurements is presented and is used to derive a representative analytic approximation for differenced Doppler measurements. The analytical models are tasked to investigate the ability of these data types to estimate spacecraft geocentric angular motion, Deep Space Network station oscillator (clock/frequency) offsets, and signal-path calibration errors over a period of a few days, in the presence of systematic station location and transmission media calibration errors. Quantitative results indicate that a few differenced Doppler plus ranging passes yield angular position estimates with a precision on the order of 0.1 to 0.4 micro-rad, and angular rate precision on the order of 10 to 25 x 10(exp -12) rad/sec, assuming no a priori information on the coordinate parameters. Sensitivity analyses suggest that troposphere zenith delay calibration error is the dominant systematic error source in most of the tracking scenarios investigated; as expected, the differenced Doppler data were found to be much more sensitive to troposphere calibration errors than differenced range. By comparison, results computed using wideband and narrowband (delta) VLBI under similar circumstances yielded angular precisions of 0.07 to 0.4 micro-rad, and angular rate precisions of 0.5 to 1.0 x 10(exp -12) rad/sec. Author

N92-29369*# Jet Propulsion Lab., California Inst. of Tech., Pasadena.

ORBITER-ORBITER AND ORBITER-LANDER TRACKING USING SAME-BEAM INTERFEROMETRY **c17**

W. M. Folkner and J. S. Border *In its* The Telecommunications and Data Acquisition Report 15 May 1992 p 74-86 (For primary document see N92-29364 20-32)
(RTOP 310-10-63-88-01)
Avail: CASI HC A03/MF A04

Two spacecraft orbiting Mars will subtend a small angle as viewed from Earth. This angle will usually be smaller than the beam width of a single radio antenna. Thus the two spacecraft may be tracked simultaneously by a single Earth-based antenna. The same-beam interferometry (SBI) technique involves using two widely separated antennas, each observing the two spacecraft, to produce a measurement of the angular separation of the two spacecraft in the plane of the sky. The information content of SBI data is thus complementary to the line-of-sight information provided by conventional Doppler data. The inclusion of SBI data with the Doppler data in a joint orbit estimation procedure can desensitize the solution to gravity mismodeling and result in improved orbit determination accuracy. This article presents an overview of the SBI technique, a measurement error analysis, and an error covariance analysis of some examples of the application of SBI to orbit determination. For hypothetical scenarios involving the Mars Observer and the Russian Mars '94 spacecraft, orbit determination accuracy improvements of up to an order of magnitude are predicted, relative to the accuracy that can be obtained by using only Doppler data acquired separately from each spacecraft. Relative tracking between a Mars orbiter and a lander fixed on the surface of Mars is also studied. Results indicate that the lander location may be determined to a few meters, while the orbiter ephemeris may be determined with accuracy similar to the orbiter-orbiter case. Author

N92-29370*# Jet Propulsion Lab., California Inst. of Tech., Pasadena.

GEOMETRIC DISTORTION ANALYSIS OF A WIDE-FIELD ASTROGRAPH **c17**

W. M. Owen, Jr. and S. B. Shaklan *In its* The Telecommunications and Data Acquisition Report 15 May 1992 p 87-93 (For primary document see N92-29364 20-32)
(RTOP 310-10-63-92-01)
Avail: CASI HC A02/MF A04

Ground-based optical navigation seeks to determine the angular position of a star, Solar System body, or laser-emitting spacecraft relative to objects with well-known coordinates. Measurement accuracies of 25 nrad would make optical techniques competitive with current radio metric technology. This article examines a proposed design for a wide-field astrograph and concludes that the deviation of an image centroid from the ideal projection can be modeled to the desired accuracy provided that the field of view does not exceed 5 deg on a side. Author

N92-29371*# Jet Propulsion Lab., California Inst. of Tech., Pasadena.

APPLICATIONS OF INERTIAL-SENSOR HIGH-INHERITANCE INSTRUMENTS TO DSN PRECISION ANTENNA POINTING **c35**

R. E. Goddard *In its* The Telecommunications and Data Acquisition Report 15 May 1992 p 94-104 (For primary

document see N92-29364 20-32)
(RTOP 310-20-65-67-00)
Avail: CASI HC A03/MF A04

Laboratory test results of the initialization and tracking performance of an existing inertial-sensor-based instrument are given. The instrument, although not primarily designed for precision antenna pointing applications, demonstrated an on-average 10-hour tracking error of several millidegrees. The system-level instrument performance is shown by analysis to be sensor limited. Simulated instrument improvements show a tracking error of less than 1 mdeg, which would provide acceptable performance, i.e., low pointing loss, for the Deep Space Network 70-m antenna subnetwork, operating at Ka-band (1-cm wavelength). Author

N92-29372*# Jet Propulsion Lab., California Inst. of Tech., Pasadena.
PERFORMANCE OF A 12-GHz FIBER-OPTIC SYSTEM FOR BEAM-WAVEGUIDE ANTENNA STABILITY TESTING c74
T. Y. Otoshi, M. M. Franco, and G. F. Lutes *In its* The Telecommunications and Data Acquisition Report 15 May 1992 p 105-113 (For primary document see N92-29364 20-32)
(RTOP 310-20-65-92-01)
Avail: CASI HC A02/MF A04

A 12-GHz fiber-optic system is a critical part of a test configuration that was proposed for measuring the fractional frequency stability of the Deep Space Station (DSS)-13 beam-waveguide (BWG) antenna. This fiber-optic system is used to carry Ku-band (12-GHz) signals from a reference antenna to the DSS-13 BWG pedestal room. Tests performed only on the fiber-optic system portion of the overall test configuration showed that the 12-GHz fiber-optic system (installed at DSS-13) has a frequency stability of about 1.1 x 10(exp -16) for sampling time tau = 1000 sec for a nighttime run. This preliminary result establishes the lowest noise floor that can probably be achieved for the test configuration that will be used to measure the frequency stability of the DSS-13 BWG antenna. Author

N92-29373*# Jet Propulsion Lab., California Inst. of Tech., Pasadena.
IMPROVEMENTS IN X-BAND TRANSMITTER PHASE STABILITY THROUGH KLYSTRON BODY TEMPERATURE REGULATION c33
R. M. Perez *In its* The Telecommunications and Data Acquisition Report 15 May 1992 p 114-120 (For primary document see N92-29364 20-32)
(RTOP 310-20-64-22-00)
Avail: CASI HC A02/MF A04

This article describes the techniques used and experimental results obtained in improving transmitter stability by control of the klystron body temperature. Related work in the measurement of klystron phase control parameters (pushing factors) is also discussed. The contribution of waveguide temperature excursions to uplink phase stability is presented. Suggestions are made as to the direction of future work in this area. Author

N92-29374*# Jet Propulsion Lab., California Inst. of Tech., Pasadena.
NOISE-OPTIMAL CONTROL OF HEMT LNA'S FOR COMPENSATION OF TEMPERATURE DEVIATIONS c33
C. MacCarley, J. J. Bautista, and P. A. Willis *In its* The Telecommunications and Data Acquisition Report 15 May 1992 p 121-129 (For primary document see N92-29364 20-32)
(RTOP 310-20-66-09-01)
Avail: CASI HC A02/MF A04

Noise-optimal control of high-electron mobility transistor low noise amplifier (HEMT LNA) bias voltage and current values was achieved at room temperature. The performance metric maximized was the amplifier gain divided by the amplifier input noise temperature, G/T(sub e). Additionally, the feasibility of automating the initial determination of bias settings was demonstrated in the laboratory. Simulation models of an HEMT were developed from available measurement data, installed on a Sun SPARC 1 workstation, and used in investigating several optimization algorithms. Simple tracking-type algorithms, which follow changes in optimum settings if started at or near the global optimum point, produced the best performance. Implementation of the optimization algorithms was performed using a three-stage Field Effect Transistor (FET) LNA and an existing test apparatus. Software was written to control the bias settings of the first stage of the LNA and to perform noise and gain measurements by using the test apparatus. The optimization control was then integrated with existing test software to create a master test and optimization program for test apparatus use. Author

N92-29375*# Jet Propulsion Lab., California Inst. of Tech., Pasadena.
GOLAY AND OTHER BOX CODES c61
G. Solomon *In its* The Telecommunications and Data Acquisition Report 15 May 1992 p 130-135 (For primary document see N92-29364 20-32)
(RTOP 310-30-71-83-02)
Avail: CASI HC A02/MF A04

The (24,12;8) extended Golay Code can be generated as a 6 x 4 binary matrix from the (15,11;3) BCH-Hamming Code, represented as a 5 x 3 matrix, by adding a row and a column, both of odd or even parity. The odd-parity case provides the additional 12th dimension. Furthermore, any three columns and five rows of the 6 x 4 Golay form a BCH-Hamming (15,11;3) Code. Similarly a (80,58;8) code can be generated as a 10 x 8 binary matrix from the (63,57;3) BCH-Hamming Code represented as a 9 x 7 matrix by adding a row and a column both of odd and even parity. Furthermore, any seven columns along with the top nine rows is a BCH-Hamming (53,57;3) Code. A (80,40;16) 10 x 8 matrix binary code with weight structure identical to the extended (80,40;16) Quadratic Residue Code is generated from a (63,39;7) binary cyclic code represented as a 9 x 7 matrix, by adding a row and a column, both of odd or even parity. Author

N92-29376*# Jet Propulsion Lab., California Inst. of Tech., Pasadena.
FIGURE OF MERIT FOR DIRECT-DETECTION OPTICAL CHANNELS c74
C.-C. Chen *In its* The Telecommunications and Data Acquisition Report 15 May 1992 p 136-151 (For primary document see N92-29364 20-32)
(RTOP 310-20-67-59-00)
Avail: CASI HC A03/MF A04

The capacity and sensitivity of a direct-detection optical channel are calculated and compared to those of a white Gaussian noise channel. Unlike Gaussian channels in which the receiver performance can be characterized using the noise temperature, the performance of the direct-detection channel depends on both signal and background noise, as well as the ratio of peak to average signal power. Because of the signal-power dependence of the optical channel, actual performance of the channel can be evaluated only by considering both transmit and receive ends of the systems. Given the background noise power and the modulation bandwidth, however, the theoretically optimum receiver sensitivity can be calculated. This optimum receiver sensitivity can be used to define the equivalent receiver noise temperature and calculate the corresponding G/T product. It should be pointed out, however, that the receiver sensitivity is a function of signal power, and care must be taken to avoid deriving erroneous projections of the direct-detection channel performance. Author

N92-29377*# Jet Propulsion Lab., California Inst. of Tech., Pasadena.
OPTIMIZING THE G/T RATIO OF THE DSS-13 34-METER BEAM-WAVEGUIDE ANTENNA
M. S. Esquivel *In its* The Telecommunications and Data Acquisition Report 15 May 1992 p 152-161 (For primary document see N92-29364 20-32)
(RTOP 310-30-69-91-02)
Avail: CASI HC A02/MF A04

Calculations using Physical Optics computer software were done to optimize the gain-to-noise-temperature (G/T) ratio of Deep Space

Station (DSS)-13, the Deep Space Network's (DSN's) 34-m beam-waveguide antenna, at X-band for operation with the ultra-low-noise amplifier maser system. A better G/T value was obtained by using a 24.2-dB far-field-gain smooth-wall dual-mode horn than by using the standard X-band 22.5-dB-gain corrugated horn. Author

N92-29378*# Jet Propulsion Lab., California Inst. of Tech., Pasadena.

DYNAMIC MODELING OF FLUID TRANSMISSION LINES OF THE DSN 70-METER ANTENNAS BY USING A LUMPED PARAMETER MODEL **c37**

R. D. Bartos *In its* The Telecommunications and Data Acquisition Report 15 May 1992 p 162-169 (For primary document see N92-29364 20-32)
(RTOP 310-30-42-10-87)
Avail: CASI HC A02/MF A04

Fluid transmission lines and fittings were found to significantly affect the dynamic and steady state operation of the engineering system in which they are incorporated. Therefore, a better understanding of the operation of a system can be obtained by including the performance of the transmission lines and fittings within the system model. The most accurate model of a transmission line or fitting is obtained by using a distributed parameter model. However, a distributed parameter model tends to be very complex. This complexity can be avoided without significant loss of model accuracy by using a lumped parameter model when the length of the fluid path through the transmission line or fitting is short. This article develops a lumped parameter model for short fluid transmission lines and fittings, describes the conditions under which the model is valid, and presents the model parameters associated with the servo hydraulic system of the Deep Space Network (DSN) 70-meter antennas. Author

N92-29379*# Jet Propulsion Lab., California Inst. of Tech., Pasadena.

BANDWIDTH COMPRESSION OF NOISY SIGNALS WITH SQUARE-WAVE SUBCARRIER

Y. Feria and J. Statman *In its* The Telecommunications and Data Acquisition Report 15 May 1992 p 170-178 (For primary document see N92-29364 20-32)
(RTOP 310-30-71-92-02)
Avail: CASI HC A02/MF A04

This article discusses a method for downconverting the square-wave subcarrier of spacecraft signals, such as the one from Galileo, which results in a compression bandwidth that lowers the sample rate significantly. The study is focused on three issues. The first is the selection of an adequate down-mixing signal for the resulting signal to have a format similar to that of the original signal, except at a lower subcarrier frequency. The second is the control of the noise level so that the signal to noise ratio is not degraded due to the downconversion. The third is to determine the bandwidth of the downconverted signal considering the uncertainty of the residual carrier frequency. Author

N92-29380*# Jet Propulsion Lab., California Inst. of Tech., Pasadena.

AN OSI ARCHITECTURE FOR THE DEEP SPACE NETWORK

W. R. Heuser *In its* The Telecommunications and Data Acquisition Report 15 May 1992 p 179-208 (For primary document see N92-29364 20-32)
(RTOP 310-40-73-89-01)
Avail: CASI HC A03/MF A04

This article presents an Open Systems Interconnection (OSI) architecture developed for the Deep Space Network. An historical review is provided to establish the context for current United States Government policy on interprocessor communication standards. An introduction to the OSI architecture, its seven-layer approach, and an overview of application service entities are furnished as a tutorial. Finally, the results of a prototype system developed for monitor and control of a Deep Space Station are also presented. Author

N92-29381*# Jet Propulsion Lab., California Inst. of Tech., Pasadena.

DSS-13 26-METER ANTENNA UPGRADED RADIOMETER SYSTEM

C. T. Stelzried, L. Skjerve, and G. Bury *In its* The Telecommunications and Data Acquisition Report 15 May 1992 p 209-220 (For primary document see N92-29364 20-32)
(RTOP 314-40-31-30-06)
Avail: CASI HC A03/MF A04

The Deep Space Station (DSS)-13 26-m antenna radiometer system was upgraded with an IBM-compatible computer-controlled configuration with improved supporting hardware and software. Software was generated to analyze results and correct for antenna mispointing, tropospheric loss, and other observing errors. This total power radiometer configuration provides a prototype for the new DSS-13 34-m antenna. The radiometer system is described in terms of the theory, instrumentation hardware, computer configuration, and operational features and performance. The system is used to obtain antenna efficiency and pointing model data and is useful for radio source calibrations required for radio astronomy. Some recent results are given. Author

N92-29382*# Jet Propulsion Lab., California Inst. of Tech., Pasadena.

SEQUENTIAL DESIGN OF A LINEAR QUADRATIC CONTROLLER FOR THE DEEP SPACE NETWORK ANTENNAS

W. Gawronski *In its* The Telecommunications and Data Acquisition Report 15 May 1992 p 221-252 (For primary document see N92-29364 20-32)
(RTOP 314-40-41-10-15)
Avail: CASI HC A03/MF A04

A new linear quadratic controller design procedure is proposed for the NASA/JPL Deep Space Network antennas. The antenna model is divided into a tracking subsystem and a flexible subsystem. Controllers for the flexible and tracking parts are designed separately by adjusting the performance index weights. Ad hoc weights are chosen for the tracking part of the controller and the weights of the flexible part are adjusted. Next, the gains of the tracking part are determined, followed by the flexible controller final tune-up. In addition, the controller for the flexible part is designed separately for each mode; thus the design procedure consists of weight adjustment for small-size subsystems. Since the controller gains are obtained by adjusting the performance index weights, determination of the weight effect on system performance is a crucial task. A method of determining this effect that allows an on-line improvement of the tracking performance is presented in this article. The procedure is illustrated with the control system design for the Deep Space Station (DSS)-13 antenna. Author

N92-29383*# Jet Propulsion Lab., California Inst. of Tech., Pasadena.

DSN ACQUISITION OF MAGELLAN HIGH-RATE TELEMETRY DATA **c17**

A. L. Berman and P. A. Au *In its* The Telecommunications and Data Acquisition Report 15 May 1992 p 253-264 (For primary document see N92-29364 20-32)
(RTOP 314-40-22-35-01)
Avail: CASI HC A03/MF A04

The Magellan Project levied the stringent requirement of a 98 percent high-rate telemetry data capture rate on the Deep Space Network (DSN) during the Magellan Prime Mapping Mission. To meet this requirement, the DSN undertook extensive development of the DSN Telemetry System, as well as extensive DSN operation planning and test and training. In actuality, the DSN substantially exceeded the requirement by achieving a Prime Mapping Mission high-rate telemetry data capture rate of 99.14 percent. This article details the DSN telemetry system development, and DSN operations planning and test and training. In addition, the actual high-rate telemetry data outages are comprehensively presented and analyzed. Author

N92-29384*# Jet Propulsion Lab., California Inst. of Tech., Pasadena.
GALILEO EARLY CRUISE, INCLUDING VENUS, FIRST EARTH, AND GASPRA ENCOUNTERS **c91**
P. E. Beyer, R. C. OConnor, and D. J. Mudgway *In its* The Telecommunications and Data Acquisition Report 15 May 1992 p 265-281 (For primary document see N92-29364 20-32)
(RTOP 314-40-22-37-01)
Avail: CASI HC A03/MF A04

This article documents Deep Space Network (DSN) support for the Galileo cruise to Jupiter. The unique trajectory affords multiple encounters during this cruise phase. Each encounter had or will have unique requirements for data acquisition and DSN support configurations. An overview of the cruise and encounters through the asteroid Gaspra encounter is provided. Author

N92-29385*# Jet Propulsion Lab., California Inst. of Tech., Pasadena.
DEEP SPACE NETWORK INFORMATION SYSTEM ARCHITECTURE STUDY
C. A. Beswick, R. W. Markley, ed., D. J. Atkinson, L. P. Cooper, R. C. Tausworthe, R. C. Masline, J. S. Jenkins, R. A. Crowe, J. L. Thomas, and M. J. Stoloff *In its* The Telecommunications and Data Acquisition Report 15 May 1992 p 282-355 (For primary document see N92-29364 20-32)
(RTOP 314-30-58-50-05)
Avail: CASI HC A04/MF A04

The purpose of this article is to describe an architecture for the Deep Space Network (DSN) information system in the years 2000-2010 and to provide guidelines for its evolution during the 1990s. The study scope is defined to be from the front-end areas at the antennas to the end users (spacecraft teams, principal investigators, archival storage systems, and non-NASA partners). The architectural vision provides guidance for major DSN implementation efforts during the next decade. A strong motivation for the study is an expected dramatic improvement in information-systems technologies, such as the following: computer processing, automation technology (including knowledge-based systems), networking and data transport, software and hardware engineering, and human-interface technology. The proposed Ground Information System has the following major features: unified architecture from the front-end area to the end user; open-systems standards to achieve interoperability; DSN production of level 0 data; delivery of level 0 data from the Deep Space Communications Complex, if desired; dedicated telemetry processors for each receiver; security against unauthorized access and errors; and highly automated monitor and control. Author

N92-29386*# Jet Propulsion Lab., California Inst. of Tech., Pasadena.
GENERALIZED PROBABILITY MODEL FOR CALCULATION OF INTERFERENCE TO THE DEEP SPACE NETWORK DUE TO CIRCULARLY EARTH-ORBITING SATELLITES
C. J. Ruggier *In its* The Telecommunications and Data Acquisition Report 15 May 1992 p 356-366 (For primary document see N92-29364 20-32)
(RTOP 315-20-50-00-06)
Avail: CASI HC A03/MF A04

The probability of exceeding interference power levels and the duration of interference at the Deep Space Network (DSN) antenna is calculated parametrically when the state vector of an Earth-orbiting satellite over the DSN station view area is not known. A conditional probability distribution function is derived, transformed, and then convolved with the interference signal uncertainties to yield the probability distribution of interference at any given instant during the orbiter's mission period. The analysis is applicable to orbiting satellites having circular orbits with known altitude and inclination angle. Author

N92-29387*# Jet Propulsion Lab., California Inst. of Tech., Pasadena.
Ka-BAND FEED ARRAYS FOR SPACECRAFT REFLECTOR ANTENNAS WITH LIMITED SCAN CAPABILITY: AN OVERVIEW
V. Jamnejad *In its* The Telecommunications and Data Acquisition Report 15 May 1992 p 367-376 (For primary document see N92-29364 20-32)
(RTOP 315-91-50-20-04)
Avail: CASI HC A02/MF A04

JPL and NASA are in the process of developing ground and spacecraft antenna systems at Ka-band frequencies for future deep space applications. The use of Ka-band (32-GHz down) communication will result in smaller ground and spacecraft antennas and associated equipment, and will provide larger bandwidths necessary for very high data rate communication and radio navigation. In this article, the use of a small phased array as a feed for a reflector antenna system with limited scan capability is addressed. Different feed and antenna configurations, as well as array architectures, are examined. Some theoretical and experimental parameters of a particular breadboard feed array developed by JPL and the University of Massachusetts are presented. Guidelines for the future direction of this effort are provided. Author

N92-29388*# Jet Propulsion Lab., California Inst. of Tech., Pasadena.
DSN OBSERVATIONS OF TITAN **c91**
R. M. Goldstein and R. F. Jurgens *In its* The Telecommunications and Data Acquisition Report 15 May 1992 p 377-379 (For primary document see N92-29364 20-32)
(RTOP 196-41-73-02-00)
Avail: CASI HC A01/MF A04

When using Deep Space Station (DSS)-14 in a monostatic configuration, radar observations of Titan show that Titan is a diffuse reflector with a relative radar cross section of 0.14 +/- 0.03. No hot spots were observed. Author

N92-29389*# Jet Propulsion Lab., California Inst. of Tech., Pasadena.
GOLDSTONE SOLAR SYSTEM RADAR SIGNAL PROCESSING
R. Jurgens, E. Satorius, and O. Sanchez *In its* The Telecommunications and Data Acquisition Report 15 May 1992 p 380-397 (For primary document see N92-29364 20-32)
(RTOP 196-41-73-02-00)
Avail: CASI HC A03/MF A04

A performance analysis of the planetary radar data acquisition system is presented. These results extend previous computer simulation analysis and are facilitated by the development of a simple analytical model that predicts radar system performance over a wide range of operational parameters. The results of this study are useful to both the radar system designer and the science investigator in establishing operational radar data acquisition parameters which result in the best systems performance for a given set of input conditions. Author

N92-29395# Naval Ocean Systems Center, San Diego, CA.
USER'S GUIDE FOR THE VTRPE (VARIABLE TERRAIN RADIO PARABOLIC EQUATION) COMPUTER MODEL Final Report, May 1990 - Sep. 1991
Frank J. Ryan Oct. 1991 58 p
(AD-A248112; NOSC/TR-1456) Avail: CASI HC A04/MF A01

This report is a user's guide to the VTRPE (variable terrain radio parabolic equation) computer model. It is designed to provide the reader with a summary of the physics and numerical methods used in the VTRPE model, along with detailed instructions on the model's use and operation. The VTRPE computer program is a range-dependent, tropospheric microwave propagation model that is based upon the split-step Fourier parabolic wave equation algorithm. The nominal applicable frequency range of the model is VHF to K-band. The VTRPE program is able to make predictions for microwave propagation over both land and water. The VTRPE code is a full-wave propagation model that solves the

electromagnetic wave equations for the complex electric and magnetic radiation fields. The model accounts for the effects of nonuniform atmospheric refractivity fields, variable surface terrain, and varying surface dielectric properties on microwave propagation. The code is written in ANSI-77 FORTRAN with MILSPEC-1753 FORTRAN language extensions. The VTRPE program is currently configured to run under the UNIX operating system on SUN minicomputers and CONVEX supercomputers, and under MS-DOS on 80386/80486-based PC's. GRA

N92-29406# Air Force Inst. of Tech., Wright-Patterson AFB, OH.
DEVELOPING CMMCA FLIGHT PROFILES FOR CRUISE MISSILE TRACKING M.S. Thesis
Andrew C. Hachman Mar. 1992 277 p
(AD-A248183; AFIT/GOR/ENS/92M-13) Avail: CASI HC A13/MF A03

The Air Force has recently acquired two aircraft specifically for cruise missile tracking. These aircraft, known as the Cruise Missile Mission Control Aircraft (CMMCA), are responsible for collecting data from the missile and tracking and positively controlling the missile during live fire testing over the western United States. Due to the limited tracking radar range and the flight characteristics of the CMMCA, tracking cruise missiles through complex maneuvers is not always possible. A FORTRAN optimization, based on flight simulation and optimal control theory, was written in a prior thesis effort in order to determine optimal CMMCA flight profiles for tracking cruise missiles through certain maneuvers. The primary emphasis of this research effort was to conduct an analysis of the previously written optimization program, and to make the appropriate modifications to improve the performance and efficiency of the program. The program was tested over several different missile flight paths, using a variety of different initial program conditions and input parameters, in order to find the program modifications and parameter settings that produced the best CMMCA flight profiles in response to the given cruise missile flight path. GRA

N92-29447# Massachusetts Univ., Amherst. Dept. of Electrical and Computer Engineering.
NORMALIZED RADAR CROSS SECTION OF NATURAL SURFACES AT MILLIMETER WAVELENGTHS Final Report
Robert E. McIntosh Nov. 1991 11 p
(Contract DAAL03-88-K-0105)
(AD-A248452) Avail: CASI HC A03/MF A01

This report describes the results of research of polarimetric radar measurements performed at 95 GHz and 225 GHz by the University of Massachusetts. The targets included various tree species and snow scenes. GRA

N92-29463*# Jet Propulsion Lab., California Inst. of Tech., Pasadena.
MICROSTRIP REFLECTARRAY ANTENNA FOR THE SCANSCAT RADAR APPLICATION
John Huang 15 Nov. 1990 41 p
(Contract NAS7-918)
(NASA-CR-190453; NAS 1.26:190453; JPL-Publ-90-45) Avail: CASI HC A03/MF A01

This publication presents an antenna system that has been proposed as one of the candidates for the SCANSCAT (Scanned Scatterometer) radar application. It is the mechanically steered planar microstrip reflectarray. Due to its thin, lightweight structure, the antenna's mechanical rotation will impose minimum angular momentum for the spacecraft. Since no power-dividing circuitry is needed for its many radiating microstrip patches, this electrically large array antenna demonstrates excellent power efficiency. In addition, this fairly new antenna concept can provide many significant advantages over a conventional parabolic reflector. The basic formulation for the radiation fields of the microstrip reflectarray is presented. This formulation is based on the array theory augmented by the Uniform Geometrical Theory of Diffraction (UTD). A computer code for analyzing the microstrip reflectarray's performances, such as far-field patterns, efficiency, etc., is also listed in this report. It is proposed here that a breadboard unit of this microstrip reflectarray should be constructed and tested in the future to validate the calculated performance. The antenna concept presented here can also be applied in many other types of radars where a large array antenna is needed. Author

N92-29542# Stanford Univ., CA. Space Telecommunications and Radioscience Lab.
GLOBAL MEASUREMENTS OF LOW-FREQUENCY RADIO NOISE Final Report, 1 Mar. 1981 - 31 Oct. 1989
A. C. Fraser-Smith, P. R. McGill, A. Bernardi, R. A. Helliwell, and M. E. Ladd Feb. 1992 16 p
(Contract N00014-81-K-0382)
(AD-A248260; SU-E450-1) Avail: CASI HC A03/MF A01

We report illustrative results obtained by Stanford University's global survey of ELF/VLF radio noise (frequencies in the range 10 Hz to 32 kHz). Particular comparison is made between the noise measurements made at high (polar) latitudes with those at lower latitudes. Although most of the natural ELF/VLF noise observed everywhere in the world is lightning-generated, the high-latitude noise often contains additional components that are of magnetospheric origin. In the data we have examined, this noise consists predominantly of polar chorus, which is concentrated in the range 300 Hz to 2 kHz. It produces a characteristic signature in the noise statistics. Less frequent occurrences of broad-band (auroral) hiss can occasionally mask most or all of the lightning-generated noise in the ELF/VLF range. GRA

N92-29563# Naval Surface Warfare Center, Panama City, FL.
STATISTICS OF NARROWBAND WHITE NOISE DERIVED FROM CLIPPED BROADBAND WHITE NOISE
W. M. Wynn Feb. 1992 17 p
(AD-A248597; CSS-TM-596-92) Avail: CASI HC A03/MF A01

Broadband white Gaussian noise is modelled as a series of sine and cosine functions of discrete frequencies up to a maximum frequency. The series coefficients are Gaussian with uniform variance across the frequency band. For a given sample, the Nyquist-spaced values are generated for a full period of the lowest frequency sinusoid and a peak factor is imposed, clipping the values. The resulting signal is discrete-Fourier transformed via the fast Fourier transform, hard filtered at a prescribed bandwidth, and then inverse transformed to give a set of values for the narrow band signal sample, and these values are used to update a histogram. When a sufficient number of signal samples are generated, the resulting distribution is fitted to a Gaussian distribution by a least-squares technique. It is found that the resulting distributions are noticeably non-Gaussian down to a bandwidth ratio of 1:4, below which the distribution appears to be Gaussian with a reduced variance depending on the peak factor. For a bandwidth ratio of 1:40, it is found that peak factors as low as 1.7 or even 1.5 have little effect on the narrowband distribution. GRA

N92-29568*# Smithsonian Astrophysical Observatory, Cambridge, MA.
INVESTIGATION OF THE STRUCTURE OF THE ELECTROMAGNETIC FIELD AND RELATED PHENOMENA, GENERATED BY THE ACTIVE SATELLITE Final Report, 1 May 1990 - 30 Apr. 1992
Yakov L. Alpert Jun. 1992 40 p
(Grant NAG5-1340)
(NASA-CR-190446; NAS 1.26:190446) Avail: CASI HC A03/MF A01

A short review is given for the general frequency and angle distribution of the electric field radiated by an electric dipole E = E(sub 0)cos(omega)t, in a magnetoplasma. Detailed results of numerical calculations of (E) were made in the Very Low Frequency (VLF) and the Low Frequency (LF) bands 0.02f(sub b) is less than or equal to F is less than or equal to 0.5f(sub b) (F is approximately (4-500) kHz) in the ionosphere and magnetosphere in the altitude region Z = (800-6000) km; f(sub b) is the electron gyro-frequency of the plasmas in the discussed region f(sub b) is approximately equal to (1.1 to 0.2) MHz. The amplitudes of the

electric field have large maxima in four regions: close to the direction of the Earth's magnetic field line (B(sub 0)), it is the so called Axis field (E(sub 0)) and in the Storey (E(sub St)), Reversed Storey (E(sub RevSt)), and Resonance (E(sub Res)) Cones. The maximal values of E(sub 0), E(sub Res), and E(sub RevSt) are very pronounced close to the low hybrid frequency, F approximately F(sub L). The flux of the electric field is concentrated in very narrow regions, the apex angles of the cones delta(beta) is approximately equal to (0.1 - 1) degree. The enhancement and focusing of the electric field is growing up, especially quickly at Z greater than 800 km. At Z is greater than 1000 up to 6000 km, the relative value of (E), in comparison with its value at Z = 800 km is about (10(exp 2) to 10(exp 4)) times larger. Thus, the flux of VLF and LF electromagnetic waves in the Earth magnetoplasma produces and is guided by very narrow pencil beams, similar, let us say, to laser beams. Author

N92-29572# Department of the Army, Washington, DC.
FM VIDEO DATA LINK SPECTRUM SPREADING Patent Application
Edward M. Holliday, inventor (to Army), Phillip M. Kirshtein, inventor (to Army), and Glenn D. Weathers, inventor (to Army) 8 Oct. 1991 21 p
(AD-D015257; US-Patent-Appl-SN-772999) Avail: CASI HC A03/MF A01

A video data link system utilizes spread spectrum to decrease the susceptibility of a low power video link to radio frequency countermeasures. The video data link system utilizes a combination of spread spectrum direct-sequence modulation and frequency-hop along with frequency modulation to provide spectral spreading of radio frequency energy to a bandwidth much greater than the information bandwidth. The direct sequence modulation allows minimization of the number of frequency steps required for complete spectral filling of the operational bandwidth on an average basis. Frequency hop timing is determined from the phase of the direct sequence generator to simplify the frequency hop synchronization process in the receiver. GRA

N92-29576# Naval Postgraduate School, Monterey, CA.
DETECTION OF BINARY PHASE SHIFT KEYED SIGNALS IN EXTREMELY HIGH NOISE M.S. Thesis
John B. Scout Mar. 1992 47 p
(AD-A248552) Avail: CASI HC A03/MF A01

This thesis describes the design of a fully digital Binary Phase Shift Keyed receiver considered for use in a telemetry system in the range testing of torpedos. The method employed uses a subspace technique called Estimation of Signal Parameters via Rotational Invariant Techniques (ESPRIT) to detect the carrier frequency. This method can be used at lower than normal signal-to-noise ratio's. All results were achieved by the use of computer simulations. GRA

N92-29579# Marquette Univ., Milwaukee, WI.
DETECTING MICROWAVE EMISSIONS FROM TERRESTRIAL SOURCES: A FEASIBILITY STUDY Final Technical Report, 1 Oct. 1988 - 31 Dec. 1991
Thomas C. Ehlert and Thomas K. Ishii 1 Feb. 1992 14 p
(Grant AF-AFOSR-0257-88)
(AD-A248557; AFOSR-92-0237TR) Avail: CASI HC A03/MF A01

A Dicke receiver has been designed and constructed in our effort to detect the 22 GHz spontaneous emission from water vapor. The receiver compares the brightness temperatures of two waveguides, one containing gaseous H20 at low pressure, the other containing dry air. Each waveguide is terminated with polished brass, which provides a low background brightness temperature, at one end and connects to the input of the receiver at the other end. The system is capable of detecting a brightness temperature difference of about 0.2 K. In this experiment, the radiation from water vapor produced the brightness temperature difference between source and reference of 0.28 to 0.33 K. The experimental results proved that emission from water vapor was being detected. GRA

N92-29599# Naval Postgraduate School, Monterey, CA.
REVISING M-LAYER: COMPLEX EXPONENT REPRESENTATION M.S. Thesis
Yin Y. Han Mar. 1992 76 p
(AD-A249121) Avail: CASI HC A05/MF A01

The waveguide mode tropospheric propagation effect prediction program, M-Layer, originally written by Naval Command Control and Ocean Surveillance Center, Research, Development, Test and Engineering Division (NRaD), is revised for greater accuracy, speed and stability. The accuracy improvement is achieved first by converting the extended complex number representation into the representation by the complex exponent then by re-writing the group of Airy function computation subroutines. This accuracy improvement makes it possible to implement a self-checking procedure for determining the proper method to evaluate the height gain function. Finally, a new mode locating algorithm is introduced which improves the efficiency of mode search and eliminates the looping problem observed. The revision has been documented and the new program source code has been delivered to NRaD. It is also recommended that the mode search protocol, not just the mode locating algorithm introduced in this revision, be completely revised for better performance. GRA

N92-29658*# Johns Hopkins Univ., Baltimore, MD. Dept. of Electrical and Computer Engineering.
PERFORMANCE MEASUREMENT RESULTS FOR A 220 Mbps QPPM OPTICAL COMMUNICATION RECEIVER WITH AN EG/G SLIK APD Interim Progress Report, 16 Oct. 1991 - 15 Jul. 1992
Frederic M. Davidson and Xiaoli Sun 15 Jul. 1992 23 p
(Grant NAG5-510)
(NASA-CR-190561; NAS 1.26:190561) Avail: CASI HC A03/MF A01

The performance of a 220 Mbps quaternary pulse position modulation (QPPM) optical communication receiver with a 'Slik' silicon avalanche photodiode (APD) and a wideband transimpedance preamplifier in a small hybrid circuit module was measured. The receiver performance had been poor due to the lack of a wideband and low noise transimpedance preamplifier. With the new APB preamplifier module, the receiver achieved a bit error rate (BER) of 10 exp -6 at an average received input optical signal power of 4.2 nW, which corresponds to an average of 80 received (incident) signal photons per information bit. Author

N92-29696# Office of Technology Assessment, Washington, DC.
WORLD ADMINISTRATIVE RADIO CONFERENCE. ISSUES FOR US INTERNATIONAL SPECTRUM POLICY
Nov. 1991 145 p Conference held in Spain, Feb. 1992
(PB92-157601; OTA-BP-TCT-76; ISBN-0-16-035964-3) Avail: CASI HC A07/MF A02

U.S. preparations for the 1992 World Administrative Radio Conference to be held in Spain, February 1992 are examined. WARC-92 will attempt to reassign radio frequencies internationally in order to take advantage of new radio-based technologies and applications, such as digital audio broadcasting, high definition television, and personal communications services, while still accommodating the needs of existing users and services. The impacts of the realignment will be felt throughout the U.S. economy and around the world, and the agreements reached at WARC-92 will influence the development of radio-based systems and services well into the next century. Author

N92-29730# Laboratoire d'Automatique et d'Analyse des Systemes, Toulouse (France).
METHODOLOGY FOR THE SPECIFICATION OF COMMUNICATION ACTIVITIES WITHIN THE FRAMEWORK OF A MULTI-LAYERED ARCHITECTURE: TOWARD THE DEFINITION OF A KNOWLEDGE BASE Ph.D. Thesis - Toulouse Univ. [METHODOLOGIE DE SPECIFICATION D'ACTIVITES DE COMMUNICATION DANS UNE ARCHITECTURE MILTI-COUCHES VERS LA DEFINITION D'UNE BASE DE CONNAISSANCES]
Omar Amyay 1991 131 p In FRENCH
(LAAS-91466; ETN-92-91483) Avail: CASI HC A07/MF A02

A method defined in terms of synthesis and verification steps is presented. The specification of the services and protocols of communication within a multilayered architecture of the Open Systems Interconnection (OSI) type is an essential issue for the design of computer networks. The aim is to obtain an operational specification of the protocol service couple of a given layer. Planning synthesis and verification steps constitute a specification trajectory. The latter is based on the progressive integration of the 'initial data' constraints and verification of the specification originating from each synthesis step, through validity constraints that characterize an admissible solution. Two types of trajectories are proposed according to the style of the initial specification of the service protocol couple: operational type and service supplier viewpoint; knowledge property oriented type and service viewpoint. Synthesis and verification activities were developed and formalized in terms of labeled transition systems, temporal logic and epistemic logic. The originality of the second specification trajectory and the use of the epistemic logic are shown. An 'artificial intelligence' approach enables a conceptual model to be defined for a knowledge base system for implementing the method proposed. It is structured in three levels of representation of the knowledge relating to the domain, the reasoning characterizing synthesis and verification activities and the planning of the steps of a specification trajectory. ESA

N92-29824# Technische Univ., Eindhoven (Netherlands). Dept. of Mathematics and Computing Science.
SENSITIVITY ANALYSIS OF THE LOAD ON AN ETHERNET NETWORK
Anton Dekkers and Jan vanOorschot (Technische Univ., Delft, Netherlands) Dec. 1991 20 p Sponsored in part by Netherlands Organization for the Advancement of Scientific Research
(Memo-COSOR-91-41; ISSN-0926-4493; ETN-92-91795) Avail: CASI HC A03/MF A01

A sensitivity analysis of the load of an ethernet network is presented. The aim is to determine which parameters that characterize the workload have an influence on the performance of an ethernet segment and to get an idea about the magnitude of this influence. The performance of the network is indicated by the waiting time and the access delay. The performance is measured using a simulation model. The simulation model is a very accurate description of a real ethernet implementation and was validated with the results of real life measurements. The main advantages of simulation are the detailed information that can be obtained and the absence of expensive laboratory measurements. The importance of this sensitivity analysis is to validate future modeling assumptions and to a get a better insight into the behavior of the ethernet protocol. From the research it can be concluded that the performance is sensitive not just to the load of the ethernet, but also to the distribution of the interarrival times, the possibility of batch arrivals and the fraction of traffic arriving in large messages of a number of packets. Therefore, existing models only yield a rough performance estimation of a real ethernet segment, because they assume Poisson arrivals and do not consider batches. ESA

N92-29877# Deutsche Forschungsanstalt fuer Luft- und Raumfahrt, Oberpfaffenhofen (Germany, F.R.). Abt. Hochfrequenzphysik.
GLOBAL AND HIGH RESOLUTION RADAR CROSS SECTION MEASUREMENTS AND TWO-DIMENSIONAL MICROWAVE IMAGES OF A SCALED AIRCRAFT MODEL FROM THE TYPE AIRBUS A 310 [GLOBALE UND HOCHAUFGELOESTE RADARRUECKSTRAHLQUERSCHNITTS-MESSUNGEN UND ZWEIDIMENSIONALE MIKROWELLENABBILDUNGEN VON EINEM SKALIERTEN UND FLUGZEUGMODELL VOM TYP AIRBUSS A 310]
Karl-Heinz Bethke Jun. 1991 54 p In GEORGIAN
(DLR-Mitt-91-10; ISSN-0939-298X; ETN-92-91731) Avail: CASI HC A04/MF A01; DLR, Wissenschaftliches Berichtswesen, Postfach 90 60 58, 5000 Cologne, Fed. Republic of Germany, HC

The results from radar cross section high resolution measurements of a metallized scaled model of a usual airliner of the Airbus A310 type are presented. The measurements were performed for line polarization states by using a coherent short pulse radar at a frequency of 12.5 GHz. Two dimensional microwave images were generated for varied aspect angles by using inverse synthetic aperture principles to obtain an exact identification of each scattering center of the model. Polarization dependent back diffusions are particularly visible at the wing edges in the respective reflection images. The fins of airfoils are visible by vertical polarization for aspect angles from side views. ESA

N92-29902# Mitre Corp., Bedford, MA.
HFRAD HINDCAST: AN OTH-B RADAR AND MODEL COMPARISON STUDY
T. J. Elkins and J. Providakes Dec. 1991 21 p
(Contract F19628-89-C-0001)
(AD-A248065; M91-113) Avail: CASI HC A03/MF A01

Hindcast analysis of OTH radar data differs from purely predictive (or forecast) analysis in that it is made 'after the fact' of radar measurement, permitting the removal of a substantial part of the random variability inherent in forecasting radar performance. In this paper, hindcast analysis is used to verify the performance of the MITRE OTH radar performance model, HFRAD. Data was collected during November and December of 1990 with the AN/FPS-118 East Coast Radar System (ECRS), and during January and February of 1991 with the West Coast Radar System (WCRS). This data was analyzed and compared to hindcast estimates of performance using a new version (V507g) of HFRAD that incorporates a new and improved, clutter model. Performance was analyzed in terms of target signal-to-noise ratio (SNR), both for the aggregate data set and for the data as a function of azimuth (because of its location near the auroral oval, the ECRS is known to exhibit a strong dependence of performance on azimuth). In addition, these internal model components were analyzed in the same way: subclutter visibility (SCV), surface clutter peak, background noise (i.e., noise measured with transmitter operating), noise measured with transmitter off (ambient noise), and the ratio of background noise to ambient noise. As anticipated, the comparison is generally in good agreement, although notable discrepancies still exist, particularly near the auroral oval. Suggestions for further improvements to HFRAD are presented. GRA

N92-29909# Lawrence Livermore National Lab., CA.
THE GREEN FUNCTION CELLULAR METHOD AND ITS RELATION TO MULTIPLE SCATTERING THEORY
W. H. Butler (Oak Ridge National Lab., TN.), X. G. Zhang (Kentucky Univ., Lexington.), and A. Gonis 13 Nov. 1991 8 p Presented at the Annual Fall Meeting of the Materials Research Society, Boston, MA, 2-6 Dec. 1991
(Contracts W-7405-eng-48; DE-AC05-84OR-21400)
(DE92-011470; UCRL-JC-109001; CONF-911202-69) Avail: CASI HC A02/MF A01

We investigate techniques for solving the wave equation which are based on the idea of obtaining exact local solutions within each potential cell, which are then joined to form a global solution. We derive full potential multiple scattering theory (MST) from the

Lippmann-Schwinger equation and show that it as well as a closely related cellular method are techniques of this type. This cellular method appears to have all of the advantages of MST and the added advantage of having a secular matrix with only nearest neighbor interactions. Since this cellular method is easily linearized one can rigorously reduce electronic structure calculations to the problem of solving a nearest neighbor tight-binding problem. DOE

N92-29959# Universiteit Twente, Enschede (Netherlands). Tele-Informatics and Open Systems Group.
REAL-TIME SERVICE DEFINITION OF A COMMUNICATION NETWORK IN A MANUFACTURING ENVIRONMENT
Aiko Pras, Jeroen Schot, and Thony vanderVloedt Dec. 1991 59 p
(Memo-INF-91-84; TIOS-91/034; ISSN-0924-3755; ETN-92-91580) Copyright Avail: CASI HC A04/MF A01

A data communication service that can be used in a manufacturing automation environment is defined. This communication service is an integrated service, consisting of two service components: a component which supports an unconfirmed connectionless service (datagram), and can be used for the transfer of data that does not have strong delay requirements; and a component which supports a connection oriented service, and can be used for the one way transfer of time critical user data. This second service is designed to support real time applications that require guaranteed delay and throughput for a predetermined period of time (the life time of connection). The value of the delay and throughput parameters can be negotiated during the connection set up time. A realization of this service is to be used in a laser processing cell. A formal specification in LOTOS (Language Of Temporal Ordering Specifications) is given. ESA

N92-29978# Universiteit Twente, Enschede (Netherlands). Faculty of Applied Mathematics.
ENERGY PROPAGATION IN DISSIPATIVE SYSTEMS. PART 2: CENTROVELOCITY FOR NONLINEAR WAVE EQUATIONS
G. Derks and E. vanGroesen 2 Dec. 1991 19 p
(MEMO-1016-Pt-2; ISSN-0169-2690; ETN-92-91762) Avail: CASI HC A03/MF A01

Nonlinear wave equations, first order in time, of a specific form, are considered. In the absence of dissipation, these equations are given by a Poisson system, with the Hamiltonian that is the integral of some density. The functional I, defined to be the integral of the square of the waveform, is a constant of motion of the unperturbed system. Z, the center of gravity of this density, is shown to be canonically conjugate to I and can be used as a measure to locate the position of the waveform. By introducing new coordinates based on Z, expressions for the centrovelocity of Z and the decay of I, which compare to the lines of the previous first part of this study, in both the conservative and the dissipative case, are obtained. With the derived expressions, the decay of solitary waves of the Korterweg de Vries equation, when different kinds of dissipation are added, is investigated. ESA

N92-29984# Universiteit Twente, Enschede (Netherlands). Tele-Informatics and Open Systems Group.
CISLAN-2 EXTENSION FINAL DOCUMENT BY UNIVERSITY OF TWENTE (NETHERLANDS)
Ignas Niemegeers, Frank Baumann, ed., Wim Beuwer, Marcel Jordense, Aiko Pras, Leon Schutte, and Ian Tracey 23 Jan. 1992 105 p
(Memo-INF-92-05; TIOS-92/03; ISSN-0924-3755; ETN-92-91779) Copyright Avail: CASI HC A06/MF A02

Results of worked performed under the so called Cislan extension contract are presented. The adaptation of the Cislan 2 prototype design to an environment of interconnected Local Area Networks (LAN's) instead of a single 802.5 token ring LAN is considered. In order to extend the network architecture, the Interconnection Function (IF) protocol layer was subdivided into two protocol layers: a new IF layer, and below the Medium Enhancement (ME) protocol layer. Some small enhancements to the distributed bandwidth allocation protocol were developed, which in fact are also applicable to the 'normal' Cislan 2 system. The new services and protocols are described together with some scenarios and requirements for the new internetting Cislan 2 system. How to overcome the degradation of the quality of speech due to packet loss on the LAN subsystem was studied. Experiments were planned in order to measure this speech quality degradation. Simulations were performed of two Cislan subsystems, the bandwidth allocation protocol and the clock synchronization mechanism. Results on both simulations, performed on SUN workstations using QNAP as a simulation tool, are given. Results of the simulations of the clock synchronization mechanism, and results of the simulation of the distributed bandwidth allocation protocol are given. ESA

N92-29988# Stanford Linear Accelerator Center, CA.
HIGH RESOLVING POWER SPECTROMETER FOR BEAM ANALYSIS
H. W. Moshammer and J. E. Spencer Mar. 1992 3 p Presented at the 3rd European Particle Accelerator Conference, Berlin, Germany, 24-28 Mar. 1992
(Contract DE-AC03-76SF-00515)
(DE92-010751; SU-SLAC-PUB-5780; CONF-920315-5) Avail: CASI HC A01/MF A01

We describe a system designed to analyze the high energy, closely spaced bunches from individual RF pulses. Neither a large solid angle nor momentum range is required so this allows characteristics that appear useful for other applications such as ion beam lithography. The spectrometer is a compact, double-focusing QBQ design whose symmetry allows the Quads to range between F or D with a correspondingly large range of magnifications, dispersion, and resolving power. This flexibility insures the possibility of spatially separating all of the bunches along the focal plane with minimal transverse kicks and bending angle for differing input conditions. The symmetry of the system allows a simple geometric interpretation of the resolving power in terms of thin lenses and ray optics. We discuss the optics and the hardware that is proposed to measure emittance, energy, energy spread, and bunch length for each bunch in an RF pulse train for small bunch separations. We also discuss how to use such measurements for feedback and feedforward control of these bunch characteristics as well as maintain their stability. DOE

N92-30093# National Inst. of Standards and Technology, Boulder, CO. Electromagnetic Fields Div.
APERTURE COUPLING TO SHIELDED TRANSMISSION LINES: THEORY AND EXPERIMENT
D. A. Hill, M. L. Crawford, M. Kanda, and D. I. Wu Apr. 1992 32 p Prepared in cooperation with Colorado Univ., Boulder
(PB92-183672; NISTIR-3988; B92-0123) Avail: CASI HC A03/MF A01

Coupling through circular apertures in the shields of a coaxial air line and a TEM cell is studied theoretically and experimentally. Polarizability theory is used to compute the effective dipole moments that excite the transmission lines in the internal region. Measurements of shielding effectiveness of both structures were made in a reverberation chamber over wide frequency ranges. Agreement between theory and measurements is generally within + or - 10 dB. Recommendations for improvements in the measurements and theory are made for achieving closer agreement that would be desirable for an artifact standard for shielding effectiveness measurements. Author

N92-30103*# National Aeronautics and Space Administration. Pasadena Office, CA.
MINIATURE MODULAR MICROWAVE END-TO-END RECEIVER Patent Application
Lin M. Sukamto, inventor (to NASA) (Jet Propulsion Lab., California Inst. of Tech., Pasadena.), Thomas W. Cooley, inventor (to NASA) (Jet Propulsion Lab., California Inst. of Tech., Pasadena.), Michael A. Janssen, inventor (to NASA) (Jet Propulsion Lab., California Inst. of Tech., Pasadena.), and Gary S. Parks, inventor (to NASA) (Jet Propulsion Lab., California Inst. of Tech., Pasadena.) 3 Dec. 1991 28 p

(Contract NAS7-918)
(NASA-Case-NPO-18713-1-CU; NAS 1.71:NPO-18713-1-CU; US-Patent-Appl-SN-802078) Avail: CASI HC A03/MF A01

An end-to-end microwave receiver system contained in a single miniature hybrid package mounted on a single heatsink is presented. It includes an input end connected to a microwave receiver antenna and an output end which produces a digital count proportional to the amplitude of a signal of a selected microwave frequency band received at the antenna and corresponding to one of the water vapor absorption lines near frequencies of 20 GHz or 30 GHz. The hybrid package is on the order of several centimeters in length and a few centimeters in height and width. The package includes an L-shaped carrier having a base surface, a vertical wall extending up from the base surface and forming a corner therewith, and connection pins extending through the vertical wall. Modular blocks rest on the base surface against the vertical wall and support microwave monolithic integrated circuits on top surfaces thereof connected to the external connection pins. The modular blocks lie end-to-end on the base surface so as to be modularly removable by sliding along the base surface beneath the external connection pins away from the vertical wall. NASA

N92-30170# Universiteit Twente, Enschede (Netherlands). Tele-Informatics and Open Systems Group.
VARIABLE BANDWIDTH CONNECTIONS FOR A CONNECTIONLESS SERVICE ON ATM: PERFORMANCE MODELLING AND EVALUATION
Geert J. Heijenk and Ignas G. Niemegeers Dec. 1991 17 p Presented at the IFIP Workshop on Broadband Communications, Estoril, Portugal, 20-22 Jan. 1992 Submitted for publication
(Memo-INF-91-83; TIOS-91/033; ISSN-0924-3755; ETN-92-91773) Copyright Avail: CASI HC A03/MF A01

In order to cope with the demand for a connectionless broadband service, a connectionless protocol for the Broadband-Integrated Services Digital Network (B-ISDN) needs to be designed. Such a protocol should make use of Asynchronous Transfer Mode (ATM) and the ATM adaptation layer. It needs to specify destination and bandwidth of connections to the ATM network without advance knowledge of the traffic that has to be transferred over these connections. A possible mechanism, a Variable Bandwidth Connection (VBC) mechanism, is described. It is based on the assumption that there exists a certain correlation between subsequently arriving connectionless packets. The workload on the system is described as a Markov Modulated Poisson Process (MMPP) which represents a superposition of traffic streams with three hierarchical levels. The VBC mechanism is modeled and evaluated using Generalized Stochastic Petri Nets (GSPNs). Compared to a permanent connection mechanism, bandwidth reductions from 30 to 80 percent can be obtained without affecting the average node delay. For a certain permitted average node delay, the VBC mechanism is especially advantageous in situations where either the number of communicating users is relatively low, or where the number of users is unknown or changing in time. ESA

N92-30198# National Inst. of Standards and Technology, Boulder, CO. Electromagnetic Fields Div.
STANDARD SPHERICAL DIPOLE SOURCE
G. Koepke, L. D. Driver, K. Cavcey, K. Masterson, and R. Johnk Dec. 1991 133 p
(PB92-187020; NIST/TN-1351; B91-0278) Avail: CASI HC A07/MF A02; SOD HC

A spherical dipole was developed to provide a source that can be characterized both by theory and experiment and integrated into modern automated test systems. The frequency and amplitude of the radiated electromagnetic field are established remotely using a signal generator. The signal and all other control features are transmitted to and from sphere using fiber optic cable. The field measurements show good agreement with predictions over much of the frequency band. Author

N92-30004*# Rider Coll., Lawrenceville, NJ. Dept. of Physics.
DO RECENT OBSERVATIONS OF VERY LARGE ELECTROMAGNETIC DISSOCIATION CROSS SECTIONS SIGNIFY A TRANSITION TOWARDS NON-PERTURBATIVE QED?
John W. Norbury *In its* Electromagnetic Processes in Nucleus-Nucleus Collisions Relating to Space Radiation Research 1992 15 p (For primary document see N92-30001 20-72)
(Grant NAG1-1134)
Avail: CASI HC A03/MF A03

N92-30015*# Rider Coll., Lawrenceville, NJ. Dept. of Physics.
A LETTER OF INTENT FOR AN EXPERIMENT TO STUDY STRONG ELECTROMAGNETIC FIELDS AT RHIC VIA MULTIPLE ELECTROMAGNETIC PROCESSES
M. Fatyga (Brookhaven National Lab., Upton, NY.) and John W. Norbury *In its* Electromagnetic Processes in Nucleus-Nucleus Collisions Relating to Space Radiation Research 1992 31 p (For primary document see N92-30001 20-72)
Avail: CASI HC A03/MF A03

33 ELECTRONICS AND ELECTRICAL ENGINEERING

Includes test equipment and maintainability; components, e.g., tunnel diodes and transistors; microminiaturization; and integrated circuitry.

For related information see also *60 Computer Operations and Hardware* and *76 Solid-State Physics.*

N92-29339# Lawrence Livermore National Lab., CA.
A MECHANICAL CONNECTOR DESIGN FOR HIGH-CURRENT, HIGH-COULOMB PULSED POWER SYSTEMS
A. R. Susoeff, R. S. Hawke, and K. S. Leighton 25 Feb. 1992 8 p Presented at the 6th Symposium on Electromagnetic Launch Technology, Austin, TX, 28-30 Apr. 1992
(Contracts W-7405-eng-48; DE-AC04-76DP-00789)
(DE92-012678; UCRL-JC-109672; CONF-9204102-7) Avail: CASI HC A02/MF A01

A technique to make reliable high-current, high-coulomb electrical contacts was developed for transmitting power into railguns. The method uses spring loaded removable connectors that are installed independently from the launcher. The simple rod-type design and absence of fastener holes allow maximum utilization of material mechanical properties. Repeated experiments with 9.5-mm diameter connectors demonstrated reliable pulsed charge transfer of 200 coulombs at currents of over 400kA. DOE

N92-29404# Superconductor Technologies, Inc., Santa Barbara, CA.
THE PROCESSING OF HIGH TEMPERATURE CERAMIC SUPERCONDUCTING DEVICES, VOLUME 1 Final Report
James H. Long, Jr. 31 Jan. 1992 118 p
(Contract N00014-88-C-0713; ARPA Order 6268)
(AD-A248176) Avail: CASI HC A06/MF A02

This report describes the objectives and the results achieved in a three-year research effort. The goals of the program included the following: (1) development of a process to grow high critical current, low surface resistance high temperature superconducting thin films on 2 substrates; (2) development of fabrication processes to support the development of passive microwave and IR focal plane interconnect devices; (3) design and implementation of passive microwave and IR focal plane interconnect devices; and (4) theoretical analysis of microwave losses in HTS thin films. High performance, microwave TlCaBaCuO thin films were developed and put into pilot production in a 2 wafer process. Films are made in both single and double side configurations. The films have the lowest surface resistance, at 77 K, of any material in existence, nearly 100 times better than OFHC Cu at 10 GHz and 77 K. Fabrication processes to produce passive microwave and IR focal plane interconnect devices have been

developed: patterning, contacts, bonding, passivation, crossover metallization, and die attach. Passive microwave devices were demonstrated that show orders of magnitude improvement over conventional technologies including resonators, bandpass filters, bandreject filters, delay lines, couplers, and resonator-stabilized oscillators. GRA

N92-29405# Air Force Inst. of Tech., Wright-Patterson AFB, OH.
EXPERIMENTAL EVALUATION OF INCORPORATING DIGITAL AND ANALOG INTEGRATED CIRCUIT DIE ON A COMMON SUBSTRATE UTILIZING SILICON-HYBRID WAFER-SCALE INTEGRATION TECHNOLOGY M.S. Thesis
Philip C. Reamy Mar. 1992 298 p
(AD-A248182; AFIT/GE/ENG/92M-07) Avail: CASI HC A13/MF A03

The objective of this research effort was to investigate the implementation of analog circuits in a wafer scale integration system. A test circuit composed of analog and digital subsystems was designed and tested through simulation. IC die containing this test circuit were utilized in the WSI system fabrication. Preliminary investigations were conducted to evaluate the potential improvements to the IC die mounting procedure, a key step in fabricating functional WSI systems. These investigations demonstrated a procedure which produced repeatable results in achieving acceptable planarization of IC die and host substrate surfaces. These investigations also demonstrated the successful application of a barrier coating material to prevent adhesion between the IC die adhesive and the reference flat during the IC die mounting procedure. An evaluation of candidate polyimides to be used as the interlevel dielectric in the WSI systems was also performed. Test samples for each of the WSI configurations were fabricated and tested for electrical continuity. Additional electrical characterization measurements were conducted on two of the test samples. GRA

N92-29414# General Electric Co., Largo, FL. Neutron Devices Dept.
LI/SO2 CELLS AND LI/SOCI2 CELLS: SAFE USE AND TESTING
C. G. Wagner May 1992 5 p Presented at the 35th International Power Sources Symposium, Cherry Hill, NJ, 22-25 Jun. 1992
(Contract DE-AC04-76DP-00656)
(DE92-013508; GEPP-CP-1297; CONF-920669-5) Avail: CASI HC A01/MF A01

Most lithium/sulfur dioxide (Li/SO2) cells and lithium/thionyl chloride (Li/SOCl2)) cells have pressure relief safety devices called vents built into them. These vents are designed to open under conditions of increasing internal cell pressure. The likelihood of cell venting has been reduced to very low levels by optimizing cell designs. If fully developed Li/SO2 cells or Li/SOCl2 cells (or batteries) are discharged within the intended design limits, they are essentially nonhazardous. In addition, the consequences of cell ventings are being minimized by use of appropriate absorbant materials and protective coatings. During battery assembly and test, detection and monitoring equipment is used to sense the presence of vented gases. Tester data analysis techniques have been developed to foresee either an increasing likelihood of a vent or the presence of a vented cell. Standard cleanup procedures have been developed to safely decontaminate the assembly or test area following a cell vent. DOE

N92-29443# Air Force Inst. of Tech., Wright-Patterson AFB, OH.
DESIGN AND CONSTRUCTION OF A CHANNEL ELECTRON MULTIPLIER BASED MOSSBAUER SPECTROSCOPY SYSTEM M.S. Thesis
Daniel J. Robbins Mar. 1992 59 p
(AD-A248154; AFIT/GNE/ENP/92M-9) Avail: CASI HC A04/MF A01

A channel electron multiplier (cem) detector system was designed and built to provide a signal to a Mossbauer spectroscopy system in an effort to obtain a better signal-to-noise ratio than achievable with a proportional counter system. Three cems are contained in a vacuum chamber built using standard components. Gamma rays of 14.4-keV energy from a Co-57 source enter from outside the chamber through a window and are absorbed by an Fe-57 target near the cems. The target emits internal conversion electrons which are collected by the cems, and a Mossbauer spectrometer collects the signal. The system produces a usable signal, but the signal-to-noise ratio is unacceptably high. The strongest peak has a maximum count only 2.1 percent of the total background count. The corresponding peak in a spectrum collected using the proportional detector system is 3.4 percent of the total background count. One possible cause is that some gamma rays are striking two of the cems, producing ionizations in the detectors. The cems need to be repositioned. A screen should be added in front of the cems and grounded to reduce counting of low energy electrons. These improvements should reduce the background count rate. GRA

N92-29452# Massachusetts Inst. of Tech., Cambridge. Research Lab. of Electronics.
FEMTOSECOND STUDIES OF CARRIER DYNAMICS IN COMPOUND SEMICONDUCTORS Annual Technical Report, 25 Apr. 1991 - 24 Apr. 1992
James Fujimoto 6 May 1992 38 p
(Contract N00014-91-J-1956)
(AD-A250584) Avail: CASI HC A03/MF A01

During the past year we have initiated a new research program to experimentally and theoretically investigate ultrafast processes and carrier dynamics in compound semiconductors. The objective of our program is to apply state of the art femtosecond measurement techniques including high resolution pump-probe absorption spectroscopy and time division interferometry measurements of nonlinear index as well as advanced theoretical techniques including ensemble Monte Carlo calculations and analytic solutions of rate equation models to study transient processes in semiconductors. The combination of experimental and theoretical approaches can be used to provide fundamental information about the physics of excited carriers in semiconductors and how they impact on electronic and optoelectronic device performance. Experimental efforts at MIT have centered on the development of new techniques for measurement of ultrafast processes in semiconductors and their application to study transient processes in AlGaAs. Studies focus on both femtosecond measurements of nonlinear index as well as absorption. GRA

N92-29455# Sandia National Labs., Albuquerque, NM.
LATENT INTERFACE-TRAP BUILDUP: ISSUES FOR LONG-TERM DEVICE RESPONSE
J. R. Schwank, D. M. Fleetwood, M. R. Shaneyfelt, and P. S. Winokur 1992 5 p Presented at the Nuclear and Space Radiation Effects Conference, New Orleans, LA, 13-17 Jul. 1992
(Contract DE-AC04-76DP-00789)
(DE92-003148; SAND-92-0357C; CONF-920716-1) Avail: CASI HC A01/MF A01

A large buildup in interface traps has been observed in commercial and radiation-hardened MOS transistors at very long times after irradiation (greater than 10(exp 6) s). This latent buildup may have important implications for CMOS response in space. DOE

N92-29498# Army Lab. Command, Fort Monmouth, NJ. Electronics Technology and Devices Lab.
INTRODUCTION TO QUARTZ FREQUENCY STANDARDS
John R. Vig Mar. 1992 56 p
(DA Proj. 1L1-62705-AH-94)
(AD-A248503; SLCET-TR-92-1) Avail: CASI HC A04/MF A01

The fundamentals of quartz frequency standards are reviewed. The subjects discussed include: crystal resonators and oscillators, oscillator types, and the characteristics arid limitations of temperature-compensated crystal oscillators (TCXO) and oven-controlled crystal oscillators (OCXO). The oscillator instabilities discussed include: aging, noise, frequency vs. temperature, warmup, acceleration effects, magnetic field effects,

atmospheric pressure effects, radiation effects, and interactions among the various effects. Guidelines are provided for oscillator comparison and selection. Discussions of specifications are also included, as are references and suggestions for further reading. GRA

N92-29518# Sandia National Labs., Albuquerque, NM.
MATERIAL-DEPOSITION PROCESSES IN THE SEPARATOR OF Li-ALLOY/FeS2 THERMAL CELLS
M. C. Hash (Argonne National Lab., IL.), J. A. Smaga (Argonne National Lab., IL.), R. A. Guidotti, and F. W. Reinhardt 1991 17 p Presented at the 8th International Symposium on Molten Salts, Saint Louis, MO, 17-22 May 1992
(Contract DE-AC04-76DP-00789)
(DE92-013669; SAND-91-2346C; CONF-9205102-2) Avail: CASI HC A03/MF A01

The deposition of Li2S and Fe in the separator layer of Li-alloy/FeS2 thermal cells during discharge was studied. The parameters having the most impact included: anode Li activity, catholyte treatment (fused vs. unfused, lithiated vs. unlithiated), and electrolyte composition. The quenched cells were subjected to detailed postmortem examination by optical microscopy to measure the distribution and amount of deposition products in the separator layer. Complementary examination of select cells was also conducted using scanning electron microscopy and energy dispersive spectroscopy. DOE

N92-29523# Pennsylvania State Univ., University Park. Dept. of Chemistry.
PULSE VOLTAMMETRY IN SINGLE CELLS USING PLATINUM MICROELECTRODES
T. K. Chen, Y. Y. Lau, D. K. Wong, and A. G. Ewing 22 Nov. 1991 28 p
(Contract N00014-90-J-1161)
(AD-A248080) Avail: CASI HC A03/MF A01

Multiple pulse voltammetry at platinum microelectrodes is described for intracellular measurements. In this technique, a sequence of three potential pulses is used for each current point measured. This pulse sequence provides a fixed cathodic activation potential and a fixed anodic cleaning potential before a varying detection potential, at which the current is measured. Voltammetric information is obtained by ramping the detection potential stepwise through the potential range of interest. The multiple pulse voltammetry technique was applied to the study of the oxidation of potassium ferrocyanide, glucose, and several catechols at platinum microdisk electrodes. In addition, this technique has been applied at ultrasmall platinum ring electrodes to reduce electrode fouling during intracellular voltammetry. In these in vivo experiments, the electrode response is degraded by only 30 percent after 40 minutes of intracellular multiple pulse. GRA

N92-29526# Air Force Inst. of Tech., Wright-Patterson AFB, OH. School of Engineering.
DESIGN AND ANALYSIS OF ELECTRICAL CIRCUITS THAT PRODUCE FRACTIONAL-ORDER DIFFERENTIATION M.S. Thesis
Richard N. Hughes Mar. 1992 742 p
(AD-A248085; AFIT/GE/ENG/92M-05) Avail: CASI HC A99/MF A06

Two half-order differentiator circuit designs were investigated and their electrical performance evaluated. Initially, each circuit design was computer modelled and simulated using the HSPICE computer analysis program. Then, each circuit design was fabricated with two different component technologies. This resulted in four circuits, realized on printed circuit boards, to be evaluated--Oldham discrete component; Oldham hybrid component; Oldfield discrete component; and Oldfield surface mount component. The characterizations of each circuit's electrical performance is documented with time, phase, gain, noise, and spectrum responses. A comparison of each circuit's performance versus the design criteria and computer model performance is presented. Based upon the comparison of the circuit's electrical performances, the circuits were rank ordered as follows: (1) Oldham integrated chip technology (hybrid) component circuit design; (2) Oldham discrete component circuit design; (3) Oldfield surface mount component circuit design; (4) Oldfield discrete component design. GRA

N92-29529# Air Force Inst. of Tech., Wright-Patterson AFB, OH. School of Engineering.
A RESPONSE SURFACE METHODOLOGY STUDY OF FERROELECTRIC MEMORY DEVICES M.S. Thesis
Kevin C. Smith Mar. 1992 187 p
(AD-A248094; AFIT/GST/ENS/92M-7) Avail: CASI HC A09/MF A02

Fatigue in ferroelectric memory devices was studied. The application of fatigue pulses to a ferroelectric sample was controlled by the RT-66 Ferroelectric Tester, a variation of the Sawyer-Tower circuit. The RT-66 also controlled data collection following the fatiguing process. Seven variables were evaluated for their potential-affect on fatigue. A sequence of fatigue tests, which varied the settings of these variables, was developed using Response Surface Methodology (RSM) experimental designs. Least-squares regression models were developed once a particular RSM set of design experiments was completed. These models were evaluated using RSM tools, and the analysis of these models allowed the iterative development of new RSM designs. Within the experimental operating region it was determined that aging did not affect fatigue, and that differences in ferroelectric materials and electrode materials were the most important factors in determining fatigue. First-order models failed to fit the data for any of the RSM designs. The final model developed had two pure quadratic terms and three first-order terms. However, this design only involved one type of ferroelectric. Further testing is necessary before the findings of this study can be extended to modeling fatigue in other ferroelectric materials. GRA

N92-29564# Naval Postgraduate School, Monterey, CA.
USING OBJECT-ORIENTED DATABASES FOR IMPLEMENTATION OF INTERACTIVE ELECTRONIC TECHNICAL MANUALS M.S. Thesis
Evyatar Chelouche Mar. 1992 102 p
(AD-A248135) Avail: CASI HC A06/MF A02

Computer-aided Acquisition and Logistic Support (CALS) is a Department of Defense (DoD) and Industry strategy to transition from paper-intensive acquisition and logistic processes to a highly automated and integrated mode of weapon system acquisition and operation. A newly demonstrated technology in the context of the CALS initiative is the Interactive Electronic Technical Manual (IETM), which is a portable computer system developed for use of technicians maintaining weapon systems. The introduction of IETM systems will relieve the technician from the need to carry extensive volumes of hardcopy technical manuals, provide him with easy interactive access to the required technical data and is expected to have a profound impact on the way weapon systems maintenance is conducted and the costs associated with it. Object Oriented Database Management Systems (OODBMS) is a new technology that marries the characteristics of object-oriented programming languages and data persistence provided by database systems. This thesis explores issues related to the utilization of OODBMS for the implementation of IETM databases, discusses the benefits of this approach and addresses some architectural issues of OODBMS in the context of IETM implementation. Author (GRA)

N92-29575# Texas Univ., Austin. Dept. of Chemical Engineering.
ELECTRICAL CONNECTION OF ENZYME REDOX CENTERS TO ELECTRODES Technical Report, Oct. 1991 - Mar. 1992
Adam Heller 20 Mar. 1992 53 p Sponsored in part by Navy; NSF; The Welch Foundation; and the Texas Advanced Research Program
(AD-A248545) Avail: CASI HC A04/MF A01

Electrically insulating proteins can be made redox-conducting through incorporation of a high density of electron relaying redox centers. Electrons diffuse in the resulting redox conductors by

self-exchange between identical and electron transfer between different relaying centers. When the self-exchange rate of the relays and their density are high, the flux of electrons through a 1 micro-m thick film of a 3-dimensional macromolecular network can match or exceed the rate of supply of electrons to or from the ensemble of enzyme molecules covalently bound to it. The network now molecularly wires the enzyme molecules to the electrode and the current measures the turnover of the wired enzyme molecules. When the enzyme turnover is substrate-flux, i.e. concentration limited, the current increases with the concentration of the substrate. GRA

N92-29612# Grenoble-1 Univ. (France). Techniques de l'Informatique, des Mathematiques, de la Microelectronique et de la Microscopie Quant.

B(EXP 2)UBIST: A STRATEGY FOR BOUNDARY SCAN BOARD UNIFIED BIST

M. Lubaszewski (Universidade Federal do Rio Grand do Sul, Porto Alegre, Brazil) and B. Courtois Jun. 1991 19 p

(IMAG-RR-862-I; ETN-92-91475) Avail: CASI HC A03/MF A01

A hierarchical strategy unifying online and offline tests at the circuit and board levels is proposed. Boundary scan and UBUST (Unified Built In Self Test) techniques are combined in order to propose a solution to obtain an efficient test strategy for circuits and boards. This results in a hierarchical strategy covering all types of tests necessary to boards, for example offline test and concurrent error detection for circuits and connections. Fault diagnosis is addressed. ESA

N92-29613# Grenoble-1 Univ. (France). Techniques de l'Informatique, des Mathematiques, de la Microelectronique et de la Microscopie Quant.

HARDENING TECHNIQUES TO COUNTER CUMULATED DOSE ON SEU AND SEL IN SPACE ENVIRONMENT [TECHNIQUES DE DURCISSEMENT FACE A LA DOSE CUMULEE, AU SEU ET SEL EN ENVIRONNEMENT SPACIAL]

D. Bessot Apr. 1991 153 p In FRENCH

(IMAG-RR-863-I; ETN-92-91476) Avail: CASI HC A08/MF A02

The total dose effect of space particles acting on semiconductor devices by creating charges in the silicon and the silicon dioxide and by creating displacement damage, from the beginning of charge creation to the parameter shifts, is reviewed. Detailed investigations on three phenomena are described: the Single Event Upset (SEU) caused by the heavy ions and the protons which come from the galactic rays and resulting in a transient upset of a critical node voltage; the Single Event Latchup (SEL) caused by the galactic and solar flares cosmic heavy ions and which may be destructive; the displacement damage induced by high energy trapped protons lying in the radiation belts (Van Allen), which involves the creation of permanent defaults over time which act on the mean carrier life, the carrier mobility and the resistivity, thus increasing either generation or recombination rate. These studies allow definition of techniques for the design and fabrication of circuits that are the least vulnerable to radiation. Simulation and test give guarantee that these new techniques assure the margins of the desired specification in space applications. ESA

N92-29729# Laboratoire d'Automatique et d'Analyse des Systemes, Toulouse (France).

STUDY AND REALIZATION OF GaAs PNP HOMOJUNCTION BIPOLAR TRANSISTORS USING ION IMPLEMENTATION Ph.D. Thesis - Toulouse Univ. [ETUDE ET REALISATION DE TRANSISTORS BIPOLAIRES PNP A HOMOJONCTION SUR ARSENIURE DE GALLIUM PAR IMPLANTATION IONIQUE]

Ana Suely Ferreira 1991 174 p In FRENCH

(LAAS-91433; ETN-92-91482) Avail: CASI HC A08/MF A02

The PNP homojunction bipolar transistor and the use of ion implantation to the device manufacture are considered. The study is based on Vannel's work on 2L integrated circuits based on GaAlAs/GaAs. In this type of logic, the basic cell is an NPN transistor with a current source which can be either a resistance or a PNP bipolar transistor. The mechanisms which guide the PNP homojunction transistor behavior are discussed. Several theories for each ion studied, that is, silicon as N type and magnetism as P type are presented. The software developed from modeling are described. The different technological ways available for the ion implantation analysis and for the characterization of implanted layers are described. The experimental study of Mg and Si implants is carried out. The implanted profiles were compared to those obtained from the modeling. The GaAs PNP bipolar transistor manufacture is presented. The technological process are described for two structure types, planar and mesa, and results from the electrical characterization associated are included. ESA

N92-29796# Allied-Signal Aerospace Co., Kansas City, MO.

ROBOTIC WORKCELL FOR WIRE WRAPPING INTEGRATED CIRCUITS

D. O. Law May 1992 23 p

(Contract DE-AC04-76DP-00613)

(DE92-013999; KCP-613-4035) Avail: CASI HC A03/MF A01

A robotic workcell was developed that electrically shorts the leads of integrated circuits by weaving a 0.005-in. copper wire around individual leads. This workcell has the capability to manipulate 13 different integrated circuit body styles including 14- to 64-lead flatpacks, 14- to 40-pin dual inline packages, and 3- to 10-pin cans. Features of the system include automatic program selection based on the particular body style provided, combined with automatic modification of the program to compensate for subtle differences between components supplied by various manufacturers of a given body style. Additionally, the workcell prepared and packages devices for storage by placing conductive foam on the leads of the device, inserting the device/foam into a plastic bag, and heat sealing the bag. DOE

N92-29854# European Space Agency. European Space Research and Technology Center, ESTEC, Noordwijk (Netherlands). Product Assurance and Safety Dept.

DESIGN GUIDELINES FOR CAPABILITY APPROVAL OF FILM HYBRID MICROCIRCUITS AND MICROWAVE HYBRID INTEGRATED CIRCUITS (MHICS)

Nov. 1991 57 p

(ESA-PSS-01-610-Issue-1; ISSN-0379-4059; ETN-92-91384)

Copyright Avail: CASI HC A04/MF A01

Design guidelines for thick and thin film hybrid microcircuits (including microwave hybrid integrated circuits) are presented. The document serves as a reference document when a manufacturer's design rules and production processes are considered for the purpose of the capability approval program defined in ESA PSS-01-605, ESA PSS-01-606 and ESA PSS-01-612. ESA

N92-29900# Department of the Navy, Washington, DC.

INTERFACE BOARD FOR PROVIDING TIME SIGNALS TO A SUPER MINICOMPUTER Patent Application

Robert J. Reid, inventor (to Navy) 7 Oct. 1991 15 p

(AD-D015198; US-Patent-Appl-SN-771928; Navy-Case-73128)

Avail: CASI HC A03/MF A01

This invention relates generally to signal interface circuit boards and more particularly to an interface board providing timing signals from a timing source to a super minicomputer (Q Bus compatible). In developing acoustic signatures for underwater vehicles, it is necessary to have accurate range and bearing data to the vehicle and have that data time correlated with the acoustic signals. Present equipment used for these purposes includes the Atlantic Undersea Test and Evaluation Center (AUTEC) Tracking System for providing three-dimensional positional information and the Acoustic Measurement Array for receiving the acoustic signals that are generated by the underwater vehicle. The tracking system determines the position of the underwater vehicle by the use of a pinger attached to the vehicle and bottom mounted hydrophones. GRA

N92-29912# Helsinki Univ. of Technology, Otaniemi (Finland). Lab. of Thermal Engineering.

EXPERIMENTAL STUDY OF CYLINDRICAL AIR ELECTRODES

M. Viitanen, J. Lamminen, and M. J. Lampinen 1991 13 p
(DE92-506507; TKK-KO/LTK-67) Avail: CASI HC A03/MF A01

The electrodes studied here are cylindrical and prepared to be placed inside the inner surface of a sintered brass tube, which is nickel-plated. Previously we have reported on the preparation of flat air electrodes and also on long run tests carried out with these electrodes. The electrode material was prepared by the so-called wet method to obtain a carbon dough which is easy to handle. The material preparation remains the same, but owing to the different geometrical shape, the preparation of the electrode itself is quite different. We have studied here the long-term performance of these new cylindrical air electrodes and at the same time measured the carbonate content of the electrolyte. We have also analyzed by comparative methods which property of the electrode lowers the performance after a fairly long period. DOE

N92-29914# Grumman Aerospace Corp., Bethpage, NY.
SMART BIT/TSMD INTEGRATION Final Report, Sep. 1989 - Jan. 1991
Charles Cooper, Kenneth A. Haller, Victor G. Zourides, Paul Skeberdis, and White Gibson Dec. 1991 193 p
(Contract F30602-89-C-0155)
(AD-A247192; RL-TR-91-353) Avail: CASI HC A09/MF A03

The problem of false alarms and intermittent failures of electronics continually manifest themselves in high levels of Cannot Duplicate (CND) and Retest OK (RETOK) reports. These conditions lead to an excessive drain on resources including spares, manpower and test equipment and ultimately produce a negative impact on mission readiness. A major contributor of false alarms/intermittents is that of external environmental factors. Smart Built-in Test (Smart BIT) uses environmental stress data as inputs to its artificial intelligence based reasoning process for detecting false alarms, and Time Stress Measurement Device (TSMD) technology provides a capability to measure, collect and store stress data for failure correlation, although with minimal attention to date to real-time applications. Until now, these technologies were independent research and development activities. This report discusses the integration of these technologies. A self contained laboratory testbed was developed to support this research. Hardware and software computer design and development necessary to investigate and complete the integration are detailed. Methods for simulating the environment based on real world data as well as actual sensor hardware implementations were developed. Guidelines for installing actual electronics in the testbed are provided along with conclusions and recommendations for fielding an integrated capability. GRA

N92-29935# Honeywell, Inc., Bloomington, MN. Sensor and System Development Center.
RF VACUUM ELECTRONICS Quarterly Technical Report, 1 Jan. - 31 Mar. 1992
T. Akinwande, P. Bauhahn, T. Ohnstein, J. Holmen, and D. Arch 8 Apr. 1992 23 p
(Contract MDA972-91-C-0030)
(AD-A248857) Avail: CASI HC A03/MF A01

We summarize our second quarter progress and discuss third quarter plans for the development of an edge emitter based vacuum triode with performance goals of 10 micro-A/micron emission current density at less than 250 V and which can be modulated at 1 GHz for 1 hour. Design and layout of the emitter test mask was completed and fabrication of two process runs of edge emitter diodes were completed. These diode emitters utilize a comb emitter design where high resistivity TaN thin films act as current limiters to prevent edge burnout. Testing of these devices will start during the third quarter. Initial design work on the edge emitter triode was started and is described. Extensive finite element modeling (FEM) and analysis to aid in the triode design took place and is described. Significant process development also took place. Experimental studies of dielectrics such as sputtered SiO2, Si3N4, and PECVD SiO2 and Si3N4 were carried out to understand their leakage characteristics and, thus, to understand their impact on emitter performance. A description of our vacuum test station is also given. GRA

N92-29936# Illinois Univ., Urbana. Coordinated Science Lab.
OPTOELECTRONIC INTEGRATION Final Report
Hadis Morkoc 20 Mar. 1992 47 p
(Contract N00014-88-K-0724)
(AD-A248950) Avail: CASI HC A03/MF A01

In the past three year period, we have tackled several related projects towards the integration optical and electronic devices. We have studied different material combinations and novel device structures. Our significant accomplishments can be grouped into seven categories. These deal with the issues related to the investigation of electronic devices such as GaAs HBT's on InP substrates, quantum well optical modulators, resonant cavity-enhanced photodetectors, wavelength selective optoelectronic switching, computers simulation of optoelectronic devices, simulation of electronic states in quantum wells and superlattices under electrical field, and the efforts in growing high quality heterostructures using new material combinations. We address the progress in each one of the four categories mentioned above. Following a brief introduction, abstracts of publications resulting from research carried out under the ONR sponsorship are enclosed for more details. We also enclose a complete list of our publications and presentations. GRA

N92-30032# National Inst. of Standards and Technology, Gaithersburg, MD. Semiconductor Electronics Div.
THE 36TH ISSUE OF ELECTRONICS AND ELECTRICAL ENGINEERING LABORATORY TECHNICAL PROGRESS BULLETIN COVERING LABORATORY PROGRAMS, JULY TO SEPTEMBER 1991, WITH 1992 EEEL EVENTS CALENDAR
J. A. Gonzales Feb. 1992 39 p
(PB92-164672; NISTIR-4726) Avail: CASI HC A03/MF A01

This is the thirty-sixth issue of a quarterly publication providing information on the technical work of the National Institute of Standards and Technology (NIST), Electronics and Electrical Engineering Laboratory (EEEL). The issue of the EEEL Technical Progress Bulletin covers the third quarter of calendar year 1991. Abstracts are provided by technical area for both published papers and papers approved by NIST for publication. Topics covered include the following: antennas; electrical engineering; electrical power; electromagnetic interference; electronics; instrumentation; laser; magnetics; microwave; optical fibers; semiconductors; and superconductors. Author

N92-30086*# National Aeronautics and Space Administration. Pasadena Office, CA.
NONVOLATILE PROGRAMMABLE NEURAL NETWORK SYNAPTIC ARRAY Patent Application
Raoul Tawel, inventor (to NASA) (Jet Propulsion Lab., California Inst. of Tech., Pasadena.) 8 Jul. 1992 20 p
(Contract NAS7-918)
(NASA-Case-NPO-18578-1-CU; NAS 1.71:NPO-18578-1-CU; US-Patent-Appl-SN-912956) Avail: CASI HC A03/MF A01

A floating-gate metal oxide semiconductor (MOS) transistor is implemented for use as a nonvolatile analog storage element of a synaptic cell used to implement an array of processing synaptic cells. These cells are based on a four-quadrant analog multiplier requiring both X and Y differential inputs, where one Y input is UV programmable. These nonvolatile synaptic cells are disclosed fully connected in a 32 x 32 synaptic cell array using standard very large scale integration (VLSI) complementary MOS (CMOS) technology. NASA

N92-30089# Helsinki Univ. of Technology, Otaniemi (Finland). Lab. of Thermal Engineering.
A MATHEMATICAL MODEL FOR METAL HYDRIDE ELECTRODES
M. Viitanen 1991 19 p
(DE92-506506; TKK-KO/LTK-66) Avail: CASI HC A03/MF A01

A model describing the discharge process of a metal hydride electrode is developed. The electrode is used as an anode in different types of electrochemical cells. The electrode studied is cylindrical and the metal hydride is in the form of powder. In the model the electrode consists of spherical particles with an electrolyte between the particles. A special case of the model is considered to demonstrate the maximum current density which can be obtained from the metal hydride electrode, i.e., in the most favorable circumstances, where the only limiting factor is the diffusion of hydrogen in metal. DOE

N92-30092# Research Triangle Inst., Research Triangle Park, NC.
FUZZY LOGIC CONTROL OF AC INDUCTION MOTORS
J. Cleland, W. Turner, P. Wang, T. Espy, and P. J. Chappell 1992 10 p Presented at the IEEE International Conference on Fuzzy Systems, San Diego, CA, 8-12 Mar. 1992 Prepared in cooperation with Duke Univ., Durham, NC; and Tennessee Univ., Knoxville
(Grant EPA-R81-4169-03)
(PB92-180207; EPA/600/A-92/101) Avail: CASI HC A02/MF A01

The fuzzy logic control (FLC) of electric motors, being investigated under the sponsorship of the U.S. EPA to reduce energy consumption when motors are operated at less than rated speeds and loads is discussed. Electric motors use 60 percent of the electrical energy generated in the U.S. An improvement of 1 percent in operating efficiency of all electric motors could result in savings of 17 billion kWh per year in the U.S. New techniques are required to extract maximum performance from modern motors. One possibility, FLC, has recently demonstrated success in solving control problems of nonlinear, multivariable systems such as ac induction motors and adjustable motor-speed drives. Simulated results of a microprocessor-based fuzzy logic motor controller (FLMC) are described. The investigation includes a motor stator voltage control scheme to minimize motor input power at specified speed/torque conditions; simulation of ac motor performance; and development of a FLMC for optimized motor efficiency. Simulated FLMC results compare favorably with other motor control approaches. Potential energy savings are quantitated based on the preliminary predictions of FLMC performance. Author

N92-30094# Helsinki Univ. of Technology, Espoo (Finland). Electron Physics Lab.
SIMULATIONS ON THE ELECTRICAL CHARACTERISTICS OF Si, SiC AND DIAMOND JUNCTION AND SCHOTTKY POWER DIODES
S. Eraenen, K. Grahn, and P. Kuivalainen 1992 50 p
(PB92-177872; Rept-1992/5) Avail: CASI HC A03/MF A01

The direct current properties of the alpha(6H)-SiC and diamond pin-junction diodes and Schottky diodes were studied. The studies have been made by using the simulation program SCORPIO, which solves the Poisson equation and the current continuity equations for the electrons and holes. The simulations are carried out for the temperatures 300, 500, and 900 K. The results of the SiC and diamond diodes are compared with those of the structurally equivalent silicon structures. Usually, the comparison between the silicon and SiC/diamond power structures are made by considering the devices with equivalent breakdown voltages. In the simulation work it is easier to consider devices which are structurally similar. So, the authors have chosen the similar structure approach over the equivalent breakdown voltage approach, although the latter points have also received some attention in their calculations. Author

N92-30176# Joint Inst. for Lab. Astrophysics, Boulder, CO.
OPTICAL AND ELECTRICAL CHARACTERISTICS OF THE CATHODE FALL Final Report, Oct. 1989 - Sep. 1990
Z. L. Petrovic and A. V. Phelps Jan. 1992 30 p
(AF Proj. 2301)
(AD-A249010; WL-TR-91-2094) Avail: CASI HC A03/MF A01

Experiments with hydrogen discharges dominated by the cathode fall show the following: (1) these discharges are unstable for wide ranges of current and circuit resistance; (2) increasing the circuit capacitance expanded the region of instabilities to lower currents; (3) lateral constrictions of the discharge occur over a much more limited range of currents and pressures than do oscillations; (4) laser-induced photoelectron pulses produce damped oscillations for discharge currents below those at which self-sustained oscillations are observed; (5) the frequency of the induced oscillations varies approximately as the square root of the discharge current; and (6) the damping of the oscillations increases with discharge current in an as yet unexplained manner. Measurements of the electronic charge multiplication at voltages below and above the breakdown or low-current-maintenance voltage showed an unexpected discontinuity at the breakdown voltage. GRA

N92-29373*# Jet Propulsion Lab., California Inst. of Tech., Pasadena.
IMPROVEMENTS IN X-BAND TRANSMITTER PHASE STABILITY THROUGH KLYSTRON BODY TEMPERATURE REGULATION
R. M. Perez *In its* The Telecommunications and Data Acquisition Report 15 May 1992 p 114-120 (For primary document see N92-29364 20-32)
(RTOP 310-20-64-22-00)
Avail: CASI HC A02/MF A04

N92-29374*# Jet Propulsion Lab., California Inst. of Tech., Pasadena.
NOISE-OPTIMAL CONTROL OF HEMT LNA'S FOR COMPENSATION OF TEMPERATURE DEVIATIONS
C. MacCarley, J. J. Bautista, and P. A. Willis *In its* The Telecommunications and Data Acquisition Report 15 May 1992 p 121-129 (For primary document see N92-29364 20-32)
(RTOP 310-20-66-09-01)
Avail: CASI HC A02/MF A04

34 FLUID MECHANICS AND HEAT TRANSFER

Includes boundary layers; hydrodynamics; fluidics; mass transfer; and ablation cooling.

For related information see also *02 Aerodynamics* and *77 Thermodynamics and Statistical Physics.*

N92-29394*# National Aeronautics and Space Administration. Ames Research Center, Moffett Field, CA.
A THEORETICAL APPROACH FOR ANALYZING THE RESTABILIZATION OF WAKES
D. C. Hill Apr. 1992 11 p
(RTOP 505-59-53)
(NASA-TM-103858; A-91119; NAS 1.15:103858) Avail: CASI HC A03/MF A01

Recently reported experimental results demonstrate that restabilization of the low-Reynolds-number flow past a circular cylinder can be achieved by the placement of a smaller cylinder in the wake of the first at particular locations. Traditional numerical procedures for modeling such phenomena are computationally expensive. An approach is presented here in which the properties of the adjoint solutions to the linearized equations of motion are exploited to map quickly the best positions for the small cylinder's placement. Comparisons with experiment and previous computations are favorable. The approach is shown to be applicable to general flows, illustrating how strongly control mechanisms that involve sources of momentum couple to unstable (or stable) modes of the system. Author

N92-29458# North Carolina State Univ., Raleigh.
VISCOUS PROFILES AND NUMERICAL METHODS FOR SHOCK WAVES Final Report
Michael Shearer 6 Jun. 1991 3 p

(Contract DAAL03-90-G-0011)
(AD-A246110) Avail: CASI HC A01/MF A01

A workshop on shock waves was held at North Carolina State University, May 23-25, 1990. The workshop brought together mathematicians interested in the following areas related to shock waves: the theory of hyperbolic conservation laws, numerical methods for hyperbolic and parabolic systems of equations, the theory of travelling waves (viscous profiles) for parabolic systems, and applications. GRA

N92-29524# Naval Postgraduate School, Monterey, CA.
TWO-DIMENSIONAL BOUNDARY SURFACES FOR PLANAR EXTERNAL TRANSONIC FLOWS M.S. Thesis
Aharon Salama Mar. 1992 66 p
(AD-A248083) Avail: CASI HC A04/MF A01

The small perturbation, two-dimensional transonic equation is manipulated with a separation-of-variables approach to obtain two ordinary, nonlinear, differential equations. Numerical integration of these differential equations results in new transonic boundary surfaces for planar external flows. A key ingredient in these solutions is the identification of dependence of two integrations constants, Alpha and Beta, on the parameter (1-M(exp 2)). The anticipated behavior for both the Mach number and the pressure coefficient is used as a guide in the actual selection of the adjustable constants in the problem. The physical reality of our boundary surfaces is examined by displaying the boundary conditions they satisfy. The strictly sonic flow (M =1.0) has an analytic representation corresponding to a divergent surface which goes supersonic. This sonic solution is compared with an Euler-CFD approach confirming the validity of our results over the region where small perturbations apply. Solutions are also shown for M = 0.8, 0.9, 1.1, and 1.2. These results are consistent with known behavior for both subsonic and supersonic external flow. Since the results of this work yield actual transonic contours, we can examine shockless surfaces for design applications. The possibility of starting with transonic surface is of interest to present day CFD approach. Finally an entire transonic upper surface is presented for M = 0.8. GRA

N92-29683# Manchester Univ. (England). Aeroanutical Engineering Group.
AERONAUTICAL ENGINEERING GROUP PUBLICATIONS, 1950 - PRESENT
1989 19 p
(Aero-Rept-8907; ETN-92-91342) Avail: CASI HC A03/MF A01

A list of 232 publications of the aeronautical engineering group is presented. For each entry the author(s), source and date of publication, and article title, are presented. ESA

N92-29692*# Institute for Computer Applications in Science and Engineering, Hampton, VA.
STREAMWISE VORTICES IN HEATED BOUNDARY LAYERS Final Report
Philip Hall (Manchester Univ., England) Jun. 1992 40 p Submitted for publication
(Contract NAS1-18605; RTOP 505-90-52-01)
(NASA-CR-189661; NAS 1.26:189661; ICASE-92-23) Avail: CASI HC A03/MF A01

The nonlinear instability of the boundary layer on a heated flat plate placed in an oncoming flow is investigated. Such flows are unstable to stationary vortex instabilities and inviscid traveling wave disturbances governed by the Taylor-Goldstein equation. For small temperature differences the Taylor-Goldstein equation reduces to Rayleigh's equation. When the temperature difference between the wall and free stream is small the preferred mode of instability is a streamwise vortex. It is shown in this case that the vortex, assumed to be of small wavelength, restructures the underlying mean flow to produce a profile which can be massively unstable to inviscid traveling waves. The mean state is shown to be destabilized or stabilized to inviscid waves depending on whether the Prandtl number is less or greater than unity. Author

N92-29721# Texas Univ., Austin. Inst. for Computational Mechanics.
MODELING AND COMPUTATIONAL ANALYSIS OF MULTISCALE PHENOMENA IN FLUID-STRUCTURE INTERACTION PROBLEMS Final Report, 14 Jun. 1989 - 14 Dec. 1991
J. T. Oden Mar. 1992 112 p
(Contract N00014-89-J-3109)
(AD-A248723) Avail: CASI HC A06/MF A02

This document summarizes research done during the period 14 Jun. 1989 - 14 Dec. 1991 on a project aimed at the development of advanced computational methods for modeling multiscale fluid-structure interaction phenomena. The major thrust of the work reported is the development of the component parts of a new family of computational schemes that could be used to study large-scale problems in fluid-structure interaction. The overall theme of the project was the optimization of the computational process through the development of new adaptive techniques, data structures, a posteriori error estimates, and high-order solvers. The premise behind studying these types of high-order methods is that, with proper data structures, they could lead to exponential rates of convergence and thereby allow one to numerically solve very large problems, with features covering many different physical scales, using many fewer degrees of freedom than that required by conventional methods. In this spirit, the project was an ambitious one for it involved developing not only new adaptive algorithms for simulating the motion of elastic structures, but also techniques for fluid structure interaction and for modeling various regimes of incompressible viscous flows. Presumably, these methods could also be used to model the transition to turbulence and ultimately turbulent boundary layers on compliant surfaces. GRA

N92-29752# Technische Univ., Eindhoven (Netherlands).
THE DEPENDENCE OF TRANSPORT COEFFICIENTS OF SUSPENSIONS IN QUASISTATIC AND RETARDED HYDRODYNAMIC INTERACTIONS Ph.D. Thesis
Hermanus Johannes Hu Clercx 1991 209 p
(ETN-92-91624) Avail: CASI HC A10/MF A03

A theoretical study of the effects on some transport coefficients of both quasistatic and retarded hydrodynamic interactions among spherical particles in a suspension is presented. The method to solve the problem of N particles, interacting hydrodynamically, in an unbounded fluid with an externally imposed flow, is shown. The results of this method, in the case of the two particle problem, are presented. Many results are already known and this enables testing of the convergence behavior of the method. Some new results are given and an alternative approach to the calculation of the effective viscosity of a hard sphere suspension as function of volume fraction, based on ideas produced by Saito, is given. The results of a study of the three particle cluster in an unbounded fluid are presented. Virial expansions of some transport coefficients, including three particle effects, are described. The problem of one particle in an externally imposed flow is addressed. The fluid motion is described by the time dependent incompressible linearized Navier-Stokes equations. The results of a study in retarded hydrodynamic interactions between two spherical particles are given. ESA

N92-29763# Technische Univ., Delft (Netherlands). Faculty of Technical Mathematics and Informatics.
FIRST ORDER APPROXIMATION TO THE AVERAGE VELOCITY OF RISE OF BUBBLES IN FLUID NOT INCLUDING INERTIAL FORCES
P. vanBeek 1991 24 p
(Rept-91-51; ISSN-0922-5641; ETN-92-91420) Copyright Avail: CASI HC A03/MF A01

A homogeneous swarm of massless bubbles rising under gravity and filling an infinitely large container is considered. The prediction of the ensemble averaged steady velocity of rise is addressed. The prediction requires an analysis of the hydrodynamic interaction between the bubbles in the swarm. The behavior of bubbles rising in potential flow is compared to that of (heavy) particles settling

under the Stokes regime. An analysis of two particles in unbounded potential flow is made. ESA

N92-29775# Technische Univ., Eindhoven (Netherlands).
THE INFLUENCE OF TURBULENCE ON AGGREGATION OF SMALL PARTICLES IN AGITATED VESSELS Ph.D. Thesis
Karel Antonius Kusters 1991 216 p
(ETN-92-91629) Avail: CASI HC A10/MF A03

The influence of the hydrodynamics in baffled turbine agitated vessels on the turbulent coagulation of small solid particles is studied, with focus on the dependence of the aggregate size on stirrer speed, concentration of solids, destabilizer concentration, and vessel size. The following studies are presented: aggregation theory; hydrodynamics in stirred tanks; numerical particle tracking in a turbine agitated vessel; aggregation kinetics in stirred tanks; and maximum aggregate size in stirred tanks. The application of the model to describe the aggregation process in strirred tanks to experimental conditions other than those tested and to particulate systems with different physical properties is discussed. ESA

N92-29784# Massachusetts Inst. of Tech., Cambridge.
FORCES ON A PIPE BEND RESULTING FROM CLEARING A POOL OF LIQUID UPSTREAM
Andrew S. Neumann (Schlumberger Technologies Corp., Billerica, MA.) and Peter Griffith 1991 22 p Presented at the American Society of Mechanical Engineers Pressure Vessel and Piping Conference, New Orleans, LA, 21-25 Jun. 1992
(Contract DE-FG07-88ER-12822)
(DE92-004179; CONF-920631-3) Avail: CASI HC A03/MF A01

The forces experienced by a bend in a pipe when a pool of water upstream is cleared by a rush of air have been measured. These forces are found to be negligible as long as a transition to slug flow does not occur. This transition does not occur as long as the maximum liquid fraction in the pool is less than 20 percent. The forces experienced at the bend are greatly reduced if the slug has traveled more than 6 L/D's, a distance which is more than sufficient to insure that the slug has entrained air. The effect of an upstream expansion on the force experienced by the bend as a cleared air-water plug passes through it has also been measured. A conservative estimate of the maximum force can be made by assuming that the plug is composed entirely of liquid and moves at the mixture velocity characteristic of the small pipe. The measured maximum force decreases rapidly with increasing distance. These measurements will help in designing piping supports for lines which cannot be properly sloped or are downstream of a pressure relief valve. DOE

N92-29830*# National Aeronautics and Space Administration. Langley Research Center, Hampton, VA.
AERODYNAMIC DESIGN OPTIMIZATION USING SENSITIVITY ANALYSIS AND COMPUTATIONAL FLUID DYNAMICS Patent Application
Oktay Baysal, inventor (to NASA) (Old Dominion Univ., Norfolk, VA.) and Mohamad E. Eleshaky, inventor (to NASA) (Old Dominion Univ., Norfolk, VA.) 3 Jan. 1992 24 p
(Grant NAG1-1188)
(NASA-Case-LAR-14815-1-CU; NAS 1.71:LAR-14815-1-CU; US-Patent-Appl-SN-820432) Avail: CASI HC A03/MF A01

An efficient aerodynamic shape optimization method based on a computational fluid dynamics/sensitivity analysis algorithm has been developed which determines automatically the geometrical definition of an optimal surface starting from any initial arbitrary geometry. This method is not limited to any number of design variables or to any class of surfaces for shape definition. NASA

N92-29857# Universiteit Twente, Enschede (Netherlands). Faculty of Applied Mathematics.
MATHEMATICAL MODELLING OF SATURATED AND UNSATURATED GROUNDWATER FLOW
B. H. Gilding Aug. 1991 169 p
(MEMO-987; ISSN-0169-2690; ETN-92-91593) Avail: CASI HC A08/MF A02

Lectures concerning the practical application of mathematical models for ground water resources evaluation and their theoretical analysis are presented. The occurrence of groundwater in the Earth's subsurface, the distinction between saturated and unsaturated soils, and the derivation of an equation of motion for groundwater flow, are discussed. From the latter, it is shown how equations which are practical for modeling groundwater movement in a saturated soil on a regional scale can be obtained; the numerical solution of these equations using the finite element method is outlined. The application of a computer program to a case study, a general strategy, and tips for the application of such models, are described. A review of techniques for mathematically modeling groundwater flow in an unsaturated soil profile is given. A survey of recent results on the analysis of one of the partial differential equations, introduced as a model for the one dimensional flow of water in an unsaturated soil, is given. Particular attention is paid to the analysis of the qualitative behavior of solutions of the equation and the physical interpretation of the results. The use of similarity solutions in analyzing partial differential equations is addressed. The porous media equation is a prototype for the equations considered. The derivation and analysis of a class of similarity solutions of this equation are studied. ESA

N92-29926# Technische Univ., Brunswick (Germany, F.R.). Fakultaet fuer Maschinenbau und Elektrotechnik.
EXPERIMENTAL EXAMINATION OF HEAVY LOADED AXIAL FANS WITH ROTATIONAL SYMMETRICAL DISTORTION OF THE INFLOW Ph.D. Thesis [EXPERIMENTELLE UNTERSUCHUNGEN HOCHBELASTETER AXIALVENTILATOREN BEI ROTATIONSSYMMETRISCHER STOERUNG DER ZUSTROEMUNG]
Roland Koerner 1991 199 p In GERMAN
(ETN-92-91489) Avail: CASI HC A09/MF A03

The effects of rotational symmetrical inflow distortions on three aerodynamic heavy loaded bladings are experimentally examined with various design flow coefficients and various design pressure coefficients. It is shown that an additional overall pressure loss in the ventilator installation is related to the production of various flow profiles. The variation of velocity energy in the test levels zero and six, is to be taken into account for rotational symmetrical distortion of the flow. ESA

N92-29933# Pennsylvania State Univ., University Park. Turbomachinery Lab.
EXPLICIT NAVIER-STOKES COMPUTATION OF TURBOMACHINERY FLOWS Final Report, 1 Aug. 1986 - 31 Dec. 1991
Robert F. Kunz and Budugur Lakshminarayana Jan. 1992 23 p
(Contract DAAL03-86-G-0044)
(AD-A248458; PSU-TURBO-9201) Avail: CASI HC A03/MF A01

A new three-dimensional explicit Navier-Stokes procedure was developed for computation of turbulent turbomachinery flows. Several numerical strategies and modelling techniques were developed and incorporated which enable convergent and accurate predictions of high Reynolds number flow fields across a wide range of Mach numbers. These include incorporation of a compressible low Reynolds number form of the k-e turbulence model in a fully explicit fashion, appropriate stability bound treatment of the transport turbulence model and other physical and solution parameters, eigenvalue and local velocity artificial dissipation scalings, a compact flux evaluation procedure and a hybrid low Reynolds number kappa-sigma/algebraic Reynolds stress model. This report provides a summary of this research. In what follows, primary research findings are summarized (details provided in cited references by the present authors), and several sample turbomachinery application results are provided. Specifically, two-dimensional results are provided for a supersonic compressor cascade operating at unique incidence condition. Three-dimensional validation is provided by a high Reynolds number axial rotor flow, for which extensive experimental data is available. This large scale computation is shown to capture rotational inviscid, blade and endwall boundary layer and wake flow physics, including

spanwise mixing effects, with good accuracy. Finally, a backswept transonic centrifugal compressor flow, for which L2F meridional passage velocity measurements are available, are computed.
GRA

N92-29944# Center for Mathematics and Computer Science, Amsterdam (Netherlands). Dept. of Numerical Mathematics.
NUMERICAL METHODS FOR THE 3D SHALLOW WATER EQUATIONS ON VECTOR AND PARALLEL COMPUTERS
Erik D. deGoede Apr. 1991 18 p Submitted for publication
Sponsored by Ministry of Transport and Public Works and Netherlands Organization for Applied Scientific Research TNO
(CWI-NM-R9109; ETN-92-91656) Copyright Avail: CASI HC A03/MF A01

Since three dimensional models require a great computational effort, it is important to construct methods that are not only accurate, but also efficient in vector and parallel computers. The accuracy and efficiency of a conditionally stable and an unconditionally stable method are compared on a minisupercomputer with four vector processors. The unconditionally stable method consist of two stages and required the solution of a sequence of linear systems. For the solution of these systems, a Jacobi type iteration method and a conjugate gradient iteration method are applied. The performance of both iteration methods is accelerated by a technique based on smoothing. Both explicit and implicit smoothing is examined. It turns out that the unconditionally stable method is more efficient than the conditionally stable method. ESA

N92-29945# Center for Mathematics and Computer Science, Amsterdam (Netherlands). Dept. of Numerical Mathematics.
ON THE NUMERICAL TREATMENT OF THE ADVECTIVE TERMS IN 3D SHALLOW WATER MODELS
Erik D. deGoede Apr. 1991 15 p Submitted for publication
Sponsored by Ministry of Transport and Public Works and Netherlands Organization for Applied Scientific Research TNO
(CWI-NM-R9110; ETN-92-91657) Copyright Avail: CASI HC A03/MF A01

A numerical method for the three dimensional shallow water equations is developed. These equations describe flows in for example, shallow seas, rivers, and estuaries. Since three dimensional models require a great computational effort, the method is constructed in such a way that it fully exploits the facilities of vector and parallel computers. The two stage method, which is unconditionally stable, is applied to a problem involving the development of a circulation in a rectangular basin and to a river problem in which a jetty was situated. ESA

N92-29947# Center for Mathematics and Computer Science, Amsterdam (Netherlands). Dept. of Numerical Mathematics.
APPLICATION OF A MOVING-GRID METHOD TO A CLASS OF 1D BRINE TRANSPORT PROBLEMS IN POROUS MEDIA
Paul A. Zegeling, J. G. Verwer, and J. C. H. vanEijkeren (National Inst. of Public Health, Bilthoven, Netherlands) Jun. 1991 29 p Submitted for publication
(Contract STW-CWI-59-0922)
(CWI-NM-R9112; ETN-92-91659) Copyright Avail: CASI HC A03/MF A01

The application of a numerical method for predicting transport of pollutants to a class of nonlinear, brine transport problems in one space dimension is illustrated. The moving grid method is described and the most important properties and principles of this numerical method are outlined. The class of one dimensional fluid flow/salt transport problems is discussed. Results of a number of illustrative tests are presented. ESA

N92-29954*# National Aeronautics and Space Administration. Langley Research Center, Hampton, VA.
ACTIVE THERMAL ISOLATION FOR TEMPERATURE RESPONSIVE SENSORS Patent Application
Scott D. Martinson, inventor (to NASA), David L. Gray, inventor (to NASA), Debra L. Carraway, inventor (to NASA), and Daniel C. Reda, inventor (to NASA) 2 Jan. 1992 16 p
(NASA-Case-LAR-14612-1; NAS 1.71:LAR-14612-1; US-Patent-Appl-SN-820431) Avail: CASI HC A03/MF A01

The detection of flow transition between laminar and turbulent flow and of shear stress or skin friction of airfoils is important in basic research for validation of airfoil theory and design. These values are conventionally measured using hot film nickel sensors deposited on a polyimide substrate. The substrate electrically insulates the sensor and underlying airfoil but is prevented from thermally isolating the sensor by thickness constraints necessary to avoid flow contamination. Proposed heating of the model surface is difficult to control, requires significant energy expenditures, and may alter the basic flow state of the airfoil. A temperature responsive sensor is located in the airflow over the specified surface of a body and is maintained at a constant temperature. An active thermal isolator is located between this temperature responsive sensor and the specific surface of the body. The total thickness of the isolator and sensor avoid any contamination of the flow. The temperature of this isolator is controlled to reduce conductive heat flow from the temperature responsive sensor to the body. This temperature control includes (1) operating the isolator at the same temperature as the constant temperature of the sensor; and (2) establishing a fixed boundary temperature which is either (a) less than or equal to or (b) slightly greater than the sensor constant temperature. The present invention accordingly thermally isolates a temperature responsive sensor in an energy efficient, controllable manner while avoiding any contamination of the flow. NASA

N92-29968# Technische Univ., Berlin (Germany, F.R.). Inst. fuer Mechanik.
THEORETICAL AND EXPERIMENTAL ASPECTS OF VELOCITY SLIP BY FLOWS ALONG SOLID WALLS Ph.D. Thesis [GESCHWINDIGKEITSSLIP BEI STROEMUNGEN LAENGS FESTER WAENDE]
Seied Mohammad Nasseri 1991 162 p In GERMAN
(ISBN-3-7983-1446-2; ISSN-0170-8902; ETN-92-91735) Avail: CASI HC A08/MF A02

The solution of linearized Navier-Stokes theory is presented in a spherical coordinate system for the stationary flow around a sphere by using product formulations represented as exponential, Legendre, and Bessel functions. Because of the rotation symmetry, the problem was considered as an analytical specific biharmonic boundary value problem by using the generalized boundary conditions which contain all relative velocity variables between wall and fluid such as ideal slip and wall adhesion. The analytical results were graphically discussed and evaluated for the flow field and velocities for varied Reynolds numbers. Tests in plane laminar channel flows for varied structured channel surfaces validate the slip assumption. ESA

N92-29972# Universiteit Twente, Enschede (Netherlands). Faculty of Applied Mathematics.
A FINITE VOLUME APPROACH TO LARGE EDDY SIMULATION OF COMPRESSIBLE, HOMOGENEOUS, ISOTROPIC, DECAYING TURBULENCE
A. W. Vreman, B. J. Geurts, J. G. M. Kuerten, and P. J. Zandbergen 28 Oct. 1991 28 p
(MEMO-1009; ISSN-0169-2690; ETN-92-91756) Avail: CASI HC A03/MF A01

Large eddy simulation (LES) of compressible, homogeneous, isotropic, decaying turbulence in a rectangular box is performed using finite volume techniques. Spectral analysis of the results of the simulations shows that an agreement with the Kolmogorov law for the inertial range can be reproduced only when an appropriate spatial discretization method is used. This agreement is obtained both for a low (0.05) and a moderate (0.6) Mach number when Smagorinsky's subgridmodel is employed. ESA

N92-29977# Universiteit Twente, Enschede (Netherlands). Faculty of Applied Mathematics.
MONOPOLAR VORTICES AS RELATIVE EQUILIBRIA AND THEIR DISSIPATIVE DECAY

B. W. vandeFliert and E. W. C. vanGroesen Nov. 1991 26 p (MEMO-1015; ISSN-0169-2690; ETN-92-91761) Avail: CASI HC A03/MF A01

Families of confined rotating monopolar vortices are characterized using a variational formulation with the angular momentum as the driving force for confinement. The characterization for positive monopolar vortices given, can be extended to negative vortices or to vortices within a rotating frame of reference. Besides the uniform Kirchhoff paths, new branches of vorticity solutions are found restricting the dynamics to levelsets of both the angular momentum and the quadratic anisotropy. The rotation rate of the smooth vorticity structures depends on the vorticity profile. This is made perceptible by considering both minimum energy vortices and minimizing vortices, rotating counterclockwise and clockwise respectively. An approximation for the decay of the vortices due to dissipation is given in terms of the dissipation of the integrals in the inviscid system. This description enables us to consider dissipation of vortices without loss of confinement. The elliptical Kirchhoff patches are found to symmetrize into circular patches. The minimum energy vortices gradually diminish while expending their support, while the maximum energy vortices are unstable for the dissipative evolution. ESA

N92-29998# Deutsche Forschungsanstalt fuer Luft- und Raumfahrt, Lampoldshausen (Germany, F.R.). Inst. fuer Chemische Antriebe und Verfahrenstechnik.

A NUMERICAL AND EXPERIMENTAL INVESTIGATION OF THE THRUST VECTOR CONTROL BY SECONDARY GAS INJECTION Ph.D. Thesis - Tech. Univ. Munich [NUMERISCHE UND EXPERIMENTELLE UNTERSUCHUNGEN ZUR SCHUBVEKTORSTEUERUNG DURCH SEKUNDAERINJEKTION]

Winfried Waidmann Jul. 1991 128 p In GERMAN (DLR-FB-91-31; ISSN-0939-2963; ETN-92-91734) Avail: CASI HC A07/MF A02; DLR Wissenschaftlisches Berichtswesen, Postfach 90 60 58, 5000 Cologne, Fed. Republic of Germany, HC

A numerical and experimental analysis of the cross injection of secondary gas stream into a supersonic flow is presented. The two dimensional compressible Navier-Stokes equations were solved by the explicit Runge-Kutta finite volume method. The equations describing the turbulent flow are closed by an algebraic turbulence model. The results of the numerical calculations are compared with experimental results performed in a rectangular expansion nozzle with a two dimensional injector. Shadow graphs, wall pressure, and side thrust measurements were used as diagnostic tools. A parametric study concerning the influence of different injection conditions and gas media delivers the best injection conditions for a maximal side thust. The effect of the different jet injection conditions is discussed in connection with the corresponding flow structure. ESA

N92-30023# Helsinki Univ. of Technology, Espoo (Finland). Lab. of Thermal Engineering.

THE 2D-COMPUTATION OF AN AXIAL FAN WITH FINFLO

K. Eriksson 1992 16 p

(PB92-180678; Rept-68) Avail: CASI HC A03/MF A01

The flow pattern of an axial fan was simulated with a flow calculation program called FINFLO. The original program was modified. The modified version can handle internal two-dimensional viscous calculation. The modification concerning the boundary conditions is discussed. Author

N92-30024*# National Aeronautics and Space Administration. Langley Research Center, Hampton, VA.

HEAT EXCHANGER WITH OSCILLATING FLOW Patent Application

Stephen J. Scotti, inventor (to NASA), Max L. Blosser, inventor (to NASA), and Charles J. Camarda, inventor (to NASA) 24 Feb. 1992 21 p

(NASA-Case-LAR-14033-2; NAS 1.71:LAR-14033-2; US-Patent-Appl-SN-843653) Avail: CASI HC A03/MF A01

Various heat exchange apparatuses are described in which an oscillating flow of primary coolant is used to dissipate an incident heat flux. The oscillating flow may be imparted by a reciprocating piston, a double action twin reciprocating piston, fluidic oscillators or electromagnetic pumps. The oscillating fluid flows through at least one conduit in either an open loop or a closed loop. A secondary flow of coolant may be used to flow over the outer walls of at least one conduit to remove heat transferred from the primary coolant to the walls of the conduit. Author

N92-30036# National Inst. of Standards and Technology, Gaithersburg, MD. Chemical Engineering Div.

HEAT TRANSFER IN AN ALUMINUM HEAT EXCHANGER USING NORMAL HYDROGEN GAS Final Report

D. A. Olson Mar. 1992 170 p Sponsored in part by AF (Contract FY1456-91-N0054)

(PB92-172832; NISTIR-3987) Avail: CASI HC A08/MF A02

The report describes measured heat transfer and pressure drop in a flat aluminum heat exchanger in normal hydrogen gas at 10.3 MPa and Reynolds numbers of 6600 to 24,600. The heat exchanger was 3.7 mm thick and contained 13 parallel flow channels of rectangular cross section, 1.32 mm wide and 2.64 mm high. The heat exchanger was insulated on the back and radiatively heated on the top with heat fluxes up to 88 W/sq cm. The measured Nusselt number was independent of heating rate and was a function of Reynolds number only. Comparison of data to correlations from past studies, along with a numerical analysis, indicated large temperature variations from the heated side to the insulated side. Because the heat exchanger was brazed to a thick base, head conduction along the flow direction appeared to be significant. Author

N92-30041*# Stanford Univ., CA. Center for Turbulence Research.

ANNUAL RESEARCH BRIEFS, 1991

Debra Spinks, comp. Dec. 1991 394 p

(Contract NCC2-460)

(NASA-CR-189967; NAS 1.26:189967) Avail: CASI HC A17/MF A04

Given here are 1991 annual progress reports of the research fellows and students of the Center for Turbulence Research. Topics addressed include turbulence modeling and simulation, local isotropy in high Reynolds number flow, small-scale vortices in vortex flow, turbulence and vortex structures, dynamic models for large eddy simulation, Monte Carlo implementation of mapping closures, flame ignition in a premixed turbulent flow, streaks in turbulent boundary layers, and linear stability analysis of hypersonic boundary layers. For individual titles, see N92-30042 through N92-30071.

N92-30042*# Stanford Univ., CA. Center for Turbulence Research.

A PRELIMINARY EXPERIMENTAL INVESTIGATION OF LOCAL ISOTROPY IN HIGH-REYNOLDS-NUMBER TURBULENCE

Srinivas V. Veeravalli and Seyed G. Saddoughi *In its* Annual Research Briefs, 1991 Dec. 1991 p 3-20 (For primary document see N92-30041 20-34)

Avail: CASI HC A03/MF A04

Detailed measurements of the velocity field were made in the wall boundary layer of the 80 by 120 foot facility at NASA Ames. The Reynolds Number R(sub lambda), based on the Taylor microscale lambda at the measurement location, was approximately 1450, one of the largest attained in laboratory flows. The data indicate that to within measurement accuracy, the w-spectrum follows, but the v-spectrum deviates from, the isotropic relation in the inertial subrange. No definite statement can be made regarding local isotropy for the dissipating scales because the spectral measurements were contaminated by high-frequency electrical noise, but it appears that the inertial-subrange anisotropy persists in the dissipation region. Author

N92-30043*# Stanford Univ., CA. Center for Turbulence Research.

LOCAL ISOTROPY IN BUOYANCY-GENERATED TURBULENCE

Jeffrey R. Chasnov *In its* Annual Research Briefs, 1991 Dec. 1991 p 21-29 (For primary document see N92-30041 20-34)
Avail: CASI HC A02/MF A04

Batchelor et al. (1992) recently considered the turbulent motion generated by buoyancy forces acting on random fluctuations in the density of an infinite fluid. This homogeneous buoyancy-generated flow field with zero mean density gradient was conceived as an idealized system which, like isotropic turbulence, may be useful as a vehicle for the general study of turbulence. The Batchelor et al. study relied partly on theoretical analysis and partly on direct and large-eddy numerical simulations of the flow field. To this mix, we add here a two-point closure study based on the eddy-damped quasi-normal Markovian (EDQNM) closure model applied to axisymmetric turbulence. The EDQNM model has been shown to yield reasonably accurate quantitative results for a variety of problems in homogeneous turbulence (Lesieur 1987). The main advantage here in applying EDQNM to the buoyancy-driven flow field is the wide range of wavenumbers over which a solution of the EDQNM equations may be solved. Whereas a typical large-eddy simulation using 128(exp 3) grid points has a wavenumber range of only 60, the EDQNM calculation can be easily run with a wavenumber range of several decades. Because of the growth in length scales in the buoyancy-driven flow field, this large wavenumber range allows for a solution of the flow field well into its asymptotic regime. Recent comparisons between large-eddy simulations and closure theory (Herring 1990) indicate that a time longer than that attainable by current large-eddy simulations is required to reach flow asymptotics and that conclusions based on large-eddy simulation results may be based only on an intermediate transient state. We briefly introduce the EDQNM equations for the buoyancy-generated flow field. We then present a Kolmogorov-like theoretical argument on the scaling of the small-scale spectra. This scaling is then confirmed by numerical solution of the EDQNM equations. We briefly conclude with possible future research directions. Author

N92-30044*# Stanford Univ., CA. Center for Turbulence Research.
NON-LINEAR INTERACTIONS IN HOMOGENEOUS TURBULENCE WITH AND WITHOUT BACKGROUND ROTATION
Fabian Waleffe *In its* Annual Research Briefs, 1991 Dec. 1991 p 31-43 (For primary document see N92-30041 20-34)
Avail: CASI HC A03/MF A04

Domaradzki et al. concluded (1988, 1990 a,b) that turbulent transfers are dominated by non-local interactions with local energy transfer. This is only partly consistent with the common wisdom that local interactions with local energy transfer dominate the inertial cascade. Brasseur et al. (1991 a,b,c) then called on this predominance of non-local interactions to refute the Kolmogorov assumption of local isotropy at the small scales. The inertial wave decomposition showed features observed in the simulations. A deeper analysis was undertaken in search of a better understanding of triad interactions and of the significance of the numerical results. The helical (or inertial wave) decomposition of the velocity field clearly identified two types of triadic transfers depending on whether the small scale helical modes have helicities of the same or the opposite sign. Only one type of interaction shows local transfer when the triads are non-local. In those cases, the local cascade to higher wavenumber must always be accompanied by a feedback on the large scale. An instability principle, suggested by the stability characteristics of triad interactions, has been introduced and predicts the direction of the energy transfers. These predictions agree with DNS and the Test Field Model. Author

N92-30045*# Stanford Univ., CA. Center for Turbulence Research.
ON SMALL SCALE VORTICES IN TURBULENT FLOWS
J. Jimenez *In its* Annual Research Briefs, 1991 Dec. 1991 p 45-56 (For primary document see N92-30041 20-34)
Avail: CASI HC A03/MF A04

Douady et al., 1991 produced direct experimental visualizations of strong concentrated persistent vortices in homogeneous turbulence, and (Schwarz, 1990) published pictures of organized strain structures which show up as alternating bands of consistent orientation of flakes suspended in a grid-stirred flow. It is not clear how or whether these structures are connected to the vortex tubes, but they are persistent and seem to have comparable dimensions. We summarize here the experimental evidence available for compact, small scale vorticity structures, using both published results and other available numerical flow fields. That evidence shows that there is a certain homogeneity of the small structures across flows whose large scale character is very different. We use those general characteristics to define a simple model for the small scale vortices and, in particular, to explain some of the experimental observed relations between the vorticity and the rate of strain tensor. Our main result is that many of those properties turns out to be essentially kinematic. Author

N92-30046*# Stanford Univ., CA. Center for Turbulence Research.
SCALING ANALYSIS OF ENERGY TRANSFER IN THE INERTIAL RANGE
Ye Zhou *In its* Annual Research Briefs, 1991 Dec. 1991 p 57-66 (For primary document see N92-30041 20-34)
Avail: CASI HC A02/MF A04

Addressed here is a fundamental question regarding the energy transfer process. At issue is the appropriate choice of a statistical quantity to indicate the nature of energy transfer across the spectrum. Basically, the problem is that the system is conservative, with T(k) less than 0 for small k and T(k) greater than 0 for large k, but since we cannot tag energy, we cannot follow its flow. Our investigation indicates that although the quantity measured by cited papers is a mathematical building block in the energy transfer process, it is not the appropriate physical quantity one should use to determine whether the nonlinear interactions are local or nonlocal. With the use of an existing DNS flow database, we have clarified these issues by making measurements of quantities that directly reflect the actual scale disparity of the interactions contributing to the energy transfer process. We found that the net flux results primarily from interaction in which the ratio of largest to smallest scale is less than 10. Author

N92-30047*# Stanford Univ., CA. Center for Turbulence Research.
LAGRANGIAN VELOCITY CORRELATION AND SPECTRUM IN HOMOGENEOUS ISOTROPIC TURBULENCE
T. Gotoh, R. S. Rogallo (National Aeronautics and Space Administration. Ames Research Center, Moffett Field, CA.), and J. R. Herring (National Center for Atmospheric Research, Boulder, CO.) *In its* Annual Research Briefs, 1991 Dec. 1991 p 67-84 (For primary document see N92-30041 20-34)
Avail: CASI HC A03/MF A04

The Lagrangian velocity correlation and its spectrum are computed by direct numerical simulation (DNS) using the passive vector method (PVM), and the validity of the method is studied. It is found that the PVM is accurate when K(sub max)/K(sub d) is greater than or equal to 2 where k(sub max) is the maximum wavenumber carried in the simulation and K(sub d) is the Kolmogorov wavenumber. The Eulerian and Lagrangian velocity correlations for various wavenumber bands are compared. At moderate to high wavenumber, the Eulerian velocity correlation decays faster than the Lagrangian, and the effect of sweep on the former is observed. The time scale of the Eulerian correlation is found to be (kU sub 0)(exp -1) and that of the Lagrangian to be ((integral limits k,0) p squared E(p)dp)(exp 1/2). The Markovianized Lagrangian renormalized approximation (MLRA) is compared to the DNS, and good agreement is found for one-time quantities in decaying turbulence at low Reynolds numbers and for the Lagrangian velocity autocorrelation in steady turbulence at moderate Reynolds number. The effect of intermittency on the Lagrangian correlation is discussed. Author

N92-30048*# Stanford Univ., CA. Center for Turbulence Research.
TURBULENCE AND VORTEX STRUCTURES

Eliot Dresselhaus *In its* Annual Research Briefs, 1991 Dec. 1991 p 85-92 (For primary document see N92-30041 20-34)
Avail: CASI HC A02/MF A04

The presence of vortex structures makes it tempting to view high Reynolds numbers velocity fields as some sort of spatial and temporal superposition of structured and random regions (She, Jackson, Orszag 1990). In this view, random regions contain most of the turbulent kinetic energy of the fluid; structured regions, on the other hand, contain little kinetic energy but do contain most of the flow's viscous energy dissipation. Thus, vortex structures are skeletons of non-limear dynamic activity which separate regions of relatively strong kinetic energy from regions of relatively strong viscous dissipation and dynamically moderate energy transfers from large to small scales. Seen in this way, the traditional picture of a spatially fractal energy cascade, in which eddies interact with smaller eddies which interact with smaller eddies and so on until being dissipated at viscous scales, is likely wrong. Energy can certainly be transmitted directly from large to small scales, presumably via vortex structures and their dynamical interactions, without necessarily being moderated by a recursive hierarchy of intermediate scales. If this is the case, then what is it about the nonlinear interactions which makes turbulence self-similar? As a starting point for these more general issues, the following questions need to be answered. What are vortex structures? How are they born? How do they die? What Navier-Stokes dynamics generate them? These questions have been the subject of previous work (Dresselhaus and Tabor, 1991) and are the subject of present investigations whose progress is briefly described here. Author

N92-30049*# Stanford Univ., CA. Center for Turbulence Research.
VORTICITY MATCHING IN SUPERFLUID HELIUM
David C. Samuels *In its* Annual Research Briefs, 1991 Dec. 1991 p 93-104 (For primary document see N92-30041 20-34)
Avail: CASI HC A03/MF A04

Recent experiments have rekindled interest in high Reynolds number flows using superfluid helium. In a continuing series of experiments, the flow of helium II through various devices (smooth pipes, corrugated pipes, valves, venturies, turbine flowmeters, and coanda flowmeters for example) was investigated. In all cases, the measured values (typically, mass flow rates and pressure drops) were found to be well described by classical relations for high Reynolds flows. This is unexpected since helium II consists of two interpenetrating fluids; one fluid with nonzero viscosity (the normal fluid) and one with zero viscosity (the superfluid). Only the normal fluid component should directly obey classical relations. Since the experiments listed above only measure the external behavior of the flow (i.e., pressure drops over devices), there is a great deal of room for interpretation of their results. One possible interpretation is that in turbulent flows the normal fluid and the superfluid velocity fields are somehow 'locked' together, presumably by the mutual friction force between the superfluid vortex filaments and the normal fluid. We refer to this locking together of the two fluids as 'vorticity matching.' Author

N92-30050*# Stanford Univ., CA. Center for Turbulence Research.
THE ROLE OF PRESSURE-DILATATION CORRELATION IN RAPIDLY COMPRESSED TURBULENCE AND IN BOUNDARY LAYERS
O. Zeman *In its* Annual Research Briefs, 1991 Dec. 1991 p 105-117 (For primary document see N92-30041 20-34)
Avail: CASI HC A03/MF A04

This work is a result of a continuing effort to advance our understanding of the compressibility effects on turbulence and to develop new, and improve the old, models for compressible turbulent flows. A specific goal reported here was the investigation of the role of pressure-dilatation correlation in rapidly compressed turbulence and in boundary layers in general. The rapid compression process is present in flows of practical importance such as in internal combustion engines and in boundary layer/shock interactions. Author

N92-30051*# Stanford Univ., CA. Center for Turbulence Research.
ANALYSES AND MODELING OF EVOLVING TURBULENT FLOW
P. A. Durbin *In its* Annual Research Briefs, 1991 Dec. 1991 p 119-135 (For primary document see N92-30041 20-34)
Avail: CASI HC A03/MF A04

Work done during this year includes the following: an asymptotic analysis of adverse pressure gradient boundary layers; and a rapid-distortion analysis of homogeneous, compressed turbulence and formulation of a new pressure-dilatation model therefrom. Additionally, a refinement of the kappa-epsilon-nu near-wall model, with an extension to calculations of heat transfer, is presented. Author

N92-30052*# Stanford Univ., CA. Center for Turbulence Research.
NEAR-WALL TURBULENCE MODELING FOR BOUNDARY LAYERS WITH SEPARATION
S. H. Ko *In its* Annual Research Briefs, 1991 Dec. 1991 p 137-146 (For primary document see N92-30041 20-34)
Avail: CASI HC A02/MF A04

As a turbulent boundary layer undergoes a strong adverse pressure gradient, the flow may separate from the wall, and the use of empirical wall functions is inappropriate. The turbulence transport equations as well as the momentum equations must be solved through the laminar sublayer to the wall. The laminar sublayer encompasses a region where viscous effects become increasingly important. For the past two decades, many proposals for near-wall turbulence models of the kappa-epsilon type have been presented for calculating near-wall flows. A thorough review and a systematic evaluation of these models was previously given. It was found that some of the models tested failed to reproduce even the simple flat-plate boundary layer flow. Overall, the authors concluded that the near-wall turbulence models needed further refinement if they were to be used with confidence to calculate near-wall flows. Recently, the use of a direct numerical simulation (DNS) data base has provided new insight and data for development and testing of near-wall turbulence models. Author

N92-30053*# Stanford Univ., CA. Center for Turbulence Research.
MODELING TURBULENT BOUNDARY LAYERS IN ADVERSE PRESSURE GRADIENTS
S. E. Belcher *In its* Annual Research Briefs, 1991 Dec. 1991 p 147-157 (For primary document see N92-30041 20-34)
Avail: CASI HC A03/MF A04

The phenomenon of separation of a turbulent boundary layer has important implications for practical applications but remains little understood. The overall aims of this research are to gain theoretical understanding of the physical processes that are important in governing the separation and thence to develop closure models to predict these flows. Author

N92-30054*# National Aeronautics and Space Administration. Ames Research Center, Moffett Field, CA.
SINGLE POINT MODELING OF INITIALLY ISOTROPIC TURBULENCE UNDER UNIFORM ROTATION
N. N. Mansour, C. Cambon (Ecole Centrale de Lyon, France), and C. G. Speziale (Institute for Computer Applications in Science and Engineering, Hampton, VA.) *In* Stanford Univ., Annual Research Briefs, 1991 Dec. 1991 p 159-167 (For primary document see N92-30041 20-34)
Avail: CASI HC A02/MF A04

Direct numerical simulations (DNS) of initially isotropic turbulence in a rotating frame were conducted, and comparisons were made with the predictions of generalized Eddy-Damped Quasi-Normal Markovian (EDQNM) approximations. It was found that for increasing rotation rates the non-linear triad interactions are reduced, causing a reduction in the energy cascade and the turbulence decay rate. At small Rossby numbers (R(sub 0) less than 0.01), the transfer of energy is essentially shut-off. The effects of rotation on one-point statistics are reflected in a reduction of

the production of enstrophy on a time scale of O(1/omega), while the destruction of enstrophy is affected on a time scale of O(kappa/epsilon). A one-point closure model that properly simulates these effects is presented and comparisons are made with DNS results. Author

N92-30055*# Stanford Univ., CA. Center for Turbulence Research.
DERIVATION OF THE KAPPA-EPSILON MODEL EQUATIONS USING THE RENORMALIZATION GROUP METHOD
L. M. Smith *In its* Annual Research Briefs, 1991 Dec. 1991 p 169-176 (For primary document see N92-30041 20-34)
Avail: CASI HC A02/MF A04

We have made a critical study of the renormalization group (RNG) theory of turbulence proposed in an earlier study. The results of that study were reported in full detail. Our independent study led to confirmation of the previous study's basic theory of the Navier-Stokes equations, but errors were found in their derivations of the velocity-derivative skewness and the model transport equation for the mean dissipation rate of energy, epsilon. The most consequential changes over the earlier report were in the epsilon model equation. As will be explained, our efforts have led to a reformulation of the previous study's RNG method for derivation of model transport equations. Author

N92-30056*# Stanford Univ., CA. Center for Turbulence Research.
ON DYNAMIC MODELS FOR LARGE EDDY SIMULATION
T. S. Lund *In its* Annual Research Briefs, 1991 Dec. 1991 p 177-190 (For primary document see N92-30041 20-34)
Avail: CASI HC A03/MF A04

The restriction to low Reynolds numbers is a well known limitation of the direct numerical simulation (DNS) technique. It is easy to show that the number of grid points required to resolve all the scales of motion increases with the 9/4 power of the Reynolds number. It is clear that direct simulation of the high Reynolds number flows found in engineering applications will continue to exceed computer hardware limitations for the foreseeable future. Author

N92-30057*# Stanford Univ., CA. Center for Turbulence Research.
LARGE EDDY SIMULATIONS OF PASSIVE AND BUOYANT SCALARS WITH DYNAMIC SUBGRID-SCALE MODELS
W. Cabot *In its* Annual Research Briefs, 1991 Dec. 1991 p 191-205 (For primary document see N92-30041 20-34)
Avail: CASI HC A03/MF A04

The immediate goal of this work is to test the performance of the dynamic subgrid-scale (SGS) model and some of its possible variants in incompressible channel flow with passive scalars and with Boussinesq buoyancy. The large eddy simulation (LES) results with the dynamic SGS model will be compared with low Reynolds number direct numerical simulation (DNS) data and with higher Reynolds number laboratory data. The consequences of implementing the dynamics SGS model at a local level rather than using globally averaged coefficients, which would be useful for applications with more complex geometries, will also be explored. A longer range goal of this work will be to test the performance of SGS models in the LES of flows with more complicated physics (e.g., rotation and density stratification), applicable to geophysical and astrophysical systems. Author

N92-30058*# Stanford Univ., CA. Center for Turbulence Research.
DYNAMIC SUBGRID-SCALE MODELING OF COMPRESSIBLE TURBULENCE
Kyle D. Squires *In its* Annual Research Briefs, 1991 Dec. 1991 p 207-223 (For primary document see N92-30041 20-34)
Avail: CASI HC A03/MF A04

The dynamic subgrid-scale modeling concept formulated by Germano et al. (1991) for incompressible flows was successfully extended to compressible turbulence. Most of the results of this extension have been reported by Moin et al. (1991). The main accomplishments and unresolved issues are highlighted, and possible directions for future work and improvements to the concept of dynamic modeling for large eddy simulation are provided. Author

N92-30059*# Stanford Univ., CA. Center for Turbulence Research.
PROBABILITY DENSITY FUNCTION APPROACH AND RELATED CLOSURES FOR TURBULENT SCALAR FIELDS
Feng Gao *In its* Annual Research Briefs, 1991 Dec. 1991 p 225-236 (For primary document see N92-30041 20-34)
Avail: CASI HC A03/MF A04

Our current study generally concerns the development of probability density function (PDF) methodology in turbulence research. More specifically, our efforts were focused on various aspects of the mapping closure models in PDF approach. The results of mapping closure are tested against the available direct numerical simulation (DNS) data to further validate the model. Encouraged by the success of single scalar mapping closure, we have extended the same idea to cases with more than one species, which is a rather natural step because most reactions involve many reacting species. Author

N92-30060*# Stanford Univ., CA. Center for Turbulence Research.
MONTE-CARLO IMPLEMENTATION OF MAPPING CLOSURES: APPLICATION TO CHEMICAL REACTING FLOWS
Luis Valino *In its* Annual Research Briefs, 1991 Dec. 1991 p 237-249 Sponsored in part by the Spanish government (For primary document see N92-30041 20-34)
Avail: CASI HC A03/MF A04

The first objective of this research is to solve the probability density function (PDF) equation of one reacting scalar in a constant density homogeneous turbulent field with a Monte-Carlo technique, using a mapping closure for the diffusion term. The second objective is to solve a similar problem for the multispecies case. The choice of a suitable method to calculate the needed characteristic time-scale should follow the accomplishment of these two objectives. Further extensions to more complex flows are also the aim of this research. Author

N92-30061*# Stanford Univ., CA. Center for Turbulence Research.
FLAME IGNITION IN A PREMIXED TURBULENT FLOW
T. J. Poinsot (Centre National de la Recherche Scientifique, Paris, France) *In its* Annual Research Briefs, 1991 Dec. 1991 p 251-272 (For primary document see N92-30041 20-34)
Avail: CASI HC A03/MF A04

A preliminary study of the ignition of a premixed flame front in a 2-D turbulent flow is presented. Flame ignition is studied using full numerical simulation including heat release, variable fluid properties, and one-step Arrhenius chemistry. The effects of turbulence on the flame growth as well as the effects of the flame on the surrounding turbulence are described. It is shown that, if combustion is successfully initiated, the initial growth is always laminar-like mainly because of dilatation effects through the flame front. Later, the turbulent fluctuations begin to wrinkle the flame and transition to turbulent propagation takes place. The influence of numerical parameters such as boundary and initial conditions is considered. The effect of Lewis number is evidenced by comparing the growth of two flames with the same flame speeds in the same turbulence but with different Lewis numbers (Le = 1.2 and Le = 0.53). Author

N92-30062*# Stanford Univ., CA. Center for Turbulence Research.
SIMULATION OF FLAME-TURBULENCE INTERACTIONS IN PREMIXED COMBUSTION
A. Trouve *In its* Annual Research Briefs, 1991 Dec. 1991 p 273-286 (For primary document see N92-30041 20-34)
Avail: CASI HC A03/MF A04

Turbulent combustion is a challenging practical problem where

fluid-mechanics and chemistry are strongly coupled. The general motivation of this work is to increase our basic understanding of flame-flow interactions under turbulent conditions. The approach consists of applying direct numerical simulation (DNS) methods of turbulent combustion. The objectives in 1991 were twofold: (1) to investigate the flamelet models used in engineering calculations of turbulent combustion with the objective of studying the combined effects of flame curvature and hydrodynamic straining on the structure of premixed turbulent flames with non-unity Lewis number; and (2) to develop a new 3-D data base of premixed flames embedded in a variety of basic turbulent flow fields. Author

N92-30063*# Stanford Univ., CA. Center for Turbulence Research.

LINEAR STABILITY ANALYSIS OF HYPERSONIC BOUNDARY LAYERS

E. Guilyardi, J. J. W. vanderVegt, and J. H. Ferziger *In its* Annual Research Briefs, 1991 Dec. 1991 p 287-298 Sponsored in part by Dassault Aviation, France (For primary document see N92-30041 20-34)

Avail: CASI HC A03/MF A04

With the aid of temporal linear stability code COSAL, our goal is to generate profiles of the most unstable waves to provide initial data for the direct numerical simulation code written by van der Vegt (1990). The COSAL code was modified in several ways to meet this requirement. Improvements needed in the accuracy of the computation of the eigenfunction were noted in van der Vegt and Ferziger (1990). Various numerical methods and grid adaptation were applied in order to increase the accuracy of the results produced by the linear stability code. Author

N92-30064*# Stanford Univ., CA. Center for Turbulence Research.

METHODS FOR DIRECT SIMULATION OF TRANSITION IN HYPERSONIC BOUNDARY LAYERS 2

J. J. W. vanderVegt *In its* Annual Research Briefs, 1991 Dec. 1991 p 299-307 (For primary document see N92-30041 20-34)

Avail: CASI HC A02/MF A04

The prediction of transition to turbulence in compressible boundary layers currently receives significant attention due to its importance in the design of high speed transport vehicles. Drag, lift, and heat transfer strongly depend on whether the boundary layer is laminar or turbulent. The study of transition in compressible boundary layers by means of direct numerical simulation (DNS) provides information not available from the commonly used linear and nonlinear stability theories. We want to study flows with both strong shocks and boundary layers, but, unfortunately, most shock capturing schemes are very dissipative in the boundary layer. We have previously presented a fully implicit finite volume method, and significant progress was made in improving the efficiency of a fully implicit method without using the approximate factorization method of Beam and Warming (1978). The finite volume method, however, is only second order accurate, and it was felt that higher order accuracy is necessary in order for success in direct numerical simulation of transition. The construction of an implicit and time accurate fourth order scheme is discussed. Author

N92-30065*# Stanford Univ., CA. Center for Turbulence Research.

EFFECT OF WALLS ON THE SUPERSONIC REACTING MIXING LAYER

D. S. Shin and J. H. Ferziger *In its* Annual Research Briefs, 1991 Dec. 1991 p 309-330 (For primary document see N92-30041 20-34)

Avail: CASI HC A03/MF A04

Most stability analyses of supersonic mixing layers have considered unconfined shear layers. However, the supersonic mixing layers in ramjet combustors and most experiments are confined by solid walls. To include the effect of chemical reactions, the authors consider a reacting mixing layer in a channel. The chemistry model is a finite rate single step irreversible reaction with Arrhenius kinetics. All flow variables are nondimensionalized by their fast-stream values. The effects of heat release, Mach number, frequency, wavenumber, thickness of shear layer, as well as distance between walls and direction of wave propagation are considered. H.A.

N92-30066*# Stanford Univ., CA. Center for Turbulence Research.

DIRECT NUMERICAL SIMULATION OF INSTABILITY AND NOISE GENERATION OF HOT JETS

M. C. Jacob *In its* Annual Research Briefs, 1991 Dec. 1991 p 331-341 (For primary document see N92-30041 20-34)

Avail: CASI HC A03/MF A04

The goal of the current investigation is to numerically simulate convectively and absolutely unstable jet flows in order to give a new insight into the underlying mechanisms of jet instabilities and their contributions to sound generation: DNS codes available at CTR solve the compressible Navier-Stokes equations and provide a very accurate flow representation. They have been able to simulate sound radiation and scattering (without an acoustical analogy or approximation). An application of these codes to heated 2-D jets has been started in this study and modifications have been made in order to allow for temperature dependent viscosity. Author

N92-30067*# Stanford Univ., CA. Center for Turbulence Research.

MIXING MEASUREMENTS OF STRAIGHT AND CURVED SHEAR LAYERS

P. S. Karasso and M. G. Mungal *In its* Annual Research Briefs, 1991 Dec. 1991 p 343-348 (For primary document see N92-30041 20-34)

Avail: CASI HC A02/MF A04

In the present study we are interested in measuring the concentration of probability density function (PDF) of mixing layers spanning the Reynolds number regime from 25,000 to about 90,000. The studies will occur in curved as well as straight layers so that firm conclusions can be reached about the effect of the two instabilities on the development of mixing layers and the effect of curvature on mixing efficiency. Finally, the issue of how resolution affects the outcome of a PDF measurement will be addressed via chemical reaction techniques and via relative resolution changes of acquired data. Author

N92-30068*# Stanford Univ., CA. Center for Turbulence Research.

PROGRESS TOWARD IDENTIFICATION OF STREAMWISE VORTICITY MEANDER IN A PLANE MIXING LAYER

R. L. LeBoeuf *In its* Annual Research Briefs, 1991 Dec. 1991 p 349-354 (For primary document see N92-30041 20-34)

Avail: CASI HC A02/MF A04

The main objective of the current project is to experimentally investigate streamwise vortical structures in mixing layers. This research program intends to clarify whether the observed decrease in mean streamwise vorticity in the far-field of mixing layers is due primarily to the 'smearing' caused by vortex meander or diffusion. The effects of vortex meander on the velocity statistics of a nominally linear array of simulated inviscid line vortices were examined. The two-point transverse velocity cross-correlations were deemed potentially useful for the identification of streamwise vortex meander in a plane mixing layer. Comparisons of these results to forthcoming simultaneous two-point cross-wire measurements in a plane mixing layer should shed some insight into the kinematics of mixing layer streamwise vorticity. Author

N92-30069*# Stanford Univ., CA. Center for Turbulence Research.

STREAKS IN TURBULENT BOUNDARY LAYERS

James M. Hamilton *In its* Annual Research Briefs, 1991 Dec. 1991 p 355-361 (For primary document see N92-30041 20-34)

Avail: CASI HC A02/MF A04

The objective of the present study is to pursue this idea of imposing symmetries on the marginal flow in an effort to identify

and understand the basic processes involved in the self-sustenance of turbulence. The simplest flow for the study of streak formation is the plane Couette flow, which has only a single sign of mean spanwise vorticity. The symmetries to be imposed on this flow are consistent with the expected structure. The computations are made with a slightly different version of the spectral code of Kim, Moin, and Moser. In addition to being consistent with streamwise vortices, the imposed symmetries must satisfy continuity, the Navier-Stokes equations, and the boundary conditions. Author

N92-30070*# Paris-Sud Univ., Orsay (France).
SOME FEEDBACK PROCEDURES FOR CONTROL OF FLOWS
Roger Temam *In* Stanford Univ., Annual Research Briefs, 1991 Dec. 1991 p 363-373 Prepared in cooperation with Indiana Univ., Bloomington (For primary document see N92-30041 20-34)
Avail: CASI HC A03/MF A04

In this article, we present some avenues concerning the application of the mathematical methods of control theory to the difficult and challenging problem of the control of turbulent flows. The effective implementation of these methods for the Burger's and Navier-Stokes equations is in progress at this time, with very satisfactory results already obtained in the case of the stochastic Burgers equation. Effective implementation and discussion of the physical relevance of the results will be presented elsewhere. Author

N92-30071*# Stanford Univ., CA. Center for Turbulence Research.
AN EXACT TURBULENT CLOSURE FOR THE HYDROMAGNETIC DYNAMO
Hubert H. Shen *In its* Annual Research Briefs, 1991 Dec. 1991 p 375-397 (For primary document see N92-30041 20-34)
Avail: CASI HC A03/MF A04

In the following we consider the hydromagnetic dynamo from the Hopf functional point of view. In the present paper, buoyancy, rotation, electrical conductivity, scalar diffusion, and source are incorporated. No perturbative, phenomenological or statistical assumptions or variational arguments are invoked; we seek an exact turbulent closure of the magnetohydrodynamic (MHD) equations. Equilibrium, stationary nonequilibrium, and time dependent solutions are proposed. No claim is made for uniqueness or completeness; however, the fact that (1) exact statistical solutions can be obtained at all, and that (2) in fact more than one class of solutions appears to emerge from this approach, seems sufficiently promising to warrant further investigation. Author

N92-30140# Mitre Corp., McLean, VA. Program Office.
CONTINUUM APPROACHES FOR DESCRIBING SOLID-GAS AND SOLID-LIQUID FLOW
P. Diamond, J. Harvey, H. Levine, P. Steinhardt, and R. Westervelt Feb. 1992 53 p
(Contract DE-AI05-90ER-30174)
(DE92-013601; JSR-90-310) Avail: CASI HC A04/MF A01

Two-phase continuum models have been used to describe the multiphase flow properties of solid-gas and solid-liquid mixtures. The approach is limited in that it requires many fitting functions and parameters to be determined empirically, and it does not provide natural explanations for some of the qualitative behavior of solid-fluid flow. In this report, we explore a more recent single-phase continuum model proposed by Jenkins and Savage to describe granular flow. Jenkins and McTigue have proposed a modified model to describe the flow of dense suspensions, and hence, many of our results can be straight-forwardly extended to this flow regime as well. The solid-fluid mixture is treated as a homogeneous, compressible fluid in which the particle fluctuations about the mean flow are described in terms of an effective temperature. The particle collisions are treated as inelastic. After an introduction in which we briefly comment on the present status of the field, we describe the details of the single-phase continuum model and analyze the microscopic and macroscopic flow conditions required for the approach to be valid. We then derive numerous qualitative predictions which can be empirically verified in small-scale experiments. The flow profiles are computed for simple boundary conditions, plane Couette flow and channel flow. Segregaion effects when there are two (or more) particle sizes are considered. The acoustic dispersion relation is derived and shown to predict that granular flow is supersonic. We point out that the analysis of flow instabilities is complicated by the finite compressibility of the solid-fluid mixture. For example, the large compressibility leads to interchange (Rayleigh-Taylor instabilities) in addition to the usual angular momentum interchange in standard (cylindrical) Couette flow. We conclude by describing some of the advantages and limitations of experimental techniques that might be used to test predictions for solid-fluid flow. DOE

N92-30149*# Stanford Univ., CA. Center for Turbulence Research.
ANNUAL RESEARCH BRIEFS, 1989
Debra Spinks, comp. Feb. 1990 274 p
(Contract NCC2-460)
(NASA-CR-189024; NAS 1.26:189024) Avail: CASI HC A12/MF A03

This report contains the 1989 annual progress reports of the Research Fellows of the Center for Turbulence Research. It is intended as a year end report to NASA, Ames Research Center which supports this group through core funding and by making available physical and intellectual resources. The Center for Turbulence Research is devoted to the fundamental study of turbulent flows; its objectives are to simulate advances in the physical understanding of turbulence, in turbulence modeling and simulation, and in turbulence control. The reports appearing in the following pages are grouped in the general areas of modeling, experimental research, theory, simulation and numerical methods, and compressible and reacting flows. For individual titles, see N92-30150 through N92-30169.

N92-30150*# Stanford Univ., CA. Center for Turbulence Research.
MODELING OF COMPRESSIBLE TURBULENCE
O. Zeman *In its* Annual Research Briefs, 1989 Feb. 1990 p 3-12 (For primary document see N92-30149 20-34)
Avail: CASI HC A02/MF A03

The work is directed toward understanding and modeling compressibility effects in turbulent flows. The primary objective is to investigate how compressibility influences the basic turbulence processes such as turbulence production and dissipation, length scale modification, spectral energy transfer, etc. The second objective is to develop parameterization schemes and models to incorporate compressibility into one-point closure models and into the subgrid scale models for LES techniques. The ultimate purpose of this research is to develop compressible turbulence models which are capable of handling the hypersonic regime. Specifically, the emphasis will be on the model capability of predicting: (1) heat and momentum transfer in hypersonic boundary layers; and (2) mixing and growth of high Mach number shear layers, jet and wakes. Author

N92-30151*# Stanford Univ., CA. Center for Turbulence Research.
TURBULENCE MODELING: NEAR-WALL TURBULENCE AND EFFECTS OF ROTATION ON TURBULENCE
T.-H. Shih *In its* Annual Research Briefs, 1989 Feb. 1990 p 13-26 (For primary document see N92-30149 20-34)
Avail: CASI HC A03/MF A03

Many Reynolds averaged Navier-Stokes solvers use closure models in conjunction with 'the law of the wall', rather than deal with a thin, viscous sublayer near the wall. This work is motivated by the need for better models to compute near wall turbulent flow. The authors use direct numerical simulation of fully developed channel flow and one of three dimensional turbulent boundary layer flow to develop new models. These direct numerical simulations provide detailed data that experimentalists have not been able to measure directly. Another objective of the work is to

examine analytically the effects of rotation on turbulence, using Rapid Distortion Theory (RDT). This work was motivated by the observation that the pressure strain models in all current second order closure models are unable to predict the effects of rotation on turbulence. H.A.

N92-30152*# Stanford Univ., CA. Center for Turbulence Research.
AN EXPERIMENTAL STUDY OF SCALAR MIXING IN CURVED SHEAR LAYERS
P. S. Karasso and M. G. Mungal *In its* Annual Research Briefs, 1989 Feb. 1990 p 27-35 (For primary document see N92-30149 20-34)
Avail: CASI HC A02/MF A03

This report describes the work being undertaken to study the scalar mixing in curved shear layers. First, the motivation for this work and its objectives are described. Second, a description of the experimental rig that has been built is given. Third, some preliminary results (flow visualizations) are discussed, and finally, future steps that will be taken to complete the study are outlined. Author

N92-30153*# Stanford Univ., CA. Center for Turbulence Research.
AN EXPERIMENTAL INVESTIGATION OF A LOW REYNOLDS NUMBER TURBULENT BOUNDARY LAYER SUBJECT TO AN ADVERSE PRESSURE GRADIENT
J. H. Watmuff *In its* Annual Research Briefs, 1989 Feb. 1990 p 37-49 (For primary document see N92-30149 20-34)
Avail: CASI HC A03/MF A03

The evolution of a low Re(sub theta) turbulent boundary layer in an adverse pressure gradient (APG) is being studied for comparison with direct numerical simulations by Spalart. A short region of favorable pressure gradient (FPG) is applied first to establish a self preserving layer with Re(sub theta) equals approx. 600, which is a suitable initial condition for simulations. The APG is then applied rapidly such that beta equals approx. 2 at Re(sub theta) equals approx. 1500. The streamwise extent of the measurements exceeds the current capabilities of direct simulation so that the results should also serve as a useful data base for Reynolds averaged boundary layer prediction methods and in the future for direct simulation schemes as computer technology evolves. Author

N92-30154*# Stanford Univ., CA. Center for Turbulence Research.
AN EXPERIMENTAL STUDY OF THE EFFECTS OF RAPID ROTATION ON TURBULENCE
S. V. Veeravalli *In its* Annual Research Briefs, 1989 Feb. 1990 p 51-57 (For primary document see N92-30149 20-34)
Avail: CASI HC A02/MF A03

Experiments, large eddy simulations and direct numerical simulations all show that rapid rotation has a striking effect on homogeneous nearly isotropic turbulence. The cascade process is effectively inhibited by rotation, and thus dissipation is greatly reduced. Some attempts have been made to incorporate this effect in turbulence models. Numerical simulation further showed the somewhat surprising result that anisotropic homogeneous turbulence subjected to rotation tended towards an isotropic state; however, the residual anisotropy was not zero. Reynolds (1989) performed a detailed analysis using Rapid Distortion Theory (RDT) and showed that a reduction in the anisotropy is indeed expected and if the anisotropy is produced by irrotational strain then the anisotropy tensor b(sub ij) is asymptotically driven to half its initial value. Our objective is to extend the work of the experiments mentioned above to lower turbulent Rossby numbers and to confirm some of the results obtained by Reynolds (1989) for anisotropic turbulence. Author

N92-30155*# Stanford Univ., CA. Center for Turbulence Research.
AN EXPERIMENTAL STUDY OF SECONDARY VORTEX STRUCTURE IN MIXING LAYERS
J. H. Bell and Rabindra D. Mehta *In its* Annual Research Briefs, 1989 Feb. 1990 p 59-79 (For primary document see N92-30149 20-34)
(Contract NCC2-55)
Avail: CASI HC A03/MF A03

This report covers the first eight months of an experimental research project on the secondary vortex structure in plane mixing layers. The aim of the project is to obtain quantitative data on the behavior of the secondary structure in a turbulent mixing layer at reasonable reynolds numbers (Re(sub delta(sub w)) approx. 50,000). In particular, we hope to resolve the questions of how the scale of the secondary vortex structure changes with the scale of the mixing layer, and whether the structures are fixed in space, or whether they 'meander' in the spanwise direction. Author

N92-30156*# Stanford Univ., CA. Center for Turbulence Research.
DEVELOPMENT OF RENORMALIZATION GROUP ANALYSIS OF TURBULENCE
L. M. Smith *In its* Annual Research Briefs, 1989 Feb. 1990 p 81-95 (For primary document see N92-30149 20-34)
Avail: CASI HC A03/MF A03

The renormalization group (RG) procedure for nonlinear, dissipative systems is now quite standard, and its applications to the problem of hydrodynamic turbulence are becoming well known. In summary, the RG method isolates self similar behavior and provides a systematic procedure to describe scale invariant dynamics in terms of large scale variables only. The parameterization of the small scales in a self consistent manner has important implications for sub-grid modeling. This paper develops the homogeneous, isotropic turbulence and addresses the meaning and consequence of epsilon-expansion. The theory is then extended to include a weak mean flow and application of the RG method to a sequence of models is shown to converge to the Navier-Stokes equations. H.A.

N92-30157*# Stanford Univ., CA. Center for Turbulence Research.
SHORT-TIME LYAPUNOV EXPONENT ANALYSIS
J. A. Vastano *In its* Annual Research Briefs, 1989 Feb. 1990 p 97-106 (For primary document see N92-30149 20-34)
Avail: CASI HC A02/MF A03

A new technique for analyzing complicated fluid flows in numerical simulations has been successfully tested. The analysis uses short time Lyapunov exponent contributions and the associated Lyapunov perturbation fields. A direct simulation of the Taylor-Couette flow just past the onset of chaos demonstrated that this new technique marks important times during the system evolution and identifies the important flow features at those times. This new technique will now be applied to a 'minimal' turbulent channel. Author

N92-30158*# Stanford Univ., CA. Center for Turbulence Research.
ORGANIZED MOTIONS UNDERLYING TURBULENT SHEAR FLOWS
F. Waleffe *In its* Annual Research Briefs, 1989 Feb. 1990 p 107-115 (For primary document see N92-30149 20-34)
Avail: CASI HC A02/MF A03

The objective of this project is to determine the nature and significance of the organized motions underlying turbulent shear flow. There is considerable experimental evidence for the existence of such motions. In particular, one consistently observes longitudinal streaks with a spacing of about 100 in wall units in the near-wall region of wall-bounded shear flows. Recently, an analysis based on the direct resonance mechanism has predicted the appearance of streaks with precisely such a spacing. Also, the minimum channel simulations of Jimenez and Moin have given a strong dynamical significance to that spanwise length scale. They have shown that turbulent-like flows can not be maintained when the spanwise wavelength of the motion is constrained to be less than about that critical number. A critical review of the direct resonance ideas and the non-linear theory of Benney and

Gustavsson is presented first. It is shown how this leads to the later mean flow-first harmonic theory of Benney. Finally, we note that a different type of analysis has led to the prediction streaks with a similar spacing. This latter approach consists of looking for optimum fields and directly provides deep insights into why a particular structure or a particular scale should be preferred.
Author

N92-30159*# Stanford Univ., CA. Center for Turbulence Research.
TURBULENCE DYNAMICS IN THE WAVELET REPRESENTATION
C. Meneveau *In its* Annual Research Briefs, 1989 Feb. 1990 p 117-130 (For primary document see N92-30149 20-34)
Avail: CASI HC A03/MF A03

The phenomenon of small-scale intermittency is shown to motivate the decomposition of the velocity fields into modes that exhibit both localization in wavenumber and physical space. We review some basic properties of such a decomposition, called the wavelet transform. The wavelet-transformed Navier-Stokes equations are derived, and we define a new quantity Pi(r, vector-x, t), which is the flux of kinetic energy to scales smaller than r at position vector-x (at time t). The main goals of this research are also summarized.
Author

N92-30160*# Stanford Univ., CA. Center for Turbulence Research.
DIRECT SIMULATION OF TURBULENT COMBUSTION
T. J. Poinsot *In its* Annual Research Briefs, 1989 Feb. 1990 p 131-156 (For primary document see N92-30149 20-34)
Avail: CASI HC A03/MF A03

Understanding and modeling of turbulent combustion are key-problems in the computation of numerous practical systems. Because of the lack of analytical theories in this field and of the difficulty of performing precise experiments, direct simulation appears to be one of the most attractive tools to use in addressing this problem. The present work can be split into two parts: (1) Development and validation of a direct simulation method for turbulent combustion; (2) Applications of the method to premixed turbulent combustion problems. The goal of part 1 is to define and to test a numerical method for direct simulation of reacting flows. A high level of confidence should be attached to direct simulation results, and this can only be achieved through extensive validation tests. In part 2, direct simulation is used to address some of the many critical problems related to turbulent combustion. At the present time, I have limited this work to premixed combustion and considered only four basic issues: (1) The effect of pressure waves on flame propagation; (2) The interaction between flame fronts and vortices; (3) The influence of curvature on premixed flame fronts; and (4) The validation of flamelet models for premixed turbulent combustion.
Author

N92-30161*# Stanford Univ., CA. Center for Turbulence Research.
TRANSITION TO TURBULENCE IN HYPERSONIC FLOW
J. J. W. vanderVegt *In its* Annual Research Briefs, 1989 Feb. 1990 p 157-168 (For primary document see N92-30149 20-34)
Avail: CASI HC A03/MF A03

An outline of the project and recent progress toward the study of transition in hypersonic boundary layers is given. Aspects of the numerical method and the results of test computations are presented. At present the laminar flows over a flat plate have been computed for M less than or equal to 5.
Author

N92-30162*# Stanford Univ., CA. Center for Turbulence Research.
DIRECT SIMULATIONS OF WALL-BOUNDED COMPRESSIBLE TURBULENCE
J. C. Buell *In its* Annual Research Briefs, 1989 Feb. 1990 p 169-173 (For primary document see N92-30149 20-34)
Avail: CASI HC A01/MF A03

A study has been initiated on the effects of compressibility (Mach number) on turbulent boundary layers. An understanding of both qualitative (turbulence structures, physical processes) and quantitative (turbulence statistics) effects are desired. This understanding should lead to better turbulence models for applications involving supersonic wall-bounded flows. Direct numerical simulations of an idealized problem will be used to accomplish these objectives. Among several possibilities we chose plane Couette flow with constant-temperature walls as the first problem to be studied. The lack of mean streamwise pressure gradient plus isothermal walls implies that both horizontal directions can be assumed to be homogeneous and that the flow can reach a statistically steady state. Together, these features greatly simplify the calculations and analyses of the results. To date, an algorithm has been developed and implemented (but not yet fully tested) for the accurate solution of the Navier-Stokes equations with the assumptions noted above.
Author

N92-30163*# Stanford Univ., CA. Center for Turbulence Research.
TURBULENT TRANSPORT IN THE SOLAR NEBULA **c92**
K. W. Thompson *In its* Annual Research Briefs, 1989 Feb. 1990 p 175-184 (For primary document see N92-30149 20-34)
Avail: CASI HC A02/MF A03

This paper describes the current state of an ongoing project to simulate turbulent flow in a solar nebula, which is the flattened disk of dust and gas out of which a solar system forms. The goal of this project is to determine a model for the transport of mass and angular momentum in the nebula. The nebula flow exhibits compressibility, thermal conduction, viscosity, internal heating through viscous dissipation, a stable shear due to Keplerian rotation, and a gravitational acceleration in the vertical direction which is linear with altitude. These properties combine to give flow patterns not seen in terrestrial applications. Primordial solar systems are known to exist and are presumably undergoing an evolution similar to the early stages of our own solar system; for example, the IRAS infrared telescope has discovered such a protoplanetary system around the star Vega. Solar nebula evolution is the subject of much research in the astrophysical community. In the long run, researchers hope to gain a better understanding of planetary formation and the processes which dissipate the solar nebula with time.
Author

N92-30164*# Stanford Univ., CA. Center for Turbulence Research.
A NUMERICAL METHOD FOR PREDICTION OF COMPRESSIBLE TURBULENT FLOWS WITH CLOSURE MODELS
P. G. Huang *In its* Annual Research Briefs, 1989 Feb. 1990 p 185-193 (For primary document see N92-30149 20-34)
Avail: CASI HC A02/MF A03

A new computer code to solve the time averaged Navier-Stokes equations is developed. Many of the state-of-the-art numerical techniques and algorithms have been tested and implemented in the program in order to achieve a better numerical accuracy and code efficiency. Various turbulence models are tested for a wide range of flows. The initial focus has been on two-equation eddy-viscosity models, which are the most advanced available in current compressible flow codes. The long term goal will be to test Reynolds-Stress models and to explore their performance in the high Mach number range. Although testing and improvement of turbulence models for supersonic and hypersonic flows is the primary objective of this research, part of the effort has been devoted to analyzing the vortex breakdown phenomena using new computer programs. Some preliminary results on the breakdown of a vortex flow in a tube are reported. Present calculations are restricted to two dimensional flow geometry.
Author

N92-30165*# Stanford Univ., CA. Center for Turbulence Research.
INCOMPRESSIBLE SPATIALLY-DEVELOPING FREE-SHEAR FLOWS

J. C. Buell *In its* Annual Research Briefs, 1989 Feb. 1990 p 195-213 (For primary document see N92-30149 20-34)
Avail: CASI HC A03/MF A03

The first goal of this research is to understand the dynamics of three dimensional vortical structures, especially the interaction of the ribs and two dimensional rollers. Because of vortex stretching effects, this requires accurate and well resolved simulations. Another goal is to distinguish temporally- and spatially-growing shear layers in terms of the dynamics and observed vortical structures. This is important since the former is much easier to compute, but the error incurred in using temporal results for certain applications is unknown. The third goal is to investigate the effects of asymmetry on passive scalar mixing and fast-chemistry product formation. In this report a brief summary of a new numerical method is presented, followed by results for mixing layers and wake flows. Author

N92-30166*# Stanford Univ., CA. Center for Turbulence Research.
A NUMERICAL METHOD FOR DIRECT SIMULATION OF TURBULENCE IN COMPLEX GEOMETRIES
P. Orlandi *In its* Annual Research Briefs, 1989 Feb. 1990 p 215-229 (For primary document see N92-30149 20-34)
Avail: CASI HC A03/MF A03

The ultimate goal of this work is to study the flow inside a channel with riblets on one of the two walls. The method has been tested for two dimensional flows in the presence of bodies with a geometrical singularity and for three dimensional flows inside domains described by Cartesian coordinates. The results have been compared with previous numerical simulations and with experimental results. The cases considered are: (1) the growth of Orr-Sommerfield waves in plane Poiseulle flow; (2) the flow over a backward facing step; (3) the flow past a wedge; and (4) the flow inside a narrow channel. Finally, the case of a channel with two large riblets on a wall has been simulated. In this case a limited number of grid points is sufficient, and in spite of the slow convergence for the pressure solver, one is able to obtain solutions with a reasonable amount of computer time. At present solutions with very fine grids in all three directions can not be obtained, due to lack of a fast pressure solver for general curvilinear coordinates. Author

N92-30167*# Stanford Univ., CA. Center for Turbulence Research.
THE LARGE-SCALE STRUCTURES IN TURBULENT PLANE COUETTE FLOW
M. J. Lee *In its* Annual Research Briefs, 1989 Feb. 1990 p 231-245 (For primary document see N92-30149 20-34)
Avail: CASI HC A03/MF A03

Turbulent plane Couette flow has been numerically simulated at a Reynolds number, Re = U(sub w)(h)/nu = 6000. Preliminary examinations of the instantaneous velocity and vorticity fields revealed the existence of large scale eddies which grow in the flow direction with time and have the spanwise scale as large as the channel height. The persistence of the longitudinal eddies was not observed when the small scales in the spanwise direction were not well resolved, indicating that the growth of the large scale longitudinal eddies requires the contribution from the small scale motions in the spanwise direction. The statistical correlation in the flow agree well with the experimental results. Author

N92-30168*# Stanford Univ., CA. Center for Turbulence Research.
TURBULENT THERMAL CONVECTION IN A DIFFERENTIALLY ROTATING CHANNEL
W. Cabot, J. B. Pollack (National Aeronautics and Space Administration. Ames Research Center, Moffett Field, CA.), P. Cassen (National Aeronautics and Space Administration. Ames Research Center, Moffett Field, CA.), and K. W. Thompson *In its* Annual Research Briefs, 1989 Feb. 1990 p 247-259 (For primary document see N92-30149 20-34)
Avail: CASI HC A03/MF A03

Differentially rotating disks of gases and solids occur in several astrophysical systems, in particular in the inner parts of protostellar nebulae, of which our own solar system is thought to be a relic. The objectives of this paper are to: (1) study localized turbulence in circumstances approximating those found in accretion disks using previously existing expertise in performing direct numerical simulation of turbulent, incompressible channel flows with low Reynolds numbers; (2) determine the limitations of such calculations; and (3) extend the type of numerical simulation (e.g., to include density and stratification and compressibility effects and to accommodate higher Reynolds numbers with sub-grid scale modeling) so that the relevant physical effects are realistically captured. Author

N92-30169*# Stanford Univ., CA. Center for Turbulence Research.
PATTERNS IN SIMULATED TURBULENT CHANNEL FLOW
D. Stretch *In its* Annual Research Briefs, 1989 Feb. 1990 p 261-279 (For primary document see N92-30149 20-34)
Avail: CASI HC A03/MF A03

The surface stress is a key diagnostic in wall bounded turbulent flows. Large fluctuations in the stress are believed to be associated with intermittent 'bursting' events during which a large proportion of the turbulence production takes place. If this is so, then a detailed investigation of the structure of the surface stress and its spatial relationship to events within the flow could have wide application in drag reduction and other aspects of flow control. The initial phase of this project, therefore, concentrated on the surface stress field. The first objective is to carry out a statistical analysis of the instantaneous surface stress in a simulated turbulent channel flow, including comparison with multipoint experimental data from a zero pressure gradient turbulent boundary layer. The second objective is to apply a simple pattern recognition procedure to educe the characteristic spatial structure of various flow diagnostics. The final objective is to extend the pattern recognition analysis to examine the whole three dimensional structure of the flow. H.A.

N92-30190*# Institute for Computer Applications in Science and Engineering, Hampton, VA.
CROSSFLOW EFFECTS ON THE GROWTH RATE OF INVISCID GOERTLER VORTICES IN A HYPERSONIC BOUNDARY LAYER Final Report
Yibin Fu and Philip Hall Jun. 1992 37 p Submitted for publication
(Contracts NAS1-18605; NAS1-8107; AF-AFOSR-89-0042; RTOP 505-90-52-01)
(NASA-CR-189667; ICASE-92-26; NAS 1.26:189667) Avail: CASI HC A03/MF A01

The effects of crossflow on the growth rate of inviscid Goertler vortices in a hypersonic boundary layer with pressure gradient are studied. Attention is focused on the inviscid mode trapped in the temperature adjustment layer; this mode has greater growth rate than any other mode. The eigenvalue problem which governs the relationship between the growth rate, the crossflow amplitude, and the wavenumber is solved numerically, and the results are then used to clarify the effects of crossflow on the growth rate of inviscid Goertler vortices. It is shown that crossflow effects on Goertler vortices are fundamentally different for incompressible and hypersonic flows. The neutral mode eigenvalue problem is found to have an exact solution, and as a by-product, we have also found the exact solution to a neutral mode eigenvalue problem which was formulated, but unsolved before, by Bassom and Hall (1991). Author

N92-30192*# Institute for Computer Applications in Science and Engineering, Hampton, VA.
STABILITY OF A PREMIXED FLAME IN STAGNATION-POINT FLOW AGAINST GENERAL DISTURBANCES Final Report
Thomas L. Jackson (Old Dominion Univ., Norfolk, VA.) and Moshe Matalon (Northwestern Univ., Evanston, IL.) Jun. 1992 34 p Submitted for publication
(Contracts NAS1-18605; NAS1-19480; AF-AFOSR-0180-91; NSF

DMS-91-04029; RTOP 505-90-52-01)
(NASA-CR-189666; NAS 1.26:189666; ICASE-92-25) Avail: CASI HC A03/MF A01

Previously, the stability of a premixed flame in a stagnation flow was discussed for a restricted class of disturbances that are self-similar to the basic undisturbed flow; thus, flame fronts with corrugations only in the cross stream direction were considered. Here, we consider a more general class of three-dimensional flame front perturbations which also permits corrugations in the streamwise direction. It is shown that, because of the stretch experienced by the flame, the hydrodynamic instability is limited only to disturbances of short wavelength. If in addition diffusion effects have a stabilizing influence, as would be the case of mixtures with Lewis number greater than one, a stretched flame could be absolutely stable. Instabilities occur when the Lewis number is below some critical value less than one. Neutral stability boundaries are presented in terms of the Lewis number, the strain rate, and the appropriate wavenumbers. Beyond the stability threshold, the two-dimensional self-similar modes always grow first. However, if disturbances of long wavelength are excluded, it is possible for the three-dimensional modes to be the least stable one. Accordingly, the pattern that will be observed on the flame front, at the onset of instability, will consist of either ridges in the direction of stretch or the more common three-dimensional cellular structure. Author

35 INSTRUMENTATION AND PHOTOGRAPHY

Includes remote sensors; measuring instruments and gages; detectors; cameras and photographic supplies; and holography.

For aerial photography see *43 Earth Resources and Remote Sensing.* For related information see also *06 Aircraft Instrumentation,* and *19 Spacecraft Instrumentation.*

N92-29228*# National Aeronautics and Space Administration. Langley Research Center, Hampton, VA.
SIXTEENTH INTERNATIONAL LASER RADAR CONFERENCE, PART 1
M. Patrick McCormick, ed. Washington Jul. 1992 407 p Conference held in Cambridge, MA, 20-24 Jul. 1992; sponsored by NASA. Langley Research Center, AFOSR, AF Phillips Lab., American Meteorological Society, and the Optical Society of America
(RTOP 665-45-20-21)
(NASA-CP-3158-Pt-1; L-17126-Pt-1; NAS 1.55:3158-Pt-1) Avail: CASI HC A18/MF A04

This publication contains extended abstracts of papers presented at the 16th International Laser Radar Conference. One-hundred ninety-five papers were presented in both oral and poster sessions. The topics of the conference sessions were: (1) Mt. Pinatubo Volcanic Dust Layer Observations; (2) Global Change/Ozone Measurements; (3) GLOBE/LAWS/LITE; (4) Mesospheric Measurements and Measurement Systems; (5) Middle Atmosphere; (6) Wind Measurements and Measurement Systems; (7) Imaging and Ranging; (8) Water Vapor Measurements; (9) Systems and Facilities; and (10) Laser Devices and Technology. This conference reflects the breadth of research activities being conducted in the lidar field. These abstracts address subjects from lidar-based atmospheric investigations relating to global change to the development of new lidar systems and technology. For individual titles, see N92-29229 through N92-29328.

N92-29229*# Fukuoka Univ. (Japan). Dept. of Applied Physics.
LONG TERM STRATOSPHERIC AEROSOL LIDAR MEASUREMENTS IN KYUSHU **c45**
Motowo Fujiwara *In* NASA. Langley Research Center, Sixteenth International Laser Radar Conference, Part 1 Jul. 1992 p 1-2 (For primary document see N92-29228 20-35)
Avail: CASI HC A01/MF A04

Lidar soundings of the stratospheric aerosols have been made since 1972 at Fukuoka, Kyushu Island of Japan. Volcanic clouds from eruptions of La Soufriere, Sierra Negra, St. Helens, Uluwan, Alaid, unknown volcano, and El Chichon were detected one after another in only three years from 1979 to 1982. In july 1991 strong scattering layers which were originated from the serious eruptions of Pinatubo in June and were almost comparable to the El Chichon clouds were detected. Volcanic clouds from pinatubo and other volcanos mentioned are examined and carefully compared to each other and to the wind and temperature which was measured by Fukuoka Meteorological Observatory almost at the same time as the lidar observation was made. H.A.

N92-29230*# Commonwealth Scientific and Industrial Research Organization, Mordialoc (Australia). Div. of Atmospheric Research.
SOUTHERN HEMISPHERE LIDAR MEASUREMENTS OF THE AEROSOL CLOUDS FROM MT. PINATUBO AND MT. HUDSON **c45**
Stuart A. Young, Peter J. Manson, and Graeme R. Patterson *In* NASA. Langley Research Center, Sixteenth International Laser Radar Conference, Part 1 Jul. 1992 p 3-6 (For primary document see N92-29228 20-35)
Avail: CASI HC A01/MF A04

On 19 Jul., 1991, during tests to determine the ability of the newly-modified CSIRO Ns:YAG lidar to measure signals from the stratosphere before the arrival of dust from the eruption of Mt. Pinatubo, a strongly scattering layer was detected at an altitude of 2 km. That evening, the spectacular sunset and twilight were typical of volcanically disturbed conditions. Lidar measurements at 532 nm were made between 1400 and 1500 EST (0400-0500 UT) on 19 Jul. through broken cloud. Approximately 3800 laser firings were averaged in 256 shot blocks. These and subsequent data have been analyzed to produce profiles of aerosol volume backscatter function and scattering ratio. Clouds again prevented a clear view of the twilights on the next two nights, although there was some evidence for an enhanced glow. The evidence suggested that the aerosol layer had disappeared. An explanation for this disappearance and the earlier than expected arrival of the layer over Melbourne was required. Nimbus 7 TOMS data for 23 Jun. showed that the SO2 from the eruption had extended at least 11000 km to the west and that the southern boundary of the cloud had reached 15 degrees S just 8 days after the climactic eruption. It can be assumed that this cloud also contained dust and sulphuric acid aerosol. It was proposed that a section had then been broken away from the main cloud and carried south by a large scale eddy between the low latitude easterlies and the strong mid-latitude westerlies which finally carried the aerosol cloud over southern Australia. Accompanying 30 mb wind data showed a counter clockwise circulation, responsible for the transport, located in the South Atlantic Ocean. Author

N92-29231*# Gesellschaft fuer Kernenergieverwertung in Schiffbau und Schiffahrt m.b.H., Geesthacht (Germany, F.R.).
STRATOSPHERIC BACKSCATTER, EXTINCTION, AND LIDAR RATIO PROFILING AFTER THE MT. PINATUBO ERUPTIONS **c45**
Albert Ansmann, Christoph Schulze, Ulla Wandinger, Claus Weitkamp, and Walfried Michaelis *In* NASA. Langley Research Center, Sixteenth International Laser Radar Conference, Part 1 Jul. 1992 p 7-10 (For primary document see N92-29228 20-35)
Avail: CASI HC A01/MF A04

Since August 1991 the stratospheric aerosol layer is continuously monitored with a combination Raman elastic-backscatter lidar, groundbased systems. XeCl excimer laser is used as the radiation source. Signals elastically backscattered from air molecules and particles and inelastically Raman backscattered from nitrogen molecules are detected. The measurements of these two signal profiles up to 35 km height allows the separate and independent determination of aerosol extinction and backscatter properties in the perturbed lower stratosphere. The extinction coefficient is derived from the nitrogen Raman signal profile, while the backscatter coefficient is obtained

from the elastic-to-inelastic backscatter signal ratio. In this way, also the extinction-to-backscatter, or lidar, ratio profile is determined. For the first time, lidar ratios are determined in the perturbed stratospheric layer by the use of remote sensing only. The lidar ratio contains information about the size range of the stratospheric particles which are assumed to be sulfuric acid droplets, and it is needed in the calculation of aerosol optical properties from data taken with a typical backscatter lidar.
Author

N92-29232*# Tokyo Metropolitan Univ. (Japan). Dept. of Electronics and Information Engineering.
MEASUREMENTS OF STRATOSPHERIC PINATUBO AEROSOL EXTINCTION PROFILES BY A RAMAN LIDAR **c45**
Makoto Abo and Chikao Nagasawa *In* NASA. Langley Research Center, Sixteenth International Laser Radar Conference, Part 1 Jul. 1992 p 11-12 (For primary document see N92-29228 20-35)
Avail: CASI HC A01/MF A04

The Raman lidar has been used for remote measurements of water vapor, ozone and atmospheric temperature in the lower troposphere because the Raman cross section is three orders smaller than the Rayleigh cross section. We estimated the extinction coefficients of the Pinatubo volcanic aerosol in the stratosphere using a Raman lidar. If the precise aerosol extinction coefficients are derived, the backscatter coefficient of a Mie scattering lidar will be more accurately estimated. The Raman lidar has performed to measure density profiles of some species using Raman scattering. Here we used a frequency-doubled Nd:YAG laser for transmitter and received nitrogen vibrational Q-branch Raman scattering signal. Ansmann et al. (1990) derived tropospherical aerosol extinction profiles with a Raman lidar. We think that this method can apply to dense stratospheric aerosols such as Pinatubo volcanic aerosols. As dense aerosols are now accumulated in the stratosphere by Pinatubo volcanic eruption, the error of Ramen lidar signal regarding the fluctuation of air density can be ignored.
Author

N92-29233*# National Aeronautics and Space Administration. Goddard Space Flight Center, Greenbelt, MD.
RAMAN LIDAR MEASUREMENTS OF PINATUBO AEROSOLS OVER SOUTHEASTERN KANSAS DURING NOVEMBER-DECEMBER 1991 **c45**
R. A. Ferrare (Universities Space Research Association, Greenbelt, MD.), S. H. Melfi, D. N. Whiteman, and K. D. Evans (Hughes STX, Inc., Lanham, MD.) *In* NASA. Langley Research Center, Sixteenth International Laser Radar Conference, Part 1 Jul. 1992 p 13-16 (For primary document see N92-29228 20-35)
Avail: CASI HC A01/MF A04

The eruptions of the Philippine volcano Pinatubo during June 1991 produced large amounts of stratospheric aerosols that could significantly affect earth's climate as well as trigger stratospheric ozone depletion through heterogeneous chemical reactions. Information regarding the physical and optical properties of these aerosols is required to quantify those effects. By measuring both the elastically backscattered signal and the inelastic signal produced by Raman scattering from nitrogen molecules, Raman lidar can provide some of this information. In this presentation we discuss Raman lidar measurements of the scattering ratio, backscattering, extinction, extinction/backscattering ratio, and optical thickness of the Pinatubo aerosols over southeastern Kansas made on 10 nights during November and December, 1991. The Raman lidar developed at GSFC is a trailer-based system which uses an XeF excimer laser to transmit light at 351 nm. The light backscattered by molecules and aerosols at this wavelength is detected as well as Raman scattered light from water vapor, nitrogen, and oxygen molecules. Since background skylights interfere with the detection of the Raman signals the data discussed in this paper were acquired only at night.
Author

N92-29234*# Meteorological Research Inst., Tsukuba (Japan).
LIDAR OBSERVATIONS OF STRATOSPHERIC AEROSOL LAYER AFTER THE MT. PINATUBO VOLCANIC ERUPTION **c45**
Tomohiro Nagai, Osamu Uchino, and Toshifumi Fujimoto *In* NASA. Langley Research Center, Sixteenth International Laser Radar Conference, Part 1 Jul. 1992 p 17-20 (For primary document see N92-29228 20-35)
Avail: CASI HC A01/MF A04

The volcano Mt. Pinatubo located on the Luzon Island, Philippines, had explosively erupted on June 15, 1991. The volcanic eruptions such as volcanic ash, SO2 and H2O reached into the stratosphere over 30 km altitude by the NOAA-11 satellite observation and this is considered one of the biggest volcanic eruptions in this century. A grandiose volcanic eruption influences the atmosphere seriously and causes many climatic effects globally. There had been many impacts on radiation, atmospheric temperature and stratospheric ozone after some past volcanic eruptions. The main cause of volcanic influence depends on stratospheric aerosol, that stay long enough to change climate and other meteorological conditions. Therefore it is very important to watch stratospheric aerosol layers carefully and continuously. Standing on this respect, we do not only continue stratospheric aerosol observation at Tsukuba but also have urgently developed another lidar observational point at Naha in Okinawa Island. This observational station could be thought valuable since there is no lidar observational station in this latitudinal zone and it is much nearer to Mt. Pinatubo. Especially, there is advantage to link up these two stations on studying the transportation mechanism in the stratosphere. In this paper, we present the results of lidar observations at Tsukuba and Naha by lidar systems with Nd:YAG laser.
Author

N92-29235*# Massachusetts Inst. of Tech., Cambridge. Center for Global Change Science.
THE ROLE OF LIDARS IN GLOBAL CHANGE RESEARCH **c45**
Ronald G. Prinn *In* NASA. Langley Research Center, Sixteenth International Laser Radar Conference, Part 1 Jul. 1992 p 21-22 (For primary document see N92-29228 20-35)
Avail: CASI HC A01/MF A04

Recent research has solidified a view of the Earth as a global scale interactive system with complex chemical, physical, biological, and dynamical processes that link the ocean, atmosphere, land, and marine terrestrial living organisms. An important aspect of Earth System Science studies in the future is the need to observe simultaneously the physical, chemical, biological, and dynamical processes involved in highly coupled phenomena such as those mentioned. Lidars operating from the surface, aircraft, and satellites provide a powerful observational technique to study the processes and observe trends important to global change. Lidar observations have already played important roles in helping understand processes controlling stratospheric ozone and aerosols, tropospheric clouds, water vapor, ozone, gaseous pollutants, and aerosols, and winds and temperatures throughout the atmosphere. In this paper the author reviews the science of global change and highlights the potential roles for lidar in studying the Earth system.
H.A.

N92-29236*# National Aeronautics and Space Administration. Langley Research Center, Hampton, VA.
INTERPRETATION OF DIAL MEASUREMENTS OF LOWER STRATOSPHERIC OZONE IN REGIONS WITH PINATUBO AEROSOLS **c45**
William B. Grant (ST Systems Corp., Hampton, VA.), Edward V. Browell (ST Systems Corp., Hampton, VA.), Marta A. Fenn (ST Systems Corp., Hampton, VA.), Carolyn F. Butler (ST Systems Corp., Hampton, VA.), Vincent G. Brackett (ST Systems Corp., Hampton, VA.), Robert E. Veiga (ST Systems Corp., Hampton, VA.), Shane D. Mayor (ST Systems Corp., Hampton, VA.), Jack Fishman, D. Nganga (Maien-Ngouabi Univ., Brazzaville, Congo), and A. Minga (Maien-Ngouabi Univ., Brazzaville, Congo) *In its* Sixteenth International Laser Radar Conference, Part 1 Jul.

1992 p 23-26 Prepared in cooperation with NATO, Washington, DC (For primary document see N92-29228 20-35)
Avail: CASI HC A01/MF A04

The influence of volcanic aerosols on stratospheric ozone is a topic of current interest, especially with the June 15, 1991 eruption of Mt. Pinatubo in the Philippines. Lidar has been used in the past to provide aerosol profiles which could be compared with ozone profiles measured using ozonesondes to look for coincidences between volcanic aerosols and ozone decreases. The differential absorption lidar (DIAL) technique has the advantages of being able to measure ozone and aerosol profiles simultaneously as well as being able to cover large geographical regions rapidly. While there are problems associated with correcting the ozone profiles for the presence of aerosols, the corrections can be made reliably when the wavelengths are closely spaced and the Bernoulli method is applied. The DIAL measurements considered in this paper are those obtained in the tropical stratosphere in January 1992 during the Airborne Arctic Stratospheric Expedition (AASE-II). The determination of ozone profiles in the presence of Pinatubo aerosols is discussed in a companion paper. Author

N92-29237*# York Univ. (Ontario). Inst. for Space and Terrestrial Science.
CORRECTING FOR INTERFERENCE OF MT. PINATUBO AEROSOLS ON DIAL MEASUREMENTS OF STRATOSPHERIC OZONE **c45**
W. Steinbrecht and A. I. Carswell *In* NASA. Langley Research Center, Sixteenth International Laser Radar Conference, Part 1 Jul. 1992 p 27-30 (For primary document see N92-29228 20-35)
Avail: CASI HC A01/MF A04

Since March 1991 our group has been routinely operating a Differential Absorption Lidar system in Toronto, Canada. The system is based on a XeCl Excimer laser and the main system parameters are reported. In all measurements after July 21, 1991 we have observed aerosol layers in the stratosphere, resulting from the Mt. Pinatubo eruptions around June 15, 1991. These aerosol layers have increased in size since they were first observed and backscatter ratios of more than 5 to 353 nm have been observed. They interfere significantly with any optical ozone measurement. In this paper we will describe our work to quantify the effects of the additional aerosol on differential absorption measurements and the attempt to correct for them. Author

N92-29238*# National Aeronautics and Space Administration. Goddard Space Flight Center, Greenbelt, MD.
A NEW RAMAN DIAL TECHNIQUE FOR MEASURING STRATOSPHERIC OZONE IN THE PRESENCE OF VOLCANIC AEROSOLS **c45**
Upendra N. Singh (Hughes STX, Inc., Lanham, MD.), Thomas J. McGee, Michael Gross (Hughes STX, Inc., Lanham, MD.), William S. Heaps, and Richard Ferrare *In* NASA. Langley Research Center, Sixteenth International Laser Radar Conference, Part 1 Jul. 1992 p 31-33 (For primary document see N92-29228 20-35)
Avail: CASI HC A01/MF A04

This paper describes a new lidar scheme to measure stratospheric ozone in the presence of heavy volcanic aerosol loading. The eruptions of the Philippine volcano Pinatubo during June 1991 ejected large amounts of sulfur dioxide into the atmosphere to altitudes of at least 30 km. The resulting aerosols have severely affected the measurements of stratospheric ozone when using traditional Rayleigh differential absorption lidar (DIAL) technique, in which the scattering mechanism is almost entirely Rayleigh and which assumes a small amount or no aerosols. In order to extract an ozone profile in the regions below about 30 km where the Rayleigh lidar returns are contaminated by aerosol scattering from Mt. Pinatubo cloud, we have used a Raman lidar technique, where the scattering mechanism depends solely on molecular nitrogen. In this scheme there is no aerosol scattering component to the backscattered lidar return. Using this technique in conjunction with the Rayleigh DIAL measurement, the GSFC stratospheric ozone lidar has measured ozone profiles between 15 and 50 km during the recently held UARS correlative measurement campaign (February-March 1992) at JPL's Table Mountain Facility in California. Author

N92-29239*# Jet Propulsion Lab., California Inst. of Tech., Pasadena. Table Mountain Facility.
THE JPL TABLE MOUNTAIN AND MAUNA LOA STRATOSPHERIC OZONE LIDARS **c45**
I. Stuart McDermid *In* NASA. Langley Research Center, Sixteenth International Laser Radar Conference, Part 1 Jul. 1992 p 35-38 (For primary document see N92-29228 20-35)
Avail: CASI HC A01/MF A04

The development of a differential absorption lidar (DIAL) system for long-term measurements of stratospheric ozone and for potential inclusion in the Network for the Detection of Stratospheric Change (NDSC) began at JPL in 1986, concurrent with the first workshop that considered the priorities and appropriate measurement techniques for such a network. The DIAL system at the JPL Table Mountain Facility (TMF) was developed specifically to have characteristics suitable for longterm measurements as proposed for NDSC. Regular measurements of stratospheric ozone concentration profiles commenced in February 1988 and this system has been fully described elsewhere. Author

N92-29240*# Paris VI Univ. (France).
THE NDSC PRIMARY SITE AT THE OBSERVATOIRE DE HAUTE-PROVENCE: OZONE AND AEROSOLS OBSERVATIONS (1986-1992) **c45**
G. Megie, S. Godin, G. Ancellet, M. Beekmann, and A. M. Lacoste *In* NASA. Langley Research Center, Sixteenth International Laser Radar Conference, Part 1 Jul. 1992 p 39-41 (For primary document see N92-29228 20-35)
Avail: CASI HC A01/MF A04

The primary site of the newly implemented Network for Detection of Stratospheric Changes (NDSC) includes three main sites in the alpine regions of southern Europe. At one of these observatories, a coherent set of experimental systems has been established to monitor on a long-term basis ozone, aerosols, minor constituents, and temperature vertical distributions in the troposphere and stratosphere. Such techniques include several lidar systems, balloon-borne sondes and ultraviolet visible spectrometry. Lidar measurements of stratospheric aerosols are performed on a routine basis, since 1980. These include the vertical distribution of the extinction and backscattering coefficients from the tropopause. Recently, measurements performed following the eruption of Mount Pinatubo, have allowed researchers to follow the time evolution of the aerosol cloud in middle latitude regions. H.A.

N92-29241*# Optech, Inc., Downsview (Ontario).
LIDAR ATMOSPHERIC OBSERVATORY IN THE CANADIAN ARCTIC **c45**
Arkady Ulitsky, Tin-Yu Wang, Martin Flood, and Brent Smith *In* NASA. Langley Research Center, Sixteenth International Laser Radar Conference, Part 1 Jul. 1992 p 43-44 (For primary document see N92-29228 20-35)
Avail: CASI HC A01/MF A04

During the last decade there have been growing concerns about a broad variety of atmospheric properties. Among these, a depletion of the stratospheric ozone layer has attracted considerable attention from the general public, politicians and scientists due to its vital impact for the entire global biosphere. One of the major warning signs was the discovery of the 'ozone hole' in the Antarctic region where the concentration of the ozone in the stratosphere was significantly reduced. At present the stratospheric ozone layer in this region is being continuously monitored by groups of scientists from around the world and numerous observations of the ozone layer on the global scale have clearly demonstrated the process of ozone depletion. Recent observations by NASA have shown significant depletion in the Arctic region. This paper provides an initial description of two lidars that are planned to be installed in a new observatory for

atmospheric studies in the Canadian Arctic. This observatory is being constructed under the supervision of the Atmospheric Environment Services (AES) of Canada as a part of Green Plan - an initiative of the Federal Government of Canada. The station is located at Eureka on Ellesmere Island at a latitude of 80 degrees N and a longitude of 86 degrees W. Author

N92-29242*# National Inst. for Environmental Studies, Tsukuba (Japan).
OBSERVATION OF STRATOSPHERIC OZONE WITH NIES LIDAR SYSTEM IN TSUKUBA, JAPAN **c45**
H. Nakane, S. Hayashida, Y. Sasano, N. Sugimoto, I. Matsui, and A. Minato *In* NASA. Langley Research Center, Sixteenth International Laser Radar Conference, Part 1 Jul. 1992 p 45-48 (For primary document see N92-29228 20-35)
Avail: CASI HC A01/MF A04

Lidars are expected to play important roles in an international monitoring network of the stratosphere such as the Network for the Detection of Stratospheric Change (NDSC). The National Institute for Environmental Studies (NIES) in Tsukuba constructed an ozone lidar system in March 1988 and started observation in August 1988. The lidar system has a 2-m telescope and injection locked XeCl and XeF excimer lasers which can measure ozone profiles (15-45 km) and temperature profiles (30-80 km). From December 1991, lidar observations have been carried out in which the second Stokes line of the stimulated Raman scattering of a KrF laser has been used. Ozone profiles obtained with the NIES lidar system are compared with the data provided by the SAGE II satellite sensor. Results showed good agreement for the individual and the zonal mean profiles. Variations of ozone with various time scales at each altitude can be studied using the data obtained with the NIES ozone lidar system. Seasonal variations are easily found at 20 km, 30 km, and 35 km, which are qualitatively understood as a result of dynamical and photochemical effects. Systematic errors of ozone profiles due to the Pinatubo stratospheric aerosols have been detected using multi-wavelength observation. Author

N92-29243*# La Sapienza Univ., Rome (Italy).
OBSERVATIONS OF OZONE-AEROSOL CORRELATED BEHAVIOUR IN THE LOWER STRATOSPHERE DURING THE EASOE CAMPAIGN **c45**
P. DiGirolamo, M. Cacciani, A. diSarra, G. Fiocco, D. Fua, T. S. Joergensen (Danish Meteorological Inst., Copenhagen.), B. Knudsen (Danish Meteorological Inst., Copenhagen.), and N. Larsen (Danish Meteorological Inst., Copenhagen.) *In* NASA. Langley Research Center, Sixteenth International Laser Radar Conference, Part 1 Jul. 1992 p 49-51 Prepared in cooperation with Rome Univ., Italy and Inst. di Fisica dell Atmosfera, Rome, Italy (For primary document see N92-29228 20-35)
Avail: CASI HC A01/MF A04

The question of possible interactions between ozone and stratospheric aerosol has been open for a long time. Measurements carried out after the Mt. Agung and El Chicon eruptions showed evidence of negative correlations between the presence of volcanic stratospheric aerosols and ozone concentration. Evidence for negative correlations in the polar winter has been also found. It is only after the discovery of the Antarctic ozone hole that catalytic effects related to low temperature heterogeneous chemistry have become the object of much investigation, now extended to the role of volcanic aerosol in the ozone reduction. These phenomena can be the object of various interpretations, not mutually exclusive, including the effect of transport, diffuse radiation as well as heterogeneous chemistry. The present paper provides preliminary results of simultaneous measurements of ozone and aerosol, carried out at Thule, Greenland, during the winter 1991-92. The European Stratospheric Ozone Experiment (EASOE) was aimed at monitoring the winter Arctic stratosphere in order to obtain a deeper insight of the ozone destruction processes taking place in the polar regions. A large amount of aerosol was injected into the lower stratosphere by the recent eruption of Volcano Pinatubo. A lidar system, already operational in Thule since November 1990, has provided detailed measurements of the stratospheric aerosol concentration during EASOE. In the same period, a large number of ozonesondes were launched. Although no PSC formation was detected over Thule, the simultaneous measurement of the stratospheric aerosol and ozone profiles give the possibility to study interactions occurring in the stratosphere between these two constituents. Author

N92-29244*# Rijksinstituut voor Volksgezondheid en Milieuhygieene, Bilthoven (Netherlands).
FIRST RESULTS FROM TROLIX 1991: AN INTERCOMPARISON OF TROPOSPHERIC OZONE LIDARS **c45**
A. Apituley, J. Boesenberg (Max-Planck-Inst. fuer Meteorologie, Hamburg, Germany, F.R.), G. Ancellet (Centre National de la Recherche Scientifique, Paris, France), H. Edner (Lund Inst. of Tech., Sweden), B. Galle (Institutet foer Vatten-Och Luftvaardsforskning, Goeteborg, Sweden), J. B. Bergwerff, G. vonCossart (Institut fuer Atmosphaerenphysik Kuehlungsborn, Germany, F.R), J. Fiedler (Institut fuer Atmosphaerenphysik Kuehlungsborn, Germany, F.R), C. N. deJonge, and J. Mellquist (Institutet foer Vatten-Och Luftvaardsforskning, Goeteborg, Sweden) *In* NASA. Langley Research Center, Sixteenth International Laser Radar Conference, Part 1 Jul. 1992 p 53-55 (For primary document see N92-29228 20-35)
Avail: CASI HC A01/MF A04

Within the framework of the European environmental research programme EUROTRAC, lidar systems for routine measurements of vertical ozone profiles throughout the planetary boundary layer and the free troposphere are currently under development. Several of these systems are now operational and an intercomparison experiment was undertaken in the period from June 10 to June 28, 1991 in Bilthoven, the Netherlands. The main scientific objectives defined for the campaign are: (1) compare the lidar measurements to in situ measurements of the ozone concentration; (2) determine how many and which wavelengths are needed for a sufficiently accurate ozone retrieval in the lower troposphere under realistic conditions; (3) assess the accuracy that can be achieved under realistic conditions; and (4) compare the performance of the participating systems. Author

N92-29245*# Alabama Univ., Huntsville. Earth System Science Lab.
GLOBAL BACKSCATTER EXPERIMENT (GLOBE) RESULTS: AEROSOL BACKSCATTER GLOBAL DISTRIBUTION AND WAVELENGTH DEPENDENCE **c45**
David A. Bowdle *In* NASA. Langley Research Center, Sixteenth International Laser Radar Conference, Part 1 Jul. 1992 p 57-60 (For primary document see N92-29228 20-35)
Avail: CASI HC A01/MF A04

The GLObal Backscatter Experiment (GLOBE) was initiated by NASA in 1986 as an interagency and international research effort to characterize tropospheric backscatter properties. The primary objective of the program is to develop realistic aerosol backscatter inputs for design and simulation studies for NASA's prospective Laser Atmospheric Wind Sounder (LAWS). To achieve this, GLOBE incorporates several different types of aerosol sensors, which operate from a variety of sensor platforms, covering a wide range of spatial and temporal scales, and measure a diverse set of aerosol physical, chemical, and optical properties. The results of this analysis have provided important new information on the life cycles and physicochemical properties of global scale tropospheric aerosol systems. In addition, GLOBE analytical methods will be useful for the Earth Observing System (EOS) and other studies that involve the assimilation of large, complex atmospheric aerosol databases. Author

N92-29246*# National Aeronautics and Space Administration. Goddard Space Flight Center, Greenbelt, MD.
THE GLOBAL BACKSCATTER EXPERIMENT AIRBORNE PULSED LIDAR MEASUREMENTS **c45**
James D. Spinhirne, S. Chudamani, Robert T. Menzies (Jet Propulsion Lab., California Inst. of Tech., Pasadena.), and David Tratt (Jet Propulsion Lab., California Inst. of Tech., Pasadena.)

In NASA. Langley Research Center, Sixteenth International Laser Radar Conference, Part 1 Jul. 1992 p 61-62 (For primary document see N92-29228 20-35)
Avail: CASI HC A01/MF A04

The Global Backscatter Experiment (GLOBE) was intended to provide data on prevailing values of atmospheric backscatter cross section. The primary intent was predicting the performance of space-borne lidar systems. A second and related goal was to understand the source and characteristics of atmospheric aerosol particles. In this paper the authors give a summary of measurement results with emphasis on the magnitude, structure, characteristics and variability of the observed atmospheric aerosol and cloud scattering. The GLOBE pulsed lidar measurements provide an extensive data set on the magnitude and variability of aerosol and cloud backscatter of the atmosphere. The data defines atmospheric aerosol scattering characteristics and should prove to be an important resource for determination of the performance and design of laser remote sensing instruments. H.A.

N92-29247*# National Aeronautics and Space Administration. Goddard Space Flight Center, Greenbelt, MD.
MULTI-WAVELENGTH AIRBORNE LIDAR INTERCOMPARISONS OF AEROSOL AND CIRRUS BACKSCATTER OVER THE PACIFIC OCEAN c45
Robert T. Menzies (Jet Propulsion Lab., California Inst. of Tech., Pasadena.), David M. Tratt (Jet Propulsion Lab., California Inst. of Tech., Pasadena.), James D. Spinhirne, and S. Chudamani *In* NASA. Langley Research Center, Sixteenth International Laser Radar Conference, Part 1 Jul. 1992 p 63-65 (For primary document see N92-29228 20-35)
Avail: CASI HC A01/MF A04

Airborne CO2 and Nd:YAG lidar instruments were flown on the NASA DC-8 research aircraft during two extended missions over the Pacific. The objectives during these flights were to characterize aerosol backscatter levels at infrared wavelengths in relatively pristine regions of the troposphere, and to observe cloud effects on lidar signals. In addition, the three wavelength Nd:YAG data were processed using independent temperature profile information, in order to deduce the Rayleigh scattering component of the total backscatter at each wavelength. The data can be used to better understand the capabilities of various airborne or Earth-orbiting lidar designs to provide backscatter information from aerosols and clouds, or to provide Doppler or DIAL information from aerosol and cloud backscatter. H.A.

N92-29248*# National Aeronautics and Space Administration. Langley Research Center, Hampton, VA.
AIRBORNE LIDAR OBSERVATIONS OF THE STRATOSPHERE AFTER THE PINATUBO ERUPTION c45
David M. Winker, Mary T. Osborn (Hughes STX, Inc., Lanham, MD.), and Robert J. DeCoursey (Hughes STX, Inc., Lanham, MD.) *In its* Sixteenth International Laser Radar Conference, Part 1 Jul. 1992 p 67-70 (For primary document see N92-29228 20-35)
Avail: CASI HC A01/MF A04

The eruption of Mt. Pinatubo in June 1991 injected the largest mass of gases and ash into the stratosphere observed since lidar and satellite monitoring of the stratosphere became possible in the middle 1960's. Because of early indications of the significance of the eruption, NASA mounted an airborne mission to survey the stratospheric plume soon after the eruption. The NASA Wallops Electra aircraft was outfitted with a depolarization lidar, a correlation spectrometer (for SO2 measurements), a total-direct-diffuse spectral radiometer, and a Fourier transform spectrometer. Six flights were made during the period July 7-14. Author

N92-29249*# Science and Technology Corp., Hampton, VA.
MULTI-WAVELENGTH MEASUREMENTS OF THE STRATOSPHERIC AEROSOL LAYER MADE AT HAMPTON, VIRGINIA (37N, 76W) c45
G. S. Kent, G. M. Hansen, and K. M. Skeens *In* NASA. Langley Research Center, Sixteenth International Laser Radar Conference, Part 1 Jul. 1992 p 71-74 (For primary document see N92-29228 20-35)
(Contract NAS1-18851)
Avail: CASI HC A01/MF A04

Atmospheric observations have recently commenced using a new lidar system. The lidar, intended for the study of clouds and aerosols in the upper troposphere and stratosphere, is presently being installed at NASA Langley. Although all the lidar subsystems are not yet in place, a program of three wavelength observations of the stratospheric layer was begun in late Feb. 1992. The present observations are continuing and work is currently in progress to improve the inversion algorithm used to obtain the backscatter profiles. The profiles will then be further used, in conjunction with suitable aerosol models, to derive the size distribution parameters and to make estimates of the column mass loading. H.A.

N92-29250*# National Inst. for Environmental Studies, Tsukuba (Japan).
THREE-WAVELENGTH LIDAR MEASUREMENTS OF PINATUBO AEROSOL AND ITS OPTICAL PROPERTIES c45
Y. Sasano, I. Matsui, and S. Hayashida *In* NASA. Langley Research Center, Sixteenth International Laser Radar Conference, Part 1 Jul. 1992 p 75-78 (For primary document see N92-29228 20-35)
Avail: CASI HC A01/MF A04

Enhanced stratospheric aerosols due to Mt. Pinatubo eruption have been measured using a YAG laser-based three wavelength lidar and a YAG laser-based large-scale lidar. Temporal variation of the integrated backscatter coefficient derived from the backscatter coefficient profiles were obtained. The present paper describes some results of optical properties analysis using lidar data obtained since Dec., 1991 when the main body of aerosols started to appear over Japan. The derived properties of the Pinatubo aerosols are extinction to backscatter ratios, wavelength dependencies of backscatter coefficients and extinction coefficients, and optical thickness. The analysis is based on the assumption of similarity in backscatter profiles for three wavelengths which are derived from lidar signals using the Fernald equation with assumed extinction to backscatter ratios. H.A.

N92-29251*# Consiglio Nazionale delle Ricerche, Frascati (Italy).
LIDAR OBSERVATIONS OF THE PINATUBO STRATOSPHERIC AEROSOL CLOUD OVER FRASCATI, ITALY c45
Fernando Congeduti, Alberto Adriani, Gian Paolo Gobbi, and Sante Centurioni *In* NASA. Langley Research Center, Sixteenth International Laser Radar Conference, Part 1 Jul. 1992 p 79-81 (For primary document see N92-29228 20-35)
Avail: CASI HC A01/MF A04

The Pinatubo eruption of June 1991 introduced large plumes into the local stratosphere. On several occasions, volcanic gases and particles reached altitudes of about 30 km, and spread towards the west. A lidar system has been operating to monitor the evolution of the stratospheric aerosol cloud. The backscattering ratio profiles of eight different measurements were chosen to summarize the most significant occurrences of the event. Since the beginning of the winter planetary wave activity, the Pinatubo cloud integrated backscatter exceeded El Chichon's. In this context, the perturbation generated by El Chichon can only be assumed as a lower limit of the one which will follow the Pinatubo eruption. Observations of the event are still in progress. H.A.

N92-29252*# Anhui Inst. of Optics and Fine Mechanics, Hefei (China).
L625 LIDAR MEASUREMENTS OF PINATUBO VOLCANIC CLOUD AT HEFEI c45
Huanling Hu and Jun Zhou *In* NASA. Langley Research Center, Sixteenth International Laser Radar Conference, Part 1 Jul. 1992 p 83-86 (For primary document see N92-29228 20-35)
Avail: CASI HC A01/MF A04

The Pinatubo volcano erupted violently between June 9-17, 1991. This eruption was much larger than the El Chichon volcanic eruption in April, 1982. Because of the effects on the global environment, much attention was focused on the measurements

of the volcanic cloud. The 84 scattering-ratio profiles of the volcanic cloud have been obtained by our L625 lidar system. The conclusions from studies of the data are: (1) Pinatubo volcanic cloud was present over Hefei after 40 days from eruption; (2) the peak scattering ratio varied violently in July and August of 1991; (3) the height of the peak scattering ratio is between about 18 to 25 km; and (4) since August 28, 1991, the optical depth was about one order of magnitude larger than before the eruption.
Author

N92-29253*# York Univ. (Ontario). Inst. for Space and Terrestrial Science.
TWO WAVELENGTH MEASUREMENTS OF THE PINATUBO AEROSOL ABOVE TORONTO, CANADA **c45**
W. Steinbrecht, D. Donovan, and A. I. Carswell *In* NASA. Langley Research Center, Sixteenth International Laser Radar Conference, Part 1 Jul. 1992 p 87-90 (For primary document see N92-29228 20-35)
Avail: CASI HC A01/MF A04

Since March 1991 our group has been routinely operating a Differential Absorption Lidar system in Toronto, Canada. The system is based on a XeCl Excimer laser. We have also been running a Backscatter Lidar based on a NdYAG laser. In the period from March 1991 to March 1992 measurements have been taken during about 40 nights with the DIAL system and more than 90 nights with the NdYAG system. In all measurements after July 21, 1991 we have observed aerosol layers in the stratosphere, resulting from the Mt. Pinatubo eruptions around June 15, 1992. These aerosol layers interfere significantly with many optical remote sensing techniques, and we have been investigating their properties with our two Lidar systems. In this paper we present a summary of these measurements. Author

N92-29254*# National Aeronautics and Space Administration. Langley Research Center, Hampton, VA.
LIDAR OBSERVATIONS OF THE PINATUBO VOLCANIC CLOUD OVER HAMPTON, VIRGINIA **c45**
M. T. Osborn (Hughes STX, Inc., Lanham, MD.), D. M. Winker, D. C. Woods, and R. J. DeCoursey (Hughes STX, Inc., Lanham, MD.) *In its* Sixteenth International Laser Radar Conference, Part 1 Jul. 1992 p 91-94 (For primary document see N92-29228 20-35)
Avail: CASI HC A01/MF A04

A series of eruptions of Mt. Pinatubo climaxed in a cataclysmic eruption on June 15-16, which greatly perturbed the stratospheric aerosol layer. These eruptions yielded an estimated 20 megatons of SO2, which is three times the amount produced by El Chichon. Lidar measurements taken by the 48-inch lidar system at Langley Research Center show the vertical distribution, intensity and spread of the Pinatubo aerosol layers over the middle latitude locations. A few observations have also been made using an airborne lidar system which measures scattering and depolarization. The magnitude and transport time of the volcanic aerosols following Pinatubo and El Chichon are compared. In addition, comparisons are made between the ground-based lidar measurements and near-coincident Stratospheric Aerosol and Gas Experiment (SAGE) 2 satellite observations of the Pinatubo aerosol layers. Author

N92-29255*# Nevada Univ., Las Vegas.
OZONE MEASUREMENTS WITH THE US EPA UV-DIAL: PRELIMINARY RESULTS **c45**
H. Moosmueller, D. Diebel, D. H. Bundy (Environmental Protection Agency, Las Vegas, NV.), M. P. Bristow (Environmental Protection Agency, Las Vegas, NV.), R. J. Alvarez, II (Environmental Protection Agency, Las Vegas, NV.), V. A. Kovalev (Environmental Protection Agency, Las Vegas, NV.), C. M. Edmonds (Environmental Protection Agency, Las Vegas, NV.), R. M. Turner, and J. L. McElroy (Environmental Protection Agency, Las Vegas, NV.) *In* NASA. Langley Research Center, Sixteenth International Laser Radar Conference, Part 1 Jul. 1992 p 95-98 (For primary document see N92-29228 20-35)
Avail: CASI HC A01/MF A04

A compact airborne down-looking lidar system was developed at the Environmental Protection Agency in Las Vegas. This differential absorption lidar (DIAL) was designed to simultaneously measure range-resolved concentrations of ozone (O3) and sulfur dioxide (SO2) in the lower troposphere, together with an indication of the aerosol distribution. The five laser wavelengths (i.e., lambda(sub 1) = 277 nm, lambda(sub 2) = 292 nm, lambda(sub 3) = 313 nm, lambda(sub4) = 319 nm, lambda(sub 5) = 369 nm) were generated via Raman conversion of a focused KrF excimer laser. The system is currently installed in a truck-based mobile laboratory. For the ground testing, an opening in the truck floor together with a folding mirror under the truck makes a horizontal, or upwardly inclined direction of measurement possible. Initial ground testing has been performed in the vicinity of a Desert Research Institute (DRI) ambient air monitoring site, located at Cottonwood Cove approximately 85 km south east of Las Vegas, Nevada. At this site O3 and SO2 concentrations are continuously monitored with an average accuracy better than +/- 10 percent. A temporary ozone measurement station with identical accuracy was set up at a distance to get a second point of comparison for the range-resolved DIAL measurements. Author

N92-29256*# Pacific Northwest Lab., Richland, WA. Applied Physics Center.
LIDAR DEVELOPMENT FOR THE ATMOSPHERIC RADIATION MEASUREMENT (ARM) PROGRAM **c45**
J. Griffin and M. Lapp (Sandia National Labs., Livermore, CA.) *In* NASA. Langley Research Center, Sixteenth International Laser Radar Conference, Part 1 Jul. 1992 p 99-101 (For primary document see N92-29228 20-35)
Avail: CASI HC A01/MF A04

The Atmospheric Radiation Measurement (ARM) Program was initiated by the Department of Energy's Atmospheric and Climate Research Division (DOE/ACRD) to improve parameterizations of cloud radiative effects in general circulation models of the Earth's climate. The Instrument Development Program (IDP), a major component of ARM, is directed toward the improvement of radiometric and remote sensing instrumentation pertinent to near real-time characterizations of atmospheric parameters. The ultimate goal of this program is to provide state-of-the-art instruments suitable for installation and extended use in ARM's field measurement component, the Cloud and Radiation Testbed (CART). Author

N92-29257*# National Aeronautics and Space Administration. Goddard Space Flight Center, Greenbelt, MD.
LIDAR MEASUREMENTS OF STRATOSPHERIC OZONE, TEMPERATURE AND AEROSOL DURING 1992 UARS CORRELATIVE MEASUREMENT CAMPAIGN **c45**
Thomas J. McGee, Upendra N. Singh (Hughes STX, Inc., Lanham, MD.), Michael Gross (Hughes STX, Inc., Lanham, MD.), William S. Heaps, and Richard Ferrare (Universities Space Research Association, Greenbelt, MD.) *In* NASA. Langley Research Center, Sixteenth International Laser Radar Conference, Part 1 Jul. 1992 p 103-106 (For primary document see N92-29228 20-35)
Avail: CASI HC A01/MF A04

Measurements of stratospheric ozone, temperature, and aerosols were made by the NASA/GSFC mobile stratospheric lidar during the UARS (Upper Atmospheric Research Satellite) Correlative Measurement Campaign at the JPL-Table Mountain Facility in Feb. and Mar. 1992. Due to the presence of substantial amounts of residual volcanic aerosol from the eruption of Mt. Pinatubo, the GSFC lidar system was modified for an accurate measurement of ozone concentration in the stratosphere. While designed primarily for the measurement of stratospheric ozone, this lidar system was also used to measure middle atmosphere temperature and density from 30 to 65 km and stratospheric aerosol from 15 to 35 km. In the following sections, we will briefly describe and present some typical measurements made during this campaign. Stratospheric ozone, temperature, and aerosols profiles derived from data taken between 15 Feb. and 20 Mar., 1992 will be presented at the conference. Author

N92-29258*# Deutsche Forschungsanstalt fuer Luft- und Raumfahrt, Oberpfaffenhofen (Germany, F.R.). Inst. fuer Physik der Atmosphaere.

AIRBORNE DIAL REMOTE SENSING OF THE ARCTIC OZONE LAYER **c45**

Martin Wirth, Wolfgang Renger, and Gerhard Ehret *In* NASA. Langley Research Center, Sixteenth International Laser Radar Conference, Part 1 Jul. 1992 p 107-108 (For primary document see N92-29228 20-35)

Avail: CASI HC A01/MF A04

A combined ozone and aerosol LIDAR was developed at the Institute of Physics of the Atmosphere at the DLR in Oberpfaffenhofen. It is an airborne version, that, based on the DIAL-principle, permits the recording of two-dimensional ozone profiles. This presentation will focus on the ozone-part; the aerosol subsection will be treated later. Author

N92-29259*# Meteorologisches Observatorium, Hohenpeissenberg (Germany, F.R.).

LIDAR MEASUREMENT OF STRATOSPHERIC OZONE AT HOHENPEISSENBERG: AN IMPROVED EVALUATION METHOD **c45**

W. Vandersee, F. Schoenenborn, and H. Claude *In* NASA. Langley Research Center, Sixteenth International Laser Radar Conference, Part 1 Jul. 1992 p 109-112 (For primary document see N92-29228 20-35)

Avail: CASI HC A01/MF A04

In 1987, the schedule of long-term ozone monitoring at the Meteorological Observatory Hohenpeissenberg was extended by operational DIAL measurements. A detailed description of the system is given in earlier works. An improved evaluation method will be described, which allows the calculation of stratospheric ozone distribution up to 50 km. A good balance between precision and range resolution is achieved. The evaluation begins with the calculation of the relative error for each channel in accordance with the Poisson distribution. During the following evaluation an error calculation is performed according to the Gaussian error propagation. After normalization of the backscatter profiles to count per shot and kilometer, an empirical function is applied to correct non-linearities of the photomultipliers. Author

N92-29260*# Centre National de la Recherche Scientifique, Paris (France).

A MULTI-WAVELENGTH OZONE LIDAR FOR THE EASOE EXPERIMENT **c45**

S. Godin, G. Ancellet, C. David, J. Porteneuve, C. Leroy, V. Mitev (Cantonal Observatory, Neuchatel, Switzerland), Y. Emery (Cantonal Observatory, Neuchatel, Switzerland), C. Flesia (Cantonal Observatory, Neuchatel, Switzerland), V. Rizi (Aquila Univ., Italy), and G. Visconti (Aquila Univ., Italy) et al *In* NASA. Langley Research Center, Sixteenth International Laser Radar Conference, Part 1 Jul. 1992 p 113-115 Prepared in cooperation with Consiglio Nazionale delle Ricerche, Florence, Italy (For primary document see N92-29228 20-35)

Avail: CASI HC A01/MF A04

The study of the ozone layer during winter and springtime in high latitude regions is a major issue in atmospheric research. For a better understanding of these problems, an important experimental campaign called EASOE (European Arctic Stratospheric Ozone Experiment) was organized by the European Community during the winter 1991-1992. Its main objective was to establish a budget of the ozone destruction processes on the whole northern hemisphere. This implied the simultaneous operation of different types of instruments located in both high and mid-latitude regions in order to study the destruction processes as well as the evolution of the ozone layer during the period of the campaign. A description will be given here of a mobile ozone lidar instrument specially designed for operation during the EASOE campaign. This system, which performs ozone measurements in the 5 to 40 km altitude range was located in Sodankyla, Finland as part of the ELSA experiment which also includes operation of another multi-wavelength lidar designed for polar stratospheric cloud measurements. Author

N92-29261*# National Aeronautics and Space Administration. Langley Research Center, Hampton, VA.

CORRECTION OF DIAL STRATOSPHERIC OZONE MEASUREMENTS IN THE PRESENCE OF PINATUBO AEROSOLS **c45**

Marta A. Fenn (Hughes STX, Inc., Lanham, MD.), Syed Ismail, Edward V. Browell, and Carolyn F. Butler (Hughes STX, Inc., Lanham, MD.) *In its* Sixteenth International Laser Radar Conference, Part 1 Jul. 1992 p 117-120 (For primary document see N92-29228 20-35)

Avail: CASI HC A01/MF A04

NASA Langley's airborne lidar system measured aerosol and ozone distributions in the stratosphere from Jan. - Mar. 1992 as part of the Airborne Arctic Stratospheric expedition (AASE-2). The eruption of Mount Pinatubo in Jun. 1991 has increased the aerosol burden of the stratosphere and thereby increased the importance of applying an aerosol correction to the ozone measurements. The correction relies on a Bernoulli solution to derive a backscatter correction to the differential absorption lidar (DIAL) returns at two wavelengths in the ultraviolet spectral region (lambda(sub on) = 301.5 nm, lambda(sub off) = 310.87 nm) as described in earlier works. This paper discusses how the parameters for the correction were optimized for application to the AASE-2 data set. Author

N92-29262*# General Electric Co., Princeton, NJ. Astro Space Div.

THE LASER ATMOSPHERIC WIND SOUNDER (LAWS) PRELIMINARY ERROR BUDGET AND PERFORMANCE ESTIMATE **c45**

David L. Kenyon and Kent Anderson *In* NASA. Langley Research Center, Sixteenth International Laser Radar Conference, Part 1 Jul. 1992 p 121-123 (For primary document see N92-29228 20-35)

Avail: CASI HC A01/MF A04

The Laser Atmospheric Wind Sounder (LAWS) study phase has resulted in a preliminary error budget and an estimate of the instrument performance. This paper will present the line-of-sight (LOS) Velocity Measurement Error Budget, the instrument Boresight Error Budget, and the predicted signal-to-noise ratio (SNR) performance. The measurement requirements and a preliminary design for the LAWS instrument are presented in a companion paper. Author

N92-29263*# Hughes Danbury Optical Systems, Inc., CT.

LAG ANGLE COMPENSATION IN A SPACE BORNE SCANNING LIDAR **c45**

A. B. Wissinger *In* NASA. Langley Research Center, Sixteenth International Laser Radar Conference, Part 1 Jul. 1992 p 125-128 (For primary document see N92-29228 20-35)

Avail: CASI HC A01/MF A04

The so-called 'lag angle' is inherent in any spaceborne scanning lidar system. It is also important in systems where the scanning causes a significant pointing error during the laser interrogating pulse echo time. In a heterodyne lidar system, the lag angle, if uncompensated, will significantly reduce the signal-to-noise ratio. An investigation of lag angle is presented. Author

N92-29264*# National Aeronautics and Space Administration. Langley Research Center, Hampton, VA.

LIDAR IN-SPACE TECHNOLOGY EXPERIMENT (LITE) ELECTRONICS OVERVIEW

Michael P. Blythe, Richard H. Couch, Carroll W. Rowland, Wayne L. Kitchen, Curtis P. Regan, Michael R. Koch, Charles W. Antill, William T. Stevens, Courtney H. Rollins, and Edward H. Kist et al *In its* Sixteenth International Laser Radar Conference, Part 1 Jul. 1992 p 129-132 (For primary document see N92-29228 20-35)

Avail: CASI HC A01/MF A04

The LITE electronics system consists of the following seven subsystems: Laser Transmitter Module (LTM), Boresight Assembly (BA), Aft-Optics Electronics (AOE), Digital Data Handling Unit (DDHU), Engineering Data System (EDS), Instrument Controller

(IC), and the Ground Support Equipment (GSE). Each of these subsystems is discussed. Author

N92-29265*# Titan Spectron Div., Costa Mesa, CA.
LASER TRANSMITTER MODULE (LTM) FOR LITE
John Chang (Gemstar Development Corp., Pasadena, CA.), Marc Cimolino (Science and Technology Corp., Hampton, VA.), Edmond Joe (A, E and M, Hampton, VA.), Mulgeta Petros (Science and Technology Corp., Hampton, VA.), Karl Reithmaier (California Inst. of Tech., Pasadena.), Ray Thompson, and Ron Villane *In* NASA. Langley Research Center, Sixteenth International Laser Radar Conference, Part 1 Jul. 1992 p 133-136 (For primary document see N92-29228 20-35)
Avail: CASI HC A01/MF A04

In Dec. 1991 TITAN SPECTRON successfully completed its six year effort to design, build, space qualify, test, and deliver the Laser Transmitter Module (LTM) for NASA LaRC's LITE program. The delivered LTM is a three color Q-switched flashlamp pumped Nd:YAG laser that is described as the first true world-class lidar in space. The preliminary design and verification tests results were first presented at the 14th International Laser Radar Conference (ILRC) in 1988. This paper describes not only the delivered product but also the verification and space qualification processes that resulted in the world's first space qualified high powered laser system for environmental exploration from space. Video of the laser operating in a Class 100 clean room and subsystems undergoing 10 G vibration tests will provide a vivid illustration of the key elements that separate a space qualified system from its laboratory counterpart. Flight laser performance measurements form the baseline in post-delivery test results to be presented at this conference. Author

N92-29266*# National Aeronautics and Space Administration. Goddard Space Flight Center, Greenbelt, MD.
INTERCOMPARISONS OF LIDAR BACKSCATTER MEASUREMENTS AND IN-SITU DATA FROM GLOBE c45
S. Chudamani and James D. Spinhirne *In* NASA. Langley Research Center, Sixteenth International Laser Radar Conference, Part 1 Jul. 1992 p 137-139 (For primary document see N92-29228 20-35)
Avail: CASI HC A01/MF A04

The Global Backscatter Experiment (GLOBE) took place during Nov. 1989 and May - Jun. 1990 and involved flight surveys of the Pacific region by the NASA DC-8 aircraft. The experimental instruments were lidars operating at wavelengths ranging from the visible to the thermal infrared and various optical particle counters for in-situ measurements. The primary motivation for GLOBE was the development of spaceborne wind sensing lidar. This paper will concern a comparison of direct backscatter measurements and backscatter calculated from particle counter data. Of special interest is that the particle measurements provided data on composition, and thus refractive index variation may be included in the analysis. Author

N92-29267*# Ecole Polytechnique, Palaiseau (France). Lab. de Meteorologie Dynamique.
SIMULATION OF THE PERFORMANCES OF WIND, AN AIRBORNE CO2 LIDAR
D. Oh, A. Dabas, F. Lieutaud, C. Loth, and P. H. Flamant *In* NASA. Langley Research Center, Sixteenth International Laser Radar Conference, Part 1 Jul. 1992 p 141-143 (For primary document see N92-29228 20-35)
Avail: CASI HC A01/MF A04

An airborne Doppler coherent lidar is under development as a joint project between France and Germany. The instrument is designed around CO2 laser technology, heterodyne detection, and a conical scanning of the line-of-site. The 10 micron domain is suitable for long range measurements due to the maturity of the technology and because it corresponds to an atmospheric window. The objectives of WIND are twofold: (1) to conduct mesoscale scientific studies in particular over oceanic and inhomogeneous terrain areas; and (2) to support the Earth-orbiting wind lidar projects. Author

N92-29268*# Ecole Polytechnique, Palaiseau (France).
SAMPLING AND REPRESENTATIVENESS FOR A SPACEBORNE WIND LIDAR
F. Lieutaud, A. Dabas, P. H. Flamant, G. Seze, and Ph. Courtier (Direction de la Meteorologie Nationale, Paris, France) *In* NASA. Langley Research Center, Sixteenth International Laser Radar Conference, Part 1 Jul. 1992 p 145-148 Sponsored in part by CNES/ESA (For primary document see N92-29228 20-35)
Avail: CASI HC A01/MF A04

The capability of an Earth-orbiting lidar to produce a reliable windfield sampling with an error of 1-3 ms(exp -1) and that is relevant to numerical forecasting and climate studies is discussed. The spatial and temporal resolutions range from 100 km to 1000 km and 3 hr to 1 month respectively. In this respect cloud obstruction is of great concern, as it can prevent the lidar probing whole parts of the atmosphere, for both short and long periods of time. A worldwide analysis of cloudiness from either visual observations made from the ground or else from the Stratospheric Aerosol and Gas Experiment (SAGE) instrument, has shown that the average cloud cover is 60 percent. This analysis is only valid at large scales (time and space) compatible with the currently operating satellites. However, a lidar footprint is only about a hundred meters or less, and it was observed from ground based lidars that, even when the cloudiness is 100 percent, some lidar shots get through. A complete analysis of the probability of probing through clouds by a spaceborne lidar is presently beyond our capacities. Hence, no small scale cloudiness data set is yet available representing all kinds of meteorological situations at all latitudes. Author

N92-29269*# National Aeronautics and Space Administration. Goddard Space Flight Center, Greenbelt, MD.
LABORATORY VELOCIMETER MEASUREMENTS USING THE EDGE TECHNIQUE
Bruce M. Gentry and C. Laurence Korb *In* NASA. Langley Research Center, Sixteenth International Laser Radar Conference, Part 1 Jul. 1992 p 149-152 (For primary document see N92-29228 20-35)
Avail: CASI HC A01/MF A04

We have developed a simple but powerful measurement methodology using the edge technique to measure the Doppler shift of backscatter laser radiation. With this method, instantaneous velocity information, including wind measurements, can be obtained with sub-meter-per-second accuracy and with high range resolution using a pulsed lidar system. This paper describes laboratory experiments that demonstrate the basic principles of the edge technique. These experiments demonstrate the sensitivity of the technique and the high velocity accuracy which can be obtained. In addition, many of the characteristics which make the edge technique a powerful method for use in lidar wind application were verified. These include the insensitivity of the measurement to laser and/or edge filter frequency jitter and drift, and the ability to make Doppler shift measurements which are of the order of 100 times better than the spectral bandwidth of the measurement (the combined spectral width of the laser and edge filter). Author

N92-29270*# Simpson Weather Associates, Inc., Charlottesville, VA.
IDENTIFICATION OF CRITICAL DESIGN POINTS FOR THE EAP OF A SPACE-BASED DOPPLER LIDAR WIND SOUNDER
G. D. Emmitt and S. A. Wood *In* NASA. Langley Research Center, Sixteenth International Laser Radar Conference, Part 1 Jul. 1992 p 153-156 (For primary document see N92-29228 20-35)
Avail: CASI HC A01/MF A04

The feasibility of making tropospheric wind measurements with a space-based Doppler lidar was studied by a number of agencies over the past 10-15 years. Currently NASA has a plan to launch such an instrument, the Laser Atmospheric Wind Sounder (LAWS), within the next decade. The design of the LAWS continues to undergo a series of iterations common to most instruments targeted for a space platform. In general, the constraints of available platform

power, weight allowance, and project funds continue to change. With these changes the performance and design specifications also must change. Author

N92-29271*# Wisconsin Univ., Madison.
WIND PROFILES DERIVED FROM VOLUME IMAGING LIDAR DATA: ENHANCEMENTS TO THE ALGORITHM AND COMPARISONS WITH INSITU OBSERVATIONS **c47**
A. K. Piironen and E. W. Eloranta *In* NASA. Langley Research Center, Sixteenth International Laser Radar Conference, Part 1 Jul. 1992 p 157-160 (For primary document see N92-29228 20-35)
Avail: CASI HC A01/MF A04

This paper presents wind measurements made with the University of Wisconsin Volume Imaging Lidar (VIL) during Aug. 1989 as part of the First ISLSCP (International Satellite Land Surface Climatology Project) Field Experiment (FIFE). Enhancements to the algorithm are described. Comparisons of these results to aircraft, balloon, and surface based wind measurements are presented. Observations of the spatial variance of aerosol backscatter are also compared to measurements of the convective boundary layer depth. Measurements are based on two-dimensional cross correlations between horizontal image planes showing the spatial distribution of aerosol scattering observed by the lidar at intervals of approximately 3 minutes. Each image plane covers an area of 500-1000 sq km and the winds calculated represent area averages. Author

N92-29272*# Wisconsin Univ., Platteville. Dept. of Physics.
MEASUREMENTS OF WIND DIVERGENCE WITH VOLUME IMAGING LIDAR **c47**
P. W. Young and E. W. Eloranta (Wisconsin Univ., Madison.) *In* NASA. Langley Research Center, Sixteenth International Laser Radar Conference, Part 1 Jul. 1992 p 161-164 (For primary document see N92-29228 20-35)
Avail: CASI HC A01/MF A04

Mesoscale horizontal divergence and vertical motion in the boundary layer are key ingredients in atmospheric and climate modeling. These quantities are very difficult to measure. This paper presents a technique for determining the divergence over a 10 km x 5 km area from lidar images depicting the spatial distribution of the naturally occurring atmospheric aerosols. Author

N92-29273*# Lund Inst. of Tech. (Sweden). Dept. of Physics.
DIAL MAPPING OF ATMOSPHERIC ATOMIC MERCURY OF GEOPHYSICAL ORIGIN **c45**
H. Edner, P. Ragnarson, S. Svanberg, and E. Wallinder *In* NASA. Langley Research Center, Sixteenth International Laser Radar Conference, Part 1 Jul. 1992 p 165-168 Sponsored in part by Swedish Natural Science Research Council; and the Swedish Board for Space Activities (For primary document see N92-29228 20-35)
Avail: CASI HC A01/MF A04

The atmospheric distribution of atomic mercury is studied with the differential absorption lidar technique using the 253.6 nm Hg resonance line. Using a mobile lidar system employing a Nd:YAG-pumped dye laser, studies were performed in Italian geothermal and mining areas. Concentrations ranging from the background value 2 ng/m(exp 3) to several micro-g/m(exp 3) were measured. Author

N92-29274*# National Oceanic and Atmospheric Administration, Boulder, CO. Wave Propagation Lab.
LIDAR TRACKING OF MULTIPLE FLUORESCENT TRACERS: METHOD AND FIELD TEST **c45**
Wynn L. Eberhard and Ron J. Willis (Colorado Univ., Boulder.) *In* NASA. Langley Research Center, Sixteenth International Laser Radar Conference, Part 1 Jul. 1992 p 169-172 Sponsored in part by EPA (For primary document see N92-29228 20-35)
(Contract DW13932524-01)
Avail: CASI HC A01/MF A04

Past research and applications have demonstrated the advantages and usefulness of lidar detection of a single fluorescent tracer to track air motions. Earlier researchers performed an analytical study that showed good potential for lidar discrimination and tracking of two or three different fluorescent tracers at the same time. The present paper summarizes the multiple fluorescent tracer method, discusses its expected advantages and problems, and describes our field test of this new technique. Author

N92-29275*# Los Alamos National Lab., NM.
LIDAR MONITORING OF MEXICO CITY'S ATMOSPHERE DURING HIGH AIR POLUTION EPISODES **c45**
C. R. Quick, Jr., F. L. Archuleta, D. E. Hof, R. R. Karl, Jr., J. J. Tiee, Jr., W. E. Eichinger, D. B. Holtkamp, and L. Tellier *In* NASA. Langley Research Center, Sixteenth International Laser Radar Conference, Part 1 Jul. 1992 p 173-175 (For primary document see N92-29228 20-35)
Avail: CASI HC A01/MF A04

Over the last two decades, Mexico City, like many large industrial and populous urban areas, has developed a serious air pollution problem, especially during the winter months when there are frequent temperature inversions and weak winds. The deteriorating air quality is the result of several factors. The basin within which Mexico City lies in Mexico's center of political, administrative and economic activity, generating 34 percent of the gross domestic product and 42 percent of the industrial revenue, and supporting a population which is rapidly approaching the 20 million mark. The basin is surrounded by mountains on three sides which end up preventing rapid dispersal of pollutants. Emissions from the transportation fleet (more than 3 million vehicles) are one of the primary pollution sources, and most are uncontrolled. Catalytic converters are just now working their way into the fleet. The Mexico City Air Quality Research Initiative in an international collaboration project between the Los Alamos National Laboratory and the Mexican Petroleum Institute are dedicated to the investigation of the air quality problem in Mexico City. The main objective of the project is to identify and assess the cost and benefits of major options being proposed to improve the air quality. The project is organized into three main activity areas: (1) modeling and simulation; (2) characterization and measurements; and (3) strategic evaluation. Author

N92-29276*# Consiglio Nazionale delle Ricerche, Naples (Italy).
LAB-SCALE LIDAR SENSING OF DIESEL ENGINES EXHAUSTS **c45**
A. Borghese *In* NASA. Langley Research Center, Sixteenth International Laser Radar Conference, Part 1 Jul. 1992 p 177-180 (For primary document see N92-29228 20-35)
Avail: CASI HC A01/MF A04

Combustion technology and its environmental concerns are being considered with increasing attention, not only for global-scale effects, but also for toxicological implications, particularly in the lift conditions of traffic-congested areas and industrial sites. Majority combustion by-products (CO, NO(sub x)) and unburned hydrocarbons (HC), are already subject to increasingly severe regulations; however other, non-regulated minority species, mainly soot and heavy aromatic molecules, involve higher health risks, as they are suspected to be agents of serious pathologies and even mutagenic effects. This is but one of the reasons why much research work is being carried out worldwide on the physical properties of these substances. Correspondingly, the need arises to detect their presence in urban environments, with as high a sensitivity as is required by their low concentrations, proper time- and space-resolutions, and 'real-time' capabilities. Lidar techniques are excellent candidates to this purpose, although severe constraints limit their applicability, eye-safety problems and aerosol Mie scattering uncertainties above all. At CNR's Istituto Motori in Napels, a Lidar-like diagnostic system is being developed, aimed primarily at monitoring the dynamic behavior of internal combustion engines, particularly diesel exhausts, and at exploring the feasibility of a so-called 'Downtown Lidar'. Author

N92-29277*# National Inst. for Environmental Studies, Tsukuba (Japan).
INFRARED PULSE-LASER LONG-PATH ABSORPTION MEASUREMENT OF CARBON DIOXIDE USING A RAMAN-SHIFTED DYE LASER **c45**
Atsushi Minato, Nobuo Sugimoto, and Yasuhiro Sasano *In* NASA. Langley Research Center, Sixteenth International Laser Radar Conference, Part 1 Jul. 1992 p 181-183 (For primary document see N92-29228 20-35)
Avail: CASI HC A01/MF A04

A pulsed laser source is effective in infrared laser long-path absorption measurements when the optical path length is very long or the reflection from a hard target is utilized, because higher signal-to-noise ratio is obtained in the detection of weak return signals. We have investigated the performance of a pulse-laser long-path absorption system using a hydrogen Raman shifter and a tunable dye laser pumped by a Nd:YAG laser, which generates second Stokes radiation in the 2-micron region. Author

N92-29278*# Colorado Univ., Boulder.
TRANSPORTABLE LIDAR FOR THE MEASUREMENT OF OZONE CONCENTRATION AND FLUX PROFILES IN THE LOWER TROPOSPHERE
Yanzeng Zhao, James N. Howell, and R. Michael Hardesty (National Oceanic and Atmospheric Administration, Boulder, CO.) *In* NASA. Langley Research Center, Sixteenth International Laser Radar Conference, Part 1 Jul. 1992 p 185-187 (For primary document see N92-29228 20-35)
Avail: CASI HC A01/MF A04

In many areas of the United States, as well as in other industrial areas (such as Europe), elevated and potentially harmful levels of ozone are being measured during summer. Most of this ozone is photochemically produced. The relatively long lifetime of ozone allows industrially produced ozone to be transported on a hemispheric scale. Since the trends of tropospheric ozone are very likely dependent on the source strengths and distributions of the pollutants and the chemical/ transport process involved, a predictive understanding of tropospheric ozone climatology requires a focus on the chemical and transport processes that link regional emissions to hemispheric ozone trends and distributions. Of critical importance to these studies is a satisfactory data base of tropospheric ozone distribution from which global and regional tropospheric ozone climatology can be derived, and the processes controlling tropospheric ozone can be better understood. A transportable lidar for measuring ozone concentration and flux profiles in the lower troposphere is needed. One such system is being developed at the National Oceanic and Atmospheric Administration/Earth Resources Laboratory (NOAA/ERL) Wave Propagation Laboratory (WPL). Author

N92-29279*# Los Alamos National Lab., NM. Chemical and Laser Sciences Div.
REMOTE DETECTION OF BIOLOGICAL PARTICLES AND CHEMICAL PLUMES USING UV FLUORESCENCE LIDAR **c45**
J. J. Tiee, D. E. Hof, R. R. Karl, R. J. Martinez, C. R. Quick, D. I. Cooper, W. E. Eichinger, and D. B. Holtkamp *In* NASA. Langley Research Center, Sixteenth International Laser Radar Conference, Part 1 Jul. 1992 p 189-192 Sponsored in part by Army; and by Los Alamos National Lab., NM (For primary document see N92-29228 20-35)
Avail: CASI HC A01/MF A04

A lidar system based on ultraviolet (UV) laser induced fluorescence (LIF) was developed for the remote detection of atmospherically dispersed biological particles and chemical vapors. This UV fluorescence lidar has many potential applications for monitoring environmental pollution, industrial waste emission, agricultural insect control, illicit chemical processing, and military defense operations. The general goal of this work is to investigate the research issues associated with the long range detection and identification of chemicals, e.g. aromatic solvents and chemical precursors, and biological materials, e.g. bacillus thuringiensis (BT) and bacillus globiggi (BG). In the detection of biological particulates, we are particularly interested in extending the detection range of an existing solar-blind 248-nm lidar system. We are investigating the use of longer excitation laser wavelengths (i.e. lambda greater than 280-nm to have more favorable atmospheric light transmission characteristics) for improving detection range to better than 10 km. In the detection of chemical plumes, our main research objectives are to determine how accurately and sensitively a chemical plume can be located at range, and how well spectrally the chemical species can be measured to allow their identification. Author

N92-29280*# Israel Inst. for Biological Research, Ness-Ziona.
SIGNAL QUALITY INFLUENCE ON AVERAGING PROCEDURE FOR DIAL POLLUTION MONITORING **c45**
S. Egert, D. Peri, and L. Berg (Laser Science, Inc., Newton, MA.) *In* NASA. Langley Research Center, Sixteenth International Laser Radar Conference, Part 1 Jul. 1992 p 193-194 (For primary document see N92-29228 20-35)
Avail: CASI HC A01/MF A04

Presented here is an analysis of the relative effect of each stochastic phenomenon on the accuracy of LIDAR measurements. The preferred averaging procedure to be applied is noted. The analysis takes into account the temporal correlation of the transmitted power variations which are associated with laser modal noise, short term temporal correlation of atmospheric turbulence, and 'white' additive noise. A distinction is made between two types of systems, one that transmits a sequence of pulses tuned into two wavelengths, but with a relatively large time separation, and another that transmits pulses in two wavelengths almost coincidentally. This distinction is important because the effect of speckle noise can be minimized when the pulses at two wavelengths are sent within the correlation time of the atmospheric turbulence. The presented analysis compares the signal to noise ratio in the calculation of the ratio beta (sub 1)/beta (sub 2), as achieved by using two methods of calculations: first averaging the data related to each wavelength and then taking the ratio, and first taking the ratio and then averaging. For both methods, normalization with respect to the transmitted power is considered, either prior to or after the averaging of the signals in each wavelength. Author

N92-29281*# Michigan Univ., Ann Arbor. Dept. of Atmospheric, Oceanic and Space Sciences.
EXTRACTION OF AEROSOL AND RAYLEIGH COMPONENTS FROM DOPPLER LIDAR RETURN SIGNAL **c45**
John E. Barnes, Ken W. Fischer, Vincent J. Abreu, and Wilbert R. Skinner *In* NASA. Langley Research Center, Sixteenth International Laser Radar Conference, Part 1 Jul. 1992 p 195-197 (For primary document see N92-29228 20-35)
Avail: CASI HC A01/MF A04

One of the most significant problems which limits the applicability of lidar systems for pressure and density profile measurements below 30 km altitude is the presence of atmospheric aerosols which contaminate the molecular or Rayleigh return signal. A new technique is described which allows for the separation of the return signal into aerosol and molecular scattered components. The technique was applied to data from the University of Michigan's High Resolution Doppler Lidar (HRDL). Author

N92-29282*# Sparta, Inc., Lexington, MA.
APPLICATION OF LASER IMAGING FOR BIO/GEOPHYSICAL STUDIES **c36**
J. R. Hummel, S. M. Goltz, N. L. DePiero, D. P. DeGloria, and F. M. Pagliughi *In* NASA. Langley Research Center, Sixteenth International Laser Radar Conference, Part 1 Jul. 1992 p 199-200 (For primary document see N92-29228 20-35)
Avail: CASI HC A01/MF A04

SPARTA, Inc. has developed a low-cost, portable laser imager that, among other applications, can be used in bio/geophysical applications. In the application to be discussed here, the system was utilized as an imaging system for background features in a forested locale. The SPARTA mini-ladar system was used at the International Paper Northern Experimental Forest near Howland, Maine to assist in a project designed to study the thermal and

radiometric phenomenology at forest edges. The imager was used to obtain data from three complex sites, a 'seed' orchard, a forest edge, and a building. The goal of the study was to demonstrate the usefulness of the laser imager as a tool to obtain geometric and internal structure data about complex 3-D objects in a natural background. The data from these images have been analyzed to obtain information about the distributions of the objects in a scene. A range detection algorithm has been used to identify individual objects in a laser image and an edge detection algorithm then applied to highlight the outlines of discrete objects. An example of an image processed in such a manner is shown. Described here are the results from the study. In addition, results are presented outlining how the laser imaging system could be used to obtain other important information about bio/geophysical systems, such as the distribution of woody material in forests. Author

N92-29283*# SRI International Corp., Menlo Park, CA. Geoscience and Engineering Center.

ARCLITE: THE ARCTIC LIDAR TECHNOLOGY FACILITY AT SONDRE STROMFJORD, GREENLAND **c09**

J. P. Thayer *In* NASA. Langley Research Center, Sixteenth International Laser Radar Conference, Part 1 Jul. 1992 p 201-203 (For primary document see N92-29228 20-35)
Avail: CASI HC A01/MF A04

SRI International is presently developing an Arctic lidar (ARCLITE) facility at the incoherent-scatter radar site in Sondre Stromfjord, Greenland (67.0 degrees N, 209.2 degrees W). The project, funded by NSF through the CEDAR (Coupling Energetics and Dynamics of Atmospheric Regions) initiative, is to perform high-altitude molecular/aerosol backscatter measurements in the Arctic covering the stratosphere/mesosphere region during nighttime and daytime conditions. The lidar system employs an injection seeded, high-energy GCR-5 Spectra Physics Nd:YAG laser for primary operation at 532 nm (550 mJ per pulse at 30 Hz). The receiver system is designed around a 36-inch Cassegrainian telescope of astronomical quality with receiver components and photon-counting electronics for day and night operations. The Rayleigh backscatter measurements will conduct investigations concerning long-term studies of the basic density and temperature structure of the Arctic stratosphere/mesosphere region; effects of stratospheric warming on the structure of the stratosphere/mesosphere region; occurrence and properties of polar stratospheric clouds; occurrence of noctilucent clouds and their properties at high latitudes; and dynamic and thermodynamic coupling between the stratosphere/mesosphere region and the lower thermosphere. Author

N92-29284*# Fukui Univ. (Japan).

ROTATIONAL RAMAN LIDAR FOR LOWER TROPOSPHERIC TEMPERATURE PROFILING

Takao Kobayashi, Takunori Taira, Takanobu Yamamoto, Akihiro Hori (Kansai Electric Power Corp. Ltd., Amagasaki, Japan), and Toshinobu Kitada (Kansai Electric Power Corp. Ltd., Amagasaki, Japan) *In* NASA. Langley Research Center, Sixteenth International Laser Radar Conference, Part 1 Jul. 1992 p 205-208 (For primary document see N92-29228 20-35)
Avail: CASI HC A01/MF A04

Accurate sensing of the tropospheric temperature profile is basically needed in meteorology and 3D mapping of the boundary layer atmospheric temperature over urban and industrial areas. Several temperature lidar techniques were investigated, including Differential Absorption Lidar (DIAL), rotational and vibrational Raman, Rayleigh and high resolution Rayleigh schemes. For the tropospheric applications, the rotational Raman scheme looks potentially advantageous, but several stringent technical problems still remain to be solved. Reported here are the continuing efforts of the system development of the rotational Raman lidar. Author

N92-29285*# York Univ. (Ontario). Dept. of Physics and Astronomy.

ONE YEAR OF RAYLEIGH LIDAR MEASUREMENTS AT TORONTO **c45**

James A. Whiteway and Allan I. Carswell *In* NASA. Langley Research Center, Sixteenth International Laser Radar Conference, Part 1 Jul. 1992 p 209-212 (For primary document see N92-29228 20-35)
Avail: CASI HC A01/MF A04

The Rayleigh lidar technique is being used at York University to study middle atmospheric thermal structure with particular emphasis on the properties and influence of internal gravity waves. These measurements are now carried out on a routine basis (every clear night) in order to determine seasonal variability and, eventually, long term trends. The transmitter consists of a doubled Nd:YAG laser with an output of 0.4 Joules per pulse at 20Hz (8 Watts) which is expanded to obtain a divergence of 0.4 milliradians. Backscattered photons are collected by a half meter cassegrain telescope, filtered to a bandwidth of 1nm, detected by a PMT, and counted with a multi-channel scaling averager. Strong backscatter from lower altitudes is blocked using a rotating chopper (25000rpm) which triggers the laser. The range gate and hardware averaging interval are variable but typically 300m and 5 minutes. Relative density profiles are obtained by simply normalizing to a model (eg. CIRA) at some altitude. Absolute temperature is derived using the hydrostatic equation, ideal gas law, and a model pressure value at the altitude where the photocount statistical uncertainty is about 15 percent - typically 90km for the entire night's average. The lower limit is currently about 30-35km due the presence aerosol from the volcanic eruption of Mt. Pinatubo. Author

N92-29286*# Bulgarian Academy of Sciences, Sofia. Inst. of Electronics.

LIDAR OBSERVATION OF AEROSOL AND TEMPERATURE STRATIFICATION OVER URBAN AREA DURING THE FORMATION OF A STABLE ATMOSPHERIC PBL **c45**

I. Kolev, O. Parvanov, B. Kaprielov, V. Mitev, V. Simeonov, and I. Grigorov *In* NASA. Langley Research Center, Sixteenth International Laser Radar Conference, Part 1 Jul. 1992 p 213-216 (For primary document see N92-29228 20-35)
Avail: CASI HC A01/MF A04

In recent years, the processes in the atmospheric planetary boundary layer (PBL) over urban areas were intensely investigated, due to ecological problems related to the air, soil, and water pollution. New pollution sources in new residential districts, when in contradiction to the microclimate and topography requirements of that region, create a number of considerable hazards and problems. The present study is a continuation of our preceding investigations and aims at revealing the aerosol structure and stratification during the transition after sunset as measured by two lidars. Such observation of the nocturnal, stable PBL formation over an urban area in Bulgaria has not been reported before. The lidars' high time and spatial resolutions allow the changes of the internal structure of the PBL's part located above the surface layer to be observed. Author

N92-29287*# Bulgarian Academy of Sciences, Sofia. Inst. of Electronics.

A COMPARISON BETWEEN RAMAN LIDAR AND CONVENTIONAL CONTACT MEASUREMENTS OF ATMOSPHERIC TEMPERATURE **c45**

V. M. Mitev, V. B. Simeonov, and I. V. Grigorov *In* NASA. Langley Research Center, Sixteenth International Laser Radar Conference, Part 1 Jul. 1992 p 217-220 (For primary document see N92-29228 20-35)
Avail: CASI HC A01/MF A04

Described here are the results of comparison between lidar and conventional contact measurements of the vertical temperature profile of the atmosphere. The lidar measurements are based on the method of temperature dependence of pure rotational Raman scattering of nitrogen and oxygen molecules. The presented results show that, as a whole, the motion of the lidar and conventional profiles coincide in the confidence intervals. Still there are districts in which the differences lay out of the confidence intervals. In analysis and estimation of the coincidence and the distinction in moving the profiles, we must take into account the differences between the methods for measuring the temperature profiles by

lidar and contact methods, i.e. the next additional factors. The tied balloon meter gives the momentary values of the temperature in particular points of the profile, as these momentary values are the results of consequent, but not simultaneous measurements. In the case of free flying balloon, the time of measuring the lower several hundred meters is little because of high vertical velocity (about 300 m/min). This leads to an indefinite increase of the measuring error. The complete space coincidence between the lidar's and conventional profiles isn't possible. The contribution of the factors mentioned above about the error of comparison could increase because of nonstable layers in the planetary boundary layer of the atmosphere as well as by the influence of the mountains and the city situated nearby. Author

N92-29288*# Bulgarian Academy of Sciences, Sofia. Inst. of Electronics.

EFFICIENCIES OF ROTATIONAL RAMAN AND RAYLEIGH TECHNIQUES FOR LASER REMOTE SENSING OF THE ATMOSPHERIC TEMPERATURE **c45**

I. D. Ivanova, L. L. Gurdev, and V. M. Mitev *In* NASA. Langley Research Center, Sixteenth International Laser Radar Conference, Part 1 Jul. 1992 p 221-224 (For primary document see N92-29228 20-35)

Avail: CASI HC A01/MF A04

Various lidar methods have been developed for measuring the atmospheric temperature, making use of the temperature dependant characteristics of rotational Raman scattering (RRS) from nitrogen and oxygen, and Rayleigh or Rayleigh-Brillowin scattering (RS or RBS). These methods have various advantages and disadvantages as compared to each other but their potential accuracies are principal characteristics of their efficiency. No systematic attempt has been undertaken so far to compare the efficiences, in the above meaning, of different temperature lidar methods. Two RRS techniques have been compared. Here, we do such a comparison using two methods based on the detection and analysis of RS (RBS) spectra. Four methods are considered here for measuring the atmospheric temperature. One of them (Schwiesow and Lading, 1981) is based on an analysis of the RS linewidth with two Michelson interferometers (MI) in parallel. The second method (Shimisu et al., 1986) employs a high-resolution analysis of the RBS line shape. The third method (Cooney, 1972) employs the temperature dependance of the RRS spectrum envelope. The fourth method (Armstrong, 1974) makes use of a scanning Fabry-Perot interferometer (FPI) as a comb filter for processing the periodic RRS spectrum of the nitrogen. Let us denote the corresponding errors in measuring the temperature by sigma(sub MI), sigma(sub HR), sigma(sub ENV), and sigma(sub FPI). Let us also define the ratios chi(sub 1) = sigma(sub MI)/sigma(sub ENV), chi(sub 2) = sigma(sub HR)/sigma(sub ENV), and chi(sub 3) = sigma(sub FPI)/sigma(sub ENV) interpreted as relative errors with respect to sigma(sub ENV). Author

N92-29289*# Bulgarian Academy of Sciences, Sofia. Inst. of Electronics.

LIDAR INVESTIGATION OF AEROSOL POLLUTION DISTRIBUTION NEAR A COAL POWER PLANT **c45**

Ts. Mitsev and G. Kolarov *In* NASA. Langley Research Center, Sixteenth International Laser Radar Conference, Part 1 Jul. 1992 p 225-228 (For primary document see N92-29228 20-35)

Avail: CASI HC A01/MF A04

Using aerosol lidars with high spatial and temporal resolution with the possibility of real-time data interpretation can solve a large number of ecological problems related to the aerosol-field distribution and variation and the structure of convective flows. Significantly less expensive specialized lidars are used in studying anthropogenic aerosols in the planetary boundary layer. Here, we present results of lidar measurements of the mass-concentration field around a coal-fired power plant with intensive local aerosol sources. We studied the pollution evolution as a function of the emission dynamics and the presence of retaining layers. The technique used incorporates complex analysis of three types of lidar mapping: horizontal map of the aerosol field, vertical cross-section map, and a series of profiles along a selected path. The lidar-sounding cycle was performed for the time of atmosphere's quasi-stationarity. Author

N92-29290*# Academy of Sciences (USSR), Moscow. Inst. of General Physics.

LASER REMOTE SENSING OF POLLUTION ON WATER SURFACES **c45**

A. F. Bunkin and Aleksander L. Surovegin (RADIAN, Moscow, USSR) *In* NASA. Langley Research Center, Sixteenth International Laser Radar Conference, Part 1 Jul. 1992 p 229-232 (For primary document see N92-29228 20-35)

Avail: CASI HC A01/MF A04

One of the most important problems of modern environmental science is the detection and identification of various impurities in the ocean. Sources of impurities in sea water are diverse. The most common of them are accidental transport, agricultural, and oil industry spills. Once the ecological balance is disturbed, biological processes in sea water become affected, resulting in changes in chlorophyll concentrations, water turbidity, and temperature. During the last few years, we have created new types of lidars and arranged nearly ten aircraft and shipboard expeditions. Some aircraft expeditions dealt with terrestrial investigations. Others were devoted to oceanological research, the results of which are discussed here. Emphasis is on the detection of phytoplankton chlorophyll and hydrocarbon in sea water. Author

N92-29291*# Bulgarian Academy of Sciences, Sofia. Inst. of Electronics.

CORRELATION ANALYSIS OF WIND LIDAR DATA **c47**

R. P. Avramova *In* NASA. Langley Research Center, Sixteenth International Laser Radar Conference, Part 1 Jul. 1992 p 233-236 (For primary document see N92-29228 20-35)

Avail: CASI HC A01/MF A04

The proposed correlation analysis represents an analysis of time sequences of lidar returns from observing points situated at the corners of right angle triangles in horizontal planes, spaced by altitude. The purpose here is to examine the choice of optical correlation techniques for lidar data to increase the number of successful measurements of wind velocity in a wide variety of meteorological conditions. Author

N92-29292*# Academia Sinica, Beijing (China). Inst. of Atmospheric Physics.

A DEVELOPING MULTIPLE-WAVELENGTH LIDAR FOR DETECTING MAINLY OZONE AND AEROSOL DISTRIBUTIONS IN THE STRATOSPHERE **c45**

Siping Zheng, Jinhuan Qiu, Shufang Wang, Qirong Huang, Wenming Wang, and Shaoming Wu *In* NASA. Langley Research Center, Sixteenth International Laser Radar Conference, Part 1 Jul. 1992 p 237 (For primary document see N92-29228 20-35)

Avail: CASI HC A01/MF A04

A multiple wavelength lidar is being developed at the Institute of Atmospheric Physics, Beijing, China, for measuring mainly ozone and aerosol distributions in the stratosphere. The system is based on a XecI excimer laser operating at 308nm and an Nd-YAG laser with three wavelengths of 1060nm, 532nm, and 355nm. The specifications of the lidar system are given in tabular form. The system is designed to measure the following parameters: 1) ozone vertical distribution (15-45km); 2) aerosol distribution (6-35km); 3) atmospheric temperature (30-70km); and 4) high clouds. The expected performances of the lidar system are simulated.

Author

N92-29293*# Academy of Sciences (USSR), Tomsk. Inst. of Atmospheric Optics.

AN EXTENSION OF THE RAMAN-LIDAR TECHNIQUE TO MEASURE THE VELOCITY AND TEMPERATURE OF THE ATMOSPHERIC EMISSION JETS FROM STACKS **c45**

Yu. F. Arshinov, S. M. Bobrovnikov, V. K. Shumskii, A. G. Popov, and I. B. Serikov *In* NASA. Langley Research Center, Sixteenth

International Laser Radar Conference, Part 1 Jul. 1992 p 239-242 (For primary document see N92-29228 20-35)
Avail: CASI HC A01/MF A04

If a Raman lidar possesses a proper spatial resolution sufficient for acquiring profiles of return signals across an emission jet, then the difference in number densities of nitrogen molecules within the jet and outside it will cause a dip in the lidar return signal from nitrogen. Experimentation showed that the Raman lidar technique can accurately measure the velocity and temperature of atmospheric emission from smoke stacks. Author

N92-29294*# Academia Sinica, Beijing (China). Inst. of Atmospheric Physics.
LIDAR OBSERVATIONS OF STRATOSPHERIC CLOUDS AFTER VOLCANIC ERUPTION OF PINATUBO c45
Jinhui Sun, Jinhuan Qiu, Qilin Xia, and Jinding Zhang *In* NASA. Langley Research Center, Sixteenth International Laser Radar Conference, Part 1 Jul. 1992 p 243-245 (For primary document see N92-29228 20-35)
Avail: CASI HC A01/MF A04

A very large increase of backscattered light from the stratospheric aerosol layer was observed by using a ruby laser in Beijing (39 degrees 54 minutes N, 116 degrees 27 minutes E) from the end of July 1991 to March 1992. It was concluded that this increase was almost certainly due to the volcanic eruption of Mt. Pinatubo in the Philippines in June 1991. The measuring instruments used are described. Information is given in graphical form for vertical profiles, fluctuation of the maximum backscattering ratio above 20 km during the nine month period, and the time variation of the integrated backscattering coefficient at a height of 15 to 30 km. Author

N92-29295*# Moscow State Univ. (USSR). Dept. of Physics.
IN VIVO AND IN VITRO CHLOROPHYLL-A AND PHEOPHYTIN-A CONCENTRATION MEASUREMENTS BY LASER FLUOROMETRY c48
A. A. Demidov, E. V. Baulin, and E. A. Chernyavskaya *In* NASA. Langley Research Center, Sixteenth International Laser Radar Conference, Part 1 Jul. 1992 p 247-250 (For primary document see N92-29228 20-35)
Avail: CASI HC A01/MF A04

Discussed here is the application of a laser fluorescent technique in in vivo and in vitro phyto- and zooplankton analysis involving popular lasers, an impulse YAG laser (lambda = 532 nm) and a steady state He-Cd (lambda = 440 nm). The YAG laser is widely used in laser remote sensing of seawater photoplankton in situ mode, but here we give special attention to its use in the precise estimation of phytoplankton pigments using laser induced fluorescence. The He-Cd laser is a novice in this field and, we believe, very promising. Our methods enable one to detect, in viro, chlorophyll-a (Chl-a) concentration in the water probe up to 10 nanograms per liter, and to measure, in vitro, Chl-a and pheophytin-a (Ph-a) concentrations in acetone extracts of phyto- and zooplankton up to 1 nanogram per liter. Author

N92-29296*# National Meteorological Center, Washington, DC. Development Div.
SCIENCE GOALS AND MISSION OBJECTIVES OF NASA'S LASER ATMOSPHERIC WIND SOUNDER PROGRAM c47
Wayman E. Baker *In* NASA. Langley Research Center, Sixteenth International Laser Radar Conference, Part 1 Jul. 1992 p 251-255 (For primary document see N92-29228 20-35)
Avail: CASI HC A01/MF A04

Knowledge of the global wind field is widely recognized as fundamental to advancing our understanding and prediction of the total Earth system. Yet, because wind profiles are primarily measured by land-based rawinsondes, the oceanic areas (covering three quarters of the Earth's surface) and many regions of the less developed southern hemisphere land areas are poorly observed. The gap between our requirements for wind data and their availability continues to widen. For example, as faster computers become available to model the atmosphere with ever increasing resolution and sophistication, our ability to model the atmosphere will be hampered by a lack of data, particularly wind profiles. In order to address this important deficiency in wind observations, NASA plans to construct the Laser Atmospheric Wind Sounder (LAWS) instrument, with deployment tentatively scheduled between 2002 and 2005 as part of NASA's Earth Observing System (EOS) mission. Addressed here is the importance of wind measurements for advancing our understanding and prediction of the total Earth System. The current characteristics of the LAWS instrument under study are also summarized. Author

N92-29297*# General Electric Co., Princeton, NJ. Astro Space Div.
THE LASER ATMOSPHERIC WIND SOUNDER (LAWS) PHASE 2 PRELIMINARY SYSTEM DESIGN
John C. Petheram, David L. Kenyon, Alan B. Wissinger (Hughes Danbury Optical Systems, Inc., CT.), and T. Rhidian Lawrence (STI Optronics, Bellevue, WA.) *In* NASA. Langley Research Center, Sixteenth International Laser Radar Conference, Part 1 Jul. 1992 p 257-259 (For primary document see N92-29228 20-35)
Avail: CASI HC A01/MF A04

The laser Atmospheric Wind Sounder (LAWS) is intended to measure global wind profiles in the lower and upper troposphere as part of the Earth Observing System (EOS). Global scale wind profiles will lead to a better understanding of large scale circulation processes and climate dynamics, an understanding of mesoscale phenomena, improved numerical weather prediction, and further insights into the coupling of the atmosphere/oceans/biosphere system. Here, details are given of the Phase 2 preliminary design. Author

N92-29298*# STI Optronics, Bellevue, WA.
THE LASER ATMOSPHERIC WIND SOUNDER (LAWS) PHASE 2 PRELIMINARY LASER DESIGN
T. Rhidian Lawrence, Albert L. Pindroh, Mark S. Bowers, Terence E. DeHart, Kenneth F. McDonald, Ananda Cousins, and Stephen E. Moody *In* NASA. Langley Research Center, Sixteenth International Laser Radar Conference, Part 1 Jul. 1992 p 261-264 (For primary document see N92-29228 20-35)
(Contracts NAS8-37589; A28-W20233)
Avail: CASI HC A01/MF A04

The requirements for the Laser Atmospheric Wind Sounder (LAWS) were determined from system considerations and are summarized in tabular form. The laser subsystem provides for the generation and frequency control of two beams, the transmit high power and local oscillator beams, which are delivered to the optical and receiver subsystems, respectively. In our baseline approach, the excitation of the gain section is achieved by a self-sustaining uv-(corona) preionized discharge. Gas is recirculated within the laser loop using a transverse flow fan. An intra-flow-loop heat exchanger, catalyst monolith, and acoustic attenuators condition the gas to ensure uniform energy output and high beam quality during high pulse repetition rate operation. The baseline LAWS laser pulse temporal profile as calculated by in-house laser codes is given in graphical form. Author

N92-29299*# General Electric Co., Philadelphia, PA. Astro Space Div.
GE'S MOBILE, COHERENT DOPPLER LIDAR TEST/EVALUATION FACILITIES c09
J. T. Sroga, J. W. Scott, S. C. Kiernan, F. J. Weaver, J. E. Trotta, and J. C. Petheram *In* NASA. Langley Research Center, Sixteenth International Laser Radar Conference, Part 1 Jul. 1992 p 265-267 (For primary document see N92-29228 20-35)
Avail: CASI HC A01/MF A04

The primary objective of this independent research and development (IR and D) program in support of the Laser Atmospheric Wind Sounder (LAWS) program is to develop and evaluate technologies with direct applications to spaceborne laser wind sensing, and to develop system level engineering experience in designing, operating, and modeling a coherent Doppler lidar. GE is developing a mobile, ground based coherent Doppler lidar as an end-to-end system level test facility to evaluate applicable

technologies, verify system level performance issues, perform instrument calibration, and validate end-to-end system performance model predictions. Here, the primary focus is on a description of the ground based lidar system and the performance during the initial shakedown operation after system integration. Author

N92-29300*# GEC-Marconi Ltd., Borehamwood (England).
THE e-BEAM SUSTAINED LASER TECHNOLOGY FOR SPACE-BASED DOPPLER WIND LIDAR c47
M. J. Brown, W. Holman, R. J. Robinson, P. M. Schwarzenberger, I. M. Smith, S. Wallace, M. R. Harris (Defence Research Agency, Malvern, England), D. V. Willetts (Defence Research Agency, Malvern, England), and S. C. Kurzius (Lockheed Missiles and Space Co., Huntsville, AL.) *In* NASA. Langley Research Center, Sixteenth International Laser Radar Conference, Part 1 Jul. 1992 p 269-272 (For primary document see N92-29228 20-35)
Avail: CASI HC A01/MF A04

An overview is presented of GEC Avionics activities relating to the Spaceborne Doppler Wind Lidar. In particular, the results of design studies into the use of an e-beam sustained CO2 laser for spaceborne applications, and experimental work on a test bed system are discussed. Author

N92-29301*# National Aeronautics and Space Administration. Langley Research Center, Hampton, VA.
THE LIDAR IN-SPACE TECHNOLOGY EXPERIMENT (LITE)
M. Patrick McCormick *In its* Sixteenth International Laser Radar Conference, Part 1 Jul. 1992 p 273-276 (For primary document see N92-29228 20-35)
Avail: CASI HC A01/MF A04

The primary goals of the Lidar In-Space Technology Experiment (LITE) are to demonstrate the maturity of space-based lidar technology, to provide some unique measurements, and to provide a platform for the development of technology for future space-based systems. LITE is currently scheduled to fly on the Shuttle in early 1994. Approval has recently been given for the first of several planned follow-on missions at 2-year intervals. The first mission will be used to develop experience in operating a lidar system in a space environment and to evaluate the sensitivity of the instrument for performing scientific studies. The second mission will focus on scientific studies of clouds, aerosols, and the middle atmosphere. On subsequent follow-on missions, LITE will be used as a test bed for demonstrating more advanced measurement capabilities. Author

N92-29302*# Science and Technology Corp., Hampton, VA.
SYSTEM TESTING AND PERFORMANCE CHARACTERIZATION OF THE LITE LASER TRANSMITTER MODULE AT NASA
Marc C. Cimolino and Mulugeta Petros *In* NASA. Langley Research Center, Sixteenth International Laser Radar Conference, Part 1 Jul. 1992 p 277-280 (For primary document see N92-29228 20-35)
Avail: CASI HC A01/MF A04

The Laser Transmitter Module (LTM) is a three-color Q-switched flashlamp pumped Nd:YAG laser. The original design concept was to package commercially available optics and flashlamp electronics for spaceflight with a power consumption goal of 2200 W and a weight goal of 600 lbs. The optical output was to exceed 200 mJ of IR, 400 mJ of green, and 150 mJ of UV per pulse at 10 Hz. The new space qualified laser exceeds the optical output requirements by 188 percent, 50 percent, and 13 percent in the UR, green, and UV respectively. This output needs only 1500 W at a weight of only 500 lbs. The LTM was delivered to the NASA Langley Research Center in December 1991. Optical characterization is now being completed. Author

N92-29303*# National Aeronautics and Space Administration. Langley Research Center, Hampton, VA.
MECHANICAL AND THERMAL ISSUES IN THE DEVELOPMENT OF A SPACEBORNE LIDAR SYSTEM
Joseph F. DeLorme *In its* Sixteenth International Laser Radar Conference, Part 1 Jul. 1992 p 281-284 (For primary document see N92-29228 20-35)
Avail: CASI HC A01/MF A04

The Lidar In-space Technology Experiment (LITE) is being developed by NASA's Langley Research Center (LaRC) to conduct spaceborne remote sensing of the Earth's atmosphere from the Space Shuttle. LITE is currently manifested as the primary payload on STS-63 to be launched in February 1994. Addressed here are some of the key mechanical and thermal issues in the design and development of this spaceborne lidar system. Author

N92-29304*# National Aeronautics and Space Administration. Langley Research Center, Hampton, VA.
LIDAR MEASUREMENTS OF AEROSOL AND OZONE DISTRIBUTIONS DURING THE 1992 AIRBORNE ARCTIC STRATOSPHERIC EXPEDITION c45
E. V. Browell, C. F. Butler (ST Systems Corp., Hampton, VA.), M. A. Fenn, W. B. Grant, and A. F. Carter *In its* Sixteenth International Laser Radar Conference, Part 1 Jul. 1992 p 285-288 (For primary document see N92-29228 20-35)
Avail: CASI HC A01/MF A04

The LaRC airborne lidar system was operated from the ARC DC-8 aircraft during the 1992 Airborne Arctic Stratospheric Expedition (ASEE-2) to investigate the distribution of stratospheric aerosols and O3 across the Arctic vortex from Jan. to Mar. 1992. Monthly flights were made across the Arctic vortex from Anchorage, Alaska, to Stavanger, Norway, and then back to Bangor, Maine, and additional round-trip flights north into the vortex were made each month from either Stavanger or Bangor depending on the location of the vortex that month. The airborne lidar system uses the differential absorption lidar (DIAL) technique at laser wavelengths of 301.5 and 310.8 nm to measure O3 profiles above the DC-8 over the 12-25 km altitude range. Lidar measurements of aerosol backscatter and depolarization profiles over the 12-30 km altitude range are made simultaneously with the O3 measurements using infrared (IR) and visible (VIS) laser wavelengths of 603 and 1064 nm, respectively. The measurements of Pinatubo aerosols, polar stratospheric clouds, and O3 made with the airborne DIAL system during the AASE-2 expedition and to chemical and dynamical process that contribute to O3 depletion in the wintertime Arctic stratosphere. Author

N92-29305*# Deutsche Forschungsanstalt fuer Luft- und Raumfahrt, Oberpfaffenhofen (Germany, F.R.).
AIRBORNE LIDAR MEASUREMENTS OF STRATOSPHERIC AEROSOLS DURING THE EUROPEAN ARCTIC STRATOSPHERIC OZONE EXPERIMENT (EASOE) Abstract Only c45
Wolfgang Renger, Gerhard Ehret, Peter Moerl, and Martin Wirth *In* NASA. Langley Research Center, Sixteenth International Laser Radar Conference, Part 1 Jul. 1992 p 289-290 (For primary document see N92-29228 20-35)
Avail: CASI HC A01/MF A04

The European Arctic Statospheric Ozone Experiment was performed during the winter of 1991/1992 to study processes in the Arctic Stratosphere, which possibly might result in an ozone depletion similar to what has been found in the Antarctic. Besides a number of ground observations at several locations and numerous balloon borne in situ and remote sensing experiments, three aircrafts were operating from the airport of Kiruna, Sweden, two of them equipped with lidars. Various aspects of this investigation are presented. Author

N92-29306*# Paris VI Univ. (France). Service d'Aeronomie.
AEROSOLS AND POLAR STRATOSPHERIC CLOUDS MEASUREMENTS DURING THE EASOE CAMPAIGN Abstract Only c45
D. Haner, S. Godin, G. Megie, C. David, and V. Mitev *In* NASA. Langley Research Center, Sixteenth International Laser Radar Conference, Part 1 Jul. 1992 p 291 (For primary document see N92-29228 20-35)
Avail: CASI HC A01/MF A04

Preliminary results of observations performed using two

different lidar systems during the EASOE (European Arctic Stratospheric Ozone Experiment), which has taken place in the winter of 1991-1992 in the northern hemisphere lattitude regions, are presented. The first system is a ground based multiwavelength lidar intended to perform measurements of the ozone vertical distribution in the 5 km to 40 km altitude range. It was located in Sodankyla (67 degrees N, 27 degrees E) as part of the ELSA experiment. The objectives of the ELSA cooperative project is to study the relation between polar stratospheric cloud events and ozone depletion with high vertical resolution and temporal continuity, and the evolution of the ozone distribution in relation to the position of the polar vortex. The second system is an airborne backscatter lidar (Leandre) which allows for the study of the 3-D structure and the optical properties of polar stratospheric clouds. The Leandre instrument is a dual-polarization lidar system, emitting at 532 nm, which allows for the determination of the type of clouds observed, according to the usual classification of polar stratospheric clouds. More than 60 hours of flight were performed in Dec. 1991, and Jan. and Feb. 1992 in Kiruna, Sweden. The operation of the Leandre instrument has led to the observation of the short scale variability of the Pinatubo volcanic cloud in the high latitude regions and to several episodes of polar stratospheric clouds. Preliminary analysis of the data is presented. Author

N92-29307*# Illinois Univ., Urbana-Champaign. Dept. of Atmospheric Sciences.

LIDAR OBSERVATIONS OF POLAR STRATOSPHERIC CLOUDS AND STRATOSPHERIC TEMPERATURES AT THE SOUTH POLE **c45**

Richard L. Collins, Kenneth P. Bowman, and Chester S. Gardner *In* NASA. Langley Research Center, Sixteenth International Laser Radar Conference, Part 1 Jul. 1992 p 293-295 (For primary document see N92-29228 20-35)
Avail: CASI HC A01/MF A04

Polar stratospheric clouds (PSC's) play a crucial role in the ozone chemistry of the polar regions. Current chemical models rely on the presence of these clouds to explain the rapid destruction of ozone observed each spring in Antarctica. We present lidar observations of PCS's and stratospheric temperatures at the South Pole throughout the Antarctic winter and spring of 1990. Author

N92-29308*# Massachusetts Inst. of Tech., Lexington. Lincoln Lab.

DEVELOPMENT OF MESOSPHERIC SODIUM LASER BEACON FOR ATMOSPHERIC ADAPTIVE OPTICS

T. H. Jeys *In* NASA. Langley Research Center, Sixteenth International Laser Radar Conference, Part 1 Jul. 1992 p 297-299 Sponsored in part by AF (For primary document see N92-29228 20-35)
Avail: CASI HC A01/MF A04

A solid-state source of long pulse length, sodium-resonance radiation was developed for the purpose of generating an artificial star in the earth's mesospheric sodium layer. This radiation is generated by sum-frequency mixing the output of a 1.064 micron Nd:YAG laser with the output of a 1.319-micron Nd:YAG laser. By operating these lasers at wavelengths very close to the peak of their tuning curves, it is possible to match the wavelength of the sum-frequency radiation to that of the sodium D2 adsorption wavelength. Two pulsed laser systems were constructed, one producing as much as 0.6 J of sodium resonance radiation at a 10-Hz repetition rate and another producing as much as 24 mJ at a 840-Hz repetition rate. In both laser systems, the 1.06-micron and 1.32-micron Nd:YAG lasers are configured as mode-locked master oscillators followed by power amplifiers. Other aspects of this project are presented. Author

N92-29309*# Phillips Lab., Kirkland AFB, NM. Starfire Optical Range.

CHARACTERIZATION OF ARTIFICIAL GUIDESTARS GENERATED IN THE MESOSPHERIC SODIUM LAYER **c46**

M. P. Jelonek, R. Q. Fugate, W. J. Lange, A. C. Slavin, R. E. Ruane (Rockwell Power Systems, Albuquerque, NM.), and R. A. Cleis (Optical Sciences Co., Placentia, CA.) *In* NASA. Langley Research Center, Sixteenth International Laser Radar Conference, Part 1 Jul. 1992 p 301-304 (For primary document see N92-29228 20-35)
Avail: CASI HC A01/MF A04

Using a 10 W average power sum-frequency laser, we have generated resonant fluorescence beacons in the mesospheric sodium layer and are currently evaluating them for use as an artificial guidestar for atmospheric compensation using adaptive optics. Two flashlamp pumped Nd:YAG lasers operating at 1.064 and 1.319 microns are mixed in a lithium triborate crystal to produce 589 nm light at 840 Hz. The laser emits 47.5 microsec mode-locked pulse trains at 11-14 mJ per pulse and is tuned to the sodium resonance transition with intracavity etalons. Author

N92-29310*# Massachusetts Inst. of Tech., Lexington. Lincoln Lab.

OPTICAL PUMPING OF MESOSPHERIC SODIUM: A NEW MEASUREMENT CAPABILITY **c46**

R. M. Heinrichs, T. H. Jeys, K. F. Wall, J. Korn, and T. C. Hotaling *In* NASA. Langley Research Center, Sixteenth International Laser Radar Conference, Part 1 Jul. 1992 p 305-308 (For primary document see N92-29228 20-35)
Avail: CASI HC A01/MF A04

The first observation of laser-induced optical pumping in a remote sensing application is reported. We have observed a large variation in the amount of laser light resonantly backscattered from the earth's mesospheric sodium layer depending on the laser polarization. This is consistent with optical pumping of the mesospheric sodium atoms. A new lidar capability is being developed based on measurements of the rethermalization rate of the optically pumped sodium atoms. These measurements have potential applications in the fields of global warming research, spacecraft re-entry, and upper atmospheric dynamics. Author

N92-29311*# Illinois Univ., Urbana-Champaign. Dept of Electrical and Computer Engineering.

LIDAR PROBING OF THE MESOSPHERE: SIMULTANEOUS OBSERVATIONS OF SPORADIC SODIUM AND IRON FORMATIONS, CALCIUM ION LAYERS, NEUTRAL TEMPERATURE AND WINDS **c46**

Timothy J. Kane, Jun Qian, Daniel R. Scherrer, Daniel C. Senft, W. Matthew Pfenninger, George C. Papen, and Chester S. Gardner *In* NASA. Langley Research Center, Sixteenth International Laser Radar Conference, Part 1 Jul. 1992 p 309-312 (For primary document see N92-29228 20-35)
Avail: CASI HC A01/MF A04

Meteoritic ablation in the upper atmosphere is the commonly accepted source of the mesospheric metals between 80 and 105 km. The vertical and temporal behavior of some of these metals can be probed with high accuracy and resolution using resonance fluorescence lidar techniques. Of considerable interest in recent years has been the sporadic and rapid formation of thin, dense enhancements in these metallic layers. Since late Mar. 1991, the UIUC CEDAR lidar system, located at the Urbana Atmospheric Observatory, has been routinely operating at the Fe resonance line of 372 nm in order to probe the mesospheric Fe layer. In Nov. 1991, the capability to investigate mesospheric Ca(+) at the resonance line of 393.4 nm was added. The lidar's eximer-pumped dye laser uses Exciton QUI laser dye dissolved in p-dioxane, which can lase at both the Fe and Ca(+) frequencies. Various aspects of this investigation are discussed. Author

N92-29312*# Tokyo Metropolitan Univ. (Japan). Dept. of Electronics and Information Engineering.

LIDAR MEASUREMENTS OF METALLIC SPECIES IN MESOPAUSE REGION **c46**

Chikao Nagasawa and Makoto Abo *In* NASA. Langley Research Center, Sixteenth International Laser Radar Conference, Part 1 Jul. 1992 p 313-316 (For primary document see N92-29228 20-35)
Avail: CASI HC A01/MF A04

Sodium density distributions were measured over more than 20 nights since Jul. 1991 at Tokyo Metropolitan University. Our

sodium lidar specifications are shown. The lidar consists of a dye laser that is pumped by a pulsed Nd:YAG laser. The dye laser is tuned to the D2 resonant absorption line of Na at the wavelength of 589 nm. A small fraction of the output beam is directed to a hollow-cathode lamp. The precise tuning of the Na D2 line is accomplished by monitoring the signal obtained from the hollow-cathode lamp and controlling the grating in the dye laser oscillator cavity. The raw data for each profile were obtained by firing the laser 5000 times for approximately 8.5 minutes. We have observed the sporadic sodium layers three times during the observation period. Recently, lidar measurements of iron atoms were also performed. Other aspects of this investigation are presented. Author

N92-29313*# Illinois Univ., Urbana-Champaign. Dept. of Electrical and Computer Engineering.

ERROR ANALYSIS OF WIND MEASUREMENTS FOR THE UNIVERSITY OF ILLINOIS SODIUM DOPPLER TEMPERATURE SYSTEM **c47**

W. Matthew Pfenninger and George C. Papen *In* NASA. Langley Research Center, Sixteenth International Laser Radar Conference, Part 1 Jul. 1992 p 317-320 (For primary document see N92-29228 20-35)

Avail: CASI HC A01/MF A04

Four-frequency lidar measurements of temperature and wind velocity require accurate frequency tuning to an absolute reference and long term frequency stability. We quantify frequency tuning errors for the Illinois sodium system, to measure absolute frequencies and a reference interferometer to measure relative frequencies. To determine laser tuning errors, we monitor the vapor cell and interferometer during lidar data acquisition and analyze the two signals for variations as functions of time. Both sodium cell and interferometer are the same as those used to frequency tune the laser. By quantifying the frequency variations of the laser during data acquisition, an error analysis of temperature and wind measurements can be calculated. These error bounds determine the confidence in the calculated temperatures and wind velocities. Author

N92-29314*# Illinois Univ., Urbana-Champaign. Dept. of Electrical and Computer Engineering.

SODIUM DOPPLER TEMPERATURE LIDAR OBSERVATIONS OF THE MESOPAUSE REGION TEMPERATURE AND WIND STRUCTURE **c46**

Daniel C. Senft, Daniel R. Scherrer, and Chester S. Gardner *In* NASA. Langley Research Center, Sixteenth International Laser Radar Conference, Part 1 Jul. 1992 p 321-323 (For primary document see N92-29228 20-35)

Avail: CASI HC A01/MF A04

Measurements of the mesopause region temperature structure are being routinely conducted at Urbana, Illinois with the University of Illinois (UIUC) Sodium Doppler Temperature Lidar. The first measurements were taken with this system in Jan. 1991 and are now being made, and will soon be done routinely in conjunction with the temperature measurements. The results obtained with the UIUC Sodium Doppler Temperature Lidar (SDTL) are presented. A description of the system is given in accompanying articles. Author

N92-29315*# Illinois Univ., Urbana-Champaign. Dept. of Electrical and Computer Engineering.

AIRBORNE SODIUM AND RAYLEIGH LIDAR OBSERVATIONS FROM ALOHA-90 **c46**

Chris A. Hostetler and Chester S. Gardner *In* NASA. Langley Research Center, Sixteenth International Laser Radar Conference, Part 1 Jul. 1992 p 325-328 (For primary document see N92-29228 20-35)

Avail: CASI HC A01/MF A04

Airborne Na and Rayleigh lidar observations from the Airborne Lidar and Observations of Hawaiian Airglow Campaign (ALOHA-90) campaign are described. We present gravity wave vertical and horizontal wave number spectra from the upper stratosphere and the upper mesosphere. Also, we document the occurrence of a large amplitude short horizontal scale quasi-monochromatic gravity wave event and discuss the implications of the event in light of recently developed gravity wave horizontal wave number spectra models. Finally, we discuss observations of sporadic Na layer events. Author

N92-29316*# Phillips Lab., Hanscom AFB, MA. Ionospheric Physics Div.

RAYLEIGH/RAMAN GREENLAND LIDAR OBSERVATIONS OF ATMOSPHERIC TEMPERATURE DURING A MAJOR ARCTIC STRATOSPHERIC WARMING EVENT **c47**

John W. Meriwether, Robert Farley, R. McNutt, Phan D. Dao, and Warren P. Moskowitz (Photometrics, Inc., Woburn, MA.) *In* NASA. Langley Research Center, Sixteenth International Laser Radar Conference, Part 1 Jul. 1992 p 329-332 (For primary document see N92-29228 20-35)

Avail: CASI HC A01/MF A04

Between Jan. 22 1991 to Feb. 5 1991, we made numerous observations of atmospheric temperature profiles between 10 and 70 km by using the combination of Rayleigh and Raman lidar systems contained in the PL Mobile Lidar Facility located at the National Science Foundation Incoherent Radar Facility of Sondrestrom in Greenland. The purpose of these measurements was to observe the dynamics of the winter Arctic stratosphere and mesosphere regions during a winter period from the succession of temperature profiles obtained in our campaign observations. Various aspects of this investigation are presented. Author

N92-29317*# Photometrics, Inc., Woburn, MA.

ELASTIC AND RAMAN LIDAR TEMPERATURE MEASUREMENTS FROM POKER FLAT, ALASKA DURING FEBRUARY 1992 **c46**

Michael Burka, Phan Dao (Phillips Lab., Hanscom AFB, MA.), Gilbert Davidson, Robert Farley (Phillips Lab., Hanscom AFB, MA.), John Meriwether (Phillips Lab., Hanscom AFB, MA.), and Alex Wilson (Phillips Lab., Hanscom AFB, MA.) *In* NASA. Langley Research Center, Sixteenth International Laser Radar Conference, Part 1 Jul. 1992 p 333-336 (For primary document see N92-29228 20-35)

Avail: CASI HC A01/MF A04

Ground-based lidar observations are increasingly used to elucidate the dynamical structure of the stratosphere and mesosphere. Observations made from Poker Flat, Alaska during Feb. 1992 using the Phillips Laboratory Mobile Lidar Facility are reported. Author

N92-29318*# Centre National de la Recherche Scientifique, Verrieres-Le Buisson (France). Service d'Aeronomie.

RAYLEIGH/RAMAN LIDARS: INTERCOMPARISONS AND VALIDATION **c46**

Marie-Lise Chanin *In* NASA. Langley Research Center, Sixteenth International Laser Radar Conference, Part 1 Jul. 1992 p 337-340 (For primary document see N92-29228 20-35)

Avail: CASI HC A01/MF A04

Vertical sounding of the atmosphere by Rayleigh lidar was exclusively used in France to study the structure, the dynamics as well as the long term trend of the middle atmosphere. More recently, the addition of a rotational-Raman mode fills the gap between the ground and 30 km in such a way that the whole altitude range from ground up to 90-100 km can be studied with a unique instrument. The growing need of absolute measurement of temperature with high precision for climatic purpose led us to perform critical review of all the sources of error which can occur in this type of measurement. This is the subject of a recent paper which shows that the increase of the performances of the instrument in the last decade was successfully obtained without compromising the accuracy. It is briefly reviewed. Concern is with the presentation of the recent improvements of the technique and of the results of intercomparisons and validation of new satellites data. Author

N92-29319*# Centre National de la Recherche Scientifique, Verrieres-Le Buisson (France). Service d'Aeronomie.
WIND MEASUREMENTS FROM 15 TO 50 KM WITH A DOPPLER RAYLEIGH LIDAR **c47**
A. Garnier and M. L. Chanin *In* NASA. Langley Research Center, Sixteenth International Laser Radar Conference, Part 1 Jul. 1992 p 341-344 (For primary document see N92-29228 20-35)
Avail: CASI HC A01/MF A04

The possibility to measure the mean wind in the high stratosphere using a Doppler Rayleigh lidar was demonstrated in 1989, and the Observatory of Haute Province (44 deg N, 6 deg E). It was originally developed to cover the height range 25-60 km, a region where the radars cannot operate; therefore, the system was designed to cover altitudes where the signal is only due to the Rayleigh backscattering. The instrument is currently set up at the Center d'Essais des Landes (44 deg N, 1 deg W) where it operated during the Dynamic Adapted Network for the Atmosphere Campaign in 1990. As the contribution of the Mie scattering was very low during this period above southern France, we have obtained vertical wind profiles in the stratosphere down to 15 km. Since the eruption of the Pinatubo volcano in Jun. 1991, the contribution of Mie scattering has increased between 15 and 30 km and it was very difficult with the original system to obtain wind measurements below 30 km. We will show that by using the same method with slightly different characteristics of the system, it is possible to measure the wind in the presence of Mie scattering. The first experimental results are presented. Author

N92-29320*# Commonwealth Scientific and Industrial Research Organization, Mordialoc (Australia). Div. of Atmospheric Research.
LIDAR STUDIES OF EXTINCTION IN CLOUDS IN THE ECLIPS PROJECT **c47**
C. Martin, R. Platt, Stuart A. Young, and Graeme P. Patterson *In* NASA. Langley Research Center, Sixteenth International Laser Radar Conference, Part 1 Jul. 1992 p 345-348 (For primary document see N92-29228 20-35)
Avail: CASI HC A01/MF A04

The Experimental Cloud Lidar Pilot Study (ECLIPS) project has now had two active phases in 1989 and 1991. A number of laboratories around the world have taken part in the study. The observations have yielded new data on cloud height and structure, and have yielded some useful new information on the retrieval of cloud optical properties, together with the uncertainties involved. Clouds have a major impact on the climate of the earth. They have the effect of reducing the mean surface temperature from 30 C for a cloudless planet to a value of about 15 C for present cloud conditions. However, it is not at all certain how clouds would react to a change in the planetary temperature in the event of climate change due to a radiative forcing from greenhouse gases. Clouds both reflect out sunlight (negative feedback) and enhance the greenhouse effect (positive feedback), but the ultimate sign of cloud feedback is unknown. Because of these uncertainties, campaigns to study clouds intensely were initiated. The International Satellite Cloud Climatology (ISCPP) and the FIRE Campaigns (cirrus and stratocumulus) are examples. The ECLIPS was set up similarly to the above experiments to obtain information specifically on cloud base, but also cloud top (where possible), optical properties, and cloud structure. ECLIPS was designed to allow as many laboratories as possible globally to take part to get the largest range of clouds. It involves observations with elastic backscatter lidar, supported by infrared fluxes at the ground and radiosonde data, as basic instrumentation. More complex experiments using beam filter radiometers, solar pyranometers, and satellite data and often associated with other campaigns were also encouraged to join ECLIPS. Two periods for observation were chosen, Sep. - Dec. 1989 and Apr. - Jul. 1992 into which investigators were requested to fit 30 days of observations. These would be either continuous, or arranged to coincide with NOAA satellite overpasses to obtain AVHRR data. The distribution of the ECLIPS international effort as in 1991 is shown. The main gaps in the global distribution are in the tropics and the Southern Hemisphere. Author

N92-29321*# York Univ. (Ontario). Dept. of Physics and Astronomy.
LIDAR STUDIES OF CLOUDS AT TORONTO DURING THE ECLIPS PROGRAM **c47**
S. R. Pal, A. I. Carswell, A. Y. Fong, I. Pribluda, and W. Steinbrecht *In* NASA. Langley Research Center, Sixteenth International Laser Radar Conference, Part 1 Jul. 1992 p 349-352 (For primary document see N92-29228 20-35)
Avail: CASI HC A01/MF A04

The Experimental Cloud Lidar Pilot Study (ECLIPS) measurement program involves the measurement of cloud optical and physical parameters with vertically pointing ground-based lidars simultaneously with satellites observing the same cloud system from above. Our frequency doubled Nd:YAG lidar transmits about 500 mJ of linearly polarized radiation at each wavelength (532, 1064 nm) with a prf of 20 Hz. An overview of the statistical behavior of cloud physical parameters and optical parameters is presented. Author

N92-29322*# Wisconsin Univ., Madison. Dept. of Meteorology.
ADAPTATION OF THE UNIVERSITY OF WISCONSIN HIGH SPECTRAL RESOLUTION LIDAR FOR POLARIZATION AND MULTIPLE SCATTERING MEASUREMENTS
E. W. Eloranta and P. K. Piironen *In* NASA. Langley Research Center, Sixteenth International Laser Radar Conference, Part 1 Jul. 1992 p 353-356 (For primary document see N92-29228 20-35)
Avail: CASI HC A01/MF A04

A new implementation of the High Spectral Resolution Lidar (HSRL) in an instrument van which allows measurements during field experiments is described. The instrument was modified to provide measurements of depolarization. In addition, both the signal amplitude and depolarization variations with receiver field of view are simultaneously measured. These modifications allow discrimination of ice clouds from water clouds and observation of multiple scattering contributions to the lidar return. Author

N92-29323*# Utah Univ., Salt Lake City. Dept. of Meteorology.
POLARIZATION LIDAR LIQUID CLOUD DETECTION ALGORITHM FOR WINTER MOUNTAIN STORMS **c47**
Kenneth Sassen and Hongjie Zhao *In* NASA. Langley Research Center, Sixteenth International Laser Radar Conference, Part 1 Jul. 1992 p 357-359 (For primary document see N92-29228 20-35)
Avail: CASI HC A01/MF A04

We have collected an extensive polarization lidar dataset from elevated sites in the Tushar Mountains of Utah in support of winter storm cloud seeding research and experiments. Our truck-mounted ruby lidar collected zenith, dual-polarization lidar data through a roof window equipped with a wiper system to prevent snowfall accumulation. Lidar returns were collected at a rate of one shot every 1 to 5 min during declared storm periods over the 1985 and 1987 mid-Jan. to mid-Mar. Field seasons. The mid-barrier remote sensor field site was located at 2.57 km MSL. Of chief interest to weather modification efforts are the heights of supercooled liquid water (SLW) clouds, which must be known to assess their 'seedability' (i.e., temperature and height suitability for artificially increasing snowfall). We are currently re-examining out entire dataset to determine the climatological properties of SLW clouds in winter storms using an autonomous computer algorithm. Author

N92-29324*# National Oceanic and Atmospheric Administration, Boulder, CO. Wave Propagation Lab.
MEASUREMENT OF MEAN OR EFFECTIVE RADIUS OF CLOUD DROP SIZE DISTRIBUTIONS WITH A 10.6-MICRON WAVELENGTH LIDAR **c47**
Wynn L. Eberhard *In* NASA. Langley Research Center, Sixteenth International Laser Radar Conference, Part 1 Jul. 1992 p 361-364 Sponsored in part by NOAA (For primary document

see N92-29228 20-35)
(Contract DE-FG02-90ER-61059)
Avail: CASI HC A01/MF A04

Platt and Takashima (1987) proposed and analytically evaluated a technique to observe the mode radius R sub p of drop size distributions in clouds using the backscatter detected by a CO2 lidar. The scheme depends on fortuitous relationships between the backscatter and extinction properties of common drop size distributions when probed with wavelengths between about 9 and 11 microns, which is the range of CO2 laser transitions. This study extends their work to measurement of mean and effective radius and presents experimental results that demonstrate that the technique is practical. Author

N92-29325*# National Aeronautics and Space Administration. Langley Research Center, Hampton, VA.
OBSERVATIONS OF CIRRUS CLOUDS OVER THE PACIFIC REGION BY THE NASA MULTIWAVELENGTH LIDAR SYSTEM **c47**
Syed Ismail, Edward V. Browell, Marta A. Fenn (STX Corp., Hampton, VA.), and Greg D. Nowicki (STX Corp., Hampton, VA.) *In its* Sixteenth International Laser Radar Conference, Part 1 Jul. 1992 p 365-368 (For primary document see N92-29228 20-35)
Avail: CASI HC A01/MF A04

As part of the Pacific Exploratory Mission-West Campaign that took place during 16 Sep. - 21 Oct. 1991, lidar measurements were made from the ARC DC-8 aircraft at an altitude of approximately 9 km. This mission provided a unique opportunity to make cirrus cloud observations around the Pacific region covering the latitude range from 5 to 55 deg N and the longitude range from -114 to 120 deg E. Cirrus clouds were observed on most of these flights providing a unique data base. The latitudinal coverage of cirrus observations was further extended to -5 deg S from observations on 30 Jan. 1992 as part of the Airborne Arctic Stratospheric Expedition 2. During this latter mission, aerosol depolarizations at 622 and 1064 nm were also measured. The optical characteristics and statistics related to these cirrus cloud observations are summarized. Author

N92-29326*# Messerschmitt-Boelkow-Blohm G.m.b.H., Munich (Germany, F.R.).
DIODE-PUMPED Nd:YAG LIDAR FOR AIRBORNE CLOUD MEASUREMENTS
A. Mehnert, Th. Halldorsson, H. Herrmann (Deutsche Forschungsanstalt fuer Luft- und Raumfahrt, Oberpfaffenhofen, Germany, F.R.), R. Haering (Deutsche Forschungsanstalt fuer Luft- und Raumfahrt, Oberpfaffenhofen, Germany, F.R.), W. Krichbaumer (Deutsche Forschungsanstalt fuer Luft- und Raumfahrt, Oberpfaffenhofen, Germany, F.R.), J. Streicher (Deutsche Forschungsanstalt fuer Luft- und Raumfahrt, Oberpfaffenhofen, Germany, F.R.), and Ch. Werner (Deutsche Forschungsanstalt fuer Luft- und Raumfahrt, Oberpfaffenhofen, Germany, F.R.) *In* NASA. Langley Research Center, Sixteenth International Laser Radar Conference, Part 1 Jul. 1992 p 369-371 (For primary document see N92-29228 20-35)
Avail: CASI HC A01/MF A04

This work is concerned with the experimental method used to separate scattering and to use it for the determination of cloud microphysical parameters. It is also the first airborne test of a lidar version related to the ATLID Program - ESA's scheduled spaceborne lidar. The already tested DLR microlidar was modified with the new diode-pumped laser and a faster data recording system was added. The system was used during the CLEOPATRA campaign in the DLR research aircraft Falcon 20 to measure cloud parameters. The diode pumped Nd:YAG laser we developed for the microlidar is a modification of the laser we introduced at the Lidar Congress at 'Laser 1991' in Munich. Various aspects of this work are discussed. Author

N92-29327*# Arizona Univ., Tucson. Dept. of Electrical and Computer Engineering.
REMOTE SENSING BY SPACEBORNE LIDAR AIDED BY SURFACE RETURNS **c47**
J. A. Reagan and T. W. Cooley *In* NASA. Langley Research Center, Sixteenth International Laser Radar Conference, Part 1 Jul. 1992 p 373-376 (For primary document see N92-29228 20-35)
Avail: CASI HC A01/MF A04

Spaceborne lidar offers the possibility of global mapping of clouds and atmospheric aerosols. Mapping of cloud-top heights, multiple layers of thin clouds and the depth of the planetary boundary layer (PBL), given sufficient aerosols, are applications that should be fairly easy to accomplish from space with even a modest lidar system. However, the constraints imposed on spaceborne lidar by large ranging distances, limited available power/weight, and fast moving platforms present significant challenges to achieving more quantitative retrievals such as extracting aerosol extinction profiles, PBL optical depths and cloud optical depths. Ways to take advantage of the strong signals available from ground/sea reflections to improve upon atmospheric aerosol and cloud retrievals as well as to distinguish certain surface types are explored. Author

N92-29328*# Atmospheric and Environmental Research, Inc., Cambridge, MA.
NWP IMPACT OF CLOUD TOP AND BOUNDARY LAYER WINDS FROM A SATELLITE BORNE LIDAR: AN OBSERVING SYSTEM SIMULATION EXPERIMENT **c47**
R. G. Isaacs, C. Grassotti, R. N. Hoffman, M. Mickelson, T. Nehrkorn, and J.-F. Louis *In* NASA. Langley Research Center, Sixteenth International Laser Radar Conference, Part 1 Jul. 1992 p 377-380 (For primary document see N92-29228 20-35)
(Contract F19628-89-C-0137)
Avail: CASI HC A01/MF A04

Observing systems simulation experiments (OSSE's) provide a powerful tool to assess the impact of proposed satellite borne observing systems on meteorological applications models. We describe the results of an OSSE conducted to assess the impact of data from a low power lidar wind sensor on the forecast accuracy of a global spectral numerical weather prediction (NWP) model, the Air Force Geophysics Laboratory Global Data Assimilation System. The instrument would be operating at near-infrared wavelengths thereby increasing the backscatter signal relative to comparable infrared lidar. Author

N92-29469# Oesterreichisches Forschungszentrum Seibersdorf G.m.b.H., Vienna.
MIGMAS/A: TEST OF A SCANNING ION MICROSCOPE ON THE SOVIET SPACE STATION MIR [MIGMAS/A: TEST EINES RASTER-IONENMIKROSKOPS AUF DER SOWJETISCHEN WELTRAUMSTATION MIR]
Willibald Riedler, Friedrich G. Ruedenauer (Technische Univ., Graz, Austria), Peter Beck (Technische Univ., Graz, Austria), M. Fehringer (Technische Univ., Graz, Austria), R. Finsterbusch, R. Pammer, F. Puerstl, and W. Steiger Jan. 1992 27 p In GERMAN
(OEFZS-4615; ETN-92-91505) Copyright Avail: CASI HC A03/MF A01

The scanning ion microscope described consists of a liquid metal ion emitter, an electrostatic focusing system, and a scanning and image recording system mounted in a hermetic vacuum enclosure. Data obtained by telemetry show excellent operational stability of the microscope under microgravity conditions. Data recorded on memcards show that imaging properties of the microscope remained unimpaired by mechanical loads experienced during a space flight. Migmas is intended to be used mainly for analysis of space corrosion, e.g. the degrading action of space exposure on materials. ESA

N92-29571# Department of the Army, Washington, DC.
MODULATED HIGH SENSITIVITY INFRARED POLARIMETER Patent Application
John A. Grisham, inventor (to Army), Frederick W. Clarke, inventor (to Army), Charles R. Christensen, inventor (to Army), and John L. Stenby, inventor (to Army) 24 Feb. 1992 10 p
(AD-D015256; US-Patent-Appl-SN-839627) Avail: CASI HC A02/MF A01

A modulated Faraday rotation signal is produced by passing a linearly polarized laser beam through a semiconductor wafer sample in a modulated magnetic field that is induced in a electromagnet by a sine wave generator and driver coupled thereto. The rotation signal is normalized by dividing by a transmission signal produced by modulating the beam with a chopper that operates at a different frequency from the frequency of the driver. The result is a Faraday rotation measurement with high signal-to-noise ratio and compensation for laser drift in intensity and beam direction.
Author (GRA)

N92-29731# Technische Univ., Brunswick (Germany, F.R.). Fakultaet fuer Maschinenbau und Elektrotechnik.
MOTION RESTORATION OF LONG TIME EXPOSED IMAGES WITH SATELLITE-BORNE CAMERAS Ph.D. Thesis [BEWEGUNGSKORREKTUR LANGZEITBELICHTETER BILDER BEI SATELLITENGESTUETZTEN KAMERAS]
Harald Michalik 1991 186 p In GERMAN
(ETN-92-91490) Avail: CASI HC A09/MF A02

Two main different processes for motion restoration in satellite cameras were examined and compared, with regard to obtainable image quality, e.g., signal/signal to noise ratio and resolution, and hardware expenditure. Linear models were used for camera components and long time exposure for mobile objects. It is shown that motion compensation is a simple process for motion restoration. Long time exposure is resolved in many short time exposed single images which are accumulated in a digital memory. Another process, image restoration, is used only for restoration of motion distortion inferior to two picture points. A comparison of expenditure is given for both processes. ESA

N92-29942# General Atomic Co., San Diego, CA.
SHORT WAVELENGTH INTERFEROMETER FOR ITER
R. T. Snider and T. N. Carlstrom Apr. 1992 14 p Presented at the 9th Topical Conference on High-Temperature Plasma Diagnostics, Santa Fe, NM, 15-19 Mar. 1992
(Contract DE-AC03-89ER-51114)
(DE92-013008; GA-A-20855; CONF-920362-25) Avail: CASI HC A03/MF A01

There is a need for a real time, reliable density measurement compatible with the restricted access and radiation environment on ITER. Due to the large plasma path length, high density and field, refraction and Faraday rotation effects makes the use of contemporary long wavelength (greater than 50 microns) interferometers impractical. In this paper we consider the design of a short wavelength vibration compensated interferometer which allows operation without a prohibitively large vibration isolated structure and permits the optics to be conveniently mounted directly in or on the tokamak. A density interferometer design for ITER incorporating a 10.6 micron CO2 interferometer with vibration compensation provided by a 3.39 micron HeNe laser is discussed. The proposed interferometer design requires only a small intrusion into the ITER tokamak without a large support structure. Refraction and Faraday rotation problems are avoided, and it provides a density resolution of at least 0.5 percent. Results are presented from an interferometer installed on the DIII-D tokamak incorporating essential elements of the proposed ITER design including 10.6 and 3.39 micron lasers, a retro-reflector mounted on the vacuum wall of the DIII-D tokamak and real-time density feedback control. In this paper we consider a short wavelength interferometer design that incorporates vibration compensation for use on ITER. Our primary concern is to develop a interferometer design that will produce a reliable real time density monitor. We use the ITER conceptual design activity report as the basis of the design.
DOE

N92-29952*# National Aeronautics and Space Administration. Lyndon B. Johnson Space Center, Houston, TX.
ACCELEROMETER METHOD AND APPARATUS FOR INTEGRAL DISPLAY AND CONTROL FUNCTIONS Patent Application
Richard J. Bozeman, Jr., inventor (to NASA) 19 Jun. 1992 20 p
(NASA-Case-MSC-21961-1; NAS 1.71:MSC-21961-1;
US-Patent-Appl-SN-901626) Avail: CASI HC A03/MF A01

Vibration analysis has been used for years to provide a determination of the proper functioning of different types of machinery, including rotating machinery and rocket engines. A determination of a malfunction, if detected at a relatively early stage in its development, will allow changes in operating mode or a sequenced shutdown of the machinery prior to a total failure. Such preventative measures result in less extensive and/or less expensive repairs, and can also prevent a sometimes catastrophic failure of equipment. Standard vibration analyzers are generally rather complex, expensive, and of limited portability. They also usually result in displays and controls being located remotely from the machinery being monitored. Consequently, a need exists for improvements in accelerometer electronic display and control functions which are more suitable for operation directly on machines and which are not so expensive and complex. The invention includes methods and apparatus for detecting mechanical vibrations and outputting a signal in response thereto. The apparatus includes an accelerometer package having integral display and control functions. The accelerometer package is suitable for mounting upon the machinery to be monitored. Display circuitry provides signals to a bar graph display which may be used to monitor machine condition over a period of time. Control switches may be set which correspond to elements in the bar graph to provide an alert if vibration signals increase over the selected trip point. The circuitry is shock mounted within the accelerometer housing. The method provides for outputting a broadband analog accelerometer signal, integrating this signal to produce a velocity signal, integrating and calibrating the velocity signal before application to a display driver, and selecting a trip point at which a digitally compatible output signal is generated. The benefits of a vibration recording and monitoring system with controls and displays readily mountable on the machinery being monitored and having capabilities described will be appreciated by those working in the art. NASA

N92-30030*# National Aeronautics and Space Administration. Langley Research Center, Hampton, VA.
CALIBRATION APPARATUS FOR RECESS MOUNTED PRESSURE TRANSDUCERS Patent Application
Michael A. Marcolini, inventor (to NASA), William T. Miller, Jr., inventor (to NASA), Robert A. Baals, inventor (to NASA), and Ruth M. Martin, inventor (to NASA) 29 Apr. 1992 25 p
(NASA-Case-LAR-14724-1; NAS 1.71:LAR-14724-1;
US-Patent-Appl-SN-876592) Avail: CASI HC A03/MF A01

Measurement of surface pressure fluctuations is important in aerodynamic studies and is conventionally accomplished via thin surface mounted transducers. These transducers contaminate the airflow, leading to the use of transducers located beneath the surface and communicating thereto via a pipette. This solution creates its own problem of transducer calibration due to the structure of the pipette. A calibration apparatus and method for calibrating a pressure transducer are provided. The pressure transducer is located within a test structure having a pipette leading from an outer structure surface to the pressure transducer. The calibration apparatus defines an acoustic cavity. A first end of the acoustic cavity is adapted to fluidly communicate with the pipette leading to the pressure transducer, wherein a channel is formed from the acoustic cavity to the transducer. An acoustic driver is provided for acoustically exciting fluid in the acoustic cavity to generate pressure waves which propagate to the pressure transducer. A pressure sensing microphone is provided for sensing the pressure fluctuations in the cavity near the cavity end, whereby this sensed pressure is compared with a simultaneously pressure sensed by the pressure transducer to permit calibration of the

pressure transducer sensings. Novel aspects of the present invention include its use of a calibration apparatus to permit in-situ calibration of recess mounted pressure transducers. NASA

N92-30090# Oak Ridge National Lab., TN.
SUB-ANGSTROM MICROSCOPY THROUGH INCOHERENT IMAGING AND IMAGE RECONSTRUCTION
S. J. Pennycook, D. E. Jesson, M. F. Chisholm, A. G. Ferridge (Wellcome Research Labs., Beckenham, England), and M. J. Seddon (Wellcome Research Labs., Beckenham, England) Mar. 1992 28 p Presented at the 10th Pfefferkorn Conference on Signal and Image Processing in Microscopy and Microanalysis, Cambridge, England, 16-19 Sep. 1991
(Contract DE-AC05-84OR-21400)
(DE92-011787; CONF-9109256-2) Avail: CASI HC A03/MF A01

Z-contrast scanning transmission electron microscopy (STEM) with a high-angle annular detector breaks the coherence of the imaging process, and provides an incoherent image of a crystal projection. Even in the presence of strong dynamical diffraction, the image can be accurately described as a convolution between an object function, sharply peaked at the projected atomic sites, and the probe intensity profile. Such an image can be inverted intuitively without the need for model structures, and therefore provides the important capability to reveal unanticipated interfacial arrangements. It represents a direct image of the crystal projection, revealing the location of the atomic columns and their relative high-angle scattering power. Since no phase is associated with a peak in the object function or the contrast transfer function, extension to higher resolution is also straightforward. Image restoration techniques such as maximum entropy, in conjunction with the 1.3 (Angstrom) probe anticipated for a 300 kV STEM, appear to provide a simple and robust route to the achievement of sub-(Angstrom) resolution electron microscopy. DOE

N92-30202# Department of the Navy, Washington, DC.
FRICTION DRIVE POSITION TRANSDUCER Patent Application
Ronald E. Waclawik, inventor (to Navy), James L. Cayer, inventor (to Navy), and Kenneth M. LaPointe, inventor (to Navy) 28 Oct. 1991 15 p
(AD-D015205; US-Patent-Appl-SN-783660; Navy-Case-72831)
Avail: CASI HC A03/MF A01

A spring force loaded contact wheel mounted in a stationary position relative to a reciprocating shaft is disclosed. The apparatus of the present invention includes a tensioning assembly for maintaining absolute contact between the contact wheel and the reciprocating shaft wherein the tensioning assembly urges the contact wheel against the shaft to maintain contact therebetween so that the wheel turns as the shaft is linearly displaced. A rotary encoding device is coupled to the wheel for translating the angular and rotational movement thereof into an electronic signal for providing linear displacement information and derivative data with respect to displacement of the shaft. Absolute friction contact and cooperative interaction between the shaft and the contact wheel is further enhanced in the preferred embodiment by advantageously selecting the types of surface finish and the amount of surface area of the contact wheel relative to the surface condition of the shaft as well as by reducing the moment of inertia of the contact wheel. GRA

N92-29371*# Jet Propulsion Lab., California Inst. of Tech., Pasadena.
APPLICATIONS OF INERTIAL-SENSOR HIGH-INHERITANCE INSTRUMENTS TO DSN PRECISION ANTENNA POINTING
R. E. Goddard *In its* The Telecommunications and Data Acquisition Report 15 May 1992 p 94-104 (For primary document see N92-29364 20-32)
(RTOP 310-20-65-67-00)
Avail: CASI HC A03/MF A04

36 LASERS AND MASERS

Includes parametric amplifiers.
For related information see also *76 Solid-State Physics.*

N92-29332# Naval Ocean Systems Center, San Diego, CA. Research, Development, Test, and Evaluation Div.
PHASE CONJUGATION IN BaTiO3 AT 830 NANOMETERS
I. Bendall and D. M. Gookin Mar. 1992 7 p
(AD-A250240) Avail: CASI HC A02/MF A01

We have demonstrated self-pumped phase conjugation of semiconductor lasers at 830 nanometers in barium titanate using a self-contained geometry. The reflectivities and response times of this geometry are compared to those reported for self-pumped ring passive phase conjugate mirrors. GRA

N92-29340# Lawrence Livermore National Lab., CA.
LASER-INDUCED DESORPTION FROM SAPPHIRE SURFACES
A. V. Hamza and M. A. Schildbach Mar. 1992 4 p Presented at the Workshop on Disabsorption Induced by Electronic Transitions, Taos, NM, 1-4 Apr. 1992
(Contract W-7405-eng-48)
(DE92-012698; UCRL-JC-110159; CONF-920462-1) Avail: CASI HC A01/MF A01

Laser-induced desorption of energetic (approx. 7eV) aluminum ions was observed from clean and water-covered sapphire (1102) surfaces using time-of-flight mass spectrometry with laser wavelengths of 1064, 355, and 266 nm. In sharp contrast, O(+) (H(+) and OH(+)) ions were observed in electron-induced desorption measurements with 300 eV electrons from the bare (water-covered) (1102) surface. Sapphire surfaces were characterized with low energy electron diffraction, reflection electron energy loss spectroscopy, and Auger electron spectroscopy. DOE

N92-29358# Lawrence Livermore National Lab., CA.
ACTIVE MODELOCKING AND PHASE STABILIZATION OF A CAVITY DUMPED DIODE PUMPED Nd:YAG MINI-LASER
A. J. Ruggiero Mar. 1992 6 p Presented at the CLEO/QELS 1992, Anaheim, CA, 10-17 May 1992
(Contract W-7405-eng-48)
(DE92-011946; UCRL-JC-110158; CONF-920573-7) Avail: CASI HC A02/MF A01

The design and operation of a variable repetition rate, acousto-optically cavity dumped, actively modelocked and phase stabilized diode pumped Nd:YAG mini-laser is reported. Use of a piezoelectrically induced strain optic (PESO) loss modulator for modelocking results in stable 20psec pulses at 1064nm over a range of repetition rates from single shot to the 100MHz oscillator frequency. DOE

N92-29396# Royal Signals and Radar Establishment, Malvern (England).
LASER DIODE END-PUMPED Nd:YAG LASER
Ian F. Elder Jan. 1992 49 p
(AD-A248123; RSRE-MEMO-4564; DRIC-BR-309213) Avail: CASI HC A03/MF A01

The 100 Hz operation of a Nd:YAG laser longitudinally pumped by a 1 W peak power quasi-cw laser diode was investigated theoretically and experimentally. An optical-to-optical slope efficiency of 33 percent, indicating a wall-plug efficiency of 7 percent, was exhibited, but the threshold optical power of 330 mW was high due to poor antireflection coatings on the laser rod giving a round-trip intracavity loss of 3.1 percent. The 1.064 micro output was observed to be diffraction-limited. The theoretical modelling of the laser's input/output characteristics agreed well with the experimentally obtained results. GRA

N92-29434# Sandia National Labs., Livermore, CA.
REVIEW OF POTENTIAL X RAY LASER APPLICATIONS IN MATERIALS SCIENCE AND CHEMISTRY
G. D. Kubiak 1992 7 p Presented at the X Ray Lasers Applications Workshop, San Francisco, CA, Jan. 1992

(Contract DE-AC04-76DP-00789)
(DE92-012254; SAND-92-8464C; CONF-9201103-1) Avail: CASI HC A02/MF A01

While high instantaneous brightness will be an essential attribute for certain experiments, it is not necessarily a desired one for many of the experiments commonly performed now in materials science and chemistry. High repetition-rate XUV and soft x-ray storage ring and laser plasma sources predominate in these fields because the majority of users require high average power, not high instantaneous brightness. Thus, it is envisioned that low-pulse-energy, high-repetition-rate x-ray lasers may be at least as useful within these disciplines as their more commonly discussed high-energy, low-repetition-rate counterparts. In the following, experiments in the areas of materials science and chemistry which might benefit from either of these two x-ray laser options are briefly described. DOE

N92-29472# Lawrence Livermore National Lab., CA.
X RAY LASER RESEARCH AT THE NOVA LASER
B. J. MacGowan Apr. 1992 16 p Presented at the Society of Photo-Optical Instrumentation Engineers' Symposium on Optics, Electro-Optic and Laser Applications in Science and Engineering, Los Angeles, CA, 20-24 Jan. 1992
(Contract W-7405-eng-48)
(DE92-012695; UCRL-JC-108127; CONF-920124-24) Avail: CASI HC A03/MF A01

Laboratory x-ray lasers are currently being studied by researchers by LLNL using the Nova glass laser as a pump source. Laser action has been demonstrated at wavelengths as short as 35.6 A while x-ray amplifier saturation has been observed with longer wavelength schemes. The most successful schemes to data have been collisionally pumped x-ray lasers which use the thermal electron distribution within a laser produced plasma to excite electrons from closed shells in neon- and nickel-like ions to higher energy metastable levels. The multitude of x-ray laser wavelengths produced by isoelectronic scaling of these laser schemes results in a quasi-tunable bright source of x-rays that presently spans the range 35-300 A, (40 to 350 eV). Currently attempts are being made to quantify and improve the longitudinal and transverse coherence of collisionally pumped x-ray lasers in order to increase their usefulness for specific applications. DOE

N92-29474# General Atomic Co., San Diego, CA.
DESIGN AND OPERATION OF THE MULTIPULSE THOMSON SCATTERING DIAGNOSTIC ON DIII-D
T. N. Carlstrom, G. L. Campbell, J. C. DeBoo, R. Evanko, C. M. Greenfield, J. Haskovec, C. L. Hsieh, E. McKee, R. T. Snider, and R. Stockdale et al Mar. 1992 21 p Presented at the 9th Topical Conference on High-Temperature Plasma Diagnostics, Santa Fe, NM, 15-19 Mar. 1992
(Contract DE-AC03-89ER-51114)
(DE92-011393; GA-A-20849; CONF-920362-21) Avail: CASI HC A03/MF A01

This paper describes the design and operation of a 40 spatial channel Thomson scattering system that uses multiple 20 Hz Nd:YAG lasers to measure the electron temperature and density profiles periodically throughout an entire plasma discharge. As many as eight lasers may be fired alternately for an average measurement frequency of 160 Hz, or they may be fired in rapid succession (less than 10 kHz), producing a burst of pulses for measuring transient events. The high spatial resolution (1.3 cm) and wide dynamic range (10 eV to 20 keV) enable this system to resolve large electron density and temperature gradients formed at the plasma edge and in the scrape-off-layer during H-mode operation. These features provide a formidable tool for studying L-H transitions, edge localized modes (ELMs), beta limits, transport, and disruptions in an efficient manner suitable for large tokamak operation where shot-to-shot scans are impractical. The scattered light is dispersed by interference filter polychromators and detected by silicon avalanche photodiodes. Laser control and data acquisition are performed in real-time by a VME based microcomputer. Data analysis is performed by a MicroVAX 3400. Additional features of this system include real-time analysis capability, full statistical treatment of error bars based on the measured background light, and laser beam quality and alignment monitoring during plasma operation. Results of component testing, calibration, plasma operation, and error analysis are presented. DOE

N92-29509# Lawrence Livermore National Lab., CA.
ION COLLISION EFFECTS IN HYDROGEN-LIKE RECOMBINATION X RAY LASERS
J. K. Nash, D. C. Eder, and H. A. Scott Mar. 1992 16 p Presented at the Society of Photo-Optical Instrumentation Engineers (SPIE) Meeting, San Diego, CA, 21-26 Jul. 1991
(Contract W-7405-eng-48)
(DE92-013515; UCRL-JC-110302; CONF-9107115-75) Avail: CASI HC A03/MF A01

We investigate the influence of ion collisional excitation on gain estimates for lasing between the two 3d-2p fine-structure transitions in a recombining, hydrogen-like magnesium plasma. A sizable reduction of the 3d(sub 3/2)-2p(sub 1/2) gain coefficient is found, resulting from both collisional population transfer and from lower state broadening of the emission profile. The need for care in evaluating the latter effect is discussed. DOE

N92-29516# Sandia National Labs., Livermore, CA.
USING PHASE RETRIEVAL TO DETERMINE THE INTENSITY AND PHASE OF AN ULTRASHORT LASER PULSE
R. Trebino and D. J. Kane (Southwest Sciences, Inc., Santa Fe, NM.) 1992 5 p Presented at the Signal Recovery and Synthesis Topical Meeting, New Orleans, LA, 14-16 Apr. 1992
(Contract DE-AC04-76DR-00789)
(DE92-013564; SAND-92-8509C; CONF-920496-2) Avail: CASI HC A01/MF A01

We have solved the long-standing problem of measuring the full electric field, E(t), of a single ultrashort laser pulse by reducing it to a two-dimensional phase-retrieval problem. DOE

N92-29559# General Electric Co., Schenectady, NY. Research and Development Center.
LASER PROCESSING FOR INTERCONNECT TECHNOLOGY Final Report, 1 Oct. 1985 - 30 Nov. 1991
H. S. Cole, Y. S. Liu, and K. Paik 27 Feb. 1992 132 p
(Contract N00014-85-C-0890)
(AD-A248103) Avail: CASI HC A07/MF A02

The overall objective of this program was to investigate laser-activated chemistry for fabrication of metal lines on low dielectric constant substrates. The need to provide highly conductive metal on polymeric substrates (with epsilon less than 3.5) is essential for high-speed interconnect technology. Using lasers to fabricate these interconnects offers unique possibilities and advantages over more conventional lithography approaches. Since the laser can be put under computer control, the possibility exists for rapid design modifications. Initial results of work performed on this contract were reported in a Phase 1 final report entitled, 'Laser-Activated Metal Deposition', 31 Jan. 1988. This Phase 1 report covers work during the period of 1 Oct. 1985 - 31 Dec. 1987. Work carried out during that time period included a survey of laser-driven processes for metal deposition from organometallic compounds and investigations into various gas phase and thin film metal deposition processes. The key output of that activity was the development of a process to selectively deposit copper on polyimide. The approach uses a CW laser at 351 nm to irradiate organometallic palladium compounds to selectively deposit catalytic amounts of palladium on polyimide. Subsequent immersion of the irradiated samples in an electroless copper solution resulted in selective copper deposition. GRA

N92-29581# Laser Technology, Inc., South Lyon, MI.
LASER PAINT STRIPPING Final Report, Apr. 1988 - Jan. 1991
J. D. Head and J. Peter Niedzielski Jun. 1991 102 p
(Contract F33615-88-C-5416)
(AD-A249233; WL-TR-91-4026) Avail: CASI HC A06/MF A02

A study to assess the utility of high powered CO2 pulsed laser depainting methods was conducted on aluminum and graphite

epoxy composites. The various tests were designed to detect potential forms of damage or loss of properties of various aircraft structural materials during removal of paint with pulsed laser energy. Tests for changes in physical properties, paint adhesion and corrosion protection of repainted materials showed no detectable adverse changes in any of the samples studied. GRA

N92-29787# Lawrence Livermore National Lab., CA.
PRELIMINARY CUTTING AND DRILLING STUDIES USING NEW GENERATION LASERS
D. D. Kautz, J. S. Sze, E. P. Dragon, and R. S. Hargrove 20 Feb. 1992 7 p Presented at the Lasers 1991, San Diego, CA, 8-13 Dec. 1991 Revised
(Contract W-7405-eng-48)
(DE92-010712; UCRL-JC-109918-Rev-1; CONF-911296-8-Rev-1) Avail: CASI HC A02/MF A01

High power and radiance dye lasers developed at Lawrence Livermore National Laboratory show promise for material processing tasks. Evaluation using welding heat flow models suggests significant increases in precision and speed are expected. We developed tooling and instrumentation to diagnose important parameters including spot geometry and optical train quality. We started processing studies to determine the viability of these lasers for cutting and drilling. We used titanium and stainless steel alloys for testing due to the availability of comparable parametric studies in the technical literature. Results show that cuts and holes with extremely fine features can be made with dye lasers. The high radiance beam produces low distortion and small heat-affected zone. We have accomplished very high aspect ratios and micron scale kerfs and holes. Through continued system improvement and process optimization, we believe that submicron levels will be realized. DOE

N92-29928# Retina Foundation, Boston, MA. Eye Research Inst.
CENTER OF EXCELLENCE: MICROLASER MICROSCOPE
R. H. Webb 1992 9 p
(Contract DE-FG02-91ER-61229)
(DE92-013485; DOE/ER-61229/1) Avail: CASI HC A02/MF A01

This Center-of-Excellence grant has two components: development of an imaging system based on microlaser arrays forms a central project among a group of laser diagnostic and therapeutic efforts primarily funded outside the grant. In these first 8 months we have set up the Microlaser Microscope using small microlaser arrays. We have emphasized the basics of microlaser handling and electronic addressing and the optics of the microscope. Details of electronics and optics given here will be used in the larger arrays which should be available soon. After a description of the central Microlaser Microscope project, we touch briefly on the other projects of the Center, which have been outstandingly fruitful this year. Publications are necessarily concerned with the smaller projects, since the Microlaser Microscope is in its early stages. DOE

N92-29937# Lawrence Livermore National Lab., CA.
TUNABLE DRIVER FOR THE LLNL FEL EXPERIMENT
W. C. Guss (Massachusetts Inst. of Tech., Cambridge.), M. A. Basten (Massachusetts Inst. of Tech., Cambridge.), K. E. Kreischer (Massachusetts Inst. of Tech., Cambridge.), and R. J. Temkin (Massachusetts Inst. of Tech., Cambridge.) Jul. 1991 11 p
(Contract W-7405-eng-48)
(DE92-011292; UCRL-CR-104380-Rev-1) Avail: CASI HC A03/MF A01

This report describes main activities undertaken during the period 1 June 1990 to 1 June 1991 by MIT to support the Lawrence Livermore National Laboratory tunable FEL driver project. The goal of this research was to further characterize a tunable microwave source (already identified as a BWO-gyrotron) of moderate output power (10-20 kW). In the 1989 fiscal year, the source was assembled at MIT and initial tests were conducted. Proposed for the fiscal year 1990 were analysis of the previous experimental results and the performance of new experiments designed to increase the voltage tuning range, the output efficiency, and magnetic field tuning. During the report period, the previous experimental results were analyzed and compared to computational results and new components were designed, to make the BWO ready for further experiments. In addition, the BWO-gyrotron was mounted in a new superconducting magnet and initial magnetic field profile measurements were made. DOE

N92-29948# National Oceanic and Atmospheric Administration, Boulder, CO. Wave Propagation Lab.
TURBULENCE EFFECTS ON THE GEODYNAMIC LASER RANGING SYSTEM
J. H. Churnside Jan. 1992 44 p
(PB92-166404; NOAA-TM-ERL-WPL-218) Avail: CASI HC A03/MF A01

The possible effects of refractive turbulence in the atmosphere on the Geodynamic Laser Ranging System are considered. For reasonable propagation conditions, beam steering effects can generally be neglected. Turbulence-induced beam spreading must be considered under conditions of high path-integrated turbulence. However, the most important effect is scintillation of the retroreflected beam. The weak-turbulence theory suggests that scintillations can be severe under some conditions. Under these conditions, this theory is not expected to be valid, and more work must be done to estimate the effects on system performance. Author

N92-29987# Lawrence Livermore National Lab., CA.
THE X RAY LASER COHERENCE EXPERIMENTS IN NEON-LIKE YTTRIUM
G. M. Shimkaveg, M. R. Carter, R. S. Walling, J. M. Ticehurst, J. A. Koch, S. Mrowka, J. E. Trebes, B. J. MacGowan, L. B. DaSilva, and D. L. Matthews et al Jan. 1992 11 p Presented at the Lasers 1991, San Diego, CA, 8-13 Dec. 1991
(Contract W-7405-eng-48)
(DE92-010714; UCRL-JC-107745; CONF-911296-5) Avail: CASI HC A03/MF A01

We present recent results from neon-like x-ray laser experiments conducted at the Nova laser's Two-Beam Facility. This begins a series of experiments aimed at the characterization and control of the degree of spatial coherence in our soft x-ray laser beams, important to planned application areas such as microscopy and holography. New instrumentation developed for this effort include a fully time-resolved coherence diagnostic (which records a multiple-slit diffraction pattern) and wide-angle extreme ultraviolet spectrographs and beam divergence cameras. We present new measurements of beam profiles and gain, as well as spatial coherence data such as time-resolved multi-slit diffraction patterns. This new time-resolved coherence data exhibit aperture functions which increase in size during the time of the lasing. Also, some preliminary data is given from the first 'double-foil' experiments, involving two x-ray amplifiers spatially separated by 29 cm and shot sequentially, in an 'oscillator-amplifier' configuration. DOE

N92-30135# Sandia National Labs., Albuquerque, NM.
LASER ETCHING: POSSIBILITIES AND PROBLEMS
C. I. H. Ashby 1992 13 p Presented at the 2nd International Conference on Laser Advanced Materials Processing, Nagaoka City, Japan, 7-12 Jun. 1992
(Contract DE-AC04-76DP-00789)
(DE92-010800; SAND-92-0446C; CONF-920657-1) Avail: CASI HC A03/MF A01

There are three basic categories of chemistry-based laser etching; they differ in the fundamental role of photons in enhancing the etching reaction. Laser beams are used to drive thermal chemical reactions, gas- or liquid-phase photochemical reactions, and carrier-driven reactions. Etching conditions can be selected so that more than one of these mechanisms is operative. Each of these reaction types have unique characteristics that either assist or impede their practical application. In this paper, we will examine the state of the field today and draw some conclusions about possible applications and problems that are likely to be encountered as we apply laser-based chemical etching processes. DOE

N92-29282*# Sparta, Inc., Lexington, MA.
APPLICATION OF LASER IMAGING FOR BIO/GEOPHYSICAL STUDIES
J. R. Hummel, S. M. Goltz, N. L. DePiero, D. P. DeGloria, and F. M. Pagliughi *In* NASA. Langley Research Center, Sixteenth International Laser Radar Conference, Part 1 Jul. 1992 p 199-200 (For primary document see N92-29228 20-35)
Avail: CASI HC A01/MF A04

37 MECHANICAL ENGINEERING

Includes auxiliary systems (nonpower); machine elements and processes; and mechanical equipment.

N92-29351*# National Aeronautics and Space Administration. Lewis Research Center, Cleveland, OH.
OPTIMAL DESIGN OF COMPACT SPUR GEAR REDUCTIONS
M. Savage (Akron Univ., OH.), S. B. Lattime (Akron Univ., OH.), J. A. Kimmel (Akron Univ., OH.), and H. H. Coe 1992 10 p Proposed for presentation at the Sixth International Power Transmission and Gearing Conference, Scottsdale, AZ, 13-16 Sep. 1992; sponsored by ASME
(Grant NAG3-1047; DA Proj. 1L1-62211-A-47-A; RTOP 505-63-36)
(NASA-TM-105676; E-7048; NAS 1.15:105676; AVSCOM-TR-91-C-041) Avail: CASI HC A02/MF A01

The optimal design of compact spur gear reductions includes the selection of bearing and shaft proportions in addition to gear mesh parameters. Designs for single mesh spur gear reductions are based on optimization of system life, system volume, and system weight including gears, support shafts, and the four bearings. The overall optimization allows component properties to interact, yielding the best composite design. A modified feasible directions search algorithm directs the optimization through a continuous design space. Interpolated polynomials expand the discrete bearing properties and proportions into continuous variables for optimization. After finding the continuous optimum, the designer can analyze near optimal designs for comparison and selection. Design examples show the influence of the bearings on the optimal configurations. Author

N92-29357# Argonne National Lab., IL.
ROLLING-CONTACT AND WEAR RESISTANCE OF HARD COATINGS ON BEARING-STEEL SUBSTRATES
A. Erdemir Feb. 1992 24 p Presented at the International Conference on Metallurgical Coatings and Thin Films, San Diego, CA, 6-10 Apr. 1992
(Contract W-31-109-eng-38)
(DE92-011834; ANL/CP-74638; CONF-920439-6) Avail: CASI HC A03/MF A01

Ever-increasing needs for high-performance ball- and roller-bearing components that can endure extreme applications have led to a growing interest in hard coatings for improved fatigue life and wear resistance. In particular, hard TiN and TiC coatings and, quite recently, diamond like carbon films have attracted much attention from manufacturers that produce bearing systems for both rolling- and sliding-contact applications. This paper presents an overview that highlights recent incremental progress in achieving improved fatigue and wear resistance in bearing steels through the use of hard coatings. Effects of coating adhesion, thickness, and morphology on fatigue and wear resistance of hard coatings are discussed in detail. Specific references are made to a few mechanistic models that correlate coating thickness and adhesion to improved fatigue life and wear resistance. DOE

N92-29392*# Pittsburgh Univ., PA. Dept. of Mathematics and Statistics.
MULTIDIMENSIONAL COMPUTER SIMULATION OF STIRLING CYCLE ENGINES Final Technical Report
Charles A. Hall and Thomas A. Porsching Jul. 1992 15 p
(Grant NAG3-1097)
(NASA-CR-190497; NAS 1.26:190497; ICMA-92-175) Avail: CASI HC A03/MF A01

This report summarizes the activities performed under NASA-Grant NAG3-1097 during 1991. During that period, work centered on the following tasks: (1) to investigate more effective solvers for ALGAE; (2) to modify the plotting package for ALGAE; and (3) to validate ALGAE by simulating oscillating flow problems similar to those studied by Kurzweg and Ibrahim. Author

N92-29534# Argonne National Lab., IL.
COMPUTER MODEL SIMULATION OF NULL-FLUX MAGNETIC SUSPENSION AND GUIDANCE
Jianliang He and D. M. Rote 1992 11 p Presented at the 6th World Conference on Transport Research, Lyon (France), 29 Jun. - 3 Jul. 1992
(Contract W-31-109-eng-38)
(DE92-013044; ANL/CP-73256; CONF-9206161-1) Avail: CASI HC A03/MF A01

The magnetic force computations in a null-flux suspension system using dynamic circuit theory are discussed. A computer simulation model that can be used to compute magnetic forces and predict the system performance is developed on the basis of dynamic circuit theory. Numerical examples are presented to demonstrate the application of the model. The performance of the null-flux suspension system is simulated and discussed. DOE

N92-29602# National Aerospace Lab., Amsterdam (Netherlands). Structures and Materials Div.
DSC MEASUREMENTS ON EXPERIMENTAL TGDDM/DDS RESIN SYSTEMS: THE INFLUENCE OF VARIATIONS IN RESIN COMPOSITION AND CATALYST CONTENT
W. vanderHoeven 20 Jul. 1990 59 p
(NLR-TP-90267-U; ETN-92-91443) Avail: CASI HC A04/MF A01

DSC measurements were performed on 17 resin mixtures, of which the basic constituents were Tetradiglycidyl Diaminodiphenylmethane (TGDDM) and Diglycidyl Ether of Bisphenol A (DGEBA) epoxies and Diaminodiophenylsulfone (DDS) hardener. The DDS/TGDDM and DGEBA/TGDDM ratios were systematically varied. In addition, for some of the mixtures small amounts of catalyst (0.2 and 2 weight percent) were added. The mixtures were cured in the DSC during a scan at constant heating rate (10 C/min). From the results the reaction onset temperature, the peak temperature(s) and the heat of reaction were determined. A second DSC scan was performed to determine the glass transition temperatures of the cured resin systems. The results showed that the effect of the DDS/TGDDM ratio strongly depends on the catalyst content. By increasing the catalyst content, the curing reactions are shifted to lower temperatures and become exothermic. The highest glass transition temperatures were measured for mixtures with 0.2 weight percent catalyst. ESA

N92-29697*# National Aeronautics and Space Administration. Lewis Research Center, Cleveland, OH.
VALIDATION OF FINITE ELEMENT AND BOUNDARY ELEMENT METHODS FOR PREDICTING STRUCTURAL VIBRATION AND RADIATED NOISE
A. F. Seybert (Kentucky Univ., Lexington.), X. F. Wu (Kentucky Univ., Lexington.), and Fred B. Oswald 1992 9 p Prepared for presentation at the Winter Annual Meeting of the ASME, Anaheim, CA, 8-13 Nov. 1992
(RTOP 505-63-39)
(NASA-TM-105359; AVSCOM-TR-92-C-050; E-7127; NAS 1.15:105359) Avail: CASI HC A02/MF A01

Analytical and experimental validation of methods to predict structural vibration and radiated noise are presented. A rectangular box excited by a mechanical shaker was used as a vibrating structure. Combined finite element method (FEM) and boundary element method (BEM) models of the apparatus were used to predict the noise radiated from the box. The FEM was used to predict the vibration, and the surface vibration was used as input to the BEM to predict the sound intensity and sound power. Vibration predicted by the FEM model was validated by experimental modal analysis. Noise predicted by the BEM was

validated by sound intensity measurements. Three types of results are presented for the total radiated sound power: (1) sound power predicted by the BEM modeling using vibration data measured on the surface of the box; (2) sound power predicted by the FEM/BEM model; and (3) sound power measured by a sound intensity scan. The sound power predicted from the BEM model using measured vibration data yields an excellent prediction of radiated noise. The sound power predicted by the combined FEM/BEM model also gives a good prediction of radiated noise except for a shift of the natural frequencies that are due to limitations in the FEM model. Author

N92-29762*# National Aeronautics and Space Administration. Lyndon B. Johnson Space Center, Houston, TX.
FASTENING APPARATUS HAVING SHAPE MEMORY ALLOY ACTUATOR Patent Application
Darin McKinnis, inventor (to NASA) 13 May 1992 24 p
(NASA-Case-MSC-21935-1; NAS 1.71:MSC-21935-1;
US-Patent-Appl-SN-882408) Avail: CASI HC A03/MF A01

A releasable fastening apparatus is presented. The device includes a connecting member and a housing. The housing supports a gripping mechanism that is adapted to engage the connecting member. A triggering member is movable within the housing between a first position in which it constrains the gripping mechanism in locked engagement with the connecting member, and a second position in which the gripping mechanism is disengaged from the connecting member. A shaped memory alloy actuator is employed for translating the triggering member from its first to its second position. The actuator is designed to expand longitudinally when transitioned from a martensitic to an austenitic state. NASA

N92-29765*# National Aeronautics and Space Administration. Pasadena Office, CA.
POSITION-ERROR-BASED FORCE REFLECTION AND COMPLIANCE CONTROL Patent Application
Won S. Kim, inventor (to NASA) (Jet Propulsion Lab., California Inst. of Tech., Pasadena.) 8 Jul. 1992 33 p
(Contract NAS7-918)
(NASA-Case-NPO-18668-1-CU; NAS 1.71:NPO-18668-1-CU;
US-Patent-Appl-SN-912955) Avail: CASI HC A03/MF A01

Two types of systems for force-reflecting control, which enables high force-reflection gain, are presented: (1) position-error-based force reflection and low-pass-filtered force reflection. Both of the systems are combined with shared compliance control. In the position-error-based class, the position error between the commanded and the actual position of a compliantly controlled robot is used to provide force reflection. In the low-pass-filtered force reflection class, the low-pass-filtered output of the compliance control is used to provide force reflection. The increase in force reflection gain can be more than 10-fold as compared to a conventional high-bandwidth pure force reflection system, when high compliance values are used for the compliance control. NASA

N92-29785# Naval Postgraduate School, Monterey, CA.
FULL POSE AND PARTIAL POSE CALIBRATION OF A 6 DEGREE-OF-FREEDOM ROBOT MANIPULATOR ARM M.S. Thesis
Scott A. Potter Sep. 1991 131 p
(AD-A247463) Avail: CASI HC A07/MF A02

A six degree of freedom robot manipulator arm, a PUMA 560, is calibrated using full pose and partial pose methods in order to improve the accuracy of the manipulator arm. The theory applicable to modeling of mechanisms is introduced. A thirty parameter kinematic model is developed for use in the full pose calibration method and a twenty-six parameter kinematic model is developed for the partial pose calibration. A simulation study is performed to determine the applicability and feasibility of each model. Experimental pose measurements are performed using each method to obtain data with which to perform an actual calibration of the manipulator and compare with the predicted results. The effects of noise in each measurement system employed and in the manipulator's joint position encoders are discussed. The measurement systems employed are examined in detail and a comparison between the two is performed. The measured kinematic parameters of each model are presented as results. GRA

N92-29885# National Aerospace Lab., Amsterdam (Netherlands). Space Div.
ON FICTITIOUS JOINTS MODELLING OF MANIPULATOR LINK FLEXIBILITY FOR THE HERA SIMULATION FACILITY PILOT
P. T. L. M. vanWoerkom 20 May 1988 39 p
(Contracts NIVR-2606-N; NIVR-2506-N)
(NLR-TR-88086-U; ETN-92-91548) Avail: CASI HC A03/MF A01

The way the mathematical model for the dynamics of Hermes Robotic Arm (HERA) can be simulated with rigid body simulation software through the introduction of fictitious joints, is described. Limitations and extensions are indicated. ESA

N92-30026*# National Aeronautics and Space Administration. Lyndon B. Johnson Space Center, Houston, TX.
FINGERED BOLA BODY, BOLA WITH SAME, AND METHODS OF USE Patent Application
John M. Dzenitis, inventor (to NASA) and Linda W. Billica, inventor (to NASA) 5 Jun. 1992 16 p
(NASA-Case-MSC-21967-1; NAS 1.71:MSC-21967-1;
US-Patent-Appl-SN-892053) Avail: CASI HC A03/MF A01

The present invention discloses bola bodies, bolas, and a snaring method which use such devices. A bola body, according to the present invention, is nonspherical or irregular in shape rather than a smooth sphere or ovoid body. One or more fingers extends from the bola body. These fingers may be relatively straight or they may have crooked or bent portions to enhance entanglement with a bola line or lines or with each other. Two or more of such fingers may be used and may be regularly or irregularly spaced apart on a bola body. A bola with such bodies includes lines which are connected to the other bodies. In one particular embodiment of a bola body, according to the present invention, the body has an irregular shape with a bottom rectangular portion and a top pyramid portion forming a nose. A plurality of fingers extended from the pyramidal top portion with one finger extended up and away from each of four corners of the top portion. Such a bola body tends to be initially oriented with its nose and fingers against an object being snared since the body is pulled nose first when a bola line is secured at the tip of the pyramidal portion of the bola body. With such a bola, an unwrapping bola body can slip around a target member so that two of the rod-shaped fingers catch a bola line and guide it into an area or crook between the fingers and a side of the top pyramidal portion of the bola body. Tension on the bola line maintains the line in the crook and tends to press the fingers against the unwrapped target member to stabilize the wrapping of the line about the target member. With such a bola, it is difficult for two or more lines unwrapping in different directions to move past one another without being forced together by line tension. Also, the fingers of such bola bodies may hook and hold each other. The fingers may also hook or entangle some object on or portion of the target member. A probable known target member has known dimensions and shapes so that the bola may be sized and configured to reliably snare such a known target. The bolas can be optimally sized, fashioned, and configured to contact and hold a probable target of known size, dimension, and shape. Author

N92-30082*# National Aeronautics and Space Administration. Lyndon B. Johnson Space Center, Houston, TX.
BEARING SERVICING TOOL Patent Application
Rex A. Boyce, inventor (to NASA) 31 Oct. 1991 18 p
(NASA-Case-MSC-21881-1; NAS 1.71:MSC-21881-1;
US-Patent-Appl-SN-785637) Avail: CASI HC A03/MF A01

A tool for removing and/or replacing bearings in situ is presented which comprises a brace having a first end adapted to engage a first end of the bearing housing, and a second end adapted to engage a second end of the bearing housing. If the two ends of the bearing housing are different in configuration, the

respective ends of the brace are correspondingly configured. An elongate guide member integral with the brace has two parts, each projecting endwise from a respective end of the brace. A pressure plate is alternatively removably mountable on either part of the guide member for longitudinal movement therealong, and has first and second ends of different configurations adapted to engage first and second ends respectively of the bearing. A threaded-type drive is cooperative between the guide and the pressure plate to move the pressure plate longitudinally along the guide and apply a force to the bearing, either to remove the bearing from its housing, or to emplace a new bearing in the housing. NASA

N92-30097*# National Aeronautics and Space Administration. Langley Research Center, Hampton, VA.
SHAFT MOUNT FOR DATA COUPLER SYSTEM Patent Application
James R. Elliott, Jr., inventor (to NASA) and Mark T. Lord, inventor (to NASA) 3 Oct. 1991 9 p
(NASA-Case-LAR-13805-1; NAS 1.71:LAR-13805-1;
US-Patent-Appl-SN-770509) Avail: CASI HC A02/MF A01

A device for mounting a data transmission apparatus to a rotating, tapered, and instrumented shaft is provided. This device permits attachment without interfering with shaft rotation or the accuracy of data output, and prevents both radial and axial slippage of the data transmission apparatus. The mounting device consists of a sleeve assembly which is attached to the shaft by means of clamps that are situated at some distance removed from the instrumented area of the shaft. The data transmission device is secured to the sleeve such that the entire assembly rotates with the shaft. Shim adjustments between sleeve sections assure that a minimum compressive load is transferred to the instrumented area of the shaft and a rubber lining is affixed to a large portion of the interior surface of the sleeve to absorb vibration. NASA

N92-30101*# National Aeronautics and Space Administration. Lyndon B. Johnson Space Center, Houston, TX.
CHECK VALVE WITH POPPET DAMPING MECHANISM Patent Application
Brian G. Morris, inventor (to NASA) 22 Jun. 1992 14 p
(NASA-Case-MSC-21903-1; NAS 1.71:MSC-21903-1;
US-Patent-Appl-SN-902266) Avail: CASI HC A03/MF A01

An inline check valve for a flow line is presented where the valve element is guided for inline travel forward and rearward of a valve sealing member and is spring biased to a closed sealing condition. One of the guides for the valve element includes a dashpot bore and plunger member to control the rate of travel of the valve element in either direction as well as provided a guiding function. The dashpot is not anchored to the valve body so that the valve can be functional even if the plunger member becomes jammed in the dashpot. NASA

N92-29378*# Jet Propulsion Lab., California Inst. of Tech., Pasadena.
DYNAMIC MODELING OF FLUID TRANSMISSION LINES OF THE DSN 70-METER ANTENNAS BY USING A LUMPED PARAMETER MODEL
R. D. Bartos *In its* The Telecommunications and Data Acquisition Report 15 May 1992 p 162-169 (For primary document see N92-29364 20-32)
(RTOP 310-30-42-10-87)
Avail: CASI HC A02/MF A04

38 QUALITY ASSURANCE AND RELIABILITY

Includes product sampling procedures and techniques; and quality control.

N92-29478# Lawrence Livermore National Lab., CA.
COMPUTED TOMOGRAPHY EXPERIMENTS OF PANTEX HIGH EXPLOSIVES
D. E. Perkins, H. E. Martz, L. O. Hester, G. Sobczak, and C. L. Pratt (Mason and Hanger-Silas Mason Co., Inc., Amarillo, TX.) Apr. 1992 45 p
(Contract W-7405-eng-48)
(DE92-013517; UCRL-CR-110256) Avail: CASI HC A03/MF A01

X-ray computed tomography is an advanced imaging technique which provide three-dimensional nondestructive characterization of materials, components and assemblies. The CT Project group at Lawrence Livermore National Laboratory (LLNL) and the Pantex Plant are cooperating to examine the use of CT technology to inspect and characterize high-explosives pressings (e.g., PBX-9502, LX-10-2). High-explosives pressings manufactured by Pantex must be characterized prior to assembling into weapons systems; a nondestructive examination of all assembly parts would be preferable to the current sampling and destructive testing. The earlier in the processing cycle this can be done the more cost effective it will be. We have performed experiments that show that this characterization can be performed at the pressed billet stage using CT. We have detected 2-mm inclusions in a 15-cm diameter billet and 3.5-mm voids in a 20-cm diameter billet. Based on these results we show calculations that can be used to design production CT systems for characterization of high-explosives. DOE

N92-29710# Ohio State Univ., Columbus. Dept. of Statistics.
THEORY OF SYSTEM RELIABILITY DEMONSTRATION, BURN-IN DESIGN, AND RECORD STATISTICS Final Report, 1 Jul. 1989 - 30 Jun. 1991
Saul Blumenthal Apr. 1992 6 p
(Grant AF-AFOSR-0357-89)
(AD-A250582; AFOSR-92-0359TR) Avail: CASI HC A02/MF A01

Estimations of component near-out time were improved by developing Poisson approximations to like distributions (shape-fit). The techniques were also successfully applied to burn-in distributions. GRA

N92-29829*# National Aeronautics and Space Administration. Langley Research Center, Hampton, VA.
METHOD AND APPARATUS FOR THERMOGRAPHICALLY AND QUANTITATIVELY ANALYZING A STRUCTURE FOR DISBONDS AND/OR INCLUSIONS Patent Application
Joseph S. Heyman, inventor (to NASA) and William P. Winfree, inventor (to NASA) 5 May 1992 19 p
(NASA-Case-LAR-14559-1; NAS 1.71:LAR-14559-1;
US-Patent-Appl-SN-878631) Avail: CASI HC A03/MF A01

The nondestructive detection of disbonds or inclusions in laminates is paramount to ensure mission safety in aerospace vehicles. The present invention employs a heat source such as a magnetic/induction eddy current generator to remotely heat a region of a surface of a test structure to a desired depth. The frequency of the heat source is varied to heat to the desired depth. A thermal sensor senses temperature changes in the heated region as a function of time. A computer compares these sensed temperature changes with calibration standards of a similar sample having known disbond or inclusion geography(ies) to analyze the test structure. A plurality of sensors can be arranged linearly to sense vector heat flow. NASA

N92-29873# Messerschmitt-Boelkow-Blohm G.m.b.H., Munich (Germany, F.R.). Helicopter Component Test.
COMPUTED TOMOGRAPHY (CT) AS A NONDESTRUCTIVE TEST METHOD USED FOR COMPOSITE HELICOPTER COMPONENTS
Reinhold Oster 1991 9 p Presented at the 17th European Rotorcraft Forum, Berlin, Fed. Republic of Germany, 24-27 Sep. 1991
(MBB-UD-0603-91-PUB; ETN-92-91695) Avail: CASI HC A02/MF A01

The first components of primary helicopter structures to be made of glass fiber reinforced plastics were the main and tail rotor blades of the Bo105 and BK117 helicopters. These blades

are now successfully produced in series. New developments in rotor components, e.g. the rotor blade technology of the Bo108 and PAH2 programs, make use of very complex fiber reinforced structures to achieve simplicity and strength. Computer tomography was found to be an outstanding nondestructive test method for examining the internal structure of components. A CT scanner generates x-ray attenuation measurements which are used to produce computer reconstructed images of any desired part of an object. The system images a range of flaws in composites in a number of views and planes. Several CT investigations and their results are reported taking composite helicopter components as an example. ESA

N92-29878# European Space Agency. European Space Research and Technology Center, ESTEC, Noordwijk (Netherlands). Product Assurance and Safety Dept.
MAINTAINABILITY REQUIREMENTS FOR ESA SPACE SYSTEMS
Nov. 1991 28 p
(ESA-PSS-01-50-Issue-1; ISSN-0379-4059; ETN-92-91385)
Copyright Avail: CASI HC A03/MF A01

Maintainability program management, engineering, analyses, assessment, demonstration and data collection are specified. The requirements defined apply to all systems where maintenance is to be used to achieve or sustain system capabilities for mission success. The software part of systems are not addressed. The ESA maintainability assurance policy, basic approach, quantitative maintainability requirements, and applicable documents, are outlined. ESA

N92-30116*# Federal Aviation Administration, Atlantic City, NJ.
FEDERAL AVIATION ADMINISTRATION AGING AIRCRAFT NONDESTRUCTIVE INSPECTION RESEARCH PLAN
Chris C. Seher *In* NASA. Langley Research Center, The 1991 International Conference on Aging Aircraft and Structural Airworthiness Jul. 1992 p 221-229 (For primary document see N92-30106 20-39)
Avail: CASI HC A02/MF A04

N92-30117*# Douglas Aircraft Co., Inc., Long Beach, CA.
INSPECTION OF AGING AIRCRAFT: A MANUFACTURER'S PERSPECTIVE
Donald J. Hagemaier *In* NASA. Langley Research Center, The 1991 International Conference on Aging Aircraft and Structural Airworthiness Jul. 1992 p 231-247 (For primary document see N92-30106 20-39)
Avail: CASI HC A03/MF A04

N92-30118*# National Aeronautics and Space Administration. Langley Research Center, Hampton, VA.
THERMAL QNDE DETECTION OF AIRFRAME DISBONDS
William P. Winfree *In its* The 1991 International Conference on Aging Aircraft and Structural Airworthiness Jul. 1992 p 249-260 (For primary document see N92-30106 20-39)
Avail: CASI HC A03/MF A04

N92-30119*# Iowa State Univ. of Science and Technology, Ames. Center for Aviation Systems Reliability.
NDE RESEARCH EFFORTS AT THE FAA CENTER FOR AVIATION SYSTEMS RELIABILITY
Donald O. Thompson and Lisa J. H. Brasche *In* NASA. Langley Research Center, The 1991 International Conference on Aging Aircraft and Structural Airworthiness Jul. 1992 p 261-265 (For primary document see N92-30106 20-39)
(Contract W-7405-eng-82)
Avail: CASI HC A01/MF A04

N92-30120*# Sandia National Labs., Albuquerque, NM.
AGING AIRCRAFT NDI DEVELOPMENT AND DEMONSTRATION CENTER (AANC): AN OVERVIEW
Patrick L. Walter *In* NASA. Langley Research Center, The 1991 International Conference on Aging Aircraft and Structural Airworthiness Jul. 1992 p 267-273 Sponsored in part by FAA (For primary document see N92-30106 20-39)
Avail: CASI HC A02/MF A04

N92-30121*# Sacramento Air Logistics Center, McClellan AFB, CA. Nondestructive Inspection Div.
NONDESTRUCTIVE INSPECTION PERSPECTIVES
Douglas A. Froom *In* NASA. Langley Research Center, The 1991 International Conference on Aging Aircraft and Structural Airworthiness Jul. 1992 p 275-278 (For primary document see N92-30106 20-39)
Avail: CASI HC A01/MF A04

39 STRUCTURAL MECHANICS

Includes structural element design and weight analysis; fatigue; and thermal stress.

For applications see *05 Aircraft Design, Testing and Performance* and *18 Spacecraft Design, Testing and Performance*.

N92-29338# Lawrence Livermore National Lab., CA.
AN INNOVATIVE APPROACH FOR COUPLED THERMOMECHANICAL ANALYSIS
R. G. Whirley and B. E. Engelmann Aug. 1991 9 p Presented at the American Society of Mechanical Engineers (ASME) Annual Winter Meeting, Atlanta, GA, 1-6 Dec. 1991
(Contract W-7405-eng-48)
(DE92-011467; UCRL-JC-107866; CONF-911213-25) Avail: CASI HC A02/MF A01

This paper describes a staggered step formulation for coupled thermomechanical problems, and the implementation of this approach into a new nonlinear finite element code, PALM2D. The staggered step approach considers the coupled thermomechanical response of solids, including nonlinear effects in both the thermal and mechanical aspects. The thermal problem may include temperature dependent thermal conductivities and convection boundary conditions, and the mechanical problem may include large deformations and strains as well as material nonlinearities such as plasticity. Heat generation due to mechanical plastic deformation is incorporated into the energy equation, and the energy equation is solved on the current deformed geometry. Experience to date indicates that this approach allows an inexpensive solution to many strongly nonlinear fully coupled thermomechanical problems. DOE

N92-29342*# National Aeronautics and Space Administration. Lewis Research Center, Cleveland, OH.
STRUCTURAL DURABILITY OF STIFFENED COMPOSITE SHELLS
Levon Minnetyan (Clarkson Univ., Potsdam, NY.), James M. Rivers (Clarkson Univ., Potsdam, NY.), Pappu L. N. Murthy, and Christos C. Chamis 1992 33 p Presented at the 33rd Structures, Structural Dynamics and Materials Conference, Dallas, TX, 13-15 Apr. 1992; sponsored in part by AIAA, ASME, ASCE, AHS, and ASC
(Grant NAG3-1101)
(NASA-CR-190588; NAS 1.26:190588) Avail: CASI HC A03/MF A01

The durability of a stiffened composite cylindrical shell panel is investigated under several loading conditions. An integrated computer code is utilized for the simulation of load induced structural degradation. Damage initiation, growth, and accumulation up to the stage of propagation to fracture are included in the computational simulation. Results indicate significant differences in the degradation paths for different loading cases. The effects of combined loading on structural durability and ultimate structural strength of a stiffened shell are assessed. Author

N92-29393*# National Aeronautics and Space Administration. Langley Research Center, Hampton, VA.
AN INTERLAMINAR TENSION STRENGTH SPECIMEN
Wade C. Jackson and Roderick H. Martin May 1992 50 p

Presented at the ASTM 11th Symposium on Composite Materials: Testing and Design, Pittsburgh, PA, 4-5 May 1992
(RTOP 510-02-12-10)
(NASA-TM-107623; NAS 1.15:107623; AVSCOM-TR-92-B-008)
Avail: CASI HC A03/MF A01

This paper describes a technique to determine interlaminar tension strength, sigma(sub 3c) of a fiber reinforced composite material using a curved beam. The specimen was a unidirectional curved beam, bent 90 degrees, with straight arms. Attached to each arm was a hinged loading mechanism which was held by the grips of a tensile testing machine. Geometry effects of the specimen, including the effects of loading arm length, inner radius, thickness, and width, were studied. The data sets fell into two categories: low strength corresponding to a macroscopic flaw related failure and high strength corresponding to a microscopic flaw related failure. From the data available, the loading arm length had no effect on sigma(sub 3c). The inner radius was not expected to have a significant effect on sigma(sub 3c), but this conclusion could not be confirmed because of differences in laminate quality for each curve geometry. The thicker specimens had the lowest value of sigma(sub 3c) because of poor laminate quality. Width was found to affect the value of sigma(sub 3c) only slightly. The wider specimens generally had a slightly lower strength since more material was under high stress, and hence, had a larger probability of containing a significant flaw. Author

N92-29407# Massachusetts Univ., Amherst. Dept. of Civil Engineering.
CONSTITUTIVE MODELLING FOR GRANULAR MATERIAL UNDER FINITE STRAINS WITH PARTICLE SLIDINGS AND FABRIC CHANGES Final Report, 1 May 1989 - 30 Sep. 1991
Ching S. Chang 4 Feb. 1992 85 p
(Grant AF-AFOSR-0313-89)
(AD-A248187; AFOSR-92-0200TR) Avail: CASI HC A05/MF A01

The overall objective of this research is to develop a constitutive model for granular material under finite strains with explicit consideration of particle sliding and the consequent fabric change. The specific objective of this research is focused on the development of a stress-strain theory that accounts for the microstructure and the non-uniform strain field of the particle assembly. The developed theoretical model is evaluated by results obtained from computer simulation and experiments of granular material. Mechanical behavior of granular media is important in many fields of studies such as soil mechanics, powder mechanics, and ceramic mechanics. The mechanical behavior of granular media was studied by borrowing the stress-strain models, such as elastic, elasto-plastic, or plastic models, developed for continuum materials. These continuum models consider neither the discrete nature nor the deformation mechanism of granular materials. A more rational approach should be one that considers the granular system as an assemblage of particles. The stress-strain behavior for a granular material is defined for a representative-volume which consists of a sufficiently large number of particles to be representative of the material. When subjected to loading, the deformation of the granular system results from particle deformation as well as slip between particles. GRA

N92-29535# Argonne National Lab., IL.
AN APPROXIMATION METHOD FOR DYNAMIC RESPONSE OF STRAIN-HARDENING STRUCTURES
C. K. Youngdahl Feb. 1992 10 p Presented at the 2nd International Conference on Structures Under Shock and Impact, Southampton, England, 16-18 Jun. 1992
(Contract W-31-109-eng-38)
(DE92-013053; ANL/CP-75372; CONF-9206166-1) Avail: CASI HC A02/MF A01

An approximation method is being developed to predict the dynamic plastic response of rigid, strain-hardening structures. This method is analogous to the instantaneous mode techniques used to treat rigid, perfectly plastic structures in that deflection shape involving a number of arbitrary functions of time selected, based on static deformation profiles. Two stress fields are associated with the deflection shape: one satisfies the equations of motion with appropriate boundary and continuity conditions, and the other satisfies the strain-hardening constitutive relation with appropriate boundary and smoothness conditions. The method is illustrated using the case of a simply-supported beam with a central plastic region. DOE

N92-29601# Pennsylvania Univ., Philadelphia. Dept. of Materials Science and Engineering.
MECHANISM OF DIFFUSION-CONTROLLED BRITTLE FRACTURE
C. J. McMahon Oct. 1991 4 p
(Contract DE-FG02-87ER-45290)
(DE92-011572; DOE/ER-45290/5) Avail: CASI HC A01/MF A01

Two generations of UHV testing systems were developed, one for testing pre-cracked specimens at constant displacement and the other at constant load, and they were supplemented by a computer-controlled potential-drop system for measurement of crack-growth rates. The latter system was also developed during this project. Experiments were carried out on the alloy Cu-8 percent Sn which was used as a model system for the phenomenon of diffusion-controlled fracture by intergranular decohesion resulting from the ingress of an embrittling element from a free surface as the result of an applied stress. The cracking phenomenon found earlier in alloy steels, and shown to be due to surface-adsorbed sulfur, was reproduced in the Cu-Sn alloy. This provided verification of the earlier proposed mechanism for the cracking phenomenon in the alloy steels, known as stress-relief cracking, and it also provided support for the hypothesis that the phenomenon was of a generic nature. In conjunction with the experimental work, the development of a quantitative theory of this class of brittle fracture, which we have termed 'dynamic embrittlement', was begun. DOE

N92-29603# National Aerospace Lab., Amsterdam (Netherlands). Structures and Materials Div.
SHORT CRACKS AND DURABILITY ANALYSIS OF THE FOKKER 100 WING/FUSELAGE STRUCTURE
R. J. H. Wanhill and L. Schra 2 Oct. 1990 24 p Presented at the International Conference on Short Cracks, Sheffield, England, Dec. 1990
(NLR-TP-90336-U; ETN-92-91449) Avail: CASI HC A03/MF A01

Short and long fatigue crack growth in the industry standard damage tolerant aluminum alloy 2024-T3 were compared using flight simulation loading representative for the Fokker 100 wing/fuselage structure. The results and a straightforward durability analysis showed that the behavior of short cracks is not significant for the current wing/fuselage structure. The data provide a reference for evaluating new candidate materials for durable wing/fuselage structures in transport aircraft. ESA

N92-29672 Aeronautical Research Labs., Melbourne (Australia).
STRESSES AND STRAINS IN PLAIN AND COLDWORKED ANNULI SUBJECTED TO REMOTE, INTERFERENCE OR COMBINED LOADING
G. S. Jost May 1992 56 p
(ARL-STRUC-R-446; AR-006-663) Copyright Avail: Issuing Activity

Analytical plane-strain stresses and strains have been derived for both plain and coldworked annuli subjected to remote loading, interference loading or both loadings acting together. Where required, the deformation theory of plasticity has been used. The comparitive influence of the various loading cases on the fatigue process are discussed. Under cyclic remote loading, it is predicted that the most beneficial fatigue situation will result from a combination of interference fitting and coldworking. Author

N92-29700# Technische Univ., Delft (Netherlands). Faculty of Aerospace Engineering.
THE EFFECT OF LENGTH VARIATION ON THE STABILITY OF

CIRCULAR CYLINDRICAL SHELLS UNDER PURE BENDING
E. Karyadi Dec. 1991 34 p
(LR-669; ETN-92-91406) Avail: CASI HC A03/MF A01

The effect of length variation in the stability of circular cylindrical shells is investigated by means of Flugge's equation whereby the chosen boundary conditions are satisfied rigorously. The isotropic cylinders are subjected to pure bending load. The results show that the maximum critical bending stress is only about 1.4 percent higher than the critical uniform compressive stress. ESA

N92-29708# National Aerospace Lab., Amsterdam (Netherlands). Structures and Materials Div.
FATIGUE CRACK GROWTH IN DAMAGE TOLERANT Al-Li SHEET ALLOYS
R. J. H. Wanhill 22 Mar. 1990 13 p Presented at the International Conference in Advanced Aluminum and Magnesium Alloys, Amsterdam, Netherlands, 20-22 Jun. 1990 Sponsored by Netherlands Agency for Aerospace Programs
(NLR-TP-90107-U; ETN-92-91532) Avail: CASI HC A03/MF A01

The fatigue crack growth properties of two candidate damage tolerant Al-Li sheet alloys, 2091 and 8090 are compared with those of the conventional and widely used 2024 alloy. There were three load histories: constant amplitude, gust spectrum, and constant amplitude with occasional peak loads. The results are interpreted with the aid of fractographic observations and measurements of fracture surface roughness. The practical significance of the results is assessed, and recommendations are made for further evaluations. ESA

N92-29813# National Inst. of Standards and Technology, Gaithersburg, MD. Center for Computing and Applied Mathematics.
COMPUTER PROGRAM POWNOR FOR FITTING THE POWER-NORMAL AND -LOGNORMAL MODELS TO LIFE OR STRENGTH DATA FROM SPECIMENS OF VARIOUS SIZES
W. Nelson and N. Dognanksoy Mar. 1992 33 p Sponsored in part by NSF and by American Statistical Association, Alexandria, VA
(PB92-169119; NISTIR-4760) Avail: CASI HC A03/MF A01

The power-normal and -lognormal models, which describe the effect of specimen size on the distribution of life or strength of a product or material, are presented. Such a model arises when any specimen can be regarded as a series system of smaller portions, where portions of a certain size have a normal life (or strength) distribution. Also, the report documents the first computer program that fits the model to data (including censored and interval life data) from specimens of various sizes. The program employs maximum likelihood fitting and provides approximate confidence limits, as well as estimates, for model parameters, distribution percentiles, and other quantities of interest. How to run the program is explained with an analysis of data on time to electromigration failure of aluminum conductors for microcircuits. Author

N92-29915# Naval Undersea Warfare Center, New London, CT.
A CLOSED FORM SOLUTION OF A LONGITUDINAL BEAM WITH A VISCOUS BOUNDARY CONDITION Progress Report
Andrew J. Hull 6 Apr. 1992 24 p
(AD-A248841; NUWC-NL-TR-10017) Avail: CASI HC A03/MF A01

This paper develops a closed form solution of a longitudinal beam with a viscous boundary condition subjected to point loading. A new inner product is formulated that allows the time and space modes of the beam to decouple. This expansion yields explicit eigenvalues and eigenvectors. A frequency domain example is presented, and the results are compared with finite element solutions of the same problem. It is shown that the closed form solution is computationally more efficient than a finite element solution. Additionally, truncation error at lower frequencies is shown to be extremely small. The method is easily implemented and can provide time and frequency domain solutions to this class of problems. GRA

N92-29925# Technische Univ., Brunswick (Germany, F.R.). Fakultaet fuer Maschinenbau und Elektrotechnik.
THICKNESS DEPENDENCY OF ELASTIC AFTEREFFECT OF THIN BENDING BEAMS Ph.D. Thesis
[DICKENABHAENGIGKEIT DER ELASTISCHEN NACHWIRKUNG VON DUENNEN BIEGEBALKEN]
Joerg Frank 1991 170 p In GERMAN
(ETN-92-91488) Avail: CASI HC A08/MF A02

The influence of specimen thickness on the inelastic behavior of thin bending beams at room temperature is examined. The most important theoretical relationships are phenomenologically explained: those with the mechanical time response of spring materials for quasi-static and periodic load can be described. The mechanical properties of spring materials, e.g., CuBe2, TiAl6V4, quartz glass and silicon, and the construction of bending beams, are considered. A new measuring structure with which the strain retardation of thin bending beams can be determined unidirectionally is described. The evaluation of the measuring results allows the adaptation of the model function to the retardation curves by nonlinear optimization. ESA

N92-30028*# National Aeronautics and Space Administration. Langley Research Center, Hampton, VA.
COMBINED LOAD TEST APPARATUS FOR FLAT PANELS Patent Application
Robert R. McWithey, inventor (to NASA) (AS&M, Inc., Hampton, VA.), Carl J. Martin, Jr., inventor (to NASA) (Lockheed Engineering and Sciences Co., Hampton, VA.), and Jeffrey A. Cerro, inventor (to NASA) (Lockheed Engineering and Sciences Co., Hampton, VA.) 7 Apr. 1992 16 p
(NASA-Case-LAR-14698-1; NAS 1.71:LAR-14698-1; US-Patent-Appl-SN-866769) Avail: CASI HC A03/MF A01

Future hypersonic aircraft such as the National Aero-Space Plane and a high speed civil transport will require the design and use of efficient, highly-loaded, flat structural panels to achieve mission requirements. These panels will be subjected to severe combinations of in-plane mechanical distributed loads (i.e., normal loads in two perpendicular directions plus a shear load), in addition to pressure and thermal loads. A testing apparatus is provided for applying uniform combined in-plane stresses to a flat panel containing an interior test area. Actuators cause two sets of load rods to apply loads to the edge of the flat panel. The first set applies loads which are perpendicular to and independent of the loads applied by the second set. The loads are applied according to a cosine load distribution to obtain a uniform stress field within the test area. The flat panel may be rotated with respect to the applied loads to obtain a wide range of combined stresses in the test area. Movement outside the plane of the flat panel may be selectively prevented by connecting the flat panel to a restraining disk by support rods. The support rods then define the test area. A thermal load may be applied to one side of the flat panel and a pressure load may be applied to the other side. The novelty of this method is found in providing a testing apparatus which allows mechanical, thermal and pressure loads to be applied simultaneously to a flat panel for testing purposes. NASA

N92-30099*# National Aeronautics and Space Administration. Langley Research Center, Hampton, VA.
APPARATUS FOR ELEVATED TEMPERATURE COMPRESSION OR TENSION TESTING OF SPECIMENS Patent Application
Thomas S. Gates, inventor (to NASA) 12 May 1992 8 p
(NASA-Case-LAR-14775-1; NAS 1.71:LAR-14775-1; US-Patent-Appl-SN-881912) Avail: CASI HC A02/MF A01

In order to support materials selection for the next generation supersonic civilian passenger transport aircraft, a testing apparatus was developed to evaluate certain materials under conditions of high load and elevated temperature. In order to elevate the temperature of the material during standard tension and compression testing the test specimen is surrounded by a pair of supports which include internal heating means. These supports also prevent buckling of the specimen during compression testing. NASA

N92-30106*# National Aeronautics and Space Administration. Langley Research Center, Hampton, VA.
THE 1991 INTERNATIONAL CONFERENCE ON AGING AIRCRAFT AND STRUCTURAL AIRWORTHINESS
Charles E. Harris, ed. Washington Jul. 1992 470 p Conference held in Washington, DC, 19-21 Nov. 1991; sponsored by NASA, Washington and FAA
(RTOP 538-02-10-01)
(NASA-CP-3160; L-17094; NAS 1.55:3160) Avail: CASI HC A20/MF A04

Technical sessions of the conference included structural performance, nondestructive evaluation, maintenance and repair, international activities, and commuter airlines. Each session was organized to provide a well-rounded view of the subject from the industry, regulatory, and research perspective. Thirty-four presentations were given by the international technical community. For individual titles, see N92-30107 through N92-30134.

N92-30107*# Boeing Commercial Airplane Co., Seattle, WA. Structures Engineering Div.
STRUCTURAL INTEGRITY OF FUTURE AGING AIRPLANES
Jack F. McGuire and Ulf G. Goranson *In* NASA. Langley Research Center, The 1991 International Conference on Aging Aircraft and Structural Airworthiness Jul. 1992 p 33-47 (For primary document see N92-30106 20-39)
Avail: CASI HC A03/MF A04

A multitude of design considerations is involved in ensuring the structural integrity of Boeing jet transports that have common design concepts validated by extensive analyses, tests, and three decades of service. As airplanes approach their design service objectives, the incidences of fatigue and corrosion may become widespread. Continuing airworthiness of the aging jet fleet requires diligent performance from the manufacturer, the airlines, and airworthiness authorities. Aging fleet support includes timely development of supplemental structural inspection documents applicable to selected older airplanes, teardown inspections of high-time airframes retired from service, fatigue testing of older airframes, and structural surveys of more than 130 airplanes operated throughout the world. Lessons learned from these activities are incorporated in service bulletin recommendations, production line modifications, and design manual updates. An overview of traditional Boeing fleet support activities and the anticipated benefits for future generations of commercial airplanes based on the continuous design improvement process are presented. Author

N92-30108*# Douglas Aircraft Co., Inc., Long Beach, CA. Airworthiness Assurance Programs.
MAINTAINING THE SAFETY OF AN AGING FLEET OF AIRCRAFT **c03**
Amos W. Hoggard *In* NASA. Langley Research Center, The 1991 International Conference on Aging Aircraft and Structural Airworthiness Jul. 1992 p 49-65 (For primary document see N92-30106 20-39)
Avail: CASI HC A03/MF A04

The current status of the Douglas Aging Fleet is examined in light of increasing concern for the possibility of the onset of widespread cracking and recent industry activity to minimize the concern. A fleet monitoring program together with an augmented maintenance program is proposed as a possible means to reduce the concern. Six candidate options for maintenance program augmentation are examined which have been shown to be effective in detection of widespread fatigue damage. A brief example of how this system might be applied to the DC-9 Fleet is presented. Author

N92-30109*# Boeing Commercial Airplane Co., Seattle, WA.
PERFORMANCE OF FUSELAGE PRESSURE STRUCTURE
James R. Maclin *In* NASA. Langley Research Center, The 1991 International Conference on Aging Aircraft and Structural Airworthiness Jul. 1992 p 67-74 (For primary document see N92-30106 20-39)
Avail: CASI HC A02/MF A04

There are currently more than 1,000 Boeing airplanes around the world over 20 years old. That number is expected to double by the year 1995. With these statistics comes the reality that structural airworthiness will be in the forefront of aviation issues well into the next century. The results of previous and recent test programs Boeing has implemented to study the structural performance of older airplanes relative to pressurized fuselage sections are described. Included in testing were flat panels with multiple site damage (MSD), a full-scale 737 and 2 747s as well as panels representing a 737 and 777, and a generic aircraft in large pressure-test fixtures. Because damage is a normal part of aging, focus is on the degree to which structural integrity is maintained after failure or partial failure of any structural element, including multiple site damage (MSD), and multiple element damage (MED). Author

N92-30110*# National Aeronautics and Space Administration. Langley Research Center, Hampton, VA.
FRACTURE MECHANICS RESEARCH AT NASA RELATED TO THE AGING COMMERCIAL TRANSPORT FLEET
James C. Newman, Jr. and Charles E. Harris *In its* The 1991 International Conference on Aging Aircraft and Structural Airworthiness Jul. 1992 p 75-91 (For primary document see N92-30106 20-39)
Avail: CASI HC A03/MF A04

NASA is conducting the Airframe Structural Integrity Program in support of the aging commercial transport fleet. This interdisciplinary program is being worked in cooperation with the U.S. airframe manufacturers, airline operators, and the FAA. Advanced analysis methods are under development and an extensive testing program is under way to study fatigue crack growth and fracture in complex built-up shell structures. Innovative nondestructive examination technologies are also being developed to provide large area inspection capability to detect corrosion, disbonds, and cracks. Recent fracture mechanics results applicable to predicting the growth of cracks under monotonic and cyclic loading at rivets in fuselage lap-splice joints are reviewed. Author

N92-30111*# Harvard Univ., Cambridge, MA. Div. of Applied Sciences.
PRELIMINARY RESULTS ON THE FRACTURE ANALYSIS OF MULTI-SITE CRACKING OF LAP JOINTS IN AIRCRAFT SKINS
J. L. Beuth, Jr. and John W. Hutchinson *In* NASA. Langley Research Center, The 1991 International Conference on Aging Aircraft and Structural Airworthiness Jul. 1992 p 93-110 Sponsored in part by FAA (For primary document see N92-30106 20-39)
(Grant NSF MSM-88-12779)
Avail: CASI HC A03/MF A04

Results of a fracture mechanics analysis relevant to fatigue crack growth at rivets in lap joints of aircraft skins are presented. Multi-site damage (MSD) is receiving increased attention within the context of problems of aging aircraft. Fracture analyses previously carried out include small-scale modeling of rivet/skin interactions, larger-scale two-dimensional models of lap joints similar to that developed here, and full scale three-dimensional models of large portions of the aircraft fuselage. Fatigue testing efforts have included flat coupon specimens, two-dimensional lap joint tests, and full scale tests on specimens designed to closely duplicate aircraft sections. Most of this work is documented in the proceedings of previous symposia on the aging aircraft problem. The effect MSD has on the ability of skin stiffeners to arrest the growth of long skin cracks is a particularly important topic that remains to be addressed. One of the most striking features of MSD observed in joints of some test sections and in the joints of some of the older aircraft fuselages is the relative uniformity of the fatigue cracks from rivet to rivet along an extended row of rivets. This regularity suggests that nucleation of the cracks must not be overly difficult. Moreover, it indicates that there is some mechanism which keeps longer cracks from running away from shorter ones, or, equivalently, a mechanism for shorter cracks to catch-up with longer cracks. This basic mechanism has not been

identified, and one of the objectives of the work is to see to what extent the mechanism is revealed by a fracture analysis of the MSD cracks. Another related aim is to present accurate stress intensity factor variations with crack length which can be used to estimate fatigue crack growth lifetimes once cracks have been initiated. Results are presented which illustrate the influence of load shedding from rivets with long cracks to neighboring rivets with shorter cracks. Results are also included for the effect of residual stress due to the riveting process itself. Author

N92-30112*# Federal Aviation Administration, Cambridge, MA. National Transportation Systems Center.
CURRENT DOT RESEARCH ON THE EFFECT OF MULTIPLE SITE DAMAGE ON STRUCTURAL INTEGRITY
P. Tong (Hong Kong Univ. of Science and Technology, Kowloon.), Kemal Arin, David Y. Jeong, R. Greif, John C. Brewer, Stephan N. Bobo, and Sam N. Sampath (Federal Aviation Administration, Atlantic City, NJ.) *In* NASA. Langley Research Center, The 1991 International Conference on Aging Aircraft and Structural Airworthiness Jul. 1992 p 111-157 (For primary document see N92-30106 20-39)
Avail: CASI HC A03/MF A04

Multiple site damage (MSD) is a type of cracking that may be found in aging airplanes and which may adversely affect their continuing airworthiness. The Volpe National Transportation Systems Center has supported the Federal Aviation Administration Technical Center on structural integrity research for the past two and half years. The work has focused on understanding the behavior of MSD, detection of MSD during airframe inspection, and the avoidance of MSD in future designs. These three elements of the MSD problem are addressed and a summary of the completed work, the current status, and requirements for future research is provided. Author

N92-30113*# Federal Aviation Administration, Seattle, WA.
STATUS OF THE FAA FLIGHT LOADS MONITORING PROGRAM
Terence J. Barnes and Thomas DeFiore (Federal Aviation Administration, Atlantic City, NJ.) *In* NASA. Langley Research Center, The 1991 International Conference on Aging Aircraft and Structural Airworthiness Jul. 1992 p 159-185 (For primary document see N92-30106 20-39)
Avail: CASI HC A03/MF A04

In support of the Federal Aviation Administration Aging Aircraft Research Program, the Agency has established a Flight Loads Data Collection Program for Commercial Aircraft. The objectives of this Program are as follows: (1) review existing data collected by other sources including but not limited to U.S., Foreign, Military, etc.; (2) collect current operational usage data from both large and small transport aircraft; and (3) develop criteria for future generations of transports. This paper presents the status of the various programs which are completed, underway or planned. The FAA will be collecting, storing, and analyzing the data which characterize typical commercial transport operations. The airframe manufacturers will handle the task of calculating the loads and stresses. Author

N92-30114*# Aeronautical Systems Div., Wright-Patterson AFB, OH.
DAMAGE TOLERANCE FOR COMMUTER AIRCRAFT
John W. Lincoln *In* NASA. Langley Research Center, The 1991 International Conference on Aging Aircraft and Structural Airworthiness Jul. 1992 p 187-201 (For primary document see N92-30106 20-39)
Avail: CASI HC A03/MF A04

The damage tolerance experience in the United States Air Force with military aircraft and in the commercial world with large transport category aircraft indicates that a similar success could be achieved in commuter aircraft. The damage tolerance process is described for the purpose of defining the approach that could be used for these aircraft to ensure structural integrity. Results of some of the damage tolerance assessments for this class of aircraft are examined to illustrate the benefits derived from this approach. Recommendations are given for future damage tolerance assessment of existing commuter aircraft and on the incorporation of damage tolerance capability in new designs. Author

N92-30115*# National Aeronautics and Space Administration. Langley Research Center, Hampton, VA.
DAMAGED STIFFENED SHELL RESEARCH AT NASA. LANGLEY RESEARCH CENTER
James H. Starnes, Jr. and Vicki O. Britt *In its* The 1991 International Conference on Aging Aircraft and Structural Airworthiness Jul. 1992 p 203-220 (For primary document see N92-30106 20-39)
Avail: CASI HC A03/MF A04

The structural behavior of stiffened fuselage shells with local cracks is influenced by the local deformations and stress gradients near the cracks, and this behavior must be understood to predict fuselage structural integrity and residual strength. As a crack grows, the stiffness and internal load distributions in a stiffened shell change, affecting the local deformations and stress gradients near the crack. Transport fuselage shells are designed to support internal pressure and mechanical loads which cause a geometrically nonlinear response. Research is being conducted at NASA LaRC to develop and demonstrate a verified nonlinear stiffened shell analysis methodology for accurately predicting the global and local behavior of nonlinear stiffened fuselage shells with local cracks and with combined internal pressure and mechanical loads. The nonlinear structural analysis methodology being developed and planned at NASA LaRC for damaged stiffened fuselage shells and the experiments being planned to verify this analysis methodology are summarized in the present paper. Author

N92-30116*# Federal Aviation Administration, Atlantic City, NJ.
FEDERAL AVIATION ADMINISTRATION AGING AIRCRAFT NONDESTRUCTIVE INSPECTION RESEARCH PLAN **c38**
Chris C. Seher *In* NASA. Langley Research Center, The 1991 International Conference on Aging Aircraft and Structural Airworthiness Jul. 1992 p 221-229 (For primary document see N92-30106 20-39)
Avail: CASI HC A02/MF A04

This paper highlights the accomplishments and plans of the Federal Aviation Administration (FAA) for the development of improved nondestructive evaluation (NDE) equipment, procedures, and training. The role of NDE in aircraft safety and the need for improvement are discussed. The FAA program participants, and coordination of activities within the program and with relevant organizations outside the program are also described. Author

N92-30117*# Douglas Aircraft Co., Inc., Long Beach, CA.
INSPECTION OF AGING AIRCRAFT: A MANUFACTURER'S PERSPECTIVE **c38**
Donald J. Hagemaier *In* NASA. Langley Research Center, The 1991 International Conference on Aging Aircraft and Structural Airworthiness Jul. 1992 p 231-247 (For primary document see N92-30106 20-39)
Avail: CASI HC A03/MF A04

Douglas, in conjunction with operators and regulators, has established interrelated programs to identify and address issues regarding inspection of aging aircraft. These inspection programs consist of the following: Supplemental Inspection Documents; Corrosion Prevention and Control Documents; Repair Assessment Documents; and Service Bulletin Compliance Documents. In addition, airframe manufacturers perform extended airframe fatigue tests to deal with potential problems before they can develop in the fleet. Lastly, nondestructive inspection (NDI) plays a role in all these programs through the detection of cracks, corrosion, and disbonds. However, improved and more cost effective NDI methods are needed. Some methods such as magneto-optic imaging, electronic shearography, Diffractor-Sight, and multi-parameter eddy current testing appear viable for near-term improvements in NDI of aging aircraft. Author

N92-30118*# National Aeronautics and Space Administration. Langley Research Center, Hampton, VA.
THERMAL QNDE DETECTION OF AIRFRAME DISBONDS c38
William P. Winfree *In its* The 1991 International Conference on Aging Aircraft and Structural Airworthiness Jul. 1992 p 249-260 (For primary document see N92-30106 20-39)
Avail: CASI HC A03/MF A04

Thermographic characterization of aircraft bonded lap joints offers a quick noncontacting technique to acquire information for structural integrity assessment. This paper discusses recent research to optimize the technique and determine the limits of its applicability. The temperature of the outer surface of the lap joint is increased by the application of heat flux from either flash or quartz lamp heaters. The time dependence of the surface temperature of the lap joint is imaged radiometrically. Measurements are presented for a range of specimens, ranging from samples fabricated with well characterized disbonds to actual aircraft. A technique for processing these images to enhance the contrast between bonded and disbonded regions of the lap joint is presented. Numerical models of the technique simulate the procedure. These simulations provide a cost efficient method for optimizing the technique by varying parameters such as the time for application of heat. These simulations facilitate the definition of parameters difficult to determine experimentally, such as the minimum air gap required for a disbond to be detected. Good agreement between measurements and these simulations is found. Author

N92-30119*# Iowa State Univ. of Science and Technology, Ames. Center for Aviation Systems Reliability.
NDE RESEARCH EFFORTS AT THE FAA CENTER FOR AVIATION SYSTEMS RELIABILITY c38
Donald O. Thompson and Lisa J. H. Brasche *In* NASA. Langley Research Center, The 1991 International Conference on Aging Aircraft and Structural Airworthiness Jul. 1992 p 261-265 (For primary document see N92-30106 20-39)
(Contract W-7405-eng-82)
Avail: CASI HC A01/MF A04

The Federal Aviation Administration-Center for Aviation Systems Reliability (FAA-CASR), a part of the Institute for Physical Research and Technology at Iowa State University, began operation in the Fall of 1990 with funding from the FAA. The mission of the FAA-CASR is to develop quantitative nondestructive evaluation (NDE) methods for aircraft structures and materials including prototype instrumentation, software, techniques, and procedures and to develop and maintain comprehensive education and training programs in aviation specific inspection procedures and practices. To accomplish this mission, FAA-CASR brings together resources from universities, government, and industry to develop a comprehensive approach to problems specific to the aviation industry. The problem areas are targeted by the FAA, aviation manufacturers, the airline industry and other members of the aviation business community. This consortium approach ensures that the focus of the efforts is on relevant problems and also facilitates effective transfer of the results to industry. Author

N92-30120*# Sandia National Labs., Albuquerque, NM.
AGING AIRCRAFT NDI DEVELOPMENT AND DEMONSTRATION CENTER (AANC): AN OVERVIEW c38
Patrick L. Walter *In* NASA. Langley Research Center, The 1991 International Conference on Aging Aircraft and Structural Airworthiness Jul. 1992 p 267-273 Sponsored in part by FAA (For primary document see N92-30106 20-39)
Avail: CASI HC A02/MF A04

A major center with emphasis on validation of nondestructive inspection (NDI) techniques for aging aircraft, the Aging Aircraft NDI Development and Demonstration Center (AANC), has been funded by the FAA at Sandia National Laboratories. The Center has been assigned specific tasks in developing techniques for the nondestructive inspection of static engine parts, assessing inspection reliability (POD experiments), developing testbeds for NDI validation, maintaining a FAA library of characterized aircraft structural test specimens, and leasing a hangar to house a high flight cycle transport aircraft for use as a full scale test bed. Author

N92-30121*# Sacramento Air Logistics Center, McClellan AFB, CA. Nondestructive Inspection Div.
NONDESTRUCTIVE INSPECTION PERSPECTIVES c38
Douglas A. Froom *In* NASA. Langley Research Center, The 1991 International Conference on Aging Aircraft and Structural Airworthiness Jul. 1992 p 275-278 (For primary document see N92-30106 20-39)
Avail: CASI HC A01/MF A04

This paper presents ideas for consideration by those concerned with commercial aircraft nondestructive inspection (NDI). The perspective is that of an individual with a background in military aircraft NDI, and important differences are indicated between the commercial NDI and military NDI activities. In particular, it is significantly more expensive to implement some new NDI technology, and therefore, in-depth cost-benifit studies for commercial users are recommended. Author

N92-30122*# Northwest Airlines, Inc., Minneapolis, MN.
CURRENT AND FUTURE DEVELOPMENTS IN CIVIL AIRCRAFT NON-DESTRUCTIVE EVALUATION FROM AN OPERATOR'S POINT OF VIEW c01
Jeff Register *In* NASA. Langley Research Center, The 1991 International Conference on Aging Aircraft and Structural Airworthiness Jul. 1992 p 279-282 (For primary document see N92-30106 20-39)
Avail: CASI HC A01/MF A04

In June, 1988, the first International Conference on aging aircraft was held to address nondestructive tests (NDT) of aging aircraft and other issues. From this meeting, a research program was initiated and funded by the FAA. As a result of this program, a lot of work has been done to study current NDT practices in the aviation industry and secondly, to research and develop new NDT methods to improve the reliability and efficiency of in-service inspection of aircraft structures and powerplants. The following is an overview of the current and future developments in civil aircraft NDT, as viewed by an air carrier and the concerns for NDT in the future. Author

N92-30123*# Airbus Industrie, Blagnac (France).
AGEING AIRPLANE REPAIR ASSESSMENT PROGRAM FOR AIRBUS A300 c03
J. M. Gaillardon, Hans-J. Schmidt, and B. Brandecker *In* NASA. Langley Research Center, The 1991 International Conference on Aging Aircraft and Structural Airworthiness Jul. 1992 p 283-289 (For primary document see N92-30106 20-39)
Avail: CASI HC A02/MF A04

This paper describes the current status of the repair categorization activities and includes all details about the methodologies developed for determination of the inspection program for the skin on pressurized fuselages. For inspection threshold determination two methods are defined based on fatigue life approach, a simplified and detailed method. The detailed method considers 15 different parameters to assess the influences of material, geometry, size location, aircraft usage, and workmanship on the fatigue life of the repair and the original structure. For definition of the inspection intervals a general method is developed which applies to all concerned repairs. For this the initial flaw concept is used by considering 6 parameters and the detectable flaw sizes depending on proposed nondestructive inspection methods. An alternative method is provided for small repairs allowing visual inspection with shorter intervals. Author

N92-30124*# Federal Express Corp., Memphis, TN. Aircraft Reliability Div.
COMMUNICATION: AN IMPORTANT ELEMENT OF MAINTENANCE AND REPAIR c03
James S. Tripp *In* NASA. Langley Research Center, The 1991 International Conference on Aging Aircraft and Structural

Airworthiness Jul. 1992 p 291-299 (For primary document see N92-30106 20-39)
Avail: CASI HC A02/MF A04

People from the airlines, the FAA, and the manufacturers have worked together in an effort to improve the Service Difficulty Reporting system. Their work to date is summarized as follows: (1) design a worldwide reporting system to provide safety alerts to aircraft operators, manufacturers, repair facilities, and regulatory authorities; (2) design a companion system to provide worldwide reliability experience; and (3) overhaul regulatory requirements to be consistent with (1) and (2) to provide information necessary and useful for public consumption. H.A.

N92-30125*# Federal Aviation Administration, Washington, DC. Office of Aviation Medicine.
HUMAN FACTORS IN AIRCRAFT MAINTENANCE AND INSPECTION **c54**
William T. Shepherd *In* NASA. Langley Research Center, The 1991 International Conference on Aging Aircraft and Structural Airworthiness Jul. 1992 p 301-304 (For primary document see N92-30106 20-39)
Avail: CASI HC A01/MF A04

The events which have led to the intensive study of aircraft structural problems have contributed in no less measure to the study of human factors which influence aircraft maintenance and inspection. Initial research emphasis on aging aircraft maintenance and inspection has since broadened to include all aircraft types. Technicians must be equally adept at repairing old and new aircraft. Their skills must include the ability to repair sheet metal and composite materials; control cable and fly-by-wire systems; round dials and glass cockpits. Their work performance is heavily influenced by others such as designers, technical writers, job card authors, schedulers, and trainers. This paper describes the activities concerning aircraft and maintenance human factors. Author

N92-30126*# Galaxy Scientific Corp., Atlanta, GA.
USING INTELLIGENT SIMULATION TO ENHANCE HUMAN PERFORMANCE IN AIRCRAFT MAINTENANCE **c54**
William B. Johnson and Jeffrey E. Norton *In* NASA. Langley Research Center, The 1991 International Conference on Aging Aircraft and Structural Airworthiness Jul. 1992 p 305-313 (For primary document see N92-30106 20-39)
(Contract DTFA03-89-C-00043)
Avail: CASI HC A02/MF A04

Human factors research and development investigates the capabilities and limitations of the human within a system. Of the many variables affecting human performance in the aviation maintenance system, training is among the most important. The advent of advanced technology hardware and software has created intelligent training simulations. This paper describes one advanced technology training system under development for the Federal Aviation Administration. Author

N92-30127*# Federal Aviation Administration, Washington, DC.
REVISION OF CERTIFICATION STANDARDS FOR AVIATION MAINTENANCE PERSONNEL **c53**
Leslie K. Vipond *In* NASA. Langley Research Center, The 1991 International Conference on Aging Aircraft and Structural Airworthiness Jul. 1992 p 315-319 (For primary document see N92-30106 20-39)
Avail: CASI HC A01/MF A04

Part 65, Subparts D and E, of the Federal Aviation Regulations (FAR) identify the certification requirements for aviation mechanics and aviation repairmen. The training, experience, privileges, ratings, recordkeeping, and currency requirements for aviation maintenance personnel are also addressed by those parts of the FAR. The recent emergence of the aging fleet problem and the introduction of new technologies, aircraft, engines, and aeronautical products has caused certain portions of these rules to become obsolete. Further, international political arrangements, such as bilateral airworthiness and maintenance agreements, International Civil Aviation Organization (ICAO) standards, certain international agreements for maintenance personnel training, and mechanic certificate reciprocity, have all impacted on the current regulatory policy. Author

N92-30128*# Federal Aviation Administration, Seattle, WA.
THE FAA AGING AIRPLANE PROGRAM PLAN FOR TRANSPORT AIRCRAFT **c03**
Dayton Curtis and Jess Lewis (Federal Aviation Administration, Washington, DC.) *In* NASA. Langley Research Center, The 1991 International Conference on Aging Aircraft and Structural Airworthiness Jul. 1992 p 321-325 (For primary document see N92-30106 20-39)
Avail: CASI HC A01/MF A04

The Federal Aviation Administration (FAA) Aging Airplane Program is focused on five program areas: maintenance, transport airplanes, commuter airplanes, airplane engines, and research. These programs are complementary and concurrent, and have been in effect since 1988. The programs address the aging airplane challenge through different methods, including policies, procedures, and hardware development. Each program is carefully monitored and its progress tracked to ensure that the needs of the FAA, the industry, and the flying public are being met. Author

N92-30129*# National Aerospace Lab., Emmeloord (Netherlands).
AGEING AIRCRAFT RESEARCH IN THE NETHERLANDS **c03**
J. B. deJonge and G. Bartelds *In* NASA. Langley Research Center, The 1991 International Conference on Aging Aircraft and Structural Airworthiness Jul. 1992 p 327-335 Sponsored in part by FAA and Dept. of Civil Aviation (For primary document see N92-30106 20-39)
Avail: CASI HC A02/MF A04

The problems of aging aircraft are worldwide. Hence, international cooperative actions to overcome or prevent problems should be taken. The Federal Aviation Administration (FAA) and the Netherlands Civil Aviation Department (RLD) signed a Memorandum of Cooperation in the area of structural integrity, with specific reference to research on problems in the area of aging aircraft. Here, an overview is given of aging research that is going on in the Netherlands. The work described is done largely at the National Aerospace Laboratory; much of the research is part of the foremention cooperative agreement. Author

N92-30130*# Office National d'Etudes et de Recherches Aerospatiales, Paris (France).
SURVEY OF FRENCH ACTIVITIES CONCERNING STRUCTURAL AIRWORTHINESS AND AGING AIRCRAFT **c03**
Roger Labourdette *In* NASA. Langley Research Center, The 1991 International Conference on Aging Aircraft and Structural Airworthiness Jul. 1992 p 337-360 (For primary document see N92-30106 20-39)
Avail: CASI HC A03/MF A04

French activities concerning structural airworthiness and aging aircraft are presented. Basic applied research, full-scale testing, teardown inspections, crack initiation, fatigue crack growth, fretting fatigue, non-destructive inspection, and damage tolerance are among the topics covered. Author

N92-30131*# Department of Transport, Ottawa (Ontario). Airworthiness Branch.
TRANSPORT CANADA AGING AIRCRAFT ACTIVITIES **c03**
S. R. Didrikson *In* NASA. Langley Research Center, The 1991 International Conference on Aging Aircraft and Structural Airworthiness Jul. 1992 p 361-365 (For primary document see N92-30106 20-39)
Avail: CASI HC A01/MF A04

A description is given of recent initiatives undertaken in Canada to address the problems of aging passenger airplanes. In addition to participation in and support of U.S. aging aircraft programs, independent activities were undertaken in such areas as regulatory control of nondestructive testing, aging fleet evaluations, and measures to address the airworthiness of aging Canadian-manufactured airplanes. Author

N92-30132*# Civil Aviation Authority, Canberra (Australia).
AGING COMMUTER AEROPLANES: FATIGUE EVALUATION AND CONTROL METHODS
A. J. Emmerson *In* NASA. Langley Research Center, The 1991 International Conference on Aging Aircraft and Structural Airworthiness Jul. 1992 p 367-378 (For primary document see N92-30106 20-39)
Avail: CASI HC A03/MF A04

The loss of reliability in aircraft is caused by two broad classes of problems. There are those problems which are self evident and hazardous rather than catastrophic. These are the problem areas where characteristically there have been multiple overhauls, repairs, and replacements, and where aging really means the results of repair ineffectiveness that accumulates. The other class of the problem is the insidious and potentially catastrophic class. It includes the progressive deterioration of items that are not maintained, and often cannot be maintained because the deterioration cannot be seen. It includes the loss of physical properties in adhesives and other organic compounds, corrosion, and the response of repeated loads. Dealt with here is a currently unnecessarily troublesome aspect of that response. Although we must remain concerned about those types of aircraft which have been certified under a design standard or operational rule which embodies the elementary fail-safe concept and which have not been subjected to a subsequent structural audit, the focus here is on types of aircraft for which fatigue and damage tolerance evaluation was not required as a condition of certification. Author

N92-30133*# Saab-Scania, Linkoping (Sweden). Aircraft Div.
A MANUFACTURER'S APPROACH TO ENSURE LONG TERM STRUCTURAL INTEGRITY **c03**
Hans Ansell, Billy Fredriksson, and Ingvar Holm *In* NASA. Langley Research Center, The 1991 International Conference on Aging Aircraft and Structural Airworthiness Jul. 1992 p 379-405 (For primary document see N92-30106 20-39)
Avail: CASI HC A03/MF A04

The main features of the design concepts for the Saab 340 and Saab 2000 aircraft are described with respect to structural integrity and high reliability. Also described is the approach taken at Saab Aircraft to ensure structural integrity and high reliability. The concepts of global and local loads and sequences, and the fatigue and damage tolerance sizing and their verification are discussed. Also described is quality assurance in the production and structural maintenance program. Structural repair and feedback from operators are also covered. Author

N92-30134*# Georgia Inst. of Tech., Atlanta. Computational Modeling Center.
SIMPLIFIED COMPUTATIONAL METHODS FOR ELASTIC AND ELASTIC-PLASTIC FRACTURE PROBLEMS
Satya N. Atluri *In* NASA. Langley Research Center, The 1991 International Conference on Aging Aircraft and Structural Airworthiness Jul. 1992 p 407-453 Sponsored in part by ONR and FAA (For primary document see N92-30106 20-39)
Avail: CASI HC A03/MF A04

An overview is given of some of the recent (1984-1991) developments in computational/analytical methods in the mechanics of fractures. Topics covered include analytical solutions for elliptical or circular cracks embedded in isotropic or transversely isotropic solids, with crack faces being subjected to arbitrary tractions; finite element or boundary element alternating methods for two or three dimensional crack problems; a 'direct stiffness' method for stiffened panels with flexible fasteners and with multiple cracks; multiple site damage near a row of fastener holes; an analysis of cracks with bonded repair patches; methods for the generation of weight functions for two and three dimensional crack problems; and domain-integral methods for elastic-plastic or inelastic crack mechanics. Author

N92-30214*# National Aeronautics and Space Administration. Langley Research Center, Hampton, VA.
LINEAR SYSTEM IDENTIFICATION VIA BACKWARD-TIME OBSERVER MODELS
Jer-Nan Juang and Minh Q. Phan (Lockheed Engineering and Sciences Co., Hampton, VA.) Jun. 1992 26 p
(RTOP 590-14-21-01)
(NASA-TM-107632; NAS 1.15:107632) Avail: CASI HC A03/MF A01

Presented here is an algorithm to compute the Markov parameters of a backward-time observer for a backward-time model from experimental input and output data. The backward-time observer Markov parameters are decomposed to obtain the backward-time system Markov parameters (backward-time pulse response samples) for the backward-time system identification. The identified backward-time system Markov parameters are used in the Eigensystem Realization Algorithm to identify a backward-time state-space model, which can be easily converted to the usual forward-time representation. If one reverses time in the model to be identified, what were damped true system modes become modes with negative damping, growing as the reversed time increases. On the other hand, the noise modes in the identification still maintain the property that they are stable. The shift from positive damping to negative damping of the true system modes allows one to distinguish these modes from noise modes. Experimental results are given to illustrate when and to what extent this concept works. Author

42 GEOSCIENCES (GENERAL)

No abstracts in this category.

43 EARTH RESOURCES AND REMOTE SENSING

Includes remote sensing of earth resources by aircraft and spacecraft; photogrammetry; and aerial photography.

For instrumentation see *35 Instrumentation and Photography.*

N92-29442*# National Aeronautics and Space Administration, Washington, DC.
EOS DATA AND INFORMATION SYSTEM (EOSDIS)
May 1992 36 p Original contains color illustrations
(NASA-TM-107922; NAS 1.15:107922) Avail: CASI HC A03/MF A01; 4 functional color pages

In the past decade, science and technology have reached levels that permit assessments of global environmental change. Scientific success in understanding global environmental change depends on integration and management of numerous data sources. The Global Change Data and Information System (GCDIS) must provide for the management of data, information dissemination, and technology transfer. The Earth Observing System Data and Information System (EOSDIS) is NASA's portion of this global change information system. H.A.

N92-29467# General Accounting Office, Washington, DC. Information Management and Technology Div.
EOS DATA POLICY: QUESTIONS REMAIN ABOUT US COMMERCIAL ACCESS. REPORT TO THE CHAIRMAN, COMMITTEE ON SCIENCE, SPACE, AND TECHNOLOGY, HOUSE OF REPRESENTATIVES
25 Jun. 1992 30 p Original contains color illustrations
(GAO/IMTEC-92-44; B-248072) Avail: CASI HC A03/MF A01; GAO, PO Box 6015, Gaithersburg, MD 20877 HC

The Earth Observing System (EOS) is the centerpiece of

NASA's Mission to Planet Earth program and its main contribution to the international effort to study the earth on a global scale. The goal of EOS is to create a unified scientific observing system that will permit studies of the earth's atmosphere, biosphere, oceans, land surfaces, and polar regions. This report focuses on NASA policies and international principles governing U.S. commercial access to information collected by the multibillion dollar EOS satellites. Author

N92-29493# Beleidscommissie Remote Sensing, Delft (Netherlands).
GIS FOR COASTAL MANAGEMENT
A. Reijneveld (EUROCONSULT B.V., Arnhem, Netherlands), R. Boertjes (EUROCONSULT B.V., Arnhem, Netherlands), G. Hesselmans (Delft Hydraulics Lab., Netherlands), and L. Verhage (Delft Hydraulics Lab., Netherlands) Oct. 1991 64 p
(BCRS Proj. CO-2.21)
(BCRS-90-31; ISBN-90-54-11007-4; ETN-92-91605) Avail: CASI HC A04/MF A01

A study aimed at investigating and commercializing the use of remote sensing for coastal management is reported. The use of remote sensing, conventional field surveys and Geographical Information Systems (GIS) for the technical aspects of coastal planning was demonstrated. A demonstration GIS for a pilot project in Indonesia Rawa Sragi, in which remote sensing data and other geographical data were integrated, was developed. A short introduction to the coastal zone is given and the concept of coastal zone management is introduced. A detailed description of the analysis methods applied to the more sensing imagery used in the demonstration is given. The commercialization of a Coastal Management Information System (COMIS) is explained and conclusions and recommendations formulated. ESA

N92-29494# Beleidscommissie Remote Sensing, Delft (Netherlands).
ALEXANDER: USER GUIDE (VERSION 1.0)
L. Blesius (International Inst. for Aerospace Survey and Earth Sciences, Enschede, Netherlands) and H. R. Kostwinder (International Inst. for Aerospace Survey and Earth Sciences, Enschede, Netherlands) Sep. 1991 106 p
(BCRS Proj. TE-2.3)
(BCRS-90-38; ISBN-90-54-11005-8; ETN-92-91606) Avail: CASI HC A06/MF A02

Alexander is an image processing system specifically designed for teaching the use of remote sensing and geographic information systems. The Alexander user guide is presented. Part A is intended for the supervisor of the system and a detailed description of the Alexander system structures as well as the installation of the software is given. A description of some utilities under the supervisor submenu, which are concerned with file handling and some trouble shooting procedures is also given. Part B is aimed at the more conventional user. The use of Alexander is considered and the operations of the various programs are described. ESA

N92-29495# Beleidscommissie Remote Sensing, Delft (Netherlands).
MAPPING OF GROUNDWATER LOSSES BY EVAPORATION IN THE WESTERN DESERT OF EGYPT
M. Menenti (Winand Staring Centre, Wageningen, Netherlands), W. G. M. Bastiaanssen (Winand Staring Centre, Wageningen, Netherlands), K. Hefny (Research Inst. for Groundwater, Cairo, Egypt), and M. H. AbdElKarim (Research Inst. for Groundwater, Cairo, Egypt) Sep. 1991 108 p Sponsored in part by Netherlands Ministry for Development Cooperation and Beleidscommissie Remote Sensing
(BCRS Proj. OP-3.2)
(BCRS-91-01; Rept-43; ISBN-90-54-11004-X; ISSN-0924-3062; ETN-92-91607) Copyright Avail: CASI HC A06/MF A02

The results of an indepth investigation in the western desert of Egypt to map ground water losses by evaporation are presented. The knowledge of the terms of the waterbalance of the vast groundwater reservoir underneath the western desert of Egypt is rather scarce, and as a rule, based on indirect estimations. The evaporation of this fossil groundwater occurs in depressions where groundwater is present at shallow depths, the so called playas or sebkhas. Space measurements of land surface properties were deemed necessary to study the spatial variability of soil properties and surface energy balances. The natural evaporation losses mapped were 3 to 30 times higher in comparison with figures published in former groundwater studies. ESA

N92-29688# Beleidscommissie Remote Sensing, Delft (Netherlands).
[ACTIVITIES REPORT OF THE NETHERLANDS REMOTE SENSING BOARD (WITH ABRIDGED VERSION)] Annual Report, 1990
1991 140 p In DUTCH
(ETN-92-91352) Avail: CASI HC A07/MF A02

The main activities carried out by the Netherlands Remote Sensing Board within the executional limits of the Dutch National Remote Sensing Program are overviewed. This five year program proceeded along the guidelines of its four basic objectives: to prepare operational remote sensing techniques, and put them on a viable commercial basis; to prepare for the ERS-1 project; to apply remote sensing for the benefit of developing countries to build up and extend the Dutch remote sensing user community by constructing and developing the proper national infrastructure for this purpoose. ESA

N92-29693# Beleidscommissie Remote Sensing, Delft (Netherlands).
MONITORING OF GRASS DOMINANCE ON DUTCH HEATHLANDS USING REMOTE SENSING AND A GEOGRAPHIC INFORMATION SYSTEM (HEIMON) [MONITORING VAN HEIDEVERGRASSING MET BEHULP VAN REMOTE SENSING EN EEN GEOGRAFISCH INFORMATIESYSTEEM (HEIMON)]
J. P. Moen (Utrecht State Univ., Netherlands), F. J. M. vanderWel (Utrecht State Univ., Netherlands), J. T. deSmidt (Utrecht State Univ., Netherlands), L. L. Vels (Research Inst. for Nature Management, Arnhem, Netherlands), and D. J. Harms (Eurosense B.V., The Hague, Netherlands) Sep. 1991 99 p In DUTCH and ENGLISH
(BCRS Proj. OP-2.11)
(BCRS-91-12; ISBN-90-54-11003-1; ETN-92-91608) Avail: CASI HC A05/MF A02

The HEIMON project (Dutch acronym for the monitoring of heather vegetation) was carried out using image processing and GIS (Geographic Information System) techniques, in order to investigate the dominance of grass growth. Bands 5 and 7 (mid infrared) of LANDSAT TM (Thematic Mapper) data proved to be useful to distinguish grass and heath dominance (classification). The monitoring of the process is possible using classified satellite images obtained at different points in time. However, reliable interpretation is only possible if the satellite results can be related to additional local information (in a supporting GIS). The HEIMON project also provides interesting cartographic data. In a national, regional as well as local level, monitoring offers a powerful tool that permits an efficient management policy regarding heather areas. ESA

N92-29701# New Mexico State Univ., Las Cruces. Dept. of Agronomy.
FIELD STUDY OF MULTIDIMENSIONAL FLOW AND TRANSPORT IN THE VADOSE ZONE
R. S. Bowman, D. B. Stephens, P. Arnet, D. P. Grabka, and R. I. Schmidt-Petersen Dec. 1991 143 p Sponsored in part by Geological Survey, Reston, VA
(Contract DI-14-08-0001-G1645)
(PB92-161363; WRRI-262; USGS/G-1645) Avail: CASI HC A07/MF A02

A comprehensive field experiment was conducted to determine geologic controls on water flow and solute transport in a heterogeneous vadose zone. The experiment was conducted on a 10 m by 10 m plot underlain by heterogeneous beds of clays, sands, gravels, and cobbles of alluvial and fluvial origin. The plot

and surrounding area were instrumented with 21 neutron probe access tubes, 168 tensiometers, and 62 solution samplers. Steady water application was provided by a drip irrigation system. Measurements of subsurface wetting and drainage, a multitracer transport experiment, in situ and laboratory determinations of hydraulic parameters, and destructive geologic characterization were conducted. The results of all determinations reflected the extreme short-scale geologic variability of the subsurface material. Attempts to model the flow and transport behavior were only partially successful. The project provided a detailed characterization of a vadose zone typical of those found throughout the western U.S. The extensive data base developed under controlled conditions may be useful for future modeling activities. Author

N92-29707# National Aerospace Lab., Amsterdam (Netherlands). Space Div.
CAESAR: A CCD AIRBORNE EXPERIMENTAL SCANNER FOR APPLICATIONS IN REMOTE SENSING RADIOMETRIC AND GEOMETRIC CALIBRATION
W. J. Looyen and R. W. vanSwol 14 Mar. 1989 30 p
(NLR-TP-89103-U; ETN-92-91517) Avail: CASI HC A03/MF A01

The project concerning a multispectral scanner named, CAESAR, Charge Couple Device (CCD) Airborne Experimental Scanner for Application in Remote Sensing is presented. The objectives of the project were to increase technical knowledge of and practical experience with the application of linear CCD detectors in remote sensing for land and sea observation. With this scanner two objectives were fulfilled: technical knowledge about CCD detectors and practical experience with their application in remote sensing were gained and an important research tool was made available to remote sensing scientists. CAESAR was designed to make land and sea (water) observations in up to nine different wavelength bands. The application of CCD arrays in CAESAR required radiometric calibration of all individual CCD elements in order to meet the important user requirements on the minimum detectable ground reflectance variation. Since CAESAR is an airborne scanner geometric corrections are required, as well, to compensate for image distortions due to aircraft motions. Both radiometric and geometric corrections are applied during the preprocessing of the data. The results of performance tests show that the design goals were met and that an advanced airborne scanner for land and marine applications can be offered to the remote sensing community. ESA

N92-29717# Winand Staring Centre, Wageningen (Netherlands). Agricultural Research Dept.
MAPPING AGROECOLOGICAL ZONES AND TIME LAG IN VEGETATION GROWTH BY MEANS OF FOURIER ANALYSIS OF TIME SERIES OF NDVI IMAGES
M. Menenti, S. Azzali, W. Verhoef (National Aerospace Lab., Emmeloord, Netherlands), and R. vanSwol (National Aerospace Lab., Emmeloord, Netherlands) 1991 35 p Sponsored by Beleidscommissie Remote Sensing
(Rept-32; BCRS-91-22; ISSN-0924-3062; ETN-92-91611)
Copyright Avail: CASI HC A03/MF A01

A method which gives a quantitative meaning to general concepts such as 'variability of vegetation growth', 'growth cycle', and 'early or late growing season' is presented. This was accomplished by applying Fourier analysis to time series of 10 day composites of Normalized Difference Vegetation Index (NDVI) images of Zambia and Somalia. Time series of NDVI images are deconvoluted in a set of harmonic functions having different periods (or fequency). The amplitude of each harmonic gives the contribution of NDVI variation in time of the actual observations; for each harmonic the timelag with respect to the origin in time on the observations is obtained. Since the technique was applied on a pixel by pixel basis, maps were obtained of amplitude and time lag for each period. Different techniques are compared to map zones wherein vegetation development is similar and which will be termed 'isogrowth' zones. The obtained results indicate that differences in vegetation development among map units of an existing agroclimatic map are not significant, while reliable differences are observed among the map units obtained by means of the described procedure. ESA

N92-29728# Delft Hydraulics Lab. (Netherlands).
RIVER HYDROMETRY BY PATTERN RECOGNITION IN REMOTE SENSING IMAGES
J. R. Moll and J. F. M. Overmars Dec. 1990 12 p Presented at International Symposium on Remote Sensing and Water Resources, Enschede, Netherlands, 20-24 Aug. 1990
(Publ-445; ISSN-0166-7521; ETN-92-91466) Avail: CASI HC A03/MF A01

Remote sensing technology offers new possibilities to monitor river behavior in large areas that are often difficult to access. A system is developed for monitoring of river floods and river planform. Dedicated mathematical model of river hydraulics, hydrology, and morphology can be implemented within the system. Results of the proof of concept phase of this project are presented. Data processing techniques for automatic pattern recognition and river hydrometry are illustrated with examples from a case study of a flood in the river Waal in the Netherlands. From a LANDSAT TM (Thematic Mapper) image, the river axis, and river width are derived. The results are compared with data from a digitized topographic map and with computational results of a none dimensional flood routing model. An outline of the system development phase is given in conclusion. The implementation of the system in Bangladesh is scheduled for 1991. ESA

N92-30017# Committee on Commerce, Science, and Transportation (U.S. Senate).
NASA'S EARTH OBSERVING SYSTEM
Washington GAO 1992 87 p
(S-Hrg-102-647; GPO-55-802cc; ISBN-0-16-038754-X) Avail: CASI HC A05/MF A01; Subcommittee on Science, Technology, and Space, Senate, Washington DC 20515 HC

The U.S. Senate, Subcommittee on Science, Technology, and Space of the Committee on Commerce, Science, and Transportation met on February 26, 1992 to discuss NASA's Mission to Planet Earth and within that mission, the Earth Observing System (EOS). Questions were asked by Senators Gore and Pressler to various scientists about the EOS's mission capabilities, present status, and budgetary needs. H.A.

N92-30022# Oregon State Univ., Newport. Marine Science Center.
APPLICATION OF REMOTE SENSING METHODS FOR TRACKING LARGE CETACEANS: NORTH ATLANTIC RIGHT WHALES EUBALAENA GLACIALIS Final Report
B. R. Mate, S. Nieukirk, R. Mesecar, and T. Martin Feb. 1992 182 p Sponsored in part by Minerals Management Service, Herndon, VA
(Contract DI-14-12-0001-30411)
(PB92-185016; OCS/MMS-91/0069) Avail: CASI HC A09/MF A02

The main objectives of the study were to develop a satellite-monitored radio tag for use on right whales; tag up to 10 right whales; periodically relocate, observe, and examine tagged whales in order to assess the accuracy of locations and evaluate the performance of the tag and deployment mechanisms; provide photo documentation of the attachment methods and possible effects of the tag on the animal's physical well being and behavior; document right whale movements including residency times, migration pathways, timing and speeds; and relate the location of animals to known habitat characteristics and locations of other tagged whales to identify habitat preferences. Author

N92-30088# Mitre Corp., McLean, VA. Program Office.
SMALL SATELLITES AND RPAS IN GLOBAL-CHANGE RESEARCH: SUMMARY AND CONCLUSIONS
P. Banks, J. M. Cornwall, F. Dyson, N. Fortson, S. Koonin, C. Max, G. MacDonald, S. Ride, M. Ruderman, and S. Treiman et al Jan. 1992 25 p

(Contract DE-AI05-90ER-30174)
(DE92-013602; JSR-91-330A) Avail: CASI HC A03/MF A01

JASON has now conducted two studies on the use of small satellites and remotely-piloted aircraft (RPAs) in global change research, with special reference to the DOE Atmospheric Radiation Measurement (ARM) program and to DARPA's Small Satellite program. The studies centered around meetings, one in January and the other in June 1991, to which we invited representatives of all areas of the global change program and of the DOD satellite science and technology community. We have already issued a report on the January study. Here we summarize the main themes and results of our Summer Study; the full report will be issued shortly. DOE

N92-30105# National Center for Atmospheric Research, Boulder, CO. Atmospheric Technology Div.
A SPECTRAL VEGETATION RADIOMETER FOR AIRBORNE BOUNDARY-LAYER RESEARCH
Lutz Bannehr and Vince Glover Feb. 1992 50 p Sponsored by NSF
(PB92-186113; NCAR/TN-370+STR) Avail: CASI HC A03/MF A01

The Technical Note presents a comprehensive description of the Spectral Vegetation Radiometer (SVR) used on National Center for Atmospheric Research (NCAR) aircraft to derive information about the vegetation cover. The information presented here is more detailed than is possible in a journal article. The Technical Note is structured to first provide the reader with background information of the vegetation index. Next, applications ae discussed, and finally the problems involved in analyzing the vegetation index are described. Furthermore, the reader obtains an inside view of the instrument design and how the calibration should be performed. The examples of the spectral vegetation radiometer presented explore the utility of remote sensing method for meteorological research in the planetary boundary layer. Author

N92-30210*# National Aeronautics and Space Administration. Goddard Space Flight Center, Greenbelt, MD.
BIOPHYSICAL, MORPHOLOGICAL, CANOPY OPTICAL PROPERTY, AND PRODUCTIVITY DATA FROM THE SUPERIOR NATIONAL FOREST
F. G. Hall, K. F. Huemmrich (Hughes STX, Inc., Lanham, MD.), D. E. Strebel (Versar, Inc., Columbia, MD.), S. J. Goetz (Hughes STX, Inc., Lanham, MD.), J. E. Nickeson (Hughes STX, Inc., Lanham, MD.), and K. D. Woods (California Univ., Santa Barbara.) Jul. 1992 137 p
(NASA-TM-104568; NAS 1.15:104568; Rept-92B00092) Avail: CASI HC A07/MF A02

Described here are the results of a NASA field experiment conducted in the Superior National Forest near Ely, Minnesota, during the summers of 1983 and 1984. The purpose of the experiment was to examine the use of remote sensing to provide measurements of biophysical parameters in the boreal forests. Leaf area index, biomass, net primary productivity, canopy coverage, overstory and understory species composition data are reported for about 60 sites, representing a range of stand density and age for aspen and spruce. Leaf, needle, and bark high-resolution spectral reflectance and transmittance data are reported for the major boreal forest species. Canopy bidirectional reflectance measurements are provided from a helicopter-mounted Barnes Multiband Modular Radiometer (MMR) and the Thematic Mapper Simulator (TMS) on the NASA C-130 aircraft. Author

N92-30230# Beleidscommissie Remote Sensing, Delft (Netherlands).
COMPARISON OF IN SITU, AIRCRAFT- AND SATELLITE DERIVED SURFACE REFLECTANCES IN FLEVOLAND (NETHERLANDS). A VALIDATION EXPERIMENT
J. M. M. Kokke (Rijkswaterstaat, Delft, Netherlands) Nov. 1991 34 p
(BCRS Proj. IS-3.9)
(BCRS-91-28; ISBN-90-5411-010-4; ETN-92-91877) Avail: CASI HC A03/MF A01

In order to evaluate a complete atmospheric correction method for multispectral spaceborne imagery, a validation campaign was set up in one of the Dutch polders. A ground based radiometer measured total and diffuse spectral irradiance simultaneous with Thematic Mapper (TM) data acquisition for purposes of atmospheric correction of observed satellite radiances. The experiment included the use of data of the Dutch CAESAR (CCD (Charge Coupled Device) Airborne Experimental Scanner) to compare measured reflectances from several altitude levels. To assess the surface reflectance factors in the test area, a hand held field radiometer was used. Reference panels with known reflectances served for calibration of in situ and airborne data. Differences between satellite derived reflectances and ground based reflectances were quite small. Somewhat larger deviations occurred in airborne derived reflectances, which could not accurately be explained because of insufficient knowledge of some instrumental factors, e.g., field radiometer spectral response. ESA

N92-30231# Beleidscommissie Remote Sensing, Delft (Netherlands).
TERS PRODUCT DEVELOPMENT PLAN FOR URBAN PLANNING OF BANDUNG, INDONESIA
A. vanDijk (DHV Consultants, Malang, Indonesia) and V. Polle (International Inst. for Aerial Survey and Earth Sciences, Delft, Netherlands) Mar. 1992 113 p
(BCRS Proj. CO-2.22)
(BCRS-91-30; ISBN-90-5411-032-5; ETN-92-91879) Avail: CASI HC A06/MF A02

The objective of the project was to reveal the utility of TERS-like high resolution satellite data (such as the French SPOT) as an instrument for actual urban expansion mapping in Indonesia. Thematic maps, on a scale of 1:50,000 for the metropolitan area, and on a scale of 1:100,000 for the urban and the suburban areas of Greater Bandung, were prepared. The maps were overlayed with existing information (streetplans etc.) and field checks of the existing maps were performed. A final product, intended as a planning tool for local government agencies, was prepared in close cooperation with the users. The product and its application are outlined and discussed. ESA

44 ENERGY PRODUCTION AND CONVERSION

Includes specific energy conversion systems, e.g., fuel cells; global sources of energy; geophysical conversion; and windpower.

For related information see also *07 Aircraft Propulsion and Power, 20 Spacecraft Propulsion and Power,* and *28 Propellants and Fuels.*

N92-29454# Midwest Research Inst., Golden, CO.
TOMORROW'S ENERGY TODAY: ENERGY EFFICIENCY AND RENEWABLE ENERGY
A. Brennan Apr. 1992 15 p
(Contract DE-AC02-83CH-10093)
(DE91-002110; DOE/CH-10093/90) Avail: CASI HC A03/MF A01

This broad overview of energy programs of the Office of Conservation and Renewable Energy of the U.S. DOE emphasizes means of promoting energy efficiency for the next generation. Current research goals to reduce energy consumption in industry, buildings, and the transportation sector are presented. A doubling of economic growth without depleting fossil fuels by the year 2030 is conceivable. DOE

N92-29476# Yardney Technical Products, Inc., Pawcatuck, CT.
ADVANCED RECHARGEABLE LITHIUM SULFUR DIOXIDE CELL Final Report, Sep. 1988 - Feb. 1991
R. C. McDonald, P. Harris, F. Goebel, S. Hossain, and R. Vierra Nov. 1991 126 p
(Contract DAAL01-88-C-0849)

(AD-A250027; SLCET-TR-88-0849-F) Avail: CASI HC A07/MF A02

The electrochemical performance and safety of the rechargeable lithium sulfur dioxide system has been investigated in laboratory cells and in high rate D cells. Small design and active materials were optimized to that cathode utilization of 1.6Ah/grams of carbon and 0.19Ah/cm3 of cathode were achieved with 100-200 cycles. Discharge and charge of cells at temperatures down to -30 C were examined, as were pulse discharge, storage, high temperature, and voltage delay. Analytical techniques were developed for determination of SO2 electrolyte phase behavior and analysis of lithium dithionate degradation product. Cell venting, shorting, and over-heating remain persistent problems as the testing proceeds to the larger spiral-wound cell. Cell venting seems to occur the most on charge, or shortly thereafter, and is associated with accumulation of reactive side-products. Large cell electrodes are pyrophoric when examined in air after extensive cycling. GRA

N92-29519# Texas A&M Univ., College Station. Dept. of Chemistry.

NEW DIRECTIONS FOR THE CATALYTIC CONVERSION OF METHANE Annual Report, Dec. 1990 - Nov. 1991

J. H. Lunsford Feb. 1992 31 p

(Contract GRI-5086-260-1326)

(PB92-172360; GRI-92/0074) Avail: CASI HC A03/MF A01

The addition of chlorine via HCl to a Li(+)-MgO catalyst improves its activity for the oxidative dehydrogenation (OXD) of ethane. The latter effect is greater than ethylene-to-ethane ratio (greater than 5) observed during the oxidative coupling reaction. During the OXD reaction at 620 C, an 80 percent conversion of C2H6 was achieved with 77 percent selectivity to C2H4 after 40 h on stream. To attain these favorable results, the Cl/Li ratio must be greater than or = 0.9. The absolute amounts of Li and Cl are of secondary importance, although an excess amount of promoters may serve to replace that which is slowly lost during the reaction. In the presence of chlorine, LiCl is formed rather than Li2CO3. The carbonate phase spreads over the surface and presumably blocks active sites. The chlorine in the catalyst also modifies the gross basicity of the catalyst, thus, making it less effective for the future oxidation of ethylene, which is the desired product. Author

N92-29636# Helsinki Univ. of Technology, Otaniemi (Finland). Dept. of Technical Physics.

SOLCHIPS: A FAST PREDESIGN AND OPTIMIZATION TOOL FOR SOLAR HEATING WITH SEASONAL STORAGE

P. D. Lund and S. S. Peltola 1991 31 p

(DE92-506509; TKK-F-A669) Avail: CASI HC A03/MF A01

A new version of the SOLCHIPS predisign and optimization tool for solar heating systems with seasonal storage is described. The tool comprises a user friendly interface with a minimal input requirement. The tool is here applied to the redesign of an existing solar heating installation and to the predesign of a completely new solar plant. The evaluation and dimensioning of one CSHPSS configuration can now be done in 10 to 20 seconds, thus enabling fast optimization in respect to several parameters. A case study of an existing CSHPSS plant shows a 50 percent decrease in the annual energy price when the system is redesigned using the SOLCHIPS tool. DOE

N92-29646# Pacific Northwest Lab., Richland, WA.

THERMAL ENERGY STORAGE FOR COGENERATION APPLICATIONS

M. K. Drost and Z. I. Antoniak Apr. 1992 16 p Presentcd at the Cogeneration Technical Conference, Scottsdale, AZ, 13-15 Apr. 1992

(Contract DE-AC06-76RL-01830)

(DE92-012339; PNL-SA-20771; CONF-9204130-1) Avail: CASI HC A03/MF A01

Cogeneration is playing an increasingly important role in providing energy efficient power generation and thermal energy for space heating and industrial process heat applications. However, the range of applications for cogeneration could be further increased if the generation of electricity could be decoupled from the generation of process heat. Thermal energy storage (TES) can decouple power generation from the production of process heat, allowing the production of dispatchable power while fully utilizing the thermal energy available from the prime mover. The Pacific Northwest Laboratory (PNL) leads the US Department of Energy's Thermal Energy Storage Program. The program focuses on developing TES for daily cycling (diurnal storage), annual cycling (seasonal storage), and utility applications (utility thermal energy storage (UTES)). Several of these technologies can be used in a cogeneration facility. This paper discusses TES concepts relevant to cogeneration and describes the current status of these TES systems. DOE

N92-29662*# National Aeronautics and Space Administration. Lewis Research Center, Cleveland, OH.

DESIGN CHARACTERISTICS OF A HEAT PIPE TEST CHAMBER

Karl W. Baker, J. Hoon Jang (Sverdrup Technology, Inc., Brook Park, OH.), and Juin S. Yu (West Virginia Inst. of Tech., Montgomery.) Jul. 1992 26 p Proposed for presentation at the First International Conference on Aerospace Heat Exchanger Technology, Palo Alto, CA, 15-17 Feb. 1993; sponsored by ASME and IAAA

(RTOP 506-41-51)

(NASA-TM-105737; E-7142; NAS 1.15:105737) Avail: CASI HC A03/MF A01

LeRC has designed a heat pipe test facility which will be used to provide data for validating heat pipe computer codes. A heat pipe test chamber that uses helium gas for enhancing heat transfer was investigated. The conceptual design employs the technique of guarded heating and guarded cooling to facilitate accurate measurements of heat transfer rates to the evaporator and from the condenser. The design parameters are selected for a baseline heat pipe made of stainless steel with an inner diameter of 38.10 mm and a wall thickness of 1.016 mm. The heat pipe operates at a design temperature of 1000 K with an evaporator radial heat flux of 53 W/sq. cm. Author

45 ENVIRONMENT POLLUTION

Includes atmospheric, noise, thermal, and water pollution.

N92-29416# Office of Technology Assessment, Washington, DC.

COMBINED SUMMARIES: TECHNOLOGIES TO SUSTAIN TROPICAL FOREST RESOURCES AND BIOLOGICAL DIVERSITY

May 1992 89 p Original contains color illustrations

(OTA-F-515) Avail: CASI HC A05/MF A01

Loss of tropical forests and reduction in the Earth's biological diversity have grown from development assistance concerns to themes of global debate during the last decade. Loss of tropical forests is still associated with poverty in tropical developing nations, but it is now juxtaposed with potential disruption of global weather patterns. In the years since the Office of Technology Assessment published 'Technologies to Sustain Tropical Forest Resources' (1984) and 'Technologies to Maintain Biological Diversity' (1987), new issues have arisen, new approaches have been devised, and new policies have been adopted. Yet the technologies underlying the efforts to manage the resources sustainably have changed little. Thus, in a continuing service to Congress, we are reprinting the summaries of the two earlier assessments and are providing an introduction to the changes that have occurred since their publication. Author

N92-29430*# Bionetics Corp., Cocoa Beach, FL.

MOSQUITO LAGOON ENVIRONMENTAL RESOURCES INVENTORY

Jane A. Provancha, Carlton R. Hall, and Donna M. Oddy Mar.

1992 121 p
(Contract NAS10-11624)
(NASA-TM-107548; NAS 1.15:107548) Avail: CASI HC A06/MF A02

This document provides a synopsis of biotic and abiotic data collected in the Mosquito Lagoon area in relation to water quality. A holistic ecological approach was used in this review to allow for summaries of climate, land use, vegetation, geohydrology, water quality, fishes, sea turtles, wading birds, marine mammals, invertebrates, shellfish, and mosquito control. The document includes a bibliographic database list of 157 citations that have references to the Mosquito Lagoon, many of which were utilized in development of the text. Author

N92-29497# Beleidscommissie Remote Sensing, Delft (Netherlands).
RESEARCH PROGRAMMING STUDIES: REMOTE SENSING EMISSIONS, LAND USE AND EFFECTS, IN RELATION TO CLIMATE AND ENVIRONMENT [PROGRAMMERINGSSTUDIE: REMOTE SENSING EMISSIES, GRONDGEBRUIK EN EFFECTEN, IN RELATIE TOT KLIMAAT EN MILIEU]
P. J. vanderWiele (Ministerie van Volkshuisvesting, Ruimtelijke Ordening en Milieubeheer, The Hague, Netherlands) and P. Vellinga (Ministerie van Volkshuisvesting, Ruimtelijke Ordening en Milieubeheer, The Hague, Netherlands) Sep. 1991 30 p In DUTCH
(BCRS-91-17; ISBN-90-54-11002-3; ETN-92-91609) Avail: CASI HC A03/MF A01

A remote sensing research programming study was performed with a view to climatic and environmental investigations. The Dutch remote sensing research projects are overviewed; they mainly concern water quality, land use, and meteorological applications. In several projects, the coupling between sensing data and GIS (Geographic Information System) techniques is central. Selection criteria for the research programming are outlined. Recommendation for further remote sensing studies are given. ESA

N92-29499# Beleidscommissie Remote Sensing, Delft (Netherlands).
THE MAIN LINES OF THE RESEARCH PROGRAMS REMOTE SENSING: CLIMATE AND ENVIRONMENT [PROGRAMMA OP HOOFDLIJNEN 'REMOTE SENSING - KLIMAAT EN MILIEU']
P. J. H. Builtjes (Organisatie voor Toegepast Natuurwetenschappelijk Onderzoek, Delft, Netherlands) and M. G. M. Roemer (Organisatie voor Toegepast Natuurwetenschappelijk Onderzoek, Delft, Netherlands) Sep. 1991 13 p In DUTCH (BCRS Proj. 6.5/IS-11)
(BCRS-91-25; ISBN-90-54-11001-5; ETN-92-91610) Avail: CASI HC A03/MF A01

The main lines of a remote sensing research program were established with a view to the selection of research projects in the field of atmospheric chemistry and physics in relation to climate and environment. The research program concerns remote sensing from ground level, from balloons, and from aircraft. The relation between the current and planned research program is outlined. General considerations concerning the short term aims of the research program as well as the long term infrastructure are given. ESA

N92-29520# Environmental Protection Agency, Research Triangle Park, NC. Environmental Criteria and Assessment Office.
AIR QUALITY CRITERIA FOR OXIDES OF NITROGEN, VOLUME 1
Aug. 1991 454 p
(PB92-176361; EPA/600/8-91/049AA-Vol-1; ECAO-R-0082-Vol-1) Avail: CASI HC A20/MF A04

The revised air quality criteria document for oxides of nitrogen reviews and evaluates the scientific information on the health and welfare effects associated with exposure to concentrations of NO2 found in ambient air. Although the document is not intended to be an exhaustive literature review, it is intended to cover all the pertinent literature through early 1991. The set consists of 16 chapters which are divided into three volumes. The first volume contains the summary chapter for the entire set which is followed by a general introduction in Chapter 2. Chapter 3 through 8 then provide background information on physical and chemical properties of NO2 and related compounds; sources and emissions; atmospheric transport, transformation and fate of NO2; methods for collection and measurement of NO2; and ambient air concentrations and factors affecting exposure of the general population. Author

N92-29521# Environmental Protection Agency, Research Triangle Park, NC. Environmental Criteria and Assessment Office.
AIR QUALITY CRITERIA FOR OXIDES OF NITROGEN, VOLUME 2
Aug. 1991 647 p
(PB92-176379; EPA/600/8-91/049AB-Vol-2; ECAO-R-0082-Vol-2) Avail: CASI HC A99/MF A06

The revised air quality criteria document for oxides of nitrogen reviews and evaluates the scientific information on the health and welfare effects associated with exposure to concentrations of NO2 found in ambient air. Although the document is not intended to be an exhaustive literature review, it is intended to cover all the pertinent literature through early 1991. The set consist of 16 chapters which are divided into three volumes. The second volume contains chapters 9-12. Chapter 9 evaluates NO2 effects on crops and natural vegetation, while chapter 10 discusses effects on terrestrial and equatic ecosystems. Chapter 11 describes effects on visibility, and chapter 12 describes damage to materials attributable to NO2. Author

N92-29522# Environmental Protection Agency, Research Triangle Park, NC. Environmental Criteria and Assessment Office.
AIR QUALITY CRITERIA FOR OXIDES OF NITROGEN, VOLUME 3
Aug. 1991 527 p
(PB92-176387; EPA/600/8-91/049CA-Vol-3; ECAO-R-0082-Vol-3) Avail: CASI HC A23/MF A04

The revised air quality document for oxides of nitrogen reviews and evaluates the scientific information on the health and welfare effects associated with exposure to concentrations of NO2 found in ambient air. Although the document is not intended to be an exhaustive literature review, it is intended to cover all the pertinent literature through early 1991. The set consist of 16 chapters which are divided into three volumes. The third volume contains chapters 13-16. The volume evaluates information concerning the health effects of NO2. The topics covered include: studies of the effects of nitrogen compounds on animals; epidemiology studies of oxides of nitrogen; controlled human exposure studies of oxides of nitrogen; human effects associated with exposure to nitrogen dioxide; and a glossary of terms and symbols. Author

N92-29597# California Univ., Davis.
NATIONAL INSTITUTE FOR GLOBAL ENVIRONMENTAL CHANGE Semiannual Report, 1 Jul. - 31 Dec. 1991
G. C. Werth 1 Apr. 1992 160 p
(Contract DE-FC03-90ER-61010)
(DE92-013487; DOE/ER-61010/T1) Avail: CASI HC A08/MF A02

This document is the Semi-Annual Report of the National Institute for Global Environmental Change for the reporting period July 1 to December 31, 1991. The report is in two parts. Part 1 presents the mission of the institute, examples of progress toward that mission, a brief description of the revised management plan, and the financial report. Part 2 presents the statements of the Regional Center Directors along with progress reports of the projects written by the researchers themselves. DOE

N92-29638# Institute of Energy Economics of Japan.
GLOBAL-WARMING PROBLEM AND GLOBAL ECONOMIC MODELS
30 Sep. 1991 200 p
(DE92-514557; IEE-SR-225) Avail: CASI HC A09/MF A03

This report describes results of investigation, comparison and

analysis of various global models to analyze what policies are effective for reduction of greenhouse effect gases as measures for prevention of the global warming and building of a well-balanced energy supply structure. The paper deals with global models like a general equilibrium macroeconomic model on a cost for reduction of CO2 emission and an energy economy simulation model. The results of the simulation of global models indicate that there are big differences in optimum carbon tax rate between the models, but a drop in GDP growth rate affected by emission control is very low in each model. These results seem to be attractive. However, in the method using these models in which improvement of energy efficiency is regarded as a main factor, there is still some doubt whether CO2 emission can be practically controlled in the long term. DOE

N92-29668 Commonwealth Scientific and Industrial Research Organization, Mordialoc (Australia). Div. of Atmospheric Research.

CONSTRAINING THE ATMOSPHERIC CARBON BUDGET: A PRELIMINARY ASSESSMENT

I. G. Enting 1992 31 p

(CSIRO-TP-25; ISBN-0-643-05249-6) Copyright Avail: CASI HC A03/MF A01

Direct observations show that the concentration of CO2 in the atmosphere has been increasing over the last three decades (from about 315 ppmv in 1959 to 350 ppmv in 1990) and that the rate of increase has grown. Measurements of gas trapped in bubbles in polar ice show that the concentrations were around 280 ppmv at the beginning of the last century and have grown at a generally increasing rate over the last two hundred years. The current rate of increase of atmospheric CO2 represents about half of the rate at which carbon is released due to the use of fossil fuels. While it is generally assumed that the world's oceans represent the sink for much of the fossil carbon that leaves the atmosphere, the role of the terrestrial biota in the atmospheric carbon budget is the subject of considerable uncertainty. In particular, the study by Tans et al. (1990) raised the possibility that the oceanic uptake of CO2 might be only half as much as determined by conventional carbon cycle modelling, implying very large biotic uptakes. Author

N92-29698# Council on Environmental Quality, Washington, DC.

ENVIRONMENTAL QUALITY: REPORT OF THE COUNCIL ON ENVIRONMENTAL QUALITY Annual Report No. 22

1991 404 p

(PB92-154954) Avail: CASI HC A18/MF A04

The annual report is divided into two parts. Part 1 outlines key environmental and conservation issues facing the United States today in the following areas: agriculture, air quality, biodiversity, budget, coasts and oceans, data collection and analysis, economics, education, energy, enforcement, federal facilities management, fisheries and marine mammals, forestry, hazardous and solid wastes, international issues, mission to planet earth, National Environmental Policy Act, pollution prevention, private sector initiatives, public lands, science and technology, transportation, water, and wetlands. Part 2 contains over 100 tables and figures providing additional detail about conditions and trends in the environment. Author

N92-29746# Colorado State Univ., Fort Collins. Dept. of Civil Engineering.

MODEL FOR REGIONAL SOLUTE TRANSPORT SUITED FOR CALIBRATION AND MANAGEMENT Final Report

H. J. Morel-Seytoux Sep. 1991 29 p

(Contract DI-14-08-0001-G1637)

(PB92-161371; USGS/G-1637) Avail: CASI HC A03/MF A01

A Purely Advective Approach is followed to develop a practical model for regional solute transport. First, it is shown that it is not theoretically sound to use the traditional advective-dispersive governing equation. The stochastic approach demonstrates that a dispersion coefficient can be defined only under extremely rare and unpractical conditions. Thus a detailed velocity field must be determined. To define such a velocity field, the hydraulic conductivity field itself must be well defined. Calibration techniques to determine such a field were investigated which can, at least in principle, obtain it continuously in space. A model was developed which is purely advective. The model was compared to the United States Geological Survey (USGS) model MOC (Method of Characteristics). The results indicate that the model works as well as MOC, but not better. This was a disappointment and is due to a procedure (Kriging) which introduced numerical dispersion. A new approach was devised to avoid it and is being implemented. Author

N92-29790# Lawrence Livermore National Lab., CA.

INTERCOMPARISON OF GLOBAL MARINE CLIMATOLOGIES

S. L. Grotch Mar. 1992 8 p Presented at the International Comprehensive Ocean Atmosphere Data Set Workshop, Boulder, CO, 13-15 Jan. 1992

(Contract W-7405-eng-48)

(DE92-011389; UCRL-JC-109501; CONF-9201100-1) Avail: CASI HC A02/MF A01

One of the major goals of the Program for Climate Model Diagnosis and Intercomparison at LLNL is the development and application of statistical/graphical methods for the intercomparison of GCMs among themselves and with observational data. Consequently, it is important to have available datasets that represent 'current climate' and a range of tools with which to perform detailed intercomparisons. This work reports on an intercomparison of four historical climatologies for surface winds (focusing on zonal u-wind) and illustrates a variety of statistical/graphical tools that can be used to quantitatively determine the differences/similarities among these datasets. DOE

N92-30018# ManTech Environmental Technology, Inc., Corvallis, OR.

NATO WORKSHOP ON THE ATMOSPHERIC METHANE CYCLE. WORKING GROUP REPORT ON METHANE SOURCES AND SINKS

D. Bachelet and H. U. Neue 1992 17 p Workshop held in Mt. Hood, OR, 6-11 Oct. 1991 Prepared in cooperation with International Rice Research Inst., Manila, Philippines

(Contract EPA/68-C8-0006)

(PB92-180256; EPA/600/A-92/106) Avail: CASI HC A03/MF A01

Methane concentrations in the atmosphere have increased form about 0.75 to 1.7 ppmv since preindustrial times. The authors have tried to concisely summarize the discussions that took place at Timberline, October 8-10, 1991 to quantify the size of the global 'Methane Sources and Sinks' that may contribute to the atmospheric increase. Several 'specialty' groups emerged during the workshop and it is their conclusions that are presented here. Each paragraph is also the focus of an individual chapter and of usually several manuscripts that were submitted to Chemosphere. The authors have tried to cite these documents in the relevant sections and they refer the reader to these sources for detailed explanations of each source and sink. Author

N92-30019# National Oceanic and Atmospheric Administration, Washington, DC. Office of the Chief Scientist.

NOAA ENVIRONMENTAL DIGEST: SELECTED INDICATORS OF THE UNITED STATES AND THE GLOBAL ENVIRONMENT, DECEMBER 1991 Final Report

I. C. Sheifer Dec. 1991 205 p

(PB92-185073) Avail: CASI HC A10/MF A03

The global environment is an interrelated system that includes the atmosphere, oceans, ice, and biota. These components are coupled through a complex, even chaotic, combination of biological, chemical, and physical processes occurring over the spectrum of time and space scales. The natural coupling of these processes requires that the Earth be studied in an interdisciplinary fashion as a single system with global dimensions. The purpose here is to divide the global environment into the categories of atmosphere, ocean, cryosphere (ice), and biosphere. The parameters presented

here were chosen because of their potential influence on the global environment or because they are considered indicators of system change. Author

N92-30021# ManTech Environmental Technology, Inc., Corvallis, OR.
POTENTIAL IMPACTS OF CLIMATE CHANGE ON PACIFIC NORTHWEST FOREST VEGETATION
G. A. King and D. T. Tingey May 1992 45 p
(Contract EPA-68-C8-0006)
(PB92-184985; EPA/600/R-92/095) Avail: CASI HC A03/MF A01

Despite the limitations of the models used in the climate change analyses, some overall conclusions can be made concerning climate change impacts on Northwest forests. The foremost of these is that the distribution and composition of forests in Washington and Oregon could change substantially under the GCM scenarios of regional climate change. The Holdridge, climate/forest correlations, and forest gap models (except for the CLIMACS results) all forecast shifts to forests better adapted to warmer and drier conditions. Temperate forests in the Holdridge scenarios are generally restricted to upper elevations and total forest acreage decreases by 5 to 25 percent depending on the climate scenario used. In central Oregon, total forested area is projected to decrease by almost half under a 5C warming. Oak woodlands and dry Douglas-fir dominated forests are likely to increase in areal extent, while the more productive western hemlock - Douglas-fir forest will undergo significant contraction. Subalpine and alpine vegetation are likely to be reduced substantially. Declines in moisture availability would decrease forest productivity and long-term timber production. Author

N92-30031# Environmental Protection Agency, Research Triangle Park, NC. Air and Energy Engineering Research Lab.
NEW DEVELOPMENTS IN EMISSION PROJECTION METHODOLOGIES Report, Apr. - Sep. 1991
L. G. Jones and D. C. Misenheimer 1992 10 p Presented at EI Conference, Durham, NC, 9-12 Sep. 1991
(PB92-139393; EPA/600/A-92/002) Avail: CASI HC A02/MF A01

Described here is the scope of an EPA research program to develop the Economic Growth Analysis System (EGAS) that will be operated to provide economic inputs for EPA's Regional Oxidant Model (ROM) and Urban Airshed Model (UAM). The Clean Air Act requires states to reduce ozone atmospheric concentrations in areas exceeding the primary ambient standard of 0.120 ppm, and to model their future ozone concentrations to demonstrate the effectiveness of their control programs to attain the primary standard. To assist state and local agency authorities in preparing these ozone predictions, EPA has sponsored the development of the UAM, an atmospheric chemistry model, and has published guidance on its operation and use by state and local authorities. The UAM requires boundary conditions, which include the amount of pollutants crossing the boundaries of the area being modeled. Boundary conditions will be supplied from the operation of the ROM. The emissions preprocessor modules for UAM and ROM require various model input parameters for the projection of emissions, including anticipated future year economic activities for all pollutant source categories in the area being modeled. To fulfill the need, EPA has initiated a research program to produce a system (EGAS) for supplying default economic activity inputs in a format usable by UAM and ROM. Author

N92-30173# ManTech Environmental Technology, Inc., Corvallis, OR.
WHAT IS THE POTENTIAL OF FOREST MANAGEMENT TO SLOW THE INCREASE OF ATMOSPHERIC CO2?
P. Schroeder, J. K. Winjum, and R. K. Dixon Feb. 1992 19 p Presented at the 17th Annual Conference of National Association of Environmental Professionals, Seattle, WA, 5-8 May 1992 Prepared in cooperation with National Council for Air and Stream Improvement, Inc., Corvallis, OR
(Contract EPA-68-C8-0006)
(PB92-180249; EPA/600/A-92/105) Avail: CASI HC A03/MF A01

Forests are a major sink for carbon and play an important role in the global carbon cycle. Not only do forests contain huge amounts of carbon, they exchange it very actively with the atmosphere. On average, the equivalent of the entire CO2 content of the atmosphere passes through the earth's terrestrial vegetation every 7 years, and about 70 percent of the entire exchange occurs through forest ecosystems. Because this exchange is so active, expanding the world's forests could present an opportunity to increase the terrestrial carbon sink, and slow the increase in atmospheric CO2 concentration. Average standing stock of carbon over a stand life cycle can range from less than 40 tons C/ha in boreal regions to over 100 tons C/ha in humid temperate regions. Values for tree plantations in the tropics are intermediate because they are often grown on short cycles that preclude high levels of biomass accumulation. Accumulation of biomass and carbon is controlled not only by growth rate, but also by the length of the rotation or life cycle. Costs varied from $99-637/ha and $3-10/ton of stored carbon. An important uncertainty in assessing the total potential of forest management to store atmospheric carbon is the area of land that is both suitable and available for establishing forests. Published estimates of suitable land area in the tropics, for example, vary by a factor of three. Author

N92-30200# Environmental Protection Agency, Research Triangle Park, NC. Office of Air Quality Planning and Standards.
HUMAN EXPOSURE MODEL-2: USER'S GUIDE
Feb. 1991 164 p
(PB92-186246; EPA/450/3-91/0100) Avail: CASI HC A08/MF A02

The document is a guide to the Human Exposure Model-II (HEM-II) computer software. The HEM-II software is an effective tool for screening point sources of hazardous air pollutants and ranking individual sources and source categories in terms of their relative carcinogenic risks. Author

N92-30211# Lawrence Livermore National Lab., CA.
ELECTROCHEMICAL ARRAY SENSORS FOR PLATING WASTE STREAM MONITORING
R. S. Glass, K. C. Hong, J. C. Estill, R. A. Reibold, W. M. Thompson, D. W. OBrien, D. R. Ciarlo, and V. E. Granstaff (Sandia National Labs., Albuquerque, NM.) Mar. 1992 22 p Presented at the 1992 American Electroplaters and Surface Finishers Society Conference (AESF SUR/FIN 92), Atlanta, GA, 22-25 Jun. 1992
(Contract W-7405-eng-48)
(DE92-011446; UCRL-JC-108819; CONF-9206129-3) Avail: CASI HC A03/MF A01

Electrochemical sensors are being developed to aid in waste reduction efforts for plating operations and in environmental remediation. An important feature of these sensor systems are solid-state multielement microelectrode arrays. The individual elements of these arrays will be selected so that a variety of chemical species can be detected using a single device. In addition, we are developing a compact electronics package, consisting of a potentiostat, signal generator, and microcomputer with user-friendly software to use in conjunction with the arrays. This report discusses the selection process for array elements, advantages of the use of microelectrodes, and application to the analysis of actual plating rinse tank systems. DOE

N92-30226# Technische Univ., Delft (Netherlands). Faculty of Technical Mathematics and Information.
EXPERT JUDGMENT STUDY ON ATMOSPHERIC DISPERSION AND DEPOSITION: MAIN REPORT AND ANNEXES
Roger Cooke 1991 241 p
(Contract EEC-90-ET-011)
(Rept-91-81; ISSN-0922-5641; ETN-92-91831) Copyright Avail: CASI HC A11/MF A03

Research on the use of structured expert judgement in the assessment of uncertainty in the MARIA program package COSYMA is documented. Detailed analyses and data on the

following are given: parameter fitting for uncertain models; expert judgement for uncertainty analysis of accident consequence codes; experts' method of assessment, overview of selected variables; seed variables, meteorological data; combination of experts' assessments, graphic representation; optical decision maker's assessments; definition of terms; and EXCALIBR data files. ESA

N92-29229*# Fukuoka Univ. (Japan). Dept. of Applied Physics.
LONG TERM STRATOSPHERIC AEROSOL LIDAR MEASUREMENTS IN KYUSHU
Motowo Fujiwara *In* NASA. Langley Research Center, Sixteenth International Laser Radar Conference, Part 1 Jul. 1992 p 1-2 (For primary document see N92-29228 20-35)
Avail: CASI HC A01/MF A04

N92-29230*# Commonwealth Scientific and Industrial Research Organization, Mordialoc (Australia). Div. of Atmospheric Research.
SOUTHERN HEMISPHERE LIDAR MEASUREMENTS OF THE AEROSOL CLOUDS FROM MT. PINATUBO AND MT. HUDSON
Stuart A. Young, Peter J. Manson, and Graeme R. Patterson *In* NASA. Langley Research Center, Sixteenth International Laser Radar Conference, Part 1 Jul. 1992 p 3-6 (For primary document see N92-29228 20-35)
Avail: CASI HC A01/MF A04

N92-29231*# Gesellschaft fuer Kernenergieverwertung in Schiffbau und Schiffahrt m.b.H., Geesthacht (Germany, F.R.).
STRATOSPHERIC BACKSCATTER, EXTINCTION, AND LIDAR RATIO PROFILING AFTER THE MT. PINATUBO ERUPTIONS
Albert Ansmann, Christoph Schulze, Ulla Wandinger, Claus Weitkamp, and Walfried Michaelis *In* NASA. Langley Research Center, Sixteenth International Laser Radar Conference, Part 1 Jul. 1992 p 7-10 (For primary document see N92-29228 20-35)
Avail: CASI HC A01/MF A04

N92-29232*# Tokyo Metropolitan Univ. (Japan). Dept. of Electronics and Information Engineering.
MEASUREMENTS OF STRATOSPHERIC PINATUBO AEROSOL EXTINCTION PROFILES BY A RAMAN LIDAR
Makoto Abo and Chikao Nagasawa *In* NASA. Langley Research Center, Sixteenth International Laser Radar Conference, Part 1 Jul. 1992 p 11-12 (For primary document see N92-29228 20-35)
Avail: CASI HC A01/MF A04

N92-29233*# National Aeronautics and Space Administration. Goddard Space Flight Center, Greenbelt, MD.
RAMAN LIDAR MEASUREMENTS OF PINATUBO AEROSOLS OVER SOUTHEASTERN KANSAS DURING NOVEMBER-DECEMBER 1991
R. A. Ferrare (Universities Space Research Association, Greenbelt, MD.), S. H. Melfi, D. N. Whiteman, and K. D. Evans (Hughes STX, Inc., Lanham, MD.) *In* NASA. Langley Research Center, Sixteenth International Laser Radar Conference, Part 1 Jul. 1992 p 13-16 (For primary document see N92-29228 20-35)
Avail: CASI HC A01/MF A04

N92-29234*# Meteorological Research Inst., Tsukuba (Japan).
LIDAR OBSERVATIONS OF STRATOSPHERIC AEROSOL LAYER AFTER THE MT. PINATUBO VOLCANIC ERUPTION
Tomohiro Nagai, Osamu Uchino, and Toshifumi Fujimoto *In* NASA. Langley Research Center, Sixteenth International Laser Radar Conference, Part 1 Jul. 1992 p 17-20 (For primary document see N92-29228 20-35)
Avail: CASI HC A01/MF A04

N92-29235*# Massachusetts Inst. of Tech., Cambridge. Center for Global Change Science.
THE ROLE OF LIDARS IN GLOBAL CHANGE RESEARCH
Ronald G. Prinn *In* NASA. Langley Research Center, Sixteenth International Laser Radar Conference, Part 1 Jul. 1992 p 21-22 (For primary document see N92-29228 20-35)
Avail: CASI HC A01/MF A04

N92-29236*# National Aeronautics and Space Administration. Langley Research Center, Hampton, VA.
INTERPRETATION OF DIAL MEASUREMENTS OF LOWER STRATOSPHERIC OZONE IN REGIONS WITH PINATUBO AEROSOLS
William B. Grant (ST Systems Corp., Hampton, VA.), Edward V. Browell (ST Systems Corp., Hampton, VA.), Marta A. Fenn (ST Systems Corp., Hampton, VA.), Carolyn F. Butler (ST Systems Corp., Hampton, VA.), Vincent G. Brackett (ST Systems Corp., Hampton, VA.), Robert E. Veiga (ST Systems Corp., Hampton, VA.), Shane D. Mayor (ST Systems Corp., Hampton, VA.), Jack Fishman, D. Nganga (Maien-Ngouabi Univ., Brazzaville, Congo), and A. Minga (Maien-Ngouabi Univ., Brazzaville, Congo) *In its* Sixteenth International Laser Radar Conference, Part 1 Jul. 1992 p 23-26 Prepared in cooperation with NATO, Washington, DC (For primary document see N92-29228 20-35)
Avail: CASI HC A01/MF A04

N92-29237*# York Univ. (Ontario). Inst. for Space and Terrestrial Science.
CORRECTING FOR INTERFERENCE OF MT. PINATUBO AEROSOLS ON DIAL MEASUREMENTS OF STRATOSPHERIC OZONE
W. Steinbrecht and A. I. Carswell *In* NASA. Langley Research Center, Sixteenth International Laser Radar Conference, Part 1 Jul. 1992 p 27-30 (For primary document see N92-29228 20-35)
Avail: CASI HC A01/MF A04

N92-29238*# National Aeronautics and Space Administration. Goddard Space Flight Center, Greenbelt, MD.
A NEW RAMAN DIAL TECHNIQUE FOR MEASURING STRATOSPHERIC OZONE IN THE PRESENCE OF VOLCANIC AEROSOLS
Upendra N. Singh (Hughes STX, Inc., Lanham, MD.), Thomas J. McGee, Michael Gross (Hughes STX, Inc., Lanham, MD.), William S. Heaps, and Richard Ferrare *In* NASA. Langley Research Center, Sixteenth International Laser Radar Conference, Part 1 Jul. 1992 p 31-33 (For primary document see N92-29228 20-35)
Avail: CASI HC A01/MF A04

N92-29239*# Jet Propulsion Lab., California Inst. of Tech., Pasadena. Table Mountain Facility.
THE JPL TABLE MOUNTAIN AND MAUNA LOA STRATOSPHERIC OZONE LIDARS
I. Stuart McDermid *In* NASA. Langley Research Center, Sixteenth International Laser Radar Conference, Part 1 Jul. 1992 p 35-38 (For primary document see N92-29228 20-35)
Avail: CASI HC A01/MF A04

N92-29240*# Paris VI Univ. (France).
THE NDSC PRIMARY SITE AT THE OBSERVATOIRE DE HAUTE-PROVENCE: OZONE AND AEROSOLS OBSERVATIONS (1986-1992)
G. Megie, S. Godin, G. Ancellet, M. Beekmann, and A. M. Lacoste *In* NASA. Langley Research Center, Sixteenth International Laser Radar Conference, Part 1 Jul. 1992 p 39-41 (For primary document see N92-29228 20-35)
Avail: CASI HC A01/MF A04

N92-29241*# Optech, Inc., Downsview (Ontario).
LIDAR ATMOSPHERIC OBSERVATORY IN THE CANADIAN ARCTIC
Arkady Ulitsky, Tin-Yu Wang, Martin Flood, and Brent Smith *In* NASA. Langley Research Center, Sixteenth International Laser Radar Conference, Part 1 Jul. 1992 p 43-44 (For primary document see N92-29228 20-35)
Avail: CASI HC A01/MF A04

N92-29242*# National Inst. for Environmental Studies, Tsukuba (Japan).
OBSERVATION OF STRATOSPHERIC OZONE WITH NIES LIDAR SYSTEM IN TSUKUBA, JAPAN
H. Nakane, S. Hayashida, Y. Sasano, N. Sugimoto, I. Matsui, and A. Minato *In* NASA. Langley Research Center, Sixteenth International Laser Radar Conference, Part 1 Jul. 1992 p 45-48 (For primary document see N92-29228 20-35)
Avail: CASI HC A01/MF A04

N92-29243*# La Sapienza Univ., Rome (Italy).
OBSERVATIONS OF OZONE-AEROSOL CORRELATED BEHAVIOUR IN THE LOWER STRATOSPHERE DURING THE EASOE CAMPAIGN
P. DiGirolamo, M. Cacciani, A. diSarra, G. Fiocco, D. Fua, T. S. Joergensen (Danish Meteorological Inst., Copenhagen.), B. Knudsen (Danish Meteorological Inst., Copenhagen.), and N. Larsen (Danish Meteorological Inst., Copenhagen.) *In* NASA. Langley Research Center, Sixteenth International Laser Radar Conference, Part 1 Jul. 1992 p 49-51 Prepared in cooperation with Rome Univ., Italy and Inst. di Fisica dell Atmosfera, Rome, Italy (For primary document see N92-29228 20-35)
Avail: CASI HC A01/MF A04

N92-29244*# Rijksinstituut voor Volksgezondheid en Milieuhygieene, Bilthoven (Netherlands).
FIRST RESULTS FROM TROLIX 1991: AN INTERCOMPARISON OF TROPOSPHERIC OZONE LIDARS
A. Apituley, J. Boesenberg (Max-Planck-Inst. fuer Meteorologie, Hamburg, Germany, F.R.), G. Ancellet (Centre National de la Recherche Scientifique, Paris, France), H. Edner (Lund Inst. of Tech., Sweden), B. Galle (Institutet foer Vatten-Och Luftvaardsforskning, Goeteborg, Sweden), J. B. Bergwerff, G. vonCossart (Institut fuer Atmosphaerenphysik Kuehlungsborn, Germany, F.R), J. Fiedler (Institut fuer Atmosphaerenphysik Kuehlungsborn, Germany, F.R), C. N. deJonge, and J. Mellquist (Institutet foer Vatten-Och Luftvaardsforskning, Goeteborg, Sweden) *In* NASA. Langley Research Center, Sixteenth International Laser Radar Conference, Part 1 Jul. 1992 p 53-55 (For primary document see N92-29228 20-35)
Avail: CASI HC A01/MF A04

N92-29245*# Alabama Univ., Huntsville. Earth System Science Lab.
GLOBAL BACKSCATTER EXPERIMENT (GLOBE) RESULTS: AEROSOL BACKSCATTER GLOBAL DISTRIBUTION AND WAVELENGTH DEPENDENCE
David A. Bowdle *In* NASA. Langley Research Center, Sixteenth International Laser Radar Conference, Part 1 Jul. 1992 p 57-60 (For primary document see N92-29228 20-35)
Avail: CASI HC A01/MF A04

N92-29246*# National Aeronautics and Space Administration. Goddard Space Flight Center, Greenbelt, MD.
THE GLOBAL BACKSCATTER EXPERIMENT AIRBORNE PULSED LIDAR MEASUREMENTS
James D. Spinhirne, S. Chudamani, Robert T. Menzies (Jet Propulsion Lab., California Inst. of Tech., Pasadena.), and David Tratt (Jet Propulsion Lab., California Inst. of Tech., Pasadena.) *In* NASA. Langley Research Center, Sixteenth International Laser Radar Conference, Part 1 Jul. 1992 p 61-62 (For primary document see N92-29228 20-35)
Avail: CASI HC A01/MF A04

N92-29247*# National Aeronautics and Space Administration. Goddard Space Flight Center, Greenbelt, MD.
MULTI-WAVELENGTH AIRBORNE LIDAR INTERCOMPARISONS OF AEROSOL AND CIRRUS BACKSCATTER OVER THE PACIFIC OCEAN
Robert T. Menzies (Jet Propulsion Lab., California Inst. of Tech., Pasadena.), David M. Tratt (Jet Propulsion Lab., California Inst. of Tech., Pasadena.), James D. Spinhirne, and S. Chudamani *In* NASA. Langley Research Center, Sixteenth International Laser Radar Conference, Part 1 Jul. 1992 p 63-65 (For primary document see N92-29228 20-35)
Avail: CASI HC A01/MF A04

N92-29248*# National Aeronautics and Space Administration. Langley Research Center, Hampton, VA.
AIRBORNE LIDAR OBSERVATIONS OF THE STRATOSPHERE AFTER THE PINATUBO ERUPTION
David M. Winker, Mary T. Osborn (Hughes STX, Inc., Lanham, MD.), and Robert J. DeCoursey (Hughes STX, Inc., Lanham, MD.) *In its* Sixteenth International Laser Radar Conference, Part 1 Jul. 1992 p 67-70 (For primary document see N92-29228 20-35)
Avail: CASI HC A01/MF A04

N92-29249*# Science and Technology Corp., Hampton, VA.
MULTI-WAVELENGTH MEASUREMENTS OF THE STRATOSPHERIC AEROSOL LAYER MADE AT HAMPTON, VIRGINIA (37N, 76W)
G. S. Kent, G. M. Hansen, and K. M. Skeens *In* NASA. Langley Research Center, Sixteenth International Laser Radar Conference, Part 1 Jul. 1992 p 71-74 (For primary document see N92-29228 20-35)
(Contract NAS1-18851)
Avail: CASI HC A01/MF A04

N92-29250*# National Inst. for Environmental Studies, Tsukuba (Japan).
THREE-WAVELENGTH LIDAR MEASUREMENTS OF PINATUBO AEROSOL AND ITS OPTICAL PROPERTIES
Y. Sasano, I. Matsui, and S. Hayashida *In* NASA. Langley Research Center, Sixteenth International Laser Radar Conference, Part 1 Jul. 1992 p 75-78 (For primary document see N92-29228 20-35)
Avail: CASI HC A01/MF A04

N92-29251*# Consiglio Nazionale delle Ricerche, Frascati (Italy).
LIDAR OBSERVATIONS OF THE PINATUBO STRATOSPHERIC AEROSOL CLOUD OVER FRASCATI, ITALY
Fernando Congeduti, Alberto Adriani, Gian Paolo Gobbi, and Sante Centurioni *In* NASA. Langley Research Center, Sixteenth International Laser Radar Conference, Part 1 Jul. 1992 p 79-81 (For primary document see N92-29228 20-35)
Avail: CASI HC A01/MF A04

N92-29252*# Anhui Inst. of Optics and Fine Mechanics, Hefei (China).
L625 LIDAR MEASUREMENTS OF PINATUBO VOLCANIC CLOUD AT HEFEI
Huanling Hu and Jun Zhou *In* NASA. Langley Research Center, Sixteenth International Laser Radar Conference, Part 1 Jul. 1992 p 83-86 (For primary document see N92-29228 20-35)
Avail: CASI HC A01/MF A04

N92-29253*# York Univ. (Ontario). Inst. for Space and Terrestrial Science.
TWO WAVELENGTH MEASUREMENTS OF THE PINATUBO AEROSOL ABOVE TORONTO, CANADA
W. Steinbrecht, D. Donovan, and A. I. Carswell *In* NASA. Langley Research Center, Sixteenth International Laser Radar Conference, Part 1 Jul. 1992 p 87-90 (For primary document see N92-29228 20-35)
Avail: CASI HC A01/MF A04

N92-29254*# National Aeronautics and Space Administration. Langley Research Center, Hampton, VA.
LIDAR OBSERVATIONS OF THE PINATUBO VOLCANIC CLOUD OVER HAMPTON, VIRGINIA
M. T. Osborn (Hughes STX, Inc., Lanham, MD.), D. M. Winker, D. C. Woods, and R. J. DeCoursey (Hughes STX, Inc., Lanham, MD.) *In its* Sixteenth International Laser Radar Conference, Part 1 Jul. 1992 p 91-94 (For primary document see N92-29228

20-35)
Avail: CASI HC A01/MF A04

N92-29255*# Nevada Univ., Las Vegas.
OZONE MEASUREMENTS WITH THE US EPA UV-DIAL: PRELIMINARY RESULTS
H. Moosmueller, D. Diebel, D. H. Bundy (Environmental Protection Agency, Las Vegas, NV.), M. P. Bristow (Environmental Protection Agency, Las Vegas, NV.), R. J. Alvarez, II (Environmental Protection Agency, Las Vegas, NV.), V. A. Kovalev (Environmental Protection Agency, Las Vegas, NV.), C. M. Edmonds (Environmental Protection Agency, Las Vegas, NV.), R. M. Turner, and J. L. McElroy (Environmental Protection Agency, Las Vegas, NV.) *In* NASA. Langley Research Center, Sixteenth International Laser Radar Conference, Part 1 Jul. 1992 p 95-98 (For primary document see N92-29228 20-35)
Avail: CASI HC A01/MF A04

N92-29256*# Pacific Northwest Lab., Richland, WA. Applied Physics Center.
LIDAR DEVELOPMENT FOR THE ATMOSPHERIC RADIATION MEASUREMENT (ARM) PROGRAM
J. Griffin and M. Lapp (Sandia National Labs., Livermore, CA.) *In* NASA. Langley Research Center, Sixteenth International Laser Radar Conference, Part 1 Jul. 1992 p 99-101 (For primary document see N92-29228 20-35)
Avail: CASI HC A01/MF A04

N92-29257*# National Aeronautics and Space Administration. Goddard Space Flight Center, Greenbelt, MD.
LIDAR MEASUREMENTS OF STRATOSPHERIC OZONE, TEMPERATURE AND AEROSOL DURING 1992 UARS CORRELATIVE MEASUREMENT CAMPAIGN
Thomas J. McGee, Upendra N. Singh (Hughes STX, Inc., Lanham, MD.), Michael Gross (Hughes STX, Inc., Lanham, MD.), William S. Heaps, and Richard Ferrare (Universities Space Research Association, Greenbelt, MD.) *In* NASA. Langley Research Center, Sixteenth International Laser Radar Conference, Part 1 Jul. 1992 p 103-106 (For primary document see N92-29228 20-35)
Avail: CASI HC A01/MF A04

N92-29258*# Deutsche Forschungsanstalt fuer Luft- und Raumfahrt, Oberpfaffenhofen (Germany, F.R.). Inst. fuer Physik der Atmosphaere.
AIRBORNE DIAL REMOTE SENSING OF THE ARCTIC OZONE LAYER
Martin Wirth, Wolfgang Renger, and Gerhard Ehret *In* NASA. Langley Research Center, Sixteenth International Laser Radar Conference, Part 1 Jul. 1992 p 107-108 (For primary document see N92-29228 20-35)
Avail: CASI HC A01/MF A04

N92-29259*# Meteorologisches Observatorium, Hohenpeissenberg (Germany, F.R.).
LIDAR MEASUREMENT OF STRATOSPHERIC OZONE AT HOHENPEISSENBERG: AN IMPROVED EVALUATION METHOD
W. Vandersee, F. Schoenenborn, and H. Claude *In* NASA. Langley Research Center, Sixteenth International Laser Radar Conference, Part 1 Jul. 1992 p 109-112 (For primary document see N92-29228 20-35)
Avail: CASI HC A01/MF A04

N92-29260*# Centre National de la Recherche Scientifique, Paris (France).
A MULTI-WAVELENGTH OZONE LIDAR FOR THE EASOE EXPERIMENT
S. Godin, G. Ancellet, C. David, J. Porteneuve, C. Leroy, V. Mitev (Cantonal Observatory, Neuchatel, Switzerland), Y. Emery (Cantonal Observatory, Neuchatel, Switzerland), C. Flesia (Cantonal Observatory, Neuchatel, Switzerland), V. Rizi (Aquila Univ., Italy), and G. Visconti (Aquila Univ., Italy) et al *In* NASA. Langley Research Center, Sixteenth International Laser Radar Conference, Part 1 Jul. 1992 p 113-115 Prepared in cooperation with Consiglio Nazionale delle Ricerche, Florence, Italy (For primary document see N92-29228 20-35)
Avail: CASI HC A01/MF A04

N92-29261*# National Aeronautics and Space Administration. Langley Research Center, Hampton, VA.
CORRECTION OF DIAL STRATOSPHERIC OZONE MEASUREMENTS IN THE PRESENCE OF PINATUBO AEROSOLS
Marta A. Fenn (Hughes STX, Inc., Lanham, MD.), Syed Ismail, Edward V. Browell, and Carolyn F. Butler (Hughes STX, Inc., Lanham, MD.) *In its* Sixteenth International Laser Radar Conference, Part 1 Jul. 1992 p 117-120 (For primary document see N92-29228 20-35)
Avail: CASI HC A01/MF A04

N92-29262*# General Electric Co., Princeton, NJ. Astro Space Div.
THE LASER ATMOSPHERIC WIND SOUNDER (LAWS) PRELIMINARY ERROR BUDGET AND PERFORMANCE ESTIMATE
David L. Kenyon and Kent Anderson *In* NASA. Langley Research Center, Sixteenth International Laser Radar Conference, Part 1 Jul. 1992 p 121-123 (For primary document see N92-29228 20-35)
Avail: CASI HC A01/MF A04

N92-29263*# Hughes Danbury Optical Systems, Inc., CT.
LAG ANGLE COMPENSATION IN A SPACE BORNE SCANNING LIDAR
A. B. Wissinger *In* NASA. Langley Research Center, Sixteenth International Laser Radar Conference, Part 1 Jul. 1992 p 125-128 (For primary document see N92-29228 20-35)
Avail: CASI HC A01/MF A04

N92-29266*# National Aeronautics and Space Administration. Goddard Space Flight Center, Greenbelt, MD.
INTERCOMPARISONS OF LIDAR BACKSCATTER MEASUREMENTS AND IN-SITU DATA FROM GLOBE
S. Chudamani and James D. Spinhirne *In* NASA. Langley Research Center, Sixteenth International Laser Radar Conference, Part 1 Jul. 1992 p 137-139 (For primary document see N92-29228 20-35)
Avail: CASI HC A01/MF A04

N92-29273*# Lund Inst. of Tech. (Sweden). Dept. of Physics.
DIAL MAPPING OF ATMOSPHERIC ATOMIC MERCURY OF GEOPHYSICAL ORIGIN
H. Edner, P. Ragnarson, S. Svanberg, and E. Wallinder *In* NASA. Langley Research Center, Sixteenth International Laser Radar Conference, Part 1 Jul. 1992 p 165-168 Sponsored in part by Swedish Natural Science Research Council; and the Swedish Board for Space Activities (For primary document see N92-29228 20-35)
Avail: CASI HC A01/MF A04

N92-29274*# National Oceanic and Atmospheric Administration, Boulder, CO. Wave Propagation Lab.
LIDAR TRACKING OF MULTIPLE FLUORESCENT TRACERS: METHOD AND FIELD TEST
Wynn L. Eberhard and Ron J. Willis (Colorado Univ., Boulder.) *In* NASA. Langley Research Center, Sixteenth International Laser Radar Conference, Part 1 Jul. 1992 p 169-172 Sponsored in part by EPA (For primary document see N92-29228 20-35)
(Contract DW13932524-01)
Avail: CASI HC A01/MF A04

N92-29275*# Los Alamos National Lab., NM.
LIDAR MONITORING OF MEXICO CITY'S ATMOSPHERE DURING HIGH AIR POLUTION EPISODES
C. R. Quick, Jr., F. L. Archuleta, D. E. Hof, R. R. Karl, Jr., J. J. Tiee, Jr., W. E. Eichinger, D. B. Holtkamp, and L. Tellier *In* NASA. Langley Research Center, Sixteenth International Laser

Radar Conference, Part 1 Jul. 1992 p 173-175 (For primary document see N92-29228 20-35)
Avail: CASI HC A01/MF A04

N92-29276*# Consiglio Nazionale delle Ricerche, Naples (Italy).
LAB-SCALE LIDAR SENSING OF DIESEL ENGINES EXHAUSTS
A. Borghese *In* NASA. Langley Research Center, Sixteenth International Laser Radar Conference, Part 1 Jul. 1992 p 177-180 (For primary document see N92-29228 20-35)
Avail: CASI HC A01/MF A04

N92-29277*# National Inst. for Environmental Studies, Tsukuba (Japan).
INFRARED PULSE-LASER LONG-PATH ABSORPTION MEASUREMENT OF CARBON DIOXIDE USING A RAMAN-SHIFTED DYE LASER
Atsushi Minato, Nobuo Sugimoto, and Yasuhiro Sasano *In* NASA. Langley Research Center, Sixteenth International Laser Radar Conference, Part 1 Jul. 1992 p 181-183 (For primary document see N92-29228 20-35)
Avail: CASI HC A01/MF A04

N92-29279*# Los Alamos National Lab., NM. Chemical and Laser Sciences Div.
REMOTE DETECTION OF BIOLOGICAL PARTICLES AND CHEMICAL PLUMES USING UV FLUORESCENCE LIDAR
J. J. Tiee, D. E. Hof, R. R. Karl, R. J. Martinez, C. R. Quick, D. I. Cooper, W. E. Eichinger, and D. B. Holtkamp *In* NASA. Langley Research Center, Sixteenth International Laser Radar Conference, Part 1 Jul. 1992 p 189-192 Sponsored in part by Army; and by Los Alamos National Lab., NM (For primary document see N92-29228 20-35)
Avail: CASI HC A01/MF A04

N92-29280*# Israel Inst. for Biological Research, Ness-Ziona.
SIGNAL QUALITY INFLUENCE ON AVERAGING PROCEDURE FOR DIAL POLLUTION MONITORING
S. Egert, D. Peri, and L. Berg (Laser Science, Inc., Newton, MA.) *In* NASA. Langley Research Center, Sixteenth International Laser Radar Conference, Part 1 Jul. 1992 p 193-194 (For primary document see N92-29228 20-35)
Avail: CASI HC A01/MF A04

N92-29281*# Michigan Univ., Ann Arbor. Dept. of Atmospheric, Oceanic and Space Sciences.
EXTRACTION OF AEROSOL AND RAYLEIGH COMPONENTS FROM DOPPLER LIDAR RETURN SIGNAL
John E. Barnes, Ken W. Fischer, Vincent J. Abreu, and Wilbert R. Skinner *In* NASA. Langley Research Center, Sixteenth International Laser Radar Conference, Part 1 Jul. 1992 p 195-197 (For primary document see N92-29228 20-35)
Avail: CASI HC A01/MF A04

N92-29285*# York Univ. (Ontario). Dept. of Physics and Astronomy.
ONE YEAR OF RAYLEIGH LIDAR MEASUREMENTS AT TORONTO
James A. Whiteway and Allan I. Carswell *In* NASA. Langley Research Center, Sixteenth International Laser Radar Conference, Part 1 Jul. 1992 p 209-212 (For primary document see N92-29228 20-35)
Avail: CASI HC A01/MF A04

N92-29286*# Bulgarian Academy of Sciences, Sofia. Inst. of Electronics.
LIDAR OBSERVATION OF AEROSOL AND TEMPERATURE STRATIFICATION OVER URBAN AREA DURING THE FORMATION OF A STABLE ATMOSPHERIC PBL
I. Kolev, O. Parvanov, B. Kaprielov, V. Mitev, V. Simeonov, and I. Grigorov *In* NASA. Langley Research Center, Sixteenth International Laser Radar Conference, Part 1 Jul. 1992 p 213-216 (For primary document see N92-29228 20-35)
Avail: CASI HC A01/MF A04

N92-29287*# Bulgarian Academy of Sciences, Sofia. Inst. of Electronics.
A COMPARISON BETWEEN RAMAN LIDAR AND CONVENTIONAL CONTACT MEASUREMENTS OF ATMOSPHERIC TEMPERATURE
V. M. Mitev, V. B. Simeonov, and I. V. Grigorov *In* NASA. Langley Research Center, Sixteenth International Laser Radar Conference, Part 1 Jul. 1992 p 217-220 (For primary document see N92-29228 20-35)
Avail: CASI HC A01/MF A04

N92-29288*# Bulgarian Academy of Sciences, Sofia. Inst. of Electronics.
EFFICIENCIES OF ROTATIONAL RAMAN AND RAYLEIGH TECHNIQUES FOR LASER REMOTE SENSING OF THE ATMOSPHERIC TEMPERATURE
I. D. Ivanova, L. L. Gurdev, and V. M. Mitev *In* NASA. Langley Research Center, Sixteenth International Laser Radar Conference, Part 1 Jul. 1992 p 221-224 (For primary document see N92-29228 20-35)
Avail: CASI HC A01/MF A04

N92-29289*# Bulgarian Academy of Sciences, Sofia. Inst. of Electronics.
LIDAR INVESTIGATION OF AEROSOL POLLUTION DISTRIBUTION NEAR A COAL POWER PLANT
Ts. Mitsev and G. Kolarov *In* NASA. Langley Research Center, Sixteenth International Laser Radar Conference, Part 1 Jul. 1992 p 225-228 (For primary document see N92-29228 20-35)
Avail: CASI HC A01/MF A04

N92-29290*# Academy of Sciences (USSR), Moscow. Inst. of General Physics.
LASER REMOTE SENSING OF POLLUTION ON WATER SURFACES
A. F. Bunkin and Aleksander L. Surovegin (RADIAN, Moscow, USSR) *In* NASA. Langley Research Center, Sixteenth International Laser Radar Conference, Part 1 Jul. 1992 p 229-232 (For primary document see N92-29228 20-35)
Avail: CASI HC A01/MF A04

N92-29292*# Academia Sinica, Beijing (China). Inst. of Atmospheric Physics.
A DEVELOPING MULTIPLE-WAVELENGTH LIDAR FOR DETECTING MAINLY OZONE AND AEROSOL DISTRIBUTIONS IN THE STRATOSPHERE
Siping Zheng, Jinhuan Qiu, Shufang Wang, Qirong Huang, Wenming Wang, and Shaoming Wu *In* NASA. Langley Research Center, Sixteenth International Laser Radar Conference, Part 1 Jul. 1992 p 237 (For primary document see N92-29228 20-35)
Avail: CASI HC A01/MF A04

N92-29293*# Academy of Sciences (USSR), Tomsk. Inst. of Atmospheric Optics.
AN EXTENSION OF THE RAMAN-LIDAR TECHNIQUE TO MEASURE THE VELOCITY AND TEMPERATURE OF THE ATMOSPHERIC EMISSION JETS FROM STACKS
Yu. F. Arshinov, S. M. Bobrovnikov, V. K. Shumskii, A. G. Popov, and I. B. Serikov *In* NASA. Langley Research Center, Sixteenth International Laser Radar Conference, Part 1 Jul. 1992 p 239-242 (For primary document see N92-29228 20-35)
Avail: CASI HC A01/MF A04

N92-29294*# Academia Sinica, Beijing (China). Inst. of Atmospheric Physics.
LIDAR OBSERVATIONS OF STRATOSPHERIC CLOUDS AFTER VOLCANIC ERUPTION OF PINATUBO
Jinhui Sun, Jinhuan Qiu, Qilin Xia, and Jinding Zhang *In* NASA. Langley Research Center, Sixteenth International Laser Radar

Conference, Part 1 Jul. 1992 p 243-245 (For primary document see N92-29228 20-35)
Avail: CASI HC A01/MF A04

N92-29304*# National Aeronautics and Space Administration. Langley Research Center, Hampton, VA.
LIDAR MEASUREMENTS OF AEROSOL AND OZONE DISTRIBUTIONS DURING THE 1992 AIRBORNE ARCTIC STRATOSPHERIC EXPEDITION
E. V. Browell, C. F. Butler (ST Systems Corp., Hampton, VA.), M. A. Fenn, W. B. Grant, and A. F. Carter *In its* Sixteenth International Laser Radar Conference, Part 1 Jul. 1992 p 285-288 (For primary document see N92-29228 20-35)
Avail: CASI HC A01/MF A04

N92-29305*# Deutsche Forschungsanstalt fuer Luft- und Raumfahrt, Oberpfaffenhofen (Germany, F.R.).
AIRBORNE LIDAR MEASUREMENTS OF STRATOSPHERIC AEROSOLS DURING THE EUROPEAN ARCTIC STRATOSPHERIC OZONE EXPERIMENT (EASOE) Abstract Only
Wolfgang Renger, Gerhard Ehret, Peter Moerl, and Martin Wirth *In* NASA. Langley Research Center, Sixteenth International Laser Radar Conference, Part 1 Jul. 1992 p 289-290 (For primary document see N92-29228 20-35)
Avail: CASI HC A01/MF A04

N92-29306*# Paris VI Univ. (France). Service d'Aeronomie.
AEROSOLS AND POLAR STRATOSPHERIC CLOUDS MEASUREMENTS DURING THE EASOE CAMPAIGN Abstract Only
D. Haner, S. Godin, G. Megie, C. David, and V. Mitev *In* NASA. Langley Research Center, Sixteenth International Laser Radar Conference, Part 1 Jul. 1992 p 291 (For primary document see N92-29228 20-35)
Avail: CASI HC A01/MF A04

N92-29307*# Illinois Univ., Urbana-Champaign. Dept. of Atmospheric Sciences.
LIDAR OBSERVATIONS OF POLAR STRATOSPHERIC CLOUDS AND STRATOSPHERIC TEMPERATURES AT THE SOUTH POLE
Richard L. Collins, Kenneth P. Bowman, and Chester S. Gardner *In* NASA. Langley Research Center, Sixteenth International Laser Radar Conference, Part 1 Jul. 1992 p 293-295 (For primary document see N92-29228 20-35)
Avail: CASI HC A01/MF A04

46 GEOPHYSICS

Includes aeronomy; upper and lower atmosphere studies; ionospheric and magnetospheric physics; and geomagnetism.

For space radiation see *93 Space Radiation.*

N92-29513# Los Alamos National Lab., NM.
POLEWARD LEAPING AURORAS, THE SUBSTORM EXPANSIVE AND RECOVERY PHASES, AND THE RECOVERY OF THE PLASMA SHEET
E. W. Hones 1992 8 p Presented at the International Conference on Substorms, Kiruna (Sweden), 23-28 Mar. 1992
(Contract W-7405-eng-36)
(DE92-013530; LA-UR-92-1330; CONF-9203149-1) Avail: CASI HC A02/MF A01

The auroral motions and geomagnetic changes the characterize the substorm's expansive phase, maximum epoch, and recovery phase are discussed in the context of their possible associations with the dropout and, especially, the recovery of the magnetotail plasma sheet. The evidence that there may be an inordinately sudden large poleward excursion or displacement (a poleward leap) of the electrojet and the auroras at the expansive phase-recovery phase transition is described. The close temporal association of these signatures with the recovery of the plasma sheet, observed on many occasions, suggests a causal relationship between substorm maximum epoch and recovery phase on the one hand and plasma sheet recovery on the other. DOE

N92-29536# Los Alamos National Lab., NM.
LOW ENERGY NEUTRAL ATOMS IN THE EARTH'S MAGNETOSPHERE: MODELING
K. R. Moore, D. J. McComas, H. O. Funsten, and M. F. Thomsen 1992 12 p Presented at the 1992 SPIE International Symposium on Optical Applied Science and Engineering, San Diego, CA, 19-24 Jul. 1992
(Contract W-7405-eng-36)
(DE92-013240; LA-UR-92-1442; CONF-920792-1) Avail: CASI HC A03/MF A01

Detection of low energy neutral atoms (LENA's) produced by the interaction of the Earth's geocorona with ambient space plasma has been proposed as a technique to obtain global information about the magnetosphere. Recent instrumentation advances reported previously and in these proceedings provide an opportunity for detecting LENA's in the energy range of less than 1 keV to approximately 50 keV. We present results from a numerical model which calculates line of sight LENA fluxes expected at a remote orbiting spacecraft for various magnetospheric plasma regimes. This model uses measured charge exchange cross sections, either of two neural hydrogen geocorona models, and various empirical modes of the ring current and plasma sheet to calculate the contribution to the integrated directional flux from each point along the line of sight of the instrument. We discuss implications for LENA imaging of the magnetosphere based on these simulations. DOE

N92-29670 Commonwealth Scientific and Industrial Research Organization, Mordialoc (Australia). Div. of Atmospheric Research.
A SOIL-CANOPY SCHEME FOR USE IN A NUMERICAL MODEL OF THE ATMOSPHERE: 1D STAND-ALONE MODEL
E. A. Kowalczyk, J. R. Garratt, and P. B. Krummel 1991 59 p
(CSIRO-TP-23; ISBN-0-643-05248-8) Copyright Avail: CASI HC A04/MF A01

We provide a detailed description of a soil-canopy scheme for use in the CSIRO general circulation models (GCMs) (CSIRO-4 and CSIRO-9), in the form of a one-dimensional stand-alone model. In addition, the paper documents the model's ability to simulate realistic surface fluxes by comparison with mesoscale model simulations (involving more sophisticated soil and boundary-layer treatments) and observations, and the diurnal range in surface quantities, including extreme maximum surface temperatures. The sensitivity of the model to values of the surface resistance is also quantified. The model represents phase 1 of a longer-term plan to improve the atmospheric boundary layer (ABL) and surface schemes in the CSIRO GCMs. Author

N92-29690# Kernforschungszentrum G.m.b.H., Karlsruhe (Germany, F.R.). Inst. fuer Meteorologie und Klimaforschung.
COMPARISON OF TURBULENCE PARAMETERS MEASURED BY SODAR AND SONIC ANEMOMETER
H. Gentou (Remtech, S.A., Paris, France), P. Thomas, and S. Vogt Sep. 1991 71 p
(KfK-4890; ISSN-0303-4003; ETN-92-91501) Copyright Avail: CASI HC A04/MF A01

A monostatic Doppler sodar and a sonic anemometer measured 30 min values of the vertical wind speed and its standard deviation at 100 m above ground level. Other meteorological parameters were additionally measured by the sodar and at a 200 m high tower. During seven runs lasting about two hours each and covering different atmospheric stability conditions, instantaneous values of the vertical wind speed were measured by both instruments, from which logarithmic power spectra were calculated. From these spectra, the logarithmic spectral peak, the corresponding outer turbulent scale wavelength, and the integral scale of turbulence were determined. The long term comparison of the standard deviation measured by both instruments was quantified by the bias, the root mean square error, the precision, and the correlation

coefficient. The agreement of the data sets varies as a function of horizontal wind speed and atmospheric stability. In general, there is a better agreement during low wind situation and during nighttime. The sodar is underestimating high values of the standard deviation. The power spectra yielded by both instruments are generally well comparable in all atmospheric stability conditions. In particular, the logarithmic spectral peaks derived from sodar and sonic data are almost coincident. During windy conditions, the inertial subrange slope of the sodar spectra is not detailed and the definition of the spectral peak is difficult. In some cases, the spectra derived from sodar data are underestimated. ESA

N92-29950# California Univ., Irvine. Dept. of Civil Engineering.
INSTANTANEOUS OPTIMAL CONTROL FOR LINEAR, NONLINEAR AND HYSTERETIC STRUCTURES: STABLE CONTROLLERS
J. N. Yang and Z. Li 15 Nov. 1991 57 p Sponsored in part by National Center for Earthquake Engineering Research, Buffalo, NY
(Grants NSF BCS-91-96089; NSF ECE-86-07591)
(PB92-163807; NCEER-91/0026) Avail: CASI HC A04/MF A01

Recently, instantaneous optimal control algorithms have been proposed and developed for applications to control of seismic-excited linear, nonlinear and hysteretic structural systems. In particular, these control algorithms are suitable for aseismic hybrid control systems for which the linear quadratic optimal control theory is not applicable. Within the framework of instantaneous optimal control, the weighting matrix Q should be assigned to guarantee the stability of the controlled structure. A systematic way of assigning the weighting matrix by use of the Lyapunov direct method is investigated. Based on the Lyapunov method, several possible choices for the weighting matrix are presented, and their control performances are examined and compared for active and hybrid control systems under seismic loads. For the particular structures considered, the simplest choice for the Q matrix seems to result in a good performance. Author

N92-30087# Naval Command, Control and Ocean Surveillance Center, San Diego, CA.
EVALUATION OF AN AUREOLE LIDAR TECHNIQUE FOR ESTIMATING EXTINCTION PROFILES
D. R. Jensen Feb. 1992 20 p
(AD-A249740; NCCOSC/RDT/E-TR-1483) Avail: CASI HC A03/MF A01

An aureole lidar technique for estimating extinction profiles was developed at the Naval Research Laboratory, Washington, DC. This technique was evaluated by making nearly simultaneous measurements of atmospheric extinction from the NRL airborne Aureole Lidar Platform and the NOSC Airborne Platform, which utilizes the Particle Measuring Systems (PMS), Inc., aerosol spectrometers. Profiles of measured aerosol-size distributions were used to calculate extinction coefficients and were compared with the aureole lidar estimations. Aureole lidar estimated extinction coefficient profiles are similar in structure to the PMS-measured profiles and agreed well in extinction magnitude. When the near-surface aircraft aerosol measurements are averaged over a longer time, excellent agreement exists between the aureole lidar and the PMS-measured values. GRA

N92-29309*# Phillips Lab., Kirkland AFB, NM. Starfire Optical Range.
CHARACTERIZATION OF ARTIFICIAL GUIDESTARS GENERATED IN THE MESOSPHERIC SODIUM LAYER
M. P. Jelonek, R. Q. Fugate, W. J. Lange, A. C. Slavin, R. E. Ruane (Rockwell Power Systems, Albuquerque, NM.), and R. A. Cleis (Optical Sciences Co., Placentia, CA.) *In* NASA. Langley Research Center, Sixteenth International Laser Radar Conference, Part 1 Jul. 1992 p 301-304 (For primary document see N92-29228 20-35)
Avail: CASI HC A01/MF A04

N92-29310*# Massachusetts Inst. of Tech., Lexington. Lincoln Lab.
OPTICAL PUMPING OF MESOSPHERIC SODIUM: A NEW MEASUREMENT CAPABILITY
R. M. Heinrichs, T. H. Jeys, K. F. Wall, J. Korn, and T. C. Hotaling *In* NASA. Langley Research Center, Sixteenth International Laser Radar Conference, Part 1 Jul. 1992 p 305-308 (For primary document see N92-29228 20-35)
Avail: CASI HC A01/MF A04

N92-29311*# Illinois Univ., Urbana-Champaign. Dept of Electrical and Computer Engineering.
LIDAR PROBING OF THE MESOSPHERE: SIMULTANEOUS OBSERVATIONS OF SPORADIC SODIUM AND IRON FORMATIONS, CALCIUM ION LAYERS, NEUTRAL TEMPERATURE AND WINDS
Timothy J. Kane, Jun Qian, Daniel R. Scherrer, Daniel C. Senft, W. Matthew Pfenninger, George C. Papen, and Chester S. Gardner *In* NASA. Langley Research Center, Sixteenth International Laser Radar Conference, Part 1 Jul. 1992 p 309-312 (For primary document see N92-29228 20-35)
Avail: CASI HC A01/MF A04

N92-29312*# Tokyo Metropolitan Univ. (Japan). Dept. of Electronics and Information Engineering.
LIDAR MEASUREMENTS OF METALLIC SPECIES IN MESOPAUSE REGION
Chikao Nagasawa and Makoto Abo *In* NASA. Langley Research Center, Sixteenth International Laser Radar Conference, Part 1 Jul. 1992 p 313-316 (For primary document see N92-29228 20-35)
Avail: CASI HC A01/MF A04

N92-29314*# Illinois Univ., Urbana-Champaign. Dept. of Electrical and Computer Engineering.
SODIUM DOPPLER TEMPERATURE LIDAR OBSERVATIONS OF THE MESOPAUSE REGION TEMPERATURE AND WIND STRUCTURE
Daniel C. Senft, Daniel R. Scherrer, and Chester S. Gardner *In* NASA. Langley Research Center, Sixteenth International Laser Radar Conference, Part 1 Jul. 1992 p 321-323 (For primary document see N92-29228 20-35)
Avail: CASI HC A01/MF A04

N92-29315*# Illinois Univ., Urbana-Champaign. Dept. of Electrical and Computer Engineering.
AIRBORNE SODIUM AND RAYLEIGH LIDAR OBSERVATIONS FROM ALOHA-90
Chris A. Hostetler and Chester S. Gardner *In* NASA. Langley Research Center, Sixteenth International Laser Radar Conference, Part 1 Jul. 1992 p 325-328 (For primary document see N92-29228 20-35)
Avail: CASI HC A01/MF A04

N92-29317*# Photometrics, Inc., Woburn, MA.
ELASTIC AND RAMAN LIDAR TEMPERATURE MEASUREMENTS FROM POKER FLAT, ALASKA DURING FEBRUARY 1992
Michael Burka, Phan Dao (Phillips Lab., Hanscom AFB, MA.), Gilbert Davidson, Robert Farley (Phillips Lab., Hanscom AFB, MA.), John Meriwether (Phillips Lab., Hanscom AFB, MA.), and Alex Wilson (Phillips Lab., Hanscom AFB, MA.) *In* NASA. Langley Research Center, Sixteenth International Laser Radar Conference, Part 1 Jul. 1992 p 333-336 (For primary document see N92-29228 20-35)
Avail: CASI HC A01/MF A04

N92-29318*# Centre National de la Recherche Scientifique, Verrieres-Le Buisson (France). Service d'Aeronomie.
RAYLEIGH/RAMAN LIDARS: INTERCOMPARISONS AND VALIDATION
Marie-Lise Chanin *In* NASA. Langley Research Center, Sixteenth International Laser Radar Conference, Part 1 Jul. 1992

p 337-340 (For primary document see N92-29228 20-35)
Avail: CASI HC A01/MF A04

47 METEOROLOGY AND CLIMATOLOGY

Includes weather forecasting and modification.

N92-29424# Naval Postgraduate School, Monterey, CA.
MULTI-FRACTAL ANALYSIS OF NOCTURNAL BOUNDARY LAYER TIME SERIES FROM THE BOULDER ATMOSPHERIC OBSERVATORY M.S. Thesis
Alex J. DeCaria Mar. 1992 58 p
(AD-A248347) Avail: CASI HC A04/MF A01

Time series from a nocturnal boundary layer are analyzed using fractal techniques. The behavior of the self-affine fractal dimension, D(sub A), is found to drop during a gravity wave train and rise with turbulence. D(sub A) is proposed as a time series conditional sampling criterion for distinguishing waves from turbulence. Only weak correlations are found between D(sub A) bulk turbulence measures such as Brunt-Vaisala frequency, Richardson number and buoyancy length. The advantages of analysis over turbulent kinetic energy (TKE), its component variances, FFT spectra, and self-similar fractals are also discussed in terms of local versus global basis functions, dimensional suitability, noise, algorithm complexity, and other factors. D(sub A) was found to be the only measure capable of reliably distinguishing the wave from turbulence. GRA

N92-29565# Army Lab. Command, White Sands Missile Range, NM. Atmospheric Sciences Lab.
SENSITIVITY OF C2 SUB n TO RANDOM VARIATIONS OF WINDSPEED, SENSIBLE HEAT FLUX, AND LATENT HEAT FLUX Final Report
Henry Rachele and Arnold Tunick Mar. 1992 29 p
(AD-A248696; ASL-TR-0308) Avail: CASI HC A03/MF A01

The optical turbulence structure parameter, (C sub n) sq, is a primary parameter in expressions used to characterize electromagnetic energy and image propagation through the atmosphere. Examples of these expressions include the receiver coherence diameter and the atmospheric modulation transfer function. In this analysis, the authors write (C sub n) sq in terms of windspeed (V), sensible heat flux (H), and latent heat flux (L'E) assuming that their values are measured or modeled. Then the authors consider the effect on 2 (C sub n) sq if estimates of H, L'E, and V are assumed to be in error or vary (that is, due to sensor error and/or natural atmospheric variations). Micrometeorological data from Davis, California, are used to comprise two case studies. The results presented include bar charts of the modeled distributions of H; L'E; the surface friction velocity, U; the temperature and specific humidity scaling parameters, T and q; the Obukhov scaling length, L; the reference level (1 m) windspeed, V sub r; and finally (C sub n) sq for each case. GRA

N92-29653*# National Aeronautics and Space Administration. Goddard Space Flight Center, Greenbelt, MD.
MONTHLY MEANS OF SELECTED CLIMATE VARIABLES FOR 1985 - 1989
S. Schubert, C.-Y. Wu (General Sciences Corp., Laurel, MD.), J. Zero (General Sciences Corp., Laurel, MD.), J.-K. Schemm (General Sciences Corp., Laurel, MD.), C.-K. Park (Universities Space Research Association, Columbia, MD.), and M. Suarez Jun. 1992 390 p
(RTOP 578-41-07-20)
(NASA-TM-104565; NAS 1.15:104565; Rept-92B00088) Avail: CASI HC A17/MF A04

Meteorologists are accustomed to viewing instantaneous weather maps, since these contain the most relevant information for the task of producing short-range weather forecasts. Climatologists, on the other hand, tend to deal with long-term means, which portray the average climate. The recent emphasis on dynamical extended-range forecasting and, in particular measuring and predicting short term climate change makes it important that we become accustomed to looking at variations on monthly and longer time scales. A convenient toll for researchers to familiarize themselves with the variability which occurs in selected parameters on these time scales is provided. The format of the document was chosen to help facilitate the intercomparison of various parameters and highlight the year-to-year variability in monthly means. Author

N92-29666# Meteorological Satellite Center, Tokyo (Japan).
TAPERING CLOUDS AND THEIR CLASSIFICATION DUE MAINLY TO THE SURROUNDING CLOUD PATTERN IN THE GMS IMAGERY Technical Note No. 24
Hideki Itoh, Tadashi Asoh, and Masami Sakurada Mar. 1992 33 p In JAPANESE; In ENGLISH and JAPANESE
(ISSN-0388-9653) Avail: CASI HC A03/MF A01

Active convective clouds developed into an elongated triangular pattern is called Tapering Cloud (later referred to as TC) owing to the cloud shape in the satellite imagery. TC is closely associated with severe weather, such as heavy rain, tornados, and so on. We investigated the meteorological conditions and sub-synoptical cloud pattern where TC is involved, with GMS-4 satellite imagery over one year. Main results from this survey are as follows: (1) TC evolves mostly over the sea and occurred largely around Sakisima Islands in the southern part of the East China Sea; (2) Latitudinal locations of TC occurrence show a seasonal variation; (3) On about 80 percent of TCs, life time is shorter than 10 hours; (4) Approximately 80 percent of TCs can be identified in the satellite imagery to have a Cu line extending windward from the point of elongated triangular TC; (5) According to the surface weather chart of JMA, approximately half of TCs evolve near the front and another half evolve in the warm sector; and (6) All TCs evolve in the ascending area on the 700 mb P-velocity map.
Author

N92-29743# National Weather Service, Honolulu, HI.
TROPICAL CYCLONES: CENTRAL NORTH PACIFIC, 1991
A. K. T. Chun, R. T. Martin, H. E. Rosendal, and G. H. Trapp Apr. 1992 28 p
(PB92-167345; NOAA-TM-NWSTM-PR-37) Avail: CASI HC A03/MF A01

The Central Pacific Hurricane Season ended with just three tropical systems in the area. All three systems were hurricanes while they were in the eastern Pacific with ENRIQUE weakening to the depression state before entering the central Pacific. The season started out rather slowly with very little activity in June and early July. ENRIQUE was the first system to reach the central Pacific and continued to be an unusual system after developing into a hurricane for a short six hour period over the eastern Pacific on 17 Jul. 1991. Author

N92-29799# National Oceanic and Atmospheric Administration, Boulder, CO. Forecast Systems Lab.
LAPS SPECIFIC HUMIDITY ANALYSIS
D. L. Birkenheuer Feb. 1992 46 p
(PB92-163575; NOAA-TM-ERL-1; FSL-1) Avail: CASI HC A03/MF A01

This technical memorandum explains one aspect of the Local Analysis and Prediction System (LAPS) - the treatment of water vapor. LAPS is a collection of algorithms that has two major functions. One is to analyze atmospheric state variables from data germane to a forecast office. The second function derives fields from the state variables to help answer specific forecast questions. To date, the LAPS moisture analysis includes a cloud analysis of liquid and frozen water and a specific humidity (SH) analysis for the vapor phase. The SH analysis starts with the data source and analysis algorithm and is followed by example analyses (a clear case and one illustrating cloud treatment). Then current work and future plans of the SH analysis package are summarized. An appendix describes the horizontal shape matching (HSM) algorithm applied to this problem including the rationale used to choose the various HSM weighting coefficients. The technique to choose the HSM weighting coefficients can apply to other applications of variational analysis. Author

N92-29800# National Oceanic and Atmospheric Administration, Boulder, CO. Wave Propagation Lab.
TRACKING HURRICANE CLAUDETTE WITH THE US AIR FORCE OTH-B RADAR
T. M. Georges, J. A. Harlan, L. R. Meyer, and R. G. Peer Jan. 1992 45 p Prepared in cooperation with Colorado Univ., Boulder
(PB92-164524; NOAA-TM-ERL-WPL-219) Avail: CASI HC A03/MF A01

Hurricane Claudette was successfully tracked for three days using the 0.5-Hz (7-m) surface-wave-direction field mapping by the U.S. Air Force OTH-B over-the-horizon radar 2400 km away on the coast of Maine. Surface wave direction is displayed with 60-km resolution in the vicinity of the storm for five radar runs. The radar-derived track is compared with that published by the NOAA National Hurricane Center. Skewness and asymmetries in the apparent wave-direction field are noted. Author

N92-29801# National Weather Service, Washington, DC. Climate Analysis Center.
PROCEEDINGS OF THE 16TH ANNUAL CLIMATE DIAGNOSTICS WORKSHOP
Mar. 1992 476 p Workshop held in Los Angeles, CA, 28 Oct. - 28 Nov. 1991
(PB92-167378) Avail: CASI HC A21/MF A04

The Sixteenth Annual Climate Diagnostics Workshop was hosted by the Department of Atmospheric Sciences at the University of California in Los Angeles. The workshop consisted of 10 sessions, entitled: ENSO; low frequency variability; stratosphere; ocean circulations; ocean-atmosphere interaction; special section on contemporary climate-variations, problems, and issues; global climate change; hydrology and precipitation; ENSO and seasonal forecasts; and climate prediction. Author

N92-30034# National Oceanic and Atmospheric Administration, Oak Ridge, TN. Atmospheric Turbulence and Diffusion Div.
PRELIMINARY ANALYSIS OF WIND DATA FROM THE OAK RIDGE SITE SURVEY
R. M. Eckman, R. J. Dobosy, and W. R. Pendergrass Feb. 1992 54 p Sponsored by DOE
(PB92-174564; NOAA-TM-ERL-ARL-193) Avail: CASI HC A04/MF A01

The U.S. Department of Energy operates six nuclear-material plants that fall under the jurisdiction of Oak Ridge Operation (ORO), which is headquartered in Oak Ridge, Tennessee. All of the plants store chemicals that could produce a toxic atmospheric cloud during an accident. Although each plant had independently developed a capability to model and deal with hazardous atmospheric releases, ORO decided in 1986 to upgrade and integrate its emergency-response capability. Part of the upgrade involves the development and implementation of improved computer models for simulating atmospheric diffusion. Here, a preliminary analysis of wind data from the Oak Ridge site survey is presented. The survey began in the fall of 1989 and ended in December 1990. Since the three Oak Ridge plants are relatively close together, one meteorological survey was conducted for the entire Oak Ridge Reservation. Like the preliminary reports from the earlier site surveys, the primary goal is a recommendation on the number and general location of permanent meteorological towers.
Author

N92-30171# World Meteorological Organization, Geneva (Switzerland). World Climate Data Program.
CLICOM-NEWS, ISSUE 7
Feb. 1992 24 p
Avail: CASI HC A03/MF A01; WMO, Geneva, Switzerland

The Climate Computing (CLICOM) Newsletter is intended to keep countries informed of developments within the CLICOM project relating to the following: (1) the current status of the implemented systems; (2) implementation schedules and strategies; (3) hardware improvements; (4) software and manual up-grades; (5) product and application developments; and (6) problems. The Newsletter is issued in English only. However a section may be devoted to inputs from users in French and Spanish. These items are printed as received. Translation of the entire newsletter into other languages, by donor countries, will be welcomed. All CLICOM users are encouraged to contribute imformation and/or to write to the World Climate Data and Monitoring Program Office of the World Meteorological Organization (WMO) Secretariat concerning problems encountered or lessons learned with the CLICOM systems. Author

N92-29271*# Wisconsin Univ., Madison.
WIND PROFILES DERIVED FROM VOLUME IMAGING LIDAR DATA: ENHANCEMENTS TO THE ALGORITHM AND COMPARISONS WITH INSITU OBSERVATIONS
A. K. Piironen and E. W. Eloranta *In* NASA. Langley Research Center, Sixteenth International Laser Radar Conference, Part 1 Jul. 1992 p 157-160 (For primary document see N92-29228 20-35)
Avail: CASI HC A01/MF A04

N92-29272*# Wisconsin Univ., Platteville. Dept. of Physics.
MEASUREMENTS OF WIND DIVERGENCE WITH VOLUME IMAGING LIDAR
P. W. Young and E. W. Eloranta (Wisconsin Univ., Madison.) *In* NASA. Langley Research Center, Sixteenth International Laser Radar Conference, Part 1 Jul. 1992 p 161-164 (For primary document see N92-29228 20-35)
Avail: CASI HC A01/MF A04

N92-29291*# Bulgarian Academy of Sciences, Sofia. Inst. of Electronics.
CORRELATION ANALYSIS OF WIND LIDAR DATA
R. P. Avramova *In* NASA. Langley Research Center, Sixteenth International Laser Radar Conference, Part 1 Jul. 1992 p 233-236 (For primary document see N92-29228 20-35)
Avail: CASI HC A01/MF A04

N92-29296*# National Meteorological Center, Washington, DC. Development Div.
SCIENCE GOALS AND MISSION OBJECTIVES OF NASA'S LASER ATMOSPHERIC WIND SOUNDER PROGRAM
Wayman E. Baker *In* NASA. Langley Research Center, Sixteenth International Laser Radar Conference, Part 1 Jul. 1992 p 251-255 (For primary document see N92-29228 20-35)
Avail: CASI HC A01/MF A04

N92-29300*# GEC-Marconi Ltd., Borehamwood (England).
THE e-BEAM SUSTAINED LASER TECHNOLOGY FOR SPACE-BASED DOPPLER WIND LIDAR
M. J. Brown, W. Holman, R. J. Robinson, P. M. Schwarzenberger, I. M. Smith, S. Wallace, M. R. Harris (Defence Research Agency, Malvern, England), D. V. Willetts (Defence Research Agency, Malvern, England), and S. C. Kurzius (Lockheed Missiles and Space Co., Huntsville, AL.) *In* NASA. Langley Research Center, Sixteenth International Laser Radar Conference, Part 1 Jul. 1992 p 269-272 (For primary document see N92-29228 20-35)
Avail: CASI HC A01/MF A04

N92-29313*# Illinois Univ., Urbana-Champaign. Dept. of Electrical and Computer Engineering.
ERROR ANALYSIS OF WIND MEASUREMENTS FOR THE UNIVERSITY OF ILLINOIS SODIUM DOPPLER TEMPERATURE SYSTEM
W. Matthew Pfenninger and George C. Papen *In* NASA. Langley Research Center, Sixteenth International Laser Radar Conference, Part 1 Jul. 1992 p 317-320 (For primary document see N92-29228 20-35)
Avail: CASI HC A01/MF A04

N92-29316*# Phillips Lab., Hanscom AFB, MA. Ionospheric Physics Div.
RAYLEIGH/RAMAN GREENLAND LIDAR OBSERVATIONS OF ATMOSPHERIC TEMPERATURE DURING A MAJOR ARCTIC STRATOSPHERIC WARMING EVENT

John W. Meriwether, Robert Farley, R. McNutt, Phan D. Dao, and Warren P. Moskowitz (Photometrics, Inc., Woburn, MA.) *In* NASA. Langley Research Center, Sixteenth International Laser Radar Conference, Part 1 Jul. 1992 p 329-332 (For primary document see N92-29228 20-35)
Avail: CASI HC A01/MF A04

N92-29319*# Centre National de la Recherche Scientifique, Verrieres-Le Buisson (France). Service d'Aeronomie.
WIND MEASUREMENTS FROM 15 TO 50 KM WITH A DOPPLER RAYLEIGH LIDAR
A. Garnier and M. L. Chanin *In* NASA. Langley Research Center, Sixteenth International Laser Radar Conference, Part 1 Jul. 1992 p 341-344 (For primary document see N92-29228 20-35)
Avail: CASI HC A01/MF A04

N92-29320*# Commonwealth Scientific and Industrial Research Organization, Mordialoc (Australia). Div. of Atmospheric Research.
LIDAR STUDIES OF EXTINCTION IN CLOUDS IN THE ECLIPS PROJECT
C. Martin, R. Platt, Stuart A. Young, and Graeme P. Patterson *In* NASA. Langley Research Center, Sixteenth International Laser Radar Conference, Part 1 Jul. 1992 p 345-348 (For primary document see N92-29228 20-35)
Avail: CASI HC A01/MF A04

N92-29321*# York Univ. (Ontario). Dept. of Physics and Astronomy.
LIDAR STUDIES OF CLOUDS AT TORONTO DURING THE ECLIPS PROGRAM
S. R. Pal, A. I. Carswell, A. Y. Fong, I. Pribluda, and W. Steinbrecht *In* NASA. Langley Research Center, Sixteenth International Laser Radar Conference, Part 1 Jul. 1992 p 349-352 (For primary document see N92-29228 20-35)
Avail: CASI HC A01/MF A04

N92-29323*# Utah Univ., Salt Lake City. Dept. of Meteorology.
POLARIZATION LIDAR LIQUID CLOUD DETECTION ALGORITHM FOR WINTER MOUNTAIN STORMS
Kenneth Sassen and Hongjie Zhao *In* NASA. Langley Research Center, Sixteenth International Laser Radar Conference, Part 1 Jul. 1992 p 357-359 (For primary document see N92-29228 20-35)
Avail: CASI HC A01/MF A04

N92-29324*# National Oceanic and Atmospheric Administration, Boulder, CO. Wave Propagation Lab.
MEASUREMENT OF MEAN OR EFFECTIVE RADIUS OF CLOUD DROP SIZE DISTRIBUTIONS WITH A 10.6-MICRON WAVELENGTH LIDAR
Wynn L. Eberhard *In* NASA. Langley Research Center, Sixteenth International Laser Radar Conference, Part 1 Jul. 1992 p 361-364 Sponsored in part by NOAA (For primary document see N92-29228 20-35)
(Contract DE-FG02-90ER-61059)
Avail: CASI HC A01/MF A04

N92-29325*# National Aeronautics and Space Administration. Langley Research Center, Hampton, VA.
OBSERVATIONS OF CIRRUS CLOUDS OVER THE PACIFIC REGION BY THE NASA MULTIWAVELENGTH LIDAR SYSTEM
Syed Ismail, Edward V. Browell, Marta A. Fenn (STX Corp., Hampton, VA.), and Greg D. Nowicki (STX Corp., Hampton, VA.) *In its* Sixteenth International Laser Radar Conference, Part 1 Jul. 1992 p 365-368 (For primary document see N92-29228 20-35)
Avail: CASI HC A01/MF A04

N92-29327*# Arizona Univ., Tucson. Dept. of Electrical and Computer Engineering.
REMOTE SENSING BY SPACEBORNE LIDAR AIDED BY SURFACE RETURNS
J. A. Reagan and T. W. Cooley *In* NASA. Langley Research Center, Sixteenth International Laser Radar Conference, Part 1 Jul. 1992 p 373-376 (For primary document see N92-29228 20-35)
Avail: CASI HC A01/MF A04

N92-29328*# Atmospheric and Environmental Research, Inc., Cambridge, MA.
NWP IMPACT OF CLOUD TOP AND BOUNDARY LAYER WINDS FROM A SATELLITE BORNE LIDAR: AN OBSERVING SYSTEM SIMULATION EXPERIMENT
R. G. Isaacs, C. Grassotti, R. N. Hoffman, M. Mickelson, T. Nehrkorn, and J.-F. Louis *In* NASA. Langley Research Center, Sixteenth International Laser Radar Conference, Part 1 Jul. 1992 p 377-380 (For primary document see N92-29228 20-35)
(Contract F19628-89-C-0137)
Avail: CASI HC A01/MF A04

48 OCEANOGRAPHY

Includes biological, dynamic, and physical oceanography; and marine resources.

For related information see also *43 Earth Resources and Remote Sensing.*

N92-29345# North Carolina Univ., Greensboro. Dept. of Biology.
OCEAN OPTICAL MODELING: LIGHT FIELD STRUCTURE, INTERNAL RADIANT EMISSION, AND VERTICAL INHOMOGENEITIES Annual Letter Report
Robert H. Stavn 1992 8 p
(Contract N00014-89-J-3137)
(AD-A248272) Avail: CASI HC A02/MF A01

The overall goals of this project are the determination of the most significant optical parameters needed for the modeling and prediction of the penetration and second-order reemission of light in the sea. This problem is confounded by the multiple scattering of the penetrating and secondarily emitted photons. This multiple scattering phenomenon creates non-linearities in the submarine photic field which dictates that the most efficient approach to solve the problem is the Monte Carlo simulation of photon penetration. I have been developing code for Monte Carlo simulations of photon penetration and an exciting development is the porting of this code to the Cray Y-MP supercomputer. I have been given computer time for this development at the North Carolina Supercomputer Center, and I have also done development on the Primary Oceanographic Prediction System (POPS) at the Cray Y-MP of the U.S. Naval Oceanographic Office, Stennis Space Center, Bay St. Louis, MS. In the short term the operational limits for the optical parameters used to characterize the light climate for the open ocean will be established. These limits on the parameters that can be conveniently measured (apparent optical properties) will be determined from the Monte Carlo simulations employing the inherent optical properties. That is, the apparent optical properties can be derived from the Monte Carlo simulations using the inherent optical properties. Thus, reliable links will be established between the easily measured apparent optical properties and the more difficult inherent optical properties. The end result of this effort connecting the inherent and apparent optical properties will be a robust and reliable 'standard ocean model'. GRA

N92-29439# Columbia Univ., Palisades, NY. Geological Observatory.
CIRCULATION AND EXCHANGE AT THE CONTINENTAL SHELF AND SLOPE SEEP-2
R. W. Houghton and Hsien-Wang Ou 1991 5 p
(Contract DE-FG02-89ER-60818)
(DE92-013500; DOE/ER-60818/3) Avail: CASI HC A01/MF A01

This project was a component of the SEEP-2 program. It

contributed to the instrumentation of the SEEP-2 moored array to the processing and analysis of the time-series data of water temperature and currents, and to a theoretical modeling study of the circulation on the continental margin. We are responsible for nearly half of the current meters and thermistor chains that were deployed in the SEEP-2 moored array on the continental margin off the Delmarva peninsula. Data tapes derived from three deployments of the instruments in this array were processed. A second component of this project was a theoretical study of the interaction of the Gulf Stream with the continental margin north of Cape Hatteras. The model shows how the topographic influence on the local vorticity balance leads to back-folding filaments of Gulf Stream water and to the Slope Sea gyre circulation. DOE

N92-29554# Washington Univ., Seattle. Applied Research Lab.
SOUND SPEED, REFLECTIVITY, AND ABSORPTION MEASUREMENTS IN ARCTIC ICE IN 1988
T. Wen, G. R. Garrison, R. E. Francois, R. P. Stein, and W. J. Felton Mar. 1991 147 p
(Contract N00039-88-C-0054)
(AD-A246293; APL-UW-TR-9005) Avail: CASI HC A07/MF A02

Acoustic measurements at 20-300 kHz were made in the Arctic in Spring 1988 to study sound speed and absorption within the ice canopy and the reflectivity of the water-ice interface. An average sound speed of 3669 + or - 29 m/s was found for first-year ice, with evidence that the speed varied from 3800 m/s in solid ice to 2000 m/s in the socalled skeletal layer at the lower boundary. The absorption, alpha, for vertical transmissions was found to be three times as high as that given in the literature for horizontal transmissions; the recommended frequency and temperature dependence is alpha = 0.19f(-6/T)(to the 2/3 power) for temperatures between T = -2 and T = -20 C. The reflectivity of the lower surface of the ice decreased from 0.2 at 20 KHz to 0.04 at 200 kHz for sound impinging at normal incidence. A simple model that treats the echoes as the sum of reflections from two surfaces, one at the interface between the water and the skeletal layer and one at the transition from the porous skeletal layer to solid ice, matches the experimental results with reasonable accuracy. GRA

N92-29562# RASCON Associates, West Falmouth, MA.
FINITE DIFFERENCE MODELLING OF SEISMIC WAVE PROPAGATION AT THE SEAFLOOR Final Report
R. A. Stephen 1991 29 p
(Contract N00014-88-M-6610)
(AD-A248345; NOARL-CR-026-91) Avail: CASI HC A03/MF A01

The objectives of this study were (1) to implement the WHOI finite difference code on the CONVEX computer at NORDA and (2) to run a suite of models on the effects of lateral heterogeneity on the primary response from the seafloor. Finite difference solutions to the elastic wave equation accurately predict the response of impulsive and continuous waves sources. Wave types included are reflections, refractions, diffractions, Stoneley and pseudo-Rayleigh waves, evanescent waves and head waves. The primary disadvantage of the method is that it is very computation intensive and it is generally limited to problems with dimensions of only a few tens of wavelengths. This can be partially alleviated by using powerful computers such as the CONVEX at NORDA. GRA

N92-29618# Teledyne Geotechnical, Alexandria, VA.
LAND-BASED SEISMIC ARRAY STUDIES OF LOW FREQUENCY AMBIENT OCEANIC NOISE Final Report
Robert K. Cessaro Feb. 1992 44 p
(Contract N00014-90-C-0118)
(AD-A248255; TGAL-92-13) Avail: CASI HC A03/MF A01

Low frequency (0.01 to 0.2 Hz) seismic noise, arising from pelagic storms, is commonly observed as microseisms in seismic records from land and ocean bottom detectors. One principal research objective, in the study of microseisms, has been to locate their sources. This paper reports on an analysis of primary and secondary microseisms recorded simultaneously on three land-based long-period arrays (Alaskan Long Period Array, Montana Large Aperture Seismic Array, and Norwegian Seismic Array) during the early 1970's. Reliable microseism source locations are determined by wide-angle triangulation, using the azimuths of approach obtained from frequency wave-number analysis of the records of microseisms propagating across these arrays. Two near-shore sources of both primary and secondary microseisms appear to be persistent in the sense that they are associated with essentially constant near-shore locations. Secondary microseisms are observed to emanate from wide ranging pelagic locations in addition to the same near-shore locations determined for the primary microseisms. GRA

N92-29684# Bidston Observatory, Merseyside (England).
CLASS A NETWORK DATARING GAUGES: 1989 DATA PROCESSING AND ANALYSIS
S. M. Shaw 1991 133 p Sponsored by MAAF
(Rept-18-1991; ETN-92-91343) Avail: CASI HC A07/MF A02; Proudman Oceanographic Lab., Bidston Observatory, Birkenhead, Merseyside L43 7RA, England, HC

The sea level data processing for 1989 from 20 modernized Dataring sites around the United Kingdom coast is reported. The results for 1989 from these sites, each with percentage returns of data in excess of 86 percent are presented. A general description of the system configuration and methods of recording elevations at each site is presented. Details of site visits, processing details, harmonic constants from an independent analysis, frequency distribution curves and cumulative frequency curves are included. The 1989 statistics for extreme and mean sea levels, and surge residuals for all 20 sites are given. ESA

N92-29686*# National Aeronautics and Space Administration. Goddard Space Flight Center, Greenbelt, MD.
SeaWiFS TECHNICAL REPORT SERIES. VOLUME 1: AN OVERVIEW OF SeaWiFS AND OCEAN COLOR
Stanford B. Hooker, ed., Elaine R. Firestone, ed. (General Sciences Corp., Laurel, MD.), Wayne E. Esaias, Gene C. Feldman, Watson W. Gregg, and Charles R. McClain Jul. 1992 28 p
(NASA-TM-104566-Vol-1; Rept-92B00089; NAS 1.15:104566-Vol-1) Avail: CASI HC A03/MF A01

The purpose of this series of technical reports is to provide current documentation of the Sea-viewing Wide Field-of-view Sensor (SeaWiFS) Project activities, instrument performance, algorithms, and operations. This documentation is necessary to ensure that critical information related to the quality and calibration of the satellite data is available to the scientific community. SeaWiFS will bring to the ocean community a welcomed and improved renewal of the ocean color remote sensing capability lost when the Nimbus-7 Coastal Zone Color Scanner (CZCS) ceased operating in 1986. The goal of SeaWiFS, scheduled to be launched in August 1993, is to examine oceanic factors that affect global change. Because of the role of phytoplankton in the global carbon cycle, data obtained from SeaWiFS will be used to assess the ocean's role in this cycle, as well as other biogeochemical cycles. SeaWiFS data will be used to help elucidate the magnitude and variability of the annual cycle of primary production by marine phytoplankton and to determine the distribution and timing of spring blooms. The observations will help to visualize the dynamics of ocean and costal currents, the physics of mixing, and the relationships between ocean physics and large-scale patterns of productivity. The data will help fill the gap in ocean biological observations between those of the CZCS and the upcoming Moderate Resolution Imaging Spectrometer (MODIS) on the Earth Observing System-A (EOS-A) satellite. Author

N92-29704# Florida State Univ., Tallahassee. Dept. of Oceanography.
NUMERICAL MODELING STUDIES OF THE GULF OF MEXICO AND THE CARIBBEAN SEA USING THE BRYAN-COX MODEL Final Report
W. Sturges and S. Welsh Dec. 1991 109 p Sponsored in part by Minerals Management Service, New Orleans, LA

(Contract DI-14-12-0001-30363)
(PB92-164987; OCS/MMS-91/0061) Avail: CASI HC A06/MF A02

A numerical model of the Gulf Stream formation region was developed, based on the Bryan-Cox-Semtner, or 'DFDL', primitive equation formulation. It is fully nonlinear with 12 levels and has realistic topography in each level. It includes the western North Atlantic from the mid-Atlantic ridge into the Caribbean Sea, the Gulf of Mexico, and the east coast of the United States to Cape Hatteras. A new feature of the model is the manner of forcing along the boundary. The vertical shear is set by the historical (observed) mean density field at the eastern boundary, and the total transport by the curl of the wind stress. The model was initialized with the mean density field and is forced by mean winds. The following seven years of model runs are the basis of the work reported here, when the model appears to have reached statistical equilibrium and the flow in the Straits of Florida is no longer increasing. Author

N92-29805# Woods Hole Oceanographic Inst., MA.
SHELF MIXED LAYER EXPERIMENT (SMILE) PROGRAM DESCRIPTION AND COASTAL AND MOORED ARRAY DATA REPORT
C. A. Alessi, S. J. Lentz, and R. C. Beardsley Dec. 1991 210 p
(Grant NSF OCE-87-16937)
(PB92-170281; WHOI-91-39) Avail: CASI HC A10/MF A03

The Shelf Mixed Layer Experiment (SMILE) was designed to study the response of the oceanic surface boundary layer over the continental shelf to atmospheric forcing. The SMILE field program was conducted over the northern California shelf between Pt. Arena and Pt. Reyes from mid-November 1988 to mid-May 1989. The field program consisted of five main components: (1) a long-term moored array to obtain current, temperature, and conductivity time series observations in the upper ocean over the shelf; (2) a short-term moored instrument deployment to measure the vertical current shear and stratification in the top 6 m of the water column; (3) shipboard CTD and acoustic Doppler current profiler (ADCP) surveys over the shelf and adjacent slope to map regional water property and current distributions; (4) a long-term moored and coastal meteorological array including one sounding station to obtain time series observations of the atmospheric surface forcing and monitor the structure of the marine boundary layer; and (5) overflights with an instrumented aircraft to measure the spatial structure of the surface wind, wind stress, and heat flux fields under different atmospheric conditions. The objectives are to describe the SMILE field program, including overviews of the five components, and to present a statistical and graphical summary of the atmospheric (wind, air temperature, pressure, relative humidity, short- and long-wave radiation) and oceanic (current, water temperature, and conductivity) long-term array measurements made as part of SMILE. Author

N92-29806# Woods Hole Oceanographic Inst., MA.
OCEANUS 218: WARM RING INERTIAL CRITICAL LAYER EXPERIMENT (WRINCLE) Technical Report, 20 Mar. - 9 Apr. 1990
R. W. Schmitt and E. T. Montgomery Nov. 1991 40 p
(Grant NSF OCE-89-11053)
(PB92-170299; WHOI-91-33) Avail: CASI HC A03/MF A01

The scientific objective of the Warm Ring Inertial Critical Layer Experiment (WRINCLE) was to study the phenomenon of inertial-internal wave trapping in anticyclonic rings and the associated mixing. High resolution profiler (HRP) casts provided fine- and microstructure data, and the Richardson Number float and expendable current profiler (XCP) surveys provided velocity and density finestructure measurements. During the time R/V Oceanus was in and around the ring, 78 HRP drops to 1000 m were completed, and data from 55 XCP's, 26 conductivity temperature and depth profiler (CTD) casts, and 59 expendable bathythermographs (XBT's) were logged. The report documents the work performed at sea, and summarizes some of the data collected. Author

N92-30193*# National Aeronautics and Space Administration. Goddard Space Flight Center, Greenbelt, MD.
SeaWIFS TECHNICAL REPORT SERIES. VOLUME 5: OCEAN OPTICS PROTOCOLS FOR SeaWIFS VALIDATION
James L. Mueller (San Diego State Univ., CA.), Roswell W. Austin (San Diego State Univ., CA.), Stanford B. Hooker, ed., and Elaine R. Firestone, ed. (General Sciences Corp., Laurel, MD.) Jul. 1992 48 p Workshop held in Monterey, CA, 9-12 Apr. 1991; sponsored by SeaWiFS Project Office
(NASA-TM-104566; NAS 1.15:104566; Rept-92B00097-Vol-5)
Avail: CASI HC A03/MF A01

Protocols are presented for measuring optical properties, and other environmental variables, to validate the radiometric performance of the Sea-viewing Wide Field-of-view Sensor (SeaWiFS), and to develop and validate bio-optical algorithms for use with SeaWiFS data. The protocols are intended to establish foundations for a measurement strategy to verify the challenging SeaWiFS accuracy goals of 5 percent in water-leaving radiances and 35 percent in chlorophyll alpha concentration. The protocols first specify the variables which must be measured, and briefly review rationale. Subsequent chapters cover detailed protocols for instrument performance specifications, characterizing and calibration instruments, methods of making measurements in the field, and methods of data analysis. These protocols were developed at a workshop sponsored by the SeaWiFS Project Office (SPO) and held at the Naval Postgraduate School in Monterey, California (9-12 April, 1991). This report is the proceedings of that workshop, as interpreted and expanded by the authors and reviewed by workshop participants and other members of the bio-optical research community. The protocols are a first prescription to approach unprecedented measurement accuracies implied by the SeaWiFS goals, and research and development are needed to improve the state-of-the-art in specific areas. The protocols should be periodically revised to reflect technical advances during the SeaWiFS Project cycle. Author

N92-29295*# Moscow State Univ. (USSR). Dept. of Physics.
IN VIVO AND IN VITRO CHLOROPHYLL-A AND PHEOPHYTIN-A CONCENTRATION MEASUREMENTS BY LASER FLUOROMETRY
A. A. Demidov, E. V. Baulin, and E. A. Chernyavskaya *In* NASA. Langley Research Center, Sixteenth International Laser Radar Conference, Part 1 Jul. 1992 p 247-250 (For primary document see N92-29228 20-35)
Avail: CASI HC A01/MF A04

51 LIFE SCIENCES (GENERAL)

N92-29397*# National Aeronautics and Space Administration. Ames Research Center, Moffett Field, CA.
IN VITRO MEASUREMENT OF NUCLEUS PULPOSUS SWELLING PRESSURE: A NEW TECHNIQUE FOR STUDIES OF SPINAL ADAPTATION TO GRAVITY
A. R. Hargens, M. G. Glover (California Univ., San Diego.), M. M. Mahmood (California Univ., San Diego.), S. Gott (California Univ., San Diego.), S. R. Garfin (California Univ., San Diego.), R. Ballard, G. Murthy, and M. D. Brown (Miami Univ., FL.) Jan. 1992 10 p
(RTOP 199-14-12-04)
(NASA-TM-103853; A-91108; NAS 1.15:103853) Avail: CASI HC A02/MF A01

Swelling of the intervertebral disc nucleus pulposus is altered by posture and gravity. We have designed and tested a new osmometer for in vitro determination of nucleus pulposus swelling pressure. The functional principle of the osmometer involves compressing a sample of nucleus pulposus with nitrogen gas until saline pressure gradients across a 0.45 microns Millipore filter are eliminated. Swelling pressure of both pooled dog and pooled pig lumbar disc nucleus pulposus were measured on the new osmometer and compared to swelling pressures determined using the equilibrium dialysis technique. The osmometer measured

swelling pressures comparable to those obtained by the dialysis technique. This osmometer provides a rapid, direct, and accurate measurement of swelling pressure of the nucleus pulposus.
Author

N92-29410# Johns Hopkins Univ., Baltimore, MD. School of Medicine.
EFFECTS OF IONIZING RADIATION ON AUDITORY AND VISUAL THRESHOLDS Technical Report, 9 Oct. 1987 - 28 May 1991
Robert D. Hienz Mar. 1992 47 p
(Contract DNA001-87-C-0277)
(AD-A248199) Avail: CASI HC A03/MF A01

An experimental analysis of the effects of low-dose ionizing radiation on sensory and motor function was conducted in baboons. Animals were trained using a reaction time procedure to respond to near-threshold acoustic and visual stimuli, and quantitative assessments were made of radiation-induced changes in absolute auditory and visual thresholds and reaction times. Animals received multiple exposures at single fractionated dose levels of 1, 2, and 5 Gy. Single exposures at higher exposure levels of 10 and 15 Gy were also examined. 100-200 cGy exposures produced transient changes in reaction times. Transient increases in reaction times occurred following low-dose exposures, usually within 1-3 weeks following the exposure. These increases typically recovered to normal baseline levels within 2-3 weeks. 1000 and 1500 cGy exposures produced long-term hearing deficits which were not frequency-specific. The severe hearing loss was most likely due to a sensorineural deficit, since complete loss of function of the tympanic membrane or middle ear ossicles would be expected to produce a hearing loss about 50-55 dB. These higher radiation doses have had less of an effect on visual intensity thresholds, producing a 5-1O dB deficit in visual thresholds. No physical damage to the cornea, iris, lens, or retina was observed. GRA

N92-29732# Technische Univ., Delft (Netherlands). Dept. of Biochemical Engineering.
METHODOLOGY ON MONITORING AND MODELLING OF MICROBIAL METABOLISM Ph.D. Thesis
Hendrik Jan Noorman 1991 255 p
(ETN-92-91745) Avail: CASI HC A12/MF A03

The methodology to obtain mechanistical, dynamical microbial system descriptions is described. The energetics and regulation of the metabolism of Acinetobacter calcoaceticus, grown in the presence of acetate and xylose are investigated. Mathematical modeling and experimental verification are combined. The reactor is considered and the development of some practical tools is described. Mathematical methods to analyze microbial system descriptions and experimental data are given. The stoichiometric and kinetic parameters of the Acinetobacter system are studied. For individual titles, see N92-29733 through N92-29740.

N92-29733# Technische Univ., Delft (Netherlands).
LINEAR RELATIONS IN MICROBIAL REACTION SYSTEMS: A GENERAL OVERVIEW OF THEIR ORIGIN, FORM, AND USE
Hendrik Jan Noorman, J. J. Heijnen, and K. C. A. M. Luyben *In its* Methodology on Monitoring and Modelling of Microbial Metabolism 1991 p 25-61 Submitted for publication (For primary document see N92-29732 20-51)
Avail: CASI HC A03/MF A03

In microbial reaction systems, there are a number of linear relations among net conversion rates, useful in the analysis of experimental data. A general approach for the formulation and application of the linear relations is provided. Two types of system descriptions, one considering the biomass as a black box and the other based on metabolic pathways, are defined in a linear vector and matrix algebra framework. A correct a priori description can be obtained by three useful tests: the independency, consistency and observability tests. The sets of linear relations obtained from the two system descriptions are different. Conservation relations, derived from element, electrical charge, energy and Gibbs energy balances are provided by the black box approach. In addition to the conservation relations, metabolic and reaction relations are provided by the metabolic approach. A number of different types of linear relations given in the literature are reviewed. They are classified according to the different categories that result from the black box or the metabolic system description. Validation of hypotheses related to metabolic pathways are supported by experimental validation of the linear metabolic relations. ESA

N92-29734# Technische Univ., Delft (Netherlands).
MODELLING AND EXPERIMENTAL VALIDATION OF CARBON DIOXIDE EVOLUTION IN ALKALOPHILIC CULTURES
Hendrik Jan Noorman, G. C. A. Luijkx, K. C. A. M. Luyben, and J. J. Heijnen *In its* Methodology on Monitoring and Modelling of Microbial Metabolism 1991 p 65-93 Submitted for publication (For primary document see N92-29732 20-51)
Avail: CASI HC A03/MF A03

The chemical reactions involving carbon dioxide in mineral culture media are considered. A mathematical model is set up. The reactions were studied in three different aqueous solutions, being water, mineral salt medium and a suspension with nongrowing bacterial cells. For each situation, three methods were compared for the determination of the bicarbonate concentration on the solution: equilibrium state total carbon analysis, dynamic monitoring of the rate of acid or alkali addition, and dynamic measurement of the carbon dioxide gas phase mole fraction. In a batch stirred tank reactor, the equilibrium constant agreed with the published value, and the three bicarbonate analysis methods gave the same results. A real alkalophilic process, using Acinetobacter calcoaceticus in a continuous stirred tank reactor at steady state, gave results in accord with the literature. However, the results do not allow validation of the equation expressing the nonideality. The steady state in the batch system and in continuous culture is well described with the mathematical model. However, in the transient state some unexplained differences between simulation and measurement, are noted. ESA

N92-29735# Technische Univ., Delft (Netherlands).
MICROBIAL ALDONOLACTONE FORMATION AND HYDROLYSIS: KINETIC AND BIOENERGETIC ASPECTS
Hendrik Jan Noorman, J. L. L. Rakels, J. G. Kuenen, K. C. A. M. Luyben, and J. J. Heijnen *In its* Methodology on Monitoring and Modelling of Microbial Metabolism 1991 p 97-126 Submitted for publication (For primary document see N92-29732 20-51)
Avail: CASI HC A03/MF A03

During growth in mixtures of acetate and aldose sugars, the growth yield of the bacterium Acinetobacter caloaceticus was increased when aldonolactone hydrolysis occurred. The underlying mechanism was investigated by studying the relationship between cellular yield and lactone hydrolysis in a quantitative way. The literature on the kinetics of acid formation from aldonolactones was reviewed. The reaction pattern is composed of lactone isomerization and hydrolysis steps which occur in series. In the acid pH range, lactone interconversion is the slowest step, whereas above pH 7 hydrolysis is rate/limiting for acid formation. Only for D-gluconolactone could a detailed mechanistic model be constructed. For a number of other aldonolactones including D-xylono and D-galactono lactone, an empirical kinetic equation was derived. The rate constants of these lactones are much smaller than for gluconolactone. The kinetic model of the hydrolysis of xylonolactone was tested, using the electrical charge balance in the Acinetobacter system. The published biomass yield data and the rate of lactone hydrolysis were compared. The observed relation seems to be only apparent. The electrical charge balance in the study of processes in which charged compounds are being converted is shown to be powerful. ESA

N92-29736# Technische Univ., Delft (Netherlands).
THE BIOREACTOR OVERFLOW DEVICE: AN UNDESIRED SELECTIVE SEPARATOR IN CONTINUOUS CULTURES?
Hendrik Jan Noorman, J. Baksteen, J. J. Heijnen, and K. C. A. M. Luyben *In its* Methodology on Monitoring and Modelling of Microbial Metabolism 1991 p 129-145 Submitted for publication (For primary document see N92-29732 20-51)
Avail: CASI HC A03/MF A03

Nonhomogeneous cell suspensions in a continuous culture may result in a difference between the biomass concentrations in the culture vessel and the effluent. This will have important consequences for values calculated for stoichiometric and kinetic coefficients. For the bacterium Acinetobacter calcoaceticus, the cells were shown to tend to be buoyant, and because of this, if the vessel overflow device is not designed properly, cells will be selectively removed from the reactor. Two different effluent removal devices were compared, only one of which functioned well. The experimental results obtained for this microbial system are described. ESA

N92-29737# Technische Univ., Delft (Netherlands).
CLASSIFICATION, ERROR DETECTION, AND RECONCILIATION OF MEASUREMENTS IN COMPLEX BIOCHEMICAL SYSTEMS
Hendrik Jan Noorman, K. C. A. M. Luyben, and J. J. Heijnen *In its* Methodology on Monitoring and Modelling of Microbial Metabolism 1991 p 149-178 Submitted for publication (For primary document see N92-29732 20-51)
Avail: CASI HC A03/MF A03

The applicability of the balancing method to a relatively complex microbial reaction system was investigated. The bacterium is used as a model system for energetic studies because its cellular energy balance can be manipulated. The balancing method, comprising rate classification measurement error detection and data reconciliation, is outlined. A black box and a metabolic description of the Acinetobacter system are made. Experiments using continuous cultures in steady state are described and the results are reported. The balancing method is applied to the experimental data. ESA

N92-29738# Technische Univ., Delft (Netherlands).
ON THE ESTIMATION OF BIOENERGETIC PARAMETERS
Hendrik Jan Noorman, B. Romein, K. C. A. M. Luyben, and J. J. Heijnen *In its* Methodology on Monitoring and Modelling of Microbial Metabolism 1991 p 181-203 Submitted for publication (For primary document see N92-29732 20-51)
Avail: CASI HC A03/MF A03

The occurrence and magnitude of the cell yield increase was studied over a broad range of specific growth rates. The effect was described with a mathematical model, where the energetics are covered by three basic parameters: the efficiency of oxidative phosphorylation, the yield of biomass in Adenosine Triphosphate (ATP), and the ATP turnover constant. The Acinetobacter system is described, leading to the formulation of the ATP balance. Experiments, using continuous cultures in steady state, are described. Macroscopic parameters and ATP coefficients are estimated for the Acinetobacter systems. The results are interpreted in physiological terms. ESA

N92-29739# Technische Univ., Delft (Netherlands).
FLUX-CAPACITY RELATIONSHIPS OF ACINETOBACTER CALCOACETICUS ENZYMES DURING XYLOSE OXIDATION
Hendrik Jan Noorman, G. Lukito, J. J. Heijnen, and K. C. A. M. Luyben *In its* Methodology on Monitoring and Modelling of Microbial Metabolism 1991 p 207-225 Submitted for publication (For primary document see N92-29732 20-51)
Avail: CASI HC A03/MF A03

The regulation of acetate consumption, xylose oxidation via glucose dehydrogenase, Isocitrate Lyase (ICL) activity and NADPH dependent Isocitrate Dehydrogenase (ICDPH) activity on Acinetobacter is described as a function of the specific growth rate and the presence of xylose. The ability to oxidize xylose was constitutively present, but could be further induced by the supply of xylose. The maximum acetate conversion rate increased with increasing specific growth rates, and showed an overcapacity at low dilution rates. The substrate flow through ICDPH and ICL increased at higher increasing specific growth rates, although only 20 percent of the capacity was used. Under some conditions, ICDPH activity was reduced by the supply of xylose to the culture. The results are discussed in relation to the cellular energy budget, and simple kinetic expressions are developed to describe the observations. ESA

N92-29740# Technische Univ., Delft (Netherlands).
ANALYSIS AND EXPERIMENTAL TESTING OF A BOTTLENECK MODEL FOR THE DESCRIPTION OF MICROBIAL DYNAMICS
Hendrik Jan Noorman, J. A. C. Langerak, M. G. Musch, J. J. Heijnen, and K. C. A. M. Luyben *In its* Methodology on Monitoring and Modelling of Microbial Metabolism 1991 p 229-257 Submitted for publication (For primary document see N92-29732 20-51)
Avail: CASI HC A03/MF A03

Cellular control mechanisms play an important role in the productivity of large scale biotechnological processes. They can be studied in isolation in small scale reactors, by monitoring the microbial response after a deliberate disturbance of a steady state. Generally, a two phase response is observed, involving a rapid utilization of a metabolic overcapacity and a slow subsequent reorganization of the macromolecular composition. This was quantified in a mathematical bottleneck model, with a simple representation of enzyme activation and deactivation phenomena. Steady and transient states were described with the same model, where, for each substrate, the dynamic state allows the separate determination of the activation and deactivation parameters which are pumped on the steady state. This model was experimentally tested, using Acinetobacter calcoaceticus in continuous cultures, supplied with acetate and xylose. Transient states were obtained by a stepwise shift of the dilution rate and the xylose/acetate feed ratio. A strong dependency of the regulatory parameters of acetate and xylose conversion on the presence of xylose is reported. ESA

N92-29754# Technische Univ., Delft (Netherlands).
STATE ESTIMATION AND ERROR DIAGNOSIS FOR BIOTECHNOLOGICAL PROCESSES Ph.D. Thesis
Reinier Thomas Jacob vanderHeijden 1991 192 p (ETN-92-91744) Avail: CASI HC A09/MF A02

A means of obtaining a more accurate and reliable characterization of the process state, without additional process information, and an improvement of the possibilities for process control are discussed. The currenty available methods for state estimation are overviewed. The application of a state estimation within a process controller is described. An analytical approach is used to develop an insensitive state estimator. Systematic methods to check the consistency of the measurements are discussed. For individual titles, see N92-29755 through N92-29760.

N92-29755# Technische Univ., Delft (Netherlands).
THE USE OF STATE ESTIMATORS (OBSERVERS) FOR ON-LINE ESTIMATION OF NON-MEASURABLE PROCESS VARIABLES
Reinier Thomas Jacob vanderHeijden, C. Hellinga, K. C. A. M. Luyben, and G. Honderd *In its* State Estimation and Error Diagnosis for Biotechnological Processes 1991 p 17-29 (For primary document see N92-29754 20-51)
Avail: CASI HC A03/MF A02

An approach to the measurement of key variables in bioprocess control, which uses direct online measurements made in conjunction with a computational model of the process to obtain estimates for the values of less easily measurable variables, is considered. This information can be used to control the process. The combination of model and measurement is known as an observer. The measurements taken are used to correct the state estimates provided by the model. The art of using observers lies in the development of good models and appropriate corrections. Several alternatives for the tuning of observers are presented. Attention is paid to the effect of model errors. Adaptive structures, used to correct the model, may be helpful in solving the bias caused in the estimates. Some recent developments are discussed. ESA

N92-29756# Technische Univ., Delft (Netherlands).
STATE ESTIMATION AND CONTROL OF THE IBE-FERMENTATION WITH PRODUCT RECOVERY
Reinier Thomas Jacob vanderHeijden, W. J. Groot, C. Hellinga, G. Honderd, and K. C. A. M. Luyben *In its* State Estimation and Error Diagnosis for Biotechnological Processes 1991 p 31-45 (For primary document see N92-29754 20-51)
Avail: CASI HC A03/MF A02

The control of the combined process for the continuous production of Isopropanol, Butanol, and Ethanol (IBE) from whey permeate is discussed. This process consists of a fluidized bed reactor coupled with a product recovery unit. Immobilized clostridia are used for this fermentation. The process combined a high biomass retention with relatively low product concentrations. The experimental setup is described. The mathematical model is presented and the state observer is examined. The two different control strategies are developed and the results of both control strategies are compared. ESA

N92-29757# Technische Univ., Delft (Netherlands).
A LOW SENSITIVITY OBSERVER FOR COMPLEX BIOTECHNOLOGICAL PROCESSES
Reinier Thomas Jacob vanderHeijden, P. F. W. Goverde, C. Hellinga, K. C. A. M. Luyben, and G. Honderd *In its* State Estimation and Error Diagnosis for Biotechnological Processes 1991 p 47-66 (For primary document see N92-29754 20-51)
Avail: CASI HC A03/MF A02

Process monitoring and control are frequently hindered by a lack of on-line information. State estimators may be used to estimate the actual values of unmeasurable process variables. However, errors in the process model incorporated in the estimator can easily cause a bias in the estimated variables. Sometimes, these errors are successfully reduced by implementation of a parameter estimator. An alternative approach: the low sensitivity observer is presented. This estimator is so tuned as to minimize sensitivity to certain errors in the process model. A low sensitivity observer was developed for a relatively complex process with five state variables, fourteen model parameters, and two online measurements. A numerical solution is presented. The problem of analyzing the large amount of simulation data was solved. An example of how such a low sensitivity observer can be made insensitive with respect to the given model errors is presented. This low sensitivity observer is used with experimental data to show that it is insensitive as required during the steady state. This result indicates that the theory of low sensitivity observers is more generally applicable than thought. ESA

N92-29758# Technische Univ., Delft (Netherlands).
ANALYTICAL TUNING OF A LOW SENSITIVITY OBSERVER APPLIED TO A CONTINUOUS ETHANOL FERMENTATION WITH PRODUCT RECOVERY
Reinier Thomas Jacob vanderHeijden, B. Romein, C. Hellinga, G. Honderd, and K. C. A. M. Luyben *In its* State Estimation and Error Diagnosis for Biotechnological Processes 1991 p 67-86 (For primary document see N92-29754 20-51)
Avail: CASI HC A03/MF A02

The influence of parameter errors in the process model used in an observer is described. In controlling a biotechnological process, the process variables of primary interest can often not be measured online. To estimate these primary control variables, an observer can be applied. However, errors may reduce the quality of the estimates. An observer insensitive to certain parameter errors in a process model was constructed. Such an observer is referred to as a low sensitivity observer. The conditions for low sensitivity were derived analytically. The general solution obtained was applied for any possible working point and parameter set. The applicability of the analytical solution was tested by using the low sensitivity observer in a feedback control loop. The process under consideration was a bench scale, continuous ethanol fermentation with product recovery. The nonmeasured substrate concentration was controlled by modifying the dilution rate. The substrate estimate obtained from this system remained correct, irrespective of the occurrence of specific model errors. A gradual decrease of the dilution rate had no significant influence on the quality of the estimate. The analytical solution is shown to function well for control purposes. ESA

N92-29759# Technische Univ., Delft (Netherlands).
IMPROVED BALANCING METHODS AND ERROR DIAGNOSIS FOR BIO(CHEMICAL) CONVERSIONS
Reinier Thomas Jacob vanderHeijden, J. J. Heijnen, B. Romein, C. Hellinga, and K. C. A. M. Luyben *In its* State Estimation and Error Diagnosis for Biotechnological Processes 1991 p 87-131 (For primary document see N92-29754 20-51)
Avail: CASI HC A03/MF A02

Balancing techniques to systematically check measurement data for the presence of errors are described. A number of equality constraints are used. The development of a new method to obtain a set of equations for balancing the measured conversion rates is described. The procedure provides an equation to give estimates of the nonmeasured conversion rates, after the measurements are balanced. A new and efficient method to determine whether or not the conversion rates are balanceable and calculable is described. The method differs from the graph/theoretical method and is implemented into a computer program. The residuals of the redundancy relations are tested by means of a chi square test, to decide whether there are significant errors in the data. A new and powerful method to locate the source of an error is presented. This method for error diagnosis is both powerful and numerically efficient. The methods described are illustrated by applying them to several sets of published data. ESA

N92-29760# Technische Univ., Delft (Netherlands).
SEQUENTIAL APPLICATION OF DATA RECONCILIATION FOR SENSITIVE DETECTION OF SYSTEMATIC ERRORS
Reinier Thomas Jacob vanderHeijden, B. Romein, J. J. Heijnen, and K. C. A. M. Luyben *In its* State Estimation and Error Diagnosis for Biotechnological Processes 1991 p 133-182 (For primary document see N92-29754 20-51)
Avail: CASI HC A03/MF A02

A method to test for the presence of relatively small systematic measurement errors (bias) is described. A balancing technique is used to check and improve the consistency of the measurements. The primary measurements are translated into observed conversions. The balancing technique was applied sequentially in time. By combining the result of the individual tests, the sensitivity of the method to measurement errors was improved. Accordingly, a rather sensitive statistical test for systematic errors was obtained. The means by which conversion terms can be obtained from primary measurements were analyzed. The expression of individual errors in the primary measurements within the vector of residuals was investigated. The error diagnostic method was adapted so as to test directly for errors in the primary measurements. A quantitative measure for error sensitivity was developed. The methods described are illustrated by applying them to data from an industrial process. ESA

52 AEROSPACE MEDICINE

Includes physiological factors; biological effects of radiation; and effects of weightlessness on man and animals.

N92-29341*# George Washington Univ., Washington, DC. Science Communication Studies.
PUBLICATIONS OF THE ENVIRONMENTAL HEALTH PROGRAM: 1980-1990
Janice Wallace-Robinson, Elizabeth Hess, and Katherine J. Dickson Washington NASA Jul. 1992 42 p
(Contract NASw-4324)
(NASA-CR-4455; NAS 1.26:4455) Avail: CASI HC A03/MF A01

A 10-year cumulative bibliography of publications resulting from research supported by the Environmental Health Program of the Life Sciences Division of NASA is given. The goals of this program are to utilize ground based studies to understand the effects of

the spacecraft and EVA environments on humans and other organisms; to specify, measure, and control these environments; and to develop countermeasures, where necessary, to optimize crew health, safety, and productivity. The primary subjects encompassed are barophysiology, toxicology, and microbiology. Principal Investigators whose research tasks resulted in publication are identified. Author

N92-29347# Army Aeromedical Research Lab., Fort Rucker, AL.
TEST AND EVALUATION REPORT OF THE PHYSIO CONTROL DEFIBRILLATOR/MONITOR MODEL LIFEPAK (TRADEMARK) 8 Final Report
Jeffrey D. Haun, Joseph R. Licina, and Bill Olding Dec. 1991 75 p
(DA Proj. 3M4-63807-D-836)
(AD-A248283; USAARL-92-5) Avail: CASI HC A04/MF A01

Physio Control Defibrillator/Monitor Model LIFEPAK 8 was tested for electromagnetic interference/compatibility in the UH-60A helicopter under the U.S. Army Program for Testing Evaluation of Equipment for Aeromedical Operations. The tests were conducted using rent military and industrial standards and procedures for electromagnetic interference/compatibility and human factors. The LIFEPAK 8 was found to be compatible with U.S. Army medical evacuation UH-60A Blackhawk. GRA

N92-29577# Gordon Research Conferences, Inc., Kingston, RI.
GORDON RESEARCH CONFERENCE ON BARRIER FUNCTION OF MAMMALIAN SKIN Final Report, 1 Jul. - 31 Dec. 1991
Russell O. Potts 31 Dec. 1991 31 p Conference held in Plymouth, NH, 12-16 Aug. 1991
(Grant AF-AFOSR-0290-91)
(AD-A248556; AFOSR-92-0261TR) Avail: CASI HC A03/MF A01

The objective of this conference was to bring together scientists so they could exchange recent research results and the conference provided a mechanism for the development of close interactions between these scientists. The quality of all of the lectures was exceptionally high and considerable discussion followed each lecture. Many of the conferees expressed very favorable comments about the intellectual stimulation provided by this conference. GRA

N92-30216# Naval Health Research Center, San Diego, CA.
EXERCISE AND THREE PSYCHOSOCIAL VARIABLES: A LONGITUDINAL STUDY Final Report
Linda Stevens and Terry L. Conway 19 Nov. 1991 44 p
(AD-A250649; NHRC-91-31) Avail: CASI HC A03/MF A01

A predominant opinion in research and society today maintains that exercise is beneficial for the reduction of depression and enhancement of self-esteem and quality of life. Yet, controversy still exists over the populations in which these phenomena occur. The purpose of this study was to identify in whom, when, and where exercise participation (EX) has significant effects on depression (DEP), self-esteem (SE), and quality of life (QOL). Data were collected on 1,292 male and female, active-duty Navy personnel in 1988 and 1989 as part of an on-going evaluation of the Navy's Health and Physical Readiness Program. Pearson's product-moment correlations revealed that EX was significantly related cross-sectionally to DEP, SE, and QOL, in the expected directions, at two separate points in time. Correlations among residualized gain scores revealed that changes in EX were significantly, negatively related to changes in DEP, and significantly, positively related to changes in SE and QOL over a one-year period, across the entire Navy sample. Tests which assessed the differences in the magnitudes of the change (i.e., residualized gain) correlations indicated significantly stronger relationships between EX and DEP SE and/or QOL in individuals with a high school education than college graduates. GRA

53 BEHAVIORAL SCIENCES

Includes psychological factors; individual and group behavior; crew training and evaluation; and psychiatric research.

N92-29334# Pittsburgh Univ., PA. Dept. of Behavioral Neuroscience.
A SYSTEMS THEORETIC INVESTIGATION OF NEURONAL NETWORK PROPERTIES OF THE HIPPOCAMPAL FORMATION Final Report, 1 Dec. 1988 - 30 Nov. 1991
Theodore W. Berger 30 Nov. 1991 15 p
(Grant AF-AFOSR-0197-89)
(AD-A250246; AFOSR-92-0363TR) Avail: CASI HC A03/MF A01

The following Progress Report describes the results of the majority of our AFOSR-supported research for Year 3 of the project entitled A Systems Theoretic Investigation of Neuronal Network Properties of the Hippocampal Formation. The Progress Report is divided into six sections: a brief statement of the research objectives, an overview of general experimental and analytical procedures; research characterizing nonlinear response properties of the in vivo dentate gyrus; the extension of this research to the in vitro hippocampal slice; computer simulations of nonlinear response properties of the dentate based on the experimental work; and a listing of publications during the past year of support. GRA

N92-29398# Pennsylvania Univ., Philadelphia.
BIOLOGICALLY-BASED NEURAL NETWORK MODEL OF COLOR CONSTANCY AND COLOR CONTRAST
Susan M. Courtney, Gershon Buchsbaum, and Leif H. Finkel 1992 6 p
(Contract N00014-90-J-1864)
(AD-A248128) Avail: CASI HC A02/MF A01

The light which reaches the eye, or any other sensor, is the product of the reflectance and the illuminant. Therefore, in order to determine the surface reflectance of an object independent of the illuminant, a system must use the spatiochromatic context of the image. We have developed a neural network based on the anatomy and physiology of the visual projection from retina to V4. The network combines color-opponent and contrast information to achieve a good degree of color constancy. This network was tested on simulated images corresponding to the stimuli used in well established psychophysical experiments. Responses qualitatively match human responses to a variety of center-surround and Mondrian test stimuli. Color constancy is the ability to maintain an approximately constant color perception despite changes in the incident illumination of the object. Color contrast, also referred to as chromatic induction or simultaneous contrast, is the change in the (perceived) color of a surface due to the spectral composition of neighboring surface. Color perception in natural scenes depends upon both of these phenomena. Together, these two effects demonstrate that color perception does not directly depend upon the wavelength of the light reflected from a surface. GRA

N92-29420# Columbia Univ., New York, NY. Dept. of Psychology.
VISUAL PERCEPTION OF ELEVATION Annual Report, 1 Jan. - 31 Dec. 1991
Leonard Matin 20 Jan. 1992 8 p
(Grant AF-AFOSR-0146-91)
(AD-A248338; Rept-001; AFOSR-92-0206TR) Avail: CASI HC A02/MF A01

The experiments demonstrate the importance for human observers of the retinal orientation and location of individual straight lines in determining (1) the physical elevation visually perceived as being at eye level (VPEL), and (2) the orientation within a frontal plane visually perceived as being vertical (VPV). The particular depth plane is unimportant for each discrimination as shown by experiments in which stimuli at the same retinal location from differently pitched and differently rolled planes of different depth influence each discrimination identically. The laws of spatial summation for lines controlling VPEL have been determined and

are very different than for other visual discriminations: Influences for a parallel line set summate across a negatively accelerated exponential with a 15.1 degree space constant; lines from nonparallel sets make use of a mechanism that takes a weighted average of their individual influences. The time course for light and dark adaptation of VPEL for a 2-line stimulus is similar to that for a normally illuminated and fully structured pitched visual environment. The VPEL discrimination is near-spatiotopic for eye position and head orientation. The analysis of results at 1.5G has not yet been completed, but it appears that a bias with only minimal influence on the slope of the VPEL-vs-pitch function results from change of G. GRA

N92-29503# Southwest Texas State Univ., San Marcos.
THE EFFECTS OF STUDENT-INSTRUCTOR INTERACTION AND PAIRED/INDIVIDUAL STUDY ON ACHIEVEMENT IN COMPUTER-BASED TRAINING Interim Technical Paper, Jun. - Aug. 1991
Stanley D. Stephenson Mar. 1992 20 p
(Contract F49620-90-C-0076)
(AD-A248518; AL-TR-1992-0003) Avail: CASI HC A03/MF A01

Research shows that interaction between the students and instructor can improve performance in computer-based training (CBT). Small group study can also improve CBT performance. However, there is no data available on the interaction between these two variables. Therefore, a 2 x 2 factorial design experiment was conducted. Two hypotheses were tested: (1) paired learning would have a positive effect on performance; and (2) interactions between student and instructor would have a positive effect. The experimental data support the first hypothesis. They provide only moderate support for the second. Perhaps a CBT partner can provide the feedback and support usually given by the instructor in a traditional setting. More research is needed on the social aspects of learning and the role of the instructor in CBT. GRA

N92-29560# Pennsylvania Univ., Philadelphia. Dept. of Bioengineering.
OBJECT DISCRIMINATION BASED ON DEPTH-FROM-OCCLUSION
Leif H. Finkel and Paul Sajda 1991 23 p
(Contract N00014-90-J-1864)
(AD-A248104) Avail: CASI HC A03/MF A01

We present a model of how objects can be visually discriminated based on the extraction of depth from occlusion. Object discrimination requires consideration of both the binding problem and the problem of segmentation. We propose that the visual system binds contours and surfaces by identifying 'proto-objects', compact regions bounded by close contours. Proto-objects can then be linked into larger structures. The model is simulated by a system of interconnected neural networks. The networks have biologically-motivated architectures and utilize a distributed representation of depth. We present simulations that demonstrate three robust psychophysical properties of the system. In order to discriminate objects in the visual world, the nervous system must solve two fundamental problems: binding and segmentation. The binding problem addresses how the attributes of an object's shape, color, motion, and depth are linked to create an individual object. Segmentation deals with the converse problem of how separate objects are distinguished. GRA

N92-29591# Rochester Univ., NY. Center for Visual Science.
PERIPHERAL LIMITATIONS ON SPATIAL VISION Final Report, 1 Aug. 1988 - 31 Jan. 1992
David R. Williams 24 Mar. 1992 12 p
(Grant AF-AFOSR-0292-88)
(AD-A250579; AFOSR-92-0267TR) Avail: CASI HC A03/MF A01

This project employs psychophysical techniques to examine the limitations on spatial vision imposed by the first stages in the visual pathway. The appearance of very high frequency interference fringes is distorted, or aliased, by the cone mosaic. Such moire patterns allow us to assess the topography of the cone mosaic in the living eye, clarifying the relationship between cone spacing and resolution. Resolution was also measured under conditions in which only the M or L cones could detect the interference fringe. Visual acuity was little different than it was when both cone types detected the grating showing that resolution is immune to photoreceptor loss under these circumstances. We recently also established that a phenomenon known for 150 years has been misunderstood, and that it is chromatic aliasing caused by spatial sampling by M and L cones. A device has been constructed to provide objective measurements of the off-axis optical quality of the eye, and measurements show that optical quality declines surprisingly little across the visual field. In addition, we have taken advantage of an early nonlinearity in the visual system to measure the spatial responses of the earliest stages in retinal processing. GRA

N92-29592# Wisconsin Univ., Madison. Center on Mental Retardation and Human Development.
ADDITIVITY AND AUDITORY PATTERN ANALYSIS Final Report, 1 May 1987 - 31 Mar. 1991
R. Lutfi 26 Mar. 1992 5 p
(Grant AF-AFOSR-0240-87)
(AD-A250580; AFOSR-92-0303TR) Avail: CASI HC A01/MF A01

Human discrimination of complex acoustic signals typically cannot be predicted from the simple sum of the discriminabilites associated with individual components of the signal. Understanding such failures of additivity is central to our understanding of complex sound analysis. The goal of this project is to elucidate the rules and mechanisms whereby individual stimulus components combine to influence the detection and discrimination of complex sounds. The project is designed to answer specific questions regarding listeners' abilities to integrate information within and across acoustic dimensions, to extract information contained in the pattern of the acoustic signal, and to perform under conditions of stimulus uncertainty. The data are also used to determine how listeners weight the information provided by different components of the signal, and how best to package the acoustic information so as to be most effectively processed by the listener. GRA

N92-29620# Universal Energy Systems, Inc., San Antonio, TX.
ON THE EFFECT OF RANGE RESTRICTION ON CORRELATION COEFFICIENT ESTIMATION Final Report, 1 Jan. - 31 Dec. 1991
Douglas E. Jackson and Malcolm J. Ree Apr. 1992 41 p
(Contract F49620-88-C-0053)
(AD-A248956; AL-CR-1992-001) Avail: CASI HC A03/MF A01

Suppose it is desired to estimate the correlation coefficient between random variables X and Y in some population P and the only data available are from some population Q where Q is a proper subset of P. X and Y are defined on P, while X and Y will denote X and Y restricted to 0. A simulation program was written to study the effect of this restricted sampling on the estimation of correlation coefficients. The Air Force is studying the implementation of new selection devices that optimize the selection and classification of individuals. Whenever a new measurement instrument is suggested, it must be evaluated by estimating its correlation with performance criteria and with tests and selection devices that are currently part of the selection process. The difficulty is that the new test can only be administered to Air Force personnel. That is, people who have already been selected. Air Force personnel constitute the population Q and the applicants constitute the population P. It is necessary to use a sample from Q' to estimate correlations between tests that are to be used in P. This is called the range restriction problem. The purpose of this paper is to present the results of a study which addresses a number of issues related to the range restriction problem. The performance of the F-statistic, confidence intervals, and 'hidden variables' are considered. GRA

N92-29871# National Aerospace Lab., Amsterdam (Netherlands). Afdel. Vliegtuigen.
FIGHTER PILOT TRAINING: THE CONTRIBUTION OF SIMULATION [TRAINING VAN GEVECHTSVLIEGERS: DE ROL VAN SIMULATIE]
J. T. M. vanDoorn, G. J. Alders, E. W. Pijpers, and H. J. L. Vogelaar 10 Feb. 1989 33 p In DUTCH Presented at the ISSC Seminar on Simulation for Training, 's-Gravenhage, Netherlands, 18 Oct. 1989
(NLR-TP-89311-U; ETN-92-91527) Avail: CASI HC A03/MF A01

The contribution of simulation and simulators to the training of pilots of fighter aircrafts is discussed. The present training curriculum, including the use of simulation and simulators, is described. The possibilities to improve training by the increased use of simulation are discussed. The question whether simulation can replace live training, especially operational training is addressed. It can be concluded that simulation is a force multiplier with respect to training but that the effect of increased simulation on the required live training effect is not a simple matter to assess. Any such deduction should be thoroughly evaluated to guarantee operational safety and effectiveness. ESA

N92-29930# Princeton Univ., NJ.
PHYSIOLOGICAL ANALYSES OF THE AFFERENTS CONTROLLING BRAIN NEUROCHEMICAL SYSTEMS Annual Report, 1 Jun. 1990 - 31 May 1991
Barry L. Jacobs 24 Feb. 1992 3 p
(Grant AF-AFOSR-0294-90)
(AD-A248334; Rept-255-6491-1; AFOSR-92-0189TR) Avail: CASI HC A01/MF A01

These experiments are directed at the neurochemical systems and neuroanatomical pathways that control the activity of brain serotonergic (dorsal raphe nucleus) and noradrenergic (locus coeruleus) neurons. It seeks to answer these questions by studying single unit activity in combination with microiontophoresis in the awake cat during exposure to physiologically relevant conditions. Four series of studies are proposed. The first three will examine the neurochemical afferents that control the following types of activity of serotonergic and noradrenergic neurons: (1) tonic, as well as state-dependent activity; (2) phasic activity evoked by various sensory stimuli; and (3) activation in response to environmental and physiological challenges (stressors). The fourth series of studies will take results from the first three and seek to establish the nuclear site of origin of these effects by employing electrical stimulation in combination with single unit recording and microiontophoresis. This research program will provide a critical link for understanding the control of these two important neurochemical systems, and will thus help to elucidate, more broadly, their role in processes such as state-dependent changes in physiology and behavior, and arousal and attention. GRA

N92-30127*# Federal Aviation Administration, Washington, DC.
REVISION OF CERTIFICATION STANDARDS FOR AVIATION MAINTENANCE PERSONNEL
Leslie K. Vipond *In* NASA. Langley Research Center, The 1991 International Conference on Aging Aircraft and Structural Airworthiness Jul. 1992 p 315-319 (For primary document see N92-30106 20-39)
Avail: CASI HC A01/MF A04

54 MAN/SYSTEM TECHNOLOGY AND LIFE SUPPORT

Includes human engineering; biotechnology; and space suits and protective clothing.

For related information see also *16 Space Transportation.*

N92-29348# Army Aeromedical Research Lab., Fort Rucker, AL.
VISUAL ACUITY WITH SECOND AND THIRD GENERATION NIGHT VISION GOGGLES OBTAINED FROM A NEW METHOD OF NIGHT SKY SIMULATION ACROSS A WIDE RANGE OF TARGET CONTRAST Final Report
John C. Kotulak and Clarence E. Rash Jan. 1992 42 p
(DA Proj. 3M1-62787-A-79-B)
(AD-A248284; USAARL-92-9) Avail: CASI HC A03/MF A01

The purpose of this investigation was to study the primary factors which influence visual acuity (VA) with night vision goggles (NVGs). These factors are: night sky condition, target contrast, and NVG generation. Improved methods were used to simulate the night sky and to control for differences in target contrast which result from dissimilarities in spectral sensitivity between NVG generations. The new simulation method used combinations of spectrally flat (neutral density) and wavelength selective (blue glass) filters to reproduce the spectral distribution of the night sky across the entire NVG response range. Between-generation differences in target contrast were eliminated by weighting the incident radiant flux by the sensitivity of the detector. It was found that the difference in VA between the two generations widens under two conditions: (1) when target contrast is constant and night sky irradiance decreases; and (2) when night sky irradiance is constant and target contrast decreases. Furthermore, it was found that for a given NVG generation, VA falls off more rapidly for a low contrast target than for one of high contrast when night sky irradiance decreases. GRA

N92-29413*# Sterling (Walter V.), Inc., Palo Alto, CA.
ARMY-NASA AIRCREW/AIRCRAFT INTEGRATION PROGRAM: PHASE 4 A(3)I MAN-MACHINE INTEGRATION DESIGN AND ANALYSIS SYSTEM (MIDAS) SOFTWARE DETAILED DESIGN DOCUMENT
Carolyn Banda, David Bushnell, Scott Chen, Alex Chiu, Betsy Constantine, Jerry Murray, Christian Neukom, Michael Prevost, Renuka Shankar, and Lowell Staveland Dec. 1991 514 p
(Contract NAS2-13210)
(NASA-CR-177593; A-92049; NAS 1.26:177593) Avail: CASI HC A22/MF A04

The Man-Machine Integration Design and Analysis System (MIDAS) is an integrated suite of software components that constitutes a prototype workstation to aid designers in applying human factors principles to the design of complex human-machine systems. MIDAS is intended to be used at the very early stages of conceptual design to provide an environment wherein designers can use computational representations of the crew station and operator, instead of hardware simulators and man-in-the-loop studies, to discover problems and ask 'what if' questions regarding the projected mission, equipment, and environment. This document is the Software Product Specification for MIDAS. Introductory descriptions of the processing requirements, hardware/software environment, structure, I/O, and control are given in the main body of the document for the overall MIDAS system, with detailed discussion of the individual modules included in Annexes A-J. Author

N92-29538# Analysis and Technology, Inc., New London, CT.
EVALUATION OF NIGHT VISION GOGGLES (NVG) FOR MARITIME SEARCH AND RESCUE Interim Report No. 3, Mar. 1989 - Feb. 1991
R. Q. Robe, J. V. Plourde, and G. L. Hover Jun. 1991 106 p
(Contract DTCG39-89-C-80671)
(AD-A247182; CGR/DC-19/91; USCG-D-03-92) Avail: CASI HC A06/MF A02

Three experiments were conducted during 1989 and two more have been conducted during 1990 by the U.S. Coast Guard Research and Development (R&D) Center to evaluate night vision goggles (NVGs) for their effectiveness in detecting small targets at night. Three types of NVGs were evaluated: the AN/AVS-6 Aviators Night Vision Imaging System (ANVIS) NVG was tested onboard Coast Guard HH-3 and CH-3 helicopters, and the AN/PVS-5C and AN/PVS-7A NVGs were tested onboard 41-foot Coast Guard utility boats (UTBs). During the Fall 1990 experiment, 4-and 6-person unlit life rafts, with and without retro-reflective tape and 18-and 21-foot white boats were employed as targets during realistically-simulated search missions and are discussed herein. A large quantity of well moonlit data were collected during the fall 1990 experiment and this third interim report discusses target types where new information was obtained. A total of 1,612 target detection opportunities were generated for the above-mentioned target types during the five experiments. These data were analyzed to determine which of 25 search parameters of interest exerted a statistically-significant influence on target detection probability. Lateral range curves and sweep width estimates are developed for each search unit/target type combination. Human factors data are presented and discussed. Recommendations for conducting NVG searches for small targets and for additional data collection and analysis are provided. GRA

N92-29949# Texas Technological Univ., Lubbock. Dept. of Industrial Engineering.
DEVELOPMENT OF MODELS FOR PREDICTION OF OPTIMAL LIFTING MOTION Final Report
M. M. Ayoub 30 Sep. 1991 106 p Prepared for Centers for Disease Control, Atlanta, GA
(Grant NIOSH-R01-OH-02434)
(PB92-164656) Avail: CASI HC A06/MF A02

The angular movement of five human joints was simulated based on the invariant characteristics of manual lifting that are multidirectional and multiarticular and executed by large muscle groups generating within maximum torques. The study dealt with only one set of performance limitations of manual lifting, those produced by the understanding of human physical capacities and task requirements. It was assumed that the body will perform the lifting motion pattern in such a fashion so as to minimize a cost function. Therefore, the focus of the research was to identify the paths of motion of each of five selected joints (elbow, shoulder, hip, knee, and ankle) within the feasible space which will minimize the cost function. Three different optimization searching algorithms were introduced to minimize the objective function representing the total work done in lifting. These algorithms were: heuristic dynamic programming, filtering by total enumeration, and the general reduced gradient algorithm. A comparison was made between the prediction of the five selected joints to the actual paths to illustrate the validity of the model. Author

N92-30125*# Federal Aviation Administration, Washington, DC. Office of Aviation Medicine.
HUMAN FACTORS IN AIRCRAFT MAINTENANCE AND INSPECTION
William T. Shepherd *In* NASA. Langley Research Center, The 1991 International Conference on Aging Aircraft and Structural Airworthiness Jul. 1992 p 301-304 (For primary document see N92-30106 20-39)
Avail: CASI HC A01/MF A04

N92-30126*# Galaxy Scientific Corp., Atlanta, GA.
USING INTELLIGENT SIMULATION TO ENHANCE HUMAN PERFORMANCE IN AIRCRAFT MAINTENANCE
William B. Johnson and Jeffrey E. Norton *In* NASA. Langley Research Center, The 1991 International Conference on Aging Aircraft and Structural Airworthiness Jul. 1992 p 305-313 (For primary document see N92-30106 20-39)
(Contract DTFA03-89-C-00043)
Avail: CASI HC A02/MF A04

55 SPACE BIOLOGY

Includes exobiology; planetary biology; and extraterrestrial life.

No abstracts in this category.

59 MATHEMATICAL AND COMPUTER SCIENCES (GENERAL)

N92-29403*# National Aeronautics and Space Administration. Lyndon B. Johnson Space Center, Houston, TX.
MAKING INTELLIGENT SYSTEMS TEAM PLAYERS: OVERVIEW FOR DESIGNERS
Jane T. Malin and Debra L. Schreckenghost (Mitre Corp., Houston, TX.) Jun. 1992 51 p
(NASA-TM-104751; S-680; NAS 1.15:104751) Avail: CASI HC A04/MF A01

This report is a guide and companion to the NASA Technical Memorandum 104738, 'Making Intelligent Systems Team Players,' Volumes 1 and 2. The first two volumes of this Technical Memorandum provide comprehensive guidance to designers of intelligent systems for real-time fault management of space systems, with the objective of achieving more effective human interaction. This report provides an analysis of the material discussed in the Technical Memorandum. It clarifies what it means for an intelligent system to be a team player, and how such systems are designed. It identifies significant intelligent system design problems and their impacts on reliability and usability. Where common design practice is not effective in solving these problems, we make recommendations for these situations. In this report, we summarize the main points in the Technical Memorandum and identify where to look for further information. Author

60 COMPUTER OPERATIONS AND HARDWARE

Includes hardware for computer graphics, firmware, and data processing.

For components see *33 Electronics and Electrical Engineering.*

N92-29611# Grenoble-1 Univ. (France). Lab. de Genie Informatique.
SOFTWARE ARCHITECTURE MODELLING: APPLICATION TO AMODEUS DESIGN SCENARIOS
J. Couttaz and L. Nigay Sep. 1991 51 p
(IMAG-RR-860-I; ETN-92-91474) Avail: CASI HC A04/MF A01

An elaboration from the publications and working papers of the modeling activity performed in ESPRIT AMODEUS BRA 3066 during 1991 is presented. Software architecture modeling for the design and development of interactive systems is discussed. Software architecture models should support properties and constraints prescribed by the software and cognitive psychology communities. From these observations, a multiagent framework applicable to the software design of interactive systems is derived. Two design scenarios are described along the lines of the PAC model and justified with the application of the software design heuristics rules developed by the research group. These examples show how the general model can be engineered to fit practical problems. The ability of the model to support a number of properties and constraints relevant to software engineering is discussed. ESA

N92-29907# Westinghouse Savannah River Co., Aiken, SC.
REVIEWS OF COMPUTING TECHNOLOGY: FIBER DISTRIBUTED DATA INTERFACE
A. J. Johnson 1 Dec. 1991 34 p
(Contract DE-AC09-89SR-18035)
(DE92-011374; WSRC-IM-90-83-6) Avail: CASI HC A03/MF A01

Fiber Distributed Data Interface, more commonly known as FDDI, is the name of the standard that describes a new local area network (LAN) technology for the 90's. This technology is based on fiber optics communications and, at a data transmission rate of 100 million bits per second (mbps), provides a full order of magnitude improvement over previous LAN standards such as Ethernet and Token Ring. FDDI as a standard has been accepted by all major computer manufacturers and is a national standard as defined by the American National Standards Institute (ANSI). FDDI will become part of the US Government Open Systems Interconnection Profile (GOSIP) under Version 3 GOSIP and will become an international standard promoted by the International Standards Organization (ISO). It is important to note that there are no competing standards for high performance LAN's so that FDDI acceptance is nearly universal. This technology report describes FDDI as a technology, looks at the applications of this technology, examine the current economics of using it, and describe activities and plans by the Information Resource Management (IRM) department to implement this technology at the Savannah River Site. DOE

N92-29982# Universiteit Twente, Enschede (Netherlands). Tele-Informatics and Open Systems Group.
A METHOD FOR ANALYSING THE PERFORMANCE ASPECTS OF THE FAULT-TOLERANCE MECHANISMS IN FDDI
Aad P. A. vanMoorsel, Boudewijn R. Haverkort, and Ignas G. Niemegeers Dec. 1991 15 p Presented at IEEE Infocom 92, Florence, Italy, 4-8 May 1992 Submitted for publication
(Memo-INF-91-92; TIOS-91/036; ISSN-0924-3755; ETN-92-91777)
Copyright Avail: CASI HC A03/MF A01

The high speed Fiber Distributed Data Interface (FDDI) is becoming an accepted standard for many real time communication networks. One of its real time applications supporting aspects is that the fault tolerance mechanisms are fast and initiated automatically. Nevertheless, occurring errors can have great influence on performance measured such as the probability of missing a deadline. The ability of the error recovery mechanisms to make FDDI satisfy real time performance constraints in the presence of errors is analyzed. A complicating factor in these analyses is the rarity of the error occurrences, which makes direct simulation unattractive. Therefore, a fast simulation technique, called injection simulation, was developed which makes it possible to analyze the performance of FDDI including its fault tolerance behavior. The implementation of injection simulation for polling models of FDDI is discussed and simulation results are shown. ESA

N92-30145# Universiteit Twente, Enschede (Netherlands). Tele-Informatics and Open Systems Group.
CRITERIA FOR, AND EXPERIENCE WITH, ADTs IN LARGE LOTOS SPECIFICATIONS
H. Kremer Nov. 1991 17 p
(Memo-INF-91-74; TIOS-91/032; ISSN-0924-3755; ETN-92-91575)
Copyright Avail: CASI HC A03/MF A01

A set of general design criteria that can be used in the processes of designing new systems and of evaluating existing designs is presented. Rather than trying to define 'quality', a set of general quality design criteria that can be used to compare only some aspects of quality of different designs is presented. These criteria are formulated in an operationally useful manner. The use of these criteria is illustrated in the design of normal descriptions in LOTOS (Language Of Temporal Ordering Specifications) of the ISO (International Standards Organization) Transport service and protocol. The experience with the design of the Abstract Data Types (ADTs) is emphasized and some of the problems encountered are reported. ESA

61 COMPUTER PROGRAMMING AND SOFTWARE

Includes computer programs, routines, alogorithms, and specific applications, e.g., CAD/CAM.

N92-29362*# Research Inst. for Computing and Information Systems, Houston, TX.
ASV3 DIAL-IN INTERFACE RECOMMENDATION FOR THE REPOSITORY BASED SOFTWARE ENGINEERING (RBSE) PROGRAM
30 Mar. 1992 19 p Prepared in cooperation with SofTech, Inc., Houston, TX
(Contract NCC9-16; RICIS Proj. RB-06)
(NASA-CR-190500; NAS 1.26:190500; ADANET-FD-R/T-160-1)
Avail: CASI HC A03/MF A01

The purpose of this report is to provide insight into the approach and design of the Cooperative User Interface (CUI). The CUI is being developed based on Hypercard technology and will provide the same look and feel as is provided by the NASA Electronic Library System (NELS) X-Window interface. The interaction between the user and ASCII-LIB is presented as well as the set of Hypercard Cards with which the user will work. Author

N92-29363*# Research Inst. for Computing and Information Systems, Houston, TX.
ON-LINE REPLACEMENT OF PROGRAM MODULES USING AdaPT
Raymond S. Waldrop (Texas A&M Univ., College Station.), Richard A. Volz (Texas A&M Univ., College Station.), Gary W. Smith (Texas A&M Univ., College Station.), A. A. Holzbacher-Valero (Imperial Coll. of Science and Technology, London, England), and Stephen J. Goldsack (Imperial Coll. of Science and Technology, London, England) 5 Jun. 1992 32 p
(Contract NCC9-16; RICIS Proj. SE-35)
(NASA-CR-190499; NAS 1.26:190499) Avail: CASI HC A03/MF A01

One purpose of our research is the investigation of the effectiveness and expressiveness of AdaPT(1), a set of language extensions to Ada 83, for distributed systems. As a part of that effort, we are now investigating the subject of replacing, e.g., upgrading, software modules while the software system remains in operation. The AdaPT language extension provide a good basis for this investigation for several reasons: (1) they include the concept of specific, self-contained program modules which can be manipulated; (2) support for program configuration is included in the language; and (3) although the discussion will be in terms of the AdaPT language, the AdaPT to Ada 83 conversion methodology being developed as another part of this project will provide a basis for the application of our findings to Ada 83 systems. The purpose of this investigation is to explore the basic mechanisms to the replacement process. Thus, while replacement in the presence of real-time deadlines, heterogeneous systems, and unreliable networks is certainly a topic of interest, we will first gain an understanding of the basic processes in the absence of such concerns. The extension of the replacement process to more complex situations can be made later. This report will establish an overview of the on-line upgrade problem, and present a taxonomy of the various aspects of the replacement process. Author

N92-29391*# Research Inst. for Computing and Information Systems, Houston, TX.
DECISIONMAKER SOFTWARE AND EXTRACTING FUZZY RULES UNDER UNCERTAINTY
Kevin B. Walker (Houston Univ., Clear Lake, TX.) 13 May 1992 74 p
(Contract NCC9-16; RICIS Proj. SR-01)
(NASA-CR-190502; NAS 1.26:190502) Avail: CASI HC A04/MF A01

Knowledge acquisition under uncertainty is examined. Theories proposed in deKorvin's paper 'Extracting Fuzzy Rules Under

Uncertainty and Measuring Definability Using Rough Sets' are discussed as they relate to rule calculation algorithms. A data structure for holding an arbitrary number of data fields is described. Limitations of Pascal for loops in the generation of combinations are also discussed. Finally, recursive algorithms for generating all possible combination of attributes and for calculating the intersection of an arbitrary number of fuzzy sets are presented.
Author

N92-29399# Maryland Univ., College Park.
NUMERICAL PROCEDURES FOR ANALYZING DYNAMICAL PROCESSES Final Report, 1 Oct. 1990 - 29 Feb. 1992
Celso Grebogi, Edward Ott, and James A. Yorke 29 Feb. 1992 319 p LIMITED REPRODUCIBILITY: Availability: Document partially illegible
(Contract N00014-88-K-0657)
(AD-A248175) Avail: CASI HC A14/MF A03

We are delivering a tape with a software package for UNIX workstations with documentation for analyzing low dimensional dynamical behavior from time series. In particular, the Lyapunov exponent code will, together with the dimension code, permit the user to distinguish between periodic, chaotic, and random processes. 'Random processes' here means behavior whose dimension is too high to compute. The code computes the information dimension of the time series. We are also including in the same tape a noise-reduction code with documentation. We have developed a method which we believe is a potential breakthrough in the analysis of experimental data. Typically, attractors are reconstructed from a scalar time series of experimental data using time delays. Conventional signal filtering techniques are not useful in this case, because they examine only portions of the signal which are close in time. GRA

N92-29400*# Cornell Univ., Ithaca, NY. Dept. of Computer Science.
THE WEAKEST FAILURE DETECTOR FOR SOLVING CONSENSUS
Tushar Deepak Chandra, Vassos Hadzilacos, and Sam Toueg Jul. 1992 41 p Sponsored in part by IBM Endicott Programming Lab.; and Siemens Corp.; and Natural Sciences and Engineering Research Council of Canada
(Grants NAG2-593; NSF CCR-89-01780; NSF CCR-91-02231)
(NASA-CR-190545; NAS 1.26:190545; CU-TR-92-1293) Avail: CASI HC A03/MF A01

We determine what information about failures is necessary and sufficient to solve Consensus in asynchronous distributed systems subject to crash failures. Previously, we proved that W, a failure detector that provides surprisingly little information about which processes have crashed, is sufficient to solve Consensus in asynchronous systems with a majority of correct processes. In this paper, we prove that to solve Consensus, any failure detector has to provide at least as much information as W. Thus, W is indeed the weakest failure detector for solving Consensus in asynchronous systems with a majority of correct processes.
Author

N92-29409# Carnegie-Mellon Univ., Pittsburgh, PA. Dept. of Electrical and Computer Engineering.
ULTRA-DEPENDABLE REAL-TIME COMPUTING Report, 1 Oct. 1990 - 30 Sep. 1991
Jay K. Strosnider and Ron Bianchini 30 Sep. 1991 12 p
(Contract N00014-91-J-1304)
(AD-A248193) Avail: CASI HC A03/MF A01

The research effort this year focused in four major areas: (1) developing schedulable fault recovery strategies that guarantee minimum interference with fault free tasks, and graceful degradation; (2) developing analytical techniques that support quantitative analysis of computer architectures for fault-tolerant computation; (3) investigating how intelligent integrated agents can enhance distributed system's dependability; and (4) developing network diagnostic strategies with provable timing properties. The project members are also concerned with the transition of the theory to the user community, especially the U.S. Navy. For this reason, project members have a close relationship with the RTSIA (Real-Time Scheduling in Ada) project in the CMU Software Engineering Institute, and Distributed Combat Control Project at Naval Ocean Systems Center in San Diego. GRA

N92-29418# Kernforschungszentrum G.m.b.H., Karlsruhe (Germany, F.R.). Inst. fuer Reaktorentwicklung.
KISMET (KINEMATIC SIMULATION, MONITORING AND OFF-LINE PROGRAMMING ENVIRONMENTS FOR TELEROBOTICS): SIMULATION OF THE TARGET-ORIENTED DRIVING OF AN AUTONOMOUS VEHICLE IN A LABYRINTHIC ENVIRONMENT [SIMULATION DER ZIELFAHRT EINES AUTONOMEN FAHRZEUGS IN LABYRINTHARTIGER UMGEBUNG DURCH KISMET]
H. Knueppel, U. Kuehnapfel, and D. Smidt Oct. 1991 17 p In GEORGIAN
(KfK-4941; ISSN-0303-4003; ETN-92-91503) Copyright Avail: CASI HC A03/MF A01

An algorithm was developed for the collision free target oriented driving of an autonomous vehicle, using KISMET (Kinematic Simulation, Monitoring, and offline programming Environment for Telerobotics) software and hardware for geometric operations and graphical presentation. The algorithm uses a simple global route planner and creates the global path neglecting the finite vehicle dimensions as input to the sensor based local route planner. The local planner of each time step transforms the sensor pattern, received by a number of ultrasonic sensors to the movement pattern. The target oriented global information influences the local operations. Examples demonstrate that the target is reached collision free and close to the shortest path, even in a labyrinthic environment. ESA

N92-29487# Army Armament Research, Development and Engineering Center, Watervliet, NY.
MINIMAX LINEAR SPLINES Final Report
Royce W. Soanes Feb. 1992 21 p
(AD-A248077; ARCCB-TR-92006) Avail: CASI HC A03/MF A01

An algorithm is derived for obtaining a mesh that minimizes the maximum local interpolatory error for a linear spline, where the error is measured in any classical Banach norm. This algorithm is based on the standard method of approximate error equidistribution advocated by C. de Boor. GRA

N92-29527# Air Force Inst. of Tech., Wright-Patterson AFB, OH. School of Engineering.
AN EXAMINATION OF HYPERCUBE IMPLEMENTATIONS OF GENETIC ALGORITHMS M.S. Thesis
Andrew Dymek Mar. 1992 191 p
(AD-A248092; AFIT/GCS/ENG/92M-02) Avail: CASI HC A09/MF A02

Genetic algorithms are stochastic search algorithms which model natural adaptive systems. In support of the development of a genetic search package for AFIT's iPSC/2 Hypercube, this study focused on two problem areas associated with hypercube implementations. Premature convergence occurs when the population becomes dominated by locally optimal, but globally inferior, solutions. Based on an examination of past hypercube implementations, the selection and communication strategies were hypothesized as causes of premature convergence. Experiments to test these hypotheses were conducted on Rosenbrock's saddle, a function often associated with premature convergence. Communication of best solutions led to premature convergence in small population sizes, but increased the likelihood of finding the global optimal in large population sizes. Genetic algorithms using global selection were more robust than those using local selection. GA-hard problems are intrinsically difficult for standard genetic algorithms. Messy genetic algorithms are effective against GA-hard problems. The second part of this study added a parallel version of a messy genetic algorithm to the genetic algorithm package. Against a sample GA-hard problem, the parallel implementation achieved a linear speedup of the sequential bottleneck while still

finding the global optimal. The messy genetic algorithm should be applied to problems of practical importance. GRA

N92-29537# Lawrence Livermore National Lab., CA.
PROGRAM SIXPAK: A CODE DESIGNED TO CHECK DOUBLE-DIFFERENTIAL CORRELATED DATA AND CALCULATE EQUIVALENT UNCORRELATED DATA
D. E. Cullen 18 Feb. 1992 56 p
(Contract W-7405-eng-48)
(DE92-013752; UCRL-ID-110241) Avail: CASI HC A04/MF A01

The computer code SIXPAK is designed to check double-differential correlated data in the ENDF/B format and to calculate 'equivalent' uncorrelated data and output this data in the ENDF/B format. DOE

N92-29540# Carnegie-Mellon Univ., Pittsburgh, PA. Software Engineering Inst.
SUMMARY OF TECHNICAL OPERATIONS, 1991
Jan. 1992 50 p
(Contract F19628-85-C-0003)
(AD-A248153; CMU/SEI-91-CDRL-106) Avail: CASI HC A03/MF A01

The Software Process Focus Area objectives are to improve the process of software development Project members within this Focus Area are assessing the actual practice of software engineering in the defense community, training organizations to gain management control over their software development processes, supporting the use of quantitative methods and measures as a basis for process improvement, and developing improved methods for software process management. The Software Process Assessment (SPA) Project helps organizations improve their software development process by providing a structured framework for assessing their current practice. The objectives of an assessment are to determine the organization's software process maturity, identify key areas for improvement, and help the organization initiate those improvements. The SPA Project provides assessment briefings, training, and coaching services. In addition, it supports nine commercial assessment vendors. The project is currently focusing its efforts on assessments as components of comprehensive process improvement programs. Early this year, project members conducted a second vendor assessment training class for 17 people from 9 vendor organizations. During the fourth quarter, an update workshop was held for all currently licensed vendors. Workshop attendees were provided training in the revised Capability Maturity Model (CMM). GRA

N92-29544# Naval Ocean Systems Center, San Diego, CA. Research, Development, Test, and Evaluation Div.
CONTRACTING IN THE SOFTWARE ENGINEERING CRISIS
D. M. Bauman and A. E. Jensen Mar. 1992 12 p
(AD-A250241) Avail: CASI HC A03/MF A01

The Department of Defense (DoD) is currently experiencing extremely serious problems with Software Engineering. As weapons systems become increasingly more dependent upon the software programs which they employ, it becomes evermore apparent that DoD projects are consistently late and over budget because of software. To this end, software has become the dominant risk to cost and schedule and has caused the demise of more than a few DoD development projects. The DoD repeatedly demonstrates requisite experience to efficiently manage the development of hardware. Hardware development projects, for which the DoD readily implements tried and proven practices to systematically address all aspects of the development, are relatively risk free at their onset. Software development projects, on the other hand, are oftentimes initiated without the benefit of similarly institutionalized methodologies and practices. Because an understanding of proper Software Engineering practice is only now developing, standard, well-accepted measures do not yet exist. The DoD seems only to be scratching at the surface of state-of-the-art software engineering and herein lies the basis of the problem. GRA

N92-29570# Grenoble-1 Univ. (France). Reliable Integrated Systems Group.
A STRATEGY FOR MICROPROCESSOR BIST IMPLEMENTATION BASED ON DETERMINISTIC TESTING
M. Nicolaidis Mar. 1991 32 p
(IMAG-RR-844-I; ETN-92-91468) Avail: CASI HC A03/MF A01

A strategy for microprocessor BIST (Built In Self Test) implementation based on deterministic testing is presented. Each block of the sequencing part can be tested exhaustively by using an adequate sequencing part architecture. For data paths, we have proposed efficient test pattern generators allowing high fault coverage, low area overhead, and low test length. ESA

N92-29586# Air Force Inst. of Tech., Wright-Patterson AFB, OH.
OPTIMIZATION OF STOCHASTIC RESPONSE SURFACES SUBJECT TO CONSTRAINTS WITH LINEAR PROGRAMMING M.S. Thesis
Robert G. Harvey Mar. 1992 119 p
(AD-A248108; AFIT/GOR/ENS/92M-14) Avail: CASI HC A06/MF A02

This research investigated an alternative to the traditional approaches of optimizing a stochastic response surface subject to constraints. This research investigated the bias in the expected value of the solution, possible alternative decision variable settings, and a method to improve the solution. A three step process is presented to evaluate stochastic response surfaces subject to constraints. Step 1 is to use a traditional approach to estimate the response surface and a covariance matrix through regression. Step 2 samples the objective function of the linear program (i.e., response surface) and identifies the extreme points visited. Step 3 presents a method to estimate the optimal extreme point and present that information to a decision maker. GRA

N92-29608# Technische Univ., Eindhoven (Netherlands). Dept. of Mathematics and Computing Science.
CONSTRAINT CLASSIFICATION FOR MIXED INTEGER PROGRAMMING FORMULATIONS
G. L. Nemhauser (Georgia Inst. of Tech., Atlanta.), M. W. P. Savelsbergh, and G. C. Sigismondi (Georgia Inst. of Tech., Atlanta.) Nov. 1991 11 p
(Memo-COSOR-91-30; ETN-92-91463) Avail: CASI HC A03/MF A01

A classification scheme used in the mixed integer programming system MINTO is defined. The scheme's purpose is to identify important classes used in preprocessing, constraint generation, branching, etc. It is proposed as a general scheme to be evaluated, modified, and then adopted, by the mixed integer programming community. ESA

N92-29621# Grenoble-1 Univ. (France). Reliable Integrated Systems Group.
AUTOMATIC GENERATION ALGORITHMS, EXPERIMENTS, AND COMPARISONS OF SELF CHECKING PLA SCHEMES
M. Nicolaidis, M. Boudjit, and K. Torki Mar. 1991 32 p
(IMAG-RR-843-I; ETN-92-91467) Avail: CASI HC A03/MF A01

Self checking circuits ensure concurrent error detection by means of hardware redundancy. An important drawback of self checking circuits is the fact that they involve a significant increasing of the design time. Specific computer aided design tools are needed in order to cope with this drawback. A tool allowing automatic generation of self checking PLAs (Programmable Logic Arrays) is presented and validated by transforming a set of PLA benchmarks into self checking PLAs based on Berger coding or on parity coding. Stastistics concerning the required area overhead and comparison of different self checking PLA schemes are given. ESA

N92-29622# Iterations, Inc., New York, NY.
SCALABLE PARALLEL ALGORITHMS FOR MULTIDIMENSIONAL DIGITAL SIGNAL PROCESSING Final Report, 1 Jul. - 31 Dec. 1991
Martin Rofheart and John Granata 29 Jan. 1992 58 p

(Contract DAAL03-91-C-0038)
(AD-A249381; ARO-29087.1-MA-SBI) Avail: CASI HC A04/MF A01

A new algorithm for the multiprocessor computation of the multidimensional discrete Fourier transform is presented. The algorithm eliminates the need for interprocessor communication and is highly scalable. The cost of eliminating interprocessor communication by this method is that one addition must be performed at each processing element for every input loaded into the machine. The algorithm is based on a new multidimensional discrete Fourier transform algorithm that computes a d-dimensional discrete Fourier transform by a set of independent k-dimensional discrete Fourier transforms (k less than d); it is a reduction algorithm in the sense that it has lowered the dimension of the Fourier transforms that are computed. The k-dimensional discrete Fourier transforms are performed on data derived from the input using only additions, and produce k-dimensional hyperplanes of the output array. GRA

N92-29627# Technische Univ., Delft (Netherlands). Faculty of Technical Mathematics and Informatics.
ARTIBODIES: A SYSTEM FOR MODELLING ARTICULATED BODIES
J. E. Mebius 1991 17 p
(Rept-91-57; ISSN-0922-5641; ETN-92-91423) Copyright Avail: CASI HC A03/MF A01

ARTIBODIES is a software system for modeling articulated bodies with rigid links. It may be applied to a wide class of real life objects, including human and animal bodies, and robots and other artifacts. ARTIBODIES consists of a specification language for articulated bodies and a set of graphic display and manipulation routines. ESA

N92-29630*# Dartmouth Coll., Hanover, NH. Dept. of Mathematics and Computer Science.
AN OVERVIEW OF COMPUTER VIRUSES IN A RESEARCH ENVIRONMENT
Matt Bishop 1991 35 p
(Grants NAG2-328; NAG2-628)
(NASA-CR-190528; NAS 1.26:190528; PCS-TR91-156) Avail: CASI HC A03/MF A01

The threat of attack by computer viruses is in reality a very small part of a much more general threat, specifically threats aimed at subverting computer security. Here, computer viruses are examined as a malicious logic in a research and development environment. A relation is drawn between the viruses and various models of security and integrity. Current research techniques aimed at controlling the threats posed to computer systems by threatening viruses in particular and malicious logic in general are examined. Finally, a brief examination of the vulnerabilities of research and development systems that malicious logic and computer viruses may exploit is undertaken. Author

N92-29641# Sandia National Labs., Livermore, CA.
THE TWOPNT PROGRAM FOR BOUNDARY VALUE PROBLEMS: VERSION 3.10 OF MARCH 1992
J. F. Grcar Apr. 1992 92 p
(Contract DE-AC04-76DR-00789)
(DE92-013394; SAND-91-8230) Avail: CASI HC A05/MF A01

Twopnt is a computer program that finds steady state solutions for systems of differential equations, usually in one space dimension. This is a guide to the program's use and a description of its operation. DOE

N92-29665*# Hawaii Univ., Honolulu. Dept. of Electrical Engineering.
LOW COMPLEXITY, HIGH PERFORMANCE AND BANDWIDTH EFFICIENT CONCATENATED CODED 8-PSK SCHEMES FOR RELIABLE DATA COMMUNICATIONS
Shu Lin, Sandeep Rajpal, and DoJun Rhee 30 Jul. 1992 43 p
(Grant NAG5-931)
(NASA-CR-190588; NAS 1.26:190588; Rept-92-005) Avail: CASI HC A03/MF A01

Nested concatenated coded 8-phase shift keying (PSK) modulation schemes are proposed to achieve good error performance, large coding gains, and high spectral efficiency with reduced decoding complexity. In the concatenation, Reed-Solomon (RS) codes, including the NASA standard (255, 223) RS code, are used as the outer codes and multi-dimensional trellis 8-PSK codes are used as the inner codes. The inner codes are constructed from convolutional codes with good free branch distances and multidimensional 8-PSK coset codes through concatenation. These schemes are analyzed and upper bounds on their error performances are derived. Analytical and simulation results show that these schemes perform extremely well and achieve impressive coding gains over uncoded reference systems for bit-error-rates below 10 exp -3. These schemes achieve large coding gains with reduced decoding complexity. Author

N92-29694*# Research Inst. for Advanced Computer Science, Moffett Field, CA.
DIVERGENCE PRESERVING DISCRETE SURFACE INTEGRAL METHODS FOR MAXWELL'S CURL EQUATIONS USING NON-ORTHOGONAL UNSTRUCTURED GRIDS
Niel K. Madsen (California Univ., Livermore. Lawrence Livermore Lab.) Feb. 1992 41 p
(Contracts NCC2-387; W-7405-eng-48)
(NASA-CR-190555; NAS 1.26:190555; RIACS-TR-92-04) Avail: CASI HC A03/MF A01

Several new discrete surface integral (DSI) methods for solving Maxwell's equations in the time-domain are presented. These methods, which allow the use of general nonorthogonal mixed-polyhedral unstructured grids, are direct generalizations of the canonical staggered-grid finite difference method. These methods are conservative in that they locally preserve divergence or charge. Employing mixed polyhedral cells, (hexahedral, tetrahedral, etc.) these methods allow more accurate modeling of non-rectangular structures and objects because the traditional stair-stepped boundary approximations associated with the orthogonal grid based finite difference methods can be avoided. Numerical results demonstrating the accuracy of these new methods are presented. Author

N92-29695*# Illinois Univ., Urbana. Coordinated Science Lab.
DESIGN AND SCHEDULING FOR PERIODIC CONCURRENT ERROR DETECTION AND RECOVERY IN PROCESSOR ARRAYS
Yi-Min Wang, Pi-Yu Chung, and W. Kent Fuchs 22 May 1992 33 p
(Contract NAG1-613; N00014-90-J-1270)
(NASA-CR-190571; NAS 1.26:190571; UILU-ENG-92-2214; CRHC-92-08) Avail: CASI HC A03/MF A01

Periodic application of time-redundant error checking provides the trade-off between error detection latency and performance degradation. The goal is to achieve high error coverage while satisfying performance requirements. We derive the optimal scheduling of checking patterns in order to uniformly distribute the available checking capability and maximize the error coverage. Synchronous buffering designs using data forwarding and dynamic reconfiguration are described. Efficient single-cycle diagnosis is implemented by error pattern analysis and direct-mapped recovery cache. A rollback recovery scheme using start-up control for local recovery is also presented. Author

N92-29705# Universiteit Twente, Enschede (Netherlands). Tele-Informatics and Open Systems Group.
PROTOCOL CONFORMANCE TESTING: A FORMAL PERSPECTIVE IN ISO IS-9646
Jan Tretmans, Pim Kars, and Ed Brinksma 11 Nov. 1991 49 p
Sponsored in part by Commission of the European Communities
(Memo-INF-91-32; TIOS-91/010; ISSN-0924-3755; ETN-92-91465)
Avail: CASI HC A03/MF A01

Protocol conformance testing is concerned with testing whether a protocol implementation conforms to its specification. Currently, conformance testing is based on an informal, neutral language based methodology, for which the international standard ISO

IS-9646 serves as a reference point. With the increasing use in protocols, their use in protocol conformance testing is getting more attention. Conformance testing based on formal methods should be related to the existing methodology, the standard ISO IS-9646. A formal interpretation of concepts from ISO IS-9646 such as conformance, conformance requirement, test purpose, generic and abstract test case, test method, PICS (Protocol Implementation Conformation Statement), and PIXIT (PI Extra Information for Testing) under the assumption that the protocol was specified in a (standardized) formal description technique, is given. Relations with standard logical theory and with existing notions of conformance in concurrency theory are given. An application to labeled transition system specifications illustrates the presented ideas. ESA

N92-29711# Technische Univ., Delft (Netherlands). Faculty of Technical Mathematics and Informatics.
SOFTWARE QUALITY CONTROL AND REQUIREMENTS SPECIFICATION
Jacco Wesselius 1991 28 p
(Rept-91-48; ISSN-0922-5641; ETN-92-91417) Copyright Avail: CASI HC A03/MF A01

Due to the increasing impact of computer software products on human welfare the quality of these products becomes a topic ever more important. Starting from a short discussion about the meaning of 'quality', it is being argued that a method for specifying software requirements is needed that can serve as a means of communicating both a perception of the customer's problem, and an agreed upon specification of required product characteristics. Based on a classification scheme of software requirements a dependency graph of requirements classes is sketched. From this graph it is shown that the first step towards a method for requirements specification should be the development of a method for specifying product service requirements. After a discussion of the criteria for assessing methods for requirements specification, and a short discussion of existing methods, the starting point of the research is addressed: requirements specification should start with the definition of a 'problem specific terminology'. ESA

N92-29712# Technische Univ., Delft (Netherlands). Faculty of Technical Mathematics and Informatics.
ABSTRACT DATA TYPES AND ALGORITHM STRUCTURES AND A BASIS FOR COMPONENT REUSE
Haikuan Li and J. vanKatwijk 1991 25 p
(Rept-91-49; ISSN-0922-5641; ETN-92-91418) Copyright Avail: CASI HC A03/MF A01

Software reuse can be based on composition principles or on generation principles. These two approaches can complement each other, leading to an approach which supports the features of both approaches. Such a combination is discussed. Two kinds of components are described: Object oriented component (Ocomp) and Structure oriented component (Scomp). The outline of a reuse system is given. Ocomp and Scomp semantics and proposed syntax are described. A binding with C++ is given as an example. ESA

N92-29714# Stockholm Univ. (Sweden). Dept. of Physics.
SOLITON
Michael Bradley and Anna Curir (Osservatorio Astronomico, Turin, Italy) Dec. 1990 17 p
(USIP-90-09; ETN-92-91507) Avail: CASI HC A03/MF A01

The SOLITON program for generating solutions to Einstein's equations with the inverse scattering technique, by Belinskii and Zakharov is discussed. The test concerning the background matrix and the way solutions are obtained are summarized. The available functions are listed and an example of how the program works is given. The program can handle up to three real poles in the scattering matrix. ESA

N92-29745# National Inst. of Standards and Technology, Gaithersburg, MD. Advanced Systems Div.
USER'S MANUAL FOR THE NIST TTCN TRANSLATOR, VERSION 3.0
D. H. Su 31 Aug. 1991 41 p
(PB92-172493; NISTIR-4655) Avail: CASI HC A03/MF A01

Standard conformance testing is the first step in ensuring the interoperability of communications products. There has been increased interest in the development of Abstract Conformance Test Suites (ATS) in the standards community. A standard test script language called Tree and Tabular Combined Notation (TTCN) was used to specify test suites. The National Institute of Standards and Technology (NIST) has developed a TTCN to C language translator to help the industry in speeding up implementation of ATSs into executable test suites (ETS). The manual describes processes involved in implementing an ETS, how the translator is to be used, and the design of the translator itself. Author

N92-29747# Nationaal Inst. voor Kernfysica en Hoge Energiefysica, Amsterdam (Netherlands).
THE FORM VERSION OF MINCER
S. A. Larin (Academy of Sciences, USSR, Moscow), F. V. Tkachov (Fermi National Accelerator Lab., Batavia, IL.), and J. A. M. Vermaseren 1991 39 p Sponsored in part by Natural Sciences and Engineering Research Council and Quebec Committee of Education
(NIKHEF-H/91-18; ETN-92-91616) Avail: CASI HC A03/MF A01

The program MINCER for massless three loop Feynman diagrams of the propagator types was reprogrammed in the language of FORM. The new version is throughly optimized and can be run from a utility like the UNIX 'make', which allows large numbers of diagrams to be conveniently processed. It was used for some calculations that were previously not practical. ESA

N92-29749# Technische Univ., Delft (Netherlands). Faculty of Technical Mathematics and Informatics.
EFFICIENT COMPLETE RADIOSITY RAY TRACING USING A SHADOW COHERENCE METHOD
Arjan J. F. Kok, Frederik W. Jansen, and Charles Woodward (Helsinki Univ. of Technology, Espoo, Finland) 1991 25 p Sponsored in part by Helsinki Univ. of Technology Foundation
(Rept-91-63; ISSN-0922-5641; ETN-92-91427) Copyright Avail: CASI HC A03/MF A01

Most two pass radiosity methods calculate, in a preprocessing step for each patch or element in a scene, a radiosity shading that contains both the intensity of the light that is received directly from the main light sources and the intensity of the light that is received indirectly by means of diffuse and specular interreflection between patches. However, it is very difficult to represent accurately the distribution of the radiosity shading over the patch, in particular where sharp shadows exist. A better approach, therefore, is to store only the indirect reflection component, which is fairly constant over the patch, in the form of radiosity shading, and to calculate the direct reflection component, which is responsible for the larger part of the intensity variation, during the second pass by casting shadow rays. The number of shadow rays for the direct light computation can be kept low by selecting only those light sources that substantially contribute to the shading of a patch, and by applying an adaptive image refinement technique in combination with a shadow coherence method. ESA

N92-29776# Technische Univ., Eindhoven (Netherlands).
CHAIN CODING IN COMPUTER GRAPHICS Ph.D. Thesis
Hubertus Martinus Ma vandeWetering 1991 130 p Sponsored by Netherlands Foundation for Technical Research
(ETN-92-91630) Avail: CASI HC A07/MF A02

Applications of chain coding in the realm of computer graphics are discussed. The basic definitions are given and the notions of discrete curves and chain coding are introduced. Bresenham's line algorithms and algorithms for linear transformations of discrete curves given by chain codes are derived. Properties with respect to linear transformations of dicrete curves are given. As the central part of the study, operators on chains are defined, and these operators are combined into a definition for discrete curves given by three control points. These discrete curves are related to

continuous curves by computing them for different resolutions and having this resolution to go to infinity. Some algorithms for computing the so defined discrete curves are given. These themes are extended for curves with more than three control points. For this situation, two new operators are introduced. The notion of a canonic chain is introduced. An algorithm for computing the set of interior points of a given closed discrete curve is given and is used for computing thick versions of dicrete curves. Offset curves are discussed. ESA

N92-29779# Technische Univ., Delft (Netherlands). Faculty of Technical Mathematics and Informatics.
AN INTRODUCTION TO SOFTWARE REUSE
Haikuan Li 1991 14 p
(Rept-91-50; ISSN-0922-5641; ETN-92-91419) Copyright Avail: CASI HC A03/MF A01

Software reuse is the reapplication of the artifacts and the knowledge about the development of one system to another system in order to reduce the effort of software development and maintenance of that other system. The technologies applied to software reuse can be classified in different ways according to different views. The view that classifying the technologies into reuse-in-the-small and reuse-in-the-large is useful is addressed. Comparing the technologies applied to the two kinds of reuse, reuse-in-the-small is fundamentally limited by its lack of information about improving the whole process of software development and maintenance. However, these limitations may be overcome by reuse-in-the-large which is more likely to be a challenge to software crisis and is, therefore, a hot topic in the near future. What software reuse is, why software reuse is necessary, how to achieve software reuse, current achievements, problems, and future work are described. ESA

N92-29780# Stockholm Univ. (Sweden). Dept. of Physics.
DECOMPOSER: PROGRAM DOCUMENTATION
Mikael Zackrisson Dec. 1991 88 p
(USIP-91-04; ETN-92-91510) Avail: CASI HC A05/MF A01

A computer program, to be used in the process of analyzing molecular spectra, is described. The purpose of the program is to improve line position determination, by separating or decomposing congested spectra into single line profiles using the information in recorded spectra. This is accomplished by making phenomenological assumptions concerning lineshapes of rotational lines. The operations instructions, the program structure, and the data format are presented. The program is useful in cases where the recorded lines have complicated profiles. As lines overlap, bulky interference structures appear in the spectrum and the aid of a numerical bookkeeping device is required. ESA

N92-29782# Technische Univ., Eindhoven (Netherlands).
ARCHITECTURAL SYNTHESIS AND OPTIMIZATION OF DIGITAL SYSTEMS Ph.D. Thesis
Leon Stok 1991 153 p
(ISBN-90-9003966-X; ETN-92-91633) Copyright Avail: CASI HC A08/MF A02

A complete system representation to model all the levels of documentation during the various steps of an architectural synthesis for a digital system is described. A systematic partitioning of the architectural synthesis into optimization problems is featured. The mapping of the various allocation problems into graph theoretic models is shown. Several theoretical results illustrate the delimitation between NP completeness and polynomial optimization problems on data path allocation. The use of both exact and heuristic algorithms to build a practical computer aided design system, based on the system representation, is shown. Several schemes for solving specific instantiations of the synthesis problem for particular architectures are described. Algorithms for applications in which interconnect area is a major concern are given. ESA

N92-29797# Oak Ridge National Lab., TN.
REVERSE AUTOMATIC DIFFERENTIATION OF MODULAR FORTRAN PROGRAMS
J. E. Horwedel Mar. 1992 27 p
(Contract DE-AC05-84OR-21400)
(DE92-014071; ORNL/TM-12050) Avail: CASI HC A03/MF A01

Several software systems are available for implementing automatic differentiation of computer programs. The forward mode of automatic differentiation is limited by computational intensity and computer memory. The reverse mode, or adjoint approach, is limited by computer memory and disk storage. A modular technique for derivative computation that can significantly reduce memory required to compute derivatives in a complex FORTRAN model using the reverse mode of automatic differentiation is discussed and demonstrated. DOE

N92-29815# Universiteit Twente, Enschede (Netherlands). Dept. of Computer Science.
A NEW HEURISTIC FOR LOAD-BALANCED ASSIGNMENT OF OBJECTS AND MINIMIZED NETWORK COMMUNICATION IN DISTRIBUTED PROGRAMS IMPLEMENTED THROUGH INVERSE REMOTE PROCEDURE CALLS
Alexander D. Stoyenko (New Jersey Inst. of Tech., Newark.), Mehmet Aksit, and Jan Bosch Dec. 1991 37 p Sponsored in part by AT and T Technologies, Inc.; Siemens Corporate Research; New Jersey Inst. of Technology; and State of New Jersey
(Grant NATO-CRG-901077)
(Memo-INF-91-91; ISSN-0924-3755; ETN-92-91583) Copyright Avail: CASI HC A03/MF A01

A load balancing and communication minimizing heuristic used in the Inverse Remote Procedure Call (IRPC) system is introduced. The system provides compile and run time support for developing distributed applications, while shielding the programmer from the details of distribution and interconnection. The IRPC graph partitioning heuristic operates in time of O(N) in the number of communicating objects. This complexity is both independent of M, the number of network sites, and considerably better than that of previously known related algorithms, such as the A, which employs backtracking and is potentially exponential of the max-flow/min-cut class of network flow algorithms or heuristics which tend to be at least of O(M(N (exp 4))). In an extensive quantitative evaluation, the heuristic was demonstrated to perform very well, finding on the average 75 percent traffic cost reductions for over 95 percent of the programs. By employing transparent and automatic mechansims and a well performing efficient distributing heuristic, the IRPC system improves significantly on the previous systems, and serves as a useful tool for distributed application development. ESA

N92-29816# Universiteit Twente, Enschede (Netherlands). Dept. of Computer Science.
INFORMATION SYSTEMS ANALYSIS AND DESIGN BASED ON AN OBJECT-ORIENTED FRAMEWORK
Rob L. W. vandeWeg and Rolf Engmann Dec. 1991 59 p
(Memo-INF-91-93; ISSN-0924-3755; ETN-92-91584) Copyright Avail: CASI HC A04/MF A01

Four studies are presented: a framework and method of Object Oriented (OO) information Systems Analysis and Design (SAD); an architecture for information systems and CASE (Computer Aided Software Engineering) tools based on an OO framework; a grammar for OOSAD; the IFIP case. Real world entities are modeled as objects with Entity Relationship (ER) diagrams, state transition diagrams and a formal grammar. Steps in OO development are defined corresponding to the framework. This yields a method for OOSAD. An architecture for OO information systems, which is structured in layers, each layer representing specific concepts of the OOSAD framework, is described. The architecture leads to specifications for CASE tools, that may be constructed for supporting development of information systems. With these CASE tools it will be possible to specify (well known diagram techniques) information systems independently of the implementation environment (programming language and database management system). Examples of mappings of ER models and state transition diagrams to a relational database environment and object oriented programming language are described. The extended Backus-Nauer

form is used to specify a formal gammar derived from the OOSAD framework. An illustration of the application of the OOSAD method is given by means of the IFIP case. ESA

N92-29818# Technische Univ., Eindhoven (Netherlands). Dept. of Mathematics and Computing Science.
ON THE p-COVERAGE PROBLEM ON THE REAL LINE
Stan vanHoesel and Albert Wagelmans (Erasmus Univ., Rotterdam, Netherlands) Dec. 1991 27 p Sponsored in part by Netherlands Organization for Applied Scientific Research TNO
(Memo-COSOR-91-33; ETN-92-91787) Avail: CASI HC A03/MF A01

The p-coverage problem on the real line is considered. A detailed description of an algorithm to solve the coverage problem without the upper bound p on the number of open facilities is given. The change in the structure of the optimal solution when the setup costs of the facilities are all decreased by the same amount is analyzed. This result is used to develop a parametric approach to the p-coverage problem which runs in O(pnlogn) time, n being the number of clients. ESA

N92-29819# Technische Univ., Eindhoven (Netherlands). Dept. of Mathematics and Computing Science.
ON SETUP COST REDUCTION IN THE ECONOMIC LOT-SIZING MODEL WITHOUT SPECULATIVE MOTIVES
Stan vanHoesel and Albert Wagelmans (Erasmus Univ., Rotterdam, Netherlands) Dec. 1991 23 p Sponsored in part by Netherlands Organization for Applied Scientific Research TNO
(Memo-COSOR-91-34; ETN-92-91788) Avail: CASI HC A03/MF A01

An important special case of the economic lot sizing problem is the one in which there are no speculative motives to hold inventory, i.e., the marginal cost of producing one unit in some period plus the cost of holding it until some future period is at least the marginal production cost in the latter period. It is already known that this special case can be solved in linear time. The effects of reducing all setup costs by the same amount is studied. It turns out that the optimal solution changes in a very structured way. This fact will be used to develop faster algorithms for several problems that can be reformulated as parametric lot sizing problems. The result is an algorithm for the so called dynamic lot sizing problem with learning effects in setups. This algorithm has a complexity that is of the same order as the fastest algorithm known so far, but is valid for a more general class of models than usually considered. ESA

N92-29820# Technische Univ., Eindhoven (Netherlands). Dept. of Mathematics and Computing Science.
ON THE COMPLEXITY OF POSTOPTIMALITY ANALYSIS OF 0/1 PROGRAMS
Stan vanHoesel and Albert Wagelmans (Erasmus Univ., Rotterdam, Netherlands) Dec. 1991 24 p Sponsored in part by Netherlands Organization for Applied Scientific Research TNO
(Memo-COSOR-91-35; ETN-92-91789) Avail: CASI HC A03/MF A01

The complexity of postoptimality analysis of 0/1 programs with a linear objective function is addressed. After an optimal solution has been determined for a given cost vector, one may want to know how much each cost coefficient can vary individually without affecting the optimality of the solution. It is shown that, under mild conditions, the existence of a polynomial method to calculate these maximal ranges implies a polynomial method to solve the 0/1 program itself. As a consequence, postoptimality analysis of many well known NP hard problems can not be performed by polynomial methods, unless P = NP. A natural question that arises with respect to these problems is whether it is possible to calculate in polynomial time reasonable approximations of the maximal ranges. It is shown that it is equally unlikely that there exists a polynomial method that calculates conservative ranges for which the relative deviation from the true ranges is guaranteed to be, at most, some constant. The issue of postoptimality analysis of epsilon optimal solutions of NP hard 0/1 problems is addressed. It is shown that for an epsilon optimal solution that has been determined in polynomial time, it is not possible to calculate in polynomial time the maximal amount by which a cost coefficient can be increased such that the solution remains epsilon optimal, unless P = NP. ESA

N92-29855# Universiteit Twente, Enschede (Netherlands). Dept. of Computer Science.
IMPLEMENTATION OF THE OBJECT-ORIENTED DATA MODEL TM
Hennie J. Steenhagen and Peter M. G. Apers Dec. 1991 23 p
(Memo-INF-91-94; ISSN-0924-3755; ETN-92-91585) Copyright Avail: CASI HC A03/MF A01

The high level object oriented data model TM, based on an extension of the type theory of Cardelli, is addressed. TM includes a logical formalism for constraint specification, which is an important aspect of the data model, and the notion of predicative sets. Predicative set expressions provide for a high level, descriptive specification mechanism. Topics of research are the theoretical foundations of TM, as well as implementation aspects. Just as in the case of relational database systems, algebraic optimization is expected to be an important aspect of efficient implementation of the data model. With the expectation in mind, the language ADL (Algebraic Database Language), based on the Functional Programming language FP is defined. Like FP, ADL is a language in which programs are functions, built up from primitive operators and functionals (higher order functions). The translation of TM to ADL is described. An algorithm is presented to translate (safe) TM expression into ADL expressions. Optimization in ADL is discussed and some equivalence rules are given. ESA

N92-29865# Center for Mathematics and Computer Science, Amsterdam (Netherlands). Dept. of Operations Research, Statistics, and System Theory.
SOFTWARE RELIABILITY AND THE BOOTSTRAP
Mark C. vanPul Sep. 1991 11 p Sponsored by Netherlands Foundation for Applied Technology and Netherlands Organization for Applied Scientific Research TNO
(CWI-BS-R9123; ISSN-0924-0659; ETN-92-91647) Copyright Avail: CASI HC A03/MF A01

It is demonstrated that in a general framework of counting processes, the parametric bootstrap is asymptotically consistent. The general framework of counting processes and intensities as described in Van Pul (1990) are summarized. How parametric bootstrap methods could be applied is discussed. It is shown that in this general setting the parametric bootstrap is asymptotically consistent. The proof, which makes use of the Skohorod-Dudley-Wichura 'almost pure representation' theorems, is based on stronger versions of the concepts of LAN and regularity. Some applications of the developed theory in the context of software reliability are addressed. The bootstrap method is applied on simulated data according to the model of Jelinski-Moranda. ESA

N92-29868# Center for Mathematics and Computer Science, Amsterdam (Netherlands). Computer Science.
OPTIMALITY OF WAIT-FREE ATOMIC MULTIWRITER VARIABLES
Ming Li (Waterloo Univ., Ontario) and Paul M. B. Vitanyi (Amsterdam Univ., Netherlands) Jun. 1991 11 p Submitted for publication Sponsored by Netherlands Organization for Applied Scientific Research TNO
(CWI-CS-R9128; ETN-92-91785) Copyright Avail: CASI HC A03/MF A01

Known implementations of concurrent wait free atomic shared multiwriter variables use Theta(n) control bits per subvariable. Implementations of sequential time stamp systems have been shown to require Omega(n) control bits per subvariable. A sequential wait-free atomic shared multiwriter variable construction using log n control bits per subvariable is exhibited. There arises the question of the optimality of concurrent implementations of the same, and of weak time stamp systems. It is shown that the solutions are self stabilizing. ESA

N92-29869# European Space Agency. European Space Research and Technology Center, ESTEC, Noordwijk (Netherlands). Thermal Control and Life Support Div.
ESATAN USER MANUAL
Nov. 1991 444 p
(ESA-PSS-03-105-Issue-2; ISSN-0379-4059; ETN-92-91386)
Copyright Avail: CASI HC A19/MF A04

The ESATAN user manual provides a full description of the use and operation of the ESA thermal analyzer, ESATAN. It describes in detail the preprocessor, editor, SINDA to ESATAN translator, and the syntax checker. A complete list of the ESATAN library routines and their usage is given. ESA

N92-29887# Technische Univ., Delft (Netherlands). Faculty of Technical Mathematics and Informatics.
ARCHITECTURE AND USE OF DELFT DIRECT MANIPULATION MANAGER (D2M2)
Johan Versendaal, Willem Beekman, Marco Kruit, and Charles vanderMast 1991 20 p
(Rept-91-46; ISSN-0922-5641; ETN-92-91416) Copyright Avail: CASI HC A03/MF A01

A user interface management system based on an object oriented approach to the design of both the user interface and the application semantics is presented. The data for user interface and application semantics are stored and processed apart. However, the modeling technique is identical for both, using the same tool for semantic data modeling. The modeling technique supports most characteristics of the object oriented paradigm: objects, classes and inheritance. The diagrams used can describe among others the concepts classification, aggregation, decomposition, generalization specialization and role attributes. Attributes of objects can be described in propriety forms. Transition diagrams including pre and post conditions are applied to specify the interaction possible to the end use. The concepts supported by this tool are described and discussed. This tool as well as the products it can produce are based on the graphical user interface. From these specifications a run time version of the application can be generated. A protocol is used for the communication between applications and user interface manager during run time. The features of a Delft Direct Manipulation Manager are demonstrated with the design and implementation of a small application with direct manipulation. ESA

N92-29890# Center for Mathematics and Computer Science, Amsterdam (Netherlands). Dept. of Software Technology.
COMPUTING DISTINGUISHING FORMULAS FOR BRANCHING BISIMULATION
Henri P. Korver Mar. 1991 20 p Sponsored by EEC
(CWI-CS-R9121; ETN-92-91549) Copyright Avail: CASI HC A03/MF A01

Branching bisimulation is a behavioral equivalence in labeled transition systems proposed by Van Glabbeek and Weijland as an alternative to Milner's observational equivalence. An algorithm is presented which, given two branching bisimulation inequivalent finite state processes, produces a distinguishing formula in Hennessy-Milner logic extended with an 'until' operator. The algorithm, which is a modification of an algorithm due to Cleaveland, works in conjunction with a partition refinement algorithm for deciding branching bisimulation equivalence. The algorithm provides a useful extension to the algorithm for deciding equivalence because it tells a user 'why' certain finite state systems are inequivalent. ESA

N92-29891# Center for Mathematics and Computer Science, Amsterdam (Netherlands). Dept. of Algorithmics and Architecture.
FACETS OF DATABASE TRIGGERS
M. H. vanderVoort and M. L. Kersten Mar. 1991 38 p
(CWI-CS-R9122; ETN-92-91550) Copyright Avail: CASI HC A03/MF A01

Rule based programming has found wide spread use in computer science. It is disguised as exceptions in operating systems, as production systems and deamons in artificial intelligence, as actors in programming languages, and as triggers in database systems. Generally, triggers are event condition action triples, where the action is executed when the condition holds after the event has occurred. In database systems, triggers are used for integrity enforcement, to maintain materialized views, for notification of users, and to provide an abstraction level to the application programmer. Three main issues of triggers are addressed in a database context: the trigger definition language, trigger semantics, and trigger optimization. The first issue focuses on the usage of triggers and on the concepts and expressiveness of trigger languages. The second issue treats several execution models, which determine the interaction of triggers and database applications. As always, optimization of triggers is of vital importance to obtain acceptable performance. Sophisticated indexing and evaluation strategies are discussed. ESA

N92-29961# Universiteit Twente, Enschede (Netherlands). Dept. of Computer Science.
AN OBJECT-ORIENTED LANGUAGE-DATABASE INTEGRATION MODEL: THE COMPOSITION-FILTERS APPROACH
Lodewijk Bergmans, Mehmet Aksit, and Sinan Vural Dec. 1991 26 p
(Memo-INF-91-90; ISSN-0924-3755; ETN-92-91582) Copyright Avail: CASI HC A03/MF A01

A model based on so called object composition filters, that uniformly integrates database like features into an object oriented language, is introduced. The focus is on providing persistent dynamic data structures, data sharing, transactions, multiple views, and associative access, integrated with the object oriented paradigm. The main contribution is that the database like features are part of this new object oriented model; therefore, they are uniformly integrated with object oriented features such as data abstraction, encapsulation, message passing, and inheritance. This approach eliminates the problems asssociated with existing systems such as lack of reusability and extensibility for database operations, the violation of encapsulation, the need to define specific types such as sets, and the incapability to support multiple views. The model is illustrated through the object oriented language SINA. ESA

N92-29970# Universiteit Twente, Enschede (Netherlands). Dept. of Computer Science.
INVERSE REMOTE PROCEDURE CALLS
Alexander D. Stoyenko (New Jersey Inst. of Tech., Newark.), Mehmet Aksit, and Jan Bosch Dec. 1991 23 p Sponsored by AT and T; Siemens Corporate Research; New Jersey Inst. of Technol.; and State of New Jersey
(Grant NATO-CRG-901077)
(Memo-INF-91-89; ISSN-0924-3755; ETN-92-91776) Copyright Avail: CASI HC A03/MF A01

One of the challenges in RPC (Remote Procedure Call) research is to minimize expensive network traffic, found in great many distributed applications. The Inverse RPC (IRPC) System that shields the distributed program writer from this complex problem by providing transparent and automatic mechanism to do the task is introduced. Given a distributed program, the IRPC System maps it (statically or dynamically) to a graph that represents program objects and their dependencies (due to invocations and parameter passing) as nodes and edges, respectively. The IRPC graph partitioning heurtistic operates in time of O(N squared) in the number of communicating objects. This complexity is both independnt of M, the number of network sites, and considerably better than that of previously known related algorithms which tend to be at least of O(MN exp 4). In an extensive quantitative evaluation, the heuristic was demonstrated to perform very well, finding on the average 50 percent traffic cost reductions for over 90 percent of the programs. The heuristic was also demonstrated to be stable and robust, and to find cost reductions independently of the number of distributed program objects and the structure of the program. ESA

N92-29981# Universiteit Twente, Enschede (Netherlands). Tele-Informatics and Open Systems Group.
A SOFT STAIRWAY TO INSTITUTIONS
Antonino Salibra (Pisa Univ., Italy) and Giuseppe Scollo 5 Dec. 1991 22 p
(Memo-INF-91-87; TIOS-91/035; ISSN-0924-3755; ETN-92-91774) Copyright Avail: CASI HC A03/MF A01

The notion of institution is dissected into less restrictive notions. A novel notion of institution morphism is introduced and preservation of institution properties by corresponding properties of such morphisms is characterized. The target of this work is the stepwise construction of a general framework for translating logics and algebraic specifications using them. An available translation of order sorted conditional equational logic into equational type logic is revisited in this light. Model theoretic results relating to compactness are presented. ESA

N92-29989# Center for Mathematics and Computer Science, Amsterdam (Netherlands). Dept. of Computer Science.
AN ALGEBRAIC SPECIFICATION FOR THE STATIC SEMANTICS OF PASCAL
A. vanDeursen Jun. 1991 96 p Sponsored in part by Commission of the European Communities and Netherlands Organization for Applied Scientific Research TNO
(CWI-CS-R9129; ETN-92-91554) Copyright Avail: CASI HC A05/MF A01

An algebraic specification made for the complete static semantics of PASCAL as defined by the International Standardization Organization is discussed. An explanation of how the specification was set up, and how several details were dealt with in a convenient way is given. The specification is related to algebraic specifications for other aspects of (other) programming languages, and the algebraic approach is compared with the other formal specifications for PASCAL. ESA

N92-29990# Center for Mathematics and Computer Science, Amsterdam (Netherlands). Dept. of Computer Science.
LOOP CHECKING IN PARTIAL DEDUCTION
Roland N. Bol Jul. 1991 37 p Submitted for publication Sponsored in part by Commission of the European Communities and Netherlands Organization for Applied Scientific Research TNO
(CWI-CS-R9134; ETN-92-91557) Copyright Avail: CASI HC A03/MF A01

In the framework of a referenced study on partial evaluation in logic programming, partial deduction involves the creation of SLD trees for a given program and some goals, up to certain halting points. The relation between halting criteria for partial deduction and loop checking, (as formalized in a referenced study in the analysis of loop checking mechanisms for logic programs) is identified. It appears that loop checks for partial deduction must be complete, whereas traditionally the soundness of a loop check is more important. However, it is also shown that sound loop checks can contribute to improve partial deduction. A class of complete loop checks suitable for partial deduction is identified. ESA

N92-29991# Center for Mathematics and Computer Science, Amsterdam (Netherlands). Dept. of Computer Science.
RENDEZ-VOUS WITH METRIC SEMANTICS
J. W. deBakker (Vrije Univ., Amsterdam, Netherlands) and E. P. deVink (Vrije Univ., Amsterdam, Netherlands) Jul. 1991 32 p Sponsored in part by Commission of the European Communities and Netherlands Organization for Applied Scientific Research TNO
(CWI-CS-R9135; ETN-92-91558) Copyright Avail: CASI HC A03/MF A01

A comparative semantic study of an element of the family of concurrent object-oriented programming languages is made. Particular attention is paid to two notions: dynamically evolving process structures, including a mechanism to name and refer to processes and means to create new processes; and rendezvous between processes involving the sending and answering of messages and the induced execution of method calls. The methodology of metric semantics is applied in the design of operational and denotational semantics, as well as in the proof of their equivalence. Both semantics employ domains which are determined as fixed points of a contracting factor in the category of complete metric spaces. Fruitful use is made of the technique of defining semantic meaning functions as fixed points of contracting high order mappings. Syntactic and semantic continuations play a pervasive role. ESA

N92-29992# Center for Mathematics and Computer Science, Amsterdam (Netherlands). Dept. of Computer Science.
CCS FOR OO AND LP
J. W. deBakker (Vrije Univ., Amsterdam, Netherlands) and E. P. deVink (Vrije Univ., Amsterdam, Netherlands) Jul. 1991 36 p Sponsored in part by Commission of the European Communities and Netherlands Organization for Applied Scientific Research TNO
(CWI-CS-R9136; ETN-92-91559) Copyright Avail: CASI HC A03/MF A01

The design of Comparative Continuation Semantics (CCS) for Object Oriented (OO) and Logic Programming (LP) languages is illustrated by three case studies dealing with process creation, backtracking, and rendezvous. Operational and denotational semantics involving syntactic and semantic continuations are proposed, and their equivalence is shown. For the rendezvous concept, a somewhat streamlined version of earlier work in the semantics of the Parallel Object Oriented Language (POOL) is presented. The metric framework is exploited throughout, and (unique fixed points of) contracting functions are used pervasively. ESA

N92-29994# Center for Mathematics and Computer Science, Amsterdam (Netherlands). Dept. of Computer Science.
PROOF THEORY FOR MICRO CRL
Jan Friso Groote and Alban Ponse Aug. 1991 44 p Sponsored by Commission of the European Communities and Netherlands Organization of Applied Scientific Research TNO
(CWI-CS-R9138; ISSN-0169-118X; ETN-92-91561) Copyright Avail: CASI HC A03/MF A01

A proof theory for the specification language micro-CRL (Common Representation Language) is proposed. Micro-CRL consists of process algebra extended with abstract data types. The proof theory is meant to formalize the interaction between processes and data. It provides the means to prove properties about these in a precise way. The proof theory was designed such that automatic proof checking is feasible. A simple language in which basic properties of processes and of data can be expressed is defined. A proof system for this property language, comprising a rule for induction, the recursive specification principle, and process algebra axioms, is presented. The proof theory is illustrated with small examples and a case study about a bag. ESA

N92-30020# National Inst. of Standards and Technology, Gaithersburg, MD. Fabrication Technology Div.
SHOP OF THE 1990'S: THE IMPLEMENTATION OF A CAD/CAM SYSTEM FOR SMALL MACHINE SHOPS
A. Moll Mar. 1992 52 p
(PB92-181098; NISTIR-4810) Avail: CASI HC A04/MF A01

Outlined here are the logical implementation steps and procedures that should be followed after a small machine shop has purchased a computer aided design/computer aided manufacturing (CAD/CAM) system. Author

N92-30073# Universiteit Twente, Enschede (Netherlands). Dept. of Computer Science.
A CASE STUDY IN FUNCTIONAL REAL-TIME PROGRAMMING
D. H. Fijma and R. T. Udink Aug. 1991 22 p
(Memo-INF-91-62; ISSN-0924-3755; ETN-92-91566) Avail: CASI HC A03/MF A01

A case study in functional real time programming is presented. Some solutions to the lack of time expressibility in functional

languages are discussed. It was realized that not only the lack of time expressibility, but also the lack of a notion of independent parallel processes was a problem. The sorting office concept, as introduced by W. Stoye, was originally presented as a solution of the first problem. The proper notion of processes it enables is emphasized. Using this concept, a controller for a robot arm was programmed. ESA

N92-30141# Center for Mathematics and Computer Science, Amsterdam (Netherlands). Dept. of Computer Science.
TEXTURE SYNTHESIS
Michal Haindl Sep. 1991 54 p Sponsored by European Research Consortium for Informatics and Mathematics and Netherlands Organization for Applied Scientific Research TNO
(CWI-CS-R9139; ISSN-0169-118X; ETN-92-91562) Copyright Avail: CASI HC A04/MF A01

Texture synthesis methods are considered. To enhance realism in graphical systems it is necessary to cover generated surfaces with natural like textures. A texture is assumed to be a realization of a random field. Problems of parameter estimation and random field synthesis of a given random field model are studied. The most flexible models for natural like textures synthesis seem to be simultaneous autoregressive and Gaussian Markov random field models. ESA

N92-30144# Universiteit Twente, Enschede (Netherlands). Tele-Informatics and Open Systems Group.
A FORMAL DEVELOPMENT TRAJECTORY FOR OSI APPLICATION LAYER PROTOCOLS
R. E. Booth, I. Widya, V. M. Jones, R. J. Clark, F. Juillot, and G. vanderHeijden Sep. 1991 16 p
(Memo-INF-91-71; TIOS-91/026; ISSN-0924-3755; ETN-92-91572) Avail: CASI HC A03/MF A01

Experience developing Open Systems Interconnection (OSI) application layer protocols using a methodology which exploits the formal language Language, Of temporal Ordering Specification (LOTOS), for wide spectrum design is reported. LOTOS and LOTOS based development methods are described and three case studies using OSI application layer protocols are described. Each case study explores a different design solution with particular emphasis on the industrial applicability of the techniques used. ESA

N92-30146# Center for Mathematics and Computer Science, Amsterdam (Netherlands). Dept. of Computer Science.
LINEAR APPROXIMATION OF SHORTEST SUPERSTRINGS
Avrim Blum (Massachusetts Inst. of Tech., Cambridge.), Tao Jiang (McMaster Univ., Hamilton, Ontario), Ming Li (Waterloo Univ., Ontario), John Tromp, and Mihalis Yannakakis (Bell Telephone Labs., Inc., Murray Hill, NJ.) Apr. 1991 15 p Presented at the 1991 ACM Symposium on Theory of Computing Submitted for publication Sponsored in part by NSF; SERB; and McMaster Univ.
(Grants NSERC-OGP-0046613; NSERC-OGP-0036747; NSERC-OGP-0046506)
(CWI-CS-R9126; ETN-92-91639) Copyright Avail: CASI HC A03/MF A01

It is shown that the superstring problem can be approximated within a constant factor, and that algorithm GREEDY produces a superstring of length at most 4n. The algorithm, named GREEDY, repeatedly merges the pair of strings with maximum overlap until only one string remains. How well GREEDY approximates a shortest common superstring, is still an open question. A modified greedy procedure MGREEDY that achieves a bound of 4n, and another algorithm TGREEDY, based on MGREEDY, that achieves 3n, are included. Notation, definitions, and some basic facts about strings are given. The algortihm MGREEDY with its proof are presented and the 4n bound for GREEDY is given. It is shown that the superstring problem is MAX SNP-hard which implies that it is unlikely there is a polynomial time approximation scheme for the superstring problem. ESA

N92-30179# Center for Mathematics and Computer Science, Amsterdam (Netherlands). Dept. of Operations Research, Statistics, and System Theory.
SIMULATIONS ON THE JELINSKI-MORANDA MODEL OF SOFTWARE RELIABILITY
Mark C. J. vanPul Sep. 1991 18 p Sponsored by Netherlands Foundation for Applied Technology and Netherlands Organization for Applied Scientific Research TNO
(CWI-BS-R9122; ISSN-0924-0659; ETN-92-91563) Copyright Avail: CASI HC A03/MF A01

In software reliability theory many different models have been proposed and investigated. Some of these models intuitively match better with reality than others. The properties of certain static estimation procedures in connection with these models, on the contrary, are also model dependent. An investigation as to how well the maximum likelihood estimation procedure behaves in the case of the very well known software reliability model suggested by Jelinski-Moranda is presented. The Jelinski-Moranda model is described and background in counting processes and martingale theory is given. Simulation experiments are described and computations of some asymptotic expected variances are given. ESA

N92-30181# Universiteit Twente, Enschede (Netherlands). Dept. of Computer Science.
OBJECT-ORIENTED SYSTEM IMPLEMENTATION
E. G. Zondag Aug. 1991 26 p
(Memo-INF-91-67; ISSN-0924-3755; ETN-92-91569) Copyright Avail: CASI HC A03/MF A01

Issues relating to the dependence quality of system implementation on the way the system constituents and their management are modeled and developed and the benefits of object oriented approaches to both modeling and development are addressed. An object oriented development scheme is suggested. Essential elements are system structuring, an elementary graphical notation, and subjects and repositories. Object oriented analysis and design schemes are presented as short algorithms with a number of guidelines. Some state of the art material for implementing systems is surveyed, biasing object orientedness. Topics are management considerations, resources as objects, object groups (fragmentation and propagation), and system construction (customization, layers and modules, openness and minimality). A system development model based on 'fab systems' as frameworks is proposed. A fab is a general system building block. An implementation strategy is suggested. ESA

N92-30186# Universiteit Twente, Enschede (Netherlands). Faculty of Applied Mathematics
ALGORITHMS AND MIN-MAX THEOREMS FOR CERTAIN MULTIWAY CUTS
Peter L. Erdoes and Laszlo A. Szekeley (Bonn Univ., Germany, F.R.) Jan. 1992 15 p Sponsored in part by Alexander von Humboldt-Stiftung
(MEMO-1022; ISSN-0169-2690; ETN-92-91767) Avail: CASI HC A03/MF A01

A greedy type algortihm and a min-max theorem is developed for the multiway cut problems of trees. Applications to biology also require complicated edge weights that depend on the two components adjacent by the edge. A dynamic programming type algorithm for this more general problem is given and the min-max theorem is shown to be no longer valid. As a substitute, a sort of min-max theorem that seems to fit the biological applications is shown. ESA

N92-30191# Universiteit Twente, Enschede (Netherlands). Tele-Informatics and Open Systems Group.
PERFORMABILITY MODELLING TOOLS: A SURVEY
Boudewijn R. Haverkort and Ignas G. Niemegeers Nov. 1991 34 p
(Memo-INF-91-82; TIOS-91/031; ISSN-0924-3755; ETN-92-91772) Copyright Avail: CASI HC A03/MF A01

A fairly general modeling tool framework that can be used as a guide to assess the usability and structure of performability

modeling tools was developed. The mathematical aspects of performability modeling (the core of every performability modeling tool) are reviewed and this framework is discussed. Eleven recently developed tools that can all be used for aspects of performability modeling and analysis are discussed. Their structure, their capabilities in terms of measures that can be obtained, and the used modeling formalism are assessed. Directions for future work in the field of performability modeling tools are considered. ESA

N92-30195# Katholieke Univ., Nijmegen (Netherlands). Nijmeegs Inst. voor Cognitie-Onderzoek en Informatie-Technologie.
VISUAL PATTERN COMPLETION
F. Boselie and D. Wouterlood Oct. 1990 21 p
(PB92-187418; Internal-90-NICI-08) Avail: CASI HC A03/MF A01

The phenomenon of visual completion poses two problems: (1) how to tell when an occluding and a partly occluded object can be seen, as opposed to one or several non-overlapping objects; and (2) how to see behind the occluding object. These problems can be answered by prevailing specifications of minimum principles. The paper argues that the principle of good continuation plays a dominant role in the perceptual organization of completion-patterns. Author

N92-30201# Leiden Univ. (Netherlands). Dept. of Mathematics and Computer Science.
SEPARABLE MARKOVIAN DECISION PROBLEMS: THE LINEAR PROGRAMMING METHOD IN THE MULTICHAIN CASE (REVISED)
L. C. M. Kallenberg 1992 26 p
(PB92-187350; TW-91-09) Avail: CASI HC A03/MF A01

Separable Markovian decision problems have the following properties that for certain pairs (i,a) of state i and an action a: (1) the immediate reward is the sum of terms due to the current state and action (r(ia) = s(i) + t(a)); and (2) the transition probability depends only on the action and not on the state from which the transition occurs. The separable model was first studied in the late sixties. For the discounted case and the unichain undiscounted case, a reduced LP formulation was given, which involves a substantially smaller number of variables than in the LP formulation of a general Markov decision problem. It was unknown whether such an efficient formulation was also possible in the multichain case. The paper solves the problem; such an efficient formulation can be obtained. Some applications of separable models are also presented. Author

N92-30207*# Toledo Univ., OH.
USERS MANUAL FOR UPDATED COMPUTER CODE FOR AXIAL-FLOW COMPRESSOR CONCEPTUAL DESIGN Final Report
Arthur J. Glassman Jul. 1992 23 p
(Grant NAG3-1165; RTOP 505-69-50)
(NASA-CR-189171; E-7003; NAS 1.26:189171) Avail: CASI HC A03/MF A01

An existing computer code that determines the flow path for an axial-flow compressor either for a given number of stages or for a given overall pressure ratio was modified for use in air-breathing engine conceptual design studies. This code uses a rapid approximate design methodology that is based on isentropic simple radial equilibrium. Calculations are performed at constant-span-fraction locations from tip to hub. Energy addition per stage is controlled by specifying the maximum allowable values for several aerodynamic design parameters. New modeling was introduced to the code to overcome perceived limitations. Specific changes included variable rather than constant tip radius, flow path inclination added to the continuity equation, input of mass flow rate directly rather than indirectly as inlet axial velocity, solution for the exact value of overall pressure ratio rather than for any value that met or exceeded it, and internal computation of efficiency rather than the use of input values. The modified code was shown to be capable of computing efficiencies that are compatible with those of five multistage compressors and one fan that were tested experimentally. This report serves as a users manual for the revised code, Compressor Spanline Analysis (CSPAN). The modeling modifications, including two internal loss correlations, are presented. Program input and output are described. A sample case for a multistage compressor is included. Author

N92-30227# Technische Univ., Delft (Netherlands). Faculty of Technical Mathematics and Information.
A MONOTONIC BUILD-UP SIMPLEX ALGORITHM FOR LINEAR PROGRAMMING
Kurt M. Anstreicher (Iowa Univ., Iowa City.) and Tamas Terlaky 1991 20 p
(Contract OTKA-2115)
(Rept-91-82; ISSN-0922-5641; ETN-92-91832) Copyright Avail: CASI HC A03/MF A01

A simple pivot rule which has interesting theoretical properties is devised. Beginning with a basic feasible solution, and any nonbasic variable having a negative reduced cost, the pivot rule produces a sequence of pivots such that ultimately the originally chosen nonbasic variable enters the basis, and all reduced costs which were originally nonnegative remain nonnegative. Thus, the pivot rule monotonically builds up to a dual feasible, and, hence, an optimal basis. A surprising property of the pivot rule is that the pivot sequence results in intermediate bases which are neither primal nor dual feasible. Correctness of the procedure is proved, and a geometric interpretation is given and related to other pivoting rules for linear programming. ESA

N92-30228# Technische Univ., Delft (Netherlands). Faculty of Technical Mathematics and Information.
SRSM: A SOFTWARE REQUIREMENTS SPECIFICATION METHOD
Jacco Wesselius and Frans Ververs 1991 24 p
(Rept-91-84; ISSN-0922-5641; ETN-92-91834) Copyright Avail: CASI HC A03/MF A01

The argument that the specification of software requirements in a clear unambiguous way that enables communication among customers, users, specifiers, and developers is an essential step towards the achievement of software quality control is addressed. An approach to software requirements specification is presented that is centered around the definition of a problem specific language. The approach is intended to result in requirements specifications that are understandable to the customer, and that yet have a formally well defined meaning. ESA

N92-29375*# Jet Propulsion Lab., California Inst. of Tech., Pasadena.
GOLAY AND OTHER BOX CODES
G. Solomon *In its* The Telecommunications and Data Acquisition Report 15 May 1992 p 130-135 (For primary document see N92-29364 20-32)
(RTOP 310-30-71-83-02)
Avail: CASI HC A02/MF A04

62 COMPUTER SYSTEMS

Includes computer networks and special application computer systems.

N92-29353# Lawrence Livermore National Lab., CA.
CODE GENERATION IN ALPAL USING SYMBOLIC TECHNIQUES
G. O. Cook, Jr. 30 Dec. 1991 11 p Presented at the International Symposium on Symbolic and Algebraic Computation, Berkeley, CA, 27-29 Jul. 1992
(Contract W-7405-eng-48)
(DE92-011299; UCRL-JC-108973; CONF-920760-2) Avail: CASI HC A03/MF A01

In practice it takes far more time to program a numerical model than to derive it, especially for a nonlinear model or a model that is approximated by an implicit numerical technique. As part of an effort to simplify this part of the scientist's job, we have created A Livermore Physics Applications Language (ALPAL). ALPAL

automatically generates Fortran or C code to numerically solve scientific problems that involve differential and integral equations. The scientist specifies the model and, optionally, the numerical methods with ALPAL using an almost natural language like that used in journal articles. ALPAL is unique in that it can generate highly efficient code, even for the very complicated mathematical problems that arise in large scientific simulation codes. This high level of power is achieved by use of symbolic techniques, including use of computer algebra facilities. DOE

N92-29390*# Research Inst. for Computing and Information Systems, Houston, TX.
APPLICATION OF FUZZY LOGIC-NEURAL NETWORK BASED REINFORCEMENT LEARNING TO PROXIMITY AND DOCKING OPERATIONS Interim Progress Report
Yashvant Jani (Togai InfraLogic, Inc., Houston, TX.) 4 May 1992 83 p
(Contract NCC9-16; RICIS Proj. AR-06)
(NASA-CR-190504; NAS 1.26:190504) Avail: CASI HC A05/MF A01

As part of the Research Institute for Computing and Information Systems (RICIS) activity, the reinforcement learning techniques developed at Ames Research Center are being applied to proximity and docking operations using the Shuttle and Solar Max satellite simulation. This activity is carried out in the software technology laboratory utilizing the Orbital Operations Simulator (OOS). This interim report provides the status of the project and outlines the future plans. Author

N92-29555# Mentor Technologies, Inc., Rockville, MD.
MICRO-COMPUTER NETWORK ARCHITECTURE FOR RANGE INSTRUMENTATION APPLICATIONS, VOLUME 1 Final Technical Report, 9 Sep. 1989 - 18 Sep. 1991
M. Belzer, Y. Cho, and J. Han 18 Dec. 1991 170 p
(Contract DAAD07-89-C-0214)
(AD-A247836; MTI-R89-006-28-Vol-1) Avail: CASI HC A08/MF A02

First, the basic Decentralized Square Root Information Filter (DSRIF) theory was extended in 2 ways. An expression for the likelihood function in terms of DSRIF variables, and a method for distributing the prior and process noise statistics over the set of locally optimal filters were derived. Next, software developed in Phase 1 research was upgraded to enable multitarget tracking within our distributed filtering environment. Outlier detection/rejection, track initiation, measurement-to-track, and track-to-track association routines were encoded and successfully tested using real MLRS data provided by WSMR. Finally, MTI conducted experimental work wherein 2 video trackers were built and networked with a global processor. Laboratory testing showed that the 2-camera network could track a variety of objects over the entire laboratory space. Moreover, each tracker was able to aid the other in acquiring a common target. Field testing of an individual tracker showed that it could acquire and track objects similar to the SADARM submunition, and against a cloudy background. GRA

N92-29610# Grenoble-1 Univ. (France). Lab. de Genie Informatique.
A MASSIVELY PARALLEL GENETIC ALGORITHM FOR THE GRAPH PARTITIONING PROBLEM [UN ALGORITHME GENETIQUE MASSIVEMENT PARALLELE POUR LE PROBLEME DE PARTITIONNEMENT DE GRAPHES]
E. G. Talbi and P. Bessiere Mar. 1991 14 p In FRENCH
(IMAG-RR-845-I; ETN-92-91471) Avail: CASI HC A03/MF A01

A massively parallel genetic algorithm is proposed and implemented on a transputer network. The performance is evaluated by the number of processors used and the size of the initial population for the graph partitioning problem. In particular, the application of this problem to the positioning of communicating processes in a distributed memory, parallel architecture is addressed. A 'superlinear' improvement of the algorithm is shown in the sense that in multiplying the number of processors by p, the time taken to obtain a solution of a given cost is divided by kp (k greater than 1). ESA

N92-29614# Grenoble-1 Univ. (France). Lab. de Modelisation et Calcul.
PARALLELIZATION OF THE RECURSIVE GRADIENT BACKPROPAGATION ALGORITHM [PARALLELISATION DE L'ALGORITHME DE RETROPOPAGATION DU GRADIENT RECURSIF]
H. Frydlener May 1991 13 p In FRENCH
(Contract LEP-Philips-903-9P34-R0)
(IMAG-RR-854-M; ETN-92-91477) Avail: CASI HC A03/MF A01

The implementation of recurrent artificial neural nets on multiprocessor distributed memory machine is presented. Partitioning of the problem to obtain an optimal computation time is demonstrated and different allocation strategies are compared to optimize the communication time. ESA

N92-29624# Argonne National Lab., Idaho Falls, ID.
A UNIVERSAL, FAULT-TOLERANT, NON-LINEAR ANALYTIC NETWORK FOR MODELING AND FAULT DETECTION
J. E. Mott (Advanced Modeling Techniques Corp., Idaho Falls, ID.), R. W. King, L. R. Monson, D. L. Olson, and J. D. Staffon Mar. 1992 18 p Presented at the 8th Power Plant Dynamics, Control and Testing Symposium, Knoxville, TN, 27-29 May 1992
(Contract W-31-109-eng-38)
(DE92-011840; ANL/CP-75747; CONF-920538-14) Avail: CASI HC A03/MF A01

The similarities and differences of a universal network and normal neural networks are outlined. The description and application of a universal network are discussed by showing how a simple linear system is modeled by normal techniques and by universal network techniques. A full implementation of the universal network as universal process modeling software on a dedicated computer system at EBR-II is described and example results are presented. It is concluded that the universal network provides different feature recognition capabilities than a neural network and that the universal network can provide extremely fast, accurate, and fault-tolerant estimation, validation, and replacement of signals in a real system. DOE

N92-29716# Technische Univ., Delft (Netherlands). Faculty of Technical Mathematics and Informatics.
AN ANNOTATED BIBLIOGRAPHY IN PARALLEL PARSING
J. P. M. deVreught 1991 24 p
(Rept-91-64; ISSN-0922-5641; ETN-92-91428) Copyright Avail: CASI HC A03/MF A01

A bibliography divided into the following five (partly overlapping) parts is presented: theoretical results in parallel algorithms; sequential recognizing and parsing; recognizing and parsing of attribute grammars (AG's); slow parallel recognizing and parsing; and fast parallel recognizing and parsing. The main emphasis of the bibliography lies in the following topics: AGs and similar formalisms; parallel recognizing and parsing of formal languages. Since the subject of sequential recognizing and parsing is well known, the subject is not discussed further. The subject of parallel algorithms only receives minimal attention. The last three of the five parts receive most attention. ESA

N92-29825# Technische Univ., Eindhoven (Netherlands). Dept. of Mathematics and Computing Science.
MEASURING AND SIMULATING AN 802.3 CSMA/CD LAN
Anton Dekkers (Technische Univ., Delft, Netherlands) and Jan vanOorschot Dec. 1991 18 p
(Memo-COSOR-91-42; ISSN-0926-4493; ETN-92-91796) Avail: CASI HC A03/MF A01

A single 802.3 Carrier Sense Multiple Access/Collision Detection (CSMA/CD) LAN (Local Area Network) segment is measured, resulting in throughput, response times, and workstation parameters for several work nodes. During the measurements, the network carried an artificial workload with the characteristics of a real life workload. A simulation of the laboratory test is

developed using the artificial workload parameters and the 802.3 CSMA/CD standard of the Consultative Committee for International Telephony and Telegraphy (CCITT). The measurements show that it is possible to determine the workstation parameters with a great accuracy using simple throughput measurements on an otherwise empty network. It is then possible to isolate exact ethernet parameters during throughput measurements on a network with a known workload. The behavior measured is reproduced in a simple simulation. The results of the simulation conform to the measured values. Some conclusions are that 802.3 CSMA/CD segment can be measured and simulated with accurate results. The simulation environment is used to model a real life ethernet network in circumstances that cannot be measured in a real life situation. Parameters that can be used to fine tune the simulation are the interframe gap time and the workstation distance on a network. ESA

N92-29867# Center for Mathematics and Computer Science, Amsterdam (Netherlands). Dept. of Numerical Mathematics.
ANALYSIS OF PARALLEL DIAGONAL-IMPLICIT ITERATION OF RUNGE-KUTTA METHODS
P. J. vanderHouwen and B. P. Sommeijer Aug. 1991 16 p Sponsored by Netherlands Organization for Applied Scientific Research TNO
(CWI-NM-R9114; ISSN-0169-0388; ETN-92-91660) Copyright Avail: CASI HC A03/MF A01

Parallel, diagonally implicit iteration of Runge-Kutta methods (PDIRK) for solving large systems of stiff equations on parallel computers are analyzed. The Runge-Kutta corrector, the iteration scheme for solving the state vector equation, the predictor formula, and the formula for the step point values are specified. The rate of convergence, the linear stability, and the stiff error constants of PDIRK methods are investigated. ESA

N92-29880# Universiteit Twente, Enschede (Netherlands). Tele-Informatics and Open Systems Group.
PERFORMANCE OF A CONNECTIONLESS PROTOCOL OVER ATM
Geert Heijenk, Aad P. A. vanMoorsel, and Ignas G. Niemegeers Jan. 1992 13 p Presented at the International Workshop on Advanced Communications and Applications for High Speed Networks, Munich, Fed. Republic of Germany, 16-19 Mar. 1992 Submitted for publication
(Memo-INF-92-02; TIOS-92/01; ISSN-0924-3755; ETN-92-91586) Avail: CASI HC A03/MF A01

The design of a Connectionless (CL) protocol for the B-ISDN (Broadband Integrated Services Digital Network) is discussed. Such a protocol should make use of ATM (Asynchronous Transfer Mode) and the ATM Adaptation Layer. It needs to specify destination and bandwidth of connections to the ATM network without advance knowledge of the traffic that has to be transferred over these connections. A possible mechanism which can cope with this problem, the 'On-demand Connection with Delayed Release' (OCDR) mechanism, is described. Its efficient operation is based on the assumption that there exists a certain correlation between subsequently arriving CL packets. Two different arrival processes are used to evaluate the performance of the OCDR mechanism: a Poisson arrival process, and a Markov Modulated Poisson Process (MMPP) which models a bursty traffic source. Markov models of the OCDR mechanism were constructed for both arrival processes. For the model with Poisson arrivals, a closed form solution is presented. The model with MMPP arrivals is solved numerically. Compared to a 'permanent connection' mechanism, significant bandwidth reductions can be obtained provided that the offered traffic has a bursty nature. The OCDR mechanism has the advantageous property that the obtained average node delay is not strongly related to the intensity and burstiness of the offered traffic. ESA

N92-29888# Laboratoire d'Automatique et d'Analyse des Systemes, Toulouse (France).
RELIABLE PROCESSING OF CONFIDENTIAL DATA BY MEANS OF FRAGMENTATION-REDUNDANCY-SCATTERING Ph.D. Thesis - Toulouse Univ. [TRAITEMENTS FIABLES DE DONNEES CONFIDENTIELLES PAR FRAGMENTATION-REDONDANCE-DISSEMINATION]
Gilles Trouessin 1991 168 p In FRENCH
(LAAS-91412; ETN-92-91481) Avail: CASI HC A08/MF A02

Theoretical and practical results on three possible approaches for reliable processing of confidential data is presented: protection replication, encryption replication, and fragmentation redundancy scattering. These approaches are aimed at tolerating both accidental faults and intentional faults. Reliability improvement and confidentiality preservation are generally based on antagonistic techniques and are usually considered separately. Different solutions are introduced and compared with respect to a set of criteria related to dependability, openness, and performance; one of these solutions, fragmentation scattering and replication, that seems to be the most promising, is thoroughly examined. ESA

N92-29958# Universiteit Twente, Enschede (Netherlands). Tele-Informatics and Open Systems Group.
CISLAN-2 FINAL DOCUMENT BY UNIVERSITY OF TWENTE (NETHERLANDS)
Frank V. Baumann, ed., Ignas Niemegeers, Wim Beuwer, Marcel Jordense, Aiko Pras, and Leon Schutte 15 Nov. 1991 114 p
(Memo-INF-91-81; TIOS-91/030; ISSN-0924-3755; ETN-92-91579) Copyright Avail: CASI HC A06/MF A02

The aim of the Cislan-2 project is to gain insight into the problems and solutions of a future infrastructure to provide support for users of both standard integrated services and data transfer services. An introduction to Cislan-2 is given and the following are reported: CISLAN architecture, second cycle; work structure of the Cislan-2 project; Cislan service definition; the S and T service definitions; Cislan protocol, call protocol; service description of the Interconnection Function (IF); protocol definition of the IF; the IF protocol, a clock rate synchronization; the IF protocol, a distributed bandwidth allocation algorithm; and a LAN (Local Area Network) service definition. A list of Cislan documents is given. ESA

N92-29985# Universiteit Twente, Enschede (Netherlands). Tele-Informatics and Open Systems Group.
COMPARING UCN WITH FDDI AND DQDB USING A REALISTIC WORK MODEL
H. L. Pasch and Ignas G. Niemegeers Jan. 1992 16 p
(Memo-INF-92-06; TIOS-92/04; ISSN-0924-3755; ETN-92-91780) Copyright Avail: CASI HC A03/MF A01

A network design, called Universal Channel Network (UCN), is proposed. UCN is adaptive and can be made to behave either like a token ring, a slotted ring, or anything in between. The aim is to get a network that combines the advantages of both the token ring and the slotted ring. UCN is explained and its performance is compared with that of Distributed Queue Dual Bus (DQDB) and Fiber Distributed Data Interface (FDDI). The workload model used is a detailed representation of today's traffic, extrapolated into the future. ESA

N92-30074# Universiteit Twente, Enschede (Netherlands). Tele-Informatics and Open Systems Group.
A SIMULATION STUDY ON A HIGH-SPEED SLOTTED-RING ACCESS MECHANISM WITH DYNAMICALLY ADAPTIVE SLOT SIZE
H. L. Pasch and I. G. Niemegeers Aug. 1991 12 p
(Memo-INF-91-63; TIOS-91/025; ISSN-0923-1714; ETN-92-91567) Avail: CASI HC A03/MF A01

Two access mechanisms complementary in performance, the token ring and the slotted ring, are addressed. While the token ring outperforms the slotted ring for long messages, the latter performs significantly better for short messages. The factor that causes this difference is shown to be the number of tokens on the ring. A new network design in which the number of tokens is

made adaptive, resulting in a network that can be made to behave like both the token ring and the slotted ring, or anything in between (i.e., it performs optimally for any given message length) is proposed. Simulation results showing the performance gain achieved by using this principle are presented. A new priority mechanism in which an upper bound for the access delay of high priority messages is guaranteed is introduced. ESA

N92-30142# Universiteit Twente, Enschede (Netherlands). Dept. of Computer Science.
A MODEL FOR DATAFLOW QUERY EXECUTION IN A PARALLEL MAIN-MEMORY ENVIRONMENT
Annita N. Wilschut Oct. 1991 29 p
(Memo-INF-91-34; ISSN-0924-3755; ETN-92-91565) Copyright Avail: CASI HC A03/MF A01

An analytical model for the behavior and the performance of multijoin queries is developed. The model is simple, and it increases the insight in the essentials of dataflow query execution. Multijoin queries are studied using this model. The results of this study confirm the results of a previous simulation study of multijoin queries. The gained understanding of dataflow query execution will be used for the design of a query optimizer for a parallel, dataflow DBMS (Data Base Management System). ESA

N92-30183# Universiteit Twente, Enschede (Netherlands). Dept. of Computer Science.
PBT: A PARALLEL BOTTOM-UP TOMITA PARSER
Marc Lankhorst and Klaas Sikkel Sep. 1991 81 p
(Memo-INF-91-69; ISSN-0924-3755; ETN-92-91570) Copyright Avail: CASI HC A05/MF A01

The construction of a PBT algorithm on the basis of Tomita's generalized LR method is described. A correctness proof of PBT and results of an empirical comparison between PBT and Tomita's algorithms are given. On the basis of these results, the PBT is concluded to have both theoretical and practical advantages over Tomita's algorithm. Contrary to Tomita's algorithm, it can be used to parse all (including cyclic) context free languages. It not only has a smaller computational complexity, but also a better space efficiency than Tomita's algorithm. ESA

N92-30189# Universiteit Twente, Enschede (Netherlands). Dept. of Computer Science.
OPTIMAL PARALLEL PARSING OF ALMOST ALL LL(k) GRAMMARS
Paul Oude Luttighuis 7 Nov. 1991 42 p
(Memo-INF-91-78; ISSN-0924-3755; ETN-92-91770) Copyright Avail: CASI HC A03/MF A01

An optimal parallel parsing algorithm for the class LE(p, q) grammars is introduced. This class is properly contained in, but very close to, LL(q). As an application, the algorithm is used to transform (leftmost) derivations into parse trees, thus showing that, on a P-RAM (Parallel Random Access Memory), there is no essential difference in the order of complexity between parsers yielding (leftmost) derivations and those yielding parse trees. Previously, this non-trivial result was assumed in the literature. ESA

N92-30229# Technische Univ., Delft (Netherlands). Faculty of Technical Mathematics and Information.
A PARALLEL RESTRUCTURED VERSION OF GMRES(M)
E. deSturler 1991 30 p
(Rept-91-85; ISSN-0922-5641; ETN-92-91835) Copyright Avail: CASI HC A03/MF A01

A restructure version of the GMRES(m) (Generalized Minimal Residual) algorithm, referred to as modGMRES(m), is devised, which is more suited for parallel implementation. A performance model is developed for Krylov subspace methods implemented in distributed memory, MIMD computers. This performance model defines the number of processors relative to an optimal number of processors. This approach reveals a number of hidden invariances of the parallel implementation. This performance model is used to evaluate the parallel implementations of the GMRES(m) algorithms and the modGMRES(m) variant for medium to massive parallelism. The modGMRES(m) method is shown to be able to yield a substantial improvement in time per iteration over GMRES(m). The potential numerical instability, arising from the groupwise generation of the vectors that span the Krylov space, is overcome by a polynomial generation of these vectors. Numerical experiments suggest that the total number of iterations for modGMRES(m) remains about the same as the GMRES(m). ESA

63 CYBERNETICS

Includes feedback and control theory, artificial intelligence, robotics and expert systems.

For related information see also *54 Man/System Technology and Life Support.*

N92-29456# Sandia National Labs., Albuquerque, NM.
IMPROVING PATH PLANNING WITH LEARNING
P. C. Chen 16 Dec. 1991 15 p Presented at the 9th International Machine Learning Conference, Aberdeen (England), 1-3 Jul. 1992
(Contract DE-AC04-76DP-00789)
(DE92-004360; SAND-91-2808C; CONF-920740-1) Avail: CASI HC A03/MF A01

We present a learning algorithm designed to improve robot path planning. The algorithm relies on an existing path planner to provide solutions to difficult tasks. From these solutions, it learns a sparse network of useful robot subgoals which guide and support fast planning. We analyze the algorithm theoretically by developing some general techniques useful in characterizing behaviors of probabilistic learning. We also demonstrate the effectiveness of the algorithm empirically with an existing path planner in practical environments. The learning algorithm not only reduces the time cost of existing planners, but also increases their capability in solving difficult tasks. DOE

N92-29504# Oak Ridge National Lab., TN.
AN OBJECT-BASED INTERVIEWING SYSTEM
B. Tonn, R. Goeltz, and Tai-Lun Chiang (Tennessee Univ., Knoxville.) 1992 14 p Presented at the Computing for the Social Sciences Conference, Ann Arbor, MI, 4-7 May 1992
(Contract DE-AC05-84OR-21400)
(DE92-013422; CONF-9205152-1) Avail: CASI HC A03/MF A01

Oak Ridge National Laboratory (ORNL) has developed an object-based interviewing system (OBIS). The key design feature is that each survey question is a function, which is treated as an independent object. The Survey Manager (SM) module maintains a stack of questions and calls each question function when directed. Each question, when called, calls the Interaction Facility (IF) to set up the appropriate screen. This modular approach to automated survey design offers maximum flexibility for system development and maintenance. The software is written in Common Lisp and currently runs on Symbolics and VAX computers. The Bureau of Labor Statistics is funding a project to use OBIS to automate the Current Population Survey (CPS), an expenditure survey, and questions about intrahousehold communication to collect data to study communication and proxy response error. DOE

N92-29541# Army Armament Research, Development and Engineering Center, Picatinny Arsenal, NJ.
INTRODUCTION TO NEURAL NETWORKS
Nanette S. Holder Mar. 1992 18 p
(AD-A248258) Avail: CASI HC A03/MF A01

There is a great desire for engineers and scientists to model the processing functions of the nervous system. There are some who feel that these models should be directly related to the actual system, so they study the neuron, the primary element of the nervous system. These people model their neural networks after studies performed on the nervous system. Others feel that these networks should be black box models. Neural networks allow for parallel processing of information that can greatly reduce the time

required to perform operations which are needed in pattern recognition. GRA

N92-29550# Oak Ridge National Lab., TN.
USING CUSTOM-DESIGNED VLSI FUZZY INFERENCING CHIPS FOR THE AUTONOMOUS NAVIGATION OF A MOBILE ROBOT
F. G. Pin, R. S. Pattay, Hiroyuki Watanabe, and J. Symon 1991 15 p Presented at the 1992 IEEE International Conference on Intelligent Robots and Systems, Raleigh, NC, 7-10 Jul. 1992
(Contract DE-AC05-84OR-21400)
(DE92-000424; CONF-920724-1) Avail: CASI HC A03/MF A01

Two types of computer boards including custom-designed VLSI fuzzy inferencing chips have been developed to add a qualitative reasoning capability to the real-time control of autonomous mobile robots. The design and operation of these boards are first described and an example of their use for the autonomous navigation of mobile robot is presented. The development of qualitative reasoning schemes emulating human-like navigation in apriori unknown environments is discussed. An approach using superposition of elemental sensor-based behaviors is shown to allow easy development and testing of the inferencing rule base, while providing for progressive addition of behaviors to resolve situations of increasing complexity. The efficiency of such schemes, which can consist of as little as a dozen qualitative rules, is illustrated in experiments involving an autonomous mobile robot navigating on the basis of very sparse and inaccurate sensor data. DOE

N92-29561# Air Force Inst. of Tech., Wright-Patterson AFB, OH.
BOOLEAN REASONING AND INFORMED SEARCH IN THE MINIMIZATION OF LOGIC CIRCUITS Ph.D. Thesis
James J. Kainec Mar. 1992 610 p
(AD-A248110; AFIT/DS/ENG/92-02) Avail: CASI HC A99/MF A06

The minimization of logic circuits is an important area of research. The approaches taken in this field, however, have for the most part been ad hoc. Boolean techniques are employed to manipulate formulas, but not to perform symbolic reasoning. Boolean equations are employed principally as icons; they are never solved. The first objective of this dissertation is to apply Boolean reasoning systematically and uniformly to the minimization problem. Boolean reasoning entails the reduction of systems of Boolean equations to a single equation; the single equation is an abstraction, independent of the form of the original equations, upon which a variety of reasoning operations may be performed. The second objective is to apply informed search, which has arisen from research in Artificial Intelligence, to the minimization problem. A circuit specification is reduced to a single equivalent equation called a 1-normal form. It is shown that forming a particular solution for the equation corresponds to deriving a design. GRA

N92-29590# California Inst. of Tech., Pasadena. Div. of Biology.
CONTROLLING THE FLOW OF VISUAL INFORMATION THROUGH THE LATERAL GENICULATE NUCLEUS: FROM SINGLE CELLS TO NEURAL NETWORKS Final Report, 1 Nov. 1988 - 31 Oct. 1991
Christof Koch 31 Oct. 1991 8 p
(Grant AF-AFOSR-0029-89)
(AD-A250578; AFOSR-92-0309TR) Avail: CASI HC A02/MF A01

Over the last three years, we have carried out a number of projects under this grant, relating to the gating and processing of information in the mammalian visual pathway. Specifically, they have involved (1) a detailed computational investigation of the early visual system of the cat using both analytical as well as numerical tools, (2) a study of the dynamic properties of 2-D networks of coupled oscillatory neurons, and (3) the outline of a first neurobiological theory of visual awareness. GRA

N92-29644# Oak Ridge National Lab., TN.
TERRAIN FOLLOWING OF ARBITRARY SURFACES USING A HIGH INTENSITY LED PROXIMITY SENSOR
J. E. Baker 1991 20 p Presented at the 1992 IEEE International Conference on Intelligent Robots and Systems, Raleigh, NC, 7-10 Jul. 1992
(Contract DE-AC05-84OR-21400)
(DE92-004464; CONF-920724-2) Avail: CASI HC A03/MF A01

Many robotic operations, e.g., mapping, scanning, feature following, etc., require accurate surface following of arbitrary targets. This paper presents a versatile surface following and mapping system designed to promote hardware, software and application independence, modular development, and upward expandability. These goals are met by a full, a priori specification of the hardware and software interfaces; a modular system architecture; and hierarchical surface-data analysis method, permitting application specific tuning at each conceptual level of topological abstraction. This surface following system was fully designed and implemented independently of any specific robotic host, then successfully integrated with and demonstrated on a completely a priori unknown, real-time robotic system. DOE

N92-29656*# Catholic Univ. of America, Washington, DC. Dept. of Electrical Engineering.
EXPERIMENTAL INVESTIGATION OF ADAPTIVE CONTROL OF A PARALLEL MANIPULATOR Semiannual Progress Report, 1 Feb. - 31 Jul. 1992
Charles C. Nguyen and Sami S. Antrazi 31 Jul. 1992 24 p
(Grant NAG5-780)
(NASA-CR-189867; NAS 1.26:189867) Avail: CASI HC A03/MF A01

The implementation of a joint-space adaptive control scheme used to control non-compliant motion of a Stewart Platform-based Manipulator (SPBM) is presented. The SPBM is used in a facility called the Hardware Real-Time Emulator (HRTE) developed at Goddard Space Flight Center to emulate space operations. The SPBM is comprised of two platforms and six linear actuators driven by DC motors, and possesses six degrees of freedom. The report briefly reviews the development of the adaptive control scheme which is composed of proportional-derivative (PD) controllers whose gains are adjusted by an adaptation law driven by the errors between the desired and actual trajectories of the SPBM actuator lengths. The derivation of the adaptation law is based on the concept of model reference adaptive control (MRAC) and Lyapunov direct method under the assumption that SPBM motion is slow as compared to the controller adaptation rate. An experimental study is conducted to evaluate the performance of the adaptive control scheme implemented to control the SPBM to track a vertical and circular paths under step changes in payload. Experimental results show that the adaptive control scheme provides superior tracking capability as compared to fixed-gain controllers. Author

N92-29673*# San Diego State Univ., CA. Robotics and Intelligent Systems Lab.
ROBUST ADAPTIVE KINEMATIC CONTROL OF REDUNDANT ROBOTS
M. Tarokh and D. D. Zuck 1992 26 p
(Contract NAS7-1110)
(NASA-CR-190520; NAS 1.26:190520) Avail: CASI HC A03/MF A01

The paper presents a general method for the resolution of redundancy that combines the Jacobian pseudoinverse and augmentation approaches. A direct adaptive control scheme is developed to generate joint angle trajectories for achieving desired end-effector motion as well as additional user defined tasks. The scheme ensures arbitrarily small errors between the desired and the actual motion of the manipulator. Explicit bounds on the errors are established that are directly related to the mismatch between actual and estimated pseudoinverse Jacobian matrix, motion velocity and the controller gain. It is shown that the scheme is tolerant of the mismatch and consequently only infrequent pseudoinverse computations are needed during a typical robot motion. As a result, the scheme is computationally fast, and can

be implemented for real-time control of redundant robots. A method is incorporated to cope with the robot singularities allowing the manipulator to get very close or even pass through a singularity while maintaining a good tracking performance and acceptable joint velocities. Computer simulations and experimental results are provided in support of the theoretical developments. Author

N92-29675# Laboratoire d'Automatique et d'Analyse des Systemes, Toulouse (France).
RECOGNITION OF MULTI-ARTICULATED THREE-DIMENSIONAL OBJECTS USING A MULTISENSOR SYSTEM FOR ROBOTICS APPLICATIONS Ph.D. Thesis - Toulouse Univ. [RECONNAISSANCE D'OBJETS ARTICULES TRIDIMENSIONNELS A PARTIR D'INFORMATIONS MULTISENSORIELLES POUR DES APPLICATIONS ROBOTIQUES]
Joel Colly 1991 142 p In FRENCH
(LAAS-91394; ETN-92-91479) Avail: CASI HC A07/MF A02

The problem of recognition of polyhedral articulated three dimensional objects in computer vision is addressed. To achieve this a hybrid laser camera system on the mobile robot HILARE is used. Representation of the scene through pictures of depth is described, and this information is merged with the video data in order to build a metaface structure. Identification and localization of polyhedral objects is considered. The object recognition is performed in two classical steps: hypothesis generation using three dimensional features (planar faces), and hypothesis verification by additional matching using all extracted features (three dimensional faces and edges, two dimensional regions and edges). The problem of articulated object recognition is dealt with. The proposed approach is 'opportunistics'. It is based on the recognition of one of the parts of the articulated object, then identification and localization of other connected parts. An application to space robotics (localization and inspection of a satellite from a shuttle) permitted this work to be validated. ESA

N92-29678# Laboratoire d'Automatique et d'Analyse des Systemes, Toulouse (France).
SPARA: A SYSTEM OF PLANNING ROBOT MANIPULATION TASKS Ph.D. Thesis - Toulouse Univ. [SPARA: UN SYSTEME DE PROGRAMMATION AUTOMATIQUE DE TACHE DE MANIPULATION ROBOTISEE]
Pascal Violero 1991 152 p In FRENCH
(LAAS-91395; ETN-92-91480) Avail: CASI HC A08/MF A02

The planning of robot manipulation tasks in a constraint environment is considered. This problem taken as a whole is too complex; therefore, it is decomposed into subproblems: grasping, local motions, and transfer motions. Such a decomposition of the initial problem generates another problem when one tries to synthesize the different solutions because subproblems are not independent. This problem of consistency is divided in two parts: geometric constraints and uncertainty constraints. These interactions are studied so that a control structure can be built which permits the different constraints during the planning to be propagated. The state of the art in the field of automatic task level programming is reviewed. The decomposition principle used is presented which allows the modules used in the system to be presented. The grasping problem is considered and account is taken of the interdependencies induced by the decomposition of the initial task (interaction between local motions and transfer motions, and interaction between the pick operation and place operation). For more flexibility in the system, the control structure is interactive; this control structure is presented. Implementation and validation of the system is considered. ESA

N92-29764# Technische Univ., Delft (Netherlands). Faculty of Technical Mathematics and Informatics.
THE ISOPONE METHOD IN OPTIMAL CONTROL
M. B. Klompstra, P. K. G. M. vanBrunschot (Koninklijke/Shell-Lab., Amsterdam, Netherlands), and G. J. Olsder 1991 20 p
(Rept-91-52; ISSN-0922-5641; ETN-92-91421) Copyright Avail: CASI HC A03/MF A01

An extension to the minimum time problem, a well known problem in optimal control for which several solution methods are available, is presented. A specific optimal control problem is treated and the so called isopone method to determine the optimal control is proposed. In this method multidimensional reachable subsets are computed repeatedly. This method is similar to dynamic programming in that it is a recursive algorithm, but is designed to reduce the amount of calculation time. The current algorithm also yields, as a degenerate case, the time optimal route. ESA

N92-29955*# National Aeronautics and Space Administration. Pasadena Office, CA.
ELECTRONIC NEURAL NETWORK FOR SOLVING TRAVELING SALESMAN AND SIMILAR GLOBAL OPTIMIZATION PROBLEMS Patent Application
Anil P. Thakoor, inventor (to NASA) (Jet Propulsion Lab., California Inst. of Tech., Pasadena.), Alexander W. Moopenn, inventor (to NASA) (Jet Propulsion Lab., California Inst. of Tech., Pasadena.), Tuan A. Duong, inventor (to NASA) (Jet Propulsion Lab., California Inst. of Tech., Pasadena.), and Silvio P. Eberhardt, inventor (to NASA) (Jet Propulsion Lab., California Inst. of Tech., Pasadena.) 8 Nov. 1991 27 p
(Contract NAS7-918)
(NASA-Case-NPO-17807-2-CU; NAS 1.71:NPO-17807-2-CU; US-Patent-Appl-SN-789567) Avail: CASI HC A03/MF A01

This invention is a novel high-speed neural network based processor for solving the 'traveling salesman' and other global optimization problems. It comprises a novel hybrid architecture employing a binary synaptic array whose embodiment incorporates the fixed rules of the problem, such as the number of cities to be visited. The array is prompted by analog voltages representing variables such as distances. The processor incorporates two interconnected feedback networks, each of which solves part of the problem independently and simultaneously, yet which exchange information dynamically. NASA

N92-29962# Technische Univ., Delft (Netherlands). Faculty of Technical Mathematics and Informatiques.
ASYMPTOTIC RESULTS IN FEEDBACK SYSTEMS Ph.D. Thesis
Jacobus Adrianus Cor Resing 1990 102 p
(ETN-92-91702) Avail: CASI HC A06/MF A02

Feedback systems are considered. The description of feedback processes is given and the results obtained in feedback queueing studies are presented. The feedback system term is used in two different ways: in the theory of stochastic processes and queueing theory. The asymptotic behavior of discrete event dynamic systems in which the activity times are random variables are discussed. A general approach to the study of limiting behavior for interactive schemes with an i.i.d. feedback is presented. A probabilistic coupling between the M/G/1 processor sharing queue and the M/M/1 feedback queue is studied. A single server queueing system with finite waiting room is considered. For individual titles, see N92-29963 through N92-29966.

N92-29963# Technische Univ., Delft (Netherlands). Faculty of Technical Mathematics and Informatics.
ASYMPTOTIC BEHAVIOR OF RANDOM DISCRETE EVENT SYSTEMS
Jacobus Adrianus Cor Resing, R. E. deVries, G. Hooghiemstra, M. S. Keane, and G. J. Olsder *In its* Asymptotic Results in Feedback Systems 1990 p 15-41 Submitted for publication
(For primary document see N92-29962 20-63)
Avail: CASI HC A03/MF A02

Some aspects of the asymptotic behavior of Discrete Event Dynamic Systems (DEDS) in which the activity times are random variables are discussed. The main result is that a central limit theorem holds for DEDS and consequently that the cycletime of the system is asymptotically normally distributed. In other investigations a systematic theory parallel to linear algebra was developed for the max-algebra, and the use of the max-algebra in the temporal approach to DEDS was discussed and illustrated. The models for DEDS and the max-algebra will be introduced and some results on DEDS are recalled. Some models which

take this random behavior into account are considered. In particular, for a class of random discrete event systems, the expected cycle time is derived and it is shown that this cycletime is asymptotically normal. Calculations of the expectation and variance of the cycletime are given in several examples. The reducible random DEDS is considered and the asympotic behavior of random DEDS with deterministic DEDS are compared. ESA

N92-29964# Technische Univ., Delft (Netherlands). Faculty of Technical Mathematics and Informatics.
STRONG LAW AND CENTRAL LIMIT THEOREM FOR A PROCESS BETWEEN MAXIMA AND SUMS
F. denHollander, G. Hooghiemstra, M. Keane, and Jacobus Adrianus Cor Resing *In its* Asymptotic Results in Feedback Systems 1990 p 43-64 (For primary document see N92-29962 20-63)
Avail: CASI HC A03/MF A02

A general approach to the study of limiting behavior for iterative schemes with an i.i.d. feedback is presented. The skeleton of the proof is given. The basic ingredients collect what technical facts need to be verified in order to get (x(sub n)/a(sub n)) approaching 1 and ((x(sub n)-a(sub n))/b(sub n)) approaching Z, and show how a(sub n), b(sub n) and Z come out. Several standard tools, among which recursive inequalities, central limit theorem for martingale difference arrays, invariance principle and continuous mapping theorem, are used. The general skeleton to the three cases alpha(sub n) = 1-1/n; alpha(sub n) = 1-1/n to the power of l, for l between zero and 1 and for 1 greater than 1 and explicit computations are includeed. The interest in iterative schemes of the type stems from a storage problem for solar energy described by Haslett. ESA

N92-29965# Technische Univ., Delft (Netherlands). Faculty of Technical Mathematics and Informatics.
THE M/G/1 PROCESSOR SHARING QUEUE AS THE ALMOST SURE LIMIT OF FEEDBACK QUEUES
Jacobus Adrianus Cor Resing, G. Hooghiemstra, and M. S. Keane *In its* Asymptotic Results in Feedback Systems 1990 p 65-75 Submitted for publication (For primary document see N92-29962 20-63)
Avail: CASI HC A03/MF A02

A probabilistic coupling between the M/G/1 processor sharing queue and the M/M/1 feedback queue, with general feedback probabilities, is established. This coupling is used to prove the almost sure convergence of sojourn times in the feedback model to sojourn times in the M/G/1 processor sharing queue. Using the theory of regenerative processes, it follows that for stable queues the stationary distribution of the sojourn time in the feedback model converges in law to the corresponding distribution in the processor sharing model. The results do not depend on Poisson arrival times, but are valid for general arrival processes. ESA

N92-29966# Technische Univ., Delft (Netherlands). Faculty of Technical Mathematics and Informatics.
MULTITYPE BRANCHING PROCESSES IN M/G/1-QUEUEING THEORY
Jacobus Adrianus Cor Resing *In its* Asymptotic Results in Feedback Systems 1990 p 77-94 (For primary document see N92-29962 20-63)
Avail: CASI HC A03/MF A02

A single server queueing system with infinite waiting room is considered. Customers arrive at the system according to a Poisson process with intensity lambda greater than 0. Each customer requires two services: a customer who enters the queue will return to the queue (feedback) after his first service for a second one. Fed back customers return instantaneously, joining the end of the queue. Some of the terminology and theory of multitype branching processes are reviewed. A proof of a multitype version of a theorem of Pakes for single-type branching processes with state dependent immigration is given. The notion of generation times is introduced. For various multitype M/G/1 queues these generation times are used to analyze the models. Moment calculations, both for branching processes with immigration in each state and for branching processes with immigration only in state zero are performed. The results to M/G/1 queues with a countable number of customer types are extended. Conclusions and open questions are included. ESA

N92-29969# Universiteit Twente, Enschede (Netherlands). Dept. of Computer Science.
A SEVEN-LEAGUE-BOOTS ALGORITHM FOR PATH PLANNING IN CONFIGURATION SPACES
Jan M. Nauta Dec. 1991 20 p
(Memo-INF-91-88; ISSN-0924-3755; ETN-92-91775) Copyright Avail: CASI HC A03/MF A01

In the past ten years, many algorithms for robot paths planning have been published. Many of these algorithms use configuration spaces, in which the so called configuration of a robot can be represented by a single point. This means that the problem of path planning is reduced to the search for a path for a single point in configuration space. A new algorithm to find such a path is presented. The approach taken is to search within a hierarchically organized grid using the well known A(asterisk) algorithm in a bidirectional way. ESA

N92-29971# Universiteit Twente, Enschede (Netherlands). Faculty of Applied Mathematics.
POLYNOMIAL METHODS IN H(INFINITY)-OPTIMAL CONTROL
Gjerrit Meinsma 24 Oct. 1991 39 p
(MEMO-1008; ISSN-0169-2690; ETN-92-91755) Avail: CASI HC A03/MF A01

A polynomial solution of the standard H(infinity) optimal control problem is presented. Based on two polynomial J spectral factorization problems, a parameterization of all suboptimal compensators is obtained. Bounds on the McMillan degree of suboptimal compensators are derived. ESA

N92-29983# Universiteit Twente, Enschede (Netherlands). Dept. of Computer Science.
AN ANALYSIS OF MODEL-BASED DIAGNOSIS USING PROBLEM-REFORMULATION
D. J. Out and R. R. Bakker Jan. 1992 73 p
(Memo-INF-92-03; ISSN-0924-3755; ETN-92-91778) Copyright Avail: CASI HC A04/MF A01

An integrated framework of model based diagnosis, based on reformulations of the diagnostic problem is presented. It is shown how the majority of diagnostic actions can be described as reformulations of the diagnostic problem. A classification of reformulations which allows reuse of diagnostic conclusions is given. Diagnostic actions are formally described and classified according to this classification. ESA

N92-30085*# National Aeronautics and Space Administration. Pasadena Office, CA.
FAST TEMPORAL NEURAL LEARNING USING TEACHER FORCING Patent Application
Nikzad Toomarian, inventor (to NASA) (Jet Propulsion Lab., California Inst. of Tech., Pasadena.) and Jacob Bahren, inventor (to NASA) (Jet Propulsion Lab., California Inst. of Tech., Pasadena.) 29 Jun. 1992 34 p
(Contract NAS7-918)
(NASA-Case-NPO-18553-1-CU; NAS 1.71:NPO-18553-1-CU; US-Patent-Appl-SN-908677) Avail: CASI HC A03/MF A01

A neural network is trained to output a time dependent target vector defined over a predetermined time interval in response to a time dependent input vector defined over the same time interval by applying corresponding elements of the error vector, or difference between the target vector and the actual neuron output vector, to the inputs of corresponding output neurons of the network as corrective feedback. This feedback decreases the error and quickens the learning process, so that a much smaller number of training cycles are required to complete the learning process. A conventional gradient descent algorithm is employed to update the neural network parameters at the end of the predetermined time interval. The foregoing process is repeated in repetitive cycles

until the actual output vector corresponds to the target vector. In the preferred embodiment, as the overall error of the neural network output decreasing during successive training cycles, the portion of the error fed back to the output neurons is decreased accordingly, allowing the network to learn with greater freedom from teacher forcing as the network parameters converge to their optimum values. The invention may also be used to train a neural network with stationary training and target vectors. NASA

N92-30143# Universiteit Twente, Enschede (Netherlands). Knowledge-Based Systems Group.
TEMPORAL REASONING IN MODEL-BASED DIAGNOSIS
D. G. Pasman and R. R. Bakker Aug. 1991 34 p Sponsored by Stichting Knowledge Based Systems
(Memo-INF-91-66; UT-KBS-91-33; SKBS-A1/91-21; ISSN-0924-3755; ETN-92-91568) Avail: CASI HC A03/MF A01

A diagnostic method for diagnosing discrete dynamic systems is described. The basic idea for this method is symbolic simulation, as it is used for diagnosing static systems. Temporal reasoning is used partially. This method seems to be able to diagnose discrete dynamic systems rather well. When diagnosing systems with feedback, the problem concerning the low discriminating power is still prevalent. For this problem, a possible improvement is presented, but future research will still be necessary. ESA

N92-30184# Universiteit Twente, Enschede (Netherlands). Tele-Informatics and Open Systems Group.
INTEGRATED SERVICE ENGINEERING SUPPORTED BY THE FDT LOTOS
Ria Schepers and L. FerreiraPires 24 Oct. 1991 73 p
(Memo-INF-91-76; TIOS-91/028; ISSN-0924-3755; ETN-92-91576) Copyright Avail: CASI HC A04/MF A01

The use of the FDT (Formal Description Techniques) LOTOS (Language Of Temporal Ordering Specifications), in the design of Integrated Service Engineering (ISE) systems is discussed. LOTOS is used in combination with some architectural concepts and architectural components which appear to be necessary in ISE. Results from the ESPRIT ISE project and Open Distributed Processing are used as a starting point for the discussion. The conclusion is that LOTOS can be used to improve the design process of ISE systems, because it complements the development tools available in ISE by allowing modeling of concurrency and synchronization aspects of distributed systems at a high level of abstraction with respect to implementation details. ESA

64 NUMERICAL ANALYSIS

Includes iteration, difference equations, and numerical approximation.

N92-29446# Pennsylvania State Univ., University Park. Dept. of Mineral Engineering.
A GENERALIZED POLYNOMIAL FORM OF THE OBJECTIVE FUNCTION IN FLASH CALCULATIONS M.S. Thesis
Brett D. Weigle May 1992 117 p
(AD-A248160) Avail: CASI HC A06/MF A02

This work centers on the recasting of the Rachford-Rice objective function into a polynomial function of the vapor fraction. The degree of this polynomial is one less than the number of components in the system and its coefficients can be calculated from the feed composition and the equilibrium ratios. A recursive expression is developed that involves symmetric functions and can be easily programmed on a computer or scientific calculator. The principal advantage of this new form of the objective function is that the theory of polynomials is well-developed. The location of their zeroes can be predicted with confidence by techniques based on sound mathematical principles, such as the Fourier-Budan theorem. The polynomial in the vapor fraction is well-behaved over the two-phase region and its root can be quickly located by a hybrid method of interval-halving technique and Newton-Raphson procedure. The validity of the new objective function and its automatic coefficient-generating algorithm are tested using several multicomponent systems for which experimental data are available. The new objective function is not prone to the erratic behavior of the Rachford-Rice function and is not sensitive to initial guess of the root. GRA

N92-29481# Lawrence Livermore National Lab., CA.
A NEW ALGEBRA CORE FOR THE MINIMAL FORM PROBLEM
M. R. Purtill (Institute for Defense Analyses, Princeton, NJ.), J. S. Oliveira, and G. O. Cook, Jr. 20 Dec. 1991 7 p Presented at the International Symposium on Symbolic and Algebraic Computation, Berkeley, CA, 27-29 Jul. 1992
(Contract W-7405-eng-48)
(DE92-011966; UCRL-JC-109226; CONF-920760-4) Avail: CASI HC A02/MF A01

The demands of large-scale algebraic computation have led to the development of many new algorithms for manipulating algebraic objects in computer algebra systems. For instance, parallel versions of many important algorithms have been discovered. Simultaneously, more effective symbolic representations of algebraic objects have been sought. Also, while some clever techniques have been found for improving the speed of the algebraic simplification process, little attention has been given to the issue of restructuring expressions, or transforming them into 'minimal forms'. By 'minimal form', we mean that form of an expression that involves a minimum number of operations. In a companion paper, we introduce some new algorithms that are very effective at finding minimal forms of expressions. These algorithms require algebraic and combinatorial machinery that is not readily available in most algebra systems. In this paper, we describe a new algebra core that begins to provide the necessary capabilities. DOE

N92-29486# Pittsburgh Univ., PA. Learning Research and Development Center.
THE COGNITIVE FUNCTION OF THEORETICAL KNOWLEDGE IN PROCEDURAL LEARNING Report, Apr. 1991 - Mar. 1992
Stellan Ohlsson Mar. 1992 5 p
(Contract N00014-89-J-1681)
(AD-A248075) Avail: CASI HC A01/MF A01

The present project continuous work began under a previous project, 'Knowledge-based revision of cognitive procedures in response to changing task demands: Toward a theory of the nature and function of principled knowledge'. In the course of the previous project, a theory of skill acquisition was developed. The basic principles of this theory are as follows: (1) skill acquisition consists of encoding the results of problem solving for future use; and (2) that skill acquisition consists of the correction of errors, where an error is defined as a contradiction between the outcomes of problem solving steps and prior domain knowledge. The theory was embodied in a simulation model called the Heuristic Searcher (HS). The HS model was used to clarify various phenomena in the learning of elementary arithmetic. GRA

N92-29548# Yale Univ., New Haven, CT. Dept. of Computer Science.
ON THE NUMERICAL SOLUTION OF ONE-DIMENSIONAL INTEGRAL AND DIFFERENTIAL EQUATIONS Ph.D. Thesis
Harold P. Starr, Jr. Dec. 1991 105 p
(Contract N00014-86-K-0310)
(AD-A250388; YALEU/DCS/RR-888) Avail: CASI HC A06/MF A02

Many problems in mathematical physics can be formulated as one-dimensional integral equations. Examples include problems in electrostatics, crack problems in elastic bodies, and two-point boundary value problems for ordinary differential equations. Since most integral equations arising in applications do not have analytic solutions, there is considerable interest in the numerical solution of these problems. Unfortunately, discretization of integral equations leads to dense systems of linear algebraic equations, and the direct solution of a dense linear system of dimension N requires order O(N cubed) arithmetic operations. Alternatively, the solution to the linear system can be obtained using an iterative method

such as the conjugate gradient algorithm or the conjugate residual algorithm. This thesis is based on the observation that one-dimensional integral operators can be recursively decomposed into sums of products of operators of low numerical rank. A complicated analytical apparatus is then constructed which allows for the direct solution of an integral equation in order O(N) operations. The algorithms of this thesis permit the use of schemes with extremely high orders of convergence, and are quite insensitive to end-point singularities. The performance of the methods is illustrated with numerical examples. GRA

N92-29573# Grenoble-1 Univ. (France). Lab. d'Informatique Fondamentale et d'Intelligence Artificielle.
STRONG BISIMILARITY ON NETS REVISITED
C. Autant, Z. Belmesk, and P. Schnoebelen Mar. 1991 30 p Submitted for publication
(RR-847-I-IMAG-120-LIFIA; ETN-92-91469) Avail: CASI HC A03/MF A01

A previously proposed notion of bi-simulation between Petri nets which considers bi-simulations between places of nets rather than between markings is addressed. This definition leads to several problems that were not previously noticed. It turns out that the saturation is more complicated, over transition systems, than in classical bisimulation theory. A new definition which solves the problems and which is much more general is proposed. The consequences of the new definition are investigated. Many results of classical bi-simulation theory can be recovered modulo some adaptation. This indicates that the definition is 'correct' and productive. ESA

N92-29574# Grenoble-1 Univ. (France). Lab. d'Informatique Fondamentale et d'Intelligence Artificielle.
EXPERIMENTS ON PROCESSES WITH BACKTRACKING
P. Schnoebelen Jul. 1991 23 p Submitted for publication
(RR-858-I-IMAG-121-LIFIA; ETN-92-91470) Avail: CASI HC A03/MF A01

Trace, ready, and failure based equivalences of processes when the user is provided with a special 'undo' button, allowing back steps to be taken, are investigated. This gives rise to new semantic equivalences and to new characterizations of old ones. Congruence properties and full abstraction problems for a CCS (Calculus of Communicating Systems) like process algebra are investigated. ESA

N92-29589# Virginia Polytechnic Inst. and State Univ., Blacksburg. Dept. of Mathematics.
MODELLING, INFORMATION PROCESSING AND CONTROL
Final Report, 1 Nov. 1988 - 31 Oct. 1991
David L. Russell 31 Oct. 1991 37 p
(Grant AF-AFOSR-0031-89)
(AD-A250571; AFOSR-92-0270TR) Avail: CASI HC A03/MF A01

The principal investigator, his associates and research assistants have carried out a program of research in the general area of distributed parameter systems modelling, identification and control. This work has been concentrated in four main areas: (1) control of the Korteweg de Vries and other nonlinear partial differential equations exhibiting solitary waves, (2) frequency domain analysis of distributed parameter systems, (3) energy dissipation mechanisms in elastic structures, and (4) modelling and parameter estimation in elastic structures. GRA

N92-29604# National Aerospace Lab., Amsterdam (Netherlands). Fluid Dynamics Div.
HYPERBOLIC GRID GENERATION CONTROL BY PANEL METHODS
M. H. L. Hounjet 15 Feb. 1991 17 p Presented at the 3rd International Conference on Numerical Grid Generation in Computational Fluid Dynamics and Related Fields, Barcelona, Spain, 3-7 Jun. 1991
(Contract NIVR-01904-N)
(NLR-TP-91061-U; ETN-92-91453) Avail: CASI HC A03/MF A01

A method for the generation of OH type grids about transport type aircraft is presented. The method combines a hyperbolic grid generation scheme with source terms obtained with a panel method in such a way that OH type grids around fairly complex shapes with concavities can be generated easily. The components of the method, a method to generate grids with a panel method and the hyperbolic grid generation scheme, are described and applications are shown. ESA

N92-29607# Technische Univ., Eindhoven (Netherlands). Dept. of Mathematics and Computing Science.
TOOLS FOR THE INTERFACING BETWEEN DYNAMICAL PROBLEMS AND MODELS WITHIN DECISION SUPPORT SYSTEMS
Jaap Wessels (International Inst. for Applied Systems Analysis, Laxenburg, Austria) 4 Nov. 1991 18 p
(Memo-COSOR-91-29; ETN-92-91462) Avail: CASI HC A03/MF A01

The difficulties arising from formulating models for dynamical problems in such a way that they can be treated by appropriate solvers are addressed. One of these difficulties is that different types of solvers are recomendable for different questions within the same situation. Therefore it is recommended to use solver independent specification methods. Since specification and respecification can be time-consuming and boring, it is recommended that rule-based specification tools be developed. A sketch of possible specification methods for manpower policy making and for goods flow control is given as an illustration. ESA

N92-29685# Amsterdam Univ. (Netherlands). Inst. for Language, Logic and Information.
DEFAULTS IN UPDATE SEMANTICS
Frank Veltman Jun. 1991 57 p
(ITLI-LP-91-02; ISSN-0924-2082; ETN-92-91350) Avail: CASI HC A04/MF A01

Questions on logic validity are addressed. A theory which consists of update conditions rather than a specification of truth conditions is given. According to this theory the slogan 'you know the meaning of a sentence if you know the conditions under which it is true' should be replaced by this one: 'you known the meaning of a sentence if you known the change it brings about in the information state of anyone who accepts the news conveyed by it'. ESA

N92-29687# Amsterdam Univ. (Netherlands). Inst. for Language, Logic and Information.
DYNAMIC SEMANTICS AND CIRCULAR PROPOSITIONS
Willem Groeneveld Jul. 1991 44 p
(ITLI-LP-91-03; ISSN-0924-2082; ETN-92-91351) Avail: CASI HC A03/MF A01

An attempt to add another proposal to the list of solutions to the Liar paradox is made. The theory of the study is an extension of Barwise and Echtemendy's Austinian account of truth and circular propositions. The main ingredient of the study is a form of dynamic semantics (update semantics). The form of dynamic semantics used is concluded not to be final. An improvement of the theory could perhaps be a revision of the Austinian setup as a choice for a different framework. ESA

N92-29742# Technische Univ., Eindhoven (Netherlands). Dept. of Mathematics and Computing Science.
D-OPTIMAL DESIGNS FOR AN INCOMPLETE QUADRATIC MODEL
E. E. M. vanBerkum and P. M. Upperman (Quality Engineering Consultancy, Veldhoven, Netherlands) Oct. 1991 12 p
(Memo-COSOR-91-26; ETN-92-91460) Avail: CASI HC A03/MF A01

D-optimal designs for some incomplete quadratic models in linear repression are given. The quadratic models are incomplete in the sense that not all quantitative factors have quadratic terms. The experimental region is a q dimensional cube. ESA

N92-29791# Lawrence Livermore National Lab., CA.
ISLAND: INTERACTIVE SOLUTION LANGUAGE FOR AN ADAPTIVE NIKE DRIVER
B. E. Engelmann and R. G. Whirley Oct. 1991 122 p
(Contract W-7405-eng-48)
(DE92-011444; UCRL-MA-108721) Avail: CASI HC A06/MF A02

Effective solution strategies to solve the global nonlinear equations are a vital part of an implicit nonlinear finite element analysis code such as NIKE2D. Efficient strategies make good use of computational resources, and allow larger and more complex analysis models to be studied. Robust algorithms are essential to handle the complex nonlinearities which arise in many engineering applications, such as metalforming process simulation. Our research indicates that robustness can be best achieved through adaptive solution strategies. This adaptivity and flexibility has recently been incorporated into NIKE2D. Temporal and algorithmic adaptivity is achieved through the development of ISLAND (Interactive Solution Language for an Adaptive Nike Driver). This report serves as a User Manual for the ISLAND language and its application to the definition of adaptive solution strategies in NIKE2D. ISLAND substantially improves the robustness of NIKE2D when solving strongly nonlinear problems. In addition, ISLAND allows new classes of constrained problems to be solved which could not previously be studied. Applications span many process simulation problems, including superplastic forming. These new solution control features make NIKE2D a 'smart code,' and permit many new and challenging problems to be addressed. DOE

N92-29792# Lawrence Livermore National Lab., CA.
SOLUTION STRATEGIES FOR IMPLICIT NONLINEAR FINITE ELEMENT ANALYSIS
B. E. Engelmann and R. G. Whirley Aug. 1991 8 p Presented at the ASME Annual Winter Meeting, Atlanta, GA, 1-6 Dec. 1991
(Contract W-7405-eng-48)
(DE92-011466; UCRL-JC-107865; CONF-911213-24) Avail: CASI HC A02/MF A01

The development of effective solution strategies to solve the global nonlinear equations which arise in implicit finite element analysis is an important area of research. Efficient strategies make good use of computational resources, and allow larger and more complex analysis models to be studied. Robust algorithms are essential to handle the complex nonlinearities which arise in many engineering applications, such as metalforming process simulation. Our research indicates that robustness can be best achieved in a general setting through adaptive solution strategies. This adaptivity and flexibility has been incorporated into an implicit nonlinear finite element code, NIKE2D. Temporal and algorithmic adaptivity is achieved through the development of ISLAND (Interactive Solution Language for an Adaptive Nike Driver). These new solution control features make NIKE2D a 'smart code,' and permit many new and challenging problems to be addressed. DOE

N92-29793# International Centre for Theoretical Physics, Trieste (Italy).
THE EXTENDED BETHE ANSATZ FOR INFINITE S = 1/2 QUANTUM SPIN CHAINS WITH NON-NEAREST-NEIGHBOR INTERACTION
V. I. Inozemtsev Oct. 1991 19 p
(DE92-622378; IC-91/374) Avail: CASI HC A03/MF A01

It is shown that the description of the states of infinite S = 1/2 interacting spin systems with the Hamiltonian H(sub s) = -J/2 (sigma)(sub j contains I,j,I(epsilon)Z) a(exp 2) sinh(exp -2) a(j - I) ((sigma)j(sigma)I-1)/2 can be performed by studying the hyperbolic Calogero-Sutherland eigenvalue problem. The construction of multimagnon wave functions in each N-magnon sector is based on solutions of the set of linear algebraic equations which determine also the structure of zonal spherical functions on symmetric spaces X(-)(sub N) = SL(N,H)/Sp(N) of negative curvature. The usual Bethe Ansatz for the XXX Heisenberg model corresponds to asymptotic forms of these wave functions at small values of a(exp -1) or large distances between spins turned over the ferromagnetic ground state. DOE

N92-29826# Technische Univ., Eindhoven (Netherlands). Dept. of Mathematics and Computing Science.
ON THE ADDITION OF LOG-CONVEX FUNCTIONS AND SEQUENCES
F. W. Steutel Jan. 1992 5 p
(Memo-COSOR-92-01; ISSN-0926-4493; ETN-92-91797) Avail: CASI HC A01/MF A01

We give a proof of the well known fact that log-convexity of functions and sequences is preserved under addition. ESA

N92-29858# Universiteit Twente, Enschede (Netherlands). Faculty of Applied Mathematics.
CONSTRUCTION OF A VC1 INTERPOLANT OVER TRIANGLES VIA EDGE DELETION
Claudia Cottin (Duisburg Univ., Germany, F.R.) and Ruud vanDamme Aug. 1991 14 p
(MEMO-988; ISSN-0169-2690; ETN-92-91594) Avail: CASI HC A03/MF A01

A construction of a visually smooth surface which interpolates to position values and normal vectors of randomly distributed points on a three dimensional object is presented. The method is local and uses quartic triangular and bicubic quadrilateral patches without splits. It heavily relies on an edge deleting algorithm which, starting from a given triangulation, derives a suitable combination of three and foursided patches. ESA

N92-29861# Center for Mathematics and Computer Science, Amsterdam (Netherlands). Dept. of Operations Research, Statistics, and System Theory.
DISCRETIZATION OF MORPHOLOGICAL OPERATORS
H. J. A. M. Heijmans Jul. 1991 24 p Sponsored by Netherlands Organization for Applied Scientific Research TNO
(CWI-BS-R9118; ISSN-0924-0659; ETN-92-91643) Copyright Avail: CASI HC A03/MF A01

A theory of discretization of images, image operators and image functionals in mathematical morphology is presented. The procedure of image discretization consists of two steps: the definition of a sequence of discrete images obtained by sampling the original continuous image on grids with finer and finer mesh width, and the representation of the discrete images as continuous images. The hit or miss topology on the space of closed Euclidean sets is used to show that the thus obtained discretized images approach the original continuous image if the mesh width tends to zero. The image discretization procedure is then used to obtain discretizations of image operators and functionals. Particular attention is given to discretizations with nice monotonicity properties, the so-called constructing discretizations. ESA

N92-29862# Center for Mathematics and Computer Science, Amsterdam (Netherlands). Dept. of Operations Research, Statistics, and System Theory.
ON CONSTRUCTING KERNEL POLYNOMIALS OF A SPECTRAL FUNCTION: APPLICATION TO ARMA MODELS
Kacha O. Dzhaparidze Jul. 1991 21 p Sponsored by Netherlands Organization for Applied Scientific Research TNO
(CWI-BS-R9119; ISSN-0924-0659; ETN-92-91644) Copyright Avail: CASI HC A03/MF A01

Useful formulas for constructing kernel polynomials associated with a certain class of spectral functions are presented. Spectral functions with rational densities which characterize ARMA model are included. As applied to the last subclass, this formula expresses kernel polynomials of an ARMA model in terms of kernel polynomials of an AR part which are easily constructed. ESA

N92-29864# Center for Mathematics and Computer Science, Amsterdam (Netherlands). Dept. of Operations Research, Statistics, and System Theory.
NON-INTERFERING DIPATHS IN PLANAR DIGRAPHS
C. McDiarmid (Oxford Univ., England), B. Reed (Waterloo Univ., Ontario), A. Schrijver, and B. Shepherd Sep. 1991 10 p Sponsored in part by Natural Sciences and Engineering Research Council and Netherlands Organization for Applied Scientific

Research TNO
(CWI-BS-R9121; ISSN-0924-0659; ETN-92-91646) Copyright Avail: CASI HC A02/MF A01

A min-max theorem for the problem of finding the maximum number of dipaths is given. Two given vertices in a planar graph are connected so that the internal vertices of distinct dipaths are not adjacent. The theorem also yields a polynomial time algorithm for finding such a collection of dipaths. The result can be extended to the case where the internal vertices of distinct dipaths are to be separated by a larger (directed) distance d greater than 1. ESA

N92-29866# Center for Mathematics and Computer Science, Amsterdam (Netherlands). Dept. of Analysis, Algebra and Geometry.
POSITIVE CONVOLUTION STRUCTURES ASSOCIATED WITH QUANTUM GROUPS
Tom H. Koornwinder Jun. 1991 25 p Presented at the Probability Measures on Groups, Oberwolfach, Fed. Republic of Germany, 4-10 Nov. 1990 Sponsored by Netherlands Organization for Applied Scientific Research TNO
(CWI-AM-R9105; ETN-92-91648) Copyright Avail: CASI HC A03/MF A01

An introduction to quantum groups is given, and how various types of positivity results of q special functions can be obtained from a quantum group interpretation is discussed. The notion of compact quantum Gelfand pairs is introduced, and it is shown that the linearization coefficients for the corresponding spherical functions are nonnegative. The nonnegativity of linearization coefficients is obtained for little q-Legendre polynomials and for a class of Askey-Wilson polynomials. It is also shown how such properties can be derived from Rahman-Verma type addition formulas. Spherical functions for compact quantum Gelfand pairs are also shown to satisfy product formulas with positive kermel. The quantum disk polynomials are discussed, a class of orthogonal polynomials on two noncommunicating variables. ESA

N92-29872# Universiteit Twente, Enschede (Netherlands). Faculty of Applied Mathematics.
INTEGRABLE DEFORMATIONS OF MEROMORPHIC EQUATIONS ON P(EXP 1)C
G. F. Helminck Sep. 1991 13 p
(MEMO-993; ISSN-0169-2690; ETN-92-91598) Avail: CASI HC A03/MF A01

A study concerning a holomorphic vectorbundle over P(exp 1)(C) and meromorphic connection of the vectorbundle is presented. Under some restrictions on the parameters space of the deformation, deformations of meromorphic equations on P(exp 1)(C) are constructed. They give rise locally on the parameters space of the deformation to solutions of nonlinear equations. If the original system on P(exp 1)(C) had a logarithmic pole at infinity, then the solutions of the nonlinear equations are shown to extend meromorphically to the whole parameter space of the deformation. ESA

N92-29881# Center for Mathematics and Computer Science, Amsterdam (Netherlands). Dept. of Analysis, Algebra and Geometry.
GAARDING INEQUALITIES FOR SYSTEMS OF PSEUDO-DIFFERENTIAL OPERATORS
Raymond G. M. Brummelhuis (Universidad Autonoma de Madrid, Cantoblanco, Spain) Sep. 1991 32 p Sponsored in part by Netherlands Organization for Applied Scientific Research TNO and Ministerio de Educacion y Ciencias
(CWI-AM-R9111; ISSN-0924-2953; ETN-92-91653) Copyright Avail: CASI HC A03/MF A01

A generalization of Melin's inequality to systems is given. The symbols used are assumed to be Hermitean. This subject is sophisticated for scalar operators. The classical Gaarding inequality for elliptic systems of pseudodifferential operators is mentioned and also the various improvements: the inequalities of Hoermlander, Melin, and Fefferman and Phong. ESA

N92-29882# Center for Mathematics and Computer Science, Amsterdam (Netherlands). Dept. of Analysis, Algebra and Geometry.
ASKEY-WILSON POLYNOMIALS FOR ROOT SYSTEMS OF TYPE BC
Tom H. Koornwinder Sep. 1991 19 p Presented at the AMS Meeting and Special Session on Hypergeometric Functions on Domains of Positivity, Jack Polynomials, and Applications, Tampa, FL, 22-23 Mar. 1991 Sponsored by Netherlands Organization for Applied Scientific Research TNO
(CWI-AM-R9112; ISSN-0924-2953; ETN-92-91654) Copyright Avail: CASI HC A03/MF A01

A family of Askey-Wilson type orthogonal polynomials on n variables associated with a root system of type BC(sub n) is introduced. Macdonald's results are summarized. The family depends, apart from q, on 5 parameters. For n = 1 it specializes to the four parameter family of one variable Askey-Wilson polynomials. For any n it contains Macdonald's two three parameter families of orthogonal polynomials associated with a root system of type BC(sub n) as special cases. The special case BC(sub n) and the further specialization to BC(sub 1) are discussed. Askey-Wilson polynomials for root system BC(sub n) are shown to be eigenfunctions of a certain difference operator and the full orthogonality of the polynomials is established. ESA

N92-29883# Center for Mathematics and Computer Science, Amsterdam (Netherlands). Dept. of Numerical Mathematics.
SOLVING PARABOLIC INTEGRO-DIFFERENTIAL EQUATIONS BY AN EXPLICIT INTEGRATION METHOD
A. S. VasudevaMurthy (Bangalore Univ., India) and J. G. Verwer Apr. 1991 14 p Submitted for publication Sponsored in part by NUFFIC and Netherlands Organization for Applied Scientific Research TNO
(CWI-NM-R9108; ISSN-0169-0388; ETN-92-91655) Copyright Avail: CASI HC A03/MF A01

The numerical integration in time of nonclassical parabolic initial boundary value problems which involve nonlocal integral terms over the spatial domain is described. The integral terms may appear in the boundary conditions and/or on the governing partial differential equation itself. These terms generally complicate the application of standard methods. An explicit method, the Runge/Kutta/Chebyshev method, whose application remains straightforward in many cases of practical interest is reviewed. Two numerical examples are discussed. A comparison is made, respectively, with the inplicit backward differentiation code DASSL and with the Keller box scheme. ESA

N92-29892# Center for Mathematics and Computer Science, Amsterdam (Netherlands). Dept. of Interactive Systems.
REAL-TIME QUADRATIC SHADING
V. C. J. Disselkoen Apr. 1991 17 p
(CWI-CS-R9123; ETN-92-91551) Copyright Avail: CASI HC A03/MF A01

A technique generating quadratic shading functions for scanlines when using a shading model closely related to Phong shading is described. The specular term is expressed using quadratic curves, obviating the need for pixel time exponentiation. The method combines concepts from vector coordinate interpolation and vector rotation techniques. ESA

N92-29893# Center for Mathematics and Computer Science, Amsterdam (Netherlands). Dept. of Analysis, Algebra and Geometry.
ASYMPTOTIC INVERSION OF THE INCOMPLETE BETA FUNCTION
N. M. Temme Jul. 1991 16 p Sponsored by National Organization for Applied Scientific Research TNO
(CWI-AM-R9106; ETN-92-91649) Copyright Avail: CASI HC A03/MF A01

The normalized incomplete beta function I(sub x)(a,b) is inverted for large values of the parameter a and b. The approximations are obtained by using uniform asymptotic expansions of the incomplete beta function, in which an error function or an

incomplete gamma function is the dominant term. The inversion problem is started by inverting this dominant term. Further terms in the expansion are obtained by using standard perturbation methods, which were recently introduced in a paper describing a method for asymptotic inversion of the incomplete gamma functions. Numerical results indicate that to obtain an accuracy of four correct digits the asymptotic method can already be used for a + b greater than or equal to 5. ESA

N92-29894# Center for Mathematics and Computer Science, Amsterdam (Netherlands). Dept. of Analysis, Algebra and Geometry.
HYPERASYMPTOTIC EXPANSIONS OF CONFLUENT HYPERGEOMETRIC FUNCTIONS
A. B. OldeDaalhuis Jul. 1991 13 p Sponsored by Netherlands Organization for Applied Scientific Research TNO
(CWI-AM-R9107; ETN-92-91650) Copyright Avail: CASI HC A03/MF A01

A new method for obtaining hyperasymptotic expansions for integrals representing the confluent hypergeometric U function is reported. At each level, the remainder is exponentially small compared with the previous remainders, and the number of new terms increases. Two numerical illustrations confirm these exponential improvements. ESA

N92-29895# Center for Mathematics and Computer Science, Amsterdam (Netherlands). Dept. of Analysis, Algebra and Geometry.
DIFFUSION APPROXIMATION OF STOCHASTIC INTEGRAL FUNCTIONALS OF JUMP MARKOV PROCESSES
V. V. Korolyuk (Kiev Univ., USSR) Jul. 1991 10 p Sponsored by Netherlands Organization for Applied Scientific Research TNO
(CWI-AM-R9108; ISSN-0924-2953; ETN-92-91651) Copyright Avail: CASI HC A02/MF A01

The problem of a diffusion approximation for stochastic integral functionals with rapid ergodic and splitting Markov Switchings is considered under some balance conditions. ESA

N92-29896# Center for Mathematics and Computer Science, Amsterdam (Netherlands). Dept. of Analysis, Algebra and Geometry.
DIFFUSION APPROXIMATION OF STOCHASTIC ADDITIVE FUNCTIONALS OF JUMP MARKOV PROCESSES
V. V. Korolyuk (Kiev Univ., USSR) Aug. 1991 10 p Sponsored by Netherlands Organization for Applied Scientific Research TNO
(CWI-AM-R9110; ISSN-0924-2953; ETN-92-91652) Copyright Avail: CASI HC A02/MF A01

The problem of diffusion approximation for stochastic additive functionals of jump Markov processes with splitting phase space on the series scheme is considered under some balance conditions. The proofs of the limit results are based on the martingale approach. ESA

N92-29898# Technische Univ., Eindhoven (Netherlands). Dept. of Mathematics and Computing Science.
DECISION SYSTEMS; THE RELATION BETWEEN PROBLEM SPECIFICATION AND MATHEMATICAL ANALYSIS
Jaap Wessels (International Inst. for Applied Systems Analysis, Laxenburg, Austria) Dec. 1991 24 p
(Memo-COSOR-91-37; ISSN-0926-4493; ETN-92-91791) Avail: CASI HC A03/MF A01

A demonstration that automated support for decision making of a tactical or strategic nature requires a solver independent medium for describing decision situations is presented. Such a medium may be specific for one environment, but it is also possible to develop media for certain types of environments. By using such a medium one obtains a decoupling of problem formulation and method of analysis. This makes it possible to use parts of the problem formulation as input for different types of models. Such problem formulations may provide mathematical models themselves, although they might also contain some less formal features. The decoupling makes it possible to choose problem formulations which are much closer to the original decision situation than would otherwise be possible with formulations in terms of a preselected solver. The argumentation is illustrated by treating a language for specifying goods flow problems in some detail. This language is based on timed colored Petri nets. ESA

N92-29919# Technische Univ., Delft (Netherlands). Faculty of Technical Mathematics and Informatics.
A MODEL FOR NO BOREL LIFTINGS
A. Dow and J. Vermeer 1991 26 p
(Rept-91-37; ISSN-0922-5641; ETN-92-91410) Copyright Avail: CASI HC A03/MF A01

Presented here is a study aimed at giving a self contained and complete proof of Shelah's result, that there is a model in which there is no (strong) lifting of the category algebra. The construction of the model follows a standard pattern. A method of coding Borel sets is described and P names of Borel codes, where P is some forcing poset, are discussed. Basic facts about the oracle chain condition are recalled and the single step iteration is addressed. ESA

N92-29920# Technische Univ., Delft (Netherlands). Faculty of Technical Mathematics and Informatics.
EXTREMALLY DISCONNECTED SPACES, SUBSPACES AND RETRACTIONS
A. Dow and J. Vermeer 1991 22 p
(Rept-91-38; ISSN-0922-5641; ETN-92-91411) Copyright Avail: CASI HC A03/MF A01

A study where a characterization of the class of compact subspaces of extremally disconnected spaces is found is presented. The characterization is shown to be useful, but is not suggested as 'satisfactory', since it is not an internal characterization. It has the property of being 'projective' with respect to the class of absolute retracts. By applying this to the basically disconnected question, an equivalent formulation which makes the question much more concrete is found. ESA

N92-29921# Technische Univ., Delft (Netherlands). Faculty of Technical Mathematics and Informatics.
LIMIT THEOREMS FOR FUNCTIONALS OF CONVEX HULLS
A. J. Cabo and P. Groeneboom 1991 24 p
(Rept-91-39; ISSN-0922-5641; ETN-92-91412) Copyright Avail: CASI HC A03/MF A01

In a previous paper a central limit theorem for the number of vertices of the convex hull of a uniform sample from the interior of a convex polygon is derived. This is done by approximating the process of vertices of the convex hull by the process of extreme points of a Poisson point process and by considering the latter process of extreme points as a Markov process (for a particular parameterization). This method is shown to be also applicable to derive limit theorems for the boundary length and for the area of the convex hull. This extends results of previous studies and shows that the boundary length and the area have a strikingly different probabilistic behavior. ESA

N92-29922# Technische Univ., Delft (Netherlands). Faculty of Technical Mathematics and Informatics.
A METHOD FOR CONVERTING THE SURFACE OF A GENERALIZED CYLINDER INTO A B-SPLINE SURFACE
Willem F. Bronsvoort and Jacob J. Waarts 1991 14 p
(Rept-91-40; ISSN-0922-5641; ETN-92-91413) Copyright Avail: CASI HC A03/MF A01

Generalized cylinders are objects defined by sweeping an arbitrary two dimensional closed contour along an arbitrary three dimensional trajectory, while simultaneously scaling the contour in two perpendicular directions. A simple method that converts the surface of a generalized cylinder of which the contour, the trajectory and the scale functions are defined by BB spline curves, into a B spline surface, is presented. ESA

N92-29923# Technische Univ., Delft (Netherlands). Faculty of Technical Mathematics and Informatics.
ABSTRACT QUASILINEAR EQUATIONS AND APPLICATION TO A GROUNDWATER FLOW PROBLEM

Philippe Clement and Shuanhu Li 1991 24 p
(Rept-91-41; ISSN-0922-5641; ETN-92-91414) Copyright Avail: CASI HC A03/MF A01

An approach under strong assumption on the operator is given for an abstract quasilinear differential equation. The result relies heavily on the maximal regularity for linear differential equations; the approach is somehow more direct. The theorem is applied to a quasilinear elliptic parabolic partial differential equation system arising in a two dimensional groundwater flow problem. ESA

N92-29924# Technische Univ., Delft (Netherlands). Faculty of Technical Mathematics and Informatics.
MINIMAL-CHANGE CODES AND NUMBER SYSTEMS
A. J. vanZanten 1991 53 p
(Rept-91-42; ISSN-0922-5641; ETN-92-91415) Copyright Avail: CASI HC A04/MF A01

The index system for various combinatorial objects ordered in minimal change order is addressed. For practical reasons, the index system for the Gray code of those objects is studied. It turns out that for each case studied a certain number system exists that is very suitable to express the indices of the objects in order to solve the ranking and unranking problems. In all cases the objects are represented by strings of numbers, hence, lexicographically. The index system related to a lexicographically ordered list usually gives an indication of the structure of the index system belonging to the Gray code of the same objects. The lexicographic codes are discussed in the various cases. ESA

N92-29946# Center for Mathematics and Computer Science, Amsterdam (Netherlands). Dept. of Numerical Mathematics.
AN IMPROVED ACCURACY VERSION OF THE MIXED FINITE ELEMENT METHOD FOR A SECOND ORDER ELLIPTIC EQUATION
R. R. P. vanNooyen May 1991 22 p Submitted for publication Sponsored by Netherlands Organization for Applied Scientific Research TNO
(CWI-NM-R9111; ETN-92-91658) Copyright Avail: CASI HC A03/MF A01

A new variant of the mixed finite element method for a second order elliptic problem is discussed. By using an appropriate quadrature rule to compute the coefficient matrix an improvement in the order of approximation of local averages is obtained. The new method can be used to obtain an a posteriori error estimate for a lower order method. ESA

N92-29956# Universiteit Twente, Enschede (Netherlands). Dept. of Computer Science.
THE PRIMORDIAL SOUP ALGORITHM: A SYSTEMATIC APPROACH TO THE SPECIFICATION AND DESIGN OF PARALLEL PARSERS
Wil Janssen, Mannes Poel, Klaas Sikkel, and Job Zwiers Nov. 1991 34 p
(Memo-INF-91-77; ISSN-0924-3755; ETN-92-91577) Copyright Avail: CASI HC A03/MF A01

A general framework for parallel parsing is presented, which allows for a unified, systematic approach to parallel parsing. The Primordial Soup Algorithm (PSA) creates trees by allowing partial parse trees to combine arbitrarily. A large class of parallel parsing strategies can be defined by adding constraints to the general algorithm. This is exemplified by strategies for parsers based on the algorithms of Cocke-Younger-Kasami (CYK), Earley, de Vreught, and Honig and Rytter. From such a parsing strategy, algorithms for various machine architectures can be derived in a systematic way. As an example, the CYK case is treated in full detail. The PS framework can be used to derive sequential algorithms, and there is no fundamental difference between sequential and parallel processing. In an appendix, a prototype PROLOG implementation of the PSA is transformed into an Earley parser. ESA

N92-29979# Universiteit Twente, Enschede (Netherlands). Center for Theoretical Physics.
APPROXIMATION IN A DAMPED HAMILTONIAN SYSTEM BY SUCCESSIVE RELATIVE EQUILIBRIA
G. Derks and T. P. Valkering 2 Dec. 1991 22 p
(MEMO-1017; ISSN-0169-2690; ETN-92-91763) Avail: CASI HC A03/MF A01

An (N + 1) dimensional Hamiltonian system with a cyclic coordinate and uniform friction added is considered. With aid of the constant of motion of the system without friction, induced by the cyclic coordinate, a collection of special solutions of the nondissipative system, called the Manifold of Relative Equilibria (MRE), depending on 2 parameters, is defined. For some classes of Hamiltonian, it is possible to approximate the solutions of the dissipative system, that started in the neighborhood of the MRE, with the points of the MRE (hence with 2 parameters). The spherical pendulum is shown to be such a Hamiltonian system. Central in the analysis is that the dissipative autonomous problem is transformed to a Hamiltonian nonautonomous one. For such a system, a generalization of the well known fact that the minimum of an autonomous Hamiltonian system is stable, is proved under certain assumptions. ESA

N92-29993# Center for Mathematics and Computer Science, Amsterdam (Netherlands). Dept. of Computer Science.
UNDECIDABLE EQUIVALENCES FOR BASIC PROCESS ALGEBRA
Jan Friso Groote and Hans Huettel (Edinburgh Univ., Scotland) Aug. 1991 19 p Sponsored in part by Commission of the European Communities; Aalborg Univ.; Danish Research Academy; and Netherlands Organization for Applied Scientific Research TNO
(CWI-CS-R9137; ECS-LFCS-91-169; ISSN-0169-118X; ETN-92-91560) Copyright Avail: CASI HC A03/MF A01

A recent theorem shows that strong bisimilarity is decidable for the class of 'normed' BPA (Basic Process Algebra) processes, which correspond to context free grammars. Huynh and Tian showed that readiness and failure equivalence are undecidable for BPA processes. An examination of all other equivalences in the linear/branching time hierarchy is presented. It is shown that none of them are decidable for normed BPA processes. ESA

N92-29995# Universiteit Twente, Enschede (Netherlands). Dept. of Computer Science.
PARTIAL LOGIC AS A SIMPLE RESTRICTION OF STANDARD LOGIC
Jan Kuper 24 Sep. 1991 19 p
(Memo-INF-91-73; ISSN-0924-3755; ETN-92-91574) Copyright Avail: CASI HC A03/MF A01

The concise axiomatization of partial logic, which appears to be a simple restriction of ordinary first order predicate logic, is given. Its semantics are formulated as a natural adaptation of ordinary Tarski semantics of the first order logic, and the soundness and completeness of the system are proved. The logic is well suited to describe partial functions. A first order formulation of the lambda calculus is given as an example. ESA

N92-29999# Universiteit Twente, Enschede (Netherlands). Faculty of Applied Mathematics.
RANDOM WALK POLYNOMIALS AND RANDOM WALK MEASURES
Erik A. vanDoorn and Pauline Schrijner Oct. 1991 14 p
(MEMO-1007; ISSN-0169-2690; ETN-92-91754) Avail: CASI HC A03/MF A01

Random walk polynomials and random walk measures play a prominent role in the analysis of a class of Markov chains called random walks. Without any reference to random walks, however, a random walk polynomial sequence can be defined, and is defined in this study, as an orthogonal polynomial sequence (P(sub n)(x)), which is such that the parameters alpha(sub n) in the recurrence relations P(sub n + 1)(x) = (x - alpha(sub n))P(sub n)(x) - beta(sub n)P(sub n - 1)(x) are nonnegative. Any measure with respect to which a random walk polynomial sequence is orthogonal is a

random walk measure. Some properties of random walk measures and polynomials are collected and these findings are used to obtain a limit theorem for random walk measures which is of interest in the study of random walks. A conjecture in random walk measures involving Christoffel functions is given in conclusion. ESA

N92-30075# Universiteit Twente, Enschede (Netherlands). Dept. of Computer Science.
A CLOSER LOOK AT A FIBONACCI-LIKE ITERATED NONLINEAR MAP: MORE CHAOS AND ORDER
Peter R. J. Asveld Sep. 1991 70 p
(Memo-INF-91-70; ISSN-0924-3755; ETN-92-91571) Copyright Avail: CASI HC A04/MF A01

The continuation of a study of a Fibonacci like analog of the well known iterated nonlinear map x(sub n+1) = lambda x(sub n)(1- x(sub n)) is presented. This second order variant contains two parameters: one which corresponds to lambda, and a second one denoted by alpha that determined the relative influence of the two previous values. As in the earlier study, lambda is fixed to 3.9999 and the parameter alpha is varied in between 0 and 1. Many subintervals of alpha that exhibit interesting types of behavior (regular patterns, periodic limit cycles, 'intermediate stages', etc.), are considered. The effect of the initial conditions on the ultimate behavior of this iterated mapping is discussed. ESA

N92-30077# Universiteit Twente, Enschede (Netherlands). Faculty of Applied Mathematics.
PORT-CONTROLLED HAMILTONIAN SYSTEMS: MODELLING ORIGINS AND SYSTEMTHEORETIC PROPERTIES
B. M. Maschke (Conservatoire National des Arts et Metiers, Paris, France) and A. J. vanderSchaft Oct. 1991 16 p
(MEMO-1001; ISSN-0169-2690; ETN-92-91748) Avail: CASI HC A03/MF A01

A study which shows that the network representation (as obtained through the generalized bond graph formalism) of nonresistive physical systems in interaction with their environment leads to a well defined class of (nonlinear) control systems, called port controlled Hamiltonian systems, is presented. A first basic feature of these systems is that their internal dynamics is Hamiltonian with respect to a Poisson structure determined by the topology of the network and to a Hamiltonian given by the stored energy. Secondly, the network representation provides automatically (intrinsically to the notation) to every port control variable (input) a port conjugated variable as output. This definition of port conjugated input and output variables, based on energy considerations, is shown to have important consequences for the observability and controllability properties, as well as the external characterization of port controlled Hamiltonian systems. ESA

N92-30078# Universiteit Twente, Enschede (Netherlands). Faculty of Applied Mathematics.
SUPERSYMMETRIC EXTENSIONS OF THE NONLINEAR SCHROEDINGER EQUATION: SYMMETRIES AND COVERINGS
Marcel Roelofs and Paul H. M. Kersten 11 Oct. 1991 32 p
(MEMO-1002; ISSN-0169-2690; ETN-92-91749) Avail: CASI HC A03/MF A01

A construction for a supersymmetric generalization of the cubic Schroedinger equation, resulting in two supersymmetric systems, one of which contains a free parameter, is proposed. Both systems are proven to admit an infinite set of (higher order) local and nonlocal symmetries and a seemingly infinite set of conservation laws, the lowest order terms of which are given explicitly. Moreover, the theory of coverings (equivalent to the prolongation method of Wahlquist and Estabrook) is applied to both systems. Both are seen to admit an infinite dimensional covering algebra, the structure of which is determined explicitly, resulting in a related supersymmetric system of differential equations, as well as an auto Baecklund transformation for each equation. This indicates the complete integrability of both systems. ESA

N92-30080# Universiteit Twente, Enschede (Netherlands). Faculty of Applied Mathematics.
CLASSIFICATION OF A-GRADED ALGEBRAS WITH 3 GENERATORS
E. Korkina (Institute of New Technologies, Moscow, USSR) Oct. 1991 16 p
(MEMO-1004; ISSN-0169-2690; ETN-92-91751) Avail: CASI HC A03/MF A01

Further to V. I. Arnold's notion of A graded algebras, where a complete classification was made for the case of 3 generators, but no proofs of statement were presented, a study to construct the proof of the classification is presented. Commutative associative N graded algebras over C having a finite number of generators and with homogeneous subspaces of dimension 0 or 1 are considered. ESA

N92-30081# Universiteit Twente, Enschede (Netherlands). Faculty of Applied Mathematics.
OPTIMAL COPYING STRATEGIES
H. J. Broersma and F. Goebel Oct. 1991 9 p
(MEMO-1005; ISSN-0169-2690; ETN-92-91752) Avail: CASI HC A02/MF A01

Some examples of problems arising in optimal strategy for making copies of another tape, assuming that not only the copy is a little worse than the original but also the mother tape (or any other tape) incurs a loss of quality when it is copied, are shown. A special strategy is defined and its optimality is proved. Two variations of the original problem formulation are mentioned. The asymptotic behavior of the quality loss as the number of required copies tends to infinity is given. ESA

N92-30096# Institut des Hautes Etudes Scientifiques, Bures-sur-Yvette (France).
SPECTRAL TYPE OF ORNSTEIN'S CLASS ONE TRANSFORMATIONS
J. Bourgain Mar. 1992 13 p
(PB92-178292; IHES/M/92/14) Avail: CASI HC A03/MF A01

Concern is with the spectral analysis of a class of transformations introduced in a paper by D. Ornstein. These transformations called class one or rank one have spectral multiplicity one. It is apparently an unsolved problem whether the spectral type may be absolutely continuous with respect to Lebesgue measure (such an example would be very meaningful to Banach's well known problem whether a dynamical system (Omega,mu,T) may have simple Lebesgue spectrum). In the paper by Ornstein, an example of a mixing rank one transformation is obtained. The construction makes essential use of probabilistic techniques. It is shown that for such a random construction the maximal spectral type is always singular. The investigation will be mainly oriented towards harmonic analysis. Author

N92-30147# Universiteit Twente, Enschede (Netherlands). Faculty of Applied Mathematics.
CHEBYSHEV LINE APPROXIMATION: A SENSITIVITY ANALYSIS
P. Jonker, M. Streng, and F. Twilt Dec. 1991 23 p
(MEMO-1020; ISSN-0169-2690; ETN-92-91765) Avail: CASI HC A03/MF A01

The Chebyshev approximation of finite sets of points in the plane by straight lines is considered. This problem can be written as an optimization problem, which, in the generic case, is shown to be structurally stable. In the special case of three data points, an overview of possible bifurcations of the corresponding optimization problems, including transitions of the Morse indices for the critical points, is given. ESA

N92-30177# Center for Mathematics and Computer Science, Amsterdam (Netherlands). Dept. of Computer Science.
TERM REWRITING ANALYSIS IN PROCESS ALGEBRA
G. J. Akkerman (Utrecht State Univ., Netherlands) and J. C. M. Baeten (Amsterdam Univ., Netherlands) Jun. 1991 12 p
Sponsored in part by Commission of the European Communities and Netherlands Organization for Applied Scientific Research

TNO
(CWI-CS-R9130; ETN-92-91555) Copyright Avail: CASI HC A03/MF A01

The application of term rewriting analysis to theories of communicating concurrent systems is discussed. Turning such a theory into a canonical term rewriting system yields decidability and is essential for implementation. This is carried out for the theory ACP (Algebra of Communication Processes) with a silent step in the setting of branching bisimulation. It is necessary to consider rewriting modulo equalities. Knuth-Bendix completion, and a Peterson-Stickel complete term rewriting system which has the same term algebra as the fragment of ACP(tau) it corresponds with, are considered. The termination of this rewrite system is proved. ESA

N92-30178# Center for Mathematics and Computer Science, Amsterdam (Netherlands). Dept. of Computer Science.
REAL SPACE PROCESS ALGEBRA
J. C. M. Baeten (Amsterdam Univ., Netherlands) and J. A. Bergstra (Amsterdam Univ., Netherlands) Jun. 1991 18 p Sponsored in part by Commission of the Economic Communities and Netherlands Organization for Applied Scientific Research TNO
(CWI-CW-R9131; ETN-92-91556) Copyright Avail: CASI HC A03/MF A01

A real time process algebra is extended to real space time process algebra, where actions are not just parametrized by a time coordinate, but also by three spatial coordinates. Two versions are described: classical space time, where all equations are invariant Galilei transformations, and relativistic space time, where all equations are invariant under Lorentz transformations. The latter case in turn splits into two subcases: the temporal interleaving model and the true concurrency model. ESA

N92-30185# Universiteit Twente, Enschede (Netherlands). Faculty of Applied Mathematics.
SUFFICIENT CONDITIONS FOR DOMINATING CLIQUES
Cornelis Hoede and Li Xueliang (Xinjiang Univ., Urumchi, China) Oct. 1991 14 p
(MEMO-1006; ISSN-0169-2690; ETN-92-91753) Avail: CASI HC A03/MF A01

Sufficient conditions for 'dominating cliques' are addressed, considering simple finite undirected connected graphs. A set of vertices is a 'dominating set' in a graph if every vertex not in the dominating set is adjacent to one or more vertices in the dominating set. A 'dominating clique' is a dominating set that induces a complete subgraph. Various conditions for the occurrence of a dominating clique are presented. ESA

65 STATISTICS AND PROBABILITY

Includes data sampling and smoothing; Monte Carlo method; and stochastic processes.

N92-29419# Oesterreichisches Forschungszentrum Seibersdorf G.m.b.H., Vienna. Bereich Systemforschung Technik-Wirtschaft-Umwelt.
THE DETERMINATION OF STOCHASTIC MODELS AND AREAS OF CONFIDENCE [UEBER DIE BESTIMMUNG VON STOCHASTISCHEN MODELLEN UND VERTRAUENSBEREICHEN]
Alexander Kopcsa Dec. 1991 39 p In GEORGIAN
(OEFZS-4612; ETN-92-91504) Copyright Avail: CASI HC A03/MF A01

A method to find a stochastic model describing a stochastic variable, under the assumption that data exist, is described. Some possibilities of estimating the parameters of the model and calculating areas of confidence are given. The stochastic model is determined using the Pearson diagram. ESA

N92-29491# Grenoble-1 Univ. (France).
SOME APPLICATIONS OF ORTHOGONAL FUNCTIONS TO PROBABILITY AND STATISTICS Ph.D. Thesis [QUELQUES APPLICATIONS DES FONCTIONS ORTHOGONALES END PROBABILITE ET STATISTIQUE]
Rene Blacher 1990 141 p In ENGLISH and FRENCH
(ETN-92-91741) Avail: CASI HC A07/MF A02

The study of the correlation of superior order is continued. The asymptotic distribution of the empirical correlation coefficients are obtained. An Hilbertian independence test is deduced. The Hermite polynomials and the Laguerre polynomials are shown to be equal to any moments. The distributions of a sum of n random vectors and of their quadratic forms are deduced. For individual titles, see N92-29492 through N92-29492.

N92-29492# Grenoble-1 Univ. (France). Univ. Scientifique et Medicale.
A NEW FORM FOR THE CHI-SQUARED TEST OF INDEPENDENCE (DOCUMENT 2)
Rene Blacher *In its* Some Applications of Orthogonal Functions to Probability and Statistics 1990 19 p Repr. from Statistics, v. 19, no. 4, 1988 p 519-536 (For primary document see N92-29491 20-65)
Avail: CASI HC A03/MF A02

The chi squared tests of independence are studied: tests with and without estimated marginal distributions; and the chi squared restricted test, for which the statistic test is simplified. A new form of the chi squared tests of independence which simplifies their presentation is thus obtained. The method highlights the difference of these tests and produces examples of minimum chi squared estimators, Hilbertian tests, and different chi squared tests. ESA

N92-29500# Stanford Univ., CA. Dept. of Operations Research.
LIMIT THEOREMS FOR CUMULATIVE PROCESSES
Peter W. Glynn and Ward Whitt (Bell Telephone Labs., Inc., Murray Hill, NJ.) Oct. 1991 31 p
(Contract DAAL03-91-G-0101)
(AD-A248507; TR-72) Avail: CASI HC A03/MF A01

Necessary and sufficient conditions are established for cumulative processes (associated with regenerative processes) to obey several classical limit theorems; e.g., a strong law of large numbers, a law of the iterated logarithm and a functional central limit theorem. The key random variables are the integral of the regenerative process over one cycle and the supremum of the absolute value of this integral over all possible initial segments of a cycle. The tail behavior of the distribution of the second random variable determines whether the cumulative process obeys the same limit theorem as the partial sums of the cycle integrals. Interesting open problems are the necessary conditions for the weak law of large numbers and the ordinary central limit theorem. GRA

N92-29501# Stanford Univ., CA. Dept. of Statistics.
A SAMPLE-SIZE OPTIMAL BAYESIAN PROCEDURE FOR SEQUENTIAL PHARMACEUTICAL TRIALS
Noel Cressie and Jonathan Biele 5 Mar. 1992 20 p
(Contract N00025-92-J-1264)
(AD-A248512; TR-451) Avail: CASI HC A03/MF A01

Consider a pharmaceutical trial where the consequences of different decisions are expressed on a financial sale. The efficacy of the new drug under consideration has a prior distribution obtained from the underlying biological process, animal experiments, clinical experience, and so forth. In an important paper, Berry and Ho (1988) show how these components are used to establish an optimal (Bayes) sequential procedure, assuming a known constant size at each decision point. We show in this article how it is also possible to optimize with respect to the sample-size rule. This last component of the design, which is missing from most sequential procedures, has the potential to yield considerably larger expected net gains. GRA

N92-29585# Air Force Inst. of Tech., Wright-Patterson AFB, OH.
A SENSITIVITY ANALYSIS OF CIRCULAR ERROR PROBABLE APPROXIMATION TECHNIQUES M.S. Thesis
Peter Puhek Mar. 1992 185 p
(AD-A248105; AFIT/GOR/ENS/92M-23) Avail: CASI HC A09/MF A02

Several algebraic CEP estimates models were examined in this study. Each assumes that the crossrange and downrange miss distances of the sample data follow a bivariate normal distribution. The analysis determined the sensitivities of these models to changes in the parameters of sample size, bias, correlation, and ellipticity. The accuracy of each model is expressed in terms of relative error, and the parameter regions in which a certain method dominated as the most accurate were noted. In general, it was found that bias was the most significant parameter in determining the best CEP method. A simple method, based on the Rayleigh distribution dominated as the best when bias was 0, .25, .5, .75, or 1, and the Grubbs-Patnaik/chi-square method dominated for the bias setting of 2 regardless of the settings of the other parameters. Levels of bias greater than 2 were not addressed. GRA

N92-29606# Technische Univ., Eindhoven (Netherlands). Dept. of Mathematics and Computing Science.
A COMPENSATION APPROACH FOR TWO-DIMENSIONAL MARKOV PROCESSES
I. J. B. F. Adan, J. Wessels (International Inst. for Applied Systems Analysis, Laxenburg, Austria), and W. H. M. Zijm (Universiteit Twente, Enschede, Netherlands) 26 Oct. 1991 35 p
(Memo-COSOR-91-28; ETN-92-91461) Avail: CASI HC A03/MF A01

Several queueing processes may be modeled as random walks in a multidimensional grid. The equilibrium distribution for the case of a two dimensional grid is considered. In previous research it was shown that for some two dimensional random walks the equilibrium distribution has the form of an infinite series of product of powers which can be constructed with a compensation procedure. The object of the study is to investigate under which conditions such an elegant solution exists and may be found with a compensation approach. The conditions can be easily formulated in terms of the random behavior in the inner area and the drift on the boundaries. ESA

N92-29609# Technische Univ., Eindhoven (Netherlands). Dept. of Mathematics and Computing Science.
TAGUCHI METHODS
Jack T. M. Wijnen Nov. 1991 13 p
(Memo-COSOR-91-31; ETN-92-91464) Avail: CASI HC A03/MF A01

An introduction to Taguchi's quality engineering ideas and statistical procedures is presented. Taguchi was asked in 1949 to improve productivity in research and development and his ideas and statistical procedures have been used in Japan for decades. Quality, orthogonal arrays, and direct product arrays are described. ESA

N92-29626# Technische Univ., Delft (Netherlands). Faculty of Technical Mathematics and Informatics.
NONPARAMETRIC MAXIMUM LIKELIHOOD ESTIMATORS FOR INTERVAL CENSORING AND DECONVOLUTION
Piet Groeneboom 1991 94 p Prepared in cooperation with Stanford Univ., CA
(Rept-91-53; ISSN-0922-5641; ETN-92-91422) Copyright Avail: CASI HC A05/MF A01

An attempt to develop theory for Non Parametric Maximum Likelihood Estimators (NPMLE's) for the distribution function in certain inverse problems is presented. The interval censoring problem is addressed. In this case, one only has information about an interval to which the variable of interest belongs, a situation quite common in medical research. The classical approach is to use the EM algorithm. This is shown to correspond to the so called self consistency equations for the NPMLE. These equations yield necessary but not sufficient conditions for the characterization of the NPMLE and have (so far) not been very useful in developing distribution theory. For this reason another approach, based on isotonic regression theory, which gives necessary and sufficient conditions, and which yields efficient algorithms and also leads to distribution theory is addressed. Consistency is proved for the NPMLE in all situations discussed. Distribution theory is addressed and open problems and conjectures are discussed. ESA

N92-29718# Stanford Univ., CA. Dept. of Statistics.
ACCURATE PROCEDURES FOR APPROXIMATE BAYESIAN AND CONDITIONAL INFERENCE WITHOUT THE NEED FOR ORTHOGONAL PARAMETERS
Thomas J. DiCiccio, Joseph B. Keller, and Michael A. Martin 24 Feb. 1992 26 p
(Contract N00025-92-J-1264)
(AD-A248662) Avail: CASI HC A03/MF A01

This paper concerns methods to construct approximate confidence limits for a scalar parameter in the presence of nuisance parameters. The methods are based on Bayesian procedures in which prior density is chosen so that the posterior quantiles of iP are approximate confidence limits with coverage error of order 0(n-1)) under repeated sampling. Multidimensional integration of the posterior density is avoided by using approximations of marginal densities and distribution functions; thus, adjustments are obtained that improve the standard normal approximation to the distributions of signed roots of the profile and conditional likelihood ratio statistics for psi. The necessary prior densities are easy to specify when the nuisance parameters are orthogonal to the parameter of interest, and this simplicity is exploited in developing the methods. However, the need for explicit specification of an orthogonal parameterization is alleviated by approximating the Jacobian of a transformation to orthogonality. The methods are illustrated and compared with other procedures in some examples involving exponential families. GRA

N92-29774# Technische Univ., Eindhoven (Netherlands).
A COMPENSATION APPROACH FOR QUEUEING PROBLEMS Ph.D. Thesis
Ivo Jean-Baptiste Fr Adan 1991 190 p
(ETN-92-91628) Avail: CASI HC A09/MF A02

A fairly general class of two dimensional Markov processes is considered in order to investigate under what conditions these processes have a solution in the form of a series of products of powers which can be found by a compensation approach. The symmetric shortest queue problem is treated as an application of the theory. For this problem some special properties are worked out in detail and used for numerical purposes. The general theory is applied to a queueing model for multiprogramming queues. The general compensation approach is further extended to the symmetric shortest queue problem. Conclusions and comments are given and in particular the approach is sketched for the symmetric shortest delay problem with Erlang servers and the M/E(sub r)/c. ESA

N92-29817# Technische Univ., Eindhoven (Netherlands). Dept. of Mathematics and Computing Science.
THE THEORY OF IMPRECISE PROBABILITIES: SOME RESULTS FOR DISTRIBUTION FUNCTIONS, DENSITIES, HAZARD RATES, AND HAZARD FUNCTIONS
F. P. A. Coolen Nov. 1991 35 p
(Memo-COSOR-91-32; ETN-92-91786) Avail: CASI HC A03/MF A01

The theory of imprecise probabilities is discussed, and some relations are derived for lower and upper cumulative distribution functions and densities. To introduce the concept in the theory of reliability, lower and upper hard rates and hazard functions are defined. Some aspects of updating lower and upper prior densities in light of new information are described. ESA

N92-29821# Technische Univ., Eindhoven (Netherlands). Dept. of Mathematics and Computing Science.
ON THE ASYMPTOTICALLY UNIFORM DISTRIBUTION MODULO 1 OF EXTREME ORDER STATISTICS
J. J. A. M. Brands and R. J. G. Wilms Dec. 1991 18 p Submitted for publication
(Memo-COSOR-91-38; ISSN-0926-4493; ETN-92-91792) Avail: CASI HC A03/MF A01

A sequence of independent and identically distributed random variables is addressed: (x(sub m))(exp 1)(sup infinity). Sufficient conditions for the fractional part of max (x(sub 1), ..., x(sub n)) to converge in distribution, as n approaches infinity, to a random variable with a uniform distribution on the half open interval (1,1) (open to the right), are given. Some properties of Fourier-Stieljes sequences and Brands' property are given. ESA

N92-29827# Technische Univ., Eindhoven (Netherlands). Dept. of Mathematics and Computing Science.
SELECTION CONSTANTS FOR UNIFORM POPULATIONS
Paul vanderLaan Jan. 1992 17 p
(Memo-COSOR-92-02; ISSN-0926-4493; ETN-92-91798) Avail: CASI HC A03/MF A01

Using the subset selection approach, selection constants are determined for uniform populations. Tables with exact results are presented. Comparisons are made with approximate values and with selection constants for normal populations. ESA

N92-29828# Technische Univ., Eindhoven (Netherlands). Dept. of Mathematics and Computing Science.
DATA REDUCTION IN STATISTICAL INFERENCE
E. E. M. vanBerkum, H. N. Linssen, and D. A. Overdijk Feb. 1992 26 p
(Memo-COSOR-92-03; ISSN-0926-4493; ETN-92-91799) Avail: CASI HC A03/MF A01

Generalized definitions of the invariance, (partial) sufficiency and ancillarity principles are given in a measure-theoretic context. Data reduction in statistical inference is described in terms of these principles. ESA

N92-29856# Universiteit Twente, Enschede (Netherlands). Faculty of Applied Mathematics.
PARAMETER IDENTIFICATION IN TIDAL MODELS WITH UNCERTAIN BOUNDARIES
Arunabha Bagchi and Paul tenBrummelhuis Jul. 1991 21 p Presented at the 9th IFAC/IFORS Symposium on Identification System Parameter Estimation, Budapest, Hungary, 8-12 Jul. 1991
(MEMO-983; ISSN-0169-2690; ETN-92-91590) Avail: CASI HC A03/MF A01

A simultaneous state and parameter estimation procedure for tidal models with random inputs, which is formulated as a minimization problem, is considered. It is assumed that some system parameters are unknown and that the random noise inputs act only on the open boundaries. In estimating the states, the hyperbolic nature of the governing dynamical equations is exploited, which makes the procedure also suitable for use in nonlinear tidal models without an excessive computational load. The method of Chavent, used to calculate the gradient of a criterion that is to be minimized, is now applied on a stochastic environment and the estimation method can also be applied to practical, large scale problems. ESA

N92-29860# Center for Mathematics and Computer Science, Amsterdam (Netherlands). Dept. of Operations Research, Statistics, and System Theory.
ASYMPTOTIC OPTIMALITY OF THE CHI-SQUARE TEST WITH LARGE NUMBER OF DEGREES OF FREEDOM WITHIN THE CLASS OF SYMMETRIC TESTS
D. M. Chibisov (Steklov Mathematical Inst., Moscow, USSR) Jul. 1991 25 p Sponsored by Netherlands Organization for Applied Scientific Research TNO
(CWI-BS-R9116; ETN-92-91642) Copyright Avail: CASI HC A03/MF A01

The problem of testing an hypothesis against an alternative hypothesis for independent variables having normal distributions is considered. The objective is to prove the corresponding property of the chi-square test in the problem of testing equiprobability of outcomes in a multinomial distribution when the number of outcomes, N, grows to infinity together with the number of trials, n. The method of asymptotic analysis of the 'symmetrized' likelihood ratio developed provides a basic tool for this problem. ESA

N92-29863# Center for Mathematics and Computer Science, Amsterdam (Netherlands). Dept. of Operations Research, Statistics, and System Theory.
U-STATISTICS OF INCREASING DEGREES WITH ASYMPTOTICALLY POISSON DISTRIBUTIONS
V. S. Korolyuk (Academy of Sciences of the Ukrainian SSR, Kiev.) and Y. V. Borovskikh (Academy of Sciences, USSR, Leningrad) Aug. 1991 7 p Sponsored by Netherlands Organization for Applied Scientific Research TNO
(CWI-BS-R9120; ISSN-0924-0659; ETN-92-91645) Copyright Avail: CASI HC A02/MF A01

The limit theorem for U statistics with increasing degrees, provided that the counting measure of sampling variables has asymptotically Poisson distribution, is addressed. A sequence of independent identically distributed random variables taking values in a measurable space and having a common distribution is considered. The asymptotics of the U statistics under a given condition are studied. ESA

N92-29897# Technische Univ., Eindhoven (Netherlands). Dept. of Mathematics and Computing Science.
IMPRECISE CONJUGATE PRIOR DENSITIES FOR THE ONE-PARAMETER EXPONENTIAL FAMILY OF DISTRIBUTIONS
F. P. A. Coolen Dec. 1991 31 p
(Memo-COSOR-91-36; ETN-92-91790) Avail: CASI HC A03/MF A01

A generalization of the standard Bayesian theory of statistical inference is presented for members of the one parameter exponential family of distributions, such that imprecise prior densities are allowed. This enables representation for the parameter of interest. A model is suggested with imprecise conjugate prior densities to enable simple updating of the prior densities if new data become available. ESA

N92-29974# Universiteit Twente, Enschede (Netherlands). Faculty of Applied Mathematics.
A SIMPLE APPROXIMATION TO THE BIVARIATE NORMAL DISTRIBUTION WITH LARGE CORRELATION COEFFICIENT
Willem Albers and Wilbert C. M. Kallenberg Nov. 1991 18 p
(MEMO-1011; ISSN-0169-2690; ETN-92-91758) Avail: CASI HC A03/MF A01

The bivariate normal distribution function is approximated with emphasis on situations where the correlation coefficient is large. The high accuracy of the approximation is illustrated by numerical examples. Moreover, exact upper and lower bounds are presented as well as asymptotic results on the error terms. ESA

N92-29975# Universiteit Twente, Enschede (Netherlands). Faculty of Applied Mathematics.
A TWO-STAGE ESTIMATOR FOR GENERALIZED LINEAR MODELS WITH NONCONSTANT DISPERSION PARAMETER
Klaas Poortema Nov. 1991 16 p
(MEMO-1012; ISSN-0169-2690; ETN-92-91759) Avail: CASI HC A03/MF A01

A two stage estimator to estimate beta in generalized linear models where the dispersion parameter is a linear function of covariates is proposed. Asymptotic normality is proved not only for an exact likelihood of the dependent variables, instead expressions for expectation and variance are presumed together with some regularity conditions. In the first stage (square root of n), consistent estimators are constructed. The second stage consists of a single iteration step which suffices to obtain the desired asymptotic covariance matrix for the beta estimator. ESA

N92-29976# Universiteit Twente, Enschede (Netherlands). Faculty of Applied Mathematics.
TESTING EQUALITY OF VARIANCES IN THE ANALYSIS OF REPEATED MEASUREMENTS
Wilbert C. M. Kallenberg, Govind S. Mudholkar (Rochester Univ., NY.), and Perla Subbaiah (Oakland Univ., Rochester, MI.) Nov. 1991 30 p
(MEMO-1013; ISSN-0169-2690; ETN-92-91760) Avail: CASI HC A03/MF A01

The problem of comparing the precisions of two instruments using repeated measurements can be cast as an extension of the Pitman-Morgan problem of testing equality of variances of a bivariate normal distribution. Hawkins (1981) decomposes the hypothesis of equal variances in this model into two subhypotheses for which simple tests exist. For the overall hypothesis, he proposes to combine the tests of the subhypotheses using Fisher's method and empirically compares the component tests and their combination with the likelihood ratio test. A study which attempts to resolve some discrepancies and puzzling conclusions in Hawkin's study and to propose simple modifications is presented. The new tests are compared to the test discussed by Hawkins and to each other both in terms of the finite sample power (estimated by Monte Carlo simulation) and theoretically in terms of asymptotic relative efficiencies. ESA

N92-29980# Universiteit Twente, Enschede (Netherlands). Faculty of Applied Mathematics.
POWER APPROXIMATIONS TO AND POWER COMPARISON OF CERTAIN GOODNESS-OF-FIT TESTS
Tadeusz Inglot (Technical Univ. of Wroclaw, Poland), Wilbert C. M. Kallenberg, and Teresa Ledwina (Technical Univ. of Wroclaw, Poland) Dec. 1991 29 p
(MEMO-1019; ISSN-0169-2690; ETN-92-91764) Avail: CASI HC A03/MF A01

A global power approximation approach is extended to a large class of goodness of fit test statistics, including Neyman's smooth tests. A criterion which makes a power comparison possible, at least in a rough sense, is proposed. It turns out that for most alternatives indeed there is not much difference between both tests in taking a large or a small number of components. Surprisingly, on the (small) set of alternatives where there is a difference, Neyman's smooth test requires the larger number of components. The criterion may be of independent interest and may also be applied in other situations where (noncentral) chi-square distributions occur. The method is illustrated by numerical results. ESA

N92-30174# Maryland Univ., College Park. Inst. for Physical Science and Technology.
BASIC PROBLEMS OF A-POSTERIORI ERROR ESTIMATION
I. Babuska, L. Plank, and R. Rodriguez Feb. 1992 31 p
(Contract N00014-90-J-1090; NSF CCR-88-20279)
(AD-A248986) Avail: CASI HC A03/MF A01

This paper addresses basic questions regarding reliability of a-posteriori error estimation. It analyzes in detail an a-posteriori estimator for linear elements on triangular meshes. It gives the bounds of the effectivity index depending on the geometry of the triangles and smoothness of the approximated solution. The theoretical results are in concordance with the results of our numerical experiments. The second part analyzes in one dimensional setting a one parametric family of the estimators and their optimal selection for adaptively constructed meshes. GRA

N92-30180# Center for Mathematics and Computer Science, Amsterdam (Netherlands). Dept. of Operations Research, Statistics, and System Theory.
ANALYSIS OF A THREE-DIMENSIONAL POINT PATTERN WITH REPLICATION
A. J. Baddeley, R. A. Moyeed (Bath Univ., England), C. V. Howard (Liverpool Univ., England), and A. Boyde (University Coll., London, England) Sep. 1991 41 p Submitted for publication
Sponsored by Netherlands Organization for Applied Scientific Research TNO
(CWI-BS-R9124; ISSN-0924-0659; ETN-92-91564) Copyright Avail: CASI HC A03/MF A01

Techniques for analyzing three dimensional spatial point patterns are demonstrated on data from a confocal microscope recording the locations of cells in three dimensions. New computational techniques for edge corrections and empty space measurements are proposed. A novel feature of the data is replication and nesting in a sampling design: multiple spatial patterns were observed from each of several animals. A ratio regression approach was developed for this. ESA

N92-30188# Universiteit Twente, Enschede (Netherlands). Faculty of Applied Mathematics.
A RANDOM POLYNOMIAL TIME ALGORITHM FOR WELL-ROUNDING CONVEX BODIES
U. Faigle, N. Gademann, and W. Kern Jan. 1992 34 p
(MEMO-1023; ISSN-0169-2690; ETN-92-91768) Avail: CASI HC A03/MF A01

The problem of approximately computing the volume of convex bodies is addressed. A randomized polynomial time algorithm for well rounding a convex body is derived, based on the method of rapidly mixing Markov chains for generating approximately uniformly distributed points. A series of test runs of the algorithm as a subroutine of a probabilistic LP algorithm are performed on both standard and randomly generated problems. Typically, problems of dimension n approximately equal to 300 are solved optimally within a few minutes on a slow machine. ESA

66 SYSTEMS ANALYSIS

Includes mathematical modeling; network analysis; and operations research.

N92-29973# Universiteit Twente, Enschede (Netherlands). Faculty of Applied Mathematics.
PUZZLES 3 HANOI-VARIATIONS IN DIGRAPHS
F. Goebel Nov. 1991 13 p
(MEMO-1010; ISSN-0169-2690; ETN-92-91757) Avail: CASI HC A03/MF A01

Two variations of the Hanoi puzzle are treated. In both cases, the moves are restricted by prohibiting certain transitions between squares. These restrictions can be indicated by a digraph with the set of pegs or squares as the point set. In the first variation, the digraph is the directed cycle on 3 points. The existence of a solution is proved and the minimum number of moves is determined. In the second variation, the digraph is the acyclic tournament. In this case, a solution exists only if for a given number of disks, the number of squares is sufficiently large. A recurrence for this number is presented and its asymptotic behavior is determined. ESA

N92-30079# Universiteit Twente, Enschede (Netherlands). Faculty of Applied Mathematics.
A SURVEY ON MINIMUM COST SPANNING TREE GAMES
Harry Aarts and Theo Driessen Oct. 1991 41 p
(MEMO-1003; ISSN-0169-2690; ETN-92-91750) Avail: CASI HC A03/MF A01

A survey on known results on Minimum Cost Spanning Tree (MCST) games is presented. These games represent a special class of cooperative games in characteristic function form and arise in certain cost allocation problems in networks. Special attention is paid to the existence and the structure of the core of MCST games. Some extreme points of the core are directly deducible from minimum cost spanning trees in the corresponding network (MCST allocation; weak demand allocation). Some results on the solution concept called the irreducible core are treated. ESA

N92-30138# Los Alamos National Lab., NM.
BURROS: SIMPLE, AFFORDABLE, EFFECTIVE SPACE TRANSPORTATION

G. H. Canavan May 1992 23 p
(Contract W-7405-eng-36)
(DE92-013553; LA-12197-MS) Avail: CASI HC A03/MF A01

This note argues that space is the best place to put not only the sensors, but also the Spare Based Interceptors (SBIs) and Directed-Energy Weapons (DEWs) needed to address long-range, intra- and inter-theater missiles efficiently. There are real threats; they are likely to worsen. Ground-based defenses cannot handle them all affordably. Mixes are generally appropriate. There is a role for SBIs, but it doesn't appear to require all of the capabilities built into the current SBIs at the outset. The SBIs that are needed now could be no more than cheap burros that were amenable to joint development and robust command for the protection of all. Their deployment for Global Protection Against Limited Strikes should not adversely impact the arms control or crisis stability of the strategic balance with the Soviet Union in any rational, concrete calculus, including that used by the Soviet Union. Deployment at low latitudes should give them adequate capability against theater launches but none against Soviet International Ballist Missiles and only marginal, residual impact on Submarine-Launched Ballistics Missiles. They should not either leave hot production capability of anything threatening or provoke untoward responses. We have a hot production line on Chevrolets that would pose more of a threat to the Soviet Union. Their inability to overcome even crude Soviet countermeasures would be an asset in this light. A companion effort could develop the brilliant eyes needed to guide them. A similar logic is possible with DEWs, but they are less developed and hence less at issue. DOE

N92-30139# Los Alamos National Lab., NM.
PHASE-SPACE ESTIMATE OF SATELLITE COVERAGE TIME
G. H. Canavan May 1992 6 p
(Contract W-7405-eng-36)
(DE92-013555; LA-12298-MS) Avail: CASI HC A02/MF A01

This note derives a phase-space estimate of the overlap in satellite coverage and evaluates its impact on the time for a constellation to cover some specified area. The satellites' motion is treated as random in the calculation of the overlaps. Enough passes are prescribed to assure that an adequate probability of observing each area is accumulated. For 0.9-0.99 probabilities of coverage, overlaps increase the time for coverage by factors of 2-4 over no-overlap estimates. This model also gives the probability of different vintages of data. If a given constellation covers the whole Earth in the no-overlap time T(sub 0), the average vintage of the data over the earth will then be the average (T), which is essentially the same as T(sub 0). Overlap over the poles might be wasteful, but overlap in areas of interest by inclined orbits just causes measurements to be more current in areas of interest. DOE

67 THEORETICAL MATHEMATICS

Includes topology and number theory.

No abstracts in this category.

70 PHYSICS (GENERAL)

For precision time and time interval (PTTI) see *35 Instrumentation and Photography;* for geophysics, astrophysics or solar physics see *46 Geophysics, 90 Astrophysics,* or *92 Solar Physics.*

N92-29354# Northwestern Univ., Evanston, IL.
STRUCTURE AND SHEAR RESPONSE OF LIPID MONOLAYERS
P. Dutta and J. B. Ketterson Feb. 1992 7 p
(Contract DE-FG02-84ER-45125)
(DE92-011633; DOE/ER-45125/9) Avail: CASI HC A02/MF A01

We have been studying lipid monolayers both on the surface of water and after transfer to solid substrates. On the surface of water, we have determined in detail the structure of heneicosanoic acid monolayers along a high-pressure isobar, and correlated this information with viscosity data. We have also determined the effect of ions in the subphase on acid monolayer structure (as a function of pH). We have studied capillary waves on monolayer-covered water surfaces, and we find that these monolayers can be quite anisotropic in some phases, so that the monolayer 'pressure' is always a meaningful quantity. Using atomic force microscopy, we have seen 'islands' in Langmuir-Blodgett monolayers without the need for a dye, plus features that are to visible using fluorescence microscopy. DOE

N92-29802# National Inst. of Standards and Technology, Gaithersburg, MD. Precision Engineering Div.
CHALLENGES TO NIST IN DIMENSIONAL METROLOGY: THE IMPACT OF TIGHTENING TOLERANCES IN THE US DISCRETE-PART MANUFACTURING INDUSTRY
D. A. Swyt Jan. 1992 30 p
(PB92-164680; NISTIR-4757) Avail: CASI HC A03/MF A01

The report looks at recent changes in dimensional tolerances in a number of U.S. discrete-parts manufacturing industries and the measurement challenges to the National Institute of Standards and Technology (NIST) they pose. The changes in tolerances have been shown to be part of a long-term trend by which tolerances have been decreasing at the rate of approximately a factor of three every ten years. The report has also shown that whether by the twice-applied Gage-Makers factor-of-ten or Military-Standard factor-of-four relationship of measurement accuracy to manufacturing tolerances, NIST needs to be more accurate than these moving-target tolerances by factors of sixteen to one hundred. Since NIST does not have the current capability to adequately address such needs, it needs to develop new laboratory-based capability in each of the three tolerance regimes: the normal-tolerance regime of metal-cutting machine tools and coordinate measuring machines; the precision-tolerance regime of diamond slicing and advanced interferometers; and the ultraprecision-tolerance regime of scanning tunneling lithography and microscopy. Author

N92-30035# National Inst. of Standards and Technology, Gaithersburg, MD.
PHYSICS LABORATORY TECHNICAL ACTIVITIES, 1991 Final Report
K. B. Gebbie Feb. 1992 181 p Presented at the Board on Assessment of NIST Programs, National Research Council, Washington, DC, 24-25 Feb. 1992
(PB92-172824; NISTIR-4741) Avail: CASI HC A09/MF A02

The report summarizes research projects, measurement method development, calibration and testing, and data evaluation activities that were carried out during calendar year 1991 in the National Institute of Standards and Technology (NIST) Physics Laboratory. These activities fall in the following areas: electron and optical physics; atomic physics; molecular physics; radiometric physics; quantum metrology; ionizing radiation; time and frequency; quantum physics; and fundamental constants. Author

N92-30095# Institut des Hautes Etudes Scientifiques, Bures-sur-Yvette (France).
SWIRLS AND WHEELS
B. Maskit Feb. 1992 37 p
(Grant NSF DMS-90-03361)
(PB92-173251; IHES/M/92/12) Avail: CASI HC A03/MF A01

There are several standard splittings of Kleinian groups using multiple combination theorems; these are the splitting of a function group into basic groups, the more general splitting of an analytically finite group into web groups, and the splitting given by Thurston of a Haken hyperbolic manifold. These splitting all use a finite set of combination theorems, where the order is, in some sense, irrelevant (the first two splittings mentioned above use only one

such set; the Thurston splitting uses a finite sequence of these). A general theory of these finite sets of commuting splittings is built in the context of an arbitrary Kleinian group, and a descriptive language for these splittings is constructed. The point is decomposition rather than construction. One needs to be able to say that a given group could have been built up by using a commuting set of combination theorems, from certain subgroups, without specifying the subgroups. The description is given in terms of a system of swirls and wheels. Swirls are simple closed curves with certain additional properties, and wheels are generalized simple closed curves; these will be described. A system of these is a G-invariant collection, where no element of the system crosses any other element of the system, although they may touch at carefully controlled points. Author

71 ACOUSTICS

Includes sound generation, transmission and attenuation. For noise pollution see *45 Environmental Pollution.*

N92-29346# Woods Hole Oceanographic Inst., MA.
ACOUSTIC SCATTERING FROM ELASTIC ICE: A FINITE DIFFERENCE SOLUTION Ph.D. Thesis
J. Robert Fricke Jun. 1991 277 p
(AD-A248281; WHOI-91-10) Avail: CASI HC A13/MF A03

In this thesis I consider acoustic scattering from Arctic ice. No analytic scattering theories are able to explain the observed low frequency (10-100 Hz) loss measured in long-range propagation experiments. Reasoning that a full-wave solution holds the key, I use the finite difference method to solve the elastodynamic equations. This technique allows arbitrary roughness, unrestricted in slope, displacement, or radius of curvature and provides direct, physical insight into the rough ice scattering mechanism. The underlying partial differential equations treat the air-ice-water complex as a heterogeneous continuum in three dimensions. A plane strain approximation reduces the formation to two dimensions, which limits the computational burden, while permitting the salient features of the scattering process to be studied. Broadband numerical scattering experiments are conducted using two classes of roughness features: ice edges and pressure ridges. Specular loss due to an ice edge is found to be too low to explain the observed scattering loss in the central Arctic. The loss due to a ridge is affected by three phenomena: mass loading, excitation of plate waves, and a material dependent power law. The first two affect the magnitude of the loss, while the last affects the frequency dependence. The observed loss is best explained by scatter from relatively young, large pressure ridges, which are modeled as fluid structures. GRA

N92-29441# Massachusetts Univ., Amherst. Dept. of Mathematics and Statistics.
COMPUTATIONAL ACOUSTICS Final Report, 1 Feb. 1988 - 31 Jan. 1990
Donald F. StMary 8 Feb. 1992 3 p
(Contract N00014-88-K-0264)
(AD-A247688) Avail: CASI HC A01/MF A01

The development of accurate and efficient numerical models for the acoustic propagation problem is discussed. There were five main considerations: (1) long range propagation; (2) short range propagation; (3) one-way outgoing or incoming (no backscatter - PE's); (4) two-way (backscatter - Elliptics); and (5) liquid/solid interface. To model the physical phenomena, we used partial differential equations and modern numerical methods of scientific computing. The following were the main considerations: stability, convergence, accuracy, efficiency, error estimates, well-posedness, and applicability. GRA

N92-29543# Northwestern Univ., Evanston, IL. Dept. of Engineering Science and Applied Mathematics.
ASYMPTOTIC AND NUMERICAL METHODS IN APPLIED WAVE PROPAGATION Final Technical Report
Gregory A. Kriegsmann (New Jersey Inst. of Tech., Newark.) and Edward L. Reiss 31 Dec. 1991 7 p
(Contract N00014-90-J-1746)
(AD-A250227) Avail: CASI HC A02/MF A01

The initial thrust of our research program was to study the propagation of acoustic waves from a time periodic point source in an ocean whose properties vary slowly with range, and which rests on an elastic bottom (whose properties may also vary slowly with range). The motivations for these investigations were to study the propagation of sound in realistic ocean environments and to specifically understand the physics of mode cut-off. In this important situation, it is imperative to know the amount of energy lost to the ocean bottom and the amount converted into the reflected modes. The detailed knowledge of the reflected acoustic wave is important in target acquisition and determination, i.e., in inverse problems. Our research program evolved over the last part of the contract period to address and study certain types of inverse problems which may prove useful in target determination and acquisition. Appendix A contains a bibliography of papers published, submitted for publication, or in preparation that have been supported by this contract. GRA

N92-29588# Virginia Polytechnic Inst. and State Univ., Blacksburg. Dept. of Mechanical Engineering.
ACTIVE STRUCTURAL ACOUSTIC CONTROL AND SMART STRUCTURES Final Technical Report
Chris R. Fuller 1 Sep. 1991 188 p
(Contract N00014-88-K-0721)
(AD-A248341) Avail: CASI HC A09/MF A02

This final technical report for the DARPA/ONR Advanced Submarine Technology (AST) Program concerns recent VPI&SU research in the area of active structural acoustic control with active/adaptive structures. The material is divided into progress in the areas of structural acoustics, actuators, sensors, and control approaches. Due to the coupled nature of the problem, considerable effort throughout the VPI&SU program has been given to the interaction of these areas with each other, and their integration. The focus is analytical. Experimental investigations involve active control of sound radiation from simple panels, as well as panels with some added complexity, using point and distributed control forces and sensors on the plates. The results presented show that significant progress has been made towards controlling structurally radiated noise by active/adaptive means applied directly to the structure. The demonstrated technology is highly applicable to acoustic quieting in advanced submarine designs. GRA

N92-29628# Technische Univ., Delft (Netherlands). Faculty of Technical Mathematics and Informatics.
MATCHED ASYMPTOTIC EXPANSIONS SOLUTION FOR LOW-FREQUENCY SOUND RADIATION FROM FLUID-LOADED, BAFFLED PLATES: AXISYMMETRIC CASE
Christiaan Kauffmann 1991 26 p Presented at 121st Acoustical Society of America Meeting, Baltimore, MD, 29 Apr. - 3 May 1991
(Rept-91-60; ISSN-0922-5641; ETN-92-91424) Copyright Avail: CASI HC A03/MF A01

The method of matched asymptotic expansions is used to investigate sound radiation from fluid loaded, baffled, thin elastic plates of dimensions which are compared to the acoustic wavelength. In this low frequency region both nearfield quantities (plate response and surface pressure) as well as farfield radiation properties are obtained. At low frequencies, the plate radiates sound like a monopole with the strength of it being proportional to the net volume velocity of the plate. By using a structural reciprocity relation, the method is shown to be consistent with respect to power balance up to leading order. The validity of the results is demonstrated by comparison with exact results. ESA

N92-29748# Technische Univ., Delft (Netherlands). Faculty of Technical Mathematics and Informatics.
MATCHED ASYMPTOTIC EXPANSIONS SOLUTION FOR LOW-FREQUENCY SOUND RADIATION FROM FLUID-LOADED, BAFFLED PLATES: TWO-DIMENSIONAL CASE

Christiaan Kauffmann 1991 31 p
(Rept-91-62; ISSN-0922-5641; ETN-92-91426) Copyright Avail: CASI HC A03/MF A01

The method of matched asymptotic expansions is used to investigate sound radiation from fluid loaded, baffled, thin elastic plates of dimensions which are small compared to the acoustic wavelength. In this low frequency region, both nearfield quantities (plate response and surface pressure) as well as farfield radiation properties are obtained. For the two dimensional case, logarithmic gauge functions are introduced into the asymptotic expansions and a restricted matching rule is applied. At low frequencies, the plate radiates sound like a monopole, the strength of it being proportional to the net volume velocity of the plate. By using a structural reciprocity relation, the method is shown to be consistent with respect to power balance up to leading orders. The validity of the results is demonstrated by comparison with exact results. ESA

N92-29814# Southampton Univ. (England). Inst. of Sound and Vibration Research.
REALISTIC MODELS FOR PREDICTING SOUND PROPAGATION IN FLOW DUCT SYSTEMS
P. O. A. L. Davies Dec. 1991 21 p
(ISVR-TR-204; ETN-92-91370) Avail: CASI HC A03/MF A01

Progress in the development of theoretical and experimental methods for studying sound generation and propagation in flow duct systems is reviewed. Relevant physical factors which must be taken into account when adopting the well documented analogy with electrical networks to model the acoustic characteristics of mufflers and silencers are set out. This includes, for example, those circumstances where the necessity to satisfy momentum conversation presents an additional relevant constraint in the formulation of physically realistic acoustic models. The discussion is illustrated by a sequence of practical examples, where the predictions of sound propagation derived with appropriate linearized acoustic models are compared with experimental observations. ESA

N92-29918# Technische Univ., Delft (Netherlands). Faculty of Technical Mathematics and Informatics.
ESTIMATION OF THE INVERSE ACOUSTIC TRANSMISSION OPERATOR OF A HETEROGENEOUS REGION DIRECTLY FROM ITS REFLECTION OPERATOR
Gerard C. Herman 1991 22 p
(Rept-91-36; ISSN-0922-5641; ETN-92-91409) Copyright Avail: CASI HC A03/MF A01

A method for estimating the inverse acoustic transmission operator of a heterogeneous model directly from its reflection operator (without determining the model itself) is discussed. The method can be used for removing certain near surface effects from seismic data and is illustrated with a one dimensional example. ESA

N92-29997# Deutsche Forschungsanstalt fuer Luft- und Raumfahrt, Brunswick (Germany, F.R.). Abteilung Technische Akustik.
JET AIRCRAFT NOISE AT HIGH SUBSONIC FLIGHT MACH NUMBERS [DER LAERM VON STRAHLFLUGZEUGEN BEI HOHEN UNTERSCHALL-FLUGMACHZAHLEN]
Jan Boettcher and Ulf Michel Aug. 1991 94 p In GEORGIAN
(DLR-FB-91-28; ISSN-0939-2963; ETN-92-91733) Avail: CASI HC A05/MF A01; DLR, Wissenschaftlisches Berichtswesen, Postfach 90 60 58, 5000 Cologne, Fed. Republic of Germany, HC

Acoustic overfly measurements are carried out and analyzed to identify the sound sources of the noise development by means of their spectral radiation properties. The extension of existing prediction schemes for the radiation mixing and the broadband shock noise is discussed on the basis of experimental results. Measure and calculation results were compared and a good agreement was found for the time profiles of noise levels, the frequency spectra, and the total sound pressure level as a function of emission angle. The prediction schema could be used to demonstrate the influence of operational parameters and quantify the noise production. It is shown that a decrease in flight Mach number and an increase of flight height cause an important noise reduction. ESA

72 ATOMIC AND MOLECULAR PHYSICS

Includes atomic structure, electron properties, and molecular spectra.

N92-29350# Washington State Univ., Pullman. Dept. of Chemistry.
RARE GAS CLUSTERS CONTAINING CHARGED ATOMS
Isidore Last and Thomas F. George Mar. 1992 58 p
(Contract N00014-90-J-1193)
(AD-A248299; WSU/DC/92-TR-80) Avail: CASI HC A04/MF A01

Three kinds of rare gas (R) containing clusters are considered in this article: (1) ionic clusters Rn+ and (R M)+, M being another atom or a molecule, (2) neutral rare gas-halogen n n clusters R n X with R X electron transfer, and (3) Rydberg excited R n clusters. These clusters have much in common, as all of them contain ions or ionic cores, with the positive charge delocalized mostly between some number of atoms. Such systems can be treated by the semiempirical diatomics-in-ionic-systems (DIIS) method. We present in this article a brief description of the DIIS method and the results of its applications to the kinds of clusters mentioned above. The article also presents discussions of results obtained by other theoretical methods and experimental studies. GRA

N92-29356# Argonne National Lab., IL.
PROSPECTS FOR LONG BASELINE NEUTRINO OSCILLATION EXPERIMENTS
M. Goodman 1991 37 p Presented at the Workshop on Long-Baseline Neutrino Oscillations, Batavia, IL, 17-20 Nov. 1991
(Contract W-31-109-eng-38)
(DE92-011833; ANL-HEP-CP-92-17; CONF-9111141-7) Avail: CASI HC A03/MF A01

Several recent developments have motivated consideration of neutrino experiments located hundreds or thousands of kilometers from an accelerator. The motivations and experimental challenges for such experiments are examined. Three proposals for using the Fermilab Main Injector are compared. The requirements on mass, distance, and resolution for an 'ideal' detector are considered. DOE

N92-29415# Academy of Sciences of the Ukrainian SSR, Kiev. Inst. Teoreticheskoj Fiziki.
ELECTRON SPECTRA OF ADATOMIC STRUCTURES
O. I. Gerasimov and T. Ya. Shvets 1991 17 p
(DE92-625013; ITP-91-6) Avail: CASI HC A03/MF A01

Within the framework of statistical theory of line-shape in electron elastic scattering and high resolution electron energy loss spectroscopy, electronic spectra are studied concerning the problem of the detection of scattering from adatomic complexes and determination of parameters of simple models for the surface structure. DOE

N92-29488# Rutherford Appleton Lab., Chilton (England).
CONTRIBUTIONS TO HADRON 1991: 1) TESTING THE NATURE OF THE F(0)(S ASTERISK). 2) GAMMA GAMMA TO PI(EXP 0) PI(EXP 0): DISPERSIVE ANALYSIS COMPARED TO CHIRAL PERTURBATION THEORY
D. Morgan and M. R. Pennington Oct. 1991 14 p Presented at 4th International Conference on Hadron Spectroscopy, College Park, MD, 12-16 Aug. 1991
(RAL-91-070; ETN-92-91718) Copyright Avail: CASI HC A03/MF A01

A method to distinguish regular quark model partonic compounds from molecular states in a model independent way is presented. Applying the method to existing data, f(0)(S asterisk) is concluded as unlikely to be a molecule. A study showing that the principles of gauge invariance, the Partially Conserved Axial

vector Current hypothesis (PCAC), and requirements of analyticity and unitarity, combined with standard pi pi phase shift information, are sufficient to predict the low energy cross section for gamma gamma to pi(0) pi(0), in agreement with experiment, is presented. For individual titles, see N92-29489 through N92-29490.

N92-29489# Rutherford Appleton Lab., Chilton (England).
TESTING THE NATURE OF THE f(0)(S ASTERISK)
D. Morgan and M. R. Pennington (Durham Univ., England) *In its* Contributions to Hadron 1991: 1) Testing the Nature of the f(0)(S asterisk). 2) Gamma Gamma to Pi(exp 0) Pi(exp 0): Dispersive Analysis Compared to Chiral Perturbation Theory Oct. 1991 p 1-7 (For primary document see N92-29488 20-72)
Copyright Avail: CASI HC A02/MF A01

A way to distinguish regular quark model partonic compounds from molecular states in a model independent way is considered. The issue arises in evaluating the proposed K(bar-K) molecule assignment for f(0)(S asterisk) alias f(0)(975). A method whereby in favorable circumstances the above alternative can be distinguished by objective appeal to data is described. Applying this to existing data, f(0)(S asterisk) is concluded as unlikely to be a molecule. ESA

N92-29490# Rutherford Appleton Lab., Chilton (England).
GAMMA GAMMA TO PI(EXP 0) PI(EXP 0): DISPERSIVE ANALYSIS COMPARED TO CHIRAL PERTURBATION THEORY
D. Morgan and M. R. Pennington (Durham Univ., England) *In its* Contributions to Hadron 1991: 1) Testing the Nature of the f(0)(S asterisk). 2) Gamma Gamma to Pi(exp 0) Pi(exp 0): Dispersive Analysis Compared to Chiral Perturbation Theory Oct. 1991 p 9-12 (For primary document see N92-29488 20-72)
Copyright Avail: CASI HC A01/MF A01

The process gamma gamma to pi pi is strongly constrained by gauge invariance, Partially Conserved Axial vector Current hypothesis (PCAC), and requirements of analyticality and unitarity. Combined with standard pi pi phase shift information, these principles are shown to be sufficient to predict the low energy cross section for gamma gamma to pi(0) pi(0) in agreement with experiment. The failure of the lowest order in chiral perturbation theory, which also makes a specific prediction for this process, to reproduce the detailed cross section is discussed. Future very high precision measurements of gamma gamma to pi(0) pi(0) and gamma gamma to pi(+) pi(-) could contain low energy pi pi parameters appreciably. ESA

N92-29507# Superconducting Super Collider Lab., Dallas, TX.
HYDROGEN DESORPTION AND THE SEARCH FOR THE HIGGS
A. W. Maschke Mar. 1992 3 p Presented at the 5th International Workshop on Desorption Induced by Electronic Transitions, Taos, NM, 1-4 Apr. 1992 Submitted for publication
(Contract DE-AC35-89ER-40486)
(DE92-013464; SSCL-Preprint-86; CONF-9204137-1) Avail: CASI HC A01/MF A01

Two large proton colliding beam projects are now under way, with their main goal being the discovery of the Higgs boson, the key to symmetry breaking in the Standard Model of strong and electroweak interactions. Both the Large Hadron Collider (LHC), to be built in the LEP tunnel at CERN, and the Superconducting Super Collider (SSC) underway in Texas require superconducting magnets; therefore, they can tolerate only very small losses from beam-gas interactions before energy deposition in the magnets becomes prohibitive. Therefore, a very good vacuum is required. The biggest obstacle to achieving good vacuum is photodesorption of hydrogen from synchrotron radiation emitted by the proton beams. DOE

N92-29515# Los Alamos National Lab., NM.
MULTIPHOTON PROCESSES IN SCATTERING AND IONIZATION IN AN INTENSE LINEARLY-POLARIZED RADIATION FIELD
L. A. Collins and G. Csanak (Tsukuba Univ., Ibaraki, Japan) 1992 7 p Presented at the Physics of High Power Laser Matter Interactions, Kyoto (Japan), 9-13 Mar. 1992
(Contract W-7405-eng-36)
(DE92-013546; LA-UR-92-1230; CONF-9203152-1) Avail: CASI HC A02/MF A01

We have employed the Gavrila-Kaminski formulation for the conversion of the time-dependent Schrodinger equation to a set of coupled differential equations that describe the interaction of an electron with a proton in the presence of an intense linearly-polarized radiation field in the Kramers-Henneberger gauge. The differential equations are solved numerically by a linear algebraic prescription effectively applied to electron-molecule collisions. We studied both electron-proton collisions assisted by the laser field and multiphoton ionization of H. In the former, we observed the capture-escape resonances while in the latter, we found evidence of the stabilization mechanism as the intensity reaches 10(exp 18) W/cm(exp 2). DOE

N92-29582# Brookhaven National Lab., Upton, NY.
FREE ION YIELDS IN LIQUIDS: MOLECULAR STRUCTURE AND TRACK EFFECTS
R. Holroyd 1992 10 p Presented at the International Conference on Liquid Radiation Detectors: Their Fundamental Properties and Applications, Tokyo (Japan), 7-10 Apr. 1992
(Contract DE-AC02-76CH-00016)
(DE92-012208; BNL-47420; CONF-920480-1) Avail: CASI HC A02/MF A01

The signal generated in a liquid-filled ionization chamber is proporational to the ions that escape, the free ion yield or G(sub fi). Recent results show how molecular structure, rate of energy loss (dE/dx) and pressure affect G(sub fi) and give further insight into the ionization process in liquids. As a consequence of the passage of high energy charged particles through a liquid, molecules are ionized and excited. The electrons have kinetic energy initially which allow them to travel some distance away from their geminate cations. The electrons may lose energy to vibrational modes but a significant fraction of the separation occurs while the electrons have subvibrational (near thermal) energy. When the electron finally thermalizes it is within the coulombic field of its parent cation and the two ions constitute a geminate pair. The free ion yield is determined by the fraction of geminate pairs which separate to form free ions as against those that recombine to form excited states. DOE

N92-29634# Los Alamos National Lab., NM.
SYNTHESIS AND CHARACTERIZATION OF A COVALENTLY BOUND SELF-ASSEMBLED MACROCYCLE MONOLAYER THIN FILM FOR NONLINEAR OPTICAL MATERIALS
DeQuan Li, B. I. Swanson, J. M. Robinson, and M. A. Hoffbauer 1992 9 p Presented at the Society of Photo-Optical Instrumentation Engineers' International Symposium on Laser Spectroscopy as Part of SPIE's Symposium on Optics, Electro-Optics and Laser Applications in Science and Engineering, Los Angeles, CA, 20-22 Jan. 19
(Contract W-7405-eng-36)
(DE92-011353; LA-UR-92-748; CONF-920124-20) Avail: CASI HC A02/MF A01

Synthesis and characterization of covalently bound self-assembled, 5,10,15,20 Tetra(4-pyridyl) 21H,23H porphine monolayer superlattices on various oxide surfaces such as fused silica, glass or silicon are described. The mono-molecular thin film structures are characterized by UV-visible, lambda (sub max) = 447 nm, and FTIR-ATR spectroscopy. In addition, X-ray photoelectron spectroscopy and secondary ion mass spectroscopy studies are used to confirm the formation of a self-assembled monolayer on the fused-silica surface. Attractive features in these complexes are their second-order nonlinear optical properties, enhanced by the completely delocalized pi-electrons. Second harmonic generation measurements have been used to determine the uniformity of the film, the relative and absolute magnitudes of nonzero elements of the nonlinear susceptibility, chi (exp 2), and the average molecular orientation of the chromophores. DOE

N92-29642# University of Western Michigan, Kalamazoo.
CORRELATED CHARGE-CHANGING ION-ATOM COLLISIONS
J. A. Tanis Apr. 1992 9 p
(Contract DE-FG02-87ER-13778)
(DE92-013473; DOE/ER-13778/5) Avail: CASI HC A02/MF A01

This report summarizes the progress and accomplishments in accelerator atomic physics research supported by DOE grant DE-FG02-87ER13778 from March 16, 1991 through March 15, 1992. This work involves the experimental investigation of fundamental atomic processes in collisions of charged projectiles with neutral targets or electrons, with particular emphasis on two-electron interactions and electron correlation effects. Processes involving combinations of excitation, ionization, and charge transfer are investigated utilizing coincidence techniques in which projectile charge-changing events are associated with x-ray emission, target recoil ions, or electron emission. New results have been obtained for studies involving (1) resonant recombination of atomic ions, (2) double ionization of helium, and (3) continuum electron emission. Experiments were conducted using accelerators at the Lawrence Berkeley Laboratory, Argonne National Laboratory, Michigan State University, Western Michigan University, and the Institute of Nuclear Research, Debrecen, Hungary. Brief summaries of work completed and work in progress are given in this report. DOE

N92-29715# Stockholm Univ. (Sweden). Dept. of Physics.
EXPLORATORY STUDY FOR A SOLID-STATE CHARGED-PARTICLE SPECTROMETER INSIDE THE CELSIUS RING: ALPHA AND HYDROGEN REACTIONS AT 1.7 AND 2.2 GeV/c
C. Bargholtz, K. Fransson, L. Holmberg, K. Lindh, L. Sandberg, P.-E. Tegner, P. Thoerngren-Engblom, and D. Vojdani Aug. 1991 31 p Sponsored by Swedish Natural Research Council
(USIP-91-02; ETN-92-91508) Avail: CASI HC A03/MF A01

Charged particles emitted in the extreme forward direction can be detected in a particle telescope mounted inside the Celsius ring in one of the dipole magnets following the target. Results of a test with a plastic scintillator telescope for alpha + H reactions at 1.7 and 2.2 GeV/c are reported. The purpose of the experiment was to learn about possible problems such as background and bursts of high count rates at the intended position of the forward spectrometer. The experiment and the equipment used are described. ESA

N92-29750# Nationaal Inst. voor Kernfysica en Hoge Energiefysica, Amsterdam (Netherlands).
THE O(ALPHA(s) CUBED) QCD CORRECTION TO THE LOWEST MOMENT OF THE LONGITUDINAL STRUCTURE FUNCTION IN DEEP INELASTIC ELECTRON-NUCLEON SCATTERING
S. A. Larin (Academy of Sciences, USSR, Moscow), F. V. Tkachov (Fermi National Accelerator Lab., Batavia, IL.), and J. A. M. Vermaseren 1991 9 p Sponsored in part by Natural Sciences and Engineering Research Council and Quebec Committee of Education
(NIKHEF-H/91-19; ETN-92-91617) Avail: CASI HC A02/MF A01

The analytic leading twist three loop perturbative QCD (Quantum-Chromo-Dynamic) correction to the moment integral upper limit 1, lower limit 0, dx F(L)(sup p-n) (x, Q squared) of the nonsinglet longitudinal structure function F(L) of the deep inelastic electron-nucleon scattering is presented. It provides quantitative information on uncertainties of pQCD predictions for R(x, Q squared) = sigma (L)/sigma(T). ESA

N92-29751# Nationaal Inst. voor Kernfysica en Hoge Energiefysica, Amsterdam (Netherlands).
CLASSICAL ASPECTS OF WEAK INTERACTIONS
F. R. Klinkhamer Oct. 1991 11 p Presented at the EPS Conference on Hadronic Structure and Electroweak Interactions, Amsterdam, Netherlands, 5-10 Aug. 1991 Submitted for publication Sponsored by Royal Netherlands Academy of Arts and Sciences
(NIKHEF-H/91-25; ETN-92-91623) Avail: CASI HC A03/MF A01

The classical physics of the electroweak standard model and its possible implications for cosmology and future particle collider experiments are discussed. It was seen that the classical field theory of electroweak interactions has an energy scale set by the sphaleron Es = O(Mw/alpha(weak)). Up till now small fluctuations around the vacuum at energies approximately alpha(weak)Es were probed. Under extreme conditions the nontrivial structure of configuration space may become important. An example of this may be anamalous B + h violation on an early epoch of the hot big bang. Whether or not similar conditions could be created in high energy particle colliders remains to be seen. ESA

N92-29777# Technische Univ., Eindhoven (Netherlands).
DIFFUSION AND PHASE RELATIONS IN THE SYSTEMS Ti-Si-C AND Ti-Si-N Ph.D. Thesis
Wilhelmus Jacobus Jo Wakelkamp 1991 126 p Sponsored by Netherlands Foundation for Chemical Research and Netherlands Organization for Applied Scientific Research TNO
(ETN-92-91631) Avail: CASI HC A07/MF A02

The interaction between titanium and the ceramics silicon carbide or silicon nitride is addressed. A literature review of the subject is given, all binary and ternary systems involved are treated, and some properties of the materials of interest are shown. Facts about the diffusion in these systems are given. The relation between thermodynamics and phase diagrams is explained. For some applications, phase diagrams are shown to be representable in more useful forms than the usually known form in which the temperature is plotted versus the mole fraction of one of the compounds. The selection of the proper thermodynamic data is shown to be important and difficult, and the solution of this problem is shown. A model developed in literature to predict the layer sequence between two materials in a diffusion couple in a ternary system is extended with regard to the formation of a ternary compound. Attempts are made to confirm this model experimentally. The conditions under which the experiments and analysis are performed are summarized. The results of respectively the Ti-Si-C and the Ti-Si-N systems where the phase equilibria and the diffusion processes were studied, are given. ESA

N92-29778# Technische Univ., Eindhoven (Netherlands).
ORIENTED STRUCTURES BASED ON TRANS-1,4-POLYBUTADIENE Ph.D. Thesis
Yvonne Maria Theodor Tervoort-Engelen 1991 136 p
(ETN-92-91632) Avail: CASI HC A07/MF A02

Oriented structures based on trans 1,4 polybutadiene (t-1,4-PB) are explored in view of the enhancement of intermolecular interactions in fibrous systems. The deformation behavior and properties of both melt and solution crystallized t-1,4-PB films are presented and crosslinking of the oriented structures is discussed. The solution blending of t-1,4-PB and UHMW-PE, and the resulting morphology of the solution crystallized blends as a function of t-1,4-PBN content, are described. Drawing of the solution crystallized blends and the resulting fiber properties, in relation to the fiber morphology, is discussed. The network formation by electron beam irradiation in drawn UHMW-PE/t-1,4-Pb blends is discussed. Results are interpreted in view of the study objective. Some aspects of the morphology of nascent UHMW-PE reactor powders are discussed, focusing on the question of whether chain extended or chain folded crystals prevail in these samples. ESA

N92-29899# Massachusetts Univ., Amherst. Dept. of Chemistry.
THEORY OF THE DISSOCIATION DYNAMICS OF SMALL MOLECULES ON METAL SURFACES: FINITE TEMPERATURE STUDIES
B. E. Jackson Feb. 1992 6 p
(Contract DE-FG02-87ER-13744)
(DE92-011188; DOE/ER-13744/12) Avail: CASI HC A02/MF A01

The goal of this study is to gain a better understanding of

metal-catalyzed reactions via a detailed examination of the dynamics of molecule-metal interactions. Much effort has focused on treating the molecule as quantum mechanically as possible, and including the effects of finite surface temperature. Recently developed time dependent quantum techniques have been used to compute the dissociative sticking probability of H2 on various metal surfaces. All molecular degrees of freedom are included either quantum mechanically or classically. The dependence upon translational and internal molecular energy, the angle and site of the surface impact, and the details of the molecule-metal interaction potential were examined. Similar techniques have been used to study the Eley-Rideal mechanism for the recombinative desorption of adsorbed H atoms with gas phase H atoms. Extremely accurate methods for coupling the molecule to the thermal vibrations of the solid have been developed. They are being used in a general study of sticking, as well as to examine the trapping of H2 and other diatomics in weakly bound molecular precursors to dissociative adsorption. DOE

N92-29910# Oak Ridge National Lab., TN.
PROCEEDINGS OF THE THIRD CONFERENCE ON RADIATION PROTECTION AND DOSIMETRY
R. E. Swaja, ed., C. S. Sims, ed., and W. H. Casson, ed. Oct. 1991 169 p Presented at the Third Conference on Radiation Protection and Dosimetry, Orlando, FL, 21-24 Oct. 1991
(Contract DE-AC05-84OR-21400)
(DE92-011502; ORNL/TM-11882; CONF-911004) Avail: CASI HC A08/MF A02

The Third Conference on Radiation Protection and Dosimetry was held during October 21-24, 1991, at the Sheraton Plaza Hotel in Orlando, Florida. This meeting was designed with the objectives of promoting communication among applied, research, regulatory, and standards personnel involved in radiation protection, and providing them with sufficient information to evaluate their programs. To meet these objectives, a technical program consisting of more than 75 invited and contributed oral presentations encompassing all aspects of radiation protection was prepared. General topics considered in the technical session included external dosimetry, internal dosimetry, instruments, accident dosimetry, regulations and standards, research advances, and applied program experience. In addition, special sessions were held to afford attendees the opportunity to make short presentations of recent work or to discuss topics of general interest. Individual reports are processed separately on the database. DOE

N92-30001*# Rider Coll., Lawrenceville, NJ. Dept. of Physics.
[ELECTROMAGNETIC PROCESSES IN NUCLEUS-NUCLEUS COLLISIONS RELATING TO SPACE RADIATION RESEARCH] Final Report, 1990-1992
John W. Norbury 1992 244 p
(Grant NAG1-1134)
(NASA-CR-190533; NAS 1.26:190533) Avail: CASI HC A11/MF A03

Most of the papers within this report deal with electromagnetic processes in nucleus-nucleus collisions which are of concern in the space radiation program. In particular, the removal of one and two nucleons via both electromagnetic and strong interaction processes has been extensively investigated. The theory of relativistic Coulomb fission has also been developed. Several papers on quark models also appear. Finally, note that the theoretical methods developed in this work have been directly applied to the task of radiation protection of astronauts. This has been done by parameterizing the theoretical formalism in such a fashion that it can be used in cosmic ray transport codes. For individual titles, see N92-30002 through N92-30015.

N92-30002*# Rider Coll., Lawrenceville, NJ. Dept. of Physics.
CROSS SECTION PARAMETERIZATIONS FOR COSMIC RAY NUCLEI. 1: SINGLE NUCLEON REMOVAL **c93**
John W. Norbury and Lawrence W. Townsend (National Aeronautics and Space Administration. Langley Research Center, Hampton, VA.) *In its* Electromagnetic Processes in Nucleus-Nucleus Collisions Relating to Space Radiation Research 1992 24 p (For primary document see N92-30001 20-72)
(Grant NAG1-1134)
Avail: CASI HC A03/MF A03

Parameterizations of single nucleon removal from electromagnetic and strong interactions of cosmic rays with nuclei are presented. These parameterizations are based upon the most accurate theoretical calculations available to date. They should be very suitable for use in cosmic ray propagation through interstellar space, the Earth's atmosphere, lunar samples, meteorites, spacecraft walls and lunar and martian habitats.
Author

N92-30003*# Rider Coll., Lawrenceville, NJ. Dept. of Physics.
SOLUTION OF TWO-BODY RELATIVISTIC BOUND STATE EQUATIONS WITH CONFINING PLUS COULOMB INTERACTIONS
Khin Maung Maung (Hampton Inst., VA.), David E. Kahana (Continuous Electron Beam Accelerator Facility, Newport New, VA.), and John W. Norbury *In its* Electromagnetic Processes in Nucleus-Nucleus Collisions Relating to Space Radiation Research 1992 25 p (For primary document see N92-30001 20-72)
(Grant NAG1-1134)
Avail: CASI HC A03/MF A03

Studies of meson spectroscopy have often employed a nonrelativistic Coulomb plus Linear Confining potential in position space. However, because the quarks in mesons move at an appreciable fraction of the speed of light, it is necessary to use a relativistic treatment of the bound state problem. Such a treatment is most easily carried out in momentum space. However, the position space Linear and Coulomb potentials lead to singular kernels in momentum space. Using a subtraction procedure we show how to remove these singularities exactly and thereby solve the Schroedinger equation in momentum space for all partial waves. Furthermore, we generalize the Linear and Coulomb potentials to relativistic kernels in four dimensional momentum space. Again we use a subtraction procedure to remove the relativistic singularities exactly for all partial waves. This enables us to solve three dimensional reductions of the Bethe-Salpeter equation. We solve six such equations for Coulomb plus Confining interactions for all partial waves. Author

N92-30004*# Rider Coll., Lawrenceville, NJ. Dept. of Physics.
DO RECENT OBSERVATIONS OF VERY LARGE ELECTROMAGNETIC DISSOCIATION CROSS SECTIONS SIGNIFY A TRANSITION TOWARDS NON-PERTURBATIVE QED? **c32**
John W. Norbury *In its* Electromagnetic Processes in Nucleus-Nucleus Collisions Relating to Space Radiation Research 1992 15 p (For primary document see N92-30001 20-72)
(Grant NAG1-1134)
Avail: CASI HC A03/MF A03

The very large electromagnetic dissociation (EMD) cross section recently observed by Hill, Wohn, Schwellenbach, and Smith do not agree with Weizsacker-Williams (WW) theory or any simple modification thereof. Calculations are presented for the reaction probabilities for this experiment and the entire single and double nucleon removal EMD data set. It is found that for those few reactions where theory and experiment disagree, the probabilities are exceptionally large. This indicates that WW theory is not valid for these reactions and that one must consider higher order corrections and perhaps even a non-perturbative approach to quantum electrodynamics (QED). Author

N92-30005*# Rider Coll., Lawrenceville, NJ. Dept. of Physics.
EFFECTS OF RETARDATION IN RELATIVISTIC EQUATIONS WITH CONFINING INTERACTION **c77**
Khin Maung Maung (Hampton Inst., VA.), David E. Kahana (Continuous Electron Beam Accelerator Facility, Newport New, VA.), and John W. Norbury *In its* Electromagnetic Processes in Nucleus-Nucleus Collisions Relating to Space Radiation Research 1992 6 p (For primary document see N92-30001 20-72)
(Grants NAG1-477; NAG1-1134)
Avail: CASI HC A02/MF A03

A method has been developed for solving two body relativistic bound state equations in momentum space with a confining interaction. A total of six different three dimensional reductions of the Bethe-Salpeter equations are studied with particular emphasis placed on the competing roles of relativistic kinematics and retardation. The results indicate that these two effects counteract each other and this sheds some light on why nonrelativistic models of meson spectroscopy have been quite successful. Author

N92-30006*# Rider Coll., Lawrenceville, NJ. Dept. of Physics.
TWO NEUTRON REMOVAL IN RELATIVISTIC NUCLEUS-NUCLEUS REACTIONS
John W. Norbury *In its* Electromagnetic Processes in Nucleus-Nucleus Collisions Relating to Space Radiation Research 1992 3 p Repr. from the American Physical Society, Physical Review C, v. 45, no. 6, Jun. 1992 p 3024-3026 (For primary document see N92-30001 20-72)
(Grant NAG1-1134)
Avail: CASI HC A01/MF A03

Significant discrepancies between theory and experiment have previously been noted for double neutron removal via electromagnetic processes in relativistic nucleus-nucleus collisions. The present work examines the cause of these discrepancies and systematically investigates whether the problem might be due to electromagnetic theory, nuclear contributions, or an underestimate of experimental error. Using cross section systematics from other reactions it is found that the discrepancies can be resolved in a plausible manner. Author

N92-30007*# Rider Coll., Lawrenceville, NJ. Dept. of Physics.
CONFINING POTENTIAL IN MOMENTUM SPACE
John W. Norbury, David E. Kahana (Continuous Electron Beam Accelerator Facility, Newport New, VA.), and Khin Maung Maung (Hampton Inst., VA.) *In its* Electromagnetic Processes in Nucleus-Nucleus Collisions Relating to Space Radiation Research 1992 4 p Sponsored in part by DOE (For primary document see N92-30001 20-72)
(Grants NAG1-477; NAG1-1134)
Avail: CASI HC A01/MF A03

A method is presented for the solution in momentum space of the bound state problem with a linear potential in r space. The potential is unbounded at large r leading to a singularity at small q. The singularity is integrable, when regulated by exponentially screening the r-space potential, and is removed by a subtraction technique. The limit of zero screening is taken analytically, and the numerical solution of the subtracted integral equation gives eigenvalues and wave functions in good agreement with position space calculations. Author

N92-30008*# Rider Coll., Lawrenceville, NJ. Dept. of Physics.
RELATIVISTIC COULOMB FISSION
John W. Norbury *In its* Electromagnetic Processes in Nucleus-Nucleus Collisions Relating to Space Radiation Research 1992 3 p Repr. from the American Physical Society, Physical Review C, v. 43, no. 2, Feb. 1991 p R368-R370 (For primary document see N92-30001 20-72)
(Grant NAG1-1134)
Avail: CASI HC A01/MF A03

Nuclear fission reactions induced by the electromagnetic field of relativistic nuclei are studied for energies relevant to present and future relativistic heavy ion accelerators. Cross sections are calculated for U-238 and Pu-239 fission induced by C-12, Si-28, Au-197, and U-238 projectiles. It is found that some of the cross sections can exceed 10 b. Author

N92-30009*# Rider Coll., Lawrenceville, NJ. Dept. of Physics.
HIGGS-BOSON PRODUCTION IN NUCLEUS-NUCLEUS COLLISIONS
John W. Norbury *In its* Electromagnetic Processes in Nucleus-Nucleus Collisions Relating to Space Radiation Research 1992 3 p Repr. from the American Physical Society, Physical Review D, v. 42, no. 11, 1 Dec. 1990 p 3696-3698 (For primary document see N92-30001 20-72)
(Grant NAG1-1134)
Avail: CASI HC A01/MF A03

Cross section calculations are presented for the production of intermediate-mass Higgs bosons produced in ultrarelativistic nucleus-nucleus collisions via two photon fusion. The calculations are performed in position space using Baur's method for folding together the Weizsacker-Williams virtual-photon spectra of the two colliding nuclei. It is found that two photon fusion in nucleus-nucleus collisions is a plausible way of finding intermediate-mass Higgs bosons at the Superconducting Super Collider or the CERN Large Hadron Collider. Author

N92-30010*# Rider Coll., Lawrenceville, NJ. Dept. of Physics.
CHARGE DEPENDENCE AND ELECTRIC QUADRUPOLE EFFECTS ON SINGLE-NUCLEON REMOVAL IN RELATIVISTIC AND INTERMEDIATE ENERGY NUCLEAR COLLISIONS
John W. Norbury *In its* Electromagnetic Processes in Nucleus-Nucleus Collisions Relating to Space Radiation Research 1992 4 p Repr. from the American Physical Society, Physical Review C, v. 42, no. 5, Nov. 1990 p 2259-2262 (For primary document see N92-30001 20-72)
(Grant NAG1-1134)
Avail: CASI HC A01/MF A03

Single nucleon removal in relativistic and intermediate energy nucleus-nucleus collisions is studied using a generalization of Weizsacker-Williams theory that treats each electromagnetic multipole separately. Calculations are presented for electric dipole and quadrupole excitations and incorporate a realistic minimum impact parameter, Coulomb recoil corrections, and the uncertainties in the input photonuclear data. Discrepancies are discussed. The maximum quadrupole effect to be observed in future experiments is estimated and also an analysis of the charge dependence of the electromagnetic cross sections down to energies as low as 100 MeV/nucleon is made. Author

N92-30011*# National Aeronautics and Space Administration. Langley Research Center, Hampton, VA.
SINGLE NUCLEON EMISSION IN RELATIVISTIC NUCLEUS-NUCLEUS REACTIONS
John W. Norbury (Rider Coll., Lawrenceville, NJ.) and Lawrence W. Townsend *In* Rider Coll., Electromagnetic Processes in Nucleus-Nucleus Collisions Relating to Space Radiation Research 1992 3 p Repr. from the American Physical Society, Physical Review C, v. 42, no. 4, Oct. 1990 p 1775-1777 (For primary document see N92-30001 20-72)
(Grant NAG1-1134)
Avail: CASI HC A01/MF A03

Significant discrepancies between theory and experiment have previously been noted for nucleon emission via electromagnetic processes in relativistic nucleus-nucleus collisions. The present work investigates the hypothesis that these discrepancies have arisen due to uncertainties about how to deduce the experimental electromagnetic cross section from the total measured cross section. An optical-model calculation of single neutron removal is added to electromagnetic cross sections and compared to the total experimental cross sections. Good agreement is found thereby resolving some of the earlier noted discrepancies. A detailed comparison to the recent work of Benesh, Cook, and Vary is made for both the impact parameter and the nuclear cross section. Good agreement is obtained giving an independent confirmation of the parameterized formulas developed by those authors.
Author

N92-30012*# Rider Coll., Lawrenceville, NJ. Dept. of Physics.
STOPPING POWERS AND CROSS SECTIONS DUE TO TWO-PHOTON PROCESSES IN RELATIVISTIC NUCLEUS-NUCLEUS COLLISION
Wang K. Cheung and John W. Norbury *In its* Electromagnetic Processes in Nucleus-Nucleus Collisions Relating to Space Radiation Research 1992 59 p (For primary document see N92-30001 20-72)
Avail: CASI HC A04/MF A03

The radiation dose received from high energy galactic cosmic rays (GCR) is a limiting factor in the design of long duration space flights and the building of lunar and martian habitats. It is of vital importance to have an accurate understanding of the interactions of GCR in order to assess the radiation environment that the astronauts will be exposed to. Although previous studies have concentrated on the strong interaction process in GCR, there are also very large effects due to electromagnetic (EM) interactions. In this report we describe our first efforts at understanding these EM production processes due to two-photon collisions. More specifically, we shall consider particle production processes in relativistic heavy ion collisions (RHICs) through two-photon exchange. Author

N92-30013*# Rider Coll., Lawrenceville, NJ. Dept. of Physics.
AN INTRODUCTION TO USING THE FORTRAN PROGRAMS PROVIDED WITH COMPUTATIONAL NUCLEAR PHYSICS 1 NUCLEAR STRUCTURE
Matthew A. Boytos and John W. Norbury *In its* Electromagnetic Processes in Nucleus-Nucleus Collisions Relating to Space Radiation Research 1992 18 p Repr. from Computational Nuclear Physics 1 Nuclear Structure, Springer-Varlag, Berlin, Fed. Republic of Germany, 1991 (For primary document see N92-30001 20-72)
Avail: CASI HC A03/MF A03

The authors of this paper have provided a set of ready-to-run FORTRAN programs that should be useful in the field of theoretical nuclear physics. The purpose of this document is to provide a simple synopsis of the programs and their use. A separate section is devoted to each program set and includes: abstract; files; compiling, linking, and running; obtaining results; and a tutorial. H.A.

N92-30014*# Brookhaven National Lab., Upton, NY.
FOURTH WORKSHOP ON EXPERIMENTS AND DETECTORS FOR A RELATIVISTIC HEAVY ION COLLIDER c73
M. Fatyga, ed. and B. Moskowitz, ed. *In* Rider Coll., Electromagnetic Processes in Nucleus-Nucleus Collisions Relating to Space Radiation Research 1992 24 p Workshop held in Upton, NY, 2-7 Jul. 1990 (For primary document see N92-30001 20-72)
(BNL-52262; DOE/OSTI-4500-R75) Avail: CASI HC A03/MF A03

We present a description of an experiment which can be used to search for effects of strong electromagnetic fields on the production of e(sup +) e(sup -) pairs in the elastic scattering of two heavy ions at the Relativistic Heavy Ion Collider (RHIC). A very brief discussion of other possible studies of electromagnetic phenomena at RHIC is also presented. Author

N92-30015*# Rider Coll., Lawrenceville, NJ. Dept. of Physics.
A LETTER OF INTENT FOR AN EXPERIMENT TO STUDY STRONG ELECTROMAGNETIC FIELDS AT RHIC VIA MULTIPLE ELECTROMAGNETIC PROCESSES c32
M. Fatyga (Brookhaven National Lab., Upton, NY.) and John W. Norbury *In its* Electromagnetic Processes in Nucleus-Nucleus Collisions Relating to Space Radiation Research 1992 31 p (For primary document see N92-30001 20-72)
Avail: CASI HC A03/MF A03

An experimental program at the Relativistic Heavy Ion Collider (RHIC) which is designed to study nonperturbative aspects of electrodynamics is outlined. Additional possibilities for new studies of electrodynamics via multiple electromagnetic processes are also described. Author

N92-30213# Australian National Univ., Canberra. Research School of Physical Sciences.
SPECTROSCOPY OF W-183; MEASURED MAGNETIC MOMENTS AND ROTATION-PARTICLE COUPLING
G. J. Lampard, H. H. Bolotin (Melbourne Univ., Parkville, Australia), and A. E. Stuchbery Sep. 1991 36 p Submitted for publication
(DE92-624790; ANU-P-1092) Avail: CASI HC A03/MF A01

The gyromagnetic ratios of 6 excited levels in the lowest K = 1/2 and 3/2 bands of W-183 were measured using the thin-foil transient-field technique. The level scheme was extended to spin 17/2(sup -) and multipole mixing ratios measured for several transitions. Detailed comparisons of the spectroscopic data on W-183 with the rotation-particle coupling model show good agreement, but favor a Coriolis mixing strength much larger than predicted by previous Nilsson model calculations in which hexadecapole deformation was neglected. DOE

73 NUCLEAR AND HIGH-ENERGY PHYSICS

Includes elementary and nuclear particles; and reactor theory.

For space radiation see *93 Space Radiation.*

N92-29457# EG and G Energy Measurements, Inc., Las Vegas, NV.
HIGH INTENSITY SOURCE LABORATORY (HISL)
15 Jan. 1992 29 p
(Contract DE-AC08-88NV-10617)
(DE92-011173; EGG-10617-1199) Avail: CASI HC A03/MF A01

The High Intensity Source Laboratory (HISL) is a laboratory facility operated for the US Department of Energy (DOE) by EG&G, Energy Measurements (EG&G/EM). This document is intended as an overview -- primarily for external users -- of the general purposes and capabilities of HISL; numerous technical details are beyond its scope. Moreover, systems at HISL are added, deleted, and modified to suit current needs, and upgraded with continuing development. Consequently, interested parties are invited to contact the HISL manager for detailed, current, technical, and administrative information. The HISL develops and operates pulsed radiation sources with energies, intensities, and pulse widths appropriate for several applications. Principal among these are development, characterization, and calibration of various high-bandwidth radiation detectors and diagnostic systems. Hardness/vulnerability of electronic or other sensitive components to radiation is also tested. In this connection, source development generally focuses on attending (1) the highest possible intensities with (2) reasonably short pulse widths, and (3) comprehensive output characterization. DOE

N92-29477# Brookhaven National Lab., Upton, NY.
LONGITUDINAL BUNCH PROFILE MEASUREMENTS WITH STRIPLINES
S. L. Kramer 1992 3 p Presented at the 3rd European Particle Accelerator Conference, Berlin (Germany), 24-28 Mar. 1992
(Contract DE-AC02-76CH-00016)
(DE92-013035; BNL-47378; CONF-920315-28) Avail: CASI HC A01/MF A01

Striplines beam position monitors are normally considered low frequency devices with at best an octave bandwidth. Some attempts to make them very high frequency and broadband have led to long and complicated tapered construction. However, conventional uniform coupling striplines can provide very high frequency and broadband response, if the downstream induced signal is gated out electronically. In this case, the leading edge beam signal can provide bunch length and even current profile information for bunch lengths shorter than the length of the stripline. Recent improvement in transient digitizers have made these measurements possible for accelerator operations. Measurements of bunch lengths down to 50 psec are presented. Improvements to striplines and measurement systems are discussed, that could lead to bunch length resolutions approx. 10 psec. DOE

N92-29502# EG and G Energy Measurements, Inc., Las Vegas, NV.
THE 20 ELEMENT HgI2 ENERGY DISPERSIVE X RAY ARRAY DETECTOR SYSTEM

J. A. Iwanczyk (XSIRIUS Scientific, Inc., Marina Del Ray, CA.), N. Dorri (XSIRIUS Scientific, Inc., Marina Del Ray, CA.), M. Wang (XSIRIUS Scientific, Inc., Marina Del Ray, CA.), R. W. Szczebiot (XSIRIUS Scientific, Inc., Marina Del Ray, CA.), A. J. Dabrowski (XSIRIUS Scientific, Inc., Marina Del Ray, CA.), B. Hedman (Stanford Univ., CA.), K. O. Hodgson (Stanford Univ., CA.), and B. E. Patt (EG and G Energy Measurements, Inc., Goleta, CA.) 1991 5 p Presented at the IEEE Nuclear Science Symposium, Santa Fe, NM, 5-9 Nov. 1991
(Contract DE-AC08-88NV-10617)
(DE92-013356; EGG-10617-2135; CONF-911106-94) Avail: CASI HC A01/MF A01

This paper describes recent progress in the development of HgI2 energy dispersive x-ray detector arrays and associated miniaturized processing electronics for synchrotron radiation research applications. The experimental results with a 20 element array detector were obtained under realistic synchrotron beam conditions at SSRL. An energy resolution of 250 eV (FWHM) at 5.9 keV (Mn-K(sub a)) was achieved. Energy resolution and throughput measurements versus input count rate and energy of incoming radiation have been measured. Extended X-ray Absorption Fine Structure (EXAFS) spectra were taken from diluted samples simulating proteins with nickel. DOE

N92-29532# Oregon Univ., Eugene.
THEORY OF ELEMENTARY PARTICLES STUDIES IN WEAK INTERACTION AND GRAND UNIFICATION AND STUDIES IN ACCELERATOR DESIGN
1991 16 p
(Contract DE-FG06-85ER-40224)
(DE92-014309; DOE/ER-40224/185) Avail: CASI HC A03/MF A01

This report discusses research in high energy physics on the following topics: rare b decays; flavor changing top decays; neutrino physics; standard model; cp violation; heavy ion collisions; electron-positron interactions; electron-hadron interactions; hadron-hadron interactions; deep inelastic scattering; and grand unified models. DOE

N92-29788# Stanford Linear Accelerator Center, CA.
TRANSVERSE WAKEFIELDS AT HIGH DISPERSION
F. J. Decker Mar. 1992 4 p Presented at the 3rd European Particle Accelerator Conference, Berlin, Germany, 24-28 Mar. 1992
(Contract DE-AC03-76SF-00515)
(DE92-010752; SU-SLAC-PUB-5784; CONF-920315-4) Avail: CASI HC A01/MF A01

In high energy linear colliders, the transverse beam emittance has to be preserved in order to achieve small interaction spots. If the beam is off-center in an accelerating cavity, it excites transverse wakefields, mainly the dipole mode, which deflects the tail of the beam leading to an emittance growth. In a high dispersive region, even a well centered beam can excite wakefields of higher order modes since the energy spread of the beam causes a transverse beam size which is comparable with the beam pipe. During the bunch length compression in the ring-to-linac (RTL) section of the Stanford Linear Collider (SLC), the beam pipe of 75 mm diameter is practically filled in the horizontal plane. Especially, if beam losses start to be involved, the very outer parts of the beam excite wakefields at any pipe irregularities like bellows, diameter steps, etc. Measured evidences, theoretical estimates, and comparisons to other effects, like higher order magnet optics, are presented. DOE

N92-29938# Westinghouse Hanford Co., Richland, WA.
SP-100 W/Re THERMOCOUPLE CALIBRATION TECHNIQUES
N. S. Cannon and R. C. Knight Jan. 1992 9 p Presented at the 7th International Symposium on Temperature: Its Measurement and Control in Science and Industry, Toronto, Ontario, 28 Apr. - 1 May 1992
(Contract DE-AC06-87RL-10930)
(DE92-011302; WHC-SA-1258; CONF-920423-3) Avail: CASI HC A02/MF A01

The accuracy requirement of the SP-100 Temperature Sensor Program for the reference tungsten/rhenium metal-sheathed thermocouple sensor is +/- 1.4 percent of the reading (in Kelvin) at space reactor operating temperature (nominally 1375 K) over the operating life of the reactor. This is a stringent requirement considering that the as-fabricated base wire 'limits of error' are generally specified at roughly +/- 1.0 percent for exposure temperatures above 700 K. Although the thermocouples will be located out of the reactor's neutron field so that irradiation decalibration is expected to be negligible, thermal exposure effects will probably cause the thermocouple to drift out of specification during the 10-yr reactor operating life. A plan to accurately quantify thermocouple drift with aging time, and provide on-board calibration for the sensor is described. DOE

N92-30014*# Brookhaven National Lab., Upton, NY.
FOURTH WORKSHOP ON EXPERIMENTS AND DETECTORS FOR A RELATIVISTIC HEAVY ION COLLIDER
M. Fatyga, ed. and B. Moskowitz, ed. *In* Rider Coll., Electromagnetic Processes in Nucleus-Nucleus Collisions Relating to Space Radiation Research 1992 24 p Workshop held in Upton, NY, 2-7 Jul. 1990 (For primary document see N92-30001 20-72)
(BNL-52262; DOE/OSTI-4500-R75) Avail: CASI HC A03/MF A03

74 OPTICS

Includes light phenomena; and optical devices.
For lasers see *36 Lasers and Masers.*

N92-29331*# Virginia Polytechnic Inst. and State Univ., Blacksburg. Dept. of Electrical Engineering.
MICRO-DEVICE FOR COUPLING, MULTIPLEXING AND DEMULTIPLEXING USING ELLIPTICAL-CORE TWO-MODE FIBER
A. Wang, K. A. Murphy, G. Z. Wang, A. M. Vengsarkar (Bell Telephone Labs., Inc., Murray Hill, NJ.), and R. O. Claus 1990 6 p
(Grant NAG1-1348)
(NASA-CR-190496; NAS 1.26:190496) Avail: CASI HC A02/MF A01

We propose and demonstrate experimentally a fiber optic micro-device that is capable of tunably splitting, multiplexing, and demultiplexing optical signals using elliptical-core two-mode optical fiber. A crosstalk of 15 dB with an insertion loss of 1.2 dB was obtained. Author

N92-29337# Lawrence Livermore National Lab., CA.
NEAR-VISIBLE RAMAN INSTRUMENTATION FOR REMOTE MULTI-POINT PROCESS MONITORING USING OPTICAL FIBERS AND OPTICAL MULTIPLEXING
T. M. Vess and S. M. Angel Mar. 1992 8 p Presented at the Soc. of Photo-Optical Instrumentation Engineers' International Symposium on Laser Spectroscopy as Part of SPIE's Symposium on Optics, Electro-Optics and Laser Applications in Science and Engineering, Los Angeles, CA, 20-24 Jan. 1992
(Contract W-7405-eng-48)
(DE92-011287; UCRL-JC-109754; CONF-920124-22) Avail: CASI HC A02/MF A01

A portable Raman instrument is presented which measures spectra simultaneously from 10 separate fiber-optic probes. The instrument is being developed for a number of applications including multi-point process monitoring and characterizing mixed waste tanks. DOE

N92-29475# Brookhaven National Lab., Upton, NY.
TRANSITION CROSSING IN THE RHIC
Jie Wei 1992 3 p Presented at the 3rd European Particle Accelerator Conference, Berlin (Germany), 24-28 Mar. 1992
(Contract DE-AC02-76CH-00016)

(DE92-013031; BNL-46683; CONF-920315-30) Avail: CASI HC A01/MF A01

This report summarizes the study of various longitudinal problems pertaining to the transition-energy crossing in the proposed Relativistic Heavy Ion Collider. Scaling laws are provided for the effects of chromatic nonlinearity, self-field mismatch, and microwave instability. It is indicated that the beam loss and bunch-area growth are mainly caused by the chromatic nonlinear effort, which is enhanced by the space-charge force near transition. Computer simulation using the program TIBETAN shows that a '(gamma)T-jump' of about 0.8 unit within a time period of 60 ms is adequate to achieve a 'clean' crossing, provided that the remnant voltage of the 160 MHz rf system is less than 10 kV. DOE

N92-29484# Lawrence Livermore National Lab., CA.
CONDENSER OPTICS, PARTIAL COHERENCE, AND IMAGING FOR SOFT X RAY PROJECTION LITHOGRAPHY
G. E. Sommargren and L. G. Seppala Mar. 1992 5 p Presented at the Soft X Ray Projection Lithography Topical Meeting, Monterey, CA, 6-8 Apr. 1992
(Contract W-7405-eng-48)
(DE92-011762; UCRL-JC-110134; CONF-9204120-1) Avail: CASI HC A01/MF A01

In this paper we have concentrated on the design and implications of condenser systems for an all reflective soft x-ray projection lithography system having five main components: the source, condenser (illumination system), mask, imaging system and wafer. DOE

N92-29530# State Univ. of New York, Albany. Atmospheric Sciences Research Center.
COSINE RESPONSE CHARACTERISTICS OF RADIOMETRIC AND PHOTOMETRIC SENSORS
J. J. Michalsky, L. C. Harrison, and W. E. Berkheiser, III 1992 5 p Presented at the National Solar Energy Conference, Cocoa Beach, FL, 13-18 Jun. 1992
(Contract DE-FG02-90ER-61072)
(DE92-011437; DOE/ER-61072/4; CONF-920678-2) Avail: CASI HC A01/MF A01

Global and diffuse irradiance and illuminance are measured with instruments that are assumed to have true cosine responses. It is known, largely from reports with a limited distribution or by word of mouth, that no instrument is perfect in this regard. This paper reports on measurements of cosine responses for several instrument types and manufacture familiar to the solar radiation measurement community. The measurements were made with an automated cosine response test bench using the same protocol for each instrument. The cosine bench measures with variable angular resolution as fine as 0.25 degrees. The automated rotation is in one plane. A manual rotation allows measurements for other azimuths. DOE

N92-29546# California Univ., Irvine.
DIFFRACTION OF LIGHT FROM RANDOMLY ROUGH SURFACES
Alexei A. Maradudin 16 Mar. 1992 13 p
(Contract DAAL03-88-K-0067)
(AD-A250261; ARO-25464.11-PH) Avail: CASI HC A03/MF A01

A combined theoretical and experimental investigation of the scattering of light from randomly rough metallic, dielectric, and perfectly conducting surfaces has been carried out. A major goal of this research program has been an increased understanding of the phenomenon of the enhanced backscattering of light from such surfaces, viz. the narrow peak in the angular distribution of the intensity of the incoherent component of the scattered light in the retroreflection (backscattering) direction. At the same time, a new effect has been predicted and observed in the transmission of light through a thin metal film with random surfaces. This is enhanced transmission, viz. a narrow peak in the angular distribution of the intensity of the incoherent component of the transmitted light in the antispecular direction. Both enhanced backscattering and enhanced transmission are examples of the weak localization of classical (electromagnetic) waves due to their interaction with a random medium. GRA

N92-29578# Lawrence Livermore National Lab., CA.
CURSORY EXAMINATION OF THE ZETA POTENTIAL BEHAVIORS OF TWO OPTICAL MATERIALS
A. Tesar and T. Oja (Matec Applied Sciences, Inc., Hopkinton, MA.) 2 Jan. 1992 9 p
(Contract W-7405-eng-48)
(DE92-011588; UCRL-ID-109373) Avail: CASI HC A02/MF A01

When an oxide surface is placed in water, a difference in potential across the interface occurs due to dipole orientation. Hydroxyl groups or bound oxygen atoms on the oxide surface will orient adjacent water molecules which balance the dipole charge. This occurs over some small distance called the electrical double layer. Trace amounts of high field strength ions present in the vicinity of the double layer can have significant effects on the double layer. When there is movement of the oxide surface with respect to the water, a shearing of the double layer occurs. The electrical potential at this surface of shear is termed the zeta potential. The impetus for this study was to document the zeta potential behavior in water of two optical materials, a multicomponent phosphate glass and Zerodur, a silicate glass-ceramic. DOE

N92-29652*# Virginia Polytechnic Inst. and State Univ., Blacksburg. Dept. of Electrical Engineering.
ANALYSES OF NEAR- AND FAR-FIELD TWO-LOBE PATTERNS OUTSIDE THE OUTPUT ENDFACE OF A TWO-MODE FIBER
A. Wang, G. Z. Wang, and R. O. Claus 1991 6 p
(Grant NAG1-1348)
(NASA-CR-190494; NAS 1.26:190494) Avail: CASI HC A02/MF A01

The behaviors of the near- and far-field two-lobe radiation patterns from a circular-core two-mode fiber are studied by using both the mode and Kirchhoff diffraction theories. The electric field outside the output endface of the fiber is derived from the electric field distribution of the LP sub 01 and LP sub 11 modes at the fiber endface using the Kirchhoff diffraction formula. Different phenomena are studied by solving this expression numerically at near-and far-fields. The Gouy phase shifts are quantitatively evaluated at cross-sections of the near field. The results reveal the distortion and dislocation of the far-field two-lobe pattern induced by an inclination angle of the fiber endface. Author

N92-29679*# Jet Propulsion Lab., California Inst. of Tech., Pasadena.
DEVELOPMENTS IN FIBER OPTICS FOR DISTRIBUTION AUTOMATION
H. Kirkham, H. Friend, S. Jackson, and A. Johnston 1 Dec. 1991 64 p
(Contracts NAS7-918; DE-AI01-79ET-29372)
(NASA-CR-190454; NAS 1.26:190454; JPL-Publ-90-2) Avail: CASI HC A04/MF A01

An optical fiber based communications system of unusual design is described. The system consists of a network of optical fibers overlaid on the distribution system. It is configured as a large number of interconnected rings, with some spurs. Protocols for access to and control of the network are described. Because of the way they function, the protocols are collectively called AbNET, in commemoration of the microbiologists' abbreviation Ab for antibody. Optical data links that could be optically powered are described. There are two versions, each of which has a good frequency response and minimal filtering requirements. In one, a conventional FM pulse train is used at the transmitter, and a novel form of phase-locked loop is used as demodulator. In the other, the FM transmitter is replaced with a pulse generator arranged so that the period between pulses represents the modulating signal. Transmitter and receiver designs, including

temperature compensation methods, are presented. Experimental results are given. Author

N92-29681*# Virginia Polytechnic Inst. and State Univ., Blacksburg. Fiber and Electro-Optics Research Center.
ERBIUM-DOPED FIBER AMPLIFIER ELEMENTS FOR STRUCTURAL ANALYSIS SENSORS
P. Hanna-Hawver, K. D. Kamdar, S. Mehta, S. Nagarajan, M. H. Nasta, and R. O. Claus 1992 5 p
(Grant NAG1-1348)
(NASA-CR-190491; NAS 1.26:190491) Avail: CASI HC A01/MF A01

The use of erbium-doped fiber amplifiers (EDFA's) in optical fiber sensor systems for structural analysis is described. EDFA's were developed for primary applications as periodic regenerator amplifiers in long-distance fiber-based communication systems. Their in-line amplification performance also makes them attractive for optical fiber sensor systems which require long effective lengths or the synthesis of special length-dependent signal processing functions. Sensor geometries incorporating EDFA's in recirculating and multiple loop sensors are discussed. Noise and polarization birefringence are also considered, and the experimental development of system components is discussed. Author

N92-29726# Johns Hopkins Univ., Laurel, MD. Applied Physics Lab.
A WAVE THEORY FOR NON-IMAGING CONCENTRATORS
William H. Carter Apr. 1992 26 p
(Contracts N00039-91-C-0001; N00039-91-C-5301)
(AD-A248865; JHU/APL-TG-1382) Avail: CASI HC A03/MF A01

An expression is derived for propagation of the radiance function for light in any state of coherence through a concentrator that can be represented by a linear, stationary optical system. For light from a quasi-homogeneous source, this expression can be somewhat simplified by an approximation. It is shown that the radiance function is invariant for a large class of optical systems. It is also shown that fundamental limitations for the concentration of light follow from the uncertainty principle and the second law of thermodynamics, which apply quite generally. These relations show why quasi-homogeneous light (such as light from thermal sources) can not be concentrated as well as light from some other sources (such as light from a laser). GRA

N92-29727# Oregon Graduate Inst. of Science and Technology, Beaverton.
INTERNATIONAL CONFERENCE TOPICAL MEETING ON ATMOSPHERIC, VOLUME, AND SURFACE SCATTERING AND PROPAGATION Final Report, 30 Sep. 1990 - 29 Jan. 1992
J. F. Holmes Jan. 1992 285 p Conference held in Florence, Italy, 27-30 Aug. 1991
(Contract DAAL03-90-G-0219)
(AD-A248881; ARO-28415.1-GS-CF) Avail: CASI HC A13/MF A03

The meeting was held as scheduled. A Digest of the meeting was published and contains copies of the presentations. GRA

N92-29832*# National Aeronautics and Space Administration. Pasadena Office, CA.
IMPROVED REAL-TIME IMAGING SPECTROMETER Patent Application
James L. Lambert, inventor (to NASA) (Jet Propulsion Lab., California Inst. of Tech., Pasadena.), Tien-Hsin Chao, inventor (to NASA) (Jet Propulsion Lab., California Inst. of Tech., Pasadena.), Jeffrey W. Yu, inventor (to NASA) (Jet Propulsion Lab., California Inst. of Tech., Pasadena.), and Li-Jen Cheng, inventor (to NASA) (Jet Propulsion Lab., California Inst. of Tech., Pasadena.) 9 Dec. 1991 39 p
(Contract NAS7-918)
(NASA-Case-NPO-18410-1-CU; NAS 1.71:NPO-18410-1-CU)
Avail: CASI HC A03/MF A01

An improved AOTF-based imaging spectrometer that offers several advantages over prior art AOTF imaging spectrometers is presented. The ability to electronically set the bandpass wavelength provides observational flexibility. Various improvements in optical architecture provide simplified magnification variability, improved image resolution and light throughput efficiency and reduced sensitivity to ambient light. Two embodiments of the invention are: (1) operation in the visible/near-infrared domain of wavelength range 0.48 to 0.76 microns; and (2) infrared configuration which operates in the wavelength range of 1.2 to 2.5 microns. NASA

N92-29859# Technische Univ., Eindhoven (Netherlands).
THE OPTICAL DESIGN OF AmPS: ELEMENTS OF THE DESIGN OF A PULSE STRETCHER Ph.D. Thesis
Yunyan Wu 1991 113 p Sponsored by Stichting voor Fundamenteel Onderzoek der Materie and Nederlandse Organisatie voor Wetenschappelijk Onderzoek
(ETN-92-91626) Avail: CASI HC A06/MF A02

The optical design of the AmPS (Amsterdam Pulse Stretcher) is addressed. The basic concepts of circular machine theory are presented and the structure of the AmPS is described. The considerations which led to this design are given; the resulting parameters of the ring (both geometric and optical) are shown; the parameters chosen for the ring main magnets (dipoles, quadrupoles and sextupoles) are given. Misalignments and mis-settings of the magnetic elements can cause beam loss. An orbit correction scheme, designed to cancel the effects of these misalignments, is discussed. The resonant extraction concept is detailed. The injection process, in which a 'hollow' beam in phase space is created, is explained. Some methods to obtain a uniform extracted beam current are investigated; the bases of these methods and simulation results showing the properties of the extracted beam are given. Numerical simulation played an important role in the optical design of the AmPS. The whole design concept and the parameters chosen for the stretcher ring were numerically checked. The simulation results show that the lattice design and the element parameter chosen for the AmPS fulfill the specifications. The AmPS is expected to provide a state of the art high duty factor beam for nuclear physics experiments. ESA

N92-29951*# National Aeronautics and Space Administration. Langley Research Center, Hampton, VA.
MULTIRESPONSE IMAGER AND IMAGING PROCESS FOR IMPROVED RESOLUTION Patent Application
Carl E. Fales, inventor (to NASA) and Fredrich O. Huck, inventor (to NASA) 14 May 1992 16 p
(NASA-Case-LAR-14779-1; NAS 1.71:LAR-14779-1;
US-Patent-Appl-SN-885714) Avail: CASI HC A03/MF A01

The implementation of this invention consists of two elements, the image gathering device and an image restoration filter algorithm. The image gathering device is implemented with an optical aperture control that allows one to change the spatial frequency response of the image gathering device for each one of the successive image acquisitions; the image restoration algorithm unscrambles the within-passband and aliased signal components in the presence of photosensor noise to produce an image with an increased resolution. The upper limit of the increase in resolution is 1/square root of A times the sampling interval of the image gathering device for A image gathering events. The image gathering device and the target must be stationary with respect to each other during the image gathering process. NASA

N92-30027*# National Aeronautics and Space Administration. Lyndon B. Johnson Space Center, Houston, TX.
POLARIZATION PERCEPTION DEVICE Patent Application
Victor S. Whitehead, inventor (to NASA) and Kinsel L. Coulson, inventor (to NASA) (California Univ., Davis.) 6 Apr. 1992 20 p
(NASA-Case-MSC-21915-1; NAS 1.71:MSC-21915-1;
US-Patent-Appl-SN-863883) Avail: CASI HC A03/MF A01

A polarization perception device comprises a base and a polarizing filter having opposite broad sides and a centerline perpendicular thereto. The filter is mounted on the base for relative rotation and with a major portion of the area of the filter substantially unobstructed on either side. A motor on the base automatically moves the filter angularly about its centerline at a speed slow

enough to permit changes in light transmission by virtue of such movement to be perceived as light-dark pulses by a human observer, but fast enough so that the light phase of each such pulse occurs prior to fading of the light phase image of the preceding pulse from the observer's retina. In addition to an observer viewing a scene in real time through the filter while it is so angularly moved, or instead of such observation, the scene can be photographed, filmed or taped by a camera whose lens is positioned behind the filter. Author

N92-30029*# National Aeronautics and Space Administration. Langley Research Center, Hampton, VA.
OPTICAL FIBER SENSOR HAVING AN ACTIVE CORE Patent Application
Claudio Oliveira Egalon, inventor (to NASA) (Analytical Services and Materials, Inc., Hampton, VA.) and Robert S. Rogowski, inventor (to NASA) 18 Mar. 1992 17 p
(NASA-Case-LAR-14607-1SB; NAS 1.71:LAR-14607-1SB; US-Patent-Appl-SN-855363) Avail: CASI HC A03/MF A01

An optical fiber is provided comprising an active fiber core which produces waves of light upon excitation. A factor ka is identified and increased until a desired improvement in power efficiency is obtained. The variable a is the radius of the active fiber core and k is defined as 2 pi/lambda wherein lambda is the wavelength of the light produced by the active fiber core. In one embodiment, the factor ka is increased until the power efficiency stabilizes. In addition to a bare fiber core embodiment, a two-stage fluorescent fiber is provided wherein an active cladding surrounds a portion of the active fiber core having an improved ka factor. The power efficiency of the embodiment is further improved by increasing a difference between the respective indices of refraction of the active cladding and the active fiber core. Author

N92-30084*# National Aeronautics and Space Administration. Pasadena Office, CA.
DYNAMIC APERTURE FRINGE DISCRIMINATOR Patent Application
Lawrence J. Steimle, inventor (to NASA) (Jet Propulsion Lab., California Inst. of Tech., Pasadena.) and David L. Thiessen, inventor (to NASA) (Jet Propulsion Lab., California Inst. of Tech., Pasadena.) 15 May 1992 27 p
(Contract NAS7-918)
(NASA-Case-NPO-18478-1-CU; NAS 1.71:NPO-18478-1-CU; US-Patent-Appl-SN-883957) Avail: CASI HC A03/MF A01

A device for eliminating unwanted reflections from refractive optical elements in an optical system is provided. The device operates to prevent desired multiple fringe patterns from being obscured by reflections from refractive elements positioned in proximity to a focal plane of the system. The problem occurs when an optical beam is projected into, and reflected back out of, the optical system. Surfaces of the refractive elements reflect portions of the beam which interfere with portions of the beam which are transmitted through the refractive elements. Interference between the reflected and transmitted portions of the beam produce multiple fringe sets which tend to obscure desired interference fringes. With the refractive optical element in close proximity to the focal plane of the system, the undesired reflected light reflects at an angle 180 degrees opposite from the desired transmitted beam. The device exploits the 180-degree offset, or rotational shear, of the undesired reflected light by providing an optical stop for blocking one-half of the cross-section of the test beam. By blocking one-half of the test beam, the undesired offset beam is blocked, while the returning transmitted beam passes into the optical system unaffected. An image is thereby produced from only the desired transmitted beam. In one configuration, the blocking device includes a semicircular aperture which is caused to rotate about the axis of the test beam. By rotating, all portions of the test beam are cyclically projected into the optical system to thereby produce a complete test image. The rotating optical stop is preferably caused to rotate rapidly to eliminate flicker in the resulting image. NASA

N92-30104*# National Aeronautics and Space Administration. Pasadena Office, CA.
PROGRAMMABLE HYPERSPECTRAL IMAGE MAPPER WITH ON-ARRAY PROCESSING Patent Application
James A. Cutts, inventor (to NASA) (Jet Propulsion Lab., California Inst. of Tech., Pasadena.) 22 Jun. 1992 36 p
(Contract NAS7-918)
(NASA-Case-NPO-17794-1-CU; NAS 1.71:NPO-17794-1-CU; US-Patent-Appl-SN-904550) Avail: CASI HC A03/MF A01

A hyperspectral imager includes a focal plane having an array of spaced image recording pixels receiving light from a scene moving relative to the focal plane in a longitudinal direction, the recording pixels being transportable at a controllable rate in the focal plane in the longitudinal direction, an electronic shutter for adjusting an exposure time of the focal plane, whereby recording pixels in an active area of the focal plane are removed therefrom and stored upon expiration of the exposure time, an electronic spectral filter for selecting a spectral band of light received by the focal plane from the scene during each exposure time and an electronic controller connected to the focal plane, to the electronic shutter and to the electronic spectral filter for controlling (1) the controllable rate at which the recording is transported in the longitudinal direction, (2) the exposure time, and (3) the spectral band so as to record a selected portion of the scene through M spectral bands with a respective exposure time t(sub q) for each respective spectral band q. NASA

N92-29372*# Jet Propulsion Lab., California Inst. of Tech., Pasadena.
PERFORMANCE OF A 12-GHz FIBER-OPTIC SYSTEM FOR BEAM-WAVEGUIDE ANTENNA STABILITY TESTING
T. Y. Otoshi, M. M. Franco, and G. F. Lutes *In its* The Telecommunications and Data Acquisition Report 15 May 1992 p 105-113 (For primary document see N92-29364 20-32)
(RTOP 310-20-65-92-01)
Avail: CASI HC A02/MF A04

N92-29376*# Jet Propulsion Lab., California Inst. of Tech., Pasadena.
FIGURE OF MERIT FOR DIRECT-DETECTION OPTICAL CHANNELS
C.-C. Chen *In its* The Telecommunications and Data Acquisition Report 15 May 1992 p 136-151 (For primary document see N92-29364 20-32)
(RTOP 310-20-67-59-00)
Avail: CASI HC A03/MF A04

75 PLASMA PHYSICS

Includes magnetohydrodynamics and plasma fusion.

For ionospheric plasmas see *46 Geophysics*. For space plasmas see *90 Astrophysics*.

N92-29336# Massachusetts Inst. of Tech., Cambridge. Plasma Fusion Center.
EXPERIMENTAL AND THEORETICAL RESEARCH IN APPLIED PLASMA PHYSICS
M. Porkolab 1992 161 p
(Contract DE-FG02-91ER-54109)
(DE92-013587; DOE/ER-54109/2) Avail: CASI HC A08/MF A02

This report discusses research in the following areas: fusion theory and computations; theory of thermonuclear plasmas; user service center; high poloidal beta studies on PBX-M; fast ECE fluctuation diagnostic for ballooning mode studies; x-ray imaging diagnostic; millimeter/submillimeter-wave fusion ion diagnostics; small scale turbulence and nonlinear dynamics in plasmas; plasma turbulence and transport; phase contrast interferometer diagnostic for long wavelength fluctuations in DIII-D; and charged and neutral fusion production for fusion plasmas. DOE

N92-29412# General Atomic Co., San Diego, CA.
MULTICHORD SPECTROSCOPY OF THE D3-D DIVERTOR REGION
N. H. Brooks, A. Howald, K. Klepper, and P. West Apr. 1992 7 p Presented at the 9th Topical Conference on High-Temperature Plasma Diagnostics, Santa Fe, NM, 15-19 Mar. 1992
(Contract DE-AC03-89ER-51114)
(DE92-013507; GA-A-20872; CONF-920362-27) Avail: CASI HC A02/MF A01

A multichannel spectrometer with high spectral resolution (0.01 nm) and high temporal resolution (0.5 msec) has been configured to collect data simultaneously from eight viewchords spanning the divertor region of D3-D. Fiberoptically coupled to a wide-field lens with a vertical view of the vessel floor, the instrument will be capable of differentiating the behavior of impurity line emission at the inner and outer divertor strike points, on and off the Advanced Divertor Program (ADP) ring, on the face of the Divertor Material Exposure System (DIMES) probe, and in the region of the lower centerpost. Used with a coarse grating (300 grooves/mm), spectral coverage of each spatial channel is 15 nm with 0.3 nm resolution; used in high order with a 1200 groove/nm grating, the instrument is capable of resolving Doppler profiles. Spatial variation of gas recycling and impurity influx is studied for both single- and double-null divertor configurations in low and high density operating regimes. DOE

N92-29438# Georgia Inst. of Tech., Atlanta.
ANALYSIS OF A DEDICATED ROTATION EXPERIMENT IN TFTR
W. M. Stacey Mar. 1992 88 p
(Contract DE-FG05-87ER-51112)
(DE92-013463; GTFR-100) Avail: CASI HC A05/MF A01

The results and analysis of a well-diagnosed, dedicated rotation experiment in TFTR are presented. Various neoclassical and anomalous theories for momentum transport are described and compared with the experimental data. The gyroviscocity theory is able to predict the measured central toroidal rotation speed, momentum confinement time and radial torque flow profile reasonably well when a poloidal asymmetry factor (tilde (theta)) = 1.5 is used. The cold-ion-perpendicular-viscocity theory requires the assumption of an implausibly large number of cold ions in order to predict the magnitude of the experimental torque flow. The ion-temperature-gradient-mode theory, the untrapped-particle-electrostatic-mode theory and the stochastic-magnetic-perturbation theory all predict torque flows that differ greatly in magnitude, radial profile, and parametric dependence from the experimental values. DOE

N92-29450# Rutgers - The State Univ., New Brunswick, NJ. Dept. of Physics.
STATISTICAL MECHANICS OF COLLECTIVE PHENOMENA IN PLASMAS Final Report, 1 Nov. 1990 - 31 Oct. 1991
Joel L. Lebowitz 31 Oct. 1991 7 p
(Grant AF-AFOSR-0010-87)
(AD-A250581; AFOSR-92-0277TR) Avail: CASI HC A02/MF A01

We have carried out theoretical studies of equilibrium and nonequilibrium properties of strongly coupled particle systems, and of the phenomena which take place when neutral or partially ionized atoms interact strongly with external fields and with each other in a plasma. The main tools of our study are statistical mechanics and kinetic theory, including the transition from a microscopic to a hydrodynamic description. Quantum mechanics plays a central role in many of these problems, and is an important ingredient in our work. GRA

N92-29510# Ballistic Research Labs., Aberdeen Proving Ground, MD.
SPATIAL AND TEMPORAL TEMPERATURE STUDIES OF ELECTROTHERMAL CHEMICAL (ETC) PLASMAS Final Technical Report, Dec. 1989 - Oct. 1990
Richard A. Beyer and Steven W. Bunte Mar. 1992 23 p
(DA Proj. 1L1-62618-AH-80)
(AD-A248541; BRL-TR-3324) Avail: CASI HC A03/MF A01

Atomic spectroscopy has been used to measure plasma temperatures in the exit flow of polyethylene capillary. Typical events involve the deposition of about 300 J of energy. Temperature values observed range from 10,000 K to almost 50,000 K, the latter the result of shock wave heating of the supersonic exit flow. Under the most favorable signal to noise conditions, uncertainties are estimated at 5 percent. GRA

N92-29528# Air Force Inst. of Tech., Wright-Patterson AFB, OH. School of Engineering.
NUMERICAL ANALYSIS OF PLASMA TRANSPORT IN TANDEM VOLUME MAGNETIC MULTICUSP ION SOURCES M.S. Thesis
Todd R. Vitko Mar. 1992 136 p
(AD-A248093; AFIT/GEP/ENP/92M-01) Avail: CASI HC A07/MF A02

A one-dimensional fluid model of plasma transport in tandem volume magnetic multicusp ion sources is explored. The model, a positive ion source code, calculates plasma density, drift velocity, electron temperature, and ion temperature in an ion source. The usefulness of the model is limited in the following ways: (1) the plasma density trend runs opposite to experimental results, and electron temperatures are an order of magnitude higher than experimentally observed; (2) simplification of the reaction chemistry leads to a plasma balance between ionization and outflow instead of the correct balance between ionization and recombination; (3) wall losses are neglected; (4) there are inconsistencies in the derivations of some equations; (5) the final solution depends on the choice of an initial estimated solution; (6) results of the model are not totally reproducible; and (7) numerical instabilities develop upon modification of terms or variation of initial conditions outside of a narrow range. Calculations of the plasma potential from the results of the model are qualitatively correct. GRA

N92-29531# Lawrence Livermore National Lab., CA.
LLE-LLNL PROGRESS REPORT ON STUDIES IN NONLOCAL HEAT TRANSPORT IN SPHERICAL PLASMAS USING THE FOKKER-PLANCK CODE SPARK
E. M. Epperlein (Rochester Univ., NY.), P. Amendt, L. Powers, and L. J. Suter 22 Apr. 1992 37 p
(Contracts DE-FC03-85DP-40200; W-7405-eng-48)
(DE92-014093; UCRL-ID-110314) Avail: CASI HC A03/MF A01

Preliminary 1-D studies of nonlocal heat transport in spherical plasmas based on the Fokker-Planck code SPARK indicate significant levels of electron preheat and radial heat flux across a spherical heat sink surface kept at fixed temperature. However, the diffusive approximation to the Fokker-Planck equation is shown to be particularly sensitive to the nature of the inner surface boundary condition chosen. A suggested remedy is the inclusion of a target capsule in future simulations studies with SPARK. DOE

N92-29640# TRW Space Technology Labs., Redondo Beach, CA. Applied Technology Div.
MHD TECHNOLOGY TRANSFER, INTEGRATION AND REVIEW COMMITTEE
Jan. 1992 128 p
(Contract DE-AC22-87PC-90274)
(DE92-012687; DOE/PC-90274/T12; MHD-ITC-91-021) Avail: CASI HC A07/MF A02

This fifth semi-annual status report of the MHD Technology Transfer, Integration, and Review Committee (TTIRC) summarizes activities of the TTIRC during the period April 1990 through September 1990. It includes summaries and minutes of committee meetings, progress summaries of ongoing Proof-of-Concept (POC) contracts, discussions pertaining to technical integration issues in the POC program, and planned activities for the next six months. DOE

N92-29761# Technische Univ., Eindhoven (Netherlands).
THE EXPANDING PLASMA JET: EXPERIMENTS AND MODEL Ph.D. Thesis
Mauritius Cornelius vandeSanden 1991 190 p
(ETN-92-91627) Avail: CASI HC A09/MF A02

The fundamental aspects of an argon plasma expanding from a cascaded arc, a type of plasma used for fundamental research and for technologically orientated research on plasma deposition and plasma sources, are addressed. A thermodynamic study of the influence of the temperature nonequilibrium on the ionization equilibrium is discussed. A more rigorous study of the same problem using the Zubarev formalism is given. The presentation of the model for the plasma expanding from a cascaded arc is addressed. The cascaded arc setup is discussed. For the study of transport processes and the nonequilibrium state of the expanding plasma, the knowledge of the important plasma parameters, the electron density and temperature, and the neutral particle density are essential. Therefore, a designed and constructed Thomson-Rayleigh scattering setup is discussed. The light emission and the Fabry-Perot experiment are discussed. Results and conclusions are given. ESA

N92-29789# Los Alamos National Lab., NM.
X RAY STREAK CAMERA DIAGNOSTICS OF PICOSECOND LASER-PLASMA INTERACTIONS
J. A. Cobble, R. D. Fulton, L. A. Jones, G. A. Kyrala, G. T. Schappert, A. J. Taylor, and E. K. Wahlin 1992 10 p Presented at the 9th Topical Conference on High-Temperature Plasma Diagnostics, Santa Fe, NM, 15-19 Mar. 1992
(Contract W-7405-eng-36)
(DE92-011371; LA-UR-92-792; CONF-920362-14) Avail: CASI HC A02/MF A01

An x-ray streak camera is used to diagnose a laser-produced Al plasma with time resolution of (approximately)10 ps. A streak record of filtered emission and a time-integrated transmission grating spectrum reveal that the plasma radiation is dominated by emission from He- and H-like resonance lines. DOE

N92-29798# Lawrence Livermore National Lab., CA.
ESTIMATING PLASMA TEMPERATURES
J. K. Nash, C. A. Iglesias, M. H. Chen, and F. J. Rogers Apr. 1992 10 p
(Contract W-7405-eng-48)
(DE92-014092; UCRL-ID-110284) Avail: CASI HC A02/MF A01

Recent laser-produced plasma experiments have relied on spectroscopic comparisons with models to infer plasma temperatures. The models use an experimentally determined value for the matter density as input and treat the temperature as a free parameter to obtain a best fit to the experimental absorption spectrum. However, uncertainties in the ionization balance theories lead to inferred temperatures that are model dependent. We report results of a new approach which combines high quality atomic data with an ionization balance obtained from systematic expansions of the grand canonical ensemble. The latter avoids the ad hoc cutoffs required in free energy minimization schemes and includes Coulomb corrections usually neglected in other models. Comparisons to experimental spectra show excellent agreement. DOE

N92-29917# Los Alamos National Lab., NM.
OPTICAL DIAGNOSTICS ON DENSE Z-PINCH PLASMAS
R. A. Riley, Jr., R. H. Lovberg, J. S. Shlachter, and D. W. Scudder 1992 15 p Presented at the 9th Topical Conference on High-Temperature Plasma Diagnostics, Santa Fe, NM, 15-19 Mar. 1992
(Contract W-7405-eng-36)
(DE92-011228; LA-UR-92-1043; CONF-920362-18) Avail: CASI HC A03/MF A01

A novel 'point-diffraction' interferometer has been implemented on the Los Alamos Solid Fiber Z-Pinch experiment. The laser beam is split into two legs after passing through the plasma. The reference leg is filtered with a pin-hole aperture and recombined with the other leg to form an interferogram. This allows compact mounting of the optics and relative ease of alignment. The Z-Pinch experiment employs a pulsed-power generator that delivers up to 700 KA with a 100ns rise-time through a fiber of deuterium or deuterated polyethylene (CD(sub s)) that is 5-cm long and initially solid with radius of approx. 15 microns. The interferometer, using a triangle of approx. 200ps pulse from a Nd:YAG laser frequency doubled to (lambda) = 532nm, measures the electronline density and, assuming azimuthal symmetry, the density as a function of radial and axial position. Calculations predict Faraday rotations of order pi/2 for plasma and current densities that this experiment was designed to produce. The resulting periodic loss of fringes would provide the current density distribution. DOE

N92-30072# Rochester Univ., NY. Lab. for Laser Energetics.
LLE REVIEW
R. L. Keck, ed. 1991 65 p
(Contract DE-FC03-85DP-40200)
(DE92-011614; DOE/DP-40200/188) Avail: CASI HC A04/MF A01

This volume of the LLE Review, covering the period October-December 1991, contains articles on the analysis of argon-filled target experiments, and a theoretical analysis of the impact of nonlocal heat transport in laser filamentation in plasmas. In the Advanced Technology section there is an article on mechanisms that affect thin-film conductivity, and a report on the gain characteristics of the 20-cm SSA prototype amplifier to be used in the OMEGA Upgrade. Finally, the activities of the National Laser Users Facility and the GDL and OMEGA laser facilities are summarized. Highlights of the research are reported. Argon radiation from argon-filled, polymer-shell targets is used as a core-temperature diagnostic and density diagnostic of the surrounding region in a regime where the argon line radiation is strongly absorbed. A theoretical analysis of the impact of nonlocal heat transport on laser filamentation in plasmas is developed. The resulting model is compared with experimental observations, and the implications for ICF are discussed. A study of thermal conductivity in thin films seeks to identify mechanisms that result in degradation of thin-film conductivity. Identifying these mechanisms can lead to changes in the thin-film manufacturing that will improve their resistance to laser damage. DOE

N92-30091# National Inst. for Fusion Science, Nagoya (Japan).
FORMATION OF PRESHEATH AND CURRENT-FREE DOUBLE LAYER IN A TWO-ELECTRON-TEMPERATURE PLASMA
Kunihiro Sato (Himeji Inst. of Tech., Japan) and Fujio Miyawaki (Himeji Inst. of Tech., Japan) Feb. 1992 36 p Submitted for publication
(NIFS-132; ISSN-0915-633X) Avail: CASI HC A03/MF A01

Development of the steady-state potential in a two-temperature-electron plasma in contact with the wall is investigated analytically. It is shown that if the hot- to cold electron temperature ratio is greater than ten, the potential drop in the presheath, which is allowed to have either a small value characterized by the cold electrons or a large value by the hot electrons, discontinuously changes at a critical value for the hot- to total electron density ratio. It is also found that the monotonically decreasing potential structure which consists of the first presheath, a current-free double layer, the second presheath, and the sheath can be steadily formed in a lower range of the hot- to total electron density ratio around the critical value. The current-free double layer is set up due to existence of the two electron species and cold ions generated by ionization so as to connect two presheath potentials at different levels. Author

N92-30172# National Inst. for Fusion Science, Nagoya (Japan).
HEAT FLOW OF A TWO-ELECTRON-TEMPERATURE PLASMA THROUGH THE SHEATH IN THE PRESENCE OF ELECTRON EMISSION
Kunihiro Sato (Himeji Inst. of Tech., Japan) and Fujio Miyawaki (Himeji Inst. of Tech., Japan) Mar. 1992 17 p Submitted for publication
(NIFS-136; ISSN-0915-633X) Avail: CASI HC A03/MF A01

The electrostatic sheath and the heat flow of a two-electron-temperature plasma in the presence of electron emission is investigated analytically. It is shown that the energy flux is remarkably enhanced up to a value near the electron free-flow energy flux as a result of considerable reduction of the sheath potential due to electron emission if the fraction of hot electrons at the sheath edge is much smaller than one. If the hot- to cold-electron temperature is of the order of ten and the hot electron density is comparable with the cold electron density, the action of the sheath as a thermal insulator is improved as a result of suppression of electron emission due to the space-charge effect of hot electrons. Author

N92-30203# Los Alamos National Lab., NM.
INTENSE DIAGNOSTIC NEUTRAL BEAM DEVELOPMENT FOR ITER
D. J. Rej, I. Henins (Oak Ridge National Lab., TN.), R. J. Fonck, and Y. J. Kim 1992 11 p Presented at the 9th Topical Conference on High-Temperature Plasma Diagnostics, Santa Fe, NM, 15-19 Mar. 1991
(Contract W-7405-eng-36)
(DE92-011262; LA-UR-92-826; CONF-920362-16) Avail: CASI HC A03/MF A01

For the next-generation, burning tokamak plasmas such as ITER, diagnostic neutral beams and beam spectroscopy will continue to be used to determine a variety of plasma parameters such as ion temperature, rotation, fluctuations, impurity content, current density profile, and confined alpha particle density and energy distribution. Present-day low-current, long-pulse beam technology will be unable the provision of the required signal intensities because of higher beam attenuation and background bremsstrahlung radiation in these larger, higher-density plasmas. To address this problem, we are developing a short-pulse, intense diagnostic neutral beam. Protons or deuterons are accelerated using magnetic-insulated ion-diode technology, and neutralized in a transient gas cell. A prototype 25-kA, 100-kV, 1 microsecond accelerator is under construction at Los Alamos. Initial experiments will focus on ITER-related issues of beam energy distribution, current density, pulse length, divergence, propagation, impurity content, reproducibility, and maintenance. DOE

76 SOLID-STATE PHYSICS

Includes superconductivity.

For related information, see also *33 Electronics and Electrical Engineering* and *36 Lasers and Masers.*

N92-29429# Utah Univ., Salt Lake City. Dept. of Materials Science and Engineering.
THERMODYNAMIC AND KINETIC ASPECTS OF 3/5 EPITAXY
G. B. Stringfellow 22 May 1992 16 p
(Contract N00014-91-J-1447)
(AD-A250632; TR-32) Avail: CASI HC A03/MF A01

Crystal growth processes in general and epitaxial processes in particular are often discussed in terms of three disciplines: thermodynamics, mass transport and hydrodynamics, and chemical reaction kinetics. This paper will concentrate on two of these, the thermodynamic and kinetic aspects of epitaxy. Three major influences of thermodynamics will be discussed: (1) Thermodynamics defines the driving force and hence the upper limit of growth rate. This occurs only when all reactants in the system are allowed to equilibrate with the substrate. (2) Thermodynamics often controls stoichiometry and the solid composition of alloys. An understanding of thermodynamic and kinetic constraints can lead to the growth of metastable alloys. (3) The driving force for ordering into natural superlattice structures during growth is also governed by thermodynamics. The actual ordered structures observed are dependent on the surface kinetics. This aspect of kinetics will be addressed in addition to the kinetics of both homogeneous and heterogeneous chemical reactions occurring during growth. Each of these topics is addressed in terms of fundamental concepts, with examples from recent research on the epitaxial growth of 3/5 semiconductor compounds and alloys. GRA

N92-29437# Brookhaven National Lab., Upton, NY.
X RAY STUDY OF INTERFACIAL INTERACTIONS IN HIGHLY MILLED Sn-Ge POWDERS
J. K. D. S. Jayanetti, S. M. Heald, and Z. Tan 1991 4 p Presented at the Annual Fall Meeting of the Materials Research Society, Boston, MA, 2-6 Dec. 1991
(Contracts DE-AC02-76CH-00016; DE-AS05-80ER-10742)
(DE92-012518; BNL-47382; CONF-911202-78) Avail: CASI HC A01/MF A01

We have studied possible structural changes occurring at the Sn/Ge interface of highly milled Sn/Ge composites. EXAFS and x-ray diffraction measurements were made on mechanically milled powders having compositions ranging from 20 to 50 vol. percent Sn. X-ray diffraction measurements indicate the increasing amorphization of Sn as the Sn content is decreased. EXAFS results indicate that this amorphous phase is due to the formation of an alpha-Sn/Ge alloy. The EXAFS from this alloy did not change significantly at the Sn melting point. X-ray diffraction measurements made at room temperature show a systematic decrease in the intensity of Sn peaks and broadening of Ge peaks with the decreasing Sn content. DOE

N92-29473# Lawrence Livermore National Lab., CA.
THE REAL-SPACE MULTIPLE-SCATTERING THEORY AND THE ELECTRONIC STRUCTURE OF GRAIN BOUNDARIES
E. C. Sowa, A. Gonis, and X. G. Zhang (California Univ., Berkeley. Lawrence Berkeley Lab.) May 1991 11 p Presented at the Spring Meeting of the Materials Research Society (MRS), Anaheim, CA, 29 Apr. - 3 May 1991
(Contract W-7405-eng-48)
(DE92-013006; UCRL-JC-106149; CONF-910406-40) Avail: CASI HC A03/MF A01

We describe the recently developed real-space multiple-scattering theory (RSMST). The theory is designed for performing first-principles electronic-structure calculations of extended defects, such as surfaces and interfaces, including atomic relaxations and with or without impurities, without using artificial periodic boundary conditions. We present the results of non-charge-self-consistent RSMST calculations of the local electronic densities of states at twist and tilt grain boundaries in fcc Cu and bcc Nb, and report on progress towards the implementation of charge self-consistency and total-energy capabilities. DOE

N92-29485# Princeton Univ., NJ. Dept. of Geological and Geophysical Sciences.
THERMOCHEMISTRY OF PHASES RELATED TO OXIDE SUPERCONDUCTORS
1991 14 p
(Contract DE-FG02-89ER-45394)
(DE92-011811; DOE/ER-45394/3) Avail: CASI HC A03/MF A01

The aim of this project has been to understand the crystal-chemical and energetic constraints on the stability of phases related to oxide superconductors, using high temperature reaction calorimetry and the unique expertise of this laboratory, coupled with synthesis and structural studies. The YBCO (Y2O3BaOCuO) system has been studied in detail by Zhou for his Ph.D. thesis, while DiCarlo has been studying alkaline earth doped lanthanium cuprates of the series La(2-x)A(x)CuO(4-y) having structures related to K2NiF4. DOE

N92-29558# Brigham Young Univ., Provo, UT. Dept. of Chemistry.
SOLID STATE STRUCTURES OF SOME DITHIONOAMIDO-18-CROWN-6 LIGANDS Interim Report
P. Huszthy, J. S. Bradshaw, N. K. Dalley, and R. M. Izatt 24 Mar. 1992 5 p

(Contract N00014-91-J-1710)
(AD-A248098; TR-8) Avail: CASI HC A01/MF A01

The structures of three Dithionoamido-18-crown-6 ligands were determined by x-ray diffraction studies. The results show that the carbon and oxygen atoms on the macro-ring opposite the pyridine ring are disordered. A serious conformation change is noted when methyl substituents are bonded to the amide nitrogen atoms. The structures were determined by x-ray diffraction studies. The discussion of the experimental procedures used in these studies and tables of structure determination summaries, atomic parameters, and torsion angles are included in the supplementary material. The molecule contained a 2-fold axis. The unit cells of both contain two chemically similar but crystallographically distinct molecules. GRA

N92-29583# Honeywell, Inc., Minneapolis, MN. Sensor and System Development Center.
MONOLITHIC INTEGRATION OF SEMICONDUCTOR AND SUPERCONDUCTOR COMPONENTS Report, 1 Oct. - 31 Dec. 1991
Burgess Johnson 31 Dec. 1991 10 p
(Contract N00014-90-C-0226)
(AD-A245351) Avail: CASI HC A02/MF A01

The goal of the program is to develop transistor technology compatible with high transition temperature superconductor technology so that transistor pixel switches can be integrated with yttrium barium copper oxide superconducting microbolometers in the same silicon substrate. A 4x4 matrix-addressable superconducting microbolometer array will be delivered at the completion of the program. Superconducting films of YBa2Cu3O7 were grown in-situ on 3-inch silicon wafers coated amorphous silicon nitride and polycrystalline yttria stabilized zirconia. GRA

N92-29584# Midwest Research Inst., Golden, CO. National Renewable Energy Lab.
NOVEL THIN-FILM CuInSe2 FABRICATION
G. D. Mooney (Colorado Univ., Boulder.) and A. M. Hermann (Colorado Univ., Boulder.) Mar. 1992 58 p
(Contract DE-AC02-83CH-10093)
(DE92-001222; NREL/TP-411-4752) Avail: CASI HC A04/MF A01

This report describes research in Rapid Thermal Processing (RTP), a process that allows the formation of CuInSe2 without the use of H2Se. RTP is a well-established method of rapidly achieving temperatures necessary to melt and recrystallize materials such as Si and silicides. RTP processes can rapidly and uniformly heat large surface areas to hundreds of degrees Celsius. RTP is the most promising method of rapid recrystallization studied to date, being readily scalable from the research to the production level. The approach to the experiment was divided into two sections: (1) fabricating the precursor film and (2) processing the precursor film. The objective of the first phase of the work was to fabricate the thin films by RTP, then fully characterize them, to demonstrate the viability of the process as a method by which to make device-quality CuInSe2. The second phase was to demonstrate that material made by this method could be used to make an active photovoltaic device. DOE

N92-29635# Utah Univ., Salt Lake City. Dept. of Materials Science and Engineering.
OMVPE GROWTH OF InAsSbBi AND RELATED ALLOYS USING NEW ORGANOMETALLIC GROUP 5 SOURCES End-of-the-year Report
G. B. Stringfellow 1 Jun. 1992 14 p
(Contract N00014-91-J-1447)
(AD-A250631) Avail: CASI HC A03/MF A01

The major goal of the project is the organometallic vapor phase epitaxial (OMVPE) growth of a new III/V alloy, InAsSbBi, with a band gap of less than 0.1 eV at 77 K. This material is expected to be useful for infrared detectors with response in the wavelength range from 8 to 12 microns. The alloy is metastable, but for certain growth conditions it can be produced by OMVPE. This requires very low growth temperatures of 250-350 C. This, in turn requires that new organometallic In and Sb precursors be developed which pyrolyze at lower temperatures than the conventional sources trimethylindium (TMIn) and trimethylantimony (TMSb). A related goal is to produce materials suitable for device fabrication. GRA

N92-29676*# Clemson Univ., SC. Dept. of Ceramic Engineering.
DEVELOPMENT OF HIGH T(SUB c) (GREATER THAN 110 K) Bi, Tl, AND Y-BASED MATERIALS AS SUPERCONDUCTING CIRCUIT ELEMENTS Annual Report, Feb. 1991 - Feb. 1992
Gene H. Haertling, Gregory Grabert, and Phillip Gilmour 12 May 1992 92 p
(Grant NAG1-1108)
(NASA-CR-190311; NAS 1.26:190311) Avail: CASI HC A05/MF A01

Experimental work has continued on the development and characterization of bulk and hot pressed powders and tapecast materials in the Bi-Sr-Ca-Cu-O and Tl-Ba-Ca-Cu-O systems. A process for producing warp-free, sintered, superconducting tapes of Bi composition Bi2Sr2Ca2Cu3O(x) with a mixed oxide process was established. This procedure required a triple calcination at 830 C for 24 hours and sintering at 845 C from 20 to 200 hours. Hot pressing the triple calcined powder at 845 C for 6 hours at 5000 psi yielded a dense material which on further heat treatment at 845 C for 24 hours exhibited a Tc of 108.2 K. A further improvement in the processing of the bismuth materials was achieved via a chemical coprecipitation process wherein the starting nitrate materials were coprecipitated with oxalic acid, thus yielding a more chemically homogeneous, more reactive powder. With the coprecipitated powders, only one calcine at 830 C for 12 hours and a final sinter at 845 C for 30 hours was sufficient to produce a bulk superconducting material with a Tc of 108.4 K. SAFIRE-type grounding links were successfully fabricated from sintered, tapecast, coprecipitated BSCCO 2223 powders. Compositional and processing investigations were continued on the Tl-based superconductors. Manganese and lithium additions and sintering temperature and time were examined to determine their influence on superconducting properties. It was found that lithium substitutions for copper enhance the transition temperatures while manganese additions produced deleterious effects on the superconducting properties. A suitable procedure for producing reproducible bulk and tapecast material of Tl composition Tl2Ba2Ca2Cu3O(x) was developed and used in fabricating uniform superconducting tapes. The highest transition temperature for Tl-based tapes was measured at 110.2 K. Thallium superconducting SAFIRE-type grounding links were fabricated from the tapes.
Author

N92-29722# Illinois Univ., Urbana. Dept. of Electrical and Computer Engineering.
VARIABLE TEMPERATURE SCANNING TUNNELING MICROSCOPY Final Report, 21 Jul. 1988 - 20 Jul. 1991
Joseph W. Lyding Jul. 1991 24 p
(Contract N00014-88-K-0416)
(AD-A248725) Avail: CASI HC A03/MF A01

Variable temperature STM/STS was used over the 4.2 - 400 K temperature range to study CDW formation and spatial variations of the superconducting energy gap in Pb films. Topographic variations of the superconducting energy gap in Pb films show an intriguing transition from superconducting to normal behavior over distances much less than the bulk coherence length. More recently, efforts were focused on the development of a multi-chamber UHV-STM system that will couple a wide range of STM/STS capability with sample and tip preparation and characterization facilities. The first chamber of this system is fully functional and is being used to study and modify semiconductor surfaces. Other chambers will be specialized for STM nanolithography and cryogenic UHV-STM. This system accommodates UHV sample and tip transfer between chambers in addition to independent chamber operation modes. STM modification of H-passivated silicon surfaces was accomplished using techniques developed at NIST. A unique STM lateral coarse translation system was developed and used to locate and modify SiMOSFET structures fabricated for this

project. Gratings written by STM within the gate region are being evaluated for the creation of finished devices that will exhibit quantum interference effects at higher temperatures than previously observed. Work is also underway to fabricate planar tunnel junction structures that utilize coulomb charging effects to realize logic functions. GRA

N92-29753# Technische Univ., Eindhoven (Netherlands). Dept. of Physics.
TIME-OF-FLIGHT EXPERIMENTS ON GaAs/Al(x)Ga(x-1)As HETEROSTRUCTURES Ph.D. Thesis
Enneliena Aaffiena E Zwaal 1991 147 p
(ETN-92-91625) Avail: CASI HC A07/MF A02

The possibilities and limitations of time-of-flight experiments in two dimensional semiconductor structures, in particular the transport properties of GaAs/Al(x)Ga(1-x)As heterostructure at high electric fields, are studied. Results on the following are discussed: high electric field effects; time of flight experiments; current instabilities; and imaging of current instabilities. ESA

N92-29766# Technische Univ., Delft (Netherlands). Physical Chemistry of the Solid State Div.
AMORPHIZATION BY INTERDIFFUSION IN METALLIC MULTILAYERS Ph.D. Thesis [AMORFISATIE DOOR INTERDIFFUSIE IN METALLISCHE MULTILAGEN]
Marcus Antonius Hollanders 1990 193 p Sponsored by Netherlands Organization for Scientific Research
(ETN-92-91743) Copyright Avail: CASI HC A09/MF A03

Studies on interdiffusion induced amorphization in Ni/Ti and Ni/Ta multilayers are described. The formation of amorphous phases in multilayers at elevated temperatures is studied. The main experimental method used is X-ray diffraction. The effect of random variations of the layer thickness is reviewed. A generalization of the Darwin-Prins treatment is presented. The results of the X-ray diffraction measurements are presented. The analysis leads to a model that allows determination of the effective diffusion coefficients. Furthermore, multilayers with different composition are studied by differential scanning calorimetry and layers with different composition modulation lengths are investigated by resistivity measurements. For individual titles, see N92-29767 through N92-29773.

N92-29767# Technische Univ., Delft (Netherlands). Metallurgy Lab.
LAYER-THICKNESS VARIATIONS AND X RAY DIFFRACTION PATTERNS, A GENERAL TREATMENT
Marcus Antonius Hollanders and Barend J. Thijsse *In its* Amorphization by Interdiffusion in Metallic Multilayers 1990 p 19-29 (For primary document see N92-29766 20-76)
Copyright Avail: CASI HC A03/MF A03

The effects of random thickness variations in a compositionally modulated material on the X-ray diffraction pattern is expressed in terms of the distribution function. This distribution is incorporated via its Fourier transform in a function describing the phase relations between the individual layers. Features of multilayer diffraction patterns, such as the presence or absence of superlattice peaks, are explained. If the Fourier transform of the thickness variation distribution changes sign from positive to negative, the superlattice peaks change position from integral to half integral order. ESA

N92-29768# Technische Univ., Delft (Netherlands). Metallurgy Lab.
LOW-ANGLE X RAY DIFFRACTION STUDY OF SOLID STATE AMORPHIZATION IN A Ni/Ti MULTILAYER
Marcus Antonius Hollanders and Barend J. Thijsse *In its* Amorphization by Interdiffusion in Metallic Multilayers 1990 p 30-55 Sponsored by Netherlands Organization for the Advancement of Pure Research (For primary document see N92-29766 20-76)
Copyright Avail: CASI HC A03/MF A03

Successive stages in the annealing of a Ni/Ti mulytilayer at 523 K were studied by X-ray diffraction at small scattering angles. For a correct interpretation, the Darwin-Prins dynamical scattering theory was generalized by removing discretization errors. The problem of extracting a composition profile from a diffraction pattern and the influence of diffusion on a diffraction pattern are discussed. The results indicate that planar layer growth is the dominant mechanism for amorphization: sharp interfaces and a regular periodicity are maintained throughout all stages of annealing. The first internal Ni/Ti interface remained inactive. ESA

N92-29769# Technische Univ., Delft (Netherlands). Metallurgy Lab.
AMORPHIZATION ALONG INTERFACES AND GRAIN BOUNDARIES IN POLYCRYSTALLINE MULTILAYERS: AN X RAY DIFFRACTION STUDY OF Ni/Ti MULTILAYERS
Marcus Antonius Hollanders, Barend J. Thijsse, and Eric J. Mittemeijer *In its* Amorphization by Interdiffusion in Metallic Multilayers 1990 p 59-93 Sponsored by Stichting voor Fundamenteel Onderzoek der Materie (For primary document see N92-29766 20-76)
Copyright Avail: CASI HC A03/MF A03

The diffusion induced Solid State Amorphization (SSA) was studied in face centered cubic (fcc)-Ni/hexagonal close packed (hcp)-Ti multilayers at 523 K. The phase changes, composition changes, and strain development were studied for annealing times up to 220 h, using X-ray diffraction methods. Diffusion coefficients were determined. The interdiffusion coefficient for the amorphous phase is smaller than the tracer diffusion coefficient of Ni in hcp-Ti and larger than the chemical diffusion coefficient in fcc (Ni, Ti) solid solutions. Both the dissolution of Ti in crystalline Ni and the amorphization are associated with the development of stress profiles in the multilayer. These are quantitatively discussed and analyzed using the X-ray diffraction and Fizeau interferometric data. Results on the kinetics of SSA are presented. ESA

N92-29770# Technische Univ., Delft (Netherlands). Metallurgy Lab.
INTERDIFFUSION REACTIONS IN Ni/Ta MULTILAYERS STUDIED BY X RAY DIFFRACTION
Marcus Antonius Hollanders, Caroline G. Duterloo, Barend J. Thijsse, and Eric J. Mittemeijer *In its* Amorphization by Interdiffusion in Metallic Multilayers 1990 p 94-121 Sponsored by Netherlands Organization for Applied Scientific Research TNO (For primary document see N92-29766 20-76)
Copyright Avail: CASI HC A03/MF A03

The results of an analogous interdiffusion study on Ni/Ta multilayers are reported. Diffusion induced phase transformations were studied in Ni/beta-Ta multilayers between 523 and 823 K, using X-ray diffraction. The multilayers had a modulation length, of 20.3 nm and a composition of Ni48Ta52. They were crystalline without coherency between the Ni and Ta sublayers. Upon annealing at relatively low temperatures (up to 723 K), Ta dissolved in crystalline Ni concurrently with the formation of an amorphous phase. The interdiffusion reactions did not only take place at the Ni/Ta interfaces, but also along the grain boundaries on the sublayers. The chemical diffusion coefficient in the amorphous phase was determined at 673 K. The results were compared with experiments on Ni/Ti multilayers, which show similar reactions. At 723 K and higher temperatures the face centered cubic (Ni, Ta) solid solution transformed into the stable Ni3Ta compound. ESA

N92-29771# Technische Univ., Delft (Netherlands). Metallurgy Lab.
A MODEL FOR INTERDIFFUSION IN POLYCRYSTALLINE MULTILAYERS AND ITS APPLICATION TO SOLID STATE AMORPHIZATION
Marcus Antonius Hollanders, Barend J. Thijsse, and Eric J. Mittemeijer *In its* Amorphization by Interdiffusion in Metallic Multilayers 1990 p 122-142 Sponsored by Netherlands Organization for Applied Scientific Research TNO (For primary document see N92-29766 20-76)
Copyright Avail: CASI HC A03/MF A03

A model for analyzing the growth of the intermediate (amorphous) phase and the formation of a solid solution along both the interfaces and the grain boundaries in multilayers was

developed. The model is valid up to moderate stages of isothermal annealing, when the multilayer can be conceived as a stack of infinite diffusion couples. Continued amorphization along the grain boundaries implies that fast diffusion paths remain active on the amorphous phase. The model was applied to experimental data obtained for Ni-Ti and Ni-Ta multilayers, showing solid state amorphization and solid solution formations. The chemical diffusion coefficient of the amorphous phase is much smaller in the Ni-Ta system than in the Ni-Ti system, resulting in less amorphization, and a much larger ratio of the grain boundary diffusion coefficient and the chemical diffusion coefficient of the amorphous phase in Ni-Ta. ESA

N92-29772# Technische Univ., Delft (Netherlands). Metallurgy Lab.

AMORPHIZATION AND RELATED EFFECTS IN Ni/Ti MULTILAYERS STUDIED BY DIFFERENTIAL SCANNING CALORIMETRY

Marcus Antonius Hollanders, Barend J. Thijsse, and Eric J. Mittemeijer *In its* Amorphization by Interdiffusion in Metallic Multilayers 1990 p 145-160 Sponsored by Stichting voor Fundamenteel Onderzoek der Materie (For primary document see N92-29766 20-76)

Copyright Avail: CASI HC A03/MF A03

Ni/Ti multilayers of three different gross compositions, all having a composition modulation wavelength of approximately 20 nm, were studied by differential scanning calorimetry. In order to associate the observed heat effects with phase transitions, duplicate samples were heated to selected temperatures and analyzed by X-ray diffraction. Amorphization and dissolution of Ti in Ni occurs in overlapping temperature ranges. Both processes have different activation energies, as revealed by a novel kinetic analysis. Crystallization of the amorphous phase is observed between 650 and 750 K. In two of the three specimens (Ni45Ti55 and Ni71Ti29) large endothermal effects are found. ESA

N92-29773# Technische Univ., Delft (Netherlands). Metallurgy Lab.

EVIDENCE FOR AMORPHIZATION IN Ni/Ti MULTILAYERS FROM ELECTRICAL RESISTIVITY CHANGES

Anja vanderGraaf, Marcus Antonius Hollanders, Barend J. Thijsse, and Eric J. Mittemeijer *In its* Amorphization by Interdiffusion in Metallic Multilayers 1990 p 161-170 Sponsored by Stichting voor Fundamenteel Onderzoek der Materie (For primary document see N92-29766 20-76)

Copyright Avail: CASI HC A02/MF A03

Ni/Ti multilayers of various composition modulation lengths were annealed and studied with in situ electrical resistivity measurements. The resistivity was measured at different temperatures. The temperature coefficient of the resistivity at the annealing temperature was determined as a function of annealing time by correlating temperature and resistivity noise. Specimens were characterized before and after annealing by X-ray diffraction analysis. The temperature coefficient of the resistivity changed sign from positive to negative on annealing, demonstrating that amorphization took place. As a result of amorphization, the resistivity increased on annealing. The kinetics of the resistivity change for small composition modulation lengths indicate that amorphization takes place along the interfaces and along the grain boundaries on the sublayers. ESA

N92-29783# Technische Univ., Eindhoven (Netherlands).

SMALL ELECTROSTRICTIVE DILATIONS OF CUBIC CRYSTALS Ph.D. Thesis

Stefanus Wolfgang Pa vanSterkenburg 1991 104 p

(ISBN-90-9004374-8; ETN-92-91634) Avail: CASI HC A06/MF A02

The electrostriction of simple cubic crystals is addressed. An improved measurement setup, consisting of two Michelson interferometers, is described. The electrostriction of eight alkali halides, three alkaline earth fluorides, and two materials with the diamond structure, was measured. In all the measurements, the frequency independence of the measured expansion in the frequency range from 40 Hz to 10 kHz, the reproducibility of the measurements, and a mathematically well defined anisotropic behavior of the crystals are guaranteed, thus, entrusting reliable measurements. A theory about the origin and magnitude of electrostriction is discussed. A model based on classical mechanics is used. A relation is shown between the electrostriction, on one hand, and dielectric and elastic material properties on the other. From this model, a physical insight can be obtained as to the internal forces in a lattice in a polarized state, leading to an electrostictive strain. ESA

N92-29911# Lawrence Livermore National Lab., CA.

THE ROLE OF CHEMICAL INTERACTIONS IN THE STABILITY OF ARTIFICIAL METALLIC SUPERLATTICES

M. Sluiter and P. E. A. Turchi 23 Dec. 1991 8 p Presented at the Annual Fall Meeting of the Materials Research Society, Boston, MA, 2-6 Dec. 1991

(Contract W-7405-eng-48)

(DE92-011528; UCRL-JC-107696; CONF-911202-70) Avail: CASI HC A02/MF A01

Atom by atom deposition techniques, such as magnetron sputtering, make possible the synthesis of artificial superlattices with composition modulations in one dimension on an atomic scale. Generally, elastic effects (lattice mismatch) and chemical affinity (ordering or clustering tendencies) are recognized as the most important driving forces for the thermodynamic stability of such materials. In this study the chemical aspect of stability will be examined using a formalism based on the first-principles electronic structure calculations developed originally for bulk alloys. The formalism has been applied to a number of systems with fcc and bcc transition metals as constituents. In some cases the stability of artificial superlattices was found to depend in a rather surprising and unexpected way on the direction and wavelength of the composition modulation. DOE

N92-29939# Ames Lab., IA.

NEUTRON DIFFRACTION STUDY OF THE ELECTRONIC STRUCTURE OF HIGH T(SUB c) SUPERCONDUCTOR-RELATED COMPOUNDS Ph.D. Thesis

Xun-Li Wang 16 Mar. 1992 161 p

(Contract W-7405-eng-82)

(DE92-012587; IS-T-1580) Avail: CASI HC A08/MF A02

Neutron diffraction techniques have been used to study the electronic structure of La2NiO4 and Sr2CuO2Cl2 by measuring the antiferromagnetic form factor of the single-crystal samples at 15 K. The antiferromagnetic form factor was obtained from the integrated intensities of several magnetic reflections. In both cases, the experimentally determined form factor exhibits a plateau at low Q values (up to 3 Angstrom (exp -1)), similar to that observed for La2CuO4. Detailed modeling of the experimental data of these three compounds suggests that the observed plateau may be accounted for by including the covalency effects in the Ni-O or Cu-O plane. The experimental data are also compared with spin-polarized band calculations. DOE

N92-30102*# National Aeronautics and Space Administration. Pasadena Office, CA.

METHOD OF FORMING SILICON STRUCTURES WITH SELECTABLE OPTICAL CHARACTERISTICS Patent Application

Robert W. Fathauer, inventor (to NASA) (Jet Propulsion Lab., California Inst. of Tech., Pasadena.) 10 Jul. 1992 14 p

(Contract NAS7-918)

(NASA-Case-NPO-18625-1-CU; NAS 1.71:NPO-18625-1-CU; US-Patent-Appl-SN-912981) Avail: CASI HC A03/MF A01

Silicon and metal are coevaporated onto a silicon substrate in a molecular beam epitaxy system with a larger than stoichiometric amount of silicon so as to epitaxially grow particles of metal silicide embedded in a matrix of single crystal epitaxially grown silicon. The particles interact with incident photons by resonant optical absorption at the surface plasmon resonance frequency. Controlling the substrate temperature and deposition rate and time allows the aspect ratio of the particles to be tailored to desired wavelength

photons and polarizations. The plasmon energy may decay as excited charge carriers or phonons, either of which can be monitored to indicate the amount of incident radiation at the selected frequency and polarization. NASA

N92-30175# North Carolina State Univ., Raleigh. Dept. of Materials Science and Engineering.
GROWTH, CHARACTERIZATION, AND DEVICE DEVELOPMENT IN MONOCRYSTALLINE DIAMOND FILMS
Quarterly Letter Report, 1 Jan. - 31 Mar. 1992
Robert F. Davis Mar. 1992 33 p
(Contract N00014-90-J-1604)
(AD-A248993) Avail: CASI HC A03/MF A01

The effects of hydrogen on cluster binding energy and growth mode of diamond, the determination of the Schottky barrier height for Ti on (111) diamond, and models for MESFET devices in diamond were the subjects addressed in this reporting period. Capillarity and atomistic formulations for determining diamond thin film growth modes were compared. Arguments are presented based on simple atomistic cluster binding energy calculations that suggest hydrogen should play an important role in stabilizing the 2-dimensional cluster configuration and thus promote layered diamond growth, assuming that the interfacial strain and misfit energies are not too high. Assumptions which may cause this model to break down experimentally are also discussed. The Ti-natural IIB(111) diamond interface was investigated using UV photo-emission produced by a 21.2 eV light source. The chemically cleaned diamond showed a sharp (0.5 eV FWHM) peak at the position of the conduction band indicating a negative electron affinity surface. By determining the relative positions of the diamond valence band edge and the titanium Fermi level, the Schottky barrier height of titanium on diamond (111) was measured and found to be 1.0 +/- 0.2 eV. A model for the observed titanium induced negative electron affinity is proposed, based on the Schottky barrier height of titanium on diamond, and the work function of titanium. A detailed, theoretical model for p-type diamond MESFETs is being developed. GRA

77 THERMODYNAMICS AND STATISTICAL PHYSICS

Includes quantum mechanics; theoretical physics; and Bose and Fermi statistics.

For related information see also *25 Inorganic and Physical Chemistry* and *34 Fluid Mechanics and Heat Transfer.*

N92-29517# Washington Univ., Seattle. Inst. for Nuclear Theory.
THEORETICAL OVERVIEW: HOT AND DENSE QCD IN EQUILIBRIUM
Tetsuo Hatsuda Nov. 1991 21 p Presented at the Quark Matter 1991, Gatlinburg, TN, 11-15 Nov. 1991
(Contract DE-FG06-90ER-40561)
(DE92-013665; DOE/ER-40561/038; CONF-9111165-13) Avail: CASI HC A03/MF A01

Static and dynamical properties of QCD at finite temperature and density are reviewed. Non-perturbative aspects of the QCD plasma and modification of the hadron properties associated with the chiral transition are discussed on the basis of lattice data, effective theories, and QCD sum rules. Special emphasis is laid on the importance of the finite baryon density to see the effects of the restoration of chiral symmetry in experiment. DOE

N92-29533# Moscow State Univ. (USSR). Nauchno-Issledovatel'skij Inst. Yadernoj Fiziki.
ON THE PARITY OF FUNDAMENTAL SOLUTIONS FOR ONE-DIMENSIONAL SCATTERING PROBLEM WITH INVERSE SQUARE POTENTIAL
V. S. Mineev 1991 13 p
(DE92-624511; INP-MSU-91-2-206; NIIYaF-MGU-91-2-206)
Avail: CASI HC A03/MF A01

Admissible techniques used to continue the fundamental solution for the stationary Schroedinger equation of inverse square potential through singular point x = 0 are analyzed in detail. Two types of self-adjoint extensions of the Schroedinger operator are shown to be admissible. The first type corresponds to the Schroedinger equation proper and defines the case of absolutely penetrable inverse square potential. The second type requires that a (delta)-shaped induced potential should be introduced in the equation and defines the case of absolutely impenetrable potential. DOE

N92-29781# Stockholm Univ. (Sweden). Dept. of Physics.
INTRODUCTION TO SO(3) MONOPOLE
Toshihiko Mori Dec. 1991 17 p
(USIP-91-05; ETN-92-91511) Avail: CASI HC A03/MF A01

The existence of the magnetic monopole is discussed. In Dirac's theory, the existence of a magnetic monopole may explain the quantization of electric charge. Years later, it was discovered that the time independent and spherically symmetric Higgs type SO(3) theory had a magnetic monopole solution. In the present investigation, concerning the t'Hooft monopole theory, the following topics are reviewed: the field theoretical model, the standard vacuum, the perturbation on the standard vacuum and the definition of an electromagnetic field tensor, the t'Hooft-Polyakov ansatz, the physical meaning of the spherically symmetric solution, the total magnetic charge, and the stability of the solution. The symmetrization and antisymmetrization of an arbitrary SO(3) gauge potential is discussed. ESA

N92-29996# Rutherford Appleton Lab., Chilton (England).
POLE COUNTING AND RESONANCE CLASSIFICATION
D. Morgan Jan. 1992 18 p
(RAL-92-004; ETN-92-91720) Avail: CASI HC A03/MF A01

S wave resonances occurring close to an inelastic threshold can be classified according to the number of nearby poles they posses, giving a useful possibility of distinguishing dynamical alternatives by objective appeal to data. Making this quantitative entails developing suitable effective range expansions for various realizations of potential scattering. A key application is deciding the make up of f(0)(976)(S*). ESA

N92-30148# Universiteit Twente, Enschede (Netherlands). Faculty of Applied Mathematics.
ON THE ENTROPY PRODUCTION OF DISSIPATION MODELS
J. W. vanderBurg, J. G. M. Kuerten, R. M. J. vanDamme, and P. J. Zandbergen 6 Jan. 1992 30 p Sponsored in part by NAL
(MEMO-1021; ISSN-0169-2690; ETN-92-91766) Avail: CASI HC A03/MF A01

A discrete version of the second law of thermodynamics is used to examine the existence of nonophysical expansion shocks in the discrete solution of the Cauchy problem for a hyperbolic conservation law. Four numerical schemes are investigated including Roe's scheme and Jameson's scheme. The discrete entropy condition is used to show that the entropy fix in Roe's scheme is necessary. A priori bounds in the dissipative parameters in Jameson's scheme are derived. ESA

N92-30212# Academy of Sciences (USSR), Novosibirsk. Inst. Yadernoj Fiziki.
ON THE TWO-DIMENSIONAL MODEL OF QUANTUM REGGE GRAVITY
V. M. Khatsimovskij 1991 15 p
(DE92-624516; IYaF-91-40) Avail: CASI HC A03/MF A01

The Ashtekar-like variables are introduced in the Regge calculus. A simplified model of the resulting theory is quantized canonically. The consequences related to quantization of Regge areas are obtained. DOE

N92-30005*# Rider Coll., Lawrenceville, NJ. Dept. of Physics.
EFFECTS OF RETARDATION IN RELATIVISTIC EQUATIONS WITH CONFINING INTERACTION
Khin Maung Maung (Hampton Inst., VA.), David E. Kahana (Continuous Electron Beam Accelerator Facility, Newport New, VA.), and John W. Norbury *In its* Electromagnetic Processes in

Nucleus-Nucleus Collisions Relating to Space Radiation Research 1992 6 p (For primary document see N92-30001 20-72)
(Grants NAG1-477; NAG1-1134)
Avail: CASI HC A02/MF A03

80 SOCIAL SCIENCES (GENERAL)

Includes educational matters.

No abstracts in this category.

81 ADMINISTRATION AND MANAGEMENT

Includes management planning and research.

N92-29822# Technische Univ., Eindhoven (Netherlands). Dept. of Mathematics and Computing Science.
THE CAPACITATED MULTI-ECHELON INVENTORY SYSTEM WITH SERIAL STRUCTURE: 1: THE PUSH AHEAD-EFFECT
C. J. Speck and J. vanderWal Dec. 1991 16 p
(Memo-COSOR-91-39; ISSN-0926-4493; ETN-92-91793) Avail: CASI HC A03/MF A01

A multi echelon, periodic review inventory model with discrete demand is considered. Finite capacities on various production/order sizes and backordering of excess demand are assumed. It is shown that under the average cost criterion the optimal order strategy may be characterized by a so called 'push ahead' effect. A modified base stock policy is found to approximate the optimal policy quite well. ESA

N92-29823# Technische Univ., Eindhoven (Netherlands). Dept. of Mathematics and Computing Science.
THE CAPACITATED MULTI-ECHELON INVENTORY SYSTEM WITH SERIAL STRUCTURE: 2: AN AVERAGE COST APPROXIMATION METHOD
C. J. Speck and J. vanderWal Dec. 1991 20 p
(Memo-COSOR-91-40; ISSN-0926-4493; ETN-92-91794) Avail: CASI HC A03/MF A01

A multi-echelon, periodic review inventory model with discrete demand is considered. Finite capacities on various production/order sizes and back ordering of excess demand are assumed. It has already been seen that the modified base stock policies work quite well under an average cost criterion. A method which provides an approximation of the average costs corresponding to a modified base stock policy in a certain class of multi-echelon serial systems is presented. In this, the moment iteration method developed by De Kok plays a central role. ESA

N92-29886# Oesterreichisches Forschungszentrum Seibersdorf G.m.b.H., Vienna. Hauptabt. Technologieforschung.
DIVERSIFICATION AND PRODUCT INNOVATION: A CHALLENGE FOR MODERN MANAGEMENT [DIVERSIFIKATION UND PRODUKTINNOVATION: EINE HERAUSFORDERUNG FUER DAS MODERNE MANAGEMENT]
Reinhard Herdin and Siegfried Huemer Feb. 1991 51 p In GERMAN
(OEFZS-4570; ETN-92-91337) Copyright Avail: CASI HC A04/MF A01

Requirements for successful innovation are worked out with reference to innovation as a process of learning and creating resources. A multistage module for technology oriented product finding and diversification is developed. Specific business areas are generated and assessed with regard to their attractiveness. The searching areas is screened for feasible new product ideas, which are assessed and selected with respect to the criteria of technological feasibility, market and product attractiveness. This results in suggestions for new products, which are selected according to their order of priority. ESA

82 DOCUMENTATION AND INFORMATION SCIENCE

Includes information management; information storage and retrieval technology; technical writing; graphic arts; and micrography.

For computer documentation see *61 Computer Programming and Software.*

N92-29552# Sandia National Labs., Albuquerque, NM.
A LOOK AT THE DEVELOPMENT ENVIRONMENT AND TOOLS USED IN A LARGE INGRES ABF APPLICATION PROJECT
M. J. Eaton 1991 9 p Presented at the North American Ingres Users Association (NAIUA) Meeting, Tarpan Springs, FL, May 1992
(Contract DE-AC04-76DP-00789)
(DE92-012632; SAND-91-2790C; CONF-9205138-2) Avail: CASI HC A02/MF A01

The organization of the INGRES ABF developer's environment tends to be an overlooked aspect of the application development process. Very often this environment develops haphazardly over time as deficiencies and new requirements are identified. This paper will describe some of the problems encountered and the solutions devised. The topics to be discussed are the following: the directory structure used to segregate the multitude of different files required by a large development effort; initialization command procedures for users and developers used to define the various symbols and logical names; file naming conventions; techniques used for configuration management and version control of ABF applications; procedures to assist the developers in quickly switching between the development and production versions of the databases; and tools developed to automate the generation of table and form documentation. DOE

N92-29553*# Research Inst. for Computing and Information Systems, Houston, TX.
NASA VISUAL THESAURUS MAINTENANCE DOCUMENTATION Interim Report
Jul. 1989 197 p Prepared in cooperation with Texas Univ., Austin
(Contract NCC9-16; RICIS Proj. IM-10)
(NASA-CR-190282; NAS 1.26:190282) Avail: CASI HC A09/MF A03

The following document is presented in six sections: (1) introduction; (2) a diagram showing how the various routines are grouped together into functional modules; (3) a printout of all the layouts in the system along with their associated layout procedures; (4) listings of all the global procedures in the system; (5) a cross-reference of all identifiers used in the system; and (6) descriptions of the external procedures used in the system. The document was prepared at the Project ICON Image Scaling Laboratory. Author

N92-29663# Office of Management and Budget, Washington, DC. Office of Information and Regulatory Affairs.
CURRENT INFORMATION TECHNOLOGY RESOURCE REQUIREMENTS OF THE FEDERAL GOVERNMENT: FISCAL YEAR 1992 Annual Report
Dec. 1991 357 p Prepared in cooperation with General Services Administration, Washington, DC; and Commerce Dept., Washington, DC
(PB92-147180) Avail: CASI HC A16/MF A03

The document is based on information submitted in support of the budget of the United States Government fiscal year 1992, and consists of a compilation of individual Federal agency information technology acquisition plans for the fiscal years 1991 through 1996. It should be noted that the resources data contained in the document is subject to change and was prepared prior to the enactment of fiscal year 1992 appropriations. The Office of

Management and Budget's purpose in making this information available is twofold: to encourage and support public and oversight agency participation in the important decision-making process of how best to use information technology to improve the responsiveness and efficiency of the Federal government; and to encourage competition in the Federal information technology market by providing information on opportunities to potential vendors. Author

N92-29699# Honeywell, Inc., Saint Louis Park, MN. Military Avionics Div.
ENHANCED EVALUATION, SELECTION AND ACCEPTANCE CRITERIA FOR THE CONTRACTOR INTEGRATED TECHNICAL INFORMATION SERVICE (CITIS)
C. P. Gehan 1992 12 p
(PB92-163856) Avail: CASI HC A03/MF A01

The purpose of the paper is as follows: recommended approaches which may be applied to assure successful data exchange for near term Computer Aided Logistic Support (CALS) deliverables (that is, those which preserve data content and format and maximize use of CALS digital interchange standards); recommend approaches which may be applied to assure successful access to and use of information which resides within the Contractor's Integrated Technical Information System (CITIS) for its intended purposes; and provide for any given type of CALS deliverable, a framework for determining the following: what the evaluation method options are, what the acceptance criteria should be, and what the selection criteria should be. Author

N92-29720# South Carolina Research Authority. Charleston.
PDES APPLICATION PROTOCOL SUITE FOR COMPOSITES (PAS-C): IDEFO ACTIVITY MODELS AND INFORMATION NEEDS FOR THE PAS-C PROGRAM Report, Jul. - Dec. 1991
Mike Stowe, Ray Grella, Keith Hunten, Floyd Ganus, and Dennis Biddle Mar. 1992 260 p
(Contract F33615-91-C-5713)
(AD-A248714; PASC006.01.00; WL-TR-92-8018) Avail: CASI HC A12/MF A03

This document addresses the requirements gathering process of an informational needs analysis for composite parts. A standard set of composite terminology and informational constructs were updated based on expert review and a comparison to other standards organizations' composite terminology. This updated terminology provides a framework for organizing and capturing the information into a usable/reusable structure. The scope of the needs analysis focused in the areas of Analysis, Design, and Manufacturing. An overall functional node tree and IDEFO models that establish the informational requirements are included. An attempt was also made to extract from composite experts a set of unique composite part characteristics. GRA

N92-29794# Los Alamos National Lab., NM.
ON THE ABSTRACTED DATAFLOW COMPLEXITY OF FAST FOURIER TRANSFORMS
A. P. W. Boehm (Colorado State Univ., Fort Collins.), R. E. Hiromoto, K. A. Kelly, and J. M. Ashley (Indiana Univ., Bloomington.) 1992 21 p Presented at the ACM SIGARCH International Conference on Supercomputing, Washington, DC, 19-24 Jul. 1992
(Contract W-7405-eng-36)
(DE92-011372; LA-UR-92-805; CONF-920730-3) Avail: CASI HC A03/MF A01

We develop and analyze the simulated performance of codes for the Fast Fourier Transform written in Id and targeted for execution on Motorola's dataflow machine Monsoon. The FFT application is of interest because of its computational parallelism, its requirement for global communications, and its array element data dependences. We use the parallel profiling simulator Id World to study the dataflow performance of various implementations. Our approach is comparative. We study two approaches, a recursive and an iterative one, and in each version we examine the effect of a variety of implementations. We contend that only through such comparative evaluations can significant insight be gained in understanding the computational and structural details of functional algorithms. DOE

N92-29934# Logistics Management Inst., Bethesda, MD.
APPLICATION CENTER OF EXCELLENCE (ACE) PROGRAM Final Report
Dennis J. OConnor Oct. 1991 22 p
(Contract MDA903-90-C-0006)
(AD-A248694; LMI-PL019R1) Avail: CASI HC A03/MF A01

The Application Center of Excellence (ACE) program increases the effectiveness of the Office of the Assistant Secretary of Defense (Production and Logistics) OASD (P and L) by exploiting the capabilities of installed computing equipment and augmenting those capabilities of installed computing equipment and/augmenting those capabilities with new technologies. In FY91, its first year of operation, the program has developed capabilities for more effective management presentations and improved connectivity to external systems. The OASD (P and L) staff is now able to produce engaging presentations in a variety of media and to connect to many external systems from the desktop. For OASD (P and L) to derive the full benefits of the program, the ACE program manager should establish guidelines for future operations. Our recommendations pertain to guidelines on the ACE infrastructure (program participants and resources) and the process used to conduct ACE business. GRA

N92-29957# Universiteit Twente, Enschede (Netherlands). Dept. of Computer Science.
INTEGRITY CONTROL IN RELATIONAL DATABASE SYSTEMS: AN OVERVIEW
Paul W. P. J. Grefen 13 Nov. 1991 54 p
(Memo-INF-91-80; ISSN-0924-3755; ETN-92-91578) Avail: CASI HC A04/MF A01

An overview of research regarding integrity control or integrity constraint handling in relational database management systems, including concepts and techniques of other types of database systems, where necessary, is given. The topic of constraint handling is discussed from two points of view: by identifying a number of important research issues and by treating each issue in detail; and by describing a number of projects that have resulted in the realization of database management systems supporting integrity constraints, where the various projects are compared with respect to a number of system characteristics. Together, both approaches give a complete overview of the state of the art in the field at this moment. An extensive bibliography with index is included. ESA

N92-30000# Universiteit Twente, Enschede (Netherlands). Tele-Informatics and Open Systems Group.
WHAT IS THE METHOD IN FORMAL METHODS?
Ed Brinksma Nov. 1991 22 p Presented at the FORTE 1991 Conference, Sydney, Australia, 19-22 Nov. 1991 Sponsored in part by Commission of the European Communities
(Memo-INF-91-79; TIOS-91/029; ISSN-0924-3755; ETN-92-91771) Copyright Avail: CASI HC A03/MF A01

An attempt to analyze the difficulties of obtaining formal methods by taking a look at the tension between the two fundamental approaches that underly the engineering of information systems (the 'formal' approach, i.e., the internally consistent description of virtual objects, based on the principle of analysis by logical deduction, and the 'scientific' approach, i.e., the externally consistent description of physical objects, based on the principle of validation (or refutation) by experimentation) is presented. One conclusion is that there is a need to be able to combine formal validation of designs, i.e., by mathematical means, with experimental validation of designs, i.e., by testing, within a single methodological framework. Some first ideas of what such a framework could look like are given. ESA

N92-30033# Department of Agriculture, Beltsville, MD. Cooperative State Research Service.
CRIS/USDA ONLINE ACCESS GUIDE. REVISION 1: FILE 60 ON DIALOG Final Report

Nov. 1991 175 p
(PB92-172857; USDA/CRIS/AG-91/11) Avail: CASI HC A08/MF A02

The report is a guide to searching the Current Research Information System (CRIS)/U.S. Department of Agriculture (USDA) online database on DIALOG. CRIS is the USDA documentation and reporting system for publicly supported agricultural, food and nutrition, and forestry research in the United States. The CRIS database consists of descriptions of research projects conducted or sponsored by the USDA, the State agricultural experiment stations and land-grant institutions, State forestry schools, Tuskegee University, U.S. schools of veterinary medicine, and participants in the competitive research grants program of the Department. Projects on human nutrition research and other Federal agencies are also included in CRIS in the Human Nutrition Research and Information Management System (HNRIMS) subfile. The guide is designed to assist online users in acquiring a fuller understanding of the CRIS online file. Intended for the practitioner familiar with the basic commands and search features of the DIALOG system, it provides the in-depth coverage needed for developing more effective and efficient searches of the CRIS/USDA database. Author

N92-30038# National Academy of Public Administration, Washington, DC.
ARCHIVES OF THE FUTURE: ARCHIVAL STRATEGIES FOR THE TREATMENT OF ELECTRONIC DATABASES
2 Dec. 1991 156 p
(Contract NAXXOP9000159)
(PB92-178631) Avail: CASI HC A08/MF A02

The purpose was to provide the National Archives and Records Administration (NARA) with criteria to assist it in the appraisal of electronic databases for transfer to the National Archives. It resulted in the compilation of an inventory of major program-related databases that in turn informs NARA about the present database environment and identifies issues in building an electronic archive of the nation's history. With respect to recommendations, NARA should adopt a more active stance of pursuing agency data that may not have been scheduled, a strategy that entails an expansion of its present outreach program. NARA should develop guidelines and standards to create more uniform agency behavior and should establish a directory of the Archives' databases. NARA should investigate the possibilities for decentralized archives. Author

N92-30039# National Inst. of Standards and Technology, Gaithersburg, MD.
OVERVIEW OF THE DOCUMENT STYLE SEMANTICS AND SPECIFICATION LANGUAGE AND THE MIL-M-28001A OUTPUT SPECIFICATION
R. B. Wilson Mar. 1992 17 p
(PB92-181122; NISTIR-4800) Avail: CASI HC A03/MF A01

Compared here are functional similarities between the Document Style Semantics and Specification Language (DSSSL) and the Output Specification (OS) of MIL-M-28001A. It is envisioned that when DSSSL becomes an International Standard (IS), it will assume the responsibilities of the OS and be referenced by MIL-M-28001A. Therefore, an initial examination of each standard's capabilities is warranted. The discussion is intended for persons with some working knowledge of the Standard Generalized Markup Language (SGML) and a minimal knowledge of DSSSL and OS. Author

N92-30040# Geological Survey, Reston, VA.
LEXICON OF NEW FORMAL GEOLOGIC NAMES OF THE UNITED STATES, 1981-1985
G. W. Luttrell, M. L. Hubert, and C. R. Murdock 1991 382 p
(PB92-181320; USGS-BULL-1565; LC-91-22753) Avail: CASI HC A17/MF A03

Brief descriptions are given of new formal geologic names in the United States and Puerto Rico that were introduced between 1981 and 1985. Information given for each name includes geologic age, geographic location, geologic province, type locality, subunits, and a summary of the lithology, genesis, structure, adjoining units, correlations, and thickness. Author

N92-30194# Space Environment Services Center, Boulder, CO.
SESC GLOSSARY OF SOLAR-TERRESTRIAL TERMS
Feb. 1992 78 p Revised
(PB92-185305) Avail: CASI HC A05/MF A01

The National Plan for Space Environment Services and Supporting Research stipulates that the Space Environment Services Center (SESC) provide space environment services to meet the common needs of all Federal Agencies and public users. The SESC collects observations and compiles a real-time data base in the Space Environment Laboratory Data Acquisition and Display System (SELDADS). The data are used by the SESC to monitor solar and geomagnetic activity and radiation levels, to issue indexes and alerts describing current conditions, and to make forecasts of future conditions. The users of these services include, among others, customers concerned with satellite monitoring, national defense, and scientific research ranging from solar to seismic physics. A common vocabulary is necessary to help such a diverse variety of customers achieve the best use of the services. The manual provides a collection of customized definitions and standardized terms specifically used by the SESC in its products, publications, and user support services. Author

83 ECONOMICS AND COST ANALYSIS

Includes cost effectiveness studies.

No abstracts in this category.

84 LAW, POLITICAL SCIENCE AND SPACE POLICY

Includes NASA appropriation hearings; aviation law; space law and policy; international law; international cooperation; and patent policy.

No abstracts in this category.

85 URBAN TECHNOLOGY AND TRANSPORTATION

Includes applications of space technology to urban problems; technology transfer; technology assessment; and surface and mass transportation.

For related information see also *03 Air Transportation and Safety, 16 Space Transportation,* and *44 Energy Production and Conversion.*

N92-29671# Office of Technology Assessment, Washington, DC.
GLOBAL STANDARDS: BUILDING BLOCKS FOR THE FUTURE
Mar. 1992 122 p
(PB92-167352; OTA-TCT-512) Avail: CASI HC A06/MF A02

The study considers the U.S. standards setting process in light of the changing economic and technological environment. Looking across industry sectors, the study compares the U.S. system with those of other countries, particularly the European Economic Community (EEC). Where remedies seem to be warranted, the Office of Technology Assessment (OTA) suggests alternative strategies and options that the U.S. might pursue. Author

N92-29808# Federal Aviation Administration, Cambridge, MA. National Transportation Systems Center.
HIGH-SPEED MAGLEV TRAINS: GERMAN SAFETY REQUIREMENTS RW-MSB
Jan. 1992 261 p Transl. into ENGLISH of Magnetschnellbannen: Sicherheitstechnische Anforderungen (Fed. Republic of Germany), Mar. 1991 261 p Sponsored in part by Federal Railroad Administration, Washington DC
(PB92-167006; DOT-VNTSC-FRA-92-1; DOT/FRA/ORD-92/01)
Avail: CASI HC A12/MF A03

This is a translation of technology-specific safety requirements developed for the German Transrapid Maglev technology. These requirements were developed by a working group composed of representatives of German Federal Railways (DB), Testing and Planning Company for Maglev System (MVO), industry, Institute Railway Technology (IFB), and safety experts of TUV Rheinland and TUV Hannover headed by TUV Rheinland and sponsored by the German Federal Ministry of Research and Technology. Topic areas covered include: levitation, propulsion, energy and control systems, load assumptions and vehicle and guideway stability, design, production and quality assurance of mechanical structures, switches, lighting protection, electromagnetic compatibility, electrostatic discharge, fire protection, and rescue plan. Author

N92-29809# Federal Aviation Administration, Cambridge, MA. National Transportation Systems Center.
GERMAN HIGH-SPEED MAGLEV TRAIN SAFETY REQUIREMENTS: POTENTIAL FOR APPLICATION IN THE UNITED STATES Interim Report, Jan. 1991 - Jan. 1992
R. M. Dorer, S. H. Markos, R. A. Wlodyka, H. S. Lee, and M. Coltman Feb. 1992 248 p Sponsored in part by Federal Railroad Administration, Washington, DC
(PB92-167014; DOT-VNTSC-FRA-92-3; DOT/FRA/ORD-92/3)
Avail: CASI HC A11/MF A03

The report is the second in a series of reports addressing the safety of high-speed maglev trains and presents the results of the review to determine the suitability of German safety requirements for application to maglev systems as proposed for U.S. operations. The intent of the review was to compare the German and U.S. safety requirements in order to assist the Federal Railroad Administration (FRA) in determining what regulations and guidelines may be necessary to ensure a high level of safety for U.S. passenger service. The German safety requirements were reviewed in terms of safety related functional areas of the following seven maglev system elements: vehicles; guideway; passenger stations; signal, control, and communications (SCC); plans and procedures; personnel; and operating environment. Potential safety concerns for each of the maglev system functional areas were identified. The German safety requirements and the applicable U.S. safety requirements are described and then compared to determine their applicability to proposed U.S. maglev system operations. Recommendations are also included for FRA consideration. In general, the German effort appears to ensure the same high level of safety for maglev trains that is expected in the U.S. for similar ground transportation technologies. The challenge lies in transferring the experience of Germany to the U.S. regulatory environment. Author

N92-30037# Grumman Aerospace Corp., Bethpage, NY. Space and Electronics Div.
NEW YORK STATE TECHNICAL AND ECONOMIC MAGLEV EVALUATION Final Report
Jun. 1991 271 p Sponsored by New York State Energy Research and Development Authority
(PB92-174119; NYSERDA-91-5) Avail: CASI HC A12/MF A03

The study is the preliminary evaluation of magnetically levitated (MAGLEV) ground transportation systems. The evaluation focuses on using the New York State Thruway right-of-way in combination with MAGLEV systems currently in development in Germany and Japan and those proposed for development in the United States. The Energy Authority's goal in cosponsoring the study was to determine if MAGLEV offered the potential to meet future New York State transportation demands cost-effectively, and to evaluate the benefits that the State might expect from supporting MAGLEV technology development and system implementation. According to the preliminary report, substantial economic benefits could accrue to the state through MAGLEV-related research, development, manufacturing, and construction. Implementation would have a favorable impact on issues related to transportation, the environment, and energy conservation. With the exception of the German Transrapid system, developing a domestic prototype MAGLEV vehicle would take seven to nine years; no insurmountable technical barriers are apparent. EMF (electromagnetic fields) shielding is, however, a concern. It will cost an estimated one billion dollars to develop a new MAGLEV system design; however, innovative designs may reduce the price. Author

88 SPACE SCIENCES (GENERAL)

No abstracts in this category.

89 ASTRONOMY

Includes radio, gamma-ray, and infrared astronomy, and astrometry.

N92-29359*# TRW, Inc., Redondo Beach, CA. Space and Technology Group.
IMAGE INVERSION ANALYSIS OF THE HST OTA (HUBBLE SPACE TELESCOPE OPTICAL TELESCOPE ASSEMBLY), PHASE A Final Technical Report
M. M. Litvak 18 Jul. 1991 35 p Revised
(Contract JPL-958888)
(NASA-CR-190483; JPL-9950-1381; NAS 1.26:190483; TRW-SN-57661) Avail: CASI HC A03/MF A01

Technical work during September-December 1990 consisted of: (1) analyzing HST point source images obtained from JPL; (2) retrieving phase information from the images by a direct (noniterative) technique; and (3) characterizing the wavefront aberration due to the errors in the Hubble Space Telescope (HST) mirrors, in a preliminary manner. This work was in support of JPL design of compensating optics for the next generation wide-field planetary camera on HST. This digital technique for phase retrieval from pairs of defocused images, is based on the energy transport equation between these image planes. In addition, an end-to-end wave optics routine, based on the JPL Code 5 prescription of the unaberrated HST and WFPC, was derived for output of the reference phase front when mirror error is absent. Also, the Roddier routine unwrapped the retrieved phase by inserting the required jumps of +/- 2(pi) radians for the sake of smoothness. A least-squares fitting routine, insensitive to phase unwrapping, but nonlinear, was used to obtain estimates of the Zernike polynomial coefficients that describe the aberration. The phase results were close to, but higher than, the expected error in conic constant of the primary mirror suggested by the fossil evidence. The analysis of aberration contributed by the camera itself could be responsible for the small discrepancy, but was not verified by analysis.
Author

N92-29468# Tuebingen Univ. (Germany, F.R.). Fakultaet fuer Physik.
ANALYSIS OF HIGH ENERGY X RAY OBSERVATIONS OF LONG PERIODIC PULSARS Ph.D. Thesis [ANALYSE VON HOCHENERGIE-ROENTGENBEOBACHTUNGEN LANGPERIODISCHER PULSARE]
Bruno Mony 1991 112 p In GERMAN
(ETN-92-91494) Avail: CASI HC A06/MF A02

The high energy x-ray observations of the three long periodic x-ray pulsars, GX 1+4, Vela X-1, and A0535 +26, carried out on

the Space Station Mir with the High Energy X-ray Experiment (HEXE) were analyzed. Phenomena, which were unknown up to now, were identified for each pulsar. From the measured spectra, GX 1+4 is deduced to have a relatively strong magnetic field. A common characteristic of Vela X-1 and A0535 +26 is the variability of the spectral hardness over the pulse phase. Using theories describing the spin up and spin down behavior of pulsars, a value was deducted for the magnetic field hardness. ESA

N92-29596# Virginia Univ., Charlottesville. Dept. of Astronomy.
THE 12 MICRON CONTRIBUTION OF NEARBY GALAXIES TO THE INFRARED BACKGROUND Annual Report, 1 Aug. 1990 - 30 Sep. 1991
Trinh X. Thuan 30 Sep. 1991 3 p
(Grant AF-AFOSR-0467-89)
(AD-A250623; AFOSR-92-0422TR) Avail: CASI HC A01/MF A01

The forty ultraluminous galaxies in the IRAS Bright Galaxy Sample of sources were mapped with 0.25 second resolution at 8.44 gigahertz. Twenty five contain diffuse radio sources. These are almost certainly starburst galaxies. The IRAS flux densities for all galaxies detected in the Faint Source Survey have been obtained. The data contains a total of 1544 galaxies. The detection rate in the FSS improves substantially by a factor of three or more for the short wavelength bands at 12 and 25 microns. This sample will form the basis for studies of the far infrared properties of optically selected galaxies. GRA

N92-29682# Royal Observatory, Edinburgh (Scotland).
UNITED KINGDOM INFRARED TELESCOPE Annual Report, 1990
1990 57 p Prepared in cooperation with Joint Astronomy Centre, Hilo, HI
(ETN-92-91341) Avail: CASI HC A04/MF A01

The scientific and operations reports for the United Kingdom Infrared Telescope (UKIRT) on Mauna Kea (Hawaii) are presented. The historical development of UKIRT is outlined. The instrumentation development is described. Two highlights of the instrumentation program in 1990 were the Cooled Grating Spectrometer (CGS3) for the 10 and 20 micrometer windows and CGS4 for the 1 to 5 micrometer waveband using array detectors. A financial statement is given. ESA

90 ASTROPHYSICS

Includes cosmology; celestial mechanics; space plasmas; and interstellar and interplanetary gases and dust.

For related information see also *75 Plasma Physics*.

N92-29833# Max-Planck-Inst. fuer Physik und Astrophysik, Garching (Germany, F.R.).
TRACES OF THE PRIMORDIAL STRUCTURE IN THE UNIVERSE
Hans Boehringer, ed. and Rudolf A. Treumann, ed. May 1991 197 p Workshop held in Tegernsee, Fed. Republic of Germany, 1-5 Oct. 1990
(MPE-227; ISSN-0178-0719; ETN-92-91737) Avail: CASI HC A09/MF A03

Twenty papers presented at the Workshop on Traces and Primordial Structure in the Universe are enclosed. The observation of large structure in the Universe as reflected in the distribution of the galaxies is discussed and the distribution and evolution of clusters of galaxies is considered. The theory of the evolution of large scale structure in the Universe, including observational evidence, is also discussed. Some early results obtained by the x-ray telescope on Rosat (x-ray astronomy satellite) are considered. For individual titles, see N92-29834 through N92-29853.

N92-29834# Tartu Astronoomia Observatooriumi (USSR).
RECONSTRUCTION OF DENSITY AND POTENTIAL FIELDS OF THE UNIVERSE
Mirt Gramann and Jaan Einasto *In* MPI fuer Physik und Astrophysik, Traces of the Primordial Structure in the Universe May 1991 p 7-19 (For primary document see N92-29833 20-90)
Avail: CASI HC A03/MF A03

Model and galaxy samples are analyzed in an attempt to see how galaxy and cluster samples could be used to characterize the total mass distribution of the Universe. A model which satisfactorily reproduces the basic properties of the observed structure is used to investigate how the distributions for the total matter, galaxies, and clusters in this model are mutually related. The relation between the distributions of galaxies and clusters in the real Universe is studied. The potential reconstruction method to restore the spectrum density fluctuations and potential field for the total matter starting from the distribution of clusters is proposed and results of the application of this method are analyzed. ESA

N92-29835# Max-Planck-Inst. fuer Astrophysik, Garching (Germany, F.R.).
CDM WITH THERMAL HISTORY OF BARYONS: HIGH-RESOLUTION 2-D AND 3-D SIMULATIONS
Ronald E. Kates and Alexander A. Klypin (Academy of Sciences, USSR, Moscow) *In* MPI fuer Physik und Astrophysik, Traces of the Primordial Structure in the Universe May 1991 p 21-30 (For primary document see N92-29833 20-90)
Avail: CASI HC A02/MF A03

Results of recent two dimensional and three dimensional simulations of gravitational and thermal processes involved in galaxy formation are described and compared. The physics is simplified in the simulations discussed by the assumption that baryons move along the same trajectories as dark matter, i.e., the density ratio of dark matter to baryons is taken to be a constant. To the extent that deviations from this assumption occur over scales smaller than those of interest, the technique makes new and reliable predictions relevant to temperature and emission properties of hot gas in superclusters and to galaxy formation in Cold Dark Matter (CDM). In particular, gas present in superclusters should have a characteristic temperature of approximately 1,000,000 K, which is ten times lower than estimated previously. The most favorable range for observing this radiation is about 100 to 300 eV. Soft x-rays emitted from hot gas in known superclusters may be detectable at the limits of sensitivity of Rosat (x-ray astronomy satellite) by averaging position sensitive proportional counters counts over a sufficiently large region. ESA

N92-29836# Edinburgh Univ. (Scotland). Dept. of Astronomy.
THE SIGNIFICANCE OF LARGE-SCALE FLOWS INTO THE GREAT ATTRACTOR
Alan Heavens *In* MPI fuer Physik und Astrophysik, Traces of the Primordial Structure in the Universe May 1991 p 31-37 (For primary document see N92-29833 20-90)
Avail: CASI HC A02/MF A03

A method which uses the flow of galaxies from all directions into the Great Attractor as a simple but powerful test for the spectrum of density fluctuations and the value of the density parameter, is discussed. The most straightforward interpretation of the depth of the potential well at the Great Attractor is that the density parameter is rather high, and there is some strong observational evidence supporting the theoretical prejudice that the density parameter equals 1. This test is particularly effective because it probes the regime in which the perturbations are still linear, very few assumptions are required, and there are few of the uncertainties which beset other tests. Provided only that the perturbations are gravitational and Gaussian, and that galaxies trace the velocity field, the depth of the potential at the Great Attractor, plus the degree of nonlinearity of the density field, can be used to put tight constraints on models of galaxy formation. For example, limiting the nonlinearity of the density field by current microwave background limits constrains the density parameter to be approximately greater than 0.5 for cold dark matter models. Using the Infrared Astronomy Satellite (IRAS) density field to fix the level of nonlinearity as well argues that, on large scales, IRAS galaxies trace the mass density. Consideration of a wider range

of power law fluctuation spectra allows the density parameter to be reduced to around 0.2 to 0.3, but values as low as required by nucleosynthesis for a baryonic Universe are strongly excluded. ESA

N92-29837# Johns Hopkins Univ., Baltimore, MD.
CLUSTER CORRELATIONS FROM N-POINT CORRELATION AMPLITUDES
I. Szapudi (Space Telescope Science Inst., Baltimore, MD.), Alexander S. Szalay (Eoetvoes Lorand Univ., Budapest, Hungary), and Peter Boschan (Eoetvoes Lorand Univ., Budapest, Hungary) *In* MPI fuer Physik und Astrophysik, Traces of the Primordial Structure in the Universe May 1991 p 39-56 Sponsored by NSF and OTKA (For primary document see N92-29833 20-90)
Avail: CASI HC A03/MF A03

It is shown, by using a new technique, how the much debated cluster correlation function is directly related to the higher order galaxy correlations. Mathematical techniques from biased galaxy formation are adopted: the biasing simulates the detection of the clusters, rather than their dynamic formation. A simple, analytical example is given. As a practical application of the simplified model, a novel method to determine the amplitudes of the irreducible N point correlation functions in the gravitational clustering hierarchy is presented. The corrected Lick catalog is used to obtain values of qN up to N = 8, considerably beyond previous attempts. The catalog, obtained from the Lick sample, has amplifications similar to the rich clusters, and the galaxy 'cluster' cross correlation is close to the geometric mean of the galaxy and cluster autocorrelations. ESA

N92-29838# Osservatorio Astronomico, Bologna (Italy).
ABELL CLUSTERS OF GALAXIES: CATALOGS AND LARGE-SCALE STRUCTURES
Giovanni Zamorani (Consiglio Nazionale delle Ricerche, Bologna, Italy), R. Scaramella (Osservatorio Astronomico, Rome, Italy), G. Vettolani (Consiglio Nazionale delle Ricerche, Bologna, Italy), and Guido Chincarini (Milan Univ., Italy) *In* MPI fuer Physik und Astrophysik, Traces of the Primordial Structure in the Universe May 1991 p 59-68 (For primary document see N92-29833 20-90)
Avail: CASI HC A02/MF A03

Results of a statistical analysis of the ACO (Abell, Corwin, and Olowin) and Abell catalogs of clusters of galaxies are summarized together with results on the large scaler distribution of these clusters. New estimates of distances, surface and radial densities are described that were derived for both catalogs. On both catalogs the effects of large scale angular gradients were studied. The ACO catalog appears to be more complete, with a larger volume density of clusters than the Abell catalog. The number density of clusters derived after corrections for angular incompleteness for both catalogs is higher than the value usually used in the literature for the volume density of rich clusters. It is shown with a check made on new redshifts that the distance estimates agree well, within the estimated uncertainties, with measured ones. Figures of the distribution of clusters in the Super Galactic plane, up to distances of 300/h Mpc are summarized and major features of this large scale distribution are outlined. These are especially important also in the light of the issue of large scale peculiar motions. ESA

N92-29839# Osservatorio Meteorologico di Brera, Milan (Italy).
SCALE-INVARIANT GALAXY CLUSTERING ON LARGE SCALES
Luigi Guzzo, Guido Chincarini (Milan Univ., Italy), Angela Iovino, Riccardo Giovanelli (Arecibo Ionospheric Observatory, Puerto Rico.), and Martha P. Haynes (Cornell Univ., Ithaca, NY.) *In* MPI fuer Physik und Astrophysik, Traces of the Primordial Structure in the Universe May 1991 p 69-73 (For primary document see N92-29833 20-90)
Avail: CASI HC A01/MF A03

The scaling properties of galaxy clustering at large separations were explored using the Perseus-Pisces region redshift catalog and other correlation results from the literature. The analysis reveals that the distribution of galaxies in scales much larger than the correlation length still obeys a very small defined scaling law, characterized by a fractal dimension D approximately equal to 2.2. Homogeneity seems to be reached for separations greater than 30/h Mpc, while for r less than 4/h Mpc the large scale symmetry is broken into the 'standard' D approximately equal to 1.2 clustering usually evidenced by two point correlation analyses. These features are presented in all the different redshift surveys analyzed. It is argued that this result could be explained as the consequence of gravitational small scale amplification of an initially scale invariant distribution with D approximately equal to 2, corresponding to a spectrum of fluctuations with (the absolute value of delta k) squared proportional to 1/(k squared). ESA

N92-29840# Max-Planck-Inst. fuer Astrophysik, Garching (Germany, F.R.).
MORPHOLOGICAL SEGREGATION OF GALAXIES ON LARGE SCALES
Hou-Jun Mo *In* MPI fuer Physik und Astrophysik, Traces of the Primordial Structure in the Universe May 1991 p 75-83 (For primary document see N92-29833 20-90)
Avail: CASI HC A02/MF A03

To test possible morphological segregation of galaxies on large scales, pair count ratio (between early type and late type galaxies) and clustering analysis were used to galaxy redshift samples formed in both supercluster regions and in regions where there is no apparent large concentration of galaxy distribution, and to galaxy samples in which galaxies in clusters and groups of galaxies are removed. It was found that systematic segregation by morphology exists on scales up to approximately 10/h Mpc. ESA

N92-29841# Muenster Univ. (Germany, F.R.). Inst. fuer Astronomie.
SCALES OF UNIVERSAL HOMOGENEITY FROM GALAXY COUNTS
Peter Schuecker and Heinz-Albert Ott *In* MPI fuer Physik und Astrophysik, Traces of the Primordial Structure in the Universe May 1991 p 85-87 (For primary document see N92-29833 20-90)
Avail: CASI HC A01/MF A03

Using subsamples of galaxies the following are determined: mean variances of galaxy number densities, scales of homogeneity, and the presence of large scale structures. Details of the homogeneity analysis and fluctuation analysis are given and the results graphically illustrated. ESA

N92-29842# European Southern Observatory, Garching (Germany, F.R.).
THE SPACE DISTRIBUTION OF LOCAL RADIO GALAXIES
Peter A. Shaver *In* MPI fuer Physik und Astrophysik, Traces of the Primordial Structure in the Universe May 1991 p 89-97 (For primary document see N92-29833 20-90)
Avail: CASI HC A02/MF A03

An analysis of the Molonglo Catalogue indicated that significant departures from isotropy are present in the sky distribution of strong extragalactic radio sources. This was shown to be due to local large scale structure, specifically a concentration to the supergalactic plane, which also influences the slope of the source counts. A study of the three dimensional distribution of local radio galaxies shows that they are more strongly concentrated to the supergalactic plane than are optically selected galaxies, and that the supergalactic concentration is more extensive than hitherto believed. It appears that radio galaxies (and clusters of galaxies) trace the 'skeleton' of large structure, about which normal galaxies are more loosely distributed. ESA

N92-29843# Durham Univ. (England). Dept. of Physics.
STUDIES OF DISTANT CLUSTERS OF GALAXIES
Richard S. Ellis *In* MPI fuer Physik und Astrophysik, Traces of the Primordial Structure in the Universe May 1991 p 101-111 (For primary document see N92-29833 20-90)
Avail: CASI HC A03/MF A03

The following topics are discussed: recent developments in

understanding the origin of the 'Butcher-Oemler' effect, arising from detailed optical and infrared studies of galaxies in selected clusters; a new catalog of southern clusters, complementing the northern catalog of Gunn, Hoessel and Oke (1986), which provides an estimate of the space density tool clusters to redshift z approximately equal to 0.5; the properties of early type galaxies in an extensive optical infrared survey of clusters with z(bar) = 0.75; the prospects for finding clusters with red shift z greater than 1 (if they exist) and the likely role of Rosat (x-ray astronomy satellite) in such programs. ESA

N92-29844*# National Aeronautics and Space Administration. Goddard Space Flight Center, Greenbelt, MD.
EVIDENCE FOR EVOLUTION OF THE LUMINOSITY FUNCTION OF CLUSTERS OF GALAXIES
Alastair C. Edge (Cambridge Univ., England), G. C. Stewart (Leicester Univ., England), A. C. Fabian (Cambridge Univ., England), and K. A. Arnaud *In* MPI fuer Physik und Astrophysik, Traces of the Primordial Structure in the Universe May 1991 p 113-117 Sponsored in part by Royal Society and Science Research Council (For primary document see N92-29833 20-90)
Avail: CASI HC A01/MF A03

From an all sky, x-ray flux limited sample of clusters of galaxies evidence for a significant deficit in the number of high luminosity clusters is found in the redshift range z approximately 0.1 to 0.2 compared with numbers of nearby clusters. This indicates that the x-ray luminous clusters are undergoing strong evolution. The strength of the effect is consistent with hierarchical merging models. The implications of such strong evolution for clusters are discussed. ESA

N92-29845# Max-Planck-Inst. fuer Physik und Astrophysik, Garching (Germany, F.R.). Inst. fuer Extraterrestrische Physik.
CONSTRAINTS ON THE MASS FLUCTUATION SPECTRUM FROM X RAY OBSERVATIONS OF CLUSTERS OF GALAXIES
Abstract Only
J. Patrick Henry (Hawaii Univ., Honolulu.) *In its* Traces of the Primordial Structure in the Universe May 1991 p 119 (For primary document see N92-29833 20-90)
Avail: CASI HC A01/MF A03

Two independent constraints on the mass fluctuation spectrum of the Universe are reported. Both constraints use x-ray measurements of clusters of galaxies. A statistically complete sample of galaxy clusters which also have complete x-ray temperature information is presented. Using this sample the cluster temperature function was derived. A sample of clusters was extracted from the Einstein Medium sensitivity survey whose flow was limited and 98.4 percent identified. It contained 93 x-ray selected clusters out to a redshift of z = 0.58. Using this sample the x-ray luminosity function was obtained at three cosmic epochs. ESA

N92-29846# Rome Univ. (Italy). Dipartimento di Fisica.
CLUSTERS OF GALAXIES IN DEPTH
Alfonso Cavaliere and S. Colafrancesco *In* MPI fuer Physik und Astrophysik, Traces of the Primordial Structure in the Universe May 1991 p 123-125 (For primary document see N92-29833 20-90)
Avail: CASI HC A01/MF A03

The distribution in depth of clusters of galaxies with large velocity dispersions, as measured in the optical band, may be consistent with approximate uniformity. In x-rays, preliminary evidence suggested a substantial dearth of luminous cluster sources in the past which has now been confirmed. X-ray and optical luminosities are linked to the dynamical masses. The (comoving) mass distribution is considered. It is concluded that fast x-ray and slower optical anti evolution at redshift z approximately equal to 0.5 will point to direct hierarchical collapse of biased overdensities in a dense universe to produce structures with increasing gas content and temperature. Additional implications include L/L(sub 0) proportional to M(sup 2/3), only limited cooling flows, and Fe/H decreasing towards us. ESA

N92-29847# Michigan Univ., Ann Arbor. Dept. of Physics.
X RAY CLUSTER COUNTS: WHAT ROSAT SHOULD SEE
August E. Evrard and J. Patrick Henry (Max-Planck-Inst. fuer Extraterrestrische Physik, Garching, Germany, F.R.) *In* MPI fuer Physik und Astrophysik, Traces of the Primordial Structure in the Universe May 1991 p 127-142 (For primary document see N92-29833 20-90)
Avail: CASI HC A03/MF A03

Expectations for characteristics of the x-ray cluster population observable by Rosat (x-ray astronomy satellite) are presented. The modeling requires an initial fluctuation spectrum and relations describing the behavior of cluster x-ray luminosity and core radius with cluster binding mass and red shift. ESA

N92-29848# Max-Planck-Inst. fuer Extraterrestrische Physik, Garching (Germany, F.R.).
THE EVOLUTION OF THE X RAY LUMINOSITY FUNCTION OF GALAXY CLUSTERS
Hans Boehringer *In* MPI fuer Physik und Astrophysik, Traces of the Primordial Structure in the Universe May 1991 p 143-152 (For primary document see N92-29833 20-90)
Avail: CASI HC A03/MF A03

It is assumed that clusters of galaxies evolve from high peaks in the primordial density fluctuation field which can be described by a Gaussian field. From a statistical analysis of peaks in the fluctuation field and the assumption of linear evolution of the density fluctuations a distribution function for the mass and amplitude of protocluster density fluctuations can be derived. Using plausible physical scaling laws and observationally determined parameters these distribution functions can be converted into the x-ray luminosity function of galaxy clusters which can in turn be compared with observations. The goal of this analysis (which is still in progress) is a theoretical model that allows for direct comparison with x-ray observations and involves only one scaling factor as open parameter once the form of the power spectrum of the primordial density fluctuations have been chosen. ESA

N92-29849# Max-Planck-Inst. fuer Astrophysik, Garching (Germany, F.R.).
N-BODY SIMULATIONS OF THE EVOLUTION OF CLUSTERS OF GALAXIES
Sabine Schindler *In* MPI fuer Physik und Astrophysik, Traces of the Primordial Structure in the Universe May 1991 p 153-160 (For primary document see N92-29833 20-90)
Avail: CASI HC A02/MF A03

Several models for the formation of clusters of galaxies with different initial conditions are presented: spherical collapse models, a steady infall model and a collision model. For each of these models the evolution and the phase space distribution of the virialized state was investigated. It is shown that the phase space distribution in the virial equilibrium still contains information on the different types of initial conditions. ESA

N92-29850# Max-Planck-Inst. fuer Extraterrestrische Physik, Garching (Germany, F.R.).
ROSAT: EARLY RESULTS
Joachim E. Truemper *In* MPI fuer Physik und Astrophysik, Traces of the Primordial Structure in the Universe May 1991 p 163-181 (For primary document see N92-29833 20-90)
Avail: CASI HC A03/MF A03

The general scientific objectives of ROSAT (x-ray astronomy satellite) are to perform the first all sky surveys using imaging x-ray and EUV (Extreme Ultraviolet) telescopes, and to perform detailed investigations of interest sources in a guest investigator program. A few details on the scientific instruments on the ROSAT spacecraft are given and results obtained by the x-ray telescope are summarized. Position Sensitive Proportional Counters (PSPC) maps of Orion, Cygnus loop soft band, Auriga and the all sky survey are enclosed. ESA

N92-29851*# Max-Planck-Inst. fuer Physik und Astrophysik, Garching (Germany, F.R.). Inst. fuer Extraterrestriche Physik.
THE X RAY MORPHOLOGY OF THE RELAXED CLUSTER OF GALAXIES A2256. 1: EVIDENCE FOR A MERGER EVENT
U. G. Briel, J. Patrick Henry, Raimund A. Schwarz, Hans Boehringer, Harald Ebeling, Alastair C. Edge, Gisela D. Hartner, Sabine Schindler, Joachim E. Truemper, and Wolfgang Voges *In its* Traces of the Primordial Structure in the Universe May 1991 p 183-195 Sponsored in part by BMFT; Royal Society; and Science Research Council (For primary document see N92-29833 20-90)
(Grants NAG5-1256; NSF INT-89-12660)
Avail: CASI HC A03/MF A03

The rich cluster of galaxies A2256 was studied utilizing the imaging proportional counter (PSPC (Position Sensitive Proportional Counters)) on board the x-ray observatory ROSAT. A2256 is considered to be a relaxed, Comalike cluster which is dynamically well evolved. However, clear evidence for substructure in A2256 was found. The x-ray surface brightness distribution reveals two separate maxima in the center, one of which is coincident with the central cD galaxy while the morphology of the other shows indications that it is merging with the main cluster body. The x-ray temperatures of the two maxima are different; the probable merging object being about a factor of five cooler than the cluster. The previously measured broad velocity distribution supports the idea that a merger in this cluster is being observed. ESA

N92-29852*# Max-Planck-Inst. fuer Physik und Astrophysik, Garching (Germany, F.R.). Inst. fuer Extraterrestrische Physik.
THE X RAY MORPHOLOGY OF THE RELAXED CLUSTER OF GALAXIES A2256. 2: SOURCES AROUND THE EXTENDED CLUSTER EMISSION
J. Patrick Henry and U. G. Briel *In its* Traces of the Primordial Structure in the Universe May 1991 p 197-203 Sponsored in part by BMFT (For primary document see N92-29833 20-90)
(Grants NAG5-1256; NSF INT-89-12660)
Avail: CASI HC A02/MF A03

X-ray emission from cluster galaxies as well as from 'dark objects' (i.e. not visible on the Palomar Observatory Sky Survey (POSS)) seen in the x-ray observation of A2256 with the imaging proportional counter on board ROSAT (x-ray astronomy satellite), is reported. This observation revealed significantly more sources in the field around the extended cluster emission than one would expect by chance. In a preliminary investigation, 14 sources were discovered at the limiting flux for this exposure, whereas about 7 sources would have been expected by chance. At least two of those sources are coincident with cluster member galaxies, having x-ray luminosities of approximately 10(exp +42) erg/s in the ROSAT energy band from 0.1 to 2.4 keV, but at least four more are from 'dark' objects. The similarity of these objects to those in A1367 suggests the existence of a new class of x-ray sources in clusters. ESA

N92-29853# Naval Research Lab., Washington, DC.
OPTICAL SEARCHES FOR ROSAT X RAY CLUSTER SOURCES
Ray G. Cruddace and H. T. MacGillivray (Royal Observatory, Edinburgh, Scotland) *In* MPI fuer Physik und Astrophysik, Traces of the Primordial Structures in the Universe May 1991 p 205-221 (For primary document see N92-29833 20-90)
Avail: CASI HC A03/MF A03

The identification of x-ray sources in the ROSAT (x-ray astronomy satellite) all sky survey relies heavily on comparison of the x-ray positions with those of objects found at other wavelengths. The use of Schmidt telescope surveys, which have achieved the most detailed description of the whole sky to date, is described. The data base which summarizes the characteristics of some 500 million objects identified on the United Kingdom Schmidt plates, is considered. This data base is interrogated routinely in identifying ROSAT sources. A study of x-ray clusters of galaxies in the southern sky is being carried out and automatic techniques used to search for clusters on a Schmidt plate at the location of a ROSAT source are described. ESA

91 LUNAR AND PLANETARY EXPLORATION

Includes planetology; and manned and unmanned flights. For spacecraft design or space stations see *18 Spacecraft Design, Testing and Performance.*

N92-29401*# Wisconsin Univ., Madison. Space Science and Engineering Center.
VENUS IN MOTION: AN ANIMATED VIDEO CATALOG OF PIONEER VENUS ORBITER CLOUD PHOTOPOLARIMETER IMAGES Progress Report, 15 Jun. - 31 Dec. 1991
Sanjay S. Limaye 17 Jul. 1992 15 p
(Grant NAG5-1609)
(NASA-CR-190543; NAS 1.26:190543) Avail: CASI HC A03/MF A01

Images of Venus acquired by the Pioneer Venus Orbiter Cloud Photopolarimeter (OCPP) during the 1982 opportunity have been utilized to create a short video summary of the data. The raw roll by roll images were first navigated using the spacecraft attitude and orbit information along with the CPP instrument pointing information. The limb darkening introduced by the variation of solar illumination geometry and the viewing angle was then modelled and removed. The images were then projected to simulate a view obtained from a fixed perspective with the observer at 10 Venus radii away and located above a Venus latitude of 30 degrees south and a longitude 60 degrees west. A total of 156 images from the 1982 opportunity have been animated at different dwell rates. Author

N92-29432*# Arizona Univ., Tucson. Lunar and Planetary Lab.
ORIGIN AND EVOLUTION OF PLANETARY ATMOSPHERES Final Report, 1 Jul. 1982 - 30 Apr. 1992
John S. Lewis 30 May 1992 114 p
(Grant NAGw-340)
(NASA-CR-190579; NAS 1.26:190579) Avail: CASI HC A06/MF A02

This report concerns several research tasks related to the origin and evolution of planetary atmospheres and the large-scale distribution of volatile elements in the Solar System. These tasks and their present status are as follows: (1) we have conducted an analysis of the volatility and condensation behavior of compounds of iron, aluminum, and phosphorus in the atmosphere of Venus in response to publish interpretations of the Soviet Venera probe XRF experiment data, to investigate the chemistry of volcanic gases, injection of volatiles by cometary and asteroidal impactors, and reactions in the troposphere; (2) we have completed and are now writing up our research on condensation-accretion modeling of the terrestrial planets; (3) we have laid the groundwork for a detailed study of the effects of water transport in the solar nebula on the bulk composition, oxidation state, and volatile content of preplanetary solids; (4) we have completed an extensive laboratory study of cryovolcanic materials in the outer solar system; (5) we have begun to study the impact erosion and shock alteration of the atmosphere of Mars resulting from cometary and asteroidal bombardment; and (6) we have developed a new Monte Carlo model of the cometary and asteroidal bombardment flux on the terrestrial planets, including all relevant chemical and physical processes associated with atmospheric entry and impact, to assess both the hazards posed by this bombardment to life on Earth and the degree of cross-correlation between the various phenomena (NO(x) production, explosive yield, crater production, iridium signature, etc.) that characterize this bombardment. The purpose of these investigations has been to contribute to the developing understanding of both the dynamics of long-term planetary atmosphere evolution and the short-term stability of planetary surface environments. Author

N92-29451*# State Univ. of New York, Stony Brook. Inst. for Terrestrial and Planetary Atmospheres.
ANALYSIS OF EUV DAYGLOW SPECTRA OF TRITON, TITAN AND EARTH Annual Progress Report
Jane Lee Fox Jul. 1992 22 p

(Grant NAGw-2483)
(NASA-CR-190586; NAS 1.26:190586) Avail: CASI HC A03/MF A01

We have begun our studies of Titan and Triton by setting up a coupled ion and neutral chemical model of the ionosphere and thermosphere of Titan. The chemical scheme employs over 100 reactions and 46 species. Transport by diffusion and eddy diffusion of neutrals is included along with ambipolar diffusion of ions. We have computed the photoionization, photodissociations, electron impact excitation and ionization rates for the most important species, and the densities of ions and neutrals for a dayside model. We have computed the heating rates as a function of altitude and the heating efficiencies. We find that the heating efficiency in our standard model varies from about 30 percent near 800 km to 22 percent near 2000 km. We report here also on some photoelectron impact excitation rates for band systems of N2 in the Titan atmosphere. In the future, we propose to polish and publish our model, extend it to Triton, and look into excitation and emission of the N2 and N2(+) band systems. Author

N92-29600# Pacific Northwest Lab., Richland, WA.
BEAM-POWERED LUNAR ROVER DESIGN
J. E. Dagle, E. P. Coomes, Z. I. Antoniak, J. A. Bamberger, J. M. Bates, M. A. Chiu, R. E. Dodge, and J. A. Wise Mar. 1992 45 p
(Contract DE-AC06-76RL-01830)
(DE92-011511; PNL-8053) Avail: CASI HC A03/MF A01

Manned exploration of our nearest neighbors in the solar systems is the primary goal of the Space Exploration Initiative (SEI). An integral part of any manned lunar or planetary outpost will be a system for manned excursions over the surface of the planet. This report presents a preliminary design for a lunar rover capable of supporting four astronauts on long-duration excursions across the lunar landscape. The distinguishing feature of this rover design is that power is provided to the rover via a laser beam from an independent orbiting power satellite. This system design provides very high power availability with minimal mass on the rover vehicle. With this abundance of power, and with a relatively small power-system mass contained in the rover, the vehicle can perform an impressive suite of mission-related activity. The rover might be used as the first outpost for the lunar surface (i.e., a mobile base). A mobile base has the advantage of providing extensive mission activities without the expense of establishing a fixed base. This concept has been referred to as 'Rove First'. A manned rover, powered by a laser beam, has been designed for travel on the lunar surface for round-trip distances in the range of 1000 km, although the actual distance traveled is not crucial since the propulsion system does not rely on energy storage. The life support system can support a 4-person crew for up to 30 days, and ample power is available for mission-related activities. The 8000-kg rover has 30 kW of continuous power available via a laser transmitter located at the Earth-moon L1 libration point, about 50,000 km above the surface of the moon. This rover, which is designed to operate in either day or night conditions, has the flexibility to perform a variety of power-intensive missions. DOE

N92-30199*# Space Physics Research Inst., Sunnyvale, CA.
DIURNAL FORCING OF PLANETARY ATMOSPHERES
Semiannual Status Report, 1 Jul. - 31 Dec. 1991
Howard C. Houben 31 Dec. 1991 33 p
(Contract NCC2-680)
(NASA-CR-190262; NAS 1.26:190262) Avail: CASI HC A03/MF A01

A free convection parameterization has been introduced into the Mars Planetary Boundary Layer Model (MPBL). Previously, the model would fail to generate turbulence under conditions of zero wind shear, even when statically unstable. This in turn resulted in erroneous results at the equator, for example, when the lack of Coriolis forcing allowed zero wind conditions. The underlying cause of these failures was the level 2 second-order turbulence closure scheme which derived diffusivities as algebraic functions of the Richardson number (the ratio of static stability to wind shear). In the previous formulation, the diffusivities were scaled by the wind shear--a convenient parameter since it is non-negative. This was the drawback that all diffusivities are zero under conditions of zero shear (viz., the free convection case). The new scheme tests for the condition of zero shear in conjunction with static instability and recalculates the diffusivities using a static stability scaling. The results for a simulation of the equatorial boundary layer at autumnal equinox are presented. (Note that after some wind shear is generated, the model reverts to the traditional diffusivity calculation.) Author

N92-29384*# Jet Propulsion Lab., California Inst. of Tech., Pasadena.
GALILEO EARLY CRUISE, INCLUDING VENUS, FIRST EARTH, AND GASPRA ENCOUNTERS
P. E. Beyer, R. C. OConnor, and D. J. Mudgway *In its* The Telecommunications and Data Acquisition Report 15 May 1992 p 265-281 (For primary document see N92-29364 20-32)
(RTOP 314-40-22-37-01)
Avail: CASI HC A03/MF A04

N92-29388*# Jet Propulsion Lab., California Inst. of Tech., Pasadena.
DSN OBSERVATIONS OF TITAN
R. M. Goldstein and R. F. Jurgens *In its* The Telecommunications and Data Acquisition Report 15 May 1992 p 377-379 (For primary document see N92-29364 20-32)
(RTOP 196-41-73-02-00)
Avail: CASI HC A01/MF A04

92 SOLAR PHYSICS

Includes solar activity, solar flares, solar radiation and sunspots.

For related information see *93 Space Radiation.*

N92-29421# Stanford Univ., CA. Center for Space Science and Astrophysics.
GLOBAL SOLAR MAGNETIC FIELDS
J. T. Hoeksema 1991 12 p
(Contract N00014-89-J-1024; NSF ATM-86-18263)
(AD-A248340) Avail: CASI HC A03/MF A01

The global solar magnetic field greatly affects the corona, heliosphere, and terrestrial environment as well as revealing much about the Sun itself. It may be useful to think of the global field in two ways: as an aggregate of many small scale processes and as an entity. When considering the origin and evolution of the global field, one immediately focuses on the smaller-scale features and processes that it comprises. These include the emergence of active regions, the interaction of new and existing flux patterns, the distortion and dispersal of flux over the surface by convective motions, the phenomena that produce the emergence of patterns with various periods, and the influence of convection and rotation at various depths on flux tubes. When contemplating the effects of the global field, one often focuses on it as an entity or on its large-scale features. Examples are the reversal of the polar fields, the asymmetry between the north and south hemispheres, the dipole or quadrupole structure of the coronal field and its observation of the Earth as 2 or 4 polarity sectors, and the rigid rotation seen in coronal holes. Both views help us appreciate the significance of the global field. GRA

N92-29631*# Iowa Univ., Iowa City. Dept. of Physics and Astronomy.
A STUDY OF SHOCK-ASSOCIATED MAGNETOHYDRODYNAMIC WAVES IN THE SOLAR WIND
Final Report
Steven R. Spangler Jun. 1992 12 p
(Grant NAGw-1594)
(NASA-CR-190567; NAS 1.26:190567) Avail: CASI HC A03/MF A01

Three major topics were addressed, one theoretical and two observational. The topics were: (1) an attempt to understand the

evolution of the large-amplitude magnetohydrodynamic (MHD) waves in the foreshock, using a nonlinear wave equation called the Derivative Nonlinear Schrodinger equation (henceforth DNLS) as a model, (2) using the extensive set of ISE data to test for the presence of various nonlinear wave processes which might be present, and (3) a study of plasma turbulence in the interstellar medium which might be physically similar to that in the solar wind. For these investigations we used radioastronomical techniques. Good progress was made in each of these areas and a separate discussion of each is given. Author

N92-29632# Tufts Univ., Medford, MA. Dept. of Physics and Astronomy.
COMSTOC 4: MULTIWAVEBAND OBSERVATIONS OF SUNSPOT AND PLAGE-ASSOCIATED CORONAL EMISSION Interim Report
Jeffrey W. Brosius, Robert F. Willson, Gordon D. Holman, and Joan T. Schmelz 22 Jan. 1992 37 p
(Grant AF-AFOSR-0147-89)
(AD-A248344; AFOSR-92-0192TR) Avail: CASI HC A03/MF A01

Simultaneous observations of an active region located near the central meridian were obtained with the Very Large Array, the Solar Maximum Mission X-ray Polychromator, and the Beijing Observatory magnetograph on 18 December 1987, during the Coronal Magnetic Structures Observing Campaign (COMSTOC). An asymmetric loop-like structure connects the strong leading sunspot with a nearby region of opposite polarity. Both 6 and 20 cm emission lies along this structure, rather than over the sunspot, with higher frequency emission originating closer to the footpoint inside the sunspot. The 20 cm emission is due to a superposition of 2nd and 3rd harmonic gyroemission, where the field strength is 16- G- 300 G, while the 6 cm emission is due to the 3rd harmonic gyroemission from a region where the magnetic field strength ranges from 547 583 G. A high value of the Alfven speed of 40,000 km/sec, is obtained at the location of the 6 cm source, with somewhat lower values of 10,000 - 20,000 km/sec, at the location of the 20 cm emission. At the location of the 6 cm source, the plasma temperature diminishes with height from 2,500,000 K at 5000 km to 1,300,000 K at 15,000 km. GRA

N92-30204*# Lockheed Missiles and Space Co., Palo Alto, CA. Research and Development Div.
INVESTIGATION OF SOLAR ACTIVE REGIONS AT HIGH RESOLUTION BY BALLOON FLIGHTS OF THE SOLAR OPTICAL UNIVERSAL POLARIMETER, DEFINITION PHASE Final Report, Jul. 1989 - Mar. 1992
Theodore D. Tarbell and Kenneth P. Topka Mar. 1992 45 p
(Contract NAS8-38106)
(NASA-CR-184339; NAS 1.26:184339; LMSC/P009805) Avail: CASI HC A03/MF A01

The definition phase of a scientific study of active regions on the sun by balloon flight of a former Spacelab instrument, the Solar Optical Universal Polarimeter (SOUP) is described. SOUP is an optical telescope with image stabilization, tunable filter and various cameras. After the flight phase of the program was cancelled due to budgetary problems, scientific and engineering studies relevant to future balloon experiments of this type were completed. High resolution observations of the sun were obtained using SOUP components at the Swedish Solar Observatory in the Canary Islands. These were analyzed and published in studies of solar magnetic fields and active regions. In addition, testing of low-voltage piezoelectric transducers was performed, which showed they were appropriate for use in image stabilization on a balloon. Author

N92-30163*# Stanford Univ., CA. Center for Turbulence Research.
TURBULENT TRANSPORT IN THE SOLAR NEBULA
K. W. Thompson *In its* Annual Research Briefs, 1989 Feb. 1990 p 175-184 (For primary document see N92-30149 20-34)
Avail: CASI HC A02/MF A03

93 SPACE RADIATION

Includes cosmic radiation; and inner and outer earth's radiation belts.

For biological effects of radiation see *52 Aerospace Medicine.* For theory see *73 Nuclear and High-Energy Physics.*

N92-29360*# Southwest Research Inst., San Antonio, TX. Instrumentation and Space Research Div.
SOURCE LOCATION DETERMINATION OF URANIAN KILOMETRIC RADIATION FROM RAY TRACING AND EMISSION LOBE MODELLING Final Report
J. D. Menietti Sep. 1991 17 p Original contains color illustrations
(Contract JPL-958828; SwRI Proj. 15-3679)
(NASA-CR-190482; JPL-9950-1369; NAS 1.26:190482) Avail: CASI HC A03/MF A01; 1 functional color page

We use an analytical fit to an emission lobe profile together with three-dimensional ray tracing to model the broad-banded smooth Uranian kilometric radiation (UKR). We assume the radiation is gyroemission from sources along magnetic field lines. Using an iterative technique that modifies the lobe function and source region, the results are compared to observations at a frequency of 481 kHz. The best-fit calculations are compared to previously published models and to recent ultraviolet (UV) observations. Author

N92-29366*# Jet Propulsion Lab., California Inst. of Tech., Pasadena.
OCCULTATION OF A COMPACT RADIO SOURCE BY VENUS
R. Linfield *In its* The Telecommunications and Data Acquisition Report 15 May 1992 p 22-39 (For primary document see N92-29364 20-32)
(RTOP 310-10-60-60-00)
Avail: CASI HC A03/MF A04

N92-29367*# Jet Propulsion Lab., California Inst. of Tech., Pasadena.
A NANORADIAN DIFFERENTIAL VLBI TRACKING DEMONSTRATION
R. N. Treuhaft and S. T. Lowe *In its* The Telecommunications and Data Acquisition Report 15 May 1992 p 40-55 (For primary document see N92-29364 20-32)
(RTOP 310-10-60-86-02)
Avail: CASI HC A03/MF A04

N92-30002*# Rider Coll., Lawrenceville, NJ. Dept. of Physics.
CROSS SECTION PARAMETERIZATIONS FOR COSMIC RAY NUCLEI. 1: SINGLE NUCLEON REMOVAL
John W. Norbury and Lawrence W. Townsend (National Aeronautics and Space Administration. Langley Research Center, Hampton, VA.) *In its* Electromagnetic Processes in Nucleus-Nucleus Collisions Relating to Space Radiation Research 1992 24 p (For primary document see N92-30001 20-72)
(Grant NAG1-1134)
Avail: CASI HC A03/MF A03

99 GENERAL

N92-29464# Air Force Office of Scientific Research, Bolling AFB, Washington, DC.
THE 1991 RESEARCH HIGHLIGHTS
1991 81 p
(AD-A247865; AFOSR-92-0217TR) Avail: CASI HC A05/MF A01

This year the Air Force Office of Scientific Research (AFOSR) marks its 40th anniversary. For four decades, AFOSR scientists and engineers have ensured that cutting edge science and technology is available to Air Force and Department of Defense

(DoD) laboratories and U.S. industry. This document provides an outline of the basic research that is being undertaken by the AFOSR. GRA

N92-29471# Japan Broadcasting Corp., Tokyo. Science and Technical Research Lab.
THE 1990 ANNUAL REPORT, APRIL 1990 - MARCH 1991
Mar. 1991 26 p Original contains color illustrations
Avail: CASI HC A03/MF A01

This annual report briefly describes research results and activities of 1990 (from April, 1990 to March, 1991) of the NHK Science and Technical Research Laboratories. The Laboratories are engaged in wide-ranging research and development, including the analysis of human visual and auditory sensation, research into image pickup devices and recording materials, research into signal transmission and compression systems, and research into program production systems. These activities are categorized into three major research goals; 'new broadcast services,' 'improving existing broadcast services,' and 'basic technology to support future broadcasting.' Our research efforts over two decades were enabled to start to serve the direct satellite broadcasting and Hi-Vision (HDTV of Japan). Direct satellite broadcasting began with 24-hour service in June, 1989 on two channels of the present TV system and experimental Hi-Vision service was started via DBS. Furthermore, we are engaged in the development of new broadcast media for the early 21st century. Author

N92-29689*# National Aeronautics and Space Administration, Washington, DC.
RESEARCH IN NASA HISTORY: A GUIDE TO THE NASA HISTORY PROGRAM
May 1992 72 p
(NASA-TM-107953; NASA-HHR-55; NAS 1.15:107953) Avail: CASI HC A04/MF A01

This report describes the research opportunities and accomplishments of NASA's agency wide history program. It also offers a concise guide to the historical documentary resources available at NASA Headquarters in Washington D.C., at NASA facilities located around the country, and through the federal records system. In addition, this report contains expanded contributions by Lee D. Saegessor and other members of the NASA Headquarters History Division and by those responsible for historical documents and records at some NASA centers. H.A.

N92-29724# Research and Development Labs., Culver City, CA.
THE 1991 SUMMER FACULTY RESEARCH PROGRAM (SFRP), VOLUME 2 Report, 30 Sep. 1990 - 30 Sep. 1991
Gary Moore 9 Jan. 1992 785 p
(Contract F49620-90-C-0076)
(AD-A248764; AFOSR-92-0168TR-Vol-2) Avail: CASI HC A99/MF A10

The objectives of this program are as follows: to develop a basis for continuing research of interest to the Air Force at the institution of the faculty member; to stimulate continuing relations among faculty members and professional peers in the Air Force; to enhance the research interests and capabilities of scientific and engineering educators; and to provide follow-on funding for research of particular promise that was started at an Air Force laboratory under the Summer Faculty Research Program. During the summer of 1991 170 university faculty conducted research at Air Force laboratories for a period of 10 weeks. Each participant provided a report of their research, and these reports are consolidated into this annual report. GRA

N92-29725# Research and Development Labs., Culver City, CA.
THE 1991 SUMMER FACULTY RESEARCH PROGRAM (SFRP), VOLUME 3 Report, 30 Sep. 1990 - 30 Sep. 1991
Gary Moore 9 Jan. 1992 772 p
(Contract F49620-90-C-0076)
(AD-A248765; AFOSR-92-0169TR-Vol-3) Avail: CASI HC A99/MF A10

The objectives of this program were as follows: to develop the basis for continuing research of interest to the Air Force at the institution of the faculty member; to stimulate continuing relations among faculty members and professional peers in the Air Force; to enhance the research interests and capabilities of scientific and engineering educators; and to provide follow-on funding for research of particular promise that was started at an Air Force laboratory under the Summer Faculty Research Program. During the summer of 1991 170 university faculty conducted research at Air Force laboratories for a period of 10 weeks. Each participant provided a report of their research, and these reports are consolidated into this annual report. GRA

N92-30197*# National Aeronautics and Space Administration. John C. Stennis Space Center, Bay Saint Louis, MS.
RESEARCH AND TECHNOLOGY ANNUAL REPORT, FY 1990
1990 100 p
(NASA-TM-107807; NAS 1.15:107807) Avail: CASI HC A05/MF A02

Given here is the annual report of the John C. Stennis Space Center (SSC), a NASA center responsible for testing NASA's large propulsion systems, developing supporting test technologies, conducting research in a variety of earth science disciplines, and facilitating the commercial uses of NASA-developed technologies. Described here are activities of the Earth Sciences Research Program, the Technology Development Program, commercial programs, the Technology Utilization Program, and the Information Systems Program. Work is described in such areas as forest ecosystems, land-sea interface, wetland biochemical flux, thermal imaging of crops, gas detectors, plume analysis, synthetic aperture radar, forest resource management, applications engineering, and the Earth Observations Commercial Applications Program.
Author

SUBJECT INDEX

Typical Subject Index Listing

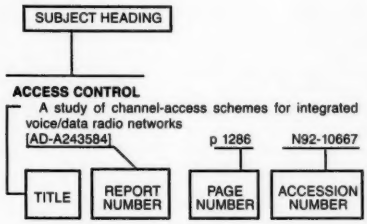

The subject heading is a key to the subject content of the document. Titles, report numbers, and accession numbers of pertinent documents are provided under each subject heading. When the title is insufficiently descriptive of the document content, a title extension has been added, separated from the title by three hyphens. The report number helps to indicate the type of document cited (e.g., NASA report, NASA translation, NASA contractor report). The accession number is the number by which the document abstracts are arranged in this journal and by which the document is sold or requested. The page number helps you locate the the citation in the abstract section. The titles, with title extensions if present, are arranged under each subject heading in ascending accession number order. The subject headings have been selected from the latest revision of the *NASA Thesaurus*.

A

A-300 AIRCRAFT
Ageing airplane repair assessment program for Airbus A300 p 3402 N92-30123

ABERRATION
Image inversion analysis of the HST OTA (Hubble Space Telescope Optical Telescope Assembly), phase A
[NASA-CR-190483] p 3564 N92-29359

ABRASIVES
Characterization of fracture in (0/90)3s SiC/1723 composites
[AD-A250612] p 3414 N92-29453

ABSORPTION SPECTRA
Femtosecond studies of carrier dynamics in compound semiconductors
[AD-A250584] p 3439 N92-29452
The 20 element HgI2 energy dispersive x ray array detector system
[DE92-013356] p 3549 N92-29502
Estimating plasma temperatures
[DE92-014092] p 3555 N92-29798

ABSORPTION SPECTROSCOPY
Infrared pulse-laser long-path absorption measurement of carbon dioxide using a Raman-shifted dye laser p 3465 N92-29277
Sound speed, reflectivity, and absorption measurements in Arctic ice in 1988
[AD-A246293] p 3505 N92-29554
Synthesis and characterization of a covalently bound self-assembled macrocycle monolayer thin film for nonlinear optical materials
[DE92-011353] p 3545 N92-29634
Estimating plasma temperatures
[DE92-014092] p 3555 N92-29798

ABSTRACTS
The 36th issue of Electronics and Electrical Engineering Laboratory Technical Progress Bulletin covering laboratory programs, July to September 1991, with 1992 EEEL events calendar
[PB92-164672] p 3442 N92-30032

ACCELEROMETERS
Accelerometer method and apparatus for integral display and control functions
[NASA-CASE-MSC-21961-1] p 3474 N92-29952

ACCEPTABILITY
Enhanced evaluation, selection and acceptance criteria for the Contractor Integrated Technical Information Service (CITIS)
[PB92-163856] p 3562 N92-29699

ACCESS CONTROL
Developments in fiber optics for distribution automation
[NASA-CR-190454] p 3551 N92-29679
A simulation study on a high-speed slotted-ring access mechanism with dynamically adaptive slot size
[MEMO-INF-91-63] p 3526 N92-30074

ACCIDENTS
Guide for evaluating 12 inch Substantial Dividing Walls (SDWs) to provide protection from remote operation, volume 1
[AD-A250251] p 3428 N92-29545
Final Environmental Impact Statement (EIS) for the Space Nuclear Thermal Propulsion (SNTP) program
[AD-A248408] p 3413 N92-29903
Final Environmental Impact Statement (EIS) for the Space Nuclear Thermal Propulsion (SNTP) program: Appendices
[AD-A248409] p 3413 N92-29904

ACCRETION DISKS
Turbulent thermal convection in a differentially rotating channel p 3455 N92-30168

ACETATES
Acetate in hydrothermal solutions: Decomposition kinetics and metal complexation
[DE92-010542] p 3417 N92-29551

ACETONITRILE
A study of the adsorption of acetonitrile on a gold electrode from aqueous solutions using in situ vibrational spectroscopy
[AD-A250191] p 3417 N92-29514

ACHIEVEMENT
The effects of student-instructor interaction and paired/individual study on achievement in computer-based training
[AD-A248518] p 3511 N92-29503

ACIDS
Polybenzimidazoles via aromatic nucleophilic displacement
[NASA-CASE-LAR-14643-1] p 3426 N92-29953

ACOUSTIC MEASUREMENT
Sound speed, reflectivity, and absorption measurements in Arctic ice in 1988
[AD-A246293] p 3505 N92-29554
Interface board for providing time signals to a super minicomputer
[AD-D015198] p 3441 N92-29900

ACOUSTIC PROPAGATION
Computational acoustics
[AD-A247688] p 3543 N92-29441

ACOUSTIC PROPERTIES
Active structural acoustic control and smart structures
[AD-A248341] p 3543 N92-29588
Interface board for providing time signals to a super minicomputer
[AD-D015198] p 3441 N92-29900

ACOUSTIC SCATTERING
Acoustic scattering from elastic ice: A finite difference solution
[AD-A248281] p 3543 N92-29346
Direct numerical simulation of instability and noise generation of hot jets p 3451 N92-30066

ACOUSTIC VELOCITY
Sound speed, reflectivity, and absorption measurements in Arctic ice in 1988
[AD-A246293] p 3505 N92-29554

ACOUSTICS
Adaptive signal processing at NOSC
[AD-A250245] p 3429 N92-29333
Computational acoustics
[AD-A247688] p 3543 N92-29441
Active structural acoustic control and smart structures
[AD-A248341] p 3543 N92-29588
Additivity and auditory pattern analysis
[AD-A250580] p 3511 N92-29592
Matched asymptotic expansions solution for low-frequency sound radiation from fluid-loaded, baffled plates: Axisymmetric case
[REPT-91-60] p 3543 N92-29628
Matched asymptotic expansions solution for low-frequency sound radiation from fluid-loaded, baffled plates: Two-dimensional case
[REPT-91-62] p 3543 N92-29748
Realistic models for predicting sound propagation in flow duct systems
[ISVR-TR-204] p 3544 N92-29814
Interface board for providing time signals to a super minicomputer
[AD-D015198] p 3441 N92-29900
Nonlinear analyses of composite aerospace structures in sonic fatigue
[NASA-CR-190565] p 3404 N92-30209

ACOUSTO-OPTICS
Programmable hyperspectral image mapper with on-array processing
[NASA-CASE-NPO-17794-1-CU] p 3553 N92-30104

ACTIVE CONTROL
Ultra-dependable real-time computing
[AD-A248193] p 3515 N92-29409
Spacecraft dynamics characterization and control system failure detection, volume 1
[NASA-CR-190517] p 3409 N92-29422
Active structural acoustic control and smart structures
[AD-A248341] p 3543 N92-29588
Instantaneous optimal control for linear, nonlinear and hysteretic structures: Stable controllers
[PB92-163807] p 3501 N92-29950

ACTIVE SATELLITES
Investigation of the structure of the electromagnetic field and related phenomena, generated by the active satellite
[NASA-CR-190446] p 3434 N92-29568

ACTUATORS
Active structural acoustic control and smart structures
[AD-A248341] p 3543 N92-29588
Experimental investigation of adaptive control of a parallel manipulator
[NASA-CR-189867] p 3528 N92-29656
Fastening apparatus having shape memory alloy actuator
[NASA-CASE-MSC-21935-1] p 3479 N92-29762
Combined load test apparatus for flat panels
[NASA-CASE-LAR-14698-1] p 3483 N92-30028

ADA (PROGRAMMING LANGUAGE)
On-line replacement of program modules using AdaPT
[NASA-CR-190499] p 3514 N92-29363

ADAPTIVE CONTROL
An examination of hypercube implementations of genetic algorithms
[AD-A248092] p 3515 N92-29527
Active structural acoustic control and smart structures
[AD-A248341] p 3543 N92-29588
Experimental investigation of adaptive control of a parallel manipulator
[NASA-CR-189867] p 3528 N92-29656
Robust adaptive kinematic control of redundant robots
[NASA-CR-190520] p 3528 N92-29673

ADAPTIVE OPTICS
Development of mesospheric sodium laser beacon for atmospheric adaptive optics p 3470 N92-29308
Characterization of artificial guidestars generated in the mesospheric sodium layer p 3470 N92-29309

ADDITIVES
Erbium-doped fiber amplifier elements for structural analysis sensors
[NASA-CR-190491] p 3552 N92-29681

Role of polyelectrolytes in barium sulphate precipitation
[PB92-184761] p 3419 N92-30196

ADIABATIC CONDITIONS
Hypersonic flow past radiation-cooled surfaces
[MBB-FE-202-S-PUB-0468-A] p 3401 N92-29713

ADSORPTION
A study of the adsorption of acetonitrile on a gold electrode from aqueous solutions using in situ vibrational spectroscopy
[AD-A250191] p 3417 N92-29514
Theory of the dissociation dynamics of small molecules on metal surfaces: Finite temperature studies
[DE92-011188] p 3546 N92-29899

ADSORPTIVITY
Theory of the dissociation dynamics of small molecules on metal surfaces: Finite temperature studies
[DE92-011188] p 3546 N92-29899

ADVECTION
Model for regional solute transport suited for calibration and management
[PB92-161371] p 3494 N92-29746

AERIAL RECONNAISSANCE
Airborne lidar observations of the stratosphere after the Pinatubo eruption p 3460 N92-29248

AERODYNAMIC CHARACTERISTICS
A comparison of the calculated and experimental off-design performance of a radial flow turbine
[NASA-CR-189207] p 3399 N92-29402
Spatial and temporal adaptive procedures for the unsteady aerodynamic analysis of airfoils using unstructured meshes
[NASA-TM-107635] p 3400 N92-29445
Computation of three-dimensional effects on two dimensional wings
[NASA-CR-190576] p 3401 N92-29691

AERODYNAMIC COEFFICIENTS
Determination of aerodynamic sensitivity coefficients for wings in transonic flow
[NASA-CR-190570] p 3401 N92-29657

AERODYNAMIC CONFIGURATIONS
Aerodynamic design optimization using sensitivity analysis and computational fluid dynamics
[NASA-CASE-LAR-14815-1-CU] p 3445 N92-29830

AERODYNAMIC DRAG
Methods for direct simulation of transition in hypersonic boundary layers 2 p 3451 N92-30064

AERODYNAMIC INTERFERENCE
Evaluation of measured-boundary-condition methods for 3D subsonic wall interference
[NLR-TR-88072-U] p 3401 N92-29884

AERODYNAMIC LOADS
Status of the FAA flight loads monitoring program p 3485 N92-30113

AERODYNAMICS
Parameter identification for nonlinear aerodynamic systems
[NASA-CR-190264] p 3399 N92-29329
Second-order shock-expansion theory extended to include real gas effects
[AD-A247191] p 3400 N92-29539
Aerodynamic design optimization using sensitivity analysis and computational fluid dynamics
[NASA-CASE-LAR-14815-1-CU] p 3445 N92-29830
A preliminary experimental investigation of local isotropy in high-Reynolds-number turbulence p 3447 N92-30042
Non-linear interactions in homogeneous turbulence with and without background rotation p 3448 N92-30044

AEROELASTICITY
Buffet test in the National Transonic Facility
[NASA-CR-189595] p 3406 N92-29352

AERONAUTICAL ENGINEERING
Aeronautical Engineering Group publications, 1950 - present
[AERO-REPT-8907] p 3444 N92-29683
Revision of certification standards for aviation maintenance personnel p 3487 N92-30127

AEROSOLS
Long term stratospheric aerosol lidar measurements in Kyushu p 3456 N92-29229
Southern Hemisphere lidar measurements of the aerosol clouds from Mt. Pinatubo and Mt. Hudson p 3456 N92-29230
Measurements of stratospheric Pinatubo aerosol extinction profiles by a Raman lidar p 3457 N92-29232
Raman lidar measurements of Pinatubo aerosols over southeastern Kansas during November-December 1991 p 3457 N92-29233
Lidar observations of stratospheric aerosol layer after the Mt. Pinatubo volcanic eruption p 3457 N92-29234
Interpretation of DIAL measurements of lower stratospheric ozone in regions with Pinatubo aerosols p 3457 N92-29236
Correcting for interference of Mt. Pinatubo aerosols on DIAL measurements of stratospheric ozone p 3458 N92-29237
A new Raman DIAL technique for measuring stratospheric ozone in the presence of volcanic aerosols p 3458 N92-29238
The NDSC primary site at the Observatoire de Haute-Provence: Ozone and aerosols observations (1986-1992) p 3458 N92-29240
Observation of stratospheric ozone with NIES lidar system in Tsukuba, Japan p 3459 N92-29242
Observations of ozone-aerosol correlated behaviour in the lower stratosphere during the EASOE campaign p 3459 N92-29243
GLObal Backscatter Experiment (GLOBE) results: Aerosol backscatter global distribution and wavelength dependence p 3459 N92-29245
Multi-wavelength airborne lidar intercomparisons of aerosol and cirrus backscatter over the Pacific Ocean p 3460 N92-29247
Multi-wavelength measurements of the stratospheric aerosol layer made at Hampton, Virginia (37N, 76W) p 3460 N92-29249
Three-wavelength lidar measurements of Pinatubo aerosol and its optical properties p 3460 N92-29250
Lidar observations of the Pinatubo stratospheric aerosol cloud over Frascati, Italy p 3460 N92-29251
L625 lidar measurements of Pinatubo volcanic cloud at Hefei p 3460 N92-29252
Two wavelength measurements of the Pinatubo aerosol above Toronto, Canada p 3461 N92-29253
Lidar observations of the Pinatubo volcanic cloud over Hampton, Virginia p 3461 N92-29254
Lidar measurements of stratospheric ozone, temperature and aerosol during 1992 UARS correlative measurement campaign p 3461 N92-29257
Airborne dial remote sensing of the Arctic ozone layer p 3462 N92-29258
Correction of DIAL stratospheric ozone measurements in the presence of Pinatubo aerosols p 3462 N92-29261
Intercomparisons of lidar backscatter measurements and in-situ data from GLOBE p 3463 N92-29266
Wind profiles derived from volume imaging lidar data: Enhancements to the algorithm and comparisons with insitu observations p 3464 N92-29271
DIAL mapping of atmospheric atomic mercury of geophysical origin p 3464 N92-29273
Extraction of aerosol and Rayleigh components from Doppler lidar return signal p 3465 N92-29281
One year of Rayleigh lidar measurements at Toronto p 3466 N92-29285
Lidar observation of aerosol and temperature stratification over urban area during the formation of a stable atmospheric PBL p 3466 N92-29286
Lidar investigation of aerosol pollution distribution near a coal power plant p 3467 N92-29289
A developing multiple-wavelength lidar for detecting mainly ozone and aerosol distributions in the stratosphere p 3467 N92-29292
Lidar observations of stratospheric clouds after volcanic eruption of Pinatubo p 3468 N92-29294
The Lidar In-Space Technology Experiment (LITE) p 3469 N92-29301
Lidar measurements of aerosol and ozone distributions during the 1992 Airborne Arctic Stratospheric Expedition p 3469 N92-29304
Aerosols and polar stratospheric clouds measurements during the EASOE campaign p 3469 N92-29306
Remote sensing by spaceborne lidar aided by surface returns p 3473 N92-29327
Evaluation of an aureole lidar technique for estimating extinction profiles
[AD-A249740] p 3501 N92-30087

AEROSPACE ENGINEERING
Maintainability requirements for ESA space systems
[ESA-PSS-01-50-ISSUE-1] p 3481 N92-29878
Fourth Meeting of the Space Agency Forum on the International Space Year (SAFISY-4)
[ESA-SP-1141] p 3407 N92-29879
A new HyperVelocity Launcher (HVL) for space science application
[DE92-010670] p 3408 N92-29986
NASA-UVA light aerospace alloy and structures technology program (LA2ST)
[NASA-CR-190538] p 3423 N92-30206

AEROSPACE ENVIRONMENTS
Surface reactions in the space environment
[AD-A250624] p 3428 N92-29428
SESC glossary of solar-terrestrial terms
[PB92-185305] p 3563 N92-30194

AEROSPACE MEDICINE
Publications of the environmental health program: 1980-1990
[NASA-CR-4455] p 3509 N92-29341
Test and evaluation report of the physio control defibrillator/monitor model LIFEPAK (trademark) 8
[AD-A248283] p 3510 N92-29347

AEROSPACE PLANES
Saenger: The reference concept and its technological requirements - aerothermodynamics
[MBB-FE-202-S-PUB-0463-A] p 3408 N92-29629
Technology programme: Aerothermodynamics and propulsion integration. Numerical and experimental aerothermodynamics
[MBB-FE-202-S-PUB-0464-A] p 3400 N92-29648
Aerothermodynamics and propulsion integration in the Saenger technology programme
[MBB-FE-202-S-PUB-0469-A] p 3400 N92-29649
Aerothermodynamic challenges of the Saenger space-transportation system
[MBB-FE-202-S-PUB-0462-A] p 3409 N92-29680

AEROSPACE SYSTEMS
Evaluating the military potential of a developing nation's space program: A case study of Brazil
[AD-A245978] p 3407 N92-29929

AEROTHERMODYNAMICS
Saenger: The reference concept and its technological requirements - aerothermodynamics
[MBB-FE-202-S-PUB-0463-A] p 3408 N92-29629
Technology programme: Aerothermodynamics and propulsion integration. Numerical and experimental aerothermodynamics
[MBB-FE-202-S-PUB-0464-A] p 3400 N92-29648
Aerothermodynamics and propulsion integration in the Saenger technology programme
[MBB-FE-202-S-PUB-0469-A] p 3400 N92-29649
Aerothermodynamic challenges of the Saenger space-transportation system
[MBB-FE-202-S-PUB-0462-A] p 3409 N92-29680
Hypersonic flow past radiation-cooled surfaces
[MBB-FE-202-S-PUB-0468-A] p 3401 N92-29713
Acquisition of an aerothermodynamic data base by means of a winged experimental reentry vehicle
[MBB/FE202/S/PUB/461] p 3399 N92-30232

AGGLOMERATION
Role of polyelectrolytes in barium sulphate precipitation
[PB92-184761] p 3419 N92-30196

AGING
The FAA aging airplane program plan for transport aircraft p 3402 N92-30128
Ageing aircraft research in the Netherlands p 3402 N92-30129
Survey of French activities concerning structural airworthiness and aging aircraft p 3402 N92-30130
Transport Canada aging aircraft activities p 3403 N92-30131

AGING (MATERIALS)
Theory of system reliability demonstration, burn-in design, and record statistics
[AD-A250582] p 3480 N92-29710
The 1991 International Conference on Aging Aircraft and Structural Airworthiness
[NASA-CP-3160] p 3484 N92-30106
Structural integrity of future aging airplanes p 3484 N92-30107
Performance of fuselage pressure structure p 3484 N92-30109
Federal Aviation Administration aging aircraft nondestructive inspection research plan p 3481 N92-30116

AGING (METALLURGY)
Microcalorimetric study of the aging reactions of atomized magnesium powder
[AD-A247932] p 3427 N92-29786

AGREEMENTS
Revision of certification standards for aviation maintenance personnel p 3487 N92-30127
Ageing aircraft research in the Netherlands p 3402 N92-30129

AGRICULTURE
CRIS/USDA online access guide. Revision 1: File 60 on DIALOG
[PB92-172857] p 3562 N92-30033

AIR
Structure of a methanol/air coaxial reacting spray near the stabilization region by OH fluorescence imaging and two-component phase-Doppler interferometry
[DE92-005328] p 3417 N92-29431
Forces on a pipe bend resulting from clearing a pool of liquid upstream
[DE92-004179] p 3445 N92-29784
Experimental study of cylindrical air electrodes
[DE92-506507] p 3441 N92-29912
Mechanical properties of coated titanium Beta-21S after exposure to air at 700 and 800 C
[NASA-TM-104220] p 3423 N92-30205

AIR BREATHING ENGINES
Users manual for updated computer code for axial-flow compressor conceptual design
[NASA-CR-189171] p 3524 N92-30207
AIR FLOW
Active thermal isolation for temperature responsive sensors
[NASA-CASE-LAR-14612-1] p 3446 N92-29954
Calibration apparatus for recess mounted pressure transducers
[NASA-CASE-LAR-14724-1] p 3474 N92-30030
AIR NAVIGATION
European studies to investigate the feasibility of using 1000 ft vertical separation minima above FL 290. Part 1: Overview of organisation, techniques employed, and conclusions
[NLR-TP-91062-U-PT-1] p 3403 N92-29605
AIR POLLUTION
Lidar monitoring of Mexico City's atmosphere during high air polution episodes p 3464 N92-29275
Lidar observation of aerosol and temperature stratification over urban area during the formation of a stable atmospheric PBL p 3466 N92-29286
Lidar investigation of aerosol pollution distribution near a coal power plant p 3467 N92-29289
Lidar observations of stratospheric clouds after volcanic eruption of Pinatubo p 3468 N92-29294
Air quality criteria for oxides of nitrogen, volume 1
[PB92-176361] p 3493 N92-29520
Air quality criteria for oxides of nitrogen, volume 2
[PB92-176379] p 3493 N92-29521
Air quality criteria for oxides of nitrogen, volume 3
[PB92-176387] p 3493 N92-29522
Global-warming problem and global economic models
[DE92-514557] p 3493 N92-29638
NATO workshop on the Atmospheric Methane Cycle. Working group report on methane sources and sinks
[PB92-180256] p 3494 N92-30018
Human exposure model-2: User's guide
[PB92-186246] p 3495 N92-30200
AIR QUALITY
Lidar monitoring of Mexico City's atmosphere during high air polution episodes p 3464 N92-29275
Air quality criteria for oxides of nitrogen, volume 1
[PB92-176361] p 3493 N92-29520
Air quality criteria for oxides of nitrogen, volume 2
[PB92-176379] p 3493 N92-29521
Air quality criteria for oxides of nitrogen, volume 3
[PB92-176387] p 3493 N92-29522
Final Environmental Impact Statement (EIS) for the Space Nuclear Thermal Propulsion (SNTP) program: Appendices
[AD-A248409] p 3413 N92-29904
New developments in emission projection methodologies
[PB92-139393] p 3495 N92-30031
AIR SAMPLING
Ozone measurements with the US EPA UV-DIAL: Preliminary results p 3461 N92-29255
A preliminary design and analysis of an advanced heat-rejection system for an extreme altitude advanced variable cycle diesel engine installed in a high-altitude advanced research platform
[NASA-CR-186021] p 3405 N92-29427
Microcalorimetric study of the aging reactions of atomized magnesium powder
[AD-A247932] p 3427 N92-29786
AIR TRAFFIC
European studies to investigate the feasibility of using 1000 ft vertical separation minima above FL 290. Part 1: Overview of organisation, techniques employed, and conclusions
[NLR-TP-91062-U-PT-1] p 3403 N92-29605
AIR TRAFFIC CONTROL
Application of VME-technology on an airborne data link processor unit
[NLR-MP-88040-U] p 3403 N92-29615
AIR WATER INTERACTIONS
Constraining the atmospheric carbon budget: A preliminary assessment
[CSIRO-TP-25] p 3494 N92-29668
AIRBORNE EQUIPMENT
The global backscatter experiment airborne pulsed lidar measurements p 3459 N92-29246
Multi-wavelength airborne lidar intercomparisons of aerosol and cirrus backscatter over the Pacific Ocean p 3460 N92-29247
Airborne lidar observations of the stratosphere after the Pinatubo eruption p 3460 N92-29248
Simulation of the performances of WIND, an airborne CO2 lidar p 3463 N92-29267
Lidar measurements of aerosol and ozone distributions during the 1992 Airborne Arctic Stratospheric Expedition p 3469 N92-29304
Airborne lidar measurements of stratospheric aerosols during the European Arctic Stratospheric Ozone Experiment (EASOE) p 3469 N92-29305
Diode-pumped Nd:YAG lidar for airborne cloud measurements p 3473 N92-29326
Comparison of in situ, aircraft- and satellite derived surface reflectances in Flevoland (Netherlands). A validation experiment
[BCRS-91-28] p 3491 N92-30230
AIRBORNE/SPACEBORNE COMPUTERS
Application of VME-technology on an airborne data link processor unit
[NLR-MP-88040-U] p 3403 N92-29615
AIRCRAFT CONSTRUCTION MATERIALS
Apparatus for elevated temperature compression or tension testing of specimens
[NASA-CASE-LAR-14775-1] p 3483 N92-30099
Human factors in aircraft maintenance and inspection p 3487 N92-30125
NASA-UVA light aerospace alloy and structures technology program (LA2ST)
[NASA-CR-190538] p 3423 N92-30206
AIRCRAFT CONTROL
Feedback control laws for highly maneuverable aircraft
[NASA-CR-190535] p 3406 N92-29654
AIRCRAFT DESIGN
Improving designer productivity --- artificial intelligence
[NASA-TM-103929] p 3404 N92-29417
Concurrent engineering in design of aircraft structures
[MBB-FE-2-S-PUB-472] p 3404 N92-29650
AIRCRAFT ENGINES
Flight evaluation of an extended engine life mode on an F-15 airplane
[NASA-TM-104240] p 3405 N92-29659
Current and future developments in civil aircraft non-destructive evaluation from an operator's point of view p 3399 N92-30122
AIRCRAFT GUIDANCE
On the optimization of windshear warning and guidance systems
[NLR-TP-90196-U] p 3402 N92-29703
AIRCRAFT INDUSTRY
The 1991 International Conference on Aging Aircraft and Structural Airworthiness
[NASA-CP-3160] p 3484 N92-30106
NDE research efforts at the FAA Center for Aviation Systems Reliability p 3481 N92-30119
Current and future developments in civil aircraft non-destructive evaluation from an operator's point of view p 3399 N92-30122
AIRCRAFT INSTRUMENTS
Sensor fault detection on board an aircraft with observer and polynomial classifier
[DLR-FB-91-34] p 3404 N92-29870
AIRCRAFT MAINTENANCE
Bearing servicing tool
[NASA-CASE-MSC-21881-1] p 3479 N92-30082
The 1991 International Conference on Aging Aircraft and Structural Airworthiness
[NASA-CP-3160] p 3484 N92-30106
Maintaining the safety of an aging fleet of aircraft p 3402 N92-30108
Current DOT research on the effect of multiple site damage on structural integrity p 3485 N92-30112
Inspection of aging aircraft: A manufacturer's perspective p 3481 N92-30117
Human factors in aircraft maintenance and inspection p 3487 N92-30125
Using intelligent simulation to enhance human performance in aircraft maintenance p 3487 N92-30126
Revision of certification standards for aviation maintenance personnel p 3487 N92-30127
The FAA aging airplane program plan for transport aircraft p 3402 N92-30128
Ageing aircraft research in the Netherlands p 3402 N92-30129
Survey of French activities concerning structural airworthiness and aging aircraft p 3402 N92-30130
Transport Canada aging aircraft activities p 3403 N92-30131
Aging commuter aeroplanes: Fatigue evaluation and control methods p 3488 N92-30132
A manufacturer's approach to ensure long term structural integrity p 3403 N92-30133
AIRCRAFT MANEUVERS
Feedback control laws for highly maneuverable aircraft
[NASA-CR-190535] p 3406 N92-29654
AIRCRAFT PERFORMANCE
The 1991 International Conference on Aging Aircraft and Structural Airworthiness
[NASA-CP-3160] p 3484 N92-30106
Performance of fuselage pressure structure p 3484 N92-30109
AIRCRAFT RELIABILITY
The 1991 International Conference on Aging Aircraft and Structural Airworthiness
[NASA-CP-3160] p 3484 N92-30106
Structural integrity of future aging airplanes p 3484 N92-30107
Performance of fuselage pressure structure p 3484 N92-30109
Current DOT research on the effect of multiple site damage on structural integrity p 3485 N92-30112
Federal Aviation Administration aging aircraft nondestructive inspection research plan p 3481 N92-30116
NDE research efforts at the FAA Center for Aviation Systems Reliability p 3481 N92-30119
Survey of French activities concerning structural airworthiness and aging aircraft p 3402 N92-30130
Transport Canada aging aircraft activities p 3403 N92-30131
AIRCRAFT SAFETY
Maintaining the safety of an aging fleet of aircraft p 3402 N92-30108
Status of the FAA flight loads monitoring program p 3485 N92-30113
Damage tolerance for commuter aircraft p 3485 N92-30114
Federal Aviation Administration aging aircraft nondestructive inspection research plan p 3481 N92-30116
AIRCRAFT STRUCTURES
Concurrent engineering in design of aircraft structures
[MBB-FE-2-S-PUB-472] p 3404 N92-29650
The 1991 International Conference on Aging Aircraft and Structural Airworthiness
[NASA-CP-3160] p 3484 N92-30106
Structural integrity of future aging airplanes p 3484 N92-30107
Maintaining the safety of an aging fleet of aircraft p 3402 N92-30108
Performance of fuselage pressure structure p 3484 N92-30109
Fracture mechanics research at NASA related to the aging commercial transport fleet p 3484 N92-30110
Preliminary results on the fracture analysis of multi-site cracking of lap joints in aircraft skins p 3484 N92-30111
Current DOT research on the effect of multiple site damage on structural integrity p 3485 N92-30112
Damage tolerance for commuter aircraft p 3485 N92-30114
Inspection of aging aircraft: A manufacturer's perspective p 3481 N92-30117
NDE research efforts at the FAA Center for Aviation Systems Reliability p 3481 N92-30119
Aging aircraft NDI Development and Demonstration Center (AANC): An overview --- nondestructive inspection p 3481 N92-30120
Nondestructive inspection perspectives p 3481 N92-30121
Current and future developments in civil aircraft non-destructive evaluation from an operator's point of view p 3399 N92-30122
Human factors in aircraft maintenance and inspection p 3487 N92-30125
Nonlinear analyses of composite aerospace structures in sonic fatigue
[NASA-CR-190565] p 3404 N92-30209
AIRFOILS
Fatigue in single crystal nickel superalloys
[AD-A248190] p 3420 N92-29408
Spatial and temporal adaptive procedures for the unsteady aerodynamic analysis of airfoils using unstructured meshes
[NASA-TM-107635] p 3400 N92-29445
Computation of three-dimensional effects on two dimensional wings
[NASA-CR-190576] p 3401 N92-29691
Active thermal isolation for temperature responsive sensors
[NASA-CASE-LAR-14612-1] p 3446 N92-29954
Experimental investigation of the flowfield of an oscillating airfoil
[NASA-TM-105675] p 3402 N92-30182
AIRFRAMES
Thermal QNDE detection of airframe disbonds p 3481 N92-30118
AIRGLOW
An extension of the Raman-lidar technique to measure the velocity and temperature of the atmospheric emission jets from stacks p 3467 N92-29293
Airborne sodium and Rayleigh lidar observations from ALOHA-90 p 3471 N92-29315

AIRLINE OPERATIONS
European studies to investigate the feasibility of using 1000 ft vertical separation minima above FL 290. Part 1: Overview of organisation, techniques employed, and conclusions
[NLR-TP-91062-U-PT-1] p 3403 N92-29605
Structural integrity of future aging airplanes
p 3484 N92-30107
Communication: An important element of maintenance and repair p 3402 N92-30124
ALGEBRA
A new algebra core for the minimal form problem
[DE92-011966] p 3531 N92-29481
Experiments on processes with backtracking
[RR-858-I-IMAG-121-LIFIA] p 3532 N92-29574
Implementation of the object-oriented data model TM
[MEMO-INF-91-94] p 3520 N92-29855
A model for no Borel liftings
[REPT-91-37] p 3535 N92-29919
An algebraic specification for the static semantics of Pascal
[CWI-CS-R9129] p 3522 N92-29989
Undecidable equivalences for basic process algebra
[CWI-CS-R9137] p 3536 N92-29993
Proof theory for micro CRL
[CWI-CS-R9138] p 3522 N92-29994
Classification of A-graded algebras with 3 generators
[MEMO-1004] p 3537 N92-30080
Term rewriting analysis in process algebra
[CWI-CS-R9130] p 3537 N92-30177
Real space process algebra
[CWI-CW-R9131] p 3538 N92-30178
ALGORITHMS
Application of laser imaging for bio/geophysical studies p 3465 N92-29282
Polarization lidar liquid cloud detection algorithm for winter mountain storms p 3472 N92-29323
Adaptive signal processing at NOSC
[AD-A250245] p 3429 N92-29333
Multi-fractal analysis of nocturnal boundary layer time series from the Boulder Atmospheric Observatory
[AD-A248347] p 3502 N92-29424
A generalized polynomial form of the objective function in flash calculations
[AD-A248160] p 3531 N92-29446
Improving path planning with learning
[DE92-004360] p 3527 N92-29456
An examination of hypercube implementations of genetic algorithms
[AD-A248092] p 3515 N92-29527
Low energy neutral atoms in the Earth's magnetosphere: Modeling
[DE92-013240] p 3500 N92-29536
A massively parallel genetic algorithm for the graph partitioning problem
[IMAG-RR-845-I] p 3525 N92-29610
Parallelization of the recursive gradient backpropagation algorithm
[IMAG-RR-854-M] p 3525 N92-29614
Automatic generation algorithms, experiments, and comparisons of self checking PLA schemes
[IMAG-RR-843-I] p 3516 N92-29621
Scalable parallel algorithms for multidimensional digital signal processing
[AD-A249381] p 3516 N92-29622
Abstract data types and algorithm structures and a basis for component reuse
[REPT-91-49] p 3518 N92-29712
Efficient complete radiosity ray tracing using a shadow coherence method
[REPT-91-63] p 3518 N92-29749
The isopone method in optimal control
[REPT-91-52] p 3529 N92-29764
Chain coding in computer graphics
[ETN-92-91630] p 3518 N92-29776
Architectural synthesis and optimization of digital systems
[ISBN-90-9003966-X] p 3519 N92-29782
ISLAND: Interactive Solution Language for an Adaptive NIKE Driver
[DE92-011444] p 3533 N92-29791
Solution strategies for implicit nonlinear finite element analysis
[DE92-011466] p 3533 N92-29792
On the p-coverage problem on the real line
[MEMO-COSOR-91-33] p 3520 N92-29818
On setup cost reduction in the economic lot-sizing model without speculative motives
[MEMO-COSOR-91-34] p 3520 N92-29819
On the complexity of postoptimality analysis of 0/1 programs
[MEMO-COSOR-91-35] p 3520 N92-29820
The capacitated multi-echelon inventory system with serial structure: 1: The push ahead-effect
[MEMO-COSOR-91-39] p 3561 N92-29822
Aerodynamic design optimization using sensitivity analysis and computational fluid dynamics
[NASA-CASE-LAR-14815-1-CU] p 3445 N92-29830
Construction of a VC1 interpolant over triangles via edge deletion
[MEMO-988] p 3533 N92-29858
Non-interfering dipaths in planar digraphs
[CWI-BS-R9121] p 3533 N92-29864
Optimality of wait-free atomic multiwriter variables
[CWI-CS-R9128] p 3520 N92-29868
Reliable processing of confidential data by means of fragmentation-redundancy-scattering
[LAAS-91412] p 3526 N92-29888
Computing distinguishing formulas for branching bisimulation
[CWI-CS-R9121] p 3521 N92-29890
Facets of database triggers
[CWI-CS-R9122] p 3521 N92-29891
Multiresponse imager and imaging process for improved resolution
[NASA-CASE-LAR-14779-1] p 3552 N92-29951
The primordial soup algorithm: A systematic approach to the specification and design of parallel parsers
[MEMO-INF-91-77] p 3536 N92-29956
A seven-league-boots algorithm for path planning in configuration spaces
[MEMO-INF-91-88] p 3530 N92-29969
Inverse remote procedure calls
[MEMO-INF-91-89] p 3521 N92-29970
Linear approximation of shortest superstrings
[CWI-CS-R9126] p 3523 N92-30146
Algorithms and min-max theorems for certain multiway cuts
[MEMO-1022] p 3523 N92-30186
A random polynomial time algorithm for well-rounding convex bodies
[MEMO-1023] p 3541 N92-30188
A parallel restructured version of GMRES(m)
[REPT-91-85] p 3527 N92-30229
ALKALINE BATTERIES
The O2 reduction at the IFC modified O2 fuel cell electrode
[NASA-TM-105691] p 3413 N92-29667
ALLOYS
Magnetic properties of nano-heterogeneous amorphous thin films
[AD-A250570] p 3420 N92-29426
Processing and properties of mechanically alloyed sintered steels with hard inclusions
[KFK-4909] p 3422 N92-29651
ALLUVIUM
Field study of multidimensional flow and transport in the vadose zone
[PB92-161363] p 3489 N92-29701
ALPHA PARTICLES
The comparative effects of gamma radiation and in situ alpha particles on five strong-base anion exchange resins
[DE92-000177] p 3425 N92-29643
ALTERNATING CURRENT
Fuzzy logic control of AC induction motors
[PB92-180207] p 3443 N92-30092
ALTITUDE CONTROL
European studies to investigate the feasibility of using 1000 ft vertical separation minima above FL 290. Part 1: Overview of organisation, techniques employed, and conclusions
[NLR-TP-91062-U-PT-1] p 3403 N92-29605
ALUMINIDES
Mechanical properties of coated titanium Beta-21S after exposure to air at 700 and 800 C
[NASA-TM-104220] p 3423 N92-30205
ALUMINUM
Laser-induced desorption from sapphire surfaces
[DE92-012698] p 3475 N92-29340
Laser paint stripping
[AD-A249233] p 3476 N92-29581
Evaluation of aluminum ion vapor deposition as a replacement for cadmium electroplating at Anniston Army Depot
[AD-A250063] p 3423 N92-29940
Heat transfer in an aluminum heat exchanger using normal hydrogen gas
[PB92-172832] p 3447 N92-30036
ALUMINUM ALLOYS
A study of the influence of alloying additions on the passivity of aluminum
[AD-A248339] p 3421 N92-29587
Short cracks and durability analysis of the Fokker 100 wing/fuselage structure
[NLR-TP-90336-U] p 3482 N92-29603
Structure and stability of Al-Cu-Ru face-centered icosahedral alloys
[DE92-012550] p 3422 N92-29706
ALUMINUM GALLIUM ARSENIDES
Study and realization of GaAs PNP homojunction bipolar transistors using ion implementation
[LAAS-91433] p 3441 N92-29729
Time-of-flight experiments on GaAs/Al(x)Ga(x-1)As heterostructures
[ETN-92-91625] p 3558 N92-29753
ALUMINUM OXIDES
Electron microscopy study on zirconia and alumina ceramic powders synthesized by microwave plasma pyrolysis
[DE92-013385] p 3424 N92-29479
Effect of whisker orientation on the mechanical properties of silicon carbide/alumina composites
[AD-A248737] p 3415 N92-29723
ALUMINUM-LITHIUM ALLOYS
Fatigue crack growth in damage tolerant Al-Li sheet alloys
[NLR-TP-90107-U] p 3483 N92-29708
Aluminum-lithium alloys: Surface-cracked tension fracture tests and physical and thermal properties at cryogenic temperatures
[PB92-172477] p 3422 N92-29803
AMIDES
Solid state structures of some Dithionoamido-18-crown-6 ligands
[AD-A248098] p 3556 N92-29558
AMORPHOUS MATERIALS
Magnetic properties of nano-heterogeneous amorphous thin films
[AD-A250570] p 3420 N92-29426
X ray study of interfacial interactions in highly milled Sn-Ge powders
[DE92-012518] p 3556 N92-29437
Amorphization by interdiffusion in metallic multilayers
[ETN-92-91743] p 3558 N92-29766
AMORPHOUS SEMICONDUCTORS
Monolithic integration of semiconductor and superconductor components
[AD-A245351] p 3557 N92-29583
AMORPHOUS SILICON
Monolithic amorphous silicon modules on continuous polymer substrate
[DE92-001163] p 3425 N92-29598
ANALOG CIRCUITS
Experimental evaluation of incorporating digital and analog integrated circuit die on a common substrate utilizing silicon-hybrid wafer-scale integration technology
[AD-A248182] p 3439 N92-29405
Nonvolatile programmable neural network synaptic array
[NASA-CASE-NPO-18578-1-CU] p 3442 N92-30086
ANALYSIS (MATHEMATICS)
Modeling and computational analysis of multiscale phenomena in fluid-structure interaction problems
[AD-A248723] p 3444 N92-29721
Microbial aldonolactone formation and hydrolysis: Kinetic and bioenergetic aspects p 3507 N92-29735
Askey-Wilson polynomials for root systems of type BC
[CWI-AM-R9112] p 3534 N92-29882
Phase-space estimate of satellite coverage time
[DE92-013555] p 3542 N92-30139
ANALYSIS OF VARIANCE
Testing equality of variances in the analysis of repeated measurements
[MEMO-1013] p 3541 N92-29976
Analysis of a three-dimensional point pattern with replication
[CWI-BS-R9124] p 3541 N92-30180
ANALYTIC FUNCTIONS
Integrable deformations of meromorphic equations on P(exp 1)C
[MEMO-993] p 3534 N92-29872
ANALYTIC GEOMETRY
A method for converting the surface of a generalized cylinder into a B-spline surface
[REPT-91-40] p 3535 N92-29922
ANALYZERS
High resolving power spectrometer for beam analysis
[DE92-010751] p 3437 N92-29988
ANGLE OF ATTACK
Study of optical techniques for the Ames unitary wind tunnels. Part 3: Angle of attack
[NASA-CR-190541] p 3406 N92-29655
ANGULAR VELOCITY
A nanoradian differential VLBI tracking demonstration
p 3430 N92-29367
Deep-space navigation with differenced data types. Part 3: An expanded information content and sensitivity analysis p 3409 N92-29368
ANIMATION
Venus in motion: An animated video catalog of Pioneer Venus Orbiter Cloud Photopolarimeter images
[NASA-CR-190543] p 3568 N92-29401

ANIONS
The comparative effects of gamma radiation and in situ alpha particles on five strong-base anion exchange resins
[DE92-000177] p 3425 N92-29643
ANISOTROPY
Manufacturing of components of fibre-metal laminates: An overview
[LR-670] p 3415 N92-29702
ANNEALING
Evidence for amorphization in Ni/Ti multilayers from electrical resistivity changes p 3559 N92-29773
ANNUAL VARIATIONS
One year of Rayleigh lidar measurements at Toronto p 3466 N92-29285
Tapering clouds and their classification due mainly to the surrounding cloud pattern in the GMS imagery
[ISSN-0388-9653] p 3502 N92-29666
ANNULI
Stresses and strains in plain and coldworked annuli subjected to remote, interference or combined loading
[ARL-STRUC-R-446] p 3482 N92-29672
ANODES
Pulse voltammetry in single cells using platinum microelectrodes
[AD-A248080] p 3440 N92-29523
ANTARCTIC REGIONS
Airborne lidar measurements of stratospheric aerosols during the European Arctic Stratospheric Ozone Experiment (EASOE) p 3469 N92-29305
Aerosols and polar stratospheric clouds measurements during the EASOE campaign p 3469 N92-29306
Lidar observations of polar stratospheric clouds and stratospheric temperatures at the South Pole p 3470 N92-29307
ANTENNA ARRAYS
Applications of inertial-sensor high-inheritance instruments to DSN precision antenna pointing p 3430 N92-29371
Ka-band feed arrays for spacecraft reflector antennas with limited scan capability: An overview p 3433 N92-29387
Microstrip reflectarray antenna for the SCANSCAT radar application
[NASA-CR-190453] p 3434 N92-29463
ANTENNA DESIGN
Performance of a 12-GHz fiber-optic system for beam-waveguide antenna stability testing p 3431 N92-29372
Dynamic modeling of fluid transmission lines of the DSN 70-meter antennas by using a lumped parameter model p 3432 N92-29378
DSS-13 26-meter antenna upgraded radiometer system p 3432 N92-29381
Sequential design of a linear quadratic controller for the Deep Space Network antennas p 3432 N92-29382
Ka-band feed arrays for spacecraft reflector antennas with limited scan capability: An overview p 3433 N92-29387
Microstrip reflectarray antenna for the SCANSCAT radar application
[NASA-CR-190453] p 3434 N92-29463
ANTENNA RADIATION PATTERNS
Microstrip reflectarray antenna for the SCANSCAT radar application
[NASA-CR-190453] p 3434 N92-29463
Analyses of near- and far-field two-lobe patterns outside the output endface of a two-mode fiber
[NASA-CR-190494] p 3551 N92-29652
ANTENNAS
Applications of inertial-sensor high-inheritance instruments to DSN precision antenna pointing p 3430 N92-29371
ANTICYCLONES
OCEANUS 218: Warm Ring Inertial Critical Layer Experiment (WRINCLE)
[PB92-170299] p 3506 N92-29806
ANTIFERROMAGNETISM
Neutron diffraction study of the electronic structure of high T(sub c) superconductor-related compounds
[DE92-012587] p 3559 N92-29939
ANTIMISSILE DEFENSE
Burros: Simple, affordable, effective space transportation
[DE92-013553] p 3541 N92-30138
Phase-space estimate of satellite coverage time
[DE92-013555] p 3542 N92-30139
ANTIPROTONS
Feasibility of an antiproton catalyzed fission fragment rocket
[AD-A248157] p 3412 N92-29444
ANTIREFLECTION COATINGS
Laser diode end-pumped Nd:YAG laser
[AD-A248123] p 3475 N92-29396
APERTURES
Dynamic aperture fringe discriminator
[NASA-CASE-NPO-18478-1-CU] p 3553 N92-30084
Aperture coupling to shielded transmission lines: Theory and experiment
[PB92-183672] p 3437 N92-30093
APPLICATIONS PROGRAMS (COMPUTERS)
An OSI architecture for the Deep Space Network p 3432 N92-29380
Numerical procedures for analyzing dynamical processes
[AD-A248175] p 3515 N92-29399
Reverse automatic differentiation of modular FORTRAN programs
[DE92-014071] p 3519 N92-29797
An introduction to using the FORTRAN programs provided with Computational Nuclear Physics 1 Nuclear Structure p 3549 N92-30013
APPROPRIATIONS
Current information technology resource requirements of the Federal Government: Fiscal year 1992
[PB92-147180] p 3561 N92-29663
NASA's Earth Observing System
[S-HRG-102-647] p 3490 N92-30017
APPROXIMATION
An approximation method for dynamic response of strain-hardening structures
[DE92-013053] p 3482 N92-29535
Divergence preserving discrete surface integral methods for Maxwell's curl equations using non-orthogonal unstructured grids
[NASA-CR-190555] p 3517 N92-29694
Theory of system reliability demonstration, burn-in design, and record statistics
[AD-A250582] p 3480 N92-29710
First order approximation to the average velocity of rise of bubbles in fluid not including inertial forces
[REPT-91-51] p 3444 N92-29763
Asymptotic inversion of the incomplete beta function
[CWI-AM-R9106] p 3534 N92-29893
Diffusion approximation of stochastic integral functionals of jump Markov processes
[CWI-AM-R9108] p 3535 N92-29895
Diffusion approximation of stochastic additive functionals of jump Markov processes
[CWI-AM-R9110] p 3535 N92-29896
An improved accuracy version of the mixed finite element method for a second order elliptic equation
[CWI-NM-R9111] p 3536 N92-29946
A simple approximation to the bivariate normal distribution with large correlation coefficient
[MEMO-1011] p 3540 N92-29974
Power approximations to and power comparison of certain goodness-of-fit tests
[MEMO-1019] p 3541 N92-29980
Linear approximation of shortest superstrings
[CWI-CS-R9126] p 3523 N92-30146
A random polynomial time algorithm for well-rounding convex bodies
[MEMO-1023] p 3541 N92-30188
An approximate solution for interlaminar stresses in laminated composites: Applied mechanics program
[NASA-CR-190537] p 3416 N92-30208
AQUEOUS SOLUTIONS
A study of the adsorption of acetonitrile on a gold electrode from aqueous solutions using in situ vibrational spectroscopy
[AD-A250191] p 3417 N92-29514
Role of polyelectrolytes in barium sulphate precipitation
[PB92-184761] p 3419 N92-30196
ARCHITECTURE (COMPUTERS)
An OSI architecture for the Deep Space Network p 3432 N92-29380
Deep Space Network information system architecture study p 3433 N92-29385
Making intelligent systems team players: Overview for designers
[NASA-TM-104751] p 3513 N92-29403
Ultra-dependable real-time computing
[AD-A248193] p 3515 N92-29409
Introduction to neural networks
[AD-A248258] p 3527 N92-29541
Software architecture modelling: Application to AMODEUS design scenarios
[IMAG-RR-860-I] p 3513 N92-29611
Application of VME-technology on an airborne data link processor unit
[NLR-MP-88040-U] p 3403 N92-29615
Methodology for the specification of communication activities within the framework of a multi-layered architecture: Toward the definition of a knowledge base
[LAAS-91466] p 3436 N92-29730
Architectural synthesis and optimization of digital systems
[ISBN-90-9003966-X] p 3519 N92-29782
Information systems analysis and design based on an object-oriented framework
[MEMO-INF-91-93] p 3519 N92-29816
Architecture and use of Delft Direct Manipulation Manager (D2M2)
[REPT-91-46] p 3521 N92-29887
Electronic neural network for solving traveling salesman and similar global optimization problems
[NASA-CASE-NPO-17807-2-CU] p 3529 N92-29955
Cislan-2 final document by University of Twente (Netherlands)
[MEMO-INF-91-81] p 3526 N92-29958
Integrated service engineering supported by the FDT LOTOS
[MEMO-INF-91-76] p 3531 N92-30184
ARCTIC OCEAN
Acoustic scattering from elastic ice: A finite difference solution
[AD-A248281] p 3543 N92-29346
ARCTIC REGIONS
Lidar atmospheric observatory in the Canadian Arctic p 3458 N92-29241
Airborne dial remote sensing of the Arctic ozone layer p 3462 N92-29258
ARCLITE: The Arctic Lidar Technology Facility at Sondre Stromfjord, Greenland p 3407 N92-29283
Lidar measurements of aerosol and ozone distributions during the 1992 Airborne Arctic Stratospheric Expedition p 3469 N92-29304
Airborne lidar measurements of stratospheric aerosols during the European Arctic Stratospheric Ozone Experiment (EASOE) p 3469 N92-29305
Rayleigh/Raman Greenland lidar observations of atmospheric temperature during a major Arctic stratospheric warming event p 3471 N92-29316
Sound speed, reflectivity, and absorption measurements in Arctic ice in 1988
[AD-A246293] p 3505 N92-29554
AREA
Phase-space estimate of satellite coverage time
[DE92-013555] p 3542 N92-30139
ARGON PLASMA
The expanding plasma jet: Experiments and model
[ETN-92-91627] p 3555 N92-29761
ARITHMETIC AND LOGIC UNITS
A strategy for microprocessor BIST implementation based on deterministic testing
[IMAG-RR-844-I] p 3516 N92-29570
ARMED FORCES (UNITED STATES)
The 1991 Summer Faculty Research Program (SFRP), volume 2
[AD-A248764] p 3571 N92-29724
The 1991 Summer Faculty Research Program (SFRP), volume 3
[AD-A248765] p 3571 N92-29725
ARMOR
Optimization of armored spherical tanks for storage on the lunar surface
[NASA-TM-105700] p 3414 N92-30187
ARRAYS
Interface board for providing time signals to a super minicomputer
[AD-D015198] p 3441 N92-29900
ARTIFICIAL INTELLIGENCE
Making intelligent systems team players: Overview for designers
[NASA-TM-104751] p 3513 N92-29403
Improving designer productivity --- artificial intelligence
[NASA-TM-103929] p 3404 N92-29417
Improving path planning with learning
[DE92-004360] p 3527 N92-29456
An object-based interviewing system
[DE92-013422] p 3527 N92-29504
Introduction to neural networks
[AD-A248258] p 3527 N92-29541
Boolean reasoning and informed search in the minimization of logic circuits
[AD-A248110] p 3528 N92-29561
Smart BIT/TSMD integration
[AD-A247192] p 3442 N92-29914
An analysis of model-based diagnosis using problem-reformulation
[MEMO-INF-92-03] p 3530 N92-29983
Fast temporal neural learning using teacher forcing
[NASA-CASE-NPO-18553-1-CU] p 3530 N92-30085
Temporal reasoning in model-based diagnosis
[MEMO-INF-91-66] p 3531 N92-30143
ARTIFICIAL SATELLITES
OFFEQ-1: Preliminary flight evaluation results
[ITN-92-85126] p 3410 N92-29480
Small satellites and RPAS in global-change research: Summary and conclusions
[DE92-013602] p 3490 N92-30088
ASTEROIDS
Galileo early cruise, including Venus, first Earth, and Gaspra encounters p 3433 N92-29384

ASTROGRAPHY
Geometric distortion analysis of a wide-field astrograph p 3409 N92-29370
ASTRONOMICAL CATALOGS
Abell clusters of galaxies: Catalogs and large-scale structures p 3566 N92-29838
ASTRONOMICAL COORDINATES
Geometric distortion analysis of a wide-field astrograph p 3409 N92-29370
ASTRONOMICAL MODELS
CDM with thermal history of baryons: High-resolution 2-D and 3-D simulations p 3565 N92-29835
N-body simulations of the evolution of clusters of galaxies p 3567 N92-29849
ASTRONOMY
ARCLITE: The Arctic Lidar Technology Facility at Sondre Stromfjord, Greenland p 3407 N92-29283
The 12 micron contribution of nearby galaxies to the infrared background
[AD-A250623] p 3565 N92-29596
United Kingdom Infrared Telescope
[ETN-92-91341] p 3565 N92-29682
ASYMPTOTIC METHODS
Asymptotic optimality of the chi-square test with large number of degrees of freedom within the class of symmetric tests
[CWI-BS-R9116] p 3540 N92-29860
U-statistics of increasing degrees with asymptotically Poisson distributions
[CWI-BS-R9120] p 3540 N92-29863
Asymptotic inversion of the incomplete beta function
[CWI-AM-R9106] p 3534 N92-29893
Hyperasymptotic expansions of confluent hypergeometric functions
[CWI-AM-R9107] p 3535 N92-29894
ASYMPTOTIC PROPERTIES
On the asymptotically uniform distribution modulo 1 of extreme order statistics
[MEMO-COSOR-91-38] p 3540 N92-29821
Asymptotic results in feedback systems
[ETN-92-91702] p 3529 N92-29962
Asymptotic behavior of random discrete event systems p 3529 N92-29963
A simple approximation to the bivariate normal distribution with large correlation coefficient
[MEMO-1011] p 3540 N92-29974
A two-stage estimator for generalized linear models with nonconstant dispersion parameter
[MEMO-1012] p 3540 N92-29975
Testing equality of variances in the analysis of repeated measurements
[MEMO-1013] p 3541 N92-29976
Approximation in a damped Hamiltonian system by successive relative equilibria
[MEMO-1017] p 3536 N92-29979
Optimal copying strategies
[MEMO-1005] p 3537 N92-30081
Simulations on the Jelinski-Moranda model of software reliability
[CWI-BS-R9122] p 3523 N92-30179
ASYMPTOTIC SERIES
Matched asymptotic expansions solution for low-frequency sound radiation from fluid-loaded, baffled plates: Axisymmetric case
[REPT-91-60] p 3543 N92-29628
Matched asymptotic expansions solution for low-frequency sound radiation from fluid-loaded, baffled plates: Two-dimensional case
[REPT-91-62] p 3543 N92-29748
ATMOSPHERIC BOUNDARY LAYER
Lidar observation of aerosol and temperature stratification over urban area during the formation of a stable atmospheric PBL p 3466 N92-29286
The Lidar In-Space Technology Experiment (LITE) p 3469 N92-29301
A soil-canopy scheme for use in a numerical model of the atmosphere: 1D stand-alone model
[CSIRO-TP-23] p 3500 N92-29670
Shelf Mixed Layer Experiment (SMILE) program description and coastal and moored array data report
[PB92-170281] p 3506 N92-29805
ATMOSPHERIC CHEMISTRY
Analysis of EUV dayglow spectra of Triton, Titan and Earth
[NASA-CR-190586] p 3568 N92-29451
Constraining the atmospheric carbon budget: A preliminary assessment
[CSIRO-TP-25] p 3494 N92-29668
Proceedings of the 16th Annual Climate Diagnostics Workshop
[PB92-167378] p 3503 N92-29801
New developments in emission projection methodologies
[PB92-139393] p 3495 N92-30031
What is the potential of forest management to slow the increase of atmospheric CO2?
[PB92-180249] p 3495 N92-30173
ATMOSPHERIC CIRCULATION
Sixteenth International Laser Radar Conference, part 1
[NASA-CP-3158-PT-1] p 3456 N92-29228
GLObal Backscatter Experiment (GLOBE) results: Aerosol backscatter global distribution and wavelength dependence p 3459 N92-29245
The Laser Atmospheric Wind Sounder (LAWS) preliminary error budget and performance estimate p 3462 N92-29262
Identification of critical design points for the EAP of a space-based Doppler lidar wind sounder p 3463 N92-29270
Science goals and mission objectives of NASA's laser atmospheric wind sounder program p 3468 N92-29296
The Laser Atmospheric Wind Sounder (LAWS) phase 2 preliminary system design p 3468 N92-29297
The Laser Atmospheric Wind Sounder (LAWS) phase 2 preliminary laser design p 3468 N92-29298
GE's mobile, coherent Doppler lidar test/evaluation facilities p 3407 N92-29299
Air quality criteria for oxides of nitrogen, volume 1
[PB92-176361] p 3493 N92-29520
Sensitivity of C2 sub n to random variations of windspeed, sensible heat flux, and latent heat flux
[AD-A248696] p 3502 N92-29565
Intercomparison of global marine climatologies
[DE92-011389] p 3494 N92-29790
ATMOSPHERIC COMPOSITION
The role of lidars in global change research p 3457 N92-29235
Interpretation of DIAL measurements of lower stratospheric ozone in regions with Pinatubo aerosols p 3457 N92-29236
A new Raman DIAL technique for measuring stratospheric ozone in the presence of volcanic aerosols p 3458 N92-29238
The JPL Table Mountain and Mauna Loa stratospheric ozone lidars p 3458 N92-29239
Lidar atmospheric observatory in the Canadian Arctic p 3458 N92-29241
Observation of stratospheric ozone with NIES lidar system in Tsukuba, Japan p 3459 N92-29242
Observations of ozone-aerosol correlated behaviour in the lower stratosphere during the EASOE campaign p 3459 N92-29243
GLObal Backscatter Experiment (GLOBE) results: Aerosol backscatter global distribution and wavelength dependence p 3459 N92-29245
Airborne lidar observations of the stratosphere after the Pinatubo eruption p 3460 N92-29248
Two wavelength measurements of the Pinatubo aerosol above Toronto, Canada p 3461 N92-29253
Lidar measurements of stratospheric ozone, temperature and aerosol during 1992 UARS correlative measurement campaign p 3461 N92-29257
Lidar measurement of stratospheric ozone at Hohenpeissenberg: An improved evaluation method p 3462 N92-29259
A multi-wavelength ozone lidar for the EASOE experiment p 3462 N92-29260
Correction of DIAL stratospheric ozone measurements in the presence of Pinatubo aerosols p 3462 N92-29261
DIAL mapping of atmospheric atomic mercury of geophysical origin p 3464 N92-29273
Lidar investigation of aerosol pollution distribution near a coal power plant p 3467 N92-29289
Optical pumping of mesospheric sodium: A new measurement capability p 3470 N92-29310
Lidar probing of the mesosphere: Simultaneous observations of sporadic sodium and iron formations, calcium ion layers, neutral temperature and winds p 3470 N92-29311
Lidar measurements of metallic species in mesopause region p 3470 N92-29312
Error analysis of wind measurements for the University of Illinois sodium Doppler temperature system p 3471 N92-29313
Sodium Doppler temperature lidar observations of the mesopause region temperature and wind structure p 3471 N92-29314
Airborne sodium and Rayleigh lidar observations from ALOHA-90 p 3471 N92-29315
Air quality criteria for oxides of nitrogen, volume 1
[PB92-176361] p 3493 N92-29520
Constraining the atmospheric carbon budget: A preliminary assessment
[CSIRO-TP-25] p 3494 N92-29668
NATO workshop on the Atmospheric Methane Cycle. Working group report on methane sources and sinks
[PB92-180256] p 3494 N92-30018
NOAA environmental digest: Selected indicators of the United States and the global environment, December 1991
[PB92-185073] p 3494 N92-30019
New developments in emission projection methodologies
[PB92-139393] p 3495 N92-30031
What is the potential of forest management to slow the increase of atmospheric CO2?
[PB92-180249] p 3495 N92-30173
Support activities to maintain SUMS flight readiness
[NASA-CR-189656-VOL-1] p 3410 N92-30217
Support activities to maintain SUMS flight readiness, volume 2. Attachment A: Flight 61-C report
[NASA-CR-189656-VOL-2] p 3411 N92-30218
Support activities to maintain SUMS flight readiness, volume 3. Attachment B: Flight STS-35 report, section A
[NASA-CR-189656-VOL-3] p 3411 N92-30219
Support activities to maintain SUMS flight readiness, volume 4. Attachment B: Flight STS-35 report, section B
[NASA-CR-189656-VOL-4] p 3411 N92-30220
Support activities to maintain SUMS flight readiness, volume 5. Attachment B: Flight STS-35 report, section C
[NASA-CR-189656-VOL-5] p 3411 N92-30221
Support activities to maintain SUMS flight readiness, volume 6. Attachment B: Flight STS-35 report, section D
[NASA-CR-189656-VOL-6] p 3411 N92-30222
Support activities to maintain SUMS flight readiness, volume 7. Attachment B: Flight STS-35 report, section E
[NASA-CR-189656-VOL-7] p 3412 N92-30223
Support activities to maintain SUMS flight readiness, volume 8. Attachment B: Flight STS-35 report, section F
[NASA-CR-189656-VOL-8] p 3412 N92-30224
Support activities to maintain SUMS flight readiness, volume 9. Attachment C: Flight STS-40 report. Attachment D: SUMS software listing
[NASA-CR-189656-VOL-9] p 3412 N92-30225
ATMOSPHERIC CORRECTION
Comparison of in situ, aircraft- and satellite derived surface reflectances in Flevoland (Netherlands). A validation experiment
[BCRS-91-28] p 3491 N92-30230
ATMOSPHERIC DIFFUSION
Preliminary analysis of wind data from the Oak Ridge site survey
[PB92-174564] p 3503 N92-30034
ATMOSPHERIC EFFECTS
Sixteenth International Laser Radar Conference, part 1
[NASA-CP-3158-PT-1] p 3456 N92-29228
ATMOSPHERIC ENTRY
Support activities to maintain SUMS flight readiness
[NASA-CR-189656-VOL-1] p 3410 N92-30217
Support activities to maintain SUMS flight readiness, volume 2. Attachment A: Flight 61-C report
[NASA-CR-189656-VOL-2] p 3411 N92-30218
Support activities to maintain SUMS flight readiness, volume 3. Attachment B: Flight STS-35 report, section A
[NASA-CR-189656-VOL-3] p 3411 N92-30219
Support activities to maintain SUMS flight readiness, volume 4. Attachment B: Flight STS-35 report, section B
[NASA-CR-189656-VOL-4] p 3411 N92-30220
Support activities to maintain SUMS flight readiness, volume 5. Attachment B: Flight STS-35 report, section C
[NASA-CR-189656-VOL-5] p 3411 N92-30221
Support activities to maintain SUMS flight readiness, volume 6. Attachment B: Flight STS-35 report, section D
[NASA-CR-189656-VOL-6] p 3411 N92-30222
Support activities to maintain SUMS flight readiness, volume 7. Attachment B: Flight STS-35 report, section E
[NASA-CR-189656-VOL-7] p 3412 N92-30223
Support activities to maintain SUMS flight readiness, volume 8. Attachment B: Flight STS-35 report, section F
[NASA-CR-189656-VOL-8] p 3412 N92-30224
Support activities to maintain SUMS flight readiness, volume 9. Attachment C: Flight STS-40 report. Attachment D: SUMS software listing
[NASA-CR-189656-VOL-9] p 3412 N92-30225
ATMOSPHERIC GENERAL CIRCULATION MODELS
Lidar development for the Atmospheric Radiation Measurement (ARM) Program p 3461 N92-29256
A soil-canopy scheme for use in a numerical model of the atmosphere: 1D stand-alone model
[CSIRO-TP-23] p 3500 N92-29670
ATMOSPHERIC MODELS
Measurements of wind divergence with volume imaging lidar p 3464 N92-29272
Science goals and mission objectives of NASA's laser atmospheric wind sounder program p 3468 N92-29296
User's guide for the VTRPE (Variable Terrain Radio Parabolic Equation) computer model
[AD-A248112] p 3433 N92-29395
National Institute for Global Environmental Change
[DE92-013487] p 3493 N92-29597

Constraining the atmospheric carbon budget: A preliminary assessment
[CSIRO-TP-25] p 3494 N92-29668
On the optimization of windshear warning and guidance systems
[NLR-TP-90196-U] p 3402 N92-29703
Intercomparison of global marine climatologies
[DE92-011389] p 3494 N92-29790
Diurnal forcing of planetary atmospheres
[NASA-CR-190262] p 3569 N92-30199

ATMOSPHERIC MOISTURE
LAPS specific humidity analysis
[PB92-163575] p 3502 N92-29799

ATMOSPHERIC OPTICS
Development of mesospheric sodium laser beacon for atmospheric adaptive optics p 3470 N92-29308
International conference topical meeting on atmospheric, volume, and surface scattering and propagation
[AD-A248881] p 3552 N92-29727

ATMOSPHERIC PHYSICS
A developing multiple-wavelength lidar for detecting mainly ozone and aerosol distributions in the stratosphere p 3467 N92-29292
Proceedings of the 16th Annual Climate Diagnostics Workshop
[PB92-167378] p 3503 N92-29801
Evaluation of an aureole lidar technique for estimating extinction profiles
[AD-A249740] p 3501 N92-30087
Expert judgment study on atmospheric dispersion and deposition: Main report and annexes
[REPT-91-81] p 3495 N92-30226

ATMOSPHERIC RADIATION
Lidar development for the Atmospheric Radiation Measurement (ARM) Program p 3461 N92-29256
Surface reactions in the space environment
[AD-A250624] p 3428 N92-29428

ATMOSPHERIC REFRACTION
User's guide for the VTRPE (Variable Terrain Radio Parabolic Equation) computer model
[AD-A248112] p 3433 N92-29395

ATMOSPHERIC SCATTERING
Long term stratospheric aerosol lidar measurements in Kyushu p 3456 N92-29229
The global backscatter experiment airborne pulsed lidar measurements p 3459 N92-29246
International conference topical meeting on atmospheric, volume, and surface scattering and propagation
[AD-A248881] p 3552 N92-29727

ATMOSPHERIC SOUNDING
Lidar measurements of metallic species in mesopause region p 3470 N92-29312
Sodium Doppler temperature lidar observations of the mesopause region temperature and wind structure p 3471 N92-29314
Airborne sodium and Rayleigh lidar observations from ALOHA-90 p 3471 N92-29315
Rayleigh/Raman lidars: Intercomparisons and validation p 3471 N92-29318
Lidar studies of clouds at Toronto during the ECLIPS program p 3472 N92-29321
Observations of cirrus clouds over the Pacific region by the NASA multiwavelength lidar system p 3473 N92-29325
Remote sensing by spaceborne lidar aided by surface returns p 3473 N92-29327

ATMOSPHERIC STRATIFICATION
Characterization of artificial guidestars generated in the mesospheric sodium layer p 3470 N92-29309
Optical pumping of mesospheric sodium: A new measurement capability p 3470 N92-29310

ATMOSPHERIC TEMPERATURE
Lidar measurements of stratospheric ozone, temperature and aerosol during 1992 UARS correlative measurement campaign p 3461 N92-29257
ARCLITE: The Arctic Lidar Technology Facility at Sondre Stromfjord, Greenland p 3407 N92-29283
Rotational Raman lidar for lower tropospheric temperature profiling p 3466 N92-29284
One year of Rayleigh lidar measurements at Toronto p 3466 N92-29285
A comparison between Raman lidar and conventional contact measurements of atmospheric temperature p 3466 N92-29287
Efficiencies of rotational Raman and Rayleigh techniques for laser remote sensing of the atmospheric temperature p 3467 N92-29288
Error analysis of wind measurements for the University of Illinois sodium Doppler temperature system p 3471 N92-29313
Sodium Doppler temperature lidar observations of the mesopause region temperature and wind structure p 3471 N92-29314
Rayleigh/Raman Greenland lidar observations of atmospheric temperature during a major Arctic stratospheric warming event p 3471 N92-29316
Elastic and Raman lidar temperature measurements from Poker Flat, Alaska during February 1992 p 3471 N92-29317
Rayleigh/Raman lidars: Intercomparisons and validation p 3471 N92-29318
A soil-canopy scheme for use in a numerical model of the atmosphere: 1D stand-alone model
[CSIRO-TP-23] p 3500 N92-29670

ATMOSPHERIC TURBULENCE
Signal quality influence on averaging procedure for DIAL pollution monitoring p 3485 N92-29280
Comparison of turbulence parameters measured by SODAR and sonic anemometer
[KFK-4890] p 3500 N92-29690

ATMOSPHERIC WINDOWS
Simulation of the performances of WIND, an airborne CO2 lidar p 3463 N92-29267

ATOMIC CLOCKS
Introduction to quartz frequency standards
[AD-A248503] p 3439 N92-29498

ATOMIC STRUCTURE
MNDO study of boron-nitrogen analogues of buckminsterfullerene
[AD-A247777] p 3414 N92-29460
The real-space multiple-scattering theory and the electronic structure of grain boundaries
[DE92-013006] p 3556 N92-29473
Theoretical/experimental investigations of the structure and dynamics of highly energetic dication species
[AD-A247050] p 3418 N92-29901
The Green Function Cellular Method and its relation to multiple scattering theory
[DE92-011470] p 3436 N92-29909
The role of chemical interactions in the stability of artificial metallic superlattices
[DE92-011528] p 3559 N92-29911
Neutron diffraction study of the electronic structure of high T(sub c) superconductor-related compounds
[DE92-012587] p 3559 N92-29939

ATOMS
Theory of the dissociation dynamics of small molecules on metal surfaces: Finite temperature studies
[DE92-011188] p 3546 N92-29899

AUDITORY DEFECTS
Effects of ionizing radiation on auditory and visual thresholds
[AD-A248199] p 3507 N92-29410

AUDITORY SIGNALS
Additivity and auditory pattern analysis
[AD-A250580] p 3511 N92-29592

AUGER SPECTROSCOPY
Quasi-static intergranular cracking in a Cu-Sn alloy: An analog of stress relief cracking of steels
[DE92-011646] p 3420 N92-29483

AURORAS
Poleward leaping auroras, the substorm expansive and recovery phases, and the recovery of the plasma sheet
[DE92-013530] p 3500 N92-29513

AUSTENITE
Fastening apparatus having shape memory alloy actuator
[NASA-CASE-MSC-21935-1] p 3479 N92-29762

AUSTENITIC STAINLESS STEELS
Corrosion resistance of stainless steels and high Ni-Cr alloys to acid fluoride wastes
[DE92-012338] p 3420 N92-29436

AUTOCORRELATION
Lagrangian velocity correlation and spectrum in homogeneous isotropic turbulence p 3448 N92-30047

AUTOMATIC CONTROL
Robotic workcell for wire wrapping integrated circuits
[DE92-013999] p 3441 N92-29796

AUTONOMOUS NAVIGATION
A systems analysis of the impact of navigation instrumentation on-board a Mars rover, based on a covariance analysis of navigation performance
[NASA-CR-189868] p 3403 N92-29440
Using custom-designed VLSI fuzzy inferencing chips for the autonomous navigation of a mobile robot
[DE92-000424] p 3528 N92-29550
Path tracking using simple planar curves
[AD-A248252] p 3403 N92-29617
Incorporation of GPS/INS into small autonomous underwater vehicle navigation
[AD-A248884] p 3403 N92-29906

AUTONOMY
KISMET (kinematic simulation, monitoring and off-line programming environments for telerobotics): Simulation of the target-oriented driving of an autonomous vehicle in a labyrinthic environment
[KFK-4941] p 3515 N92-29418

AXIAL FLOW
Experimental examination of heavy loaded axial fans with rotational symmetrical distortion of the inflow
[ETN-92-91489] p 3445 N92-29926

AXIOMS
Partial logic as a simple restriction of standard logic
[MEMO-INF-91-73] p 3536 N92-29995

B

BABOONS
Effects of ionizing radiation on auditory and visual thresholds
[AD-A248199] p 3507 N92-29410

BACKGROUND NOISE
Figure of merit for direct-detection optical channels p 3431 N92-29376

BACKGROUND RADIATION
The 12 micron contribution of nearby galaxies to the infrared background
[AD-A250623] p 3565 N92-29596

BACKSCATTERING
Sixteenth International Laser Radar Conference, part 1
[NASA-CP-3158-PT-1] p 3456 N92-29228
Long term stratospheric aerosol lidar measurements in Kyushu p 3456 N92-29229
Stratospheric backscatter, extinction, and lidar ratio profiling after the Mt. Pinatubo eruptions p 3456 N92-29231
Raman lidar measurements of Pinatubo aerosols over southeastern Kansas during November-December 1991 p 3457 N92-29233
The NDSC primary site at the Observatoire de Haute-Provence: Ozone and aerosols observations (1986-1992) p 3458 N92-29240
GLObal Backscatter Experiment (GLOBE) results: Aerosol backscatter global distribution and wavelength dependence p 3459 N92-29245
The global backscatter experiment airborne pulsed lidar measurements p 3459 N92-29246
Multi-wavelength airborne lidar intercomparisons of aerosol and cirrus backscatter over the Pacific Ocean p 3460 N92-29247
Multi-wavelength measurements of the stratospheric aerosol layer made at Hampton, Virginia (37N, 76W) p 3460 N92-29249
Three-wavelength lidar measurements of Pinatubo aerosol and its optical properties p 3460 N92-29250
Lidar observations of the Pinatubo stratospheric aerosol cloud over Frascati, Italy p 3460 N92-29251
L625 lidar measurements of Pinatubo volcanic cloud at Hefei p 3460 N92-29252
Lidar observations of the Pinatubo volcanic cloud over Hampton, Virginia p 3461 N92-29254
Intercomparisons of lidar backscatter measurements and in-situ data from GLOBE p 3463 N92-29266
Laboratory velocimeter measurements using the edge technique p 3463 N92-29269
One year of Rayleigh lidar measurements at Toronto p 3466 N92-29285
Lidar observations of stratospheric clouds after volcanic eruption of Pinatubo p 3468 N92-29294
Wind measurements from 15 to 50 km with a Doppler Rayleigh lidar p 3472 N92-29319
Computational acoustics
[AD-A247688] p 3543 N92-29441
Diffraction of light from randomly rough surfaces
[AD-A250261] p 3551 N92-29546

BACTERIA
Classification, error detection, and reconciliation of measurements in complex biochemical systems p 3508 N92-29737

BACTERIOLOGY
Microbial aldonolactone formation and hydrolysis: Kinetic and bioenergetic aspects p 3507 N92-29735

BALLOON FLIGHT
Investigation of solar active regions at high resolution by balloon flights of the solar optical universal polarimeter, definition phase
[NASA-CR-184339] p 3570 N92-30204

BANACH SPACE
Minimax linear splines
[AD-A248077] p 3515 N92-29487

BANDPASS FILTERS
Improved real-time imaging spectrometer
[NASA-CASE-NPO-18410-1-CU] p 3552 N92-29832

BANDWIDTH
Bandwidth compression of noisy signals with square-wave subcarrier p 3432 N92-29379
Variable bandwidth connections for a connectionless service on ATM: Performance modelling and evaluation
[MEMO-INF-91-83] p 3438 N92-30170

BARIUM
Role of polyelectrolytes in barium sulphate precipitation
[PB92-184761] p 3419 N92-30196
BARIUM TITANATES
Phase conjugation in BaTiO3 at 830 nanometers
[AD-A250240] p 3475 N92-29332
BARYONS
Theoretical overview: Hot and dense QCD in equilibrium
[DE92-013665] p 3560 N92-29517
CDM with thermal history of baryons: High-resolution 2-D and 3-D simulations p 3565 N92-29835
BATHYTHERMOGRAPHS
OCEANUS 218: Warm Ring Inertial Critical Layer Experiment (WRINCLE)
[PB92-170299] p 3506 N92-29806
BAYES THEOREM
A sample-size optimal bayesian procedure for sequential pharmaceutical trials
[AD-A248512] p 3538 N92-29501
Accurate procedures for approximate Bayesian and conditional inference without the need for orthogonal parameters
[AD-A248662] p 3539 N92-29718
Imprecise conjugate prior densities for the one-parameter exponential family of distributions
[MEMO-COSOR-91-36] p 3540 N92-29897
BCH CODES
Golay and other box codes p 3431 N92-29375
BEACONS
Development of mesospheric sodium laser beacon for atmospheric adaptive optics p 3470 N92-29308
Characterization of artificial guidestars generated in the mesospheric sodium layer p 3470 N92-29309
BEAM INJECTION
The optical design of AmPS: Elements of the design of a pulse stretcher
[ETN-92-91626] p 3552 N92-29859
BEAM WAVEGUIDES
Performance of a 12-GHz fiber-optic system for beam-waveguide antenna stability testing
p 3431 N92-29372
Optimizing the G/T ratio of the DSS-13 34-meter beam-waveguide antenna p 3431 N92-29377
BEAMS (RADIATION)
Transition crossing in the RHIC
[DE92-013031] p 3550 N92-29475
Longitudinal bunch profile measurements with striplines
[DE92-013035] p 3549 N92-29477
High resolving power spectrometer for beam analysis
[DE92-010751] p 3437 N92-29988
BEAMS (SUPPORTS)
A closed form solution of a longitudinal beam with a viscous boundary condition
[AD-A248841] p 3483 N92-29915
Thickness dependency of elastic aftereffect of thin bending beams
[ETN-92-91488] p 3483 N92-29925
BEARINGS
Bearing servicing tool
[NASA-CASE-MSC-21881-1] p 3479 N92-30082
BEHAVIOR
Physiological analyses of the afferents controlling brain neurochemical systems
[AD-A248334] p 3512 N92-29930
BEND TESTS
The effect of length variation on the stability of circular cylindrical shells under pure bending
[LR-669] p 3482 N92-29700
BENDING
Thickness dependency of elastic aftereffect of thin bending beams
[ETN-92-91488] p 3483 N92-29925
Fundamental study of compressive strength development in PAN-based carbon fibers
[AD-A250285] p 3416 N92-30137
An approximate solution for interlaminar stresses in laminated composites: Applied mechanics program
[NASA-CR-190537] p 3416 N92-30208
BENZENE
Polybenzimidazoles via aromatic nucleophilic displacement
[NASA-CASE-LAR-14643-1] p 3426 N92-29953
BETHE-SALPETER EQUATION
Solution of two-body relativistic bound state equations with confining plus Coulomb interactions
p 3547 N92-30003
Effects of retardation in relativistic equations with confining interaction p 3547 N92-30005
BIBLIOGRAPHIES
Publications of the environmental health program: 1980-1990
[NASA-CR-4455] p 3509 N92-29341
An annotated bibliography in parallel parsing
[REPT-91-64] p 3525 N92-29716
The 36th issue of Electronics and Electrical Engineering Laboratory Technical Progress Bulletin covering laboratory programs, July to September 1991, with 1992 EEEL events calendar
[PB92-164672] p 3442 N92-30032
BIDIRECTIONAL REFLECTANCE
Biophysical, morphological, canopy optical property, and productivity data from the Superior National Forest
[NASA-TM-104568] p 3491 N92-30210
BINARY ALLOYS
The role of chemical interactions in the stability of artificial metallic superlattices
[DE92-011528] p 3559 N92-29911
BINARY CODES
Golay and other box codes p 3431 N92-29375
BINARY DATA
Golay and other box codes p 3431 N92-29375
Detection of binary phase shift keyed signals in extremely high noise
[AD-A248552] p 3435 N92-29576
BINOMIALS
Minimal-change codes and number systems
[REPT-91-42] p 3536 N92-29924
BIOASSAY
Proceedings of the Third Conference on Radiation Protection and Dosimetry
[DE92-011502] p 3547 N92-29910
BIOCHEMISTRY
Classification, error detection, and reconciliation of measurements in complex biochemical systems
p 3508 N92-29737
Research and technology annual report, FY 1990
[NASA-TM-107807] p 3571 N92-30197
BIOCONVERSION
Flux-capacity relationships of Acinetobacter calcoaceticus enzymes during xylose oxidation
p 3508 N92-29739
State estimation and control of the IBE-fermentation with product recovery p 3509 N92-29756
Improved balancing methods and error diagnosis for bio(chemical) conversions p 3509 N92-29759
BIODYNAMICS
ARTIBODIES: A system for modelling articulated bodies
[REPT-91-57] p 3517 N92-29627
BIOGEOCHEMISTRY
SeaWiFS technical report series. Volume 1: An overview of SeaWiFS and ocean color
[NASA-TM-104566-VOL-1] p 3505 N92-29686
BIOINSTRUMENTATION
Electrical connection of enzyme redox centers to electrodes
[AD-A248545] p 3440 N92-29575
BIOLOGICAL EVOLUTION
Algorithms and min-max theorems for certain multiway cuts
[MEMO-1022] p 3523 N92-30186
BIOLOGICAL MODELS (MATHEMATICS)
The use of state estimators (observers) for on-line estimation of non-measurable process variables
p 3508 N92-29755
BIOLOGY
Combined summaries: Technologies to sustain tropical forest resources and biological diversity
[OTA-F-515] p 3492 N92-29416
BIOMASS
On the estimation of bioenergetic parameters
p 3508 N92-29738
BIOPHYSICS
Biophysical, morphological, canopy optical property, and productivity data from the Superior National Forest
[NASA-TM-104568] p 3491 N92-30210
BIOPROCESSING
State estimation and error diagnosis for biotechnological processes
[ETN-92-91744] p 3508 N92-29754
The use of state estimators (observers) for on-line estimation of non-measurable process variables
p 3508 N92-29755
State estimation and control of the IBE-fermentation with product recovery p 3509 N92-29756
A low sensitivity observer for complex biotechnological processes p 3509 N92-29757
Analytical tuning of a low sensitivity observer applied to a continuous ethanol fermentation with product recovery p 3509 N92-29758
BIOREACTORS
The bioreactor overflow device: An undesired selective separator in continuous cultures? p 3507 N92-29736
BIOSPHERE
NOAA environmental digest: Selected indicators of the United States and the global environment, December 1991
[PB92-185073] p 3494 N92-30019
BIOTECHNOLOGY
Analysis and experimental testing of a bottleneck model for the description of microbial dynamics
p 3508 N92-29740
A low sensitivity observer for complex biotechnological processes p 3509 N92-29757
Analytical tuning of a low sensitivity observer applied to a continuous ethanol fermentation with product recovery p 3509 N92-29758
Sequential application of data reconciliation for sensitive detection of systematic errors p 3509 N92-29760
BIPOLAR TRANSISTORS
Study and realization of GaAs PNP homojunction bipolar transistors using ion implementation
[LAAS-91433] p 3441 N92-29729
Optoelectronic integration
[AD-A248950] p 3442 N92-29936
BLACK HOLES (ASTRONOMY)
The significance of large-scale flows into the Great Attractor p 3565 N92-29836
BLAST LOADS
Guide for evaluating 12 inch Substantial Dividing Walls (SDWs) to provide protection from remote operation, volume 2
[AD-A250252] p 3428 N92-29335
Guide for evaluating 12 inch Substantial Dividing Walls (SDWs) to provide protection from remote operation, volume 1
[AD-A250251] p 3428 N92-29545
BLOWDOWN WIND TUNNELS
Production of periodical Mach number variations in high subsonic flow in a blow down wind tunnel, and its influence on profile measurements
[ETN-92-91492] p 3401 N92-29889
BLUNT BODIES
Second-order shock-expansion theory extended to include real gas effects
[AD-A247191] p 3400 N92-29539
BOATS
Evaluation of Night Vision Goggles (NVG) for maritime search and rescue
[AD-A247182] p 3512 N92-29538
BODIES OF REVOLUTION
Second-order shock-expansion theory extended to include real gas effects
[AD-A247191] p 3400 N92-29539
BODY CENTERED CUBIC LATTICES
The real-space multiple-scattering theory and the electronic structure of grain boundaries
[DE92-013006] p 3556 N92-29473
The role of chemical interactions in the stability of artificial metallic superlattices
[DE92-011528] p 3559 N92-29911
BODY TEMPERATURE
Improvements in X-band transmitter phase stability through klystron body temperature regulation
p 3431 N92-29373
BOEING AIRCRAFT
Structural integrity of future aging airplanes
p 3484 N92-30107
Performance of fuselage pressure structure
p 3484 N92-30109
BONDING
Theoretical/experimental investigations of the structure and dynamics of highly energetic dication species
[AD-A247050] p 3418 N92-29901
Vibrational spectrum and structure of 1,2-dimethyl-1,2-disila-closo-dodecaborane
[AD-A250235] p 3419 N92-29941
BOOLEAN ALGEBRA
Boolean reasoning and informed search in the minimization of logic circuits
[AD-A248110] p 3528 N92-29561
Extremally disconnected spaces, subspaces and retractions
[REPT-91-38] p 3535 N92-29920
BORESIGHTS
Lidar In-space Technology Experiment (LITE) electronics overview p 3462 N92-29264
BORON
MNDO study of boron-nitrogen analogues of buckminsterfullerene
[AD-A247777] p 3414 N92-29460
BOSONS
Hydrogen desorption and the search for the Higgs
[DE92-013464] p 3545 N92-29507
Higgs-boson production in nucleus-nucleus collisions
p 3548 N92-30009
BOUNDARIES
Variational formulation and finite element implementation of Pagano's theory of laminated plates
[AD-A250592] p 3415 N92-29594
A closed form solution of a longitudinal beam with a viscous boundary condition
[AD-A248841] p 3483 N92-29915

BOUNDARY CONDITIONS
Two-dimensional boundary surfaces for planar external transonic flows
[AD-A248083] p 3444 N92-29524
Parameter identification in tidal models with uncertain boundaries
[MEMO-983] p 3540 N92-29856
Evaluation of measured-boundary-condition methods for 3D subsonic wall interference
[NLR-TR-88072-U] p 3401 N92-29884
A closed form solution of a longitudinal beam with a viscous boundary condition
[AD-A248841] p 3483 N92-29915

BOUNDARY ELEMENT METHOD
Validation of finite element and boundary element methods for predicting structural vibration and radiated noise
[NASA-TM-105359] p 3478 N92-29697
Nonlinear analyses of composite aerospace structures in sonic fatigue
[NASA-CR-190565] p 3404 N92-30209

BOUNDARY LAYER FLOW
Near-wall turbulence modeling for boundary layers with separation p 3449 N92-30052

BOUNDARY LAYER STABILITY
Mixing measurements of straight and curved shear layers p 3451 N92-30067

BOUNDARY LAYERS
Rotational Raman lidar for lower tropospheric temperature profiling p 3466 N92-29284
Streamwise vortices in heated boundary layers
[NASA-CR-189661] p 3444 N92-29692
A preliminary experimental investigation of local isotropy in high-Reynolds-number turbulence p 3447 N92-30042
The role of pressure-dilatation correlation in rapidly compressed turbulence and in boundary layers p 3449 N92-30050
Analyses and modeling of evolving turbulent flow p 3449 N92-30051
Near-wall turbulence modeling for boundary layers with separation p 3449 N92-30052

BOUNDARY VALUE PROBLEMS
On the numerical solution of one-dimensional integral and differential equations
[AD-A250388] p 3531 N92-29548
The twopnt program for boundary value problems: Version 3.10 of March 1992
[DE92-013394] p 3517 N92-29641
Divergence preserving discrete surface integral methods for Maxwell's curl equations using non-orthogonal unstructured grids
[NASA-CR-190555] p 3517 N92-29694
A closed form solution of a longitudinal beam with a viscous boundary condition
[AD-A248841] p 3483 N92-29915

BRAIN
Physiological analyses of the afferents controlling brain neurochemical systems
[AD-A248334] p 3512 N92-29930

BRANCHING (MATHEMATICS)
Computing distinguishing formulas for branching bisimulation
[CWI-CS-R9121] p 3521 N92-29890
Multitype branching processes in M/G/1-queueing theory p 3530 N92-29966
A closer look at a Fibonacci-like iterated nonlinear map: More chaos and order
[MEMO-INF-91-70] p 3537 N92-30075

BRAZIL
Evaluating the military potential of a developing nation's space program: A case study of Brazil
[AD-A245978] p 3407 N92-29929

BREMSSTRAHLUNG
CoMStOC 4: Multiwaveband observations of sunspot and plage-associated coronal emission
[AD-A248344] p 3570 N92-29632

BRIGHTNESS TEMPERATURE
Detecting microwave emissions from terrestrial sources: A feasibility study
[AD-A248557] p 3435 N92-29579
CoMStOC 4: Multiwaveband observations of sunspot and plage-associated coronal emission
[AD-A248344] p 3570 N92-29632

BRINES
Acetate in hydrothermal solutions: Decomposition kinetics and metal complexation
[DE92-010542] p 3417 N92-29551
Application of a moving-grid method to a class of 1D brine transport problems in porous media
[CWI-NM-R9112] p 3446 N92-29947

BRITTLENESS
Mechanism of diffusion-controlled brittle fracture
[DE92-011572] p 3482 N92-29601

BROADBAND
Statistics of narrowband white noise derived from clipped broadband white noise
[AD-A248597] p 3434 N92-29563
Performance of a connectionless protocol over ATM
[MEMO-INF-92-02] p 3526 N92-29880

BROADCASTING
The 1990 annual report, April 1990 - March 1991 p 3571 N92-29471
World Administrative Radio Conference. Issues for US International Spectrum Policy
[PB92-157601] p 3435 N92-29696
Sensitivity analysis of the load on an ethernet network
[MEMO-COSOR-91-41] p 3436 N92-29824

BROKEN SYMMETRY
Hydrogen desorption and the search for the Higgs
[DE92-013464] p 3545 N92-29507

BUBBLES
First order approximation to the average velocity of rise of bubbles in fluid not including inertial forces
[REPT-91-51] p 3444 N92-29763

BUCKLING
The effect of length variation on the stability of circular cylindrical shells under pure bending
[LR-669] p 3482 N92-29700

BUCKMINSTERFULLERENE
MNDO study of boron-nitrogen analogues of buckminsterfullerene
[AD-A247777] p 3414 N92-29460

BUFFETING
Buffet test in the National Transonic Facility
[NASA-CR-189595] p 3406 N92-29352

BUNCHING
Transition crossing in the RHIC
[DE92-013031] p 3550 N92-29475
Longitudinal bunch profile measurements with striplines
[DE92-013035] p 3549 N92-29477

BUOYANCY
Local isotropy in buoyancy-generated turbulence p 3447 N92-30043
Large eddy simulations of passive and buoyant scalars with dynamic subgrid-scale models p 3450 N92-30057

BURN-IN
Theory of system reliability demonstration, burn-in design, and record statistics
[AD-A250582] p 3480 N92-29710

BURNING RATE
Microcalorimetric study of the aging reactions of atomized magnesium powder
[AD-A247932] p 3427 N92-29786

C

C++ (PROGRAMMING LANGUAGE)
Abstract data types and algorithm structures and a basis for component reuse
[REPT-91-49] p 3518 N92-29712

CADMIUM
Evaluation of aluminum ion vapor deposition as a replacement for cadmium electroplating at Anniston Army Depot
[AD-A250063] p 3423 N92-29940

CALCIUM
Lidar probing of the mesosphere: Simultaneous observations of sporadic sodium and iron formations, calcium ion layers, neutral temperature and winds p 3470 N92-29311

CALCULUS
Experiments on processes with backtracking
[RR-858-I-IMAG-121-LIFIA] p 3532 N92-29574
Partial logic as a simple restriction of standard logic
[MEMO-INF-91-73] p 3536 N92-29995
On the two-dimensional model of quantum Regge gravity
[DE92-624516] p 3560 N92-30212

CALIBRATING
CAESAR: A CCD airborne experimental scanner for applications in remote sensing radiometric and geometric calibration
[NLR-TP-89103-U] p 3490 N92-29707
Model for regional solute transport suited for calibration and management
[PB92-161371] p 3494 N92-29746
Full pose and partial pose calibration of a 6 degree-of-freedom robot manipulator arm
[AD-A247463] p 3479 N92-29785
SP-100 W/Re thermocouple calibration techniques
[DE92-011302] p 3550 N92-29938
Calibration apparatus for recess mounted pressure transducers
[NASA-CASE-LAR-14724-1] p 3474 N92-30030
Physics Laboratory technical activities, 1991
[PB92-172824] p 3542 N92-30035
SeaWiFS technical report series. Volume 5: Ocean optics protocols for SeaWiFS validation
[NASA-TM-104566] p 3506 N92-30193

CALIFORNIA
Shelf Mixed Layer Experiment (SMILE) program description and coastal and moored array data report
[PB92-170281] p 3506 N92-29805

CAMERAS
Study of optical techniques for the Ames unitary wind tunnels. Part 3: Angle of attack
[NASA-CR-190541] p 3406 N92-29655
Motion restoration of long time exposed images with satellite-borne cameras
[ETN-92-91490] p 3474 N92-29731
Improved real-time imaging spectrometer
[NASA-CASE-NPO-18410-1-CU] p 3552 N92-29832
Polarization perception device
[NASA-CASE-MSC-21915-1] p 3552 N92-30027
Investigation of solar active regions at high resolution by balloon flights of the solar optical universal polarimeter, definition phase
[NASA-CR-184339] p 3570 N92-30204

CANADA
One year of Rayleigh lidar measurements at Toronto p 3466 N92-29285

CANOPIES (VEGETATION)
Biophysical, morphological, canopy optical property, and productivity data from the Superior National Forest
[NASA-TM-104568] p 3491 N92-30210

CAPACITANCE
Optical and electrical characteristics of the cathode fall
[AD-A249010] p 3443 N92-30176

CARBON
Hydrogenation reactions of neutral carbon clusters: C(sub n) (n = 6-75) + D(sub 2)
[DE92-005330] p 3417 N92-29459

CARBON CYCLE
Constraining the atmospheric carbon budget: A preliminary assessment
[CSIRO-TP-25] p 3494 N92-29668
What is the potential of forest management to slow the increase of atmospheric CO2?
[PB92-180249] p 3495 N92-30173

CARBON DIOXIDE
Infrared pulse-laser long-path absorption measurement of carbon dioxide using a Raman-shifted dye laser p 3465 N92-29277
National Institute for Global Environmental Change
[DE92-013487] p 3493 N92-29597
Global-warming problem and global economic models
[DE92-514557] p 3493 N92-29638
Modelling and experimental validation of carbon dioxide evolution in alkalophilic cultures p 3507 N92-29734
Converting a CO2 atmosphere to a high-purity O2 supply
[NASA-CASE-LAR-14398-1] p 3419 N92-30098
What is the potential of forest management to slow the increase of atmospheric CO2?
[PB92-180249] p 3495 N92-30173

CARBON DIOXIDE CONCENTRATION
Constraining the atmospheric carbon budget: A preliminary assessment
[CSIRO-TP-25] p 3494 N92-29668
What is the potential of forest management to slow the increase of atmospheric CO2?
[PB92-180249] p 3495 N92-30173

CARBON DIOXIDE LASERS
Simulation of the performances of WIND, an airborne CO2 lidar p 3463 N92-29267
The e-beam sustained laser technology for space-based Doppler wind lidar p 3469 N92-29300
Laser paint stripping
[AD-A249233] p 3476 N92-29581

CARBON FIBERS
Development and characterization of oxidation-protected CFC
[MBB-Z-0395-91-PUB] p 3416 N92-29876
Fundamental study of compressive strength development in PAN-based carbon fibers
[AD-A250285] p 3416 N92-30137

CARBON-CARBON COMPOSITES
Review of temperature dependent effects on the oxidation protection of carbon/carbon
[DE92-012333] p 3415 N92-29645

CARBONATES
New directions for the catalytic conversion of methane
[PB92-172380] p 3492 N92-29519
Experimental study of cylindrical air electrodes
[DE92-506507] p 3441 N92-29912

CARBORANE
Vibrational spectrum and structure of 1,2-dimethyl-1,2-disila-closo-dodecaborane
[AD-A250235] p 3419 N92-29941

CARCINOGENS
Human exposure model-2: User's guide
[PB92-186246] p 3495 N92-30200
CARDS
The effect of yaw cards on the pitching and yawing motion of symmetric projectiles
[AD-A250021] p 3406 N92-29449
CARIBBEAN SEA
Numerical modeling studies of the Gulf of Mexico and the Caribbean Sea using the Bryan-Cox model
[PB92-164987] p 3505 N92-29704
CARRIER FREQUENCIES
Bandwidth compression of noisy signals with square-wave subcarrier p 3432 N92-29379
CARRIER WAVES
Bandwidth compression of noisy signals with square-wave subcarrier p 3432 N92-29379
CASCADE FLOW
Development of a multigrid transonic potential flow code for cascades
[NASA-CR-190480] p 3399 N92-29361
Examination of the main error factors with regards to secondary losses in compression and turbine cascades by variations of the blade picture ratio
[ETN-92-91493] p 3405 N92-29927
CASE HISTORIES
Evaluating the military potential of a developing nation's space program: A case study of Brazil
[AD-A245978] p 3407 N92-29929
CASSEGRAIN OPTICS
ARCLITE: The Arctic Lidar Technology Facility at Sondre Stromfjord, Greenland p 3407 N92-29283
One year of Rayleigh lidar measurements at Toronto p 3466 N92-29285
CATALYSIS
Acetate in hydrothermal solutions: Decomposition kinetics and metal complexation
[DE92-010542] p 3417 N92-29551
DSC measurements on experimental TGDDM/DDS resin systems: The influence of variations in resin composition and catalyst content
[NLR-TP-90267-U] p 3478 N92-29602
CATALYSTS
New directions for the catalytic conversion of methane
[PB92-172360] p 3492 N92-29519
CATHODES
Optical and electrical characteristics of the cathode fall
[AD-A249010] p 3443 N92-30176
CATIONS
Theoretical/experimental investigations of the structure and dynamics of highly energetic dication species
[AD-A247050] p 3418 N92-29901
CATS
Controlling the flow of visual information through the lateral geniculate nucleus: From single cells to neural networks
[AD-A250578] p 3528 N92-29590
CAUCHY PROBLEM
On the entropy production of dissipation models
[MEMO-1021] p 3560 N92-30148
CAVITY RESONATORS
Active modelocking and phase stabilization of a cavity dumped diode pumped Nd:YAG mini-laser
[DE92-011946] p 3475 N92-29358
CELL CATHODES
Advanced rechargeable lithium sulfur dioxide cell
[AD-A250027] p 3491 N92-29476
CELLS (BIOLOGY)
Pulse voltammetry in single cells using platinum microelectrodes
[AD-A248080] p 3440 N92-29523
On the estimation of bioenergetic parameters p 3508 N92-29738
CENSORED DATA (MATHEMATICS)
Computer program POWNOR for fitting the power-normal and -lognormal models to life or strength data from specimens of various sizes
[PB92-169119] p 3483 N92-29813
CENTRAL PROCESSING UNITS
Terrain following of arbitrary surfaces using a high intensity LED proximity sensor
[DE92-004464] p 3528 N92-29644
The M/G/1 processor sharing queue as the almost sure limit of feedback queues p 3530 N92-29965
CENTRIFUGAL COMPRESSORS
Explicit Navier-Stokes computation of turbomachinery flows
[AD-A248458] p 3445 N92-29933
CERAMIC MATRIX COMPOSITES
Characterization of fracture in (0/90)3s SiC/1723 composites
[AD-A250612] p 3414 N92-29453
Micromechanisms of cyclic and environmentally-assisted subcritical crack growth in ceramic-matrix composites
[AD-A248067] p 3414 N92-29556
Approaches to polymer-derived CMC matrices
[NASA-TM-105754] p 3415 N92-29660
CERAMICS
The processing of high temperature ceramic superconducting devices, volume 1
[AD-A248176] p 3438 N92-29404
Electron microscopy study on zirconia and alumina ceramic powders synthesized by microwave plasma pyrolysis
[DE92-013385] p 3424 N92-29479
Synthesis and useful reactions of organosilicon polymeric precursors for ceramics
[AD-A248500] p 3424 N92-29496
Cursory examination of the zeta potential behaviors of two optical materials
[DE92-011588] p 3551 N92-29578
Survey of research into electromagnetic and other wave effects on mechanical behavior and processing of materials
[AD-A248614] p 3426 N92-29905
An ontology of ceramics
[MEMO-INF-91-85] p 3426 N92-29960
CERTIFICATION
Revision of certification standards for aviation maintenance personnel p 3487 N92-30127
CHANNEL FLOW
Large eddy simulations of passive and buoyant scalars with dynamic subgrid-scale models p 3450 N92-30057
Some feedback procedures for control of flows p 3452 N92-30070
Turbulence modeling: Near-wall turbulence and effects of rotation on turbulence p 3452 N92-30151
A numerical method for direct simulation of turbulence in complex geometries p 3455 N92-30166
Turbulent thermal convection in a differentially rotating channel p 3455 N92-30168
Patterns in simulated turbulent channel flow p 3455 N92-30169
CHANNEL MULTIPLIERS
Design and construction of a channel electron multiplier based Mossbauer spectroscopy system
[AD-A248154] p 3439 N92-29443
CHANNEL NOISE
Design and construction of a channel electron multiplier based Mossbauer spectroscopy system
[AD-A248154] p 3439 N92-29443
CHANNELS (DATA TRANSMISSION)
Figure of merit for direct-detection optical channels p 3431 N92-29376
Comparing UCN with FDDI and DQDB using a realistic work model
[MEMO-INF-92-06] p 3526 N92-29985
CHAOS
Modeling deterministic chaos in thermally-pulsed combustion
[DE92-011756] p 3416 N92-29355
A closer look at a Fibonacci-like iterated nonlinear map: More chaos and order
[MEMO-INF-91-70] p 3537 N92-30075
CHARGE CARRIERS
Femtosecond studies of carrier dynamics in compound semiconductors
[AD-A250584] p 3439 N92-29452
CHARGE COUPLED DEVICES
CAESAR: A CCD airborne experimental scanner for applications in remote sensing radiometric and geometric calibration
[NLR-TP-89103-U] p 3490 N92-29707
Center of excellence: Microlaser microscope
[DE92-013485] p 3477 N92-29928
CHARGED PARTICLES
Rare gas clusters containing charged atoms
[AD-A248299] p 3544 N92-29350
Free ion yields in liquids: Molecular structure and track effects
[DE92-012208] p 3545 N92-29582
CHEBYSHEV APPROXIMATION
Chebyshev line approximation: A sensitivity analysis
[MEMO-1020] p 3537 N92-30147
CHEMICAL ANALYSIS
Computed tomography experiments of Pantex high explosives
[DE92-013517] p 3480 N92-29478
CHEMICAL BONDS
The activation of chemical bonds at surfaces
[AD-A248666] p 3418 N92-29719
CHEMICAL EQUILIBRIUM
A generalized polynomial form of the objective function in flash calculations
[AD-A248160] p 3531 N92-29446
CHEMICAL EXPLOSIONS
Computed tomography experiments of Pantex high explosives
[DE92-013517] p 3480 N92-29478
Strategies for understanding the deflagration-to-detonation transition
[DE92-013528] p 3427 N92-29512
CHEMICAL PROPERTIES
Air quality criteria for oxides of nitrogen, volume 1
[PB92-176361] p 3493 N92-29520
CHEMICAL REACTIONS
Thermodynamic and kinetic aspects of 3/5 epitaxy
[AD-A250632] p 3556 N92-29429
Synthesis of a naphthalene-hydroxynaphthalene polymer model compound
[DE92-012264] p 3423 N92-29435
The development of a fiber optic Raman temperature measurement system for rocket flows
[NASA-CR-189200] p 3413 N92-29448
Hydrogenation reactions of neutral carbon clusters: C(sub n) (n = 6-75) + D(sub 2)
[DE92-005330] p 3417 N92-29459
Modeling of the role of atomic hydrogen in heat transfer during hot filament assisted deposition of diamond
[AD-A250607] p 3418 N92-29595
Review of temperature dependent effects on the oxidation protection of carbon/carbon
[DE92-012333] p 3415 N92-29645
Modelling and experimental validation of carbon dioxide evolution in alkalophilic cultures p 3507 N92-29734
Finite-rate diffusion-controlled reaction in a vortex
[PB92-172006] p 3418 N92-29744
Polybenzimidazoles via aromatic nucleophilic displacement
[NASA-CASE-LAR-14643-1] p 3426 N92-29953
Monte-Carlo implementation of mapping closures: Application to chemical reacting flows p 3450 N92-30060
Effect of walls on the supersonic reacting mixing layer p 3451 N92-30065
CHEMILUMINESCENCE
Shock enhancement and control of hypersonic combustion
[AD-A248558] p 3418 N92-29580
CHEMISORPTION
Acetate in hydrothermal solutions: Decomposition kinetics and metal complexation
[DE92-010542] p 3417 N92-29551
The activation of chemical bonds at surfaces
[AD-A248666] p 3418 N92-29719
CHEMISTRY
Review of potential x ray laser applications in materials science and chemistry
[DE92-012254] p 3475 N92-29434
CHEMOSPHERE
NATO workshop on the Atmospheric Methane Cycle. Working group report on methane sources and sinks
[PB92-180256] p 3494 N92-30018
CHIPS (ELECTRONICS)
Using custom-designed VLSI fuzzy inferencing chips for the autonomous navigation of a mobile robot
[DE92-000424] p 3528 N92-29550
CHIRAL DYNAMICS
Contributions to Hadron 1991: 1) Testing the nature of the f(0)(S asterisk). 2) Gamma gamma to pi(exp 0) pi(exp 0): Dispersive analysis compared to chiral perturbation theory
[RAL-91-070] p 3544 N92-29488
Gamma gamma to pi(exp 0) pi(exp 0): Dispersive analysis compared to chiral perturbation theory p 3545 N92-29490
Theoretical overview: Hot and dense QCD in equilibrium
[DE92-013665] p 3560 N92-29517
CHLOROPHYLLS
In vivo and in vitro chlorophyll-a and pheophytin-a concentration measurements by laser fluorometry p 3468 N92-29295
SeaWiFS technical report series. Volume 5: Ocean optics protocols for SeaWiFS validation
[NASA-TM-104566] p 3506 N92-30193
CHROMIUM STEELS
Corrosion resistance of stainless steels and high Ni-Cr alloys to acid fluoride wastes
[DE92-012338] p 3420 N92-29436
CIRCUIT BOARDS
Design and analysis of electrical circuits that produce fractional-order differentiation
[AD-A248085] p 3440 N92-29526
B(exp 2)UBIST: A strategy for boundary scan board unified BIST
[IMAG-RR-862-I] p 3441 N92-29612
Interface board for providing time signals to a super minicomputer
[AD-D015198] p 3441 N92-29900

CIRCUITS
Computer model simulation of null-flux magnetic suspension and guidance
[DE92-013044] p 3478 N92-29534
Development of high T(sub c) (greater than 110 K) Bi, Tl, and Y-based materials as superconducting circuit elements
[NASA-CR-190311] p 3557 N92-29676
CIRCULAR CYLINDERS
A theoretical approach for analyzing the restabilization of wakes
[NASA-TM-103858] p 3443 N92-29394
A method for converting the surface of a generalized cylinder into a B-spline surface
[REPT-91-40] p 3535 N92-29922
CIRCULAR ORBITS
Generalized probability model for calculation of interference to the Deep Space Network due to circularly Earth-orbiting satellites p 3433 N92-29386
CIRRUS CLOUDS
Observations of cirrus clouds over the Pacific region by the NASA multiwavelength lidar system p 3473 N92-29325
CITIES
Lidar monitoring of Mexico City's atmosphere during high air polution episodes p 3464 N92-29275
Lidar observation of aerosol and temperature stratification over urban area during the formation of a stable atmospheric PBL p 3466 N92-29286
CIVIL AVIATION
European studies to investigate the feasibility of using 1000 ft vertical separation minima above FL 290. Part 1: Overview of organisation, techniques employed, and conclusions
[NLR-TP-91062-U-PT-1] p 3403 N92-29605
Current and future developments in civil aircraft non-destructive evaluation from an operator's point of view p 3399 N92-30122
Communication: An important element of maintenance and repair p 3402 N92-30124
Ageing aircraft research in the Netherlands p 3402 N92-30129
CLASSIFICATIONS
On the effect of range restriction on correlation coefficient estimation
[AD-A248956] p 3511 N92-29620
Tapering clouds and their classification due mainly to the surrounding cloud pattern in the GMS imagery
[ISSN-0388-9653] p 3502 N92-29666
Classification, error detection, and reconciliation of measurements in complex biochemical systems p 3508 N92-29737
Pole counting and resonance classification
[RAL-92-004] p 3560 N92-29996
Classification of A-graded algebras with 3 generators
[MEMO-1004] p 3537 N92-30080
CLASSIFIERS
Sensor fault detection on board an aircraft with observer and polynomial classifier
[DLR-FB-91-34] p 3404 N92-29870
CLIMATE
Mosquito Lagoon environmental resources inventory
[NASA-TM-107548] p 3492 N92-29430
Monthly means of selected climate variables for 1985 - 1989
[NASA-TM-104565] p 3502 N92-29653
Intercomparison of global marine climatologies
[DE92-011389] p 3494 N92-29790
Proceedings of the 16th Annual Climate Diagnostics Workshop
[PB92-167378] p 3503 N92-29801
Potential impacts of climate change on Pacific Northwest forest vegetation
[PB92-184985] p 3495 N92-30021
CLICOM-news, issue 7 p 3503 N92-30171
CLIMATE CHANGE
Sixteenth International Laser Radar Conference, part 1
[NASA-CP-3158-PT-1] p 3456 N92-29228
Lidar observations of stratospheric aerosol layer after the Mt. Pinatubo volcanic eruption p 3457 N92-29234
The role of lidars in global change research p 3457 N92-29235
Combined summaries: Technologies to sustain tropical forest resources and biological diversity
[OTA-F-515] p 3492 N92-29416
National Institute for Global Environmental Change
[DE92-013487] p 3493 N92-29597
Monthly means of selected climate variables for 1985 - 1989
[NASA-TM-104565] p 3502 N92-29653
Proceedings of the 16th Annual Climate Diagnostics Workshop
[PB92-167378] p 3503 N92-29801
ATLAS 1: Encountering planet Earth
[NASA-TM-107956] p 3408 N92-30016
NASA's Earth Observing System
[S-HRG-102-647] p 3490 N92-30017
Potential impacts of climate change on Pacific Northwest forest vegetation
[PB92-184985] p 3495 N92-30021
CLIMATOLOGY
Rayleigh/Raman lidars: Intercomparisons and validation p 3471 N92-29318
Polarization lidar liquid cloud detection algorithm for winter mountain storms p 3472 N92-29323
Research programming studies: Remote sensing emissions, land use and effects, in relation to climate and environment
[BCRS-91-17] p 3493 N92-29497
The main lines of the research programs remote sensing: Climate and environment
[BCRS-91-25] p 3493 N92-29499
National Institute for Global Environmental Change
[DE92-013487] p 3493 N92-29597
Intercomparison of global marine climatologies
[DE92-011389] p 3494 N92-29790
Proceedings of the 16th Annual Climate Diagnostics Workshop
[PB92-167378] p 3503 N92-29801
CLICOM-news, issue 7 p 3503 N92-30171
CLINICAL MEDICINE
A sample-size optimal bayesian procedure for sequential pharmaceutical trials
[AD-A248512] p 3538 N92-29501
CLOSURE LAW
Single point modeling of initially isotropic turbulence under uniform rotation p 3449 N92-30054
CLOSURES
Probability density function approach and related closures for turbulent scalar fields p 3450 N92-30059
Monte-Carlo implementation of mapping closures: Application to chemical reacting flows p 3450 N92-30060
CLOUD COVER
Sampling and representativeness for a spaceborne wind lidar p 3463 N92-29268
NWP impact of cloud top and boundary layer winds from a satellite borne lidar: An observing system simulation experiment p 3473 N92-29328
CLOUD PHYSICS
Lidar studies of extinction in clouds in the ECLIPS project p 3472 N92-29320
CLOUDS (METEOROLOGY)
The Lidar In-Space Technology Experiment (LITE) p 3469 N92-29301
Lidar studies of extinction in clouds in the ECLIPS project p 3472 N92-29320
Lidar studies of clouds at Toronto during the ECLIPS program p 3472 N92-29321
Adaptation of the University of Wisconsin high spectral resolution lidar for polarization and multiple scattering measurements p 3472 N92-29322
Polarization lidar liquid cloud detection algorithm for winter mountain storms p 3472 N92-29323
Measurement of mean or effective radius of cloud drop size distributions with a 10.6-micron wavelength lidar p 3472 N92-29324
Diode-pumped Nd:YAG lidar for airborne cloud measurements p 3473 N92-29326
Remote sensing by spaceborne lidar aided by surface returns p 3473 N92-29327
NWP impact of cloud top and boundary layer winds from a satellite borne lidar: An observing system simulation experiment p 3473 N92-29328
Tapering clouds and their classification due mainly to the surrounding cloud pattern in the GMS imagery
[ISSN-0388-9653] p 3502 N92-29666
CLUMPS
Hydrogenation reactions of neutral carbon clusters: C(sub n) (n = 6-75) + D(sub 2)
[DE92-005330] p 3417 N92-29459
CMOS
Latent interface-trap buildup: Issues for long-term device response
[DE92-003148] p 3439 N92-29455
Nonvolatile programmable neural network synaptic array
[NASA-CASE-NPO-18578-1-CU] p 3442 N92-30086
COAGULATION
The influence of turbulence on aggregation of small particles in agitated vessels
[ETN-92-91629] p 3445 N92-29775
COAL
Lidar investigation of aerosol pollution distribution near a coal power plant p 3467 N92-29289
COASTAL ECOLOGY
GIS for coastal management
[BCRS-90-31] p 3489 N92-29493
COASTAL WATER
Class A network Dataring gauges: 1989 data processing and analysis
[REPT-18-1991] p 3505 N92-29684
COASTAL ZONE COLOR SCANNER
SeaWiFS technical report series. Volume 1: An overview of SeaWiFS and ocean color
[NASA-TM-104566-VOL-1] p 3505 N92-29686
SeaWiFS technical report series. Volume 5: Ocean optics protocols for SeaWiFS validation
[NASA-TM-104566] p 3506 N92-30193
COASTS
Shelf Mixed Layer Experiment (SMILE) program description and coastal and moored array data report
[PB92-170281] p 3506 N92-29805
COATINGS
Rolling-contact and wear resistance of hard coatings on bearing-steel substrates
[DE92-011834] p 3478 N92-29357
COCKPIT SIMULATORS
Army-NASA aircrew/aircraft integration program: Phase 4 A(3)I Man-Machine Integration Design and Analysis System (MIDAS) software detailed design document
[NASA-CR-177593] p 3512 N92-29413
Transport delay measurements: Methodology and analysis for the F-16C combat engagement trainer, the display for advanced research and training, and the F-16A limited field of view
[AD-A248519] p 3406 N92-29505
CODING
The cognitive function of theoretical knowledge in procedural learning
[AD-A248075] p 3531 N92-29486
Chain coding in computer graphics
[ETN-92-91630] p 3518 N92-29776
COEFFICIENTS
The effect of yaw cards on the pitching and yawing motion of symmetric projectiles
[AD-A250021] p 3406 N92-29449
Statistics of narrowband white noise derived from clipped broadband white noise
[AD-A248597] p 3434 N92-29563
A semi empirical method for the analytical representation of stationary measured profile coefficients for applications of rotary wing aerodynamics
[ETN-92-91491] p 3401 N92-29741
The dependence of transport coefficients of suspensions in quasistatic and retarded hydrodynamic interactions
[ETN-92-91624] p 3444 N92-29752
On the asymptotically uniform distribution modulo 1 of extreme order statistics
[MEMO-COSOR-91-38] p 3540 N92-29821
COGENERATION
Thermal energy storage for cogeneration applications
[DE92-012339] p 3492 N92-29646
COGNITIVE PSYCHOLOGY
The cognitive function of theoretical knowledge in procedural learning
[AD-A248075] p 3531 N92-29486
Visual pattern completion
[PB92-187418] p 3524 N92-30195
COHERENT RADIATION
The x ray laser coherence experiments in neon-like yttrium
[DE92-010714] p 3477 N92-29987
COLD PLASMAS
Analysis of a dedicated rotation experiment in TFTR
[DE92-013463] p 3554 N92-29438
COLD WORKING
Stresses and strains in plain and coldworked annuli subjected to remote, interference or combined loading
[ARL-STRUC-R-446] p 3482 N92-29672
COLLISION PARAMETERS
Electron spectra of adatomic structures
[DE92-625013] p 3544 N92-29415
Exploratory study for a solid-state charged-particle spectrometer inside the Celsius ring: Alpha and hydrogen reactions at 1.7 and 2.2 GeV/c
[USIP-91-02] p 3546 N92-29715
Charge dependence and electric quadrupole effects on single-nucleon removal in relativistic and intermediate energy nuclear collisions p 3548 N92-30010
COLLISIONAL PLASMAS
Ion collision effects in hydrogen-like recombination x ray lasers
[DE92-013515] p 3476 N92-29509
COLLISIONS
Continuum approaches for describing solid-gas and solid-liquid flow
[DE92-013601] p 3452 N92-30140

COLLOIDS
Electrochemistry in colloids and dispersions. Volume 1: Electroanalytical methods and applications, electrosynthesis and electrocatalysis, polymers and latexes
[AD-A248335] p 3418 N92-29557
Electrochemistry in colloids and dispersions. Volume 2: Solute distribution, diffusion, and transport colloidal metals
[AD-A248336] p 3419 N92-29931
Electrochemistry in colloids and dispersions. Volume 3: Colloidal semiconductors
[AD-A248337] p 3419 N92-29932

COLOR
Biologically-based neural network model of color constancy and color contrast
[AD-A248128] p 3510 N92-29398
Object discrimination based on depth-from-occlusion
[AD-A248104] p 3511 N92-29560

COLOR VISION
Biologically-based neural network model of color constancy and color contrast
[AD-A248128] p 3510 N92-29398
Peripheral limitations on spatial vision
[AD-A250579] p 3511 N92-29591

COMBAT
Transport delay measurements: Methodology and analysis for the F-16C combat engagement trainer, the display for advanced research and training, and the F-16A limited field of view
[AD-A248519] p 3406 N92-29505

COMBINATORIAL ANALYSIS
Minimal-change codes and number systems
[REPT-91-42] p 3536 N92-29924

COMBINED CYCLE POWER GENERATION
Thermal energy storage for cogeneration applications
[DE92-012339] p 3492 N92-29646

COMBINED STRESS
Stresses and strains in plain and coldworked annuli subjected to remote, interference or combined loading
[ARL-STRUC-R-446] p 3482 N92-29672
Combined load test apparatus for flat panels
[NASA-CASE-LAR-14698-1] p 3483 N92-30028

COMBUSTIBLE FLOW
Simulation of flame-turbulence interactions in premixed combustion p 3450 N92-30062
Direct simulation of turbulent combustion p 3454 N92-30160

COMBUSTION
Modeling deterministic chaos in thermally-pulsed combustion
[DE92-011756] p 3416 N92-29355
Structure of a methanol/air coaxial reacting spray near the stabilization region by OH fluorescence imaging and two-component phase-Doppler interferometry
[DE92-005328] p 3417 N92-29431
A linear eddy sub-grid model for turbulent reacting flows: Application to hydrogen-air combustion
[DE92-006699] p 3417 N92-29433
On transient flamelets and their relationship to turbulent methane-air jet flames
[DE92-006705] p 3419 N92-29943

COMBUSTION CHAMBERS
Applied analytical combustion/emissions research at the NASA Lewis Research Center
[NASA-TM-105731] p 3412 N92-29343
The development of a fiber optic Raman temperature measurement system for rocket flows
[NASA-CR-189200] p 3413 N92-29448

COMBUSTION CHEMISTRY
Progress on combustion mechanisms of solid propellants
[AD-A248146] p 3427 N92-29330
Synthesis of a naphthalene-hydroxynaphthalene polymer model compound
[DE92-012264] p 3423 N92-29435

COMBUSTION CONTROL
Shock enhancement and control of hypersonic combustion
[AD-A248558] p 3418 N92-29580

COMBUSTION PHYSICS
Progress on combustion mechanisms of solid propellants
[AD-A248146] p 3427 N92-29330
Modeling deterministic chaos in thermally-pulsed combustion
[DE92-011756] p 3416 N92-29355
Flame ignition in a premixed turbulent flow p 3450 N92-30061
Simulation of flame-turbulence interactions in premixed combustion p 3450 N92-30062

COMBUSTION PRODUCTS
Lab-scale lidar sensing of diesel engines exhausts p 3464 N92-29276

COMMAND AND CONTROL
An analysis of the endurance of mobile satellite command and control systems
[AD-A248084] p 3410 N92-29525

COMMAND LANGUAGES
ASV3 dial-in interface recommendation for the Repository Based Software Engineering (RBSE) program
[NASA-CR-190500] p 3514 N92-29362

COMMERCIAL AIRCRAFT
Structural integrity of future aging airplanes p 3484 N92-30107
Fracture mechanics research at NASA related to the aging commercial transport fleet p 3484 N92-30110
Status of the FAA flight loads monitoring program p 3485 N92-30113
Nondestructive inspection perspectives p 3481 N92-30121

COMMUNICATING
Experiments on processes with backtracking
[RR-858-I-IMAG-121-LIFIA] p 3532 N92-29574
A massively parallel genetic algorithm for the graph partitioning problem
[IMAG-RR-845-I] p 3525 N92-29610
Parallelization of the recursive gradient backpropagation algorithm
[IMAG-RR-854-M] p 3525 N92-29614
Communication: An important element of maintenance and repair p 3402 N92-30124

COMMUNICATION EQUIPMENT
Erbium-doped fiber amplifier elements for structural analysis sensors
[NASA-CR-190491] p 3552 N92-29681

COMMUNICATION NETWORKS
Developments in fiber optics for distribution automation
[NASA-CR-190454] p 3551 N92-29679
User's manual for the NIST TTCN translator, version 3.0
[PB92-172493] p 3518 N92-29745
Real-time service definition of a communication network in a manufacturing environment
[MEMO-INF-91-84] p 3437 N92-29959
A simulation study on a high-speed slotted-ring access mechanism with dynamically adaptive slot size
[MEMO-INF-91-63] p 3526 N92-30074
Variable bandwidth connections for a connectionless service on ATM: Performance modelling and evaluation
[MEMO-INF-91-83] p 3438 N92-30170

COMMUNICATION THEORY
Improving the LAMP Mk 3 SH-60B HF communication system
[AD-A245970] p 3429 N92-29344
Golay and other box codes p 3431 N92-29375

COMMUTER AIRCRAFT
Damage tolerance for commuter aircraft p 3485 N92-30114

COMPACTING
A study of the influence of alloying additions on the passivity of aluminum
[AD-A248339] p 3421 N92-29587

COMPARISON
Comparison of turbulence parameters measured by SODAR and sonic anemometer
[KFK-4890] p 3500 N92-29690
Comparing UCN with FDDI and DQDB using a realistic work model
[MEMO-INF-92-06] p 3526 N92-29985
Comparison of in situ, aircraft- and satellite derived surface reflectances in Flevoland (Netherlands). A validation experiment
[BCRS-91-28] p 3491 N92-30230

COMPLETENESS
Partial logic as a simple restriction of standard logic
[MEMO-INF-91-73] p 3536 N92-29995

COMPLEX COMPOUNDS
Acetate in hydrothermal solutions: Decomposition kinetics and metal complexation
[DE92-010542] p 3417 N92-29551

COMPLEX NUMBERS
Revising M-layer: Complex exponent representation
[AD-A249121] p 3435 N92-29599

COMPLEXITY
On setup cost reduction in the economic lot-sizing model without speculative motives
[MEMO-COSOR-91-34] p 3520 N92-29819
On the complexity of postoptimality analysis of 0/1 programs
[MEMO-COSOR-91-35] p 3520 N92-29820
On the addition of log-convex functions and sequences
[MEMO-COSOR-92-01] p 3533 N92-29826

COMPONENT RELIABILITY
An analysis of the endurance of mobile satellite command and control systems
[AD-A248084] p 3410 N92-29525

COMPOSITE MATERIALS
A perspective on MoSi2 based composites
[DE92-013434] p 3415 N92-29795
Status and perspectives of modern composite materials
[MBB-Z-0380-91-PUB] p 3416 N92-29875
Survey of research into electromagnetic and other wave effects on mechanical behavior and processing of materials
[AD-A248614] p 3426 N92-29905
NASA-UVA light aerospace alloy and structures technology program (LA2ST)
[NASA-CR-190538] p 3423 N92-30206

COMPOSITE STRUCTURES
Structural durability of stiffened composite shells
[NASA-CR-190588] p 3481 N92-29342
Compressive response of debonded thick composite shells including the effects of transient moisture sorption
[AD-A250080] p 3414 N92-29462
Computed Tomography (CT) as a nondestructive test method used for composite helicopter components
[MBB-UD-0603-91-PUB] p 3480 N92-29873
Nonlinear analyses of composite aerospace structures in sonic fatigue
[NASA-CR-190565] p 3404 N92-30209

COMPRESSIBILITY
Compressive response of debonded thick composite shells including the effects of transient moisture sorption
[AD-A250080] p 3414 N92-29462
Direct simulations of wall-bounded compressible turbulence p 3454 N92-30162

COMPRESSIBILITY EFFECTS
The role of pressure-dilatation correlation in rapidly compressed turbulence and in boundary layers p 3449 N92-30050
Modeling of compressible turbulence p 3452 N92-30150
Turbulent thermal convection in a differentially rotating channel p 3455 N92-30168

COMPRESSIBLE BOUNDARY LAYER
Methods for direct simulation of transition in hypersonic boundary layers 2 p 3451 N92-30064

COMPRESSIBLE FLOW
The role of pressure-dilatation correlation in rapidly compressed turbulence and in boundary layers p 3449 N92-30050
Dynamic subgrid-scale modeling of compressible turbulence p 3450 N92-30058
Modeling of compressible turbulence p 3452 N92-30150
A numerical method for prediction of compressible turbulent flows with closure models p 3454 N92-30164

COMPRESSION LOADS
Strategies for understanding the deflagration-to-detonation transition
[DE92-013528] p 3427 N92-29512
Apparatus for elevated temperature compression or tension testing of specimens
[NASA-CASE-LAR-14775-1] p 3483 N92-30099

COMPRESSION TESTS
Apparatus for elevated temperature compression or tension testing of specimens
[NASA-CASE-LAR-14775-1] p 3483 N92-30099

COMPRESSIVE STRENGTH
Fundamental study of compressive strength development in PAN-based carbon fibers
[AD-A250285] p 3416 N92-30137

COMPRESSOR BLADES
Examination of the main error factors with regards to secondary losses in compression and turbine cascades by variations of the blade picture ratio
[ETN-92-91493] p 3405 N92-29927

COMPUTATION
Second-order shock-expansion theory extended to include real gas effects
[AD-A247191] p 3400 N92-29539
Revising M-layer: Complex exponent representation
[AD-A249121] p 3435 N92-29599
Parallelization of the recursive gradient backpropagation algorithm
[IMAG-RR-854-M] p 3525 N92-29614
The twopnt program for boundary value problems: Version 3.10 of March 1992
[DE92-013394] p 3517 N92-29641
On the p-coverage problem on the real line
[MEMO-COSOR-91-33] p 3520 N92-29818
On setup cost reduction in the economic lot-sizing model without speculative motives
[MEMO-COSOR-91-34] p 3520 N92-29819
On the complexity of postoptimality analysis of 0/1 programs
[MEMO-COSOR-91-35] p 3520 N92-29820
An introduction to using the FORTRAN programs provided with Computational Nuclear Physics 1 Nuclear Structure p 3549 N92-30013

Simplified computational methods for elastic and elastic-plastic fracture problems p 3488 N92-30134

COMPUTATIONAL FLUID DYNAMICS

Applied analytical combustion/emissions research at the NASA Lewis Research Center
[NASA-TM-105731] p 3412 N92-29343

Development of a multigrid transonic potential flow code for cascades
[NASA-CR-190480] p 3399 N92-29361

A comparison of the calculated and experimental off-design performance of a radial flow turbine
[NASA-CR-189207] p 3399 N92-29402

Spatial and temporal adaptive procedures for the unsteady aerodynamic analysis of airfoils using unstructured meshes
[NASA-TM-107635] p 3400 N92-29445

Hyperbolic grid generation control by panel methods
[NLR-TP-91061-U] p 3532 N92-29604

NASA Workshop on future directions in surface modeling and grid generation
[NASA-CP-10092] p 3400 N92-29625

Dynamic solder management
[AD-A250564] p 3422 N92-29647

Aeronautical Engineering Group publications, 1950 - present
[AERO-REPT-8907] p 3444 N92-29683

A semi empirical method for the analytical representation of stationary measured profile coefficients for applications of rotary wing aerodynamics
[ETN-92-91491] p 3401 N92-29741

Aerodynamic design optimization using sensitivity analysis and computational fluid dynamics
[NASA-CASE-LAR-14815-1-CU] p 3445 N92-29830

Production of periodical Mach number variations in high subsonic flow in a blow down wind tunnel, and its influence on profile measurements
[ETN-92-91492] p 3401 N92-29889

Experimental examination of heavy loaded axial fans with rotational symmetrical distortion of the inflow
[ETN-92-91489] p 3445 N92-29926

Explicit Navier-Stokes computation of turbomachinery flows
[AD-A248458] p 3445 N92-29933

The 2D-computation of an axial fan with FINFLO
[PB92-180678] p 3447 N92-30023

Local isotropy in buoyancy-generated turbulence p 3447 N92-30043

Streaks in turbulent boundary layers p 3451 N92-30069

Transition to turbulence in hypersonic flow p 3454 N92-30161

Turbulent transport in the solar nebula p 3454 N92-30163

Incompressible spatially-developing free-shear flows p 3454 N92-30165

A numerical method for direct simulation of turbulence in complex geometries p 3455 N92-30166

The large-scale structures in turbulent plane Couette flow p 3455 N92-30167

COMPUTATIONAL GRIDS

Spatial and temporal adaptive procedures for the unsteady aerodynamic analysis of airfoils using unstructured meshes
[NASA-TM-107635] p 3400 N92-29445

Hyperbolic grid generation control by panel methods
[NLR-TP-91061-U] p 3532 N92-29604

A compensation approach for two-dimensional Markov processes
[MEMO-COSOR-91-28] p 3539 N92-29606

Discretization of morphological operators
[CWI-BS-R9118] p 3533 N92-29861

Local isotropy in buoyancy-generated turbulence p 3447 N92-30043

On dynamic models for large eddy simulation p 3450 N92-30056

A numerical method for direct simulation of turbulence in complex geometries p 3455 N92-30166

Basic problems of a-posteriori error estimation
[AD-A248986] p 3541 N92-30174

COMPUTER AIDED DESIGN

Army-NASA aircrew/aircraft integration program: Phase 4 A(3)I Man-Machine Integration Design and Analysis System (MIDAS) software detailed design document
[NASA-CR-177593] p 3512 N92-29413

Improving designer productivity --- artificial intelligence
[NASA-TM-103929] p 3404 N92-29417

SOLCHIPS: A fast predesign and optimization tool for solar heating with seasonal storage
[DE92-506509] p 3492 N92-29636

SPARA: A system of planning robot manipulation tasks
[LAAS-91395] p 3529 N92-29678

Shop of the 1990's: The implementation of a CAD/CAM system for small machine shops
[PB92-181098] p 3522 N92-30020

COMPUTER AIDED MANUFACTURING

Improving designer productivity --- artificial intelligence
[NASA-TM-103929] p 3404 N92-29417

Robotic workcell for wire wrapping integrated circuits
[DE92-013999] p 3441 N92-29796

Real-time service definition of a communication network in a manufacturing environment
[MEMO-INF-91-84] p 3437 N92-29959

Shop of the 1990's: The implementation of a CAD/CAM system for small machine shops
[PB92-181098] p 3522 N92-30020

COMPUTER AIDED TOMOGRAPHY

Computed tomography experiments of Pantex high explosives
[DE92-013517] p 3480 N92-29478

Computed Tomography (CT) as a nondestructive test method used for composite helicopter components
[MBB-UD-0603-91-PUB] p 3480 N92-29873

COMPUTER ASSISTED INSTRUCTION

The effects of student-instructor interaction and paired/individual study on achievement in computer-based training
[AD-A248518] p 3511 N92-29503

COMPUTER COMPONENTS

Application Center of Excellence (ACE) program
[AD-A248694] p 3562 N92-29934

COMPUTER DESIGN

DSS-13 26-meter antenna upgraded radiometer system p 3432 N92-29381

COMPUTER GRAPHICS

Software architecture modelling: Application to AMODEUS design scenarios
[IMAG-RR-860-I] p 3513 N92-29611

ARTIBODIES: A system for modelling articulated bodies
[REPT-91-57] p 3517 N92-29627

Efficient complete radiosity ray tracing using a shadow coherence method
[REPT-91-63] p 3518 N92-29749

Chain coding in computer graphics
[ETN-92-91630] p 3518 N92-29776

Real-time quadratic shading
[CWI-CS-R9123] p 3534 N92-29892

Texture synthesis
[CWI-CS-R9139] p 3523 N92-30141

COMPUTER INFORMATION SECURITY

An overview of computer viruses in a research environment
[NASA-CR-190528] p 3517 N92-29630

Reliable processing of confidential data by means of fragmentation-redundancy-scattering
[LAAS-91412] p 3526 N92-29888

COMPUTER NETWORKS

A systems theoretic investigation of neuronal network properties of the hippocampal formation
[AD-A250246] p 3510 N92-29334

ASV3 dial-in interface recommendation for the Repository Based Software Engineering (RBSE) program
[NASA-CR-190500] p 3514 N92-29362

A universal, fault-tolerant, non-linear analytic network for modeling and fault detection
[DE92-011840] p 3525 N92-29624

Class A network Dataring gauges: 1989 data processing and analysis
[REPT-18-1991] p 3505 N92-29684

Performance of a connectionless protocol over ATM
[MEMO-INF-92-02] p 3526 N92-29880

Reviews of computing technology: Fiber distributed data interface
[DE92-011374] p 3514 N92-29907

Inverse remote procedure calls
[MEMO-INF-91-89] p 3521 N92-29970

Comparing UCN with FDDI and DQDB using a realistic work model
[MEMO-INF-92-06] p 3526 N92-29985

A simulation study on a high-speed slotted-ring access mechanism with dynamically adaptive slot size
[MEMO-INF-91-63] p 3526 N92-30074

COMPUTER PROGRAM INTEGRITY

Software reliability and the bootstrap
[CWI-BS-R9123] p 3520 N92-29865

Integrity control in relational database systems: An overview
[MEMO-INF-91-80] p 3562 N92-29957

Simulations on the Jelinski-Moranda model of software reliability
[CWI-BS-R9122] p 3523 N92-30179

COMPUTER PROGRAMMING

Summary of technical operations, 1991 --- software development
[AD-A248153] p 3516 N92-29540

Contracting in the software engineering crisis
[AD-A250241] p 3516 N92-29544

A look at the development environment and tools used in a large INGRES ABF application project
[DE92-012632] p 3561 N92-29552

Constraint classification for mixed integer programming formulations
[MEMO-COSOR-91-30] p 3516 N92-29608

Developments in fiber optics for distribution automation
[NASA-CR-190454] p 3551 N92-29679

Protocol conformance testing: A formal perspective in ISO IS-9646
[MEMO-INF-91-32] p 3517 N92-29705

Software quality control and requirements specification
[REPT-91-48] p 3518 N92-29711

An object-oriented language-database integration model: The composition-filters approach
[MEMO-INF-91-90] p 3521 N92-29961

CCS for OO and LP
[CWI-CS-R9136] p 3522 N92-29992

A case study in functional real-time programming
[MEMO-INF-91-62] p 3522 N92-30073

A formal development trajectory for OSI application layer protocols
[MEMO-INF-91-71] p 3523 N92-30144

Object-oriented system implementation
[MEMO-INF-91-67] p 3523 N92-30181

COMPUTER PROGRAMS

An innovative approach for coupled thermomechanical analysis
[DE92-011467] p 3481 N92-29338

On-line replacement of program modules using AdaPT
[NASA-CR-190499] p 3514 N92-29363

Alexander: User guide (version 1.0)
[BCRS-90-38] p 3489 N92-29494

Program SIXPAK: A code designed to check double-differential correlated data and calculate equivalent uncorrelated data
[DE92-013752] p 3516 N92-29537

Summary of technical operations, 1991 --- software development
[AD-A248153] p 3516 N92-29540

Micro-computer network architecture for range instrumentation applications, volume 1
[AD-A247836] p 3525 N92-29555

SOLCHIPS: A fast predesign and optimization tool for solar heating with seasonal storage
[DE92-506509] p 3492 N92-29636

The twopnt program for boundary value problems: Version 3.10 of March 1992
[DE92-013394] p 3517 N92-29641

Design characteristics of a heat pipe test chamber
[NASA-TM-105737] p 3492 N92-29662

Software quality control and requirements specification
[REPT-91-48] p 3518 N92-29711

SOLITON
[USIP-90-09] p 3518 N92-29714

User's manual for the NIST TTCN translator, version 3.0
[PB92-172493] p 3518 N92-29745

The FORM version of MINCER
[NIKHEF-H/91-18] p 3518 N92-29747

An introduction to software reuse
[REPT-91-50] p 3519 N92-29779

Decomposer: Program documentation
[USIP-91-04] p 3519 N92-29780

On the abstracted dataflow complexity of fast Fourier transforms
[DE92-011372] p 3562 N92-29794

Reverse automatic differentiation of modular FORTRAN programs
[DE92-014071] p 3519 N92-29797

Computer program POWNOR for fitting the power-normal and -lognormal models to life or strength data from specimens of various sizes
[PB92-169119] p 3483 N92-29813

Implementation of the object-oriented data model TM
[MEMO-INF-91-94] p 3520 N92-29855

ESATAN user manual
[ESA-PSS-03-105-ISSUE-2] p 3521 N92-29869

A method for computing the 3-dimensional flow about wings with leading-edge vortex separation. Part 2: Description of computer program VORSEP
[NLR-TR-86006-U] p 3402 N92-29916

Experience with piloted simulation in the development of helicopters
[MBB-UD-0610-91-PUB] p 3407 N92-30076

Users manual for updated computer code for axial-flow compressor conceptual design
[NASA-CR-189171] p 3524 N92-30207

Support activities to maintain SUMS flight readiness, volume 9. Attachment C: Flight STS-40 report. Attachment D: SUMS software listing
[NASA-CR-189656-VOL-9] p 3412 N92-30225

Expert judgment study on atmospheric dispersion and deposition: Main report and annexes
[REPT-91-81] p 3495 N92-30226

COMPUTER STORAGE DEVICES
A response surface methodology study of ferroelectric memory devices
[AD-A248094] p 3440 N92-29529
COMPUTER SYSTEMS DESIGN
ASV3 dial-in interface recommendation for the Repository Based Software Engineering (RBSE) program
[NASA-CR-190500] p 3514 N92-29362
Deep Space Network information system architecture study p 3433 N92-29385
Automatic generation algorithms, experiments, and comparisons of self checking PLA schemes
[IMAG-RR-843-I] p 3516 N92-29621
Information systems analysis and design based on an object-oriented framework
[MEMO-INF-91-93] p 3519 N92-29816
Cislan-2 final document by University of Twente (Netherlands)
[MEMO-INF-91-81] p 3526 N92-29958
What is the method in formal methods?
[MEMO-INF-91-79] p 3562 N92-30000
Criteria for, and experience with, ADTs in large LOTOS specifications
[MEMO-INF-91-74] p 3514 N92-30145
Object-oriented system implementation
[MEMO-INF-91-67] p 3523 N92-30181
COMPUTER SYSTEMS PERFORMANCE
Design and scheduling for periodic concurrent error detection and recovery in processor arrays
[NASA-CR-190571] p 3517 N92-29695
Measuring and simulating an 802.3 CSMA/CD LAN
[MEMO-COSOR-91-42] p 3525 N92-29825
A method for analysing the performance aspects of the fault-tolerance mechanisms in FDDI
[MEMO-INF-91-92] p 3514 N92-29982
Performability modelling tools: A survey
[MEMO-INF-91-82] p 3523 N92-30191
COMPUTER SYSTEMS SIMULATION
A method for analysing the performance aspects of the fault-tolerance mechanisms in FDDI
[MEMO-INF-91-92] p 3514 N92-29982
Performability modelling tools: A survey
[MEMO-INF-91-82] p 3523 N92-30191
COMPUTER TECHNIQUES
ASV3 dial-in interface recommendation for the Repository Based Software Engineering (RBSE) program
[NASA-CR-190500] p 3514 N92-29362
The weakest failure detector for solving consensus
[NASA-CR-190545] p 3515 N92-29400
The effects of student-instructor interaction and paired/individual study on achievement in computer-based training
[AD-A248518] p 3511 N92-29503
Using object-oriented databases for implementation of interactive electronic technical manuals
[AD-A248135] p 3440 N92-29564
COMPUTER VIRUSES
An overview of computer viruses in a research environment
[NASA-CR-190528] p 3517 N92-29630
COMPUTER VISION
Recognition of multi-articulated three-dimensional objects using a multisensor system for robotics applications
[LAAS-91394] p 3529 N92-29675
COMPUTERIZED SIMULATION
Progress on combustion mechanisms of solid propellants
[AD-A248146] p 3427 N92-29330
A systems theoretic investigation of neuronal network properties of the hippocampal formation
[AD-A250246] p 3510 N92-29334
Structural durability of stiffened composite shells
[NASA-CR-190588] p 3481 N92-29342
Ocean optical modeling: Light field structure, internal radiant emission, and vertical inhomogeneities
[AD-A248272] p 3504 N92-29345
Multidimensional computer simulation of Stirling cycle engines
[NASA-CR-190497] p 3478 N92-29392
KISMET (kinematic simulation, monitoring and off-line programming environments for telerobotics): Simulation of the target-oriented driving of an autonomous vehicle in a labyrinthic environment
[KFK-4941] p 3515 N92-29418
A linear eddy sub-grid model for turbulent reacting flows: Application to hydrogen-air combustion
[DE92-006699] p 3417 N92-29433
Ion collision effects in hydrogen-like recombination x ray lasers
[DE92-013515] p 3476 N92-29509
Computer model simulation of null-flux magnetic suspension and guidance
[DE92-013044] p 3478 N92-29534
Detection of binary phase shift keyed signals in extremely high noise
[AD-A248552] p 3435 N92-29576
A universal, fault-tolerant, non-linear analytic network for modeling and fault detection
[DE92-011840] p 3525 N92-29624
The twopnt program for boundary value problems: Version 3.10 of March 1992
[DE92-013394] p 3517 N92-29641
Dynamic solder management
[AD-A250564] p 3422 N92-29647
On fictitious joints modelling of manipulator link flexibility for the HERA simulation facility pilot
[NLR-TR-88086-U] p 3479 N92-29885
On transient flamelets and their relationship to turbulent methane-air jet flames
[DE92-006705] p 3419 N92-29943
Undecidable equivalences for basic process algebra
[CWI-CS-R9137] p 3536 N92-29993
Large eddy simulations of passive and buoyant scalars with dynamic subgrid-scale models p 3450 N92-30057
Dynamic subgrid-scale modeling of compressible turbulence p 3450 N92-30058
Simulation of flame-turbulence interactions in premixed combustion p 3450 N92-30062
Linear stability analysis of hypersonic boundary layers p 3451 N92-30063
Methods for direct simulation of transition in hypersonic boundary layers 2 p 3451 N92-30064
Direct numerical simulation of instability and noise generation of hot jets p 3451 N92-30066
Streaks in turbulent boundary layers p 3451 N92-30069
Texture synthesis
[CWI-CS-R9139] p 3523 N92-30141
Annual research briefs, 1989
[NASA-CR-189024] p 3452 N92-30149
Short-time Lyapunov exponent analysis p 3453 N92-30157
Direct simulation of turbulent combustion p 3454 N92-30160
Direct simulations of wall-bounded compressible turbulence p 3454 N92-30162
Turbulent transport in the solar nebula p 3454 N92-30163
Incompressible spatially-developing free-shear flows p 3454 N92-30165
A numerical method for direct simulation of turbulence in complex geometries p 3455 N92-30166
The large-scale structures in turbulent plane Couette flow p 3455 N92-30167
Patterns in simulated turbulent channel flow p 3455 N92-30169
COMPUTERS
An overview of computer viruses in a research environment
[NASA-CR-190528] p 3517 N92-29630
CONCATENATED CODES
Low complexity, high performance and bandwidth efficient concatenated coded 8-PSK schemes for reliable data communications
[NASA-CR-190588] p 3517 N92-29665
CONCENTRATION (COMPOSITION)
In vivo and in vitro chlorophyll-a and pheophytin-a concentration measurements by laser fluorometry p 3468 N92-29295
DSC measurements on experimental TGDDM/DDS resin systems: The influence of variations in resin composition and catalyst content
[NLR-TP-90267-U] p 3478 N92-29602
New developments in emission projection methodologies
[PB92-139393] p 3495 N92-30031
CONCENTRATORS
A wave theory for non-imaging concentrators
[AD-A248865] p 3552 N92-29726
CONCRETES
Guide for evaluating 12 inch Substantial Dividing Walls (SDWs) to provide protection from remote operation, volume 2
[AD-A250252] p 3428 N92-29335
Guide for evaluating 12 inch Substantial Dividing Walls (SDWs) to provide protection from remote operation, volume 1
[AD-A250251] p 3428 N92-29545
CONCURRENT PROCESSING
Design and scheduling for periodic concurrent error detection and recovery in processor arrays
[NASA-CR-190571] p 3517 N92-29695
Optimality of wait-free atomic multiwriter variables
[CWI-CS-R9128] p 3520 N92-29868
Computing distinguishing formulas for branching bisimulation
[CWI-CS-R9121] p 3521 N92-29890
Rendez-vous with metric semantics
[CWI-CS-R9135] p 3522 N92-29991
CCS for OO and LP
[CWI-CS-R9136] p 3522 N92-29992
Term rewriting analysis in process algebra
[CWI-CS-R9130] p 3537 N92-30177
Real space process algebra
[CWI-CW-R9131] p 3538 N92-30178
CONDENSING
Polybenzimidazoles via aromatic nucleophilic displacement
[NASA-CASE-LAR-14643-1] p 3426 N92-29953
CONDITIONS
Sufficient conditions for dominating cliques
[MEMO-1006] p 3538 N92-30185
CONDUCTION BANDS
Growth, characterization, and device development in monocrystalline diamond films
[AD-A248993] p 3560 N92-30175
CONFERENCES
Viscous profiles and numerical methods for shock waves
[AD-A246110] p 3443 N92-29458
Gordon research conference on Barrier Function of Mammalian Skin
[AD-A248556] p 3510 N92-29577
NASA Workshop on future directions in surface modeling and grid generation
[NASA-CP-10092] p 3400 N92-29625
International conference topical meeting on atmospheric, volume, and surface scattering and propagation
[AD-A248881] p 3552 N92-29727
Fourth Meeting of the Space Agency Forum on the International Space Year (SAFISY-4)
[ESA-SP-1141] p 3407 N92-29879
Proceedings of the Third Conference on Radiation Protection and Dosimetry
[DE92-011502] p 3547 N92-29910
The 1991 International Conference on Aging Aircraft and Structural Airworthiness
[NASA-CP-3160] p 3484 N92-30106
CONFIDENCE LIMITS
The determination of stochastic models and areas of confidence
[OEFZS-4612] p 3538 N92-29419
Accurate procedures for approximate Bayesian and conditional inference without the need for orthogonal parameters
[AD-A248662] p 3539 N92-29718
Computer program POWNOR for fitting the power-normal and -lognormal models to life or strength data from specimens of various sizes
[PB92-169119] p 3483 N92-29813
CONICAL SCANNING
Simulation of the performances of WIND, an airborne CO2 lidar p 3463 N92-29267
CONIFERS
Potential impacts of climate change on Pacific Northwest forest vegetation
[PB92-184985] p 3495 N92-30021
CONNECTORS
Fastening apparatus having shape memory alloy actuator
[NASA-CASE-MSC-21935-1] p 3479 N92-29762
Combined load test apparatus for flat panels
[NASA-CASE-LAR-14698-1] p 3483 N92-30028
CONSERVATION
Environmental quality: Report of the Council on Environmental Quality
[PB92-154954] p 3494 N92-29698
CONSERVATION LAWS
Supersymmetric extensions of the nonlinear Schroedinger equation: Symmetries and coverings
[MEMO-1002] p 3537 N92-30078
On the entropy production of dissipation models
[MEMO-1021] p 3560 N92-30148
CONSTRAINTS
Peripheral limitations on spatial vision
[AD-A250579] p 3511 N92-29591
Constraint classification for mixed integer programming formulations
[MEMO-COSOR-91-30] p 3516 N92-29608
Software architecture modelling: Application to AMODEUS design scenarios
[IMAG-RR-860-I] p 3513 N92-29611
CONTAMINANTS
Applied analytical combustion/emissions research at the NASA Lewis Research Center
[NASA-TM-105731] p 3412 N92-29343
New developments in emission projection methodologies
[PB92-139393] p 3495 N92-30031

CONTINENTAL SHELVES
Circulation and exchange at the continental shelf and slope SEEP-2
[DE92-013500] p 3504 N92-29439
Shelf Mixed Layer Experiment (SMILE) program description and coastal and moored array data report
[PB92-170281] p 3506 N92-29805
CONTINUOUS WAVE LASERS
Laser diode end-pumped Nd:YAG laser
[AD-A248123] p 3475 N92-29396
Laser processing for interconnect technology
[AD-A248103] p 3476 N92-29559
CONTINUUM FLOW
Continuum approaches for describing solid-gas and solid-liquid flow
[DE92-013601] p 3452 N92-30140
CONTINUUM MODELING
Constitutive modelling for granular material under finite strains with particle slidings and fabric changes
[AD-A248187] p 3482 N92-29407
CONTRACTORS
Enhanced evaluation, selection and acceptance criteria for the Contractor Integrated Technical Information Service (CITIS)
[PB92-163856] p 3562 N92-29699
CONTROL SURFACES
Computation of three-dimensional effects on two dimensional wings
[NASA-CR-190576] p 3401 N92-29691
CONTROL SYSTEMS DESIGN
Results of a flight simulator experiment to establish handling quality guidelines for the design of future transport aircraft
[NLR-MP-88044-U] p 3404 N92-29616
Experimental investigation of adaptive control of a parallel manipulator
[NASA-CR-189867] p 3528 N92-29656
SPARA: A system of planning robot manipulation tasks
[LAAS-91395] p 3529 N92-29678
State estimation and control of the IBE-fermentation with product recovery p 3509 N92-29756
Full pose and partial pose calibration of a 6 degree-of-freedom robot manipulator arm
[AD-A247463] p 3479 N92-29785
Fuzzy logic control of AC induction motors
[PB92-180207] p 3443 N92-30092
CONTROL THEORY
Developing CMMCA flight profiles for cruise missile tracking
[AD-A248183] p 3434 N92-29406
Some feedback procedures for control of flows p 3452 N92-30070
CONTROLLABILITY
Results of a flight simulator experiment to establish handling quality guidelines for the design of future transport aircraft
[NLR-MP-88044-U] p 3404 N92-29616
CONTROLLERS
Sequential design of a linear quadratic controller for the Deep Space Network antennas p 3432 N92-29382
Experimental investigation of adaptive control of a parallel manipulator
[NASA-CR-189867] p 3528 N92-29656
State estimation and error diagnosis for biotechnological processes
[ETN-92-91744] p 3508 N92-29754
Instantaneous optimal control for linear, nonlinear and hysteretic structures: Stable controllers
[PB92-163807] p 3501 N92-29950
Programmable hyperspectral image mapper with on-array processing
[NASA-CASE-NPO-17794-1-CU] p 3553 N92-30104
CONVECTION
Global solar magnetic fields
[AD-A248340] p 3569 N92-29421
CONVERGENCE
An examination of hypercube implementations of genetic algorithms
[AD-A248092] p 3515 N92-29527
Modeling and computational analysis of multiscale phenomena in fluid-structure interaction problems
[AD-A248723] p 3444 N92-29721
ISLAND: Interactive Solution Language for an Adaptive NIKE Driver
[DE92-011444] p 3533 N92-29791
U-statistics of increasing degrees with asymptotically Poisson distributions
[CWI-BS-R9120] p 3540 N92-29863
Hyperasymptotic expansions of confluent hypergeometric functions
[CWI-AM-R9107] p 3535 N92-29894
CONVERSION
A method for converting the surface of a generalized cylinder into a B-spline surface
[REPT-91-40] p 3535 N92-29922
CONVEXITY
Limit theorems for functionals of convex hulls
[REPT-91-39] p 3535 N92-29921
A random polynomial time algorithm for well-rounding convex bodies
[MEMO-1023] p 3541 N92-30188
CONVOLUTION INTEGRALS
Nonparametric maximum likelihood estimators for interval censoring and deconvolution
[REPT-91-53] p 3539 N92-29626
Positive convolution structures associated with quantum groups
[CWI-AM-R9105] p 3534 N92-29866
COOLANTS
Heat exchanger with oscillating flow
[NASA-CASE-LAR-14033-2] p 3447 N92-30024
COOLING SYSTEMS
Contingency power for a small turboshaft engine by using water injection into turbine cooling air
[NASA-TM-105680] p 3405 N92-29661
COORDINATES
A determination of the radio-planetary frame tie from comparison of Earth orientation parameters p 3409 N92-29365
COPOLYMERIZATION
Molecular engineering of liquid crystalline polymers
[AD-A248996] p 3427 N92-30136
COPOLYMERS
Molecular engineering of liquid crystalline polymers by living polymerization. 22: Synthesis and characterization of binary copolymers
[AD-A248287] p 3425 N92-29567
COPPER
The real-space multiple-scattering theory and the electronic structure of grain boundaries
[DE92-013006] p 3556 N92-29473
Robotic workcell for wire wrapping integrated circuits
[DE92-013999] p 3441 N92-29796
COPPER ALLOYS
Quasi-static intergranular cracking in a Cu-Sn alloy: An analog of stress relief cracking of steels
[DE92-011646] p 3420 N92-29483
Structure and stability of Al-Cu-Ru face-centered icosahedral alloys
[DE92-012550] p 3422 N92-29706
Thickness dependency of elastic aftereffect of thin bending beams
[ETN-92-91488] p 3483 N92-29925
COPPER SELENIDES
Novel thin-film CuInSe2 fabrication
[DE92-001222] p 3557 N92-29584
CORIOLIS EFFECT
Diurnal forcing of planetary atmospheres
[NASA-CR-190262] p 3569 N92-30199
CORRECTION
Correcting for interference of Mt. Pinatubo aerosols on DIAL measurements of stratospheric ozone p 3458 N92-29237
CORRELATION
Correlation analysis of wind lidar data p 3467 N92-29291
Program SIXPAK: A code designed to check double-differential correlated data and calculate equivalent uncorrelated data
[DE92-013752] p 3516 N92-29537
Cluster correlations from N-point correlation amplitudes p 3566 N92-29837
CORRELATION COEFFICIENTS
A new form for the chi-squared test of independence (document 2) p 3538 N92-29492
On the effect of range restriction on correlation coefficient estimation
[AD-A248956] p 3511 N92-29620
A simple approximation to the bivariate normal distribution with large correlation coefficient
[MEMO-1011] p 3540 N92-29974
CORROSION
Migmas/A: Test of a scanning ion microscope on the Soviet Space Station Mir
[OEFZS-4615] p 3473 N92-29469
Laser paint stripping
[AD-A249233] p 3476 N92-29581
A study of the influence of alloying additions on the passivity of aluminum
[AD-A248339] p 3421 N92-29587
CORROSION PREVENTION
Inspection of aging aircraft: A manufacturer's perspective p 3481 N92-30117
CORROSION RESISTANCE
Irradiation effects on the electrochemistry and corrosion resistance of stainless steel
[DE92-013504] p 3420 N92-29411
Corrosion resistance of stainless steels and high Ni-Cr alloys to acid fluoride wastes
[DE92-012338] p 3420 N92-29436
COSMIC RAYS
Electromagnetic processes in nucleus-nucleus collisions relating to space radiation research
[NASA-CR-190533] p 3547 N92-30001
Cross section parameterizations for cosmic ray nuclei. 1: Single nucleon removal p 3547 N92-30002
Stopping powers and cross sections due to two-photon processes in relativistic nucleus-nucleus collision p 3548 N92-30012
COSMOLOGY
Classical aspects of weak interactions
[NIKHEF-H/91-25] p 3546 N92-29751
COST ANALYSIS
Geostationary Operational Environmental Satellite(GEOS-N report)
[NASA-TM-107919] p 3410 N92-29810
Geostationary Operational Environmental Satellite (GOES-N report). Volume 1: Technical
[NASA-TM-107918] p 3410 N92-29811
COST ESTIMATES
The capacitated multi-echelon inventory system with serial structure: 2: An average cost approximation method
[MEMO-COSOR-91-40] p 3561 N92-29823
COST REDUCTION
Geostationary Operational Environmental Satellite (GOES-N report). Volume 1: Technical
[NASA-TM-107918] p 3410 N92-29811
On setup cost reduction in the economic lot-sizing model without speculative motives
[MEMO-COSOR-91-34] p 3520 N92-29819
COSTS
On setup cost reduction in the economic lot-sizing model without speculative motives
[MEMO-COSOR-91-34] p 3520 N92-29819
COUETTE FLOW
Streaks in turbulent boundary layers p 3451 N92-30069
Short-time Lyapunov exponent analysis p 3453 N92-30157
The large-scale structures in turbulent plane Couette flow p 3455 N92-30167
COULOMB COLLISIONS
Relativistic Coulomb fission p 3548 N92-30008
COULOMB POTENTIAL
Solution of two-body relativistic bound state equations with confining plus Coulomb interactions p 3547 N92-30003
Confining potential in momentum space p 3548 N92-30007
COUPLERS
Shaft mount for data coupler system
[NASA-CASE-LAR-13805-1] p 3480 N92-30097
COUPLING
Aperture coupling to shielded transmission lines: Theory and experiment
[PB92-183672] p 3437 N92-30093
COVARIANCE
A systems analysis of the impact of navigation instrumentation on-board a Mars rover, based on a covariance analysis of navigation performance
[NASA-CR-189868] p 3403 N92-29440
Optimization of stochastic response surfaces subject to constraints with linear programming
[AD-A248108] p 3516 N92-29586
CRACK ARREST
Tear straps in airplane fuselage
[AD-A248543] p 3404 N92-29511
CRACK INITIATION
Structural durability of stiffened composite shells
[NASA-CR-190588] p 3481 N92-29342
CRACK PROPAGATION
Structural durability of stiffened composite shells
[NASA-CR-190588] p 3481 N92-29342
Quasi-static intergranular cracking in a Cu-Sn alloy: An analog of stress relief cracking of steels
[DE92-011646] p 3420 N92-29483
Micromechanisms of cyclic and environmentally-assisted subcritical crack growth in ceramic-matrix composites
[AD-A248067] p 3414 N92-29556
Mechanism of diffusion-controlled brittle fracture
[DE92-011572] p 3482 N92-29601
Fatigue crack growth in damage tolerant Al-Li sheet alloys
[NLR-TP-90107-U] p 3483 N92-29708
Preliminary results on the fracture analysis of multi-site cracking of lap joints in aircraft skins p 3484 N92-30111
CRACKS
Characterization of fracture in (0/90)3s SiC/1723 composites
[AD-A250612] p 3414 N92-29453
Quasi-static intergranular cracking in a Cu-Sn alloy: An analog of stress relief cracking of steels
[DE92-011646] p 3420 N92-29483

Tear straps in airplane fuselage
[AD-A248543] p 3404 N92-29511
Federal Aviation Administration aging aircraft nondestructive inspection research plan
p 3481 N92-30116
Inspection of aging aircraft: A manufacturer's perspective p 3481 N92-30117
Simplified computational methods for elastic and elastic-plastic fracture problems p 3488 N92-30134

CREEP PROPERTIES
Strengthening mechanisms, creep and fatigue processes in dispersion hardened niobium alloy
[AD-A250282] p 3421 N92-29547

CREEP STRENGTH
A perspective on MoSi2 based composites
[DE92-013434] p 3415 N92-29795

CRITERIA
Criteria for, and experience with, ADTs in large LOTOS specifications
[MEMO-INF-91-74] p 3514 N92-30145

CRITICAL POINT
Identification of critical design points for the EAP of a space-based Doppler lidar wind sounder
p 3463 N92-29270

CROSS FLOW
Crossflow effects on the growth rate of inviscid Goertler vortices in a hypersonic boundary layer
[NASA-CR-189667] p 3455 N92-30190

CROSS SECTIONS
Do recent observations of very large electromagnetic dissociation cross sections signify a transition towards non-perturbative QED? p 3438 N92-30004

CRUISE MISSILES
Developing CMMCA flight profiles for cruise missile tracking
[AD-A248183] p 3434 N92-29406

CRYOGENIC COMPUTER STORAGE
Pressurization of cryogens: A review of current technology and its applicability to low-gravity conditions
[NASA-TM-105746] p 3427 N92-29669

CRYOGENIC FLUIDS
Pressurization of cryogens: A review of current technology and its applicability to low-gravity conditions
[NASA-TM-105746] p 3427 N92-29669

CRYOGENIC STORAGE
Optimization of armored spherical tanks for storage on the lunar surface
[NASA-TM-105700] p 3414 N92-30187

CRYOGENIC TEMPERATURE
Aluminum-lithium alloys: Surface-cracked tension fracture tests and physical and thermal properties at cryogenic temperatures
[PB92-172477] p 3422 N92-29803

CRYOGENICS
Final Environmental Impact Statement (EIS) for the Space Nuclear Thermal Propulsion (SNTP) program
[AD-A248408] p 3413 N92-29903

CRYSTAL LATTICES
Sub-angstrom microscopy through incoherent imaging and image reconstruction
[DE92-011787] p 3475 N92-30090

CRYSTAL OSCILLATORS
Introduction to quartz frequency standards
[AD-A248503] p 3439 N92-29498

CRYSTAL STRUCTURE
LiMoN2: The first metallic layered nitride
[AD-A248446] p 3418 N92-29619
Structure and stability of Al-Cu-Ru face-centered icosahedral alloys
[DE92-012550] p 3422 N92-29706
Amorphization along interfaces and grain boundaries in polycrystalline multilayers: An x ray diffraction study of Ni/Ti multilayers p 3558 N92-29769
Interdiffusion reactions in Ni/Ta multilayers studied by x ray diffraction p 3558 N92-29770
Sub-angstrom microscopy through incoherent imaging and image reconstruction
[DE92-011787] p 3475 N92-30090

CRYSTAL SURFACES
Thermodynamic and kinetic aspects of 3/5 epitaxy
[AD-A250632] p 3556 N92-29429
A response surface methodology study of ferroelectric memory devices
[AD-A248094] p 3440 N92-29529

CRYSTALLINITY
Molecular engineering of liquid crystalline polymers by living polymerization. 19: Synthesis and characterization of poly 2-(4-biphenyloxy)ethyl vinyl etherby
[AD-A248285] p 3423 N92-29349
Molecular engineering of side chain liquid crystalline polymers
[AD-A248540] p 3424 N92-29508
Molecular engineering of liquid crystalline polymers by living polymerization. 20: Synthesis and characterization of binary copolymers of 11-(4-cyano-4'-biphenyl) oxy)undecanyl vinyl ether with n-butyl vinyl ether and of 2-(4-cyano-4'-biphenyl) oxy)ethyl vinyl ether with n-butyl vinyl ether
[AD-A248286] p 3425 N92-29566
Molecular engineering of liquid crystalline polymers by living polymerization. 22: Synthesis and characterization of binary copolymers
[AD-A248287] p 3425 N92-29567

CRYSTALLIZATION
Molecular engineering of liquid crystalline polymers by living polymerization. 19: Synthesis and characterization of poly 2-(4-biphenyloxy)ethyl vinyl etherby
[AD-A248285] p 3423 N92-29349
Molecular engineering of liquid crystalline polymers by living polymerization. 22: Synthesis and characterization of binary copolymers
[AD-A248287] p 3425 N92-29567
Novel thin-film CuInSe2 fabrication
[DE92-001222] p 3557 N92-29584
Oriented structures based on trans-1,4-polybutadiene
[ETN-92-91632] p 3546 N92-29778

CRYSTALS
A response surface methodology study of ferroelectric memory devices
[AD-A248094] p 3440 N92-29529

CUBIC LATTICES
Small electrostrictive dilations of cubic crystals
[ISBN-90-9004374-8] p 3559 N92-29783

CULTURE TECHNIQUES
Modelling and experimental validation of carbon dioxide evolution in alkalophilic cultures p 3507 N92-29734
Microbial aldonolactone formation and hydrolysis: Kinetic and bioenergetic aspects p 3507 N92-29735
The bioreactor overflow device: An undesired selective separator in continuous cultures? p 3507 N92-29736
Classification, error detection, and reconciliation of measurements in complex biochemical systems
p 3508 N92-29737

CUMULATIVE DAMAGE
Short cracks and durability analysis of the Fokker 100 wing/fuselage structure
[NLR-TP-90336-U] p 3482 N92-29603

CURING
DSC measurements on experimental TGDDM/DDS resin systems: The influence of variations in resin composition and catalyst content
[NLR-TP-90267-U] p 3478 N92-29602

CURRENT DISTRIBUTION
Shelf Mixed Layer Experiment (SMILE) program description and coastal and moored array data report
[PB92-170281] p 3506 N92-29805

CURVATURE
Mixing measurements of straight and curved shear layers p 3451 N92-30067

CURVED BEAMS
An interlaminar tension strength specimen
[NASA-TM-107623] p 3481 N92-29393

CURVES (GEOMETRY)
Real-time quadratic shading
[CWI-CS-R9123] p 3534 N92-29892

CYANATES
Nonideal formation of network polymers
[AD-A248072] p 3424 N92-29465

CYCLIC LOADS
Short cracks and durability analysis of the Fokker 100 wing/fuselage structure
[NLR-TP-90336-U] p 3482 N92-29603
Stresses and strains in plain and coldworked annuli subjected to remote, interference or combined loading
[ARL-STRUC-R-446] p 3482 N92-29672

CYCLONES
Tropical cyclones: Central North Pacific, 1991
[PB92-167345] p 3502 N92-29743

CYCLOTRON RESONANCE DEVICES
Tunable driver for the LLNL FEL experiment
[DE92-011292] p 3477 N92-29937

CYLINDRICAL SHELLS
Structural durability of stiffened composite shells
[NASA-CR-190588] p 3481 N92-29342
The effect of length variation on the stability of circular cylindrical shells under pure bending
[LR-669] p 3482 N92-29700
Damaged stiffened shell research at NASA Langley Research Center p 3485 N92-30115

D

DAMAGE
Current DOT research on the effect of multiple site damage on structural integrity p 3485 N92-30112
Aging commuter aeroplanes: Fatigue evaluation and control methods p 3488 N92-30132

DAMAGE ASSESSMENT
Repair procedures for advanced composites for helicopters
[MBB-UD-0606-91-PUB] p 3399 N92-29874
Current DOT research on the effect of multiple site damage on structural integrity p 3485 N92-30112
Damage tolerance for commuter aircraft
p 3485 N92-30114

DAMPING
Check valve with poppet damping mechanism
[NASA-CASE-MSC-21903-1] p 3480 N92-30101

DARK MATTER
CDM with thermal history of baryons: High-resolution 2-D and 3-D simulations p 3565 N92-29835

DATA ACQUISITION
The Telecommunications and Data Acquisition Report
[NASA-CR-190460] p 3429 N92-29364
Galileo early cruise, including Venus, first Earth, and Gaspra encounters p 3433 N92-29384
Goldstone solar system radar signal processing
p 3433 N92-29389
EOS data policy: Questions remain about US commercial access. Report to the Chairman, Committee on Science, Space, and Technology, House of Representatives
[GAO/IMTEC-92-44] p 3488 N92-29467
Design and operation of the multipulse Thomson scattering diagnostic on DIII-D
[DE92-011393] p 3476 N92-29474
Status of the FAA flight loads monitoring program
p 3485 N92-30113
SESC glossary of solar-terrestrial terms
[PB92-185305] p 3563 N92-30194
Comparison of in situ, aircraft- and satellite derived surface reflectances in Flevoland (Netherlands). A validation experiment
[BCRS-91-28] p 3491 N92-30230
Acquisition of an aerothermodynamic data base by means of a winged experimental reentry vehicle
[MBB/FE202/S/PUB/461] p 3399 N92-30232

DATA BASE MANAGEMENT SYSTEMS
An object-based interviewing system
[DE92-013422] p 3527 N92-29504
A look at the development environment and tools used in a large INGRES ABF application project
[DE92-012632] p 3561 N92-29552
Using object-oriented databases for implementation of interactive electronic technical manuals
[AD-A248135] p 3440 N92-29564
Integrity control in relational database systems: An overview
[MEMO-INF-91-80] p 3562 N92-29957
An object-oriented language-database integration model: The composition-filters approach
[MEMO-INF-91-90] p 3521 N92-29961

DATA BASES
Observations of cirrus clouds over the Pacific region by the NASA multiwavelength lidar system
p 3473 N92-29325
A look at the development environment and tools used in a large INGRES ABF application project
[DE92-012632] p 3561 N92-29552
NASA visual thesaurus maintenance documentation
[NASA-CR-190282] p 3561 N92-29553
Using object-oriented databases for implementation of interactive electronic technical manuals
[AD-A248135] p 3440 N92-29564
Marine structural steel toughness data bank (abridged edition)
[PB92-163294] p 3422 N92-29807
Facets of database triggers
[CWI-CS-R9122] p 3521 N92-29891
CRIS/USDA online access guide. Revision 1: File 60 on DIALOG
[PB92-172857] p 3562 N92-30033
Archives of the future: Archival strategies for the treatment of electronic databases
[PB92-178631] p 3563 N92-30038
Status of the FAA flight loads monitoring program
p 3485 N92-30113
Communication: An important element of maintenance and repair p 3402 N92-30124
SESC glossary of solar-terrestrial terms
[PB92-185305] p 3563 N92-30194
Acquisition of an aerothermodynamic data base by means of a winged experimental reentry vehicle
[MBB/FE202/S/PUB/461] p 3399 N92-30232

DATA COMPRESSION
Bandwidth compression of noisy signals with square-wave subcarrier p 3432 N92-29379

DATA FLOW ANALYSIS
On the abstracted dataflow complexity of fast Fourier transforms
[DE92-011372] p 3562 N92-29794
A model for dataflow query execution in a parallel main-memory environment
[MEMO-INF-91-34] p 3527 N92-30142

DATA LINKS
FM video data link spectrum spreading
[AD-D015257] p 3435 N92-29572
Application of VME-technology on an airborne data link processor unit
[NLR-MP-88040-U] p 3403 N92-29615
Developments in fiber optics for distribution automation
[NASA-CR-190454] p 3551 N92-29679
DATA MANAGEMENT
EOS data policy: Questions remain about US commercial access. Report to the Chairman, Committee on Science, Space, and Technology, House of Representatives
[GAO/IMTEC-92-44] p 3488 N92-29467
PDES application protocol suite for composites (PAS-C): IDEFO activity models and information needs for the PAS-C program
[AD-A248714] p 3562 N92-29720
Facets of database triggers
[CWI-CS-R9122] p 3521 N92-29891
DATA PROCESSING
Circulation and exchange at the continental shelf and slope SEEP-2
[DE92-013500] p 3504 N92-29439
A look at the development environment and tools used in a large INGRES ABF application project
[DE92-012632] p 3561 N92-29552
Modelling, information processing and control
[AD-A250571] p 3532 N92-29589
Class A network Dataring gauges: 1989 data processing and analysis
[REPT-18-1991] p 3505 N92-29684
Classification, error detection, and reconciliation of measurements in complex biochemical systems
p 3508 N92-29737
Reliable processing of confidential data by means of fragmentation-redundancy-scattering
[LAAS-91412] p 3526 N92-29888
DATA REDUCTION
Data reduction in statistical inference
[MEMO-COSOR-92-03] p 3540 N92-29828
DATA STORAGE
Nonvolatile programmable neural network synaptic array
[NASA-CASE-NPO-18578-1-CU] p 3442 N92-30086
DATA STRUCTURES
DecisionMaker software and extracting fuzzy rules under uncertainty
[NASA-CR-190502] p 3514 N92-29391
Abstract data types and algorithm structures and a basis for component reuse
[REPT-91-49] p 3518 N92-29712
Modeling and computational analysis of multiscale phenomena in fluid-structure interaction problems
[AD-A248723] p 3444 N92-29721
Object-oriented system implementation
[MEMO-INF-91-67] p 3523 N92-30181
DATA SYSTEMS
Lidar In-space Technology Experiment (LITE) electronics overview p 3462 N92-29264
The Telecommunications and Data Acquisition Report
[NASA-CR-190460] p 3429 N92-29364
EOS Data and Information System (EOSDIS) --- landsat satellites
[NASA-TM-107922] p 3488 N92-29442
Program SIXPAK: A code designed to check double-differential correlated data and calculate equivalent uncorrelated data
[DE92-013752] p 3516 N92-29537
Shaft mount for data coupler system
[NASA-CASE-LAR-13805-1] p 3480 N92-30097
Criteria for, and experience with, ADTs in large LOTOS specifications
[MEMO-INF-91-74] p 3514 N92-30145
CLICOM-news, issue 7 p 3503 N92-30171
DATA TRANSFER (COMPUTERS)
Enhanced evaluation, selection and acceptance criteria for the Contractor Integrated Technical Information Service (CITIS)
[PB92-163856] p 3562 N92-29699
Architectural synthesis and optimization of digital systems
[ISBN-90-9003966-X] p 3519 N92-29782
Cislan-2 final document by University of Twente (Netherlands)
[MEMO-INF-91-81] p 3526 N92-29958
Real-time service definition of a communication network in a manufacturing environment
[MEMO-INF-91-84] p 3437 N92-29959
Inverse remote procedure calls
[MEMO-INF-91-89] p 3521 N92-29970
Comparing UCN with FDDI and DQDB using a realistic work model
[MEMO-INF-92-06] p 3526 N92-29985
Criteria for, and experience with, ADTs in large LOTOS specifications
[MEMO-INF-91-74] p 3514 N92-30145
Variable bandwidth connections for a connectionless service on ATM: Performance modelling and evaluation
[MEMO-INF-91-83] p 3438 N92-30170
DATA TRANSMISSION
Low complexity, high performance and bandwidth efficient concatenated coded 8-PSK schemes for reliable data communications
[NASA-CR-190588] p 3517 N92-29665
Reviews of computing technology: Fiber distributed data interface
[DE92-011374] p 3514 N92-29907
Shaft mount for data coupler system
[NASA-CASE-LAR-13805-1] p 3480 N92-30097
DAWN CHORUS
Global measurements of low-frequency radio noise
[AD-A248260] p 3434 N92-29542
DAYGLOW
Analysis of EUV dayglow spectra of Triton, Titan and Earth
[NASA-CR-190586] p 3568 N92-29451
DC 9 AIRCRAFT
Maintaining the safety of an aging fleet of aircraft
p 3402 N92-30108
DECARBOXYLATION
Acetate in hydrothermal solutions: Decomposition kinetics and metal complexation
[DE92-010542] p 3417 N92-29551
DECISION MAKING
DecisionMaker software and extracting fuzzy rules under uncertainty
[NASA-CR-190502] p 3514 N92-29391
A sample-size optimal bayesian procedure for sequential pharmaceutical trials
[AD-A248512] p 3538 N92-29501
Optimization of stochastic response surfaces subject to constraints with linear programming
[AD-A248108] p 3516 N92-29586
Decision systems; the relation between problem specification and mathematical analysis
[MEMO-COSOR-91-37] p 3535 N92-29898
Separable Markovian decision problems: The linear programming method in the multichain case (revised)
[PB92-187350] p 3524 N92-30201
Expert judgment study on atmospheric dispersion and deposition: Main report and annexes
[REPT-91-81] p 3495 N92-30226
DECISION THEORY
Tools for the interfacing between dynamical problems and models within decision support systems
[MEMO-COSOR-91-29] p 3532 N92-29607
DEDUCTION
Loop checking in partial deduction
[CWI-CS-R9134] p 3522 N92-29990
DEEP SPACE NETWORK
The Telecommunications and Data Acquisition Report
[NASA-CR-190460] p 3429 N92-29364
Deep-space navigation with differenced data types. Part 3: An expanded information content and sensitivity analysis p 3409 N92-29368
Applications of inertial-sensor high-inheritance instruments to DSN precision antenna pointing
p 3430 N92-29371
Dynamic modeling of fluid transmission lines of the DSN 70-meter antennas by using a lumped parameter model
p 3432 N92-29378
An OSI architecture for the Deep Space Network
p 3432 N92-29380
DSS-13 26-meter antenna upgraded radiometer system p 3432 N92-29381
Sequential design of a linear quadratic controller for the Deep Space Network antennas p 3432 N92-29382
DSN acquisition of Magellan high-rate telemetry data
p 3409 N92-29383
Deep Space Network information system architecture study p 3433 N92-29385
Generalized probability model for calculation of interference to the Deep Space Network due to circularly Earth-orbiting satellites p 3433 N92-29386
DSN observations of Titan p 3433 N92-29388
DEFECTS
Compressive response of debonded thick composite shells including the effects of transient moisture sorption
[AD-A250080] p 3414 N92-29462
Method and apparatus for thermographically and quantitatively analyzing a structure for disbonds and/or inclusions
[NASA-CASE-LAR-14559-1] p 3480 N92-29829
Thermal QNDE detection of airframe disbonds
p 3481 N92-30118
DEFENSE PROGRAM
The 1991 research highlights
[AD-A247865] p 3570 N92-29464
Burros: Simple, affordable, effective space transportation
[DE92-013553] p 3541 N92-30138
DEFORMATION
An innovative approach for coupled thermomechanical analysis
[DE92-011467] p 3481 N92-29338
Compressive response of debonded thick composite shells including the effects of transient moisture sorption
[AD-A250080] p 3414 N92-29462
Strengthening mechanisms, creep and fatigue processes in dispersion hardened niobium alloy
[AD-A250282] p 3421 N92-29547
A consistent shear deformable theory for laminated plates
[AD-A250591] p 3415 N92-29593
Variational formulation and finite element implementation of Pagano's theory of laminated plates
[AD-A250592] p 3415 N92-29594
Effect of grain size on deformation stability of copper under quasi-static and dynamic tensile loading
[DE92-012677] p 3421 N92-29639
Integrable deformations of meromorphic equations on P(exp 1)C
[MEMO-993] p 3534 N92-29872
DEGRADATION
Surface reactions in the space environment
[AD-A250624] p 3428 N92-29428
Advanced rechargeable lithium sulfur dioxide cell
[AD-A250027] p 3491 N92-29476
DEHYDROGENATION
New directions for the catalytic conversion of methane
[PB92-172360] p 3492 N92-29519
DELAMINATING
Compressive response of debonded thick composite shells including the effects of transient moisture sorption
[AD-A250080] p 3414 N92-29462
A consistent shear deformable theory for laminated plates
[AD-A250591] p 3415 N92-29593
Variational formulation and finite element implementation of Pagano's theory of laminated plates
[AD-A250592] p 3415 N92-29594
DELAY
Real-time service definition of a communication network in a manufacturing environment
[MEMO-INF-91-84] p 3437 N92-29959
DELTA WINGS
A method for computing the 3-dimensional flow about wings with leading-edge vortex separation. Part 2: Description of computer program VORSEP
[NLR-TR-86006-U] p 3402 N92-29916
DEMOGRAPHY
Exercise and three psychosocial variables: A longitudinal study
[AD-A250649] p 3510 N92-30216
DEMULTIPLEXING
Micro-device for coupling, multiplexing and demultiplexing using elliptical-core two-mode fiber
[NASA-CR-190496] p 3550 N92-29331
DENSE PLASMAS
Optical diagnostics on dense Z-pinch plasmas
[DE92-011228] p 3555 N92-29917
DENSITY DISTRIBUTION
The significance of large-scale flows into the Great Attractor p 3565 N92-29836
Scales of universal homogeneity from galaxy counts
p 3566 N92-29841
On constructing kernel polynomials of a spectral function: Application to ARMA models
[CWI-BS-R9119] p 3533 N92-29862
DENSITY MEASUREMENT
Extraction of aerosol and Rayleigh components from Doppler lidar return signal p 3465 N92-29281
DEPLOYMENT
An analysis of the endurance of mobile satellite command and control systems
[AD-A248084] p 3410 N92-29525
DEPOSITION
Material-deposition processes in the separator of Li-alloy/FeS2 thermal cells
[DE92-013669] p 3440 N92-29518
Novel thin-film CuInSe2 fabrication
[DE92-001222] p 3557 N92-29584
Modeling of the role of atomic hydrogen in heat transfer during hot filament assisted deposition of diamond
[AD-A250607] p 3418 N92-29595
Monolithic amorphous silicon modules on continuous polymer substrate
[DE92-001163] p 3425 N92-29598
Role of polyelectrolytes in barium sulphate precipitation
[PB92-184761] p 3419 N92-30196
DEPTH
Object discrimination based on depth-from-occlusion
[AD-A248104] p 3511 N92-29560

DESERTS
Mapping of groundwater losses by evaporation in the western desert of Egypt
[BCRS-91-01] p 3489 N92-29495
DESIGN ANALYSIS
Optimal design of compact spur gear reductions
[NASA-TM-105676] p 3478 N92-29351
Making intelligent systems team players: Overview for designers
[NASA-TM-104751] p 3513 N92-29403
A preliminary design and analysis of an advanced heat-rejection system for an extreme altitude advanced variable cycle diesel engine installed in a high-altitude advanced research platform
[NASA-CR-186021] p 3405 N92-29427
Technology programme: Aerothermodynamics and propulsion integration. Numerical and experimental aerothermodynamics
[MBB-FE-202-S-PUB-0464-A] p 3400 N92-29648
Concurrent engineering in design of aircraft structures
[MBB-FE-2-S-PUB-472] p 3404 N92-29650
Design characteristics of a heat pipe test chamber
[NASA-TM-105737] p 3492 N92-29662
Aerodynamic design optimization using sensitivity analysis and computational fluid dynamics
[NASA-CASE-LAR-14815-1-CU] p 3445 N92-29830
Experience with piloted simulation in the development of helicopters
[MBB-UD-0610-91-PUB] p 3407 N92-30076
Users manual for updated computer code for axial-flow compressor conceptual design
[NASA-CR-189171] p 3524 N92-30207
DESORPTION
Laser-induced desorption from sapphire surfaces
[DE92-012698] p 3475 N92-29340
Hydrogen desorption and the search for the Higgs
[DE92-013464] p 3545 N92-29507
Theory of the dissociation dynamics of small molecules on metal surfaces: Finite temperature studies
[DE92-011188] p 3546 N92-29899
DETECTION
A developing multiple-wavelength lidar for detecting mainly ozone and aerosol distributions in the stratosphere p 3467 N92-29292
Prospects for long baseline neutrino oscillation experiments
[DE92-011833] p 3544 N92-29356
Low energy neutral atoms in the Earth's magnetosphere: Modeling
[DE92-013240] p 3500 N92-29536
Evaluation of Night Vision Goggles (NVG) for maritime search and rescue
[AD-A247182] p 3512 N92-29538
A universal, fault-tolerant, non-linear analytic network for modeling and fault detection
[DE92-011840] p 3525 N92-29624
On the optimization of windshear warning and guidance systems
[NLR-TP-90196-U] p 3402 N92-29703
Smart BIT/TSMD integration
[AD-A247192] p 3442 N92-29914
Accelerometer method and apparatus for integral display and control functions
[NASA-CASE-MSC-21961-1] p 3474 N92-29952
Phase-space estimate of satellite coverage time
[DE92-013555] p 3542 N92-30139
Electrochemical array sensors for plating waste stream monitoring
[DE92-011446] p 3495 N92-30211
DETERIORATION
Aging commuter aeroplanes: Fatigue evaluation and control methods p 3488 N92-30132
DETONATION
Guide for evaluating 12 inch Substantial Dividing Walls (SDWs) to provide protection from remote operation, volume 2
[AD-A250252] p 3428 N92-29335
Strategies for understanding the deflagration-to-detonation transition
[DE92-013528] p 3427 N92-29512
Guide for evaluating 12 inch Substantial Dividing Walls (SDWs) to provide protection from remote operation, volume 1
[AD-A250251] p 3428 N92-29545
DIAGNOSIS
State estimation and error diagnosis for biotechnological processes
[ETN-92-91744] p 3508 N92-29754
Improved balancing methods and error diagnosis for bio(chemical) conversions p 3509 N92-29759
An analysis of model-based diagnosis using problem-reformulation
[MEMO-INF-92-03] p 3530 N92-29983
DIAMOND FILMS
Raman features of CVD diamond films
[DE92-011381] p 3426 N92-29908
Growth, characterization, and device development in monocrystalline diamond films
[AD-A248993] p 3560 N92-30175
DIAMONDS
Characterization of fracture in (0/90)3s SiC/1723 composites
[AD-A250612] p 3414 N92-29453
Modeling of the role of atomic hydrogen in heat transfer during hot filament assisted deposition of diamond
[AD-A250607] p 3418 N92-29595
Simulations on the electrical characteristics of Si, SiC and diamond junction and Schottky power diodes
[PB92-177872] p 3443 N92-30094
DIAPHRAGMS (MECHANICS)
Bladder operated robotic joint
[NASA-CASE-MFS-28682-1] p 3426 N92-29831
DIELECTRIC PROPERTIES
User's guide for the VTRPE (Variable Terrain Radio Parabolic Equation) computer model
[AD-A248112] p 3433 N92-29395
DIELECTRICS
Diffraction of light from randomly rough surfaces
[AD-A250261] p 3551 N92-29546
RF vacuum electronics
[AD-A248857] p 3442 N92-29935
DIESEL ENGINES
Lab-scale lidar sensing of diesel engines exhausts p 3464 N92-29276
A preliminary design and analysis of an advanced heat-rejection system for an extreme altitude advanced variable cycle diesel engine installed in a high-altitude advanced research platform
[NASA-CR-186021] p 3405 N92-29427
DIFFERENTIAL EQUATIONS
On the numerical solution of one-dimensional integral and differential equations
[AD-A250388] p 3531 N92-29548
Variational formulation and finite element implementation of Pagano's theory of laminated plates
[AD-A250592] p 3415 N92-29594
The twopnt program for boundary value problems: Version 3.10 of March 1992
[DE92-013394] p 3517 N92-29641
Mathematical modelling of saturated and unsaturated groundwater flow
[MEMO-987] p 3445 N92-29857
Gaarding inequalities for systems of pseudo-differential operators
[CWI-AM-R9111] p 3534 N92-29881
On the entropy production of dissipation models
[MEMO-1021] p 3560 N92-30148
DIFFERENTIATORS
Design and analysis of electrical circuits that produce fractional-order differentiation
[AD-A248085] p 3440 N92-29526
DIFFRACTION
Optical diagnostics on dense Z-pinch plasmas
[DE92-011228] p 3555 N92-29917
DIFFRACTION PATTERNS
Layer-thickness variations and x ray diffraction patterns, a general treatment p 3558 N92-29767
Low-angle x ray diffraction study of solid state amorphization in a Ni/Ti multilayer p 3558 N92-29768
Dynamic aperture fringe discriminator
[NASA-CASE-NPO-18478-1-CU] p 3553 N92-30084
DIFFUSE RADIATION
Cosine response characteristics of radiometric and photometric sensors
[DE92-011437] p 3551 N92-29530
DIFFUSION
Electrochemistry in colloids and dispersions. Volume 1: Electroanalytical methods and applications, electrosynthesis and electrocatalysis, polymers and latexes
[AD-A248335] p 3418 N92-29557
Finite-rate diffusion-controlled reaction in a vortex
[PB92-172006] p 3418 N92-29744
Amorphization by interdiffusion in metallic multilayers
[ETN-92-91743] p 3558 N92-29766
Electrochemistry in colloids and dispersions. Volume 2: Solute distribution, diffusion, and transport colloidal metals
[AD-A248336] p 3419 N92-29931
Electrochemistry in colloids and dispersions. Volume 3: Colloidal semiconductors
[AD-A248337] p 3419 N92-29932
On transient flamelets and their relationship to turbulent methane-air jet flames
[DE92-006705] p 3419 N92-29943
DIGITAL COMPUTERS
A universal, fault-tolerant, non-linear analytic network for modeling and fault detection
[DE92-011840] p 3525 N92-29624
DIGITAL DATA
Enhanced evaluation, selection and acceptance criteria for the Contractor Integrated Technical Information Service (CITIS)
[PB92-163856] p 3562 N92-29699
Discretization of morphological operators
[CWI-BS-R9118] p 3533 N92-29861
DIGITAL SYSTEMS
World Administrative Radio Conference. Issues for US International Spectrum Policy
[PB92-157601] p 3435 N92-29696
Architectural synthesis and optimization of digital systems
[ISBN-90-9003966-X] p 3519 N92-29782
DIGITAL TECHNIQUES
Image inversion analysis of the HST OTA (Hubble Space Telescope Optical Telescope Assembly), phase A
[NASA-CR-190483] p 3564 N92-29359
B(exp 2)UBIST: A strategy for boundary scan board unified BIST
[IMAG-RR-862-I] p 3441 N92-29612
DIMENSIONAL ANALYSIS
Acoustic scattering from elastic ice: A finite difference solution
[AD-A248281] p 3543 N92-29346
On the two-dimensional model of quantum Regge gravity
[DE92-624516] p 3560 N92-30212
DIODES
RF vacuum electronics
[AD-A248857] p 3442 N92-29935
DIRECT CURRENT
Simulations on the electrical characteristics of Si, SiC and diamond junction and Schottky power diodes
[PB92-177872] p 3443 N92-30094
DIRECTIONAL ANTENNAS
Sequential design of a linear quadratic controller for the Deep Space Network antennas p 3432 N92-29382
DIRECTIONAL STABILITY
The effect of yaw cards on the pitching and yawing motion of symmetric projectiles
[AD-A250021] p 3406 N92-29449
DIRECTORIES
A look at the development environment and tools used in a large INGRES ABF application project
[DE92-012632] p 3561 N92-29552
Archives of the future: Archival strategies for the treatment of electronic databases
[PB92-178631] p 3563 N92-30038
DISCONNECT DEVICES
Fastening apparatus having shape memory alloy actuator
[NASA-CASE-MSC-21935-1] p 3479 N92-29762
DISCRIMINATION
Additivity and auditory pattern analysis
[AD-A250580] p 3511 N92-29592
DISCRIMINATORS
Dynamic aperture fringe discriminator
[NASA-CASE-NPO-18478-1-CU] p 3553 N92-30084
DISILICIDES
A perspective on MoSi2 based composites
[DE92-013434] p 3415 N92-29795
DISPERSIONS
Electrochemistry in colloids and dispersions. Volume 2: Solute distribution, diffusion, and transport colloidal metals
[AD-A248336] p 3419 N92-29931
Electrochemistry in colloids and dispersions. Volume 3: Colloidal semiconductors
[AD-A248337] p 3419 N92-29932
DISPLAY DEVICES
Accelerometer method and apparatus for integral display and control functions
[NASA-CASE-MSC-21961-1] p 3474 N92-29952
DISSIPATION
Monopolar vortices as relative equilibria and their dissipative decay
[MEMO-1015] p 3446 N92-29977
Energy propagation in dissipative systems. Part 2: Centrovelocity for nonlinear wave equations
[MEMO-1016-PT-2] p 3437 N92-29978
Approximation in a damped Hamiltonian system by successive relative equilibria
[MEMO-1017] p 3536 N92-29979
Modeling of compressible turbulence p 3452 N92-30150
DISSOCIATION
Theory of the dissociation dynamics of small molecules on metal surfaces: Finite temperature studies
[DE92-011188] p 3546 N92-29899
Do recent observations of very large electromagnetic dissociation cross sections signify a transition towards non-perturbative QED? p 3438 N92-30004
Two neutron removal in relativistic nucleus-nucleus reactions p 3548 N92-30006

Converting a CO2 atmosphere to a high-purity O2 supply
[NASA-CASE-LAR-14398-1] p 3419 N92-30098

DISTORTION
Geometric distortion analysis of a wide-field astrograph p 3409 N92-29370

DISTRIBUTED PARAMETER SYSTEMS
Ultra-dependable real-time computing
[AD-A248193] p 3515 N92-29409

DISTRIBUTED PROCESSING
An OSI architecture for the Deep Space Network p 3432 N92-29380
The weakest failure detector for solving consensus
[NASA-CR-190545] p 3515 N92-29400
A massively parallel genetic algorithm for the graph partitioning problem
[IMAG-RR-845-I] p 3525 N92-29610
Developments in fiber optics for distribution automation
[NASA-CR-190454] p 3551 N92-29679
Methodology for the specification of communication activities within the framework of a multi-layered architecture: Toward the definition of a knowledge base
[LAAS-91466] p 3436 N92-29730
Reviews of computing technology: Fiber distributed data interface
[DE92-011374] p 3514 N92-29907
Integrated service engineering supported by the FDT LOTOS
[MEMO-INF-91-76] p 3531 N92-30184
A parallel restructured version of GMRES(m)
[REPT-91-85] p 3527 N92-30229

DISTRIBUTION FUNCTIONS
Nonparametric maximum likelihood estimators for interval censoring and deconvolution
[REPT-91-53] p 3539 N92-29626
Theory of system reliability demonstration, burn-in design, and record statistics
[AD-A250582] p 3480 N92-29710
Accurate procedures for approximate Bayesian and conditional inference without the need for orthogonal parameters
[AD-A248662] p 3539 N92-29718
U-statistics of increasing degrees with asymptotically Poisson distributions
[CWI-BS-R9120] p 3540 N92-29863

DIURNAL VARIATIONS
Diurnal forcing of planetary atmospheres
[NASA-CR-190262] p 3569 N92-30199

DIVERGENCE
Measurements of wind divergence with volume imaging lidar p 3464 N92-29272
Divergence preserving discrete surface integral methods for Maxwell's curl equations using non-orthogonal unstructured grids
[NASA-CR-190555] p 3517 N92-29694

DIVERTERS
Multichord spectroscopy of the D3-D divertor region
[DE92-013507] p 3554 N92-29412

DOCUMENTS
Aeronautical Engineering Group publications, 1950 - present
[AERO-REPT-8907] p 3444 N92-29683

DOPED CRYSTALS
Erbium-doped fiber amplifier elements for structural analysis sensors
[NASA-CR-190491] p 3552 N92-29681

DOPPLER RADAR
GLObal Backscatter Experiment (GLOBE) results: Aerosol backscatter global distribution and wavelength dependence p 3459 N92-29245
The Laser Atmospheric Wind Sounder (LAWS) preliminary error budget and performance estimate p 3462 N92-29262
Simulation of the performances of WIND, an airborne CO2 lidar p 3463 N92-29267
Identification of critical design points for the EAP of a space-based Doppler lidar wind sounder p 3463 N92-29270
Extraction of aerosol and Rayleigh components from Doppler lidar return signal p 3465 N92-29281
Science goals and mission objectives of NASA's laser atmospheric wind sounder program p 3468 N92-29296
The Laser Atmospheric Wind Sounder (LAWS) phase 2 preliminary system design p 3468 N92-29297
The Laser Atmospheric Wind Sounder (LAWS) phase 2 preliminary laser design p 3468 N92-29298
GE's mobile, coherent Doppler lidar test/evaluation facilities p 3407 N92-29299
The e-beam sustained laser technology for space-based Doppler wind lidar p 3469 N92-29300
Error analysis of wind measurements for the University of Illinois sodium Doppler temperature system p 3471 N92-29313
Sodium Doppler temperature lidar observations of the mesopause region temperature and wind structure p 3471 N92-29314
Wind measurements from 15 to 50 km with a Doppler Rayleigh lidar p 3472 N92-29319

DOSIMETERS
Proceedings of the Third Conference on Radiation Protection and Dosimetry
[DE92-011502] p 3547 N92-29910

DOUBLE STARS
Analysis of high energy x ray observations of long periodic pulsars
[ETN-92-91494] p 3564 N92-29468

DOWN-CONVERTERS
Bandwidth compression of noisy signals with square-wave subcarrier p 3432 N92-29379

DOWNRANGE
A sensitivity analysis of circular error probable approximation techniques
[AD-A248105] p 3539 N92-29585

DRAG REDUCTION
Patterns in simulated turbulent channel flow p 3455 N92-30169

DROP SIZE
Measurement of mean or effective radius of cloud drop size distributions with a 10.6-micron wavelength lidar p 3472 N92-29324

DUCTED FLOW
Realistic models for predicting sound propagation in flow duct systems
[ISVR-TR-204] p 3544 N92-29814

DURABILITY
Structural durability of stiffened composite shells
[NASA-CR-190588] p 3481 N92-29342

DYE LASERS
Infrared pulse-laser long-path absorption measurement of carbon dioxide using a Raman-shifted dye laser p 3465 N92-29277
Preliminary cutting and drilling studies using new generation lasers
[DE92-010712] p 3477 N92-29787

DYNAMIC CHARACTERISTICS
Elastic and Raman lidar temperature measurements from Poker Flat, Alaska during February 1992 p 3471 N92-29317
Studies of distant clusters of galaxies p 3566 N92-29843

DYNAMIC CONTROL
Spacecraft dynamics characterization and control system failure detection, volume 1
[NASA-CR-190517] p 3409 N92-29422

DYNAMIC LOADS
Effect of grain size on deformation stability of copper under quasi-static and dynamic tensile loading
[DE92-012677] p 3421 N92-29639

DYNAMIC MODELS
On fictitious joints modelling of manipulator link flexibility for the HERA simulation facility pilot
[NLR-TR-88086-U] p 3479 N92-29885
On dynamic models for large eddy simulation p 3450 N92-30056
Large eddy simulations of passive and buoyant scalars with dynamic subgrid-scale models p 3450 N92-30057
Dynamic subgrid-scale modeling of compressible turbulence p 3450 N92-30058

DYNAMIC PROGRAMMING
Tools for the interfacing between dynamical problems and models within decision support systems
[MEMO-COSOR-91-29] p 3532 N92-29607
On the p-coverage problem on the real line
[MEMO-COSOR-91-33] p 3520 N92-29818
On setup cost reduction in the economic lot-sizing model without speculative motives
[MEMO-COSOR-91-34] p 3520 N92-29819

DYNAMIC RESPONSE
Buffet test in the National Transonic Facility
[NASA-CR-189595] p 3406 N92-29352
An approximation method for dynamic response of strain-hardening structures
[DE92-013053] p 3482 N92-29535
A closed form solution of a longitudinal beam with a viscous boundary condition
[AD-A248841] p 3483 N92-29915

DYNAMIC STABILITY
A study of the influence of alloying additions on the passivity of aluminum
[AD-A248339] p 3421 N92-29587

DYNAMIC STRUCTURAL ANALYSIS
Buffet test in the National Transonic Facility
[NASA-CR-189595] p 3406 N92-29352
Spacecraft dynamics characterization and control system failure detection, volume 1
[NASA-CR-190517] p 3409 N92-29422
Accelerometer method and apparatus for integral display and control functions
[NASA-CASE-MSC-21961-1] p 3474 N92-29952

DYNAMICAL SYSTEMS
Numerical procedures for analyzing dynamical processes
[AD-A248175] p 3515 N92-29399
Parameter identification in tidal models with uncertain boundaries
[MEMO-983] p 3540 N92-29856
Energy propagation in dissipative systems. Part 2: Centrovelocity for nonlinear wave equations
[MEMO-1016-PT-2] p 3437 N92-29978
Approximation in a damped Hamiltonian system by successive relative equilibria
[MEMO-1017] p 3536 N92-29979
Port-controlled Hamiltonian systems: Modelling origins and systemtheoretic properties
[MEMO-1001] p 3537 N92-30077
Temporal reasoning in model-based diagnosis
[MEMO-INF-91-66] p 3531 N92-30143

DYNAMO THEORY
An exact turbulent closure for the hydromagnetic dynamo p 3452 N92-30071

E

EARTH (PLANET)
Analysis of EUV dayglow spectra of Triton, Titan and Earth
[NASA-CR-190586] p 3568 N92-29451
NOAA environmental digest: Selected indicators of the United States and the global environment, December 1991
[PB92-185073] p 3494 N92-30019

EARTH ATMOSPHERE
Mechanical and thermal issues in the development of a spaceborne lidar system p 3469 N92-29303
EOS data policy: Questions remain about US commercial access. Report to the Chairman, Committee on Science, Space, and Technology, House of Representatives
[GAO/IMTEC-92-44] p 3488 N92-29467
National Institute for Global Environmental Change
[DE92-013487] p 3493 N92-29597
Global-warming problem and global economic models
[DE92-514557] p 3493 N92-29638
Intercomparison of global marine climatologies
[DE92-011389] p 3494 N92-29790
ATLAS 1: Encountering planet Earth
[NASA-TM-107956] p 3408 N92-30016
NOAA environmental digest: Selected indicators of the United States and the global environment, December 1991
[PB92-185073] p 3494 N92-30019
Small satellites and RPAS in global-change research: Summary and conclusions
[DE92-013602] p 3490 N92-30088

EARTH MAGNETOSPHERE
Low energy neutral atoms in the Earth's magnetosphere: Modeling
[DE92-013240] p 3500 N92-29536

EARTH OBSERVATIONS (FROM SPACE)
Fourth Meeting of the Space Agency Forum on the International Space Year (SAFISY-4)
[ESA-SP-1141] p 3407 N92-29879
ATLAS 1: Encountering planet Earth
[NASA-TM-107956] p 3408 N92-30016
NASA's Earth Observing System
[S-HRG-102-647] p 3490 N92-30017

EARTH OBSERVING SYSTEM (EOS)
Science goals and mission objectives of NASA's laser atmospheric wind sounder program p 3468 N92-29296
The Laser Atmospheric Wind Sounder (LAWS) phase 2 preliminary system design p 3468 N92-29297
EOS Data and Information System (EOSDIS) — landsat satellites
[NASA-TM-107922] p 3488 N92-29442
EOS data policy: Questions remain about US commercial access. Report to the Chairman, Committee on Science, Space, and Technology, House of Representatives
[GAO/IMTEC-92-44] p 3488 N92-29467
NASA's Earth Observing System
[S-HRG-102-647] p 3490 N92-30017

EARTH ORIENTATION
A determination of the radio-planetary frame tie from comparison of Earth orientation parameters p 3409 N92-29365

EARTH SCIENCES
The role of lidars in global change research p 3457 N92-29235
Research and technology annual report, FY 1990
[NASA-TM-107807] p 3571 N92-30197

EARTH SURFACE
Wind profiles derived from volume imaging lidar data: Enhancements to the algorithm and comparisons with insitu observations p 3464 N92-29271
DIAL mapping of atmospheric atomic mercury of geophysical origin p 3464 N92-29273
A soil-canopy scheme for use in a numerical model of the atmosphere: 1D stand-alone model
[CSIRO-TP-23] p 3500 N92-29670

ECOLOGY
Mosquito Lagoon environmental resources inventory
[NASA-TM-107548] p 3492 N92-29430

ECONOMIC ANALYSIS
Global standards: Building blocks for the future
[PB92-167352] p 3563 N92-29671
On setup cost reduction in the economic lot-sizing model without speculative motives
[MEMO-COSOR-91-34] p 3520 N92-29819
New developments in emission projection methodologies
[PB92-139393] p 3495 N92-30031
New York State technical and economic MAGLEV evaluation
[PB92-174119] p 3564 N92-30037

ECONOMICS
Lidar monitoring of Mexico City's atmosphere during high air polution episodes p 3464 N92-29275
Global standards: Building blocks for the future
[PB92-167352] p 3563 N92-29671

ECOSYSTEMS
Air quality criteria for oxides of nitrogen, volume 2
[PB92-176379] p 3493 N92-29521
Research and technology annual report, FY 1990
[NASA-TM-107807] p 3571 N92-30197

EDDY CURRENTS
Magnetic properties of nano-heterogeneous amorphous thin films
[AD-A250570] p 3420 N92-29426
Method and apparatus for thermographically and quantitatively analyzing a structure for disbonds and/or inclusions
[NASA-CASE-LAR-14559-1] p 3480 N92-29829

EDDY VISCOSITY
A numerical method for prediction of compressible turbulent flows with closure models
p 3454 N92-30164

EDGE DETECTION
Application of laser imaging for bio/geophysical studies p 3465 N92-29282
Analysis of a three-dimensional point pattern with replication
[CWI-BS-R9124] p 3541 N92-30180

EDGE DISLOCATIONS
Strengthening mechanisms, creep and fatigue processes in dispersion hardened niobium alloy
[AD-A250282] p 3421 N92-29547

EDUCATION
Exercise and three psychosocial variables: A longitudinal study
[AD-A250649] p 3510 N92-30216

EFFECTS
Effects of bleed air extraction on thrust levels on the F404-GE-400 turbofan engine
[NASA-TM-104247] p 3405 N92-29425
The effects of student-instructor interaction and paired/individual study on achievement in computer-based training
[AD-A248518] p 3511 N92-29503
The effect of length variation on the stability of circular cylindrical shells under pure bending
[LR-669] p 3482 N92-29700
Effects of retardation in relativistic equations with confining interaction p 3547 N92-30005

EFFICIENCY
Efficiencies of rotational Raman and Rayleigh techniques for laser remote sensing of the atmospheric temperature p 3467 N92-29288

EGYPT
Mapping of groundwater losses by evaporation in the western desert of Egypt
[BCRS-91-01] p 3489 N92-29495

EIGENVALUES
The extended Bethe Ansatz for infinite S = 1/2 quantum spin chains with non-nearest-neighbor interaction
[DE92-622378] p 3533 N92-29793
A closed form solution of a longitudinal beam with a viscous boundary condition
[AD-A248841] p 3483 N92-29915

EIGENVECTORS
A closed form solution of a longitudinal beam with a viscous boundary condition
[AD-A248841] p 3483 N92-29915

EINSTEIN EQUATIONS
SOLITON
[USIP-90-09] p 3518 N92-29714

ELASTIC DEFORMATION
Thickness dependency of elastic aftereffect of thin bending beams
[ETN-92-91488] p 3483 N92-29925

ELASTIC SCATTERING
Electron spectra of adatomic structures
[DE92-625013] p 3544 N92-29415
Fourth workshop on Experiments and Detectors for a Relativistic Heavy Ion Collider
[BNL-52262] p 3549 N92-30014

ELASTIC WAVES
Finite difference modelling of seismic wave propagation at the seafloor
[AD-A248345] p 3505 N92-29562

ELASTOPLASTICITY
Constitutive modelling for granular material under finite strains with particle slidings and fabric changes
[AD-A248187] p 3482 N92-29407

ELECTRIC CONNECTORS
Electrical connection of enzyme redox centers to electrodes
[AD-A248545] p 3440 N92-29575

ELECTRIC CONTACTS
A mechanical connector design for high-current, high-coulomb pulsed power systems
[DE92-012678] p 3438 N92-29339

ELECTRIC DIPOLES
Investigation of the structure of the electromagnetic field and related phenomena, generated by the active satellite
[NASA-CR-190446] p 3434 N92-29568
Charge dependence and electric quadrupole effects on single-nucleon removal in relativistic and intermediate energy nuclear collisions p 3548 N92-30010
Standard spherical dipole source
[PB92-187020] p 3438 N92-30198

ELECTRIC FIELDS
Using phase retrieval to determine the intensity and phase of an ultrashort laser pulse
[DE92-013564] p 3476 N92-29516
Investigation of the structure of the electromagnetic field and related phenomena, generated by the active satellite
[NASA-CR-190446] p 3434 N92-29568
Analyses of near- and far-field two-lobe patterns outside the output endface of a two-mode fiber
[NASA-CR-190494] p 3551 N92-29652
Effect of whisker orientation on the mechanical properties of silicon carbide/alumina composites
[AD-A248737] p 3415 N92-29723

ELECTRIC MOTORS
Beam-powered lunar rover design
[DE92-011511] p 3569 N92-29600

ELECTRIC POTENTIAL
Cursory examination of the zeta potential behaviors of two optical materials
[DE92-011588] p 3551 N92-29578
Optical and electrical characteristics of the cathode fall
[AD-A249010] p 3443 N92-30176

ELECTRIC POWER PLANTS
Tomorrow's energy today: Energy efficiency and renewable energy
[DE91-002110] p 3491 N92-29454

ELECTRIC PULSES
A mechanical connector design for high-current, high-coulomb pulsed power systems
[DE92-012678] p 3438 N92-29339

ELECTRIC WIRE
Robotic workcell for wire wrapping integrated circuits
[DE92-013999] p 3441 N92-29796

ELECTRICAL ENGINEERING
Hardening techniques to counter cumulated dose on SEU and SEL in space environment
[IMAG-RR-863-I] p 3441 N92-29613
The 36th issue of Electronics and Electrical Engineering Laboratory Technical Progress Bulletin covering laboratory programs, July to September 1991, with 1992 EEEL events calendar
[PB92-164672] p 3442 N92-30032

ELECTRICAL PROPERTIES
Design and analysis of electrical circuits that produce fractional-order differentiation
[AD-A248085] p 3440 N92-29526
LiMoN2: The first metallic layered nitride
[AD-A248446] p 3418 N92-29619
A study and feasibility of ultra thin silica layers by rapid thermal processing
[LAAS-91393] p 3422 N92-29674
Simulations on the electrical characteristics of Si, SiC and diamond junction and Schottky power diodes
[PB92-177872] p 3443 N92-30094

ELECTRICAL RESISTIVITY
Electrical, optical, and magnetic resonance studies of novel pi-conjugated polymers
[DE92-012548] p 3424 N92-29482
Evidence for amorphization in Ni/Ti multilayers from electrical resistivity changes p 3559 N92-29773

ELECTROACOUSTIC TRANSDUCERS
Interface board for providing time signals to a super minicomputer
[AD-D015198] p 3441 N92-29900
Calibration apparatus for recess mounted pressure transducers
[NASA-CASE-LAR-14724-1] p 3474 N92-30030

ELECTROCATALYSTS
The O2 reduction at the IFC modified O2 fuel cell electrode
[NASA-TM-105691] p 3413 N92-29667

ELECTROCHEMICAL CELLS
Material-deposition processes in the separator of Li-alloy/FeS2 thermal cells
[DE92-013669] p 3440 N92-29518
Experimental study of cylindrical air electrodes
[DE92-506507] p 3441 N92-29912
A mathematical model for metal hydride electrodes
[DE92-506506] p 3442 N92-30089

ELECTROCHEMICAL OXIDATION
Pulse voltammetry in single cells using platinum microelectrodes
[AD-A248080] p 3440 N92-29523

ELECTROCHEMISTRY
Irradiation effects on the electrochemistry and corrosion resistance of stainless steel
[DE92-013504] p 3420 N92-29411
Electrochemistry in colloids and dispersions. Volume 1: Electroanalytical methods and applications, electrosynthesis and electrocatalysis, polymers and latexes
[AD-A248335] p 3418 N92-29557
Electrochemistry in colloids and dispersions. Volume 2: Solute distribution, diffusion, and transport colloidal metals
[AD-A248336] p 3419 N92-29931
Electrochemistry in colloids and dispersions. Volume 3: Colloidal semiconductors
[AD-A248337] p 3419 N92-29932

ELECTRODE MATERIALS
A response surface methodology study of ferroelectric memory devices
[AD-A248094] p 3440 N92-29529

ELECTRODES
A study of the adsorption of acetonitrile on a gold electrode from aqueous solutions using in situ vibrational spectroscopy
[AD-A250191] p 3417 N92-29514
Material-deposition processes in the separator of Li-alloy/FeS2 thermal cells
[DE92-013669] p 3440 N92-29518
Pulse voltammetry in single cells using platinum microelectrodes
[AD-A248080] p 3440 N92-29523
Electrical connection of enzyme redox centers to electrodes
[AD-A248545] p 3440 N92-29575
Metal vapor plasma behavior during vacuum arc remelting of alloy 718
[DE92-011761] p 3421 N92-29623
The O2 reduction at the IFC modified O2 fuel cell electrode
[NASA-TM-105691] p 3413 N92-29667
Experimental study of cylindrical air electrodes
[DE92-506507] p 3441 N92-29912
A mathematical model for metal hydride electrodes
[DE92-506506] p 3442 N92-30089
Electrochemical array sensors for plating waste stream monitoring
[DE92-011446] p 3495 N92-30211

ELECTRODYNAMICS
A letter of intent for an experiment to study strong electromagnetic fields at RHIC via multiple electromagnetic processes p 3438 N92-30015

ELECTROLESS DEPOSITION
Laser processing for interconnect technology
[AD-A248103] p 3476 N92-29559

ELECTROLYTES
Advanced rechargeable lithium sulfur dioxide cell
[AD-A250027] p 3491 N92-29476
Electrochemistry in colloids and dispersions. Volume 1: Electroanalytical methods and applications, electrosynthesis and electrocatalysis, polymers and latexes
[AD-A248335] p 3418 N92-29557
Experimental study of cylindrical air electrodes
[DE92-506507] p 3441 N92-29912

ELECTROMAGNETIC COMPATIBILITY
Test and evaluation report of the physio control defibrillator/monitor model LIFEPAK (trademark) 8
[AD-A248283] p 3510 N92-29347
Test and evaluation report of the IMED volumetric infusion pump model 960A
[AD-A248538] p 3404 N92-29506

ELECTROMAGNETIC FIELDS
Investigation of the structure of the electromagnetic field and related phenomena, generated by the active satellite
[NASA-CR-190446] p 3434 N92-29568
Transverse wakefields at high dispersion
[DE92-010752] p 3550 N92-29788
Fourth workshop on Experiments and Detectors for a Relativistic Heavy Ion Collider
[BNL-52262] p 3549 N92-30014
A letter of intent for an experiment to study strong electromagnetic fields at RHIC via multiple electromagnetic processes p 3438 N92-30015
New York State technical and economic MAGLEV evaluation
[PB92-174119] p 3564 N92-30037
Standard spherical dipole source
[PB92-187020] p 3438 N92-30198

ELECTROMAGNETIC INTERACTIONS
Electromagnetic processes in nucleus-nucleus collisions relating to space radiation research
[NASA-CR-190533] p 3547 N92-30001
Cross section parameterizations for cosmic ray nuclei. 1: Single nucleon removal p 3547 N92-30002
Do recent observations of very large electromagnetic dissociation cross sections signify a transition towards non-perturbative QED? p 3438 N92-30004
Two neutron removal in relativistic nucleus-nucleus reactions p 3548 N92-30006
Stopping powers and cross sections due to two-photon processes in relativistic nucleus-nucleus collision p 3548 N92-30012
Fourth workshop on Experiments and Detectors for a Relativistic Heavy Ion Collider
[BNL-52262] p 3549 N92-30014

ELECTROMAGNETIC INTERFERENCE
Test and evaluation report of the physio control defibrillator/monitor model LIFEPAK (trademark) 8
[AD-A248283] p 3510 N92-29347

ELECTROMAGNETIC NOISE
Introduction to quartz frequency standards
[AD-A248503] p 3439 N92-29498
Jet aircraft noise at high subsonic flight Mach numbers
[DLR-FB-91-28] p 3544 N92-29997

ELECTROMAGNETIC NOISE MEASUREMENT
Global measurements of low-frequency radio noise
[AD-A248260] p 3434 N92-29542

ELECTROMAGNETIC PROPERTIES
Global solar magnetic fields
[AD-A248340] p 3569 N92-29421

ELECTROMAGNETIC RADIATION
Investigation of the structure of the electromagnetic field and related phenomena, generated by the active satellite
[NASA-CR-190446] p 3434 N92-29568

ELECTROMAGNETISM
Survey of research into electromagnetic and other wave effects on mechanical behavior and processing of materials
[AD-A248614] p 3426 N92-29905

ELECTROMIGRATION
Computer program POWNOR for fitting the power-normal and -lognormal models to life or strength data from specimens of various sizes
[PB92-169119] p 3483 N92-29813

ELECTRON ACCELERATORS
Transverse wakefields at high dispersion
[DE92-010752] p 3550 N92-29788

ELECTRON BEAMS
Transverse wakefields at high dispersion
[DE92-010752] p 3550 N92-29788

ELECTRON BUNCHING
Transverse wakefields at high dispersion
[DE92-010752] p 3550 N92-29788

ELECTRON CYCLOTRON HEATING
Tunable driver for the LLNL FEL experiment
[DE92-011292] p 3477 N92-29937

ELECTRON EMISSION
Heat flow of a two-electron-temperature plasma through the sheath in the presence of electron emission
[NIFS-136] p 3555 N92-30172

ELECTRON ENERGY
Electron spectra of adatomic structures
[DE92-625013] p 3544 N92-29415

ELECTRON MICROSCOPY
Electron microscopy study on zirconia and alumina ceramic powders synthesized by microwave plasma pyrolysis
[DE92-013385] p 3424 N92-29479
Sub-angstrom microscopy through incoherent imaging and image reconstruction
[DE92-011787] p 3475 N92-30090

ELECTRON MOBILITY
Free ion yields in liquids: Molecular structure and track effects
[DE92-012208] p 3545 N92-29582

ELECTRON PLASMA
Investigation of the structure of the electromagnetic field and related phenomena, generated by the active satellite
[NASA-CR-190446] p 3434 N92-29568
Formation of presheath and current-free double layer in a two-electron-temperature plasma
[NIFS-132] p 3555 N92-30091
Heat flow of a two-electron-temperature plasma through the sheath in the presence of electron emission
[NIFS-136] p 3555 N92-30172

ELECTRON SPECTROSCOPY
Quasi-static intergranular cracking in a Cu-Sn alloy: An analog of stress relief cracking of steels
[DE92-011646] p 3420 N92-29483

ELECTRON SPIN
The extended Bethe Ansatz for infinite S = 1/2 quantum spin chains with non-nearest-neighbor interaction
[DE92-622378] p 3533 N92-29793

ELECTRON STATES
Surface reactions in the space environment
[AD-A250624] p 3428 N92-29428

ELECTRON TRANSFER
Electrical connection of enzyme redox centers to electrodes
[AD-A248545] p 3440 N92-29575
Correlated charge-changing ion-atom collisions
[DE92-013473] p 3546 N92-29642

ELECTRON TUNNELING
Zee star analysis
[AD-A248342] p 3417 N92-29423
Variable temperature scanning tunneling microscopy
[AD-A248725] p 3557 N92-29722

ELECTRONIC EQUIPMENT
Introduction to neural networks
[AD-A248258] p 3527 N92-29541
Smart BIT/TSMD integration
[AD-A247192] p 3442 N92-29914

ELECTRONIC FILTERS
Programmable hyperspectral image mapper with on-array processing
[NASA-CASE-NPO-17794-1-CU] p 3553 N92-30104

ELECTRONS
Rare gas clusters containing charged atoms
[AD-A248299] p 3544 N92-29350
Zee star analysis
[AD-A248342] p 3417 N92-29423
Surface reactions in the space environment
[AD-A250624] p 3428 N92-29428
Theory of elementary particles studies in weak interaction and grand unification and studies in accelerator design
[DE92-014309] p 3550 N92-29532
The O(alpha(s) cubed) QCD correction to the lowest moment of the longitudinal structure function in deep inelastic electron-nucleon scattering
[NIKHEF-H/91-19] p 3546 N92-29750

ELECTROPLATING
Evaluation of aluminum ion vapor deposition as a replacement for cadmium electroplating at Anniston Army Depot
[AD-A250063] p 3423 N92-29940

ELECTROSTATICS
Electrostatic ion thruster optics calculations
[DE92-006608] p 3413 N92-29461
On the numerical solution of one-dimensional integral and differential equations
[AD-A250388] p 3531 N92-29548

ELECTROSTRICTION
Small electrostrictive dilations of cubic crystals
[ISBN-90-9004374-8] p 3559 N92-29783

ELEMENTARY PARTICLE INTERACTIONS
Theory of elementary particles studies in weak interaction and grand unification and studies in accelerator design
[DE92-014309] p 3550 N92-29532
The extended Bethe Ansatz for infinite S = 1/2 quantum spin chains with non-nearest-neighbor interaction
[DE92-622378] p 3533 N92-29793

ELEVATION
Visual perception of elevation
[AD-A248338] p 3510 N92-29420

ELLIPTIC DIFFERENTIAL EQUATIONS
Abstract quasilinear equations and application to a groundwater flow problem
[REPT-91-41] p 3535 N92-29923
An improved accuracy version of the mixed finite element method for a second order elliptic equation
[CWI-NM-R9111] p 3536 N92-29946

EMBRITTLEMENT
Mechanism of diffusion-controlled brittle fracture
[DE92-011572] p 3482 N92-29601

EMITTERS
RF vacuum electronics
[AD-A248857] p 3442 N92-29935

EMULSIONS
Electrochemistry in colloids and dispersions. Volume 1: Electroanalytical methods and applications, electrosynthesis and electrocatalysis, polymers and latexes
[AD-A248335] p 3418 N92-29557
Electrochemistry in colloids and dispersions. Volume 2: Solute distribution, diffusion, and transport colloidal metals
[AD-A248336] p 3419 N92-29931
Electrochemistry in colloids and dispersions. Volume 3: Colloidal semiconductors
[AD-A248337] p 3419 N92-29932

ENCOUNTERS
Galileo early cruise, including Venus, first Earth, and Gaspra encounters p 3433 N92-29384

END EFFECTORS
Experimental investigation of adaptive control of a parallel manipulator
[NASA-CR-189867] p 3528 N92-29656

END-TO-END DATA SYSTEMS
Miniature modular microwave end-to-end receiver
[NASA-CASE-NPO-18713-1-CU] p 3437 N92-30103

ENERGY CONSERVATION
Tomorrow's energy today: Energy efficiency and renewable energy
[DE91-002110] p 3491 N92-29454
Global-warming problem and global economic models
[DE92-514557] p 3493 N92-29638
New York State technical and economic MAGLEV evaluation
[PB92-174119] p 3564 N92-30037

ENERGY CONSUMPTION
Tomorrow's energy today: Energy efficiency and renewable energy
[DE91-002110] p 3491 N92-29454

ENERGY CONVERSION
Tomorrow's energy today: Energy efficiency and renewable energy
[DE91-002110] p 3491 N92-29454

ENERGY DISSIPATION
Free ion yields in liquids: Molecular structure and track effects
[DE92-012208] p 3545 N92-29582
Turbulence and vortex structures p 3448 N92-30048
Derivation of the kappa-epsilon model equations using the renormalization group method p 3450 N92-30055

ENERGY LEVELS
Correlated charge-changing ion-atom collisions
[DE92-013473] p 3546 N92-29642
Spectroscopy of W-183; measured magnetic moments and rotation-particle coupling
[DE92-624790] p 3549 N92-30213

ENERGY SPECTRA
Electron spectra of adatomic structures
[DE92-625013] p 3544 N92-29415

ENERGY STORAGE
Thermal energy storage for cogeneration applications
[DE92-012339] p 3492 N92-29646

ENERGY TRANSFER
Non-linear interactions in homogeneous turbulence with and without background rotation p 3448 N92-30044
Scaling analysis of energy transfer in the inertial range p 3448 N92-30046
Turbulence and vortex structures p 3448 N92-30048
Turbulence dynamics in the wavelet representation p 3454 N92-30159

ENGINE DESIGN
Contingency power for a small turboshaft engine by using water injection into turbine cooling air
[NASA-TM-105680] p 3405 N92-29661
Users manual for updated computer code for axial-flow compressor conceptual design
[NASA-CR-189171] p 3524 N92-30207

ENGINE PARTS
Aging aircraft NDI Development and Demonstration Center (AANC): An overview — nondestructive inspection p 3481 N92-30120

ENGINE TESTS
A comparison of the calculated and experimental off-design performance of a radial flow turbine
[NASA-CR-189207] p 3399 N92-29402
Effects of bleed air extraction on thrust levels on the F404-GE-400 turbofan engine
[NASA-TM-104247] p 3405 N92-29425
The development of a fiber optic Raman temperature measurement system for rocket flows
[NASA-CR-189200] p 3413 N92-29448

ENGINEERING MANAGEMENT
Summary of technical operations, 1991 --- software development
[AD-A248153] p 3516 N92-29540
ENTROPY
On the entropy production of dissipation models
[MEMO-1021] p 3560 N92-30148
ENVIRONMENT EFFECTS
Lidar observations of stratospheric aerosol layer after the Mt. Pinatubo volcanic eruption p 3457 N92-29234
L625 lidar measurements of Pinatubo volcanic cloud at Hefei p 3460 N92-29252
Air quality criteria for oxides of nitrogen, volume 2
[PB92-176379] p 3493 N92-29521
National Institute for Global Environmental Change
[DE92-013487] p 3493 N92-29597
Potential impacts of climate change on Pacific Northwest forest vegetation
[PB92-184985] p 3495 N92-30021
ENVIRONMENT MANAGEMENT
GIS for coastal management
[BCRS-90-31] p 3489 N92-29493
Environmental quality: Report of the Council on Environmental Quality
[PB92-154954] p 3494 N92-29698
ENVIRONMENT POLLUTION
Remote detection of biological particles and chemical plumes using UV fluorescence lidar
p 3465 N92-29279
National Institute for Global Environmental Change
[DE92-013487] p 3493 N92-29597
ENVIRONMENTAL CONTROL
Final Environmental Impact Statement (EIS) for the Space Nuclear Thermal Propulsion (SNTP) program
[AD-A248408] p 3413 N92-29903
What is the potential of forest management to slow the increase of atmospheric CO2?
[PB92-180249] p 3495 N92-30173
ENVIRONMENTAL MONITORING
Ozone measurements with the US EPA UV-DIAL: Preliminary results p 3461 N92-29255
Research programming studies: Remote sensing emissions, land use and effects, in relation to climate and environment
[BCRS-91-17] p 3493 N92-29497
The main lines of the research programs remote sensing: Climate and environment
[BCRS-91-25] p 3493 N92-29499
ENVIRONMENTAL QUALITY
Environmental quality: Report of the Council on Environmental Quality
[PB92-154954] p 3494 N92-29698
ENVIRONMENTAL SURVEYS
Final Environmental Impact Statement (EIS) for the Space Nuclear Thermal Propulsion (SNTP) program
[AD-A248408] p 3413 N92-29903
Final Environmental Impact Statement (EIS) for the Space Nuclear Thermal Propulsion (SNTP) program: Appendices
[AD-A248409] p 3413 N92-29904
ENVIRONMENTAL TESTS
Compressive response of debonded thick composite shells including the effects of transient moisture sorption
[AD-A250080] p 3414 N92-29462
ENZYME ACTIVITY
Methodology on monitoring and modelling of microbial metabolism
[ETN-92-91745] p 3507 N92-29732
Flux-capacity relationships of Acinetobacter calcoaceticus enzymes during xylose oxidation
p 3508 N92-29739
ENZYMES
Electrical connection of enzyme redox centers to electrodes
[AD-A248545] p 3440 N92-29575
EPHEMERIDES
Orbiter-orbiter and orbiter-lander tracking using same-beam interferometry p 3409 N92-29369
EPIDEMIOLOGY
Air quality criteria for oxides of nitrogen, volume 3
[PB92-176387] p 3493 N92-29522
EPITAXY
Thermodynamic and kinetic aspects of 3/5 epitaxy
[AD-A250632] p 3556 N92-29429
EPOXY MATRIX COMPOSITES
DSC measurements on experimental TGDDM/DDS resin systems: The influence of variations in resin composition and catalyst content
[NLR-TP-90267-U] p 3478 N92-29602
EPOXY RESINS
A consistent shear deformable theory for laminated plates
[AD-A250591] p 3415 N92-29593
DSC measurements on experimental TGDDM/DDS resin systems: The influence of variations in resin composition and catalyst content
[NLR-TP-90267-U] p 3478 N92-29602
EQUATIONS OF MOTION
Solution strategies for implicit nonlinear finite element analysis
[DE92-011466] p 3533 N92-29792
Mathematical modelling of saturated and unsaturated groundwater flow
[MEMO-987] p 3445 N92-29857
EQUATIONS OF STATE
Solution of two-body relativistic bound state equations with confining plus Coulomb interactions
p 3547 N92-30003
Effects of retardation in relativistic equations with confining interaction p 3547 N92-30005
Confining potential in momentum space
p 3548 N92-30007
EQUATORS
Diurnal forcing of planetary atmospheres
[NASA-CR-190262] p 3569 N92-30199
EQUILIBRIUM EQUATIONS
A compensation approach for two-dimensional Markov processes
[MEMO-COSOR-91-28] p 3539 N92-29606
EQUILIBRIUM FLOW
Dynamic solder management
[AD-A250564] p 3422 N92-29647
Numerical modeling studies of the Gulf of Mexico and the Caribbean Sea using the Bryan-Cox model
[PB92-164987] p 3505 N92-29704
EQUIVALENCE
Experiments on processes with backtracking
[RR-858-I-IMAG-121-LIFIA] p 3532 N92-29574
ERBIUM
Erbium-doped fiber amplifier elements for structural analysis sensors
[NASA-CR-190491] p 3552 N92-29681
ERROR ANALYSIS
Lidar measurement of stratospheric ozone at Hohenpeissenberg: An improved evaluation method
p 3462 N92-29259
The Laser Atmospheric Wind Sounder (LAWS) preliminary error budget and performance estimate
p 3462 N92-29262
Error analysis of wind measurements for the University of Illinois sodium Doppler temperature system
p 3471 N92-29313
The cognitive function of theoretical knowledge in procedural learning
[AD-A248075] p 3531 N92-29486
Minimax linear splines
[AD-A248077] p 3515 N92-29487
A sensitivity analysis of circular error probable approximation techniques
[AD-A248105] p 3539 N92-29585
Design and scheduling for periodic concurrent error detection and recovery in processor arrays
[NASA-CR-190571] p 3517 N92-29695
Sensor fault detection on board an aircraft with observer and polynomial classifier
[DLR-FB-91-34] p 3404 N92-29870
Basic problems of a-posteriori error estimation
[AD-A248986] p 3541 N92-30174
ERROR CORRECTING CODES
Golay and other box codes p 3431 N92-29375
ERROR DETECTION CODES
Golay and other box codes p 3431 N92-29375
B(exp 2)UBIST: A strategy for boundary scan board unified BIST
[IMAG-RR-862-I] p 3441 N92-29612
Automatic generation algorithms, experiments, and comparisons of self checking PLA schemes
[IMAG-RR-843-I] p 3516 N92-29621
ERRORS
Minimax linear splines
[AD-A248077] p 3515 N92-29487
A universal, fault-tolerant, non-linear analytic network for modeling and fault detection
[DE92-011840] p 3525 N92-29624
Classification, error detection, and reconciliation of measurements in complex biochemical systems
p 3508 N92-29737
A compensation approach for queueing problems
[ETN-92-91628] p 3539 N92-29774
ERS-1 (ESA SATELLITE)
Activities report of the Netherlands Remote Sensing Board (with abridged version)
[ETN-92-91352] p 3489 N92-29688
ESTIMATES
New developments in emission projection methodologies
[PB92-139393] p 3495 N92-30031
ESTIMATING
Optimization of stochastic response surfaces subject to constraints with linear programming
[AD-A248108] p 3516 N92-29586
Estimating plasma temperatures
[DE92-014092] p 3555 N92-29798
Estimation of the inverse acoustic transmission operator of a heterogeneous region directly from its reflection operator
[REPT-91-36] p 3544 N92-29918
A two-stage estimator for generalized linear models with nonconstant dispersion parameter
[MEMO-1012] p 3540 N92-29975
Basic problems of a-posteriori error estimation
[AD-A248986] p 3541 N92-30174
ESTIMATORS
Nonparametric maximum likelihood estimators for interval censoring and deconvolution
[REPT-91-53] p 3539 N92-29626
ETCHING
Monolithic amorphous silicon modules on continuous polymer substrate
[DE92-001163] p 3425 N92-29598
Laser etching: Possibilities and problems
[DE92-010800] p 3477 N92-30135
ETHANE
New directions for the catalytic conversion of methane
[PB92-172360] p 3492 N92-29519
ETHERS
Structural rearrangements during mesomorphic phase transitions in poly(10-((4-cyano-4' biphenyl)oxy)decanyl vinyl ether)
[AD-A248306] p 3425 N92-29569
ETHYL COMPOUNDS
Molecular engineering of liquid crystalline polymers by living polymerization. 20: Synthesis and characterization of binary copolymers of 11-(4-cyano-4'-biphenyl) oxy)undecanyl vinyl ether with n-butyl vinyl ether and of 2-(4-cyano-4'-biphenyl) oxy)ethyl vinyl ether with n-butyl vinyl ether
[AD-A248286] p 3425 N92-29566
ETHYLENE
New directions for the catalytic conversion of methane
[PB92-172360] p 3492 N92-29519
EULER EQUATIONS OF MOTION
Spatial and temporal adaptive procedures for the unsteady aerodynamic analysis of airfoils using unstructured meshes
[NASA-TM-107635] p 3400 N92-29445
EUROPEAN SPACE AGENCY
Fourth Meeting of the Space Agency Forum on the International Space Year (SAFISY-4)
[ESA-SP-1141] p 3407 N92-29879
EVAPORATION
Mapping of groundwater losses by evaporation in the western desert of Egypt
[BCRS-91-01] p 3489 N92-29495
EVAPORATORS
Design characteristics of a heat pipe test chamber
[NASA-TM-105737] p 3492 N92-29662
EXCIMER LASERS
Ozone measurements with the US EPA UV-DIAL: Preliminary results p 3461 N92-29255
EXCITATION
Free ion yields in liquids: Molecular structure and track effects
[DE92-012208] p 3545 N92-29582
Correlated charge-changing ion-atom collisions
[DE92-013473] p 3546 N92-29642
Optical fiber sensor having an active core
[NASA-CASE-LAR-14607-1SB] p 3553 N92-30029
EXHAUST EMISSION
Applied analytical combustion/emissions research at the NASA Lewis Research Center
[NASA-TM-105731] p 3412 N92-29343
Research programming studies: Remote sensing emissions, land use and effects, in relation to climate and environment
[BCRS-91-17] p 3493 N92-29497
EXOTHERMIC REACTIONS
DSC measurements on experimental TGDDM/DDS resin systems: The influence of variations in resin composition and catalyst content
[NLR-TP-90267-U] p 3478 N92-29602
EXPERIMENT DESIGN
An analysis of the endurance of mobile satellite command and control systems
[AD-A248084] p 3410 N92-29525
Definition and design of an experiment to test raster scanning with rotating unbalanced-mass devices on gimbaled payloads
[NASA-TP-3249] p 3429 N92-29677
The expanding plasma jet: Experiments and model
[ETN-92-91627] p 3555 N92-29761

EXPERIMENTATION
Fourth workshop on Experiments and Detectors for a Relativistic Heavy Ion Collider
[BNL-52262] p 3549 N92-30014
A letter of intent for an experiment to study strong electromagnetic fields at RHIC via multiple electromagnetic processes p 3438 N92-30015
Annual research briefs, 1989
[NASA-CR-189024] p 3452 N92-30149
EXPERT SYSTEMS
Deep Space Network information system architecture study p 3433 N92-29385
DecisionMaker software and extracting fuzzy rules under uncertainty
[NASA-CR-190502] p 3514 N92-29391
An object-based interviewing system
[DE92-013422] p 3527 N92-29504
Methodology for the specification of communication activities within the framework of a multi-layered architecture: Toward the definition of a knowledge base
[LAAS-91466] p 3436 N92-29730
An ontology of ceramics
[MEMO-INF-91-85] p 3426 N92-29960
EXPLOSIONS
Guide for evaluating 12 inch Substantial Dividing Walls (SDWs) to provide protection from remote operation, volume 2
[AD-A250252] p 3428 N92-29335
Guide for evaluating 12 inch Substantial Dividing Walls (SDWs) to provide protection from remote operation, volume 1
[AD-A250251] p 3428 N92-29545
EXPLOSIVES
Guide for evaluating 12 inch Substantial Dividing Walls (SDWs) to provide protection from remote operation, volume 2
[AD-A250252] p 3428 N92-29335
Computed tomography experiments of Pantex high explosives
[DE92-013517] p 3480 N92-29478
Strategies for understanding the deflagration-to-detonation transition
[DE92-013528] p 3427 N92-29512
Guide for evaluating 12 inch Substantial Dividing Walls (SDWs) to provide protection from remote operation, volume 1
[AD-A250251] p 3428 N92-29545
EXPONENTS
Numerical procedures for analyzing dynamical processes
[AD-A248175] p 3515 N92-29399
Revising M-layer: Complex exponent representation
[AD-A249121] p 3435 N92-29599
EXPOSURE
Human exposure model-2: User's guide
[PB92-186246] p 3495 N92-30200
Mechanical properties of coated titanium Beta-21S after exposure to air at 700 and 800 C
[NASA-TM-104220] p 3423 N92-30205
EXTINCTION
Stratospheric backscatter, extinction, and lidar ratio profiling after the Mt. Pinatubo eruptions p 3456 N92-29231
Measurements of stratospheric Pinatubo aerosol extinction profiles by a Raman lidar p 3457 N92-29232
Lidar studies of extinction in clouds in the ECLIPS project p 3472 N92-29320
EXTRATERRESTRIAL RADIATION
Electromagnetic processes in nucleus-nucleus collisions relating to space radiation research
[NASA-CR-190533] p 3547 N92-30001
EXTRAVEHICULAR ACTIVITY
Publications of the environmental health program: 1980-1990
[NASA-CR-4455] p 3509 N92-29341
EXTREME ULTRAVIOLET RADIATION
Review of potential x ray laser applications in materials science and chemistry
[DE92-012254] p 3475 N92-29434
Analysis of EUV dayglow spectra of Triton, Titan and Earth
[NASA-CR-190586] p 3568 N92-29451
EXTREMELY HIGH FREQUENCIES
Applications of inertial-sensor high-inheritance instruments to DSN precision antenna pointing p 3430 N92-29371
Ka-band feed arrays for spacecraft reflector antennas with limited scan capability: An overview p 3433 N92-29387
EXTREMUM VALUES
Extremally disconnected spaces, subspaces and retractions
[REPT-91-38] p 3535 N92-29920
EYE (ANATOMY)
Biologically-based neural network model of color constancy and color contrast
[AD-A248128] p 3510 N92-29398
Visual perception of elevation
[AD-A248338] p 3510 N92-29420
Peripheral limitations on spatial vision
[AD-A250579] p 3511 N92-29591

F

F-15 AIRCRAFT
Flight evaluation of an extended engine life mode on an F-15 airplane
[NASA-TM-104240] p 3405 N92-29659
F-16 AIRCRAFT
Transport delay measurements: Methodology and analysis for the F-16C combat engagement trainer, the display for advanced research and training, and the F-16A limited field of view
[AD-A248519] p 3406 N92-29505
F-18 AIRCRAFT
Parameter identification for nonlinear aerodynamic systems
[NASA-CR-190264] p 3399 N92-29329
FABRICATION
Laser processing for interconnect technology
[AD-A248103] p 3476 N92-29559
Novel thin-film CuInSe2 fabrication
[DE92-001222] p 3557 N92-29584
FABRY-PEROT INTERFEROMETERS
Efficiencies of rotational Raman and Rayleigh techniques for laser remote sensing of the atmospheric temperature p 3467 N92-29288
FACE CENTERED CUBIC LATTICES
The real-space multiple-scattering theory and the electronic structure of grain boundaries
[DE92-013006] p 3556 N92-29473
FAILURE
Smart BIT/TSMD integration
[AD-A247192] p 3442 N92-29914
Fundamental study of compressive strength development in PAN-based carbon fibers
[AD-A250285] p 3416 N92-30137
FAILURE ANALYSIS
The weakest failure detector for solving consensus
[NASA-CR-190545] p 3515 N92-29400
Aluminum-lithium alloys: Surface-cracked tension fracture tests and physical and thermal properties at cryogenic temperatures
[PB92-172477] p 3422 N92-29803
Performance of fuselage pressure structure p 3484 N92-30109
Fracture mechanics research at NASA related to the aging commercial transport fleet p 3484 N92-30110
Preliminary results on the fracture analysis of multi-site cracking of lap joints in aircraft skins p 3484 N92-30111
Current DOT research on the effect of multiple site damage on structural integrity p 3485 N92-30112
Fundamental study of compressive strength development in PAN-based carbon fibers
[AD-A250285] p 3416 N92-30137
FALSE ALARMS
Smart BIT/TSMD integration
[AD-A247192] p 3442 N92-29914
FAR FIELDS
Analyses of near- and far-field two-lobe patterns outside the output endface of a two-mode fiber
[NASA-CR-190494] p 3551 N92-29652
FARADAY EFFECT
Modulated high sensitivity infrared polarimeter
[AD-D015256] p 3474 N92-29571
FARM CROPS
Air quality criteria for oxides of nitrogen, volume 2
[PB92-176379] p 3493 N92-29521
FAST FOURIER TRANSFORMATIONS
Statistics of narrowband white noise derived from clipped broadband white noise
[AD-A248597] p 3434 N92-29563
On the abstracted dataflow complexity of fast Fourier transforms
[DE92-011372] p 3562 N92-29794
FATIGUE (MATERIALS)
Rolling-contact and wear resistance of hard coatings on bearing-steel substrates
[DE92-011834] p 3478 N92-29357
Characterization of fracture in (0/90)3s SiC/1723 composites
[AD-A250612] p 3414 N92-29453
Micromechanisms of cyclic and environmentally-assisted subcritical crack growth in ceramic-matrix composites
[AD-A248067] p 3414 N92-29556
Maintaining the safety of an aging fleet of aircraft p 3402 N92-30108
Fracture mechanics research at NASA related to the aging commercial transport fleet p 3484 N92-30110
Preliminary results on the fracture analysis of multi-site cracking of lap joints in aircraft skins p 3484 N92-30111
Aging commuter aeroplanes: Fatigue evaluation and control methods p 3488 N92-30132
FATIGUE LIFE
Optimal design of compact spur gear reductions
[NASA-TM-105676] p 3478 N92-29351
Short cracks and durability analysis of the Fokker 100 wing/fuselage structure
[NLR-TP-90336-U] p 3482 N92-29603
Aging aircraft NDI Development and Demonstration Center (AANC): An overview --- nondestructive inspection p 3481 N92-30120
Ageing airplane repair assessment program for Airbus A300 p 3402 N92-30123
FATIGUE TESTS
A response surface methodology study of ferroelectric memory devices
[AD-A248094] p 3440 N92-29529
Fatigue crack growth in damage tolerant Al-Li sheet alloys
[NLR-TP-90107-U] p 3483 N92-29708
Inspection of aging aircraft: A manufacturer's perspective p 3481 N92-30117
FAULT TOLERANCE
Ultra-dependable real-time computing
[AD-A248193] p 3515 N92-29409
A universal, fault-tolerant, non-linear analytic network for modeling and fault detection
[DE92-011840] p 3525 N92-29624
Reliable processing of confidential data by means of fragmentation-redundancy-scattering
[LAAS-91412] p 3526 N92-29888
A method for analysing the performance aspects of the fault-tolerance mechanisms in FDDI
[MEMO-INF-91-92] p 3514 N92-29982
FEASIBILITY ANALYSIS
Detecting microwave emissions from terrestrial sources: A feasibility study
[AD-A248557] p 3435 N92-29579
European studies to investigate the feasibility of using 1000 ft vertical separation minima above FL 290. Part 1: Overview of organisation, techniques employed, and conclusions
[NLR-TP-91062-U-PT-1] p 3403 N92-29605
Definition and design of an experiment to test raster scanning with rotating unbalanced-mass devices on gimbaled payloads
[NASA-TP-3249] p 3429 N92-29677
Full pose and partial pose calibration of a 6 degree-of-freedom robot manipulator arm
[AD-A247463] p 3479 N92-29785
Geostationary Operational Environmental Satellite(GEOS-N report)
[NASA-TM-107919] p 3410 N92-29810
Evaluation of aluminum ion vapor deposition as a replacement for cadmium electroplating at Anniston Army Depot
[AD-A250063] p 3423 N92-29940
FEEDBACK CONTROL
Feedback control laws for highly maneuverable aircraft
[NASA-CR-190535] p 3406 N92-29654
Asymptotic results in feedback systems
[ETN-92-91702] p 3529 N92-29962
The M/G/1 processor sharing queue as the almost sure limit of feedback queues p 3530 N92-29965
Some feedback procedures for control of flows p 3452 N92-30070
Sample positioning in microgravity
[NASA-CASE-NPO-18448-1-CU] p 3428 N92-30083
FERMENTATION
State estimation and control of the IBE-fermentation with product recovery p 3509 N92-29756
FERROELECTRICITY
A response surface methodology study of ferroelectric memory devices
[AD-A248094] p 3440 N92-29529
FERROMAGNETIC MATERIALS
The extended Bethe Ansatz for infinite S = 1/2 quantum spin chains with non-nearest-neighbor interaction
[DE92-622378] p 3533 N92-29793
FEYNMAN DIAGRAMS
The FORM version of MINCER
[NIKHEF-H/91-18] p 3518 N92-29747
FIBER COMPOSITES
An interlaminar tension strength specimen
[NASA-TM-107623] p 3481 N92-29393
A consistent shear deformable theory for laminated plates
[AD-A250591] p 3415 N92-29593

Status and perspectives of modern composite materials
[MBB-Z-0380-91-PUB] p 3416 N92-29875
Development and characterization of oxidation-protected CFC
[MBB-Z-0395-91-PUB] p 3416 N92-29876
Fundamental study of compressive strength development in PAN-based carbon fibers
[AD-A250285] p 3416 N92-30137

FIBER OPTICS
Micro-device for coupling, multiplexing and demultiplexing using elliptical-core two-mode fiber
[NASA-CR-190496] p 3550 N92-29331
Performance of a 12-GHz fiber-optic system for beam-waveguide antenna stability testing
p 3431 N92-29372
The development of a fiber optic Raman temperature measurement system for rocket flows
[NASA-CR-189200] p 3413 N92-29448
Developments in fiber optics for distribution automation
[NASA-CR-190454] p 3551 N92-29679
Reviews of computing technology: Fiber distributed data interface
[DE92-011374] p 3514 N92-29907

FIBERS
Characterization of fracture in (0/90)3s SiC/1723 composites
[AD-A250612] p 3414 N92-29453
Oriented structures based on trans-1,4-polybutadiene
[ETN-92-91632] p 3546 N92-29778

FIELD EFFECT TRANSISTORS
Noise-optimal control of HEMT LNA's for compensation of temperature deviations p 3431 N92-29374

FIELD OF VIEW
Geometric distortion analysis of a wide-field astrograph p 3409 N92-29370

FIELD THEORY (PHYSICS)
Introduction to SO(3) monopole
[USIP-91-05] p 3560 N92-29781
Probability density function approach and related closures for turbulent scalar fields p 3450 N92-30059
On the two-dimensional model of quantum Regge gravity
[DE92-624516] p 3560 N92-30212

FIGHTER AIRCRAFT
Fighter pilot training: The contribution of simulation
[NLR-TP-89311-U] p 3512 N92-29871

FIGURE OF MERIT
Figure of merit for direct-detection optical channels
p 3431 N92-29376

FILLERS
Nonideal formation of network polymers
[AD-A248072] p 3424 N92-29465

FILM THICKNESS
A study and feasibility of ultra thin silica layers by rapid thermal processing
[LAAS-91393] p 3422 N92-29674

FINE STRUCTURE
The 20 element HgI2 energy dispersive x ray array detector system
[DE92-013356] p 3549 N92-29502
Ion collision effects in hydrogen-like recombination x ray lasers
[DE92-013515] p 3476 N92-29509

FINGERS
Fingered bola body, bola with same, and methods of use
[NASA-CASE-MSC-21967-1] p 3479 N92-30026

FINITE DIFFERENCE THEORY
Acoustic scattering from elastic ice: A finite difference solution
[AD-A248281] p 3543 N92-29346
Finite difference modelling of seismic wave propagation at the seafloor
[AD-A248345] p 3505 N92-29562
Pressurization of cryogens: A review of current technology and its applicability to low-gravity conditions
[NASA-TM-105746] p 3427 N92-29669
Divergence preserving discrete surface integral methods for Maxwell's curl equations using non-orthogonal unstructured grids
[NASA-CR-190555] p 3517 N92-29694

FINITE ELEMENT METHOD
A consistent shear deformable theory for laminated plates
[AD-A250591] p 3415 N92-29593
Variational formulation and finite element implementation of Pagano's theory of laminated plates
[AD-A250592] p 3415 N92-29594
Validation of finite element and boundary element methods for predicting structural vibration and radiated noise
[NASA-TM-105359] p 3478 N92-29697
ISLAND: Interactive Solution Language for an Adaptive NIKE Driver
[DE92-011444] p 3533 N92-29791
Solution strategies for implicit nonlinear finite element analysis
[DE92-011466] p 3533 N92-29792
RF vacuum electronics
[AD-A248857] p 3442 N92-29935
An improved accuracy version of the mixed finite element method for a second order elliptic equation
[CWI-NM-R9111] p 3536 N92-29946
Nonlinear analyses of composite aerospace structures in sonic fatigue
[NASA-CR-190565] p 3404 N92-30209

FINITE VOLUME METHOD
Development of a multigrid transonic potential flow code for cascades
[NASA-CR-190480] p 3399 N92-29361
A finite volume approach to large eddy simulation of compressible, homogeneous, isotropic, decaying turbulence
[MEMO-1009] p 3446 N92-29972
A numerical and experimental investigation of the thrust vector control by secondary gas injection
[DLR-FB-91-31] p 3447 N92-29998
Methods for direct simulation of transition in hypersonic boundary layers 2 p 3451 N92-30064

FISHES
Mosquito Lagoon environmental resources inventory
[NASA-TM-107548] p 3492 N92-29430

FISSION
Feasibility of an antiproton catalyzed fission fragment rocket
[AD-A248157] p 3412 N92-29444

FITTINGS
Dynamic modeling of fluid transmission lines of the DSN 70-meter antennas by using a lumped parameter model
p 3432 N92-29378
Structural basis for the mechanical properties of polyethylenes
[PB92-164425] p 3426 N92-29804

FLAME PROPAGATION
Flame ignition in a premixed turbulent flow
p 3450 N92-30061
Stability of a premixed flame in stagnation-point flow against general disturbances
[NASA-CR-189666] p 3455 N92-30192

FLAMES
Structure of a methanol/air coaxial reacting spray near the stabilization region by OH fluorescence imaging and two-component phase-Doppler interferometry
[DE92-005328] p 3417 N92-29431
Strategies for understanding the deflagration-to-detonation transition
[DE92-013528] p 3427 N92-29512
On transient flamelets and their relationship to turbulent methane-air jet flames
[DE92-006705] p 3419 N92-29943
Simulation of flame-turbulence interactions in premixed combustion p 3450 N92-30062

FLASH LAMPS
Laser Transmitter Module (LTM) for LITE
p 3463 N92-29265
System testing and performance characterization of the LITE Laser Transmitter Module at NASA
p 3469 N92-29302
Characterization of artificial guidestars generated in the mesospheric sodium layer p 3470 N92-29309

FLASH POINT
A generalized polynomial form of the objective function in flash calculations
[AD-A248160] p 3531 N92-29446

FLAT PLATES
Streamwise vortices in heated boundary layers
[NASA-CR-189661] p 3444 N92-29692
Modeling turbulent boundary layers in adverse pressure gradients p 3449 N92-30053

FLAVOR (PARTICLE PHYSICS)
Theory of elementary particles studies in weak interaction and grand unification and studies in accelerator design
[DE92-014309] p 3550 N92-29532

FLEXIBLE SPACECRAFT
Spacecraft dynamics characterization and control system failure detection, volume 1
[NASA-CR-190517] p 3409 N92-29422

FLIGHT CONTROL
Effects of bleed air extraction on thrust levels on the F404-GE-400 turbofan engine
[NASA-TM-104247] p 3405 N92-29425

FLIGHT PATHS
Developing CMMCA flight profiles for cruise missile tracking
[AD-A248183] p 3434 N92-29406

FLIGHT SAFETY
European studies to investigate the feasibility of using 1000 ft vertical separation minima above FL 290. Part 1: Overview of organisation, techniques employed, and conclusions
[NLR-TP-91062-U-PT-1] p 3403 N92-29605
On the optimization of windshear warning and guidance systems
[NLR-TP-90196-U] p 3402 N92-29703

FLIGHT SIMULATION
Developing CMMCA flight profiles for cruise missile tracking
[AD-A248183] p 3434 N92-29406
Transport delay measurements: Methodology and analysis for the F-16C combat engagement trainer, the display for advanced research and training, and the F-16A limited field of view
[AD-A248519] p 3406 N92-29505
Results of a flight simulator experiment to establish handling quality guidelines for the design of future transport aircraft
[NLR-MP-88044-U] p 3404 N92-29616
Assessment of army aviators' ability to perform individual and collective tasks in the aviation networked simulator
[AD-A250293] p 3407 N92-29709
Experience with piloted simulation in the development of helicopters
[MBB-UD-0610-91-PUB] p 3407 N92-30076

FLIGHT SIMULATORS
Fighter pilot training: The contribution of simulation
[NLR-TP-89311-U] p 3512 N92-29871
Experience with piloted simulation in the development of helicopters
[MBB-UD-0610-91-PUB] p 3407 N92-30076

FLIGHT TESTS
Flight evaluation of an extended engine life mode on an F-15 airplane
[NASA-TM-104240] p 3405 N92-29659

FLIGHT TRAINING
Transport delay measurements: Methodology and analysis for the F-16C combat engagement trainer, the display for advanced research and training, and the F-16A limited field of view
[AD-A248519] p 3406 N92-29505

FLOW CHARACTERISTICS
An experimental study of scalar mixing in curved shear layers p 3453 N92-30152

FLOW DISTORTION
Experimental examination of heavy loaded axial fans with rotational symmetrical distortion of the inflow
[ETN-92-91489] p 3445 N92-29926
An experimental study of the effects of rapid rotation on turbulence p 3453 N92-30154

FLOW DISTRIBUTION
Computation of three-dimensional effects on two dimensional wings
[NASA-CR-190576] p 3401 N92-29691
The significance of large-scale flows into the Great Attractor p 3565 N92-29836
Explicit Navier-Stokes computation of turbomachinery flows
[AD-A248458] p 3445 N92-29933
Theoretical and experimental aspects of velocity slip by flows along solid walls
[ISBN-3-7983-1446-2] p 3446 N92-29968
The 2D-computation of an axial fan with FINFLO
[PB92-180678] p 3447 N92-30023
Local isotropy in buoyancy-generated turbulence
p 3447 N92-30043
On small scale vortices in turbulent flows
p 3448 N92-30045
Monte-Carlo implementation of mapping closures: Application to chemical reacting flows
p 3450 N92-30060
Simulation of flame-turbulence interactions in premixed combustion p 3450 N92-30062
Experimental investigation of the flowfield of an oscillating airfoil
[NASA-TM-105675] p 3402 N92-30182

FLOW EQUATIONS
Mathematical modelling of saturated and unsaturated groundwater flow
[MEMO-987] p 3445 N92-29857
Abstract quasilinear equations and application to a groundwater flow problem
[REPT-91-41] p 3535 N92-29923
Numerical methods for the 3D shallow water equations on vector and parallel computers
[CWI-NM-R9109] p 3446 N92-29944
On the numerical treatment of the advective terms in 3D shallow water models
[CWI-NM-R9110] p 3446 N92-29945

FLOW GEOMETRY
The large-scale structures in turbulent plane Couette flow p 3455 N92-30167

FLOW MEASUREMENT
Evaluation of measured-boundary-condition methods for 3D subsonic wall interference
[NLR-TR-88072-U] p 3401 N92-29884
Mixing measurements of straight and curved shear layers p 3451 N92-30067
An experimental investigation of a low Reynolds number turbulent boundary layer subject to an adverse pressure gradient p 3453 N92-30153
An experimental study of secondary vortex structure in mixing layers p 3453 N92-30155

FLOW STABILITY
A theoretical approach for analyzing the restabilization of wakes
[NASA-TM-103858] p 3443 N92-29394
Streamwise vortices in heated boundary layers
[NASA-CR-189661] p 3444 N92-29692
Linear stability analysis of hypersonic boundary layers p 3451 N92-30063
Methods for direct simulation of transition in hypersonic boundary layers 2 p 3451 N92-30064
Crossflow effects on the growth rate of inviscid Goertler vortices in a hypersonic boundary layer
[NASA-CR-189667] p 3455 N92-30190
Stability of a premixed flame in stagnation-point flow against general disturbances
[NASA-CR-189666] p 3455 N92-30192

FLOW THEORY
Development of renormalization group analysis of turbulence p 3453 N92-30156
Organized motions underlying turbulent shear flows p 3453 N92-30158

FLOW VELOCITY
An experimental investigation of a low Reynolds number turbulent boundary layer subject to an adverse pressure gradient p 3453 N92-30153

FLOW VISUALIZATION
Lidar tracking of multiple fluorescent tracers: Method and field test p 3464 N92-29274
An experimental study of scalar mixing in curved shear layers p 3453 N92-30152

FLUID DYNAMICS
A linear eddy sub-grid model for turbulent reacting flows: Application to hydrogen-air combustion
[DE92-006699] p 3417 N92-29433
Annual research briefs, 1991
[NASA-CR-189967] p 3447 N92-30041
On small scale vortices in turbulent flows p 3448 N92-30045
Scaling analysis of energy transfer in the inertial range p 3448 N92-30046
Lagrangian velocity correlation and spectrum in homogeneous isotropic turbulence p 3448 N92-30047
Turbulence and vortex structures p 3448 N92-30048

FLUID FILLED SHELLS
The influence of turbulence on aggregation of small particles in agitated vessels
[ETN-92-91629] p 3445 N92-29775

FLUID FLOW
Modeling deterministic chaos in thermally-pulsed combustion
[DE92-011756] p 3416 N92-29355
Application of a moving-grid method to a class of 1D brine transport problems in porous media
[CWI-NM-R9112] p 3446 N92-29947
Converting a CO2 atmosphere to a high-purity O2 supply
[NASA-CASE-LAR-14398-1] p 3419 N92-30098
Short-time Lyapunov exponent analysis p 3453 N92-30157

FLUID MECHANICS
Simulation of flame-turbulence interactions in premixed combustion p 3450 N92-30062

FLUID TRANSMISSION LINES
Dynamic modeling of fluid transmission lines of the DSN 70-meter antennas by using a lumped parameter model p 3432 N92-29378

FLUORESCENCE
Lidar tracking of multiple fluorescent tracers: Method and field test p 3464 N92-29274
Structure of a methanol/air coaxial reacting spray near the stabilization region by OH fluorescence imaging and two-component phase-Doppler interferometry
[DE92-005328] p 3417 N92-29431
Optical fiber sensor having an active core
[NASA-CASE-LAR-14607-1SB] p 3553 N92-30029

FLUORIDES
Corrosion resistance of stainless steels and high Ni-Cr alloys to acid fluoride wastes
[DE92-012338] p 3420 N92-29436

FLUTTER
Buffet test in the National Transonic Facility
[NASA-CR-189595] p 3406 N92-29352

FLUX (RATE)
Flux-capacity relationships of Acinetobacter calcoaceticus enzymes during xylose oxidation p 3508 N92-29739

FLY BY WIRE CONTROL
Results of a flight simulator experiment to establish handling quality guidelines for the design of future transport aircraft
[NLR-MP-88044-U] p 3404 N92-29616

FOAMS
Robotic workcell for wire wrapping integrated circuits
[DE92-013999] p 3441 N92-29796

FOCAL PLANE DEVICES
The processing of high temperature ceramic superconducting devices, volume 1
[AD-A248176] p 3438 N92-29404
Programmable hyperspectral image mapper with on-array processing
[NASA-CASE-NPO-17794-1-CU] p 3553 N92-30104

FOKKER-PLANCK EQUATION
LLE-LLNL progress report on studies in nonlocal heat transport in spherical plasmas using the Fokker-Planck code SPARK
[DE92-014093] p 3554 N92-29531

FORECASTING
HFRAD hindcast: An OTH-B radar and model comparison study
[AD-A248065] p 3436 N92-29902
SESC glossary of solar-terrestrial terms
[PB92-185305] p 3563 N92-30194

FOREST MANAGEMENT
What is the potential of forest management to slow the increase of atmospheric CO2?
[PB92-180249] p 3495 N92-30173
Research and technology annual report, FY 1990
[NASA-TM-107807] p 3571 N92-30197

FORESTS
Application of laser imaging for bio/geophysical studies p 3465 N92-29282
Combined summaries: Technologies to sustain tropical forest resources and biological diversity
[OTA-F-515] p 3492 N92-29416
Potential impacts of climate change on Pacific Northwest forest vegetation
[PB92-184985] p 3495 N92-30021
What is the potential of forest management to slow the increase of atmospheric CO2?
[PB92-180249] p 3495 N92-30173
Research and technology annual report, FY 1990
[NASA-TM-107807] p 3571 N92-30197
Biophysical, morphological, canopy optical property, and productivity data from the Superior National Forest
[NASA-TM-104568] p 3491 N92-30210

FORM FACTORS
Neutron diffraction study of the electronic structure of high T(sub c) superconductor-related compounds
[DE92-012587] p 3559 N92-29939

FORMALISM
Protocol conformance testing: A formal perspective in ISO IS-9646
[MEMO-INF-91-32] p 3517 N92-29705
What is the method in formal methods?
[MEMO-INF-91-79] p 3562 N92-30000
Integrated service engineering supported by the FDT LOTOS
[MEMO-INF-91-76] p 3531 N92-30184

FORTRAN
Developing CMMCA flight profiles for cruise missile tracking
[AD-A248183] p 3434 N92-29406
Reverse automatic differentiation of modular FORTRAN programs
[DE92-014071] p 3519 N92-29797
An introduction to using the FORTRAN programs provided with Computational Nuclear Physics 1 Nuclear Structure p 3549 N92-30013

FOURIER ANALYSIS
Mapping agroecological zones and time lag in vegetation growth by means of Fourier analysis of time series of NDVI images
[REPT-32] p 3490 N92-29717

FOURIER TRANSFORMATION
Using phase retrieval to determine the intensity and phase of an ultrashort laser pulse
[DE92-013564] p 3476 N92-29516
Scalable parallel algorithms for multidimensional digital signal processing
[AD-A249381] p 3516 N92-29622
Synthesis and characterization of a covalently bound self-assembled macrocycle monolayer thin film for nonlinear optical materials
[DE92-011353] p 3545 N92-29634

FRACTURE MECHANICS
Characterization of fracture in (0/90)3s SiC/1723 composites
[AD-A250612] p 3414 N92-29453
Tear straps in airplane fuselage
[AD-A248543] p 3404 N92-29511
A consistent shear deformable theory for laminated plates
[AD-A250591] p 3415 N92-29593
Mechanism of diffusion-controlled brittle fracture
[DE92-011572] p 3482 N92-29601
Fracture mechanics research at NASA related to the aging commercial transport fleet p 3484 N92-30110
Preliminary results on the fracture analysis of multi-site cracking of lap joints in aircraft skins p 3484 N92-30111
Simplified computational methods for elastic and elastic-plastic fracture problems p 3488 N92-30134
Fundamental study of compressive strength development in PAN-based carbon fibers
[AD-A250285] p 3416 N92-30137

FRACTURE STRENGTH
Effect of whisker orientation on the mechanical properties of silicon carbide/alumina composites
[AD-A248737] p 3415 N92-29723
A perspective on MoSi2 based composites
[DE92-013434] p 3415 N92-29795
Aluminum-lithium alloys: Surface-cracked tension fracture tests and physical and thermal properties at cryogenic temperatures
[PB92-172477] p 3422 N92-29803
Fundamental study of compressive strength development in PAN-based carbon fibers
[AD-A250285] p 3416 N92-30137

FRACTURES (MATERIALS)
Characterization of fracture in (0/90)3s SiC/1723 composites
[AD-A250612] p 3414 N92-29453
Simplified computational methods for elastic and elastic-plastic fracture problems p 3488 N92-30134

FRACTURING
Structural durability of stiffened composite shells
[NASA-CR-190588] p 3481 N92-29342
Characterization of fracture in (0/90)3s SiC/1723 composites
[AD-A250612] p 3414 N92-29453
Mechanism of diffusion-controlled brittle fracture
[DE92-011572] p 3482 N92-29601
Aluminum-lithium alloys: Surface-cracked tension fracture tests and physical and thermal properties at cryogenic temperatures
[PB92-172477] p 3422 N92-29803
Preliminary results on the fracture analysis of multi-site cracking of lap joints in aircraft skins p 3484 N92-30111
Simplified computational methods for elastic and elastic-plastic fracture problems p 3488 N92-30134

FRAGMENTS
Guide for evaluating 12 inch Substantial Dividing Walls (SDWs) to provide protection from remote operation, volume 2
[AD-A250252] p 3428 N92-29335
Feasibility of an antiproton catalyzed fission fragment rocket
[AD-A248157] p 3412 N92-29444

FREE CONVECTION
Turbulent thermal convection in a differentially rotating channel p 3455 N92-30168

FREE ELECTRON LASERS
Tunable driver for the LLNL FEL experiment
[DE92-011292] p 3477 N92-29937

FREE FLOW
Streamwise vortices in heated boundary layers
[NASA-CR-189661] p 3444 N92-29692
Incompressible spatially-developing free-shear flows p 3454 N92-30165

FREQUENCY DISTRIBUTION
Statistics of narrowband white noise derived from clipped broadband white noise
[AD-A248597] p 3434 N92-29563

FREQUENCY MODULATION
FM video data link spectrum spreading
[AD-D015257] p 3435 N92-29572

FREQUENCY RESPONSE
Multiresponse imager and imaging process for improved resolution
[NASA-CASE-LAR-14779-1] p 3552 N92-29951

FREQUENCY STABILITY
Performance of a 12-GHz fiber-optic system for beam-waveguide antenna stability testing p 3431 N92-29372

FREQUENCY STANDARDS
Introduction to quartz frequency standards
[AD-A248503] p 3439 N92-29498

FREQUENCY SYNCHRONIZATION
FM video data link spectrum spreading
[AD-D015257] p 3435 N92-29572

FRICTION
Vorticity matching in superfluid helium p 3449 N92-30049

Friction drive position transducer
[AD-D015205] p 3475 N92-30202

FUEL CELLS
The O2 reduction at the IFC modified O2 fuel cell electrode
[NASA-TM-105691] p 3413 N92-29667

FUEL TANK PRESSURIZATION
Pressurization of cryogens: A review of current technology and its applicability to low-gravity conditions
[NASA-TM-105746] p 3427 N92-29669
National Launch System cycle 1 loads and models data book
[NASA-TM-103560] p 3408 N92-30215

FULL SCALE TESTS
Aging aircraft NDI Development and Demonstration Center (AANC): An overview --- nondestructive inspection p 3481 N92-30120

FUNCTIONAL DESIGN SPECIFICATIONS
Application of VME-technology on an airborne data link processor unit
[NLR-MP-88040-U] p 3403 N92-29615

FUNCTIONS (MATHEMATICS)
Some applications of orthogonal functions to probability and statistics
[ETN-92-91741] p 3538 N92-29491
Gaarding inequalities for systems of pseudo-differential operators
[CWI-AM-R9111] p 3534 N92-29881
Asymptotic inversion of the incomplete beta function
[CWI-AM-R9106] p 3534 N92-29893
Theoretical and experimental aspects of velocity slip by flows along solid walls
[ISBN-3-7983-1446-2] p 3446 N92-29968

FURNACES
Metal vapor plasma behavior during vacuum arc remelting of alloy 718
[DE92-011761] p 3421 N92-29623
Process of ferrochromium now and in the future
[DE92-506510] p 3421 N92-29637

FUSELAGES
Tear straps in airplane fuselage
[AD-A248543] p 3404 N92-29511
Performance of fuselage pressure structure p 3484 N92-30109
Damaged stiffened shell research at NASA. Langley Research Center p 3485 N92-30115
Ageing airplane repair assessment program for Airbus A300 p 3402 N92-30123

FUSION REACTORS
LLE review
[DE92-011614] p 3555 N92-30072

FUZZY SETS
DecisionMaker software and extracting fuzzy rules under uncertainty
[NASA-CR-190502] p 3514 N92-29391

FUZZY SYSTEMS
Application of fuzzy logic-neural network based reinforcement learning to proximity and docking operations
[NASA-CR-190504] p 3525 N92-29390
Fuzzy logic control of AC induction motors
[PB92-180207] p 3443 N92-30092

G

GALACTIC CLUSTERS
Traces of the primordial structure in the universe
[MPE-227] p 3565 N92-29833
Reconstruction of density and potential fields of the Universe p 3565 N92-29834
Cluster correlations from N-point correlation amplitudes p 3566 N92-29837
Abell clusters of galaxies: Catalogs and large-scale structures p 3566 N92-29838
Scale-invariant galaxy clustering on large scales p 3566 N92-29839
Studies of distant clusters of galaxies p 3566 N92-29843
Evidence for evolution of the luminosity function of clusters of galaxies p 3567 N92-29844
Constraints on the mass fluctuation spectrum from x ray observations of clusters of galaxies p 3567 N92-29845
Clusters of galaxies in depth p 3567 N92-29846
X ray cluster counts: What ROSAT should see p 3567 N92-29847
The evolution of the x ray luminosity function of galaxy clusters p 3567 N92-29848
N-body simulations of the evolution of clusters of galaxies p 3567 N92-29849
ROSAT: Early results p 3567 N92-29850
The x ray morphology of the relaxed cluster of galaxies A2256. 1: Evidence for a merger event p 3568 N92-29851
The x ray morphology of the relaxed cluster of galaxies A2256. 2: Sources around the extended cluster emission p 3568 N92-29852
Optical searches for ROSAT x ray cluster sources p 3568 N92-29853

GALACTIC EVOLUTION
Traces of the primordial structure in the universe
[MPE-227] p 3565 N92-29833
CDM with thermal history of baryons: High-resolution 2-D and 3-D simulations p 3565 N92-29835
Morphological segregation of galaxies on large scales p 3566 N92-29840
Evidence for evolution of the luminosity function of clusters of galaxies p 3567 N92-29844
Clusters of galaxies in depth p 3567 N92-29846
The evolution of the x ray luminosity function of galaxy clusters p 3567 N92-29848
N-body simulations of the evolution of clusters of galaxies p 3567 N92-29849

GALACTIC MASS
Cluster correlations from N-point correlation amplitudes p 3566 N92-29837
Abell clusters of galaxies: Catalogs and large-scale structures p 3566 N92-29838
Scale-invariant galaxy clustering on large scales p 3566 N92-29839
The space distribution of local radio galaxies p 3566 N92-29842
Constraints on the mass fluctuation spectrum from x ray observations of clusters of galaxies p 3567 N92-29845
Clusters of galaxies in depth p 3567 N92-29846
The evolution of the x ray luminosity function of galaxy clusters p 3567 N92-29848

GALACTIC STRUCTURE
Traces of the primordial structure in the universe
[MPE-227] p 3565 N92-29833
Reconstruction of density and potential fields of the Universe p 3565 N92-29834
CDM with thermal history of baryons: High-resolution 2-D and 3-D simulations p 3565 N92-29835
Scale-invariant galaxy clustering on large scales p 3566 N92-29839
Morphological segregation of galaxies on large scales p 3566 N92-29840
Scales of universal homogeneity from galaxy counts p 3566 N92-29841
Evidence for evolution of the luminosity function of clusters of galaxies p 3567 N92-29844
X ray cluster counts: What ROSAT should see p 3567 N92-29847

GALAXIES
The 12 micron contribution of nearby galaxies to the infrared background
[AD-A250623] p 3565 N92-29596
The significance of large-scale flows into the Great Attractor p 3565 N92-29836
Morphological segregation of galaxies on large scales p 3566 N92-29840
Scales of universal homogeneity from galaxy counts p 3566 N92-29841

GALILEO SPACECRAFT
Galileo early cruise, including Venus, first Earth, and Gaspra encounters p 3433 N92-29384

GALLIUM ARSENIDES
Study and realization of GaAs PNP homojunction bipolar transistors using ion implementation
[LAAS-91433] p 3441 N92-29729
Time-of-flight experiments on GaAs/Al(x)Ga(x-1)As heterostructures
[ETN-92-91625] p 3558 N92-29753
Laser etching: Possibilities and problems
[DE92-010800] p 3477 N92-30135

GAME THEORY
Puzzles 3 Hanoi-variations in digraphs
[MEMO-1010] p 3541 N92-29973
A survey on minimum cost spanning tree games
[MEMO-1003] p 3541 N92-30079

GAMMA RAYS
The comparative effects of gamma radiation and in situ alpha particles on five strong-base anion exchange resins
[DE92-000177] p 3425 N92-29643

GAS ANALYSIS
The development of a fiber optic Raman temperature measurement system for rocket flows
[NASA-CR-189200] p 3413 N92-29448

GAS COMPOSITION
Observations of ozone-aerosol correlated behaviour in the lower stratosphere during the EASOE campaign p 3459 N92-29243
Transportable lidar for the measurement of ozone concentration and flux profiles in the lower troposphere p 3465 N92-29278

GAS DISCHARGES
Optical and electrical characteristics of the cathode fall
[AD-A249010] p 3443 N92-30176

GAS LASERS
In vivo and in vitro chlorophyll-a and pheophytin-a concentration measurements by laser fluorometry p 3468 N92-29295

GAS PIPES
Structural basis for the mechanical properties of polyethylenes
[PB92-164425] p 3426 N92-29804

GAS PRESSURE
In vitro measurement of nucleus pulposus swelling pressure: A new technique for studies of spinal adaptation to gravity
[NASA-TM-103853] p 3506 N92-29397
Second-order shock-expansion theory extended to include real gas effects
[AD-A247191] p 3400 N92-29539
Converting a CO2 atmosphere to a high-purity O2 supply
[NASA-CASE-LAR-14398-1] p 3419 N92-30098

GAS SPECTROSCOPY
Theoretical/experimental investigations of the structure and dynamics of highly energetic dication species
[AD-A247050] p 3418 N92-29901

GAS TURBINE ENGINES
Applied analytical combustion/emissions research at the NASA Lewis Research Center
[NASA-TM-105731] p 3412 N92-29343
Fatigue in single crystal nickel superalloys
[AD-A248190] p 3420 N92-29408
Flight evaluation of an extended engine life mode on an F-15 airplane
[NASA-TM-104240] p 3405 N92-29659

GASES
Continuum approaches for describing solid-gas and solid-liquid flow
[DE92-013601] p 3452 N92-30140

GAUGE THEORY
Introduction to SO(3) monopole
[USIP-91-05] p 3560 N92-29781

GEARS
Optimal design of compact spur gear reductions
[NASA-TM-105676] p 3478 N92-29351

GEOCORONAL EMISSIONS
Low energy neutral atoms in the Earth's magnetosphere: Modeling
[DE92-013240] p 3500 N92-29536

GEODYNAMICS
Turbulence effects on the geodynamic laser ranging system
[PB92-166404] p 3477 N92-29948

GEOGRAPHIC INFORMATION SYSTEMS
GIS for coastal management
[BCRS-90-31] p 3489 N92-29493
Alexander: User guide (version 1.0)
[BCRS-90-38] p 3489 N92-29494
Monitoring of grass dominance on Dutch heathlands using remote sensing and a geographic information system (HEIMON)
[BCRS-91-12] p 3489 N92-29693

GEOMAGNETIC TAIL
Poleward leaping auroras, the substorm expansive and recovery phases, and the recovery of the plasma sheet
[DE92-013530] p 3500 N92-29513

GEOMAGNETISM
Poleward leaping auroras, the substorm expansive and recovery phases, and the recovery of the plasma sheet
[DE92-013530] p 3500 N92-29513
SESC glossary of solar-terrestrial terms
[PB92-185305] p 3563 N92-30194

GEOMETRIC ACCURACY
CAESAR: A CCD airborne experimental scanner for applications in remote sensing radiometric and geometric calibration
[NLR-TP-89103-U] p 3490 N92-29707

GEOMETRY
Construction of a VC1 interpolant over triangles via edge deletion
[MEMO-988] p 3533 N92-29858

GEOPHYSICS
Application of laser imaging for bio/geophysical studies p 3465 N92-29282

GERMANIUM
X ray study of interfacial interactions in highly milled Sn-Ge powders
[DE92-012518] p 3556 N92-29437

GETTERS
Li/SO2 cells and Li/SOCl2 cells: Safe use and testing
[DE92-013508] p 3439 N92-29414

GLASS
Cursory examination of the zeta potential behaviors of two optical materials
[DE92-011588] p 3551 N92-29578

GLASS COATINGS
Mechanical properties of coated titanium Beta-21S after exposure to air at 700 and 800 C
[NASA-TM-104220] p 3423 N92-30205
GLASS FIBER REINFORCED PLASTICS
Computed Tomography (CT) as a nondestructive test method used for composite helicopter components
[MBB-UD-0603-91-PUB] p 3480 N92-29873
GLASS TRANSITION TEMPERATURE
DSC measurements on experimental TGDDM/DDS resin systems: The influence of variations in resin composition and catalyst content
[NLR-TP-90267-U] p 3478 N92-29602
GLOBAL POSITIONING SYSTEM
Incorporation of GPS/INS into small autonomous underwater vehicle navigation
[AD-A248884] p 3403 N92-29906
GOERTLER INSTABILITY
Mixing measurements of straight and curved shear layers p 3451 N92-30067
GOES SATELLITES
Geostationary Operational Environmental Statellite(GEOS-N report)
[NASA-TM-107919] p 3410 N92-29810
Geostationary Operational Environmental Satellite (GOES-N report). Volume 1: Technical
[NASA-TM-107918] p 3410 N92-29811
Geostationary Operational Environmental Satellite (GOES-N report). Volume 2: Technical appendix
[NASA-TM-107920] p 3410 N92-29812
GOES 7
Geostationary Operational Environmental Satellite (GOES-N report). Volume 1: Technical
[NASA-TM-107918] p 3410 N92-29811
GOGGLES
Visual acuity with second and third generation night vision goggles obtained from a new method of night sky simulation across a wide range of target contrast
[AD-A248284] p 3512 N92-29348
Evaluation of Night Vision Goggles (NVG) for maritime search and rescue
[AD-A247182] p 3512 N92-29538
GOLD
A study of the adsorption of acetonitrile on a gold electrode from aqueous solutions using in situ vibrational spectroscopy
[AD-A250191] p 3417 N92-29514
GOODNESS OF FIT
Power approximations to and power comparison of certain goodness-of-fit tests
[MEMO-1019] p 3541 N92-29980
GOVERNMENT PROCUREMENT
Geostationary Operational Environmental Statellite(GEOS-N report)
[NASA-TM-107919] p 3410 N92-29810
GRAIN BOUNDARIES
Zee star analysis
[AD-A248342] p 3417 N92-29423
The real-space multiple-scattering theory and the electronic structure of grain boundaries
[DE92-013006] p 3556 N92-29473
Quasi-static intergranular cracking in a Cu-Sn alloy: An analog of stress relief cracking of steels
[DE92-011646] p 3420 N92-29483
Strengthening mechanisms, creep and fatigue processes in dispersion hardened niobium alloy
[AD-A250282] p 3421 N92-29547
Amorphization along interfaces and grain boundaries in polycrystalline multilayers: An x ray diffraction study of Ni/Ti multilayers p 3558 N92-29769
GRAIN SIZE
Effect of grain size on deformation stability of copper under quasi-static and dynamic tensile loading
[DE92-012677] p 3421 N92-29639
GRAMMARS
Optimal parallel parsing of almost all LL(k) grammars
[MEMO-INF-91-78] p 3527 N92-30189
GRANULAR MATERIALS
Constitutive modelling for granular material under finite strains with particle slidings and fabric changes
[AD-A248187] p 3482 N92-29407
GRAPH THEORY
A massively parallel genetic algorithm for the graph partitioning problem
[IMAG-RR-845-I] p 3525 N92-29610
Sufficient conditions for dominating cliques
[MEMO-1006] p 3538 N92-30185
Algorithms and min-max theorems for certain multiway cuts
[MEMO-1022] p 3523 N92-30186
GRAPHITE-EPOXY COMPOSITES
An interlaminar tension strength specimen
[NASA-TM-107623] p 3481 N92-29393
Laser paint stripping
[AD-A249233] p 3476 N92-29581
A consistent shear deformable theory for laminated plates
[AD-A250591] p 3415 N92-29593
GRAPHS (CHARTS)
A new heuristic for load-balanced assignment of objects and minimized network communication in distributed programs implemented through inverse remote procedure calls
[MEMO-INF-91-91] p 3519 N92-29815
Non-interfering dipaths in planar digraphs
[CWI-BS-R9121] p 3533 N92-29864
Inverse remote procedure calls
[MEMO-INF-91-89] p 3521 N92-29970
Puzzles 3 Hanoi-variations in digraphs
[MEMO-1010] p 3541 N92-29973
Sufficient conditions for dominating cliques
[MEMO-1006] p 3538 N92-30185
GRASSES
Monitoring of grass dominance on Dutch heathlands using remote sensing and a geographic information system (HEIMON)
[BCRS-91-12] p 3489 N92-29693
GRATINGS (SPECTRA)
Using phase retrieval to determine the intensity and phase of an ultrashort laser pulse
[DE92-013564] p 3476 N92-29516
GRAVELS
Field study of multidimensional flow and transport in the vadose zone
[PB92-161363] p 3489 N92-29701
GRAVITATIONAL EFFECTS
A nanoradian differential VLBI tracking demonstration p 3430 N92-29367
Orbiter-orbiter and orbiter-lander tracking using same-beam interferometry p 3409 N92-29369
In vitro measurement of nucleus pulposus swelling pressure: A new technique for studies of spinal adaptation to gravity
[NASA-TM-103853] p 3506 N92-29397
GRAVITY WAVES
Airborne sodium and Rayleigh lidar observations from ALOHA-90 p 3471 N92-29315
Multi-fractal analysis of nocturnal boundary layer time series from the Boulder Atmospheric Observatory
[AD-A248347] p 3502 N92-29424
GREENHOUSE EFFECT
National Institute for Global Environmental Change
[DE92-013487] p 3493 N92-29597
Global-warming problem and global economic models
[DE92-514557] p 3493 N92-29638
GREENLAND
ARCLITE: The Arctic Lidar Technology Facility at Sondre Stromfjord, Greenland p 3407 N92-29283
GRID GENERATION (MATHEMATICS)
Development of a multigrid transonic potential flow code for cascades
[NASA-CR-190480] p 3399 N92-29361
Hyperbolic grid generation control by panel methods
[NLR-TP-91061-U] p 3532 N92-29604
NASA Workshop on future directions in surface modeling and grid generation
[NASA-CP-10092] p 3400 N92-29625
Application of a moving-grid method to a class of 1D brine transport problems in porous media
[CWI-NM-R9112] p 3446 N92-29947
GROUND STATE
The extended Bethe Ansatz for infinite S = 1/2 quantum spin chains with non-nearest-neighbor interaction
[DE92-622378] p 3533 N92-29793
GROUND STATIONS
Final Environmental Impact Statement (EIS) for the Space Nuclear Thermal Propulsion (SNTP) program
[AD-A248408] p 3413 N92-29903
GROUND SUPPORT EQUIPMENT
Lidar In-space Technology Experiment (LITE) electronics overview p 3462 N92-29264
GROUND WATER
Mapping of groundwater losses by evaporation in the western desert of Egypt
[BCRS-91-01] p 3489 N92-29495
Field study of multidimensional flow and transport in the vadose zone
[PB92-161363] p 3489 N92-29701
Mathematical modelling of saturated and unsaturated groundwater flow
[MEMO-987] p 3445 N92-29857
Abstract quasilinear equations and application to a groundwater flow problem
[REPT-91-41] p 3535 N92-29923
GROUND WIND
Wind profiles derived from volume imaging lidar data: Enhanc ments to the algorithm and comparisons with insitu observations p 3464 N92-29271
GROUP THEORY
Swirls and wheels
[PB92-173251] p 3542 N92-30095
GULF OF MEXICO
Numerical modeling studies of the Gulf of Mexico and the Caribbean Sea using the Bryan-Cox model
[PB92-164987] p 3505 N92-29704
GULF STREAM
Circulation and exchange at the continental shelf and slope SEEP-2
[DE92-013500] p 3504 N92-29439
GUST LOADS
Short cracks and durability analysis of the Fokker 100 wing/fuselage structure
[NLR-TP-90336-U] p 3482 N92-29603

H

HADRONS
The FORM version of MINCER
[NIKHEF-H/91-18] p 3518 N92-29747
HAMILTONIAN FUNCTIONS
The extended Bethe Ansatz for infinite S = 1/2 quantum spin chains with non-nearest-neighbor interaction
[DE92-622378] p 3533 N92-29793
Energy propagation in dissipative systems. Part 2: Centrovelocity for nonlinear wave equations
[MEMO-1016-PT-2] p 3437 N92-29978
Approximation in a damped Hamiltonian system by successive relative equilibria
[MEMO-1017] p 3536 N92-29979
Port-controlled Hamiltonian systems: Modelling origins and systemtheoretic properties
[MEMO-1001] p 3537 N92-30077
HAZARDS
Guide for evaluating 12 inch Substantial Dividing Walls (SDWs) to provide protection from remote operation, volume 1
[AD-A250251] p 3428 N92-29545
HEALTH
Publications of the environmental health program: 1980-1990
[NASA-CR-4455] p 3509 N92-29341
Exercise and three psychosocial variables: A longitudinal study
[AD-A250649] p 3510 N92-30216
HEAT EXCHANGERS
Heat exchanger with oscillating flow
[NASA-CASE-LAR-14033-2] p 3447 N92-30024
Heat transfer in an aluminum heat exchanger using normal hydrogen gas
[PB92-172832] p 3447 N92-30036
HEAT FLUX
Sensitivity of C2 sub n to random variations of windspeed, sensible heat flux, and latent heat flux
[AD-A248696] p 3502 N92-29565
Heat exchanger with oscillating flow
[NASA-CASE-LAR-14033-2] p 3447 N92-30024
Heat transfer in an aluminum heat exchanger using normal hydrogen gas
[PB92-172832] p 3447 N92-30036
HEAT MEASUREMENT
DSC measurements on experimental TGDDM/DDS resin systems: The influence of variations in resin composition and catalyst content
[NLR-TP-90267-U] p 3478 N92-29602
Amorphization and related effects in Ni/Ti multilayers studied by differential scanning calorimetry p 3559 N92-29772
Microcalorimetric study of the aging reactions of atomized magnesium powder
[AD-A247932] p 3427 N92-29786
HEAT OF FORMATION
MNDO study of boron-nitrogen analogues of buckminsterfullerene
[AD-A247777] p 3414 N92-29460
HEAT PIPES
Design characteristics of a heat pipe test chamber
[NASA-TM-105737] p 3492 N92-29662
HEAT RESISTANT ALLOYS
Fatigue in single crystal nickel superalloys
[AD-A248190] p 3420 N92-29408
Metal vapor plasma behavior during vacuum arc remelting of alloy 718
[DE92-011761] p 3421 N92-29623
HEAT SOURCES
Method and apparatus for thermographically and quantitatively analyzing a structure for disbonds and/or inclusions
[NASA-CASE-LAR-14559-1] p 3480 N92-29829
HEAT STORAGE
SOLCHIPS: A fast predesign and optimization tool for solar heating with seasonal storage
[DE92-506509] p 3492 N92-29636
Thermal energy storage for cogeneration applications
[DE92-012339] p 3492 N92-29646

HEAT TRANSFER
LLE-LLNL progress report on studies in nonlocal heat transport in spherical plasmas using the Fokker-Planck code SPARK
[DE92-014093] p 3554 N92-29531
Second-order shock-expansion theory extended to include real gas effects
[AD-A247191] p 3400 N92-29539
Design characteristics of a heat pipe test chamber
[NASA-TM-105737] p 3492 N92-29662
ESATAN user manual
[ESA-PSS-03-105-ISSUE-2] p 3521 N92-29869
Heat exchanger with oscillating flow
[NASA-CASE-LAR-14033-2] p 3447 N92-30024
Heat transfer in an aluminum heat exchanger using normal hydrogen gas
[PB92-172832] p 3447 N92-30036
Flame ignition in a premixed turbulent flow
p 3450 N92-30061
Effect of walls on the supersonic reacting mixing layer
p 3451 N92-30065

HEAT TRANSMISSION
Second-order shock-expansion theory extended to include real gas effects
[AD-A247191] p 3400 N92-29539
Method and apparatus for thermographically and quantitatively analyzing a structure for disbonds and/or inclusions
[NASA-CASE-LAR-14559-1] p 3480 N92-29829
Heat flow of a two-electron-temperature plasma through the sheath in the presence of electron emission
[NIFS-136] p 3555 N92-30172

HEAT TREATMENT
Development of high T(sub c) (greater than 110 K) Bi, Tl, and Y-based materials as superconducting circuit elements
[NASA-CR-190311] p 3557 N92-29676

HEAVY IONS
Transition crossing in the RHIC
[DE92-013031] p 3550 N92-29475
Theory of elementary particles studies in weak interaction and grand unification and studies in accelerator design
[DE92-014309] p 3550 N92-29532
Relativistic Coulomb fission p 3548 N92-30008
Stopping powers and cross sections due to two-photon processes in relativistic nucleus-nucleus collision
p 3548 N92-30012
Fourth workshop on Experiments and Detectors for a Relativistic Heavy Ion Collider
[BNL-52262] p 3549 N92-30014
A letter of intent for an experiment to study strong electromagnetic fields at RHIC via multiple electromagnetic processes p 3438 N92-30015

HELICOPTER CONTROL
Helicopter low-speed yaw control
[NASA-CASE-LAR-14219-1] p 3406 N92-30025

HELICOPTER DESIGN
Repair procedures for advanced composites for helicopters
[MBB-UD-0606-91-PUB] p 3399 N92-29874

HELICOPTER TAIL ROTORS
A semi empirical method for the analytical representation of stationary measured profile coefficients for applications of rotary wing aerodynamics
[ETN-92-91491] p 3401 N92-29741
Computed Tomography (CT) as a nondestructive test method used for composite helicopter components
[MBB-UD-0603-91-PUB] p 3480 N92-29873

HELICOPTERS
Improving the LAMP Mk 3 SH-60B HF communication system
[AD-A245970] p 3429 N92-29344
Evaluation of Night Vision Goggles (NVG) for maritime search and rescue
[AD-A247182] p 3512 N92-29538
Helicopter low-speed yaw control
[NASA-CASE-LAR-14219-1] p 3406 N92-30025
Experience with piloted simulation in the development of helicopters
[MBB-UD-0610-91-PUB] p 3407 N92-30076

HELIUM HYDROGEN ATMOSPHERES
Modeling of the role of atomic hydrogen in heat transfer during hot filament assisted deposition of diamond
[AD-A250607] p 3418 N92-29595

HELIUM PLASMA
Transport processes in beamed energy propulsion systems
[AD-A247296] p 3413 N92-29913

HERMES MANNED SPACEPLANE
On fictitious joints modelling of manipulator link flexibility for the HERA simulation facility pilot
[NLR-TR-88086-U] p 3479 N92-29885

HETEROCYCLIC COMPOUNDS
Polybenzimidazoles via aromatic nucleophilic displacement
[NASA-CASE-LAR-14643-1] p 3426 N92-29953

HETERODYNING
Lag angle compensation in a space borne scanning lidar p 3462 N92-29263

HETEROJUNCTION DEVICES
Optoelectronic integration
[AD-A248950] p 3442 N92-29936

HEURISTIC METHODS
The cognitive function of theoretical knowledge in procedural learning
[AD-A248075] p 3531 N92-29486
A new heuristic for load-balanced assignment of objects and minimized network communication in distributed programs implemented through inverse remote procedure calls
[MEMO-INF-91-91] p 3519 N92-29815
A seven-league-boots algorithm for path planning in configuration spaces
[MEMO-INF-91-88] p 3530 N92-29969
Inverse remote procedure calls
[MEMO-INF-91-89] p 3521 N92-29970

HIERARCHIES
An analysis of model-based diagnosis using problem-reformulation
[MEMO-INF-92-03] p 3530 N92-29983

HIGH ALTITUDE
A preliminary design and analysis of an advanced heat-rejection system for an extreme altitude advanced variable cycle diesel engine installed in a high-altitude advanced research platform
[NASA-CR-186021] p 3405 N92-29427

HIGH CURRENT
The processing of high temperature ceramic superconducting devices, volume 1
[AD-A248176] p 3438 N92-29404

HIGH DEFINITION TELEVISION
World Administrative Radio Conference. Issues for US International Spectrum Policy
[PB92-157601] p 3435 N92-29696

HIGH ELECTRON MOBILITY TRANSISTORS
Noise-optimal control of HEMT LNA's for compensation of temperature deviations p 3431 N92-29374

HIGH ENERGY INTERACTIONS
Spectroscopy of W-183; measured magnetic moments and rotation-particle coupling
[DE92-624790] p 3549 N92-30213

HIGH GAIN
Position-error-based force reflection and compliance control
[NASA-CASE-NPO-18668-1-CU] p 3479 N92-29765

HIGH RESOLUTION
Adaptation of the University of Wisconsin high spectral resolution lidar for polarization and multiple scattering measurements p 3472 N92-29322
High resolving power spectrometer for beam analysis
[DE92-010751] p 3437 N92-29988
Investigation of solar active regions at high resolution by balloon flights of the solar optical universal polarimeter, definition phase
[NASA-CR-184339] p 3570 N92-30204
TERS product development plan for urban planning of Bandung, Indonesia
[BCRS-91-30] p 3491 N92-30231

HIGH REYNOLDS NUMBER
A preliminary experimental investigation of local isotropy in high-Reynolds-number turbulence
p 3447 N92-30042
Mixing measurements of straight and curved shear layers p 3451 N92-30067

HIGH STRENGTH
An interlaminar tension strength specimen
[NASA-TM-107623] p 3481 N92-29393
Manufacturing of components of fibre-metal laminates: An overview
[LR-670] p 3415 N92-29702

HIGH STRENGTH ALLOYS
Fatigue crack growth in damage tolerant Al-Li sheet alloys
[NLR-TP-90107-U] p 3483 N92-29708

HIGH TEMPERATURE
Apparatus for elevated temperature compression or tension testing of specimens
[NASA-CASE-LAR-14775-1] p 3483 N92-30099

HIGH TEMPERATURE GASES
Contingency power for a small turboshaft engine by using water injection into turbine cooling air
[NASA-TM-105680] p 3405 N92-29661

HIGH TEMPERATURE SUPERCONDUCTORS
The processing of high temperature ceramic superconducting devices, volume 1
[AD-A248176] p 3438 N92-29404
Development of high T(sub c) (greater than 110 K) Bi, Tl, and Y-based materials as superconducting circuit elements
[NASA-CR-190311] p 3557 N92-29676

HIGHLY MANEUVERABLE AIRCRAFT
Feedback control laws for highly maneuverable aircraft
[NASA-CR-190535] p 3406 N92-29654

HILSCH TUBES
On small scale vortices in turbulent flows
p 3448 N92-30045

HIPPOCAMPUS
A systems theoretic investigation of neuronal network properties of the hippocampal formation
[AD-A250246] p 3510 N92-29334

HISS
Global measurements of low-frequency radio noise
[AD-A248260] p 3434 N92-29542

HISTORIES
Research in NASA history: A guide to the NASA history program
[NASA-TM-107953] p 3571 N92-29689

HOLDERS
Fingered bola body, bola with same, and methods of use
[NASA-CASE-MSC-21967-1] p 3479 N92-30026

HOMOGENEITY
Scales of universal homogeneity from galaxy counts
p 3566 N92-29841

HOMOGENEOUS TURBULENCE
Local isotropy in buoyancy-generated turbulence
p 3447 N92-30043
Non-linear interactions in homogeneous turbulence with and without background rotation p 3448 N92-30044
On small scale vortices in turbulent flows
p 3448 N92-30045
Lagrangian velocity correlation and spectrum in homogeneous isotropic turbulence p 3448 N92-30047
Analyses and modeling of evolving turbulent flow
p 3449 N92-30051
Development of renormalization group analysis of turbulence p 3453 N92-30156
Turbulence dynamics in the wavelet representation
p 3454 N92-30159

HOOKS
Fingered bola body, bola with same, and methods of use
[NASA-CASE-MSC-21967-1] p 3479 N92-30026

HOT PRESSING
Development of high T(sub c) (greater than 110 K) Bi, Tl, and Y-based materials as superconducting circuit elements
[NASA-CR-190311] p 3557 N92-29676

HUBBLE SPACE TELESCOPE
Image inversion analysis of the HST OTA (Hubble Space Telescope Optical Telescope Assembly), phase A
[NASA-CR-190483] p 3564 N92-29359

HUMAN BEINGS
Visual perception of elevation
[AD-A248338] p 3510 N92-29420
Peripheral limitations on spatial vision
[AD-A250579] p 3511 N92-29591

HUMAN FACTORS ENGINEERING
Visual acuity with second and third generation night vision goggles obtained from a new method of night sky simulation across a wide range of target contrast
[AD-A248284] p 3512 N92-29348
Army-NASA aircrew/aircraft integration program: Phase 4 A(3)I Man-Machine Integration Design and Analysis System (MIDAS) software detailed design document
[NASA-CR-177593] p 3512 N92-29413
Human factors in aircraft maintenance and inspection
p 3487 N92-30125
Using intelligent simulation to enhance human performance in aircraft maintenance
p 3487 N92-30126

HUMAN PERFORMANCE
Development of models for prediction of optimal lifting motion
[PB92-164656] p 3513 N92-29949
Using intelligent simulation to enhance human performance in aircraft maintenance
p 3487 N92-30126

HUMIDITY
LAPS specific humidity analysis
[PB92-163575] p 3502 N92-29799

HURRICANES
Tropical cyclones: Central North Pacific, 1991
[PB92-167345] p 3502 N92-29743
Tracking hurricane Claudette with the US Air Force OTH-B radar
[PB92-164524] p 3503 N92-29800

HYBRID CIRCUITS
Design and analysis of electrical circuits that produce fractional-order differentiation
[AD-A248085] p 3440 N92-29526

Performance measurement results for a 220 Mbps QPPM optical communication receiver with an EG/G Slik APD
[NASA-CR-190561] p 3435 N92-29658
Design guidelines for capability approval of film hybrid microcircuits and Microwave Hybrid Integrated Circuits (MHICs)
[ESA-PSS-01-610-ISSUE-1] p 3441 N92-29854

HYDRAULIC JETS
Characterization of fracture in (0/90)3s SiC/1723 composites
[AD-A250612] p 3414 N92-29453

HYDROCARBON COMBUSTION
A generalized polynomial form of the objective function in flash calculations
[AD-A248160] p 3531 N92-29446

HYDROCARBONS
Lab-scale lidar sensing of diesel engines exhausts
p 3464 N92-29276

HYDRODYNAMICS
Statistical mechanics of collective phenomena in plasmas
[AD-A250581] p 3554 N92-29450
The dependence of transport coefficients of suspensions in quasistatic and retarded hydrodynamic interactions
[ETN-92-91624] p 3444 N92-29752
Continuum approaches for describing solid-gas and solid-liquid flow
[DE92-013601] p 3452 N92-30140
Development of renormalization group analysis of turbulence p 3453 N92-30156

HYDROFLUORIC ACID
Corrosion resistance of stainless steels and high Ni-Cr alloys to acid fluoride wastes
[DE92-012338] p 3420 N92-29436

HYDROGEN
Hydrogen desorption and the search for the Higgs
[DE92-013464] p 3545 N92-29507
Heat transfer in an aluminum heat exchanger using normal hydrogen gas
[PB92-172832] p 3447 N92-30036
Growth, characterization, and device development in monocrystalline diamond films
[AD-A248993] p 3560 N92-30175

HYDROGEN IONS
Multiphoton processes in scattering and ionization in an intense linearly-polarized radiation field
[DE92-013546] p 3545 N92-29515

HYDROGEN OXYGEN ENGINES
The development of a fiber optic Raman temperature measurement system for rocket flows
[NASA-CR-189200] p 3413 N92-29448

HYDROGENATION
Hydrogenation reactions of neutral carbon clusters: C(sub n) (n = 6-75) + D(sub 2)
[DE92-005330] p 3417 N92-29459

HYDROGEOLOGY
Final Environmental Impact Statement (EIS) for the Space Nuclear Thermal Propulsion (SNTP) program: Appendices
[AD-A248409] p 3413 N92-29904

HYDROLOGY
Field study of multidimensional flow and transport in the vadose zone
[PB92-161363] p 3489 N92-29701
River hydrometry by pattern recognition in remote sensing images
[PUBL-445] p 3490 N92-29728
Model for regional solute transport suited for calibration and management
[PB92-161371] p 3494 N92-29746

HYDROLYSIS
Microbial aldonolactone formation and hydrolysis: Kinetic and bioenergetic aspects p 3507 N92-29735

HYDROPHONES
Interface board for providing time signals to a super minicomputer
[AD-D015198] p 3441 N92-29900

HYDROXYL COMPOUNDS
Synthesis of a naphthalene-hydroxynaphthalene polymer model compound
[DE92-012264] p 3423 N92-29435

HYPERBOLIC FUNCTIONS
Hyperbolic grid generation control by panel methods
[NLR-TP-91061-U] p 3532 N92-29604

HYPERCUBE MULTIPROCESSORS
An examination of hypercube implementations of genetic algorithms
[AD-A248092] p 3515 N92-29527

HYPERGEOMETRIC FUNCTIONS
Hyperasymptotic expansions of confluent hypergeometric functions
[CWI-AM-R9107] p 3535 N92-29894

HYPERSONIC BOUNDARY LAYER
Linear stability analysis of hypersonic boundary layers
p 3451 N92-30063
Methods for direct simulation of transition in hypersonic boundary layers 2 p 3451 N92-30064
Transition to turbulence in hypersonic flow
p 3454 N92-30161
Crossflow effects on the growth rate of inviscid Goertler vortices in a hypersonic boundary layer
[NASA-CR-189667] p 3455 N92-30190

HYPERSONIC COMBUSTION
Shock enhancement and control of hypersonic combustion
[AD-A248558] p 3418 N92-29580

HYPERSONIC FLIGHT
Aerothermodynamics and propulsion integration in the Saenger technology programme
[MBB-FE-202-S-PUB-0469-A] p 3400 N92-29649

HYPERSONIC FLOW
Hypersonic flow past radiation-cooled surfaces
[MBB-FE-202-S-PUB-0468-A] p 3401 N92-29713
Transition to turbulence in hypersonic flow
p 3454 N92-30161
A numerical method for prediction of compressible turbulent flows with closure models
p 3454 N92-30164
Crossflow effects on the growth rate of inviscid Goertler vortices in a hypersonic boundary layer
[NASA-CR-189667] p 3455 N92-30190

HYPERSONIC HEAT TRANSFER
Hypersonic flow past radiation-cooled surfaces
[MBB-FE-202-S-PUB-0468-A] p 3401 N92-29713

HYPERSONIC VEHICLES
Acquisition of an aerothermodynamic data base by means of a winged experimental reentry vehicle
[MBB/FE202/S/PUB/461] p 3399 N92-30232

HYPERVELOCITY LAUNCHERS
A new HyperVelocity Launcher (HVL) for space science application
[DE92-010670] p 3408 N92-29986

HYSTERESIS
Instantaneous optimal control for linear, nonlinear and hysteretic structures: Stable controllers
[PB92-163807] p 3501 N92-29950

I

ICE
Acoustic scattering from elastic ice: A finite difference solution
[AD-A248281] p 3543 N92-29346
Sound speed, reflectivity, and absorption measurements in Arctic ice in 1988
[AD-A246293] p 3505 N92-29554

ICE CLOUDS
Aerosols and polar stratospheric clouds measurements during the EASOE campaign p 3469 N92-29306
Lidar observations of polar stratospheric clouds and stratospheric temperatures at the South Pole
p 3470 N92-29307
Adaptation of the University of Wisconsin high spectral resolution lidar for polarization and multiple scattering measurements p 3472 N92-29322

IGNITION
Strategies for understanding the deflagration-to-detonation transition
[DE92-013528] p 3427 N92-29512
Flame ignition in a premixed turbulent flow
p 3450 N92-30061

IMAGE ANALYSIS
Image inversion analysis of the HST OTA (Hubble Space Telescope Optical Telescope Assembly), phase A
[NASA-CR-190483] p 3564 N92-29359
Analysis of a three-dimensional point pattern with replication
[CWI-BS-R9124] p 3541 N92-30180

IMAGE FILTERS
Multiresponse imager and imaging process for improved resolution
[NASA-CASE-LAR-14779-1] p 3552 N92-29951

IMAGE PROCESSING
Condenser optics, partial coherence, and imaging for soft x ray projection lithography
[DE92-011762] p 3551 N92-29484
Alexander: User guide (version 1.0)
[BCRS-90-38] p 3489 N92-29494
River hydrometry by pattern recognition in remote sensing images
[PUBL-445] p 3490 N92-29728
Motion restoration of long time exposed images with satellite-borne cameras
[ETN-92-91490] p 3474 N92-29731
Discretization of morphological operators
[CWI-BS-R9118] p 3533 N92-29861
Real-time quadratic shading
[CWI-CS-R9123] p 3534 N92-29892
Multiresponse imager and imaging process for improved resolution
[NASA-CASE-LAR-14779-1] p 3552 N92-29951
Sub-angstrom microscopy through incoherent imaging and image reconstruction
[DE92-011787] p 3475 N92-30090
Analysis of a three-dimensional point pattern with replication
[CWI-BS-R9124] p 3541 N92-30180

IMAGE RECONSTRUCTION
Discretization of morphological operators
[CWI-BS-R9118] p 3533 N92-29861
Sub-angstrom microscopy through incoherent imaging and image reconstruction
[DE92-011787] p 3475 N92-30090

IMAGE RESOLUTION
Improved real-time imaging spectrometer
[NASA-CASE-NPO-18410-1-CU] p 3552 N92-29832
Multiresponse imager and imaging process for improved resolution
[NASA-CASE-LAR-14779-1] p 3552 N92-29951

IMAGING SPECTROMETERS
SeaWiFS technical report series. Volume 1: An overview of SeaWiFS and ocean color
[NASA-TM-104566-VOL-1] p 3505 N92-29686
Improved real-time imaging spectrometer
[NASA-CASE-NPO-18410-1-CU] p 3552 N92-29832

IMAGING TECHNIQUES
Sixteenth International Laser Radar Conference, part 1
[NASA-CP-3158-PT-1] p 3456 N92-29228
Wind profiles derived from volume imaging lidar data: Enhancements to the algorithm and comparisons with insitu observations p 3464 N92-29271
Application of laser imaging for bio/geophysical studies p 3465 N92-29282
Visual acuity with second and third generation night vision goggles obtained from a new method of night sky simulation across a wide range of target contrast
[AD-A248284] p 3512 N92-29348
Structure of a methanol/air coaxial reacting spray near the stabilization region by OH fluorescence imaging and two-component phase-Doppler interferometry
[DE92-005328] p 3417 N92-29431
Condenser optics, partial coherence, and imaging for soft x ray projection lithography
[DE92-011762] p 3551 N92-29484
Efficient complete radiosity ray tracing using a shadow coherence method
[REPT-91-63] p 3518 N92-29749
Real-time quadratic shading
[CWI-CS-R9123] p 3534 N92-29892
Multiresponse imager and imaging process for improved resolution
[NASA-CASE-LAR-14779-1] p 3552 N92-29951
Sub-angstrom microscopy through incoherent imaging and image reconstruction
[DE92-011787] p 3475 N92-30090
Programmable hyperspectral image mapper with on-array processing
[NASA-CASE-NPO-17794-1-CU] p 3553 N92-30104

IMPACT LOADS
Guide for evaluating 12 inch Substantial Dividing Walls (SDWs) to provide protection from remote operation, volume 2
[AD-A250252] p 3428 N92-29335
Guide for evaluating 12 inch Substantial Dividing Walls (SDWs) to provide protection from remote operation, volume 1
[AD-A250251] p 3428 N92-29545

IMPACT TESTS
A new HyperVelocity Launcher (HVL) for space science application
[DE92-010670] p 3408 N92-29986

IMPURITIES
Laser remote sensing of pollution on water surfaces
p 3467 N92-29290
Multichord spectroscopy of the D3-D divertor region
[DE92-013507] p 3554 N92-29412
Zee star analysis
[AD-A248342] p 3417 N92-29423

IN-FLIGHT MONITORING
Support activities to maintain SUMS flight readiness
[NASA-CR-189656-VOL-1] p 3410 N92-30217

INCLUSIONS
Processing and properties of mechanically alloyed sintered steels with hard inclusions
[KFK-4909] p 3422 N92-29651
Method and apparatus for thermographically and quantitatively analyzing a structure for disbonds and/or inclusions
[NASA-CASE-LAR-14559-1] p 3480 N92-29829

INCOHERENT SCATTER RADAR
ARCLITE: The Arctic Lidar Technology Facility at Sondre Stromfjord, Greenland p 3407 N92-29283
INCOMPRESSIBLE FLOW
A method for computing the 3-dimensional flow about wings with leading-edge vortex separation. Part 2: Description of computer program VORSEP
[NLR-TR-86006-U] p 3402 N92-29916
Modeling turbulent boundary layers in adverse pressure gradients p 3449 N92-30053
Large eddy simulations of passive and buoyant scalars with dynamic subgrid-scale models p 3450 N92-30057
Incompressible spatially-developing free-shear flows p 3454 N92-30165
INCONEL (TRADEMARK)
Metal vapor plasma behavior during vacuum arc remelting of alloy 718
[DE92-011761] p 3421 N92-29623
INDEPENDENT VARIABLES
Non-interfering dipaths in planar digraphs
[CWI-BS-R9121] p 3533 N92-29864
INDEXES (DOCUMENTATION)
Aeronautical Engineering Group publications, 1950 - present
[AERO-REPT-8907] p 3444 N92-29683
INDIUM COMPOUNDS
Novel thin-film CuInSe2 fabrication
[DE92-001222] p 3557 N92-29584
INDONESIA
TERS product development plan for urban planning of Bandung, Indonesia
[BCRS-91-30] p 3491 N92-30231
INDUCTION MOTORS
Fuzzy logic control of AC induction motors
[PB92-180207] p 3443 N92-30092
INDUSTRIAL AREAS
Lidar monitoring of Mexico City's atmosphere during high air polution episodes p 3464 N92-29275
Transportable lidar for the measurement of ozone concentration and flux profiles in the lower troposphere p 3465 N92-29278
INDUSTRIAL PLANTS
Thermal energy storage for cogeneration applications
[DE92-012339] p 3492 N92-29646
INDUSTRIES
The 1991 research highlights
[AD-A247865] p 3570 N92-29464
Global standards: Building blocks for the future
[PB92-167352] p 3563 N92-29671
Challenges to NIST in dimensional metrology: The impact of tightening tolerances in the US discrete-part manufacturing industry
[PB92-164680] p 3542 N92-29802
INELASTIC SCATTERING
The O(alpha(s) cubed) QCD correction to the lowest moment of the longitudinal structure function in deep inelastic electron-nucleon scattering
[NIKHEF-H/91-19] p 3546 N92-29750
INEQUALITIES
Gaarding inequalities for systems of pseudo-differential operators
[CWI-AM-R9111] p 3534 N92-29881
INFERENCE
Using custom-designed VLSI fuzzy inferencing chips for the autonomous navigation of a mobile robot
[DE92-000424] p 3528 N92-29550
Accurate procedures for approximate Bayesian and conditional inference without the need for orthogonal parameters
[AD-A248662] p 3539 N92-29718
Data reduction in statistical inference
[MEMO-COSOR-92-03] p 3540 N92-29828
INFORMATION
Modelling, information processing and control
[AD-A250571] p 3532 N92-29589
INFORMATION DISSEMINATION
EOS Data and Information System (EOSDIS) --- landsat satellites
[NASA-TM-107922] p 3488 N92-29442
INFORMATION FLOW
Archives of the future: Archival strategies for the treatment of electronic databases
[PB92-178631] p 3563 N92-30038
INFORMATION MANAGEMENT
NASA visual thesaurus maintenance documentation
[NASA-CR-190282] p 3561 N92-29553
CRIS/USDA online access guide. Revision 1: File 60 on DIALOG
[PB92-172857] p 3562 N92-30033
Archives of the future: Archival strategies for the treatment of electronic databases
[PB92-178631] p 3563 N92-30038
INFORMATION SYSTEMS
The Telecommunications and Data Acquisition Report
[NASA-CR-190460] p 3429 N92-29364
Deep Space Network information system architecture study p 3433 N92-29385
EOS Data and Information System (EOSDIS) --- landsat satellites
[NASA-TM-107922] p 3488 N92-29442
Current information technology resource requirements of the Federal Government: Fiscal year 1992
[PB92-147180] p 3561 N92-29663
Information systems analysis and design based on an object-oriented framework
[MEMO-INF-91-93] p 3519 N92-29816
What is the method in formal methods?
[MEMO-INF-91-79] p 3562 N92-30000
CRIS/USDA online access guide. Revision 1: File 60 on DIALOG
[PB92-172857] p 3562 N92-30033
Archives of the future: Archival strategies for the treatment of electronic databases
[PB92-178631] p 3563 N92-30038
INFORMATION THEORY
Golay and other box codes p 3431 N92-29375
INFRARED ABSORPTION
Infrared pulse-laser long-path absorption measurement of carbon dioxide using a Raman-shifted dye laser p 3465 N92-29277
Electrical, optical, and magnetic resonance studies of novel pi-conjugated polymers
[DE92-012548] p 3424 N92-29482
INFRARED ASTRONOMY
Studies of distant clusters of galaxies p 3566 N92-29843
INFRARED DETECTORS
OMVPE growth of InAsSbBi and related alloys using new organometallic group 5 sources
[AD-A250631] p 3557 N92-29635
INFRARED RADIATION
Intercomparisons of lidar backscatter measurements and in-situ data from GLOBE p 3463 N92-29266
High Intensity Source Laboratory (HISL)
[DE92-011173] p 3549 N92-29457
Modulated high sensitivity infrared polarimeter
[AD-D015256] p 3474 N92-29571
The 12 micron contribution of nearby galaxies to the infrared background
[AD-A250623] p 3565 N92-29596
Improved real-time imaging spectrometer
[NASA-CASE-NPO-18410-1-CU] p 3552 N92-29832
INFRARED SPECTROSCOPY
A study of the adsorption of acetonitrile on a gold electrode from aqueous solutions using in situ vibrational spectroscopy
[AD-A250191] p 3417 N92-29514
Vibrational spectrum and structure of 1,2-dimethyl-1,2-disila-closo-dodecaborane
[AD-A250235] p 3419 N92-29941
INFRARED STARS
The 12 micron contribution of nearby galaxies to the infrared background
[AD-A250623] p 3565 N92-29596
INFRARED TELESCOPES
United Kingdom Infrared Telescope
[ETN-92-91341] p 3565 N92-29682
INLET FLOW
Experimental examination of heavy loaded axial fans with rotational symmetrical distortion of the inflow
[ETN-92-91489] p 3445 N92-29926
INPUT/OUTPUT ROUTINES
Multitype branching processes in M/G/1-queueing theory p 3530 N92-29966
INSECTS
Mosquito Lagoon environmental resources inventory
[NASA-TM-107548] p 3492 N92-29430
INSPECTION
Federal Aviation Administration aging aircraft nondestructive inspection research plan p 3481 N92-30116
Inspection of aging aircraft: A manufacturer's perspective p 3481 N92-30117
NDE research efforts at the FAA Center for Aviation Systems Reliability p 3481 N92-30119
Aging aircraft NDI Development and Demonstration Center (AANC): An overview --- nondestructive inspection p 3481 N92-30120
Nondestructive inspection perspectives p 3481 N92-30121
Ageing airplane repair assessment program for Airbus A300 p 3402 N92-30123
Human factors in aircraft maintenance and inspection p 3487 N92-30125
Survey of French activities concerning structural airworthiness and aging aircraft p 3402 N92-30130
Aging commuter aeroplanes: Fatigue evaluation and control methods p 3488 N92-30132
INSTITUTIONS
A soft stairway to institutions
[MEMO-INF-91-87] p 3522 N92-29981
INSTRUCTORS
The effects of student-instructor interaction and paired/individual study on achievement in computer-based training
[AD-A248518] p 3511 N92-29503
INSULATORS
A novel approach to silicon-on-insulator materials
[AD-A248074] p 3424 N92-29466
INTEGERS
Constraint classification for mixed integer programming formulations
[MEMO-COSOR-91-30] p 3516 N92-29608
INTEGRAL EQUATIONS
On the numerical solution of one-dimensional integral and differential equations
[AD-A250388] p 3531 N92-29548
Solving parabolic integro-differential equations by an explicit integration method
[CWI-NM-R9108] p 3534 N92-29883
Hyperasymptotic expansions of confluent hypergeometric functions
[CWI-AM-R9107] p 3535 N92-29894
Diffusion approximation of stochastic integral functionals of jump Markov processes
[CWI-AM-R9108] p 3535 N92-29895
Diffusion approximation of stochastic additive functionals of jump Markov processes
[CWI-AM-R9110] p 3535 N92-29896
Confining potential in momentum space p 3548 N92-30007
INTEGRATED CIRCUITS
Experimental evaluation of incorporating digital and analog integrated circuit die on a common substrate utilizing silicon-hybrid wafer-scale integration technology
[AD-A248182] p 3439 N92-29405
Monolithic integration of semiconductor and superconductor components
[AD-A245351] p 3557 N92-29583
B(exp 2)UBIST: A strategy for boundary scan board unified BIST
[IMAG-RR-862-I] p 3441 N92-29612
Robotic workcell for wire wrapping integrated circuits
[DE92-013999] p 3441 N92-29796
Design guidelines for capability approval of film hybrid microcircuits and Microwave Hybrid Integrated Circuits (MHICs)
[ESA-PSS-01-610-ISSUE-1] p 3441 N92-29854
Optoelectronic integration
[AD-A248950] p 3442 N92-29936
INTERACTIONS
Non-linear interactions in homogeneous turbulence with and without background rotation p 3448 N92-30044
INTERCALATION
LiMoN2: The first metallic layered nitride
[AD-A248446] p 3418 N92-29619
INTERCONTINENTAL BALLISTIC MISSILES
A sensitivity analysis of circular error probable approximation techniques
[AD-A248105] p 3539 N92-29585
INTERFACES
Amorphization along interfaces and grain boundaries in polycrystalline multilayers: An x ray diffraction study of Ni/Ti multilayers p 3558 N92-29769
Interface board for providing time signals to a super minicomputer
[AD-D015198] p 3441 N92-29900
A method for analysing the performance aspects of the fault-tolerance mechanisms in FDDI
[MEMO-INF-91-92] p 3514 N92-29982
INTERFACIAL TENSION
Growth, characterization, and device development in monocrystalline diamond films
[AD-A248993] p 3560 N92-30175
INTERFEROMETERS
Experimental and theoretical research in applied plasma physics
[DE92-013587] p 3553 N92-29336
Femtosecond studies of carrier dynamics in compound semiconductors
[AD-A250584] p 3439 N92-29452
Study of optical techniques for the Ames unitary wind tunnels. Part 3: Angle of attack
[NASA-CR-190541] p 3406 N92-29655
Short wavelength interferometer for ITER
[DE92-013008] p 3474 N92-29942
INTERFEROMETRY
Orbiter-orbiter and orbiter-lander tracking using same-beam interferometry p 3409 N92-29369
Short wavelength interferometer for ITER
[DE92-013008] p 3474 N92-29942
INTERGRANULAR CORROSION
Irradiation effects on the electrochemistry and corrosion resistance of stainless steel
[DE92-013504] p 3420 N92-29411

INTERLAMINAR STRESS
An interlaminar tension strength specimen
[NASA-TM-107623] p 3481 N92-29393
INTERNAL COMBUSTION ENGINES
Lab-scale lidar sensing of diesel engines exhausts
p 3464 N92-29276
INTERNATIONAL COOPERATION
Combined summaries: Technologies to sustain tropical forest resources and biological diversity
[OTA-F-515] p 3492 N92-29416
World Administrative Radio Conference. Issues for US International Spectrum Policy
[PB92-157601] p 3435 N92-29696
Fourth Meeting of the Space Agency Forum on the International Space Year (SAFISY-4)
[ESA-SP-1141] p 3407 N92-29879
INTERPLANETARY SPACECRAFT
A determination of the radio-planetary frame tie from comparison of Earth orientation parameters
p 3409 N92-29365
INTERPLANETARY TRAJECTORIES
Galileo early cruise, including Venus, first Earth, and Gaspra encounters p 3433 N92-29384
INTERPOLATION
Construction of a VC1 interpolant over triangles via edge deletion
[MEMO-988] p 3533 N92-29858
INTERPROCESSOR COMMUNICATION
An OSI architecture for the Deep Space Network
p 3432 N92-29380
Application of VME-technology on an airborne data link processor unit
[NLR-MP-88040-U] p 3403 N92-29615
Methodology for the specification of communication activities within the framework of a multi-layered architecture: Toward the definition of a knowledge base
[LAAS-91466] p 3436 N92-29730
A new heuristic for load-balanced assignment of objects and minimized network communication in distributed programs implemented through inverse remote procedure calls
[MEMO-INF-91-91] p 3519 N92-29815
Cislan-2 final document by University of Twente (Netherlands)
[MEMO-INF-91-81] p 3526 N92-29958
A case study in functional real-time programming
[MEMO-INF-91-62] p 3522 N92-30073
Term rewriting analysis in process algebra
[CWI-CS-R9130] p 3537 N92-30177
INTERSTELLAR MATTER
A study of shock-associated magnetohydrodynamic waves in the solar wind
[NASA-CR-190567] p 3569 N92-29631
INTERVALS
Nonparametric maximum likelihood estimators for interval censoring and deconvolution
[REPT-91-53] p 3539 N92-29626
INTRUSION
Reliable processing of confidential data by means of fragmentation-redundancy-scattering
[LAAS-91412] p 3526 N92-29888
INVARIANCE
Data reduction in statistical inference
[MEMO-COSOR-92-03] p 3540 N92-29828
INVENTORIES
Archives of the future: Archival strategies for the treatment of electronic databases
[PB92-178631] p 3563 N92-30038
INVENTORY MANAGEMENT
The capacitated multi-echelon inventory system with serial structure: 1: The push ahead-effect
[MEMO-COSOR-91-39] p 3561 N92-29822
The capacitated multi-echelon inventory system with serial structure: 2: An average cost approximation method
[MEMO-COSOR-91-40] p 3561 N92-29823
INVERSE SCATTERING
On the parity of fundamental solutions for one-dimensional scattering problem with inverse square potential
[DE92-624511] p 3560 N92-29533
SOLITON
[USIP-90-09] p 3518 N92-29714
Estimation of the inverse acoustic transmission operator of a heterogeneous region directly from its reflection operator
[REPT-91-36] p 3544 N92-29918
INVERSIONS
Image inversion analysis of the HST OTA (Hubble Space Telescope Optical Telescope Assembly), phase A
[NASA-CR-190483] p 3564 N92-29359
INVISCID FLOW
A comparison of the calculated and experimental off-design performance of a radial flow turbine
[NASA-CR-189207] p 3399 N92-29402
Streamwise vortices in heated boundary layers
[NASA-CR-189661] p 3444 N92-29692
Progress toward identification of streamwise vorticity meander in a plane mixing layer p 3451 N92-30068
Crossflow effects on the growth rate of inviscid Goertler vortices in a hypersonic boundary layer
[NASA-CR-189667] p 3455 N92-30190
ION ACCELERATORS
Relativistic Coulomb fission p 3548 N92-30008
ION ATOM INTERACTIONS
Correlated charge-changing ion-atom collisions
[DE92-013473] p 3546 N92-29642
ION BEAMS
Neutralizer and sample chamber for the Atomic Oxygen Simulation System (AOSS)
[NASA-CR-184343] p 3407 N92-29664
ION EMISSION
Logion: The operation of liquid metal ion emitters under weightlessness
[OEFZS-4616] p 3428 N92-29470
ION ENGINES
Electrostatic ion thruster optics calculations
[DE92-006608] p 3413 N92-29461
ION EXCHANGING
The comparative effects of gamma radiation and in situ alpha particles on five strong-base anion exchange resins
[DE92-000177] p 3425 N92-29643
ION IMPLANTATION
Study and realization of GaAs PNP homojunction bipolar transistors using ion implementation
[LAAS-91433] p 3441 N92-29729
ION MICROSCOPES
Migmas/A: Test of a scanning ion microscope on the Soviet Space Station Mir
[OEFZS-4615] p 3473 N92-29469
ION PROPULSION
Electrostatic ion thruster optics calculations
[DE92-006608] p 3413 N92-29461
ION RECOMBINATION
Ion collision effects in hydrogen-like recombination x ray lasers
[DE92-013515] p 3476 N92-29509
ION SOURCES
Numerical analysis of plasma transport in tandem volume magnetic multicusp ion sources
[AD-A248093] p 3554 N92-29528
ION TEMPERATURE
Numerical analysis of plasma transport in tandem volume magnetic multicusp ion sources
[AD-A248093] p 3554 N92-29528
IONIC COLLISIONS
Ion collision effects in hydrogen-like recombination x ray lasers
[DE92-013515] p 3476 N92-29509
Correlated charge-changing ion-atom collisions
[DE92-013473] p 3546 N92-29642
IONIZATION
Multiphoton processes in scattering and ionization in an intense linearly-polarized radiation field
[DE92-013546] p 3545 N92-29515
The expanding plasma jet: Experiments and model
[ETN-92-91627] p 3555 N92-29761
IONIZATION POTENTIALS
Hydrogenation reactions of neutral carbon clusters: C(sub n) (n = 6-75) + D(sub 2)
[DE92-005330] p 3417 N92-29459
IONIZING RADIATION
Effects of ionizing radiation on auditory and visual thresholds
[AD-A248199] p 3507 N92-29410
IONOSPHERES
Analysis of EUV dayglow spectra of Triton, Titan and Earth
[NASA-CR-190586] p 3568 N92-29451
IONS
Rare gas clusters containing charged atoms
[AD-A248299] p 3544 N92-29350
Free ion yields in liquids: Molecular structure and track effects
[DE92-012208] p 3545 N92-29582
IRON
Lidar probing of the mesosphere: Simultaneous observations of sporadic sodium and iron formations, calcium ion layers, neutral temperature and winds
p 3470 N92-29311
Lidar measurements of metallic species in mesopause region p 3470 N92-29312
Material-deposition processes in the separator of Li-alloy/FeS2 thermal cells
[DE92-013669] p 3440 N92-29518
IRON COMPOUNDS
Material-deposition processes in the separator of Li-alloy/FeS2 thermal cells
[DE92-013669] p 3440 N92-29518
Process of ferrochromium now and in the future
[DE92-506510] p 3421 N92-29637
IRRADIATION
Irradiation effects on the electrochemistry and corrosion resistance of stainless steel
[DE92-013504] p 3420 N92-29411
Surface reactions in the space environment
[AD-A250624] p 3428 N92-29428
Hydrogenation reactions of neutral carbon clusters: C(sub n) (n = 6-75) + D(sub 2)
[DE92-005330] p 3417 N92-29459
ISOLATION
Active thermal isolation for temperature responsive sensors
[NASA-CASE-LAR-14612-1] p 3446 N92-29954
ISOLATORS
Active thermal isolation for temperature responsive sensors
[NASA-CASE-LAR-14612-1] p 3446 N92-29954
ISOMORPHISM
Molecular engineering of liquid crystalline polymers
[AD-A248996] p 3427 N92-30136
ISOTHERMAL PROCESSES
A study and feasibility of ultra thin silica layers by rapid thermal processing
[LAAS-91393] p 3422 N92-29674
ISOTROPIC TURBULENCE
A finite volume approach to large eddy simulation of compressible, homogeneous, isotropic, decaying turbulence
[MEMO-1009] p 3446 N92-29972
A preliminary experimental investigation of local isotropy in high-Reynolds-number turbulence
p 3447 N92-30042
Local isotropy in buoyancy-generated turbulence
p 3447 N92-30043
Lagrangian velocity correlation and spectrum in homogeneous isotropic turbulence p 3448 N92-30047
Single point modeling of initially isotropic turbulence under uniform rotation p 3449 N92-30054
An experimental study of the effects of rapid rotation on turbulence p 3453 N92-30154
Development of renormalization group analysis of turbulence p 3453 N92-30156
Turbulence dynamics in the wavelet representation
p 3454 N92-30159
ITERATION
A closer look at a Fibonacci-like iterated nonlinear map: More chaos and order
[MEMO-INF-91-70] p 3537 N92-30075
ITERATIVE SOLUTION
ISLAND: Interactive Solution Language for an Adaptive NIKE Driver
[DE92-011444] p 3533 N92-29791
Solution strategies for implicit nonlinear finite element analysis
[DE92-011466] p 3533 N92-29792
A two-stage estimator for generalized linear models with nonconstant dispersion parameter
[MEMO-1012] p 3540 N92-29975

J

JET AIRCRAFT NOISE
Jet aircraft noise at high subsonic flight Mach numbers
[DLR-FB-91-28] p 3544 N92-29997
JET FLOW
On transient flamelets and their relationship to turbulent methane-air jet flames
[DE92-006705] p 3419 N92-29943
Direct numerical simulation of instability and noise generation of hot jets p 3451 N92-30066
JOINTS (JUNCTIONS)
Bladder operated robotic joint
[NASA-CASE-MFS-28682-1] p 3426 N92-29831
On fictitious joints modelling of manipulator link flexibility for the HERA simulation facility pilot
[NLR-TR-88086-U] p 3479 N92-29885
JUNCTION DIODES
Simulations on the electrical characteristics of Si, SiC and diamond junction and Schottky power diodes
[PB92-177872] p 3443 N92-30094
JUPITER (PLANET)
A nanoradian differential VLBI tracking demonstration
p 3430 N92-29367

K

K-EPSILON TURBULENCE MODEL
Analyses and modeling of evolving turbulent flow
p 3449 N92-30051
Derivation of the kappa-epsilon model equations using the renormalization group method p 3450 N92-30055

Turbulence modeling: Near-wall turbulence and effects of rotation on turbulence p 3452 N92-30151
Development of renormalization group analysis of turbulence p 3453 N92-30156

KANSAS
Raman lidar measurements of Pinatubo aerosols over southeastern Kansas during November-December 1991 p 3457 N92-29233

KERNEL FUNCTIONS
On constructing kernel polynomials of a spectral function: Application to ARMA models
[CWI-BS-R9119] p 3533 N92-29862

KILOMETRIC WAVES
Source location determination of Uranian kilometric radiation from ray tracing and emission lobe modelling
[NASA-CR-190482] p 3570 N92-29360

KINEMATICS
ARTIBODIES: A system for modelling articulated bodies
[REPT-91-57] p 3517 N92-29627
Robust adaptive kinematic control of redundant robots
[NASA-CR-190520] p 3528 N92-29673

KINETIC ENERGY
Feasibility of an antiproton catalyzed fission fragment rocket
[AD-A248157] p 3412 N92-29444
Turbulence and vortex structures p 3448 N92-30048
Turbulence dynamics in the wavelet representation p 3454 N92-30159

KINETIC EQUATIONS
Microbial aldonolactone formation and hydrolysis: Kinetic and bioenergetic aspects p 3507 N92-29735

KINETICS
Multi-fractal analysis of nocturnal boundary layer time series from the Boulder Atmospheric Observatory
[AD-A248347] p 3502 N92-29424
Statistical mechanics of collective phenomena in plasmas
[AD-A250581] p 3554 N92-29450
Theoretical/experimental investigations of the structure and dynamics of highly energetic dication species
[AD-A247050] p 3418 N92-29901
Electrochemistry in colloids and dispersions. Volume 3: Colloidal semiconductors
[AD-A248337] p 3419 N92-29932

KLYSTRONS
Improvements in X-band transmitter phase stability through klystron body temperature regulation p 3431 N92-29373

KNOWLEDGE BASES (ARTIFICIAL INTELLIGENCE)
Methodology for the specification of communication activities within the framework of a multi-layered architecture: Toward the definition of a knowledge base
[LAAS-91466] p 3436 N92-29730

KNOWLEDGE REPRESENTATION
An ontology of ceramics
[MEMO-INF-91-85] p 3426 N92-29960

KOLMOGOROFF THEORY
Non-linear interactions in homogeneous turbulence with and without background rotation p 3448 N92-30044
Lagrangian velocity correlation and spectrum in homogeneous isotropic turbulence p 3448 N92-30047

L

LABORATORIES
High Intensity Source Laboratory (HISL)
[DE92-011173] p 3549 N92-29457
Physics Laboratory technical activities, 1991
[PB92-172824] p 3542 N92-30035

LAGOONS
Mosquito Lagoon environmental resources inventory
[NASA-TM-107548] p 3492 N92-29430

LAMINAR FLOW
On transient flamelets and their relationship to turbulent methane-air jet flames
[DE92-006705] p 3419 N92-29943
Active thermal isolation for temperature responsive sensors
[NASA-CASE-LAR-14612-1] p 3446 N92-29954
Transition to turbulence in hypersonic flow p 3454 N92-30161

LAMINATES
An interlaminar tension strength specimen
[NASA-TM-107623] p 3481 N92-29393
A consistent shear deformable theory for laminated plates
[AD-A250591] p 3415 N92-29593
Variational formulation and finite element implementation of Pagano's theory of laminated plates
[AD-A250592] p 3415 N92-29594
Manufacturing of components of fibre-metal laminates: An overview
[LR-670] p 3415 N92-29702
Layer-thickness variations and x ray diffraction patterns, a general treatment p 3558 N92-29767
Low-angle x ray diffraction study of solid state amorphization in a Ni/Ti multilayer p 3558 N92-29768
Method and apparatus for thermographically and quantitatively analyzing a structure for disbonds and/or inclusions
[NASA-CASE-LAR-14559-1] p 3480 N92-29829
Repair procedures for advanced composites for helicopters
[MBB-UD-0606-91-PUB] p 3399 N92-29874
An approximate solution for interlaminar stresses in laminated composites: Applied mechanics program
[NASA-CR-190537] p 3416 N92-30208

LAND USE
Mosquito Lagoon environmental resources inventory
[NASA-TM-107548] p 3492 N92-29430
Research programming studies: Remote sensing emissions, land use and effects, in relation to climate and environment
[BCRS-91-17] p 3493 N92-29497
Final Environmental Impact Statement (EIS) for the Space Nuclear Thermal Propulsion (SNTP) program
[AD-A248408] p 3413 N92-29903
Final Environmental Impact Statement (EIS) for the Space Nuclear Thermal Propulsion (SNTP) program: Appendices
[AD-A248409] p 3413 N92-29904

LANDSAT SATELLITES
EOS Data and Information System (EOSDIS) --- landsat satellites
[NASA-TM-107922] p 3488 N92-29442

LANGUAGE PROGRAMMING
Implementation of the object-oriented data model TM
[MEMO-INF-91-94] p 3520 N92-29855
CCS for OO and LP
[CWI-CS-R9136] p 3522 N92-29992
Proof theory for micro CRL
[CWI-CS-R9138] p 3522 N92-29994

LAP JOINTS
Preliminary results on the fracture analysis of multi-site cracking of lap joints in aircraft skins p 3484 N92-30111
Thermal QNDE detection of airframe disbonds p 3481 N92-30118

LARGE APERTURE SEISMIC ARRAY
Land-based seismic array studies of low frequency ambient oceanic noise
[AD-A248255] p 3505 N92-29618

LARGE SPACE STRUCTURES
Spacecraft dynamics characterization and control system failure detection, volume 1
[NASA-CR-190517] p 3409 N92-29422

LASER APPLICATIONS
Development of mesospheric sodium laser beacon for atmospheric adaptive optics p 3470 N92-29308
Characterization of artificial guidestars generated in the mesospheric sodium layer p 3470 N92-29309
Optical pumping of mesospheric sodium: A new measurement capability p 3470 N92-29310
Lidar probing of the mesosphere: Simultaneous observations of sporadic sodium and iron formations, calcium ion layers, neutral temperature and winds p 3470 N92-29311
Lidar measurements of metallic species in mesopause region p 3470 N92-29312
Lidar studies of clouds at Toronto during the ECLIPS program p 3472 N92-29321
Diode-pumped Nd:YAG lidar for airborne cloud measurements p 3473 N92-29326
Laser-induced desorption from sapphire surfaces
[DE92-012698] p 3475 N92-29340
Review of potential x ray laser applications in materials science and chemistry
[DE92-012254] p 3475 N92-29434
X ray laser research at the Nova laser
[DE92-012695] p 3476 N92-29472
Laser processing for interconnect technology
[AD-A248103] p 3476 N92-29559
Study of optical techniques for the Ames unitary wind tunnels. Part 3: Angle of attack
[NASA-CR-190541] p 3406 N92-29655

LASER BEAMS
Laser-induced desorption from sapphire surfaces
[DE92-012698] p 3475 N92-29340
Modulated high sensitivity infrared polarimeter
[AD-D015256] p 3474 N92-29571
The x ray laser coherence experiments in neon-like yttrium
[DE92-010714] p 3477 N92-29987
Sample positioning in microgravity
[NASA-CASE-NPO-18448-1-CU] p 3428 N92-30083

LASER CUTTING
Preliminary cutting and drilling studies using new generation lasers
[DE92-010712] p 3477 N92-29787

LASER DOPPLER VELOCIMETERS
Laboratory velocimeter measurements using the edge technique p 3463 N92-29269

LASER DRILLING
Preliminary cutting and drilling studies using new generation lasers
[DE92-010712] p 3477 N92-29787

LASER FUSION
LLE review
[DE92-011614] p 3555 N92-30072

LASER INDUCED FLUORESCENCE
Lidar tracking of multiple fluorescent tracers: Method and field test p 3464 N92-29274
Remote detection of biological particles and chemical plumes using UV fluorescence lidar p 3465 N92-29279
In vivo and in vitro chlorophyll-a and pheophytin-a concentration measurements by laser fluorometry p 3468 N92-29295

LASER OUTPUTS
System testing and performance characterization of the LITE Laser Transmitter Module at NASA p 3469 N92-29302
Laser diode end-pumped Nd:YAG laser
[AD-A248123] p 3475 N92-29396

LASER PLASMAS
Review of potential x ray laser applications in materials science and chemistry
[DE92-012254] p 3475 N92-29434
High Intensity Source Laboratory (HISL)
[DE92-011173] p 3549 N92-29457
X ray laser research at the Nova laser
[DE92-012695] p 3476 N92-29472
X ray streak camera diagnostics of picosecond laser-plasma interactions
[DE92-011371] p 3555 N92-29789
Estimating plasma temperatures
[DE92-014092] p 3555 N92-29798
LLE review
[DE92-011614] p 3555 N92-30072

LASER PUMPING
Optical pumping of mesospheric sodium: A new measurement capability p 3470 N92-29310
Laser diode end-pumped Nd:YAG laser
[AD-A248123] p 3475 N92-29396
X ray laser research at the Nova laser
[DE92-012695] p 3476 N92-29472

LASER RANGE FINDERS
Turbulence effects on the geodynamic laser ranging system
[PB92-166404] p 3477 N92-29948

LASER SPECTROSCOPY
Infrared pulse-laser long-path absorption measurement of carbon dioxide using a Raman-shifted dye laser p 3465 N92-29277

LASER TARGETS
LLE review
[DE92-011614] p 3555 N92-30072

LASER WEAPONS
Burros: Simple, affordable, effective space transportation
[DE92-013553] p 3541 N92-30138

LASER WELDING
Preliminary cutting and drilling studies using new generation lasers
[DE92-010712] p 3477 N92-29787

LASERS
Signal quality influence on averaging procedure for DIAL pollution monitoring p 3465 N92-29280
Application of laser imaging for bio/geophysical studies p 3465 N92-29282
Efficiencies of rotational Raman and Rayleigh techniques for laser remote sensing of the atmospheric temperature p 3467 N92-29288
Laser remote sensing of pollution on water surfaces p 3467 N92-29290
In vivo and in vitro chlorophyll-a and pheophytin-a concentration measurements by laser fluorometry p 3468 N92-29295
GE's mobile, coherent Doppler lidar test/evaluation facilities p 3407 N92-29299
A wave theory for non-imaging concentrators
[AD-A248865] p 3552 N92-29726
Short wavelength interferometer for ITER
[DE92-013008] p 3474 N92-29942
Laser etching: Possibilities and problems
[DE92-010800] p 3477 N92-30135

LATENT HEAT
Sensitivity of C2 sub n to random variations of windspeed, sensible heat flux, and latent heat flux
[AD-A248696] p 3502 N92-29565

LEADING EDGES
A method for computing the 3-dimensional flow about wings with leading-edge vortex separation. Part 2: Description of computer program VORSEP
[NLR-TR-86006-U] p 3402 N92-29916

LEAF AREA INDEX
Biophysical, morphological, canopy optical property, and productivity data from the Superior National Forest
[NASA-TM-104568] p 3491 N92-30210
LEARNING
Linear approximation of shortest superstrings
[CWI-CS-R9126] p 3523 N92-30146
LEARNING THEORY
The cognitive function of theoretical knowledge in procedural learning
[AD-A248075] p 3531 N92-29486
LEAST SQUARES METHOD
Statistics of narrowband white noise derived from clipped broadband white noise
[AD-A248597] p 3434 N92-29563
LEBESGUE THEOREM
Spectral type of Ornstein's class one transformations
[PB92-178292] p 3537 N92-30096
LENGTH
The effect of length variation on the stability of circular cylindrical shells under pure bending
[LR-669] p 3482 N92-29700
LENSES
Polarization perception device
[NASA-CASE-MSC-21915-1] p 3552 N92-30027
LIAPUNOV FUNCTIONS
Numerical procedures for analyzing dynamical processes
[AD-A248175] p 3515 N92-29399
Short-time Lyapunov exponent analysis
p 3453 N92-30157
LIBRARIES
ASV3 dial-in interface recommendation for the Repository Based Software Engineering (RBSE) program
[NASA-CR-190500] p 3514 N92-29362
LIFE RAFTS
Evaluation of Night Vision Goggles (NVG) for maritime search and rescue
[AD-A247182] p 3512 N92-29538
LIFE SCIENCES
Molecular engineering of liquid crystalline polymers by living polymerization. 19: Synthesis and characterization of poly 2-(4-biphenyloxy)ethyl vinyl etherby
[AD-A248285] p 3423 N92-29349
LIFT
Development of models for prediction of optimal lifting motion
[PB92-164656] p 3513 N92-29949
Experimental investigation of the flowfield of an oscillating airfoil
[NASA-TM-105675] p 3402 N92-30182
LIGANDS
Solid state structures of some Dithionoamido-18-crown-6 ligands
[AD-A248098] p 3556 N92-29558
LIGHT ALLOYS
NASA-UVA light aerospace alloy and structures technology program (LA2ST)
[NASA-CR-190538] p 3423 N92-30206
LIGHT BEAMS
Electrostatic ion thruster optics calculations
[DE92-006608] p 3413 N92-29461
Transition crossing in the RHIC
[DE92-013031] p 3550 N92-29475
LIGHT EMISSION
Ocean optical modeling: Light field structure, internal radiant emission, and vertical inhomogeneities
[AD-A248272] p 3504 N92-29345
LIGHT GAS GUNS
A new HyperVelocity Launcher (HVL) for space science application
[DE92-010670] p 3408 N92-29986
LIGHT SCATTERING
Extraction of aerosol and Rayleigh components from Doppler lidar return signal p 3465 N92-29281
Ocean optical modeling: Light field structure, internal radiant emission, and vertical inhomogeneities
[AD-A248272] p 3504 N92-29345
Diffraction of light from randomly rough surfaces
[AD-A250261] p 3551 N92-29546
LIGHT SOURCES
A wave theory for non-imaging concentrators
[AD-A248865] p 3552 N92-29726
LIGHT TRANSMISSION
Diffraction of light from randomly rough surfaces
[AD-A250261] p 3551 N92-29546
Polarization perception device
[NASA-CASE-MSC-21915-1] p 3552 N92-30027
Evaluation of an aureole lidar technique for estimating extinction profiles
[AD-A249740] p 3501 N92-30087
LIKELIHOOD RATIO
Accurate procedures for approximate Bayesian and conditional inference without the need for orthogonal parameters
[AD-A248662] p 3539 N92-29718
Testing equality of variances in the analysis of repeated measurements
[MEMO-1013] p 3541 N92-29976
LIMITER CIRCUITS
RF vacuum electronics
[AD-A248857] p 3442 N92-29935
LIMITS (MATHEMATICS)
Limit theorems for cumulative processes
[AD-A248507] p 3538 N92-29500
Limit theorems for functionals of convex hulls
[REPT-91-39] p 3535 N92-29921
LINEAR ACCELERATORS
Transverse wakefields at high dispersion
[DE92-010752] p 3550 N92-29788
LINEAR EQUATIONS
D-optimal designs for an incomplete quadratic model
[MEMO-COSOR-91-26] p 3532 N92-29742
Abstract quasilinear equations and application to a groundwater flow problem
[REPT-91-41] p 3535 N92-29923
LINEAR FILTERS
Motion restoration of long time exposed images with satellite-borne cameras
[ETN-92-91490] p 3474 N92-29731
LINEAR PROGRAMMING
Optimization of stochastic response surfaces subject to constraints with linear programming
[AD-A248108] p 3516 N92-29586
Separable Markovian decision problems: The linear programming method in the multichain case (revised)
[PB92-187350] p 3524 N92-30201
A monotonic build-up simplex algorithm for linear programming
[REPT-91-82] p 3524 N92-30227
LINEAR QUADRATIC REGULATOR
Sequential design of a linear quadratic controller for the Deep Space Network antennas p 3432 N92-29382
LINEAR SYSTEMS
Linear relations in microbial reaction systems: A general overview of their origin, form, and use
p 3507 N92-29733
Instantaneous optimal control for linear, nonlinear and hysteretic structures: Stable controllers
[PB92-163807] p 3501 N92-29950
Linear approximation of shortest superstrings
[CWI-CS-R9126] p 3523 N92-30146
Linear system identification via backward-time observer models
[NASA-TM-107632] p 3488 N92-30214
A parallel restructured version of GMRES(m)
[REPT-91-85] p 3527 N92-30229
LINEARIZATION
Positive convolution structures associated with quantum groups
[CWI-AM-R9105] p 3534 N92-29866
LIPIDS
Structure and shear response of lipid monolayers
[DE92-011633] p 3542 N92-29354
LIQUID CRYSTALS
Molecular engineering of liquid crystalline polymers by living polymerization. 19: Synthesis and characterization of poly 2-(4-biphenyloxy)ethyl vinyl etherby
[AD-A248285] p 3423 N92-29349
Molecular engineering of side chain liquid crystalline polymers
[AD-A248540] p 3424 N92-29508
Molecular engineering of liquid crystalline polymers by living polymerization. 20: Synthesis and characterization of binary copolymers of 11-(4-cyano-4'-biphenyl) oxy)undecanyl vinyl ether with n-butyl vinyl ether and of 2-(4-cyano-4'-biphenyl) oxy)ethyl vinyl ether with n-butyl vinyl ether
[AD-A248286] p 3425 N92-29566
Molecular engineering of liquid crystalline polymers by living polymerization. 22: Synthesis and characterization of binary copolymers
[AD-A248287] p 3425 N92-29567
Molecular engineering of liquid crystalline polymers
[AD-A248996] p 3427 N92-30136
LIQUID HELIUM 2
Vorticity matching in superfluid helium
p 3449 N92-30049
LIQUID METALS
Logion: The operation of liquid metal ion emitters under weightlessness
[OEFZS-4616] p 3428 N92-29470
LIQUID PHASES
A generalized polynomial form of the objective function in flash calculations
[AD-A248160] p 3531 N92-29446
LIQUID SLOSHING
Pressurization of cryogens: A review of current technology and its applicability to low-gravity conditions
[NASA-TM-105746] p 3427 N92-29669
LIQUIDS
Continuum approaches for describing solid-gas and solid-liquid flow
[DE92-013601] p 3452 N92-30140
LITHIUM
Advanced rechargeable lithium sulfur dioxide cell
[AD-A250027] p 3491 N92-29476
Material-deposition processes in the separator of Li-alloy/FeS2 thermal cells
[DE92-013669] p 3440 N92-29518
LiMoN2: The first metallic layered nitride
[AD-A248446] p 3418 N92-29619
LITHIUM CHLORIDES
New directions for the catalytic conversion of methane
[PB92-172360] p 3492 N92-29519
LITHIUM COMPOUNDS
Material-deposition processes in the separator of Li-alloy/FeS2 thermal cells
[DE92-013669] p 3440 N92-29518
LITHIUM SULFUR BATTERIES
Li/SO2 cells and Li/SOCl2 cells: Safe use and testing
[DE92-013508] p 3439 N92-29414
LITHOGRAPHY
Condenser optics, partial coherence, and imaging for soft x ray projection lithography
[DE92-011762] p 3551 N92-29484
LITHOLOGY
Lexicon of new formal geologic names of the United States, 1981-1985
[PB92-181320] p 3563 N92-30040
LOAD TESTING MACHINES
Apparatus for elevated temperature compression or tension testing of specimens
[NASA-CASE-LAR-14775-1] p 3483 N92-30099
LOAD TESTS
Combined load test apparatus for flat panels
[NASA-CASE-LAR-14698-1] p 3483 N92-30028
Apparatus for elevated temperature compression or tension testing of specimens
[NASA-CASE-LAR-14775-1] p 3483 N92-30099
LOADS (FORCES)
Combined load test apparatus for flat panels
[NASA-CASE-LAR-14698-1] p 3483 N92-30028
An approximate solution for interlaminar stresses in laminated composites: Applied mechanics program
[NASA-CR-190537] p 3416 N92-30208
National Launch System cycle 1 loads and models data book
[NASA-TM-103560] p 3408 N92-30215
LOCAL AREA NETWORKS
Measuring and simulating an 802.3 CSMA/CD LAN
[MEMO-COSOR-91-42] p 3525 N92-29825
Cislan-2 final document by University of Twente (Netherlands)
[MEMO-INF-91-81] p 3526 N92-29958
Cislan-2 extension final document by University of Twente (Netherlands)
[MEMO-INF-92-05] p 3437 N92-29984
LOGARITHMS
On the addition of log-convex functions and sequences
[MEMO-COSOR-92-01] p 3533 N92-29826
LOGIC CIRCUITS
Experimental evaluation of incorporating digital and analog integrated circuit die on a common substrate utilizing silicon-hybrid wafer-scale integration technology
[AD-A248182] p 3439 N92-29405
Boolean reasoning and informed search in the minimization of logic circuits
[AD-A248110] p 3528 N92-29561
LOGIC DESIGN
Fuzzy logic control of AC induction motors
[PB92-180207] p 3443 N92-30092
LOGIC PROGRAMMING
A soft stairway to institutions
[MEMO-INF-91-87] p 3522 N92-29981
Loop checking in partial deduction
[CWI-CS-R9134] p 3522 N92-29990
LOGISTICS
Enhanced evaluation, selection and acceptance criteria for the Contractor Integrated Technical Information Service (CITIS)
[PB92-163856] p 3562 N92-29699
LOGISTICS MANAGEMENT
Application Center of Excellence (ACE) program
[AD-A248694] p 3562 N92-29934
LOOPS
Loop checking in partial deduction
[CWI-CS-R9134] p 3522 N92-29990
LOSSES
Examination of the main error factors with regards to secondary losses in compression and turbine cascades by variations of the blade picture ratio
[ETN-92-91493] p 3405 N92-29927

LOW FREQUENCIES
Global measurements of low-frequency radio noise
[AD-A248260] p 3434 N92-29542
Land-based seismic array studies of low frequency ambient oceanic noise
[AD-A248255] p 3505 N92-29618
LOW PASS FILTERS
Position-error-based force reflection and compliance control
[NASA-CASE-NPO-18668-1-CU] p 3479 N92-29765
LOW REYNOLDS NUMBER
A theoretical approach for analyzing the restabilization of wakes
[NASA-TM-103858] p 3443 N92-29394
On dynamic models for large eddy simulation
p 3450 N92-30056
An experimental investigation of a low Reynolds number turbulent boundary layer subject to an adverse pressure gradient p 3453 N92-30153
The large-scale structures in turbulent plane Couette flow p 3455 N92-30167
Turbulent thermal convection in a differentially rotating channel p 3455 N92-30168
LOW SPEED
Helicopter low-speed yaw control
[NASA-CASE-LAR-14219-1] p 3406 N92-30025
LUMINOSITY
The evolution of the x ray luminosity function of galaxy clusters p 3567 N92-29848
LUMPED PARAMETER SYSTEMS
Dynamic modeling of fluid transmission lines of the DSN 70-meter antennas by using a lumped parameter model
p 3432 N92-29378
LUNAR BASED EQUIPMENT
Optimization of armored spherical tanks for storage on the lunar surface
[NASA-TM-105700] p 3414 N92-30187
LUNAR ROVING VEHICLES
Beam-powered lunar rover design
[DE92-011511] p 3569 N92-29600

M

MACH NUMBER
Production of periodical Mach number variations in high subsonic flow in a blow down wind tunnel, and its influence on profile measurements
[ETN-92-91492] p 3401 N92-29889
MACHINE LEARNING
Application of fuzzy logic-neural network based reinforcement learning to proximity and docking operations
[NASA-CR-190504] p 3525 N92-29390
DecisionMaker software and extracting fuzzy rules under uncertainty
[NASA-CR-190502] p 3514 N92-29391
Fast temporal neural learning using teacher forcing
[NASA-CASE-NPO-18553-1-CU] p 3530 N92-30085
MACHINING
Preliminary cutting and drilling studies using new generation lasers
[DE92-010712] p 3477 N92-29787
MAGELLAN PROJECT (NASA)
DSN acquisition of Magellan high-rate telemetry data
p 3409 N92-29383
MAGELLANIC CLOUDS
ROSAT: Early results p 3567 N92-29850
MAGNESIUM
Ion collision effects in hydrogen-like recombination x ray lasers
[DE92-013515] p 3476 N92-29509
Microcalorimetric study of the aging reactions of atomized magnesium powder
[AD-A247932] p 3427 N92-29786
MAGNETIC DIPOLES
Standard spherical dipole source
[PB92-187020] p 3438 N92-30198
MAGNETIC EFFECTS
Introduction to quartz frequency standards
[AD-A248503] p 3439 N92-29498
MAGNETIC FIELDS
Survey of research into electromagnetic and other wave effects on mechanical behavior and processing of materials
[AD-A248614] p 3426 N92-29905
MAGNETIC LEVITATION VEHICLES
Computer model simulation of null-flux magnetic suspension and guidance
[DE92-013044] p 3478 N92-29534
High-speed Maglev trains: German safety requirements RW-MSB
[PB92-167006] p 3564 N92-29808
German high-speed Maglev train safety requirements: Potential for application in the United States
[PB92-167014] p 3564 N92-29809
New York State technical and economic MAGLEV evaluation
[PB92-174119] p 3564 N92-30037
MAGNETIC MEASUREMENT
OFFEQ-1: Preliminary flight evaluation results
[ITN-92-85126] p 3410 N92-29480
MAGNETIC MOMENTS
Spectroscopy of W-183; measured magnetic moments and rotation-particle coupling
[DE92-624790] p 3549 N92-30213
MAGNETIC MONOPOLES
Introduction to SO(3) monopole
[USIP-91-05] p 3560 N92-29781
MAGNETIC POLES
Global solar magnetic fields
[AD-A248340] p 3569 N92-29421
MAGNETIC PROPERTIES
Magnetic properties of nano-heterogeneous amorphous thin films
[AD-A250570] p 3420 N92-29426
LiMoN2: The first metallic layered nitride
[AD-A248446] p 3418 N92-29619
MAGNETIC RESONANCE
Electrical, optical, and magnetic resonance studies of novel pi-conjugated polymers
[DE92-012548] p 3424 N92-29482
MAGNETIC STORMS
Poleward leaping auroras, the substorm expansive and recovery phases, and the recovery of the plasma sheet
[DE92-013530] p 3500 N92-29513
MAGNETIC SUSPENSION
Computer model simulation of null-flux magnetic suspension and guidance
[DE92-013044] p 3478 N92-29534
MAGNETOHYDRODYNAMIC FLOW
Transport processes in beamed energy propulsion systems
[AD-A247296] p 3413 N92-29913
An exact turbulent closure for the hydromagnetic dynamo p 3452 N92-30071
MAGNETOHYDRODYNAMIC GENERATORS
MHD Technology Transfer, Integration and Review Committee
[DE92-012687] p 3554 N92-29640
MAGNETOHYDRODYNAMIC STABILITY
Experimental and theoretical research in applied plasma physics
[DE92-013587] p 3553 N92-29336
Numerical analysis of plasma transport in tandem volume magnetic multicusp ion sources
[AD-A248093] p 3554 N92-29528
Optical diagnostics on dense Z-pinch plasmas
[DE92-011228] p 3555 N92-29917
MAGNETOHYDRODYNAMIC WAVES
A study of shock-associated magnetohydrodynamic waves in the solar wind
[NASA-CR-190567] p 3569 N92-29631
MAGNETOHYDRODYNAMICS
MHD Technology Transfer, Integration and Review Committee
[DE92-012687] p 3554 N92-29640
An exact turbulent closure for the hydromagnetic dynamo p 3452 N92-30071
MAINTENANCE
An analysis of the endurance of mobile satellite command and control systems
[AD-A248084] p 3410 N92-29525
NASA visual thesaurus maintenance documentation
[NASA-CR-190282] p 3561 N92-29553
Repair procedures for advanced composites for helicopters
[MBB-UD-0606-91-PUB] p 3399 N92-29874
Maintainability requirements for ESA space systems
[ESA-PSS-01-50-ISSUE-1] p 3481 N92-29878
Ageing airplane repair assessment program for Airbus A300 p 3402 N92-30123
Communication: An important element of maintenance and repair p 3402 N92-30124
MAINTENANCE TRAINING
Using intelligent simulation to enhance human performance in aircraft maintenance
p 3487 N92-30126
Revision of certification standards for aviation maintenance personnel p 3487 N92-30127
MALFUNCTIONS
Accelerometer method and apparatus for integral display and control functions
[NASA-CASE-MSC-21961-1] p 3474 N92-29952
MAMMALS
Gordon research conference on Barrier Function of Mammalian Skin
[AD-A248556] p 3510 N92-29577
MAN MACHINE SYSTEMS
Making intelligent systems team players: Overview for designers
[NASA-TM-104751] p 3513 N92-29403
Army-NASA aircrew/aircraft integration program: Phase 4 A(3)I Man-Machine Integration Design and Analysis System (MIDAS) software detailed design document
[NASA-CR-177593] p 3512 N92-29413
MAN-COMPUTER INTERFACE
ASV3 dial-in interface recommendation for the Repository Based Software Engineering (RBSE) program
[NASA-CR-190500] p 3514 N92-29362
Making intelligent systems team players: Overview for designers
[NASA-TM-104751] p 3513 N92-29403
Architecture and use of Delft Direct Manipulation Manager (D2M2)
[REPT-91-46] p 3521 N92-29887
MANAGEMENT
MHD Technology Transfer, Integration and Review Committee
[DE92-012687] p 3554 N92-29640
Diversification and product innovation: A challenge for modern management
[OEFZS-4570] p 3561 N92-29886
MANAGEMENT INFORMATION SYSTEMS
PDES application protocol suite for composites (PAS-C): IDEFO activity models and information needs for the PAS-C program
[AD-A248714] p 3562 N92-29720
Architecture and use of Delft Direct Manipulation Manager (D2M2)
[REPT-91-46] p 3521 N92-29887
MANAGEMENT SYSTEMS
Geostationary Operational Environmental Satellite (GOES-N report). Volume 2: Technical appendix
[NASA-TM-107920] p 3410 N92-29812
CRIS/USDA online access guide. Revision 1: File 60 on DIALOG
[PB92-172857] p 3562 N92-30033
MANIFOLDS (MATHEMATICS)
Swirls and wheels
[PB92-173251] p 3542 N92-30095
MANIPULATORS
Experimental investigation of adaptive control of a parallel manipulator
[NASA-CR-189867] p 3528 N92-29656
Position-error-based force reflection and compliance control
[NASA-CASE-NPO-18668-1-CU] p 3479 N92-29765
Full pose and partial pose calibration of a 6 degree-of-freedom robot manipulator arm
[AD-A247463] p 3479 N92-29785
On fictitious joints modelling of manipulator link flexibility for the HERA simulation facility pilot
[NLR-TR-88086-U] p 3479 N92-29885
MANUFACTURING
Novel thin-film CuInSe2 fabrication
[DE92-001222] p 3557 N92-29584
Monolithic amorphous silicon modules on continuous polymer substrate
[DE92-001163] p 3425 N92-29598
Hardening techniques to counter cumulated dose on SEU and SEL in space environment
[IMAG-RR-863-I] p 3441 N92-29613
Manufacturing of components of fibre-metal laminates: An overview
[LR-670] p 3415 N92-29702
PDES application protocol suite for composites (PAS-C): IDEFO activity models and information needs for the PAS-C program
[AD-A248714] p 3562 N92-29720
Challenges to NIST in dimensional metrology: The impact of tightening tolerances in the US discrete-part manufacturing industry
[PB92-164680] p 3542 N92-29802
Survey of research into electromagnetic and other wave effects on mechanical behavior and processing of materials
[AD-A248614] p 3426 N92-29905
A manufacturer's approach to ensure long term structural integrity p 3403 N92-30133
MAPPING
Mapping of groundwater losses by evaporation in the western desert of Egypt
[BCRS-91-01] p 3489 N92-29495
Terrain following of arbitrary surfaces using a high intensity LED proximity sensor
[DE92-004464] p 3528 N92-29644
Mapping agroecological zones and time lag in vegetation growth by means of Fourier analysis of time series of NDVI images
[REPT-32] p 3490 N92-29717
Monte-Carlo implementation of mapping closures: Application to chemical reacting flows
p 3450 N92-30060
A closer look at a Fibonacci-like iterated nonlinear map: More chaos and order
[MEMO-INF-91-70] p 3537 N92-30075

Programmable hyperspectral image mapper with on-array processing
[NASA-CASE-NPO-17794-1-CU] p 3553 N92-30104

MARINE ENVIRONMENTS
Asymptotic and numerical methods in applied wave propagation
[AD-A250227] p 3543 N92-29543

MARINE MAMMALS
Mosquito Lagoon environmental resources inventory
[NASA-TM-107548] p 3492 N92-29430

MARINE METEOROLOGY
OCEANUS 218: Warm Ring Inertial Critical Layer Experiment (WRINCLE)
[PB92-170299] p 3506 N92-29806

MARINE TECHNOLOGY
Marine structural steel toughness data bank (abridged edition)
[PB92-163294] p 3422 N92-29807

MARKET RESEARCH
Diversification and product innovation: A challenge for modern management
[OEFZS-4570] p 3561 N92-29886

MARKING
Application of remote sensing methods for tracking large cetaceans: North Atlantic right whales Eubalaena Glacialis
[PB92-185016] p 3490 N92-30022

MARKOV CHAINS
Separable Markovian decision problems: The linear programming method in the multichain case (revised)
[PB92-187350] p 3524 N92-30201

MARKOV PROCESSES
A compensation approach for two-dimensional Markov processes
[MEMO-COSOR-91-28] p 3539 N92-29606
A compensation approach for queueing problems
[ETN-92-91628] p 3539 N92-29774
Diffusion approximation of stochastic integral functionals of jump Markov processes
[CWI-AM-R9108] p 3535 N92-29895
Diffusion approximation of stochastic additive functionals of jump Markov processes
[CWI-AM-R9110] p 3535 N92-29896
Single point modeling of initially isotropic turbulence under uniform rotation p 3449 N92-30054
Linear system identification via backward-time observer models
[NASA-TM-107632] p 3488 N92-30214

MARS SURFACE
A systems analysis of the impact of navigation instrumentation on-board a Mars rover, based on a covariance analysis of navigation performance
[NASA-CR-189868] p 3403 N92-29440

MARTINGALES
Software reliability and the bootstrap
[CWI-BS-R9123] p 3520 N92-29865
Diffusion approximation of stochastic integral functionals of jump Markov processes
[CWI-AM-R9108] p 3535 N92-29895
Diffusion approximation of stochastic additive functionals of jump Markov processes
[CWI-AM-R9110] p 3535 N92-29896

MASERS
Optimizing the G/T ratio of the DSS-13 34-meter beam-waveguide antenna p 3431 N92-29377

MASS DISTRIBUTION
Reconstruction of density and potential fields of the Universe p 3565 N92-29834
Cluster correlations from N-point correlation amplitudes p 3566 N92-29837
Abell clusters of galaxies: Catalogs and large-scale structures p 3566 N92-29838
Scale-invariant galaxy clustering on large scales p 3566 N92-29839
The space distribution of local radio galaxies p 3566 N92-29842
Constraints on the mass fluctuation spectrum from x ray observations of clusters of galaxies p 3567 N92-29845
Clusters of galaxies in depth p 3567 N92-29846
The evolution of the x ray luminosity function of galaxy clusters p 3567 N92-29848
National Launch System cycle 1 loads and models data book
[NASA-TM-103560] p 3408 N92-30215

MASS FLOW RATE
Vorticity matching in superfluid helium p 3449 N92-30049

MASS SPECTRA
Constraints on the mass fluctuation spectrum from x ray observations of clusters of galaxies p 3567 N92-29845

MASS SPECTROMETERS
Support activities to maintain SUMS flight readiness
[NASA-CR-189656-VOL-1] p 3410 N92-30217
Support activities to maintain SUMS flight readiness, volume 2. Attachment A: Flight 61-C report
[NASA-CR-189656-VOL-2] p 3411 N92-30218
Support activities to maintain SUMS flight readiness, volume 3. Attachment B: Flight STS-35 report, section A
[NASA-CR-189656-VOL-3] p 3411 N92-30219
Support activities to maintain SUMS flight readiness, volume 4. Attachment B: Flight STS-35 report, section B
[NASA-CR-189656-VOL-4] p 3411 N92-30220
Support activities to maintain SUMS flight readiness, volume 5. Attachment B: Flight STS-35 report, section C
[NASA-CR-189656-VOL-5] p 3411 N92-30221
Support activities to maintain SUMS flight readiness, volume 6. Attachment B: Flight STS-35 report, section D
[NASA-CR-189656-VOL-6] p 3411 N92-30222
Support activities to maintain SUMS flight readiness, volume 7. Attachment B: Flight STS-35 report, section E
[NASA-CR-189656-VOL-7] p 3412 N92-30223
Support activities to maintain SUMS flight readiness, volume 8. Attachment B: Flight STS-35 report, section F
[NASA-CR-189656-VOL-8] p 3412 N92-30224
Support activities to maintain SUMS flight readiness, volume 9. Attachment C: Flight STS-40 report. Attachment D: SUMS software listing
[NASA-CR-189656-VOL-9] p 3412 N92-30225

MASS TRANSFER
Thermodynamic and kinetic aspects of 3/5 epitaxy
[AD-A250632] p 3556 N92-29429

MATERIAL BALANCE
The bioreactor overflow device: An undesired selective separator in continuous cultures? p 3507 N92-29736

MATERIALS SCIENCE
Review of potential x ray laser applications in materials science and chemistry
[DE92-012254] p 3475 N92-29434
NASA-UVA light aerospace alloy and structures technology program (LA2ST)
[NASA-CR-190538] p 3423 N92-30206

MATHEMATICAL LOGIC
Defaults in update semantics
[ITLI-LP-91-02] p 3532 N92-29685
Dynamic semantics and circular propositions
[ITLI-LP-91-03] p 3532 N92-29687
A soft stairway to institutions
[MEMO-INF-91-87] p 3522 N92-29981
Partial logic as a simple restriction of standard logic
[MEMO-INF-91-73] p 3536 N92-29995
Fuzzy logic control of AC induction motors
[PB92-180207] p 3443 N92-30092

MATHEMATICAL MODELS
Acoustic scattering from elastic ice: A finite difference solution
[AD-A248281] p 3543 N92-29346
Code generation in ALPAL using symbolic techniques
[DE92-011299] p 3524 N92-29353
Development of a multigrid transonic potential flow code for cascades
[NASA-CR-190480] p 3399 N92-29361
A theoretical approach for analyzing the restabilization of wakes
[NASA-TM-103858] p 3443 N92-29394
Electron spectra of adatomic structures
[DE92-625013] p 3544 N92-29415
The determination of stochastic models and areas of confidence
[OEFZS-4612] p 3538 N92-29419
Spacecraft dynamics characterization and control system failure detection, volume 1
[NASA-CR-190517] p 3409 N92-29422
Origin and evolution of planetary atmospheres
[NASA-CR-190579] p 3568 N92-29432
Circulation and exchange at the continental shelf and slope SEEP-2
[DE92-013500] p 3504 N92-29439
Tear straps in airplane fuselage
[AD-A248543] p 3404 N92-29511
Computer model simulation of null-flux magnetic suspension and guidance
[DE92-013044] p 3478 N92-29534
Low energy neutral atoms in the Earth's magnetosphere: Modeling
[DE92-013240] p 3500 N92-29536
Path tracking using simple planar curves
[AD-A248252] p 3403 N92-29617
Global-warming problem and global economic models
[DE92-514557] p 3493 N92-29638
Pressurization of cryogens: A review of current technology and its applicability to low-gravity conditions
[NASA-TM-105746] p 3427 N92-29669
A soil-canopy scheme for use in a numerical model of the atmosphere: 1D stand-alone model
[CSIRO-TP-23] p 3500 N92-29670
The effect of length variation on the stability of circular cylindrical shells under pure bending
[LR-669] p 3482 N92-29700
Numerical modeling studies of the Gulf of Mexico and the Caribbean Sea using the Bryan-Cox model
[PB92-164987] p 3505 N92-29704
River hydrometry by pattern recognition in remote sensing images
[PUBL-445] p 3490 N92-29728
Study and realization of GaAs PNP homojunction bipolar transistors using ion implementation
[LAAS-91433] p 3441 N92-29729
Methodology on monitoring and modelling of microbial metabolism
[ETN-92-91745] p 3507 N92-29732
Linear relations in microbial reaction systems: A general overview of their origin, form, and use p 3507 N92-29733
Modelling and experimental validation of carbon dioxide evolution in alkalophilic cultures p 3507 N92-29734
The bioreactor overflow device: An undesired selective separator in continuous cultures? p 3507 N92-29736
On the estimation of bioenergetic parameters p 3508 N92-29738
Analysis and experimental testing of a bottleneck model for the description of microbial dynamics p 3508 N92-29740
A semi empirical method for the analytical representation of stationary measured profile coefficients for applications of rotary wing aerodynamics
[ETN-92-91491] p 3401 N92-29741
The expanding plasma jet: Experiments and model
[ETN-92-91627] p 3555 N92-29761
Full pose and partial pose calibration of a 6 degree-of-freedom robot manipulator arm
[AD-A247463] p 3479 N92-29785
Reverse automatic differentiation of modular FORTRAN programs
[DE92-014071] p 3519 N92-29797
Parameter identification in tidal models with uncertain boundaries
[MEMO-983] p 3540 N92-29856
Mathematical modelling of saturated and unsaturated groundwater flow
[MEMO-987] p 3445 N92-29857
Discretization of morphological operators
[CWI-BS-R9118] p 3533 N92-29861
On fictitious joints modelling of manipulator link flexibility for the HERA simulation facility pilot
[NLR-TR-88086-U] p 3479 N92-29865
A method for converting the surface of a generalized cylinder into a B-spline surface
[REPT-91-40] p 3535 N92-29922
Thickness dependency of elastic aftereffect of thin bending beams
[ETN-92-91488] p 3483 N92-29925
On the numerical treatment of the advective terms in 3D shallow water models
[CWI-NM-R9110] p 3446 N92-29945
Development of models for prediction of optimal lifting motion
[PB92-164656] p 3513 N92-29949
A finite volume approach to large eddy simulation of compressible, homogeneous, isotropic, decaying turbulence
[MEMO-1009] p 3446 N92-29972
A two-stage estimator for generalized linear models with nonconstant dispersion parameter
[MEMO-1012] p 3540 N92-29975
An analysis of model-based diagnosis using problem-reformulation
[MEMO-INF-92-03] p 3530 N92-29983
Cross section parameterizations for cosmic ray nuclei. 1: Single nucleon removal p 3547 N92-30002
Solution of two-body relativistic bound state equations with confining plus Coulomb interactions p 3547 N92-30003
Two neutron removal in relativistic nucleus-nucleus reactions p 3548 N92-30006
Higgs-boson production in nucleus-nucleus collisions p 3548 N92-30009
Stopping powers and cross sections due to two-photon processes in relativistic nucleus-nucleus collision p 3548 N92-30012
Large eddy simulations of passive and buoyant scalars with dynamic subgrid-scale models p 3450 N92-30057
Dynamic subgrid-scale modeling of compressible turbulence p 3450 N92-30058
A mathematical model for metal hydride electrodes
[DE92-506506] p 3442 N92-30089
Texture synthesis
[CWI-CS-R9139] p 3523 N92-30141
An experimental study of the effects of rapid rotation on turbulence p 3453 N92-30154
Short-time Lyapunov exponent analysis p 3453 N92-30157
Organized motions underlying turbulent shear flows p 3453 N92-30158

Turbulent transport in the solar nebula
p 3454 N92-30163
Simulations on the Jelinski-Moranda model of software reliability
[CWI-BS-R9122] p 3523 N92-30179
Linear system identification via backward-time observer models
[NASA-TM-107632] p 3488 N92-30214
National Launch System cycle 1 loads and models data book
[NASA-TM-103560] p 3408 N92-30215

MATRICES (MATHEMATICS)
Linear relations in microbial reaction systems: A general overview of their origin, form, and use
p 3507 N92-29733
Positive convolution structures associated with quantum groups
[CWI-AM-R9105] p 3534 N92-29866
A monotonic build-up simplex algorithm for linear programming
[REPT-91-82] p 3524 N92-30227

MATRIX MATERIALS
Approaches to polymer-derived CMC matrices
[NASA-TM-105754] p 3415 N92-29660
A perspective on MoSi2 based composites
[DE92-013434] p 3415 N92-29795

MAXIMA
Non-interfering dipaths in planar digraphs
[CWI-BS-R9121] p 3533 N92-29864
Strong law and central limit theorem for a process between maxima and sums p 3530 N92-29964

MAXIMUM LIKELIHOOD ESTIMATES
Nonparametric maximum likelihood estimators for interval censoring and deconvolution
[REPT-91-53] p 3539 N92-29626
Computer program POWNOR for fitting the power-normal and -lognormal models to life or strength data from specimens of various sizes
[PB92-169119] p 3483 N92-29813
Parameter identification in tidal models with uncertain boundaries
[MEMO-983] p 3540 N92-29856
Software reliability and the bootstrap
[CWI-BS-R9123] p 3520 N92-29865
Simulations on the Jelinski-Moranda model of software reliability
[CWI-BS-R9122] p 3523 N92-30179

MAXIMUM PRINCIPLE
Abstract quasilinear equations and application to a groundwater flow problem
[REPT-91-41] p 3535 N92-29923

MAXWELL EQUATION
Divergence preserving discrete surface integral methods for Maxwell's curl equations using non-orthogonal unstructured grids
[NASA-CR-190555] p 3517 N92-29694

MEANDERS
Progress toward identification of streamwise vorticity meander in a plane mixing layer p 3451 N92-30068

MEASUREMENT
A letter of intent for an experiment to study strong electromagnetic fields at RHIC via multiple electromagnetic processes p 3438 N92-30015

MEASURING INSTRUMENTS
Error analysis of wind measurements for the University of Illinois sodium Doppler temperature system
p 3471 N92-29313
Sequential application of data reconciliation for sensitive detection of systematic errors p 3509 N92-29760
Sensor fault detection on board an aircraft with observer and polynomial classifier
[DLR-FB-91-34] p 3404 N92-29870
Electrochemical array sensors for plating waste stream monitoring
[DE92-011446] p 3495 N92-30211

MECHANICAL ENGINEERING
Repair procedures for advanced composites for helicopters
[MBB-UD-0606-91-PUB] p 3399 N92-29874
Penguin extruded aluminium box launcher for marine application
[FFI-91/4001] p 3408 N92-29967

MECHANICAL PROPERTIES
Rolling-contact and wear resistance of hard coatings on bearing-steel substrates
[DE92-011834] p 3478 N92-29357
Processing and properties of mechanically alloyed sintered steels with hard inclusions
[KFK-4909] p 3422 N92-29651
Fatigue crack growth in damage tolerant Al-Li sheet alloys
[NLR-TP-90107-U] p 3483 N92-29708
Effect of whisker orientation on the mechanical properties of silicon carbide/alumina composites
[AD-A248737] p 3415 N92-29723
Structural basis for the mechanical properties of polyethylenes
[PB92-164425] p 3426 N92-29804
Development and characterization of oxidation-protected CFC
[MBB-Z-0395-91-PUB] p 3416 N92-29876

MEDICAL EQUIPMENT
Test and evaluation report of the physio control defibrillator/monitor model LIFEPAK (trademark) 8
[AD-A248283] p 3510 N92-29347
Test and evaluation report of the IMED volumetric infusion pump model 960A
[AD-A248538] p 3404 N92-29506

MEDICAL SERVICES
Test and evaluation report of the physio control defibrillator/monitor model LIFEPAK (trademark) 8
[AD-A248283] p 3510 N92-29347
Test and evaluation report of the IMED volumetric infusion pump model 960A
[AD-A248538] p 3404 N92-29506

MELTING
Metal vapor plasma behavior during vacuum arc remelting of alloy 718
[DE92-011761] p 3421 N92-29623

MEMBRANES
A method for making biocompatible polymer articles using atomic oxygen
[NASA-CASE-MSC-21529-1] p 3427 N92-30100

MEMORY
A systems theoretic investigation of neuronal network properties of the hippocampal formation
[AD-A250246] p 3510 N92-29334

MERCURY (METAL)
DIAL mapping of atmospheric atomic mercury of geophysical origin p 3464 N92-29273

MEROMORPHIC FUNCTIONS
Integrable deformations of meromorphic equations on P(exp 1)C
[MEMO-993] p 3534 N92-29872

MESONS
Solution of two-body relativistic bound state equations with confining plus Coulomb interactions
p 3547 N92-30003
Effects of retardation in relativistic equations with confining interaction p 3547 N92-30005

MESOPAUSE
Lidar measurements of metallic species in mesopause region p 3470 N92-29312
Sodium Doppler temperature lidar observations of the mesopause region temperature and wind structure
p 3471 N92-29314

MESOSCALE PHENOMENA
Simulation of the performances of WIND, an airborne CO2 lidar p 3463 N92-29267
Measurements of wind divergence with volume imaging lidar p 3464 N92-29272
The Laser Atmospheric Wind Sounder (LAWS) phase 2 preliminary system design p 3468 N92-29297
A soil-canopy scheme for use in a numerical model of the atmosphere: 1D stand-alone model
[CSIRO-TP-23] p 3500 N92-29670

MESOSPHERE
Development of mesospheric sodium laser beacon for atmospheric adaptive optics p 3470 N92-29308
Characterization of artificial guidestars generated in the mesospheric sodium layer p 3470 N92-29309
Optical pumping of mesospheric sodium: A new measurement capability p 3470 N92-29310
Lidar probing of the mesosphere: Simultaneous observations of sporadic sodium and iron formations, calcium ion layers, neutral temperature and winds
p 3470 N92-29311
Elastic and Raman lidar temperature measurements from Poker Flat, Alaska during February 1992
p 3471 N92-29317

METABOLISM
Methodology on monitoring and modelling of microbial metabolism
[ETN-92-91745] p 3507 N92-29732
On the estimation of bioenergetic parameters
p 3508 N92-29738

METAL COATINGS
Mechanical properties of coated titanium Beta-21S after exposure to air at 700 and 800 C
[NASA-TM-104220] p 3423 N92-30205

METAL CRYSTALS
Amorphization by interdiffusion in metallic multilayers
[ETN-92-91743] p 3558 N92-29766
Amorphization along interfaces and grain boundaries in polycrystalline multilayers: An x ray diffraction study of Ni/Ti multilayers p 3558 N92-29769
A model for interdiffusion in polycrystalline multilayers and its application to solid state amorphization
p 3558 N92-29771
Amorphization and related effects in Ni/Ti multilayers studied by differential scanning calorimetry
p 3559 N92-29772
Evidence for amorphization in Ni/Ti multilayers from electrical resistivity changes p 3559 N92-29773

METAL FATIGUE
Strengthening mechanisms, creep and fatigue processes in dispersion hardened niobium alloy
[AD-A250282] p 3421 N92-29547
Stresses and strains in plain and coldworked annuli subjected to remote, interference or combined loading
[ARL-STRUC-R-446] p 3482 N92-29672

METAL FILMS
Diffraction of light from randomly rough surfaces
[AD-A250261] p 3551 N92-29546
LiMoN2: The first metallic layered nitride
[AD-A248446] p 3418 N92-29619
Evaluation of aluminum ion vapor deposition as a replacement for cadmium electroplating at Anniston Army Depot
[AD-A250063] p 3423 N92-29940

METAL FUELS
Microcalorimetric study of the aging reactions of atomized magnesium powder
[AD-A247932] p 3427 N92-29786

METAL HYDRIDES
A mathematical model for metal hydride electrodes
[DE92-506506] p 3442 N92-30089

METAL IONS
Lidar probing of the mesosphere: Simultaneous observations of sporadic sodium and iron formations, calcium ion layers, neutral temperature and winds
p 3470 N92-29311
Laser-induced desorption from sapphire surfaces
[DE92-012698] p 3475 N92-29340
Correlated charge-changing ion-atom collisions
[DE92-013473] p 3546 N92-29642
Evaluation of aluminum ion vapor deposition as a replacement for cadmium electroplating at Anniston Army Depot
[AD-A250063] p 3423 N92-29940

METAL MATRIX COMPOSITES
Status and perspectives of modern composite materials
[MBB-Z-0380-91-PUB] p 3416 N92-29875

METAL OXIDE SEMICONDUCTORS
Nonvolatile programmable neural network synaptic array
[NASA-CASE-NPO-18578-1-CU] p 3442 N92-30086

METAL OXIDES
Mechanical properties of coated titanium Beta-21S after exposure to air at 700 and 800 C
[NASA-TM-104220] p 3423 N92-30205

METAL PLATES
A new HyperVelocity Launcher (HVL) for space science application
[DE92-010670] p 3408 N92-29986

METAL POWDER
X ray study of interfacial interactions in highly milled Sn-Ge powders
[DE92-012518] p 3556 N92-29437
Microcalorimetric study of the aging reactions of atomized magnesium powder
[AD-A247932] p 3427 N92-29786

METAL SHEETS
Manufacturing of components of fibre-metal laminates: An overview
[LR-670] p 3415 N92-29702
Fatigue crack growth in damage tolerant Al-Li sheet alloys
[NLR-TP-90107-U] p 3483 N92-29708

METAL SURFACES
Diffraction of light from randomly rough surfaces
[AD-A250261] p 3551 N92-29546
Neutralizer and sample chamber for the Atomic Oxygen Simulation System (AOSS)
[NASA-CR-184343] p 3407 N92-29664
Theory of the dissociation dynamics of small molecules on metal surfaces: Finite temperature studies
[DE92-011188] p 3546 N92-29899

METAL VAPORS
Metal vapor plasma behavior during vacuum arc remelting of alloy 718
[DE92-011761] p 3421 N92-29623

METALLIC PLASMAS
Metal vapor plasma behavior during vacuum arc remelting of alloy 718
[DE92-011761] p 3421 N92-29623

METEOROID PROTECTION
Optimization of armored spherical tanks for storage on the lunar surface
[NASA-TM-105700] p 3414 N92-30187

METEOROLOGICAL INSTRUMENTS
Preliminary analysis of wind data from the Oak Ridge site survey
[PB92-174564] p 3503 N92-30034

METEOROLOGICAL PARAMETERS
Lidar development for the Atmospheric Radiation Measurement (ARM) Program p 3461 N92-29256
Lidar studies of clouds at Toronto during the ECLIPS program p 3472 N92-29321
Monthly means of selected climate variables for 1985 - 1989
[NASA-TM-104565] p 3502 N92-29653
Comparison of turbulence parameters measured by SODAR and sonic anemometer
[KFK-4890] p 3500 N92-29690
METEOROLOGICAL RADAR
Laboratory velocimeter measurements using the edge technique p 3463 N92-29269
Identification of critical design points for the EAP of a space-based Doppler lidar wind sounder p 3463 N92-29270
Lidar studies of clouds at Toronto during the ECLIPS program p 3472 N92-29321
Adaptation of the University of Wisconsin high spectral resolution lidar for polarization and multiple scattering measurements p 3472 N92-29322
Polarization lidar liquid cloud detection algorithm for winter mountain storms p 3472 N92-29323
Measurement of mean or effective radius of cloud drop size distributions with a 10.6-micron wavelength lidar p 3472 N92-29324
Observations of cirrus clouds over the Pacific region by the NASA multiwavelength lidar system p 3473 N92-29325
Diode-pumped Nd:YAG lidar for airborne cloud measurements p 3473 N92-29326
Remote sensing by spaceborne lidar aided by surface returns p 3473 N92-29327
NWP impact of cloud top and boundary layer winds from a satellite borne lidar: An observing system simulation experiment p 3473 N92-29328
METEOROLOGICAL RESEARCH AIRCRAFT
A spectral vegetation radiometer for airborne boundary-layer research
[PB92-186113] p 3491 N92-30105
METEOROLOGICAL SERVICES
Geostationary Operational Environmental Satellite (GOES-N report). Volume 1: Technical
[NASA-TM-107918] p 3410 N92-29811
METEOROLOGY
Lidar measurement of stratospheric ozone at Hohenpeissenberg: An improved evaluation method p 3462 N92-29259
Sampling and representativeness for a spaceborne wind lidar p 3463 N92-29268
Multi-fractal analysis of nocturnal boundary layer time series from the Boulder Atmospheric Observatory
[AD-A248347] p 3502 N92-29424
Proceedings of the 16th Annual Climate Diagnostics Workshop
[PB92-167378] p 3503 N92-29801
Preliminary analysis of wind data from the Oak Ridge site survey
[PB92-174564] p 3503 N92-30034
CLICOM-news, issue 7 p 3503 N92-30171
METHANE
New directions for the catalytic conversion of methane
[PB92-172360] p 3492 N92-29519
Modeling of the role of atomic hydrogen in heat transfer during hot filament assisted deposition of diamond
[AD-A250607] p 3418 N92-29595
NATO workshop on the Atmospheric Methane Cycle. Working group report on methane sources and sinks
[PB92-180256] p 3494 N92-30018
METHODOLOGY
Methodology on monitoring and modelling of microbial metabolism
[ETN-92-91745] p 3507 N92-29732
METHYL ALCOHOL
Structure of a methanol/air coaxial reacting spray near the stabilization region by OH fluorescence imaging and two-component phase-Doppler interferometry
[DE92-005328] p 3417 N92-29431
METHYL COMPOUNDS
Vibrational spectrum and structure of 1,2-dimethyl-1,2-disila-closo-dodecaborane
[AD-A250235] p 3419 N92-29941
METROLOGY
Challenges to NIST in dimensional metrology: The impact of tightening tolerances in the US discrete-part manufacturing industry
[PB92-164680] p 3542 N92-29802
MICHELSON INTERFEROMETERS
Efficiencies of rotational Raman and Rayleigh techniques for laser remote sensing of the atmospheric temperature p 3467 N92-29288
MICROBIOLOGY
Publications of the environmental health program: 1980-1990
[NASA-CR-4455] p 3509 N92-29341
Linear relations in microbial reaction systems: A general overview of their origin, form, and use p 3507 N92-29733
MICROCLIMATOLOGY
Lidar observation of aerosol and temperature stratification over urban area during the formation of a stable atmospheric PBL p 3466 N92-29286
MICROCOMPUTERS
Micro-computer network architecture for range instrumentation applications, volume 1
[AD-A247836] p 3525 N92-29555
MICROELECTRONICS
Using custom-designed VLSI fuzzy inferencing chips for the autonomous navigation of a mobile robot
[DE92-000424] p 3528 N92-29550
Monolithic integration of semiconductor and superconductor components
[AD-A245351] p 3557 N92-29583
Electrochemical array sensors for plating waste stream monitoring
[DE92-011446] p 3495 N92-30211
MICROMECHANICS
Micromechanisms of cyclic and environmentally-assisted subcritical crack growth in ceramic-matrix composites
[AD-A248067] p 3414 N92-29556
MICROMETEOROLOGY
Sensitivity of C2 sub n to random variations of windspeed, sensible heat flux, and latent heat flux
[AD-A248696] p 3502 N92-29565
MICROPROCESSORS
A strategy for microprocessor BIST implementation based on deterministic testing
[IMAG-RR-844-I] p 3516 N92-29570
MICROSCOPES
Center of excellence: Microlaser microscope
[DE92-013485] p 3477 N92-29928
MICROSCOPY
Structure and shear response of lipid monolayers
[DE92-011633] p 3542 N92-29354
MICROSEISMS
Land-based seismic array studies of low frequency ambient oceanic noise
[AD-A248255] p 3505 N92-29618
MICROSTRIP ANTENNAS
Microstrip reflectarray antenna for the SCANSCAT radar application
[NASA-CR-190453] p 3434 N92-29463
MICROSTRUCTURE
Constitutive modelling for granular material under finite strains with particle slidings and fabric changes
[AD-A248187] p 3482 N92-29407
OCEANUS 218: Warm Ring Inertial Critical Layer Experiment (WRINCLE)
[PB92-170299] p 3506 N92-29806
MICROWAVE AMPLIFIERS
Tunable driver for the LLNL FEL experiment
[DE92-011292] p 3477 N92-29937
MICROWAVE ANTENNAS
Ka-band feed arrays for spacecraft reflector antennas with limited scan capability: An overview p 3433 N92-29387
MICROWAVE CIRCUITS
Design guidelines for capability approval of film hybrid microcircuits and Microwave Hybrid Integrated Circuits (MHICs)
[ESA-PSS-01-610-ISSUE-1] p 3441 N92-29854
MICROWAVE EMISSION
Detecting microwave emissions from terrestrial sources: A feasibility study
[AD-A248557] p 3435 N92-29579
MICROWAVE EQUIPMENT
The processing of high temperature ceramic superconducting devices, volume 1
[AD-A248176] p 3438 N92-29404
Miniature modular microwave end-to-end receiver
[NASA-CASE-NPO-18713-1-CU] p 3437 N92-30103
MICROWAVE IMAGERY
Global and high resolution radar cross section measurements and two-dimensional microwave images of a scaled aircraft model from the type Airbus A 310
[DLR-MITT-91-10] p 3436 N92-29877
MICROWAVES
Electron microscopy study on zirconia and alumina ceramic powders synthesized by microwave plasma pyrolysis
[DE92-013385] p 3424 N92-29479
Survey of research into electromagnetic and other wave effects on mechanical behavior and processing of materials
[AD-A248614] p 3426 N92-29905
Transport processes in beamed energy propulsion systems
[AD-A247296] p 3413 N92-29913
MIDDLE ATMOSPHERE
The Lidar In-Space Technology Experiment (LITE) p 3469 N92-29301
Rayleigh/Raman lidars: Intercomparisons and validation p 3471 N92-29318
MIE SCATTERING
Wind measurements from 15 to 50 km with a Doppler Rayleigh lidar p 3472 N92-29319
MIGRATION
Application of remote sensing methods for tracking large cetaceans: North Atlantic right whales Eubalaena Glacialis
[PB92-185016] p 3490 N92-30022
MILITARY HELICOPTERS
Army-NASA aircrew/aircraft integration program: Phase 4 A(3)I Man-Machine Integration Design and Analysis System (MIDAS) software detailed design document
[NASA-CR-177593] p 3512 N92-29413
MILITARY OPERATIONS
Burros: Simple, affordable, effective space transportation
[DE92-013553] p 3541 N92-30138
MILLIMETER WAVES
United Kingdom Infrared Telescope
[ETN-92-91341] p 3565 N92-29682
MIMD (COMPUTERS)
A parallel restructured version of GMRES(m)
[REPT-91-85] p 3527 N92-30229
MINIATURIZATION
Miniature modular microwave end-to-end receiver
[NASA-CASE-NPO-18713-1-CU] p 3437 N92-30103
MINIMAX TECHNIQUE
Minimax linear splines
[AD-A248077] p 3515 N92-29487
Algorithms and min-max theorems for certain multiway cuts
[MEMO-1022] p 3523 N92-30186
MIR SPACE STATION
Migmas/A: Test of a scanning ion microscope on the Soviet Space Station Mir
[OEFZS-4615] p 3473 N92-29469
Logion: The operation of liquid metal ion emitters under weightlessness
[OEFZS-4616] p 3428 N92-29470
MISS DISTANCE
A sensitivity analysis of circular error probable approximation techniques
[AD-A248105] p 3539 N92-29585
MISSILE CONTROL
Developing CMMCA flight profiles for cruise missile tracking
[AD-A248183] p 3434 N92-29406
MISSILE LAUNCHERS
Penguin extruded aluminium box launcher for marine application
[FFI-91/4001] p 3408 N92-29967
MISSILE TRACKING
Developing CMMCA flight profiles for cruise missile tracking
[AD-A248183] p 3434 N92-29406
MISSILES
Evaluating the military potential of a developing nation's space program: A case study of Brazil
[AD-A245978] p 3407 N92-29929
Burros: Simple, affordable, effective space transportation
[DE92-013553] p 3541 N92-30138
MISSION PLANNING
Fourth Meeting of the Space Agency Forum on the International Space Year (SAFISY-4)
[ESA-SP-1141] p 3407 N92-29879
NASA's Earth Observing System
[S-HRG-102-647] p 3490 N92-30017
MIXING LAYERS (FLUIDS)
Effect of walls on the supersonic reacting mixing layer p 3451 N92-30065
Mixing measurements of straight and curved shear layers p 3451 N92-30067
Progress toward identification of streamwise vorticity meander in a plane mixing layer p 3451 N92-30068
An experimental study of scalar mixing in curved shear layers p 3453 N92-30152
An experimental study of secondary vortex structure in mixing layers p 3453 N92-30155
Incompressible spatially-developing free-shear flows p 3454 N92-30165
MOBILITY
Using custom-designed VLSI fuzzy inferencing chips for the autonomous navigation of a mobile robot
[DE92-000424] p 3528 N92-29550
MODEL REFERENCE ADAPTIVE CONTROL
Experimental investigation of adaptive control of a parallel manipulator
[NASA-CR-189867] p 3528 N92-29656

MODULATION
Modulated high sensitivity infrared polarimeter
[AD-D015256] p 3474 N92-29571
MODULATORS
Optoelectronic integration
[AD-A248950] p 3442 N92-29936
MODULES
System testing and performance characterization of the LITE Laser Transmitter Module at NASA
p 3469 N92-29302
On-line replacement of program modules using AdaPT
[NASA-CR-190499] p 3514 N92-29363
Monolithic amorphous silicon modules on continuous polymer substrate
[DE92-001163] p 3425 N92-29598
MOISTURE
Compressive response of debonded thick composite shells including the effects of transient moisture sorption
[AD-A250080] p 3414 N92-29462
Potential impacts of climate change on Pacific Northwest forest vegetation
[PB92-184985] p 3495 N92-30021
MOLECULAR BEAM EPITAXY
A novel approach to silicon-on-insulator materials
[AD-A248074] p 3424 N92-29466
Method of forming silicon structures with selectable optical characteristics
[NASA-CASE-NPO-18625-1-CU] p 3559 N92-30102
MOLECULAR BEAMS
Hydrogenation reactions of neutral carbon clusters: C(sub n) (n = 6-75) + D(sub 2)
[DE92-005330] p 3417 N92-29459
MOLECULAR CHAINS
Molecular engineering of side chain liquid crystalline polymers
[AD-A248540] p 3424 N92-29508
Molecular engineering of liquid crystalline polymers
[AD-A248996] p 3427 N92-30136
MOLECULAR COLLISIONS
Free ion yields in liquids: Molecular structure and track effects
[DE92-012208] p 3545 N92-29582
MOLECULAR INTERACTIONS
Oriented structures based on trans-1,4-polybutadiene
[ETN-92-91632] p 3546 N92-29778
MOLECULAR SPECTRA
Decomposer: Program documentation
[USIP-91-04] p 3519 N92-29780
MOLECULAR STRUCTURE
Molecular engineering of liquid crystalline polymers by living polymerization. 19: Synthesis and characterization of poly 2-(4-biphenyloxy)ethyl vinyl etherby
[AD-A248285] p 3423 N92-29349
Molecular engineering of side chain liquid crystalline polymers
[AD-A248540] p 3424 N92-29508
Molecular engineering of liquid crystalline polymers by living polymerization. 20: Synthesis and characterization of binary copolymers of 11-(4-cyano-4'-biphenyl) oxy)undecanyl vinyl ether with n-butyl vinyl ether and of 2-(4-cyano-4'-biphenyl) oxy)ethyl vinyl ether with n-butyl vinyl ether
[AD-A248286] p 3425 N92-29566
Molecular engineering of liquid crystalline polymers by living polymerization. 22: Synthesis and characterization of binary copolymers
[AD-A248287] p 3425 N92-29567
Free ion yields in liquids: Molecular structure and track effects
[DE92-012208] p 3545 N92-29582
Oriented structures based on trans-1,4-polybutadiene
[ETN-92-91632] p 3546 N92-29778
MOLECULAR THEORY
Contributions to Hadron 1991: 1) Testing the nature of the f(0)(S asterisk). 2) Gamma gamma to pi(exp 0) pi(exp 0): Dispersive analysis compared to chiral perturbation theory
[RAL-91-070] p 3544 N92-29488
Testing the nature of the f(0)(S asterisk)
p 3545 N92-29489
Gamma gamma to pi(exp 0) pi(exp 0): Dispersive analysis compared to chiral perturbation theory
p 3545 N92-29490
MOLECULAR WEIGHT
Nonideal formation of network polymers
[AD-A248072] p 3424 N92-29465
MOLECULES
The activation of chemical bonds at surfaces
[AD-A248666] p 3418 N92-29719
Finite-rate diffusion-controlled reaction in a vortex
[PB92-172006] p 3418 N92-29744
Theory of the dissociation dynamics of small molecules on metal surfaces: Finite temperature studies
[DE92-011188] p 3546 N92-29899
MOLYBDENUM
LiMoN2: The first metallic layered nitride
[AD-A248446] p 3418 N92-29619
MOLYBDENUM COMPOUNDS
A perspective on MoSi2 based composites
[DE92-013434] p 3415 N92-29795
MOMENTUM
Confining potential in momentum space
p 3548 N92-30007
MOMENTUM TRANSFER
Analysis of a dedicated rotation experiment in TFTR
[DE92-013463] p 3554 N92-29438
MONATOMIC GASES
Rare gas clusters containing charged atoms
[AD-A248299] p 3544 N92-29350
MONITORS
Near-visible Raman instrumentation for remote multi-point process monitoring using optical fibers and optical multiplexing
[DE92-011287] p 3550 N92-29337
Longitudinal bunch profile measurements with striplines
[DE92-013035] p 3549 N92-29477
Accelerometer method and apparatus for integral display and control functions
[NASA-CASE-MSC-21961-1] p 3474 N92-29952
High resolving power spectrometer for beam analysis
[DE92-010751] p 3437 N92-29988
MONOMERS
Nonideal formation of network polymers
[AD-A248072] p 3424 N92-29465
Polybenzimidazoles via aromatic nucleophilic displacement
[NASA-CASE-LAR-14643-1] p 3426 N92-29953
MONTE CARLO METHOD
Ocean optical modeling: Light field structure, internal radiant emission, and vertical inhomogeneities
[AD-A248272] p 3504 N92-29345
Femtosecond studies of carrier dynamics in compound semiconductors
[AD-A250584] p 3439 N92-29452
Testing equality of variances in the analysis of repeated measurements
[MEMO-1013] p 3541 N92-29976
Monte-Carlo implementation of mapping closures: Application to chemical reacting flows
p 3450 N92-30060
Analysis of a three-dimensional point pattern with replication
[CWI-BS-R9124] p 3541 N92-30180
MOON
Beam-powered lunar rover design
[DE92-011511] p 3569 N92-29600
MORPHOLOGY
Rolling-contact and wear resistance of hard coatings on bearing-steel substrates
[DE92-011834] p 3478 N92-29357
The x ray morphology of the relaxed cluster of galaxies A2256. 1: Evidence for a merger event
p 3568 N92-29851
The x ray morphology of the relaxed cluster of galaxies A2256. 2: Sources around the extended cluster emission
p 3568 N92-29852
Discretization of morphological operators
[CWI-BS-R9118] p 3533 N92-29861
MOTION STABILITY
The effect of yaw cards on the pitching and yawing motion of symmetric projectiles
[AD-A250021] p 3406 N92-29449
MOUNTAINS
Polarization lidar liquid cloud detection algorithm for winter mountain storms p 3472 N92-29323
MOUNTING
Experimental evaluation of incorporating digital and analog integrated circuit die on a common substrate utilizing silicon-hybrid wafer-scale integration technology
[AD-A248182] p 3439 N92-29405
MOVING TARGET INDICATORS
Micro-computer network architecture for range instrumentation applications, volume 1
[AD-A247836] p 3525 N92-29555
MTBF
B(exp 2)UBIST: A strategy for boundary scan board unified BIST
[IMAG-RR-862-I] p 3441 N92-29612
MULTIGRID METHODS
Application of a moving-grid method to a class of 1D brine transport problems in porous media
[CWI-NM-R9112] p 3446 N92-29947
MULTILAYER INSULATION
Amorphization by interdiffusion in metallic multilayers
[ETN-92-91743] p 3558 N92-29766
Layer-thickness variations and x ray diffraction patterns, a general treatment p 3558 N92-29767
Low-angle x ray diffraction study of solid state amorphization in a Ni/Ti multilayer p 3558 N92-29768
Interdiffusion reactions in Ni/Ta multilayers studied by x ray diffraction p 3558 N92-29770
A model for interdiffusion in polycrystalline multilayers and its application to solid state amorphization
p 3558 N92-29771
Amorphization and related effects in Ni/Ti multilayers studied by differential scanning calorimetry
p 3559 N92-29772
Evidence for amorphization in Ni/Ti multilayers from electrical resistivity changes p 3559 N92-29773
MULTIPHOTON ABSORPTION
Multiphoton processes in scattering and ionization in an intense linearly-polarized radiation field
[DE92-013546] p 3545 N92-29515
MULTIPLEXING
Micro-device for coupling, multiplexing and demultiplexing using elliptical-core two-mode fiber
[NASA-CR-190496] p 3550 N92-29331
Near-visible Raman instrumentation for remote multi-point process monitoring using optical fibers and optical multiplexing
[DE92-011287] p 3550 N92-29337
MULTIPROCESSING (COMPUTERS)
Code generation in ALPAL using symbolic techniques
[DE92-011299] p 3524 N92-29353
Scalable parallel algorithms for multidimensional digital signal processing
[AD-A249381] p 3516 N92-29622
Design and scheduling for periodic concurrent error detection and recovery in processor arrays
[NASA-CR-190571] p 3517 N92-29695
MULTIPROGRAMMING
A compensation approach for queueing problems
[ETN-92-91628] p 3539 N92-29774
MULTISENSOR APPLICATIONS
Recognition of multi-articulated three-dimensional objects using a multisensor system for robotics applications
[LAAS-91394] p 3529 N92-29675
MULTISPECTRAL BAND SCANNERS
CAESAR: A CCD airborne experimental scanner for applications in remote sensing radiometric and geometric calibration
[NLR-TP-89103-U] p 3490 N92-29707
MUSCLES
Development of models for prediction of optimal lifting motion
[PB92-164656] p 3513 N92-29949
MUTAGENS
Lab-scale lidar sensing of diesel engines exhausts
p 3464 N92-29276

N

NAPHTHALENE
Synthesis of a naphthalene-hydroxynaphthalene polymer model compound
[DE92-012264] p 3423 N92-29435
NARROWBAND
Statistics of narrowband white noise derived from clipped broadband white noise
[AD-A248597] p 3434 N92-29563
NASA PROGRAMS
Multi-wavelength measurements of the stratospheric aerosol layer made at Hampton, Virginia (37N, 76W)
p 3460 N92-29249
NASA Workshop on future directions in surface modeling and grid generation
[NASA-CP-10092] p 3400 N92-29625
Research in NASA history: A guide to the NASA history program
[NASA-TM-107953] p 3571 N92-29689
NASA SPACE PROGRAMS
EOS Data and Information System (EOSDIS) --- landsat satellites
[NASA-TM-107922] p 3488 N92-29442
ATLAS 1: Encountering planet Earth
[NASA-TM-107956] p 3408 N92-30016
NASA's Earth Observing System
[S-HRG-102-647] p 3490 N92-30017
NATIONAL LAUNCH VEHICLE PROGRAM
National Launch System cycle 1 loads and models data book
[NASA-TM-103560] p 3408 N92-30215
NATURAL LANGUAGE (COMPUTERS)
An ontology of ceramics
[MEMO-INF-91-85] p 3426 N92-29960
NAVIER-STOKES EQUATION
Monopolar vortices as relative equilibria and their dissipative decay
[MEMO-1015] p 3446 N92-29977
Derivation of the kappa-epsilon model equations using the renormalization group method p 3450 N92-30055
Turbulence dynamics in the wavelet representation
p 3454 N92-30159

A numerical method for prediction of compressible turbulent flows with closure models
p 3454 N92-30164

NAVIGATION
Improving path planning with learning
[DE92-004360] p 3527 N92-29456

NAVIGATION AIDS
A systems analysis of the impact of navigation instrumentation on-board a Mars rover, based on a covariance analysis of navigation performance
[NASA-CR-189868] p 3403 N92-29440

NEAR FIELDS
Analyses of near- and far-field two-lobe patterns outside the output endface of a two-mode fiber
[NASA-CR-190494] p 3551 N92-29652

NEGATIVE ELECTRON AFFINITY
Growth, characterization, and device development in monocrystalline diamond films
[AD-A248993] p 3560 N92-30175

NEGATIVE IONS
Nonideal formation of network polymers
[AD-A248072] p 3424 N92-29465

NEODYMIUM LASERS
Development of mesospheric sodium laser beacon for atmospheric adaptive optics p 3470 N92-29308
Active modelocking and phase stabilization of a cavity dumped diode pumped Nd:YAG mini-laser
[DE92-011946] p 3475 N92-29358
Design and operation of the multipulse Thomson scattering diagnostic on DIII-D
[DE92-011393] p 3476 N92-29474
Synthesis and characterization of a covalently bound self-assembled macrocycle monolayer thin film for nonlinear optical materials
[DE92-011353] p 3545 N92-29634
Optical diagnostics on dense Z-pinch plasmas
[DE92-011228] p 3555 N92-29917

NETWORK ANALYSIS
A massively parallel genetic algorithm for the graph partitioning problem
[IMAG-RR-845-I] p 3525 N92-29610
Parallelization of the recursive gradient backpropagation algorithm
[IMAG-RR-854-M] p 3525 N92-29614
Sensitivity analysis of the load on an ethernet network
[MEMO-COSOR-91-41] p 3436 N92-29824
Port-controlled Hamiltonian systems: Modelling origins and systemtheoretic properties
[MEMO-1001] p 3537 N92-30077
A survey on minimum cost spanning tree games
[MEMO-1003] p 3541 N92-30079

NETWORK CONTROL
Ultra-dependable real-time computing
[AD-A248193] p 3515 N92-29409

NEURAL NETS
A systems theoretic investigation of neuronal network properties of the hippocampal formation
[AD-A250246] p 3510 N92-29334
Application of fuzzy logic-neural network based reinforcement learning to proximity and docking operations
[NASA-CR-190504] p 3525 N92-29390
Biologically-based neural network model of color constancy and color contrast
[AD-A248128] p 3510 N92-29398
Introduction to neural networks
[AD-A248258] p 3527 N92-29541
Object discrimination based on depth-from-occlusion
[AD-A248104] p 3511 N92-29560
Controlling the flow of visual information through the lateral geniculate nucleus: From single cells to neural networks
[AD-A250578] p 3528 N92-29590
Parallelization of the recursive gradient backpropagation algorithm
[IMAG-RR-854-M] p 3525 N92-29614
A universal, fault-tolerant, non-linear analytic network for modeling and fault detection
[DE92-011840] p 3525 N92-29624
Electronic neural network for solving traveling salesman and similar global optimization problems
[NASA-CASE-NPO-17807-2-CU] p 3529 N92-29955
Fast temporal neural learning using teacher forcing
[NASA-CASE-NPO-18553-1-CU] p 3530 N92-30085
Nonvolatile programmable neural network synaptic array
[NASA-CASE-NPO-18578-1-CU] p 3442 N92-30086

NEURONS
Controlling the flow of visual information through the lateral geniculate nucleus: From single cells to neural networks
[AD-A250578] p 3528 N92-29590
Physiological analyses of the afferents controlling brain neurochemical systems
[AD-A248334] p 3512 N92-29930

NEUROPHYSIOLOGY
A systems theoretic investigation of neuronal network properties of the hippocampal formation
[AD-A250246] p 3510 N92-29334

NEUTRAL ATOMS
Rare gas clusters containing charged atoms
[AD-A248299] p 3544 N92-29350
Statistical mechanics of collective phenomena in plasmas
[AD-A250581] p 3554 N92-29450
Low energy neutral atoms in the Earth's magnetosphere: Modeling
[DE92-013240] p 3500 N92-29536

NEUTRAL BEAMS
Intense diagnostic neutral beam development for ITER
[DE92-011262] p 3556 N92-30203

NEUTRALIZERS
Neutralizer and sample chamber for the Atomic Oxygen Simulation System (AOSS)
[NASA-CR-184343] p 3407 N92-29664

NEUTRINOS
Theory of elementary particles studies in weak interaction and grand unification and studies in accelerator design
[DE92-014309] p 3550 N92-29532

NEUTRON CROSS SECTIONS
Two neutron removal in relativistic nucleus-nucleus reactions p 3548 N92-30006
Relativistic Coulomb fission p 3548 N92-30008
Higgs-boson production in nucleus-nucleus collisions p 3548 N92-30009
Charge dependence and electric quadrupole effects on single-nucleon removal in relativistic and intermediate energy nuclear collisions p 3548 N92-30010
Single nucleon emission in relativistic nucleus-nucleus reactions p 3548 N92-30011

NEUTRON DIFFRACTION
LiMoN2: The first metallic layered nitride
[AD-A248446] p 3418 N92-29619
Neutron diffraction study of the electronic structure of high T(sub c) superconductor-related compounds
[DE92-012587] p 3559 N92-29939

NEUTRONS
Two neutron removal in relativistic nucleus-nucleus reactions p 3548 N92-30006

NICKEL
Neutralizer and sample chamber for the Atomic Oxygen Simulation System (AOSS)
[NASA-CR-184343] p 3407 N92-29664
Low-angle x ray diffraction study of solid state amorphization in a Ni/Ti multilayer p 3558 N92-29768

NICKEL ALLOYS
Fatigue in single crystal nickel superalloys
[AD-A248190] p 3420 N92-29408

NICKEL STEELS
Corrosion resistance of stainless steels and high Ni-Cr alloys to acid fluoride wastes
[DE92-012338] p 3420 N92-29436

NIGHT VISION
Visual acuity with second and third generation night vision goggles obtained from a new method of night sky simulation across a wide range of target contrast
[AD-A248284] p 3512 N92-29348
Evaluation of Night Vision Goggles (NVG) for maritime search and rescue
[AD-A247182] p 3512 N92-29538

NIOBIUM
The real-space multiple-scattering theory and the electronic structure of grain boundaries
[DE92-013006] p 3556 N92-29473

NIOBIUM ALLOYS
Strengthening mechanisms, creep and fatigue processes in dispersion hardened niobium alloy
[AD-A250282] p 3421 N92-29547

NITRIC ACID
The comparative effects of gamma radiation and in situ alpha particles on five strong-base anion exchange resins
[DE92-000177] p 3425 N92-29643

NITRIDES
LiMoN2: The first metallic layered nitride
[AD-A248446] p 3418 N92-29619

NITROGEN ATOMS
MNDO study of boron-nitrogen analogues of buckminsterfullerene
[AD-A247777] p 3414 N92-29460

NITROGEN COMPOUNDS
Air quality criteria for oxides of nitrogen, volume 3
[PB92-176387] p 3493 N92-29522

NITROGEN DIOXIDE
Air quality criteria for oxides of nitrogen, volume 3
[PB92-176387] p 3493 N92-29522

NITROGEN OXIDES
Air quality criteria for oxides of nitrogen, volume 1
[PB92-176361] p 3493 N92-29520
Air quality criteria for oxides of nitrogen, volume 2
[PB92-176379] p 3493 N92-29521
Air quality criteria for oxides of nitrogen, volume 3
[PB92-176387] p 3493 N92-29522

NOCTILUCENT CLOUDS
ARCLITE: The Arctic Lidar Technology Facility at Sondre Stromfjord, Greenland p 3407 N92-29283

NOISE (SOUND)
Active structural acoustic control and smart structures
[AD-A248341] p 3543 N92-29588

NOISE GENERATORS
Direct numerical simulation of instability and noise generation of hot jets p 3451 N92-30066

NOISE INTENSITY
Bandwidth compression of noisy signals with square-wave subcarrier p 3432 N92-29379

NOISE MEASUREMENT
Noise-optimal control of HEMT LNA's for compensation of temperature deviations p 3431 N92-29374
Global measurements of low-frequency radio noise
[AD-A248260] p 3434 N92-29542

NOISE PREDICTION
Validation of finite element and boundary element methods for predicting structural vibration and radiated noise
[NASA-TM-105359] p 3478 N92-29697

NOISE PREDICTION (AIRCRAFT)
Jet aircraft noise at high subsonic flight Mach numbers
[DLR-FB-91-28] p 3544 N92-29997

NOISE REDUCTION
Numerical procedures for analyzing dynamical processes
[AD-A248175] p 3515 N92-29399
Active structural acoustic control and smart structures
[AD-A248341] p 3543 N92-29588
Geostationary Operational Environmental Satellite (GOES-N report). Volume 2: Technical appendix
[NASA-TM-107920] p 3410 N92-29812
Jet aircraft noise at high subsonic flight Mach numbers
[DLR-FB-91-28] p 3544 N92-29997

NOISE SPECTRA
Multi-fractal analysis of nocturnal boundary layer time series from the Boulder Atmospheric Observatory
[AD-A248347] p 3502 N92-29424
Design and analysis of electrical circuits that produce fractional-order differentiation
[AD-A248085] p 3440 N92-29526

NOISE TEMPERATURE
Noise-optimal control of HEMT LNA's for compensation of temperature deviations p 3431 N92-29374
Figure of merit for direct-detection optical channels p 3431 N92-29376
Optimizing the G/T ratio of the DSS-13 34-meter beam-waveguide antenna p 3431 N92-29377

NOMENCLATURES
A look at the development environment and tools used in a large INGRES ABF application project
[DE92-012632] p 3561 N92-29552
Lexicon of new formal geologic names of the United States, 1981-1985
[PB92-181320] p 3563 N92-30040

NONDESTRUCTIVE TESTS
Method and apparatus for thermographically and quantitatively analyzing a structure for disbonds and/or inclusions
[NASA-CASE-LAR-14559-1] p 3480 N92-29829
Computed Tomography (CT) as a nondestructive test method used for composite helicopter components
[MBB-UD-0603-91-PUB] p 3480 N92-29873
Repair procedures for advanced composites for helicopters
[MBB-UD-0606-91-PUB] p 3399 N92-29874
The 1991 International Conference on Aging Aircraft and Structural Airworthiness
[NASA-CP-3160] p 3484 N92-30106
Federal Aviation Administration aging aircraft nondestructive inspection research plan p 3481 N92-30116
Inspection of aging aircraft: A manufacturer's perspective p 3481 N92-30117
Thermal QNDE detection of airframe disbonds p 3481 N92-30118
NDE research efforts at the FAA Center for Aviation Systems Reliability p 3481 N92-30119
Aging aircraft NDI Development and Demonstration Center (AANC): An overview --- nondestructive inspection p 3481 N92-30120
Nondestructive inspection perspectives p 3481 N92-30121
Current and future developments in civil aircraft non-destructive evaluation from an operator's point of view p 3399 N92-30122
Ageing airplane repair assessment program for Airbus A300 p 3402 N92-30123

Transport Canada aging aircraft activities p 3403 N92-30131

NONEQUILIBRIUM PLASMAS
Transport processes in beamed energy propulsion systems
[AD-A247296] p 3413 N92-29913

NONEQUILIBRIUM THERMODYNAMICS
The expanding plasma jet: Experiments and model
[ETN-92-91627] p 3555 N92-29761

NONLINEAR EQUATIONS
Two-dimensional boundary surfaces for planar external transonic flows
[AD-A248083] p 3444 N92-29524
A study of shock-associated magnetohydrodynamic waves in the solar wind
[NASA-CR-190567] p 3569 N92-29631
ISLAND: Interactive Solution Language for an Adaptive NIKE Driver
[DE92-011444] p 3533 N92-29791
Integrable deformations of meromorphic equations on P(exp 1)C
[MEMO-993] p 3534 N92-29872
Energy propagation in dissipative systems. Part 2: Centrovelocity for nonlinear wave equations
[MEMO-1016-PT-2] p 3437 N92-29978

NONLINEAR OPTICS
Transition crossing in the RHIC
[DE92-013031] p 3550 N92-29475
Synthesis and characterization of a covalently bound self-assembled macrocycle monolayer thin film for nonlinear optical materials
[DE92-011353] p 3545 N92-29634

NONLINEAR SYSTEMS
Parameter identification for nonlinear aerodynamic systems
[NASA-CR-190264] p 3399 N92-29329
Solution strategies for implicit nonlinear finite element analysis
[DE92-011466] p 3533 N92-29792
Instantaneous optimal control for linear, nonlinear and hysteretic structures: Stable controllers
[PB92-163807] p 3501 N92-29950

NONLINEARITY
Numerical modeling studies of the Gulf of Mexico and the Caribbean Sea using the Bryan-Cox model
[PB92-164987] p 3505 N92-29704
Non-linear interactions in homogeneous turbulence with and without background rotation p 3448 N92-30044
Turbulence and vortex structures p 3448 N92-30048
Single point modeling of initially isotropic turbulence under uniform rotation p 3449 N92-30054
A closer look at a Fibonacci-like iterated nonlinear map: More chaos and order
[MEMO-INF-91-70] p 3537 N92-30075
Organized motions underlying turbulent shear flows p 3453 N92-30158
Nonlinear analyses of composite aerospace structures in sonic fatigue
[NASA-CR-190565] p 3404 N92-30209

NOREPINEPHRINE
Physiological analyses of the afferents controlling brain neurochemical systems
[AD-A248334] p 3512 N92-29930

NORMAL DENSITY FUNCTIONS
A sensitivity analysis of circular error probable approximation techniques
[AD-A248105] p 3539 N92-29585
Computer program POWNOR for fitting the power-normal and -lognormal models to life or strength data from specimens of various sizes
[PB92-169119] p 3483 N92-29813
Limit theorems for functionals of convex hulls
[REPT-91-39] p 3535 N92-29921
A simple approximation to the bivariate normal distribution with large correlation coefficient
[MEMO-1011] p 3540 N92-29974
Testing equality of variances in the analysis of repeated measurements
[MEMO-1013] p 3541 N92-29976
Progress toward identification of streamwise vorticity meander in a plane mixing layer p 3451 N92-30068

NORMALIZING (STATISTICS)
Mapping agroecological zones and time lag in vegetation growth by means of Fourier analysis of time series of NDVI images
[REPT-32] p 3490 N92-29717

NUCLEAR BINDING ENERGY
Growth, characterization, and device development in monocrystalline diamond films
[AD-A248993] p 3560 N92-30175

NUCLEAR EXPLOSION EFFECT
Surface reactions in the space environment
[AD-A250624] p 3428 N92-29428

NUCLEAR FISSION
Relativistic Coulomb fission p 3548 N92-30008

NUCLEAR INTERACTIONS
Electromagnetic processes in nucleus-nucleus collisions relating to space radiation research
[NASA-CR-190533] p 3547 N92-30001
Cross section parameterizations for cosmic ray nuclei. 1: Single nucleon removal p 3547 N92-30002
Solution of two-body relativistic bound state equations with confining plus Coulomb interactions p 3547 N92-30003
Do recent observations of very large electromagnetic dissociation cross sections signify a transition towards non-perturbative QED? p 3438 N92-30004
Higgs-boson production in nucleus-nucleus collisions p 3548 N92-30009
Charge dependence and electric quadrupole effects on single-nucleon removal in relativistic and intermediate energy nuclear collisions p 3548 N92-30010
Single nucleon emission in relativistic nucleus-nucleus reactions p 3548 N92-30011
Stopping powers and cross sections due to two-photon processes in relativistic nucleus-nucleus collision p 3548 N92-30012

NUCLEAR MODELS
Classical aspects of weak interactions
[NIKHEF-H/91-25] p 3546 N92-29751
Spectroscopy of W-183; measured magnetic moments and rotation-particle coupling
[DE92-624790] p 3549 N92-30213

NUCLEAR PHYSICS
Program SIXPAK: A code designed to check double-differential correlated data and calculate equivalent uncorrelated data
[DE92-013752] p 3516 N92-29537
An introduction to using the FORTRAN programs provided with Computational Nuclear Physics 1 Nuclear Structure p 3549 N92-30013

NUCLEAR PROPULSION
Feasibility of an antiproton catalyzed fission fragment rocket
[AD-A248157] p 3412 N92-29444
Final Environmental Impact Statement (EIS) for the Space Nuclear Thermal Propulsion (SNTP) program: Appendices
[AD-A248409] p 3413 N92-29904

NUCLEAR RADIATION
Final Environmental Impact Statement (EIS) for the Space Nuclear Thermal Propulsion (SNTP) program
[AD-A248408] p 3413 N92-29903
Final Environmental Impact Statement (EIS) for the Space Nuclear Thermal Propulsion (SNTP) program: Appendices
[AD-A248409] p 3413 N92-29904

NUCLEAR REACTIONS
Program SIXPAK: A code designed to check double-differential correlated data and calculate equivalent uncorrelated data
[DE92-013752] p 3516 N92-29537

NUCLEAR REACTORS
Multichord spectroscopy of the D3-D divertor region
[DE92-013507] p 3554 N92-29412
Final Environmental Impact Statement (EIS) for the Space Nuclear Thermal Propulsion (SNTP) program
[AD-A248408] p 3413 N92-29903

NUCLEAR STRUCTURE
An introduction to using the FORTRAN programs provided with Computational Nuclear Physics 1 Nuclear Structure p 3549 N92-30013

NUCLEAR WEAPONS
Surface reactions in the space environment
[AD-A250624] p 3428 N92-29428

NUCLEON-NUCLEON INTERACTIONS
Two neutron removal in relativistic nucleus-nucleus reactions p 3548 N92-30006
Higgs-boson production in nucleus-nucleus collisions p 3548 N92-30009
Charge dependence and electric quadrupole effects on single-nucleon removal in relativistic and intermediate energy nuclear collisions p 3548 N92-30010
Single nucleon emission in relativistic nucleus-nucleus reactions p 3548 N92-30011

NUCLEONS
The O(alpha(s) cubed) QCD correction to the lowest moment of the longitudinal structure function in deep inelastic electron-nucleon scattering
[NIKHEF-H/91-19] p 3546 N92-29750
Electromagnetic processes in nucleus-nucleus collisions relating to space radiation research
[NASA-CR-190533] p 3547 N92-30001
Cross section parameterizations for cosmic ray nuclei. 1: Single nucleon removal p 3547 N92-30002
Do recent observations of very large electromagnetic dissociation cross sections signify a transition towards non-perturbative QED? p 3438 N92-30004

NUMBER THEORY
Minimal-change codes and number systems
[REPT-91-42] p 3536 N92-29924

NUMERICAL ANALYSIS
Acoustic scattering from elastic ice: A finite difference solution
[AD-A248281] p 3543 N92-29346
Viscous profiles and numerical methods for shock waves
[AD-A246110] p 3443 N92-29458
Numerical analysis of plasma transport in tandem volume magnetic multicusp ion sources
[AD-A248093] p 3554 N92-29528
On the numerical solution of one-dimensional integral and differential equations
[AD-A250388] p 3531 N92-29548
Annual research briefs, 1989
[NASA-CR-189024] p 3452 N92-30149
Expert judgment study on atmospheric dispersion and deposition: Main report and annexes
[REPT-91-81] p 3495 N92-30226

NUMERICAL CONTROL
DSS-13 26-meter antenna upgraded radiometer system p 3432 N92-29381

NUMERICAL FLOW VISUALIZATION
Patterns in simulated turbulent channel flow p 3455 N92-30169

NUMERICAL INTEGRATION
Two-dimensional boundary surfaces for planar external transonic flows
[AD-A248083] p 3444 N92-29524
Solving parabolic integro-differential equations by an explicit integration method
[CWI-NM-R9108] p 3534 N92-29883
On the numerical treatment of the advective terms in 3D shallow water models
[CWI-NM-R9110] p 3446 N92-29945

NUMERICAL WEATHER FORECASTING
Sampling and representativeness for a spaceborne wind lidar p 3463 N92-29268
The Laser Atmospheric Wind Sounder (LAWS) phase 2 preliminary system design p 3468 N92-29297
NWP impact of cloud top and boundary layer winds from a satellite borne lidar: An observing system simulation experiment p 3473 N92-29328

O

OBJECT PROGRAMS
Abstract data types and algorithm structures and a basis for component reuse
[REPT-91-49] p 3518 N92-29712

OBJECT-ORIENTED PROGRAMMING
Using object-oriented databases for implementation of interactive electronic technical manuals
[AD-A248135] p 3440 N92-29564
Abstract data types and algorithm structures and a basis for component reuse
[REPT-91-49] p 3518 N92-29712
Rendez-vous with metric semantics
[CWI-CS-R9135] p 3522 N92-29991

OBSERVABILITY (SYSTEMS)
A low sensitivity observer for complex biotechnological processes p 3509 N92-29757
Analytical tuning of a low sensitivity observer applied to a continuous ethanol fermentation with product recovery p 3509 N92-29758

OBSERVATION
Sensor fault detection on board an aircraft with observer and polynomial classifier
[DLR-FB-91-34] p 3404 N92-29870

OBSERVATORIES
The JPL Table Mountain and Mauna Loa stratospheric ozone lidars p 3458 N92-29239
The NDSC primary site at the Observatoire de Haute-Provence: Ozone and aerosols observations (1986-1992) p 3458 N92-29240
Lidar atmospheric observatory in the Canadian Arctic p 3458 N92-29241
CoMStOC 4: Multiwaveband observations of sunspot and plage-associated coronal emission
[AD-A248344] p 3570 N92-29632
ATLAS 1: Encountering planet Earth
[NASA-TM-107956] p 3408 N92-30016

OBSTACLE AVOIDANCE
Path tracking using simple planar curves
[AD-A248252] p 3403 N92-29617

OCCLUSION
Object discrimination based on depth-from-occlusion
[AD-A248104] p 3511 N92-29560
Visual pattern completion
[PB92-187418] p 3524 N92-30195

OCCULTATION
Occultation of a compact radio source by Venus p 3429 N92-29366

OCEAN BOTTOM
Circulation and exchange at the continental shelf and slope SEEP-2
[DE92-013500] p 3504 N92-29439
Finite difference modelling of seismic wave propagation at the seafloor
[AD-A248345] p 3505 N92-29562
Land-based seismic array studies of low frequency ambient oceanic noise
[AD-A248255] p 3505 N92-29618
OCEAN CURRENTS
Circulation and exchange at the continental shelf and slope SEEP-2
[DE92-013500] p 3504 N92-29439
SeaWiFS technical report series. Volume 1: An overview of SeaWiFS and ocean color
[NASA-TM-104566-VOL-1] p 3505 N92-29686
Intercomparison of global marine climatologies
[DE92-011389] p 3494 N92-29790
Shelf Mixed Layer Experiment (SMILE) program description and coastal and moored array data report
[PB92-170281] p 3506 N92-29805
OCEAN DATA ACQUISITIONS SYSTEMS
Class A network Dataring gauges: 1989 data processing and analysis
[REPT-18-1991] p 3505 N92-29684
OCEAN DYNAMICS
SeaWiFS technical report series. Volume 1: An overview of SeaWiFS and ocean color
[NASA-TM-104566-VOL-1] p 3505 N92-29686
OCEAN MODELS
Ocean optical modeling: Light field structure, internal radiant emission, and vertical inhomogeneities
[AD-A248272] p 3504 N92-29345
Finite difference modelling of seismic wave propagation at the seafloor
[AD-A248345] p 3505 N92-29562
OCEANOGRAPHY
Ocean optical modeling: Light field structure, internal radiant emission, and vertical inhomogeneities
[AD-A248272] p 3504 N92-29345
Circulation and exchange at the continental shelf and slope SEEP-2
[DE92-013500] p 3504 N92-29439
Shelf Mixed Layer Experiment (SMILE) program description and coastal and moored array data report
[PB92-170281] p 3506 N92-29805
OCEANS
Laser remote sensing of pollution on water surfaces p 3467 N92-29290
Revising M-layer: Complex exponent representation
[AD-A249121] p 3435 N92-29599
SeaWiFS technical report series. Volume 1: An overview of SeaWiFS and ocean color
[NASA-TM-104566-VOL-1] p 3505 N92-29686
NOAA environmental digest: Selected indicators of the United States and the global environment, December 1991
[PB92-185073] p 3494 N92-30019
SeaWiFS technical report series. Volume 5: Ocean optics protocols for SeaWiFS validation
[NASA-TM-104566] p 3506 N92-30193
ON-LINE SYSTEMS
On-line replacement of program modules using AdaPT
[NASA-CR-190499] p 3514 N92-29363
Sequential design of a linear quadratic controller for the Deep Space Network antennas p 3432 N92-29382
B(exp 2)UBIST: A strategy for boundary scan board unified BIST
[IMAG-RR-862-I] p 3441 N92-29612
Enhanced evaluation, selection and acceptance criteria for the Contractor Integrated Technical Information Service (CITIS)
[PB92-163856] p 3562 N92-29699
The use of state estimators (observers) for on-line estimation of non-measurable process variables p 3508 N92-29755
Sequential application of data reconciliation for sensitive detection of systematic errors p 3509 N92-29760
ONBOARD EQUIPMENT
Evaluation of Night Vision Goggles (NVG) for maritime search and rescue
[AD-A247182] p 3512 N92-29538
OPERATORS (MATHEMATICS)
On the parity of fundamental solutions for one-dimensional scattering problem with inverse square potential
[DE92-624511] p 3560 N92-29533
On the numerical solution of one-dimensional integral and differential equations
[AD-A250388] p 3531 N92-29548
Discretization of morphological operators
[CWI-BS-R9118] p 3533 N92-29861
Gaarding inequalities for systems of pseudo-differential operators
[CWI-AM-R9111] p 3534 N92-29881
OPTICAL COMMUNICATION
Micro-device for coupling, multiplexing and demultiplexing using elliptical-core two-mode fiber
[NASA-CR-190496] p 3550 N92-29331
Performance measurement results for a 220 Mbps QPPM optical communication receiver with an EG/G Slik APD
[NASA-CR-190561] p 3435 N92-29658
OPTICAL CORRECTION PROCEDURE
The optical design of AmPS: Elements of the design of a pulse stretcher
[ETN-92-91626] p 3552 N92-29859
OPTICAL EQUIPMENT
The optical design of AmPS: Elements of the design of a pulse stretcher
[ETN-92-91626] p 3552 N92-29859
Optoelectronic integration
[AD-A248950] p 3442 N92-29936
Dynamic aperture fringe discriminator
[NASA-CASE-NPO-18478-1-CU] p 3553 N92-30084
OPTICAL FIBERS
Micro-device for coupling, multiplexing and demultiplexing using elliptical-core two-mode fiber
[NASA-CR-190496] p 3550 N92-29331
Near-visible Raman instrumentation for remote multi-point process monitoring using optical fibers and optical multiplexing
[DE92-011287] p 3550 N92-29337
Developments in fiber optics for distribution automation
[NASA-CR-190454] p 3551 N92-29679
Erbium-doped fiber amplifier elements for structural analysis sensors
[NASA-CR-190491] p 3552 N92-29681
Optical fiber sensor having an active core
[NASA-CASE-LAR-14607-1SB] p 3553 N92-30029
OPTICAL MEASUREMENT
Optical pumping of mesospheric sodium: A new measurement capability p 3470 N92-29310
Magnetic properties of nano-heterogeneous amorphous thin films
[AD-A250570] p 3420 N92-29426
Improved real-time imaging spectrometer
[NASA-CASE-NPO-18410-1-CU] p 3552 N92-29832
Studies of distant clusters of galaxies p 3566 N92-29843
Clusters of galaxies in depth p 3567 N92-29846
Optical searches for ROSAT x ray cluster sources p 3568 N92-29853
Evaluation of an aureole lidar technique for estimating extinction profiles
[AD-A249740] p 3501 N92-30087
OPTICAL MEASURING INSTRUMENTS
Condenser optics, partial coherence, and imaging for soft x ray projection lithography
[DE92-011762] p 3551 N92-29484
Using phase retrieval to determine the intensity and phase of an ultrashort laser pulse
[DE92-013564] p 3476 N92-29516
Study of optical techniques for the Ames unitary wind tunnels. Part 3: Angle of attack
[NASA-CR-190541] p 3406 N92-29655
Center of excellence: Microlaser microscope
[DE92-013485] p 3477 N92-29928
High resolving power spectrometer for beam analysis
[DE92-010751] p 3437 N92-29988
OPTICAL PATHS
Infrared pulse-laser long-path absorption measurement of carbon dioxide using a Raman-shifted dye laser p 3465 N92-29277
OPTICAL POLARIZATION
Polarization perception device
[NASA-CASE-MSC-21915-1] p 3552 N92-30027
OPTICAL PROPERTIES
Three-wavelength lidar measurements of Pinatubo aerosol and its optical properties p 3460 N92-29250
Ocean optical modeling: Light field structure, internal radiant emission, and vertical inhomogeneities
[AD-A248272] p 3504 N92-29345
Method of forming silicon structures with selectable optical characteristics
[NASA-CASE-NPO-18625-1-CU] p 3559 N92-30102
Optical and electrical characteristics of the cathode fall
[AD-A249010] p 3443 N92-30176
SeaWiFS technical report series. Volume 5: Ocean optics protocols for SeaWiFS validation
[NASA-TM-104566] p 3506 N92-30193
Biophysical, morphological, canopy optical property, and productivity data from the Superior National Forest
[NASA-TM-104568] p 3491 N92-30210
OPTICAL PUMPING
Active modelocking and phase stabilization of a cavity dumped diode pumped Nd:YAG mini-laser
[DE92-011946] p 3475 N92-29358
Ion collision effects in hydrogen-like recombination x ray lasers
[DE92-013515] p 3476 N92-29509
OPTICAL RADAR
Sixteenth International Laser Radar Conference, part 1
[NASA-CP-3158-PT-1] p 3456 N92-29228
Long term stratospheric aerosol lidar measurements in Kyushu p 3456 N92-29229
Southern Hemisphere lidar measurements of the aerosol clouds from Mt. Pinatubo and Mt. Hudson p 3456 N92-29230
Stratospheric backscatter, extinction, and lidar ratio profiling after the Mt. Pinatubo eruptions p 3456 N92-29231
Measurements of stratospheric Pinatubo aerosol extinction profiles by a Raman lidar p 3457 N92-29232
Raman lidar measurements of Pinatubo aerosols over southeastern Kansas during November-December 1991 p 3457 N92-29233
Lidar observations of stratospheric aerosol layer after the Mt. Pinatubo volcanic eruption p 3457 N92-29234
The role of lidars in global change research p 3457 N92-29235
Interpretation of DIAL measurements of lower stratospheric ozone in regions with Pinatubo aerosols p 3457 N92-29236
Correcting for interference of Mt. Pinatubo aerosols on DIAL measurements of stratospheric ozone p 3458 N92-29237
A new Raman DIAL technique for measuring stratospheric ozone in the presence of volcanic aerosols p 3458 N92-29238
The JPL Table Mountain and Mauna Loa stratospheric ozone lidars p 3458 N92-29239
The NDSC primary site at the Observatoire de Haute-Provence: Ozone and aerosols observations (1986-1992) p 3458 N92-29240
Lidar atmospheric observatory in the Canadian Arctic p 3458 N92-29241
Observation of stratospheric ozone with NIES lidar system in Tsukuba, Japan p 3459 N92-29242
Observations of ozone-aerosol correlated behaviour in the lower stratosphere during the EASOE campaign p 3459 N92-29243
First results from TROLIX 1991: An intercomparison of tropospheric ozone lidars p 3459 N92-29244
The global backscatter experiment airborne pulsed lidar measurements p 3459 N92-29246
Multi-wavelength airborne lidar intercomparisons of aerosol and cirrus backscatter over the Pacific Ocean p 3460 N92-29247
Airborne lidar observations of the stratosphere after the Pinatubo eruption p 3460 N92-29248
Multi-wavelength measurements of the stratospheric aerosol layer made at Hampton, Virginia (37N, 76W) p 3460 N92-29249
Three-wavelength lidar measurements of Pinatubo aerosol and its optical properties p 3460 N92-29250
Lidar observations of the Pinatubo stratospheric aerosol cloud over Frascati, Italy p 3460 N92-29251
L625 lidar measurements of Pinatubo volcanic cloud at Hefei p 3460 N92-29252
Two wavelength measurements of the Pinatubo aerosol above Toronto, Canada p 3461 N92-29253
Lidar observations of the Pinatubo volcanic cloud over Hampton, Virginia p 3461 N92-29254
Ozone measurements with the US EPA UV-DIAL: Preliminary results p 3461 N92-29255
Lidar development for the Atmospheric Radiation Measurement (ARM) Program p 3461 N92-29256
Lidar measurements of stratospheric ozone, temperature and aerosol during 1992 UARS correlative measurement campaign p 3461 N92-29257
Airborne dial remote sensing of the Arctic ozone layer p 3462 N92-29258
A multi-wavelength ozone lidar for the EASOE experiment p 3462 N92-29260
Correction of DIAL stratospheric ozone measurements in the presence of Pinatubo aerosols p 3462 N92-29261
The Laser Atmospheric Wind Sounder (LAWS) preliminary error budget and performance estimate p 3462 N92-29262
Lag angle compensation in a space borne scanning lidar p 3462 N92-29263
Lidar In-space Technology Experiment (LITE) electronics overview p 3462 N92-29264
Laser Transmitter Module (LTM) for LITE p 3463 N92-29265
Intercomparisons of lidar backscatter measurements and in-situ data from GLOBE p 3463 N92-29266
Simulation of the performances of WIND, an airborne CO2 lidar p 3463 N92-29267

Sampling and representativeness for a spaceborne wind lidar p 3463 N92-29268
Identification of critical design points for the EAP of a space-based Doppler lidar wind sounder p 3463 N92-29270
Wind profiles derived from volume imaging lidar data: Enhancements to the algorithm and comparisons with insitu observations p 3464 N92-29271
Measurements of wind divergence with volume imaging lidar p 3464 N92-29272
DIAL mapping of atmospheric atomic mercury of geophysical origin p 3464 N92-29273
Lidar tracking of multiple fluorescent tracers: Method and field test p 3464 N92-29274
Lidar monitoring of Mexico City's atmosphere during high air polution episodes p 3464 N92-29275
Lab-scale lidar sensing of diesel engines exhausts p 3464 N92-29276
Transportable lidar for the measurement of ozone concentration and flux profiles in the lower troposphere p 3465 N92-29278
Remote detection of biological particles and chemical plumes using UV fluorescence lidar p 3465 N92-29279
Signal quality influence on averaging procedure for DIAL pollution monitoring p 3465 N92-29280
Extraction of aerosol and Rayleigh components from Doppler lidar return signal p 3465 N92-29281
ARCLITE: The Arctic Lidar Technology Facility at Sondre Stromfjord, Greenland p 3407 N92-29283
Rotational Raman lidar for lower tropospheric temperature profiling p 3466 N92-29284
One year of Rayleigh lidar measurements at Toronto p 3466 N92-29285
Lidar observation of aerosol and temperature stratification over urban area during the formation of a stable atmospheric PBL p 3466 N92-29286
A comparison between Raman lidar and conventional contact measurements of atmospheric temperature p 3466 N92-29287
Efficiencies of rotational Raman and Rayleigh techniques for laser remote sensing of the atmospheric temperature p 3467 N92-29288
Lidar investigation of aerosol pollution distribution near a coal power plant p 3467 N92-29289
Laser remote sensing of pollution on water surfaces p 3467 N92-29290
Correlation analysis of wind lidar data p 3467 N92-29291
A developing multiple-wavelength lidar for detecting mainly ozone and aerosol distributions in the stratosphere p 3467 N92-29292
An extension of the Raman-lidar technique to measure the velocity and temperature of the atmospheric emission jets from stacks p 3467 N92-29293
Lidar observations of stratospheric clouds after volcanic eruption of Pinatubo p 3468 N92-29294
GE's mobile, coherent Doppler lidar test/evaluation facilities p 3407 N92-29299
The e-beam sustained laser technology for space-based Doppler wind lidar p 3469 N92-29300
The Lidar In-Space Technology Experiment (LITE) p 3469 N92-29301
System testing and performance characterization of the LITE Laser Transmitter Module at NASA p 3469 N92-29302
Mechanical and thermal issues in the development of a spaceborne lidar system p 3469 N92-29303
Lidar measurements of aerosol and ozone distributions during the 1992 Airborne Arctic Stratospheric Expedition p 3469 N92-29304
Airborne lidar measurements of stratospheric aerosols during the European Arctic Stratospheric Ozone Experiment (EASOE) p 3469 N92-29305
Aerosols and polar stratospheric clouds measurements during the EASOE campaign p 3469 N92-29306
Lidar observations of polar stratospheric clouds and stratospheric temperatures at the South Pole p 3470 N92-29307
Optical pumping of mesospheric sodium: A new measurement capability p 3470 N92-29310
Lidar probing of the mesosphere: Simultaneous observations of sporadic sodium and iron formations, calcium ion layers, neutral temperature and winds p 3470 N92-29311
Lidar measurements of metallic species in mesopause region p 3470 N92-29312
Sodium Doppler temperature lidar observations of the mesopause region temperature and wind structure p 3471 N92-29314
Airborne sodium and Rayleigh lidar observations from ALOHA-90 p 3471 N92-29315
Rayleigh/Raman Greenland lidar observations of atmospheric temperature during a major Arctic stratospheric warming event p 3471 N92-29316
Elastic and Raman lidar temperature measurements from Poker Flat, Alaska during February 1992 p 3471 N92-29317
Rayleigh/Raman lidars: Intercomparisons and validation p 3471 N92-29318
Lidar studies of extinction in clouds in the ECLIPS project p 3472 N92-29320
Lidar studies of clouds at Toronto during the ECLIPS program p 3472 N92-29321
Adaptation of the University of Wisconsin high spectral resolution lidar for polarization and multiple scattering measurements p 3472 N92-29322
Polarization lidar liquid cloud detection algorithm for winter mountain storms p 3472 N92-29323
Measurement of mean or effective radius of cloud drop size distributions with a 10.6-micron wavelength lidar p 3472 N92-29324
Observations of cirrus clouds over the Pacific region by the NASA multiwavelength lidar system p 3473 N92-29325
Diode-pumped Nd:YAG lidar for airborne cloud measurements p 3473 N92-29326
Remote sensing by spaceborne lidar aided by surface returns p 3473 N92-29327
NWP impact of cloud top and boundary layer winds from a satellite borne lidar: An observing system simulation experiment p 3473 N92-29328
Evaluation of an aureole lidar technique for estimating extinction profiles [AD-A249740] p 3501 N92-30087

OPTICAL SCANNERS
Study of optical techniques for the Ames unitary wind tunnels. Part 3: Angle of attack [NASA-CR-190541] p 3406 N92-29655

OPTICAL SWITCHING
Optoelectronic integration [AD-A248950] p 3442 N92-29936

OPTIMAL CONTROL
Developing CMMCA flight profiles for cruise missile tracking [AD-A248183] p 3434 N92-29406
Feedback control laws for highly maneuverable aircraft [NASA-CR-190535] p 3406 N92-29654
The isopone method in optimal control [REPT-91-52] p 3529 N92-29764
On the p-coverage problem on the real line [MEMO-COSOR-91-33] p 3520 N92-29818
Instantaneous optimal control for linear, nonlinear and hysteretic structures: Stable controllers [PB92-163807] p 3501 N92-29950
Polynomial methods in H(infinity)-optimal control [MEMO-1008] p 3530 N92-29971
Some feedback procedures for control of flows p 3452 N92-30070
Separable Markovian decision problems: The linear programming method in the multichain case (revised) [PB92-187350] p 3524 N92-30201

OPTIMIZATION
Optimal design of compact spur gear reductions [NASA-TM-105676] p 3478 N92-29351
Taguchi methods [MEMO-COSOR-91-31] p 3539 N92-29609
Parallelization of the recursive gradient backpropagation algorithm [IMAG-RR-854-M] p 3525 N92-29614
SOLCHIPS: A fast predesign and optimization tool for solar heating with seasonal storage [DE92-506509] p 3492 N92-29636
Concurrent engineering in design of aircraft structures [MBB-FE-2-S-PUB-472] p 3404 N92-29650
Architectural synthesis and optimization of digital systems [ISBN-90-9003966-X] p 3519 N92-29782
On the complexity of postoptimality analysis of 0/1 programs [MEMO-COSOR-91-35] p 3520 N92-29820
Aerodynamic design optimization using sensitivity analysis and computational fluid dynamics [NASA-CASE-LAR-14815-1-CU] p 3445 N92-29830
Parameter identification in tidal models with uncertain boundaries [MEMO-983] p 3540 N92-29856
Optimality of wait-free atomic multiwriter variables [CWI-CS-R9128] p 3520 N92-29868
Optimal copying strategies [MEMO-1005] p 3537 N92-30081
Chebyshev line approximation: A sensitivity analysis [MEMO-1020] p 3537 N92-30147
Optimal parallel parsing of almost all LL(k) grammars [MEMO-INF-91-78] p 3527 N92-30189

OPTOELECTRONIC DEVICES
Optoelectronic integration [AD-A248950] p 3442 N92-29936

ORBIT CALCULATION
A determination of the radio-planetary frame tie from comparison of Earth orientation parameters p 3409 N92-29365
Orbiter-orbiter and orbiter-lander tracking using same-beam interferometry p 3409 N92-29369

ORBITAL RENDEZVOUS
Application of fuzzy logic-neural network based reinforcement learning to proximity and docking operations [NASA-CR-190504] p 3525 N92-29390

ORCHARDS
Application of laser imaging for bio/geophysical studies p 3465 N92-29282

ORDER-DISORDER TRANSFORMATIONS
Solid state structures of some Dithionoamido-18-crown-6 ligands [AD-A248098] p 3556 N92-29558

ORGANIC SEMICONDUCTORS
Electrochemistry in colloids and dispersions. Volume 1: Electroanalytical methods and applications, electrosynthesis and electrocatalysis, polymers and latexes [AD-A248335] p 3418 N92-29557

ORGANOMETALLIC COMPOUNDS
OMVPE growth of InAsSbBi and related alloys using new organometallic group 5 sources [AD-A250631] p 3557 N92-29635

ORGANOMETALLIC POLYMERS
Synthesis and useful reactions of organosilicon polymeric precursors for ceramics [AD-A248500] p 3424 N92-29496

ORTHOGONAL FUNCTIONS
Positive convolution structures associated with quantum groups [CWI-AM-R9105] p 3534 N92-29866
Askey-Wilson polynomials for root systems of type BC [CWI-AM-R9112] p 3534 N92-29882

ORTHOGONALITY
Some applications of orthogonal functions to probability and statistics [ETN-92-91741] p 3538 N92-29491
Taguchi methods [MEMO-COSOR-91-31] p 3539 N92-29609
Random walk polynomials and random walk measures [MEMO-1007] p 3536 N92-29999

OSCILLATING FLOW
Multidimensional computer simulation of Stirling cycle engines [NASA-CR-190497] p 3478 N92-29392
Heat exchanger with oscillating flow [NASA-CASE-LAR-14033-2] p 3447 N92-30024
Experimental investigation of the flowfield of an oscillating airfoil [NASA-TM-105675] p 3402 N92-30182

OSCILLATIONS
Prospects for long baseline neutrino oscillation experiments [DE92-011833] p 3544 N92-29356

OSCILLATORS
Deep-space navigation with differenced data types. Part 3: An expanded information content and sensitivity analysis p 3409 N92-29368

OSEEN APPROXIMATION
Theoretical and experimental aspects of velocity slip by flows along solid walls [ISBN-3-7983-1446-2] p 3446 N92-29968

OSMOMETERS
In vitro measurement of nucleus pulposus swelling pressure: A new technique for studies of spinal adaptation to gravity [NASA-TM-103853] p 3506 N92-29397

OVER-THE-HORIZON RADAR
Tracking hurricane Claudette with the US Air Force OTH-B radar [PB92-164524] p 3503 N92-29800
HFRAD hindcast: An OTH-B radar and model comparison study [AD-A248065] p 3436 N92-29902

OXIDATION
New directions for the catalytic conversion of methane [PB92-172360] p 3492 N92-29519
A study of the influence of alloying additions on the passivity of aluminum [AD-A248339] p 3421 N92-29587
Review of temperature dependent effects on the oxidation protection of carbon/carbon [DE92-012333] p 3415 N92-29645
A study and feasibility of ultra thin silica layers by rapid thermal processing [LAAS-91393] p 3422 N92-29674
Flux-capacity relationships of Acinetobacter calcoaceticus enzymes during xylose oxidation p 3508 N92-29739
A perspective on MoSi2 based composites [DE92-013434] p 3415 N92-29795

OXIDATION RESISTANCE
Magnetic properties of nano-heterogeneous amorphous thin films
[AD-A250570] p 3420 N92-29426
Development and characterization of oxidation-protected CFC
[MBB-Z-0395-91-PUB] p 3416 N92-29876
OXIDATION-REDUCTION REACTIONS
Electrical connection of enzyme redox centers to electrodes
[AD-A248545] p 3440 N92-29575
OXIDES
Cursory examination of the zeta potential behaviors of two optical materials
[DE92-011588] p 3551 N92-29578
OXYGEN
The O2 reduction at the IFC modified O2 fuel cell electrode
[NASA-TM-105691] p 3413 N92-29667
Converting a CO2 atmosphere to a high-purity O2 supply
[NASA-CASE-LAR-14398-1] p 3419 N92-30098
OXYGEN ATOMS
Neutralizer and sample chamber for the Atomic Oxygen Simulation System (AOSS)
[NASA-CR-184343] p 3407 N92-29664
Converting a CO2 atmosphere to a high-purity O2 supply
[NASA-CASE-LAR-14398-1] p 3419 N92-30098
A method for making biocompatible polymer articles using atomic oxygen
[NASA-CASE-MSC-21529-1] p 3427 N92-30100
OXYGEN IONS
Neutralizer and sample chamber for the Atomic Oxygen Simulation System (AOSS)
[NASA-CR-184343] p 3407 N92-29664
OXYGEN SUPPLY EQUIPMENT
Neutralizer and sample chamber for the Atomic Oxygen Simulation System (AOSS)
[NASA-CR-184343] p 3407 N92-29664
OZONE
The NDSC primary site at the Observatoire de Haute-Provence: Ozone and aerosols observations (1986-1992) p 3458 N92-29240
Observations of ozone-aerosol correlated behaviour in the lower stratosphere during the EASOE campaign p 3459 N92-29243
First results from TROLIX 1991: An intercomparison of tropospheric ozone lidars p 3459 N92-29244
Ozone measurements with the US EPA UV-DIAL: Preliminary results p 3461 N92-29255
Airborne dial remote sensing of the Arctic ozone layer p 3462 N92-29258
Lidar measurement of stratospheric ozone at Hohenpeissenberg: An improved evaluation method p 3462 N92-29259
A multi-wavelength ozone lidar for the EASOE experiment p 3462 N92-29260
Correction of DIAL stratospheric ozone measurements in the presence of Pinatubo aerosols p 3462 N92-29261
Transportable lidar for the measurement of ozone concentration and flux profiles in the lower troposphere p 3465 N92-29278
A developing multiple-wavelength lidar for detecting mainly ozone and aerosol distributions in the stratosphere p 3467 N92-29292
Lidar measurements of aerosol and ozone distributions during the 1992 Airborne Arctic Stratospheric Expedition p 3469 N92-29304
Airborne lidar measurements of stratospheric aerosols during the European Arctic Stratospheric Ozone Experiment (EASOE) p 3469 N92-29305
Aerosols and polar stratospheric clouds measurements during the EASOE campaign p 3469 N92-29306
Lidar observations of polar stratospheric clouds and stratospheric temperatures at the South Pole p 3470 N92-29307
A preliminary design and analysis of an advanced heat-rejection system for an extreme altitude advanced variable cycle diesel engine installed in a high-altitude advanced research platform
[NASA-CR-186021] p 3405 N92-29427
New developments in emission projection methodologies
[PB92-139393] p 3495 N92-30031
OZONE DEPLETION
Lidar atmospheric observatory in the Canadian Arctic p 3458 N92-29241
Airborne lidar measurements of stratospheric aerosols during the European Arctic Stratospheric Ozone Experiment (EASOE) p 3469 N92-29305
Aerosols and polar stratospheric clouds measurements during the EASOE campaign p 3469 N92-29306
Lidar observations of polar stratospheric clouds and stratospheric temperatures at the South Pole p 3470 N92-29307
OZONOMETRY
Correcting for interference of Mt. Pinatubo aerosols on DIAL measurements of stratospheric ozone p 3458 N92-29237
A new Raman DIAL technique for measuring stratospheric ozone in the presence of volcanic aerosols p 3458 N92-29238
The JPL Table Mountain and Mauna Loa stratospheric ozone lidars p 3458 N92-29239
Observation of stratospheric ozone with NIES lidar system in Tsukuba, Japan p 3459 N92-29242
First results from TROLIX 1991: An intercomparison of tropospheric ozone lidars p 3459 N92-29244
Lidar measurements of stratospheric ozone, temperature and aerosol during 1992 UARS correlative measurement campaign p 3461 N92-29257
Lidar measurement of stratospheric ozone at Hohenpeissenberg: An improved evaluation method p 3462 N92-29259
Correction of DIAL stratospheric ozone measurements in the presence of Pinatubo aerosols p 3462 N92-29261
Transportable lidar for the measurement of ozone concentration and flux profiles in the lower troposphere p 3465 N92-29278
Airborne lidar measurements of stratospheric aerosols during the European Arctic Stratospheric Ozone Experiment (EASOE) p 3469 N92-29305
Lidar observations of polar stratospheric clouds and stratospheric temperatures at the South Pole p 3470 N92-29307
OZONOSPHERE
Correcting for interference of Mt. Pinatubo aerosols on DIAL measurements of stratospheric ozone p 3458 N92-29237
Airborne dial remote sensing of the Arctic ozone layer p 3462 N92-29258
A multi-wavelength ozone lidar for the EASOE experiment p 3462 N92-29260

P

P-N-P JUNCTIONS
Study and realization of GaAs PNP homojunction bipolar transistors using ion implementation
[LAAS-91433] p 3441 N92-29729
PACIFIC OCEAN
Multi-wavelength airborne lidar intercomparisons of aerosol and cirrus backscatter over the Pacific Ocean p 3460 N92-29247
Tropical cyclones: Central North Pacific, 1991
[PB92-167345] p 3502 N92-29743
PACKETS (COMMUNICATION)
Sensitivity analysis of the load on an ethernet network
[MEMO-COSOR-91-41] p 3436 N92-29824
PAINTS
Laser paint stripping
[AD-A249233] p 3476 N92-29581
PAIR PRODUCTION
A letter of intent for an experiment to study strong electromagnetic fields at RHIC via multiple electromagnetic processes p 3438 N92-30015
PANEL METHOD (FLUID DYNAMICS)
Hyperbolic grid generation control by panel methods
[NLR-TP-91061-U] p 3532 N92-29604
A method for computing the 3-dimensional flow about wings with leading-edge vortex separation. Part 2: Description of computer program VORSEP
[NLR-TR-86006-U] p 3402 N92-29916
PANELS
Structural durability of stiffened composite shells
[NASA-CR-190588] p 3481 N92-29342
Combined load test apparatus for flat panels
[NASA-CASE-LAR-14698-1] p 3483 N92-30028
PARABOLIC DIFFERENTIAL EQUATIONS
Solving parabolic integro-differential equations by an explicit integration method
[CWI-NM-R9108] p 3534 N92-29883
Abstract quasilinear equations and application to a groundwater flow problem
[REPT-91-41] p 3535 N92-29923
PARABOLIC REFLECTORS
Microstrip reflectarray antenna for the SCANSCAT radar application
[NASA-CR-190453] p 3434 N92-29463
PARALLEL COMPUTERS
Numerical methods for the 3D shallow water equations on vector and parallel computers
[CWI-NM-R9109] p 3446 N92-29944
PARALLEL FLOW
Heat transfer in an aluminum heat exchanger using normal hydrogen gas
[PB92-172832] p 3447 N92-30036
PARALLEL PROCESSING (COMPUTERS)
Introduction to neural networks
[AD-A248258] p 3527 N92-29541
Parallelization of the recursive gradient backpropagation algorithm
[IMAG-RR-854-M] p 3525 N92-29614
Methodology for the specification of communication activities within the framework of a multi-layered architecture: Toward the definition of a knowledge base
[LAAS-91466] p 3436 N92-29730
A case study in functional real-time programming
[MEMO-INF-91-62] p 3522 N92-30073
A model for dataflow query execution in a parallel main-memory environment
[MEMO-INF-91-34] p 3527 N92-30142
PARALLEL PROGRAMMING
A massively parallel genetic algorithm for the graph partitioning problem
[IMAG-RR-845-I] p 3525 N92-29610
Parallelization of the recursive gradient backpropagation algorithm
[IMAG-RR-854-M] p 3525 N92-29614
An annotated bibliography in parallel parsing
[REPT-91-64] p 3525 N92-29716
Analysis of parallel diagonal-implicit iteration of Runge-Kutta methods
[CWI-NM-R9114] p 3526 N92-29867
The primordial soup algorithm: A systematic approach to the specification and design of parallel parsers
[MEMO-INF-91-77] p 3536 N92-29956
PBT: A Parallel Bottom-up Tomita Parser
[MEMO-INF-91-69] p 3527 N92-30183
Optimal parallel parsing of almost all LL(k) grammars
[MEMO-INF-91-78] p 3527 N92-30189
PARAMETER IDENTIFICATION
Parameter identification for nonlinear aerodynamic systems
[NASA-CR-190264] p 3399 N92-29329
Modelling, information processing and control
[AD-A250571] p 3532 N92-29589
Sensitivity analysis of the load on an ethernet network
[MEMO-COSOR-91-41] p 3436 N92-29824
Parameter identification in tidal models with uncertain boundaries
[MEMO-983] p 3540 N92-29856
PARAMETERIZATION
A soil-canopy scheme for use in a numerical model of the atmosphere: 1D stand-alone model
[CSIRO-TP-23] p 3500 N92-29670
Cross section parameterizations for cosmic ray nuclei. 1: Single nucleon removal p 3547 N92-30002
Ageing airplane repair assessment program for Airbus A300 p 3402 N92-30123
Modeling of compressible turbulence p 3452 N92-30150
PARITY
On the parity of fundamental solutions for one-dimensional scattering problem with inverse square potential
[DE92-624511] p 3560 N92-29533
PARSING ALGORITHMS
An annotated bibliography in parallel parsing
[REPT-91-64] p 3525 N92-29716
The primordial soup algorithm: A systematic approach to the specification and design of parallel parsers
[MEMO-INF-91-77] p 3536 N92-29956
PBT: A Parallel Bottom-up Tomita Parser
[MEMO-INF-91-69] p 3527 N92-30183
Optimal parallel parsing of almost all LL(k) grammars
[MEMO-INF-91-78] p 3527 N92-30189
PARTIAL DIFFERENTIAL EQUATIONS
Acoustic scattering from elastic ice: A finite difference solution
[AD-A248281] p 3543 N92-29346
Computational acoustics
[AD-A247688] p 3543 N92-29441
Viscous profiles and numerical methods for shock waves
[AD-A246110] p 3443 N92-29458
Solving parabolic integro-differential equations by an explicit integration method
[CWI-NM-R9108] p 3534 N92-29883
Abstract quasilinear equations and application to a groundwater flow problem
[REPT-91-41] p 3535 N92-29923
Supersymmetric extensions of the nonlinear Schroedinger equation: Symmetries and coverings
[MEMO-1002] p 3537 N92-30078
PARTIAL PRESSURE
Converting a CO2 atmosphere to a high-purity O2 supply
[NASA-CASE-LAR-14398-1] p 3419 N92-30098

PARTICLE ACCELERATORS
Transition crossing in the RHIC
[DE92-013031] p 3550 N92-29475
The optical design of AmPS: Elements of the design of a pulse stretcher
[ETN-92-91626] p 3552 N92-29859
PARTICLE BEAMS
Burros: Simple, affordable, effective space transportation
[DE92-013553] p 3541 N92-30138
PARTICLE COLLISIONS
Theory of elementary particles studies in weak interaction and grand unification and studies in accelerator design
[DE92-014309] p 3550 N92-29532
Cross section parameterizations for cosmic ray nuclei. 1: Single nucleon removal p 3547 N92-30002
Do recent observations of very large electromagnetic dissociation cross sections signify a transition towards non-perturbative QED? p 3438 N92-30004
Two neutron removal in relativistic nucleus-nucleus reactions p 3548 N92-30006
Higgs-boson production in nucleus-nucleus collisions p 3548 N92-30009
Single nucleon emission in relativistic nucleus-nucleus reactions p 3548 N92-30011
Stopping powers and cross sections due to two-photon processes in relativistic nucleus-nucleus collision p 3548 N92-30012
Fourth workshop on Experiments and Detectors for a Relativistic Heavy Ion Collider
[BNL-52262] p 3549 N92-30014
PARTICLE EMISSION
Single nucleon emission in relativistic nucleus-nucleus reactions p 3548 N92-30011
PARTICLE INTERACTIONS
Contributions to Hadron 1991: 1) Testing the nature of the f(0)(S asterisk). 2) Gamma gamma to pi(exp 0) pi(exp 0): Dispersive analysis compared to chiral perturbation theory
[RAL-91-070] p 3544 N92-29488
Gamma gamma to pi(exp 0) pi(exp 0): Dispersive analysis compared to chiral perturbation theory p 3545 N92-29490
The dependence of transport coefficients of suspensions in quasistatic and retarded hydrodynamic interactions
[ETN-92-91624] p 3444 N92-29752
PARTICLE PRODUCTION
Higgs-boson production in nucleus-nucleus collisions p 3548 N92-30009
PARTICLE TELESCOPES
Exploratory study for a solid-state charged-particle spectrometer inside the Celsius ring: Alpha and hydrogen reactions at 1.7 and 2.2 GeV/c
[USIP-91-02] p 3546 N92-29715
PARTICLE TRACKS
Free ion yields in liquids: Molecular structure and track effects
[DE92-012208] p 3545 N92-29582
PARTICLE TRAJECTORIES
Exploratory study for a solid-state charged-particle spectrometer inside the Celsius ring: Alpha and hydrogen reactions at 1.7 and 2.2 GeV/c
[USIP-91-02] p 3546 N92-29715
PARTICLES
The influence of turbulence on aggregation of small particles in agitated vessels
[ETN-92-91629] p 3445 N92-29775
PARTITIONS (MATHEMATICS)
A massively parallel genetic algorithm for the graph partitioning problem
[IMAG-RR-845-I] p 3525 N92-29610
A new heuristic for load-balanced assignment of objects and minimized network communication in distributed programs implemented through inverse remote procedure calls
[MEMO-INF-91-91] p 3519 N92-29815
Computing distinguishing formulas for branching bisimulation
[CWI-CS-R9121] p 3521 N92-29890
Inverse remote procedure calls
[MEMO-INF-91-89] p 3521 N92-29970
PARTONS
Testing the nature of the f(0)(S asterisk) p 3545 N92-29489
PASCAL (PROGRAMMING LANGUAGE)
An algebraic specification for the static semantics of Pascal
[CWI-CS-R9129] p 3522 N92-29989
PASSENGER AIRCRAFT
Aging commuter aeroplanes: Fatigue evaluation and control methods p 3488 N92-30132
PASSIVITY
A study of the influence of alloying additions on the passivity of aluminum
[AD-A248339] p 3421 N92-29587
PATTERN RECOGNITION
Introduction to neural networks
[AD-A248258] p 3527 N92-29541
Recognition of multi-articulated three-dimensional objects using a multisensor system for robotics applications
[LAAS-91394] p 3529 N92-29675
River hydrometry by pattern recognition in remote sensing images
[PUBL-445] p 3490 N92-29728
Patterns in simulated turbulent channel flow p 3455 N92-30169
Analysis of a three-dimensional point pattern with replication
[CWI-BS-R9124] p 3541 N92-30180
Visual pattern completion
[PB92-187418] p 3524 N92-30195
PAYLOADS
Definition and design of an experiment to test raster scanning with rotating unbalanced-mass devices on gimbaled payloads
[NASA-TP-3249] p 3429 N92-29677
PERFORMANCE PREDICTION
Sensitivity analysis of the load on an ethernet network
[MEMO-COSOR-91-41] p 3436 N92-29824
PERFORMANCE TESTS
First results from TROLIX 1991: An intercomparison of tropospheric ozone lidars p 3459 N92-29244
Test and evaluation report of the physio control defibrillator/monitor model LIFEPAK (trademark) 8
[AD-A248283] p 3510 N92-29347
Visual acuity with second and third generation night vision goggles obtained from a new method of night sky simulation across a wide range of target contrast
[AD-A248284] p 3512 N92-29348
Multidimensional computer simulation of Stirling cycle engines
[NASA-CR-190497] p 3478 N92-29392
A comparison of the calculated and experimental off-design performance of a radial flow turbine
[NASA-CR-189207] p 3399 N92-29402
Test and evaluation report of the IMED volumetric infusion pump model 960A
[AD-A248538] p 3404 N92-29506
Cosine response characteristics of radiometric and photometric sensors
[DE92-011437] p 3551 N92-29530
CAESAR: A CCD airborne experimental scanner for applications in remote sensing radiometric and geometric calibration
[NLR-TP-89103-U] p 3490 N92-29707
Exploratory study for a solid-state charged-particle spectrometer inside the Celsius ring: Alpha and hydrogen reactions at 1.7 and 2.2 GeV/c
[USIP-91-02] p 3546 N92-29715
A method for analysing the performance aspects of the fault-tolerance mechanisms in FDDI
[MEMO-INF-91-92] p 3514 N92-29982
Performability modelling tools: A survey
[MEMO-INF-91-82] p 3523 N92-30191
PERIODIC VARIATIONS
Production of periodical Mach number variations in high subsonic flow in a blow down wind tunnel, and its influence on profile measurements
[ETN-92-91492] p 3401 N92-29889
PERMEABILITY
Magnetic properties of nano-heterogeneous amorphous thin films
[AD-A250570] p 3420 N92-29426
PERMITTIVITY
Laser processing for interconnect technology
[AD-A248103] p 3476 N92-29559
PERSONAL COMPUTERS
Application Center of Excellence (ACE) program
[AD-A248694] p 3562 N92-29934
PERSONNEL
Guide for evaluating 12 inch Substantial Dividing Walls (SDWs) to provide protection from remote operation, volume 2
[AD-A250252] p 3428 N92-29335
Guide for evaluating 12 inch Substantial Dividing Walls (SDWs) to provide protection from remote operation, volume 1
[AD-A250251] p 3428 N92-29545
Exercise and three psychosocial variables: A longitudinal study
[AD-A250649] p 3510 N92-30216
PERSONNEL DEVELOPMENT
Revision of certification standards for aviation maintenance personnel p 3487 N92-30127
PERT
On-line replacement of program modules using AdaPT
[NASA-CR-190499] p 3514 N92-29363
PERTURBATION
Stability of a premixed flame in stagnation-point flow against general disturbances
[NASA-CR-189666] p 3455 N92-30192
PERTURBATION THEORY
Contributions to Hadron 1991: 1) Testing the nature of the f(0)(S asterisk). 2) Gamma gamma to pi(exp 0) pi(exp 0): Dispersive analysis compared to chiral perturbation theory
[RAL-91-070] p 3544 N92-29488
Gamma gamma to pi(exp 0) pi(exp 0): Dispersive analysis compared to chiral perturbation theory p 3545 N92-29490
Two-dimensional boundary surfaces for planar external transonic flows
[AD-A248083] p 3444 N92-29524
The FORM version of MINCER
[NIKHEF-H/91-18] p 3518 N92-29747
PETRI NETS
Strong bisimilarity on nets revisited
[RR-847-I-IMAG-120-LIFIA] p 3532 N92-29573
Decision systems; the relation between problem specification and mathematical analysis
[MEMO-COSOR-91-37] p 3535 N92-29898
Performability modelling tools: A survey
[MEMO-INF-91-82] p 3523 N92-30191
PH FACTOR
Acetate in hydrothermal solutions: Decomposition kinetics and metal complexation
[DE92-010542] p 3417 N92-29551
PHARMACOLOGY
A sample-size optimal bayesian procedure for sequential pharmaceutical trials
[AD-A248512] p 3538 N92-29501
PHASE CONJUGATION
Phase conjugation in BaTiO3 at 830 nanometers
[AD-A250240] p 3475 N92-29332
PHASE CONTROL
Improvements in X-band transmitter phase stability through klystron body temperature regulation p 3431 N92-29373
PHASE DIAGRAMS
Structure and stability of Al-Cu-Ru face-centered icosahedral alloys
[DE92-012550] p 3422 N92-29706
Diffusion and phase relations in the systems Ti-Si-C and Ti-Si-N
[ETN-92-91631] p 3546 N92-29777
PHASE SHIFT KEYING
Detection of binary phase shift keyed signals in extremely high noise
[AD-A248552] p 3435 N92-29576
Low complexity, high performance and bandwidth efficient concatenated coded 8-PSK schemes for reliable data communications
[NASA-CR-190588] p 3517 N92-29665
PHASE TRANSFORMATIONS
Thermochemistry of phases related to oxide superconductors
[DE92-011811] p 3556 N92-29485
Theoretical overview: Hot and dense QCD in equilibrium
[DE92-013665] p 3560 N92-29517
Molecular engineering of liquid crystalline polymers by living polymerization. 20: Synthesis and characterization of binary copolymers of 11-(4-cyano-4'-biphenyl) oxy)undecanyl vinyl ether with n-butyl vinyl ether and of 2-(4-cyano-4'-biphenyl) oxy)ethyl vinyl ether with n-butyl vinyl ether
[AD-A248286] p 3425 N92-29566
Structural rearrangements during mesomorphic phase transitions in poly(10-((4-cyano-4' biphenyl)oxy)decanyl vinyl ether)
[AD-A248306] p 3425 N92-29569
Omega phase formation in titanium and titanium alloys
[DE92-011138] p 3421 N92-29633
Amorphization by interdiffusion in metallic multilayers
[ETN-92-91743] p 3558 N92-29766
Amorphization along interfaces and grain boundaries in polycrystalline multilayers: An x ray diffraction study of Ni/Ti multilayers p 3558 N92-29769
Interdiffusion reactions in Ni/Ta multilayers studied by x ray diffraction p 3558 N92-29770
A model for interdiffusion in polycrystalline multilayers and its application to solid state amorphization p 3558 N92-29771
Amorphization and related effects in Ni/Ti multilayers studied by differential scanning calorimetry p 3559 N92-29772
Evidence for amorphization in Ni/Ti multilayers from electrical resistivity changes p 3559 N92-29773
Molecular engineering of liquid crystalline polymers
[AD-A248996] p 3427 N92-30136

PHASED ARRAYS
Land-based seismic array studies of low frequency ambient oceanic noise
[AD-A248255] p 3505 N92-29618
PHENYLS
Polybenzimidazoles via aromatic nucleophilic displacement
[NASA-CASE-LAR-14643-1] p 3426 N92-29953
PHOSPHATES
Cursory examination of the zeta potential behaviors of two optical materials
[DE92-011588] p 3551 N92-29578
PHOTOCHEMICAL REACTIONS
Laser etching: Possibilities and problems
[DE92-010800] p 3477 N92-30135
PHOTODIODES
Study of optical techniques for the Ames unitary wind tunnels. Part 3: Angle of attack
[NASA-CR-190541] p 3406 N92-29655
Performance measurement results for a 220 Mbps QPPM optical communication receiver with an EG/G Slik APD
[NASA-CR-190561] p 3435 N92-29658
PHOTOELECTROCHEMISTRY
Electrochemistry in colloids and dispersions. Volume 3: Colloidal semiconductors
[AD-A248337] p 3419 N92-29932
PHOTOELECTROMAGNETIC EFFECTS
Electrical, optical, and magnetic resonance studies of novel pi-conjugated polymers
[DE92-012548] p 3424 N92-29482
PHOTOELECTRON SPECTROSCOPY
Synthesis and characterization of a covalently bound self-assembled macrocycle monolayer thin film for nonlinear optical materials
[DE92-011353] p 3545 N92-29634
PHOTOELECTRONS
Optical and electrical characteristics of the cathode fall
[AD-A249010] p 3443 N92-30176
PHOTOIONIZATION
Hydrogenation reactions of neutral carbon clusters: C(sub n) (n = 6-75) + D(sub 2)
[DE92-005330] p 3417 N92-29459
Multiphoton processes in scattering and ionization in an intense linearly-polarized radiation field
[DE92-013546] p 3545 N92-29515
PHOTOLUMINESCENCE
Femtosecond studies of carrier dynamics in compound semiconductors
[AD-A250584] p 3439 N92-29452
Electrical, optical, and magnetic resonance studies of novel pi-conjugated polymers
[DE92-012548] p 3424 N92-29482
PHOTOMETERS
Venus in motion: An animated video catalog of Pioneer Venus Orbiter Cloud Photopolarimeter images
[NASA-CR-190543] p 3568 N92-29401
Cosine response characteristics of radiometric and photometric sensors
[DE92-011437] p 3551 N92-29530
Optoelectronic integration
[AD-A248950] p 3442 N92-29936
PHOTOMETRY
Cosine response characteristics of radiometric and photometric sensors
[DE92-011437] p 3551 N92-29530
PHOTOMULTIPLIER TUBES
Design and construction of a channel electron multiplier based Mossbauer spectroscopy system
[AD-A248154] p 3439 N92-29443
PHOTONUCLEAR REACTIONS
Relativistic Coulomb fission p 3548 N92-30008
Charge dependence and electric quadrupole effects on single-nucleon removal in relativistic and intermediate energy nuclear collisions p 3548 N92-30010
PHOTORECEPTORS
Peripheral limitations on spatial vision
[AD-A250579] p 3511 N92-29591
PHYSICAL EXERCISE
Exercise and three psychosocial variables: A longitudinal study
[AD-A250649] p 3510 N92-30216
PHYSICAL FACTORS
Computational acoustics
[AD-A247688] p 3543 N92-29441
PHYSICAL OPTICS
Electrostatic ion thruster optics calculations
[DE92-006608] p 3413 N92-29461
Transition crossing in the RHIC
[DE92-013031] p 3550 N92-29475
PHYSIOCHEMISTRY
Pulse voltammetry in single cells using platinum microelectrodes
[AD-A248080] p 3440 N92-29523
PHYSIOLOGY
Physiological analyses of the afferents controlling brain neurochemical systems
[AD-A248334] p 3512 N92-29930
PHYTOPLANKTON
In vivo and in vitro chlorophyll-a and pheophytin-a concentration measurements by laser fluorometry p 3468 N92-29295
PIEZOELECTRIC CRYSTALS
Small electrostrictive dilations of cubic crystals
[ISBN-90-9004374-8] p 3559 N92-29783
PIEZOELECTRIC TRANSDUCERS
Investigation of solar active regions at high resolution by balloon flights of the solar optical universal polarimeter, definition phase
[NASA-CR-184339] p 3570 N92-30204
PILOT SELECTION
On the effect of range restriction on correlation coefficient estimation
[AD-A248956] p 3511 N92-29620
PILOT TRAINING
Fighter pilot training: The contribution of simulation
[NLR-TP-89311-U] p 3512 N92-29871
Experience with piloted simulation in the development of helicopters
[MBB-UD-0610-91-PUB] p 3407 N92-30076
PILOTS (PERSONNEL)
On the effect of range restriction on correlation coefficient estimation
[AD-A248956] p 3511 N92-29620
PIONEER VENUS 1 SPACECRAFT
Venus in motion: An animated video catalog of Pioneer Venus Orbiter Cloud Photopolarimeter images
[NASA-CR-190543] p 3568 N92-29401
PIPE FLOW
Forces on a pipe bend resulting from clearing a pool of liquid upstream
[DE92-004179] p 3445 N92-29784
PITCHING MOMENTS
The effect of yaw cards on the pitching and yawing motion of symmetric projectiles
[AD-A250021] p 3406 N92-29449
PITTING
A study of the influence of alloying additions on the passivity of aluminum
[AD-A248339] p 3421 N92-29587
PIVOTS
Bladder operated robotic joint
[NASA-CASE-MFS-28682-1] p 3426 N92-29831
PLANE STRAIN
Stresses and strains in plain and coldworked annuli subjected to remote, interference or combined loading
[ARL-STRUC-R-446] p 3482 N92-29672
PLANETARY ATMOSPHERES
Origin and evolution of planetary atmospheres
[NASA-CR-190579] p 3568 N92-29432
Diurnal forcing of planetary atmospheres
[NASA-CR-190262] p 3569 N92-30199
PLANETARY BOUNDARY LAYER
Lidar observation of aerosol and temperature stratification over urban area during the formation of a stable atmospheric PBL p 3466 N92-29286
A comparison between Raman lidar and conventional contact measurements of atmospheric temperature p 3466 N92-29287
Remote sensing by spaceborne lidar aided by surface returns p 3473 N92-29327
NWP impact of cloud top and boundary layer winds from a satellite borne lidar: An observing system simulation experiment p 3473 N92-29328
A spectral vegetation radiometer for airborne boundary-layer research
[PB92-186113] p 3491 N92-30105
Diurnal forcing of planetary atmospheres
[NASA-CR-190262] p 3569 N92-30199
PLANETARY EVOLUTION
Origin and evolution of planetary atmospheres
[NASA-CR-190579] p 3568 N92-29432
PLANETARY GEOLOGY
Origin and evolution of planetary atmospheres
[NASA-CR-190579] p 3568 N92-29432
PLANETARY IONOSPHERES
Occultation of a compact radio source by Venus p 3429 N92-29366
PLANETARY NEBULAE
Origin and evolution of planetary atmospheres
[NASA-CR-190579] p 3568 N92-29432
PLANETARY RADIATION
Source location determination of Uranian kilometric radiation from ray tracing and emission lobe modelling
[NASA-CR-190482] p 3570 N92-29360
PLANETARY SURFACES
Origin and evolution of planetary atmospheres
[NASA-CR-190579] p 3568 N92-29432
PLASMA CHEMISTRY
Numerical analysis of plasma transport in tandem volume magnetic multicusp ion sources
[AD-A248093] p 3554 N92-29528
PLASMA COMPOSITION
Multichord spectroscopy of the D3-D divertor region
[DE92-013507] p 3554 N92-29412
PLASMA CONTROL
Analysis of a dedicated rotation experiment in TFTR
[DE92-013463] p 3554 N92-29438
PLASMA DENSITY
Numerical analysis of plasma transport in tandem volume magnetic multicusp ion sources
[AD-A248093] p 3554 N92-29528
PLASMA DIAGNOSTICS
Experimental and theoretical research in applied plasma physics
[DE92-013587] p 3553 N92-29336
Analysis of a dedicated rotation experiment in TFTR
[DE92-013463] p 3554 N92-29438
Design and operation of the multipulse Thomson scattering diagnostic on DIII-D
[DE92-011393] p 3476 N92-29474
X ray streak camera diagnostics of picosecond laser-plasma interactions
[DE92-011371] p 3555 N92-29789
Optical diagnostics on dense Z-pinch plasmas
[DE92-011228] p 3555 N92-29917
Short wavelength interferometer for ITER
[DE92-013008] p 3474 N92-29942
LLE review
[DE92-011614] p 3555 N92-30072
Intense diagnostic neutral beam development for ITER
[DE92-011262] p 3556 N92-30203
PLASMA DIFFUSION
LLE-LLNL progress report on studies in nonlocal heat transport in spherical plasmas using the Fokker-Planck code SPARK
[DE92-014093] p 3554 N92-29531
PLASMA EQUILIBRIUM
Theoretical overview: Hot and dense QCD in equilibrium
[DE92-013665] p 3560 N92-29517
PLASMA HEATING
Experimental and theoretical research in applied plasma physics
[DE92-013587] p 3553 N92-29336
Spatial and temporal temperature studies of electrothermal chemical (ETC) plasmas
[AD-A248541] p 3554 N92-29510
PLASMA JETS
The expanding plasma jet: Experiments and model
[ETN-92-91627] p 3555 N92-29761
PLASMA LAYERS
Poleward leaping auroras, the substorm expansive and recovery phases, and the recovery of the plasma sheet
[DE92-013530] p 3500 N92-29513
PLASMA PHYSICS
Experimental and theoretical research in applied plasma physics
[DE92-013587] p 3553 N92-29336
PLASMA POTENTIALS
Numerical analysis of plasma transport in tandem volume magnetic multicusp ion sources
[AD-A248093] p 3554 N92-29528
Formation of presheath and current-free double layer in a two-electron-temperature plasma
[NIFS-132] p 3555 N92-30091
Heat flow of a two-electron-temperature plasma through the sheath in the presence of electron emission
[NIFS-136] p 3555 N92-30172
PLASMA SHEATHS
Electrostatic ion thruster optics calculations
[DE92-006608] p 3413 N92-29461
Formation of presheath and current-free double layer in a two-electron-temperature plasma
[NIFS-132] p 3555 N92-30091
Heat flow of a two-electron-temperature plasma through the sheath in the presence of electron emission
[NIFS-136] p 3555 N92-30172
PLASMA TEMPERATURE
Spatial and temporal temperature studies of electrothermal chemical (ETC) plasmas
[AD-A248541] p 3554 N92-29510
Estimating plasma temperatures
[DE92-014092] p 3555 N92-29798
Transport processes in beamed energy propulsion systems
[AD-A247296] p 3413 N92-29913
Formation of presheath and current-free double layer in a two-electron-temperature plasma
[NIFS-132] p 3555 N92-30091
Heat flow of a two-electron-temperature plasma through the sheath in the presence of electron emission
[NIFS-136] p 3555 N92-30172

PLASMA TURBULENCE
A study of shock-associated magnetohydrodynamic waves in the solar wind
[NASA-CR-190567] p 3560 N92-29631
PLASMA WAVES
Transport processes in beamed energy propulsion systems
[AD-A247296] p 3413 N92-29913
PLASMAS (PHYSICS)
Experimental and theoretical research in applied plasma physics
[DE92-013587] p 3553 N92-29336
Statistical mechanics of collective phenomena in plasmas
[AD-A250581] p 3554 N92-29450
Electron microscopy study on zirconia and alumina ceramic powders synthesized by microwave plasma pyrolysis
[DE92-013385] p 3424 N92-29479
Spatial and temporal temperature studies of electrothermal chemical (ETC) plasmas
[AD-A248541] p 3554 N92-29510
LLE review
[DE92-011614] p 3555 N92-30072
Intense diagnostic neutral beam development for ITER
[DE92-011262] p 3556 N92-30203
PLASTIC PROPERTIES
Mechanism of diffusion-controlled brittle fracture
[DE92-011572] p 3482 N92-29601
Simplified computational methods for elastic and elastic-plastic fracture problems p 3488 N92-30134
PLATES (STRUCTURAL MEMBERS)
A consistent shear deformable theory for laminated plates
[AD-A250591] p 3415 N92-29593
Variational formulation and finite element implementation of Pagano's theory of laminated plates
[AD-A250582] p 3415 N92-29594
Nonlinear analyses of composite aerospace structures in sonic fatigue
[NASA-CR-190565] p 3404 N92-30209
PLATING
Electrochemical array sensors for plating waste stream monitoring
[DE92-011446] p 3495 N92-30211
PLATINUM
Pulse voltammetry in single cells using platinum microelectrodes
[AD-A248080] p 3440 N92-29523
PLUMES
Remote detection of biological particles and chemical plumes using UV fluorescence lidar
p 3465 N92-29279
PLUTONIUM 239
Relativistic Coulomb fission p 3548 N92-30008
PNEUMATIC CONTROL
Effects of bleed air extraction on thrust levels on the F404-GE-400 turbofan engine
[NASA-TM-104247] p 3405 N92-29425
POINT SOURCES
Image inversion analysis of the HST OTA (Hubble Space Telescope Optical Telescope Assembly), phase A
[NASA-CR-190483] p 3564 N92-29359
Human exposure model-2: User's guide
[PB92-186246] p 3495 N92-30200
POINTING CONTROL SYSTEMS
Applications of inertial-sensor high-inheritance instruments to DSN precision antenna pointing
p 3430 N92-29371
POISSON DENSITY FUNCTIONS
U-statistics of increasing degrees with asymptotically Poisson distributions
[CWI-BS-R9120] p 3540 N92-29863
POISSON EQUATION
Port-controlled Hamiltonian systems: Modelling origins and systemtheoretic properties
[MEMO-1001] p 3537 N92-30077
POLAR METEOROLOGY
A multi-wavelength ozone lidar for the EASOE experiment p 3462 N92-29260
ARCLITE: The Arctic Lidar Technology Facility at Sondre Stromfjord, Greenland p 3407 N92-29283
Lidar measurements of aerosol and ozone distributions during the 1992 Airborne Arctic Stratospheric Expedition
p 3469 N92-29304
Aerosols and polar stratospheric clouds measurements during the EASOE campaign p 3469 N92-29306
Lidar observations of polar stratospheric clouds and stratospheric temperatures at the South Pole
p 3470 N92-29307
POLAR REGIONS
Elastic and Raman lidar temperature measurements from Poker Flat, Alaska during February 1992
p 3471 N92-29317
POLARIMETERS
Venus in motion: An animated video catalog of Pioneer Venus Orbiter Cloud Photopolarimeter images
[NASA-CR-190543] p 3568 N92-29401
Modulated high sensitivity infrared polarimeter
[AD-D015256] p 3474 N92-29571
Investigation of solar active regions at high resolution by balloon flights of the solar optical universal polarimeter, definition phase
[NASA-CR-184339] p 3570 N92-30204
POLARIZATION (WAVES)
Global and high resolution radar cross section measurements and two-dimensional microwave images of a scaled aircraft model from the type Airbus A 310
[DLR-MITT-91-10] p 3436 N92-29877
Experimental study of cylindrical air electrodes
[DE92-506507] p 3441 N92-29912
POLARIZED LIGHT
Polarization perception device
[NASA-CASE-MSC-21915-1] p 3552 N92-30027
POLICIES
Combined summaries: Technologies to sustain tropical forest resources and biological diversity
[OTA-F-515] p 3492 N92-29416
EOS data policy: Questions remain about US commercial access. Report to the Chairman, Committee on Science, Space, and Technology, House of Representatives
[GAO/IMTEC-92-44] p 3488 N92-29467
Guide for evaluating 12 inch Substantial Dividing Walls (SDWs) to provide protection from remote operation, volume 1
[AD-A250251] p 3428 N92-29545
World Administrative Radio Conference. Issues for US International Spectrum Policy
[PB92-157601] p 3435 N92-29696
Revision of certification standards for aviation maintenance personnel p 3487 N92-30127
The FAA aging airplane program plan for transport aircraft p 3402 N92-30128
POLLUTION
Combined summaries: Technologies to sustain tropical forest resources and biological diversity
[OTA-F-515] p 3492 N92-29416
Intercomparison of global marine climatologies
[DE92-011389] p 3494 N92-29790
Small satellites and RPAS in global-change research: Summary and conclusions
[DE92-013602] p 3490 N92-30088
POLLUTION CONTROL
Applied analytical combustion/emissions research at the NASA Lewis Research Center
[NASA-TM-105731] p 3412 N92-29343
Air quality criteria for oxides of nitrogen, volume 1
[PB92-176361] p 3493 N92-29520
Air quality criteria for oxides of nitrogen, volume 2
[PB92-176379] p 3493 N92-29521
Air quality criteria for oxides of nitrogen, volume 3
[PB92-176387] p 3493 N92-29522
Global-warming problem and global economic models
[DE92-514557] p 3493 N92-29638
Environmental quality: Report of the Council on Environmental Quality
[PB92-154954] p 3494 N92-29698
POLLUTION MONITORING
DIAL mapping of atmospheric atomic mercury of geophysical origin p 3464 N92-29273
Remote detection of biological particles and chemical plumes using UV fluorescence lidar
p 3465 N92-29279
POLLUTION TRANSPORT
New developments in emission projection methodologies
[PB92-139393] p 3495 N92-30031
Preliminary analysis of wind data from the Oak Ridge site survey
[PB92-174564] p 3503 N92-30034
POLYBENZIMIDAZOLE
Polybenzimidazoles via aromatic nucleophilic displacement
[NASA-CASE-LAR-14643-1] p 3426 N92-29953
POLYBUTADIENE
Oriented structures based on trans-1,4-polybutadiene
[ETN-92-91632] p 3546 N92-29778
POLYCRYSTALS
Monolithic integration of semiconductor and superconductor components
[AD-A245351] p 3557 N92-29583
Amorphization along interfaces and grain boundaries in polycrystalline multilayers: An x ray diffraction study of Ni/Ti multilayers p 3558 N92-29769
A model for interdiffusion in polycrystalline multilayers and its application to solid state amorphization
p 3558 N92-29771
Raman features of CVD diamond films
[DE92-011381] p 3426 N92-29908
POLYETHYLENES
Spatial and temporal temperature studies of electrothermal chemical (ETC) plasmas
[AD-A248541] p 3554 N92-29510
Synthesis of new high performance lubricants and solid lubricants
[DE92-011940] p 3424 N92-29549
Structural basis for the mechanical properties of polyethylenes
[PB92-164425] p 3426 N92-29804
POLYMER BLENDS
A method for making biocompatible polymer articles using atomic oxygen
[NASA-CASE-MSC-21529-1] p 3427 N92-30100
POLYMER CHEMISTRY
Synthesis of a naphthalene-hydroxynaphthalene polymer model compound
[DE92-012264] p 3423 N92-29435
Fundamental study of compressive strength development in PAN-based carbon fibers
[AD-A250285] p 3416 N92-30137
POLYMER MATRIX COMPOSITES
Approaches to polymer-derived CMC matrices
[NASA-TM-105754] p 3415 N92-29660
POLYMERIC FILMS
Electrical, optical, and magnetic resonance studies of novel pi-conjugated polymers
[DE92-012548] p 3424 N92-29482
POLYMERIZATION
Molecular engineering of liquid crystalline polymers by living polymerization. 19: Synthesis and characterization of poly 2-(4-biphenyloxy)ethyl vinyl etherby
[AD-A248285] p 3423 N92-29349
Nonideal formation of network polymers
[AD-A248072] p 3424 N92-29465
Molecular engineering of side chain liquid crystalline polymers
[AD-A248540] p 3424 N92-29508
Molecular engineering of liquid crystalline polymers by living polymerization. 20: Synthesis and characterization of binary copolymers of 11-(4-cyano-4'-biphenyl) oxy)undecanyl vinyl ether with n-butyl vinyl ether and of 2-(4-cyano-4'-biphenyl) oxy)ethyl vinyl ether with n-butyl vinyl ether
[AD-A248286] p 3425 N92-29566
Molecular engineering of liquid crystalline polymers by living polymerization. 22: Synthesis and characterization of binary copolymers
[AD-A248287] p 3425 N92-29567
Structural rearrangements during mesomorphic phase transitions in poly(10-((4-cyano-4' biphenyl)oxy)decanyl vinyl ether)
[AD-A248306] p 3425 N92-29569
Molecular engineering of liquid crystalline polymers
[AD-A248996] p 3427 N92-30136
POLYMERS
Molecular engineering of liquid crystalline polymers by living polymerization. 19: Synthesis and characterization of poly 2-(4-biphenyloxy)ethyl vinyl etherby
[AD-A248285] p 3423 N92-29349
Molecular engineering of side chain liquid crystalline polymers
[AD-A248540] p 3424 N92-29508
POLYNOMIALS
A generalized polynomial form of the objective function in flash calculations
[AD-A248160] p 3531 N92-29446
On constructing kernel polynomials of a spectral function: Application to ARMA models
[CWI-BS-R9119] p 3533 N92-29862
Positive convolution structures associated with quantum groups
[CWI-AM-R9105] p 3534 N92-29866
Sensor fault detection on board an aircraft with observer and polynomial classifier
[DLR-FB-91-34] p 3404 N92-29870
Askey-Wilson polynomials for root systems of type BC
[CWI-AM-R9112] p 3534 N92-29882
Polynomial methods in H(infinity)-optimal control
[MEMO-1008] p 3530 N92-29971
Random walk polynomials and random walk measures
[MEMO-1007] p 3536 N92-29999
A random polynomial time algorithm for well-rounding convex bodies
[MEMO-1023] p 3541 N92-30188
POLYPHENYLS
Structural rearrangements during mesomorphic phase transitions in poly(10-((4-cyano-4' biphenyl)oxy)decanyl vinyl ether)
[AD-A248306] p 3425 N92-29569
POLYSILANES
Synthesis and useful reactions of organosilicon polymeric precursors for ceramics
[AD-A248500] p 3424 N92-29496

POLYSTYRENE
The comparative effects of gamma radiation and in situ alpha particles on five strong-base anion exchange resins
[DE92-000177] p 3425 N92-29643
POPULATIONS
Selection constants for uniform populations
[MEMO-COSOR-92-02] p 3540 N92-29827
POROUS MATERIALS
Mathematical modelling of saturated and unsaturated groundwater flow
[MEMO-987] p 3445 N92-29857
POSITION (LOCATION)
Orbiter-orbiter and orbiter-lander tracking using same-beam interferometry p 3409 N92-29369
Geometric distortion analysis of a wide-field astrograph p 3409 N92-29370
Application of remote sensing methods for tracking large cetaceans: North Atlantic right whales Eubalaena Glacialis
[PB92-185016] p 3490 N92-30022
Lexicon of new formal geologic names of the United States, 1981-1985
[PB92-181320] p 3563 N92-30040
POSITION ERRORS
Position-error-based force reflection and compliance control
[NASA-CASE-NPO-18668-1-CU] p 3479 N92-29765
POSITION INDICATORS
Longitudinal bunch profile measurements with striplines
[DE92-013035] p 3549 N92-29477
Study of optical techniques for the Ames unitary wind tunnels. Part 3: Angle of attack
[NASA-CR-190541] p 3406 N92-29655
POSITION SENSING
Sample positioning in microgravity
[NASA-CASE-NPO-18448-1-CU] p 3428 N92-30083
POSITIONING DEVICES (MACHINERY)
Sample positioning in microgravity
[NASA-CASE-NPO-18448-1-CU] p 3428 N92-30083
POSITRONS
Theory of elementary particles studies in weak interaction and grand unification and studies in accelerator design
[DE92-014309] p 3550 N92-29532
POSTFLIGHT ANALYSIS
Support activities to maintain SUMS flight readiness, volume 2. Attachment A: Flight 61-C report
[NASA-CR-189656-VOL-2] p 3411 N92-30218
Support activities to maintain SUMS flight readiness, volume 3. Attachment B: Flight STS-35 report, section A
[NASA-CR-189656-VOL-3] p 3411 N92-30219
Support activities to maintain SUMS flight readiness, volume 4. Attachment B: Flight STS-35 report, section B
[NASA-CR-189656-VOL-4] p 3411 N92-30220
Support activities to maintain SUMS flight readiness, volume 5. Attachment B: Flight STS-35 report, section C
[NASA-CR-189656-VOL-5] p 3411 N92-30221
Support activities to maintain SUMS flight readiness, volume 6. Attachment B: Flight STS-35 report, section D
[NASA-CR-189656-VOL-6] p 3411 N92-30222
Support activities to maintain SUMS flight readiness, volume 7. Attachment B: Flight STS-35 report, section E
[NASA-CR-189656-VOL-7] p 3412 N92-30223
Support activities to maintain SUMS flight readiness, volume 8. Attachment B: Flight STS-35 report, section F
[NASA-CR-189656-VOL-8] p 3412 N92-30224
Support activities to maintain SUMS flight readiness, volume 9. Attachment C: Flight STS-40 report. Attachment D: SUMS software listing
[NASA-CR-189656-VOL-9] p 3412 N92-30225
POTENTIAL FIELDS
Reconstruction of density and potential fields of the Universe p 3565 N92-29834
POTENTIAL FLOW
Development of a multigrid transonic potential flow code for cascades
[NASA-CR-190480] p 3399 N92-29361
First order approximation to the average velocity of rise of bubbles in fluid not including inertial forces
[REPT-91-51] p 3444 N92-29763
POWDER (PARTICLES)
Electron microscopy study on zirconia and alumina ceramic powders synthesized by microwave plasma pyrolysis
[DE92-013385] p 3424 N92-29479
Development of high T(sub c) (greater than 110 K) Bi, Tl, and Y-based materials as superconducting circuit elements
[NASA-CR-190311] p 3557 N92-29676
POWDER METALLURGY
Processing and properties of mechanically alloyed sintered steels with hard inclusions
[KFK-4909] p 3422 N92-29651
POWDERED ALUMINUM
A study of the influence of alloying additions on the passivity of aluminum
[AD-A248339] p 3421 N92-29587
POWER BEAMING
Beam-powered lunar rover design
[DE92-011511] p 3569 N92-29600
Transport processes in beamed energy propulsion systems
[AD-A247296] p 3413 N92-29913
POWER EFFICIENCY
Optical fiber sensor having an active core
[NASA-CASE-LAR-14607-1SB] p 3553 N92-30029
POWER GAIN
Optimizing the G/T ratio of the DSS-13 34-meter beam-waveguide antenna p 3431 N92-29377
PREAMPLIFIERS
Performance measurement results for a 220 Mbps QPPM optical communication receiver with an EG/G Slik APD
[NASA-CR-190561] p 3435 N92-29658
PRECIPITATION (METEOROLOGY)
Mathematical modelling of saturated and unsaturated groundwater flow
[MEMO-987] p 3445 N92-29857
PRECIPITATION HARDENING
Strengthening mechanisms, creep and fatigue processes in dispersion hardened niobium alloy
[AD-A250282] p 3421 N92-29547
PREDICTION ANALYSIS TECHNIQUES
Monthly means of selected climate variables for 1985 - 1989
[NASA-TM-104565] p 3502 N92-29653
Validation of finite element and boundary element methods for predicting structural vibration and radiated noise
[NASA-TM-105359] p 3478 N92-29697
LAPS specific humidity analysis
[PB92-163575] p 3502 N92-29799
Proceedings of the 16th Annual Climate Diagnostics Workshop
[PB92-167378] p 3503 N92-29801
Development of models for prediction of optimal lifting motion
[PB92-164656] p 3513 N92-29949
Fracture mechanics research at NASA related to the aging commercial transport fleet p 3484 N92-30110
PREDICTIONS
Contributions to Hadron 1991: 1) Testing the nature of the f(0)(S asterisk). 2) Gamma gamma to pi(exp 0) pi(exp 0): Dispersive analysis compared to chiral perturbation theory
[RAL-91-070] p 3544 N92-29488
Gamma gamma to pi(exp 0) pi(exp 0): Dispersive analysis compared to chiral perturbation theory p 3545 N92-29490
PREDICTOR-CORRECTOR METHODS
Analysis of parallel diagonal-implicit iteration of Runge-Kutta methods
[CWI-NM-R9114] p 3526 N92-29867
PREMIXED FLAMES
Flame ignition in a premixed turbulent flow p 3450 N92-30061
Simulation of flame-turbulence interactions in premixed combustion p 3450 N92-30062
Direct simulation of turbulent combustion p 3454 N92-30160
Stability of a premixed flame in stagnation-point flow against general disturbances
[NASA-CR-189666] p 3455 N92-30192
PRESSURE DEPENDENCE
Free ion yields in liquids: Molecular structure and track effects
[DE92-012208] p 3545 N92-29582
PRESSURE DISTRIBUTION
Combined load test apparatus for flat panels
[NASA-CASE-LAR-14698-1] p 3483 N92-30028
PRESSURE EFFECTS
Introduction to quartz frequency standards
[AD-A248503] p 3439 N92-29498
The role of pressure-dilatation correlation in rapidly compressed turbulence and in boundary layers p 3449 N92-30050
PRESSURE GRADIENTS
Analyses and modeling of evolving turbulent flow p 3449 N92-30051
Near-wall turbulence modeling for boundary layers with separation p 3449 N92-30052
Modeling turbulent boundary layers in adverse pressure gradients p 3449 N92-30053
An experimental investigation of a low Reynolds number turbulent boundary layer subject to an adverse pressure gradient p 3453 N92-30153
PRESSURE MEASUREMENT
In vitro measurement of nucleus pulposus swelling pressure: A new technique for studies of spinal adaptation to gravity
[NASA-TM-103853] p 3506 N92-29397
Calibration apparatus for recess mounted pressure transducers
[NASA-CASE-LAR-14724-1] p 3474 N92-30030
PRESSURE RATIO
Two-dimensional boundary surfaces for planar external transonic flows
[AD-A248083] p 3444 N92-29524
PRESSURE REDUCTION
Li/SO2 cells and Li/SOCl2 cells: Safe use and testing
[DE92-013508] p 3439 N92-29414
Effects of bleed air extraction on thrust levels on the F404-GE-400 turbofan engine
[NASA-TM-104247] p 3405 N92-29425
PRESSURE SENSORS
Calibration apparatus for recess mounted pressure transducers
[NASA-CASE-LAR-14724-1] p 3474 N92-30030
PRIMITIVE EQUATIONS
Numerical modeling studies of the Gulf of Mexico and the Caribbean Sea using the Bryan-Cox model
[PB92-164987] p 3505 N92-29704
PRINTED CIRCUITS
Design and analysis of electrical circuits that produce fractional-order differentiation
[AD-A248085] p 3440 N92-29526
PROBABILITY DENSITY FUNCTIONS
The determination of stochastic models and areas of confidence
[OEFZS-4612] p 3538 N92-29419
The theory of imprecise probabilities: Some results for distribution functions, densities, hazard rates, and hazard functions
[MEMO-COSOR-91-32] p 3539 N92-29817
Probability density function approach and related closures for turbulent scalar fields p 3450 N92-30059
Monte-Carlo implementation of mapping closures: Application to chemical reacting flows p 3450 N92-30060
Mixing measurements of straight and curved shear layers p 3451 N92-30067
PROBABILITY DISTRIBUTION FUNCTIONS
Generalized probability model for calculation of interference to the Deep Space Network due to circularly Earth-orbiting satellites p 3433 N92-29386
The theory of imprecise probabilities: Some results for distribution functions, densities, hazard rates, and hazard functions
[MEMO-COSOR-91-32] p 3539 N92-29817
PROBABILITY THEORY
Generalized probability model for calculation of interference to the Deep Space Network due to circularly Earth-orbiting satellites p 3433 N92-29386
Some applications of orthogonal functions to probability and statistics
[ETN-92-91741] p 3538 N92-29491
A sensitivity analysis of circular error probable approximation techniques
[AD-A248105] p 3539 N92-29585
The theory of imprecise probabilities: Some results for distribution functions, densities, hazard rates, and hazard functions
[MEMO-COSOR-91-32] p 3539 N92-29817
Selection constants for uniform populations
[MEMO-COSOR-92-02] p 3540 N92-29827
Imprecise conjugate prior densities for the one-parameter exponential family of distributions
[MEMO-COSOR-91-36] p 3540 N92-29897
Electronic neural network for solving traveling salesman and similar global optimization problems
[NASA-CASE-NPO-17807-2-CU] p 3529 N92-29955
An analysis of model-based diagnosis using problem-reformulation
[MEMO-INF-92-03] p 3530 N92-29983
Phase-space estimate of satellite coverage time
[DE92-013555] p 3542 N92-30139
PROBLEM SOLVING
The weakest failure detector for solving consensus
[NASA-CR-190545] p 3515 N92-29400
Improving path planning with learning
[DE92-004360] p 3527 N92-29456
Tools for the interfacing between dynamical problems and models within decision support systems
[MEMO-COSOR-91-29] p 3532 N92-29607
Solution strategies for implicit nonlinear finite element analysis
[DE92-011466] p 3533 N92-29792
Parameter identification in tidal models with uncertain boundaries
[MEMO-983] p 3540 N92-29856

Solving parabolic integro-differential equations by an explicit integration method
[CWI-NM-R9108] p 3534 N92-29883
Diffusion approximation of stochastic integral functionals of jump Markov processes
[CWI-AM-R9108] p 3535 N92-29895
Diffusion approximation of stochastic additive functionals of jump Markov processes
[CWI-AM-R9110] p 3535 N92-29896
The Green Function Cellular Method and its relation to multiple scattering theory
[DE92-011470] p 3436 N92-29909
Numerical methods for the 3D shallow water equations on vector and parallel computers
[CWI-NM-R9109] p 3446 N92-29944
An improved accuracy version of the mixed finite element method for a second order elliptic equation
[CWI-NM-R9111] p 3536 N92-29946
Application of a moving-grid method to a class of 1D brine transport problems in porous media
[CWI-NM-R9112] p 3446 N92-29947
Electronic neural network for solving traveling salesman and similar global optimization problems
[NASA-CASE-NPO-17807-2-CU] p 3529 N92-29955
Polynomial methods in H(infinity)-optimal control
[MEMO-1008] p 3530 N92-29971
An analysis of model-based diagnosis using problem-reformulation
[MEMO-INF-92-03] p 3530 N92-29983
Optimal copying strategies
[MEMO-1005] p 3537 N92-30081

PROCESS CONTROL (INDUSTRY)
Novel thin-film CuInSe2 fabrication
[DE92-001222] p 3557 N92-29584
Monolithic amorphous silicon modules on continuous polymer substrate
[DE92-001163] p 3425 N92-29598
A universal, fault-tolerant, non-linear analytic network for modeling and fault detection
[DE92-011840] p 3525 N92-29624
Process of ferrochromium now and in the future
[DE92-506510] p 3421 N92-29637
State estimation and error diagnosis for biotechnological processes
[ETN-92-91744] p 3508 N92-29754
State estimation and control of the IBE-fermentation with product recovery p 3509 N92-29756
Analytical tuning of a low sensitivity observer applied to a continuous ethanol fermentation with product recovery p 3509 N92-29758
Polybenzimidazoles via aromatic nucleophilic displacement
[NASA-CASE-LAR-14643-1] p 3426 N92-29953
A method for making biocompatible polymer articles using atomic oxygen
[NASA-CASE-MSC-21529-1] p 3427 N92-30100

PROCESS HEAT
Thermal energy storage for cogeneration applications
[DE92-012339] p 3492 N92-29646

PRODUCTION MANAGEMENT
Shop of the 1990's: The implementation of a CAD/CAM system for small machine shops
[PB92-181098] p 3522 N92-30020

PRODUCTIVITY
Improving designer productivity --- artificial intelligence
[NASA-TM-103929] p 3404 N92-29417
Biophysical, morphological, canopy optical property, and productivity data from the Superior National Forest
[NASA-TM-104568] p 3491 N92-30210

PRODUCTS
Diversification and product innovation: A challenge for modern management
[OEFZS-4570] p 3561 N92-29886

PROGRAM VERIFICATION (COMPUTERS)
Protocol conformance testing: A formal perspective in ISO IS-9646
[MEMO-INF-91-32] p 3517 N92-29705

PROGRAMMED INSTRUCTION
Automatic generation algorithms, experiments, and comparisons of self checking PLA schemes
[IMAG-RR-843-I] p 3516 N92-29621
Software reliability and the bootstrap
[CWI-BS-R9123] p 3520 N92-29865

PROGRAMMING LANGUAGES
Code generation in ALPAL using symbolic techniques
[DE92-011299] p 3524 N92-29353
Using object-oriented databases for implementation of interactive electronic technical manuals
[AD-A248135] p 3440 N92-29564
ISLAND: Interactive Solution Language for an Adaptive NIKE Driver
[DE92-011444] p 3533 N92-29791
Implementation of the object-oriented data model TM
[MEMO-INF-91-94] p 3520 N92-29855
Facets of database triggers
[CWI-CS-R9122] p 3521 N92-29891
An object-oriented language-database integration model: The composition-filters approach
[MEMO-INF-91-90] p 3521 N92-29961
An algebraic specification for the static semantics of Pascal
[CWI-CS-R9129] p 3522 N92-29989
Rendez-vous with metric semantics
[CWI-CS-R9135] p 3522 N92-29991
Proof theory for micro CRL
[CWI-CS-R9138] p 3522 N92-29994
Overview of the document style semantics and specification language and the MIL-M-28001A output specification
[PB92-181122] p 3563 N92-30039
A formal development trajectory for OSI application layer protocols
[MEMO-INF-91-71] p 3523 N92-30144

PROJECT MANAGEMENT
Modeling and computational analysis of multiscale phenomena in fluid-structure interaction problems
[AD-A248723] p 3444 N92-29721
The 1991 Summer Faculty Research Program (SFRP), volume 3
[AD-A248765] p 3571 N92-29725
Geostationary Operational Environmental Satellite(GEOS-N report)
[NASA-TM-107919] p 3410 N92-29810

PROJECT PLANNING
The FAA aging airplane program plan for transport aircraft p 3402 N92-30128

PROJECTILES
The effect of yaw cards on the pitching and yawing motion of symmetric projectiles
[AD-A250021] p 3406 N92-29449

PROPELLANTS
Strategies for understanding the deflagration-to-detonation transition
[DE92-013528] p 3427 N92-29512
Final Environmental Impact Statement (EIS) for the Space Nuclear Thermal Propulsion (SNTP) program
[AD-A248408] p 3413 N92-29903

PROPORTIONAL COUNTERS
Design and construction of a channel electron multiplier based Mossbauer spectroscopy system
[AD-A248154] p 3439 N92-29443

PROPULSION
KISMET (kinematic simulation, monitoring and off-line programming environments for telerobotics): Simulation of the target-oriented driving of an autonomous vehicle in a labyrinthic environment
[KFK-4941] p 3515 N92-29418

PROPULSION SYSTEM CONFIGURATIONS
A preliminary design and analysis of an advanced heat-rejection system for an extreme altitude advanced variable cycle diesel engine installed in a high-altitude advanced research platform
[NASA-CR-186021] p 3405 N92-29427
Beam-powered lunar rover design
[DE92-011511] p 3569 N92-29600
Flight evaluation of an extended engine life mode on an F-15 airplane
[NASA-TM-104240] p 3405 N92-29659
Transport processes in beamed energy propulsion systems
[AD-A247296] p 3413 N92-29913
Research and technology annual report, FY 1990
[NASA-TM-107807] p 3571 N92-30197

PROPULSION SYSTEM PERFORMANCE
Flight evaluation of an extended engine life mode on an F-15 airplane
[NASA-TM-104240] p 3405 N92-29659
Transport processes in beamed energy propulsion systems
[AD-A247296] p 3413 N92-29913
Research and technology annual report, FY 1990
[NASA-TM-107807] p 3571 N92-30197

PROTECTION
Guide for evaluating 12 inch Substantial Dividing Walls (SDWs) to provide protection from remote operation, volume 2
[AD-A250252] p 3428 N92-29335
Guide for evaluating 12 inch Substantial Dividing Walls (SDWs) to provide protection from remote operation, volume 1
[AD-A250251] p 3428 N92-29545
Review of temperature dependent effects on the oxidation protection of carbon/carbon
[DE92-012333] p 3415 N92-29645

PROTECTIVE CLOTHING
Li/SO2 cells and Li/SOCl2 cells: Safe use and testing
[DE92-013508] p 3439 N92-29414

PROTECTIVE COATINGS
Experimental evaluation of incorporating digital and analog integrated circuit die on a common substrate utilizing silicon-hybrid wafer-scale integration technology
[AD-A248182] p 3439 N92-29405
Review of temperature dependent effects on the oxidation protection of carbon/carbon
[DE92-012333] p 3415 N92-29645

PROTEINS
Electrical connection of enzyme redox centers to electrodes
[AD-A248545] p 3440 N92-29575

PROTOCOL (COMPUTERS)
Application of VME-technology on an airborne data link processor unit
[NLR-MP-88040-U] p 3403 N92-29615
Developments in fiber optics for distribution automation
[NASA-CR-190454] p 3551 N92-29679
Protocol conformance testing: A formal perspective in ISO IS-9646
[MEMO-INF-91-32] p 3517 N92-29705
Methodology for the specification of communication activities within the framework of a multi-layered architecture: Toward the definition of a knowledge base
[LAAS-91466] p 3436 N92-29730
User's manual for the NIST TTCN translator, version 3.0
[PB92-172493] p 3518 N92-29745
Performance of a connectionless protocol over ATM
[MEMO-INF-92-02] p 3526 N92-29880
Cislan-2 final document by University of Twente (Netherlands)
[MEMO-INF-91-81] p 3526 N92-29958
A method for analysing the performance aspects of the fault-tolerance mechanisms in FDDI
[MEMO-INF-91-92] p 3514 N92-29982
Cislan-2 extension final document by University of Twente (Netherlands)
[MEMO-INF-92-05] p 3437 N92-29984
A formal development trajectory for OSI application layer protocols
[MEMO-INF-91-71] p 3523 N92-30144
Variable bandwidth connections for a connectionless service on ATM: Performance modelling and evaluation
[MEMO-INF-91-83] p 3438 N92-30170

PROVING
PBT: A Parallel Bottom-up Tomita Parser
[MEMO-INF-91-69] p 3527 N92-30183
SeaWiFS technical report series. Volume 5: Ocean optics protocols for SeaWiFS validation
[NASA-TM-104566] p 3506 N92-30193

PSYCHOLOGICAL FACTORS
Exercise and three psychosocial variables: A longitudinal study
[AD-A250649] p 3510 N92-30216

PSYCHOLOGY
Exercise and three psychosocial variables: A longitudinal study
[AD-A250649] p 3510 N92-30216

PUBLIC HEALTH
Air quality criteria for oxides of nitrogen, volume 1
[PB92-176361] p 3493 N92-29520
Air quality criteria for oxides of nitrogen, volume 2
[PB92-176379] p 3493 N92-29521
Air quality criteria for oxides of nitrogen, volume 3
[PB92-176387] p 3493 N92-29522

PUERTO RICO
Lexicon of new formal geologic names of the United States, 1981-1985
[PB92-181320] p 3563 N92-30040

PULSARS
Analysis of high energy x ray observations of long periodic pulsars
[ETN-92-91494] p 3564 N92-29468

PULSE DURATION
The optical design of AmPS: Elements of the design of a pulse stretcher
[ETN-92-91626] p 3552 N92-29859

PULSE POSITION MODULATION
Performance measurement results for a 220 Mbps QPPM optical communication receiver with an EG/G Slik APD
[NASA-CR-190561] p 3435 N92-29658

PULSED LASERS
Lag angle compensation in a space borne scanning lidar p 3462 N92-29263
Infrared pulse-laser long-path absorption measurement of carbon dioxide using a Raman-shifted dye laser p 3465 N92-29277
The Laser Atmospheric Wind Sounder (LAWS) phase 2 preliminary laser design p 3468 N92-29298
Using phase retrieval to determine the intensity and phase of an ultrashort laser pulse
[DE92-013564] p 3476 N92-29516
Laser paint stripping
[AD-A249233] p 3476 N92-29581
Sample positioning in microgravity
[NASA-CASE-NPO-18448-1-CU] p 3428 N92-30083

PULSED RADIATION
High Intensity Source Laboratory (HISL)
[DE92-011173] p 3549 N92-29457
PUMPS
Test and evaluation report of the IMED volumetric infusion pump model 960A
[AD-A248538] p 3404 N92-29506
PURITY
Converting a CO2 atmosphere to a high-purity O2 supply
[NASA-CASE-LAR-14398-1] p 3419 N92-30098
PYRIDINES
Solid state structures of some Dithionoamido-18-crown-6 ligands
[AD-A248098] p 3556 N92-29558
PYROLYSIS
Progress on combustion mechanisms of solid propellants
[AD-A248146] p 3427 N92-29330
Electron microscopy study on zirconia and alumina ceramic powders synthesized by microwave plasma pyrolysis
[DE92-013385] p 3424 N92-29479
Synthesis and useful reactions of organosilicon polymeric precursors for ceramics
[AD-A248500] p 3424 N92-29496
PYROTECHNICS
Microcalorimetric study of the aging reactions of atomized magnesium powder
[AD-A247932] p 3427 N92-29786

Q

Q SWITCHED LASERS
Laser Transmitter Module (LTM) for LITE
p 3463 N92-29265
System testing and performance characterization of the LITE Laser Transmitter Module at NASA
p 3469 N92-29302
QUADRANTS
Real-time quadratic shading
[CWI-CS-R9123] p 3534 N92-29892
QUADRATIC EQUATIONS
D-optimal designs for an incomplete quadratic model
[MEMO-COSOR-91-26] p 3532 N92-29742
QUADRUPOLES
Charge dependence and electric quadrupole effects on single-nucleon removal in relativistic and intermediate energy nuclear collisions p 3548 N92-30010
QUALITY
Peripheral limitations on spatial vision
[AD-A250579] p 3511 N92-29591
QUALITY CONTROL
A sample-size optimal bayesian procedure for sequential pharmaceutical trials
[AD-A248512] p 3538 N92-29501
Software quality control and requirements specification
[REPT-91-48] p 3518 N92-29711
A simple approximation to the bivariate normal distribution with large correlation coefficient
[MEMO-1011] p 3540 N92-29974
A manufacturer's approach to ensure long term structural integrity p 3403 N92-30133
QUANTILES
Accurate procedures for approximate Bayesian and conditional inference without the need for orthogonal parameters
[AD-A248662] p 3539 N92-29718
QUANTUM CHROMODYNAMICS
Theoretical overview: Hot and dense QCD in equilibrium
[DE92-013665] p 3560 N92-29517
The O(alpha(s) cubed) QCD correction to the lowest moment of the longitudinal structure function in deep inelastic electron-nucleon scattering
[NIKHEF-H/91-19] p 3546 N92-29750
Confining potential in momentum space
p 3548 N92-30007
QUANTUM ELECTRODYNAMICS
Electromagnetic processes in nucleus-nucleus collisions relating to space radiation research
[NASA-CR-190533] p 3547 N92-30001
Do recent observations of very large electromagnetic dissociation cross sections signify a transition towards non-perturbative QED? p 3438 N92-30004
QUANTUM MECHANICS
On the parity of fundamental solutions for one-dimensional scattering problem with inverse square potential
[DE92-624511] p 3560 N92-29533
Variable temperature scanning tunneling microscopy
[AD-A248725] p 3557 N92-29722
Theory of the dissociation dynamics of small molecules on metal surfaces: Finite temperature studies
[DE92-011188] p 3546 N92-29899
On the two-dimensional model of quantum Regge gravity
[DE92-624516] p 3560 N92-30212
QUANTUM THEORY
The extended Bethe Ansatz for infinite S = 1/2 quantum spin chains with non-nearest-neighbor interaction
[DE92-622378] p 3533 N92-29793
On the two-dimensional model of quantum Regge gravity
[DE92-624516] p 3560 N92-30212
QUANTUM WELLS
Optoelectronic integration
[AD-A248950] p 3442 N92-29936
QUARK MODELS
Contributions to Hadron 1991: 1) Testing the nature of the f(0)(S asterisk). 2) Gamma gamma to pi(exp 0) pi(exp 0): Dispersive analysis compared to chiral perturbation theory
[RAL-91-070] p 3544 N92-29488
Testing the nature of the f(0)(S asterisk)
p 3545 N92-29489
Electromagnetic processes in nucleus-nucleus collisions relating to space radiation research
[NASA-CR-190533] p 3547 N92-30001
Confining potential in momentum space
p 3548 N92-30007
QUARKS
Theoretical overview: Hot and dense QCD in equilibrium
[DE92-013665] p 3560 N92-29517
QUARTZ CRYSTALS
Introduction to quartz frequency standards
[AD-A248503] p 3439 N92-29498
QUEUEING THEORY
A compensation approach for queueing problems
[ETN-92-91628] p 3539 N92-29774
Asymptotic results in feedback systems
[ETN-92-91702] p 3529 N92-29962
Asymptotic behavior of random discrete event systems p 3529 N92-29963
Strong law and central limit theorem for a process between maxima and sums p 3530 N92-29964
The M/G/1 processor sharing queue as the almost sure limit of feedback queues p 3530 N92-29965
Multitype branching processes in M/G/1-queueing theory p 3530 N92-29966

R

RADAR
Application of laser imaging for bio/geophysical studies p 3465 N92-29282
Normalized radar cross section of natural surfaces at millimeter wavelengths
[AD-A248452] p 3434 N92-29447
RADAR ASTRONOMY
Goldstone solar system radar signal processing
p 3433 N92-29389
RADAR CROSS SECTIONS
DSN observations of Titan p 3433 N92-29388
Normalized radar cross section of natural surfaces at millimeter wavelengths
[AD-A248452] p 3434 N92-29447
Global and high resolution radar cross section measurements and two-dimensional microwave images of a scaled aircraft model from the type Airbus A 310
[DLR-MITT-91-10] p 3436 N92-29877
RADAR DATA
Goldstone solar system radar signal processing
p 3433 N92-29389
RADAR EQUIPMENT
Microstrip reflectarray antenna for the SCANSCAT radar application
[NASA-CR-190453] p 3434 N92-29463
RADAR IMAGERY
Goldstone solar system radar signal processing
p 3433 N92-29389
RADAR MEASUREMENT
Sixteenth International Laser Radar Conference, part 1
[NASA-CP-3158-PT-1] p 3456 N92-29228
Long term stratospheric aerosol lidar measurements in Kyushu p 3456 N92-29229
Southern Hemisphere lidar measurements of the aerosol clouds from Mt. Pinatubo and Mt. Hudson
p 3456 N92-29230
Stratospheric backscatter, extinction, and lidar ratio profiling after the Mt. Pinatubo eruptions
p 3456 N92-29231
Measurements of stratospheric Pinatubo aerosol extinction profiles by a Raman lidar
p 3457 N92-29232
Raman lidar measurements of Pinatubo aerosols over southeastern Kansas during November-December 1991
p 3457 N92-29233
Lidar observations of stratospheric aerosol layer after the Mt. Pinatubo volcanic eruption p 3457 N92-29234
The role of lidars in global change research
p 3457 N92-29235
Interpretation of DIAL measurements of lower stratospheric ozone in regions with Pinatubo aerosols
p 3457 N92-29236
Correcting for interference of Mt. Pinatubo aerosols on DIAL measurements of stratospheric ozone
p 3458 N92-29237
A new Raman DIAL technique for measuring stratospheric ozone in the presence of volcanic aerosols
p 3458 N92-29238
The JPL Table Mountain and Mauna Loa stratospheric ozone lidars p 3458 N92-29239
The NDSC primary site at the Observatoire de Haute-Provence: Ozone and aerosols observations (1986-1992) p 3458 N92-29240
Lidar atmospheric observatory in the Canadian Arctic
p 3458 N92-29241
Observation of stratospheric ozone with NIES lidar system in Tsukuba, Japan p 3459 N92-29242
First results from TROLIX 1991: An intercomparison of tropospheric ozone lidars p 3459 N92-29244
The global backscatter experiment airborne pulsed lidar measurements p 3459 N92-29246
Multi-wavelength airborne lidar intercomparisons of aerosol and cirrus backscatter over the Pacific Ocean
p 3460 N92-29247
Airborne lidar observations of the stratosphere after the Pinatubo eruption p 3460 N92-29248
Multi-wavelength measurements of the stratospheric aerosol layer made at Hampton, Virginia (37N, 76W)
p 3460 N92-29249
Three-wavelength lidar measurements of Pinatubo aerosol and its optical properties p 3460 N92-29250
Lidar observations of the Pinatubo stratospheric aerosol cloud over Frascati, Italy p 3460 N92-29251
L625 lidar measurements of Pinatubo volcanic cloud at Hefei p 3460 N92-29252
Two wavelength measurements of the Pinatubo aerosol above Toronto, Canada p 3461 N92-29253
Lidar observations of the Pinatubo volcanic cloud over Hampton, Virginia p 3461 N92-29254
Lidar measurements of stratospheric ozone, temperature and aerosol during 1992 UARS correlative measurement campaign p 3461 N92-29257
Lidar measurement of stratospheric ozone at Hohenpeissenberg: An improved evaluation method
p 3462 N92-29259
Intercomparisons of lidar backscatter measurements and in-situ data from GLOBE p 3463 N92-29266
Transportable lidar for the measurement of ozone concentration and flux profiles in the lower troposphere
p 3465 N92-29278
Signal quality influence on averaging procedure for DIAL pollution monitoring p 3465 N92-29280
One year of Rayleigh lidar measurements at Toronto
p 3466 N92-29285
A comparison between Raman lidar and conventional contact measurements of atmospheric temperature
p 3466 N92-29287
Lidar investigation of aerosol pollution distribution near a coal power plant p 3467 N92-29289
Lidar measurements of aerosol and ozone distributions during the 1992 Airborne Arctic Stratospheric Expedition
p 3469 N92-29304
Airborne lidar measurements of stratospheric aerosols during the European Arctic Stratospheric Ozone Experiment (EASOE) p 3469 N92-29305
Aerosols and polar stratospheric clouds measurements during the EASOE campaign p 3469 N92-29306
Lidar observations of polar stratospheric clouds and stratospheric temperatures at the South Pole
p 3470 N92-29307
Optical pumping of mesospheric sodium: A new measurement capability p 3470 N92-29310
Lidar probing of the mesosphere: Simultaneous observations of sporadic sodium and iron formations, calcium ion layers, neutral temperature and winds
p 3470 N92-29311
Lidar measurements of metallic species in mesopause region p 3470 N92-29312
Error analysis of wind measurements for the University of Illinois sodium Doppler temperature system
p 3471 N92-29313
Airborne sodium and Rayleigh lidar observations from ALOHA-90 p 3471 N92-29315
Rayleigh/Raman Greenland lidar observations of atmospheric temperature during a major Arctic stratospheric warming event p 3471 N92-29316

Elastic and Raman lidar temperature measurements from Poker Flat, Alaska during February 1992
p 3471 N92-29317
Rayleigh/Raman lidars: Intercomparisons and validation p 3471 N92-29318
Wind measurements from 15 to 50 km with a Doppler Rayleigh lidar p 3472 N92-29319
Lidar studies of extinction in clouds in the ECLIPS project p 3472 N92-29320
Lidar studies of clouds at Toronto during the ECLIPS program p 3472 N92-29321
Polarization lidar liquid cloud detection algorithm for winter mountain storms p 3472 N92-29323
Measurement of mean or effective radius of cloud drop size distributions with a 10.6-micron wavelength lidar
p 3472 N92-29324
Observations of cirrus clouds over the Pacific region by the NASA multiwavelength lidar system
p 3473 N92-29325
Diode-pumped Nd:YAG lidar for airborne cloud measurements p 3473 N92-29326
Remote sensing by spaceborne lidar aided by surface returns p 3473 N92-29327

RADAR SCANNING
Lag angle compensation in a space borne scanning lidar p 3462 N92-29263

RADAR SCATTERING
Adaptation of the University of Wisconsin high spectral resolution lidar for polarization and multiple scattering measurements p 3472 N92-29322
Diode-pumped Nd:YAG lidar for airborne cloud measurements p 3473 N92-29326

RADAR SIGNATURES
Global and high resolution radar cross section measurements and two-dimensional microwave images of a scaled aircraft model from the type Airbus A 310
[DLR-MITT-91-10] p 3436 N92-29877

RADAR TRACKING
DSN observations of Titan p 3433 N92-29388
Tracking hurricane Claudette with the US Air Force OTH-B radar
[PB92-164524] p 3503 N92-29800

RADIAL FLOW
A comparison of the calculated and experimental off-design performance of a radial flow turbine
[NASA-CR-189207] p 3399 N92-29402

RADIANT COOLING
Hypersonic flow past radiation-cooled surfaces
[MBB-FE-202-S-PUB-0468-A] p 3401 N92-29713

RADIANT FLUX DENSITY
Efficient complete radiosity ray tracing using a shadow coherence method
[REPT-91-63] p 3518 N92-29749

RADIATION COUNTERS
Intercomparisons of lidar backscatter measurements and in-situ data from GLOBE p 3463 N92-29266

RADIATION DETECTORS
Prospects for long baseline neutrino oscillation experiments
[DE92-011833] p 3544 N92-29356
High Intensity Source Laboratory (HISL)
[DE92-011173] p 3549 N92-29457
The 20 element HgI2 energy dispersive x ray array detector system
[DE92-013356] p 3549 N92-29502
Center of excellence: Microlaser microscope
[DE92-013485] p 3477 N92-29928

RADIATION DISTRIBUTION
User's guide for the VTRPE (Variable Terrain Radio Parabolic Equation) computer model
[AD-A248112] p 3433 N92-29395
Multiphoton processes in scattering and ionization in an intense linearly-polarized radiation field
[DE92-013546] p 3545 N92-29515

RADIATION DOSAGE
Hardening techniques to counter cumulated dose on SEU and SEL in space environment
[IMAG-RR-863-I] p 3441 N92-29613
Final Environmental Impact Statement (EIS) for the Space Nuclear Thermal Propulsion (SNTP) program: Appendices
[AD-A248409] p 3413 N92-29904
Proceedings of the Third Conference on Radiation Protection and Dosimetry
[DE92-011502] p 3547 N92-29910

RADIATION EFFECTS
Laser-induced desorption from sapphire surfaces
[DE92-012698] p 3475 N92-29340
Effects of ionizing radiation on auditory and visual thresholds
[AD-A248199] p 3507 N92-29410
Irradiation effects on the electrochemistry and corrosion resistance of stainless steel
[DE92-013504] p 3420 N92-29411
Introduction to quartz frequency standards
[AD-A248503] p 3439 N92-29498
Hardening techniques to counter cumulated dose on SEU and SEL in space environment
[IMAG-RR-863-I] p 3441 N92-29613
The comparative effects of gamma radiation and in situ alpha particles on five strong-base anion exchange resins
[DE92-000177] p 3425 N92-29643

RADIATION HARDENING
Surface reactions in the space environment
[AD-A250624] p 3428 N92-29428
Latent interface-trap buildup: Issues for long-term device response
[DE92-003148] p 3439 N92-29455
High Intensity Source Laboratory (HISL)
[DE92-011173] p 3549 N92-29457

RADIATION MEASUREMENT
Lidar development for the Atmospheric Radiation Measurement (ARM) Program p 3461 N92-29256
Prospects for long baseline neutrino oscillation experiments
[DE92-011833] p 3544 N92-29356

RADIATION PROTECTION
Proceedings of the Third Conference on Radiation Protection and Dosimetry
[DE92-011502] p 3547 N92-29910
Electromagnetic processes in nucleus-nucleus collisions relating to space radiation research
[NASA-CR-190533] p 3547 N92-30001
Stopping powers and cross sections due to two-photon processes in relativistic nucleus-nucleus collision
p 3548 N92-30012

RADII
Measurement of mean or effective radius of cloud drop size distributions with a 10.6-micron wavelength lidar
p 3472 N92-29324

RADIO ANTENNAS
Orbiter-orbiter and orbiter-lander tracking using same-beam interferometry p 3409 N92-29369

RADIO ASTRONOMY
DSS-13 26-meter antenna upgraded radiometer system p 3432 N92-29381

RADIC COMMUNICATION
Ka-band feed arrays for spacecraft reflector antennas with limited scan capability: An overview
p 3433 N92-29387

RADIO EMISSION
Source location determination of Uranian kilometric radiation from ray tracing and emission lobe modelling
[NASA-CR-190482] p 3570 N92-29360

RADIO FREQUENCIES
Improving the LAMP Mk 3 SH-60B HF communication system
[AD-A245970] p 3429 N92-29344
FM video data link spectrum spreading
[AD-D015257] p 3435 N92-29572
World Administrative Radio Conference. Issues for US International Spectrum Policy
[PB92-157601] p 3435 N92-29696
RF vacuum electronics
[AD-A248857] p 3442 N92-29935
High resolving power spectrometer for beam analysis
[DE92-010751] p 3437 N92-29988

RADIO FREQUENCY INTERFERENCE
Global measurements of low-frequency radio noise
[AD-A248260] p 3434 N92-29542

RADIO GALAXIES
The space distribution of local radio galaxies
p 3566 N92-29842

RADIO RECEIVERS
Miniature modular microwave end-to-end receiver
[NASA-CASE-NPO-18713-1-CU] p 3437 N92-30103

RADIO SOURCES (ASTRONOMY)
A nanoradian differential VLBI tracking demonstration
p 3430 N92-29367

RADIO SPECTRA
World Administrative Radio Conference. Issues for US International Spectrum Policy
[PB92-157601] p 3435 N92-29696

RADIO TRACKING
Geometric distortion analysis of a wide-field astrograph p 3409 N92-29370

RADIO TRANSMISSION
Revising M-layer: Complex exponent representation
[AD-A249121] p 3435 N92-29599

RADIO TRANSMITTERS
Improvements in X-band transmitter phase stability through klystron body temperature regulation
p 3431 N92-29373

RADIOACTIVE CONTAMINANTS
Preliminary analysis of wind data from the Oak Ridge site survey
[PB92-174564] p 3503 N92-30034

RADIOACTIVE WASTES
Near-visible Raman instrumentation for remote multi-point process monitoring using optical fibers and optical multiplexing
[DE92-011287] p 3550 N92-29337

RADIOLOGY
Final Environmental Impact Statement (EIS) for the Space Nuclear Thermal Propulsion (SNTP) program
[AD-A248408] p 3413 N92-29903

RADIOMETERS
Lidar development for the Atmospheric Radiation Measurement (ARM) Program p 3461 N92-29256
Application of laser imaging for bio/geophysical studies p 3465 N92-29282
DSS-13 26-meter antenna upgraded radiometer system p 3432 N92-29381
Cosine response characteristics of radiometric and photometric sensors
[DE92-011437] p 3551 N92-29530
A wave theory for non-imaging concentrators
[AD-A248865] p 3552 N92-29726
A spectral vegetation radiometer for airborne boundary-layer research
[PB92-186113] p 3491 N92-30105
SeaWiFS technical report series. Volume 5: Ocean optics protocols for SeaWiFS validation
[NASA-TM-104566] p 3506 N92-30193
Biophysical, morphological, canopy optical property, and productivity data from the Superior National Forest
[NASA-TM-104568] p 3491 N92-30210
Comparison of in situ, aircraft- and satellite derived surface reflectances in Flevoland (Netherlands). A validation experiment
[BCRS-91-28] p 3491 N92-30230

RADIOMETRIC CORRECTION
CAESAR: A CCD airborne experimental scanner for applications in remote sensing radiometric and geometric calibration
[NLR-TP-89103-U] p 3490 N92-29707

RADIOSONDES
Lidar studies of extinction in clouds in the ECLIPS project p 3472 N92-29320

RAIL TRANSPORTATION
Computer model simulation of null-flux magnetic suspension and guidance
[DE92-013044] p 3478 N92-29534
High-speed Maglev trains: German safety requirements RW-MSB
[PB92-167006] p 3564 N92-29808
German high-speed Maglev train safety requirements: Potential for application in the United States
[PB92-167014] p 3564 N92-29809

RAILGUN ACCELERATORS
A mechanical connector design for high-current, high-coulomb pulsed power systems
[DE92-012678] p 3438 N92-29339

RAMAN SPECTRA
Measurements of stratospheric Pinatubo aerosol extinction profiles by a Raman lidar
p 3457 N92-29232
Raman lidar measurements of Pinatubo aerosols over southeastern Kansas during November-December 1991
p 3457 N92-29233
Rotational Raman lidar for lower tropospheric temperature profiling p 3466 N92-29284
A comparison between Raman lidar and conventional contact measurements of atmospheric temperature
p 3466 N92-29287
Efficiencies of rotational Raman and Rayleigh techniques for laser remote sensing of the atmospheric temperature p 3467 N92-29288
Near-visible Raman instrumentation for remote multi-point process monitoring using optical fibers and optical multiplexing
[DE92-011287] p 3550 N92-29337
The development of a fiber optic Raman temperature measurement system for rocket flows
[NASA-CR-189200] p 3413 N92-29448
Raman features of CVD diamond films
[DE92-011381] p 3426 N92-29908

RAMAN SPECTROSCOPY
Vibrational spectrum and structure of 1,2-dimethyl-1,2-disila-closo-dodecaborane
[AD-A250235] p 3419 N92-29941

RANDOM ACCESS MEMORY
Asymptotic behavior of random discrete event systems p 3529 N92-29963

RANDOM ERRORS
State estimation and error diagnosis for biotechnological processes
[ETN-92-91744] p 3508 N92-29754
The use of state estimators (observers) for on-line estimation of non-measurable process variables
p 3508 N92-29755
Improved balancing methods and error diagnosis for bio(chemical) conversions p 3509 N92-29759

Sequential application of data reconciliation for sensitive detection of systematic errors p 3509 N92-29760

RANDOM NOISE
Statistics of narrowband white noise derived from clipped broadband white noise
[AD-A248597] p 3434 N92-29563

RANDOM PROCESSES
Modeling deterministic chaos in thermally-pulsed combustion
[DE92-011756] p 3416 N92-29355
Numerical procedures for analyzing dynamical processes
[AD-A248175] p 3515 N92-29399
Sensitivity of C2 sub n to random variations of windspeed, sensible heat flux, and latent heat flux
[AD-A248696] p 3502 N92-29565
U-statistics of increasing degrees with asymptotically Poisson distributions
[CWI-BS-R9120] p 3540 N92-29863
Asymptotic behavior of random discrete event systems p 3529 N92-29963
Strong law and central limit theorem for a process between maxima and sums p 3530 N92-29964

RANDOM VARIABLES
Limit theorems for cumulative processes
[AD-A248507] p 3538 N92-29500
On the effect of range restriction on correlation coefficient estimation
[AD-A248956] p 3511 N92-29620

RANDOM WALK
Random walk polynomials and random walk measures
[MEMO-1007] p 3536 N92-29999

RANGEFINDING
Deep-space navigation with differenced data types. Part 3: An expanded information content and sensitivity analysis p 3409 N92-29368

RARE GASES
Rare gas clusters containing charged atoms
[AD-A248299] p 3544 N92-29350

RAREFIED GAS DYNAMICS
Support activities to maintain SUMS flight readiness, volume 2. Attachment A: Flight 61-C report
[NASA-CR-189656-VOL-2] p 3411 N92-30218
Support activities to maintain SUMS flight readiness, volume 3. Attachment B: Flight STS-35 report, section A
[NASA-CR-189656-VOL-3] p 3411 N92-30219
Support activities to maintain SUMS flight readiness, volume 4. Attachment B: Flight STS-35 report, section B
[NASA-CR-189656-VOL-4] p 3411 N92-30220
Support activities to maintain SUMS flight readiness, volume 5. Attachment B: Flight STS-35 report, section C
[NASA-CR-189656-VOL-5] p 3411 N92-30221
Support activities to maintain SUMS flight readiness, volume 6. Attachment B: Flight STS-35 report, section D
[NASA-CR-189656-VOL-6] p 3411 N92-30222
Support activities to maintain SUMS flight readiness, volume 7. Attachment B: Flight STS-35 report, section E
[NASA-CR-189656-VOL-7] p 3412 N92-30223
Support activities to maintain SUMS flight readiness, volume 8. Attachment B: Flight STS-35 report, section F
[NASA-CR-189656-VOL-8] p 3412 N92-30224
Support activities to maintain SUMS flight readiness, volume 9. Attachment C: Flight STS-40 report. Attachment D: SUMS software listing
[NASA-CR-189656-VOL-9] p 3412 N92-30225

RASTER SCANNING
Definition and design of an experiment to test raster scanning with rotating unbalanced-mass devices on gimbaled payloads
[NASA-TP-3249] p 3429 N92-29677

RATES (PER TIME)
DSN acquisition of Magellan high-rate telemetry data p 3409 N92-29383

RATINGS
Assessment of army aviators' ability to perform individual and collective tasks in the aviation networked simulator
[AD-A250293] p 3407 N92-29709

RAWINSONDES
Science goals and mission objectives of NASA's laser atmospheric wind sounder program p 3468 N92-29296

RAY TRACING
Source location determination of Uranian kilometric radiation from ray tracing and emission lobe modelling
[NASA-CR-190482] p 3570 N92-29360
Efficient complete radiosity ray tracing using a shadow coherence method
[REPT-91-63] p 3518 N92-29749

RAYLEIGH SCATTERING
Efficiencies of rotational Raman and Rayleigh techniques for laser remote sensing of the atmospheric temperature p 3467 N92-29288
Shock enhancement and control of hypersonic combustion
[AD-A248558] p 3418 N92-29580

RAYLEIGH WAVES
Finite difference modelling of seismic wave propagation at the seafloor
[AD-A248345] p 3505 N92-29562

REACTING FLOW
A linear eddy sub-grid model for turbulent reacting flows: Application to hydrogen-air combustion
[DE92-006699] p 3417 N92-29433
Probability density function approach and related closures for turbulent scalar fields p 3450 N92-30059
Monte-Carlo implementation of mapping closures: Application to chemical reacting flows p 3450 N92-30060
Direct simulation of turbulent combustion p 3454 N92-30160

REACTION KINETICS
Modeling deterministic chaos in thermally-pulsed combustion
[DE92-011756] p 3416 N92-29355
Thermodynamic and kinetic aspects of 3/5 epitaxy
[AD-A250632] p 3556 N92-29429
Acetate in hydrothermal solutions: Decomposition kinetics and metal complexation
[DE92-010542] p 3417 N92-29551
Review of temperature dependent effects on the oxidation protection of carbon/carbon
[DE92-012333] p 3415 N92-29645
Finite-rate diffusion-controlled reaction in a vortex
[PB92-172006] p 3418 N92-29744

REACTION TIME
Effects of ionizing radiation on auditory and visual thresholds
[AD-A248199] p 3507 N92-29410

REACTION WHEELS
Geostationary Operational Environmental Satellite (GOES-N report). Volume 2: Technical appendix
[NASA-TM-107920] p 3410 N92-29812

REACTOR DESIGN
A universal, fault-tolerant, non-linear analytic network for modeling and fault detection
[DE92-011840] p 3525 N92-29624
SP-100 W/Re thermocouple calibration techniques
[DE92-011302] p 3550 N92-29938

REAL GASES
Second-order shock-expansion theory extended to include real gas effects
[AD-A247191] p 3400 N92-29539

REAL TIME OPERATION
Adaptive signal processing at NOSC
[AD-A250245] p 3429 N92-29333
Making intelligent systems team players: Overview for designers
[NASA-TM-104751] p 3513 N92-29403
Ultra-dependable real-time computing
[AD-A248193] p 3515 N92-29409
Terrain following of arbitrary surfaces using a high intensity LED proximity sensor
[DE92-004464] p 3528 N92-29644
Robust adaptive kinematic control of redundant robots
[NASA-CR-190520] p 3528 N92-29673
Improved real-time imaging spectrometer
[NASA-CASE-NPO-18410-1-CU] p 3552 N92-29832
Smart BIT/TSMD integration
[AD-A247192] p 3442 N92-29914
Real-time service definition of a communication network in a manufacturing environment
[MEMO-INF-91-84] p 3437 N92-29959
A case study in functional real-time programming
[MEMO-INF-91-62] p 3522 N92-30073
Real space process algebra
[CWI-CW-R9131] p 3538 N92-30178
SESC glossary of solar-terrestrial terms
[PB92-185305] p 3563 N92-30194

RECEIVERS
Figure of merit for direct-detection optical channels p 3431 N92-29376
Detecting microwave emissions from terrestrial sources: A feasibility study
[AD-A248557] p 3435 N92-29579
Performance measurement results for a 220 Mbps QPPM optical communication receiver with an EG/G Slik APD
[NASA-CR-190561] p 3435 N92-29658

RECOGNITION
Sensor fault detection on board an aircraft with observer and polynomial classifier
[DLR-FB-91-34] p 3404 N92-29870

RECOMBINATION REACTIONS
Free ion yields in liquids: Molecular structure and track effects
[DE92-012208] p 3545 N92-29582
Correlated charge-changing ion-atom collisions
[DE92-013473] p 3546 N92-29642
Theory of the dissociation dynamics of small molecules on metal surfaces: Finite temperature studies
[DE92-011188] p 3546 N92-29899

RECURSIVE FUNCTIONS
The isopone method in optimal control
[REPT-91-52] p 3529 N92-29764

RED SHIFT
Evidence for evolution of the luminosity function of clusters of galaxies p 3567 N92-29844
Clusters of galaxies in depth p 3567 N92-29846
X ray cluster counts: What ROSAT should see p 3567 N92-29847

REDUCED GRAVITY
Pressurization of cryogens: A review of current technology and its applicability to low-gravity conditions
[NASA-TM-105746] p 3427 N92-29669
Sample positioning in microgravity
[NASA-CASE-NPO-18448-1-CU] p 3428 N92-30083

REDUNDANCY
Robust adaptive kinematic control of redundant robots
[NASA-CR-190520] p 3528 N92-29673

REDUNDANCY ENCODING
Automatic generation algorithms, experiments, and comparisons of self checking PLA schemes
[IMAG-RR-843-I] p 3516 N92-29621
Improved balancing methods and error diagnosis for bio(chemical) conversions p 3509 N92-29759

REENTRY VEHICLES
Acquisition of an aerothermodynamic data base by means of a winged experimental reentry vehicle
[MBB/FE202/S/PUB/461] p 3399 N92-30232

REFLECTANCE
Sound speed, reflectivity, and absorption measurements in Arctic ice in 1988
[AD-A246293] p 3505 N92-29554

REFLECTOR ANTENNAS
Ka-band feed arrays for spacecraft reflector antennas with limited scan capability: An overview p 3433 N92-29387

REFRACTION
Finite difference modelling of seismic wave propagation at the seafloor
[AD-A248345] p 3505 N92-29562

REFRACTIVITY
Dynamic aperture fringe discriminator
[NASA-CASE-NPO-18478-1-CU] p 3553 N92-30084

REFRACTORY MATERIALS
A novel approach to silicon-on-insulator materials
[AD-A248074] p 3424 N92-29466
Micromechanisms of cyclic and environmentally-assisted subcritical crack growth in ceramic-matrix composites
[AD-A248067] p 3414 N92-29556

REGENERATIVE FUEL CELLS
Optimization of armored spherical tanks for storage on the lunar surface
[NASA-TM-105700] p 3414 N92-30187

REGENERATORS
Erbium-doped fiber amplifier elements for structural analysis sensors
[NASA-CR-190491] p 3552 N92-29681

REGGE POLES
Pole counting and resonance classification
[RAL-92-004] p 3560 N92-29996

REGRESSION ANALYSIS
D-optimal designs for an incomplete quadratic model
[MEMO-COSOR-91-26] p 3532 N92-29742
Analysis of a three-dimensional point pattern with replication
[CWI-BS-R9124] p 3541 N92-30180

REGULATIONS
German high-speed Maglev train safety requirements: Potential for application in the United States
[PB92-167014] p 3564 N92-29809
Revision of certification standards for aviation maintenance personnel p 3487 N92-30127

REINFORCED SHELLS
Damaged stiffened shell research at NASA. Langley Research Center p 3485 N92-30115

REINFORCEMENT (STRUCTURES)
Guide for evaluating 12 inch Substantial Dividing Walls (SDWs) to provide protection from remote operation, volume 2
[AD-A250252] p 3428 N92-29335
Guide for evaluating 12 inch Substantial Dividing Walls (SDWs) to provide protection from remote operation, volume 1
[AD-A250251] p 3428 N92-29545

REINFORCING FIBERS
Manufacturing of components of fibre-metal laminates: An overview
[LR-670] p 3415 N92-29702

RELATIVISTIC PARTICLES
Solution of two-body relativistic bound state equations with confining plus Coulomb interactions p 3547 N92-30003
Relativistic Coulomb fission p 3548 N92-30008
Single nucleon emission in relativistic nucleus-nucleus reactions p 3548 N92-30011

Stopping powers and cross sections due to two-photon processes in relativistic nucleus-nucleus collision p 3548 N92-30012
Fourth workshop on Experiments and Detectors for a Relativistic Heavy Ion Collider [BNL-52262] p 3549 N92-30014
A letter of intent for an experiment to study strong electromagnetic fields at RHIC via multiple electromagnetic processes p 3438 N92-30015

RELATIVITY
A nanoradian differential VLBI tracking demonstration p 3430 N92-29367

RELIABILITY
Concurrent engineering in design of aircraft structures [MBB-FE-2-S-PUB-472] p 3404 N92-29650
Theory of system reliability demonstration, burn-in design, and record statistics [AD-A250582] p 3480 N92-29710
Software reliability and the bootstrap [CWI-BS-R9123] p 3520 N92-29865
Reliable processing of confidential data by means of fragmentation-redundancy-scattering [LAAS-91412] p 3526 N92-29888
Communication: An important element of maintenance and repair p 3402 N92-30124
Aging commuter aeroplanes: Fatigue evaluation and control methods p 3488 N92-30132
A manufacturer's approach to ensure long term structural integrity p 3403 N92-30133

REMOTE SENSING
Sixteenth International Laser Radar Conference, part 1 [NASA-CP-3158-PT-1] p 3456 N92-29228
Southern Hemisphere lidar measurements of the aerosol clouds from Mt. Pinatubo and Mt. Hudson p 3456 N92-29230
Stratospheric backscatter, extinction, and lidar ratio profiling after the Mt. Pinatubo eruptions p 3456 N92-29231
Measurements of stratospheric Pinatubo aerosol extinction profiles by a Raman lidar p 3457 N92-29232
Interpretation of DIAL measurements of lower stratospheric ozone in regions with Pinatubo aerosols p 3457 N92-29236
The JPL Table Mountain and Mauna Loa stratospheric ozone lidars p 3458 N92-29239
First results from TROLIX 1991: An intercomparison of tropospheric ozone lidars p 3459 N92-29244
The global backscatter experiment airborne pulsed lidar measurements p 3459 N92-29246
Two wavelength measurements of the Pinatubo aerosol above Toronto, Canada p 3461 N92-29253
Airborne dial remote sensing of the Arctic ozone layer p 3462 N92-29258
Remote detection of biological particles and chemical plumes using UV fluorescence lidar p 3465 N92-29279
Efficiencies of rotational Raman and Rayleigh techniques for laser remote sensing of the atmospheric temperature p 3467 N92-29288
Laser remote sensing of pollution on water surfaces p 3467 N92-29290
In vivo and in vitro chlorophyll-a and pheophytin-a concentration measurements by laser fluorometry p 3468 N92-29295
The Lidar In-Space Technology Experiment (LITE) p 3469 N92-29301
Mechanical and thermal issues in the development of a spaceborne lidar system p 3469 N92-29303
Airborne sodium and Rayleigh lidar observations from ALOHA-90 p 3471 N92-29315
Diode-pumped Nd:YAG lidar for airborne cloud measurements p 3473 N92-29326
Remote sensing by spaceborne lidar aided by surface returns p 3473 N92-29327
EOS Data and Information System (EOSDIS) --- landsat satellites [NASA-TM-107922] p 3488 N92-29442
GIS for coastal management [BCRS-90-31] p 3489 N92-29493
Alexander: User guide (version 1.0) [BCRS-90-38] p 3489 N92-29494
Research programming studies: Remote sensing emissions, land use and effects, in relation to climate and environment [BCRS-91-17] p 3493 N92-29497
The main lines of the research programs remote sensing: Climate and environment [BCRS-91-25] p 3493 N92-29499
SeaWiFS technical report series. Volume 1: An overview of SeaWiFS and ocean color [NASA-TM-104566-VOL-1] p 3505 N92-29686
Activities report of the Netherlands Remote Sensing Board (with abridged version) [ETN-92-91352] p 3489 N92-29688
Monitoring of grass dominance on Dutch heathlands using remote sensing and a geographic information system (HEIMON) [BCRS-91-12] p 3489 N92-29693
CAESAR: A CCD airborne experimental scanner for applications in remote sensing radiometric and geometric calibration [NLR-TP-89103-U] p 3490 N92-29707
Mapping agroecological zones and time lag in vegetation growth by means of Fourier analysis of time series of NDVI images [REPT-32] p 3490 N92-29717
River hydrometry by pattern recognition in remote sensing images [PUBL-445] p 3490 N92-29728
Geostationary Operational Environmental Satellite (GOES-N report). Volume 1: Technical [NASA-TM-107918] p 3410 N92-29811
Fourth Meeting of the Space Agency Forum on the International Space Year (SAFISY-4) [ESA-SP-1141] p 3407 N92-29879
Application of remote sensing methods for tracking large cetaceans: North Atlantic right whales Eubalaena Glacialis [PB92-185016] p 3490 N92-30022
Small satellites and RPAS in global-change research: Summary and conclusions [DE92-013602] p 3490 N92-30088
Programmable hyperspectral image mapper with on-array processing [NASA-CASE-NPO-17794-1-CU] p 3553 N92-30104
Biophysical, morphological, canopy optical property, and productivity data from the Superior National Forest [NASA-TM-104568] p 3491 N92-30210

REMOTE SENSORS
Activities report of the Netherlands Remote Sensing Board (with abridged version) [ETN-92-91352] p 3489 N92-29688

REMOTELY PILOTED VEHICLES
A preliminary design and analysis of an advanced heat-rejection system for an extreme altitude advanced variable cycle diesel engine installed in a high-altitude advanced research platform [NASA-CR-186021] p 3405 N92-29427
Path tracking using simple planar curves [AD-A248252] p 3403 N92-29617
Small satellites and RPAS in global-change research: Summary and conclusions [DE92-013602] p 3490 N92-30088

REMOVAL
Laser paint stripping [AD-A249233] p 3476 N92-29581

RENORMALIZATION GROUP METHODS
Derivation of the kappa-epsilon model equations using the renormalization group method p 3450 N92-30055
Development of renormalization group analysis of turbulence p 3453 N92-30156

REPLACING
On-line replacement of program modules using AdaPT [NASA-CR-190499] p 3514 N92-29363
Bearing servicing tool [NASA-CASE-MSC-21881-1] p 3479 N92-30082

REPLICAS
Analysis of a three-dimensional point pattern with replication [CWI-BS-R9124] p 3541 N92-30180

REPORTS
United Kingdom Infrared Telescope [ETN-92-91341] p 3565 N92-29682
Activities report of the Netherlands Remote Sensing Board (with abridged version) [ETN-92-91352] p 3489 N92-29688
The 36th issue of Electronics and Electrical Engineering Laboratory Technical Progress Bulletin covering laboratory programs, July to September 1991, with 1992 EEEL events calendar [PB92-164672] p 3442 N92-30032

REPRODUCTION (COPYING)
Optimal copying strategies [MEMO-1005] p 3537 N92-30081

REQUIREMENTS
Saenger: The reference concept and its technological requirements - aerothermodynamics [MBB-FE-202-S-PUB-0463-A] p 3408 N92-29629
Aerothermodynamic challenges of the Saenger space-transportation system [MBB-FE-202-S-PUB-0462-A] p 3409 N92-29680
Software quality control and requirements specification [REPT-91-48] p 3518 N92-29711
High-speed Maglev trains: German safety requirements RW-MSB [PB92-167006] p 3564 N92-29808
Maintainability requirements for ESA space systems [ESA-PSS-01-50-ISSUE-1] p 3481 N92-29878
SRSM: A Software Requirements Specification Method [REPT-91-84] p 3524 N92-30228

RESCUE OPERATIONS
Evaluation of Night Vision Goggles (NVG) for maritime search and rescue [AD-A247182] p 3512 N92-29538

RESEARCH
Aeronautical Engineering Group publications, 1950 - present [AERO-REPT-8907] p 3444 N92-29683
Expert judgment study on atmospheric dispersion and deposition: Main report and annexes [REPT-91-81] p 3495 N92-30226

RESEARCH AIRCRAFT
Feedback control laws for highly maneuverable aircraft [NASA-CR-190535] p 3406 N92-29654
Flight evaluation of an extended engine life mode on an F-15 airplane [NASA-TM-104240] p 3405 N92-29659

RESEARCH AND DEVELOPMENT
The 1991 research highlights [AD-A247865] p 3570 N92-29464
The 1990 annual report, April 1990 - March 1991 p 3571 N92-29471
Summary of technical operations, 1991 --- software development [AD-A248153] p 3516 N92-29540
Research in NASA history: A guide to the NASA history program [NASA-TM-107953] p 3571 N92-29689
Integrity control in relational database systems: An overview [MEMO-INF-91-80] p 3562 N92-29957
Physics Laboratory technical activities, 1991 [PB92-172824] p 3542 N92-30035
Annual research briefs, 1989 [NASA-CR-189024] p 3452 N92-30149
NASA-UVA light aerospace alloy and structures technology program (LA2ST) [NASA-CR-190538] p 3423 N92-30206

RESEARCH FACILITIES
Sixteenth International Laser Radar Conference, part 1 [NASA-CP-3158-PT-1] p 3456 N92-29228
Multi-wavelength measurements of the stratospheric aerosol layer made at Hampton, Virginia (37N, 76W) p 3460 N92-29249
United Kingdom Infrared Telescope [ETN-92-91341] p 3565 N92-29682
Research in NASA history: A guide to the NASA history program [NASA-TM-107953] p 3571 N92-29689
LLE review [DE92-011614] p 3555 N92-30072
Research and technology annual report, FY 1990 [NASA-TM-107807] p 3571 N92-30197

RESEARCH MANAGEMENT
Research programming studies: Remote sensing emissions, land use and effects, in relation to climate and environment [BCRS-91-17] p 3493 N92-29497
The main lines of the research programs remote sensing: Climate and environment [BCRS-91-25] p 3493 N92-29499
National Institute for Global Environmental Change [DE92-013487] p 3493 N92-29597
Activities report of the Netherlands Remote Sensing Board (with abridged version) [ETN-92-91352] p 3489 N92-29688
The 1991 Summer Faculty Research Program (SFRP), volume 2 [AD-A248764] p 3571 N92-29724
The 1991 Summer Faculty Research Program (SFRP), volume 3 [AD-A248765] p 3571 N92-29725

RESEARCH PROJECTS
The 1990 annual report, April 1990 - March 1991 p 3571 N92-29471
United Kingdom Infrared Telescope [ETN-92-91341] p 3565 N92-29682
Research in NASA history: A guide to the NASA history program [NASA-TM-107953] p 3571 N92-29689
The 1991 Summer Faculty Research Program (SFRP), volume 2 [AD-A248764] p 3571 N92-29724
The 1991 Summer Faculty Research Program (SFRP), volume 3 [AD-A248765] p 3571 N92-29725

RESIDUAL STRENGTH
Damaged stiffened shell research at NASA. Langley Research Center p 3485 N92-30115

RESIN MATRIX COMPOSITES
Approaches to polymer-derived CMC matrices
[NASA-TM-105754] p 3415 N92-29660
Manufacturing of components of fibre-metal laminates: An overview
[LR-670] p 3415 N92-29702
RESINS
The comparative effects of gamma radiation and in situ alpha particles on five strong-base anion exchange resins
[DE92-000177] p 3425 N92-29643
RESOLUTION
Peripheral limitations on spatial vision
[AD-A250579] p 3511 N92-29591
RESONANCE
Pole counting and resonance classification
[RAL-92-004] p 3560 N92-29996
RESONANCE FLUORESCENCE
Characterization of artificial guidestars generated in the mesospheric sodium layer p 3470 N92-29309
Lidar probing of the mesosphere: Simultaneous observations of sporadic sodium and iron formations, calcium ion layers, neutral temperature and winds p 3470 N92-29311
RESOURCES MANAGEMENT
Diversification and product innovation: A challenge for modern management
[OEFZS-4570] p 3561 N92-29886
Research and technology annual report, FY 1990
[NASA-TM-107807] p 3571 N92-30197
RESPONSES
Peripheral limitations on spatial vision
[AD-A250579] p 3511 N92-29591
RESTORATION
Multiresponse imager and imaging process for improved resolution
[NASA-CASE-LAR-14779-1] p 3552 N92-29951
RETARDING
Effects of retardation in relativistic equations with confining interaction p 3547 N92-30005
REUSE
Abstract data types and algorithm structures and a basis for component reuse
[REPT-91-49] p 3518 N92-29712
REVENUE
Lidar monitoring of Mexico City's atmosphere during high air polution episodes p 3464 N92-29275
REVERSE ENGINEERING
Reverse automatic differentiation of modular FORTRAN programs
[DE92-014071] p 3519 N92-29797
RIBLETS
A numerical method for direct simulation of turbulence in complex geometries p 3455 N92-30166
RIGID STRUCTURES
An approximation method for dynamic response of strain-hardening structures
[DE92-013053] p 3482 N92-29535
RING LASERS
Review of potential x ray laser applications in materials science and chemistry
[DE92-012254] p 3475 N92-29434
RIVERS
River hydrometry by pattern recognition in remote sensing images
[PUBL-445] p 3490 N92-29728
ROBOT ARMS
Position-error-based force reflection and compliance control
[NASA-CASE-NPO-18668-1-CU] p 3479 N92-29765
Full pose and partial pose calibration of a 6 degree-of-freedom robot manipulator arm
[AD-A247463] p 3479 N92-29785
On fictitious joints modelling of manipulator link flexibility for the HERA simulation facility pilot
[NLR-TR-88086-U] p 3479 N92-29885
ROBOT CONTROL
Experimental investigation of adaptive control of a parallel manipulator
[NASA-CR-189867] p 3528 N92-29656
Position-error-based force reflection and compliance control
[NASA-CASE-NPO-18668-1-CU] p 3479 N92-29765
Full pose and partial pose calibration of a 6 degree-of-freedom robot manipulator arm
[AD-A247463] p 3479 N92-29785
Robotic workcell for wire wrapping integrated circuits
[DE92-013999] p 3441 N92-29796
ROBOT DYNAMICS
Robust adaptive kinematic control of redundant robots
[NASA-CR-190520] p 3528 N92-29673
ROBOTICS
KISMET (kinematic simulation, monitoring and off-line programming environments for telerobotics): Simulation of the target-oriented driving of an autonomous vehicle in a labyrinthic environment
[KFK-4941] p 3515 N92-29418
Path tracking using simple planar curves
[AD-A248252] p 3403 N92-29617
ARTIBODIES: A system for modelling articulated bodies
[REPT-91-57] p 3517 N92-29627
Recognition of multi-articulated three-dimensional objects using a multisensor system for robotics applications
[LAAS-91394] p 3529 N92-29675
Robotic workcell for wire wrapping integrated circuits
[DE92-013999] p 3441 N92-29796
Bladder operated robotic joint
[NASA-CASE-MFS-28682-1] p 3426 N92-29831
ROBOTS
Improving path planning with learning
[DE92-004360] p 3527 N92-29456
Using custom-designed VLSI fuzzy inferencing chips for the autonomous navigation of a mobile robot
[DE92-000424] p 3528 N92-29550
Terrain following of arbitrary surfaces using a high intensity LED proximity sensor
[DE92-004464] p 3528 N92-29644
Robust adaptive kinematic control of redundant robots
[NASA-CR-190520] p 3528 N92-29673
SPARA: A system of planning robot manipulation tasks
[LAAS-91395] p 3529 N92-29678
Bladder operated robotic joint
[NASA-CASE-MFS-28682-1] p 3426 N92-29831
ROBUSTNESS (MATHEMATICS)
Taguchi methods
[MEMO-COSOR-91-31] p 3539 N92-29609
Robust adaptive kinematic control of redundant robots
[NASA-CR-190520] p 3528 N92-29673
ROCKET ENGINES
Feasibility of an antiproton catalyzed fission fragment rocket
[AD-A248157] p 3412 N92-29444
Accelerometer method and apparatus for integral display and control functions
[NASA-CASE-MSC-21961-1] p 3474 N92-29952
RODS
Combined load test apparatus for flat panels
[NASA-CASE-LAR-14698-1] p 3483 N92-30028
ROLLER BEARINGS
Rolling-contact and wear resistance of hard coatings on bearing-steel substrates
[DE92-011834] p 3478 N92-29357
ROOTS OF EQUATIONS
Askey-Wilson polynomials for root systems of type BC
[CWI-AM-R9112] p 3534 N92-29882
ROSAT MISSION
Traces of the primordial structure in the universe
[MPE-227] p 3565 N92-29833
CDM with thermal history of baryons: High-resolution 2-D and 3-D simulations p 3565 N92-29835
X ray cluster counts: What ROSAT should see p 3567 N92-29847
ROSAT: Early results p 3567 N92-29850
The x ray morphology of the relaxed cluster of galaxies A2256. 1: Evidence for a merger event p 3568 N92-29851
Optical searches for ROSAT x ray cluster sources p 3568 N92-29853
ROTARY STABILITY
Explicit Navier-Stokes computation of turbomachinery flows
[AD-A248458] p 3445 N92-29933
ROTARY WING AIRCRAFT
Contingency power for a small turboshaft engine by using water injection into turbine cooling air
[NASA-TM-105680] p 3405 N92-29661
ROTARY WINGS
A semi empirical method for the analytical representation of stationary measured profile coefficients for applications of rotary wing aerodynamics
[ETN-92-91491] p 3401 N92-29741
ROTATING BODIES
Definition and design of an experiment to test raster scanning with rotating unbalanced-mass devices on gimbaled payloads
[NASA-TP-3249] p 3429 N92-29677
Accelerometer method and apparatus for integral display and control functions
[NASA-CASE-MSC-21961-1] p 3474 N92-29952
ROTATING PLASMAS
Analysis of a dedicated rotation experiment in TFTR
[DE92-013463] p 3554 N92-29438
ROTATING SHAFTS
Experimental examination of heavy loaded axial fans with rotational symmetrical distortion of the inflow
[ETN-92-91489] p 3445 N92-29926
Shaft mount for data coupler system
[NASA-CASE-LAR-13805-1] p 3480 N92-30097
ROTATION
Accelerometer method and apparatus for integral display and control functions
[NASA-CASE-MSC-21961-1] p 3474 N92-29952
Non-linear interactions in homogeneous turbulence with and without background rotation p 3448 N92-30044
Turbulence modeling: Near-wall turbulence and effects of rotation on turbulence p 3452 N92-30151
An experimental study of the effects of rapid rotation on turbulence p 3453 N92-30154
Spectroscopy of W-183; measured magnetic moments and rotation-particle coupling
[DE92-624790] p 3549 N92-30213
ROUTES
The isopone method in optimal control
[REPT-91-52] p 3529 N92-29764
ROVING VEHICLES
A systems analysis of the impact of navigation instrumentation on-board a Mars rover, based on a covariance analysis of navigation performance
[NASA-CR-189868] p 3403 N92-29440
RULES
Defaults in update semantics
[ITLI-LP-91-02] p 3532 N92-29685
RUNGE-KUTTA METHOD
Analysis of parallel diagonal-implicit iteration of Runge-Kutta methods
[CWI-NM-R9114] p 3526 N92-29867
RUTHENIUM ALLOYS
Structure and stability of Al-Cu-Ru face-centered icosahedral alloys
[DE92-012550] p 3422 N92-29706

S

S MATRIX THEORY
SOLITON
[USIP-90-09] p 3518 N92-29714
S WAVES
Pole counting and resonance classification
[RAL-92-004] p 3560 N92-29996
SAAB AIRCRAFT
A manufacturer's approach to ensure long term structural integrity p 3403 N92-30133
SAFETY
Publications of the environmental health program: 1980-1990
[NASA-CR-4455] p 3509 N92-29341
Buffet test in the National Transonic Facility
[NASA-CR-189595] p 3406 N92-29352
SAFETY DEVICES
Li/SO2 cells and Li/SOCl2 cells: Safe use and testing
[DE92-013508] p 3439 N92-29414
SAFETY FACTORS
High-speed Maglev trains: German safety requirements RW-MSB
[PB92-167006] p 3564 N92-29808
German high-speed Maglev train safety requirements: Potential for application in the United States
[PB92-167014] p 3564 N92-29809
SAFETY MANAGEMENT
High-speed Maglev trains: German safety requirements RW-MSB
[PB92-167006] p 3564 N92-29808
German high-speed Maglev train safety requirements: Potential for application in the United States
[PB92-167014] p 3564 N92-29809
Maintaining the safety of an aging fleet of aircraft p 3402 N92-30108
SAMPLING
Sampling and representativeness for a spaceborne wind lidar p 3463 N92-29268
Near-visible Raman instrumentation for remote multi-point process monitoring using optical fibers and optical multiplexing
[DE92-011287] p 3550 N92-29337
Peripheral limitations on spatial vision
[AD-A250579] p 3511 N92-29591
On the effect of range restriction on correlation coefficient estimation
[AD-A248956] p 3511 N92-29620
U-statistics of increasing degrees with asymptotically Poisson distributions
[CWI-BS-R9120] p 3540 N92-29863
SAPPHIRE
Laser-induced desorption from sapphire surfaces
[DE92-012698] p 3475 N92-29340

SATELLITE CONTROL
An analysis of the endurance of mobile satellite command and control systems
[AD-A248084] p 3410 N92-29525
SATELLITE DESIGN
Geostationary Operational Environmental Satellite (GOES-N report). Volume 2: Technical appendix
[NASA-TM-107920] p 3410 N92-29812
SATELLITE IMAGERY
Tapering clouds and their classification due mainly to the surrounding cloud pattern in the GMS imagery
[ISSN-0388-9653] p 3502 N92-29666
Mapping agroecological zones and time lag in vegetation growth by means of Fourier analysis of time series of NDVI images
[REPT-32] p 3490 N92-29717
Motion restoration of long time exposed images with satellite-borne cameras
[ETN-92-91490] p 3474 N92-29731
Comparison of in situ, aircraft- and satellite derived surface reflectances in Flevoland (Netherlands). A validation experiment
[BCRS-91-28] p 3491 N92-30230
TERS product development plan for urban planning of Bandung, Indonesia
[BCRS-91-30] p 3491 N92-30231
SATELLITE INSTRUMENTS
OFFEQ-1: Preliminary flight evaluation results
[ITN-92-85126] p 3410 N92-29480
SATELLITE LIFETIME
OFFEQ-1: Preliminary flight evaluation results
[ITN-92-85126] p 3410 N92-29480
SATELLITE ORBITS
Generalized probability model for calculation of interference to the Deep Space Network due to circularly Earth-orbiting satellites p 3433 N92-29386
OFFEQ-1: Preliminary flight evaluation results
[ITN-92-85126] p 3410 N92-29480
SATELLITE TRACKING
OFFEQ-1: Preliminary flight evaluation results
[ITN-92-85126] p 3410 N92-29480
SATELLITE-BORNE INSTRUMENTS
Motion restoration of long time exposed images with satellite-borne cameras
[ETN-92-91490] p 3474 N92-29731
SATELLITES
Phase-space estimate of satellite coverage time
[DE92-013555] p 3542 N92-30139
SCALARS
A linear eddy sub-grid model for turbulent reacting flows: Application to hydrogen-air combustion
[DE92-006699] p 3417 N92-29433
Large eddy simulations of passive and buoyant scalars with dynamic subgrid-scale models
p 3450 N92-30057
Probability density function approach and related closures for turbulent scalar fields p 3450 N92-30059
An experimental study of scalar mixing in curved shear layers p 3453 N92-30152
SCALING LAWS
Scale-invariant galaxy clustering on large scales
p 3566 N92-29839
Scaling analysis of energy transfer in the inertial range
p 3448 N92-30046
SCANNERS
Lag angle compensation in a space borne scanning lidar p 3462 N92-29263
Migmas/A: Test of a scanning ion microscope on the Soviet Space Station Mir
[OEFZS-4615] p 3473 N92-29469
SCANNING TUNNELING MICROSCOPY
Variable temperature scanning tunneling microscopy
[AD-A248725] p 3557 N92-29722
SCATTERING
Femtosecond studies of carrier dynamics in compound semiconductors
[AD-A250584] p 3439 N92-29452
The real-space multiple-scattering theory and the electronic structure of grain boundaries
[DE92-013006] p 3556 N92-29473
Multiphoton processes in scattering and ionization in an intense linearly-polarized radiation field
[DE92-013546] p 3545 N92-29515
The Green Function Cellular Method and its relation to multiple scattering theory
[DE92-011470] p 3436 N92-29909
Neutron diffraction study of the electronic structure of high T(sub c) superconductor-related compounds
[DE92-012587] p 3559 N92-29939
Pole counting and resonance classification
[RAL-92-004] p 3560 N92-29996
Sub-angstrom microscopy through incoherent imaging and image reconstruction
[DE92-011787] p 3475 N92-30090
SCATTERING AMPLITUDE
Electron spectra of adatomic structures
[DE92-625013] p 3544 N92-29415
SCATTERING COEFFICIENTS
Three-wavelength lidar measurements of Pinatubo aerosol and its optical properties p 3460 N92-29250
SOLITON
[USIP-90-09] p 3518 N92-29714
SCATTERING CROSS SECTIONS
Normalized radar cross section of natural surfaces at millimeter wavelengths
[AD-A248452] p 3434 N92-29447
SOLITON
[USIP-90-09] p 3518 N92-29714
SCATTEROMETERS
Microstrip reflectarray antenna for the SCANSCAT radar application
[NASA-CR-190453] p 3434 N92-29463
SCHEDULES
Geostationary Operational Environmental Statellite(GEOS-N report)
[NASA-TM-107919] p 3410 N92-29810
SCHEDULING
Ultra-dependable real-time computing
[AD-A248193] p 3515 N92-29409
SCHOTTKY DIODES
Electrical, optical, and magnetic resonance studies of novel pi-conjugated polymers
[DE92-012548] p 3424 N92-29482
Simulations on the electrical characteristics of Si, SiC and diamond junction and Schottky power diodes
[PB92-177872] p 3443 N92-30094
SCHROEDINGER EQUATION
Electron spectra of adatomic structures
[DE92-625013] p 3544 N92-29415
On the parity of fundamental solutions for one-dimensional scattering problem with inverse square potential
[DE92-624511] p 3560 N92-29533
Supersymmetric extensions of the nonlinear Schroedinger equation: Symmetries and coverings
[MEMO-1002] p 3537 N92-30078
SCIENTISTS
The 1991 research highlights
[AD-A247865] p 3570 N92-29464
The 1991 Summer Faculty Research Program (SFRP), volume 2
[AD-A248764] p 3571 N92-29724
The 1991 Summer Faculty Research Program (SFRP), volume 3
[AD-A248765] p 3571 N92-29725
SEA ICE
NOAA environmental digest: Selected indicators of the United States and the global environment, December 1991
[PB92-185073] p 3494 N92-30019
SEA LEVEL
Class A network Dataring gauges: 1989 data processing and analysis
[REPT-18-1991] p 3505 N92-29684
SEA WATER
Laser remote sensing of pollution on water surfaces
p 3467 N92-29290
In vivo and in vitro chlorophyll-a and pheophytin-a concentration measurements by laser fluorometry
p 3468 N92-29295
SEALS (STOPPERS)
Check valve with poppet damping mechanism
[NASA-CASE-MSC-21903-1] p 3480 N92-30101
SEARCHING
A seven-league-boots algorithm for path planning in configuration spaces
[MEMO-INF-91-88] p 3530 N92-29969
SECONDARY FLOW
Examination of the main error factors with regards to secondary losses in compression and turbine cascades by variations of the blade picture ratio
[ETN-92-91493] p 3405 N92-29927
SECONDARY INJECTION
A numerical and experimental investigation of the thrust vector control by secondary gas injection
[DLR-FB-91-31] p 3447 N92-29998
SEISMIC WAVES
Finite difference modelling of seismic wave propagation at the seafloor
[AD-A248345] p 3505 N92-29562
Land-based seismic array studies of low frequency ambient oceanic noise
[AD-A248255] p 3505 N92-29618
SELECTION
Selection constants for uniform populations
[MEMO-COSOR-92-02] p 3540 N92-29827
SELF TESTS
A strategy for microprocessor BIST implementation based on deterministic testing
[IMAG-RR-844-I] p 3516 N92-29570
B(exp 2)UBIST: A strategy for boundary scan board unified BIST
[IMAG-RR-862-I] p 3441 N92-29612
Automatic generation algorithms, experiments, and comparisons of self checking PLA schemes
[IMAG-RR-843-I] p 3516 N92-29621
SEMANTICS
Experiments on processes with backtracking
[RR-858-I-IMAG-121-LIFIA] p 3532 N92-29574
Defaults in update semantics
[ITLI-LP-91-02] p 3532 N92-29685
Dynamic semantics and circular propositions
[ITLI-LP-91-03] p 3532 N92-29687
An algebraic specification for the static semantics of Pascal
[CWI-CS-R9129] p 3522 N92-29989
Rendez-vous with metric semantics
[CWI-CS-R9135] p 3522 N92-29991
CCS for OO and LP
[CWI-CS-R9136] p 3522 N92-29992
Partial logic as a simple restriction of standard logic
[MEMO-INF-91-73] p 3536 N92-29995
Overview of the document style semantics and specification language and the MIL-M-28001A output specification
[PB92-181122] p 3563 N92-30039
SEMICONDUCTOR DEVICES
Hardening techniques to counter cumulated dose on SEU and SEL in space environment
[IMAG-RR-863-I] p 3441 N92-29613
Time-of-flight experiments on GaAs/Al(x)Ga(x-1)As heterostructures
[ETN-92-91625] p 3558 N92-29753
SEMICONDUCTOR LASERS
Phase conjugation in BaTiO3 at 830 nanometers
[AD-A250240] p 3475 N92-29332
Laser diode end-pumped Nd:YAG laser
[AD-A248123] p 3475 N92-29396
SEMICONDUCTORS (MATERIALS)
Thermodynamic and kinetic aspects of 3/5 epitaxy
[AD-A250632] p 3556 N92-29429
Femtosecond studies of carrier dynamics in compound semiconductors
[AD-A250584] p 3439 N92-29452
A novel approach to silicon-on-insulator materials
[AD-A248074] p 3424 N92-29466
Electrical, optical, and magnetic resonance studies of novel pi-conjugated polymers
[DE92-012548] p 3424 N92-29482
Modulated high sensitivity infrared polarimeter
[AD-D015256] p 3474 N92-29571
Novel thin-film CuInSe2 fabrication
[DE92-001222] p 3557 N92-29584
Variable temperature scanning tunneling microscopy
[AD-A248725] p 3557 N92-29722
Electrochemistry in colloids and dispersions. Volume 2: Solute distribution, diffusion, and transport colloidal metals
[AD-A248336] p 3419 N92-29931
Electrochemistry in colloids and dispersions. Volume 3: Colloidal semiconductors
[AD-A248337] p 3419 N92-29932
Laser etching: Possibilities and problems
[DE92-010800] p 3477 N92-30135
SEMIEMPIRICAL EQUATIONS
A semi empirical method for the analytical representation of stationary measured profile coefficients for applications of rotary wing aerodynamics
[ETN-92-91491] p 3401 N92-29741
SENSITIVITY
Determination of aerodynamic sensitivity coefficients for wings in transonic flow
[NASA-CR-190570] p 3401 N92-29657
A low sensitivity observer for complex biotechnological processes p 3509 N92-29757
Chebyshev line approximation: A sensitivity analysis
[MEMO-1020] p 3537 N92-30147
SENSORIMOTOR PERFORMANCE
Effects of ionizing radiation on auditory and visual thresholds
[AD-A248199] p 3507 N92-29410
SEPARATED FLOW
A method for computing the 3-dimensional flow about wings with leading-edge vortex separation. Part 2: Description of computer program VORSEP
[NLR-TR-86006-U] p 3402 N92-29916
SEPARATORS
Material-deposition processes in the separator of Li-alloy/FeS2 thermal cells
[DE92-013669] p 3440 N92-29518
SEQUENCING
A strategy for microprocessor BIST implementation based on deterministic testing
[IMAG-RR-844-I] p 3516 N92-29570
Minimal-change codes and number systems
[REPT-91-42] p 3536 N92-29924

Linear approximation of shortest superstrings
[CWI-CS-R9126] p 3523 N92-30146

SEQUENTIAL ANALYSIS
Limit theorems for cumulative processes
[AD-A248507] p 3538 N92-29500
A sample-size optimal bayesian procedure for sequential pharmaceutical trials
[AD-A248512] p 3538 N92-29501

SERIES (MATHEMATICS)
Asymptotic optimality of the chi-square test with large number of degrees of freedom within the class of symmetric tests
[CWI-BS-R9116] p 3540 N92-29860

SERIES EXPANSION
Matched asymptotic expansions solution for low-frequency sound radiation from fluid-loaded, baffled plates: Axisymmetric case
[REPT-91-60] p 3543 N92-29628
Matched asymptotic expansions solution for low-frequency sound radiation from fluid-loaded, baffled plates: Two-dimensional case
[REPT-91-62] p 3543 N92-29748
Asymptotic inversion of the incomplete beta function
[CWI-AM-R9106] p 3534 N92-29893
Hyperasymptotic expansions of confluent hypergeometric functions
[CWI-AM-R9107] p 3535 N92-29894
Power approximations to and power comparison of certain goodness-of-fit tests
[MEMO-1019] p 3541 N92-29980

SEROTONIN
Physiological analyses of the afferents controlling brain neurochemical systems
[AD-A248334] p 3512 N92-29930

SERVICE LIFE
Theory of system reliability demonstration, burn-in design, and record statistics
[AD-A250582] p 3480 N92-29710

SERVICES
Integrated service engineering supported by the FDT LOTOS
[MEMO-INF-91-76] p 3531 N92-30184

SERVOMECHANISMS
Definition and design of an experiment to test raster scanning with rotating unbalanced-mass devices on gimbaled payloads
[NASA-TP-3249] p 3429 N92-29677
Geostationary Operational Environmental Satellite (GOES-N report). Volume 2: Technical appendix
[NASA-TM-107920] p 3410 N92-29812
Sample positioning in microgravity
[NASA-CASE-NPO-18448-1-CU] p 3428 N92-30083

SERVOMOTORS
Definition and design of an experiment to test raster scanning with rotating unbalanced-mass devices on gimbaled payloads
[NASA-TP-3249] p 3429 N92-29677

SET THEORY
A model for no Borel liftings
[REPT-91-37] p 3535 N92-29919
A soft stairway to institutions
[MEMO-INF-91-87] p 3522 N92-29981
Swirls and wheels
[PB92-173251] p 3542 N92-30095
Sufficient conditions for dominating cliques
[MEMO-1006] p 3538 N92-30185

SHAFTS (MACHINE ELEMENTS)
Optimal design of compact apur gear reductions
[NASA-TM-105676] p 3478 N92-29351
Friction drive position transducer
[AD-D015205] p 3475 N92-30202

SHALLOW WATER
Numerical methods for the 3D shallow water equations on vector and parallel computers
[CWI-NM-R9109] p 3446 N92-29944
On the numerical treatment of the advective terms in 3D shallow water models
[CWI-NM-R9110] p 3446 N92-29945

SHAPE MEMORY ALLOYS
Fastening apparatus having shape memory alloy actuator
[NASA-CASE-MSC-21935-1] p 3479 N92-29762

SHAPES
Object discrimination based on depth-from-occlusion
[AD-A248104] p 3511 N92-29560
A semi empirical method for the analytical representation of stationary measured profile coefficients for applications of rotary wing aerodynamics
[ETN-92-91491] p 3401 N92-29741

SHEAR FLOW
Progress toward identification of streamwise vorticity meander in a plane mixing layer p 3451 N92-30068
Organized motions underlying turbulent shear flows p 3453 N92-30158

SHEAR LAYERS
Effect of walls on the supersonic reacting mixing layer p 3451 N92-30065
Mixing measurements of straight and curved shear layers p 3451 N92-30067
An experimental study of scalar mixing in curved shear layers p 3453 N92-30152
An experimental study of secondary vortex structure in mixing layers p 3453 N92-30155
Incompressible spatially-developing free-shear flows p 3454 N92-30165

SHEAR PROPERTIES
Structure and shear response of lipid monolayers
[DE92-011633] p 3542 N92-29354

SHEAR STRESS
A consistent shear deformable theory for laminated plates
[AD-A250591] p 3415 N92-29593
Active thermal isolation for temperature responsive sensors
[NASA-CASE-LAR-14612-1] p 3446 N92-29954

SHELL STABILITY
The effect of length variation on the stability of circular cylindrical shells under pure bending
[LR-669] p 3482 N92-29700

SHELLS (STRUCTURAL FORMS)
Compressive response of debonded thick composite shells including the effects of transient moisture sorption
[AD-A250080] p 3414 N92-29462

SHELTERS
Guide for evaluating 12 inch Substantial Dividing Walls (SDWs) to provide protection from remote operation, volume 2
[AD-A250252] p 3428 N92-29335
Guide for evaluating 12 inch Substantial Dividing Walls (SDWs) to provide protection from remote operation, volume 1
[AD-A250251] p 3428 N92-29545

SHIPS
Marine structural steel toughness data bank (abridged edition)
[PB92-163294] p 3422 N92-29807

SHOCK RESISTANCE
Guide for evaluating 12 inch Substantial Dividing Walls (SDWs) to provide protection from remote operation, volume 2
[AD-A250252] p 3428 N92-29335

SHOCK TUBES
Shock enhancement and control of hypersonic combustion
[AD-A248558] p 3418 N92-29580

SHOCK WAVE PROFILES
Viscous profiles and numerical methods for shock waves
[AD-A246110] p 3443 N92-29458

SHOCK WAVES
Viscous profiles and numerical methods for shock waves
[AD-A246110] p 3443 N92-29458
Strategies for understanding the deflagration-to-detonation transition
[DE92-013528] p 3427 N92-29512
Second-order shock-expansion theory extended to include real gas effects
[AD-A247191] p 3400 N92-29539
Omega phase formation in titanium and titanium alloys
[DE92-011138] p 3421 N92-29633

SHOPS
Shop of the 1990's: The implementation of a CAD/CAM system for small machine shops
[PB92-181098] p 3522 N92-30020

SHORT CRACKS
Short cracks and durability analysis of the Fokker 100 wing/fuselage structure
[NLR-TP-90336-U] p 3482 N92-29603

SHOULDERS
Development of models for prediction of optimal lifting motion
[PB92-164656] p 3513 N92-29949

SIGNAL DETECTION
Additivity and auditory pattern analysis
[AD-A250580] p 3511 N92-29592
Land-based seismic array studies of low frequency ambient oceanic noise
[AD-A248255] p 3505 N92-29618

SIGNAL DETECTORS
Design and construction of a channel electron multiplier based Mossbauer spectroscopy system
[AD-A248154] p 3439 N92-29443

SIGNAL ENCODING
Friction drive position transducer
[AD-D015205] p 3475 N92-30202

SIGNAL GENERATORS
Standard spherical dipole source
[PB92-187020] p 3438 N92-30198

SIGNAL PROCESSING
Extraction of aerosol and Rayleigh components from Doppler lidar return signal p 3465 N92-29281
Adaptive signal processing at NOSC
[AD-A250245] p 3429 N92-29333
DSN acquisition of Magellan high-rate telemetry data p 3409 N92-29383
Goldstone solar system radar signal processing p 3433 N92-29389
Detection of binary phase shift keyed signals in extremely high noise
[AD-A248552] p 3435 N92-29576
Scalable parallel algorithms for multidimensional digital signal processing
[AD-A249381] p 3516 N92-29622
Performance measurement results for a 220 Mbps QPPM optical communication receiver with an EG/G Slik APD
[NASA-CR-190561] p 3435 N92-29658
Erbium-doped fiber amplifier elements for structural analysis sensors
[NASA-CR-190491] p 3552 N92-29681

SIGNAL TO NOISE RATIOS
Signal quality influence on averaging procedure for DIAL pollution monitoring p 3465 N92-29280
Design and construction of a channel electron multiplier based Mossbauer spectroscopy system
[AD-A248154] p 3439 N92-29443
Modulated high sensitivity infrared polarimeter
[AD-D015256] p 3474 N92-29571
Detection of binary phase shift keyed signals in extremely high noise
[AD-A248552] p 3435 N92-29576
Taguchi methods
[MEMO-COSOR-91-31] p 3539 N92-29609
Motion restoration of long time exposed images with satellite-borne cameras
[ETN-92-91490] p 3474 N92-29731

SIGNAL TRANSMISSION
The 1990 annual report, April 1990 - March 1991 p 3571 N92-29471

SIGNATURE ANALYSIS
A strategy for microprocessor BIST implementation based on deterministic testing
[IMAG-RR-844-I] p 3516 N92-29570

SIGNATURES
Normalized radar cross section of natural surfaces at millimeter wavelengths
[AD-A248452] p 3434 N92-29447
Interface board for providing time signals to a super minicomputer
[AD-D015198] p 3441 N92-29900

SILANES
Electrical, optical, and magnetic resonance studies of novel pi-conjugated polymers
[DE92-012548] p 3424 N92-29482

SILICATES
Cursory examination of the zeta potential behaviors of two optical materials
[DE92-011588] p 3551 N92-29578

SILICIDES
Method of forming silicon structures with selectable optical characteristics
[NASA-CASE-NPO-18625-1-CU] p 3559 N92-30102

SILICON
Variable temperature scanning tunneling microscopy
[AD-A248725] p 3557 N92-29722
Simulations on the electrical characteristics of Si, SiC and diamond junction and Schottky power diodes
[PB92-177872] p 3443 N92-30094
Method of forming silicon structures with selectable optical characteristics
[NASA-CASE-NPO-18625-1-CU] p 3559 N92-30102

SILICON CARBIDES
Synthesis and useful reactions of organosilicon polymeric precursors for ceramics
[AD-A248500] p 3424 N92-29496
Review of temperature dependent effects on the oxidation protection of carbon/carbon
[DE92-012333] p 3415 N92-29645
Effect of whisker orientation on the mechanical properties of silicon carbide/alumina composites
[AD-A248737] p 3415 N92-29723
Diffusion and phase relations in the systems Ti-Si-C and Ti-Si-N
[ETN-92-91631] p 3546 N92-29777
Simulations on the electrical characteristics of Si, SiC and diamond junction and Schottky power diodes
[PB92-177872] p 3443 N92-30094

SILICON NITRIDES
Synthesis and useful reactions of organosilicon polymeric precursors for ceramics
[AD-A248500] p 3424 N92-29496
Diffusion and phase relations in the systems Ti-Si-C and Ti-Si-N
[ETN-92-91631] p 3546 N92-29777

SILICON OXIDES
Latent interface-trap buildup: Issues for long-term device response
[DE92-003148] p 3439 N92-29455
Review of temperature dependent effects on the oxidation protection of carbon/carbon
[DE92-012333] p 3415 N92-29645
A study and feasibility of ultra thin silica layers by rapid thermal processing
[LAAS-91393] p 3422 N92-29674
SILICON POLYMERS
Synthesis and useful reactions of organosilicon polymeric precursors for ceramics
[AD-A248500] p 3424 N92-29496
Monolithic amorphous silicon modules on continuous polymer substrate
[DE92-001163] p 3425 N92-29598
SILICON TRANSISTORS
Monolithic integration of semiconductor and superconductor components
[AD-A245351] p 3557 N92-29583
SIMILARITY THEOREM
Strong bisimilarity on nets revisited
[RR-847-I-IMAG-120-LIFIA] p 3532 N92-29573
SIMPLEX METHOD
A monotonic build-up simplex algorithm for linear programming
[REPT-91-82] p 3524 N92-30227
SIMULATION
Visual acuity with second and third generation night vision goggles obtained from a new method of night sky simulation across a wide range of target contrast
[AD-A248284] p 3512 N92-29348
A systems analysis of the impact of navigation instrumentation on-board a Mars rover, based on a covariance analysis of navigation performance
[NASA-CR-189868] p 3403 N92-29440
SOLCHIPS: A fast predesign and optimization tool for solar heating with seasonal storage
[DE92-506509] p 3492 N92-29636
Simulations on the electrical characteristics of Si, SiC and diamond junction and Schottky power diodes
[PB92-177872] p 3443 N92-30094
SIMULATORS
Neutralizer and sample chamber for the Atomic Oxygen Simulation System (AOSS)
[NASA-CR-184343] p 3407 N92-29664
On the abstracted dataflow complexity of fast Fourier transforms
[DE92-011372] p 3562 N92-29794
SINGLE CRYSTALS
Fatigue in single crystal nickel superalloys
[AD-A248190] p 3420 N92-29408
Growth, characterization, and device development in monocrystalline diamond films
[AD-A248993] p 3560 N92-30175
SINGLE EVENT UPSETS
Hardening techniques to counter cumulated dose on SEU and SEL in space environment
[IMAG-RR-863-I] p 3441 N92-29613
SINGULARITY (MATHEMATICS)
Confining potential in momentum space
p 3548 N92-30007
SINKS
NATO workshop on the Atmospheric Methane Cycle. Working group report on methane sources and sinks
[PB92-180256] p 3494 N92-30018
SINTERING
Processing and properties of mechanically alloyed sintered steels with hard inclusions
[KFK-4909] p 3422 N92-29651
Development of high T(sub c) (greater than 110 K) Bi, Tl, and Y-based materials as superconducting circuit elements
[NASA-CR-190311] p 3557 N92-29676
SITE SELECTION
Final Environmental Impact Statement (EIS) for the Space Nuclear Thermal Propulsion (SNTP) program: Appendices
[AD-A248409] p 3413 N92-29904
Preliminary analysis of wind data from the Oak Ridge site survey
[PB92-174564] p 3503 N92-30034
SIZE DISTRIBUTION
Measurement of mean or effective radius of cloud drop size distributions with a 10.6-micron wavelength lidar
p 3472 N92-29324
Computer program POWNOR for fitting the power-normal and -lognormal models to life or strength data from specimens of various sizes
[PB92-169119] p 3483 N92-29813
SKEWNESS
Derivation of the kappa-epsilon model equations using the renormalization group method p 3450 N92-30055
SKIN (ANATOMY)
Gordon research conference on Barrier Function of Mammalian Skin
[AD-A248556] p 3510 N92-29577
SKIN (STRUCTURAL MEMBER)
Preliminary results on the fracture analysis of multi-site cracking of lap joints in aircraft skins
p 3484 N92-30111
Ageing airplane repair assessment program for Airbus A300 p 3402 N92-30123
SKIN FRICTION
Active thermal isolation for temperature responsive sensors
[NASA-CASE-LAR-14612-1] p 3446 N92-29954
SKY SURVEYS (ASTRONOMY)
The 12 micron contribution of nearby galaxies to the infrared background
[AD-A250623] p 3565 N92-29596
ROSAT: Early results p 3567 N92-29850
SLAGS
Process of ferrochromium now and in the future
[DE92-506510] p 3421 N92-29637
SLENDER WINGS
A method for computing the 3-dimensional flow about wings with leading-edge vortex separation. Part 2: Description of computer program VORSEP
[NLR-TR-86006-U] p 3402 N92-29916
SLIDING
Constitutive modelling for granular material under finite strains with particle slidings and fabric changes
[AD-A248187] p 3482 N92-29407
Theoretical and experimental aspects of velocity slip by flows along solid walls
[ISBN-3-7983-1446-2] p 3446 N92-29968
SMART STRUCTURES
Active structural acoustic control and smart structures
[AD-A248341] p 3543 N92-29588
SMELTING
Process of ferrochromium now and in the future
[DE92-506510] p 3421 N92-29637
SMOKE
An extension of the Raman-lidar technique to measure the velocity and temperature of the atmospheric emission jets from stacks p 3467 N92-29293
SNOW
Normalized radar cross section of natural surfaces at millimeter wavelengths
[AD-A248452] p 3434 N92-29447
SOCIAL FACTORS
Exercise and three psychosocial variables: A longitudinal study
[AD-A250649] p 3510 N92-30216
SODAR
Comparison of turbulence parameters measured by SODAR and sonic anemometer
[KFK-4890] p 3500 N92-29690
SODIUM
Development of mesospheric sodium laser beacon for atmospheric adaptive optics p 3470 N92-29308
Characterization of artificial guidestars generated in the mesospheric sodium layer p 3470 N92-29309
Optical pumping of mesospheric sodium: A new measurement capability p 3470 N92-29310
Lidar probing of the mesosphere: Simultaneous observations of sporadic sodium and iron formations, calcium ion layers, neutral temperature and winds
p 3470 N92-29311
Lidar measurements of metallic species in mesopause region p 3470 N92-29312
Error analysis of wind measurements for the University of Illinois sodium Doppler temperature system
p 3471 N92-29313
Sodium Doppler temperature lidar observations of the mesopause region temperature and wind structure
p 3471 N92-29314
Airborne sodium and Rayleigh lidar observations from ALOHA-90 p 3471 N92-29315
SOFTWARE ENGINEERING
Contracting in the software engineering crisis
[AD-A250241] p 3516 N92-29544
Software architecture modelling: Application to AMODEUS design scenarios
[IMAG-RR-860-I] p 3513 N92-29611
Reverse automatic differentiation of modular FORTRAN programs
[DE92-014071] p 3519 N92-29797
SRSM: A Software Requirements Specification Method
[REPT-91-84] p 3524 N92-30228
SOFTWARE REUSE
An introduction to software reuse
[REPT-91-50] p 3519 N92-29779
SOFTWARE TOOLS
ASV3 dial-in interface recommendation for the Repository Based Software Engineering (RBSE) program
[NASA-CR-190500] p 3514 N92-29362
Software quality control and requirements specification
[REPT-91-48] p 3518 N92-29711
Decomposer: Program documentation
[USIP-91-04] p 3519 N92-29780
Architecture and use of Delft Direct Manipulation Manager (D2M2)
[REPT-91-46] p 3521 N92-29887
Performability modelling tools: A survey
[MEMO-INF-91-82] p 3523 N92-30191
SOI (SEMICONDUCTORS)
A novel approach to silicon-on-insulator materials
[AD-A248074] p 3424 N92-29466
SOIL MECHANICS
Constitutive modelling for granular material under finite strains with particle slidings and fabric changes
[AD-A248187] p 3482 N92-29407
SOIL MOISTURE
Mathematical modelling of saturated and unsaturated groundwater flow
[MEMO-987] p 3445 N92-29857
SOLAR ACTIVITY
SESC glossary of solar-terrestrial terms
[PB92-185305] p 3563 N92-30194
Investigation of solar active regions at high resolution by balloon flights of the solar optical universal polarimeter, definition phase
[NASA-CR-184339] p 3570 N92-30204
SOLAR CELLS
Novel thin-film CuInSe2 fabrication
[DE92-001222] p 3557 N92-29584
Monolithic amorphous silicon modules on continuous polymer substrate
[DE92-001163] p 3425 N92-29598
SOLAR CORONA
Global solar magnetic fields
[AD-A248340] p 3569 N92-29421
CoMStOC 4: Multiwaveband observations of sunspot and plage-associated coronal emission
[AD-A248344] p 3570 N92-29632
Turbulent transport in the solar nebula
p 3454 N92-30163
SOLAR FLUX
Occultation of a compact radio source by Venus
p 3429 N92-29366
SOLAR HEATING
SOLCHIPS: A fast predesign and optimization tool for solar heating with seasonal storage
[DE92-506509] p 3492 N92-29636
SOLAR MAGNETIC FIELD
Global solar magnetic fields
[AD-A248340] p 3569 N92-29421
SOLAR NEUTRINOS
Prospects for long baseline neutrino oscillation experiments
[DE92-011833] p 3544 N92-29356
SOLAR OBSERVATORIES
Investigation of solar active regions at high resolution by balloon flights of the solar optical universal polarimeter, definition phase
[NASA-CR-184339] p 3570 N92-30204
SOLAR PHYSICS
SESC glossary of solar-terrestrial terms
[PB92-185305] p 3563 N92-30194
SOLAR RADIATION
Cosine response characteristics of radiometric and photometric sensors
[DE92-011437] p 3551 N92-29530
SOLAR SYSTEM
Origin and evolution of planetary atmospheres
[NASA-CR-190579] p 3568 N92-29432
SOLAR SYSTEM EVOLUTION
Turbulent transport in the solar nebula
p 3454 N92-30163
Turbulent thermal convection in a differentially rotating channel p 3455 N92-30168
SOLAR TERRESTRIAL INTERACTIONS
ATLAS 1: Encountering planet Earth
[NASA-TM-107956] p 3408 N92-30016
SOLAR WIND
Occultation of a compact radio source by Venus
p 3429 N92-29366
A study of shock-associated magnetohydrodynamic waves in the solar wind
[NASA-CR-190567] p 3569 N92-29631
SOLDERING
Dynamic solder management
[AD-A250564] p 3422 N92-29647
SOLDERS
Dynamic solder management
[AD-A250564] p 3422 N92-29647
SOLID LUBRICANTS
Synthesis of new high performance lubricants and solid lubricants
[DE92-011940] p 3424 N92-29549

SOLID MECHANICS
NASA-UVA light aerospace alloy and structures technology program (LA2ST)
[NASA-CR-190538] p 3423 N92-30206
SOLID PROPELLANT COMBUSTION
Progress on combustion mechanisms of solid propellants
[AD-A248146] p 3427 N92-29330
SOLID ROCKET PROPELLANTS
Progress on combustion mechanisms of solid propellants
[AD-A248146] p 3427 N92-29330
SOLID STATE
Solid state structures of some Dithionoamido-18-crown-6 ligands
[AD-A248098] p 3556 N92-29558
Low-angle x ray diffraction study of solid state amorphization in a Ni/Ti multilayer p 3558 N92-29768
SOLID STATE DEVICES
Exploratory study for a solid-state charged-particle spectrometer inside the Celsius ring: Alpha and hydrogen reactions at 1.7 and 2.2 GeV/c
[USIP-91-02] p 3546 N92-29715
SOLID STATE LASERS
Center of excellence: Microlaser microscope
[DE92-013485] p 3477 N92-29928
SOLID STATE PHYSICS
The 1990 annual report, April 1990 - March 1991
p 3571 N92-29471
A model for interdiffusion in polycrystalline multilayers and its application to solid state amorphization
p 3558 N92-29771
Evidence for amorphization in Ni/Ti multilayers from electrical resistivity changes p 3559 N92-29773
SOLID-SOLID INTERFACES
Sound speed, reflectivity, and absorption measurements in Arctic ice in 1988
[AD-A246293] p 3505 N92-29554
SOLIDIFICATION
Structure and stability of Al-Cu-Ru face-centered icosahedral alloys
[DE92-012550] p 3422 N92-29706
SOLIDS
An innovative approach for coupled thermomechanical analysis
[DE92-011467] p 3481 N92-29338
Surface reactions in the space environment
[AD-A250624] p 3428 N92-29428
SOLITARY WAVES
SOLITON
[USIP-90-09] p 3518 N92-29714
SOLUTES
Electrochemistry in colloids and dispersions. Volume 1: Electroanalytical methods and applications, electrosynthesis and electrocatalysis, polymers and latexes
[AD-A248335] p 3418 N92-29557
Model for regional solute transport suited for calibration and management
[PB92-161371] p 3494 N92-29746
Electrochemistry in colloids and dispersions. Volume 2: Solute distribution, diffusion, and transport colloidal metals
[AD-A248336] p 3419 N92-29931
Electrochemistry in colloids and dispersions. Volume 3: Colloidal semiconductors
[AD-A248337] p 3419 N92-29932
SONIC ANEMOMETERS
Comparison of turbulence parameters measured by SODAR and sonic anemometer
[KFK-4890] p 3500 N92-29690
SORPTION
Compressive response of debonded thick composite shells including the effects of transient moisture sorption
[AD-A250080] p 3414 N92-29462
SOUND INTENSITY
Validation of finite element and boundary element methods for predicting structural vibration and radiated noise
[NASA-TM-105359] p 3478 N92-29697
SOUND TRANSDUCERS
Calibration apparatus for recess mounted pressure transducers
[NASA-CASE-LAR-14724-1] p 3474 N92-30030
SOUND TRANSMISSION
Matched asymptotic expansions solution for low-frequency sound radiation from fluid-loaded, baffled plates: Axisymmetric case
[REPT-91-60] p 3543 N92-29628
Matched asymptotic expansions solution for low-frequency sound radiation from fluid-loaded, baffled plates: Two-dimensional case
[REPT-91-62] p 3543 N92-29748
Realistic models for predicting sound propagation in flow duct systems
[ISVR-TR-204] p 3544 N92-29814
Estimation of the inverse acoustic transmission operator of a heterogeneous region directly from its reflection operator
[REPT-91-36] p 3544 N92-29918
SOUND WAVES
Asymptotic and numerical methods in applied wave propagation
[AD-A250227] p 3543 N92-29543
Finite difference modelling of seismic wave propagation at the seafloor
[AD-A248345] p 3505 N92-29562
Direct numerical simulation of instability and noise generation of hot jets p 3451 N92-30066
SOUTHERN HEMISPHERE
Southern Hemisphere lidar measurements of the aerosol clouds from Mt. Pinatubo and Mt. Hudson
p 3456 N92-29230
SPACE BASED RADAR
Lidar In-space Technology Experiment (LITE) electronics overview p 3462 N92-29264
NWP impact of cloud top and boundary layer winds from a satellite borne lidar: An observing system simulation experiment p 3473 N92-29328
SPACE CHARGE
Electrostatic ion thruster optics calculations
[DE92-006608] p 3413 N92-29461
Heat flow of a two-electron-temperature plasma through the sheath in the presence of electron emission
[NIFS-136] p 3555 N92-30172
SPACE COMMERCIALIZATION
EOS data policy: Questions remain about US commercial access. Report to the Chairman, Committee on Science, Space, and Technology, House of Representatives
[GAO/IMTEC-92-44] p 3488 N92-29467
SPACE COMMUNICATION
The Telecommunications and Data Acquisition Report
[NASA-CR-190460] p 3429 N92-29364
Deep Space Network information system architecture study p 3433 N92-29385
SPACE DENSITY
Abell clusters of galaxies: Catalogs and large-scale structures p 3566 N92-29838
Studies of distant clusters of galaxies
p 3566 N92-29843
SPACE MECHANICS
Phase-space estimate of satellite coverage time
[DE92-013555] p 3542 N92-30139
SPACE MISSIONS
ATLAS 1: Encountering planet Earth
[NASA-TM-107956] p 3408 N92-30016
SPACE NAVIGATION
Deep-space navigation with differenced data types. Part 3: An expanded information content and sensitivity analysis p 3409 N92-29368
SPACE PERCEPTION
Visual perception of elevation
[AD-A248338] p 3510 N92-29420
Visual pattern completion
[PB92-187418] p 3524 N92-30195
SPACE PLASMAS
Low energy neutral atoms in the Earth's magnetosphere: Modeling
[DE92-013240] p 3500 N92-29536
SPACE POWER REACTORS
SP-100 W/Re thermocouple calibration techniques
[DE92-011302] p 3550 N92-29938
SPACE PROGRAMS
Final Environmental Impact Statement (EIS) for the Space Nuclear Thermal Propulsion (SNTP) program: Appendices
[AD-A248409] p 3413 N92-29904
Evaluating the military potential of a developing nation's space program: A case study of Brazil
[AD-A245978] p 3407 N92-29929
SPACE SHUTTLES
The O2 reduction at the IFC modified O2 fuel cell electrode
[NASA-TM-105691] p 3413 N92-29667
SPACE TRANSPORTATION
Saenger: The reference concept and its technological requirements - aerothermodynamics
[MBB-FE-202-S-PUB-0463-A] p 3408 N92-29629
Technology programme: Aerothermodynamics and propulsion integration. Numerical and experimental aerothermodynamics
[MBB-FE-202-S-PUB-0464-A] p 3400 N92-29648
Aerothermodynamics and propulsion integration in the Saenger technology programme
[MBB-FE-202-S-PUB-0469-A] p 3400 N92-29649
Aerothermodynamic challenges of the Saenger space-transportation system
[MBB-FE-202-S-PUB-0462-A] p 3409 N92-29680
SPACE WEAPONS
Burros: Simple, affordable, effective space transportation
[DE92-013553] p 3541 N92-30138
SPACE-TIME FUNCTIONS
Real space process algebra
[CWI-CW-R9131] p 3538 N92-30178
SPACEBORNE ASTRONOMY
Source location determination of Uranian kilometric radiation from ray tracing and emission lobe modelling
[NASA-CR-190482] p 3570 N92-29360
Analysis of high energy x ray observations of long periodic pulsars
[ETN-92-91494] p 3564 N92-29468
SPACEBORNE EXPERIMENTS
Migmas/A: Test of a scanning ion microscope on the Soviet Space Station Mir
[OEFZS-4615] p 3473 N92-29469
Logion: The operation of liquid metal ion emitters under weightlessness
[OEFZS-4616] p 3428 N92-29470
Pressurization of cryogens: A review of current technology and its applicability to low-gravity conditions
[NASA-TM-105746] p 3427 N92-29669
SPACEBORNE LASERS
Laser Transmitter Module (LTM) for LITE
p 3463 N92-29265
Sampling and representativeness for a spaceborne wind lidar p 3463 N92-29268
System testing and performance characterization of the LITE Laser Transmitter Module at NASA
p 3469 N92-29302
SPACECRAFT ANTENNAS
Ka-band feed arrays for spacecraft reflector antennas with limited scan capability: An overview
p 3433 N92-29387
SPACECRAFT CHARGING
Hardening techniques to counter cumulated dose on SEU and SEL in space environment
[IMAG-RR-863-I] p 3441 N92-29613
SPACECRAFT CONSTRUCTION MATERIALS
NASA-UVA light aerospace alloy and structures technology program (LA2ST)
[NASA-CR-190538] p 3423 N92-30206
SPACECRAFT CONTROL
Application of fuzzy logic-neural network based reinforcement learning to proximity and docking operations
[NASA-CR-190504] p 3525 N92-29390
Spacecraft dynamics characterization and control system failure detection, volume 1
[NASA-CR-190517] p 3409 N92-29422
Geostationary Operational Environmental Satellite (GOES-N report). Volume 2: Technical appendix
[NASA-TM-107920] p 3410 N92-29812
SPACECRAFT DOCKING
Application of fuzzy logic-neural network based reinforcement learning to proximity and docking operations
[NASA-CR-190504] p 3525 N92-29390
SPACECRAFT ELECTRONIC EQUIPMENT
Hardening techniques to counter cumulated dose on SEU and SEL in space environment
[IMAG-RR-863-I] p 3441 N92-29613
SPACECRAFT ENVIRONMENTS
Publications of the environmental health program: 1980-1990
[NASA-CR-4455] p 3509 N92-29341
SPACECRAFT INSTRUMENTS
ATLAS 1: Encountering planet Earth
[NASA-TM-107956] p 3408 N92-30016
Support activities to maintain SUMS flight readiness
[NASA-CR-189656-VOL-1] p 3410 N92-30217
Support activities to maintain SUMS flight readiness, volume 2. Attachment A: Flight 61-C report
[NASA-CR-189656-VOL-2] p 3411 N92-30218
Support activities to maintain SUMS flight readiness, volume 3. Attachment B: Flight STS-35 report, section A
[NASA-CR-189656-VOL-3] p 3411 N92-30219
Support activities to maintain SUMS flight readiness, volume 4. Attachment B: Flight STS-35 report, section B
[NASA-CR-189656-VOL-4] p 3411 N92-30220
Support activities to maintain SUMS flight readiness, volume 5. Attachment B: Flight STS-35 report, section C
[NASA-CR-189656-VOL-5] p 3411 N92-30221
Support activities to maintain SUMS flight readiness, volume 6. Attachment B: Flight STS-35 report, section D
[NASA-CR-189656-VOL-6] p 3411 N92-30222
Support activities to maintain SUMS flight readiness, volume 7. Attachment B: Flight STS-35 report, section E
[NASA-CR-189656-VOL-7] p 3412 N92-30223
Support activities to maintain SUMS flight readiness, volume 8. Attachment B: Flight STS-35 report, section F
[NASA-CR-189656-VOL-8] p 3412 N92-30224
Support activities to maintain SUMS flight readiness, volume 9. Attachment C: Flight STS-40 report. Attachment D: SUMS software listing
[NASA-CR-189656-VOL-9] p 3412 N92-30225

SPACECRAFT MOTION
Deep-space navigation with differenced data types. Part 3: An expanded information content and sensitivity analysis p 3409 N92-29368

SPACECRAFT ORBITS
A determination of the radio-planetary frame tie from comparison of Earth orientation parameters p 3409 N92-29365
Orbiter-orbiter and orbiter-lander tracking using same-beam interferometry p 3409 N92-29369

SPACECRAFT POWER SUPPLIES
The O2 reduction at the IFC modified O2 fuel cell electrode
[NASA-TM-105691] p 3413 N92-29667

SPACECRAFT PROPULSION
Feasibility of an antiproton catalyzed fission fragment rocket
[AD-A248157] p 3412 N92-29444
Saenger: The reference concept and its technological requirements - aerothermodynamics
[MBB-FE-202-S-PUB-0463-A] p 3408 N92-29629
Technology programme: Aerothermodynamics and propulsion integration. Numerical and experimental aerothermodynamics
[MBB-FE-202-S-PUB-0464-A] p 3400 N92-29648
Aerothermodynamics and propulsion integration in the Saenger technology programme
[MBB-FE-202-S-PUB-0469-A] p 3400 N92-29649
Final Environmental Impact Statement (EIS) for the Space Nuclear Thermal Propulsion (SNTP) program
[AD-A248408] p 3413 N92-29903
Final Environmental Impact Statement (EIS) for the Space Nuclear Thermal Propulsion (SNTP) program: Appendices
[AD-A248409] p 3413 N92-29904

SPATIAL DISTRIBUTION
Lidar investigation of aerosol pollution distribution near a coal power plant p 3467 N92-29289
Spatial and temporal temperature studies of electrothermal chemical (ETC) plasmas
[AD-A248541] p 3554 N92-29510
The space distribution of local radio galaxies p 3566 N92-29842

SPECIFICATIONS
Tools for the interfacing between dynamical problems and models within decision support systems
[MEMO-COSOR-91-29] p 3532 N92-29607
Software quality control and requirements specification
[REPT-91-48] p 3518 N92-29711
PDES application protocol suite for composites (PAS-C): IDEFO activity models and information needs for the PAS-C program
[AD-A248714] p 3562 N92-29720
Implementation of the object-oriented data model TM
[MEMO-INF-91-94] p 3520 N92-29855
An algebraic specification for the static semantics of Pascal
[CWI-CS-R9129] p 3522 N92-29989
Proof theory for micro CRL
[CWI-CS-R9138] p 3522 N92-29994
Overview of the document style semantics and specification language and the MIL-M-28001A output specification
[PB92-181122] p 3563 N92-30039
A formal development trajectory for OSI application layer protocols
[MEMO-INF-91-71] p 3523 N92-30144
Criteria for, and experience with, ADTs in large LOTOS specifications
[MEMO-INF-91-74] p 3514 N92-30145
SRSM: A Software Requirements Specification Method
[REPT-91-84] p 3524 N92-30228

SPECTRA
Lagrangian velocity correlation and spectrum in homogeneous isotropic turbulence p 3448 N92-30047
Support activities to maintain SUMS flight readiness, volume 4. Attachment B: Flight STS-35 report, section B
[NASA-CR-189656-VOL-4] p 3411 N92-30220
Support activities to maintain SUMS flight readiness, volume 5. Attachment B: Flight STS-35 report, section C
[NASA-CR-189656-VOL-5] p 3411 N92-30221
Support activities to maintain SUMS flight readiness, volume 6. Attachment B: Flight STS-35 report, section D
[NASA-CR-189656-VOL-6] p 3411 N92-30222
Support activities to maintain SUMS flight readiness, volume 7. Attachment B: Flight STS-35 report, section E
[NASA-CR-189656-VOL-7] p 3412 N92-30223
Support activities to maintain SUMS flight readiness, volume 8. Attachment B: Flight STS-35 report, section F
[NASA-CR-189656-VOL-8] p 3412 N92-30224

SPECTRAL BANDS
Programmable hyperspectral image mapper with on-array processing
[NASA-CASE-NPO-17794-1-CU] p 3553 N92-30104

SPECTRAL METHODS
On constructing kernel polynomials of a spectral function: Application to ARMA models
[CWI-BS-R9119] p 3533 N92-29862
Streaks in turbulent boundary layers p 3451 N92-30069

SPECTRAL REFLECTANCE
Biologically-based neural network model of color constancy and color contrast
[AD-A248128] p 3510 N92-29398
A spectral vegetation radiometer for airborne boundary-layer research
[PB92-186113] p 3491 N92-30105
Comparison of in situ, aircraft- and satellite derived surface reflectances in Flevoland (Netherlands). A validation experiment
[BCRS-91-28] p 3491 N92-30230

SPECTRAL RESOLUTION
Adaptation of the University of Wisconsin high spectral resolution lidar for polarization and multiple scattering measurements p 3472 N92-29322

SPECTROMETERS
Design and construction of a channel electron multiplier based Mossbauer spectroscopy system
[AD-A248154] p 3439 N92-29443
Synthesis and characterization of a covalently bound self-assembled macrocycle monolayer thin film for nonlinear optical materials
[DE92-011353] p 3545 N92-29634
United Kingdom Infrared Telescope
[ETN-92-91341] p 3565 N92-29682
High resolving power spectrometer for beam analysis
[DE92-010751] p 3437 N92-29988
Evaluation of an aureole lidar technique for estimating extinction profiles
[AD-A249740] p 3501 N92-30087

SPECTROSCOPIC ANALYSIS
Laser-induced desorption from sapphire surfaces
[DE92-012698] p 3475 N92-29340
Multichord spectroscopy of the D3-D divertor region
[DE92-013507] p 3554 N92-29412
A study of the adsorption of acetonitrile on a gold electrode from aqueous solutions using in situ vibrational spectroscopy
[AD-A250191] p 3417 N92-29514
Estimating plasma temperatures
[DE92-014092] p 3555 N92-29798
Solution of two-body relativistic bound state equations with confining plus Coulomb interactions p 3547 N92-30003
Effects of retardation in relativistic equations with confining interaction p 3547 N92-30005

SPECTROSCOPY
Multichord spectroscopy of the D3-D divertor region
[DE92-013507] p 3554 N92-29412
Intense diagnostic neutral beam development for ITER
[DE92-011262] p 3556 N92-30203
Spectroscopy of W-183; measured magnetic moments and rotation-particle coupling
[DE92-624790] p 3549 N92-30213

SPECTRUM ANALYSIS
Efficiencies of rotational Raman and Rayleigh techniques for laser remote sensing of the atmospheric temperature p 3467 N92-29288
Analysis of EUV dayglow spectra of Triton, Titan and Earth
[NASA-CR-190586] p 3568 N92-29451
Comparison of turbulence parameters measured by SODAR and sonic anemometer
[KFK-4890] p 3500 N92-29690
A preliminary experimental investigation of local isotropy in high-Reynolds-number turbulence p 3447 N92-30042
Spectral type of Ornstein's class one transformations
[PB92-178292] p 3537 N92-30096

SPHERES
Fingered bola body, bola with same, and methods of use
[NASA-CASE-MSC-21967-1] p 3479 N92-30026
Standard spherical dipole source
[PB92-187020] p 3438 N92-30198

SPHERICAL PLASMAS
LLE-LLNL progress report on studies in nonlocal heat transport in spherical plasmas using the Fokker-Planck code SPARK
[DE92-014093] p 3554 N92-29531

SPHERICAL TANKS
Optimization of armored spherical tanks for storage on the lunar surface
[NASA-TM-105700] p 3414 N92-30187

SPINE
In vitro measurement of nucleus pulposus swelling pressure: A new technique for studies of spinal adaptation to gravity
[NASA-TM-103853] p 3506 N92-29397

SPLINE FUNCTIONS
Minimax linear splines
[AD-A248077] p 3515 N92-29487
A method for converting the surface of a generalized cylinder into a B-spline surface
[REPT-91-40] p 3535 N92-29922

SPLINES
Minimax linear splines
[AD-A248077] p 3515 N92-29487

SPONTANEOUS EMISSION
Detecting microwave emissions from terrestrial sources: A feasibility study
[AD-A248557] p 3435 N92-29579

SPRAY CHARACTERISTICS
Structure of a methanol/air coaxial reacting spray near the stabilization region by OH fluorescence imaging and two-component phase-Doppler interferometry
[DE92-005328] p 3417 N92-29431

SPRAYERS
Structure of a methanol/air coaxial reacting spray near the stabilization region by OH fluorescence imaging and two-component phase-Doppler interferometry
[DE92-005328] p 3417 N92-29431

SPREAD SPECTRUM TRANSMISSION
FM video data link spectrum spreading
[AD-D015257] p 3435 N92-29572

SPUTTERING
A study of the influence of alloying additions on the passivity of aluminum
[AD-A248339] p 3421 N92-29587

SQUARE WAVES
Bandwidth compression of noisy signals with square-wave subcarrier p 3432 N92-29379

STABILITY
Effect of grain size on deformation stability of copper under quasi-static and dynamic tensile loading
[DE92-012677] p 3421 N92-29639
The role of chemical interactions in the stability of artificial metallic superlattices
[DE92-011528] p 3559 N92-29911

STABILITY TESTS
Linear stability analysis of hypersonic boundary layers p 3451 N92-30063

STACKS
An extension of the Raman-lidar technique to measure the velocity and temperature of the atmospheric emission jets from stacks p 3467 N92-29293

STAGNATION FLOW
Stability of a premixed flame in stagnation-point flow against general disturbances
[NASA-CR-189666] p 3455 N92-30192

STAINLESS STEELS
Irradiation effects on the electrochemistry and corrosion resistance of stainless steel
[DE92-013504] p 3420 N92-29411
Preliminary cutting and drilling studies using new generation lasers
[DE92-010712] p 3477 N92-29787

STANDARDS
An OSI architecture for the Deep Space Network p 3432 N92-29380
Global standards: Building blocks for the future
[PB92-167352] p 3563 N92-29671
Reviews of computing technology: Fiber distributed data interface
[DE92-011374] p 3514 N92-29907
Revision of certification standards for aviation maintenance personnel p 3487 N92-30127

STATE ESTIMATION
State estimation and error diagnosis for biotechnological processes
[ETN-92-91744] p 3508 N92-29754
The use of state estimators (observers) for on-line estimation of non-measurable process variables p 3508 N92-29755
State estimation and control of the IBE-fermentation with product recovery p 3509 N92-29756
A low sensitivity observer for complex biotechnological processes p 3509 N92-29757
Analytical tuning of a low sensitivity observer applied to a continuous ethanol fermentation with product recovery p 3509 N92-29758
Improved balancing methods and error diagnosis for bio(chemical) conversions p 3509 N92-29759
Sequential application of data reconciliation for sensitive detection of systematic errors p 3509 N92-29760

STATE VECTORS
Generalized probability model for calculation of interference to the Deep Space Network due to circularly Earth-orbiting satellites p 3433 N92-29386

STATIC LOADS
Effect of grain size on deformation stability of copper under quasi-static and dynamic tensile loading
[DE92-012677] p 3421 N92-29639

STATISTICAL ANALYSIS
Electron spectra of adatomic structures
[DE92-625013] p 3544 N92-29415
Some applications of orthogonal functions to probability and statistics
[ETN-92-91741] p 3538 N92-29491
A new form for the chi-squared test of independence (document 2) p 3538 N92-29492
Class A network Dataring gauges: 1989 data processing and analysis
[REPT-18-1991] p 3505 N92-29684
Theory of system reliability demonstration, burn-in design, and record statistics
[AD-A250582] p 3480 N92-29710
Sequential application of data reconciliation for sensitive detection of systematic errors p 3509 N92-29760
Intercomparison of global marine climatologies
[DE92-011389] p 3494 N92-29790
Data reduction in statistical inference
[MEMO-COSOR-92-03] p 3540 N92-29828
Scaling analysis of energy transfer in the inertial range p 3448 N92-30046
Texture synthesis
[CWI-CS-R9139] p 3523 N92-30141
Chebyshev line approximation: A sensitivity analysis
[MEMO-1020] p 3537 N92-30147
Basic problems of a-posteriori error estimation
[AD-A248986] p 3541 N92-30174
Simulations on the Jelinski-Moranda model of software reliability
[CWI-BS-R9122] p 3523 N92-30179
STATISTICAL DISTRIBUTIONS
The determination of stochastic models and areas of confidence
[OEFZS-4612] p 3538 N92-29419
A new form for the chi-squared test of independence (document 2) p 3538 N92-29492
Limit theorems for cumulative processes
[AD-A248507] p 3538 N92-29500
A compensation approach for two-dimensional Markov processes
[MEMO-COSOR-91-28] p 3539 N92-29606
On the asymptotically uniform distribution modulo 1 of extreme order statistics
[MEMO-COSOR-91-38] p 3540 N92-29821
Imprecise conjugate prior densities for the one-parameter exponential family of distributions
[MEMO-COSOR-91-36] p 3540 N92-29897
STATISTICAL MECHANICS
Statistical mechanics of collective phenomena in plasmas
[AD-A250581] p 3554 N92-29450
STATISTICAL TESTS
A new form for the chi-squared test of independence (document 2) p 3538 N92-29492
Power approximations to and power comparison of certain goodness-of-fit tests
[MEMO-1019] p 3541 N92-29980
STEADY STATE
Modelling and experimental validation of carbon dioxide evolution in alkalophilic cultures p 3507 N92-29734
Formation of presheath and current-free double layer in a two-electron-temperature plasma
[NIFS-132] p 3555 N92-30091
STEELS
Rolling-contact and wear resistance of hard coatings on bearing-steel substrates
[DE92-011834] p 3478 N92-29357
Process of ferrochromium now and in the future
[DE92-506510] p 3421 N92-29637
Processing and properties of mechanically alloyed sintered steels with hard inclusions
[KFK-4909] p 3422 N92-29651
Marine structural steel toughness data bank (abridged edition)
[PB92-163294] p 3422 N92-29807
STELLAR LUMINOSITY
Evidence for evolution of the luminosity function of clusters of galaxies p 3567 N92-29844
Constraints on the mass fluctuation spectrum from x ray observations of clusters of galaxies p 3567 N92-29845
STIRLING CYCLE
Multidimensional computer simulation of Stirling cycle engines
[NASA-CR-190497] p 3478 N92-29392
STIRLING ENGINES
Multidimensional computer simulation of Stirling cycle engines
[NASA-CR-190497] p 3478 N92-29392
STIRRING
The influence of turbulence on aggregation of small particles in agitated vessels
[ETN-92-91629] p 3445 N92-29775
STOCHASTIC PROCESSES
Signal quality influence on averaging procedure for DIAL pollution monitoring p 3465 N92-29280
The determination of stochastic models and areas of confidence
[OEFZS-4612] p 3538 N92-29419
Limit theorems for cumulative processes
[AD-A248507] p 3538 N92-29500
An examination of hypercube implementations of genetic algorithms
[AD-A248092] p 3515 N92-29527
Optimization of stochastic response surfaces subject to constraints with linear programming
[AD-A248108] p 3516 N92-29586
Model for regional solute transport suited for calibration and management
[PB92-161371] p 3494 N92-29746
Asymptotic results in feedback systems
[ETN-92-91702] p 3529 N92-29962
Multitype branching processes in M/G/1-queueing theory p 3530 N92-29966
A two-stage estimator for generalized linear models with nonconstant dispersion parameter
[MEMO-1012] p 3540 N92-29975
Some feedback procedures for control of flows p 3452 N92-30070
Variable bandwidth connections for a connectionless service on ATM: Performance modelling and evaluation
[MEMO-INF-91-83] p 3438 N92-30170
Performability modelling tools: A survey
[MEMO-INF-91-82] p 3523 N92-30191
STOICHIOMETRY
Thermodynamic and kinetic aspects of 3/5 epitaxy
[AD-A250632] p 3556 N92-29429
STORAGE BATTERIES
Advanced rechargeable lithium sulfur dioxide cell
[AD-A250027] p 3491 N92-29476
STORAGE RINGS (PARTICLE ACCELERATORS)
Review of potential x ray laser applications in materials science and chemistry
[DE92-012254] p 3475 N92-29434
STORAGE TANKS
Optimization of armored spherical tanks for storage on the lunar surface
[NASA-TM-105700] p 3414 N92-30187
STORMS
Polarization lidar liquid cloud detection algorithm for winter mountain storms p 3472 N92-29323
STRAIN HARDENING
An approximation method for dynamic response of strain-hardening structures
[DE92-013053] p 3482 N92-29535
STRAKES
Helicopter low-speed yaw control
[NASA-CASE-LAR-14219-1] p 3406 N92-30025
STRAPS
Tear straps in airplane fuselage
[AD-A248543] p 3404 N92-29511
STRATIFICATION
Lidar observation of aerosol and temperature stratification over urban area during the formation of a stable atmospheric PBL p 3466 N92-29286
STRATOSPHERE
Sixteenth International Laser Radar Conference, part 1
[NASA-CP-3158-PT-1] p 3456 N92-29228
Long term stratospheric aerosol lidar measurements in Kyushu p 3456 N92-29229
Southern Hemisphere lidar measurements of the aerosol clouds from Mt. Pinatubo and Mt. Hudson p 3456 N92-29230
Stratospheric backscatter, extinction, and lidar ratio profiling after the Mt. Pinatubo eruptions p 3456 N92-29231
Measurements of stratospheric Pinatubo aerosol extinction profiles by a Raman lidar p 3457 N92-29232
Raman lidar measurements of Pinatubo aerosols over southeastern Kansas during November-December 1991 p 3457 N92-29233
Lidar observations of stratospheric aerosol layer after the Mt. Pinatubo volcanic eruption p 3457 N92-29234
Interpretation of DIAL measurements of lower stratospheric ozone in regions with Pinatubo aerosols p 3457 N92-29236
Correcting for interference of Mt. Pinatubo aerosols on DIAL measurements of stratospheric ozone p 3458 N92-29237
A new Raman DIAL technique for measuring stratospheric ozone in the presence of volcanic aerosols p 3458 N92-29238
The JPL Table Mountain and Mauna Loa stratospheric ozone lidars p 3458 N92-29239
The NDSC primary site at the Observatoire de Haute-Provence: Ozone and aerosols observations (1986-1992) p 3458 N92-29240
Observation of stratospheric ozone with NIES lidar system in Tsukuba, Japan p 3459 N92-29242
Observations of ozone-aerosol correlated behaviour in the lower stratosphere during the EASOE campaign p 3459 N92-29243
Airborne lidar observations of the stratosphere after the Pinatubo eruption p 3460 N92-29248
Multi-wavelength measurements of the stratospheric aerosol layer made at Hampton, Virginia (37N, 76W) p 3460 N92-29249
Three-wavelength lidar measurements of Pinatubo aerosol and its optical properties p 3460 N92-29250
Lidar observations of the Pinatubo stratospheric aerosol cloud over Frascati, Italy p 3460 N92-29251
L625 lidar measurements of Pinatubo volcanic cloud at Hefei p 3460 N92-29252
Lidar observations of the Pinatubo volcanic cloud over Hampton, Virginia p 3461 N92-29254
Lidar measurements of stratospheric ozone, temperature and aerosol during 1992 UARS correlative measurement campaign p 3461 N92-29257
Lidar measurement of stratospheric ozone at Hohenpeissenberg: An improved evaluation method p 3462 N92-29259
A multi-wavelength ozone lidar for the EASOE experiment p 3462 N92-29260
Correction of DIAL stratospheric ozone measurements in the presence of Pinatubo aerosols p 3462 N92-29261
A developing multiple-wavelength lidar for detecting mainly ozone and aerosol distributions in the stratosphere p 3467 N92-29292
Lidar observations of stratospheric clouds after volcanic eruption of Pinatubo p 3468 N92-29294
Lidar measurements of aerosol and ozone distributions during the 1992 Airborne Arctic Stratospheric Expedition p 3469 N92-29304
Airborne lidar measurements of stratospheric aerosols during the European Arctic Stratospheric Ozone Experiment (EASOE) p 3469 N92-29305
Aerosols and polar stratospheric clouds measurements during the EASOE campaign p 3469 N92-29306
Lidar observations of polar stratospheric clouds and stratospheric temperatures at the South Pole p 3470 N92-29307
Rayleigh/Raman Greenland lidar observations of atmospheric temperature during a major Arctic stratospheric warming event p 3471 N92-29316
Elastic and Raman lidar temperature measurements from Poker Flat, Alaska during February 1992 p 3471 N92-29317
Wind measurements from 15 to 50 km with a Doppler Rayleigh lidar p 3472 N92-29319
STRATOSPHERIC WARMING
ARCLITE: The Arctic Lidar Technology Facility at Sondre Stromfjord, Greenland p 3407 N92-29283
Rayleigh/Raman Greenland lidar observations of atmospheric temperature during a major Arctic stratospheric warming event p 3471 N92-29316
STREAK CAMERAS
X ray streak camera diagnostics of picosecond laser-plasma interactions
[DE92-011371] p 3555 N92-29789
STRESS ANALYSIS
Variational formulation and finite element implementation of Pagano's theory of laminated plates
[AD-A250592] p 3415 N92-29594
STRESS CONCENTRATION
Stresses and strains in plain and coldworked annuli subjected to remote, interference or combined loading
[ARL-STRUC-R-446] p 3482 N92-29672
STRESS CORROSION
Irradiation effects on the electrochemistry and corrosion resistance of stainless steel
[DE92-013504] p 3420 N92-29411
STRESS DISTRIBUTION
Compressive response of debonded thick composite shells including the effects of transient moisture sorption
[AD-A250080] p 3414 N92-29462
Combined load test apparatus for flat panels
[NASA-CASE-LAR-14698-1] p 3483 N92-30028
Damaged stiffened shell research at NASA. Langley Research Center p 3485 N92-30115
An approximate solution for interlaminar stresses in laminated composites: Applied mechanics program
[NASA-CR-190537] p 3416 N92-30208
STRESS-STRAIN RELATIONSHIPS
Constitutive modelling for granular material under finite strains with particle slidings and fabric changes
[AD-A248187] p 3482 N92-29407
STRINGS
Linear approximation of shortest superstrings
[CWI-CS-R9126] p 3523 N92-30146

STRUCTURAL ANALYSIS
Guide for evaluating 12 inch Substantial Dividing Walls (SDWs) to provide protection from remote operation, volume 2
[AD-A250252] p 3428 N92-29335
Guide for evaluating 12 inch Substantial Dividing Walls (SDWs) to provide protection from remote operation, volume 1
[AD-A250251] p 3428 N92-29545
Erbium-doped fiber amplifier elements for structural analysis sensors
[NASA-CR-190491] p 3552 N92-29681
The effect of length variation on the stability of circular cylindrical shells under pure bending
[LR-669] p 3482 N92-29700
Structural basis for the mechanical properties of polyethylenes
[PB92-164425] p 3426 N92-29804
A closed form solution of a longitudinal beam with a viscous boundary condition
[AD-A248841] p 3483 N92-29915
Damaged stiffened shell research at NASA. Langley Research Center p 3485 N92-30115
Simplified computational methods for elastic and elastic-plastic fracture problems p 3488 N92-30134
Nonlinear analyses of composite aerospace structures in sonic fatigue
[NASA-CR-190565] p 3404 N92-30209
National Launch System cycle 1 loads and models data book
[NASA-TM-103560] p 3408 N92-30215

STRUCTURAL DESIGN
Concurrent engineering in design of aircraft structures
[MBB-FE-2-S-PUB-472] p 3404 N92-29650
A perspective on MoSi2 based composites
[DE92-013434] p 3415 N92-29795
Penguin extruded aluminium box launcher for marine application
[FFI-91/4001] p 3408 N92-29967

STRUCTURAL DESIGN CRITERIA
Short cracks and durability analysis of the Fokker 100 wing/fuselage structure
[NLR-TP-90336-U] p 3482 N92-29603

STRUCTURAL ENGINEERING
Concurrent engineering in design of aircraft structures
[MBB-FE-2-S-PUB-472] p 3404 N92-29650
Repair procedures for advanced composites for helicopters
[MBB-UD-0606-91-PUB] p 3399 N92-29874

STRUCTURAL FAILURE
Compressive response of debonded thick composite shells including the effects of transient moisture sorption
[AD-A250080] p 3414 N92-29462
Structural integrity of future aging airplanes p 3484 N92-30107
Maintaining the safety of an aging fleet of aircraft p 3402 N92-30108
Performance of fuselage pressure structure p 3484 N92-30109
Fracture mechanics research at NASA related to the aging commercial transport fleet p 3484 N92-30110
Current DOT research on the effect of multiple site damage on structural integrity p 3485 N92-30112
Damage tolerance for commuter aircraft p 3485 N92-30114
Thermal QNDE detection of airframe disbonds p 3481 N92-30118
A manufacturer's approach to ensure long term structural integrity p 3403 N92-30133

STRUCTURAL RELIABILITY
Current DOT research on the effect of multiple site damage on structural integrity p 3485 N92-30112

STRUCTURAL STABILITY
Instantaneous optimal control for linear, nonlinear and hysteretic structures: Stable controllers
[PB92-163807] p 3501 N92-29950

STRUCTURAL VIBRATION
Validation of finite element and boundary element methods for predicting structural vibration and radiated noise
[NASA-TM-105359] p 3478 N92-29697

STRUCTURED PROGRAMMING
Abstract data types and algorithm structures and a basis for component reuse
[REPT-91-49] p 3518 N92-29712

SUBGROUPS
Swirls and wheels
[PB92-173251] p 3542 N92-30095

SUBMARINES
Active structural acoustic control and smart structures
[AD-A248341] p 3543 N92-29588

SUBROUTINES
Revising M-layer: Complex exponent representation
[AD-A249121] p 3435 N92-29599

SUBSONIC FLOW
Evaluation of measured-boundary-condition methods for 3D subsonic wall interference
[NLR-TR-88072-U] p 3401 N92-29884
Production of periodical Mach number variations in high subsonic flow in a blow down wind tunnel, and its influence on profile measurements
[ETN-92-91492] p 3401 N92-29889

SUBSONIC SPEED
Jet aircraft noise at high subsonic flight Mach numbers
[DLR-FB-91-28] p 3544 N92-29997

SUBSTRATES
Experimental evaluation of incorporating digital and analog integrated circuit die on a common substrate utilizing silicon-hybrid wafer-scale integration technology
[AD-A248182] p 3439 N92-29405
Method of forming silicon structures with selectable optical characteristics
[NASA-CASE-NPO-18625-1-CU] p 3559 N92-30102

SUGARS
Microbial aldonolactone formation and hydrolysis: Kinetic and bioenergetic aspects p 3507 N92-29735

SULFATES
Role of polyelectrolytes in barium sulphate precipitation
[PB92-184761] p 3419 N92-30196

SULFIDES
Material-deposition processes in the separator of Li-alloy/FeS2 thermal cells
[DE92-013669] p 3440 N92-29518

SULFUR DIOXIDES
Ozone measurements with the US EPA UV-DIAL: Preliminary results p 3461 N92-29255
Advanced rechargeable lithium sulfur dioxide cell
[AD-A250027] p 3491 N92-29476

SULFURIC ACID
Irradiation effects on the electrochemistry and corrosion resistance of stainless steel
[DE92-013504] p 3420 N92-29411

SUM RULES
Theoretical overview: Hot and dense QCD in equilibrium
[DE92-013665] p 3560 N92-29517

SUMS
Strong law and central limit theorem for a process between maxima and sums p 3530 N92-29964

SUN
Global solar magnetic fields
[AD-A248340] p 3569 N92-29421
CoMStOC 4: Multiwaveband observations of sunspot and plage-associated coronal emission
[AD-A248344] p 3570 N92-29632
Investigation of solar active regions at high resolution by balloon flights of the solar optical universal polarimeter, definition phase
[NASA-CR-184339] p 3570 N92-30204

SUNSPOTS
CoMStOC 4: Multiwaveband observations of sunspot and plage-associated coronal emission
[AD-A248344] p 3570 N92-29632

SUPERCONDUCTING SUPER COLLIDER
Hydrogen desorption and the search for the Higgs
[DE92-013464] p 3545 N92-29507

SUPERCONDUCTIVITY
Variable temperature scanning tunneling microscopy
[AD-A248725] p 3557 N92-29722

SUPERCONDUCTORS
Thermochemistry of phases related to oxide superconductors
[DE92-011811] p 3556 N92-29485
Monolithic integration of semiconductor and superconductor components
[AD-A245351] p 3557 N92-29583

SUPERFLUIDITY
Vorticity matching in superfluid helium p 3449 N92-30049

SUPERHIGH FREQUENCIES
Performance of a 12-GHz fiber-optic system for beam-waveguide antenna stability testing p 3431 N92-29372
Optimizing the G/T ratio of the DSS-13 34-meter beam-waveguide antenna p 3431 N92-29377

SUPERLATTICES
Thermodynamic and kinetic aspects of 3/5 epitaxy
[AD-A250632] p 3556 N92-29429
The role of chemical interactions in the stability of artificial metallic superlattices
[DE92-011528] p 3559 N92-29911

SUPERSONIC AIRCRAFT
Determination of aerodynamic sensitivity coefficients for wings in transonic flow
[NASA-CR-190570] p 3401 N92-29657

SUPERSONIC FLOW
A numerical and experimental investigation of the thrust vector control by secondary gas injection
[DLR-FB-91-31] p 3447 N92-29998
Effect of walls on the supersonic reacting mixing layer p 3451 N92-30065
Continuum approaches for describing solid-gas and solid-liquid flow
[DE92-013601] p 3452 N92-30140
Direct simulations of wall-bounded compressible turbulence p 3454 N92-30162
A numerical method for prediction of compressible turbulent flows with closure models p 3454 N92-30164

SUPERSONIC TRANSPORTS
Methods for direct simulation of transition in hypersonic boundary layers 2 p 3451 N92-30064

SUPERSONIC WIND TUNNELS
Shock enhancement and control of hypersonic combustion
[AD-A248558] p 3418 N92-29580

SUPERSYMMETRY
Introduction to SO(3) monopole
[USIP-91-05] p 3560 N92-29781
Supersymmetric extensions of the nonlinear Schroedinger equation: Symmetries and coverings
[MEMO-1002] p 3537 N92-30078

SUPPORT SYSTEMS
Support activities to maintain SUMS flight readiness
[NASA-CR-189656-VOL-1] p 3410 N92-30217
Support activities to maintain SUMS flight readiness, volume 2. Attachment A: Flight 61-C report
[NASA-CR-189656-VOL-2] p 3411 N92-30218

SUPPORTS
Shaft mount for data coupler system
[NASA-CASE-LAR-13805-1] p 3480 N92-30097

SURFACE CRACKS
Aluminum-lithium alloys: Surface-cracked tension fracture tests and physical and thermal properties at cryogenic temperatures
[PB92-172477] p 3422 N92-29803

SURFACE FINISHING
Cursory examination of the zeta potential behaviors of two optical materials
[DE92-011588] p 3551 N92-29578

SURFACE LAYERS
Lidar observation of aerosol and temperature stratification over urban area during the formation of a stable atmospheric PBL p 3466 N92-29286
Non-interfering dipaths in planar digraphs
[CWI-BS-R9121] p 3533 N92-29864

SURFACE NAVIGATION
Terrain following of arbitrary surfaces using a high intensity LED proximity sensor
[DE92-004464] p 3528 N92-29644

SURFACE PROPERTIES
Biologically-based neural network model of color constancy and color contrast
[AD-A248128] p 3510 N92-29398
Surface reactions in the space environment
[AD-A250624] p 3428 N92-29428
A study of the influence of alloying additions on the passivity of aluminum
[AD-A248339] p 3421 N92-29587
Theory of the dissociation dynamics of small molecules on metal surfaces: Finite temperature studies
[DE92-011188] p 3546 N92-29899
Role of polyelectrolytes in barium sulphate precipitation
[PB92-184761] p 3419 N92-30196

SURFACE REACTIONS
Surface reactions in the space environment
[AD-A250624] p 3428 N92-29428

SURFACE ROUGHNESS
Diffraction of light from randomly rough surfaces
[AD-A250261] p 3551 N92-29546

SURFACE TEMPERATURE
The processing of high temperature ceramic superconducting devices, volume 1
[AD-A248176] p 3438 N92-29404
Mapping of groundwater losses by evaporation in the western desert of Egypt
[BCRS-91-01] p 3489 N92-29495
Second-order shock-expansion theory extended to include real gas effects
[AD-A247191] p 3400 N92-29539
Hypersonic flow past radiation-cooled surfaces
[MBB-FE-202-S-PUB-0468-A] p 3401 N92-29713

SURFACE VEHICLES
KISMET (kinematic simulation, monitoring and off-line programming environments for telerobotics): Simulation of the target-oriented driving of an autonomous vehicle in a labyrinthic environment
[KFK-4941] p 3515 N92-29418

New York State technical and economic MAGLEV evaluation
[PB92-174119] p 3564 N92-30037
SURFACE WAVES
International conference topical meeting on atmospheric, volume, and surface scattering and propagation
[AD-A248881] p 3552 N92-29727
SURVEILLANCE
Revising M-layer: Complex exponent representation
[AD-A249121] p 3435 N92-29599
SURVEYS
Tapering clouds and their classification due mainly to the surrounding cloud pattern in the GMS imagery
[ISSN-0388-9653] p 3502 N92-29666
SUSPENDING (MIXING)
The dependence of transport coefficients of suspensions in quasistatic and retarded hydrodynamic interactions
[ETN-92-91624] p 3444 N92-29752
SWELLING
In vitro measurement of nucleus pulposus swelling pressure: A new technique for studies of spinal adaptation to gravity
[NASA-TM-103853] p 3506 N92-29397
SYMBOLIC PROGRAMMING
Code generation in ALPAL using symbolic techniques
[DE92-011299] p 3524 N92-29353
A new algebra core for the minimal form problem
[DE92-011966] p 3531 N92-29481
SYMMETRICAL BODIES
Experimental examination of heavy loaded axial fans with rotational symmetrical distortion of the inflow
[ETN-92-91489] p 3445 N92-29926
SYMMETRY
Matched asymptotic expansions solution for low-frequency sound radiation from fluid-loaded, baffled plates: Axisymmetric case
[REPT-91-60] p 3543 N92-29628
Asymptotic optimality of the chi-square test with large number of degrees of freedom within the class of symmetric tests
[CWI-BS-R9116] p 3540 N92-29860
SYNCHRONISM
The weakest failure detector for solving consensus
[NASA-CR-190545] p 3515 N92-29400
Performance of a connectionless protocol over ATM
[MEMO-INF-92-02] p 3526 N92-29880
SYNCHROTRON RADIATION
The 20 element HgI2 energy dispersive x ray array detector system
[DE92-013356] p 3549 N92-29502
Hydrogen desorption and the search for the Higgs
[DE92-013464] p 3545 N92-29507
SYNCHROTRONS
Longitudinal bunch profile measurements with striplines
[DE92-013035] p 3549 N92-29477
The 20 element HgI2 energy dispersive x ray array detector system
[DE92-013356] p 3549 N92-29502
Exploratory study for a solid-state charged-particle spectrometer inside the Celsius ring: Alpha and hydrogen reactions at 1.7 and 2.2 GeV/c
[USIP-91-02] p 3546 N92-29715
SYNTAX
Defaults in update semantics
[ITLI-LP-91-02] p 3532 N92-29685
SYNTHESIS (CHEMISTRY)
Synthesis of a naphthalene-hydroxynaphthalene polymer model compound
[DE92-012264] p 3423 N92-29435
Synthesis and useful reactions of organosilicon polymeric precursors for ceramics
[AD-A248500] p 3424 N92-29496
Synthesis of new high performance lubricants and solid lubricants
[DE92-011940] p 3424 N92-29549
Structural rearrangements during mesomorphic phase transitions in poly(10-((4-cyano-4' biphenyl)oxy)decanyl vinyl ether)
[AD-A248306] p 3425 N92-29569
Synthesis and characterization of a covalently bound self-assembled macrocycle monolayer thin film for nonlinear optical materials
[DE92-011353] p 3545 N92-29634
SYNTHETIC APERTURE RADAR
Research and technology annual report, FY 1990
[NASA-TM-107807] p 3571 N92-30197
SYSTEM FAILURES
Spacecraft dynamics characterization and control system failure detection, volume 1
[NASA-CR-190517] p 3409 N92-29422
SYSTEM IDENTIFICATION
Linear system identification via backward-time observer models
[NASA-TM-107632] p 3488 N92-30214
SYSTEMS ANALYSIS
A systems analysis of the impact of navigation instrumentation on-board a Mars rover, based on a covariance analysis of navigation performance
[NASA-CR-189868] p 3403 N92-29440
Experiments on processes with backtracking
[RR-858-I-IMAG-121-LIFIA] p 3532 N92-29574
Theory of system reliability demonstration, burn-in design, and record statistics
[AD-A250582] p 3480 N92-29710
Methodology on monitoring and modelling of microbial metabolism
[ETN-92-91745] p 3507 N92-29732
Classification, error detection, and reconciliation of measurements in complex biochemical systems p 3508 N92-29737
Analysis and experimental testing of a bottleneck model for the description of microbial dynamics p 3508 N92-29740
Information systems analysis and design based on an object-oriented framework
[MEMO-INF-91-93] p 3519 N92-29816
Object-oriented system implementation
[MEMO-INF-91-67] p 3523 N92-30181
SYSTEMS ENGINEERING
The Laser Atmospheric Wind Sounder (LAWS) phase 2 preliminary system design p 3468 N92-29297
Taguchi methods
[MEMO-COSOR-91-31] p 3539 N92-29609
The optical design of AmPS: Elements of the design of a pulse stretcher
[ETN-92-91626] p 3552 N92-29859
Cislan-2 extension final document by University of Twente (Netherlands)
[MEMO-INF-92-05] p 3437 N92-29984
SYSTEMS INTEGRATION
GE's mobile, coherent Doppler lidar test/evaluation facilities p 3407 N92-29299
Using object-oriented databases for implementation of interactive electronic technical manuals
[AD-A248135] p 3440 N92-29564
SPARA: A system of planning robot manipulation tasks
[LAAS-91395] p 3529 N92-29678
Smart BIT/TSMD integration
[AD-A247192] p 3442 N92-29914
An object-oriented language-database integration model: The composition-filters approach
[MEMO-INF-91-90] p 3521 N92-29961
Variable bandwidth connections for a connectionless service on ATM: Performance modelling and evaluation
[MEMO-INF-91-83] p 3438 N92-30170
Integrated service engineering supported by the FDT LOTOS
[MEMO-INF-91-76] p 3531 N92-30184
SYSTEMS SIMULATION
Strong bisimilarity on nets revisited
[RR-847-I-IMAG-120-LIFIA] p 3532 N92-29573
Software architecture modelling: Application to AMODEUS design scenarios
[IMAG-RR-860-I] p 3513 N92-29611
The capacitated multi-echelon inventory system with serial structure: 1: The push ahead-effect
[MEMO-COSOR-91-39] p 3561 N92-29822
The capacitated multi-echelon inventory system with serial structure: 2: An average cost approximation method
[MEMO-COSOR-91-40] p 3561 N92-29823
Measuring and simulating an 802.3 CSMA/CD LAN
[MEMO-COSOR-91-42] p 3525 N92-29825
Computing distinguishing formulas for branching bisimulation
[CWI-CS-R9121] p 3521 N92-29890
Decision systems; the relation between problem specification and mathematical analysis
[MEMO-COSOR-91-37] p 3535 N92-29898
A simulation study on a high-speed slotted-ring access mechanism with dynamically adaptive slot size
[MEMO-INF-91-83] p 3526 N92-30074
A model for dataflow query execution in a parallel main-memory environment
[MEMO-INF-91-34] p 3527 N92-30142
Temporal reasoning in model-based diagnosis
[MEMO-INF-91-66] p 3531 N92-30143
Variable bandwidth connections for a connectionless service on ATM: Performance modelling and evaluation
[MEMO-INF-91-83] p 3438 N92-30170
SYSTEMS STABILITY
Performance of a 12-GHz fiber-optic system for beam-waveguide antenna stability testing p 3431 N92-29372

T

TACTICS
Phase-space estimate of satellite coverage time
[DE92-013555] p 3542 N92-30139
TANKS (CONTAINERS)
Near-visible Raman instrumentation for remote multi-point process monitoring using optical fibers and optical multiplexing
[DE92-011287] p 3550 N92-29337
TARGET RECOGNITION
Evaluation of Night Vision Goggles (NVG) for maritime search and rescue
[AD-A247182] p 3512 N92-29538
TARGETS
KISMET (kinematic simulation, monitoring and off-line programming environments for telerobotics): Simulation of the target-oriented driving of an autonomous vehicle in a labyrinthic environment
[KFK-4941] p 3515 N92-29418
Normalized radar cross section of natural surfaces at millimeter wavelengths
[AD-A248452] p 3434 N92-29447
Evaluation of Night Vision Goggles (NVG) for maritime search and rescue
[AD-A247182] p 3512 N92-29538
TASK PLANNING (ROBOTICS)
SPARA: A system of planning robot manipulation tasks
[LAAS-91395] p 3529 N92-29678
TAYLOR INSTABILITY
Mixing measurements of straight and curved shear layers p 3451 N92-30067
TECHNOLOGIES
Summary of technical operations, 1991 --- software development
[AD-A248153] p 3516 N92-29540
Human factors in aircraft maintenance and inspection p 3487 N92-30125
TECHNOLOGY ASSESSMENT
The role of lidars in global change research p 3457 N92-29235
Contracting in the software engineering crisis
[AD-A250241] p 3516 N92-29544
Saenger: The reference concept and its technological requirements - aerothermodynamics
[MBB-FE-202-S-PUB-0463-A] p 3408 N92-29629
Global standards: Building blocks for the future
[PB92-167352] p 3563 N92-29671
Manufacturing of components of fibre-metal laminates: An overview
[LR-670] p 3415 N92-29702
An introduction to software reuse
[REPT-91-50] p 3519 N92-29779
Nondestructive inspection perspectives p 3481 N92-30121
Current and future developments in civil aircraft non-destructive evaluation from an operator's point of view p 3399 N92-30122
Using intelligent simulation to enhance human performance in aircraft maintenance p 3487 N92-30126
TECHNOLOGY TRANSFER
EOS Data and Information System (EOSDIS) --- landsat satellites
[NASA-TM-107922] p 3488 N92-29442
The 1991 research highlights
[AD-A247865] p 3570 N92-29464
Application Center of Excellence (ACE) program
[AD-A248694] p 3562 N92-29934
Communication: An important element of maintenance and repair p 3402 N92-30124
TECHNOLOGY UTILIZATION
The 1991 research highlights
[AD-A247865] p 3570 N92-29464
The 1990 annual report, April 1990 - March 1991 p 3571 N92-29471
Activities report of the Netherlands Remote Sensing Board (with abridged version)
[ETN-92-91352] p 3489 N92-29688
TELECOMMUNICATION
The Telecommunications and Data Acquisition Report
[NASA-CR-190460] p 3429 N92-29364
TELEMETRY
DSN acquisition of Magellan high-rate telemetry data p 3409 N92-29383
Deep Space Network information system architecture study p 3433 N92-29385
Detection of binary phase shift keyed signals in extremely high noise
[AD-A248552] p 3435 N92-29576
TELESCOPES
ARCLITE: The Arctic Lidar Technology Facility at Sondre Stromfjord, Greenland p 3407 N92-29283

One year of Rayleigh lidar measurements at Toronto
p 3466 N92-29285
The Lidar In-Space Technology Experiment (LITE)
p 3469 N92-29301
Investigation of solar active regions at high resolution by balloon flights of the solar optical universal polarimeter, definition phase
[NASA-CR-184339] p 3570 N92-30204

TELEVISION SYSTEMS
The 1990 annual report, April 1990 - March 1991
p 3571 N92-29471

TEMPERATURE
Theory of the dissociation dynamics of small molecules on metal surfaces: Finite temperature studies
[DE92-011188] p 3546 N92-29899

TEMPERATURE COMPENSATION
Noise-optimal control of HEMT LNA's for compensation of temperature deviations p 3431 N92-29374

TEMPERATURE CONTROL
Active thermal isolation for temperature responsive sensors
[NASA-CASE-LAR-14612-1] p 3446 N92-29954

TEMPERATURE DEPENDENCE
Review of temperature dependent effects on the oxidation protection of carbon/carbon
[DE92-012333] p 3415 N92-29645
Direct numerical simulation of instability and noise generation of hot jets p 3451 N92-30066

TEMPERATURE DISTRIBUTION
One year of Rayleigh lidar measurements at Toronto
p 3466 N92-29285
Lidar observation of aerosol and temperature stratification over urban area during the formation of a stable atmospheric PBL p 3466 N92-29286
Modeling of the role of atomic hydrogen in heat transfer during hot filament assisted deposition of diamond
[AD-A250607] p 3418 N92-29595
ESATAN user manual
[ESA-PSS-03-105-ISSUE-2] p 3521 N92-29869

TEMPERATURE EFFECTS
An innovative approach for coupled thermomechanical analysis
[DE92-011467] p 3481 N92-29338
Introduction to quartz frequency standards
[AD-A248503] p 3439 N92-29498
Modeling of the role of atomic hydrogen in heat transfer during hot filament assisted deposition of diamond
[AD-A250607] p 3418 N92-29595
Review of temperature dependent effects on the oxidation protection of carbon/carbon
[DE92-012333] p 3415 N92-29645
Effect of walls on the supersonic reacting mixing layer
p 3451 N92-30065

TEMPERATURE GRADIENTS
Design and operation of the multipulse Thomson scattering diagnostic on DIII-D
[DE92-011393] p 3476 N92-29474

TEMPERATURE INVERSIONS
Lidar monitoring of Mexico City's atmosphere during high air polution episodes p 3464 N92-29275

TEMPERATURE MEASUREMENT
A comparison between Raman lidar and conventional contact measurements of atmospheric temperature
p 3466 N92-29287
Error analysis of wind measurements for the University of Illinois sodium Doppler temperature system
p 3471 N92-29313
Sodium Doppler temperature lidar observations of the mesopause region temperature and wind structure
p 3471 N92-29314
Rayleigh/Raman Greenland lidar observations of atmospheric temperature during a major Arctic stratospheric warming event p 3471 N92-29316
Elastic and Raman lidar temperature measurements from Poker Flat, Alaska during February 1992
p 3471 N92-29317
Rayleigh/Raman lidars: Intercomparisons and validation p 3471 N92-29318
Circulation and exchange at the continental shelf and slope SEEP-2
[DE92-013500] p 3504 N92-29439
The development of a fiber optic Raman temperature measurement system for rocket flows
[NASA-CR-189200] p 3413 N92-29448
Spatial and temporal temperature studies of electrothermal chemical (ETC) plasmas
[AD-A248541] p 3554 N92-29510
Estimating plasma temperatures
[DE92-014092] p 3555 N92-29798
Method and apparatus for thermographically and quantitatively analyzing a structure for disbonds and/or inclusions
[NASA-CASE-LAR-14559-1] p 3480 N92-29829
SP-100 W/Re thermocouple calibration techniques
[DE92-011302] p 3550 N92-29938

TEMPERATURE MEASURING INSTRUMENTS
SP-100 W/Re thermocouple calibration techniques
[DE92-011302] p 3550 N92-29938

TEMPERATURE PROFILES
Rotational Raman lidar for lower tropospheric temperature profiling p 3466 N92-29284
A comparison between Raman lidar and conventional contact measurements of atmospheric temperature
p 3466 N92-29287
Modeling of the role of atomic hydrogen in heat transfer during hot filament assisted deposition of diamond
[AD-A250607] p 3418 N92-29595

TEMPERATURE SENSORS
Active thermal isolation for temperature responsive sensors
[NASA-CASE-LAR-14612-1] p 3446 N92-29954

TEMPORAL DISTRIBUTION
Spatial and temporal temperature studies of electrothermal chemical (ETC) plasmas
[AD-A248541] p 3554 N92-29510

TENSILE PROPERTIES
Mechanical properties of coated titanium Beta-21S after exposure to air at 700 and 800 C
[NASA-TM-104220] p 3423 N92-30205

TENSILE STRENGTH
An interlaminar tension strength specimen
[NASA-TM-107623] p 3481 N92-29393
Fundamental study of compressive strength development in PAN-based carbon fibers
[AD-A250285] p 3416 N92-30137

TENSILE TESTS
An interlaminar tension strength specimen
[NASA-TM-107623] p 3481 N92-29393

TENSIOMETERS
Field study of multidimensional flow and transport in the vadose zone
[PB92-161363] p 3489 N92-29701

TENSION
Apparatus for elevated temperature compression or tension testing of specimens
[NASA-CASE-LAR-14775-1] p 3483 N92-30099

TERMINOLOGY
PDES application protocol suite for composites (PAS-C): IDEFO activity models and information needs for the PAS-C program
[AD-A248714] p 3562 N92-29720
Lexicon of new formal geologic names of the United States, 1981-1985
[PB92-181320] p 3563 N92-30040

TERRAIN
User's guide for the VTRPE (Variable Terrain Radio Parabolic Equation) computer model
[AD-A248112] p 3433 N92-29395
Terrain following of arbitrary surfaces using a high intensity LED proximity sensor
[DE92-004464] p 3528 N92-29644

TEST CHAMBERS
Design characteristics of a heat pipe test chamber
[NASA-TM-105737] p 3492 N92-29662

TEST FACILITIES
Design characteristics of a heat pipe test chamber
[NASA-TM-105737] p 3492 N92-29662
Final Environmental Impact Statement (EIS) for the Space Nuclear Thermal Propulsion (SNTP) program
[AD-A248408] p 3413 N92-29903

TEST PATTERN GENERATORS
A strategy for microprocessor BIST implementation based on deterministic testing
[IMAG-RR-844-I] p 3516 N92-29570

TETHERING
Fingered bola body, bola with same, and methods of use
[NASA-CASE-MSC-21967-1] p 3479 N92-30026

TEXTS
Overview of the document style semantics and specification language and the MIL-M-28001A output specification
[PB92-181122] p 3563 N92-30039

TEXTURES
Texture synthesis
[CWI-CS-R9139] p 3523 N92-30141

THEMATIC MAPPERS (LANDSAT)
Biophysical, morphological, canopy optical property, and productivity data from the Superior National Forest
[NASA-TM-104568] p 3491 N92-30210

THEMATIC MAPPING
TERS product development plan for urban planning of Bandung, Indonesia
[BCRS-91-30] p 3491 N92-30231

THEOREM PROVING
The weakest failure detector for solving consensus
[NASA-CR-190545] p 3515 N92-29400
Dynamic semantics and circular propositions
[ITLI-LP-91-03] p 3532 N92-29687
Asymptotic optimality of the chi-square test with large number of degrees of freedom within the class of symmetric tests
[CWI-BS-R9116] p 3540 N92-29860
A model for no Borel liftings
[REPT-91-37] p 3535 N92-29919
Strong law and central limit theorem for a process between maxima and sums p 3530 N92-29964
Classification of A-graded algebras with 3 generators
[MEMO-1004] p 3537 N92-30080

THEOREMS
A new form for the chi-squared test of independence (document 2) p 3538 N92-29492
Limit theorems for cumulative processes
[AD-A248507] p 3538 N92-29500
Defaults in update semantics
[ITLI-LP-91-02] p 3532 N92-29685
Dynamic semantics and circular propositions
[ITLI-LP-91-03] p 3532 N92-29687
On the addition of log-convex functions and sequences
[MEMO-COSOR-92-01] p 3533 N92-29826
Asymptotic optimality of the chi-square test with large number of degrees of freedom within the class of symmetric tests
[CWI-BS-R9116] p 3540 N92-29860
Limit theorems for functionals of convex hulls
[REPT-91-39] p 3535 N92-29921
Undecidable equivalences for basic process algebra
[CWI-CS-R9137] p 3536 N92-29993
Algorithms and min-max theorems for certain multiway cuts
[MEMO-1022] p 3523 N92-30186

THEORETICAL PHYSICS
An introduction to using the FORTRAN programs provided with Computational Nuclear Physics 1 Nuclear Structure p 3549 N92-30013

THERMAL ABSORPTION
Sound speed, reflectivity, and absorption measurements in Arctic ice in 1988
[AD-A246293] p 3505 N92-29554

THERMAL ANALYSIS
ESATAN user manual
[ESA-PSS-03-105-ISSUE-2] p 3521 N92-29869

THERMAL DECOMPOSITION
The activation of chemical bonds at surfaces
[AD-A248666] p 3418 N92-29719

THERMAL DEGRADATION
Acetate in hydrothermal solutions: Decomposition kinetics and metal complexation
[DE92-010542] p 3417 N92-29551

THERMAL EXPANSION
A novel approach to silicon-on-insulator materials
[AD-A248074] p 3424 N92-29466

THERMAL MAPPING
Research and technology annual report, FY 1990
[NASA-TM-107807] p 3571 N92-30197

THERMAL SIMULATION
CDM with thermal history of baryons: High-resolution 2-D and 3-D simulations p 3565 N92-29835

THERMAL STABILITY
Polybenzimidazoles via aromatic nucleophilic displacement
[NASA-CASE-LAR-14643-1] p 3426 N92-29953

THERMOCHEMISTRY
Thermochemistry of phases related to oxide superconductors
[DE92-011811] p 3556 N92-29485

THERMOCOUPLES
SP-100 W/Re thermocouple calibration techniques
[DE92-011302] p 3550 N92-29938

THERMODYNAMIC CYCLES
MHD Technology Transfer, Integration and Review Committee
[DE92-012687] p 3554 N92-29640

THERMODYNAMIC EQUILIBRIUM
The expanding plasma jet: Experiments and model
[ETN-92-91627] p 3555 N92-29761

THERMODYNAMIC PROPERTIES
An innovative approach for coupled thermomechanical analysis
[DE92-011467] p 3481 N92-29338
Thermochemistry of phases related to oxide superconductors
[DE92-011811] p 3556 N92-29485
Aluminum-lithium alloys: Surface-cracked tension fracture tests and physical and thermal properties at cryogenic temperatures
[PB92-172477] p 3422 N92-29803

THERMODYNAMICS
An innovative approach for coupled thermomechanical analysis
[DE92-011467] p 3481 N92-29338
Thermodynamic and kinetic aspects of 3/5 epitaxy
[AD-A250632] p 3556 N92-29429

A generalized polynomial form of the objective function in flash calculations
[AD-A248160] p 3531 N92-29446
Diffusion and phase relations in the systems Ti-Si-C and Ti-Si-N
[ETN-92-91631] p 3546 N92-29777
THERMOGRAPHY
Thermal QNDE detection of airframe disbonds p 3481 N92-30118
THERMONUCLEAR REACTIONS
Experimental and theoretical research in applied plasma physics
[DE92-013587] p 3553 N92-29336
THERMOPLASTIC RESINS
Status and perspectives of modern composite materials
[MBB-Z-0380-91-PUB] p 3416 N92-29675
THERMOREGULATION
Improvements in X-band transmitter phase stability through klystron body temperature regulation p 3431 N92-29373
THERMOSPHERE
Analysis of EUV dayglow spectra of Triton, Titan and Earth
[NASA-CR-190586] p 3568 N92-29451
THESAURI
NASA visual thesaurus maintenance documentation
[NASA-CR-190282] p 3561 N92-29553
THICK FILMS
Design guidelines for capability approval of film hybrid microcircuits and Microwave Hybrid Integrated Circuits (MHICs)
[ESA-PSS-01-610-ISSUE-1] p 3441 N92-29854
THICK WALLS
Guide for evaluating 12 inch Substantial Dividing Walls (SDWs) to provide protection from remote operation, volume 2
[AD-A250252] p 3428 N92-29335
Guide for evaluating 12 inch Substantial Dividing Walls (SDWs) to provide protection from remote operation, volume 1
[AD-A250251] p 3428 N92-29545
THICKNESS
Thickness dependency of elastic aftereffect of thin bending beams
[ETN-92-91488] p 3483 N92-29925
THICKNESS RATIO
Layer-thickness variations and x ray diffraction patterns, a general treatment p 3558 N92-29767
THIN FILMS
The processing of high temperature ceramic superconducting devices, volume 1
[AD-A248176] p 3438 N92-29404
Magnetic properties of nano-heterogeneous amorphous thin films
[AD-A250570] p 3420 N92-29426
A novel approach to silicon-on-insulator materials
[AD-A248074] p 3424 N92-29466
Laser processing for interconnect technology
[AD-A248103] p 3476 N92-29559
Novel thin-film CuInSe2 fabrication
[DE92-001222] p 3557 N92-29584
Synthesis and characterization of a covalently bound self-assembled macrocycle monolayer thin film for nonlinear optical materials
[DE92-011353] p 3545 N92-29634
A study and feasibility of ultra thin silica layers by rapid thermal processing
[LAAS-91393] p 3422 N92-29674
Design guidelines for capability approval of film hybrid microcircuits and Microwave Hybrid Integrated Circuits (MHICs)
[ESA-PSS-01-610-ISSUE-1] p 3441 N92-29854
RF vacuum electronics
[AD-A248857] p 3442 N92-29935
THIN PLATES
Thickness dependency of elastic aftereffect of thin bending beams
[ETN-92-91488] p 3483 N92-29925
THOMSON SCATTERING
Design and operation of the multipulse Thomson scattering diagnostic on DIII-D
[DE92-011393] p 3476 N92-29474
THREE DIMENSIONAL BODIES
Recognition of multi-articulated three-dimensional objects using a multisensor system for robotics applications
[LAAS-91394] p 3529 N92-29675
THREE DIMENSIONAL FLOW
Development of a multigrid transonic potential flow code for cascades
[NASA-CR-190480] p 3399 N92-29361
Evaluation of measured-boundary-condition methods for 3D subsonic wall interference
[NLR-TR-88072-U] p 3401 N92-29884
A method for computing the 3-dimensional flow about wings with leading-edge vortex separation. Part 2: Description of computer program VORSEP
[NLR-TR-86006-U] p 3402 N92-29916
Explicit Navier-Stokes computation of turbomachinery flows
[AD-A248458] p 3445 N92-29933
Numerical methods for the 3D shallow water equations on vector and parallel computers
[CWI-NM-R9109] p 3446 N92-29944
On the numerical treatment of the advective terms in 3D shallow water models
[CWI-NM-R9110] p 3446 N92-29945
Turbulence modeling: Near-wall turbulence and effects of rotation on turbulence p 3452 N92-30151
THREE DIMENSIONAL MODELS
Analysis of a three-dimensional point pattern with replication
[CWI-BS-R9124] p 3541 N92-30180
THRUST
Effects of bleed air extraction on thrust levels on the F404-GE-400 turbofan engine
[NASA-TM-104247] p 3405 N92-29425
THRUST VECTOR CONTROL
A numerical and experimental investigation of the thrust vector control by secondary gas injection
[DLR-FB-91-31] p 3447 N92-29998
TIDES
Parameter identification in tidal models with uncertain boundaries
[MEMO-983] p 3540 N92-29856
TIME
Linear system identification via backward-time observer models
[NASA-TM-107632] p 3488 N92-30214
TIME DEPENDENCE
Multidimensional computer simulation of Stirling cycle engines
[NASA-CR-190497] p 3478 N92-29392
Improving designer productivity --- artificial intelligence
[NASA-TM-103929] p 3404 N92-29417
Approximation in a damped Hamiltonian system by successive relative equilibria
[MEMO-1017] p 3536 N92-29979
Fast temporal neural learning using teacher forcing
[NASA-CASE-NPO-18553-1-CU] p 3530 N92-30085
Phase-space estimate of satellite coverage time
[DE92-013555] p 3542 N92-30139
TIME LAG
Transport delay measurements: Methodology and analysis for the F-16C combat engagement trainer, the display for advanced research and training, and the F-16A limited field of view
[AD-A248519] p 3406 N92-29505
TIME OF FLIGHT SPECTROMETERS
Time-of-flight experiments on GaAs/Al(x)Ga(x-1)As heterostructures
[ETN-92-91625] p 3558 N92-29753
TIME SERIES ANALYSIS
Numerical procedures for analyzing dynamical processes
[AD-A248175] p 3515 N92-29399
Multi-fractal analysis of nocturnal boundary layer time series from the Boulder Atmospheric Observatory
[AD-A248347] p 3502 N92-29424
Shelf Mixed Layer Experiment (SMILE) program description and coastal and moored array data report
[PB92-170281] p 3506 N92-29805
Turbulence dynamics in the wavelet representation p 3454 N92-30159
TIME SHARING
The M/G/1 processor sharing queue as the almost sure limit of feedback queues p 3530 N92-29965
TIME SIGNALS
Interface board for providing time signals to a super minicomputer
[AD-D015198] p 3441 N92-29900
TIN
X ray study of interfacial interactions in highly milled Sn-Ge powders
[DE92-012518] p 3556 N92-29437
TIN ALLOYS
Quasi-static intergranular cracking in a Cu-Sn alloy: An analog of stress relief cracking of steels
[DE92-011646] p 3420 N92-29483
TITAN
DSN observations of Titan p 3433 N92-29388
Analysis of EUV dayglow spectra of Triton, Titan and Earth
[NASA-CR-190586] p 3568 N92-29451
TITANIUM
Low-angle x ray diffraction study of solid state amorphization in a Ni/Ti multilayer p 3558 N92-29768
Diffusion and phase relations in the systems Ti-Si-C and Ti-Si-N
[ETN-92-91631] p 3546 N92-29777
Mechanical properties of coated titanium Beta-21S after exposure to air at 700 and 800 C
[NASA-TM-104220] p 3423 N92-30205
TITANIUM ALLOYS
Omega phase formation in titanium and titanium alloys
[DE92-011138] p 3421 N92-29633
Preliminary cutting and drilling studies using new generation lasers
[DE92-010712] p 3477 N92-29787
Thickness dependency of elastic aftereffect of thin bending beams
[ETN-92-91488] p 3483 N92-29925
TITANIUM CARBIDES
Rolling-contact and wear resistance of hard coatings on bearing-steel substrates
[DE92-011834] p 3478 N92-29357
TITANIUM NITRIDES
Rolling-contact and wear resistance of hard coatings on bearing-steel substrates
[DE92-011834] p 3478 N92-29357
TOKAMAK DEVICES
Experimental and theoretical research in applied plasma physics
[DE92-013587] p 3553 N92-29336
Multichord spectroscopy of the D3-D divertor region
[DE92-013507] p 3554 N92-29412
Design and operation of the multipulse Thomson scattering diagnostic on DIII-D
[DE92-011393] p 3476 N92-29474
Tunable driver for the LLNL FEL experiment
[DE92-011292] p 3477 N92-29937
Intense diagnostic neutral beam development for ITER
[DE92-011282] p 3556 N92-30203
TOLERANCES (MECHANICS)
Aging commuter aeroplanes: Fatigue evaluation and control methods p 3488 N92-30132
TOOLS
Bearing servicing tool
[NASA-CASE-MSC-21881-1] p 3479 N92-30082
TOPOGRAPHY
Numerical modeling studies of the Gulf of Mexico and the Caribbean Sea using the Bryan-Cox model
[PB92-164987] p 3505 N92-29704
TORPEDOES
Detection of binary phase shift keyed signals in extremely high noise
[AD-A248552] p 3435 N92-29576
TOUGHNESS
Characterization of fracture in (0/90)3s SiC/1723 composites
[AD-A250612] p 3414 N92-29453
Micromechanisms of cyclic and environmentally-assisted subcritical crack growth in ceramic-matrix composites
[AD-A248067] p 3414 N92-29556
Marine structural steel toughness data bank (abridged edition)
[PB92-163294] p 3422 N92-29807
TOWERS
Preliminary analysis of wind data from the Oak Ridge site survey
[PB92-174564] p 3503 N92-30034
TOXICOLOGY
Publications of the environmental health program: 1980-1990
[NASA-CR-4455] p 3509 N92-29341
TRACERS
Lidar tracking of multiple fluorescent tracers: Method and field test p 3464 N92-29274
TRACKING (POSITION)
Applications of inertial-sensor high-inheritance instruments to DSN precision antenna pointing p 3430 N92-29371
Interface board for providing time signals to a super minicomputer
[AD-D015198] p 3441 N92-29900
TRACKING FILTERS
Micro-computer network architecture for range instrumentation applications, volume 1
[AD-A247836] p 3525 N92-29555
TRACKING NETWORKS
Micro-computer network architecture for range instrumentation applications, volume 1
[AD-A247836] p 3525 N92-29555
TRAILING EDGES
Computation of three-dimensional effects on two dimensional wings
[NASA-CR-190576] p 3401 N92-29691
TRAINING ANALYSIS
Assessment of army aviators' ability to perform individual and collective tasks in the aviation networked simulator
[AD-A250293] p 3407 N92-29709
Fighter pilot training: The contribution of simulation
[NLR-TP-89311-U] p 3512 N92-29871

TRAINING DEVICES
Transport delay measurements: Methodology and analysis for the F-16C combat engagement trainer, the display for advanced research and training, and the F-16A limited field of view
[AD-A248519] p 3406 N92-29505
TRAINING SIMULATORS
Results of a flight simulator experiment to establish handling quality guidelines for the design of future transport aircraft
[NLR-MP-88044-U] p 3404 N92-29616
Assessment of army aviators' ability to perform individual and collective tasks in the aviation networked simulator
[AD-A250293] p 3407 N92-29709
Fighter pilot training: The contribution of simulation
[NLR-TP-89311-U] p 3512 N92-29871
Using intelligent simulation to enhance human performance in aircraft maintenance
p 3487 N92-30126
TRAJECTORIES
Non-interfering dipaths in planar digraphs
[CWI-BS-R9121] p 3533 N92-29864
TRAJECTORY PLANNING
Improving path planning with learning
[DE92-004360] p 3527 N92-29456
Path tracking using simple planar curves
[AD-A248252] p 3403 N92-29617
SPARA: A system of planning robot manipulation tasks
[LAAS-91395] p 3529 N92-29678
TRANSDUCERS
Friction drive position transducer
[AD-D015205] p 3475 N92-30202
TRANSFER OF TRAINING
Assessment of army aviators' ability to perform individual and collective tasks in the aviation networked simulator
[AD-A250293] p 3407 N92-29709
TRANSFORMATIONS
Spectral type of Ornstein's class one transformations
[PB92-178292] p 3537 N92-30096
TRANSISTOR AMPLIFIERS
Noise-optimal control of HEMT LNA's for compensation of temperature deviations p 3431 N92-29374
TRANSISTORS
Nonvolatile programmable neural network synaptic array
[NASA-CASE-NPO-18578-1-CU] p 3442 N92-30086
TRANSITION FLOW
Forces on a pipe bend resulting from clearing a pool of liquid upstream
[DE92-004179] p 3445 N92-29784
Transition to turbulence in hypersonic flow
p 3454 N92-30161
TRANSITION PROBABILITIES
Separable Markovian decision problems: The linear programming method in the multichain case (revised)
[PB92-187350] p 3524 N92-30201
TRANSLATING
A soft stairway to institutions
[MEMO-INF-91-87] p 3522 N92-29981
TRANSLATORS
User's manual for the NIST TTCN translator, version 3.0
[PB92-172493] p 3518 N92-29745
TRANSMISSION EFFICIENCY
Sensitivity analysis of the load on an ethernet network
[MEMO-COSOR-91-41] p 3436 N92-29824
TRANSMISSION LINES
Aperture coupling to shielded transmission lines: Theory and experiment
[PB92-183672] p 3437 N92-30093
TRANSMITTERS
Lidar In-space Technology Experiment (LITE) electronics overview p 3462 N92-29264
Laser Transmitter Module (LTM) for LITE
p 3463 N92-29265
System testing and performance characterization of the LITE Laser Transmitter Module at NASA
p 3469 N92-29302
HFRAD hindcast: An OTH-B radar and model comparison study
[AD-A248065] p 3436 N92-29902
TRANSONIC FLOW
Development of a multigrid transonic potential flow code for cascades
[NASA-CR-190480] p 3399 N92-29361
Two-dimensional boundary surfaces for planar external transonic flows
[AD-A248083] p 3444 N92-29524
Determination of aerodynamic sensitivity coefficients for wings in transonic flow
[NASA-CR-190570] p 3401 N92-29657
TRANSONIC WIND TUNNELS
Buffet test in the National Transonic Facility
[NASA-CR-189595] p 3406 N92-29352
TRANSPORT AIRCRAFT
Applied analytical combustion/emissions research at the NASA Lewis Research Center
[NASA-TM-105731] p 3412 N92-29343
Hyperbolic grid generation control by panel methods
[NLR-TP-91061-U] p 3532 N92-29604
Results of a flight simulator experiment to establish handling quality guidelines for the design of future transport aircraft
[NLR-MP-88044-U] p 3404 N92-29616
Fracture mechanics research at NASA related to the aging commercial transport fleet p 3484 N92-30110
Status of the FAA flight loads monitoring program
p 3485 N92-30113
Aging aircraft NDI Development and Demonstration Center (AANC): An overview --- nondestructive inspection p 3481 N92-30120
The FAA aging airplane program plan for transport aircraft p 3402 N92-30128
Transport Canada aging aircraft activities
p 3403 N92-30131
TRANSPORT PROPERTIES
LLE-LLNL progress report on studies in nonlocal heat transport in spherical plasmas using the Fokker-Planck code SPARK
[DE92-014093] p 3554 N92-29531
The dependence of transport coefficients of suspensions in quasistatic and retarded hydrodynamic interactions
[ETN-92-91624] p 3444 N92-29752
Transport processes in beamed energy propulsion systems
[AD-A247296] p 3413 N92-29913
TRANSPORTATION ENERGY
New York State technical and economic MAGLEV evaluation
[PB92-174119] p 3564 N92-30037
TRANSVERSE OSCILLATION
A consistent shear deformable theory for laminated plates
[AD-A250591] p 3415 N92-29593
TRAPPING
OCEANUS 218: Warm Ring Inertial Critical Layer Experiment (WRINCLE)
[PB92-170299] p 3506 N92-29806
TRAVELING SALESMAN PROBLEM
Electronic neural network for solving traveling salesman and similar global optimization problems
[NASA-CASE-NPO-17807-2-CU] p 3529 N92-29955
TRAVELING WAVES
Viscous profiles and numerical methods for shock waves
[AD-A246110] p 3443 N92-29458
Streamwise vortices in heated boundary layers
[NASA-CR-189661] p 3444 N92-29692
TREES (MATHEMATICS)
The primordial soup algorithm: A systematic approach to the specification and design of parallel parsers
[MEMO-INF-91-77] p 3536 N92-29956
A survey on minimum cost spanning tree games
[MEMO-1003] p 3541 N92-30079
Algorithms and min-max theorems for certain multiway cuts
[MEMO-1022] p 3523 N92-30186
TREES (PLANTS)
Normalized radar cross section of natural surfaces at millimeter wavelengths
[AD-A248452] p 3434 N92-29447
TRIBOLOGY
Synthesis of new high performance lubricants and solid lubricants
[DE92-011940] p 3424 N92-29549
TRIODES
RF vacuum electronics
[AD-A248857] p 3442 N92-29935
TRITON
Analysis of EUV dayglow spectra of Triton, Titan and Earth
[NASA-CR-190586] p 3568 N92-29451
TROPICAL REGIONS
Combined summaries: Technologies to sustain tropical forest resources and biological diversity
[OTA-F-515] p 3492 N92-29416
Tropical cyclones: Central North Pacific, 1991
[PB92-167345] p 3502 N92-29743
TROPICAL STORMS
Tropical cyclones: Central North Pacific, 1991
[PB92-167345] p 3502 N92-29743
TROPOSPHERE
First results from TROLIX 1991: An intercomparison of tropospheric ozone lidars p 3459 N92-29244
GLObal Backscatter Experiment (GLOBE) results: Aerosol backscatter global distribution and wavelength dependence p 3459 N92-29245
Multi-wavelength airborne lidar intercomparisons of aerosol and cirrus backscatter over the Pacific Ocean
p 3460 N92-29247
Ozone measurements with the US EPA UV-DIAL: Preliminary results p 3461 N92-29255
Transportable lidar for the measurement of ozone concentration and flux profiles in the lower troposphere
p 3465 N92-29278
Rotational Raman lidar for lower tropospheric temperature profiling p 3466 N92-29284
The Laser Atmospheric Wind Sounder (LAWS) phase 2 preliminary system design p 3468 N92-29297
User's guide for the VTRPE (Variable Terrain Radio Parabolic Equation) computer model
[AD-A248112] p 3433 N92-29395
Revising M-layer: Complex exponent representation
[AD-A249121] p 3435 N92-29599
TUNABLE LASERS
Femtosecond studies of carrier dynamics in compound semiconductors
[AD-A250584] p 3439 N92-29452
Tunable driver for the LLNL FEL experiment
[DE92-011292] p 3477 N92-29937
TUNGSTEN ALLOYS
A study of the influence of alloying additions on the passivity of aluminum
[AD-A248339] p 3421 N92-29587
TUNGSTEN ISOTOPES
Spectroscopy of W-183; measured magnetic moments and rotation-particle coupling
[DE92-624790] p 3549 N92-30213
TUNING
Analytical tuning of a low sensitivity observer applied to a continuous ethanol fermentation with product recovery p 3509 N92-29758
TURBINE BLADES
Fatigue in single crystal nickel superalloys
[AD-A248190] p 3420 N92-29408
Examination of the main error factors with regards to secondary losses in compression and turbine cascades by variations of the blade picture ratio
[ETN-92-91493] p 3405 N92-29927
TURBINE ENGINES
Contingency power for a small turboshaft engine by using water injection into turbine cooling air
[NASA-TM-105680] p 3405 N92-29661
TURBINES
A comparison of the calculated and experimental off-design performance of a radial flow turbine
[NASA-CR-189207] p 3399 N92-29402
TURBOCOMPRESSORS
Users manual for updated computer code for axial-flow compressor conceptual design
[NASA-CR-189171] p 3524 N92-30207
TURBOFAN ENGINES
Effects of bleed air extraction on thrust levels on the F404-GE-400 turbofan engine
[NASA-TM-104247] p 3405 N92-29425
TURBOMACHINE BLADES
Explicit Navier-Stokes computation of turbomachinery flows
[AD-A248458] p 3445 N92-29933
TURBOSHAFTS
Contingency power for a small turboshaft engine by using water injection into turbine cooling air
[NASA-TM-105680] p 3405 N92-29661
TURBULENCE
The influence of turbulence on aggregation of small particles in agitated vessels
[ETN-92-91629] p 3445 N92-29775
A numerical and experimental investigation of the thrust vector control by secondary gas injection
[DLR-FB-91-31] p 3447 N92-29998
Annual research briefs, 1991
[NASA-CR-189967] p 3447 N92-30041
Scaling analysis of energy transfer in the inertial range
p 3448 N92-30046
Turbulence and vortex structures
p 3448 N92-30048
Dynamic subgrid-scale modeling of compressible turbulence p 3450 N92-30058
Methods for direct simulation of transition in hypersonic boundary layers 2 p 3451 N92-30064
An exact turbulent closure for the hydromagnetic dynamo p 3452 N92-30071
Annual research briefs, 1989
[NASA-CR-189024] p 3452 N92-30149
Modeling of compressible turbulence
p 3452 N92-30150
Development of renormalization group analysis of turbulence p 3453 N92-30156
Short-time Lyapunov exponent analysis
p 3453 N92-30157
Direct simulation of turbulent combustion
p 3454 N92-30160

Transition to turbulence in hypersonic flow
p 3454 N92-30161
Direct simulations of wall-bounded compressible turbulence p 3454 N92-30162
Turbulent transport in the solar nebula
p 3454 N92-30163
A numerical method for direct simulation of turbulence in complex geometries p 3455 N92-30166
Turbulent thermal convection in a differentially rotating channel p 3455 N92-30168
Patterns in simulated turbulent channel flow
p 3455 N92-30169
Diurnal forcing of planetary atmospheres
[NASA-CR-190262] p 3569 N92-30199

TURBULENCE EFFECTS
Turbulence effects on the geodynamic laser ranging system
[PB92-166404] p 3477 N92-29948
The role of pressure-dilatation correlation in rapidly compressed turbulence and in boundary layers
p 3449 N92-30050
Analyses and modeling of evolving turbulent flow
p 3449 N92-30051
Flame ignition in a premixed turbulent flow
p 3450 N92-30061
Annual research briefs, 1989
[NASA-CR-189024] p 3452 N92-30149
Turbulence modeling: Near-wall turbulence and effects of rotation on turbulence p 3452 N92-30151
An experimental study of the effects of rapid rotation on turbulence p 3453 N92-30154
Direct simulations of wall-bounded compressible turbulence p 3454 N92-30162

TURBULENCE MODELS
Computation of three-dimensional effects on two dimensional wings
[NASA-CR-190576] p 3401 N92-29691
Annual research briefs, 1991
[NASA-CR-189967] p 3447 N92-30041
Near-wall turbulence modeling for boundary layers with separation p 3449 N92-30052
An exact turbulent closure for the hydromagnetic dynamo p 3452 N92-30071
Annual research briefs, 1989
[NASA-CR-189024] p 3452 N92-30149
Modeling of compressible turbulence
p 3452 N92-30150
Direct simulation of turbulent combustion
p 3454 N92-30160
Direct simulations of wall-bounded compressible turbulence p 3454 N92-30162
A numerical method for prediction of compressible turbulent flows with closure models
p 3454 N92-30164
A numerical method for direct simulation of turbulence in complex geometries p 3455 N92-30166

TURBULENT BOUNDARY LAYER
Multi-fractal analysis of nocturnal boundary layer time series from the Boulder Atmospheric Observatory
[AD-A248347] p 3502 N92-29424
Modeling and computational analysis of multiscale phenomena in fluid-structure interaction problems
[AD-A248723] p 3444 N92-29721
Annual research briefs, 1991
[NASA-CR-189967] p 3447 N92-30041
Near-wall turbulence modeling for boundary layers with separation p 3449 N92-30052
Modeling turbulent boundary layers in adverse pressure gradients p 3449 N92-30053
Streaks in turbulent boundary layers
p 3451 N92-30069
Turbulence modeling: Near-wall turbulence and effects of rotation on turbulence p 3452 N92-30151
An experimental investigation of a low Reynolds number turbulent boundary layer subject to an adverse pressure gradient p 3453 N92-30153
Direct simulations of wall-bounded compressible turbulence p 3454 N92-30162

TURBULENT DIFFUSION
A finite volume approach to large eddy simulation of compressible, homogeneous, isotropic, decaying turbulence
[MEMO-1009] p 3446 N92-29972

TURBULENT FLOW
A linear eddy sub-grid model for turbulent reacting flows: Application to hydrogen-air combustion
[DE92-006699] p 3417 N92-29433
Explicit Navier-Stokes computation of turbomachinery flows
[AD-A248458] p 3445 N92-29933
Active thermal isolation for temperature responsive sensors
[NASA-CASE-LAR-14612-1] p 3446 N92-29954
Annual research briefs, 1991
[NASA-CR-189967] p 3447 N92-30041
Local isotropy in buoyancy-generated turbulence
p 3447 N92-30043
On small scale vortices in turbulent flows
p 3448 N92-30045
The role of pressure-dilatation correlation in rapidly compressed turbulence and in boundary layers
p 3449 N92-30050
Analyses and modeling of evolving turbulent flow
p 3449 N92-30051
Modeling turbulent boundary layers in adverse pressure gradients p 3449 N92-30053
Single point modeling of initially isotropic turbulence under uniform rotation p 3449 N92-30054
On dynamic models for large eddy simulation
p 3450 N92-30056
Dynamic subgrid-scale modeling of compressible turbulence p 3450 N92-30058
Probability density function approach and related closures for turbulent scalar fields p 3450 N92-30059
Monte-Carlo implementation of mapping closures: Application to chemical reacting flows
p 3450 N92-30060
Flame ignition in a premixed turbulent flow
p 3450 N92-30061
Simulation of flame-turbulence interactions in premixed combustion p 3450 N92-30062
Some feedback procedures for control of flows
p 3452 N92-30070
An exact turbulent closure for the hydromagnetic dynamo p 3452 N92-30071
Annual research briefs, 1989
[NASA-CR-189024] p 3452 N92-30149
Modeling of compressible turbulence
p 3452 N92-30150
Turbulence modeling: Near-wall turbulence and effects of rotation on turbulence p 3452 N92-30151
An experimental investigation of a low Reynolds number turbulent boundary layer subject to an adverse pressure gradient p 3453 N92-30153
An experimental study of the effects of rapid rotation on turbulence p 3453 N92-30154
An experimental study of secondary vortex structure in mixing layers p 3453 N92-30155
Development of renormalization group analysis of turbulence p 3453 N92-30156
Short-time Lyapunov exponent analysis
p 3453 N92-30157
Organized motions underlying turbulent shear flows
p 3453 N92-30158
Turbulence dynamics in the wavelet representation
p 3454 N92-30159
Direct simulation of turbulent combustion
p 3454 N92-30160
Transition to turbulence in hypersonic flow
p 3454 N92-30161
Turbulent transport in the solar nebula
p 3454 N92-30163
A numerical method for prediction of compressible turbulent flows with closure models
p 3454 N92-30164
Incompressible spatially-developing free-shear flows
p 3454 N92-30165
The large-scale structures in turbulent plane Couette flow p 3455 N92-30167
Turbulent thermal convection in a differentially rotating channel p 3455 N92-30168
Patterns in simulated turbulent channel flow
p 3455 N92-30169

TURBULENT JETS
On transient flamelets and their relationship to turbulent methane-air jet flames
[DE92-006705] p 3419 N92-29943

TURBULENT MIXING
An experimental study of secondary vortex structure in mixing layers p 3453 N92-30155

TURBULENT WAKES
Explicit Navier-Stokes computation of turbomachinery flows
[AD-A248458] p 3445 N92-29933

TWO BODY PROBLEM
Solution of two-body relativistic bound state equations with confining plus Coulomb interactions
p 3547 N92-30003
Effects of retardation in relativistic equations with confining interaction p 3547 N92-30005

TWO DIMENSIONAL FLOW
A theoretical approach for analyzing the restabilization of wakes
[NASA-TM-103858] p 3443 N92-29394
Spatial and temporal adaptive procedures for the unsteady aerodynamic analysis of airfoils using unstructured meshes
[NASA-TM-107635] p 3400 N92-29445
Matched asymptotic expansions solution for low-frequency sound radiation from fluid-loaded, baffled plates: Two-dimensional case
[REPT-91-62] p 3543 N92-29748
The 2D-computation of an axial fan with FINFLO
[PB92-180678] p 3447 N92-30023
Direct numerical simulation of instability and noise generation of hot jets p 3451 N92-30066
Modeling of compressible turbulence
p 3452 N92-30150
Incompressible spatially-developing free-shear flows
p 3454 N92-30165
A numerical method for direct simulation of turbulence in complex geometries p 3455 N92-30166
Patterns in simulated turbulent channel flow
p 3455 N92-30169

TWO DIMENSIONAL MODELS
Finite-rate diffusion-controlled reaction in a vortex
[PB92-172006] p 3418 N92-29744
On the two-dimensional model of quantum Regge gravity
[DE92-624516] p 3560 N92-30212

TWO PHASE FLOW
Structure of a methanol/air coaxial reacting spray near the stabilization region by OH fluorescence imaging and two-component phase-Doppler interferometry
[DE92-005328] p 3417 N92-29431
Forces on a pipe bend resulting from clearing a pool of liquid upstream
[DE92-004179] p 3445 N92-29784
Continuum approaches for describing solid-gas and solid-liquid flow
[DE92-013601] p 3452 N92-30140

U

UH-60A HELICOPTER
Test and evaluation report of the physio control defibrillator/monitor model LIFEPAK (trademark) 8
[AD-A248283] p 3510 N92-29347
Test and evaluation report of the IMED volumetric infusion pump model 960A
[AD-A248538] p 3404 N92-29506

ULLAGE
National Launch System cycle 1 loads and models data book
[NASA-TM-103560] p 3408 N92-30215

ULTRASONIC TESTS
Nondestructive inspection perspectives
p 3481 N92-30121

ULTRASONICS
Survey of research into electromagnetic and other wave effects on mechanical behavior and processing of materials
[AD-A248614] p 3426 N92-29905

ULTRAVIOLET LASERS
Remote detection of biological particles and chemical plumes using UV fluorescence lidar
p 3465 N92-29279

UNDERWATER ACOUSTICS
Finite difference modelling of seismic wave propagation at the seafloor
[AD-A248345] p 3505 N92-29562
Active structural acoustic control and smart structures
[AD-A248341] p 3543 N92-29588

UNDERWATER OPTICS
SeaWiFS technical report series. Volume 5: Ocean optics protocols for SeaWiFS validation
[NASA-TM-104566] p 3506 N92-30193

UNDERWATER VEHICLES
Incorporation of GPS/INS into small autonomous underwater vehicle navigation
[AD-A248884] p 3403 N92-29906

UNIFIED FIELD THEORY
Theory of elementary particles studies in weak interaction and grand unification and studies in accelerator design
[DE92-014309] p 3550 N92-29532

UNITED STATES
Current information technology resource requirements of the Federal Government: Fiscal year 1992
[PB92-147180] p 3561 N92-29663
Environmental quality: Report of the Council on Environmental Quality
[PB92-154954] p 3494 N92-29698
Lexicon of new formal geologic names of the United States, 1981-1985
[PB92-181320] p 3563 N92-30040

UNIVERSE
Reconstruction of density and potential fields of the Universe p 3565 N92-29834

UNIVERSITIES
Summary of technical operations, 1991 --- software development
[AD-A248153] p 3516 N92-29540

The 1991 Summer Faculty Research Program (SFRP), volume 2
[AD-A248764] p 3571 N92-29724

UNIVERSITY PROGRAM

The 1991 Summer Faculty Research Program (SFRP), volume 2
[AD-A248764] p 3571 N92-29724
The 1991 Summer Faculty Research Program (SFRP), volume 3
[AD-A248765] p 3571 N92-29725

UNSTEADY AERODYNAMICS

Spatial and temporal adaptive procedures for the unsteady aerodynamic analysis of airfoils using unstructured meshes
[NASA-TM-107635] p 3400 N92-29445
Experimental investigation of the flowfield of an oscillating airfoil
[NASA-TM-105675] p 3402 N92-30182

UNSTEADY FLOW

Production of periodical Mach number variations in high subsonic flow in a blow down wind tunnel, and its influence on profile measurements
[ETN-92-91492] p 3401 N92-29889

UPPER ATMOSPHERE

Support activities to maintain SUMS flight readiness
[NASA-CR-189656-VOL-1] p 3410 N92-30217
Support activities to maintain SUMS flight readiness, volume 2. Attachment A: Flight 61-C report
[NASA-CR-189656-VOL-2] p 3411 N92-30218
Support activities to maintain SUMS flight readiness, volume 3. Attachment B: Flight STS-35 report, section A
[NASA-CR-189656-VOL-3] p 3411 N92-30219
Support activities to maintain SUMS flight readiness, volume 4. Attachment B: Flight STS-35 report, section B
[NASA-CR-189656-VOL-4] p 3411 N92-30220
Support activities to maintain SUMS flight readiness, volume 5. Attachment B: Flight STS-35 report, section C
[NASA-CR-189656-VOL-5] p 3411 N92-30221
Support activities to maintain SUMS flight readiness, volume 6. Attachment B: Flight STS-35 report, section D
[NASA-CR-189656-VOL-6] p 3411 N92-30222
Support activities to maintain SUMS flight readiness, volume 7. Attachment B: Flight STS-35 report, section E
[NASA-CR-189656-VOL-7] p 3412 N92-30223
Support activities to maintain SUMS flight readiness, volume 8. Attachment B: Flight STS-35 report, section F
[NASA-CR-189656-VOL-8] p 3412 N92-30224
Support activities to maintain SUMS flight readiness, volume 9. Attachment C: Flight STS-40 report. Attachment D: SUMS software listing
[NASA-CR-189656-VOL-9] p 3412 N92-30225

UPSTREAM

Forces on a pipe bend resulting from clearing a pool of liquid upstream
[DE92-004179] p 3445 N92-29784

URANIUM 238

Relativistic Coulomb fission p 3548 N92-30008

URANUS (PLANET)

Source location determination of Uranian kilometric radiation from ray tracing and emission lobe modelling
[NASA-CR-190482] p 3570 N92-29360

URBAN PLANNING

TERS product development plan for urban planning of Bandung, Indonesia
[BCRS-91-30] p 3491 N92-30231

USER MANUALS (COMPUTER PROGRAMS)

Alexander: User guide (version 1.0)
[BCRS-90-38] p 3489 N92-29494
NASA visual thesaurus maintenance documentation
[NASA-CR-190282] p 3561 N92-29553
The twopnt program for boundary value problems: Version 3.10 of March 1992
[DE92-013394] p 3517 N92-29641
User's manual for the NIST TTCN translator, version 3.0
[PB92-172493] p 3518 N92-29745
Decomposer: Program documentation
[USIP-91-04] p 3519 N92-29780
ESATAN user manual
[ESA-PSS-03-105-ISSUE-2] p 3521 N92-29869
Human exposure model-2: User's guide
[PB92-186246] p 3495 N92-30200
Users manual for updated computer code for axial-flow compressor conceptual design
[NASA-CR-189171] p 3524 N92-30207

V

VACUUM

Sample positioning in microgravity
[NASA-CASE-NPO-18448-1-CU] p 3428 N92-30083

VACUUM MELTING

Metal vapor plasma behavior during vacuum arc remelting of alloy 718
[DE92-011761] p 3421 N92-29623

VACUUM SPECTROSCOPY

Design and construction of a channel electron multiplier based Mossbauer spectroscopy system
[AD-A248154] p 3439 N92-29443

VACUUM SYSTEMS

RF vacuum electronics
[AD-A248857] p 3442 N92-29935

VADOSE WATER

Field study of multidimensional flow and transport in the vadose zone
[PB92-161363] p 3489 N92-29701

VALENCE

Zee star analysis
[AD-A248342] p 3417 N92-29423

VALVES

Check valve with poppet damping mechanism
[NASA-CASE-MSC-21903-1] p 3480 N92-30101

VAPOR DEPOSITION

A novel approach to silicon-on-insulator materials
[AD-A248074] p 3424 N92-29466
Raman features of CVD diamond films
[DE92-011381] p 3426 N92-29908
Evaluation of aluminum ion vapor deposition as a replacement for cadmium electroplating at Anniston Army Depot
[AD-A250063] p 3423 N92-29940

VAPOR PHASE EPITAXY

OMVPE growth of InAsSbBi and related alloys using new organometallic group 5 sources
[AD-A250631] p 3557 N92-29635

VAPOR PHASES

A generalized polynomial form of the objective function in flash calculations
[AD-A248160] p 3531 N92-29446
Laser processing for interconnect technology
[AD-A248103] p 3476 N92-29559

VARIABLE CYCLE ENGINES

A preliminary design and analysis of an advanced heat-rejection system for an extreme altitude advanced variable cycle diesel engine installed in a high-altitude advanced research platform
[NASA-CR-186021] p 3405 N92-29427

VARIATIONAL PRINCIPLES

A consistent shear deformable theory for laminated plates
[AD-A250591] p 3415 N92-29593
Variational formulation and finite element implementation of Pagano's theory of laminated plates
[AD-A250592] p 3415 N92-29594
Monopolar vortices as relative equilibria and their dissipative decay
[MEMO-1015] p 3446 N92-29977

VARIATIONS

Examination of the main error factors with regards to secondary losses in compression and turbine cascades by variations of the blade picture ratio
[ETN-92-91493] p 3405 N92-29927

VAX COMPUTERS

An object-based interviewing system
[DE92-013422] p 3527 N92-29504

VECTOR PROCESSING (COMPUTERS)

Numerical methods for the 3D shallow water equations on vector and parallel computers
[CWI-NM-R9109] p 3446 N92-29944

VECTOR QUANTIZATION

Real-time quadratic shading
[CWI-CS-R9123] p 3534 N92-29892

VECTOR SPACES

Extremally disconnected spaces, subspaces and retractions
[REPT-91-38] p 3535 N92-29920
Real space process algebra
[CWI-CW-R9131] p 3538 N92-30178

VEGETATION

Air quality criteria for oxides of nitrogen, volume 2
[PB92-176379] p 3493 N92-29521

VEGETATION GROWTH

Monitoring of grass dominance on Dutch heathlands using remote sensing and a geographic information system (HEIMON)
[BCRS-91-12] p 3489 N92-29693
Mapping agroecological zones and time lag in vegetation growth by means of Fourier analysis of time series of NDVI images
[REPT-32] p 3490 N92-29717

VEGETATIVE INDEX

Mapping agroecological zones and time lag in vegetation growth by means of Fourier analysis of time series of NDVI images
[REPT-32] p 3490 N92-29717
A spectral vegetation radiometer for airborne boundary-layer research
[PB92-186113] p 3491 N92-30105

VELOCITY

CoMStOC 4: Multiwaveband observations of sunspot and plage-associated coronal emission
[AD-A248344] p 3570 N92-29632

VELOCITY DISTRIBUTION

Science goals and mission objectives of NASA's laser atmospheric wind sounder program
p 3468 N92-29296
Model for regional solute transport suited for calibration and management
[PB92-161371] p 3494 N92-29746
First order approximation to the average velocity of rise of bubbles in fluid not including inertial forces
[REPT-91-51] p 3444 N92-29763
The significance of large-scale flows into the Great Attractor p 3565 N92-29836
A preliminary experimental investigation of local isotropy in high-Reynolds-number turbulence
p 3447 N92-30042
Turbulence and vortex structures
p 3448 N92-30048
Vorticity matching in superfluid helium
p 3449 N92-30049

VELOCITY MEASUREMENT

Laboratory velocimeter measurements using the edge technique p 3463 N92-29269

VENTILATION FANS

Experimental examination of heavy loaded axial fans with rotational symmetrical distortion of the inflow
[ETN-92-91489] p 3445 N92-29926

VENUS (PLANET)

Occultation of a compact radio source by Venus
p 3429 N92-29366
Galileo early cruise, including Venus, first Earth, and Gaspra encounters p 3433 N92-29384
Venus in motion: An animated video catalog of Pioneer Venus Orbiter Cloud Photopolarimeter images
[NASA-CR-190543] p 3568 N92-29401

VENUS ATMOSPHERE

Occultation of a compact radio source by Venus
p 3429 N92-29366

VENUS SURFACE

Venus in motion: An animated video catalog of Pioneer Venus Orbiter Cloud Photopolarimeter images
[NASA-CR-190543] p 3568 N92-29401

VERTICAL DISTRIBUTION

The NDSC primary site at the Observatoire de Haute-Provence: Ozone and aerosols observations (1986-1992) p 3458 N92-29240
Lidar observations of the Pinatubo volcanic cloud over Hampton, Virginia p 3461 N92-29254

VERTICAL MOTION

Measurements of wind divergence with volume imaging lidar p 3464 N92-29272

VERY LARGE SCALE INTEGRATION

Experimental evaluation of incorporating digital and analog integrated circuit die on a common substrate utilizing silicon-hybrid wafer-scale integration technology
[AD-A248182] p 3439 N92-29405
Using custom-designed VLSI fuzzy inferencing chips for the autonomous navigation of a mobile robot
[DE92-000424] p 3528 N92-29550
Nonvolatile programmable neural network synaptic array
[NASA-CASE-NPO-18578-1-CU] p 3442 N92-30086

VERY LONG BASE INTERFEROMETRY

A determination of the radio-planetary frame tie from comparison of Earth orientation parameters
p 3409 N92-29365
A nanoradian differential VLBI tracking demonstration
p 3430 N92-29367

VIBRATION

A study of the adsorption of acetonitrile on a gold electrode from aqueous solutions using in situ vibrational spectroscopy
[AD-A250191] p 3417 N92-29514
Accelerometer method and apparatus for integral display and control functions
[NASA-CASE-MSC-21961-1] p 3474 N92-29952

VIBRATIONAL SPECTRA

Vibrational spectrum and structure of 1,2-dimethyl-1,2-disila-closo-dodecaborane
[AD-A250235] p 3419 N92-29941

VIBRATIONAL STRESS

A consistent shear deformable theory for laminated plates
[AD-A250591] p 3415 N92-29593

VIDEO DATA

FM video data link spectrum spreading
[AD-D015257] p 3435 N92-29572

VIDEO SIGNALS

Motion restoration of long time exposed images with satellite-borne cameras
[ETN-92-91490] p 3474 N92-29731

VIEWING
Polarization perception device
[NASA-CASE-MSC-21915-1] p 3552 N92-30027
VINYL COPOLYMERS
Molecular engineering of liquid crystalline polymers by living polymerization. 20: Synthesis and characterization of binary copolymers of 11-(4-cyano-4'-biphenyl) oxy)undecanyl vinyl ether with n-butyl vinyl ether and of 2-(4-cyano-4'-biphenyl) oxy)ethyl vinyl ether with n-butyl vinyl ether
[AD-A248286] p 3425 N92-29566
VINYL POLYMERS
Structural rearrangements during mesomorphic phase transitions in poly(10-((4-cyano-4' biphenyl)oxy)decanyl vinyl ether)
[AD-A248306] p 3425 N92-29569
VISCOSITY
Structure and shear response of lipid monolayers
[DE92-011633] p 3542 N92-29354
Viscous profiles and numerical methods for shock waves
[AD-A246110] p 3443 N92-29458
Vorticity matching in superfluid helium
p 3449 N92-30049
VISCOUS FLOW
Modeling and computational analysis of multiscale phenomena in fluid-structure interaction problems
[AD-A248723] p 3444 N92-29721
The 2D-computation of an axial fan with FINFLO
[PB92-180678] p 3447 N92-30023
Near-wall turbulence modeling for boundary layers with separation p 3449 N92-30052
VISIBILITY
Transport delay measurements: Methodology and analysis for the F-16C combat engagement trainer, the display for advanced research and training, and the F-16A limited field of view
[AD-A248519] p 3406 N92-29505
VISION
Controlling the flow of visual information through the lateral geniculate nucleus: From single cells to neural networks
[AD-A250578] p 3528 N92-29590
VISUAL ACUITY
Visual acuity with second and third generation night vision goggles obtained from a new method of night sky simulation across a wide range of target contrast
[AD-A248284] p 3512 N92-29348
VISUAL DISCRIMINATION
Object discrimination based on depth-from-occlusion
[AD-A248104] p 3511 N92-29560
VISUAL PERCEPTION
Object discrimination based on depth-from-occlusion
[AD-A248104] p 3511 N92-29560
Controlling the flow of visual information through the lateral geniculate nucleus: From single cells to neural networks
[AD-A250578] p 3528 N92-29590
Visual pattern completion
[PB92-187418] p 3524 N92-30195
VISUAL STIMULI
Effects of ionizing radiation on auditory and visual thresholds
[AD-A248199] p 3507 N92-29410
VOICE COMMUNICATION
Improving the LAMP Mk 3 SH-60B HF communication system
[AD-A245970] p 3429 N92-29344
VOLATILITY
Origin and evolution of planetary atmospheres
[NASA-CR-190579] p 3568 N92-29432
VOLCANOES
Sixteenth International Laser Radar Conference, part 1
[NASA-CP-3158-PT-1] p 3456 N92-29228
Long term stratospheric aerosol lidar measurements in Kyushu p 3456 N92-29229
Southern Hemisphere lidar measurements of the aerosol clouds from Mt. Pinatubo and Mt. Hudson
p 3456 N92-29230
Stratospheric backscatter, extinction, and lidar ratio profiling after the Mt. Pinatubo eruptions
p 3456 N92-29231
Measurements of stratospheric Pinatubo aerosol extinction profiles by a Raman lidar
p 3457 N92-29232
Raman lidar measurements of Pinatubo aerosols over southeastern Kansas during November-December 1991
p 3457 N92-29233
Lidar observations of stratospheric aerosol layer after the Mt. Pinatubo volcanic eruption p 3457 N92-29234
Interpretation of DIAL measurements of lower stratospheric ozone in regions with Pinatubo aerosols
p 3457 N92-29236
A new Raman DIAL technique for measuring stratospheric ozone in the presence of volcanic aerosols
p 3458 N92-29238
Observations of ozone-aerosol correlated behaviour in the lower stratosphere during the EASOE campaign
p 3459 N92-29243
Airborne lidar observations of the stratosphere after the Pinatubo eruption p 3460 N92-29248
Three-wavelength lidar measurements of Pinatubo aerosol and its optical properties p 3460 N92-29250
Lidar observations of the Pinatubo stratospheric aerosol cloud over Frascati, Italy p 3460 N92-29251
L625 lidar measurements of Pinatubo volcanic cloud at Hefei p 3460 N92-29252
Two wavelength measurements of the Pinatubo aerosol above Toronto, Canada p 3461 N92-29253
Lidar observations of the Pinatubo volcanic cloud over Hampton, Virginia p 3461 N92-29254
Wind measurements from 15 to 50 km with a Doppler Rayleigh lidar p 3472 N92-29319
VOLCANOLOGY
Lidar observations of stratospheric clouds after volcanic eruption of Pinatubo p 3468 N92-29294
VORTEX BREAKDOWN
A numerical method for prediction of compressible turbulent flows with closure models
p 3454 N92-30164
VORTEX FILAMENTS
Vorticity matching in superfluid helium
p 3449 N92-30049
VORTEX SHEDDING
A theoretical approach for analyzing the restabilization of wakes
[NASA-TM-103858] p 3443 N92-29394
VORTEX SHEETS
A method for computing the 3-dimensional flow about wings with leading-edge vortex separation. Part 2: Description of computer program VORSEP
[NLR-TR-86006-U] p 3402 N92-29916
VORTICES
Lidar measurements of aerosol and ozone distributions during the 1992 Airborne Arctic Stratospheric Expedition
p 3469 N92-29304
A linear eddy sub-grid model for turbulent reacting flows: Application to hydrogen-air combustion
[DE92-006699] p 3417 N92-29433
Streamwise vortices in heated boundary layers
[NASA-CR-189661] p 3444 N92-29692
Finite-rate diffusion-controlled reaction in a vortex
[PB92-172006] p 3418 N92-29744
Explicit Navier-Stokes computation of turbomachinery flows
[AD-A248458] p 3445 N92-29933
A finite volume approach to large eddy simulation of compressible, homogeneous, isotropic, decaying turbulence
[MEMO-1009] p 3446 N92-29972
Monopolar vortices as relative equilibria and their dissipative decay
[MEMO-1015] p 3446 N92-29977
Annual research briefs, 1991
[NASA-CR-189967] p 3447 N92-30041
Local isotropy in buoyancy-generated turbulence
p 3447 N92-30043
On small scale vortices in turbulent flows
p 3448 N92-30045
Turbulence and vortex structures
p 3448 N92-30048
On dynamic models for large eddy simulation
p 3450 N92-30056
Large eddy simulations of passive and buoyant scalars with dynamic subgrid-scale models
p 3450 N92-30057
Dynamic subgrid-scale modeling of compressible turbulence p 3450 N92-30058
Progress toward identification of streamwise vorticity meander in a plane mixing layer p 3451 N92-30068
Streaks in turbulent boundary layers
p 3451 N92-30069
An experimental study of the effects of rapid rotation on turbulence p 3453 N92-30154
An experimental study of secondary vortex structure in mixing layers p 3453 N92-30155
Incompressible spatially-developing free-shear flows
p 3454 N92-30165
The large-scale structures in turbulent plane Couette flow p 3455 N92-30167
Crossflow effects on the growth rate of inviscid Goertler vortices in a hypersonic boundary layer
[NASA-CR-189667] p 3455 N92-30190
VORTICITY
Monopolar vortices as relative equilibria and their dissipative decay
[MEMO-1015] p 3446 N92-29977
On small scale vortices in turbulent flows
p 3448 N92-30045
Vorticity matching in superfluid helium
p 3449 N92-30049
Single point modeling of initially isotropic turbulence under uniform rotation p 3449 N92-30054
Progress toward identification of streamwise vorticity meander in a plane mixing layer p 3451 N92-30068
Streaks in turbulent boundary layers
p 3451 N92-30069
An experimental study of scalar mixing in curved shear layers p 3453 N92-30152
VULNERABILITY
Surface reactions in the space environment
[AD-A250624] p 3428 N92-29428
An overview of computer viruses in a research environment
[NASA-CR-190528] p 3517 N92-29630

W

WAFERS
Monolithic integration of semiconductor and superconductor components
[AD-A245351] p 3557 N92-29583
WAKES
A theoretical approach for analyzing the restabilization of wakes
[NASA-TM-103858] p 3443 N92-29394
WALL FLOW
Streamwise vortices in heated boundary layers
[NASA-CR-189661] p 3444 N92-29692
Evaluation of measured-boundary-condition methods for 3D subsonic wall interference
[NLR-TR-88072-U] p 3401 N92-29884
Theoretical and experimental aspects of velocity slip by flows along solid walls
[ISBN-3-7983-1446-2] p 3446 N92-29968
Effect of walls on the supersonic reacting mixing layer
p 3451 N92-30065
Turbulence modeling: Near-wall turbulence and effects of rotation on turbulence p 3452 N92-30151
Organized motions underlying turbulent shear flows
p 3453 N92-30158
WALLS
A preliminary experimental investigation of local isotropy in high-Reynolds-number turbulence
p 3447 N92-30042
WARNING SYSTEMS
On the optimization of windshear warning and guidance systems
[NLR-TP-90196-U] p 3402 N92-29703
Smart BIT/TSMD integration
[AD-A247192] p 3442 N92-29914
WASTE ENERGY UTILIZATION
Process of ferrochromium now and in the future
[DE92-506510] p 3421 N92-29637
WASTE HEAT
Process of ferrochromium now and in the future
[DE92-506510] p 3421 N92-29637
WASTE TREATMENT
Corrosion resistance of stainless steels and high Ni-Cr alloys to acid fluoride wastes
[DE92-012338] p 3420 N92-29436
WASTES
Electrochemical array sensors for plating waste stream monitoring
[DE92-011446] p 3495 N92-30211
WATER
Cursory examination of the zeta potential behaviors of two optical materials
[DE92-011588] p 3551 N92-29578
WATER COLOR
SeaWiFS technical report series. Volume 1: An overview of SeaWiFS and ocean color
[NASA-TM-104566-VOL-1] p 3505 N92-29686
WATER FLOW
Field study of multidimensional flow and transport in the vadose zone
[PB92-161363] p 3489 N92-29701
Forces on a pipe bend resulting from clearing a pool of liquid upstream
[DE92-004179] p 3445 N92-29784
WATER INJECTION
Contingency power for a small turboshaft engine by using water injection into turbine cooling air
[NASA-TM-105680] p 3405 N92-29661
WATER LOSS
Mapping of groundwater losses by evaporation in the western desert of Egypt
[BCRS-91-01] p 3489 N92-29495
WATER POLLUTION
Laser remote sensing of pollution on water surfaces
p 3467 N92-29290
WATER QUALITY
Mosquito Lagoon environmental resources inventory
[NASA-TM-107548] p 3492 N92-29430

WATER TUNNEL TESTS
An experimental study of scalar mixing in curved shear layers p 3453 N92-30152
WATER VAPOR
Detecting microwave emissions from terrestrial sources: A feasibility study
[AD-A248557] p 3435 N92-29579
LAPS specific humidity analysis
[PB92-163575] p 3502 N92-29799
WAVE DIFFRACTION
Diffraction of light from randomly rough surfaces
[AD-A250261] p 3551 N92-29546
Finite difference modelling of seismic wave propagation at the seafloor
[AD-A248345] p 3505 N92-29562
WAVE DISPERSION
Finite difference modelling of seismic wave propagation at the seafloor
[AD-A248345] p 3505 N92-29562
WAVE EQUATIONS
User's guide for the VTRPE (Variable Terrain Radio Parabolic Equation) computer model
[AD-A248112] p 3433 N92-29395
Finite difference modelling of seismic wave propagation at the seafloor
[AD-A248345] p 3505 N92-29562
A study of shock-associated magnetohydrodynamic waves in the solar wind
[NASA-CR-190567] p 3569 N92-29631
The Green Function Cellular Method and its relation to multiple scattering theory
[DE92-011470] p 3436 N92-29909
Energy propagation in dissipative systems. Part 2: Centrovelocity for nonlinear wave equations
[MEMO-1016-PT-2] p 3437 N92-29978
WAVE FRONTS
Image inversion analysis of the HST OTA (Hubble Space Telescope Optical Telescope Assembly), phase A
[NASA-CR-190483] p 3564 N92-29359
WAVE FUNCTIONS
The extended Bethe Ansatz for infinite S = 1/2 quantum spin chains with non-nearest-neighbor interaction
[DE92-622378] p 3533 N92-29793
WAVE PROPAGATION
Asymptotic and numerical methods in applied wave propagation
[AD-A250227] p 3543 N92-29543
Finite difference modelling of seismic wave propagation at the seafloor
[AD-A248345] p 3505 N92-29562
Realistic models for predicting sound propagation in flow duct systems
[ISVR-TR-204] p 3544 N92-29814
Transport processes in beamed energy propulsion systems
[AD-A247296] p 3413 N92-29913
Effect of walls on the supersonic reacting mixing layer p 3451 N92-30065
WAVEGUIDE ANTENNAS
Optimizing the G/T ratio of the DSS-13 34-meter beam-waveguide antenna p 3431 N92-29377
WAVEGUIDES
Improvements in X-band transmitter phase stability through klystron body temperature regulation p 3431 N92-29373
Detecting microwave emissions from terrestrial sources: A feasibility study
[AD-A248557] p 3435 N92-29579
WAVELENGTHS
The global backscatter experiment airborne pulsed lidar measurements p 3459 N92-29246
Multi-wavelength airborne lidar intercomparisons of aerosol and cirrus backscatter over the Pacific Ocean p 3460 N92-29247
Multi-wavelength measurements of the stratospheric aerosol layer made at Hampton, Virginia (37N, 76W) p 3460 N92-29249
Two wavelength measurements of the Pinatubo aerosol above Toronto, Canada p 3461 N92-29253
WEAK INTERACTIONS (FIELD THEORY)
Hydrogen desorption and the search for the Higgs
[DE92-013464] p 3545 N92-29507
Theory of elementary particles studies in weak interaction and grand unification and studies in accelerator design
[DE92-014309] p 3550 N92-29532
Classical aspects of weak interactions
[NIKHEF-H/91-25] p 3546 N92-29751
WEAPONS
Contracting in the software engineering crisis
[AD-A250241] p 3516 N92-29544
WEAR RESISTANCE
Rolling-contact and wear resistance of hard coatings on bearing-steel substrates
[DE92-011834] p 3478 N92-29357
Micromechanisms of cyclic and environmentally-assisted subcritical crack growth in ceramic-matrix composites
[AD-A248067] p 3414 N92-29556
WEATHER
Tapering clouds and their classification due mainly to the surrounding cloud pattern in the GMS imagery
[ISSN-0388-9653] p 3502 N92-29666
NOAA environmental digest: Selected indicators of the United States and the global environment, December 1991
[PB92-185073] p 3494 N92-30019
WEATHER FORECASTING
Monthly means of selected climate variables for 1985 - 1989
[NASA-TM-104565] p 3502 N92-29653
Tropical cyclones: Central North Pacific, 1991
[PB92-167345] p 3502 N92-29743
LAPS specific humidity analysis
[PB92-163575] p 3502 N92-29799
Proceedings of the 16th Annual Climate Diagnostics Workshop
[PB92-167378] p 3503 N92-29801
WEIGHTLESSNESS
Logion: The operation of liquid metal ion emitters under weightlessness
[OEFZS-4616] p 3428 N92-29470
WHALES
Application of remote sensing methods for tracking large cetaceans: North Atlantic right whales Eubalaena Glacialis
[PB92-185016] p 3490 N92-30022
WHISKER COMPOSITES
Effect of whisker orientation on the mechanical properties of silicon carbide/alumina composites
[AD-A248737] p 3415 N92-29723
WHITE NOISE
Signal quality influence on averaging procedure for DIAL pollution monitoring p 3465 N92-29280
Figure of merit for direct-detection optical channels p 3431 N92-29376
Statistics of narrowband white noise derived from clipped broadband white noise
[AD-A248597] p 3434 N92-29563
WIENER HOPF EQUATIONS
An exact turbulent closure for the hydromagnetic dynamo p 3452 N92-30071
WIND (METEOROLOGY)
The Laser Atmospheric Wind Sounder (LAWS) preliminary error budget and performance estimate p 3462 N92-29262
Laboratory velocimeter measurements using the edge technique p 3463 N92-29269
Science goals and mission objectives of NASA's laser atmospheric wind sounder program p 3468 N92-29296
The Laser Atmospheric Wind Sounder (LAWS) phase 2 preliminary system design p 3468 N92-29297
The Laser Atmospheric Wind Sounder (LAWS) phase 2 preliminary laser design p 3468 N92-29298
GE's mobile, coherent Doppler lidar test/evaluation facilities p 3407 N92-29299
The e-beam sustained laser technology for space-based Doppler wind lidar p 3469 N92-29300
Sodium Doppler temperature lidar observations of the mesopause region temperature and wind structure p 3471 N92-29314
Intercomparison of global marine climatologies
[DE92-011389] p 3494 N92-29790
WIND DIRECTION
Preliminary analysis of wind data from the Oak Ridge site survey
[PB92-174564] p 3503 N92-30034
Diurnal forcing of planetary atmospheres
[NASA-CR-190262] p 3569 N92-30199
WIND MEASUREMENT
The Laser Atmospheric Wind Sounder (LAWS) preliminary error budget and performance estimate p 3462 N92-29262
Laboratory velocimeter measurements using the edge technique p 3463 N92-29269
Identification of critical design points for the EAP of a space-based Doppler lidar wind sounder p 3463 N92-29270
Wind profiles derived from volume imaging lidar data: Enhancements to the algorithm and comparisons with insitu observations p 3464 N92-29271
Correlation analysis of wind lidar data p 3467 N92-29291
Science goals and mission objectives of NASA's laser atmospheric wind sounder program p 3468 N92-29296
The e-beam sustained laser technology for space-based Doppler wind lidar p 3469 N92-29300
Error analysis of wind measurements for the University of Illinois sodium Doppler temperature system p 3471 N92-29313
Wind measurements from 15 to 50 km with a Doppler Rayleigh lidar p 3472 N92-29319
NWP impact of cloud top and boundary layer winds from a satellite borne lidar: An observing system simulation experiment p 3473 N92-29328
On the optimization of windshear warning and guidance systems
[NLR-TP-90196-U] p 3402 N92-29703
Preliminary analysis of wind data from the Oak Ridge site survey
[PB92-174564] p 3503 N92-30034
WIND PRESSURE
Occultation of a compact radio source by Venus p 3429 N92-29366
WIND PROFILES
GLObal Backscatter Experiment (GLOBE) results: Aerosol backscatter global distribution and wavelength dependence p 3459 N92-29245
The Laser Atmospheric Wind Sounder (LAWS) preliminary error budget and performance estimate p 3462 N92-29262
Identification of critical design points for the EAP of a space-based Doppler lidar wind sounder p 3463 N92-29270
Wind profiles derived from volume imaging lidar data: Enhancements to the algorithm and comparisons with insitu observations p 3464 N92-29271
Measurements of wind divergence with volume imaging lidar p 3464 N92-29272
Science goals and mission objectives of NASA's laser atmospheric wind sounder program p 3468 N92-29296
The Laser Atmospheric Wind Sounder (LAWS) phase 2 preliminary system design p 3468 N92-29297
The Laser Atmospheric Wind Sounder (LAWS) phase 2 preliminary laser design p 3468 N92-29298
GE's mobile, coherent Doppler lidar test/evaluation facilities p 3407 N92-29299
WIND SHEAR
Sensitivity of C2 sub n to random variations of windspeed, sensible heat flux, and latent heat flux
[AD-A248696] p 3502 N92-29565
On the optimization of windshear warning and guidance systems
[NLR-TP-90196-U] p 3402 N92-29703
Diurnal forcing of planetary atmospheres
[NASA-CR-190262] p 3569 N92-30199
WIND TUNNEL APPARATUS
Study of optical techniques for the Ames unitary wind tunnels. Part 3: Angle of attack
[NASA-CR-190541] p 3406 N92-29655
WIND TUNNEL TESTS
Shock enhancement and control of hypersonic combustion
[AD-A248558] p 3418 N92-29580
Evaluation of measured-boundary-condition methods for 3D subsonic wall interference
[NLR-TR-88072-U] p 3401 N92-29884
An experimental investigation of a low Reynolds number turbulent boundary layer subject to an adverse pressure gradient p 3453 N92-30153
An experimental study of secondary vortex structure in mixing layers p 3453 N92-30155
WIND TUNNEL WALLS
Evaluation of measured-boundary-condition methods for 3D subsonic wall interference
[NLR-TR-88072-U] p 3401 N92-29884
WIND TUNNELS
Buffet test in the National Transonic Facility
[NASA-CR-189595] p 3406 N92-29352
WIND VELOCITY
Correlation analysis of wind lidar data p 3467 N92-29291
Science goals and mission objectives of NASA's laser atmospheric wind sounder program p 3468 N92-29296
Sensitivity of C2 sub n to random variations of windspeed, sensible heat flux, and latent heat flux
[AD-A248696] p 3502 N92-29565
Diurnal forcing of planetary atmospheres
[NASA-CR-190262] p 3569 N92-30199
WINGS
Determination of aerodynamic sensitivity coefficients for wings in transonic flow
[NASA-CR-190570] p 3401 N92-29657
Computation of three-dimensional effects on two dimensional wings
[NASA-CR-190576] p 3401 N92-29691
WINTER
A multi-wavelength ozone lidar for the EASOE experiment p 3462 N92-29260
Polarization lidar liquid cloud detection algorithm for winter mountain storms p 3472 N92-29323

WIRE WINDING
Robotic workcell for wire wrapping integrated circuits
[DE92-013999] p 3441 N92-29796
WORLD METEOROLOGICAL ORGANIZATION
CLICOM-news, issue 7 p 3503 N92-30171

X

X RAY ABSORPTION
The 20 element HgI2 energy dispersive x ray array detector system
[DE92-013356] p 3549 N92-29502
X RAY ANALYSIS
X ray study of interfacial interactions in highly milled Sn-Ge powders
[DE92-012518] p 3556 N92-29437
Constraints on the mass fluctuation spectrum from x ray observations of clusters of galaxies
p 3567 N92-29845
Nondestructive inspection perspectives
p 3481 N92-30121
X RAY APPARATUS
Condenser optics, partial coherence, and imaging for soft x ray projection lithography
[DE92-011762] p 3551 N92-29484
X RAY ASTRONOMY
Analysis of high energy x ray observations of long periodic pulsars
[ETN-92-91494] p 3564 N92-29468
Traces of the primordial structure in the universe
[MPE-227] p 3565 N92-29833
Studies of distant clusters of galaxies
p 3566 N92-29843
X ray cluster counts: What ROSAT should see
p 3567 N92-29847
The evolution of the x ray luminosity function of galaxy clusters p 3567 N92-29848
ROSAT: Early results p 3567 N92-29850
The x ray morphology of the relaxed cluster of galaxies A2256. 1: Evidence for a merger event
p 3568 N92-29851
The x ray morphology of the relaxed cluster of galaxies A2256. 2: Sources around the extended cluster emission
p 3568 N92-29852
X RAY DIFFRACTION
Structure and shear response of lipid monolayers
[DE92-011633] p 3542 N92-29354
X ray study of interfacial interactions in highly milled Sn-Ge powders
[DE92-012518] p 3556 N92-29437
Solid state structures of some Dithionoamido-18-crown-6 ligands
[AD-A248098] p 3556 N92-29558
Structure and stability of Al-Cu-Ru face-centered icosahedral alloys
[DE92-012550] p 3422 N92-29706
Amorphization by interdiffusion in metallic multilayers
[ETN-92-91743] p 3558 N92-29766
Layer-thickness variations and x ray diffraction patterns, a general treatment p 3558 N92-29767
Low-angle x ray diffraction study of solid state amorphization in a Ni/Ti multilayer p 3558 N92-29768
Amorphization along interfaces and grain boundaries in polycrystalline multilayers: An x ray diffraction study of Ni/Ti multilayers p 3558 N92-29769
Interdiffusion reactions in Ni/Ta multilayers studied by x ray diffraction p 3558 N92-29770
Amorphization and related effects in Ni/Ti multilayers studied by differential scanning calorimetry
p 3559 N92-29772
X RAY LASERS
Review of potential x ray laser applications in materials science and chemistry
[DE92-012254] p 3475 N92-29434
X ray laser research at the Nova laser
[DE92-012695] p 3476 N92-29472
Ion collision effects in hydrogen-like recombination x ray lasers
[DE92-013515] p 3476 N92-29509
The x ray laser coherence experiments in neon-like yttrium
[DE92-010714] p 3477 N92-29987
X RAY SOURCES
High Intensity Source Laboratory (HISL)
[DE92-011173] p 3549 N92-29457
The 20 element HgI2 energy dispersive x ray array detector system
[DE92-013356] p 3549 N92-29502
X ray cluster counts: What ROSAT should see
p 3567 N92-29847
Optical searches for ROSAT x ray cluster sources
p 3568 N92-29853
X RAY SPECTROSCOPY
X ray study of interfacial interactions in highly milled Sn-Ge powders
[DE92-012518] p 3556 N92-29437
X RAYS
Condenser optics, partial coherence, and imaging for soft x ray projection lithography
[DE92-011762] p 3551 N92-29484
The 20 element HgI2 energy dispersive x ray array detector system
[DE92-013356] p 3549 N92-29502
X ray streak camera diagnostics of picosecond laser-plasma interactions
[DE92-011371] p 3555 N92-29789
The evolution of the x ray luminosity function of galaxy clusters p 3567 N92-29848
The x ray morphology of the relaxed cluster of galaxies A2256. 2: Sources around the extended cluster emission
p 3568 N92-29852
XYLOSE
Flux-capacity relationships of Acinetobacter calcoaceticus enzymes during xylose oxidation
p 3508 N92-29739

Y

YAG LASERS
In vivo and in vitro chlorophyll-a and pheophytin-a concentration measurements by laser fluorometry
p 3468 N92-29295
Development of mesospheric sodium laser beacon for atmospheric adaptive optics p 3470 N92-29308
Active modelocking and phase stabilization of a cavity dumped diode pumped Nd:YAG mini-laser
[DE92-011946] p 3475 N92-29358
YAW
The effect of yaw cards on the pitching and yawing motion of symmetric projectiles
[AD-A250021] p 3406 N92-29449
Helicopter low-speed yaw control
[NASA-CASE-LAR-14219-1] p 3406 N92-30025
YIELD POINT
Fatigue crack growth in damage tolerant Al-Li sheet alloys
[NLR-TP-90107-U] p 3483 N92-29708
YTTRIUM
The x ray laser coherence experiments in neon-like yttrium
[DE92-010714] p 3477 N92-29987

Z

ZETA PINCH
Optical diagnostics on dense Z-pinch plasmas
[DE92-011228] p 3555 N92-29917
ZINC
Process of ferrochromium now and in the future
[DE92-506510] p 3421 N92-29637
ZIRCONIUM OXIDES
Electron microscopy study on zirconia and alumina ceramic powders synthesized by microwave plasma pyrolysis
[DE92-013385] p 3424 N92-29479

Typical Personal Author Index Listing

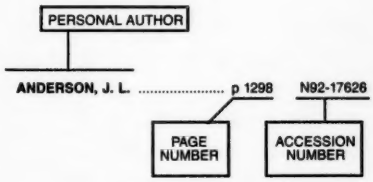

Listings in this index are arranged alphabetically by personal author. The page number helps you locate the citation in the abstract section. The accession number denotes the number by which the citation is identified.

A

AARTS, HARRY ..... p 3541 N92-30079
ABDELKARIM, M. H. ..... p 3489 N92-29495
ABHIRAMAN, A. S. ..... p 3416 N92-30137
ABO, MAKOTO ..... p 3457 N92-29232
p 3470 N92-29312
ABRESCH, RICHARD J. ..... p 3403 N92-29617
ABREU, VINCENT J. ..... p 3465 N92-29281
ACCARDI, DENISE ..... p 3408 N92-30016
ADAMS, FREDERICK C., JR. ..... p 3429 N92-29344
ADAN, I. J. B. F. ..... p 3539 N92-29606
ADAN, IVO JEAN-BAPTISTE FRANCOIS
p 3539 N92-29774
ADASCZIK, C. B. ..... p 3421 N92-29623
ADRIANI, ALBERTO ..... p 3460 N92-29251
AKINWANDE, T. ..... p 3442 N92-29935
AKKERMAN, G. J. ..... p 3537 N92-30177
AKSIT, MEHMET ..... p 3519 N92-29815
p 3521 N92-29961
p 3521 N92-29970
ALAM, M. ..... p 3426 N92-29908
ALBERS, WILLEM ..... p 3540 N92-29974
ALBERT, T. R. ..... p 3429 N92-29333
ALBRIDGE, ROYAL G. ..... p 3428 N92-29428
p 3407 N92-29664
ALDERS, G. J. ..... p 3512 N92-29871
ALESSI, C. A. ..... p 3506 N92-29805
ALHORN, D. C. ..... p 3429 N92-29677
ALPERT, YAKOV L. ..... p 3434 N92-29568
ALVAREZ, R. J., II ..... p 3461 N92-29255
AMENDT, P. ..... p 3554 N92-29531
AMYAY, OMAR ..... p 3436 N92-29730
ANCELLET, G. ..... p 3458 N92-29240
p 3459 N92-29244
p 3462 N92-29260
ANDERSON, KENT ..... p 3462 N92-29262
ANGEL, S. M. ..... p 3550 N92-29337
ANNIS, CHARLES ..... p 3420 N92-29408
ANSELL, HANS ..... p 3403 N92-30133
ANSMANN, ALBERT ..... p 3456 N92-29231
ANSTREICHER, KURT M. ..... p 3524 N92-30227
ANTILL, CHARLES W. ..... p 3462 N92-29264
ANTONIAK, Z. I. ..... p 3569 N92-29600
p 3492 N92-29646
ANTRAZI, SAMI S. ..... p 3528 N92-29656
APERS, PETER M. G. ..... p 3520 N92-29855
APITULEY, A. ..... p 3459 N92-29244
ARCH, D. ..... p 3442 N92-29935
ARCHULETA, F. L. ..... p 3464 N92-29275
AREY, B. W. ..... p 3420 N92-29411
ARIN, KEMAL ..... p 3485 N92-30112
ARMISTEAD, MICHAEL A. ..... p 3400 N92-29539
ARNAUD, K. A. ..... p 3567 N92-29844
ARNET, P. ..... p 3489 N92-29701
ARSHINOV, YU. F. ..... p 3467 N92-29293
ASAY, B. W. ..... p 3427 N92-29512
ASHBAUGH, NOEL E. ..... p 3414 N92-29453
ASHBY, C. I. H. ..... p 3477 N92-30135
ASHLEY, J. M. ..... p 3562 N92-29794
ASOH, TADASHI ..... p 3502 N92-29666
ASVELD, PETER R. J. ..... p 3537 N92-30075
ATKINSON, D. J. ..... p 3433 N92-29385
ATLURI, SATYA N. ..... p 3488 N92-30134
AU, P. A. ..... p 3409 N92-29383
AUSTIN, M. ..... p 3422 N92-29803
AUSTIN, ROSWELL W. ..... p 3506 N92-30193
AUTANT, C. ..... p 3532 N92-29573
AVRAMOVA, R. P. ..... p 3467 N92-29291
AYOUB, M. M. ..... p 3513 N92-29949
AZZALI, S. ..... p 3490 N92-29717

B

BAALS, ROBERT A. ..... p 3474 N92-30030
BABUSKA, I. ..... p 3541 N92-30174
BACHELET, D. ..... p 3494 N92-30018
BADDELEY, A. J. ..... p 3541 N92-30180
BAETEN, J. C. M. ..... p 3537 N92-30177
p 3538 N92-30178
BAGCHI, ARUNABHA ..... p 3540 N92-29856
BAHREN, JACOB ..... p 3530 N92-30085
BAKER, J. E. ..... p 3528 N92-29644
BAKER, KARL W. ..... p 3492 N92-29662
BAKER, WAYMAN E. ..... p 3468 N92-29296
BAKKER, R. R. ..... p 3530 N92-29983
p 3531 N92-30143
BAKSTEEN, J. ..... p 3507 N92-29736
BALAS, GARY J. ..... p 3406 N92-29654
BALDWIN, RICHARD S. ..... p 3413 N92-29667
BALLARD, R. ..... p 3506 N92-29397
BAMBERGER, J. A. ..... p 3569 N92-29600
BANDA, CAROLYN ..... p 3512 N92-29413
BANKS, P. ..... p 3490 N92-30088
BANNEHR, LUTZ ..... p 3491 N92-30105
BARGHOLTZ, C. ..... p 3546 N92-29715
BARLEY, M. ..... p 3410 N92-29480
BARLOW, R. S. ..... p 3419 N92-29943
BARNES, ALAN V. ..... p 3407 N92-29664
BARNES, H. L. ..... p 3417 N92-29551
BARNES, JOHN E. ..... p 3465 N92-29281
BARNES, TERENCE J. ..... p 3485 N92-30113
BARRERA, E. V. ..... p 3420 N92-29483
BARTELDS, G. ..... p 3402 N92-30129
BARTOS, R. D. ..... p 3432 N92-29378
BASTEN, M. A. ..... p 3477 N92-29937
BASTIAANSSEN, W. G. M. ..... p 3489 N92-29495
BATES, J. M. ..... p 3569 N92-29600
BATINA, JOHN T. ..... p 3400 N92-29445
BAUHAHN, P. ..... p 3442 N92-29935
BAULIN, E. V. ..... p 3468 N92-29295
BAUM, HOWARD R. ..... p 3418 N92-29744
BAUMAN, D. M. ..... p 3516 N92-29544
BAUMANN, FRANK ..... p 3437 N92-29984
BAUMANN, FRANK V. ..... p 3526 N92-29958
BAUTISTA, J. J. ..... p 3431 N92-29374
BAYSAL, OKTAY ..... p 3445 N92-29830
BEARDSLEY, R. C. ..... p 3506 N92-29805
BECK, PETER ..... p 3473 N92-29469
BEDDIN, ROBERT A ..... p 3413 N92-29913
BEEKMAN, WILLEM ..... p 3521 N92-29887
BEEKMANN, M. ..... p 3458 N92-29240
BELCHER, S. E. ..... p 3449 N92-30053
BELL, J. H. ..... p 3453 N92-30155
BELL, J. L. S. ..... p 3417 N92-29551
BELMESK, Z. ..... p 3532 N92-29573
BELZER, M. ..... p 3525 N92-29555
BENDALL, I. ..... p 3475 N92-29332
BENTS, D. J. ..... p 3414 N92-30187
BERCHTOLD, G. ..... p 3404 N92-29650
BERG, L. ..... p 3465 N92-29280
BERGER, THEODORE W. ..... p 3510 N92-29334
BERGMANS, LODEWIJK ..... p 3521 N92-29961
BERGSTRA, J. A. ..... p 3538 N92-30178
BERGWERFF, J. B. ..... p 3459 N92-29244
BERKHEISER, W. E., III ..... p 3551 N92-29530
BERMAN, A. L. ..... p 3409 N92-29383
BERNARDI, A. ..... p 3434 N92-29542
BESSIERE, P. ..... p 3525 N92-29610
BESSOT, D. ..... p 3441 N92-29613
BESWICK, C. A. ..... p 3433 N92-29385
BETHKE, KARL-HEINZ ..... p 3436 N92-29877
BEUTH, J. L., JR. ..... p 3484 N92-30111
BEUWER, WIM ..... p 3526 N92-29958
p 3437 N92-29984
BEYER, P. E. ..... p 3433 N92-29384
BEYER, RICHARD A. ..... p 3554 N92-29510
BIANCHINI, RON ..... p 3515 N92-29409
BIDDLE, DENNIS ..... p 3562 N92-29720
BIELE, JONATHAN ..... p 3538 N92-29501
BIESIADNY, THOMAS J. ..... p 3405 N92-29661
BIKA, D. ..... p 3420 N92-29483
BILLICA, LINDA W. ..... p 3479 N92-30026
BIRCKELBAW, L. D. ..... p 3400 N92-29625
BIRD, R. KEITH ..... p 3423 N92-30205
BIRKENHEUER, D. L. ..... p 3502 N92-29799
BISHOP, MATT ..... p 3517 N92-29630
BLACHER, RENE ..... p 3538 N92-29491
p 3538 N92-29492
BLADES, E. ..... p 3408 N92-30215
BLESIUS, L. ..... p 3489 N92-29494
BLOSSER, MAX L. ..... p 3447 N92-30024
BLUM, AVRIM ..... p 3523 N92-30146
BLUMENTHAL, SAUL ..... p 3480 N92-29710
BLYTHE, MICHAEL P. ..... p 3462 N92-29264
BOBO, STEPHAN N. ..... p 3485 N92-30112
BOBROVNIKOV, S. M. ..... p 3467 N92-29293
BOEHM, A. P. W. ..... p 3562 N92-29794
BOEHRINGER, HANS ..... p 3565 N92-29833
p 3567 N92-29848
p 3568 N92-29851
BOERTJES, R. ..... p 3489 N92-29493
BOESENBERG, J. ..... p 3459 N92-29244
BOETTCHER, JAN ..... p 3544 N92-29997
BOL, ROLAND N. ..... p 3522 N92-29990
BOLOTIN, H. H. ..... p 3549 N92-30213
BOOTH, R. E. ..... p 3523 N92-30144
BORDER, J. S. ..... p 3409 N92-29369
BORGHESE, A. ..... p 3464 N92-29276
BOROVSKIKH, Y. V. ..... p 3540 N92-29863
BOSCH, JAN ..... p 3519 N92-29815
p 3521 N92-29970
BOSCHAN, PETER ..... p 3566 N92-29837
BOSELIE, F. ..... p 3524 N92-30195
BOUDJIT, M. ..... p 3516 N92-29621
BOURGAIN, J. ..... p 3537 N92-30096
BOWDLE, DAVID A. ..... p 3459 N92-29245
BOWERS, MARK S. ..... p 3468 N92-29298
BOWMAN, KENNETH P. ..... p 3470 N92-29307
BOWMAN, R. S. ..... p 3489 N92-29701
BOWSER, JAMES R. ..... p 3414 N92-29460
BOYCE, REX A. ..... p 3479 N92-30082
BOYDE, A. ..... p 3541 N92-30180
BOYTOS, MATTHEW A. ..... p 3549 N92-30013
BOZEMAN, RICHARD J., JR. ..... p 3474 N92-29952
BRACKETT, VINCENT G. ..... p 3457 N92-29236
BRADLEY, MICHAEL ..... p 3518 N92-29714
BRADSHAW, J. S. ..... p 3556 N92-29558
BRANDECKER, B. ..... p 3402 N92-30123
BRANDS, J. J. A. M. ..... p 3540 N92-29821
BRASCHE, LISA J. H. ..... p 3481 N92-30119
BRENNAN, A. ..... p 3491 N92-29454
BREWER, JOHN C. ..... p 3485 N92-30112
BRIEL, U. G. ..... p 3568 N92-29851
p 3568 N92-29852
BRINKSMA, ED ..... p 3517 N92-29705
p 3562 N92-30000
BRISTOW, M. P. ..... p 3461 N92-29255
BRITT, VICKI O. ..... p 3485 N92-30115
BROERSMA, H. J. ..... p 3537 N92-30081
BRONSVOORT, WILLEM F. ..... p 3535 N92-29922
BROOKS, N. H. ..... p 3554 N92-29412
BROSIUS, JEFFREY W. ..... p 3570 N92-29632
BROWELL, E. V. ..... p 3469 N92-29304
BROWELL, EDWARD V. ..... p 3457 N92-29236
p 3462 N92-29261
p 3473 N92-29325
BROWN, M. D. ..... p 3506 N92-29397
BROWN, M. J. ..... p 3469 N92-29300
BROWN, STEVEN O. ..... p 3410 N92-29525
BRUCKART, JAMES E. ..... p 3404 N92-29506
BRUEMMER, S. M. ..... p 3420 N92-29411

BRUMMELHUIS, RAYMOND G. M. p 3534 N92-29881
BRUNTY, J. p 3408 N92-30215
BUCHHOLZ, JOERG J. p 3404 N92-29870
BUCHSBAUM, GERSHON p 3510 N92-29398
BUELL, J. C. p 3454 N92-30162
p 3454 N92-30165
BUGG, F. p 3408 N92-30215
BUILTJES, P. J. H. p 3493 N92-29499
BUKALOV, S. S. p 3419 N92-29941
BUNDY, D. H. p 3461 N92-29255
BUNKIN, A. F. p 3467 N92-29290
BUNTE, STEVEN W. p 3554 N92-29510
BURKA, MICHAEL p 3471 N92-29317
BURY, G. p 3432 N92-29381
BUSHNELL, DAVID p 3512 N92-29413
BUTENHOFF, T. J. p 3417 N92-29459
BUTLER, C. F. p 3469 N92-29304
BUTLER, CAROLYN F. p 3457 N92-29236
p 3462 N92-29261
BUTLER, THOMAS W. p 3406 N92-29352
BUTLER, W. H. p 3436 N92-29909

C

CABO, A. J. p 3535 N92-29921
CABOT, W. p 3450 N92-30057
p 3455 N92-30168
CACCIANI, M. p 3459 N92-29243
CAMARDA, CHARLES J. p 3447 N92-30024
CAMBON, C. p 3449 N92-30054
CAMPBELL, G. L. p 3476 N92-29474
CANAVAN, G. H. p 3541 N92-30138
p 3542 N92-30139
CANNON, N. S. p 3550 N92-29938
CARLSON, LELAND A. p 3401 N92-29657
CARLSTROM, T. N. p 3476 N92-29474
p 3474 N92-29942
CARR, S. H. p 3426 N92-29804
CARRAWAY, DEBRA L. p 3446 N92-29954
CARSWELL, A. I. p 3458 N92-29237
p 3461 N92-29253
p 3472 N92-29321
CARSWELL, ALLAN I. p 3466 N92-29285
CARTER, A. F. p 3469 N92-29304
CARTER, M. R. p 3477 N92-29987
CARTER, WILLIAM H. p 3552 N92-29726
CASSEN, P. p 3455 N92-30168
CASSON, W. H. p 3547 N92-29910
CAVALIERE, ALFONSO p 3567 N92-29846
CAVCEY, K. p 3438 N92-30198
CAYER, JAMES L. p 3475 N92-30202
CENTURIONI, SANTE p 3460 N92-29251
CERRO, JEFFREY A. p 3483 N92-30028
CESSARO, ROBERT K. p 3505 N92-29618
CESSOU, A. p 3417 N92-29431
CHAMIS, CHRISTOS C. p 3481 N92-29342
CHANDRA, TUSHAR DEEPAK p 3515 N92-29400
CHANG, CHING S. p 3482 N92-29407
CHANG, JOHN p 3463 N92-29265
CHANIN, M. L. p 3472 N92-29319
CHANIN, MARIE-LISE p 3471 N92-29318
CHAO, TIEN-HSIN p 3552 N92-29832
CHAPPELL, P. J. p 3443 N92-30092
CHASNOV, JEFFREY R. p 3447 N92-30043
CHELOUCHE, EVYATAR p 3440 N92-29564
CHEN, C.-C. p 3431 N92-29376
CHEN, J. Y. p 3419 N92-29943
CHEN, M. H. p 3555 N92-29798
CHEN, P. C. p 3527 N92-29456
CHEN, SCOTT p 3512 N92-29413
CHEN, T. K. p 3440 N92-29523
CHENG, LI-JEN p 3552 N92-29832
CHERNYAVSKAYA, E. A. p 3468 N92-29295
CHEUNG, WANG K. p 3548 N92-30012
CHHABILDAS, L. C. p 3408 N92-29986
CHIANG, TAI-LUN p 3527 N92-29504
CHIBISOV, D. M. p 3540 N92-29860
CHIN, ATON p 3427 N92-29786
CHINCARINI, GUIDO p 3566 N92-29838
p 3566 N92-29839
CHISHOLM, M. F. p 3475 N92-30090
CHIU, ALEX p 3512 N92-29413
CHIU, M. A. p 3569 N92-29600
CHO, Y. p 3525 N92-29555
CHOHAN, HARPAL S. p 3415 N92-29593
CHOO, Y. K. p 3400 N92-29625
CHRISTENSEN, CHARLES R. p 3474 N92-29571
CHUDAMANI, S. p 3459 N92-29246
p 3460 N92-29247
p 3463 N92-29266
CHUN, A. K. T. p 3502 N92-29743
CHUNG, PI-YU p 3517 N92-29695
CHURNSIDE, J. H. p 3477 N92-29948
CHYOU, HUI-HUANG p 3415 N92-29594
CIARLO, D. R. p 3495 N92-30211
CIMOLINO, MARC p 3463 N92-29265
CIMOLINO, MARC C. p 3469 N92-29302
CLARK, R. J. p 3523 N92-30144
CLARK, RONALD K. p 3423 N92-30205
CLARKE, FREDERICK W. p 3474 N92-29571
CLAUDE, H. p 3462 N92-29259
CLAUS, R. O. p 3550 N92-29331
p 3551 N92-29652
p 3552 N92-29681
CLEIS, R. A. p 3470 N92-29309
CLELAND, J. p 3443 N92-30092
CLEMENT, PHILIPPE p 3535 N92-29923
CLERCX, HERMANUS JOHANNES HUBERTUS p 3444 N92-29752
COBBLE, J. A. p 3555 N92-29789
COE, H. H. p 3478 N92-29351
COKER, DEMIRKAN p 3414 N92-29453
COLAFRANCESCO, S. p 3567 N92-29846
COLE, H. S. p 3476 N92-29559
COLE, J. I. p 3420 N92-29411
COLLINS, L. A. p 3545 N92-29515
COLLINS, MICHAEL J. p 3407 N92-29929
COLLINS, RICHARD L. p 3470 N92-29307
COLLY, JOEL p 3529 N92-29675
COLTMAN, M. p 3564 N92-29809
CONGEDUTI, FERNANDO p 3460 N92-29251
CONNELL, JOHN W. p 3426 N92-29953
CONNERS, TIMOTHY R. p 3405 N92-29659
CONSTANTINE, BETSY p 3512 N92-29413
CONWAY, TERRY L. p 3510 N92-30216
COOK, G. O., JR. p 3524 N92-29353
p 3531 N92-29481
COOKE, ROGER p 3495 N92-30226
COOLEN, F. P. A. p 3539 N92-29817
p 3540 N92-29897
COOLEY, T. W. p 3473 N92-29327
COOLEY, THOMAS W. p 3437 N92-30103
COOMES, E. P. p 3569 N92-29600
COOPER, CHARLES p 3442 N92-29914
COOPER, D. I. p 3465 N92-29279
COOPER, L. P. p 3433 N92-29385
CORNWALL, J. M. p 3490 N92-30088
COTTIN, CLAUDIA p 3533 N92-29858
COUCH, RICHARD H. p 3462 N92-29264
COULSON, KINSEL L. p 3552 N92-30027
COURTIER, PH. p 3463 N92-29268
COURTNEY, SUSAN M. p 3510 N92-29398
COURTOIS, B. p 3441 N92-29612
COURTRIGHT, E. L. p 3415 N92-29645
COUSINS, ANANDA p 3468 N92-29298
COUTTAZ, J. p 3513 N92-29611
COWLEY, ALAN H. p 3424 N92-29466
COX, M. E. p 3403 N92-29605
CRAWFORD, M. L. p 3437 N92-30093
CRESSIE, NOEL p 3538 N92-29501
CRIST, B. p 3426 N92-29804
CROSS, KENNETH D. p 3407 N92-29709
CROWE, R. A. p 3433 N92-29385
CROWELL, CYNTHIA A. p 3406 N92-30025
CRUDDACE, RAY G. p 3568 N92-29853
CSANAK, G. p 3545 N92-29515
CULLEN, D. E. p 3516 N92-29537
CUMMINGS, M. p 3422 N92-29647
CUMMINGS, RUSSELL M. p 3401 N92-29691
CURIR, ANNA p 3518 N92-29714
CURTIS, DAYTON p 3402 N92-30128
CUTTS, JAMES A. p 3553 N92-30104

D

DABAS, A. p 3463 N92-29267
p 3463 N92-29268
DABROWSKI, A. J. p 3549 N92-29502
DAGLE, J. E. p 3569 N92-29600
DALLEY, N. K. p 3556 N92-29558
DAO, PHAN p 3471 N92-29317
DAO, PHAN D. p 3471 N92-29316
DASILVA, L. B. p 3477 N92-29987
DAUSKARDT, R. H. p 3414 N92-29556
DAVID, C. p 3462 N92-29260
p 3469 N92-29306
DAVIDSON, FREDERIC M. p 3435 N92-29658
DAVIDSON, GILBERT p 3471 N92-29317
DAVIES, P. O. A. L. p 3544 N92-29814
DAVIS, G. D. p 3421 N92-29587
DAVIS, ROBERT F. p 3560 N92-30175
DAW, C. S. p 3416 N92-29355
DEBAKKER, J. W. p 3522 N92-29991
p 3522 N92-29992
DEBOO, J. C. p 3476 N92-29474
DEBROY, T. p 3418 N92-29595
DECARIA, ALEX J. p 3502 N92-29424
DECKER, F. J. p 3550 N92-29788
DECOURSEY, R. J. p 3461 N92-29254
DECOURSEY, ROBERT J. p 3460 N92-29248
DEFIORE, THOMAS p 3485 N92-30113
DEGLORIA, D. P. p 3465 N92-29282
DEGOEDE, ERIK D. p 3446 N92-29944
p 3446 N92-29945
DEGROOT, WIM A. p 3413 N92-29448
DEHART, TERENCE E. p 3468 N92-29298
DEJARNETTE, FRED R. p 3400 N92-29539
DEJONGE, C. N. p 3459 N92-29244
DEJONGE, J. B. p 3402 N92-30129
DEKKERS, ANTON p 3436 N92-29824
p 3525 N92-29825
DELORME, JOSEPH F. p 3469 N92-29303
DELUCA, DANIEL P. p 3420 N92-29408
DEMIDOV, A. A. p 3468 N92-29295
DENHOLLANDER, F. p 3530 N92-29964
DEPIERO, N. L. p 3465 N92-29282
DERKS, G. p 3437 N92-29978
p 3536 N92-29979
DESMIDT, J. T. p 3489 N92-29693
DESTURLER, E. p 3527 N92-30229
DEUR, J. M. p 3412 N92-29343
DEVINK, E. P. p 3522 N92-29991
p 3522 N92-29992
DEVREUGHT, J. P. M. p 3525 N92-29716
DEVRIES, R. E. p 3529 N92-29963
DIAMOND, P. p 3452 N92-30140
DICICCIO, THOMAS J. p 3539 N92-29718
DICKSON, KATHERINE J. p 3509 N92-29341
DIDRIKSON, S. R. p 3403 N92-30131
DIEBEL, D. p 3461 N92-29255
DIETRICH, GERD p 3416 N92-29876
DIGIROLAMO, P. p 3459 N92-29243
DISALVO, F. J. p 3418 N92-29619
DISARRA, A. p 3459 N92-29243
DISSELKOEN, V. C. J. p 3534 N92-29892
DIXON, R. K. p 3495 N92-30173
DOBOSY, R. J. p 3503 N92-30034
DODGE, R. E. p 3569 N92-29600
DOEHNEL, W. p 3407 N92-30076
DOERRER, LINDA H. p 3418 N92-29619
DOGNANKSOY, N. p 3483 N92-29813
DONOVAN, D. p 3461 N92-29253
DORER, R. M. p 3564 N92-29809
DORRI, N. p 3549 N92-29502
DOW, A. p 3535 N92-29919
p 3535 N92-29920
DRAGON, E. P. p 3477 N92-29787
DRESSELHAUS, ELIOT p 3448 N92-30048
DRIESSEN, THEO p 3541 N92-30079
DRIVER, L. D. p 3438 N92-30198
DROST, M. K. p 3492 N92-29646
DUONG, TUAN A. p 3529 N92-29955
DURBIN, P. A. p 3449 N92-30051
DUTERLOO, CAROLINE G. p 3558 N92-29770
DUTTA, P. p 3542 N92-29354
DYMEK, ANDREW p 3515 N92-29527
DYSON, F. p 3490 N92-30088
DZENITIS, JOHN M. p 3479 N92-30026
DZHAPARIDZE, KACHA O. p 3533 N92-29862

E

EATON, M. J. p 3561 N92-29552
EBELING, HARALD p 3568 N92-29851
EBERHARD, WYNN L. p 3464 N92-29274
p 3472 N92-29324
EBERHARDT, SILVIO P. p 3529 N92-29955
ECKMAN, R. M. p 3503 N92-30034
EDER, D. C. p 3476 N92-29509
EDGE, ALASTAIR C. p 3567 N92-29844
p 3568 N92-29851
EDMONDS, C. M. p 3461 N92-29255
EDNER, H. p 3459 N92-29244
p 3464 N92-29273
EDWARDS, C. F. p 3417 N92-29431
EGALON, CLAUDIO OLIVEIRA p 3553 N92-30029
EGERT, S. p 3465 N92-29280
EHLERT, THOMAS C. p 3435 N92-29579
EHRET, GERHARD p 3462 N92-29258
p 3469 N92-29305
EICHINGER, W. E. p 3464 N92-29275
p 3465 N92-29279
EINASTO, JAAN p 3565 N92-29834
EL-BANNA, HESHAM M. p 3401 N92-29657
ELDER, IAN F. p 3475 N92-29396
ELDER, S. H. p 3418 N92-29619
ELESHAKY, MOHAMAD E. p 3445 N92-29830
ELKINS, T. J. p 3436 N92-29902
ELLIOTT, JAMES R., JR. p 3480 N92-30097
ELLIS, RICHARD S. p 3566 N92-29843
ELORANTA, E. W. p 3464 N92-29271
p 3464 N92-29272
p 3472 N92-29322
EMERY, Y. p 3462 N92-29260

EMMERSON, A. J. p 3488 N92-30132
EMMITT, G. D. p 3463 N92-29270
ENGELMANN, B. E. p 3481 N92-29338
p 3533 N92-29791
p 3533 N92-29792
ENGMANN, ROLF p 3519 N92-29816
ENTING, I. G. p 3494 N92-29668
EPPERLEIN, E. M. p 3554 N92-29531
ERAENEN, S. p 3443 N92-30094
ERDEMIR, A. p 3478 N92-29357
ERDOES, PETER L. p 3523 N92-30186
ERIKSSON, K. p 3447 N92-30023
ERNSBERGER, G. p 3408 N92-30215
ESAIAS, WAYNE E. p 3505 N92-29686
ESCHBAUMER, HERMANN p 3399 N92-29874
ESPY, T. p 3443 N92-30092
ESQUIVEL, M. S. p 3431 N92-29377
ESTEFAN, J. A. p 3409 N92-29368
ESTILL, J. C. p 3495 N92-30211
EVANKO, R. p 3476 N92-29474
EVANS, K. D. p 3457 N92-29233
EVRARD, AUGUST E. p 3567 N92-29847
EWING, A. G. p 3440 N92-29523
EWING, CARL S. p 3428 N92-29428

F

FABIAN, A. C. p 3567 N92-29844
FAGUY, PETER W. p 3417 N92-29514
FAIGLE, U. p 3541 N92-30188
FALES, CARL E. p 3552 N92-29951
FARLEY, ROBERT p 3471 N92-29316
p 3471 N92-29317
FARSOUN, ADIB R. p 3428 N92-29335
p 3428 N92-29545
FATHAUER, ROBERT W. p 3559 N92-30102
FATYGA, M. p 3549 N92-30014
p 3433 N92-30015
FAULKNER, A. p 3407 N92-30076
FAWCETT, W. R. p 3417 N92-29514
FEHRINGER, HANS-MICHAEL p 3428 N92-29470
FEHRINGER, M. p 3473 N92-29469
FELDMAN, GENE C. p 3505 N92-29686
FELTON, W. J. p 3505 N92-29554
FENN, M. A. p 3469 N92-29304
FENN, MARTA A. p 3457 N92-29236
p 3462 N92-29261
p 3473 N92-29325
FERIA, Y. p 3432 N92-29379
FERRARE, R. A. p 3457 N92-29233
FERRARE, RICHARD p 3458 N92-29238
p 3461 N92-29257
FERREIRA, ANA SUELY p 3441 N92-29729
FERREIRAPIRES, L. p 3531 N92-30184
FERRIDGE, A. G. p 3475 N92-30090
FERRY, M. p 3421 N92-29587
FERZIGER, J. H. p 3451 N92-30063
p 3451 N92-30065
FIEDLER, J. p 3459 N92-29244
FIELDER, WILLIAM L. p 3413 N92-29667
FIJMA, D. H. p 3522 N92-30073
FINGER, M. H. p 3409 N92-29365
FINKEL, LEIF H. p 3510 N92-29398
p 3511 N92-29560
FINSTERBUSCH, R. p 3473 N92-29469
FIOCCO, G. p 3459 N92-29243
FIRESTONE, ELAINE R. p 3505 N92-29686
p 3506 N92-30193
FISCHER, KEN W. p 3465 N92-29281
FISHMAN, JACK p 3457 N92-29236
FLAMANT, P. H. p 3463 N92-29267
p 3463 N92-29268
FLEETWOOD, D. M. p 3439 N92-29455
FLESIA, C. p 3462 N92-29260
FLOOD, MARTIN p 3458 N92-29241
FOLKNER, W. M. p 3409 N92-29365
p 3409 N92-29369
FONCK, R. J. p 3556 N92-30203
FONG, A. Y. p 3472 N92-29321
FORRESTER, D. A. p 3403 N92-29605
FORTSON, N. p 3490 N92-30088
FOX, JANE LEE p 3568 N92-29451
FRANCO, M. M. p 3431 N92-29372
FRANCOIS, R. E. p 3505 N92-29554
FRANK, JOERG p 3483 N92-29925
FRANSSON, K. p 3546 N92-29715
FRASER-SMITH, A. C. p 3434 N92-29542
FREDRIKSSON, BILLY p 3403 N92-30133
FRICKE, J. ROBERT p 3543 N92-29346
FRIEND, H. p 3551 N92-29679
FROOM, DOUGLAS A. p 3481 N92-30121
FRYDLENER, H. p 3525 N92-29614
FU, YIBIN p 3455 N92-30190
FUA, D. p 3459 N92-29243
FUCHS, W. KENT p 3517 N92-29695
FUGATE, R. Q. p 3470 N92-29309
FUJIMOTO, JAMES p 3439 N92-29452
FUJIMOTO, TOSHIFUMI p 3457 N92-29234
FUJIWARA, MOTOWO p 3456 N92-29229
FULLER, CHRIS R. p 3543 N92-29588
FULTON, R. D. p 3555 N92-29789
FUNSTEN, H. O. p 3500 N92-29536

G

GADEMANN, N. p 3541 N92-30188
GAGLIANO, L. p 3408 N92-30215
GAILLARDON, J. M. p 3402 N92-30123
GALLE, B. p 3459 N92-29244
GANGLOFF, RICHARD P. p 3423 N92-30206
GANUS, FLOYD p 3562 N92-29720
GAO, FENG p 3450 N92-30059
GARDNER, CHESTER S. p 3470 N92-29307
p 3470 N92-29311
p 3471 N92-29314
p 3471 N92-29315
GARFIN, S. R. p 3506 N92-29397
GARNIER, A. p 3472 N92-29319
GARRARD, WILLIAM L. p 3406 N92-29654
GARRATT, J. R. p 3500 N92-29670
GARRISON, G. R. p 3505 N92-29554
GATES, THOMAS S. p 3483 N92-30099
GAWRONSKI, W. p 3432 N92-29382
GEBBIE, K. B. p 3542 N92-30035
GEHAN, C. P. p 3562 N92-29699
GENTOU, H. p 3500 N92-29690
GENTRY, BRUCE M. p 3463 N92-29269
GEORGE, THOMAS F. p 3544 N92-29350
p 3414 N92-29460
GEORGES, T. M. p 3503 N92-29800
GERASIMOV, O. I. p 3544 N92-29415
GEURTS, B. J. p 3446 N92-29972
GIBELING, JEFFERY C. p 3421 N92-29547
GIBSON, WHITE p 3442 N92-29914
GILDING, B. H. p 3445 N92-29857
GILMOUR, PHILLIP p 3557 N92-29676
GIOVANELLI, RICCARDO p 3566 N92-29839
GLASS, R. S. p 3495 N92-30211
GLASSMAN, ARTHUR J. p 3524 N92-30207
GLOVER, M. G. p 3506 N92-29397
GLOVER, VINCE p 3491 N92-30105
GLYNN, PETER W. p 3538 N92-29500
GOBBI, GIAN PAOLO p 3460 N92-29251
GODDARD, R. E. p 3430 N92-29371
GODIN, S. p 3458 N92-29240
p 3462 N92-29260
p 3469 N92-29306
GOEBEL, F. p 3491 N92-29476
p 3541 N92-29973
p 3537 N92-30081
GOELTZ, R. p 3527 N92-29504
GOESCHL, E. p 3428 N92-29470
GOETZ, S. J. p 3491 N92-30210
GOIX, P. J. p 3417 N92-29431
GOLDSACK, STEPHEN J. p 3514 N92-29363
GOLDSTEIN, R. M. p 3433 N92-29388
GOLTZ, S. M. p 3465 N92-29282
GONIS, A. p 3556 N92-29473
p 3436 N92-29909
GONZALES, J. A. p 3442 N92-30032
GOODMAN, M. p 3544 N92-29356
GOOKIN, D. M. p 3475 N92-29332
GORANSON, ULF G. p 3484 N92-30107
GOTOH, T. p 3448 N92-30047
GOTT, S. p 3506 N92-29397
GOURDIN, W. H. p 3421 N92-29639
GOVERDE, P. F. W. p 3509 N92-29757
GRABERT, GREGORY p 3557 N92-29676
GRABKA, D. P. p 3489 N92-29701
GRAHN, K. p 3443 N92-30094
GRALLERT, H. p 3399 N92-30232
GRAMANN, MIRT p 3565 N92-29834
GRANATA, JOHN p 3516 N92-29622
GRANSTAFF, V. E. p 3495 N92-30211
GRANT, W. B. p 3469 N92-29304
GRANT, WILLIAM B. p 3457 N92-29236
GRASSOTTI, C. p 3473 N92-29328
GRAY, DAVID L. p 3446 N92-29954
GRAY, G. T., III p 3421 N92-29633
GRCAR, J. F. p 3517 N92-29641
GREBOGI, CELSO p 3515 N92-29399
GREENFIELD, C. M. p 3476 N92-29474
GREFEN, PAUL W. P. J. p 3562 N92-29957
GREGG, WATSON W. p 3505 N92-29686
GREIF, R. p 3485 N92-30112
GRELLA, RAY p 3562 N92-29720
GRIFFIN, J. p 3461 N92-29256
GRIFFITH, PETER p 3445 N92-29784
GRIGOROV, I. p 3466 N92-29286
GRIGOROV, I. V. p 3466 N92-29287
GRIMMER, D. P. p 3425 N92-29598
GRISHAM, JOHN A. p 3474 N92-29571
GROENEBOOM, P. p 3535 N92-29921
GROENEBOOM, PIET p 3539 N92-29626
GROENEVELD, WILLEM p 3532 N92-29687
GROOT, W. J. p 3509 N92-29756
GROOTE, JAN FRISO p 3536 N92-29993
p 3522 N92-29994
GROSS, MICHAEL p 3458 N92-29238
p 3461 N92-29257
GROTCH, S. L. p 3494 N92-29790
GUIDOTTI, R. A. p 3440 N92-29518
GUILYARDI, E. p 3451 N92-30063
GURDEV, L. L. p 3467 N92-29288
GUSS, W. C. p 3477 N92-29937
GUTSFELD, C. p 3422 N92-29651
GUYENNE, T.-D. p 3407 N92-29879
GUYOMARD, D. p 3418 N92-29619
GUZZO, LUIGI p 3566 N92-29839

H

HACHMAN, ANDREW C. p 3434 N92-29406
HADZILACOS, VASSOS p 3515 N92-29400
HAERING, R. p 3473 N92-29326
HAERTLING, GENE H. p 3557 N92-29676
HAGEMAIER, DONALD J. p 3481 N92-30117
HAGLUND, RICHARD F., JR. p 3428 N92-29428
HAINDL, MICHAL p 3523 N92-30141
HALL, CARLTON R. p 3492 N92-29430
HALL, CHARLES A. p 3478 N92-29392
HALL, F. G. p 3491 N92-30210
HALL, PHILIP p 3444 N92-29692
p 3455 N92-30190
HALLDORSSON, TH. p 3473 N92-29326
HALLER, KENNETH A. p 3442 N92-29914
HAMILTON, JAMES M. p 3451 N92-30069
HAMZA, A. V. p 3475 N92-29340
HAN, J. p 3525 N92-29555
HAN, YIN Y. p 3435 N92-29599
HANER, D. p 3469 N92-29306
HANNA-HAWVER, P. p 3552 N92-29681
HANSEN, G. M. p 3460 N92-29249
HARDESTY, R. MICHAEL p 3465 N92-29278
HARGENS, A. R. p 3506 N92-29397
HARGROVE, R. S. p 3477 N92-29787
HARLAN, J. A. p 3503 N92-29800
HARMS, D. J. p 3489 N92-29693
HARRINGTON, F. p 3408 N92-30215
HARRIS, CHARLES E. p 3484 N92-30106
p 3484 N92-30110
HARRIS, M. R. p 3469 N92-29300
HARRIS, P. p 3491 N92-29476
HARRISON, L. C. p 3551 N92-29530
HARTNER, GISELA D. p 3568 N92-29851
HARVEY, J. p 3452 N92-30140
HARVEY, ROBERT G. p 3516 N92-29586
HASH, M. C. p 3440 N92-29518
HASKOVEC, J. p 3476 N92-29474
HATSUDA, TETSUO p 3560 N92-29517
HAUN, JEFFREY D. p 3510 N92-29347
HAVERKORT, BOUDEWIJN R. p 3514 N92-29982
p 3523 N92-30191
HAWKE, R. S. p 3438 N92-29339
HAYASHIDA, S. p 3459 N92-29242
p 3460 N92-29250
HAYNES, MARTHA P. p 3566 N92-29839
HE, JIANLIANG p 3478 N92-29534
HEAD, J. D. p 3476 N92-29581
HEALD, S. M. p 3556 N92-29437
HEAPS, WILLIAM S. p 3458 N92-29238
p 3461 N92-29257
HEAVENS, ALAN p 3565 N92-29836
HEDMAN, B. p 3549 N92-29502
HEFNY, K. p 3489 N92-29495
HEIJENK, GEERT p 3526 N92-29680
HEIJENK, GEERT J. p 3438 N92-30170
HEIJMANS, H. J. A. M. p 3533 N92-29861
HEIJNEN, J. J. p 3507 N92-29733
p 3507 N92-29734
p 3507 N92-29735
p 3507 N92-29736
p 3508 N92-29737
p 3508 N92-29738
p 3508 N92-29739
p 3508 N92-29740
p 3509 N92-29759
p 3509 N92-29760
HEINRICHS, R. M. p 3470 N92-29310
HELLER, ADAM p 3440 N92-29575
HELLINGA, C. p 3508 N92-29755
p 3509 N92-29756
p 3509 N92-29757
p 3509 N92-29758
p 3509 N92-29759

HELLIWELL, R. A. ..... p 3434 N92-29542
HELMINCK, G. F. ..... p 3534 N92-29872
HENINS, I. ..... p 3556 N92-30203
HENRY, J. PATRICK ..... p 3567 N92-29845
p 3567 N92-29847
p 3568 N92-29851
p 3568 N92-29852
HERAKOVICH, CARL T. ..... p 3416 N92-30208
HERDIN, REINHARD ..... p 3561 N92-29886
HERGENROTHER, PAUL M. ..... p 3426 N92-29953
HERGERT, DENNIS W. ..... p 3406 N92-29352
HERMAN, GERARD C. ..... p 3544 N92-29918
HERMANN, A. M. ..... p 3557 N92-29584
HERRING, FRED M. ..... p 3406 N92-29352
HERRING, J. R. ..... p 3448 N92-30047
HERRMANN, H. ..... p 3473 N92-29326
HESS, ELIZABETH ..... p 3509 N92-29341
HESSELMANS, G. ..... p 3489 N92-29493
HESTER, L. O. ..... p 3480 N92-29478
HEUSER, W. R. ..... p 3432 N92-29380
HEYMAN, JOSEPH S. ..... p 3480 N92-29829
HIDINGER, DAVID S. ..... p 3412 N92-29444
HIENZ, ROBERT D. ..... p 3507 N92-29410
HILL, D. A. ..... p 3437 N92-30093
HILL, D. C. ..... p 3443 N92-29394
HILL, GARY C. ..... p 3404 N92-29417
HIROMOTO, R. E. ..... p 3562 N92-29794
HIRSCHEL, E. H. ..... p 3408 N92-29629
p 3400 N92-29648
p 3400 N92-29649
p 3409 N92-29680
p 3401 N92-29713
p 3399 N92-30232
HODGSON, K. O. ..... p 3549 N92-29502
HOEDE, CORNELIS ..... p 3538 N92-30185
HOEIJMAKERS, H. W. M. ..... p 3402 N92-29916
HOEKSEMA, J. T. ..... p 3569 N92-29421
HOF, D. E. ..... p 3464 N92-29275
p 3465 N92-29279
HOFFBAUER, M. A. ..... p 3545 N92-29634
HOFFMAN, R. N. ..... p 3473 N92-29328
HOGGARD, AMOS W. ..... p 3402 N92-30108
HOLAPPA, L. ..... p 3421 N92-29637
HOLDER, NANETTE S. ..... p 3527 N92-29541
HOLLANDERS, MARCUS ANTONIUS
p 3558 N92-29766
p 3558 N92-29767
p 3558 N92-29768
p 3558 N92-29769
p 3558 N92-29770
p 3558 N92-29771
p 3559 N92-29772
p 3559 N92-29773
HOLLIDAY, EDWARD M. ..... p 3435 N92-29572
HOLM, INGVAR ..... p 3403 N92-30133
HOLMAN, GORDON D. ..... p 3570 N92-29632
HOLMAN, W. ..... p 3469 N92-29300
HOLMBERG, L. ..... p 3546 N92-29715
HOLMEN, J. ..... p 3442 N92-29935
HOLMES, J. F. ..... p 3552 N92-29727
HOLROYD, R. ..... p 3545 N92-29582
HOLTKAMP, D. B. ..... p 3464 N92-29275
p 3465 N92-29279
HOLZBACHER-VALERO, A. A. ... p 3514 N92-29363
HONDERD, G. ..... p 3508 N92-29755
p 3509 N92-29756
p 3509 N92-29757
p 3509 N92-29758
HONES, E. W. ..... p 3500 N92-29513
HONG, K. C. ..... p 3495 N92-30211
HONG, SOON J. ..... p 3415 N92-29593
HOOGHIEMSTRA, G. ..... p 3529 N92-29963
p 3530 N92-29964
p 3530 N92-29965
HOOKER, JOHN R. ..... p 3400 N92-29445
HOOKER, STANFORD B. ..... p 3505 N92-29686
p 3506 N92-30193
HORI, AKIHIRO ..... p 3466 N92-29284
HORWEDEL, J. E. ..... p 3519 N92-29797
HOSSAIN, S. ..... p 3491 N92-29476
HOSTETLER, CHRIS A. ..... p 3471 N92-29315
HOTALING, T. C. ..... p 3470 N92-29310
HOUBEN, HOWARD C. ..... p 3569 N92-30199
HOUGHTON, R. W. ..... p 3504 N92-29439
HOUNJET, M. H. L. ..... p 3532 N92-29604
HOVER, G. L. ..... p 3512 N92-29538
HOWALD, A. ..... p 3554 N92-29412
HOWARD, C. V. ..... p 3541 N92-30180
HOWELL, JAMES N. ..... p 3465 N92-29278
HSIEH, C. L. ..... p 3476 N92-29474
HU, HUANLING ..... p 3460 N92-29252
HUANG, JOHN ..... p 3434 N92-29463
HUANG, P. G. ..... p 3454 N92-30164
HUANG, QIRONG ..... p 3467 N92-29292
HUBBLE, BILL R. ..... p 3427 N92-29786
HUBERT, M. L. ..... p 3563 N92-30040
HUCK, FREDRICH O. ..... p 3552 N92-29951
HUEMER, SIEGFRIED ..... p 3561 N92-29886
HUEMMRICH, K. F. ..... p 3491 N92-30210
HUETTEL, HANS ..... p 3536 N92-29993
HUGHES, RICHARD N. ..... p 3440 N92-29526
HULL, ANDREW J. ..... p 3483 N92-29915
HUMMEL, J. R. ..... p 3465 N92-29282
HUNTEN, KEITH ..... p 3562 N92-29720
HURWITZ, FRANCES I. ..... p 3415 N92-29660
HUSZTHY, P. ..... p 3556 N92-29558
HUTCHINSON, JOHN W. ..... p 3484 N92-30111

I

IGLESIAS, C. A. ..... p 3555 N92-29798
INGLOT, TADEUSZ ..... p 3541 N92-29980
INOZEMTSEV, V. I. ..... p 3533 N92-29793
IOVINO, ANGELA ..... p 3566 N92-29839
ISAACS, R. G. ..... p 3473 N92-29328
ISHII, THOMAS K. ..... p 3435 N92-29579
ISMAIL, SYED ..... p 3462 N92-29261
p 3473 N92-29325
ITOH, HIDEKI ..... p 3502 N92-29666
IVANOVA, I. D. ..... p 3467 N92-29288
IWANCZYK, J. A. ..... p 3549 N92-29502
IZATT, R. M. ..... p 3556 N92-29558

J

JACKSON, B. E. ..... p 3546 N92-29899
JACKSON, DOUGLAS E. ..... p 3511 N92-29620
JACKSON, S. ..... p 3551 N92-29679
JACKSON, THOMAS L. ..... p 3455 N92-30192
JACKSON, WADE C. ..... p 3481 N92-29393
JACOB, M. C. ..... p 3451 N92-30066
JACOBS, BARRY L. ..... p 3512 N92-29930
JAMNEJAD, V. ..... p 3433 N92-29387
JANG, J. HOON ..... p 3492 N92-29662
JANI, YASHVANT ..... p 3525 N92-29390
JANSEN, FREDERIK W. ..... p 3518 N92-29749
JANSSEN, MICHAEL A. ..... p 3437 N92-30103
JANSSEN, WIL ..... p 3536 N92-29956
JAYANETTI, J. K. D. S. ..... p 3556 N92-29437
JELONEK, M. P. ..... p 3470 N92-29309
JELSKI, DANIEL A. ..... p 3414 N92-29460
JENKINS, J. S. ..... p 3433 N92-29385
JENSEN, A. E. ..... p 3516 N92-29544
JENSEN, D. R. ..... p 3501 N92-30087
JEONG, DAVID Y. ..... p 3485 N92-30112
JESSON, D. E. ..... p 3475 N92-30090
JEYS, T. H. ..... p 3470 N92-29308
p 3470 N92-29310
JIANG, TAO ..... p 3523 N92-30146
JIMENEZ, J. ..... p 3448 N92-30045
JOE, EDMOND ..... p 3463 N92-29265
JOERGENSEN, T. S. ..... p 3459 N92-29243
JOHNK, R. ..... p 3438 N92-30198
JOHNSON, A. J. ..... p 3514 N92-29907
JOHNSON, BURGESS ..... p 3557 N92-29583
JOHNSON, RICHARD E. ..... p 3413 N92-29667
JOHNSON, WILLIAM B. ..... p 3487 N92-30126
JOHNSTON, A. ..... p 3551 N92-29679
JOHNSTON, RICHARD P. ..... p 3405 N92-29427
JONES, L. A. ..... p 3555 N92-29789
JONES, L. G. ..... p 3495 N92-30031
JONES, RICHARD A. ..... p 3424 N92-29466
JONES, V. M. ..... p 3523 N92-30144
JONKER, P. ..... p 3537 N92-30147
JORDENSE, MARCEL ..... p 3526 N92-29958
p 3437 N92-29984
JOST, G. S. ..... p 3482 N92-29672
JUANG, JER-NAN ..... p 3488 N92-30214
JUILLOT, F. ..... p 3523 N92-30144
JURGENS, R. ..... p 3433 N92-29389
JURGENS, R. F. ..... p 3433 N92-29388

K

KAHANA, DAVID E. ..... p 3547 N92-30003
p 3547 N92-30005
p 3548 N92-30007
KAINEC, JAMES J. ..... p 3528 N92-29561
KALLENBERG, L. C. M. ..... p 3524 N92-30201
KALLENBERG, WILBERT C. M. .. p 3540 N92-29974
p 3541 N92-29976
p 3541 N92-29980
KAMDAR, K. D. ..... p 3552 N92-29681
KAMPA, K. ..... p 3407 N92-30076
KANDA, M. ..... p 3437 N92-30093
KANE, D. J. ..... p 3476 N92-29516
KANE, TIMOTHY J. ..... p 3470 N92-29311
KAPRIELOV, B. ..... p 3466 N92-29286
KARASSO, P. S. ..... p 3451 N92-30067
p 3453 N92-30152
KARDOMATEAS, GEORGE A. .... p 3414 N92-29462
KARL, R. R. ..... p 3465 N92-29279
KARL, R. R., JR. ..... p 3464 N92-29275
KARS, PIM ..... p 3517 N92-29705
KARYADI, E. ..... p 3482 N92-29700
KATES, RONALD E. ..... p 3565 N92-29835
KAUFFMANN, CHRISTIAAN ..... p 3543 N92-29628
p 3543 N92-29748
KAUFMAN, J. G. ..... p 3422 N92-29807
KAUTZ, D. D. ..... p 3477 N92-29787
KEANE, M. ..... p 3530 N92-29964
KEANE, M. S. ..... p 3529 N92-29963
p 3530 N92-29965
KECK, R. L. ..... p 3555 N92-30072
KELLER, JOSEPH B. ..... p 3539 N92-29718
KELLERER, HELMUT ..... p 3416 N92-29875
KELLEY, HENRY L. ..... p 3406 N92-30025
KELLY, K. A. ..... p 3562 N92-29794
KENT, G. S. ..... p 3460 N92-29249
KENYON, DAVID L. ..... p 3462 N92-29262
p 3468 N92-29297
KERN, W. ..... p 3541 N92-30188
KERSTEIN, A. R. ..... p 3417 N92-29433
KERSTEN, M. L. ..... p 3521 N92-29891
KERSTEN, PAUL H. M. ..... p 3537 N92-30078
KETTERSON, J. B. ..... p 3542 N92-29354
KHATSIMOVSKIJ, V. M. ..... p 3560 N92-30212
KIERNAN, S. C. ..... p 3407 N92-29299
KIM, S. ..... p 3422 N92-29803
KIM, WON S. ..... p 3479 N92-29765
KIM, Y. J. ..... p 3556 N92-30203
KIMMEL, J. A. ..... p 3478 N92-29351
KING, G. A. ..... p 3495 N92-30021
KING, R. W. ..... p 3525 N92-29624
KIRKHAM, H. ..... p 3551 N92-29679
KIRKMAN, D. A. ..... p 3413 N92-29461
KIRSHTEIN, PHILLIP M. ..... p 3435 N92-29572
KIST, EDWARD H. ..... p 3462 N92-29264
KITADA, TOSHINOBU ..... p 3466 N92-29284
KITCHEN, WAYNE L. ..... p 3462 N92-29264
KLANN, GARY A. ..... p 3405 N92-29661
KLEPPER, K. ..... p 3554 N92-29412
KLINKHAMER, F. R. ..... p 3546 N92-29751
KLOMPSTRA, M. B. ..... p 3529 N92-29764
KLYPIN, ALEXANDER A. ..... p 3565 N92-29835
KNIGHT, D. A. ..... p 3414 N92-30187
KNIGHT, R. C. ..... p 3550 N92-29938
KNUDSEN, B. ..... p 3459 N92-29243
KNUEPPEL, H. ..... p 3515 N92-29418
KO, S. H. ..... p 3449 N92-30052
KOBAYASHI, A. S. ..... p 3404 N92-29511
KOBAYASHI, TAKAO ..... p 3466 N92-29284
KOC, A. ..... p 3401 N92-29713
KOCH, CHRISTOF ..... p 3528 N92-29590
KOCH, J. A. ..... p 3477 N92-29987
KOCH, MICHAEL R. ..... p 3462 N92-29264
KOEPKE, G. ..... p 3438 N92-30198
KOERNER, ROLAND ..... p 3445 N92-29926
KOJO, M. ..... p 3421 N92-29637
KOK, ARJAN J. F. ..... p 3518 N92-29749
KOKKE, J. M. M. ..... p 3491 N92-30230
KOLAROV, G. ..... p 3467 N92-29289
KOLEV, I. ..... p 3466 N92-29286
KOONIN, S. ..... p 3490 N92-30088
KOONTZ, STEVEN ..... p 3427 N92-30100
KOORNWINDER, TOM H. ..... p 3534 N92-29866
p 3534 N92-29882
KOPCSA, ALEXANDER ..... p 3538 N92-29419
KORB, C. LAURENCE ..... p 3463 N92-29269
KORKINA, E. ..... p 3537 N92-30080
KORN, J. ..... p 3470 N92-29310
KOROLYUK, V. S. ..... p 3540 N92-29863
KOROLYUK, V. V. ..... p 3535 N92-29895
p 3535 N92-29896
KORVER, HENRI P. ..... p 3521 N92-29890
KOSAI, M. ..... p 3404 N92-29511
KOSTWINDER, H. R. ..... p 3489 N92-29494
KOTULAK, JOHN C. ..... p 3512 N92-29348
KOVALEV, V. A. ..... p 3461 N92-29255
KOWALCZYK, E. A. ..... p 3500 N92-29670
KRAMER, S. L. ..... p 3549 N92-29477
KRAMMER, J. ..... p 3404 N92-29650
KREISCHER, K. E. ..... p 3477 N92-29937
KREMER, H. ..... p 3514 N92-30145
KRICHBAUMER, W. ..... p 3473 N92-29326
KRIEGSMANN, GREGORY A. ..... p 3543 N92-29543
KROPIUNIG, C. ..... p 3428 N92-29470
KRUIT, MARCO ..... p 3521 N92-29887
KRUMMEL, P. B. ..... p 3500 N92-29670
KUBIAK, G. D. ..... p 3475 N92-29434
KUEHNAPFEL, U. ..... p 3515 N92-29418
KUENEN, J. G. ..... p 3507 N92-29735
KUERTEN, J. G. M. ..... p 3446 N92-29972
p 3560 N92-30148
KUIVALAINEN, P. ..... p 3443 N92-30094
KUNDU, K. P. ..... p 3412 N92-29343

KUNZ, ROBERT F. ..... p 3445 N92-29933
KUPER, JAN ..... p 3536 N92-29995
KURZIUS, S. C. ..... p 3469 N92-29300
KUSTERS, KAREL ANTONIUS .... p 3445 N92-29775
KYRALA, G. A. ..... p 3555 N92-29789

L

LABOURDETTE, ROGER ..... p 3402 N92-30130
LABRUJERE, T. E. ..... p 3401 N92-29884
LACOSTE, A. M. ..... p 3458 N92-29240
LADD, M. E. ..... p 3434 N92-29542
LAFON, J. ..... p 3399 N92-30232
LAGOW, R. J. ..... p 3424 N92-29549
LAKSHMINARAYANA, BUDUGUR
..... p 3445 N92-29933
LAMBERT, JAMES L. ..... p 3552 N92-29832
LAMMINEN, J. ..... p 3441 N92-29912
LAMPARD, G. J. ..... p 3549 N92-30213
LAMPINEN, M. J. ..... p 3441 N92-29912
LANGE, W. J. ..... p 3470 N92-29309
LANGERAK, J. A. C. ..... p 3508 N92-29740
LANKHORST, MARC ..... p 3527 N92-30183
LAPOINTE, KENNETH M. ..... p 3475 N92-30202
LAPP, M. ..... p 3461 N92-29256
LARIN, S. A. ..... p 3518 N92-29747
..... p 3546 N92-29750
LARSEN, N. ..... p 3459 N92-29243
LASSILA, D. H. ..... p 3421 N92-29639
LAST, ISIDORE ..... p 3544 N92-29350
LATTIME, S. B. ..... p 3478 N92-29351
LAU, Y. Y. ..... p 3440 N92-29523
LAW, D. O. ..... p 3441 N92-29796
LAWRENCE, T. RHIDIAN ..... p 3468 N92-29297
..... p 3468 N92-29298
LAWSON, A. C. ..... p 3421 N92-29633
LEBER, DOUGLAS ERIC ..... p 3403 N92-29440
LEBOEUF, R. L. ..... p 3451 N92-30068
LEBOWITZ, JOEL L. ..... p 3554 N92-29450
LEDWINA, TERESA ..... p 3541 N92-29980
LEE, GEORGE ..... p 3406 N92-29655
LEE, H. S. ..... p 3564 N92-29809
LEE, M. ..... p 3425 N92-29569
LEE, M. J. ..... p 3455 N92-30167
LEE, MYONGSOO ..... p 3423 N92-29349
..... p 3425 N92-29566
..... p 3425 N92-29567
LEIGHTON, K. S. ..... p 3438 N92-29339
LEINENWEVER, ROGER W. ..... p 3406 N92-29505
LEITES, L. A. ..... p 3419 N92-29941
LENTZ, S. J. ..... p 3506 N92-29805
LEONE, STEPHEN R. ..... p 3418 N92-29901
LERCH, MANFRED ..... p 3401 N92-29741
LEROY, C. ..... p 3462 N92-29260
LEVINE, H. ..... p 3452 N92-30140
LEWIS, JESS ..... p 3402 N92-30128
LEWIS, JOHN S. ..... p 3568 N92-29432
LI, DEQUAN ..... p 3545 N92-29634
LI, HAIKUAN ..... p 3518 N92-29712
..... p 3519 N92-29779
LI, MING ..... p 3520 N92-29868
..... p 3523 N92-30146
LI, SHUANHU ..... p 3535 N92-29923
LI, Z. ..... p 3501 N92-29950
LICINA, JOSEPH R. ..... p 3510 N92-29347
..... p 3404 N92-29506
LIEUTAUD, F. ..... p 3463 N92-29267
..... p 3463 N92-29268
LIGHTSEY, W. D. ..... p 3429 N92-29677
LIMAYE, SANJAY S. ..... p 3568 N92-29401
LIN, SHU ..... p 3517 N92-29665
LINCOLN, JOHN W. ..... p 3485 N92-30114
LINDH, K. ..... p 3546 N92-29715
LINDSAY, G. ..... p 3422 N92-29647
LINEBERGER, W. C. ..... p 3418 N92-29901
LINFIELD, R. ..... p 3429 N92-29366
LINSSEN, H. N. ..... p 3540 N92-29828
LITVAK, M. M. ..... p 3564 N92-29359
LIU, GUOJUN ..... p 3417 N92-29514
LIU, Y. S. ..... p 3476 N92-29559
LONG, JAMES H., JR. ..... p 3438 N92-29404
LOOYEN, W. J. ..... p 3490 N92-29707
LORD, MARK T. ..... p 3480 N92-30097
LOTH, C. ..... p 3463 N92-29267
LOUIS, J.-F. ..... p 3473 N92-29328
LOVBERG, R. H. ..... p 3555 N92-29917
LOWE, S. T. ..... p 3430 N92-29367
LOZIER, DANIEL W. ..... p 3418 N92-29744
LUBASZEWSKI, M. ..... p 3441 N92-29612
LUIJKX, G. C. A. ..... p 3507 N92-29734
LUKITO, G. ..... p 3508 N92-29739
LUND, P. D. ..... p 3492 N92-29636
LUND, T. S. ..... p 3450 N92-30056
LUNSFORD, J. H. ..... p 3492 N92-29519
LUTES, G. F. ..... p 3431 N92-29372
LUTFI, R. ..... p 3511 N92-29592
LUTTIGHUIS, PAUL OUDE ..... p 3527 N92-30189
LUTTRELL, G. W. ..... p 3563 N92-30040
LUYBEN, K. C. A. M. ..... p 3507 N92-29733
..... p 3507 N92-29734
..... p 3507 N92-29735
..... p 3507 N92-29736
..... p 3508 N92-29737
..... p 3508 N92-29738
..... p 3508 N92-29739
..... p 3508 N92-29740
..... p 3508 N92-29755
..... p 3509 N92-29756
..... p 3509 N92-29757
..... p 3509 N92-29758
..... p 3509 N92-29759
..... p 3509 N92-29760
LYDING, JOSEPH W. ..... p 3557 N92-29722

M

MAARSINGH, T. A. ..... p 3401 N92-29884
MACCARLEY, C. ..... p 3431 N92-29374
MACDONALD, G. ..... p 3490 N92-30088
MACGILLIVRAY, H. T. ..... p 3568 N92-29853
MACGOWAN, B. J. ..... p 3476 N92-29472
..... p 3477 N92-29987
MACKEY, D. B. ..... p 3420 N92-29436
MACLIN, JAMES R. ..... p 3484 N92-30109
MACOSKO, CHRISTOPHER ..... p 3424 N92-29465
MADSEN, NIEL K. ..... p 3517 N92-29694
MAGUIRE, M. C. ..... p 3421 N92-29623
MAHMOOD, M. M. ..... p 3506 N92-29397
MALIN, JANE T. ..... p 3513 N92-29403
MANDERS, P. J. H. M. ..... p 3403 N92-29615
MANSON, PETER J. ..... p 3456 N92-29230
MANSOUR, N. N. ..... p 3449 N92-30054
MARADUDIN, ALEXEI A. ..... p 3551 N92-29546
MARBLE, FRANK E. ..... p 3418 N92-29580
MARCOLINI, MICHAEL A. ..... p 3474 N92-30030
MARKLEY, R. W. ..... p 3433 N92-29385
MARKOS, S. H. ..... p 3564 N92-29809
MARS, NICOLAAS, J. I. ..... p 3426 N92-29960
MARSH, S. F. ..... p 3425 N92-29643
MARTIN, C. ..... p 3472 N92-29320
MARTIN, CARL J., JR. ..... p 3483 N92-30028
MARTIN, MICHAEL A. ..... p 3539 N92-29718
MARTIN, R. T. ..... p 3502 N92-29743
MARTIN, RODERICK H. ..... p 3481 N92-29393
MARTIN, RUTH M. ..... p 3474 N92-30030
MARTIN, T. ..... p 3490 N92-30022
MARTINEZ, R. J. ..... p 3465 N92-29279
MARTINSON, SCOTT D. ..... p 3446 N92-29954
MARTZ, H. E. ..... p 3480 N92-29478
MASCHKE, A. W. ..... p 3545 N92-29507
MASCHKE, B. M. ..... p 3537 N92-30077
MASKIT, B. ..... p 3542 N92-30095
MASLINE, R. C. ..... p 3433 N92-29385
MASTERSON, K. ..... p 3438 N92-30198
MATALON, MOSHE ..... p 3455 N92-30192
MATE, B. R. ..... p 3490 N92-30022
MATIN, LEONARD ..... p 3510 N92-29420
MATSUI, I. ..... p 3459 N92-29242
..... p 3460 N92-29250
MATTHEWS, D. L. ..... p 3477 N92-29987
MAUNG, KHIN MAUNG ..... p 3547 N92-30003
..... p 3547 N92-30005
..... p 3548 N92-30007
MAX, C. ..... p 3490 N92-30088
MAYER, GEORGE ..... p 3426 N92-29905
MAYOR, SHANE D. ..... p 3457 N92-29236
MCCLAIN, CHARLES R. ..... p 3505 N92-29686
MCCOMAS, D. J. ..... p 3500 N92-29536
MCCORMICK, M. PATRICK ..... p 3456 N92-29228
..... p 3469 N92-29301
MCCOY, ROBERT L. ..... p 3406 N92-29449
MCDERMID, I. STUART ..... p 3458 N92-29239
MCDIARMID, C. ..... p 3533 N92-29864
MCDONALD, KENNETH F. ..... p 3468 N92-29298
MCDONALD, R. C. ..... p 3491 N92-29476
MCELROY, J. L. ..... p 3461 N92-29255
MCGEE, THOMAS J. ..... p 3458 N92-29238
..... p 3461 N92-29257
MCGHEE, D. ..... p 3408 N92-30215
MCGILL, P. R. ..... p 3434 N92-29542
MCGUIRE, JACK F. ..... p 3484 N92-30107
MCINTOSH, ROBERT E. ..... p 3434 N92-29447
MCKEE, E. ..... p 3476 N92-29474
MCKEON, JAMES B. ..... p 3403 N92-29906
MCKINNIS, DARIN ..... p 3479 N92-29762
MCMAHAN, TRACY ..... p 3408 N92-30016
MCMAHON, C. J. ..... p 3482 N92-29601
MCMAHON, C. J., JR. ..... p 3420 N92-29483
MCMURTRY, P. A. ..... p 3417 N92-29433
MCNUTT, R. ..... p 3471 N92-29316
MCWITHEY, ROBERT R. ..... p 3483 N92-30028
MEBIUS, J. E. ..... p 3517 N92-29627
MEGIE, G. ..... p 3458 N92-29240
..... p 3469 N92-29306
MEHNERT, A. ..... p 3473 N92-29326
MEHTA, RABINDRA D. ..... p 3453 N92-30155
MEHTA, S. ..... p 3552 N92-29681
MEI, CHUH ..... p 3404 N92-30209
MEINSMA, GJERRIT ..... p 3530 N92-29971
MEISTRING, ROLF ..... p 3416 N92-29876
MELFI, S. H. ..... p 3457 N92-29233
MELLQUIST, J. ..... p 3459 N92-29244
MENENTI, M. ..... p 3489 N92-29495
..... p 3490 N92-29717
MENEVEAU, C. ..... p 3454 N92-30159
MENIETTI, J. D. ..... p 3570 N92-29360
MENON, S. ..... p 3417 N92-29433
MENYHARD, M. ..... p 3420 N92-29483
MENZIES, ROBERT T. ..... p 3459 N92-29246
..... p 3460 N92-29247
MERIWETHER, JOHN ..... p 3471 N92-29317
MERIWETHER, JOHN W. ..... p 3471 N92-29316
MESECAR, R. ..... p 3490 N92-30022
MEYER, D. ..... p 3408 N92-30215
MEYER, L. R. ..... p 3503 N92-29800
MICHAELIS, WALFRIED ..... p 3456 N92-29231
MICHALIK, HARALD ..... p 3474 N92-29731
MICHALSKY, J. J. ..... p 3551 N92-29530
MICHEL, ULF ..... p 3544 N92-29997
MICKELSON, M. ..... p 3473 N92-29328
MIKATARIAN, JEFF ..... p 3408 N92-30016
MILLER, DOUGLAS ..... p 3424 N92-29465
MILLER, WILLIAM T., JR. ..... p 3474 N92-30030
MINATO, A. ..... p 3459 N92-29242
MINATO, ATSUSHI ..... p 3465 N92-29277
MINEEV, V. S. ..... p 3560 N92-29533
MINGA, A. ..... p 3457 N92-29236
MINNETYAN, LEVON ..... p 3481 N92-29342
MISENHEIMER, D. C. ..... p 3495 N92-30031
MITEV, V. ..... p 3462 N92-29260
..... p 3466 N92-29286
..... p 3469 N92-29306
MITEV, V. M. ..... p 3466 N92-29287
..... p 3467 N92-29288
MITSEV, TS. ..... p 3467 N92-29289
MITTEMEIJER, ERIC J. ..... p 3558 N92-29769
..... p 3558 N92-29770
..... p 3558 N92-29771
..... p 3559 N92-29772
..... p 3559 N92-29773
MIYAWAKI, FUJIO ..... p 3555 N92-30091
..... p 3555 N92-30172
MO, HOU-JUN ..... p 3566 N92-29840
MOEN, J. P. ..... p 3489 N92-29693
MOERL, PETER ..... p 3469 N92-29305
MOLL, A. ..... p 3522 N92-30020
MOLL, J. R. ..... p 3490 N92-29728
MONSON, L. R. ..... p 3525 N92-29624
MONTGOMERY, E. T. ..... p 3506 N92-29806
MONY, BRUNO ..... p 3564 N92-29468
MOODY, STEPHEN E. ..... p 3468 N92-29298
MOONEY, G. D. ..... p 3557 N92-29584
MOOPENN, ALEXANDER W. ..... p 3529 N92-29955
MOORE, FRANK G. ..... p 3400 N92-29539
MOORE, GARY ..... p 3571 N92-29724
..... p 3571 N92-29725
MOORE, K. R. ..... p 3500 N92-29536
MOOSMUELLER, H. ..... p 3461 N92-29255
MORAN, SUSANNE I. ..... p 3406 N92-29505
MOREL-SEYTOUX, H. J. ..... p 3494 N92-29746
MORGAN, D. ..... p 3544 N92-29488
..... p 3545 N92-29489
..... p 3545 N92-29490
..... p 3560 N92-29996
MORI, TOSHIHIKO ..... p 3560 N92-29781
MORKOC, HADIS ..... p 3442 N92-29936
MORRIS, BRIAN G. ..... p 3480 N92-30101
MORRIS, C. E. ..... p 3421 N92-29633
MOSHAMMER, H. W. ..... p 3437 N92-29988
MOSKOWITZ, B. ..... p 3549 N92-30014
MOSKOWITZ, WARREN P. ..... p 3471 N92-29316
MOTHEO, ARTUR J. ..... p 3417 N92-29514
MOTT, J. E. ..... p 3525 N92-29624
MOYEED, R. A. ..... p 3541 N92-30180
MROWKA, S. ..... p 3477 N92-29987
MUDGWAY, D. J. ..... p 3433 N92-29384
MUDHOLKAR, GOVIND S. ..... p 3541 N92-29976
MUELLER, JAMES L. ..... p 3506 N92-30193
MUELLER, MARK J. ..... p 3413 N92-29913
MUERER, JOHAN ANDREAS ..... p 3408 N92-29967
MUKHERJEE, AMIYA K. ..... p 3421 N92-29547
MUNGAL, M. G. ..... p 3451 N92-30067
..... p 3453 N92-30152
MURDOCK, C. R. ..... p 3563 N92-30040
MURPHY, K. A. ..... p 3550 N92-29331
MURRAY, JERRY ..... p 3512 N92-29413

MURTHY, G. ..... p 3506 N92-29397
MURTHY, PAPPU L. N. ..... p 3481 N92-29342
MUSCH, M. G. ..... p 3508 N92-29740
MYERS, LAWRENCE P. ..... p 3405 N92-29659

N

NAGAI, TOMOHIRO ..... p 3457 N92-29234
NAGARAJAN, S. ..... p 3552 N92-29681
NAGASAWA, CHIKAO ..... p 3457 N92-29232
p 3470 N92-29312
NAKANE, H. ..... p 3459 N92-29242
NASH, J. K. ..... p 3476 N92-29509
p 3555 N92-29798
NASSERI, SEIED MOHAMMAD ... p 3446 N92-29968
NASTA, M. H. ..... p 3552 N92-29681
NAUTA, JAN M. ..... p 3530 N92-29969
NEHRKORN, T. ..... p 3473 N92-29328
NELSON, W. ..... p 3483 N92-29813
NEMHAUSER, G. L. ..... p 3516 N92-29608
NEUE, H. U. ..... p 3494 N92-30018
NEUKOM, CHRISTIAN ..... p 3512 N92-29413
NEUMANN, ANDREW S. ..... p 3445 N92-29784
NEWMAN, JAMES C., JR. ..... p 3484 N92-30110
NGANGA, D. ..... p 3457 N92-29236
NGUYEN, CHARLES C. ..... p 3528 N92-29656
NGUYEN, H. L. ..... p 3412 N92-29343
NI, QING-XIAO ..... p 3424 N92-29482
NICKESON, J. E. ..... p 3491 N92-30210
NICOLAIDIS, M. ..... p 3516 N92-29570
p 3516 N92-29621
NIEDZIELSKI, J. PETER ..... p 3476 N92-29581
NIEMEGEERS, I. G. ..... p 3526 N92-30074
NIEMEGEERS, IGNAS ..... p 3526 N92-29958
p 3437 N92-29984
NIEMEGEERS, IGNAS G. ..... p 3526 N92-29880
p 3514 N92-29982
p 3526 N92-29985
p 3438 N92-30170
p 3523 N92-30191
NIEUKIRK, S. ..... p 3490 N92-30022
NIGAY, L. ..... p 3513 N92-29611
NOORMAN, HENDRIK JAN ..... p 3507 N92-29732
p 3507 N92-29733
p 3507 N92-29734
p 3507 N92-29735
p 3507 N92-29736
p 3508 N92-29737
p 3508 N92-29738
p 3508 N92-29739
p 3508 N92-29740
NORBURY, JOHN W. ..... p 3547 N92-30001
p 3547 N92-30002
p 3547 N92-30003
p 3438 N92-30004
p 3547 N92-30005
p 3548 N92-30006
p 3548 N92-30007
p 3548 N92-30008
p 3548 N92-30009
p 3548 N92-30010
p 3548 N92-30011
p 3548 N92-30012
p 3549 N92-30013
p 3438 N92-30015
NORTON, JEFFREY E. ..... p 3487 N92-30126
NOWICKI, GREG D. ..... p 3473 N92-29325

O

OBERMAYER, M. ..... p 3407 N92-30076
OBRIEN, D. W. ..... p 3495 N92-30211
OCONNOR, DENNIS J. ..... p 3562 N92-29934
OCONNOR, R. C. ..... p 3433 N92-29384
ODDY, DONNA M. ..... p 3492 N92-29430
ODEN, J. T. ..... p 3444 N92-29721
OH, D. ..... p 3463 N92-29267
OHLSSON, STELLAN ..... p 3531 N92-29486
OHNSTEIN, T. ..... p 3442 N92-29935
OJA, T. ..... p 3551 N92-29578
OLDEDAALHUIS, A. B. ..... p 3535 N92-29894
OLDING, BILL ..... p 3510 N92-29347
p 3404 N92-29506
OLIVEIRA, J. S. ..... p 3531 N92-29481
OLSDER, G. J. ..... p 3529 N92-29764
p 3529 N92-29963
OLSON, D. A. ..... p 3447 N92-30036
OLSON, D. L. ..... p 3525 N92-29624
ONEIL, STEPHEN V. ..... p 3418 N92-29901
ORLANDI, P. ..... p 3455 N92-30166
OSBORN, M. T. ..... p 3461 N92-29254
OSBORN, MARY T. ..... p 3460 N92-29248
OSTER, REINHOLD ..... p 3480 N92-29873
OSWALD, FRED B. ..... p 3478 N92-29697
OTOSHI, T. Y. ..... p 3431 N92-29372
OTT, EDWARD ..... p 3515 N92-29399
OTT, HEINZ-ALBERT ..... p 3566 N92-29841
OU, HSIEN-WANG ..... p 3504 N92-29439
OUT, D. J. ..... p 3530 N92-29983
OUTLAW, RONALD A. ..... p 3419 N92-30098
OVERDIJK, D. A. ..... p 3540 N92-29828
OVERMARS, J. F. M. ..... p 3490 N92-29728
OWEN, W. M., JR. ..... p 3409 N92-29370

P

PAGLIUGHI, F. M. ..... p 3465 N92-29282
PAIK, K. ..... p 3476 N92-29559
PAL, S. R. ..... p 3472 N92-29321
PALMER, D. A. ..... p 3417 N92-29551
PAMMER, R. ..... p 3473 N92-29469
PANDA, J. ..... p 3402 N92-30182
PAPEN, GEORGE C. ..... p 3470 N92-29311
p 3471 N92-29313
PARISE, J. B. ..... p 3418 N92-29619
PARK, C.-K. ..... p 3502 N92-29653
PARKS, GARY S. ..... p 3437 N92-30103
PARVANOV, O. ..... p 3466 N92-29286
PASCH, H. L. ..... p 3526 N92-29985
p 3526 N92-30074
PASMAN, D. G. ..... p 3531 N92-30143
PATT, B. E. ..... p 3549 N92-29502
PATTAY, R. S. ..... p 3528 N92-29550
PATTERSON, GRAEME P. ..... p 3472 N92-29320
PATTERSON, GRAEME R. ..... p 3456 N92-29230
PEARSON, ALLAN E. ..... p 3399 N92-29329
PEEBLES, D. E. ..... p 3426 N92-29908
PEER, R. G. ..... p 3503 N92-29800
PELTOLA, S. S. ..... p 3492 N92-29636
PENDERGRASS, W. R. ..... p 3503 N92-30034
PENNINGTON, M. R. ..... p 3544 N92-29488
p 3545 N92-29489
p 3545 N92-29490
PENNYCOOK, S. J. ..... p 3475 N92-30090
PERCEC, V. ..... p 3425 N92-29569
PERCEC, VIRGIL ..... p 3423 N92-29349
p 3424 N92-29508
p 3425 N92-29566
p 3425 N92-29567
p 3427 N92-30136
PEREZ, R. M. ..... p 3431 N92-29373
PERI, D. ..... p 3465 N92-29280
PERKINS, D. E. ..... p 3480 N92-29478
PETHERAM, J. C. ..... p 3407 N92-29299
PETHERAM, JOHN C. ..... p 3468 N92-29297
PETROS, MULGETA ..... p 3463 N92-29265
PETROS, MULUGETA ..... p 3469 N92-29302
PETROVIC, J. J. ..... p 3415 N92-29795
PETROVIC, Z. L. ..... p 3443 N92-30176
PFENNINGER, W. MATTHEW ..... p 3470 N92-29311
p 3471 N92-29313
PHAN, MINH Q. ..... p 3488 N92-30214
PHELPS, A. V. ..... p 3443 N92-30176
PIIRONEN, A. K. ..... p 3464 N92-29271
PIIRONEN, P. K. ..... p 3472 N92-29322
PIJPERS, E. W. ..... p 3512 N92-29871
PIN, F. G. ..... p 3528 N92-29550
PINDROH, ALBERT L. ..... p 3468 N92-29298
PLANK, L. ..... p 3541 N92-30174
PLATT, R. ..... p 3472 N92-29320
PLOURDE, J. V. ..... p 3512 N92-29538
POEL, MANNES ..... p 3536 N92-29956
POINSOT, T. J. ..... p 3450 N92-30061
p 3454 N92-30160
POLITES, M. E. ..... p 3429 N92-29677
POLLACK, J. B. ..... p 3455 N92-30168
POLLE, V. ..... p 3491 N92-30231
PONSE, ALBAN ..... p 3522 N92-29994
POOL, K. H. ..... p 3420 N92-29436
POORTEMA, KLAAS ..... p 3540 N92-29975
POPOV, A. G. ..... p 3467 N92-29293
PORKOLAB, M. ..... p 3553 N92-29336
PORSCHING, THOMAS A. ..... p 3478 N92-29392
PORTENEUVE, J. ..... p 3462 N92-29260
POSNER, EDWARD C. ..... p 3429 N92-29364
POTTER, SCOTT A. ..... p 3479 N92-29785
POTTS, RUSSELL O. ..... p 3510 N92-29577
POWERS, L. ..... p 3554 N92-29531
PRAGER, M. ..... p 3422 N92-29807
PRAS, AIKO ..... p 3526 N92-29958
p 3437 N92-29959
p 3437 N92-29984
PRATT, C. L. ..... p 3480 N92-29478
PREVOST, MICHAEL ..... p 3512 N92-29413
PRIBLUDA, I. ..... p 3472 N92-29321
PRICE, E. W. ..... p 3427 N92-29330
PRINN, RONALD G. ..... p 3457 N92-29235
PROVANCHA, JANE A. ..... p 3492 N92-29430
PROVIDAKES, J. ..... p 3436 N92-29902
PUERSTL, F. ..... p 3473 N92-29469
PUHEK, PETER ..... p 3539 N92-29585
PURTILL, M. R. ..... p 3531 N92-29481
PURTSCHER, P. T. ..... p 3422 N92-29803

Q

QIAN, JUN ..... p 3470 N92-29311
QIU, JINHUAN ..... p 3467 N92-29292
p 3468 N92-29294
QUATTLEBAUM, MARTIN ..... p 3404 N92-29506
QUICK, C. R. ..... p 3465 N92-29279
QUICK, C. R., JR. ..... p 3464 N92-29275

R

RACHELE, HENRY ..... p 3502 N92-29565
RAGNARSON, P. ..... p 3464 N92-29273
RAJPAL, SANDEEP ..... p 3517 N92-29665
RAKELS, J. L. L. ..... p 3507 N92-29735
RAMULU, M. ..... p 3404 N92-29511
RAO, A. S. ..... p 3415 N92-29723
RAPUC, M. ..... p 3399 N92-30232
RARIDON, R. J. ..... p 3413 N92-29461
RASH, CLARENCE E. ..... p 3512 N92-29348
RAY, RONALD J. ..... p 3405 N92-29425
REAGAN, J. A. ..... p 3473 N92-29327
REAMY, PHILIP C. ..... p 3439 N92-29405
REDA, DANIEL C. ..... p 3446 N92-29954
REE, MALCOLM J. ..... p 3511 N92-29620
REED, B. ..... p 3533 N92-29864
REES, B. J. ..... p 3421 N92-29587
REGAN, CURTIS P. ..... p 3462 N92-29264
REGISTER, JEFF ..... p 3399 N92-30122
REHM, RONALD R. ..... p 3418 N92-29744
REIBOLD, R. A. ..... p 3495 N92-30211
REID, ROBERT J. ..... p 3441 N92-29900
REIJNEVELD, A. ..... p 3489 N92-29493
REINHARDT, F. W. ..... p 3440 N92-29518
REISS, EDWARD L. ..... p 3543 N92-29543
REITHMAIER, KARL ..... p 3463 N92-29265
REJ, D. J. ..... p 3556 N92-30203
RENGER, WOLFGANG ..... p 3462 N92-29258
p 3469 N92-29305
RESING, JACOBUS ADRIANUS CORNELIS
p 3529 N92-29962
p 3529 N92-29963
p 3530 N92-29964
p 3530 N92-29965
p 3530 N92-29966
RESSL, R. ..... p 3423 N92-29940
RHEE, DOJUN ..... p 3517 N92-29665
RICHARD, G. A. ..... p 3416 N92-29355
RIDE, S. ..... p 3490 N92-30088
RIEDELBAUCH, S. ..... p 3401 N92-29713
RIEDLER, WILLIBALD ..... p 3473 N92-29469
p 3428 N92-29470
RILEY, R. A., JR. ..... p 3555 N92-29917
RITCHIE, R. O. ..... p 3414 N92-29556
RIVERS, JAMES M. ..... p 3481 N92-29342
RIZI, V. ..... p 3462 N92-29260
ROBBINS, DANIEL J. ..... p 3439 N92-29443
ROBE, R. Q. ..... p 3512 N92-29538
ROBERTS, R. R. ..... p 3421 N92-29623
ROBERTSON, GLEN A. ..... p 3426 N92-29831
ROBINSON, J. M. ..... p 3545 N92-29634
ROBINSON, R. J. ..... p 3469 N92-29300
ROBISON, JENNIFER L. ..... p 3424 N92-29496
RODRIGUEZ, R. ..... p 3541 N92-30174
ROELOFS, MARCEL ..... p 3537 N92-30078
ROEMER, M. G. M. ..... p 3493 N92-29499
ROFHEART, MARTIN ..... p 3516 N92-29622
ROGALLO, R. S. ..... p 3448 N92-30047
ROGERS, F. J. ..... p 3555 N92-29798
ROGOWSKI, ROBERT S. ..... p 3553 N92-30029
ROHLFING, E. A. ..... p 3417 N92-29459
ROLLINS, COURTNEY H. ..... p 3462 N92-29264
ROMEIN, B. ..... p 3508 N92-29738
p 3509 N92-29758
p 3509 N92-29759
p 3509 N92-29760
ROSE, CHERYL A. ..... p 3416 N92-30208
ROSENDAL, H. E. ..... p 3502 N92-29743
ROTE, D. M. ..... p 3478 N92-29534
ROTHMAN, B. ..... p 3420 N92-29483
ROWLAND, CARROLL W. ..... p 3462 N92-29264
ROWLES, STEVE H. ..... p 3400 N92-29539
RUANE, R. E. ..... p 3470 N92-29309
RUDERMAN, M. ..... p 3490 N92-30088
RUEDENAUER, FRIEDRICH G. ... p 3473 N92-29469
p 3426 N92-29470
RUGGIER, C. J. ..... p 3433 N92-29386
RUGGIERO, A. J. ..... p 3475 N92-29358
RULE, D. ..... p 3422 N92-29803

RUSSELL, DAVID L. ..... p 3532 N92-29589
RYAN, FRANK J. ..... p 3433 N92-29395

S

SADDOUGHI, SEYED G. ..... p 3447 N92-30042
SAJDA, PAUL ..... p 3511 N92-29560
SAKURADA, MASAMI ..... p 3502 N92-29666
SALAMA, AHARON ..... p 3444 N92-29524
SALIBRA, ANTONINO ..... p 3522 N92-29981
SAMPATH, SAM N. ..... p 3485 N92-30112
SAMUELS, DAVID C. ..... p 3449 N92-30049
SANCHEZ, O. ..... p 3433 N92-29389
SANDBERG, L. ..... p 3546 N92-29715
SANDH, R. S. ..... p 3415 N92-29594
SANDHU, RANBIR S. ..... p 3415 N92-29593
SASANO, Y. ..... p 3459 N92-29242
p 3460 N92-29250
SASANO, YASUHIRO ..... p 3465 N92-29277
SASSEN, KENNETH ..... p 3472 N92-29323
SATO, KUNIHIRO ..... p 3555 N92-30091
p 3555 N92-30172
SATORIUS, E. ..... p 3433 N92-29389
SAVAGE, M. ..... p 3478 N92-29351
SAVELSBERGH, M. W. P. ..... p 3516 N92-29608
SCARAMELLA, R. ..... p 3566 N92-29838
SCHAPPERT, G. T. ..... p 3555 N92-29789
SCHEMM, J.-K. ..... p 3502 N92-29653
SCHEPERS, RIA ..... p 3531 N92-30184
SCHERRER, DANIEL R. ..... p 3470 N92-29311
p 3471 N92-29314
SCHILDBACH, M. A. ..... p 3475 N92-29340
SCHINDLER, SABINE ..... p 3567 N92-29849
p 3568 N92-29851
SCHMELZ, JOAN T. ..... p 3570 N92-29632
SCHMIDT-PETERSEN, R. I. ..... p 3489 N92-29701
SCHMIDT, HANS-J. ..... p 3402 N92-30123
SCHMITT, R. W. ..... p 3506 N92-29806
SCHNOEBELEN, P. ..... p 3532 N92-29573
p 3532 N92-29574
SCHOENENBORN, F. ..... p 3462 N92-29259
SCHOT, JEROEN ..... p 3437 N92-29959
SCHRA, L. ..... p 3482 N92-29603
SCHRECKENGHOST, DEBRA L. ..... p 3513 N92-29403
SCHRIJNER, PAULINE ..... p 3536 N92-29999
SCHRIJVER, A. ..... p 3533 N92-29864
SCHROEDER, P. ..... p 3495 N92-30173
SCHUBERT, S. ..... p 3502 N92-29653
SCHUECKER, PETER ..... p 3566 N92-29841
SCHULZE, CHRISTOPH ..... p 3456 N92-29231
SCHUTTE, LEON ..... p 3526 N92-29958
p 3437 N92-29984
SCHWANK, J. R. ..... p 3439 N92-29455
SCHWARZ, RAIMUND A. ..... p 3568 N92-29851
SCHWARZENBERGER, P. M. ..... p 3469 N92-29300
SCHWENK, E. B. ..... p 3420 N92-29436
SCOLLO, GIUSEPPE ..... p 3522 N92-29981
SCOTT, H. A. ..... p 3476 N92-29509
SCOTT, J. W. ..... p 3407 N92-29299
SCOTTI, STEPHEN J. ..... p 3447 N92-30024
SCOUT, JOHN B. ..... p 3435 N92-29576
SCUDDER, D. W. ..... p 3555 N92-29917
SEDDON, M. J. ..... p 3475 N92-30090
SEHER, CHRIS C. ..... p 3481 N92-30116
SENEKOWITSCH, JOERG ..... p 3418 N92-29901
SENFT, DANIEL C. ..... p 3470 N92-29311
p 3471 N92-29314
SENSBURG, O. ..... p 3404 N92-29650
SEPPALA, L. G. ..... p 3551 N92-29484
SERIKOV, I. B. ..... p 3467 N92-29293
SEYBERT, A. F. ..... p 3478 N92-29697
SEYFERTH, DIETMAR ..... p 3424 N92-29496
p 3419 N92-29941
SEZE, G. ..... p 3463 N92-29268
SHAKLAN, S. B. ..... p 3409 N92-29370
SHANEYFELT, M. R. ..... p 3439 N92-29455
SHANKAR, RENUKA ..... p 3512 N92-29413
SHAVER, PETER A. ..... p 3566 N92-29842
SHAW, B. A. ..... p 3421 N92-29587
SHAW, S. M. ..... p 3505 N92-29684
SHEA, CHARLOTTE ..... p 3408 N92-30016
SHEARER, MICHAEL ..... p 3443 N92-29458
SHEIFER, I. C. ..... p 3494 N92-30019
SHEN, HUBERT H. ..... p 3452 N92-30071
SHEPHERD, B. ..... p 3533 N92-29864
SHEPHERD, WILLIAM T. ..... p 3487 N92-30125
SHIELD, J. E. ..... p 3422 N92-29706
SHIH, T.-H. ..... p 3452 N92-30151
SHIMKAVEG, G. M. ..... p 3477 N92-29987
SHIN, D. S. ..... p 3451 N92-30065
SHLACHTER, J. S. ..... p 3555 N92-29917
SHORTRIDGE, ROBERT G. ..... p 3427 N92-29786
SHUMSKII, V. K. ..... p 3467 N92-29293
SHVETS, T. YA. ..... p 3544 N92-29415
SICKAFUS, K. E. ..... p 3424 N92-29479
SIGISMONDI, G. C. ..... p 3516 N92-29608
SIGMAN, R. K. ..... p 3427 N92-29330
SIKKEL, KLAAS ..... p 3536 N92-29956
p 3527 N92-30183
SIMEONOV, V. ..... p 3466 N92-29286
SIMEONOV, V. B. ..... p 3466 N92-29287
SIMS, C. S. ..... p 3547 N92-29910
SINGER, JOSEPH ..... p 3413 N92-29667
SINGH, UPENDRA N. ..... p 3458 N92-29238
p 3461 N92-29257
SINKE, J. ..... p 3415 N92-29702
SKEBERDIS, PAUL ..... p 3442 N92-29914
SKEENS, K. M. ..... p 3460 N92-29249
SKINNER, WILBERT R. ..... p 3465 N92-29281
SKJERVE, L. ..... p 3432 N92-29381
SLAVIN, A. C. ..... p 3470 N92-29309
SLUITER, M. ..... p 3559 N92-29911
SMAGA, J. A. ..... p 3440 N92-29518
SMIDT, D. ..... p 3515 N92-29418
SMITH, BETH W. ..... p 3407 N92-29709
SMITH, BRENT ..... p 3458 N92-29241
SMITH, GARY W. ..... p 3514 N92-29363
SMITH, H. D. ..... p 3420 N92-29436
SMITH, I. M. ..... p 3469 N92-29300
SMITH, J. ..... p 3401 N92-29884
SMITH, KEVIN C. ..... p 3440 N92-29529
SMITH, L. M. ..... p 3450 N92-30055
p 3453 N92-30156
SMITH, R. E. ..... p 3400 N92-29625
SNIDER, R. T. ..... p 3476 N92-29474
p 3474 N92-29942
SOANES, ROYCE W. ..... p 3515 N92-29487
SOBCZAK, G. ..... p 3480 N92-29478
SOESMAN, J. L. ..... p 3402 N92-29703
SOLOMON, G. ..... p 3431 N92-29375
SOMMARGREN, G. E. ..... p 3551 N92-29484
SOMMEIJER, B. P. ..... p 3526 N92-29867
SORBELLO, RICHARD S. ..... p 3417 N92-29423
SOWA, E. C. ..... p 3556 N92-29473
SPANGLER, STEVEN R. ..... p 3569 N92-29631
SPAULDING, GLENN ..... p 3427 N92-30100
SPECK, C. J. ..... p 3561 N92-29822
p 3561 N92-29823
SPELTEN, ROBERT ..... p 3401 N92-29889
SPENCER, J. E. ..... p 3437 N92-29988
SPESSARD, J. ..... p 3423 N92-29940
SPEZIALE, C. G. ..... p 3449 N92-30054
SPINHIRNE, JAMES D. ..... p 3459 N92-29246
p 3460 N92-29247
p 3463 N92-29266
SPINKS, DEBRA ..... p 3447 N92-30041
p 3452 N92-30149
SQUIRES, KYLE D. ..... p 3450 N92-30058
SRIDHARAN, GOVIND ..... p 3428 N92-30083
SROGA, J. T. ..... p 3407 N92-29299
STACEY, W. M. ..... p 3554 N92-29438
STAFFON, J. D. ..... p 3525 N92-29624
STARNES, JAMES H., JR. ..... p 3485 N92-30115
STARR, HAROLD P., JR. ..... p 3531 N92-29548
STATMAN, J. ..... p 3432 N92-29379
STAVELAND, LOWELL ..... p 3512 N92-29413
STAVN, ROBERT H. ..... p 3504 N92-29345
STEENHAGEN, HENNIE J. ..... p 3520 N92-29855
STEIGER, W. ..... p 3473 N92-29469
p 3428 N92-29470
STEIMLE, LAWRENCE J. ..... p 3553 N92-30084
STEIN, R. P. ..... p 3505 N92-29554
STEINBRECHT, W. ..... p 3458 N92-29237
p 3461 N92-29253
p 3472 N92-29321
STEINHARDT, P. ..... p 3452 N92-30140
STEINHOFF, JOHN ..... p 3399 N92-29361
STELZRIED, C. T. ..... p 3432 N92-29381
STENBY, JOHN L. ..... p 3474 N92-29571
STEPHEN, R. A. ..... p 3505 N92-29562
STEPHENS, D. B. ..... p 3489 N92-29701
STEPHENSON, STANLEY D. ..... p 3511 N92-29503
STEPOWSKI, D. ..... p 3417 N92-29431
STEUTEL, F. W. ..... p 3533 N92-29826
STEVENS, LINDA ..... p 3510 N92-30216
STEVENS, WILLIAM T. ..... p 3462 N92-29264
STEWART, G. C. ..... p 3567 N92-29844
STMARY, DONALD F. ..... p 3543 N92-29441
STOCKDALE, R. ..... p 3476 N92-29474
STOK, LEON ..... p 3519 N92-29782
STOLOFF, M. J. ..... p 3433 N92-29385
STOWE, MIKE ..... p 3562 N92-29720
STOYENKO, ALEXANDER D. ..... p 3519 N92-29815
p 3521 N92-29970
STREBEL, D. E. ..... p 3491 N92-30210
STREICHER, J. ..... p 3473 N92-29326
STRENG, M. ..... p 3537 N92-30147
STRETCH, D. ..... p 3455 N92-30169
STRINGFELLOW, G. B. ..... p 3556 N92-29429
p 3557 N92-29635
STROHECKER, R. ..... p 3421 N92-29623
STROHMANN, CARSTEN ..... p 3424 N92-29496
STROSNIDER, JAY K. ..... p 3515 N92-29409
STUCHBERY, A. E. ..... p 3549 N92-30213
STURGES, W. ..... p 3505 N92-29704
SU, D. H. ..... p 3518 N92-29745
SUAREZ, M. ..... p 3502 N92-29653
SUBBAIAH, PERLA ..... p 3541 N92-29976
SUGIMOTO, N. ..... p 3459 N92-29242
SUGIMOTO, NOBUO ..... p 3465 N92-29277
SUKAMTO, LIN M. ..... p 3437 N92-30103
SUN, JINHUI ..... p 3468 N92-29294
SUN, XIAOLI ..... p 3435 N92-29658
SUROVEGIN, ALEKSANDER L. ..... p 3467 N92-29290
SUSOEFF, A. R. ..... p 3438 N92-29339
SUTER, L. J. ..... p 3554 N92-29531
SVANBERG, S. ..... p 3464 N92-29273
SWAJA, R. E. ..... p 3547 N92-29910
SWANSON, B. I. ..... p 3545 N92-29634
SWYT, D. A. ..... p 3542 N92-29802
SYMON, J. ..... p 3528 N92-29550
SZAFLARSKI, DIANE M. ..... p 3418 N92-29901
SZALAY, ALEXANDER S. ..... p 3566 N92-29837
SZAPUDI, I. ..... p 3566 N92-29837
SZCZEBIOT, R. W. ..... p 3549 N92-29502
SZE, J. S. ..... p 3477 N92-29787
SZEKELEY, LASZLO A. ..... p 3523 N92-30186

T

TAIRA, TAKUNORI ..... p 3466 N92-29284
TALBI, E. G. ..... p 3525 N92-29610
TALLANT, D. R. ..... p 3426 N92-29908
TAN, Z. ..... p 3556 N92-29437
TANG, HAI C. ..... p 3418 N92-29744
TANIS, J. A. ..... p 3546 N92-29642
TANKALA, K. ..... p 3418 N92-29595
TAO, BENJAMIN ..... p 3426 N92-29905
TARBELL, THEODORE D. ..... p 3570 N92-30204
TAROKH, M. ..... p 3528 N92-29673
TAUSWORTHE, R. C. ..... p 3433 N92-29385
TAWEL, RAOUL ..... p 3442 N92-30086
TAYLOR, A. J. ..... p 3555 N92-29789
TEGNER, P.-E. ..... p 3546 N92-29715
TELLIER, L. ..... p 3464 N92-29275
TELLINGHUISEN, JOEL B. ..... p 3428 N92-29428
TEMAM, ROGER ..... p 3452 N92-30070
TEMKIN, R. J. ..... p 3477 N92-29937
TEMME, N. M. ..... p 3534 N92-29893
TENBRUMMELHUIS, PAUL ..... p 3540 N92-29856
TENHAVE, J. M. ..... p 3403 N92-29605
TERLAKY, TAMAS ..... p 3524 N92-30227
TERVOORT-ENGELEN, YVONNE MARIA THEODORA
p 3546 N92-29778
TESAR, A. ..... p 3551 N92-29578
THAKOOR, ANIL P. ..... p 3529 N92-29955
THAYER, J. P. ..... p 3407 N92-29283
THIESSEN, DAVID L. ..... p 3553 N92-30084
THIJSSE, BAREND J. ..... p 3558 N92-29767
p 3558 N92-29768
p 3558 N92-29769
p 3558 N92-29770
p 3558 N92-29771
p 3559 N92-29772
p 3559 N92-29773
THOERNGREN-ENGBLOM, P. ..... p 3546 N92-29715
THOMAS, J. F. ..... p 3416 N92-29355
THOMAS, J. L. ..... p 3433 N92-29385
THOMAS, P. ..... p 3500 N92-29690
THOMPSON, DONALD O. ..... p 3481 N92-30119
THOMPSON, K. W. ..... p 3454 N92-30163
p 3455 N92-30168
THOMPSON, RAY ..... p 3463 N92-29265
THOMPSON, W. M. ..... p 3495 N92-30211
THOMSEN, M. F. ..... p 3500 N92-29536
THUAN, TRINH X. ..... p 3565 N92-29596
THURMAN, S. W. ..... p 3409 N92-29368
TICEHURST, J. M. ..... p 3477 N92-29987
TIEE, J. J. ..... p 3465 N92-29279
TIEE, J. J., JR. ..... p 3464 N92-29275
TINGEY, D. T. ..... p 3495 N92-30021
TIRRES, LIZET ..... p 3399 N92-29402
TKACHOV, F. V. ..... p 3518 N92-29747
p 3546 N92-29750
TOLK, NORMAN H. ..... p 3428 N92-29428
p 3407 N92-29664
TOMAZOS, DIMITRIS ..... p 3424 N92-29508
p 3427 N92-30136
TONG, P. ..... p 3485 N92-30112
TONN, B. ..... p 3527 N92-29504
TOOMARIAN, NIKZAD ..... p 3530 N92-30085
TOPKA, KENNETH P. ..... p 3570 N92-30204
TORKAR, K. ..... p 3428 N92-29470
TORKI, K. ..... p 3516 N92-29621
TOUEG, SAM ..... p 3515 N92-29400
TOWNSEND, LAWRENCE W. ..... p 3547 N92-30002
p 3548 N92-30011

TRACEY, IAN ..... p 3437 N92-29984
TRACY, HENRY J. ..... p 3424 N92-29496
TRAPP, G. H. ..... p 3502 N92-29743
TRATT, DAVID ..... p 3459 N92-29246
TRATT, DAVID M. ..... p 3460 N92-29247
TREBES, J. E. ..... p 3477 N92-29987
TREBINO, R. ..... p 3476 N92-29516
TREIMAN, S. ..... p 3490 N92-30088
TRETMANS, JAN ..... p 3517 N92-29705
TREUHAFT, R. N. ..... p 3430 N92-29367
TREUMANN, RUDOLF A. ..... p 3565 N92-29833
TRIPP, JAMES S. ..... p 3402 N92-30124
TROMP, JOHN ..... p 3523 N92-30146
TROTTA, J. E. ..... p 3407 N92-29299
TROUESSIN, GILLES ..... p 3526 N92-29888
TROUVE, A. ..... p 3450 N92-30062
TRUEMPER, JOACHIM E. ..... p 3567 N92-29850
p 3568 N92-29851
TSUKRUT, V. ..... p 3425 N92-29569
TUNICK, ARNOLD ..... p 3502 N92-29565
TURCHI, P. E. A. ..... p 3559 N92-29911
TURNER, R. M. ..... p 3461 N92-29255
TURNER, W. ..... p 3443 N92-30092
TWILT, F. ..... p 3537 N92-30147
TYGIELSKI, MICHELE ..... p 3408 N92-30016

U

UCHINO, OSAMU ..... p 3457 N92-29234
UDINK, R. T. ..... p 3522 N92-30073
ULITSKY, ARKADY ..... p 3458 N92-29241
UPPERMAN, P. M. ..... p 3532 N92-29742

V

VALINO, LUIS ..... p 3450 N92-30060
VALKERING, T. P. ..... p 3536 N92-29979
VANBEEK, P. ..... p 3444 N92-29763
VANBERKUM, E. E. M. ..... p 3532 N92-29742
p 3540 N92-29828
VANBRUNSCHOT, P. K. G. M. ..... p 3529 N92-29764
VANDALSEM, W. R. ..... p 3400 N92-29625
VANDAMME, R. M. J. ..... p 3560 N92-30148
VANDAMME, RUUD ..... p 3533 N92-29858
VANDEFLIERT, B. W. ..... p 3446 N92-29977
VANDERBURG, J. W. ..... p 3560 N92-30148
VANDERGRAAF, ANJA ..... p 3559 N92-29773
VANDERHEIJDEN, G. ..... p 3523 N92-30144
VANDERHEIJDEN, REINIER THOMAS JACOBUS M.
p 3508 N92-29754
p 3508 N92-29755
p 3509 N92-29756
p 3509 N92-29757
p 3509 N92-29758
p 3509 N92-29759
p 3509 N92-29760
VANDERHOEVEN, W. ..... p 3478 N92-29602
VANDERHOUWEN, P. J. ..... p 3526 N92-29867
VANDERLAAN, PAUL ..... p 3540 N92-29827
VANDERLEEDEN, M. C. ..... p 3419 N92-30196
VANDERMAST, CHARLES ..... p 3521 N92-29887
VANDERSCHAFT, A. J. ..... p 3537 N92-30077
VANDERSEE, W. ..... p 3462 N92-29259
VANDERVEGT, J. J. W. ..... p 3451 N92-30063
p 3451 N92-30064
p 3454 N92-30161
VANDERVET, PAUL E. ..... p 3426 N92-29960
VANDERVLOEDT, THONY ..... p 3437 N92-29959
VANDERVOORT, M. H. ..... p 3521 N92-29891
VANDERWAL, J. ..... p 3561 N92-29822
p 3561 N92-29823
VANDERWEL, F. J. M. ..... p 3489 N92-29693
VANDERWIELE, P. J. ..... p 3493 N92-29497
VANDESANDEN, MAURITIUS CORNELIUS MARIA
p 3555 N92-29761
VANDEURSEN, A. ..... p 3522 N92-29989
VANDEWEG, ROB L. W. ..... p 3519 N92-29816
VANDEWETERING, HUBERTUS MARTINUS MARIA
p 3518 N92-29776
VANDIJK, A. ..... p 3491 N92-30231
VANDOORN, ERIK A. ..... p 3536 N92-29999
VANDOORN, J. T. M. ..... p 3512 N92-29871
VANDRESAR, N. T. ..... p 3427 N92-29669
VANEIJKEREN, J. C. H. ..... p 3446 N92-29947
VANENGELEN, J. A. J. ..... p 3404 N92-29616
VANGROESEN, E. ..... p 3437 N92-29978
VANGROESEN, E. W. C. ..... p 3446 N92-29977
VANHOESEL, STAN ..... p 3520 N92-29818
p 3520 N92-29819
p 3520 N92-29820
VANKATWIJK, J. ..... p 3518 N92-29712
VANMOORSEL, AAD P. A. ..... p 3526 N92-29880
p 3514 N92-29982
VANNOOYEN, R. R. P. ..... p 3536 N92-29946
VANOORSCHOT, JAN ..... p 3436 N92-29824
p 3525 N92-29825
VANPUL, MARK C. ..... p 3520 N92-29865
VANPUL, MARK C. J. ..... p 3523 N92-30179
VANSTERKENBURG, STEFANUS WOLFGANG PAULUS
p 3559 N92-29783
VANSWOL, R. ..... p 3490 N92-29717
VANSWOL, R. W. ..... p 3490 N92-29707
VANWOERKOM, P. T. L. M. ..... p 3479 N92-29885
VANZANTEN, A. J. ..... p 3536 N92-29924
VARMA, R. ..... p 3424 N92-29479
VASTANO, J. A. ..... p 3453 N92-30157
VASUDEVAMURTHY, A. S. ..... p 3534 N92-29883
VASUDEVAN, A. K. ..... p 3415 N92-29795
VEERAVALLI, S. V. ..... p 3453 N92-30154
VEERAVALLI, SRINIVAS V. ..... p 3447 N92-30042
VEIGA, ROBERT E. ..... p 3457 N92-29236
VELLINGA, P. ..... p 3493 N92-29497
VELS, L. L. ..... p 3489 N92-29693
VELTMAN, FRANK ..... p 3532 N92-29685
VENGSARKAR, A. M. ..... p 3550 N92-29331
VERHAGE, L. ..... p 3489 N92-29493
VERHOEF, W. ..... p 3490 N92-29717
VERMASEREN, J. A. M. ..... p 3518 N92-29747
p 3546 N92-29750
VERMEER, J. ..... p 3535 N92-29919
p 3535 N92-29920
VERSENDAAL, JOHAN ..... p 3521 N92-29887
VERVERS, FRANS ..... p 3524 N92-30228
VERWER, J. G. ..... p 3534 N92-29883
p 3446 N92-29947
VESS, T. M. ..... p 3550 N92-29337
VETTOLANI, G. ..... p 3566 N92-29838
VIERRA, R. ..... p 3491 N92-29476
VIG, JOHN R. ..... p 3439 N92-29498
VIITANEN, M. ..... p 3441 N92-29912
p 3442 N92-30089
VILLANE, RON ..... p 3463 N92-29265
VILSMEIER, J. ..... p 3404 N92-29650
VIOLERO, PASCAL ..... p 3529 N92-29678
VIPOND, LESLIE K. ..... p 3487 N92-30127
VISCONTI, G. ..... p 3462 N92-29260
VITANYI, PAUL M. B. ..... p 3520 N92-29868
VITKO, TODD R. ..... p 3554 N92-29528
VOGEL, A. A. ..... p 3400 N92-29625
VOGELAAR, H. J. L. ..... p 3512 N92-29871
VOGES, WOLFGANG ..... p 3568 N92-29851
VOGT, S. ..... p 3500 N92-29690
VOJDANI, D. ..... p 3546 N92-29715
VOLLATH, D. ..... p 3424 N92-29479
VOLZ, RICHARD A. ..... p 3514 N92-29363
VONCOSSART, G. ..... p 3459 N92-29244
VREMAN, A. W. ..... p 3446 N92-29972
VURAL, SINAN ..... p 3521 N92-29961

W

WAARTS, JACOB J. ..... p 3535 N92-29922
WACLAWIK, RONALD E. ..... p 3475 N92-30202
WAGELMANS, ALBERT ..... p 3520 N92-29818
p 3520 N92-29819
p 3520 N92-29820
WAGNER, C. G. ..... p 3439 N92-29414
WAHLIN, E. K. ..... p 3555 N92-29789
WAIDMANN, WINFRIED ..... p 3447 N92-29998
WAKELKAMP, WILHELMUS JACOBUS JOHANNES
p 3546 N92-29777
WALDROP, RAYMOND S. ..... p 3514 N92-29363
WALEFFE, F. ..... p 3453 N92-30158
WALEFFE, FABIAN ..... p 3448 N92-30044
WALKER, KEVIN B. ..... p 3514 N92-29391
WALL, K. F. ..... p 3470 N92-29310
WALLACE-ROBINSON, JANICE ..... p 3509 N92-29341
WALLACE, S. ..... p 3469 N92-29300
WALLACE, TERRYL A. ..... p 3423 N92-30205
WALLINDER, E. ..... p 3464 N92-29273
WALLING, R. S. ..... p 3477 N92-29987
WALSER, RODGER M. ..... p 3420 N92-29426
WALTER, PATRICK L. ..... p 3481 N92-30120
WANDINGER, ULLA ..... p 3456 N92-29231
WANG, A. ..... p 3550 N92-29331
p 3551 N92-29652
WANG, G. Z. ..... p 3550 N92-29331
p 3551 N92-29652
WANG, M. ..... p 3549 N92-29502
WANG, P. ..... p 3443 N92-30092
WANG, SHUFANG ..... p 3467 N92-29292
WANG, TIN-YU ..... p 3458 N92-29241
WANG, WENMING ..... p 3467 N92-29292
WANG, XUN-LI ..... p 3559 N92-29939
WANG, YI-MIN ..... p 3517 N92-29695
WANHILL, R. J. H. ..... p 3482 N92-29603
p 3483 N92-29708
WATANABE, HIROYUKI ..... p 3528 N92-29550
WATMUFF, J. H. ..... p 3453 N92-30153
WATZLAWICK, ROBERT ..... p 3405 N92-29927
WEATHERS, GLENN D. ..... p 3435 N92-29572
WEAVER, F. J. ..... p 3407 N92-29299
WEBB, R. H. ..... p 3477 N92-29928
WEI, JIE ..... p 3550 N92-29475
WEIGLE, BRETT D. ..... p 3531 N92-29446
WEITKAMP, CLAUS ..... p 3456 N92-29231
WELSH, S. ..... p 3505 N92-29704
WEN, T. ..... p 3505 N92-29554
WERNER, CH. ..... p 3473 N92-29326
WERTH, G. C. ..... p 3493 N92-29597
WESEMANN, LARS ..... p 3419 N92-29941
WESSELIUS, JACCO ..... p 3518 N92-29711
p 3524 N92-30228
WESSELS, J. ..... p 3539 N92-29606
WESSELS, JAAP ..... p 3532 N92-29607
p 3535 N92-29898
WEST, P. ..... p 3554 N92-29412
WESTERVELT, R. ..... p 3452 N92-30140
WHEALTON, J. H ..... p 3413 N92-29461
WHIRLEY, R. G. ..... p 3481 N92-29338
p 3533 N92-29791
p 3533 N92-29792
WHITEHEAD, VICTOR S. ..... p 3552 N92-30027
WHITEMAN, D. N. ..... p 3457 N92-29233
WHITEWAY, JAMES A. ..... p 3466 N92-29285
WHITT, WARD ..... p 3538 N92-29500
WIDYA, I. ..... p 3523 N92-30144
WIEDEMANN, KARL E. ..... p 3423 N92-30205
WIGINTON, MARGARET ..... p 3408 N92-30016
WIJNEN, JACK T. M. ..... p 3539 N92-29609
WILLETTS, D. V. ..... p 3469 N92-29300
WILLIAMS, DAVID R. ..... p 3511 N92-29591
WILLIAMS, MARC H. ..... p 3400 N92-29445
WILLIAMSON, R. L. ..... p 3421 N92-29623
WILLIS, P. A. ..... p 3431 N92-29374
WILLIS, RON J. ..... p 3464 N92-29274
WILLSON, ROBERT F. ..... p 3570 N92-29632
WILMS, R. J. G. ..... p 3540 N92-29821
WILSCHUT, ANNITA N. ..... p 3527 N92-30142
WILSON, ALEX ..... p 3471 N92-29317
WILSON, JOHN C. ..... p 3406 N92-30025
WILSON, R. B. ..... p 3563 N92-30039
WINDISCH, C. F., JR. ..... p 3420 N92-29411
WINFREE, WILLIAM P. ..... p 3480 N92-29829
p 3481 N92-30118
WINJUM, J. K. ..... p 3495 N92-30173
WINKER, D. M. ..... p 3461 N92-29254
WINKER, DAVID M. ..... p 3460 N92-29248
WINOKUR, P. S. ..... p 3439 N92-29455
WIRTH, MARTIN ..... p 3462 N92-29258
p 3469 N92-29305
WISE, J. A. ..... p 3569 N92-29600
WISSINGER, A. B. ..... p 3462 N92-29263
WISSINGER, ALAN B. ..... p 3468 N92-29297
WITTENSTEIN, J. ..... p 3410 N92-29480
WLODYKA, R. A. ..... p 3564 N92-29809
WOLFE, WILLIAM E. ..... p 3415 N92-29593
p 3415 N92-29594
WONG, D. K. ..... p 3440 N92-29523
WOOD, S. A. ..... p 3463 N92-29270
WOODS, D. C. ..... p 3461 N92-29254
WOODS, K. D. ..... p 3491 N92-30210
WOODWARD, CHARLES ..... p 3518 N92-29749
WOUTERLOOD, D. ..... p 3524 N92-30195
WRIGHT, WILLIE ..... p 3410 N92-30217
p 3411 N92-30218
p 3411 N92-30219
p 3411 N92-30220
p 3411 N92-30221
p 3411 N92-30222
p 3412 N92-30223
p 3412 N92-30224
p 3412 N92-30225
WU, C.-Y. ..... p 3502 N92-29653
WU, D. I. ..... p 3437 N92-30093
WU, SHAOMING ..... p 3467 N92-29292
WU, X. F. ..... p 3478 N92-29697
WU, YUNYAN ..... p 3552 N92-29859
WYNN, W. M. ..... p 3434 N92-29563

X

XIA, QILIN ..... p 3468 N92-29294
XIA, XINFU ..... p 3414 N92-29460
XUELIANG, LI ..... p 3538 N92-30185

Y

YAHIAMESSAOUD, ABDELLATIF ..... p 3422 N92-29674
YAMAMOTO, TAKANOBU ..... p 3466 N92-29284
YANG, J. N. ..... p 3501 N92-29950
YANNAKAKIS, MIHALIS ..... p 3523 N92-30146
YATES, JOHN T., JR. ..... p 3418 N92-29719

YORKE, JAMES A. ..... p 3515 N92-29399
YOUNG, CLARENCE P., JR. ..... p 3406 N92-29352
YOUNG, P. W. ..... p 3464 N92-29272
YOUNG, STUART A. ..... p 3456 N92-29230
p 3472 N92-29320
YOUNGDAHL, C. K. ..... p 3482 N92-29535
YU, JEFFREY W. ..... p 3552 N92-29832
YU, JUIN S. ..... p 3492 N92-29662
YUHAS, ANDREW J. ..... p 3405 N92-29425

Z

ZACKRISSON, MIKAEL ..... p 3519 N92-29780
ZAMAN, K. B. M. Q. ..... p 3402 N92-30182
ZAMORANI, GIOVANNI ..... p 3566 N92-29838
ZANDBERGEN, P. J. ..... p 3446 N92-29972
p 3560 N92-30148
ZANNER, F. J. ..... p 3421 N92-29623
ZEGELING, PAUL A. ..... p 3446 N92-29947
ZEMAN, O. ..... p 3449 N92-30050
p 3452 N92-30150
ZERO, J. ..... p 3502 N92-29653
ZHANG, JINDING ..... p 3468 N92-29294
ZHANG, X. G. ..... p 3556 N92-29473
p 3436 N92-29909
ZHAO, HONGJIE ..... p 3472 N92-29323
ZHAO, YANZENG ..... p 3465 N92-29278
ZHENG, QIANG ..... p 3425 N92-29567
ZHENG, SIPING ..... p 3467 N92-29292
ZHOU, JUN ..... p 3460 N92-29252
ZHOU, YE ..... p 3448 N92-30046
ZIJM, W. H. M. ..... p 3539 N92-29606
ZONDAG, E. G. ..... p 3523 N92-30181
ZOURIDES, VICTOR G. ..... p 3442 N92-29914
ZUCK, D. D. ..... p 3528 N92-29673
ZWAAL, ENNELIENA AAFFIENA ELFRIEDE
p 3558 N92-29753
ZWIERS, JOB ..... p 3536 N92-29956

Typical Corporate Source Index Listing

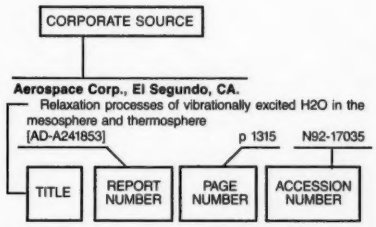

Listings in this index are arranged alphabetically by corporate source. The title of the document provides the user with a brief description of the subject matter. The report number helps to indicate the type of document cited (e.g., NASA report, translation, NASA contractor report). The accession number denotes the number by which the citation is identified. The page number helps you locate the citation in the abstract section. The titles are arranged under each corporate source in ascending accession number order.

A

ACADEMIA SINICA, BEIJING (CHINA).
A developing multiple-wavelength lidar for detecting mainly ozone and aerosol distributions in the stratosphere p 3467 N92-29292

Lidar observations of stratospheric clouds after volcanic eruption of Pinatubo p 3468 N92-29294

ACADEMY OF SCIENCES OF THE UKRAINIAN SSR, KIEV.
Electron spectra of adatomic structures
[DE92-625013] p 3544 N92-29415

ACADEMY OF SCIENCES (USSR), MOSCOW.
Laser remote sensing of pollution on water surfaces p 3467 N92-29290

ACADEMY OF SCIENCES (USSR), NOVOSIBIRSK.
On the two-dimensional model of quantum Regge gravity
[DE92-624516] p 3560 N92-30212

ACADEMY OF SCIENCES (USSR), TOMSK.
An extension of the Raman-lidar technique to measure the velocity and temperature of the atmospheric emission jets from stacks p 3467 N92-29293

AERONAUTICAL RESEARCH LABS., MELBOURNE (AUSTRALIA).
Stresses and strains in plain and coldworked annuli subjected to remote, interference or combined loading
[ARL-STRUC-R-446] p 3482 N92-29672

AERONAUTICAL SYSTEMS DIV., WRIGHT-PATTERSON AFB, OH.
Damage tolerance for commuter aircraft p 3485 N92-30114

AIR FORCE CENTER FOR ENVIRONMENTAL EXCELLENCE, BROOKS AFB, TX.
Final Environmental Impact Statement (EIS) for the Space Nuclear Thermal Propulsion (SNTP) program
[AD-A248408] p 3413 N92-29903

Final Environmental Impact Statement (EIS) for the Space Nuclear Thermal Propulsion (SNTP) program: Appendices
[AD-A248409] p 3413 N92-29904

AIR FORCE FLIGHT TEST CENTER, EDWARDS AFB, CA.
Feasibility of an antiproton catalyzed fission fragment rocket
[AD-A248157] p 3412 N92-29444

AIR FORCE INST. OF TECH., WRIGHT-PATTERSON AFB, OH.
Experimental evaluation of incorporating digital and analog integrated circuit die on a common substrate utilizing silicon-hybrid wafer-scale integration technology
[AD-A248182] p 3439 N92-29405

Developing CMMCA flight profiles for cruise missile tracking
[AD-A248183] p 3434 N92-29406

Design and construction of a channel electron multiplier based Mossbauer spectroscopy system
[AD-A248154] p 3439 N92-29443

An analysis of the endurance of mobile satellite command and control systems
[AD-A248084] p 3410 N92-29525

Design and analysis of electrical circuits that produce fractional-order differentiation
[AD-A248085] p 3440 N92-29526

An examination of hypercube implementations of genetic algorithms
[AD-A248092] p 3515 N92-29527

Numerical analysis of plasma transport in tandem volume magnetic multicusp ion sources
[AD-A248093] p 3554 N92-29528

A response surface methodology study of ferroelectric memory devices
[AD-A248094] p 3440 N92-29529

Boolean reasoning and informed search in the minimization of logic circuits
[AD-A248110] p 3528 N92-29561

A sensitivity analysis of circular error probable approximation techniques
[AD-A248105] p 3539 N92-29585

Optimization of stochastic response surfaces subject to constraints with linear programming
[AD-A248108] p 3516 N92-29586

AIR FORCE OFFICE OF SCIENTIFIC RESEARCH, BOLLING AFB, WASHINGTON, DC.
The 1991 research highlights
[AD-A247865] p 3570 N92-29464

AIRBUS INDUSTRIE, BLAGNAC (FRANCE).
Ageing airplane repair assessment program for Airbus A300 p 3402 N92-30123

ALABAMA UNIV., HUNTSVILLE.
GLObal Backscatter Experiment (GLOBE) results: Aerosol backscatter global distribution and wavelength dependence p 3459 N92-29245

ALLIED-SIGNAL AEROSPACE CO., KANSAS CITY, MO.
Robotic workcell for wire wrapping integrated circuits
[DE92-013999] p 3441 N92-29796

AMERICAN CHEMICAL SOCIETY, PRINCETON, NJ.
Electrochemistry in colloids and dispersions. Volume 1: Electroanalytical methods and applications, electrosynthesis and electrocatalysis, polymers and latexes
[AD-A248335] p 3418 N92-29557

Electrochemistry in colloids and dispersions. Volume 2: Solute distribution, diffusion, and transport colloidal metals
[AD-A248336] p 3419 N92-29931

Electrochemistry in colloids and dispersions. Volume 3: Colloidal semiconductors
[AD-A248337] p 3419 N92-29932

AMES LAB., IA.
Electrical, optical, and magnetic resonance studies of novel pi-conjugated polymers
[DE92-012548] p 3424 N92-29482

Structure and stability of Al-Cu-Ru face-centered icosahedral alloys
[DE92-012550] p 3422 N92-29706

Neutron diffraction study of the electronic structure of high T(sub c) superconductor-related compounds
[DE92-012587] p 3559 N92-29939

AMSTERDAM UNIV. (NETHERLANDS).
Defaults in update semantics
[ITLI-LP-91-02] p 3532 N92-29685

Dynamic semantics and circular propositions
[ITLI-LP-91-03] p 3532 N92-29687

ANACAPA SCIENCES, INC., FORT RUCKER, AL.
Assessment of army aviators' ability to perform individual and collective tasks in the aviation networked simulator
[AD-A250293] p 3407 N92-29709

ANALYSIS AND TECHNOLOGY, INC., NEW LONDON, CT.
Evaluation of Night Vision Goggles (NVG) for maritime search and rescue
[AD-A247182] p 3512 N92-29538

ANHUI INST. OF OPTICS AND FINE MECHANICS, HEFEI (CHINA).
L625 lidar measurements of Pinatubo volcanic cloud at Hefei p 3460 N92-29252

ARGONNE NATIONAL LAB., IDAHO FALLS, ID.
A universal, fault-tolerant, non-linear analytic network for modeling and fault detection
[DE92-011840] p 3525 N92-29624

ARGONNE NATIONAL LAB., IL.
Prospects for long baseline neutrino oscillation experiments
[DE92-011833] p 3544 N92-29356

Rolling-contact and wear resistance of hard coatings on bearing-steel substrates
[DE92-011834] p 3478 N92-29357

Computer model simulation of null-flux magnetic suspension and guidance
[DE92-013044] p 3478 N92-29534

An approximation method for dynamic response of strain-hardening structures
[DE92-013053] p 3482 N92-29535

ARIZONA UNIV., TUCSON.
Remote sensing by spaceborne lidar aided by surface returns p 3473 N92-29327

Origin and evolution of planetary atmospheres
[NASA-CR-190579] p 3568 N92-29432

ARMY AEROMEDICAL RESEARCH LAB., FORT RUCKER, AL.
Test and evaluation report of the physio control defibrillator/monitor model LIFEPAK (trademark) 8
[AD-A248283] p 3510 N92-29347

Visual acuity with second and third generation night vision goggles obtained from a new method of night sky simulation across a wide range of target contrast
[AD-A248284] p 3512 N92-29348

Test and evaluation report of the IMED volumetric infusion pump model 960A
[AD-A248538] p 3404 N92-29506

ARMY ARMAMENT RESEARCH, DEVELOPMENT AND ENGINEERING CENTER, PICATINNY ARSENAL, NJ.
Introduction to neural networks
[AD-A248258] p 3527 N92-29541

ARMY ARMAMENT RESEARCH, DEVELOPMENT AND ENGINEERING CENTER, WATERVLIET, NY.
Minimax linear splines
[AD-A248077] p 3515 N92-29487

ARMY LAB. COMMAND, FORT MONMOUTH, NJ.
Introduction to quartz frequency standards
[AD-A248503] p 3439 N92-29498

ARMY LAB. COMMAND, WHITE SANDS MISSILE RANGE, NM.
Sensitivity of C2 sub n to random variations of windspeed, sensible heat flux, and latent heat flux
[AD-A248696] p 3502 N92-29565

ATMOSPHERIC AND ENVIRONMENTAL RESEARCH, INC., CAMBRIDGE, MA.
NWP impact of cloud top and boundary layer winds from a satellite borne lidar: An observing system simulation experiment p 3473 N92-29328

AUSTRALIAN NATIONAL UNIV., CANBERRA.
Spectroscopy of W-183; measured magnetic moments and rotation-particle coupling
[DE92-624790] p 3549 N92-30213

B

BALLISTIC RESEARCH LABS., ABERDEEN PROVING GROUND, MD.
The effect of yaw cards on the pitching and yawing motion of symmetric projectiles
[AD-A250021] p 3406 N92-29449
Spatial and temporal temperature studies of electrothermal chemical (ETC) plasmas
[AD-A248541] p 3554 N92-29510

BELEIDSCOMMISSIE REMOTE SENSING, DELFT (NETHERLANDS).
GIS for coastal management
[BCRS-90-31] p 3489 N92-29493
Alexander: User guide (version 1.0)
[BCRS-90-38] p 3489 N92-29494
Mapping of groundwater losses by evaporation in the western desert of Egypt
[BCRS-91-01] p 3489 N92-29495
Research programming studies: Remote sensing emissions, land use and effects, in relation to climate and environment
[BCRS-91-17] p 3493 N92-29497
The main lines of the research programs remote sensing: Climate and environment
[BCRS-91-25] p 3493 N92-29499
Activities report of the Netherlands Remote Sensing Board (with abridged version)
[ETN-92-91352] p 3489 N92-29688
Monitoring of grass dominance on Dutch heathlands using remote sensing and a geographic information system (HEIMON)
[BCRS-91-12] p 3489 N92-29693
Comparison of in situ, aircraft- and satellite derived surface reflectances in Flevoland (Netherlands). A validation experiment
[BCRS-91-28] p 3491 N92-30230
TERS product development plan for urban planning of Bandung, Indonesia
[BCRS-91-30] p 3491 N92-30231

BIDSTON OBSERVATORY, MERSEYSIDE (ENGLAND).
Class A network Dataring gauges: 1989 data processing and analysis
[REPT-18-1991] p 3505 N92-29684

BIONETICS CORP., COCOA BEACH, FL.
Mosquito Lagoon environmental resources inventory
[NASA-TM-107548] p 3492 N92-29430

BOEING CO., SEATTLE, WA.
Buffet test in the National Transonic Facility
[NASA-CR-189595] p 3406 N92-29352

BOEING COMMERCIAL AIRPLANE CO., SEATTLE, WA.
Structural integrity of future aging airplanes
p 3484 N92-30107
Performance of fuselage pressure structure
p 3484 N92-30109

BRIGHAM YOUNG UNIV., PROVO, UT.
Solid state structures of some Dithionoamido-18-crown-6 ligands
[AD-A248098] p 3556 N92-29558

BROOKHAVEN NATIONAL LAB., UPTON, NY.
X ray study of interfacial interactions in highly milled Sn-Ge powders
[DE92-012518] p 3556 N92-29437
Transition crossing in the RHIC
[DE92-013031] p 3550 N92-29475
Longitudinal bunch profile measurements with striplines
[DE92-013035] p 3549 N92-29477
Free ion yields in liquids: Molecular structure and track effects
[DE92-012208] p 3545 N92-29582
Fourth workshop on Experiments and Detectors for a Relativistic Heavy Ion Collider
[BNL-52262] p 3549 N92-30014

BROWN UNIV., PROVIDENCE, RI.
Parameter identification for nonlinear aerodynamic systems
[NASA-CR-190264] p 3399 N92-29329

BULGARIAN ACADEMY OF SCIENCES, SOFIA.
Lidar observation of aerosol and temperature stratification over urban area during the formation of a stable atmospheric PBL p 3466 N92-29286
A comparison between Raman lidar and conventional contact measurements of atmospheric temperature
p 3466 N92-29287
Efficiencies of rotational Raman and Rayleigh techniques for laser remote sensing of the atmospheric temperature p 3467 N92-29288
Lidar investigation of aerosol pollution distribution near a coal power plant p 3467 N92-29289
Correlation analysis of wind lidar data
p 3467 N92-29291

C

CALIFORNIA INST. OF TECH., PASADENA.
Shock enhancement and control of hypersonic combustion
[AD-A248558] p 3418 N92-29580
Controlling the flow of visual information through the lateral geniculate nucleus: From single cells to neural networks
[AD-A250578] p 3528 N92-29590

CALIFORNIA POLYTECHNIC STATE UNIV., SAN LUIS OBISPO.
Computation of three-dimensional effects on two dimensional wings
[NASA-CR-190576] p 3401 N92-29691

CALIFORNIA UNIV., BERKELEY.
Micromechanisms of cyclic and environmentally-assisted subcritical crack growth in ceramic-matrix composites
[AD-A248067] p 3414 N92-29556

CALIFORNIA UNIV., DAVIS.
A study of the adsorption of acetonitrile on a gold electrode from aqueous solutions using in situ vibrational spectroscopy
[AD-A250191] p 3417 N92-29514
Strengthening mechanisms, creep and fatigue processes in dispersion hardened niobium alloy
[AD-A250282] p 3421 N92-29547
National Institute for Global Environmental Change
[DE92-013487] p 3493 N92-29597

CALIFORNIA UNIV., IRVINE.
Diffraction of light from randomly rough surfaces
[AD-A250261] p 3551 N92-29546
Instantaneous optimal control for linear, nonlinear and hysteretic structures: Stable controllers
[PB92-163807] p 3501 N92-29950

CARNEGIE-MELLON UNIV., PITTSBURGH, PA.
Ultra-dependable real-time computing
[AD-A248193] p 3515 N92-29409
Summary of technical operations, 1991
[AD-A248153] p 3516 N92-29540

CASE WESTERN RESERVE UNIV., CLEVELAND, OH.
Molecular engineering of liquid crystalline polymers by living polymerization. 19: Synthesis and characterization of poly 2-(4-biphenyloxy)ethyl vinyl etherby
[AD-A248285] p 3423 N92-29349
Molecular engineering of side chain liquid crystalline polymers
[AD-A248540] p 3424 N92-29508
Molecular engineering of liquid crystalline polymers by living polymerization. 20: Synthesis and characterization of binary copolymers of 11-(4-cyano-4'-biphenyl) oxy)undecanyl vinyl ether with n-butyl vinyl ether and of 2-(4-cyano-4'-biphenyl) oxy)ethyl vinyl ether with n-butyl vinyl ether
[AD-A248286] p 3425 N92-29566
Molecular engineering of liquid crystalline polymers by living polymerization. 22: Synthesis and characterization of binary copolymers
[AD-A248287] p 3425 N92-29567
Structural rearrangements during mesomorphic phase transitions in poly(10-((4-cyano-4' biphenyl)oxy)decanyl vinyl ether)
[AD-A248306] p 3425 N92-29569
Molecular engineering of liquid crystalline polymers
[AD-A248996] p 3427 N92-30136

CATHOLIC UNIV. OF AMERICA, WASHINGTON, DC.
Experimental investigation of adaptive control of a parallel manipulator
[NASA-CR-189867] p 3528 N92-29656

CENTER FOR MATHEMATICS AND COMPUTER SCIENCE, AMSTERDAM (NETHERLANDS).
Asymptotic optimality of the chi-square test with large number of degrees of freedom within the class of symmetric tests
[CWI-BS-R9116] p 3540 N92-29860
Discretization of morphological operators
[CWI-BS-R9118] p 3533 N92-29861
On constructing kernel polynomials of a spectral function: Application to ARMA models
[CWI-BS-R9119] p 3533 N92-29862
U-statistics of increasing degrees with asymptotically Poisson distributions
[CWI-BS-R9120] p 3540 N92-29863
Non-interfering dipaths in planar digraphs
[CWI-BS-R9121] p 3533 N92-29864
Software reliability and the bootstrap
[CWI-BS-R9123] p 3520 N92-29865
Positive convolution structures associated with quantum groups
[CWI-AM-R9105] p 3534 N92-29866
Analysis of parallel diagonal-implicit iteration of Runge-Kutta methods
[CWI-NM-R9114] p 3526 N92-29867
Optimality of wait-free atomic multiwriter variables
[CWI-CS-R9128] p 3520 N92-29868
Gaarding inequalities for systems of pseudo-differential operators
[CWI-AM-R9111] p 3534 N92-29881
Askey-Wilson polynomials for root systems of type BC
[CWI-AM-R9112] p 3534 N92-29882
Solving parabolic integro-differential equations by an explicit integration method
[CWI-NM-R9108] p 3534 N92-29883
Computing distinguishing formulas for branching bisimulation
[CWI-CS-R9121] p 3521 N92-29890
Facets of database triggers
[CWI-CS-R9122] p 3521 N92-29891
Real-time quadratic shading
[CWI-CS-R9123] p 3534 N92-29892
Asymptotic inversion of the incomplete beta function
[CWI-AM-R9106] p 3534 N92-29893
Hyperasymptotic expansions of confluent hypergeometric functions
[CWI-AM-R9107] p 3535 N92-29894
Diffusion approximation of stochastic integral functionals of jump Markov processes
[CWI-AM-R9108] p 3535 N92-29895
Diffusion approximation of stochastic additive functionals of jump Markov processes
[CWI-AM-R9110] p 3535 N92-29896
Numerical methods for the 3D shallow water equations on vector and parallel computers
[CWI-NM-R9109] p 3446 N92-29944
On the numerical treatment of the advective terms in 3D shallow water models
[CWI-NM-R9110] p 3446 N92-29945
An improved accuracy version of the mixed finite element method for a second order elliptic equation
[CWI-NM-R9111] p 3536 N92-29946
Application of a moving-grid method to a class of 1D brine transport problems in porous media
[CWI-NM-R9112] p 3446 N92-29947
An algebraic specification for the static semantics of Pascal
[CWI-CS-R9129] p 3522 N92-29989
Loop checking in partial deduction
[CWI-CS-R9134] p 3522 N92-29990
Rendez-vous with metric semantics
[CWI-CS-R9135] p 3522 N92-29991
CCS for OO and LP
[CWI-CS-R9136] p 3522 N92-29992
Undecidable equivalences for basic process algebra
[CWI-CS-R9137] p 3536 N92-29993
Proof theory for micro CRL
[CWI-CS-R9138] p 3522 N92-29994
Texture synthesis
[CWI-CS-R9139] p 3523 N92-30141
Linear approximation of shortest superstrings
[CWI-CS-R9126] p 3523 N92-30146
Term rewriting analysis in process algebra
[CWI-CS-R9130] p 3537 N92-30177
Real space process algebra
[CWI-CW-R9131] p 3538 N92-30178
Simulations on the Jelinski-Moranda model of software reliability
[CWI-BS-R9122] p 3523 N92-30179
Analysis of a three-dimensional point pattern with replication
[CWI-BS-R9124] p 3541 N92-30180

CENTERS FOR DISEASE CONTROL, ATLANTA, GA.
Development of models for prediction of optimal lifting motion
[PB92-164656] p 3513 N92-29949

CENTRE NATIONAL DE LA RECHERCHE SCIENTIFIQUE, PARIS (FRANCE).
A multi-wavelength ozone lidar for the EASOE experiment p 3462 N92-29260

CENTRE NATIONAL DE LA RECHERCHE SCIENTIFIQUE, VERRIERES-LE BUISSON (FRANCE).
Rayleigh/Raman lidars: Intercomparisons and validation p 3471 N92-29318
Wind measurements from 15 to 50 km with a Doppler Rayleigh lidar p 3472 N92-29319

CIVIL AVIATION AUTHORITY, CANBERRA (AUSTRALIA).
Aging commuter aeroplanes: Fatigue evaluation and control methods p 3488 N92-30132

CLEMSON UNIV., SC.
Development of high T(sub c) (greater than 110 K) Bi, Tl, and Y-based materials as superconducting circuit elements
[NASA-CR-190311] p 3557 N92-29676

COLORADO STATE UNIV., FORT COLLINS.
Model for regional solute transport suited for calibration and management
[PB92-161371] p 3494 N92-29746

COLORADO UNIV., BOULDER.
Transportable lidar for the measurement of ozone concentration and flux profiles in the lower troposphere p 3465 N92-29278
Tracking hurricane Claudette with the US Air Force OTH-B radar
[PB92-164524] p 3503 N92-29800
Theoretical/experimental investigations of the structure and dynamics of highly energetic dication species
[AD-A247050] p 3418 N92-29901
Aperture coupling to shielded transmission lines: Theory and experiment
[PB92-183672] p 3437 N92-30093
COLUMBIA UNIV., NEW YORK, NY.
Visual perception of elevation
[AD-A248338] p 3510 N92-29420
COLUMBIA UNIV., PALISADES, NY.
Circulation and exchange at the continental shelf and slope SEEP-2
[DE92-013500] p 3504 N92-29439
COMMERCE DEPT., WASHINGTON, DC.
Current information technology resource requirements of the Federal Government: Fiscal year 1992
[PB92-147180] p 3561 N92-29663
COMMITTEE ON COMMERCE, SCIENCE, AND TRANSPORTATION (U.S. SENATE).
NASA's Earth Observing System
[S-HRG-102-647] p 3490 N92-30017
COMMONWEALTH SCIENTIFIC AND INDUSTRIAL RESEARCH ORGANIZATION, MORDIALOC (AUSTRALIA).
Southern Hemisphere lidar measurements of the aerosol clouds from Mt. Pinatubo and Mt. Hudson p 3456 N92-29230
Lidar studies of extinction in clouds in the ECLIPS project p 3472 N92-29320
Constraining the atmospheric carbon budget: A preliminary assessment
[CSIRO-TP-25] p 3494 N92-29668
A soil-canopy scheme for use in a numerical model of the atmosphere: 1D stand-alone model
[CSIRO-TP-23] p 3500 N92-29670
CONSIGLIO NAZIONALE DELLE RICERCHE, FLORENCE (ITALY).
A multi-wavelength ozone lidar for the EASOE experiment p 3462 N92-29260
CONSIGLIO NAZIONALE DELLE RICERCHE, FRASCATI (ITALY).
Lidar observations of the Pinatubo stratospheric aerosol cloud over Frascati, Italy p 3460 N92-29251
CONSIGLIO NAZIONALE DELLE RICERCHE, NAPLES (ITALY).
Lab-scale lidar sensing of diesel engines exhausts p 3464 N92-29276
CORNELL UNIV., ITHACA, NY.
The weakest failure detector for solving consensus
[NASA-CR-190545] p 3515 N92-29400
LiMoN2: The first metallic layered nitride
[AD-A248446] p 3418 N92-29619
CORPS OF ENGINEERS, HUNTSVILLE, AL.
Guide for evaluating 12 inch Substantial Dividing Walls (SDWs) to provide protection from remote operation, volume 2
[AD-A250252] p 3428 N92-29335
Guide for evaluating 12 inch Substantial Dividing Walls (SDWs) to provide protection from remote operation, volume 1
[AD-A250251] p 3428 N92-29545
COUNCIL ON ENVIRONMENTAL QUALITY, WASHINGTON, DC.
Environmental quality: Report of the Council on Environmental Quality
[PB92-154954] p 3494 N92-29698

D

DARTMOUTH COLL., HANOVER, NH.
An overview of computer viruses in a research environment
[NASA-CR-190528] p 3517 N92-29630
DAYTON UNIV., OH.
Zee star analysis
[AD-A248342] p 3417 N92-29423
Characterization of fracture in (0/90)3s SiC/1723 composites
[AD-A250612] p 3414 N92-29453
DELFT HYDRAULICS LAB. (NETHERLANDS).
River hydrometry by pattern recognition in remote sensing images
[PUBL-445] p 3490 N92-29728
DEPARTMENT OF AGRICULTURE, BELTSVILLE, MD.
CRIS/USDA online access guide. Revision 1: File 60 on DIALOG
[PB92-172857] p 3562 N92-30033
DEPARTMENT OF THE ARMY, WASHINGTON, DC.
Modulated high sensitivity infrared polarimeter
[AD-D015256] p 3474 N92-29571
FM video data link spectrum spreading
[AD-D015257] p 3435 N92-29572
DEPARTMENT OF THE NAVY, WASHINGTON, DC.
Interface board for providing time signals to a super minicomputer
[AD-D015198] p 3441 N92-29900
Friction drive position transducer
[AD-D015205] p 3475 N92-30202
DEPARTMENT OF TRANSPORT, OTTAWA (ONTARIO).
Transport Canada aging aircraft activities p 3403 N92-30131
DEUTSCHE FORSCHUNGSANSTALT FUER LUFT- UND RAUMFAHRT, BRUNSWICK (GERMANY, F.R.).
Sensor fault detection on board an aircraft with observer and polynomial classifier
[DLR-FB-91-34] p 3404 N92-29870
Jet aircraft noise at high subsonic flight Mach numbers
[DLR-FB-91-28] p 3544 N92-29997
DEUTSCHE FORSCHUNGSANSTALT FUER LUFT- UND RAUMFAHRT, LAMPOLDSHAUSEN (GERMANY, F.R.).
A numerical and experimental investigation of the thrust vector control by secondary gas injection
[DLR-FB-91-31] p 3447 N92-29998
DEUTSCHE FORSCHUNGSANSTALT FUER LUFT- UND RAUMFAHRT, OBERPFAFFENHOFEN (GERMANY, F.R.).
Airborne dial remote sensing of the Arctic ozone layer p 3462 N92-29258
Airborne lidar measurements of stratospheric aerosols during the European Arctic Stratospheric Ozone Experiment (EASOE) p 3469 N92-29305
Global and high resolution radar cross section measurements and two-dimensional microwave images of a scaled aircraft model from the type Airbus A 310
[DLR-MITT-91-10] p 3436 N92-29877
DIESELDYNE CORP., MORROW, OH.
A preliminary design and analysis of an advanced heat-rejection system for an extreme altitude advanced variable cycle diesel engine installed in a high-altitude advanced research platform
[NASA-CR-186021] p 3405 N92-29427
DOUGLAS AIRCRAFT CO., INC., LONG BEACH, CA.
Maintaining the safety of an aging fleet of aircraft p 3402 N92-30108
Inspection of aging aircraft: A manufacturer's perspective p 3481 N92-30117
DRAPER (CHARLES STARK) LAB., INC., CAMBRIDGE, MA.
A systems analysis of the impact of navigation instrumentation on-board a Mars rover, based on a covariance analysis of navigation performance
[NASA-CR-189868] p 3403 N92-29440
DUKE UNIV., DURHAM, NC.
Fuzzy logic control of AC induction motors
[PB92-180207] p 3443 N92-30092
DURHAM UNIV. (ENGLAND).
Studies of distant clusters of galaxies p 3566 N92-29843

E

ECOLE POLYTECHNIQUE, PALAISEAU (FRANCE).
Simulation of the performances of WIND, an airborne CO2 lidar p 3463 N92-29267
Sampling and representativeness for a spaceborne wind lidar p 3463 N92-29268
EDINBURGH UNIV. (SCOTLAND).
The significance of large-scale flows into the Great Attractor p 3565 N92-29836
EG AND G ENERGY MEASUREMENTS, INC., LAS VEGAS, NV.
High Intensity Source Laboratory (HISL)
[DE92-011173] p 3549 N92-29457
The 20 element HgI2 energy dispersive x ray array detector system
[DE92-013356] p 3549 N92-29502
ENVIRONMENTAL PROTECTION AGENCY, RESEARCH TRIANGLE PARK, NC.
Air quality criteria for oxides of nitrogen, volume 1
[PB92-176361] p 3493 N92-29520
Air quality criteria for oxides of nitrogen, volume 2
[PB92-176379] p 3493 N92-29521
Air quality criteria for oxides of nitrogen, volume 3
[PB92-176387] p 3493 N92-29522
New developments in emission projection methodologies
[PB92-139393] p 3495 N92-30031
Human exposure model-2: User's guide
[PB92-186246] p 3495 N92-30200
EUROPEAN SOUTHERN OBSERVATORY, GARCHING (GERMANY, F.R.).
The space distribution of local radio galaxies p 3566 N92-29842
EUROPEAN SPACE AGENCY, PARIS (FRANCE).
Fourth Meeting of the Space Agency Forum on the International Space Year (SAFISY-4)
[ESA-SP-1141] p 3407 N92-29879
EUROPEAN SPACE AGENCY. EUROPEAN SPACE RESEARCH AND TECHNOLOGY CENTER, ESTEC, NOORDWIJK (NETHERLANDS).
Design guidelines for capability approval of film hybrid microcircuits and Microwave Hybrid Integrated Circuits (MHICs)
[ESA-PSS-01-610-ISSUE-1] p 3441 N92-29854
ESATAN user manual
[ESA-PSS-03-105-ISSUE-2] p 3521 N92-29869
Maintainability requirements for ESA space systems
[ESA-PSS-01-50-ISSUE-1] p 3481 N92-29878

F

FEDERAL AVIATION ADMINISTRATION, ATLANTIC CITY, NJ.
Federal Aviation Administration aging aircraft nondestructive inspection research plan p 3481 N92-30116
FEDERAL AVIATION ADMINISTRATION, CAMBRIDGE, MA.
High-speed Maglev trains: German safety requirements RW-MSB
[PB92-167006] p 3564 N92-29808
German high-speed Maglev train safety requirements: Potential for application in the United States
[PB92-167014] p 3564 N92-29809
Current DOT research on the effect of multiple site damage on structural integrity p 3485 N92-30112
FEDERAL AVIATION ADMINISTRATION, SEATTLE, WA.
Status of the FAA flight loads monitoring program p 3485 N92-30113
The FAA aging airplane program plan for transport aircraft p 3402 N92-30128
FEDERAL AVIATION ADMINISTRATION, WASHINGTON, DC.
Human factors in aircraft maintenance and inspection p 3487 N92-30125
Revision of certification standards for aviation maintenance personnel p 3487 N92-30127
FEDERAL EXPRESS CORP., MEMPHIS, TN.
Communication: An important element of maintenance and repair p 3402 N92-30124
FLORIDA STATE UNIV., TALLAHASSEE.
Numerical modeling studies of the Gulf of Mexico and the Caribbean Sea using the Bryan-Cox model
[PB92-164987] p 3505 N92-29704
FUKUI UNIV. (JAPAN).
Rotational Raman lidar for lower tropospheric temperature profiling p 3466 N92-29284
FUKUOKA UNIV. (JAPAN).
Long term stratospheric aerosol lidar measurements in Kyushu p 3456 N92-29229

G

GALAXY SCIENTIFIC CORP., ATLANTA, GA.
Using intelligent simulation to enhance human performance in aircraft maintenance p 3487 N92-30126
GEC-MARCONI LTD., BOREHAMWOOD (ENGLAND).
The e-beam sustained laser technology for space-based Doppler wind lidar p 3469 N92-29300
GENERAL ACCOUNTING OFFICE, WASHINGTON, DC.
EOS data policy: Questions remain about US commercial access. Report to the Chairman, Committee on Science, Space, and Technology, House of Representatives
[GAO/IMTEC-92-44] p 3488 N92-29467
GENERAL ATOMIC CO., SAN DIEGO, CA.
Multichord spectroscopy of the D3-D divertor region
[DE92-013507] p 3554 N92-29412
Design and operation of the multipulse Thomson scattering diagnostic on DIII-D
[DE92-011393] p 3476 N92-29474
Short wavelength interferometer for ITER
[DE92-013008] p 3474 N92-29942
GENERAL ELECTRIC CO., GILBERT, AZ.
Transport delay measurements: Methodology and analysis for the F-16C combat engagement trainer, the display for advanced research and training, and the F-16A limited field of view
[AD-A248519] p 3406 N92-29505
GENERAL ELECTRIC CO., LARGO, FL.
Li/SO2 cells and Li/SOCl2 cells: Safe use and testing
[DE92-013508] p 3439 N92-29414

GENERAL ELECTRIC CO., PHILADELPHIA, PA.
GE's mobile, coherent Doppler lidar test/evaluation facilities p 3407 N92-29299
GENERAL ELECTRIC CO., PRINCETON, NJ.
The Laser Atmospheric Wind Sounder (LAWS) preliminary error budget and performance estimate p 3462 N92-29262
The Laser Atmospheric Wind Sounder (LAWS) phase 2 preliminary system design p 3468 N92-29297
GENERAL ELECTRIC CO., SCHENECTADY, NY.
Laser processing for interconnect technology [AD-A248103] p 3476 N92-29559
GENERAL SERVICES ADMINISTRATION, WASHINGTON, DC.
Current information technology resource requirements of the Federal Government: Fiscal year 1992 [PB92-147180] p 3561 N92-29663
GEOLOGICAL SURVEY, RESTON, VA.
Lexicon of new formal geologic names of the United States, 1981-1985 [PB92-181320] p 3563 N92-30040
GEORGE WASHINGTON UNIV., WASHINGTON, DC.
Publications of the environmental health program: 1980-1990 [NASA-CR-4455] p 3509 N92-29341
GEORGIA INST. OF TECH., ATLANTA.
Progress on combustion mechanisms of solid propellants [AD-A248146] p 3427 N92-29330
Analysis of a dedicated rotation experiment in TFTR [DE92-013463] p 3554 N92-29438
Compressive response of debonded thick composite shells including the effects of transient moisture sorption [AD-A250080] p 3414 N92-29462
Simplified computational methods for elastic and elastic-plastic fracture problems p 3488 N92-30134
Fundamental study of compressive strength development in PAN-based carbon fibers [AD-A250285] p 3416 N92-30137
GESELLSCHAFT FUER KERNENERGIEVERWERTUNG IN SCHIFFBAU UND SCHIFFAHRT M.B.H., GEESTHACHT (GERMANY, F.R.).
Stratospheric backscatter, extinction, and lidar ratio profiling after the Mt. Pinatubo eruptions p 3456 N92-29231
GORDON RESEARCH CONFERENCES, INC., KINGSTON, RI.
Gordon research conference on Barrier Function of Mammalian Skin [AD-A248556] p 3510 N92-29577
GRENOBLE-1 UNIV. (FRANCE).
Some applications of orthogonal functions to probability and statistics [ETN-92-91741] p 3538 N92-29491
A new form for the chi-squared test of independence (document 2) p 3538 N92-29492
A strategy for microprocessor BIST implementation based on deterministic testing [IMAG-RR-844-I] p 3516 N92-29570
Strong bisimilarity on nets revisited [RR-847-I-IMAG-120-LIFIA] p 3532 N92-29573
Experiments on processes with backtracking [RR-858-I-IMAG-121-LIFIA] p 3532 N92-29574
A massively parallel genetic algorithm for the graph partitioning problem [IMAG-RR-845-I] p 3525 N92-29610
Software architecture modelling: Application to AMODEUS design scenarios [IMAG-RR-860-I] p 3513 N92-29611
B(exp 2)UBIST: A strategy for boundary scan board unified BIST [IMAG-RR-862-I] p 3441 N92-29612
Hardening techniques to counter cumulated dose on SEU and SEL in space environment [IMAG-RR-863-I] p 3441 N92-29613
Parallelization of the recursive gradient backpropagation algorithm [IMAG-RR-854-M] p 3525 N92-29614
Automatic generation algorithms, experiments, and comparisons of self checking PLA schemes [IMAG-RR-843-I] p 3516 N92-29621
GRUMMAN AEROSPACE CORP., BETHPAGE, NY.
Smart BIT/TSMD integration [AD-A247192] p 3442 N92-29914
New York State technical and economic MAGLEV evaluation [PB92-174119] p 3564 N92-30037

H

HARVARD UNIV., CAMBRIDGE, MA.
Preliminary results on the fracture analysis of multi-site cracking of lap joints in aircraft skins p 3484 N92-30111
HAWAII UNIV., HONOLULU.
Low complexity, high performance and bandwidth efficient concatenated coded 8-PSK schemes for reliable data communications [NASA-CR-190588] p 3517 N92-29665
HELSINKI UNIV. OF TECHNOLOGY, ESPOO (FINLAND).
The 2D-computation of an axial fan with FINFLO [PB92-180678] p 3447 N92-30023
Simulations on the electrical characteristics of Si, SiC and diamond junction and Schottky power diodes [PB92-177872] p 3443 N92-30094
HELSINKI UNIV. OF TECHNOLOGY, OTANIEMI (FINLAND).
SOLCHIPS: A fast predesign and optimization tool for solar heating with seasonal storage [DE92-506509] p 3492 N92-29636
Process of ferrochromium now and in the future [DE92-506510] p 3421 N92-29637
Experimental study of cylindrical air electrodes [DE92-506507] p 3441 N92-29912
A mathematical model for metal hydride electrodes [DE92-506506] p 3442 N92-30089
HONEYWELL, INC., BLOOMINGTON, MN.
RF vacuum electronics [AD-A248857] p 3442 N92-29935
HONEYWELL, INC., MINNEAPOLIS, MN.
Monolithic integration of semiconductor and superconductor components [AD-A245351] p 3557 N92-29583
HONEYWELL, INC., SAINT LOUIS PARK, MN.
Enhanced evaluation, selection and acceptance criteria for the Contractor Integrated Technical Information Service (CITIS) [PB92-163856] p 3562 N92-29699
HUGHES DANBURY OPTICAL SYSTEMS, INC., CT.
Lag angle compensation in a space borne scanning lidar p 3462 N92-29263

I

ILLINOIS UNIV., URBANA.
Design and scheduling for periodic concurrent error detection and recovery in processor arrays [NASA-CR-190571] p 3517 N92-29695
Variable temperature scanning tunneling microscopy [AD-A248725] p 3557 N92-29722
Transport processes in beamed energy propulsion systems [AD-A247296] p 3413 N92-29913
Optoelectronic integration [AD-A248950] p 3442 N92-29936
ILLINOIS UNIV., URBANA-CHAMPAIGN.
Lidar observations of polar stratospheric clouds and stratospheric temperatures at the South Pole p 3470 N92-29307
Lidar probing of the mesosphere: Simultaneous observations of sporadic sodium and iron formations, calcium ion layers, neutral temperature and winds p 3470 N92-29311
Error analysis of wind measurements for the University of Illinois sodium Doppler temperature system p 3471 N92-29313
Sodium Doppler temperature lidar observations of the mesopause region temperature and wind structure p 3471 N92-29314
Airborne sodium and Rayleigh lidar observations from ALOHA-90 p 3471 N92-29315
INDIANA UNIV., BLOOMINGTON.
Some feedback procedures for control of flows p 3452 N92-30070
INSTITUT DES HAUTES ETUDES SCIENTIFIQUES, BURES-SUR-YVETTE (FRANCE).
Swirls and wheels [PB92-173251] p 3542 N92-30095
Spectral type of Ornstein's class one transformations [PB92-178292] p 3537 N92-30096
INSTITUTE FOR COMPUTER APPLICATIONS IN SCIENCE AND ENGINEERING, HAMPTON, VA.
Streamwise vortices in heated boundary layers [NASA-CR-189661] p 3444 N92-29692
Crossflow effects on the growth rate of inviscid Goertler vortices in a hypersonic boundary layer [NASA-CR-189667] p 3455 N92-30190
Stability of a premixed flame in stagnation-point flow against general disturbances [NASA-CR-189666] p 3455 N92-30192
INSTITUTE FOR DEFENSE ANALYSES, ALEXANDRIA, VA.
Survey of research into electromagnetic and other wave effects on mechanical behavior and processing of materials [AD-A248614] p 3426 N92-29905
INSTITUTE OF ENERGY ECONOMICS OF JAPAN.
Global-warming problem and global economic models [DE92-514557] p 3493 N92-29638
INTERNATIONAL CENTRE FOR THEORETICAL PHYSICS, TRIESTE (ITALY).
The extended Bethe Ansatz for infinite S = 1/2 quantum spin chains with non-nearest-neighbor interaction [DE92-622378] p 3533 N92-29793
INTERNATIONAL RICE RESEARCH INST., MANILA (PHILIPPINES).
NATO workshop on the Atmospheric Methane Cycle. Working group report on methane sources and sinks [PB92-180256] p 3494 N92-30018
IOWA STATE UNIV. OF SCIENCE AND TECHNOLOGY, AMES.
NDE research efforts at the FAA Center for Aviation Systems Reliability p 3481 N92-30119
IOWA UNIV., IOWA CITY.
A study of shock-associated magnetohydrodynamic waves in the solar wind [NASA-CR-190567] p 3569 N92-29631
ISRAEL AIRCRAFT INDUSTRIES LTD., LOD.
OFFEQ-1: Preliminary flight evaluation results [ITN-92-85126] p 3410 N92-29480
ISRAEL INST. FOR BIOLOGICAL RESEARCH, NESS-ZIONA.
Signal quality influence on averaging procedure for DIAL pollution monitoring p 3465 N92-29280
ISTITUTO DI FISICA DELL ATMOSFERA, ROME (ITALY).
Observations of ozone-aerosol correlated behaviour in the lower stratosphere during the EASOE campaign p 3459 N92-29243
IT ENVIRONMENTAL PROGRAMS, INC., CINCINNATI, OH.
Evaluation of aluminum ion vapor deposition as a replacement for cadmium electroplating at Anniston Army Depot [AD-A250063] p 3423 N92-29940
ITERATIONS, INC., NEW YORK, NY.
Scalable parallel algorithms for multidimensional digital signal processing [AD-A249381] p 3516 N92-29622

J

JAPAN BROADCASTING CORP., TOKYO.
The 1990 annual report, April 1990 - March 1991 p 3571 N92-29471
JET PROPULSION LAB., CALIFORNIA INST. OF TECH., PASADENA.
The JPL Table Mountain and Mauna Loa stratospheric ozone lidars p 3458 N92-29239
The Telecommunications and Data Acquisition Report [NASA-CR-190460] p 3429 N92-29364
A determination of the radio-planetary frame tie from comparison of Earth orientation parameters p 3409 N92-29365
Occultation of a compact radio source by Venus p 3429 N92-29366
A nanoradian differential VLBI tracking demonstration p 3430 N92-29367
Deep-space navigation with differenced data types. Part 3: An expanded information content and sensitivity analysis p 3409 N92-29368
Orbiter-orbiter and orbiter-lander tracking using same-beam interferometry p 3409 N92-29369
Geometric distortion analysis of a wide-field astrograph p 3409 N92-29370
Applications of inertial-sensor high-inheritance instruments to DSN precision antenna pointing p 3430 N92-29371
Performance of a 12-GHz fiber-optic system for beam-waveguide antenna stability testing p 3431 N92-29372
Improvements in X-band transmitter phase stability through klystron body temperature regulation p 3431 N92-29373
Noise-optimal control of HEMT LNA's for compensation of temperature deviations p 3431 N92-29374
Golay and other box codes p 3431 N92-29375
Figure of merit for direct-detection optical channels p 3431 N92-29376
Optimizing the G/T ratio of the DSS-13 34-meter beam-waveguide antenna p 3431 N92-29377
Dynamic modeling of fluid transmission lines of the DSN 70-meter antennas by using a lumped parameter model p 3432 N92-29378
Bandwidth compression of noisy signals with square-wave subcarrier p 3432 N92-29379
An OSI architecture for the Deep Space Network p 3432 N92-29380
DSS-13 26-meter antenna upgraded radiometer system p 3432 N92-29381
Sequential design of a linear quadratic controller for the Deep Space Network antennas p 3432 N92-29382
DSN acquisition of Magellan high-rate telemetry data p 3409 N92-29383

Galileo early cruise, including Venus, first Earth, and Gaspra encounters p 3433 N92-29384
Deep Space Network information system architecture study p 3433 N92-29385
Generalized probability model for calculation of interference to the Deep Space Network due to circularly Earth-orbiting satellites p 3433 N92-29386
Ka-band feed arrays for spacecraft reflector antennas with limited scan capability: An overview p 3433 N92-29387
DSN observations of Titan p 3433 N92-29388
Goldstone solar system radar signal processing p 3433 N92-29389
Microstrip reflectarray antenna for the SCANSCAT radar application
[NASA-CR-190453] p 3434 N92-29463
Developments in fiber optics for distribution automation
[NASA-CR-190454] p 3551 N92-29679
Position-error-based force reflection and compliance control
[NASA-CASE-NPO-18668-1-CU] p 3479 N92-29765
Improved real-time imaging spectrometer
[NASA-CASE-NPO-18410-1-CU] p 3552 N92-29832
Electronic neural network for solving traveling salesman and similar global optimization problems
[NASA-CASE-NPO-17807-2-CU] p 3529 N92-29955
Sample positioning in microgravity
[NASA-CASE-NPO-18448-1-CU] p 3428 N92-30083
Dynamic aperture fringe discriminator
[NASA-CASE-NPO-18478-1-CU] p 3553 N92-30084
Fast temporal neural learning using teacher forcing
[NASA-CASE-NPO-18553-1-CU] p 3530 N92-30085
Nonvolatile programmable neural network synaptic array
[NASA-CASE-NPO-18578-1-CU] p 3442 N92-30086
Method of forming silicon structures with selectable optical characteristics
[NASA-CASE-NPO-18625-1-CU] p 3559 N92-30102
Miniature modular microwave end-to-end receiver
[NASA-CASE-NPO-18713-1-CU] p 3437 N92-30103
Programmable hyperspectral image mapper with on-array processing
[NASA-CASE-NPO-17794-1-CU] p 3553 N92-30104

JOHNS HOPKINS UNIV., BALTIMORE, MD.
Effects of ionizing radiation on auditory and visual thresholds
[AD-A248199] p 3507 N92-29410
Performance measurement results for a 220 Mbps QPPM optical communication receiver with an EG/G Slik APD
[NASA-CR-190561] p 3435 N92-29658
Cluster correlations from N-point correlation amplitudes p 3566 N92-29837

JOHNS HOPKINS UNIV., LAUREL, MD.
A wave theory for non-imaging concentrators
[AD-A248865] p 3552 N92-29726

JOINT ASTRONOMY CENTRE, HILO, HI.
United Kingdom Infrared Telescope
[ETN-92-91341] p 3565 N92-29682

JOINT INST. FOR LAB. ASTROPHYSICS, BOULDER, CO.
Optical and electrical characteristics of the cathode fall
[AD-A249010] p 3443 N92-30176

K

KARLSRUHE UNIV. (GERMANY, F.R.).
Development and characterization of oxidation-protected CFC
[MBB-Z-0395-91-PUB] p 3416 N92-29876

KATHOLIEKE UNIV., NIJMEGEN (NETHERLANDS).
Visual pattern completion
[PB92-187418] p 3524 N92-30195

KERNFORSCHUNGSZENTRUM G.M.B.H., KARLSRUHE (GERMANY, F.R.).
KISMET (kinematic simulation, monitoring and off-line programming environments for telerobotics): Simulation of the target-oriented driving of an autonomous vehicle in a labyrinthic environment
[KFK-4941] p 3515 N92-29418
Processing and properties of mechanically alloyed sintered steels with hard inclusions
[KFK-4909] p 3422 N92-29651
Comparison of turbulence parameters measured by SODAR and sonic anemometer
[KFK-4890] p 3500 N92-29690

L

LA SAPIENZA UNIV., ROME (ITALY).
Observations of ozone-aerosol correlated behaviour in the lower stratosphere during the EASOE campaign p 3459 N92-29243

LABORATOIRE D'AUTOMATIQUE ET D'ANALYSE DES SYSTEMES, TOULOUSE (FRANCE).
A study and feasibility of ultra thin silica layers by rapid thermal processing
[LAAS-91393] p 3422 N92-29674
Recognition of multi-articulated three-dimensional objects using a multisensor system for robotics applications
[LAAS-91394] p 3529 N92-29675
SPARA: A system of planning robot manipulation tasks
[LAAS-91395] p 3529 N92-29678
Study and realization of GaAs PNP homojunction bipolar transistors using ion implementation
[LAAS-91433] p 3441 N92-29729
Methodology for the specification of communication activities within the framework of a multi-layered architecture: Toward the definition of a knowledge base
[LAAS-91466] p 3436 N92-29730
Reliable processing of confidential data by means of fragmentation-redundancy-scattering
[LAAS-91412] p 3526 N92-29888

LASER TECHNOLOGY, INC., SOUTH LYON, MI.
Laser paint stripping
[AD-A249233] p 3476 N92-29581

LAWRENCE LIVERMORE NATIONAL LAB., CA.
Near-visible Raman instrumentation for remote multi-point process monitoring using optical fibers and optical multiplexing
[DE92-011287] p 3550 N92-29337
An innovative approach for coupled thermomechanical analysis
[DE92-011467] p 3481 N92-29338
A mechanical connector design for high-current, high-coulomb pulsed power systems
[DE92-012678] p 3438 N92-29339
Laser-induced desorption from sapphire surfaces
[DE92-012698] p 3475 N92-29340
Code generation in ALPAL using symbolic techniques
[DE92-011299] p 3524 N92-29353
Active modelocking and phase stabilization of a cavity dumped diode pumped Nd:YAG mini-laser
[DE92-011946] p 3475 N92-29358
X ray laser research at the Nova laser
[DE92-012695] p 3476 N92-29472
The real-space multiple-scattering theory and the electronic structure of grain boundaries
[DE92-013006] p 3556 N92-29473
Computed tomography experiments of Pantex high explosives
[DE92-013517] p 3480 N92-29478
A new algebra core for the minimal form problem
[DE92-011966] p 3531 N92-29481
Condenser optics, partial coherence, and imaging for soft x ray projection lithography
[DE92-011762] p 3551 N92-29484
Ion collision effects in hydrogen-like recombination x ray lasers
[DE92-013515] p 3476 N92-29509
LLE-LLNL progress report on studies in nonlocal heat transport in spherical plasmas using the Fokker-Planck code SPARK
[DE92-014093] p 3554 N92-29531
Program SIXPAK: A code designed to check double-differential correlated data and calculate equivalent uncorrelated data
[DE92-013752] p 3516 N92-29537
Cursory examination of the zeta potential behaviors of two optical materials
[DE92-011588] p 3551 N92-29578
Effect of grain size on deformation stability of copper under quasi-static and dynamic tensile loading
[DE92-012677] p 3421 N92-29639
Preliminary cutting and drilling studies using new generation lasers
[DE92-010712] p 3477 N92-29787
Intercomparison of global marine climatologies
[DE92-011389] p 3494 N92-29790
ISLAND: Interactive Solution Language for an Adaptive NIKE Driver
[DE92-011444] p 3533 N92-29791
Solution strategies for implicit nonlinear finite element analysis
[DE92-011466] p 3533 N92-29792
Estimating plasma temperatures
[DE92-014092] p 3555 N92-29798
The Green Function Cellular Method and its relation to multiple scattering theory
[DE92-011470] p 3436 N92-29909
The role of chemical interactions in the stability of artificial metallic superlattices
[DE92-011528] p 3559 N92-29911
Tunable driver for the LLNL FEL experiment
[DE92-011292] p 3477 N92-29937
The x ray laser coherence experiments in neon-like yttrium
[DE92-010714] p 3477 N92-29987
Electrochemical array sensors for plating waste stream monitoring
[DE92-011446] p 3495 N92-30211

LEIDEN UNIV. (NETHERLANDS).
Separable Markovian decision problems: The linear programming method in the multichain case (revised)
[PB92-187350] p 3524 N92-30201

LOCKHEED MISSILES AND SPACE CO., PALO ALTO, CA.
Investigation of solar active regions at high resolution by balloon flights of the solar optical universal polarimeter, definition phase
[NASA-CR-184339] p 3570 N92-30204

LOGISTICS MANAGEMENT INST., BETHESDA, MD.
Application Center of Excellence (ACE) program
[AD-A248694] p 3562 N92-29934

LOS ALAMOS NATIONAL LAB., NM.
Lidar monitoring of Mexico City's atmosphere during high air polution episodes p 3464 N92-29275
Remote detection of biological particles and chemical plumes using UV fluorescence lidar p 3465 N92-29279
Electron microscopy study on zirconia and alumina ceramic powders synthesized by microwave plasma pyrolysis
[DE92-013385] p 3424 N92-29479
Strategies for understanding the deflagration-to-detonation transition
[DE92-013528] p 3427 N92-29512
Poleward leaping auroras, the substorm expansive and recovery phases, and the recovery of the plasma sheet
[DE92-013530] p 3500 N92-29513
Multiphoton processes in scattering and ionization in an intense linearly-polarized radiation field
[DE92-013546] p 3545 N92-29515
Low energy neutral atoms in the Earth's magnetosphere: Modeling
[DE92-013240] p 3500 N92-29536
Omega phase formation in titanium and titanium alloys
[DE92-011138] p 3421 N92-29633
Synthesis and characterization of a covalently bound self-assembled macrocycle monolayer thin film for nonlinear optical materials
[DE92-011353] p 3545 N92-29634
The comparative effects of gamma radiation and in situ alpha particles on five strong-base anion exchange resins
[DE92-000177] p 3425 N92-29643
X ray streak camera diagnostics of picosecond laser-plasma interactions
[DE92-011371] p 3555 N92-29789
On the abstracted dataflow complexity of fast Fourier transforms
[DE92-011372] p 3562 N92-29794
A perspective on MoSi2 based composites
[DE92-013434] p 3415 N92-29795
Optical diagnostics on dense Z-pinch plasmas
[DE92-011228] p 3555 N92-29917
Burros: Simple, affordable, effective space transportation
[DE92-013553] p 3541 N92-30138
Phase-space estimate of satellite coverage time
[DE92-013555] p 3542 N92-30139
Intense diagnostic neutral beam development for ITER
[DE92-011262] p 3556 N92-30203

LUND INST. OF TECH. (SWEDEN).
DIAL mapping of atmospheric atomic mercury of geophysical origin p 3464 N92-29273

M

MANCHESTER UNIV. (ENGLAND).
Aeronautical Engineering Group publications, 1950 - present
[AERO-REPT-8907] p 3444 N92-29683

MANTECH ENVIRONMENTAL TECHNOLOGY, INC., CORVALLIS, OR.
NATO workshop on the Atmospheric Methane Cycle. Working group report on methane sources and sinks
[PB92-180256] p 3494 N92-30018
Potential impacts of climate change on Pacific Northwest forest vegetation
[PB92-184985] p 3495 N92-30021
What is the potential of forest management to slow the increase of atmospheric CO2?
[PB92-180249] p 3495 N92-30173

MARQUETTE UNIV., MILWAUKEE, WI.
Detecting microwave emissions from terrestrial sources: A feasibility study
[AD-A248557] p 3435 N92-29579
MARTIN MARIETTA LABS., BALTIMORE, MD.
A study of the influence of alloying additions on the passivity of aluminum
[AD-A248339] p 3421 N92-29587
MARYLAND UNIV., COLLEGE PARK.
Numerical procedures for analyzing dynamical processes
[AD-A248175] p 3515 N92-29399
Basic problems of a-posteriori error estimation
[AD-A248986] p 3541 N92-30174
MASSACHUSETTS INST. OF TECH., CAMBRIDGE.
The role of lidars in global change research
p 3457 N92-29235
Experimental and theoretical research in applied plasma physics
[DE92-013567] p 3553 N92-29336
Spacecraft dynamics characterization and control system failure detection, volume 1
[NASA-CR-190517] p 3409 N92-29422
Femtosecond studies of carrier dynamics in compound semiconductors
[AD-A250584] p 3439 N92-29452
Synthesis and useful reactions of organosilicon polymeric precursors for ceramics
[AD-A248500] p 3424 N92-29496
Forces on a pipe bend resulting from clearing a pool of liquid upstream
[DE92-004179] p 3445 N92-29784
Vibrational spectrum and structure of 1,2-dimethyl-1,2-disila-closo-dodecaborane
[AD-A250235] p 3419 N92-29941
MASSACHUSETTS INST. OF TECH., LEXINGTON.
Development of mesospheric sodium laser beacon for atmospheric adaptive optics p 3470 N92-29308
Optical pumping of mesospheric sodium: A new measurement capability p 3470 N92-29310
MASSACHUSETTS UNIV., AMHERST.
Constitutive modelling for granular material under finite strains with particle slidings and fabric changes
[AD-A248187] p 3482 N92-29407
Computational acoustics
[AD-A247688] p 3543 N92-29441
Normalized radar cross section of natural surfaces at millimeter wavelengths
[AD-A248452] p 3434 N92-29447
Theory of the dissociation dynamics of small molecules on metal surfaces: Finite temperature studies
[DE92-011188] p 3546 N92-29899
MAX-PLANCK-INST. FUER ASTROPHYSIK, GARCHING (GERMANY, F.R.).
CDM with thermal history of baryons: High-resolution 2-D and 3-D simulations p 3565 N92-29835
Morphological segregation of galaxies on large scales
p 3566 N92-29840
N-body simulations of the evolution of clusters of galaxies p 3567 N92-29849
MAX-PLANCK-INST. FUER EXTRATERRESTRISCHE PHYSIK, GARCHING (GERMANY, F.R.).
The evolution of the x ray luminosity function of galaxy clusters p 3567 N92-29848
ROSAT: Early results p 3567 N92-29850
MAX-PLANCK-INST. FUER PHYSIK UND ASTROPHYSIK, GARCHING (GERMANY, F.R.).
Traces of the primordial structure in the universe
[MPE-227] p 3565 N92-29833
Constraints on the mass fluctuation spectrum from x ray observations of clusters of galaxies
p 3567 N92-29845
The x ray morphology of the relaxed cluster of galaxies A2256. 1: Evidence for a merger event
p 3568 N92-29851
The x ray morphology of the relaxed cluster of galaxies A2256. 2: Sources around the extended cluster emission
p 3568 N92-29852
MCAT INST., SAN JOSE, CA.
Study of optical techniques for the Ames unitary wind tunnels. Part 3: Angle of attack
[NASA-CR-190541] p 3406 N92-29655
MENTOR TECHNOLOGIES, INC., ROCKVILLE, MD.
Micro-computer network architecture for range instrumentation applications, volume 1
[AD-A247836] p 3525 N92-29555
MESSERSCHMITT-BOELKOW-BLOHM G.M.B.H., MUNICH (GERMANY, F.R.).
Diode-pumped Nd:YAG lidar for airborne cloud measurements p 3473 N92-29326
Saenger: The reference concept and its technological requirements - aerothermodynamics
[MBB-FE-202-S-PUB-0463-A] p 3408 N92-29629
Technology programme: Aerothermodynamics and propulsion integration. Numerical and experimental aerothermodynamics
[MBB-FE-202-S-PUB-0464-A] p 3400 N92-29648
Aerothermodynamics and propulsion integration in the Saenger technology programme
[MBB-FE-202-S-PUB-0469-A] p 3400 N92-29649
Concurrent engineering in design of aircraft structures
[MBB-FE-2-S-PUB-472] p 3404 N92-29650
Aerothermodynamic challenges of the Saenger space-transportation system
[MBB-FE-202-S-PUB-0462-A] p 3409 N92-29680
Hypersonic flow past radiation-cooled surfaces
[MBB-FE-202-S-PUB-0468-A] p 3401 N92-29713
Computed Tomography (CT) as a nondestructive test method used for composite helicopter components
[MBB-UD-0603-91-PUB] p 3480 N92-29873
Repair procedures for advanced composites for helicopters
[MBB-UD-0606-91-PUB] p 3399 N92-29874
Status and perspectives of modern composite materials
[MBB-Z-0380-91-PUB] p 3416 N92-29875
Development and characterization of oxidation-protected CFC
[MBB-Z-0395-91-PUB] p 3416 N92-29876
Experience with piloted simulation in the development of helicopters
[MBB-UD-0610-91-PUB] p 3407 N92-30076
Acquisition of an aerothermodynamic data base by means of a winged experimental reentry vehicle
[MBB/FE202/S/PUB/461] p 3399 N92-30232
METEOROLOGICAL RESEARCH INST., TSUKUBA (JAPAN).
Lidar observations of stratospheric aerosol layer after the Mt. Pinatubo volcanic eruption p 3457 N92-29234
METEOROLOGICAL SATELLITE CENTER, TOKYO (JAPAN).
Tapering clouds and their classification due mainly to the surrounding cloud pattern in the GMS imagery
[ISSN-0388-9653] p 3502 N92-29666
METEOROLOGISCHES OBSERVATORIUM, HOHENPEISSENBERG (GERMANY, F.R.).
Lidar measurement of stratospheric ozone at Hohenpeissenberg: An improved evaluation method
p 3462 N92-29259
MICHIGAN UNIV., ANN ARBOR.
Extraction of aerosol and Rayleigh components from Doppler lidar return signal p 3465 N92-29281
X ray cluster counts: What ROSAT should see
p 3567 N92-29847
MIDWEST RESEARCH INST., GOLDEN, CO.
Tomorrow's energy today: Energy efficiency and renewable energy
[DE91-002110] p 3491 N92-29454
Novel thin-film CuInSe2 fabrication
[DE92-001222] p 3557 N92-29584
Monolithic amorphous silicon modules on continuous polymer substrate
[DE92-001163] p 3425 N92-29598
MINNESOTA UNIV., MINNEAPOLIS.
Nonideal formation of network polymers
[AD-A248072] p 3424 N92-29465
Feedback control laws for highly maneuverable aircraft
[NASA-CR-190535] p 3406 N92-29654
MITRE CORP., BEDFORD, MA.
HFRAD hindcast: An OTH-B radar and model comparison study
[AD-A248065] p 3436 N92-29902
MITRE CORP., MCLEAN, VA.
Small satellites and RPAS in global-change research: Summary and conclusions
[DE92-013602] p 3490 N92-30088
Continuum approaches for describing solid-gas and solid-liquid flow
[DE92-013601] p 3452 N92-30140
MORGANTOWN TECHNOLOGY CENTER, WV.
Modeling deterministic chaos in thermally-pulsed combustion
[DE92-011756] p 3416 N92-29355
MOSCOW STATE UNIV. (USSR).
In vivo and in vitro chlorophyll-a and pheophytin-a concentration measurements by laser fluorometry
p 3468 N92-29295
On the parity of fundamental solutions for one-dimensional scattering problem with inverse square potential
[DE92-624511] p 3560 N92-29533
MUENSTER UNIV. (GERMANY, F.R.).
Scales of universal homogeneity from galaxy counts
p 3566 N92-29841

N

NAPIER COLL., EDINBURGH (SCOTLAND).
Dynamic solder management
[AD-A250564] p 3422 N92-29647
NATIONAAL INST. VOOR KERNFYSICA EN HOGE ENERGIEFYSICA, AMSTERDAM (NETHERLANDS).
The FORM version of MINCER
[NIKHEF-H/91-18] p 3518 N92-29747
The O(alpha(s) cubed) QCD correction to the lowest moment of the longitudinal structure function in deep inelastic electron-nucleon scattering
[NIKHEF-H/91-19] p 3546 N92-29750
Classical aspects of weak interactions
[NIKHEF-H/91-25] p 3546 N92-29751
NATIONAL ACADEMY OF PUBLIC ADMINISTRATION, WASHINGTON, DC.
Archives of the future: Archival strategies for the treatment of electronic databases
[PB92-178631] p 3563 N92-30038
NATIONAL AERONAUTICS AND SPACE ADMINISTRATION, WASHINGTON, DC.
EOS Data and Information System (EOSDIS)
[NASA-TM-107922] p 3488 N92-29442
Research in NASA history: A guide to the NASA history program
[NASA-TM-107953] p 3571 N92-29689
NATIONAL AERONAUTICS AND SPACE ADMINISTRATION. AMES RESEARCH CENTER, MOFFETT FIELD, CA.
A theoretical approach for analyzing the restabilization of wakes
[NASA-TM-103858] p 3443 N92-29394
In vitro measurement of nucleus pulposus swelling pressure: A new technique for studies of spinal adaptation to gravity
[NASA-TM-103853] p 3506 N92-29397
Improving designer productivity
[NASA-TM-103929] p 3404 N92-29417
NASA Workshop on future directions in surface modeling and grid generation
[NASA-CP-10092] p 3400 N92-29625
Single point modeling of initially isotropic turbulence under uniform rotation p 3449 N92-30054
NATIONAL AERONAUTICS AND SPACE ADMINISTRATION. GODDARD SPACE FLIGHT CENTER, GREENBELT, MD.
Raman lidar measurements of Pinatubo aerosols over southeastern Kansas during November-December 1991
p 3457 N92-29233
A new Raman DIAL technique for measuring stratospheric ozone in the presence of volcanic aerosols
p 3458 N92-29238
The global backscatter experiment airborne pulsed lidar measurements p 3459 N92-29246
Multi-wavelength airborne lidar intercomparisons of aerosol and cirrus backscatter over the Pacific Ocean
p 3460 N92-29247
Lidar measurements of stratospheric ozone, temperature and aerosol during 1992 UARS correlative measurement campaign p 3461 N92-29257
Intercomparisons of lidar backscatter measurements and in-situ data from GLOBE p 3463 N92-29266
Laboratory velocimeter measurements using the edge technique p 3463 N92-29269
Monthly means of selected climate variables for 1985 - 1989
[NASA-TM-104565] p 3502 N92-29653
SeaWiFS technical report series. Volume 1: An overview of SeaWiFS and ocean color
[NASA-TM-104566-VOL-1] p 3505 N92-29686
Geostationary Operational Environmental Satellite(GEOS-N report)
[NASA-TM-107919] p 3410 N92-29810
Geostationary Operational Environmental Satellite (GOES-N report). Volume 1: Technical
[NASA-TM-107918] p 3410 N92-29811
Geostationary Operational Environmental Satellite (GOES-N report). Volume 2: Technical appendix
[NASA-TM-107920] p 3410 N92-29812
Evidence for evolution of the luminosity function of clusters of galaxies p 3567 N92-29844
SeaWiFS technical report series. Volume 5: Ocean optics protocols for SeaWiFS validation
[NASA-TM-104566] p 3506 N92-30193
Biophysical, morphological, canopy optical property, and productivity data from the Superior National Forest
[NASA-TM-104568] p 3491 N92-30210
NATIONAL AERONAUTICS AND SPACE ADMINISTRATION. HUGH L. DRYDEN FLIGHT RESEARCH FACILITY, EDWARDS, CA.
Effects of bleed air extraction on thrust levels on the F404-GE-400 turbofan engine
[NASA-TM-104247] p 3405 N92-29425

Flight evaluation of an extended engine life mode on an F-15 airplane
[NASA-TM-104240] p 3405 N92-29659

NATIONAL AERONAUTICS AND SPACE ADMINISTRATION. JOHN C. STENNIS SPACE CENTER, BAY SAINT LOUIS, MS.

Research and technology annual report, FY 1990
[NASA-TM-107807] p 3571 N92-30197

NATIONAL AERONAUTICS AND SPACE ADMINISTRATION. LYNDON B. JOHNSON SPACE CENTER, HOUSTON, TX.

Making intelligent systems team players: Overview for designers
[NASA-TM-104751] p 3513 N92-29403
Fastening apparatus having shape memory alloy actuator
[NASA-CASE-MSC-21935-1] p 3479 N92-29762
Accelerometer method and apparatus for integral display and control functions
[NASA-CASE-MSC-21961-1] p 3474 N92-29952
Fingered bola body, bola with same, and methods of use
[NASA-CASE-MSC-21967-1] p 3479 N92-30026
Polarization perception device
[NASA-CASE-MSC-21915-1] p 3552 N92-30027
Bearing servicing tool
[NASA-CASE-MSC-21881-1] p 3479 N92-30082
A method for making biocompatible polymer articles using atomic oxygen
[NASA-CASE-MSC-21529-1] p 3427 N92-30100
Check valve with poppet damping mechanism
[NASA-CASE-MSC-21903-1] p 3480 N92-30101

NATIONAL AERONAUTICS AND SPACE ADMINISTRATION. LANGLEY RESEARCH CENTER, HAMPTON, VA.

Sixteenth International Laser Radar Conference, part 1
[NASA-CP-3158-PT-1] p 3456 N92-29228
Interpretation of DIAL measurements of lower stratospheric ozone in regions with Pinatubo aerosols p 3457 N92-29236
Airborne lidar observations of the stratosphere after the Pinatubo eruption p 3460 N92-29248
Lidar observations of the Pinatubo volcanic cloud over Hampton, Virginia p 3461 N92-29254
Correction of DIAL stratospheric ozone measurements in the presence of Pinatubo aerosols p 3462 N92-29261
Lidar In-space Technology Experiment (LITE) electronics overview p 3462 N92-29264
The Lidar In-Space Technology Experiment (LITE) p 3469 N92-29301
Mechanical and thermal issues in the development of a spaceborne lidar system p 3469 N92-29303
Lidar measurements of aerosol and ozone distributions during the 1992 Airborne Arctic Stratospheric Expedition p 3469 N92-29304
Observations of cirrus clouds over the Pacific region by the NASA multiwavelength lidar system p 3473 N92-29325
An interlaminar tension strength specimen
[NASA-TM-107623] p 3481 N92-29393
Spatial and temporal adaptive procedures for the unsteady aerodynamic analysis of airfoils using unstructured meshes
[NASA-TM-107635] p 3400 N92-29445
Method and apparatus for thermographically and quantitatively analyzing a structure for disbonds and/or inclusions
[NASA-CASE-LAR-14559-1] p 3480 N92-29829
Aerodynamic design optimization using sensitivity analysis and computational fluid dynamics
[NASA-CASE-LAR-14815-1-CU] p 3445 N92-29830
Multiresponse imager and imaging process for improved resolution
[NASA-CASE-LAR-14779-1] p 3552 N92-29951
Polybenzimidazoles via aromatic nucleophilic displacement
[NASA-CASE-LAR-14643-1] p 3426 N92-29953
Active thermal isolation for temperature responsive sensors
[NASA-CASE-LAR-14612-1] p 3446 N92-29954
Single nucleon emission in relativistic nucleus-nucleus reactions p 3548 N92-30011
Heat exchanger with oscillating flow
[NASA-CASE-LAR-14033-2] p 3447 N92-30024
Helicopter low-speed yaw control
[NASA-CASE-LAR-14219-1] p 3406 N92-30025
Combined load test apparatus for flat panels
[NASA-CASE-LAR-14698-1] p 3483 N92-30028
Optical fiber sensor having an active core
[NASA-CASE-LAR-14607-1SB] p 3553 N92-30029
Calibration apparatus for recess mounted pressure transducers
[NASA-CASE-LAR-14724-1] p 3474 N92-30030
Shaft mount for data coupler system
[NASA-CASE-LAR-13805-1] p 3480 N92-30097
Converting a CO2 atmosphere to a high-purity O2 supply
[NASA-CASE-LAR-14398-1] p 3419 N92-30098
Apparatus for elevated temperature compression or tension testing of specimens
[NASA-CASE-LAR-14775-1] p 3483 N92-30099
The 1991 International Conference on Aging Aircraft and Structural Airworthiness
[NASA-CP-3160] p 3484 N92-30106
Fracture mechanics research at NASA related to the aging commercial transport fleet p 3484 N92-30110
Damaged stiffened shell research at NASA. Langley Research Center p 3485 N92-30115
Thermal QNDE detection of airframe disbonds p 3481 N92-30118
Mechanical properties of coated titanium Beta-21S after exposure to air at 700 and 800 C
[NASA-TM-104220] p 3423 N92-30205
Linear system identification via backward-time observer models
[NASA-TM-107632] p 3488 N92-30214

NATIONAL AERONAUTICS AND SPACE ADMINISTRATION. LEWIS RESEARCH CENTER, CLEVELAND, OH.

Structural durability of stiffened composite shells
[NASA-CR-190588] p 3481 N92-29342
Applied analytical combustion/emissions research at the NASA Lewis Research Center
[NASA-TM-105731] p 3412 N92-29343
Optimal design of compact spur gear reductions
[NASA-TM-105676] p 3478 N92-29351
Approaches to polymer-derived CMC matrices
[NASA-TM-105754] p 3415 N92-29660
Contingency power for a small turboshaft engine by using water injection into turbine cooling air
[NASA-TM-105680] p 3405 N92-29661
Design characteristics of a heat pipe test chamber
[NASA-TM-105737] p 3492 N92-29662
The O2 reduction at the IFC modified O2 fuel cell electrode
[NASA-TM-105691] p 3413 N92-29667
Pressurization of cryogens: A review of current technology and its applicability to low-gravity conditions
[NASA-TM-105746] p 3427 N92-29669
Validation of finite element and boundary element methods for predicting structural vibration and radiated noise
[NASA-TM-105359] p 3478 N92-29697
Experimental investigation of the flowfield of an oscillating airfoil
[NASA-TM-105675] p 3402 N92-30182
Optimization of armored spherical tanks for storage on the lunar surface
[NASA-TM-105700] p 3414 N92-30187

NATIONAL AERONAUTICS AND SPACE ADMINISTRATION. MARSHALL SPACE FLIGHT CENTER, HUNTSVILLE, AL.

Definition and design of an experiment to test raster scanning with rotating unbalanced-mass devices on gimbaled payloads
[NASA-TP-3249] p 3429 N92-29677
Bladder operated robotic joint
[NASA-CASE-MFS-28682-1] p 3426 N92-29831
ATLAS 1: Encountering planet Earth
[NASA-TM-107956] p 3408 N92-30016
National Launch System cycle 1 loads and models data book
[NASA-TM-103560] p 3408 N92-30215

NATIONAL AERONAUTICS AND SPACE ADMINISTRATION. PASADENA OFFICE, CA.

Position-error-based force reflection and compliance control
[NASA-CASE-NPO-18668-1-CU] p 3479 N92-29765
Improved real-time imaging spectrometer
[NASA-CASE-NPO-18410-1-CU] p 3552 N92-29832
Electronic neural network for solving traveling salesman and similar global optimization problems
[NASA-CASE-NPO-17807-2-CU] p 3529 N92-29955
Sample positioning in microgravity
[NASA-CASE-NPO-18448-1-CU] p 3428 N92-30083
Dynamic aperture fringe discriminator
[NASA-CASE-NPO-18478-1-CU] p 3553 N92-30084
Fast temporal neural learning using teacher forcing
[NASA-CASE-NPO-18553-1-CU] p 3530 N92-30085
Nonvolatile programmable neural network synaptic array
[NASA-CASE-NPO-18578-1-CU] p 3442 N92-30086
Method of forming silicon structures with selectable optical characteristics
[NASA-CASE-NPO-18625-1-CU] p 3559 N92-30102
Miniature modular microwave end-to-end receiver
[NASA-CASE-NPO-18713-1-CU] p 3437 N92-30103
Programmable hyperspectral image mapper with on-array processing
[NASA-CASE-NPO-17794-1-CU] p 3553 N92-30104

NATIONAL AEROSPACE LAB., AMSTERDAM (NETHERLANDS).

DSC measurements on experimental TGDDM/DDS resin systems: The influence of variations in resin composition and catalyst content
[NLR-TP-90267-U] p 3478 N92-29602
Short cracks and durability analysis of the Fokker 100 wing/fuselage structure
[NLR-TP-90336-U] p 3482 N92-29603
Hyperbolic grid generation control by panel methods
[NLR-TP-91061-U] p 3532 N92-29604
European studies to investigate the feasibility of using 1000 ft vertical separation minima above FL 290. Part 1: Overview of organisation, techniques employed, and conclusions
[NLR-TP-91062-U-PT-1] p 3403 N92-29605
Application of VME-technology on an airborne data link processor unit
[NLR-MP-88040-U] p 3403 N92-29615
Results of a flight simulator experiment to establish handling quality guidelines for the design of future transport aircraft
[NLR-MP-88044-U] p 3404 N92-29616
On the optimization of windshear warning and guidance systems
[NLR-TP-90196-U] p 3402 N92-29703
CAESAR: A CCD airborne experimental scanner for applications in remote sensing radiometric and geometric calibration
[NLR-TP-89103-U] p 3490 N92-29707
Fatigue crack growth in damage tolerant Al-Li sheet alloys
[NLR-TP-90107-U] p 3483 N92-29708
Fighter pilot training: The contribution of simulation
[NLR-TP-89311-U] p 3512 N92-29871
Evaluation of measured-boundary-condition methods for 3D subsonic wall interference
[NLR-TR-88072-U] p 3401 N92-29884
On fictitious joints modelling of manipulator link flexibility for the HERA simulation facility pilot
[NLR-TR-88086-U] p 3479 N92-29885
A method for computing the 3-dimensional flow about wings with leading-edge vortex separation. Part 2: Description of computer program VORSEP
[NLR-TR-86006-U] p 3402 N92-29916

NATIONAL AEROSPACE LAB., EMMELOORD (NETHERLANDS).

Ageing aircraft research in the Netherlands p 3402 N92-30129

NATIONAL CENTER FOR ATMOSPHERIC RESEARCH, BOULDER, CO.

A spectral vegetation radiometer for airborne boundary-layer research
[PB92-186113] p 3491 N92-30105

NATIONAL COUNCIL FOR AIR AND STREAM IMPROVEMENT, INC., CORVALLIS, OR.

What is the potential of forest management to slow the increase of atmospheric CO2?
[PB92-180249] p 3495 N92-30173

NATIONAL INST. FOR ENVIRONMENTAL STUDIES, TSUKUBA (JAPAN).

Observation of stratospheric ozone with NIES lidar system in Tsukuba, Japan p 3459 N92-29242
Three-wavelength lidar measurements of Pinatubo aerosol and its optical properties p 3460 N92-29250
Infrared pulse-laser long-path absorption measurement of carbon dioxide using a Raman-shifted dye laser p 3465 N92-29277

NATIONAL INST. FOR FUSION SCIENCE, NAGOYA (JAPAN).

Formation of presheath and current-free double layer in a two-electron-temperature plasma
[NIFS-132] p 3555 N92-30091
Heat flow of a two-electron-temperature plasma through the sheath in the presence of electron emission
[NIFS-136] p 3555 N92-30172

NATIONAL INST. OF STANDARDS AND TECHNOLOGY, BOULDER, CO.

Aperture coupling to shielded transmission lines: Theory and experiment
[PB92-183672] p 3437 N92-30093
Standard spherical dipole source
[PB92-187020] p 3438 N92-30198

NATIONAL INST. OF STANDARDS AND TECHNOLOGY, GAITHERSBURG, MD.

Finite-rate diffusion-controlled reaction in a vortex
[PB92-172006] p 3418 N92-29744
User's manual for the NIST TTCN translator, version 3.0
[PB92-172493] p 3518 N92-29745

Challenges to NIST in dimensional metrology: The impact of tightening tolerances in the US discrete-part manufacturing industry
[PB92-164680] p 3542 N92-29802
Aluminum-lithium alloys: Surface-cracked tension fracture tests and physical and thermal properties at cryogenic temperatures
[PB92-172477] p 3422 N92-29803
Computer program POWNOR for fitting the power-normal and -lognormal models to life or strength data from specimens of various sizes
[PB92-169119] p 3483 N92-29813
Shop of the 1990's: The implementation of a CAD/CAM system for small machine shops
[PB92-181098] p 3522 N92-30020
The 36th issue of Electronics and Electrical Engineering Laboratory Technical Progress Bulletin covering laboratory programs, July to September 1991, with 1992 EEEL events calendar
[PB92-164672] p 3442 N92-30032
Physics Laboratory technical activities, 1991
[PB92-172824] p 3542 N92-30035
Heat transfer in an aluminum heat exchanger using normal hydrogen gas
[PB92-172832] p 3447 N92-30036
Overview of the document style semantics and specification language and the MIL-M-28001A output specification
[PB92-181122] p 3563 N92-30039

NATIONAL MATERIALS PROPERTY DATA NETWORK, INC., COLUMBUS, OH.
Marine structural steel toughness data bank (abridged edition)
[PB92-163294] p 3422 N92-29807

NATIONAL METEOROLOGICAL CENTER, WASHINGTON, DC.
Science goals and mission objectives of NASA's laser atmospheric wind sounder program
p 3468 N92-29296

NATIONAL OCEANIC AND ATMOSPHERIC ADMINISTRATION, BOULDER, CO.
Lidar tracking of multiple fluorescent tracers: Method and field test p 3464 N92-29274
Measurement of mean or effective radius of cloud drop size distributions with a 10.6-micron wavelength lidar
p 3472 N92-29324
LAPS specific humidity analysis
[PB92-163575] p 3502 N92-29799
Tracking hurricane Claudette with the US Air Force OTH-B radar
[PB92-164524] p 3503 N92-29800
Turbulence effects on the geodynamic laser ranging system
[PB92-166404] p 3477 N92-29948

NATIONAL OCEANIC AND ATMOSPHERIC ADMINISTRATION, OAK RIDGE, TN.
Preliminary analysis of wind data from the Oak Ridge site survey
[PB92-174564] p 3503 N92-30034

NATIONAL OCEANIC AND ATMOSPHERIC ADMINISTRATION, WASHINGTON, DC.
Interpretation of DIAL measurements of lower stratospheric ozone in regions with Pinatubo aerosols
p 3457 N92-29236
NOAA environmental digest: Selected indicators of the United States and the global environment, December 1991
[PB92-185073] p 3494 N92-30019

NATIONAL WEATHER SERVICE, HONOLULU, HI.
Tropical cyclones: Central North Pacific, 1991
[PB92-167345] p 3502 N92-29743

NATIONAL WEATHER SERVICE, WASHINGTON, DC.
Proceedings of the 16th Annual Climate Diagnostics Workshop
[PB92-167378] p 3503 N92-29801

NAVAL COMMAND, CONTROL AND OCEAN SURVEILLANCE CENTER, SAN DIEGO, CA.
Evaluation of an aureole lidar technique for estimating extinction profiles
[AD-A249740] p 3501 N92-30087

NAVAL HEALTH RESEARCH CENTER, SAN DIEGO, CA.
Exercise and three psychosocial variables: A longitudinal study
[AD-A250649] p 3510 N92-30216

NAVAL OCEAN SYSTEMS CENTER, SAN DIEGO, CA.
Phase conjugation in BaTiO3 at 830 nanometers
[AD-A250240] p 3475 N92-29332
Adaptive signal processing at NOSC
[AD-A250245] p 3429 N92-29333
User's guide for the VTRPE (Variable Terrain Radio Parabolic Equation) computer model
[AD-A248112] p 3433 N92-29395
Contracting in the software engineering crisis
[AD-A250241] p 3516 N92-29544

NAVAL POSTGRADUATE SCHOOL, MONTEREY, CA.
Improving the LAMP Mk 3 SH-60B HF communication system
[AD-A245970] p 3429 N92-29344
Multi-fractal analysis of nocturnal boundary layer time series from the Boulder Atmospheric Observatory
[AD-A248347] p 3502 N92-29424
Two-dimensional boundary surfaces for planar external transonic flows
[AD-A248083] p 3444 N92-29524
Using object-oriented databases for implementation of interactive electronic technical manuals
[AD-A248135] p 3440 N92-29564
Detection of binary phase shift keyed signals in extremely high noise
[AD-A248552] p 3435 N92-29576
Revising M-layer: Complex exponent representation
[AD-A249121] p 3435 N92-29599
Path tracking using simple planar curves
[AD-A248252] p 3403 N92-29617
Full pose and partial pose calibration of a 6 degree-of-freedom robot manipulator arm
[AD-A247463] p 3479 N92-29785
Incorporation of GPS/INS into small autonomous underwater vehicle navigation
[AD-A248884] p 3403 N92-29906
Evaluating the military potential of a developing nation's space program: A case study of Brazil
[AD-A245978] p 3407 N92-29929

NAVAL RESEARCH LAB., WASHINGTON, DC.
Optical searches for ROSAT x ray cluster sources
p 3568 N92-29853

NAVAL SURFACE WARFARE CENTER, BETHESDA, MD.
Effect of whisker orientation on the mechanical properties of silicon carbide/alumina composites
[AD-A248737] p 3415 N92-29723

NAVAL SURFACE WARFARE CENTER, CRANE, IN.
Microcalorimetric study of the aging reactions of atomized magnesium powder
[AD-A247932] p 3427 N92-29786

NAVAL SURFACE WARFARE CENTER, DAHLGREN, VA.
Second-order shock-expansion theory extended to include real gas effects
[AD-A247191] p 3400 N92-29539

NAVAL SURFACE WARFARE CENTER, PANAMA CITY, FL.
Statistics of narrowband white noise derived from clipped broadband white noise
[AD-A248597] p 3434 N92-29563

NAVAL UNDERSEA WARFARE CENTER, NEW LONDON, CT.
A closed form solution of a longitudinal beam with a viscous boundary condition
[AD-A248841] p 3483 N92-29915

NEVADA UNIV., LAS VEGAS.
Ozone measurements with the US EPA UV-DIAL: Preliminary results p 3461 N92-29255

NEW MEXICO STATE UNIV., LAS CRUCES.
Field study of multidimensional flow and transport in the vadose zone
[PB92-161363] p 3489 N92-29701

NORTH CAROLINA STATE UNIV., RALEIGH.
Buffet test in the National Transonic Facility
[NASA-CR-189595] p 3406 N92-29352
Viscous profiles and numerical methods for shock waves
[AD-A246110] p 3443 N92-29458
Growth, characterization, and device development in monocrystalline diamond films
[AD-A248993] p 3560 N92-30175

NORTH CAROLINA UNIV., GREENSBORO.
Ocean optical modeling: Light field structure, internal radiant emission, and vertical inhomogeneities
[AD-A248272] p 3504 N92-29345

NORTHWEST AIRLINES, INC., MINNEAPOLIS, MN.
Current and future developments in civil aircraft non-destructive evaluation from an operator's point of view p 3399 N92-30122

NORTHWESTERN UNIV., EVANSTON, IL.
Structure and shear response of lipid monolayers
[DE92-011633] p 3542 N92-29354
Asymptotic and numerical methods in applied wave propagation
[AD-A250227] p 3543 N92-29543
Structural basis for the mechanical properties of polyethylenes
[PB92-164425] p 3426 N92-29804

NORWEGIAN DEFENCE RESEARCH ESTABLISHMENT, KJELLER.
Penguin extruded aluminium box launcher for marine application
[FFI-91/4001] p 3408 N92-29967

O

OAK RIDGE NATIONAL LAB., TN.
Electrostatic ion thruster optics calculations
[DE92-006608] p 3413 N92-29461
An object-based interviewing system
[DE92-013422] p 3527 N92-29504
Using custom-designed VLSI fuzzy inferencing chips for the autonomous navigation of a mobile robot
[DE92-000424] p 3528 N92-29550
Acetate in hydrothermal solutions: Decomposition kinetics and metal complexation
[DE92-010542] p 3417 N92-29551
Terrain following of arbitrary surfaces using a high intensity LED proximity sensor
[DE92-004464] p 3528 N92-29644
Reverse automatic differentiation of modular FORTRAN programs
[DE92-014071] p 3519 N92-29797
Proceedings of the Third Conference on Radiation Protection and Dosimetry
[DE92-011502] p 3547 N92-29910
Sub-angstrom microscopy through incoherent imaging and image reconstruction
[DE92-011787] p 3475 N92-30090

OESTERREICHISCHES FORSCHUNGSZENTRUM SEIBERSDORF G.M.B.H., VIENNA.
The determination of stochastic models and areas of confidence
[OEFZS-4612] p 3538 N92-29419
Migmas/A: Test of a scanning ion microscope on the Soviet Space Station Mir
[OEFZS-4615] p 3473 N92-29469
Logion: The operation of liquid metal ion emitters under weightlessness
[OEFZS-4616] p 3428 N92-29470
Diversification and product innovation: A challenge for modern management
[OEFZS-4570] p 3561 N92-29886

OFFICE NATIONAL D'ETUDES ET DE RECHERCHES AEROSPATIALES, PARIS (FRANCE).
Survey of French activities concerning structural airworthiness and aging aircraft p 3402 N92-30130

OFFICE OF MANAGEMENT AND BUDGET, WASHINGTON, DC.
Current information technology resource requirements of the Federal Government: Fiscal year 1992
[PB92-147180] p 3561 N92-29663

OFFICE OF TECHNOLOGY ASSESSMENT, WASHINGTON, DC.
Combined summaries: Technologies to sustain tropical forest resources and biological diversity
[OTA-F-515] p 3492 N92-29416
Global standards: Building blocks for the future
[PB92-167352] p 3563 N92-29671
World Administrative Radio Conference. Issues for US International Spectrum Policy
[PB92-157601] p 3435 N92-29696

OHIO STATE UNIV., COLUMBUS.
A consistent shear deformable theory for laminated plates
[AD-A250591] p 3415 N92-29593
Variational formulation and finite element implementation of Pagano's theory of laminated plates
[AD-A250592] p 3415 N92-29594
Theory of system reliability demonstration, burn-in design, and record statistics
[AD-A250582] p 3480 N92-29710

OLD DOMINION UNIV., NORFOLK, VA.
Nonlinear analyses of composite aerospace structures in sonic fatigue
[NASA-CR-190565] p 3404 N92-30209

OPTECH, INC., DOWNSVIEW (ONTARIO).
Lidar atmospheric observatory in the Canadian Arctic
p 3458 N92-29241

OREGON GRADUATE INST. OF SCIENCE AND TECHNOLOGY, BEAVERTON.
International conference topical meeting on atmospheric, volume, and surface scattering and propagation
[AD-A248881] p 3552 N92-29727

OREGON STATE UNIV., NEWPORT.
Application of remote sensing methods for tracking large cetaceans: North Atlantic right whales Eubalaena Glacialis
[PB92-185016] p 3490 N92-30022

OREGON UNIV., EUGENE.
Theory of elementary particles studies in weak interaction and grand unification and studies in accelerator design
[DE92-014309] p 3550 N92-29532

OSSERVATORIO ASTRONOMICO, BOLOGNA (ITALY).
Abell clusters of galaxies: Catalogs and large-scale structures p 3566 N92-29838

OSSERVATORIO METEOROLOGICO DI BRERA, MILAN (ITALY).
Scale-invariant galaxy clustering on large scales
p 3566 N92-29839

P

PACIFIC NORTHWEST LAB., RICHLAND, WA.
Lidar development for the Atmospheric Radiation Measurement (ARM) Program p 3461 N92-29256
Irradiation effects on the electrochemistry and corrosion resistance of stainless steel
[DE92-013504] p 3420 N92-29411
Corrosion resistance of stainless steels and high Ni-Cr alloys to acid fluoride wastes
[DE92-012338] p 3420 N92-29436
Beam-powered lunar rover design
[DE92-011511] p 3569 N92-29600
Review of temperature dependent effects on the oxidation protection of carbon/carbon
[DE92-012333] p 3415 N92-29645
Thermal energy storage for cogeneration applications
[DE92-012339] p 3492 N92-29646
PARIS-SUD UNIV., ORSAY (FRANCE).
Some feedback procedures for control of flows
p 3452 N92-30070
PARIS VI UNIV. (FRANCE).
The NDSC primary site at the Observatoire de Haute-Provence: Ozone and aerosols observations (1986-1992) p 3458 N92-29240
Aerosols and polar stratospheric clouds measurements during the EASOE campaign p 3469 N92-29306
PENNSYLVANIA STATE UNIV., UNIVERSITY PARK.
A generalized polynomial form of the objective function in flash calculations
[AD-A248160] p 3531 N92-29446
Pulse voltammetry in single cells using platinum microelectrodes
[AD-A248080] p 3440 N92-29523
Modeling of the role of atomic hydrogen in heat transfer during hot filament assisted deposition of diamond
[AD-A250607] p 3418 N92-29595
Explicit Navier-Stokes computation of turbomachinery flows
[AD-A248458] p 3445 N92-29933
PENNSYLVANIA UNIV., PHILADELPHIA.
Biologically-based neural network model of color constancy and color contrast
[AD-A248128] p 3510 N92-29398
Quasi-static intergranular cracking in a Cu-Sn alloy: An analog of stress relief cracking of steels
[DE92-011646] p 3420 N92-29483
Object discrimination based on depth-from-occlusion
[AD-A248104] p 3511 N92-29560
Mechanism of diffusion-controlled brittle fracture
[DE92-011572] p 3482 N92-29601
PHILLIPS LAB., HANSCOM AFB, MA.
Rayleigh/Raman Greenland lidar observations of atmospheric temperature during a major Arctic stratospheric warming event p 3471 N92-29316
PHILLIPS LAB., KIRKLAND AFB, NM.
Characterization of artificial guidestars generated in the mesospheric sodium layer p 3470 N92-29309
PHOTOMETRICS, INC., WOBURN, MA.
Elastic and Raman lidar temperature measurements from Poker Flat, Alaska during February 1992
p 3471 N92-29317
PITTSBURGH UNIV., PA.
A systems theoretic investigation of neuronal network properties of the hippocampal formation
[AD-A250246] p 3510 N92-29334
Multidimensional computer simulation of Stirling cycle engines
[NASA-CR-190497] p 3478 N92-29392
The cognitive function of theoretical knowledge in procedural learning
[AD-A248075] p 3531 N92-29486
The activation of chemical bonds at surfaces
[AD-A248666] p 3418 N92-29719
PRATT AND WHITNEY AIRCRAFT, WEST PALM BEACH, FL.
Fatigue in single crystal nickel superalloys
[AD-A248190] p 3420 N92-29408
PRINCETON UNIV., NJ.
Thermochemistry of phases related to oxide superconductors
[DE92-011811] p 3556 N92-29485
Physiological analyses of the afferents controlling brain neurochemical systems
[AD-A248334] p 3512 N92-29930

R

RASCON ASSOCIATES, WEST FALMOUTH, MA.
Finite difference modelling of seismic wave propagation at the seafloor
[AD-A248345] p 3505 N92-29562
RESEARCH AND DEVELOPMENT LABS., CULVER CITY, CA.
The 1991 Summer Faculty Research Program (SFRP), volume 2
[AD-A248764] p 3571 N92-29724
The 1991 Summer Faculty Research Program (SFRP), volume 3
[AD-A248765] p 3571 N92-29725
RESEARCH INST. FOR ADVANCED COMPUTER SCIENCE, MOFFETT FIELD, CA.
Divergence preserving discrete surface integral methods for Maxwell's curl equations using non-orthogonal unstructured grids
[NASA-CR-190555] p 3517 N92-29694
RESEARCH INST. FOR COMPUTING AND INFORMATION SYSTEMS, HOUSTON, TX.
ASV3 dial-in interface recommendation for the Repository Based Software Engineering (RBSE) program
[NASA-CR-190500] p 3514 N92-29362
On-line replacement of program modules using AdaPT
[NASA-CR-190499] p 3514 N92-29363
Application of fuzzy logic-neural network based reinforcement learning to proximity and docking operations
[NASA-CR-190504] p 3525 N92-29390
DecisionMaker software and extracting fuzzy rules under uncertainty
[NASA-CR-190502] p 3514 N92-29391
NASA visual thesaurus maintenance documentation
[NASA-CR-190282] p 3561 N92-29553
RESEARCH TRIANGLE INST., RESEARCH TRIANGLE PARK, NC.
Fuzzy logic control of AC induction motors
[PB92-180207] p 3443 N92-30092
RETINA FOUNDATION, BOSTON, MA.
Center of excellence: Microlaser microscope
[DE92-013485] p 3477 N92-29928
RIDER COLL., LAWRENCEVILLE, NJ.
Electromagnetic processes in nucleus-nucleus collisions relating to space radiation research
[NASA-CR-190533] p 3547 N92-30001
Cross section parameterizations for cosmic ray nuclei. 1: Single nucleon removal p 3547 N92-30002
Solution of two-body relativistic bound state equations with confining plus Coulomb interactions
p 3547 N92-30003
Do recent observations of very large electromagnetic dissociation cross sections signify a transition towards non-perturbative QED? p 3438 N92-30004
Effects of retardation in relativistic equations with confining interaction p 3547 N92-30005
Two neutron removal in relativistic nucleus-nucleus reactions p 3548 N92-30006
Confining potential in momentum space
p 3548 N92-30007
Relativistic Coulomb fission p 3548 N92-30008
Higgs-boson production in nucleus-nucleus collisions
p 3548 N92-30009
Charge dependence and electric quadrupole effects on single-nucleon removal in relativistic and intermediate energy nuclear collisions p 3548 N92-30010
Stopping powers and cross sections due to two-photon processes in relativistic nucleus-nucleus collision
p 3548 N92-30012
An introduction to using the FORTRAN programs provided with Computational Nuclear Physics 1 Nuclear Structure p 3549 N92-30013
A letter of intent for an experiment to study strong electromagnetic fields at RHIC via multiple electromagnetic processes p 3438 N92-30015
RIJKSINSTITUUT VOOR VOLKSGEZONDHEID EN MILIEUHYGIEENE, BILTHOVEN (NETHERLANDS).
First results from TROLIX 1991: An intercomparison of tropospheric ozone lidars p 3459 N92-29244
ROCHESTER UNIV., NY.
Peripheral limitations on spatial vision
[AD-A250579] p 3511 N92-29591
LLE review
[DE92-011614] p 3555 N92-30072
ROME UNIV. (ITALY).
Observations of ozone-aerosol correlated behaviour in the lower stratosphere during the EASOE campaign
p 3459 N92-29243
Clusters of galaxies in depth p 3567 N92-29846
ROYAL OBSERVATORY, EDINBURGH (SCOTLAND).
United Kingdom Infrared Telescope
[ETN-92-91341] p 3565 N92-29682
ROYAL SIGNALS AND RADAR ESTABLISHMENT, MALVERN (ENGLAND).
Laser diode end-pumped Nd:YAG laser
[AD-A248123] p 3475 N92-29396
RUTGERS - THE STATE UNIV., NEW BRUNSWICK, NJ.
Statistical mechanics of collective phenomena in plasmas
[AD-A250581] p 3554 N92-29450
RUTHERFORD APPLETON LAB., CHILTON (ENGLAND).
Contributions to Hadron 1991: 1) Testing the nature of the f(0)(S asterisk). 2) Gamma gamma to pi(exp 0) pi(exp 0): Dispersive analysis compared to chiral perturbation theory
[RAL-91-070] p 3544 N92-29488
Testing the nature of the f(0)(S asterisk)
p 3545 N92-29489
Gamma gamma to pi(exp 0) pi(exp 0): Dispersive analysis compared to chiral perturbation theory
p 3545 N92-29490
Pole counting and resonance classification
[RAL-92-004] p 3560 N92-29996

S

SAAB-SCANIA, LINKOPING (SWEDEN).
A manufacturer's approach to ensure long term structural integrity p 3403 N92-30133
SACRAMENTO AIR LOGISTICS CENTER, MCCLELLAN AFB, CA.
Nondestructive inspection perspectives
p 3481 N92-30121
SAN DIEGO STATE UNIV., CA.
Robust adaptive kinematic control of redundant robots
[NASA-CR-190520] p 3528 N92-29673
SANDIA LABS., LIVERMORE, CA.
On transient flamelets and their relationship to turbulent methane-air jet flames
[DE92-006705] p 3419 N92-29943
SANDIA NATIONAL LABS., ALBUQUERQUE, NM.
Latent interface-trap buildup: Issues for long-term device response
[DE92-003148] p 3439 N92-29455
Improving path planning with learning
[DE92-004360] p 3527 N92-29456
Material-deposition processes in the separator of Li-alloy/FeS2 thermal cells
[DE92-013669] p 3440 N92-29518
A look at the development environment and tools used in a large INGRES ABF application project
[DE92-012632] p 3561 N92-29552
Metal vapor plasma behavior during vacuum arc remelting of alloy 718
[DE92-011761] p 3421 N92-29623
Raman features of CVD diamond films
[DE92-011381] p 3426 N92-29908
A new HyperVelocity Launcher (HVL) for space science application
[DE92-010670] p 3408 N92-29986
Aging aircraft NDI Development and Demonstration Center (AANC): An overview p 3481 N92-30120
Laser etching: Possibilities and problems
[DE92-010800] p 3477 N92-30135
SANDIA NATIONAL LABS., LIVERMORE, CA.
Structure of a methanol/air coaxial reacting spray near the stabilization region by OH fluorescence imaging and two-component phase-Doppler interferometry
[DE92-005328] p 3417 N92-29431
A linear eddy sub-grid model for turbulent reacting flows: Application to hydrogen-air combustion
[DE92-006699] p 3417 N92-29433
Review of potential x ray laser applications in materials science and chemistry
[DE92-012254] p 3475 N92-29434
Hydrogenation reactions of neutral carbon clusters: C(sub n) (n = 6-75) + D(sub 2)
[DE92-005330] p 3417 N92-29459
Using phase retrieval to determine the intensity and phase of an ultrashort laser pulse
[DE92-013564] p 3476 N92-29516
The twopnt program for boundary value problems: Version 3.10 of March 1992
[DE92-013394] p 3517 N92-29641
SCHUNK KOHLENSTOFFTECHNIK G.M.B.H., GIESSEN (GERMANY, F.R.).
Development and characterization of oxidation-protected CFC
[MBB-Z-0395-91-PUB] p 3416 N92-29876
SCIENCE AND TECHNOLOGY CORP., HAMPTON, VA.
Multi-wavelength measurements of the stratospheric aerosol layer made at Hampton, Virginia (37N, 76W)
p 3460 N92-29249
System testing and performance characterization of the LITE Laser Transmitter Module at NASA
p 3469 N92-29302

SIMPSON WEATHER ASSOCIATES, INC., CHARLOTTESVILLE, VA.
Identification of critical design points for the EAP of a space-based Doppler lidar wind sounder
p 3463 N92-29270
SMITHSONIAN ASTROPHYSICAL OBSERVATORY, CAMBRIDGE, MA.
Investigation of the structure of the electromagnetic field and related phenomena, generated by the active satellite
[NASA-CR-190446] p 3434 N92-29568
SOFTECH, INC., HOUSTON, TX.
ASV3 dial-in interface recommendation for the Repository Based Software Engineering (RBSE) program
[NASA-CR-190500] p 3514 N92-29362
SOUTH CAROLINA RESEARCH AUTHORITY. CHARLESTON.
PDES application protocol suite for composites (PAS-C): IDEFO activity models and information needs for the PAS-C program
[AD-A248714] p 3562 N92-29720
SOUTHAMPTON UNIV. (ENGLAND).
Realistic models for predicting sound propagation in flow duct systems
[ISVR-TR-204] p 3544 N92-29814
SOUTHERN RESEARCH INST., BIRMINGHAM, AL.
Synthesis of a naphthalene-hydroxynaphthalene polymer model compound
[DE92-012264] p 3423 N92-29435
SOUTHWEST RESEARCH INST., SAN ANTONIO, TX.
Source location determination of Uranian kilometric radiation from ray tracing and emission lobe modelling
[NASA-CR-190482] p 3570 N92-29360
SOUTHWEST TEXAS STATE UNIV., SAN MARCOS.
The effects of student-instructor interaction and paired/individual study on achievement in computer-based training
[AD-A248518] p 3511 N92-29503
SPACE ENVIRONMENT SERVICES CENTER, BOULDER, CO.
SESC glossary of solar-terrestrial terms
[PB92-185305] p 3563 N92-30194
SPACE PHYSICS RESEARCH INST., SUNNYVALE, CA.
Diurnal forcing of planetary atmospheres
[NASA-CR-190262] p 3569 N92-30199
SPARTA, INC., LEXINGTON, MA.
Application of laser imaging for bio/geophysical studies p 3465 N92-29282
SRI INTERNATIONAL CORP., MENLO PARK, CA.
ARCLITE: The Arctic Lidar Technology Facility at Sondre Stromfjord, Greenland p 3407 N92-29283
STANFORD LINEAR ACCELERATOR CENTER, CA.
Transverse wakefields at high dispersion
[DE92-010752] p 3550 N92-29788
High resolving power spectrometer for beam analysis
[DE92-010751] p 3437 N92-29988
STANFORD UNIV., CA.
Global solar magnetic fields
[AD-A248340] p 3569 N92-29421
Limit theorems for cumulative processes
[AD-A248507] p 3538 N92-29500
A sample-size optimal bayesian procedure for sequential pharmaceutical trials
[AD-A248512] p 3538 N92-29501
Global measurements of low-frequency radio noise
[AD-A248260] p 3434 N92-29542
Accurate procedures for approximate Bayesian and conditional inference without the need for orthogonal parameters
[AD-A248662] p 3539 N92-29718
Annual research briefs, 1991
[NASA-CR-189967] p 3447 N92-30041
A preliminary experimental investigation of local isotropy in high-Reynolds-number turbulence
p 3447 N92-30042
Local isotropy in buoyancy-generated turbulence
p 3447 N92-30043
Non-linear interactions in homogeneous turbulence with and without background rotation p 3448 N92-30044
On small scale vortices in turbulent flows
p 3448 N92-30045
Scaling analysis of energy transfer in the inertial range
p 3448 N92-30046
Lagrangian velocity correlation and spectrum in homogeneous isotropic turbulence p 3448 N92-30047
Turbulence and vortex structures
p 3448 N92-30048
Vorticity matching in superfluid helium
p 3449 N92-30049
The role of pressure-dilatation correlation in rapidly compressed turbulence and in boundary layers
p 3449 N92-30050
Analyses and modeling of evolving turbulent flow
p 3449 N92-30051
Near-wall turbulence modeling for boundary layers with separation p 3449 N92-30052
Modeling turbulent boundary layers in adverse pressure gradients p 3449 N92-30053
Derivation of the kappa-epsilon model equations using the renormalization group method p 3450 N92-30055
On dynamic models for large eddy simulation
p 3450 N92-30056
Large eddy simulations of passive and buoyant scalars with dynamic subgrid-scale models
p 3450 N92-30057
Dynamic subgrid-scale modeling of compressible turbulence p 3450 N92-30058
Probability density function approach and related closures for turbulent scalar fields p 3450 N92-30059
Monte-Carlo implementation of mapping closures: Application to chemical reacting flows
p 3450 N92-30060
Flame ignition in a premixed turbulent flow
p 3450 N92-30061
Simulation of flame-turbulence interactions in premixed combustion p 3450 N92-30062
Linear stability analysis of hypersonic boundary layers
p 3451 N92-30063
Methods for direct simulation of transition in hypersonic boundary layers 2 p 3451 N92-30064
Effect of walls on the supersonic reacting mixing layer
p 3451 N92-30065
Direct numerical simulation of instability and noise generation of hot jets p 3451 N92-30066
Mixing measurements of straight and curved shear layers p 3451 N92-30067
Progress toward identification of streamwise vorticity meander in a plane mixing layer p 3451 N92-30068
Streaks in turbulent boundary layers
p 3451 N92-30069
An exact turbulent closure for the hydromagnetic dynamo p 3452 N92-30071
Annual research briefs, 1989
[NASA-CR-189024] p 3452 N92-30149
Modeling of compressible turbulence
p 3452 N92-30150
Turbulence modeling: Near-wall turbulence and effects of rotation on turbulence p 3452 N92-30151
An experimental study of scalar mixing in curved shear layers p 3453 N92-30152
An experimental investigation of a low Reynolds number turbulent boundary layer subject to an adverse pressure gradient p 3453 N92-30153
An experimental study of the effects of rapid rotation on turbulence p 3453 N92-30154
An experimental study of secondary vortex structure in mixing layers p 3453 N92-30155
Development of renormalization group analysis of turbulence p 3453 N92-30156
Short-time Lyapunov exponent analysis
p 3453 N92-30157
Organized motions underlying turbulent shear flows
p 3453 N92-30158
Turbulence dynamics in the wavelet representation
p 3454 N92-30159
Direct simulation of turbulent combustion
p 3454 N92-30160
Transition to turbulence in hypersonic flow
p 3454 N92-30161
Direct simulations of wall-bounded compressible turbulence p 3454 N92-30162
Turbulent transport in the solar nebula
p 3454 N92-30163
A numerical method for prediction of compressible turbulent flows with closure models
p 3454 N92-30164
Incompressible spatially-developing free-shear flows
p 3454 N92-30165
A numerical method for direct simulation of turbulence in complex geometries p 3455 N92-30166
The large-scale structures in turbulent plane Couette flow p 3455 N92-30167
Turbulent thermal convection in a differentially rotating channel p 3455 N92-30168
Patterns in simulated turbulent channel flow
p 3455 N92-30169
STATE UNIV. OF NEW YORK, ALBANY.
Cosine response characteristics of radiometric and photometric sensors
[DE92-011437] p 3551 N92-29530
STATE UNIV. OF NEW YORK, STONY BROOK.
Analysis of EUV dayglow spectra of Triton, Titan and Earth
[NASA-CR-190586] p 3568 N92-29451
STERLING (WALTER V.), INC., PALO ALTO, CA.
Army-NASA aircrew/aircraft integration program: Phase 4 A(3)I Man-Machine Integration Design and Analysis System (MIDAS) software detailed design document
[NASA-CR-177593] p 3512 N92-29413
STI OPTRONICS, BELLEVUE, WA.
The Laser Atmospheric Wind Sounder (LAWS) phase 2 preliminary laser design p 3468 N92-29298
STOCKHOLM UNIV. (SWEDEN).
SOLITON
[USIP-90-09] p 3518 N92-29714
Exploratory study for a solid-state charged-particle spectrometer inside the Celsius ring: Alpha and hydrogen reactions at 1.7 and 2.2 GeV/c
[USIP-91-02] p 3546 N92-29715
Decomposer: Program documentation
[USIP-91-04] p 3519 N92-29780
Introduction to SO(3) monopole
[USIP-91-05] p 3560 N92-29781
SUPERCONDUCTING SUPER COLLIDER LAB., DALLAS, TX.
Hydrogen desorption and the search for the Higgs
[DE92-013464] p 3545 N92-29507
SUPERCONDUCTOR TECHNOLOGIES, INC., SANTA BARBARA, CA.
The processing of high temperature ceramic superconducting devices, volume 1
[AD-A248176] p 3438 N92-29404
SVERDRUP TECHNOLOGY, INC., BROOK PARK, OH.
A comparison of the calculated and experimental off-design performance of a radial flow turbine
[NASA-CR-189207] p 3399 N92-29402
The development of a fiber optic Raman temperature measurement system for rocket flows
[NASA-CR-189200] p 3413 N92-29448

T

TARTU ASTRONOOMIA OBSERVATOORIUMI (USSR).
Reconstruction of density and potential fields of the Universe p 3565 N92-29834
TECHNISCHE UNIV., BERLIN (GERMANY, F.R.).
Theoretical and experimental aspects of velocity slip by flows along solid walls
[ISBN-3-7983-1446-2] p 3446 N92-29968
TECHNISCHE UNIV., BRUNSWICK (GERMANY, F.R.).
Motion restoration of long time exposed images with satellite-borne cameras
[ETN-92-91490] p 3474 N92-29731
Thickness dependency of elastic aftereffect of thin bending beams
[ETN-92-91488] p 3483 N92-29925
Experimental examination of heavy loaded axial fans with rotational symmetrical distortion of the inflow
[ETN-92-91489] p 3445 N92-29926
TECHNISCHE UNIV., DELFT (NETHERLANDS).
Nonparametric maximum likelihood estimators for interval censoring and deconvolution
[REPT-91-53] p 3539 N92-29626
ARTIBODIES: A system for modelling articulated bodies
[REPT-91-57] p 3517 N92-29627
Matched asymptotic expansions solution for low-frequency sound radiation from fluid-loaded, baffled plates: Axisymmetric case
[REPT-91-60] p 3543 N92-29628
The effect of length variation on the stability of circular cylindrical shells under pure bending
[LR-669] p 3482 N92-29700
Manufacturing of components of fibre-metal laminates: An overview
[LR-670] p 3415 N92-29702
Software quality control and requirements specification
[REPT-91-48] p 3518 N92-29711
Abstract data types and algorithm structures and a basis for component reuse
[REPT-91-49] p 3518 N92-29712
An annotated bibliography in parallel parsing
[REPT-91-64] p 3525 N92-29716
Methodology on monitoring and modelling of microbial metabolism
[ETN-92-91745] p 3507 N92-29732
Linear relations in microbial reaction systems: A general overview of their origin, form, and use
p 3507 N92-29733
Modelling and experimental validation of carbon dioxide evolution in alkalophilic cultures p 3507 N92-29734
Microbial aldonolactone formation and hydrolysis: Kinetic and bioenergetic aspects p 3507 N92-29735
The bioreactor overflow device: An undesired selective separator in continuous cultures? p 3507 N92-29736
Classification, error detection, and reconciliation of measurements in complex biochemical systems
p 3508 N92-29737
On the estimation of bioenergetic parameters
p 3508 N92-29738
Flux-capacity relationships of Acinetobacter calcoaceticus enzymes during xylose oxidation
p 3508 N92-29739
Analysis and experimental testing of a bottleneck model for the description of microbial dynamics
p 3508 N92-29740

Matched asymptotic expansions solution for low-frequency sound radiation from fluid-loaded, baffled plates: Two-dimensional case
[REPT-91-62] p 3543 N92-29748
Efficient complete radiosity ray tracing using a shadow coherence method
[REPT-91-63] p 3518 N92-29749
State estimation and error diagnosis for biotechnological processes
[ETN-92-91744] p 3508 N92-29754
The use of state estimators (observers) for on-line estimation of non-measurable process variables
p 3508 N92-29755
State estimation and control of the IBE-fermentation with product recovery p 3509 N92-29756
A low sensitivity observer for complex biotechnological processes p 3509 N92-29757
Analytical tuning of a low sensitivity observer applied to a continuous ethanol fermentation with product recovery p 3509 N92-29758
Improved balancing methods and error diagnosis for bio(chemical) conversions p 3509 N92-29759
Sequential application of data reconciliation for sensitive detection of systematic errors p 3509 N92-29760
First order approximation to the average velocity of rise of bubbles in fluid not including inertial forces
[REPT-91-51] p 3444 N92-29763
The isopone method in optimal control
[REPT-91-52] p 3529 N92-29764
Amorphization by interdiffusion in metallic multilayers
[ETN-92-91743] p 3558 N92-29766
Layer-thickness variations and x ray diffraction patterns, a general treatment p 3558 N92-29767
Low-angle x ray diffraction study of solid state amorphization in a Ni/Ti multilayer p 3558 N92-29768
Amorphization along interfaces and grain boundaries in polycrystalline multilayers: An x ray diffraction study of Ni/Ti multilayers p 3558 N92-29769
Interdiffusion reactions in Ni/Ta multilayers studied by x ray diffraction p 3558 N92-29770
A model for interdiffusion in polycrystalline multilayers and its application to solid state amorphization
p 3558 N92-29771
Amorphization and related effects in Ni/Ti multilayers studied by differential scanning calorimetry
p 3559 N92-29772
Evidence for amorphization in Ni/Ti multilayers from electrical resistivity changes p 3559 N92-29773
An introduction to software reuse
[REPT-91-50] p 3519 N92-29779
Architecture and use of Delft Direct Manipulation Manager (D2M2)
[REPT-91-46] p 3521 N92-29887
Estimation of the inverse acoustic transmission operator of a heterogeneous region directly from its reflection operator
[REPT-91-36] p 3544 N92-29918
A model for no Borel liftings
[REPT-91-37] p 3535 N92-29919
Extremally disconnected spaces, subspaces and retractions
[REPT-91-38] p 3535 N92-29920
Limit theorems for functionals of convex hulls
[REPT-91-39] p 3535 N92-29921
A method for converting the surface of a generalized cylinder into a B-spline surface
[REPT-91-40] p 3535 N92-29922
Abstract quasilinear equations and application to a groundwater flow problem
[REPT-91-41] p 3535 N92-29923
Minimal-change codes and number systems
[REPT-91-42] p 3536 N92-29924
Asymptotic results in feedback systems
[ETN-92-91702] p 3529 N92-29962
Asymptotic behavior of random discrete event systems p 3529 N92-29963
Strong law and central limit theorem for a process between maxima and sums p 3530 N92-29964
The M/G/1 processor sharing queue as the almost sure limit of feedback queues p 3530 N92-29965
Multitype branching processes in M/G/1-queueing theory p 3530 N92-29966
Role of polyelectrolytes in barium sulphate precipitation
[PB92-184761] p 3419 N92-30196
Expert judgment study on atmospheric dispersion and deposition: Main report and annexes
[REPT-91-81] p 3495 N92-30226
A monotonic build-up simplex algorithm for linear programming
[REPT-91-82] p 3524 N92-30227
SRSM: A Software Requirements Specification Method
[REPT-91-84] p 3524 N92-30228
A parallel restructured version of GMRES(m)
[REPT-91-85] p 3527 N92-30229

TECHNISCHE UNIV., EINDHOVEN (NETHERLANDS).
A compensation approach for two-dimensional Markov processes
[MEMO-COSOR-91-28] p 3539 N92-29606
Tools for the interfacing between dynamical problems and models within decision support systems
[MEMO-COSOR-91-29] p 3532 N92-29607
Constraint classification for mixed integer programming formulations
[MEMO-COSOR-91-30] p 3516 N92-29608
Taguchi methods
[MEMO-COSOR-91-31] p 3539 N92-29609
D-optimal designs for an incomplete quadratic model
[MEMO-COSOR-91-26] p 3532 N92-29742
The dependence of transport coefficients of suspensions in quasistatic and retarded hydrodynamic interactions
[ETN-92-91624] p 3444 N92-29752
Time-of-flight experiments on GaAs/Al(x)Ga(x-1)As heterostructures
[ETN-92-91625] p 3558 N92-29753
The expanding plasma jet: Experiments and model
[ETN-92-91627] p 3555 N92-29761
A compensation approach for queueing problems
[ETN-92-91628] p 3539 N92-29774
The influence of turbulence on aggregation of small particles in agitated vessels
[ETN-92-91629] p 3445 N92-29775
Chain coding in computer graphics
[ETN-92-91630] p 3518 N92-29776
Diffusion and phase relations in the systems Ti-Si-C and Ti-Si-N
[ETN-92-91631] p 3546 N92-29777
Oriented structures based on trans-1,4-polybutadiene
[ETN-92-91632] p 3546 N92-29778
Architectural synthesis and optimization of digital systems
[ISBN-90-9003966-X] p 3519 N92-29782
Small electrostrictive dilations of cubic crystals
[ISBN-90-9004374-8] p 3559 N92-29783
The theory of imprecise probabilities: Some results for distribution functions, densities, hazard rates, and hazard functions
[MEMO-COSOR-91-32] p 3539 N92-29817
On the p-coverage problem on the real line
[MEMO-COSOR-91-33] p 3520 N92-29818
On setup cost reduction in the economic lot-sizing model without speculative motives
[MEMO-COSOR-91-34] p 3520 N92-29819
On the complexity of postoptimality analysis of 0/1 programs
[MEMO-COSOR-91-35] p 3520 N92-29820
On the asymptotically uniform distribution modulo 1 of extreme order statistics
[MEMO-COSOR-91-38] p 3540 N92-29821
The capacitated multi-echelon inventory system with serial structure: 1: The push ahead-effect
[MEMO-COSOR-91-39] p 3561 N92-29822
The capacitated multi-echelon inventory system with serial structure: 2: An average cost approximation method
[MEMO-COSOR-91-40] p 3561 N92-29823
Sensitivity analysis of the load on an ethernet network
[MEMO-COSOR-91-41] p 3436 N92-29824
Measuring and simulating an 802.3 CSMA/CD LAN
[MEMO-COSOR-91-42] p 3525 N92-29825
On the addition of log-convex functions and sequences
[MEMO-COSOR-92-01] p 3533 N92-29826
Selection constants for uniform populations
[MEMO-COSOR-92-02] p 3540 N92-29827
Data reduction in statistical inference
[MEMO-COSOR-92-03] p 3540 N92-29828
The optical design of AmPS: Elements of the design of a pulse stretcher
[ETN-92-91626] p 3552 N92-29859
Imprecise conjugate prior densities for the one-parameter exponential family of distributions
[MEMO-COSOR-91-36] p 3540 N92-29897
Decision systems; the relation between problem specification and mathematical analysis
[MEMO-COSOR-91-37] p 3535 N92-29898

TELEDYNE GEOTECHNICAL, ALEXANDRIA, VA.
Land-based seismic array studies of low frequency ambient oceanic noise
[AD-A248255] p 3505 N92-29618

TENNESSEE UNIV., KNOXVILLE.
Fuzzy logic control of AC induction motors
[PB92-180207] p 3443 N92-30092

TENNESSEE UNIV., TULLAHOMA.
Development of a multigrid transonic potential flow code for cascades
[NASA-CR-190480] p 3399 N92-29361

TEXAS A&M UNIV., COLLEGE STATION.
New directions for the catalytic conversion of methane
[PB92-172360] p 3492 N92-29519
Determination of aerodynamic sensitivity coefficients for wings in transonic flow
[NASA-CR-190570] p 3401 N92-29657

TEXAS TECHNOLOGICAL UNIV., LUBBOCK.
Development of models for prediction of optimal lifting motion
[PB92-164656] p 3513 N92-29949

TEXAS UNIV., AUSTIN.
Magnetic properties of nano-heterogeneous amorphous thin films
[AD-A250570] p 3420 N92-29426
A novel approach to silicon-on-insulator materials
[AD-A248074] p 3424 N92-29466
Synthesis of new high performance lubricants and solid lubricants
[DE92-011940] p 3424 N92-29549
NASA visual thesaurus maintenance documentation
[NASA-CR-190282] p 3561 N92-29553
Electrical connection of enzyme redox centers to electrodes
[AD-A248545] p 3440 N92-29575
Modeling and computational analysis of multiscale phenomena in fluid-structure interaction problems
[AD-A248723] p 3444 N92-29721

TEXAS UNIV. AT DALLAS, RICHARDSON.
Support activities to maintain SUMS flight readiness
[NASA-CR-189656-VOL-1] p 3410 N92-30217
Support activities to maintain SUMS flight readiness, volume 2. Attachment A: Flight 61-C report
[NASA-CR-189656-VOL-2] p 3411 N92-30218
Support activities to maintain SUMS flight readiness, volume 3. Attachment B: Flight STS-35 report, section A
[NASA-CR-189656-VOL-3] p 3411 N92-30219
Support activities to maintain SUMS flight readiness, volume 4. Attachment B: Flight STS-35 report, section B
[NASA-CR-189656-VOL-4] p 3411 N92-30220
Support activities to maintain SUMS flight readiness, volume 5. Attachment B: Flight STS-35 report, section C
[NASA-CR-189656-VOL-5] p 3411 N92-30221
Support activities to maintain SUMS flight readiness, volume 6. Attachment B: Flight STS-35 report, section D
[NASA-CR-189656-VOL-6] p 3411 N92-30222
Support activities to maintain SUMS flight readiness, volume 7. Attachment B: Flight STS-35 report, section E
[NASA-CR-189656-VOL-7] p 3412 N92-30223
Support activities to maintain SUMS flight readiness, volume 8. Attachment B: Flight STS-35 report, section F
[NASA-CR-189656-VOL-8] p 3412 N92-30224
Support activities to maintain SUMS flight readiness, volume 9. Attachment C: Flight STS-40 report. Attachment D: SUMS software listing
[NASA-CR-189656-VOL-9] p 3412 N92-30225

TITAN SPECTRON DIV., COSTA MESA, CA.
Laser Transmitter Module (LTM) for LITE
p 3463 N92-29265

TOKYO METROPOLITAN UNIV. (JAPAN).
Measurements of stratospheric Pinatubo aerosol extinction profiles by a Raman lidar
p 3457 N92-29232
Lidar measurements of metallic species in mesopause region p 3470 N92-29312

TOLEDO UNIV., OH.
Users manual for updated computer code for axial-flow compressor conceptual design
[NASA-CR-189171] p 3524 N92-30207

TRW, INC., REDONDO BEACH, CA.
Image inversion analysis of the HST OTA (Hubble Space Telescope Optical Telescope Assembly), phase A
[NASA-CR-190483] p 3564 N92-29359

TRW SPACE TECHNOLOGY LABS., REDONDO BEACH, CA.
MHD Technology Transfer, Integration and Review Committee
[DE92-012687] p 3554 N92-29640

TUEBINGEN UNIV. (GERMANY, F.R.).
Analysis of high energy x ray observations of long periodic pulsars
[ETN-92-91494] p 3564 N92-29468

TUFTS UNIV., MEDFORD, MA.
CoMStOC 4: Multiwaveband observations of sunspot and plage-associated coronal emission
[AD-A248344] p 3570 N92-29632

U

UNIVERSAL ENERGY SYSTEMS, INC., SAN ANTONIO, TX.
On the effect of range restriction on correlation coefficient estimation
[AD-A248956] p 3511 N92-29620

UNIVERSITAET DER BUNDESWEHR MUENCHEN, NEUBIBERG (GERMANY, F.R.).

A semi empirical method for the analytical representation of stationary measured profile coefficients for applications of rotary wing aerodynamics
[ETN-92-91491] p 3401 N92-29741

Production of periodical Mach number variations in high subsonic flow in a blow down wind tunnel, and its influence on profile measurements
[ETN-92-91492] p 3401 N92-29889

Examination of the main error factors with regards to secondary losses in compression and turbine cascades by variations of the blade picture ratio
[ETN-92-91493] p 3405 N92-29927

UNIVERSITEIT TWENTE, ENSCHEDE (NETHERLANDS).

Protocol conformance testing: A formal perspective in ISO IS-9646
[MEMO-INF-91-32] p 3517 N92-29705

A new heuristic for load-balanced assignment of objects and minimized network communication in distributed programs implemented through inverse remote procedure calls
[MEMO-INF-91-91] p 3519 N92-29815

Information systems analysis and design based on an object-oriented framework
[MEMO-INF-91-93] p 3519 N92-29816

Implementation of the object-oriented data model TM
[MEMO-INF-91-94] p 3520 N92-29855

Parameter identification in tidal models with uncertain boundaries
[MEMO-983] p 3540 N92-29856

Mathematical modelling of saturated and unsaturated groundwater flow
[MEMO-987] p 3445 N92-29857

Construction of a VC1 interpolant over triangles via edge deletion
[MEMO-988] p 3533 N92-29858

Integrable deformations of meromorphic equations on P(exp 1)C
[MEMO-993] p 3534 N92-29872

Performance of a connectionless protocol over ATM
[MEMO-INF-92-02] p 3526 N92-29880

The primordial soup algorithm: A systematic approach to the specification and design of parallel parsers
[MEMO-INF-91-77] p 3536 N92-29956

Integrity control in relational database systems: An overview
[MEMO-INF-91-80] p 3562 N92-29957

Cislan-2 final document by University of Twente (Netherlands)
[MEMO-INF-91-81] p 3526 N92-29958

Real-time service definition of a communication network in a manufacturing environment
[MEMO-INF-91-84] p 3437 N92-29959

An ontology of ceramics
[MEMO-INF-91-85] p 3426 N92-29960

An object-oriented language-database integration model: The composition-filters approach
[MEMO-INF-91-90] p 3521 N92-29961

A seven-league-boots algorithm for path planning in configuration spaces
[MEMO-INF-91-88] p 3530 N92-29969

Inverse remote procedure calls
[MEMO-INF-91-89] p 3521 N92-29970

Polynomial methods in H(infinity)-optimal control
[MEMO-1008] p 3530 N92-29971

A finite volume approach to large eddy simulation of compressible, homogeneous, isotropic, decaying turbulence
[MEMO-1009] p 3446 N92-29972

Puzzles 3 Hanoi-variations in digraphs
[MEMO-1010] p 3541 N92-29973

A simple approximation to the bivariate normal distribution with large correlation coefficient
[MEMO-1011] p 3540 N92-29974

A two-stage estimator for generalized linear models with nonconstant dispersion parameter
[MEMO-1012] p 3540 N92-29975

Testing equality of variances in the analysis of repeated measurements
[MEMO-1013] p 3541 N92-29976

Monopolar vortices as relative equilibria and their dissipative decay
[MEMO-1015] p 3446 N92-29977

Energy propagation in dissipative systems. Part 2: Centrovelocity for nonlinear wave equations
[MEMO-1016-PT-2] p 3437 N92-29978

Approximation in a damped Hamiltonian system by successive relative equilibria
[MEMO-1017] p 3536 N92-29979

Power approximations to and power comparison of certain goodness-of-fit tests
[MEMO-1019] p 3541 N92-29980

A soft stairway to institutions
[MEMO-INF-91-87] p 3522 N92-29981

A method for analysing the performance aspects of the fault-tolerance mechanisms in FDDI
[MEMO-INF-91-92] p 3514 N92-29982

An analysis of model-based diagnosis using problem-reformulation
[MEMO-INF-92-03] p 3530 N92-29983

Cislan-2 extension final document by University of Twente (Netherlands)
[MEMO-INF-92-05] p 3437 N92-29984

Comparing UCN with FDDI and DQDB using a realistic work model
[MEMO-INF-92-06] p 3526 N92-29985

Partial logic as a simple restriction of standard logic
[MEMO-INF-91-73] p 3536 N92-29995

Random walk polynomials and random walk measures
[MEMO-1007] p 3536 N92-29999

What is the method in formal methods?
[MEMO-INF-91-79] p 3562 N92-30000

A case study in functional real-time programming
[MEMO-INF-91-62] p 3522 N92-30073

A simulation study on a high-speed slotted-ring access mechanism with dynamically adaptive slot size
[MEMO-INF-91-63] p 3526 N92-30074

A closer look at a Fibonacci-like iterated nonlinear map: More chaos and order
[MEMO-INF-91-70] p 3537 N92-30075

Port-controlled Hamiltonian systems: Modelling origins and systemtheoretic properties
[MEMO-1001] p 3537 N92-30077

Supersymmetric extensions of the nonlinear Schroedinger equation: Symmetries and coverings
[MEMO-1002] p 3537 N92-30078

A survey on minimum cost spanning tree games
[MEMO-1003] p 3541 N92-30079

Classification of A-graded algebras with 3 generators
[MEMO-1004] p 3537 N92-30080

Optimal copying strategies
[MEMO-1005] p 3537 N92-30081

A model for dataflow query execution in a parallel main-memory environment
[MEMO-INF-91-34] p 3527 N92-30142

Temporal reasoning in model-based diagnosis
[MEMO-INF-91-66] p 3531 N92-30143

A formal development trajectory for OSI application layer protocols
[MEMO-INF-91-71] p 3523 N92-30144

Criteria for, and experience with, ADTs in large LOTOS specifications
[MEMO-INF-91-74] p 3514 N92-30145

Chebyshev line approximation: A sensitivity analysis
[MEMO-1020] p 3537 N92-30147

On the entropy production of dissipation models
[MEMO-1021] p 3560 N92-30148

Variable bandwidth connections for a connectionless service on ATM: Performance modelling and evaluation
[MEMO-INF-91-83] p 3438 N92-30170

Object-oriented system implementation
[MEMO-INF-91-67] p 3523 N92-30181

PBT: A Parallel Bottom-up Tomita Parser
[MEMO-INF-91-69] p 3527 N92-30183

Integrated service engineering supported by the FDT LOTOS
[MEMO-INF-91-76] p 3531 N92-30184

Sufficient conditions for dominating cliques
[MEMO-1006] p 3538 N92-30185

Algorithms and min-max theorems for certain multiway cuts
[MEMO-1022] p 3523 N92-30186

A random polynomial time algorithm for well-rounding convex bodies
[MEMO-1023] p 3541 N92-30188

Optimal parallel parsing of almost all LL(k) grammars
[MEMO-INF-91-78] p 3527 N92-30189

Performability modelling tools: A survey
[MEMO-INF-91-82] p 3523 N92-30191

UNIVERSITY OF WESTERN MICHIGAN, KALAMAZOO.

Correlated charge-changing ion-atom collisions
[DE92-013473] p 3546 N92-29642

UTAH UNIV., SALT LAKE CITY.

Polarization lidar liquid cloud detection algorithm for winter mountain storms p 3472 N92-29323

Thermodynamic and kinetic aspects of 3/5 epitaxy
[AD-A250632] p 3556 N92-29429

OMVPE growth of InAsSbBi and related alloys using new organometallic group 5 sources
[AD-A250631] p 3557 N92-29635

V

VANDERBILT UNIV., NASHVILLE, TN.

Surface reactions in the space environment
[AD-A250624] p 3428 N92-29428

Neutralizer and sample chamber for the Atomic Oxygen Simulation System (AOSS)
[NASA-CR-184343] p 3407 N92-29664

VIRGINIA POLYTECHNIC INST. AND STATE UNIV., BLACKSBURG.

Micro-device for coupling, multiplexing and demultiplexing using elliptical-core two-mode fiber
[NASA-CR-190496] p 3550 N92-29331

Active structural acoustic control and smart structures
[AD-A248341] p 3543 N92-29588

Modelling, information processing and control
[AD-A250571] p 3532 N92-29589

Analyses of near- and far-field two-lobe patterns outside the output endface of a two-mode fiber
[NASA-CR-190494] p 3551 N92-29652

Erbium-doped fiber amplifier elements for structural analysis sensors
[NASA-CR-190491] p 3552 N92-29681

VIRGINIA UNIV., CHARLOTTESVILLE.

The 12 micron contribution of nearby galaxies to the infrared background
[AD-A250623] p 3565 N92-29596

NASA-UVA light aerospace alloy and structures technology program (LA2ST)
[NASA-CR-190538] p 3423 N92-30206

An approximate solution for interlaminar stresses in laminated composites: Applied mechanics program
[NASA-CR-190537] p 3416 N92-30208

W

WASHINGTON STATE UNIV., PULLMAN.

Rare gas clusters containing charged atoms
[AD-A248299] p 3544 N92-29350

MNDO study of boron-nitrogen analogues of buckminsterfullerene
[AD-A247777] p 3414 N92-29460

WASHINGTON UNIV., SEATTLE.

Tear straps in airplane fuselage
[AD-A248543] p 3404 N92-29511

Theoretical overview: Hot and dense QCD in equilibrium
[DE92-013665] p 3560 N92-29517

Sound speed, reflectivity, and absorption measurements in Arctic ice in 1988
[AD-A246293] p 3505 N92-29554

WESTINGHOUSE HANFORD CO., RICHLAND, WA.

SP-100 W/Re thermocouple calibration techniques
[DE92-011302] p 3550 N92-29938

WESTINGHOUSE SAVANNAH RIVER CO., AIKEN, SC.

Reviews of computing technology: Fiber distributed data interface
[DE92-011374] p 3514 N92-29907

WINAND STARING CENTRE, WAGENINGEN (NETHERLANDS).

Mapping agroecological zones and time lag in vegetation growth by means of Fourier analysis of time series of NDVI images
[REPT-32] p 3490 N92-29717

WISCONSIN UNIV., MADISON.

Wind profiles derived from volume imaging lidar data: Enhancements to the algorithm and comparisons with insitu observations p 3464 N92-29271

Adaptation of the University of Wisconsin high spectral resolution lidar for polarization and multiple scattering measurements p 3472 N92-29322

Venus in motion: An animated video catalog of Pioneer Venus Orbiter Cloud Photopolarimeter images
[NASA-CR-190543] p 3568 N92-29401

Additivity and auditory pattern analysis
[AD-A250580] p 3511 N92-29592

WISCONSIN UNIV., MILWAUKEE.

Zee star analysis
[AD-A248342] p 3417 N92-29423

WISCONSIN UNIV., PLATTEVILLE.

Measurements of wind divergence with volume imaging lidar p 3464 N92-29272

WOODS HOLE OCEANOGRAPHIC INST., MA.

Acoustic scattering from elastic ice: A finite difference solution
[AD-A248281] p 3543 N92-29346

Shelf Mixed Layer Experiment (SMILE) program description and coastal and moored array data report
[PB92-170281] p 3506 N92-29805

OCEANUS 218: Warm Ring Inertial Critical Layer Experiment (WRINCLE)
[PB92-170299] p 3506 N92-29806

WORLD METEOROLOGICAL ORGANIZATION, GENEVA (SWITZERLAND).

CLICOM-news, issue 7 p 3503 N92-30171

Y

YALE UNIV., NEW HAVEN, CT.

On the numerical solution of one-dimensional integral and differential equations
[AD-A250388] p 3531 N92-29548

YARDNEY TECHNICAL PRODUCTS, INC., PAWCATUCK, CT.
Advanced rechargeable lithium sulfur dioxide cell [AD-A250027] p 3491 N92-29476
YORK UNIV. (ONTARIO).
Correcting for interference of Mt. Pinatubo aerosols on DIAL measurements of stratospheric ozone p 3458 N92-29237
Two wavelength measurements of the Pinatubo aerosol above Toronto, Canada p 3461 N92-29253
One year of Rayleigh lidar measurements at Toronto p 3466 N92-29285
Lidar studies of clouds at Toronto during the ECLIPS program p 3472 N92-29321

Typical Contract Number Index Listing

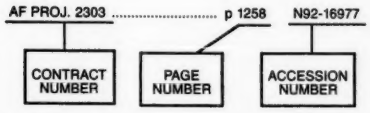

Listings in this index are arranged alphanumerically by contract number. Under each contract number the accession numbers denoting documents that have been produced as a result of research done under that contract are arranged in ascending order. The page number helps to locate the citation in the abstract section. The accession number denotes the number by which the citation is identified.

AF PROJ. 2301 ..... p 3443 N92-30176
AF PROJ. 2308 ..... p 3418 N92-29580
AF PROJ. 3405 ..... p 3407 N92-29709
AF-AFOSR-0010-87 ..... p 3554 N92-29450
AF-AFOSR-0029-89 ..... p 3528 N92-29590
AF-AFOSR-0030-90 ..... p 3428 N92-29428
AF-AFOSR-0031-89 ..... p 3532 N92-29589
AF-AFOSR-0074-89 ..... p 3418 N92-29901
AF-AFOSR-0146-91 ..... p 3510 N92-29420
AF-AFOSR-0147-89 ..... p 3570 N92-29632
AF-AFOSR-0180-91 ..... p 3455 N92-30192
AF-AFOSR-0188-90 ..... p 3418 N92-29580
AF-AFOSR-0193-89 ..... p 3416 N92-30137
AF-AFOSR-0197-89 ..... p 3510 N92-29334
AF-AFOSR-0240-87 ..... p 3511 N92-29592
AF-AFOSR-0257-88 ..... p 3435 N92-29579
AF-AFOSR-0287-89 ..... p 3421 N92-29547
AF-AFOSR-0290-91 ..... p 3510 N92-29577
AF-AFOSR-0292-88 ..... p 3511 N92-29591
AF-AFOSR-0294-90 ..... p 3512 N92-29930
AF-AFOSR-0308-89 ..... p 3413 N92-29913
AF-AFOSR-0313-89 ..... p 3482 N92-29407
AF-AFOSR-0357-89 ..... p 3480 N92-29710
AF-AFOSR-0467-89 ..... p 3565 N92-29596
AF-AFOSR-89-0042 ..... p 3455 N92-30190
ARPA ORDER 6268 ..... p 3438 N92-29404
A28-W20233 ..... p 3468 N92-29298
BCRS PROJ. CO-2.21 ..... p 3489 N92-29493
BCRS PROJ. CO-2.22 ..... p 3491 N92-30231
BCRS PROJ. IS-3.9 ..... p 3491 N92-30230
BCRS PROJ. OP-2.11 ..... p 3489 N92-29693
BCRS PROJ. OP-3.2 ..... p 3489 N92-29495
BCRS PROJ. TE-2.3 ..... p 3489 N92-29494
BCRS PROJ. 6.5/IS-11 ..... p 3493 N92-29499
DA PROJ. 1L1-62211-A-47-A ..... p 3478 N92-29351
DA PROJ. 1L1-62618-AH-80 ..... p 3554 N92-29510
DA PROJ. 1L1-62705-AH-94 ..... p 3439 N92-29498
DA PROJ. 3M1-62787-A-79-B ..... p 3512 N92-29348
DA PROJ. 3M4-63807-D-836 ..... p 3510 N92-29347
p 3404 N92-29506
DAAA15-88-D-0001 ..... p 3423 N92-29940
DAAD07-89-C-0214 ..... p 3525 N92-29555
DAAL01-88-C-0849 ..... p 3491 N92-29476
DAAL03-86-G-0044 ..... p 3445 N92-29933
DAAL03-88-K-0067 ..... p 3551 N92-29546
DAAL03-88-K-0105 ..... p 3434 N92-29447
DAAL03-89-K-0001 ..... p 3418 N92-29719
DAAL03-90-G-0011 ..... p 3443 N92-29458
DAAL03-90-G-0219 ..... p 3552 N92-29727
DAAL03-91-C-0038 ..... p 3516 N92-29622
DAAL03-91-G-0101 ..... p 3538 N92-29500
DAJA45-91-C-0016 ..... p 3422 N92-29647
DE-AC02-76CH-00016 ..... p 3556 N92-29437
p 3550 N92-29475
p 3549 N92-29477
p 3545 N92-29582
DE-AC02-83CH-10093 ..... p 3491 N92-29454
p 3557 N92-29584
p 3425 N92-29598
DE-AC03-76SF-00515 ..... p 3550 N92-29788
p 3437 N92-29988
DE-AC03-89ER-51114 ..... p 3554 N92-29412
p 3476 N92-29474
p 3474 N92-29942
DE-AC04-76DP-00613 ..... p 3441 N92-29796
DE-AC04-76DP-00656 ..... p 3439 N92-29414
DE-AC04-76DP-00789 ..... p 3438 N92-29339
p 3475 N92-29434
p 3439 N92-29455
p 3527 N92-29456
p 3440 N92-29518
p 3561 N92-29552
p 3421 N92-29623
p 3426 N92-29908
p 3408 N92-29986
p 3477 N92-30135
DE-AC04-76DR-00789 ..... p 3417 N92-29431
p 3417 N92-29433
p 3417 N92-29459
p 3476 N92-29516
p 3517 N92-29641
p 3419 N92-29943
DE-AC05-84OR-21400 ..... p 3413 N92-29461
p 3527 N92-29504
p 3528 N92-29550
p 3417 N92-29551
p 3528 N92-29644
p 3519 N92-29797
p 3436 N92-29909
p 3547 N92-29910
p 3475 N92-30090
DE-AC06-76RL-01830 ..... p 3420 N92-29411
p 3420 N92-29436
p 3569 N92-29600
p 3415 N92-29645
p 3492 N92-29646
DE-AC06-87RL-10930 ..... p 3550 N92-29938
DE-AC08-88NV-10617 ..... p 3549 N92-29457
p 3549 N92-29502
DE-AC09-89SR-18035 ..... p 3514 N92-29907
DE-AC22-87PC-90274 ..... p 3554 N92-29640
DE-AC22-90PC-90038 ..... p 3423 N92-29435
DE-AC35-89ER-40486 ..... p 3545 N92-29507
DE-AI01-79ET-29372 ..... p 3551 N92-29679
DE-AI05-90ER-30174 ..... p 3490 N92-30088
p 3452 N92-30140
DE-AS05-80ER-10742 ..... p 3556 N92-29437
DE-FC03-85DP-40200 ..... p 3554 N92-29531
p 3555 N92-30072
DE-FC03-90ER-61010 ..... p 3493 N92-29597
DE-FG02-84ER-45125 ..... p 3542 N92-29354
DE-FG02-87ER-13744 ..... p 3546 N92-29899
DE-FG02-87ER-13778 ..... p 3546 N92-29642
DE-FG02-87ER-45290 ..... p 3420 N92-29483
p 3482 N92-29601
DE-FG02-89ER-45394 ..... p 3556 N92-29485
DE-FG02-89ER-60818 ..... p 3504 N92-29439
DE-FG02-90ER-61059 ..... p 3472 N92-29324
DE-FG02-90ER-61072 ..... p 3551 N92-29530
DE-FG02-91ER-54109 ..... p 3553 N92-29336
DE-FG02-91ER-61229 ..... p 3477 N92-29928
DE-FG05-87ER-51112 ..... p 3554 N92-29438
DE-FG05-91ER-12119 ..... p 3424 N92-29549
DE-FG06-85ER-40224 ..... p 3550 N92-29532
DE-FG06-90ER-40561 ..... p 3560 N92-29517
DE-FG07-88ER-12822 ..... p 3445 N92-29784
DI-14-08-0001-G1637 ..... p 3494 N92-29746
DI-14-08-0001-G1645 ..... p 3489 N92-29701
DI-14-12-0001-30363 ..... p 3505 N92-29704
DI-14-12-0001-30411 ..... p 3490 N92-30022
DNA001-87-C-0277 ..... p 3507 N92-29410
DTCG23-86-C-20062 ..... p 3422 N92-29807
DTCG39-89-C-80671 ..... p 3512 N92-29538
DTFA03-89-C-00043 ..... p 3487 N92-30126
DW13932524-01 ..... p 3464 N92-29274
EEC-90-ET-011 ..... p 3495 N92-30226
EPA-R81-4169-03 ..... p 3443 N92-30092
EPA-68-C8-0006 ..... p 3495 N92-30021
p 3495 N92-30173
EPA/68-C8-0006 ..... p 3494 N92-30018
FY1456-91-N0054 ..... p 3447 N92-30036
F19628-85-C-0003 ..... p 3516 N92-29540
F19628-89-C-0001 ..... p 3436 N92-29902
F19628-89-C-0137 ..... p 3473 N92-29328
F30602-88-D-0028 ..... p 3417 N92-29423
F30602-89-C-0155 ..... p 3442 N92-29914
F33615-85-C-3213 ..... p 3415 N92-29593
p 3415 N92-29594
F33615-87-C-5243 ..... p 3414 N92-29453
F33615-88-C-0014 ..... p 3406 N92-29505
F33615-88-C-5416 ..... p 3476 N92-29581
F33615-91-C-5713 ..... p 3562 N92-29720
F49620-87-C-0067 ..... p 3420 N92-29426
F49620-88-C-0053 ..... p 3511 N92-29620
F49620-90-C-0076 ..... p 3511 N92-29503
p 3571 N92-29724
p 3571 N92-29725
GRI-5084-260-1051 ..... p 3426 N92-29804
GRI-5086-260-1326 ..... p 3492 N92-29519
JPL-958828 ..... p 3570 N92-29360
JPL-958888 ..... p 3564 N92-29359
LEP-PHILIPS-903-9P34-R0 ..... p 3525 N92-29614
MDA903-87-C-0523 ..... p 3407 N92-29709
MDA903-89-C-0003 ..... p 3426 N92-29905
MDA903-90-C-0006 ..... p 3562 N92-29934
MDA972-91-C-0030 ..... p 3442 N92-29935
NAGW-1594 ..... p 3569 N92-29631
NAGW-2483 ..... p 3568 N92-29451
NAGW-340 ..... p 3568 N92-29432
NAG1-1065 ..... p 3399 N92-29329
NAG1-1108 ..... p 3557 N92-29676
NAG1-1134 ..... p 3547 N92-30001
p 3547 N92-30002
p 3547 N92-30003
p 3438 N92-30004
p 3547 N92-30005
p 3548 N92-30006
p 3548 N92-30007
p 3548 N92-30008
p 3548 N92-30009
p 3548 N92-30010
p 3548 N92-30011
NAG1-1188 ..... p 3445 N92-29830
NAG1-1348 ..... p 3550 N92-29331
p 3551 N92-29652
p 3552 N92-29681
NAG1-1358 ..... p 3404 N92-30209
NAG1-1380 ..... p 3406 N92-29654
NAG1-372 ..... p 3400 N92-29445
NAG1-477 ..... p 3547 N92-30005
p 3548 N92-30007
NAG1-613 ..... p 3517 N92-29695
NAG1-745 ..... p 3423 N92-30206
NAG1-793 ..... p 3401 N92-29657
NAG1-841 ..... p 3416 N92-30208
NAG1-968 ..... p 3409 N92-29422
NAG2-328 ..... p 3517 N92-29630
NAG2-593 ..... p 3515 N92-29400
NAG2-628 ..... p 3517 N92-29630
NAG3-1047 ..... p 3478 N92-29351
NAG3-1097 ..... p 3478 N92-29392
NAG3-1101 ..... p 3481 N92-29342
NAG3-1165 ..... p 3524 N92-30207
NAG3-398 ..... p 3399 N92-29361
NAG5-1256 ..... p 3568 N92-29851
p 3568 N92-29852
NAG5-1340 ..... p 3434 N92-29568
NAG5-1609 ..... p 3568 N92-29401
NAG5-510 ..... p 3435 N92-29658
NAG5-780 ..... p 3528 N92-29656
NAG5-931 ..... p 3517 N92-29665
NASW-4324 ..... p 3509 N92-29341
NAS1-17399 ..... p 2410 N92-30217
p 3411 N92-30218
p 3411 N92-30219
p 3411 N92-30220
p 3411 N92-30221
p 3411 N92-30222
p 3412 N92-30223
p 3412 N92-30224
p 3412 N92-30225
NAS1-18605 ..... p 3444 N92-29692
p 3455 N92-30190
p 3455 N92-30192
NAS1-18851 ..... p 3460 N92-29249
NAS1-19480 ..... p 3455 N92-30192
NAS1-8107 ..... p 3455 N92-30190

NAS10-11624 ..... p 3492 N92-29430
NAS2-131313 ..... p 3405 N92-29427
NAS2-13210 ..... p 3512 N92-29413
NAS3-25266 ..... p 3399 N92-29402
p 3413 N92-29448
NAS7-1110 ..... p 3528 N92-29673
NAS7-918 ..... p 3434 N92-29463
p 3551 N92-29679
p 3479 N92-29765
p 3552 N92-29832
p 3529 N92-29955
p 3428 N92-30083
p 3553 N92-30084
p 3530 N92-30085
p 3442 N92-30086
p 3559 N92-30102
p 3437 N92-30103
p 3553 N92-30104
NAS8-37589 ..... p 3468 N92-29298
NAS8-37748 ..... p 3407 N92-29664
NAS8-38106 ..... p 3570 N92-30204
NAS9-18426 ..... p 3403 N92-29440
NATO-CRG-901077 ..... p 3519 N92-29815
p 3521 N92-29970
NAXXOP9000159 ..... p 3563 N92-30038
NCC1-141 ..... p 3406 N92-29352
NCC2-387 ..... p 3517 N92-29694
NCC2-460 ..... p 3447 N92-30041
p 3452 N92-30149
NCC2-536 ..... p 3401 N92-29691
NCC2-55 ..... p 3453 N92-30155
NCC2-680 ..... p 3569 N92-30199
NCC2-716 ..... p 3406 N92-29655
NCC9-16 ..... p 3514 N92-29362
p 3514 N92-29363
p 3525 N92-29390
p 3514 N92-29391
p 3561 N92-29553
NIOSH-R01-OH-02434 ..... p 3513 N92-29949
NIVR-01904-N ..... p 3532 N92-29604
NIVR-2506-N ..... p 3479 N92-29885
NIVR-2606-N ..... p 3479 N92-29885
NSERC-OGP-0036747 ..... p 3523 N92-30146
NSERC-OGP-0046506 ..... p 3523 N92-30146
NSERC-OGP-0046613 ..... p 3523 N92-30146
NSF ATM-86-18263 ..... p 3569 N92-29421
NSF BCS-91-96089 ..... p 3501 N92-29950
NSF CCR-88-20279 ..... p 3541 N92-30174
NSF CCR-89-01780 ..... p 3515 N92-29400
NSF CCR-91-02231 ..... p 3515 N92-29400
NSF DMS-90-03361 ..... p 3542 N92-30095
NSF DMS-91-04029 ..... p 3455 N92-30192
NSF ECE-86-07591 ..... p 3501 N92-29950
NSF INT-89-12660 ..... p 3568 N92-29851
p 3568 N92-29852
NSF MSM-88-12779 ..... p 3484 N92-30111
NSF OCE-87-16937 ..... p 3506 N92-29805
NSF OCE-89-11053 ..... p 3506 N92-29806
N00014-81-K-0382 ..... p 3434 N92-29542
N00014-85-C-0638 ..... p 3421 N92-29587
N00014-85-C-0890 ..... p 3476 N92-29559
N00014-86-K-0310 ..... p 3531 N92-29548
N00014-88-C-0713 ..... p 3438 N92-29404
N00014-88-K-0264 ..... p 3543 N92-29441
N00014-88-K-0366 ..... p 3424 N92-29465
N00014-88-K-0416 ..... p 3557 N92-29722
N00014-88-K-0657 ..... p 3515 N92-29399
N00014-88-K-0721 ..... p 3543 N92-29588
N00014-88-K-0724 ..... p 3442 N92-29936
N00014-88-M-6610 ..... p 3505 N92-29562
N00014-89-J-1024 ..... p 3569 N92-29421
N00014-89-J-1094 ..... p 3414 N92-29556
N00014-89-J-1276 ..... p 3404 N92-29511
N00014-89-J-1681 ..... p 3531 N92-29486
N00014-89-J-1767 ..... p 3424 N92-29466
N00014-89-J-1923 ..... p 3427 N92-29330
N00014-89-J-3109 ..... p 3444 N92-29721
N00014-89-J-3137 ..... p 3504 N92-29345
N00014-90-C-0118 ..... p 3505 N92-29618
N00014-90-C-0226 ..... p 3557 N92-29583
N00014-90-J-1090 ..... p 3541 N92-30174
N00014-90-J-1161 ..... p 3440 N92-29523
N00014-90-J-1193 ..... p 3544 N92-29350
p 3414 N92-29460
N00014-90-J-1235 ..... p 3417 N92-29514
N00014-90-J-1270 ..... p 3517 N92-29695
N00014-90-J-1604 ..... p 3560 N92-30175
N00014-90-J-1746 ..... p 3543 N92-29543
N00014-90-J-1828 ..... p 3423 N92-29349
p 3424 N92-29508
p 3425 N92-29566
p 3425 N92-29567
p 3425 N92-29569
p 3427 N92-30136
N00014-90-J-1864 ..... p 3510 N92-29398
p 3511 N92-29560
N00014-91-C-0124 ..... p 3420 N92-29408
N00014-91-J-1269 ..... p 3418 N92-29619
N00014-91-J-1304 ..... p 3515 N92-29409
N00014-91-J-1447 ..... p 3556 N92-29429
p 3557 N92-29635
N00014-91-J-1590 ..... p 3424 N92-29496
p 3419 N92-29941
N00014-91-J-1616 ..... p 3418 N92-29557
p 3419 N92-29931
p 3419 N92-29932
N00014-91-J-1710 ..... p 3556 N92-29558
N00014-91-J-1892 ..... p 3414 N92-29462
N00014-91-J-1956 ..... p 3439 N92-29452
N00014-92-J-1125 ..... p 3418 N92-29595
N00025-92-J-1264 ..... p 3538 N92-29501
p 3539 N92-29718
N00039-88-C-0054 ..... p 3505 N92-29554
N00039-91-C-0001 ..... p 3552 N92-29726
N00039-91-C-5301 ..... p 3552 N92-29726
OTKA-2115 ..... p 3524 N92-30227
RICIS PROJ. AR-06 ..... p 3525 N92-29390
RICIS PROJ. IM-10 ..... p 3561 N92-29553
RICIS PROJ. RB-06 ..... p 3514 N92-29362
RICIS PROJ. SE-35 ..... p 3514 N92-29363
RICIS PROJ. SR-01 ..... p 3514 N92-29391
RTOP 196-41-73-02-00 ..... p 3433 N92-29388
p 3433 N92-29389
RTOP 199-14-12-04 ..... p 3506 N92-29397
RTOP 310-10-60-50-00 ..... p 3409 N92-29365
RTOP 310-10-60-60-00 ..... p 3429 N92-29366
RTOP 310-10-60-86-02 ..... p 3430 N92-29367
RTOP 310-10-63-50-00 ..... p 3409 N92-29368
RTOP 310-10-63-88-01 ..... p 3409 N92-29369
RTOP 310-10-63-92-01 ..... p 3409 N92-29370
RTOP 310-20-64-22-00 ..... p 3431 N92-29373
RTOP 310-20-65-67-00 ..... p 3430 N92-29371
RTOP 310-20-65-92-01 ..... p 3431 N92-29372
RTOP 310-20-66-09-01 ..... p 3431 N92-29374
RTOP 310-20-67-59-00 ..... p 3431 N92-29376
RTOP 310-30-42-10-87 ..... p 3432 N92-29378
RTOP 310-30-69-91-02 ..... p 3431 N92-29377
RTOP 310-30-71-83-02 ..... p 3431 N92-29375
RTOP 310-30-71-92-02 ..... p 3432 N92-29379
RTOP 310-40-73-89-01 ..... p 3432 N92-29380
RTOP 314-30-58-50-05 ..... p 3433 N92-29385
RTOP 314-40-22-35-01 ..... p 3409 N92-29383
RTOP 314-40-22-37-01 ..... p 3433 N92-29384
RTOP 314-40-31-30-06 ..... p 3432 N92-29381
RTOP 314-40-41-10-15 ..... p 3432 N92-29382
RTOP 315-20-50-00-06 ..... p 3433 N92-29386
RTOP 315-91-50-20-04 ..... p 3433 N92-29387
RTOP 326-81-10 ..... p 3414 N92-30187
RTOP 505-59-00 ..... p 3400 N92-29625
RTOP 505-59-53 ..... p 3443 N92-29394
RTOP 505-59-85-01 ..... p 3406 N92-29352
RTOP 505-62-52 ..... p 3402 N92-30182
RTOP 505-63-36 ..... p 3478 N92-29351
RTOP 505-63-39 ..... p 3478 N92-29697
RTOP 505-63-40 ..... p 3415 N92-29660
RTOP 505-63-50-12 ..... p 3400 N92-29445
RTOP 505-68-30 ..... p 3405 N92-29425
RTOP 505-68-32 ..... p 3405 N92-29661
RTOP 505-69-14 ..... p 3405 N92-29427
RTOP 505-69-50 ..... p 3404 N92-29417
p 3524 N92-30207
RTOP 505-90-52-01 ..... p 3444 N92-29692
p 3455 N92-30190
p 3455 N92-30192
RTOP 506-41-21 ..... p 3413 N92-29667
RTOP 506-41-51 ..... p 3492 N92-29662
RTOP 506-42-31 ..... p 3413 N92-29448
RTOP 506-42-73 ..... p 3427 N92-29669
RTOP 506-43-71-01 ..... p 3423 N92-30205
RTOP 506-48-11-03 ..... p 3410 N92-30217
p 3411 N92-30218
p 3411 N92-30219
p 3411 N92-30220
p 3411 N92-30221
p 3411 N92-30222
p 3412 N92-30223
p 3412 N92-30224
p 3412 N92-30225
RTOP 510-02-12-10 ..... p 3481 N92-29393
RTOP 533-02-36 ..... p 3405 N92-29659
RTOP 535-05-10 ..... p 3399 N92-29402
RTOP 537-02-20 ..... p 3412 N92-29343
RTOP 538-02-10-01 ..... p 3484 N92-30106
RTOP 578-41-07-20 ..... p 3502 N92-29653
RTOP 590-14-21-01 ..... p 3488 N92-30214
RTOP 665-45-20-21 ..... p 3456 N92-29228
STW-CWI-59-0922 ..... p 3446 N92-29947
SWRI PROJ. 15-3679 ..... p 3570 N92-29360
W-31-109-ENG-38 ..... p 3544 N92-29356
p 3478 N92-29357
p 3478 N92-29534
p 3482 N92-29535
W-7405-ENG-36 ..... p 3525 N92-29624
p 3424 N92-29479
p 3427 N92-29512
p 3500 N92-29513
p 3545 N92-29515
p 3500 N92-29536
p 3421 N92-29633
p 3545 N92-29634
p 3425 N92-29643
p 3555 N92-29789
p 3562 N92-29794
p 3415 N92-29795
p 3555 N92-29917
p 3541 N92-30138
p 3542 N92-30139
p 3556 N92-30203
W-7405-ENG-48 ..... p 3550 N92-29337
p 3481 N92-29338
p 3438 N92-29339
p 3475 N92-29340
p 3524 N92-29353
p 3475 N92-29358
p 3476 N92-29472
p 3556 N92-29473
p 3480 N92-29478
p 3531 N92-29481
p 3551 N92-29484
p 3476 N92-29509
p 3554 N92-29531
p 3516 N92-29537
p 3551 N92-29578
p 3421 N92-29639
p 3517 N92-29694
p 3477 N92-29787
p 3494 N92-29790
p 3533 N92-29791
p 3533 N92-29792
p 3555 N92-29798
p 3436 N92-29909
p 3559 N92-29911
p 3477 N92-29937
p 3477 N92-29987
p 3495 N92-30211
W-7405-ENG-82 ..... p 3424 N92-29482
p 3422 N92-29706
p 3559 N92-29939
p 3481 N92-30119

Typical Report Number Index Listing

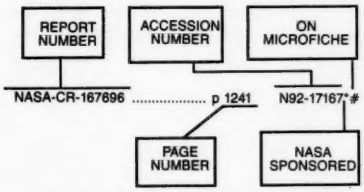

Listings in this index are arranged alphanumerically by report number. The accession number denotes the number by which the citation is identified. The page number helps to locate the citation in the abstract section. An asterisk (*) indicates that the item is a NASA report. A pound sign (#) indicates that the item is available on microfiche.

A-91108 ..... p 3506 N92-29397 * #
A-91119 ..... p 3443 N92-29394 * #
A-92049 ..... p 3512 N92-29413 * #
A-92072 ..... p 3400 N92-29625 * #
A-92081 ..... p 3404 N92-29417 * #

AAE-91-11 ..... p 3413 N92-29913 #

AD-A245351 ..... p 3557 N92-29583 #
AD-A245970 ..... p 3429 N92-29344 #
AD-A245978 ..... p 3407 N92-29929 #
AD-A246110 ..... p 3443 N92-29458 #
AD-A246293 ..... p 3505 N92-29554 #
AD-A247050 ..... p 3418 N92-29901 #
AD-A247182 ..... p 3512 N92-29538 #
AD-A247191 ..... p 3400 N92-29539 #
AD-A247192 ..... p 3442 N92-29914 #
AD-A247296 ..... p 3413 N92-29913 #
AD-A247463 ..... p 3479 N92-29785 #
AD-A247688 ..... p 3543 N92-29441 #
AD-A247777 ..... p 3414 N92-29460 #
AD-A247836 ..... p 3525 N92-29555 #
AD-A247865 ..... p 3570 N92-29464 #
AD-A247932 ..... p 3427 N92-29786 #
AD-A248065 ..... p 3436 N92-29902 #
AD-A248067 ..... p 3414 N92-29556 #
AD-A248072 ..... p 3424 N92-29465 #
AD-A248074 ..... p 3424 N92-29466 #
AD-A248075 ..... p 3531 N92-29486 #
AD-A248077 ..... p 3515 N92-29487 #
AD-A248080 ..... p 3440 N92-29523 #
AD-A248083 ..... p 3444 N92-29524 #
AD-A248084 ..... p 3410 N92-29525 #
AD-A248085 ..... p 3440 N92-29526 #
AD-A248092 ..... p 3515 N92-29527 #
AD-A248093 ..... p 3554 N92-29528 #
AD-A248094 ..... p 3440 N92-29529 #
AD-A248096 ..... p 3556 N92-29558 #
AD-A248103 ..... p 3476 N92-29559 #
AD-A248104 ..... p 3511 N92-29560 #
AD-A248105 ..... p 3539 N92-29585 #
AD-A248108 ..... p 3516 N92-29586 #
AD-A248110 ..... p 3528 N92-29561 #
AD-A248112 ..... p 3433 N92-29395 #
AD-A248123 ..... p 3475 N92-29396 #
AD-A248128 ..... p 3510 N92-29398 #
AD-A248135 ..... p 3440 N92-29564 #
AD-A248146 ..... p 3427 N92-29330 #
AD-A248153 ..... p 3516 N92-29540 #
AD-A248154 ..... p 3439 N92-29443 #
AD-A248157 ..... p 3412 N92-29444 #
AD-A248160 ..... p 3531 N92-29446 #
AD-A248175 ..... p 3515 N92-29399 #
AD-A248176 ..... p 3438 N92-29404 #
AD-A248182 ..... p 3439 N92-29405 #
AD-A248183 ..... p 3434 N92-29406 #
AD-A248187 ..... p 3482 N92-29407 #
AD-A248190 ..... p 3420 N92-29408 #
AD-A248193 ..... p 3515 N92-29409 #
AD-A248199 ..... p 3507 N92-29410 #
AD-A248252 ..... p 3403 N92-29617 #
AD-A248255 ..... p 3505 N92-29618 #
AD-A248258 ..... p 3527 N92-29541 #
AD-A248260 ..... p 3434 N92-29542 #
AD-A248272 ..... p 3504 N92-29345 #
AD-A248281 ..... p 3543 N92-29346 #
AD-A248283 ..... p 3510 N92-29347 #
AD-A248284 ..... p 3512 N92-29348 #
AD-A248285 ..... p 3423 N92-29349 #
AD-A248286 ..... p 3425 N92-29566 #
AD-A248287 ..... p 3425 N92-29567 #
AD-A248299 ..... p 3544 N92-29350 #
AD-A248306 ..... p 3425 N92-29569 #
AD-A248334 ..... p 3512 N92-29930 #
AD-A248335 ..... p 3418 N92-29557 #
AD-A248336 ..... p 3419 N92-29931 #
AD-A248337 ..... p 3419 N92-29932 #
AD-A248338 ..... p 3510 N92-29420 #
AD-A248339 ..... p 3421 N92-29587 #
AD-A248340 ..... p 3569 N92-29421 #
AD-A248341 ..... p 3543 N92-29588 #
AD-A248342 ..... p 3417 N92-29423 #
AD-A248344 ..... p 3570 N92-29632 #
AD-A248345 ..... p 3505 N92-29562 #
AD-A248347 ..... p 3502 N92-29424 #
AD-A248408 ..... p 3413 N92-29903 #
AD-A248409 ..... p 3413 N92-29904 #
AD-A248446 ..... p 3418 N92-29619 #
AD-A248452 ..... p 3434 N92-29447 #
AD-A248458 ..... p 3445 N92-29933 #
AD-A248500 ..... p 3424 N92-29496 #
AD-A248503 ..... p 3439 N92-29498 #
AD-A248507 ..... p 3538 N92-29500 #
AD-A248512 ..... p 3538 N92-29501 #
AD-A248518 ..... p 3511 N92-29503 #
AD-A248519 ..... p 3406 N92-29505 #
AD-A248538 ..... p 3404 N92-29506 #
AD-A248540 ..... p 3424 N92-29508 #
AD-A248541 ..... p 3554 N92-29510 #
AD-A248543 ..... p 3404 N92-29511 #
AD-A248545 ..... p 3440 N92-29575 #
AD-A248552 ..... p 3435 N92-29576 #
AD-A248556 ..... p 3510 N92-29577 #
AD-A248557 ..... p 3435 N92-29579 #
AD-A248558 ..... p 3418 N92-29580 #
AD-A248597 ..... p 3434 N92-29563 #
AD-A248614 ..... p 3426 N92-29905 #
AD-A248662 ..... p 3539 N92-29718 #
AD-A248666 ..... p 3418 N92-29719 #
AD-A248694 ..... p 3562 N92-29934 #
AD-A248696 ..... p 3502 N92-29565 #
AD-A248714 ..... p 3562 N92-29720 #
AD-A248723 ..... p 3444 N92-29721 #
AD-A248725 ..... p 3557 N92-29722 #
AD-A248737 ..... p 3415 N92-29723 #
AD-A248764 ..... p 3571 N92-29724 #
AD-A248765 ..... p 3571 N92-29725 #
AD-A248841 ..... p 3483 N92-29915 #
AD-A248857 ..... p 3442 N92-29935 #
AD-A248865 ..... p 3552 N92-29726 #
AD-A248881 ..... p 3552 N92-29727 #
AD-A248884 ..... p 3403 N92-29906 #
AD-A248950 ..... p 3442 N92-29936 #
AD-A248956 ..... p 3511 N92-29620 #
AD-A248986 ..... p 3541 N92-30174 #
AD-A248993 ..... p 3560 N92-30175 #
AD-A248996 ..... p 3427 N92-30136 #
AD-A249010 ..... p 3443 N92-30176 #
AD-A249121 ..... p 3435 N92-29599 #
AD-A249233 ..... p 3476 N92-29581 #
AD-A249381 ..... p 3516 N92-29622 #
AD-A249740 ..... p 3501 N92-30087 #
AD-A250021 ..... p 3406 N92-29449 #
AD-A250027 ..... p 3491 N92-29476 #
AD-A250063 ..... p 3423 N92-29940 #
AD-A250080 ..... p 3414 N92-29462 #
AD-A250191 ..... p 3417 N92-29514 #
AD-A250227 ..... p 3543 N92-29543 #
AD-A250235 ..... p 3419 N92-29941 #
AD-A250240 ..... p 3475 N92-29332 #
AD-A250241 ..... p 3516 N92-29544 #
AD-A250245 ..... p 3429 N92-29333 #
AD-A250246 ..... p 3510 N92-29334 #
AD-A250251 ..... p 3428 N92-29545 #
AD-A250252 ..... p 3428 N92-29335 #
AD-A250261 ..... p 3551 N92-29546 #
AD-A250282 ..... p 3421 N92-29547 #
AD-A250285 ..... p 3416 N92-30137 #
AD-A250293 ..... p 3407 N92-29709 #
AD-A250388 ..... p 3531 N92-29548 #
AD-A250564 ..... p 3422 N92-29647 #
AD-A250570 ..... p 3420 N92-29426 #
AD-A250571 ..... p 3532 N92-29589 #
AD-A250578 ..... p 3528 N92-29590 #
AD-A250579 ..... p 3511 N92-29591 #
AD-A250580 ..... p 3511 N92-29592 #
AD-A250581 ..... p 3554 N92-29450 #
AD-A250582 ..... p 3480 N92-29710 #
AD-A250584 ..... p 3439 N92-29452 #
AD-A250591 ..... p 3415 N92-29593 #
AD-A250592 ..... p 3415 N92-29594 #
AD-A250607 ..... p 3418 N92-29595 #
AD-A250612 ..... p 3414 N92-29453 #
AD-A250623 ..... p 3565 N92-29596 #
AD-A250624 ..... p 3428 N92-29428 #
AD-A250631 ..... p 3557 N92-29635 #
AD-A250632 ..... p 3556 N92-29429 #
AD-A250649 ..... p 3510 N92-30216 #

AD-D015198 ..... p 3441 N92-29900 #
AD-D015205 ..... p 3475 N92-30202 #
AD-D015256 ..... p 3474 N92-29571 #
AD-D015257 ..... p 3435 N92-29572 #

AD-E501508 ..... p 3426 N92-29905 #

ADANET-FD-R/T-160-1 ..... p 3514 N92-29362 * #

AERO-REPT-8907 ..... p 3444 N92-29683 #

AFIT/DS/ENG/92-02 ..... p 3528 N92-29561 #

AFIT/GCS/ENG/92M-02 ..... p 3515 N92-29527 #

AFIT/GE/ENG/92M-05 ..... p 3440 N92-29526 #
AFIT/GE/ENG/92M-07 ..... p 3439 N92-29405 #

AFIT/GEP/ENP/92M-01 ..... p 3554 N92-29528 #

AFIT/GNE/ENP/92M-03 ..... p 3412 N92-29444 #
AFIT/GNE/ENP/92M-9 ..... p 3439 N92-29443 #

AFIT/GOR/ENS/92M-03 ..... p 3410 N92-29525 #
AFIT/GOR/ENS/92M-13 ..... p 3434 N92-29406 #
AFIT/GOR/ENS/92M-14 ..... p 3516 N92-29586 #
AFIT/GOR/ENS/92M-23 ..... p 3539 N92-29585 #

AFIT/GST/ENS/92M-7 ..... p 3440 N92-29529 #

AFOSR-92-0153TR ..... p 3418 N92-29901 #
AFOSR-92-0160TR ..... p 3413 N92-29913 #
AFOSR-92-0168TR-VOL-2 ..... p 3571 N92-29724 #
AFOSR-92-0169TR-VOL-3 ..... p 3571 N92-29725 #
AFOSR-92-0189TR ..... p 3512 N92-29930 #
AFOSR-92-0192TR ..... p 3570 N92-29632 #
AFOSR-92-0200TR ..... p 3482 N92-29407 #
AFOSR-92-0206TR ..... p 3510 N92-29420 #
AFOSR-92-0217TR ..... p 3570 N92-29464 #
AFOSR-92-0237TR ..... p 3435 N92-29579 #
AFOSR-92-0238TR ..... p 3418 N92-29580 #
AFOSR-92-0261TR ..... p 3510 N92-29577 #
AFOSR-92-0267TR ..... p 3511 N92-29591 #
AFOSR-92-0270TR ..... p 3532 N92-29589 #
AFOSR-92-0277TR ..... p 3554 N92-29450 #
AFOSR-92-0281TR ..... p 3420 N92-29426 #
AFOSR-92-0302TR ..... p 3416 N92-30137 #
AFOSR-92-0303TR ..... p 3511 N92-29592 #
AFOSR-92-0309TR ..... p 3528 N92-29590 #
AFOSR-92-0359TR ..... p 3480 N92-29710 #
AFOSR-92-0363TR ..... p 3510 N92-29334 #
AFOSR-92-0387TR ..... p 3421 N92-29547 #

AFOSR-92-0422TR ..... p 3565 N92-29596 #
AFOSR-92-0424TR ..... p 3428 N92-29428 #

AIAA PAPER 91-5031 ..... p 3401 N92-29713 #
AIAA PAPER 91-5041 ..... p 3400 N92-29649 #
AIAA PAPER 92-2622-CP ..... p 3402 N92-30182 * #
AIAA PAPER 92-3061 ..... p 3427 N92-29669 * #
AIAA PAPER 92-3069 ..... p 3399 N92-29402 * #
AIAA PAPER 92-3092 ..... p 3405 N92-29425 * #
AIAA PAPER 92-3338 ..... p 3412 N92-29343 * #

AL-CR-1992-001 ..... p 3511 N92-29620 #

AL-TP-1992-0009 ..... p 3406 N92-29505 #

AL-TR-1992-0003 ..... p 3511 N92-29503 #

AM-92-02 ..... p 3416 N92-30208 * #

ANL-HEP-CP-92-17 ..... p 3544 N92-29356 #

ANL/CP-73256 ..... p 3478 N92-29534 #
ANL/CP-74638 ..... p 3478 N92-29357 #
ANL/CP-75372 ..... p 3482 N92-29535 #
ANL/CP-75747 ..... p 3525 N92-29624 #

ANU-P-1092 ..... p 3549 N92-30213 #

APL-UW-TR-9005 ..... p 3505 N92-29554 #

AR-006-663 ..... p 3482 N92-29672

ARCCB-TR-92006 ..... p 3515 N92-29487 #

ARI-RN-92-32 ..... p 3407 N92-29709 #

ARL-STRUC-R-446 ..... p 3482 N92-29672

ARO-25464.11-PH ..... p 3551 N92-29546 #
ARO-26238.19-CH ..... p 3418 N92-29719 #
ARO-28415.1-GS-CF ..... p 3552 N92-29727 #
ARO-29087.1-MA-SBI ..... p 3516 N92-29622 #

ASL-TR-0308 ..... p 3502 N92-29565 #

AVSCOM-TR-91-C-041 ..... p 3478 N92-29351 * #
AVSCOM-TR-92-B-008 ..... p 3481 N92-29393 * #
AVSCOM-TR-92-C-019 ..... p 3405 N92-29661 * #
AVSCOM-TR-92-C-050 ..... p 3478 N92-29697 * #

B-248072 ..... p 3488 N92-29467 #

BCRS-90-31 ..... p 3489 N92-29493 #
BCRS-90-38 ..... p 3489 N92-29494 #
BCRS-91-01 ..... p 3489 N92-29495 #
BCRS-91-12 ..... p 3489 N92-29693 #
BCRS-91-17 ..... p 3493 N92-29497 #
BCRS-91-22 ..... p 3490 N92-29717 #
BCRS-91-25 ..... p 3493 N92-29499 #
BCRS-91-28 ..... p 3491 N92-30230 #
BCRS-91-30 ..... p 3491 N92-30231 #

BNL-46683 ..... p 3550 N92-29475 #
BNL-47378 ..... p 3549 N92-29477 #
BNL-47382 ..... p 3556 N92-29437 #
BNL-47420 ..... p 3545 N92-29582 #
BNL-52262 ..... p 3549 N92-30014 * #

BRL-TR-3324 ..... p 3554 N92-29510 #
BRL-TR-3338 ..... p 3406 N92-29449 #

B91-0278 ..... p 3438 N92-30198 #
B92-0123 ..... p 3437 N92-30093 #

CDNSWC-SME-92-10 ..... p 3415 N92-29723 #

CETHA-TS-CR-91054 ..... p 3423 N92-29940 #

CGR/DC-19/91 ..... p 3512 N92-29538 #

CMU/SEI-91-CDRL-106 ..... p 3516 N92-29540 #

CONF-910406-40 ..... p 3556 N92-29473 #
CONF-9107115-75 ..... p 3476 N92-29509 #
CONF-9109256-2 ..... p 3475 N92-30090 #
CONF-911003-25 ..... p 3420 N92-29483 #
CONF-911003-26 ..... p 3415 N92-29645 #
CONF-911004 ..... p 3547 N92-29910 #
CONF-911106-94 ..... p 3549 N92-29502 #
CONF-9111141-7 ..... p 3544 N92-29356 #
CONF-9111165-13 ..... p 3560 N92-29517 #
CONF-911195-3 ..... p 3421 N92-29639 #
CONF-911202-69 ..... p 3436 N92-29909 #
CONF-911202-70 ..... p 3559 N92-29911 #
CONF-911202-76 ..... p 3556 N92-29437 #
CONF-911213-24 ..... p 3533 N92-29792 #
CONF-911213-25 ..... p 3481 N92-29338 #
CONF-911296-5 ..... p 3477 N92-29987 #
CONF-911296-8-REV-1 ..... p 3477 N92-29787 #
CONF-9201100-1 ..... p 3494 N92-29790 #
CONF-9201103-1 ..... p 3475 N92-29434 #
CONF-920124-20 ..... p 3545 N92-29634 #
CONF-920124-22 ..... p 3550 N92-29337 #
CONF-920124-24 ..... p 3476 N92-29472 #
CONF-9203124-1 ..... p 3426 N92-29908 #
CONF-9203147-1-VUGRAPHS ..... p 3427 N92-29512 #
CONF-9203149-1 ..... p 3500 N92-29513 #
CONF-920315-28 ..... p 3549 N92-29477 #
CONF-920315-30 ..... p 3550 N92-29475 #
CONF-920315-4 ..... p 3550 N92-29788 #
CONF-920315-5 ..... p 3437 N92-29988 #
CONF-9203152-1 ..... p 3545 N92-29515 #
CONF-920362-14 ..... p 3555 N92-29789 #
CONF-920362-16 ..... p 3556 N92-30203 #
CONF-920362-18 ..... p 3555 N92-29917 #
CONF-920362-21 ..... p 3476 N92-29474 #
CONF-920362-25 ..... p 3474 N92-29942 #
CONF-920362-27 ..... p 3554 N92-29412 #
CONF-920373-2 ..... p 3408 N92-29986 #
CONF-920402-2 ..... p 3424 N92-29479 #
CONF-920402-4 ..... p 3415 N92-29795 #
CONF-9204102-7 ..... p 3438 N92-29339 #
CONF-9204103-2 ..... p 3416 N92-29355 #
CONF-9204120-1 ..... p 3551 N92-29484 #
CONF-9204130-1 ..... p 3492 N92-29646 #
CONF-9204137-1 ..... p 3545 N92-29507 #
CONF-920423-3 ..... p 3550 N92-29938 #
CONF-920430-85 ..... p 3420 N92-29436 #
CONF-920439-6 ..... p 3478 N92-29357 #
CONF-920458-8 ..... p 3420 N92-29411 #
CONF-920462-1 ..... p 3475 N92-29340 #
CONF-920480-1 ..... p 3545 N92-29582 #
CONF-920496-2 ..... p 3476 N92-29516 #
CONF-9205102-2 ..... p 3440 N92-29518 #
CONF-9205138-2 ..... p 3561 N92-29552 #
CONF-9205142-1 ..... p 3421 N92-29623 #
CONF-9205152-1 ..... p 3527 N92-29504 #
CONF-920538-14 ..... p 3525 N92-29624 #
CONF-920573-7 ..... p 3475 N92-29358 #
CONF-920604-2 ..... p 3421 N92-29633 #
CONF-9206129-3 ..... p 3495 N92-30211 #
CONF-9206161-1 ..... p 3478 N92-29534 #
CONF-9206166-1 ..... p 3482 N92-29535 #
CONF-920631-3 ..... p 3445 N92-29784 #
CONF-920657-1 ..... p 3477 N92-30135 #
CONF-920669-5 ..... p 3439 N92-29414 #
CONF-920678-2 ..... p 3551 N92-29530 #
CONF-920703-1 ..... p 3425 N92-29643 #
CONF-920707-11 ..... p 3417 N92-29433 #
CONF-920707-15 ..... p 3419 N92-29943 #
CONF-920707-1 ..... p 3417 N92-29431 #
CONF-920707-2 ..... p 3417 N92-29459 #
CONF-920716-1 ..... p 3439 N92-29455 #
CONF-920724-1 ..... p 3528 N92-29550 #
CONF-920724-2 ..... p 3528 N92-29644 #
CONF-920730-3 ..... p 3562 N92-29794 #
CONF-920740-1 ..... p 3527 N92-29456 #
CONF-920747-1-EXTD-ABST ..... p 3413 N92-29461 #
CONF-920760-2 ..... p 3524 N92-29353 #
CONF-920760-4 ..... p 3531 N92-29481 #
CONF-920761-5 ..... p 3417 N92-29551 #
CONF-920792-1 ..... p 3500 N92-29536 #

CRHC-92-08 ..... p 3517 N92-29695 * #

CSDL-T-1126 ..... p 3403 N92-29440 * #

CSIRO-TP-23 ..... p 3500 N92-29670
CSIRO-TP-25 ..... p 3494 N92-29668

CSS-TM-596-92 ..... p 3434 N92-29563 #

CU-TR-92-1293 ..... p 3515 N92-29400 * #

CWI-AM-R9105 ..... p 3534 N92-29866 #
CWI-AM-R9106 ..... p 3534 N92-29893 #
CWI-AM-R9107 ..... p 3535 N92-29894 #
CWI-AM-R9108 ..... p 3535 N92-29895 #
CWI-AM-R9110 ..... p 3535 N92-29896 #
CWI-AM-R9111 ..... p 3534 N92-29881 #
CWI-AM-R9112 ..... p 3534 N92-29882 #

CWI-BS-R9116 ..... p 3540 N92-29860 #
CWI-BS-R9118 ..... p 3533 N92-29861 #
CWI-BS-R9119 ..... p 3533 N92-29862 #
CWI-BS-R9120 ..... p 3540 N92-29863 #
CWI-BS-R9121 ..... p 3533 N92-29864 #
CWI-BS-R9122 ..... p 3523 N92-30179 #
CWI-BS-R9123 ..... p 3520 N92-29865 #
CWI-BS-R9124 ..... p 3541 N92-30180 #

CWI-CS-R9121 ..... p 3521 N92-29890 #
CWI-CS-R9122 ..... p 3521 N92-29891 #
CWI-CS-R9123 ..... p 3534 N92-29892 #
CWI-CS-R9126 ..... p 3523 N92-30146 #
CWI-CS-R9128 ..... p 3520 N92-29868 #
CWI-CS-R9129 ..... p 3522 N92-29989 #
CWI-CS-R9130 ..... p 3537 N92-30177 #
CWI-CS-R9134 ..... p 3522 N92-29990 #
CWI-CS-R9135 ..... p 3522 N92-29991 #
CWI-CS-R9136 ..... p 3522 N92-29992 #
CWI-CS-R9137 ..... p 3536 N92-29993 #
CWI-CS-R9138 ..... p 3522 N92-29994 #
CWI-CS-R9139 ..... p 3523 N92-30141 #

CWI-CW-R9131 ..... p 3538 N92-30178 #

CWI-NM-R9108 ..... p 3534 N92-29883 #
CWI-NM-R9109 ..... p 3446 N92-29944 #
CWI-NM-R9110 ..... p 3446 N92-29945 #
CWI-NM-R9111 ..... p 3536 N92-29946 #
CWI-NM-R9112 ..... p 3446 N92-29947 #
CWI-NM-R9114 ..... p 3526 N92-29867 #

DE91-002110 ..... p 3491 N92-29454 #
DE92-000177 ..... p 3425 N92-29643 #
DE92-000424 ..... p 3528 N92-29550 #
DE92-001163 ..... p 3425 N92-29598 #
DE92-001222 ..... p 3557 N92-29584 #
DE92-003148 ..... p 3439 N92-29455 #
DE92-004179 ..... p 3445 N92-29784 #
DE92-004360 ..... p 3527 N92-29456 #
DE92-004464 ..... p 3528 N92-29644 #
DE92-005328 ..... p 3417 N92-29431 #
DE92-005330 ..... p 3417 N92-29459 #
DE92-006608 ..... p 3413 N92-29461 #
DE92-006699 ..... p 3417 N92-29433 #
DE92-006705 ..... p 3419 N92-29943 #
DE92-010542 ..... p 3417 N92-29551 #
DE92-010670 ..... p 3408 N92-29986 #
DE92-010712 ..... p 3477 N92-29787 #
DE92-010714 ..... p 3477 N92-29987 #
DE92-010751 ..... p 3437 N92-29988 #
DE92-010752 ..... p 3550 N92-29788 #
DE92-010800 ..... p 3477 N92-30135 #
DE92-011138 ..... p 3421 N92-29633 #
DE92-011173 ..... p 3549 N92-29457 #
DE92-011188 ..... p 3546 N92-29899 #
DE92-011228 ..... p 3555 N92-29917 #
DE92-011262 ..... p 3556 N92-30203 #
DE92-011287 ..... p 3550 N92-29337 #
DE92-011292 ..... p 3477 N92-29937 #
DE92-011299 ..... p 3524 N92-29353 #
DE92-011302 ..... p 3550 N92-29938 #
DE92-011353 ..... p 3545 N92-29634 #
DE92-011371 ..... p 3555 N92-29789 #
DE92-011372 ..... p 3562 N92-29794 #
DE92-011374 ..... p 3514 N92-29907 #
DE92-011381 ..... p 3426 N92-29908 #
DE92-011389 ..... p 3494 N92-29790 #
DE92-011393 ..... p 3476 N92-29474 #
DE92-011437 ..... p 3551 N92-29530 #
DE92-011444 ..... p 3533 N92-29791 #
DE92-011446 ..... p 3495 N92-30211 #
DE92-011466 ..... p 3533 N92-29792 #
DE92-011467 ..... p 3481 N92-29338 #
DE92-011470 ..... p 3436 N92-29909 #
DE92-011502 ..... p 3547 N92-29910 #
DE92-011511 ..... p 3569 N92-29600 #
DE92-011528 ..... p 3559 N92-29911 #
DE92-011572 ..... p 3482 N92-29601 #
DE92-011588 ..... p 3551 N92-29578 #
DE92-011614 ..... p 3555 N92-30072 #
DE92-011633 ..... p 3542 N92-29354 #
DE92-011646 ..... p 3420 N92-29483 #
DE92-011756 ..... p 3416 N92-29355 #
DE92-011761 ..... p 3421 N92-29623 #
DE92-011762 ..... p 3551 N92-29484 #
DE92-011787 ..... p 3475 N92-30090 #
DE92-011811 ..... p 3556 N92-29485 #
DE92-011833 ..... p 3544 N92-29356 #
DE92-011834 ..... p 3478 N92-29357 #
DE92-011840 ..... p 3525 N92-29624 #
DE92-011940 ..... p 3424 N92-29549 #
DE92-011946 ..... p 3475 N92-29358 #
DE92-011966 ..... p 3531 N92-29481 #
DE92-012208 ..... p 3545 N92-29582 #
DE92-012254 ..... p 3475 N92-29434 #
DE92-012264 ..... p 3423 N92-29435 #
DE92-012333 ..... p 3415 N92-29645 #
DE92-012338 ..... p 3420 N92-29436 #
DE92-012339 ..... p 3492 N92-29646 #
DE92-012518 ..... p 3556 N92-29437 #
DE92-012548 ..... p 3424 N92-29482 #
DE92-012550 ..... p 3422 N92-29706 #
DE92-012587 ..... p 3559 N92-29939 #
DE92-012632 ..... p 3561 N92-29552 #
DE92-012677 ..... p 3421 N92-29639 #

DE92-012678 ..... p 3438 N92-29339 #
DE92-012687 ..... p 3554 N92-29640 #
DE92-012695 ..... p 3476 N92-29472 #
DE92-012698 ..... p 3475 N92-29340 #
DE92-013006 ..... p 3556 N92-29473 #
DE92-013008 ..... p 3474 N92-29942 #
DE92-013031 ..... p 3550 N92-29475 #
DE92-013035 ..... p 3549 N92-29477 #
DE92-013044 ..... p 3478 N92-29534 #
DE92-013053 ..... p 3482 N92-29535 #
DE92-013240 ..... p 3500 N92-29536 #
DE92-013356 ..... p 3549 N92-29502 #
DE92-013385 ..... p 3424 N92-29479 #
DE92-013394 ..... p 3517 N92-29641 #
DE92-013422 ..... p 3527 N92-29504 #
DE92-013434 ..... p 3415 N92-29795 #
DE92-013463 ..... p 3554 N92-29438 #
DE92-013464 ..... p 3545 N92-29507 #
DE92-013473 ..... p 3546 N92-29642 #
DE92-013485 ..... p 3477 N92-29928 #
DE92-013487 ..... p 3493 N92-29597 #
DE92-013500 ..... p 3504 N92-29439 #
DE92-013504 ..... p 3420 N92-29411 #
DE92-013507 ..... p 3554 N92-29412 #
DE92-013508 ..... p 3439 N92-29414 #
DE92-013515 ..... p 3476 N92-29509 #
DE92-013517 ..... p 3480 N92-29478 #
DE92-013528 ..... p 3427 N92-29512 #
DE92-013530 ..... p 3500 N92-29513 #
DE92-013546 ..... p 3545 N92-29515 #
DE92-013553 ..... p 3541 N92-30138 #
DE92-013555 ..... p 3542 N92-30139 #
DE92-013564 ..... p 3476 N92-29516 #
DE92-013587 ..... p 3553 N92-29336 #
DE92-013601 ..... p 3452 N92-30140 #
DE92-013602 ..... p 3490 N92-30088 #
DE92-013665 ..... p 3560 N92-29517 #
DE92-013669 ..... p 3440 N92-29518 #
DE92-013752 ..... p 3516 N92-29537 #
DE92-013999 ..... p 3441 N92-29796 #
DE92-014071 ..... p 3519 N92-29797 #
DE92-014092 ..... p 3555 N92-29798 #
DE92-014093 ..... p 3554 N92-29531 #
DE92-014309 ..... p 3550 N92-29532 #
DE92-506506 ..... p 3442 N92-30089 #
DE92-506507 ..... p 3441 N92-29912 #
DE92-506509 ..... p 3492 N92-29636 #
DE92-506510 ..... p 3421 N92-29637 #
DE92-514557 ..... p 3493 N92-29638 #
DE92-622378 ..... p 3533 N92-29793 #
DE92-624511 ..... p 3560 N92-29533 #
DE92-624516 ..... p 3560 N92-30212 #
DE92-624790 ..... p 3549 N92-30213 #
DE92-625013 ..... p 3544 N92-29415 #

DLR-FB-91-28 ..... p 3544 N92-29997 #
DLR-FB-91-31 ..... p 3447 N92-29998 #
DLR-FB-91-34 ..... p 3404 N92-29870 #

DLR-MITT-91-10 ..... p 3436 N92-29877 #

DOE/CH-10093/90 ..... p 3491 N92-29454 #

DOE/DP-40200/188 ..... p 3555 N92-30072 #

DOE/ER-12119/1 ..... p 3424 N92-29549 #
DOE/ER-13744/12 ..... p 3546 N92-29899 #
DOE/ER-13778/5 ..... p 3546 N92-29642 #
DOE/ER-40224/185 ..... p 3550 N92-29532 #
DOE/ER-40561/038 ..... p 3560 N92-29517 #
DOE/ER-45125/9 ..... p 3542 N92-29354 #
DOE/ER-45290/5 ..... p 3482 N92-29601 #
DOE/ER-45394/3 ..... p 3556 N92-29485 #
DOE/ER-54109/2 ..... p 3553 N92-29336 #
DOE/ER-60818/3 ..... p 3504 N92-29439 #
DOE/ER-61010/T1 ..... p 3493 N92-29597 #
DOE/ER-61072/4 ..... p 3551 N92-29530 #
DOE/ER-61229/1 ..... p 3477 N92-29928 #

DOE/METC-C/92/7013 ..... p 3416 N92-29355 #

DOE/OSTI-4500-R75 ..... p 3549 N92-30014 * #

DOE/PC-90038/T1 ..... p 3423 N92-29435 #
DOE/PC-90274/T12 ..... p 3554 N92-29640 #

DOT-VNTSC-FRA-92-1 ..... p 3564 N92-29808 #
DOT-VNTSC-FRA-92-3 ..... p 3564 N92-29809 #

DOT/FRA/ORD-92/01 ..... p 3564 N92-29808 #
DOT/FRA/ORD-92/3 ..... p 3564 N92-29809 #

DRIC-BR-309213 ..... p 3475 N92-29396 #

E-7003 ..... p 3524 N92-30207 * #
E-7046 ..... p 3402 N92-30182 * #
E-7048 ..... p 3478 N92-29351 * #
E-7058 ..... p 3405 N92-29661 * #
E-7073 ..... p 3413 N92-29667 * #
E-7088 ..... p 3414 N92-30187 * #
E-7127 ..... p 3478 N92-29697 * #
E-7135 ..... p 3412 N92-29343 * #
E-7142 ..... p 3492 N92-29662 * #
E-7150 ..... p 3427 N92-29669 * #
E-7165 ..... p 3415 N92-29660 * #
E-7167 ..... p 3413 N92-29448 * #
E-7175 ..... p 3399 N92-29402 * #

ECAO-R-0082-VOL-1 ..... p 3493 N92-29520 #
ECAO-R-0082-VOL-2 ..... p 3493 N92-29521 #
ECAO-R-0082-VOL-3 ..... p 3493 N92-29522 #

ECS-LFCS-91-169 ..... p 3536 N92-29993 #

EGG-10617-1199 ..... p 3549 N92-29457 #
EGG-10617-2135 ..... p 3549 N92-29502 #

EPA/450/3-91/0100 ..... p 3495 N92-30200 #
EPA/600/A-92/002 ..... p 3495 N92-30031 #
EPA/600/A-92/101 ..... p 3443 N92-30092 #
EPA/600/A-92/105 ..... p 3495 N92-30173 #
EPA/600/A-92/106 ..... p 3494 N92-30018 #
EPA/600/R-92/095 ..... p 3495 N92-30021 #
EPA/600/8-91/049AA-VOL-1 ..... p 3493 N92-29520 #
EPA/600/8-91/049AB-VOL-2 ..... p 3493 N92-29521 #
EPA/600/8-91/049CA-VOL-3 ..... p 3493 N92-29522 #

ESA-PSS-01-50-ISSUE-1 ..... p 3481 N92-29878 #
ESA-PSS-01-610-ISSUE-1 ..... p 3441 N92-29854 #
ESA-PSS-03-105-ISSUE-2 ..... p 3521 N92-29869 #

ESA-SP-1141 ..... p 3407 N92-29879 #

ETN-92-91337 ..... p 3561 N92-29886 #
ETN-92-91341 ..... p 3565 N92-29682 #
ETN-92-91342 ..... p 3444 N92-29683 #
ETN-92-91343 ..... p 3505 N92-29684 #
ETN-92-91350 ..... p 3532 N92-29685 #
ETN-92-91351 ..... p 3532 N92-29687 #
ETN-92-91352 ..... p 3489 N92-29688 #
ETN-92-91370 ..... p 3544 N92-29814 #
ETN-92-91384 ..... p 3441 N92-29854 #
ETN-92-91385 ..... p 3481 N92-29878 #
ETN-92-91386 ..... p 3521 N92-29869 #
ETN-92-91388 ..... p 3407 N92-29879 #
ETN-92-91390 ..... p 3404 N92-29870 #
ETN-92-91406 ..... p 3482 N92-29700 #
ETN-92-91407 ..... p 3415 N92-29702 #
ETN-92-91409 ..... p 3544 N92-29918 #
ETN-92-91410 ..... p 3535 N92-29919 #
ETN-92-91411 ..... p 3535 N92-29920 #
ETN-92-91412 ..... p 3535 N92-29921 #
ETN-92-91413 ..... p 3535 N92-29922 #
ETN-92-91414 ..... p 3535 N92-29923 #
ETN-92-91415 ..... p 3536 N92-29924 #
ETN-92-91416 ..... p 3521 N92-29887 #
ETN-92-91417 ..... p 3518 N92-29711 #
ETN-92-91418 ..... p 3518 N92-29712 #
ETN-92-91419 ..... p 3519 N92-29779 #
ETN-92-91420 ..... p 3444 N92-29763 #
ETN-92-91421 ..... p 3529 N92-29764 #
ETN-92-91422 ..... p 3539 N92-29626 #
ETN-92-91423 ..... p 3517 N92-29627 #
ETN-92-91424 ..... p 3543 N92-29628 #
ETN-92-91426 ..... p 3543 N92-29748 #
ETN-92-91427 ..... p 3518 N92-29749 #
ETN-92-91428 ..... p 3525 N92-29716 #
ETN-92-91440 ..... p 3402 N92-29703 #
ETN-92-91443 ..... p 3478 N92-29602 #
ETN-92-91449 ..... p 3482 N92-29603 #
ETN-92-91453 ..... p 3532 N92-29604 #
ETN-92-91454 ..... p 3403 N92-29605 #
ETN-92-91460 ..... p 3532 N92-29742 #
ETN-92-91461 ..... p 3539 N92-29606 #
ETN-92-91462 ..... p 3532 N92-29607 #
ETN-92-91463 ..... p 3516 N92-29608 #
ETN-92-91464 ..... p 3539 N92-29609 #
ETN-92-91465 ..... p 3517 N92-29705 #
ETN-92-91466 ..... p 3490 N92-29728 #
ETN-92-91467 ..... p 3516 N92-29621 #
ETN-92-91468 ..... p 3516 N92-29570 #
ETN-92-91469 ..... p 3532 N92-29573 #
ETN-92-91470 ..... p 3532 N92-29574 #
ETN-92-91471 ..... p 3525 N92-29610 #
ETN-92-91474 ..... p 3513 N92-29611 #
ETN-92-91475 ..... p 3441 N92-29612 #
ETN-92-91476 ..... p 3441 N92-29613 #
ETN-92-91477 ..... p 3525 N92-29614 #
ETN-92-91478 ..... p 3422 N92-29674 #
ETN-92-91479 ..... p 3529 N92-29675 #
ETN-92-91480 ..... p 3529 N92-29678 #
ETN-92-91481 ..... p 3526 N92-29888 #
ETN-92-91482 ..... p 3441 N92-29729 #
ETN-92-91483 ..... p 3436 N92-29730 #
ETN-92-91488 ..... p 3483 N92-29925 #
ETN-92-91489 ..... p 3445 N92-29926 #
ETN-92-91490 ..... p 3474 N92-29731 #
ETN-92-91491 ..... p 3401 N92-29741 #
ETN-92-91492 ..... p 3401 N92-29889 #
ETN-92-91493 ..... p 3405 N92-29927 #
ETN-92-91494 ..... p 3564 N92-29468 #
ETN-92-91495 ..... p 3409 N92-29680 #
ETN-92-91496 ..... p 3408 N92-29629 #
ETN-92-91497 ..... p 3400 N92-29648 #
ETN-92-91498 ..... p 3401 N92-29713 #
ETN-92-91499 ..... p 3400 N92-29649 #
ETN-92-91500 ..... p 3404 N92-29650 #
ETN-92-91501 ..... p 3500 N92-29690 #
ETN-92-91502 ..... p 3422 N92-29651 #
ETN-92-91503 ..... p 3515 N92-29418 #
ETN-92-91504 ..... p 3538 N92-29419 #
ETN-92-91505 ..... p 3473 N92-29469 #
ETN-92-91506 ..... p 3428 N92-29470 #
ETN-92-91507 ..... p 3518 N92-29714 #
ETN-92-91508 ..... p 3546 N92-29715 #
ETN-92-91510 ..... p 3519 N92-29780 #
ETN-92-91511 ..... p 3560 N92-29781 #
ETN-92-91513 ..... p 3403 N92-29615 #
ETN-92-91514 ..... p 3404 N92-29616 #
ETN-92-91517 ..... p 3490 N92-29707 #
ETN-92-91527 ..... p 3512 N92-29871 #
ETN-92-91532 ..... p 3483 N92-29708 #
ETN-92-91546 ..... p 3402 N92-29916 #
ETN-92-91547 ..... p 3401 N92-29884 #
ETN-92-91548 ..... p 3479 N92-29885 #
ETN-92-91549 ..... p 3521 N92-29890 #
ETN-92-91550 ..... p 3521 N92-29891 #
ETN-92-91551 ..... p 3534 N92-29892 #
ETN-92-91554 ..... p 3522 N92-29969 #
ETN-92-91555 ..... p 3537 N92-30177 #
ETN-92-91556 ..... p 3538 N92-30178 #
ETN-92-91557 ..... p 3522 N92-29990 #
ETN-92-91558 ..... p 3522 N92-29991 #
ETN-92-91559 ..... p 3522 N92-29992 #
ETN-92-91560 ..... p 3536 N92-29993 #
ETN-92-91561 ..... p 3522 N92-29994 #
ETN-92-91562 ..... p 3523 N92-30141 #
ETN-92-91563 ..... p 3523 N92-30179 #
ETN-92-91564 ..... p 3541 N92-30180 #
ETN-92-91565 ..... p 3527 N92-30142 #
ETN-92-91566 ..... p 3522 N92-30073 #
ETN-92-91567 ..... p 3526 N92-30074 #
ETN-92-91568 ..... p 3531 N92-30143 #
ETN-92-91569 ..... p 3523 N92-30181 #
ETN-92-91570 ..... p 3527 N92-30183 #
ETN-92-91571 ..... p 3537 N92-30075 #
ETN-92-91572 ..... p 3523 N92-30144 #
ETN-92-91574 ..... p 3536 N92-29995 #
ETN-92-91575 ..... p 3514 N92-30145 #
ETN-92-91576 ..... p 3531 N92-30184 #
ETN-92-91577 ..... p 3536 N92-29956 #
ETN-92-91578 ..... p 3562 N92-29957 #
ETN-92-91579 ..... p 3526 N92-29958 #
ETN-92-91580 ..... p 3437 N92-29959 #
ETN-92-91581 ..... p 3426 N92-29960 #
ETN-92-91582 ..... p 3521 N92-29961 #
ETN-92-91583 ..... p 3519 N92-29815 #
ETN-92-91584 ..... p 3519 N92-29816 #
ETN-92-91585 ..... p 3520 N92-29855 #
ETN-92-91586 ..... p 3526 N92-29880 #
ETN-92-91590 ..... p 3540 N92-29856 #
ETN-92-91593 ..... p 3445 N92-29857 #
ETN-92-91594 ..... p 3533 N92-29858 #
ETN-92-91598 ..... p 3534 N92-29872 #
ETN-92-91605 ..... p 3489 N92-29493 #
ETN-92-91606 ..... p 3489 N92-29494 #
ETN-92-91607 ..... p 3489 N92-29495 #
ETN-92-91608 ..... p 3489 N92-29693 #
ETN-92-91609 ..... p 3493 N92-29497 #
ETN-92-91610 ..... p 3493 N92-29499 #
ETN-92-91611 ..... p 3490 N92-29717 #
ETN-92-91616 ..... p 3518 N92-29747 #
ETN-92-91617 ..... p 3546 N92-29750 #
ETN-92-91623 ..... p 3546 N92-29751 #
ETN-92-91624 ..... p 3444 N92-29752 #
ETN-92-91625 ..... p 3558 N92-29753 #
ETN-92-91626 ..... p 3552 N92-29859 #
ETN-92-91627 ..... p 3555 N92-29761 #
ETN-92-91628 ..... p 3539 N92-29774 #
ETN-92-91629 ..... p 3445 N92-29775 #
ETN-92-91630 ..... p 3518 N92-29776 #
ETN-92-91631 ..... p 3546 N92-29777 #
ETN-92-91632 ..... p 3546 N92-29778 #
ETN-92-91633 ..... p 3519 N92-29782 #
ETN-92-91634 ..... p 3559 N92-29783 #
ETN-92-91639 ..... p 3523 N92-30146 #
ETN-92-91642 ..... p 3540 N92-29860 #
ETN-92-91643 ..... p 3533 N92-29861 #

ETN-92-91644 ..... p 3533 N92-29862 #
ETN-92-91645 ..... p 3540 N92-29863 #
ETN-92-91646 ..... p 3533 N92-29864 #
ETN-92-91647 ..... p 3520 N92-29865 #
ETN-92-91648 ..... p 3534 N92-29866 #
ETN-92-91649 ..... p 3534 N92-29893 #
ETN-92-91650 ..... p 3535 N92-29894 #
ETN-92-91651 ..... p 3535 N92-29895 #
ETN-92-91652 ..... p 3535 N92-29896 #
ETN-92-91653 ..... p 3534 N92-29881 #
ETN-92-91654 ..... p 3534 N92-29882 #
ETN-92-91655 ..... p 3534 N92-29883 #
ETN-92-91656 ..... p 3446 N92-29944 #
ETN-92-91657 ..... p 3446 N92-29945 #
ETN-92-91658 ..... p 3536 N92-29946 #
ETN-92-91659 ..... p 3446 N92-29947 #
ETN-92-91660 ..... p 3526 N92-29867 #
ETN-92-91695 ..... p 3480 N92-29873 #
ETN-92-91696 ..... p 3399 N92-29874 #
ETN-92-91697 ..... p 3407 N92-30076 #
ETN-92-91698 ..... p 3416 N92-29875 #
ETN-92-91699 ..... p 3416 N92-29876 #
ETN-92-91702 ..... p 3529 N92-29962 #
ETN-92-91703 ..... p 3408 N92-29967 #
ETN-92-91718 ..... p 3544 N92-29488 #
ETN-92-91720 ..... p 3560 N92-29996 #
ETN-92-91731 ..... p 3436 N92-29877 #
ETN-92-91733 ..... p 3544 N92-29997 #
ETN-92-91734 ..... p 3447 N92-29998 #
ETN-92-91735 ..... p 3446 N92-29968 #
ETN-92-91737 ..... p 3565 N92-29833 #
ETN-92-91741 ..... p 3538 N92-29491 #
ETN-92-91743 ..... p 3558 N92-29766 #
ETN-92-91744 ..... p 3508 N92-29754 #
ETN-92-91745 ..... p 3507 N92-29732 #
ETN-92-91748 ..... p 3537 N92-30077 #
ETN-92-91749 ..... p 3537 N92-30078 #
ETN-92-91750 ..... p 3541 N92-30079 #
ETN-92-91751 ..... p 3537 N92-30080 #
ETN-92-91752 ..... p 3537 N92-30081 #
ETN-92-91753 ..... p 3538 N92-30185 #
ETN-92-91754 ..... p 3536 N92-29999 #
ETN-92-91755 ..... p 3530 N92-29971 #
ETN-92-91756 ..... p 3446 N92-29972 #
ETN-92-91757 ..... p 3541 N92-29973 #
ETN-92-91758 ..... p 3540 N92-29974 #
ETN-92-91759 ..... p 3540 N92-29975 #
ETN-92-91760 ..... p 3541 N92-29976 #
ETN-92-91761 ..... p 3446 N92-29977 #
ETN-92-91762 ..... p 3437 N92-29978 #
ETN-92-91763 ..... p 3536 N92-29979 #
ETN-92-91764 ..... p 3541 N92-29980 #
ETN-92-91765 ..... p 3537 N92-30147 #
ETN-92-91766 ..... p 3560 N92-30148 #
ETN-92-91767 ..... p 3523 N92-30186 #
ETN-92-91768 ..... p 3541 N92-30188 #
ETN-92-91770 ..... p 3527 N92-30189 #
ETN-92-91771 ..... p 3562 N92-30000 #
ETN-92-91772 ..... p 3523 N92-30191 #
ETN-92-91773 ..... p 3438 N92-30170 #
ETN-92-91774 ..... p 3522 N92-29981 #
ETN-92-91775 ..... p 3530 N92-29969 #
ETN-92-91776 ..... p 3521 N92-29970 #
ETN-92-91777 ..... p 3514 N92-29982 #
ETN-92-91778 ..... p 3530 N92-29983 #
ETN-92-91779 ..... p 3437 N92-29984 #
ETN-92-91780 ..... p 3526 N92-29985 #
ETN-92-91785 ..... p 3520 N92-29868 #
ETN-92-91786 ..... p 3539 N92-29617 #
ETN-92-91787 ..... p 3520 N92-29818 #
ETN-92-91788 ..... p 3520 N92-29819 #
ETN-92-91789 ..... p 3520 N92-29820 #
ETN-92-91790 ..... p 3540 N92-29897 #
ETN-92-91791 ..... p 3535 N92-29898 #
ETN-92-91792 ..... p 3540 N92-29821 #
ETN-92-91793 ..... p 3561 N92-29822 #
ETN-92-91794 ..... p 3561 N92-29823 #
ETN-92-91795 ..... p 3436 N92-29824 #
ETN-92-91796 ..... p 3525 N92-29825 #
ETN-92-91797 ..... p 3533 N92-29826 #
ETN-92-91798 ..... p 3540 N92-29827 #
ETN-92-91799 ..... p 3540 N92-29828 #
ETN-92-91831 ..... p 3495 N92-30226 #
ETN-92-91832 ..... p 3524 N92-30227 #
ETN-92-91834 ..... p 3524 N92-30228 #
ETN-92-91835 ..... p 3527 N92-30229 #
ETN-92-91877 ..... p 3491 N92-30230 #
ETN-92-91879 ..... p 3491 N92-30231 #
ETN-92-91903 ..... p 3399 N92-30232 #

FFI-91/4001 ..... p 3408 N92-29967 #

FSL-1 ..... p 3502 N92-29799 #

GA-A-20849 ..... p 3476 N92-29474 #
GA-A-20855 ..... p 3474 N92-29942 #
GA-A-20872 ..... p 3554 N92-29412 #

GAO/IMTEC-92-44 ..... p 3488 N92-29467 #

GARTEUR-TP-051 ..... p 3404 N92-29616 #

GEPP-CP-1297 ..... p 3439 N92-29414 #

GPO-55-802CC ..... p 3490 N92-30017 #

GRI-91/0178 ..... p 3426 N92-29804 #
GRI-92/0074 ..... p 3492 N92-29519 #

GTFR-100 ..... p 3554 N92-29438 #

H-1764 ..... p 3405 N92-29659 * #
H-1775 ..... p 3405 N92-29427 * #
H-1806 ..... p 3405 N92-29425 * #

IC-91/374 ..... p 3533 N92-29793 #

ICASE-92-23 ..... p 3444 N92-29692 * #
ICASE-92-25 ..... p 3455 N92-30192 * #
ICASE-92-26 ..... p 3455 N92-30190 * #

ICMA-92-175 ..... p 3478 N92-29392 * #

IDA-D-1115 ..... p 3426 N92-29905 #

IDA/HQ-92-40803 ..... p 3426 N92-29905 #

IEE-SR-225 ..... p 3493 N92-29638 #

IHES/M/92/12 ..... p 3542 N92-30095 #
IHES/M/92/14 ..... p 3537 N92-30096 #

IMAG-RR-843-I ..... p 3516 N92-29621 #
IMAG-RR-844-I ..... p 3516 N92-29570 #
IMAG-RR-845-I ..... p 3525 N92-29610 #
IMAG-RR-854-M ..... p 3525 N92-29614 #
IMAG-RR-860-I ..... p 3513 N92-29611 #
IMAG-RR-862-I ..... p 3441 N92-29612 #
IMAG-RR-863-I ..... p 3441 N92-29613 #

INP-MSU-91-2-206 ..... p 3560 N92-29533 #

INTERNAL-90-NICI-08 ..... p 3524 N92-30195 #

IS-T-1580 ..... p 3559 N92-29939 #
IS-T-1603 ..... p 3424 N92-29482 #
IS-T-1612 ..... p 3422 N92-29706 #

ISBN-0-16-035964-3 ..... p 3435 N92-29696 #
ISBN-0-16-038754-X ..... p 3490 N92-30017 #
ISBN-0-643-05248-8 ..... p 3500 N92-29670
ISBN-0-643-05249-6 ..... p 3494 N92-29668
ISBN-3-7983-1446-2 ..... p 3446 N92-29968 #
ISBN-90-54-11001-5 ..... p 3493 N92-29499 #
ISBN-90-54-11002-3 ..... p 3493 N92-29497 #
ISBN-90-54-11003-1 ..... p 3489 N92-29693 #
ISBN-90-54-11004-X ..... p 3489 N92-29495 #
ISBN-90-54-11005-8 ..... p 3489 N92-29494 #
ISBN-90-54-11007-4 ..... p 3489 N92-29493 #
ISBN-90-5411-010-4 ..... p 3491 N92-30230 #
ISBN-90-5411-032-5 ..... p 3491 N92-30231 #
ISBN-90-9003966-X ..... p 3519 N92-29782 #
ISBN-90-9004374-8 ..... p 3559 N92-29783 #
ISBN-90-9004659-3 ..... p 3419 N92-30196 #
ISBN-92-9092-140-4 ..... p 3407 N92-29879 #

ISSN-0166-7521 ..... p 3490 N92-29726 #
ISSN-0169-0388 ..... p 3526 N92-29867 #
ISSN-0169-0388 ..... p 3534 N92-29883 #
ISSN-0169-118X ..... p 3536 N92-29993 #
ISSN-0169-118X ..... p 3522 N92-29994 #
ISSN-0169-118X ..... p 3523 N92-30141 #
ISSN-0169-2690 ..... p 3540 N92-29856 #
ISSN-0169-2690 ..... p 3445 N92-29857 #
ISSN-0169-2690 ..... p 3533 N92-29858 #
ISSN-0169-2690 ..... p 3534 N92-29872 #
ISSN-0169-2690 ..... p 3530 N92-29971 #
ISSN-0169-2690 ..... p 3446 N92-29972 #
ISSN-0169-2690 ..... p 3541 N92-29973 #
ISSN-0169-2690 ..... p 3540 N92-29974 #
ISSN-0169-2690 ..... p 3540 N92-29975 #
ISSN-0169-2690 ..... p 3541 N92-29976 #
ISSN-0169-2690 ..... p 3446 N92-29977 #
ISSN-0169-2690 ..... p 3437 N92-29978 #
ISSN-0169-2690 ..... p 3536 N92-29979 #
ISSN-0169-2690 ..... p 3541 N92-29980 #
ISSN-0169-2690 ..... p 3536 N92-29999 #
ISSN-0169-2690 ..... p 3537 N92-30077 #
ISSN-0169-2690 ..... p 3537 N92-30078 #
ISSN-0169-2690 ..... p 3541 N92-30079 #
ISSN-0169-2690 ..... p 3537 N92-30080 #
ISSN-0169-2690 ..... p 3537 N92-30081 #
ISSN-0169-2690 ..... p 3537 N92-30147 #
ISSN-0169-2690 ..... p 3560 N92-30148 #
ISSN-0169-2690 ..... p 3538 N92-30185 #
ISSN-0169-2690 ..... p 3523 N92-30186 #
ISSN-0169-2690 ..... p 3541 N92-30188 #
ISSN-0170-8902 ..... p 3446 N92-29968 #
ISSN-0178-0719 ..... p 3565 N92-29833 #
ISSN-0303-4003 ..... p 3515 N92-29418 #
ISSN-0303-4003 ..... p 3422 N92-29651 #
ISSN-0303-4003 ..... p 3500 N92-29690 #
ISSN-0379-4059 ..... p 3441 N92-29854 #
ISSN-0379-4059 ..... p 3521 N92-29869 #
ISSN-0379-4059 ..... p 3481 N92-29878 #
ISSN-0388-9653 ..... p 3502 N92-29666 #
ISSN-0802-2437 ..... p 3408 N92-29967 #
ISSN-0915-633X ..... p 3555 N92-30091 #
ISSN-0915-633X ..... p 3555 N92-30172 #
ISSN-0922-5641 ..... p 3539 N92-29626 #
ISSN-0922-5641 ..... p 3517 N92-29627 #
ISSN-0922-5641 ..... p 3543 N92-29628 #
ISSN-0922-5641 ..... p 3518 N92-29711 #
ISSN-0922-5641 ..... p 3518 N92-29712 #
ISSN-0922-5641 ..... p 3525 N92-29716 #
ISSN-0922-5641 ..... p 3543 N92-29748 #
ISSN-0922-5641 ..... p 3518 N92-29749 #
ISSN-0922-5641 ..... p 3444 N92-29763 #
ISSN-0922-5641 ..... p 3529 N92-29764 #
ISSN-0922-5641 ..... p 3519 N92-29779 #
ISSN-0922-5641 ..... p 3521 N92-29887 #
ISSN-0922-5641 ..... p 3544 N92-29918 #
ISSN-0922-5641 ..... p 3535 N92-29919 #
ISSN-0922-5641 ..... p 3535 N92-29920 #
ISSN-0922-5641 ..... p 3535 N92-29921 #
ISSN-0922-5641 ..... p 3535 N92-29922 #
ISSN-0922-5641 ..... p 3535 N92-29923 #
ISSN-0922-5641 ..... p 3536 N92-29924 #
ISSN-0922-5641 ..... p 3495 N92-30226 #
ISSN-0922-5641 ..... p 3524 N92-30227 #
ISSN-0922-5641 ..... p 3524 N92-30228 #
ISSN-0922-5641 ..... p 3527 N92-30229 #
ISSN-0923-1714 ..... p 3526 N92-30074 #
ISSN-0924-0659 ..... p 3533 N92-29861 #
ISSN-0924-0659 ..... p 3533 N92-29862 #
ISSN-0924-0659 ..... p 3540 N92-29863 #
ISSN-0924-0659 ..... p 3533 N92-29864 #
ISSN-0924-0659 ..... p 3520 N92-29865 #
ISSN-0924-0659 ..... p 3523 N92-30179 #
ISSN-0924-0659 ..... p 3541 N92-30180 #
ISSN-0924-2082 ..... p 3532 N92-29685 #
ISSN-0924-2082 ..... p 3532 N92-29687 #
ISSN-0924-2953 ..... p 3534 N92-29881 #
ISSN-0924-2953 ..... p 3534 N92-29882 #
ISSN-0924-2953 ..... p 3535 N92-29895 #
ISSN-0924-2953 ..... p 3535 N92-29896 #
ISSN-0924-3062 ..... p 3489 N92-29495 #
ISSN-0924-3062 ..... p 3490 N92-29717 #
ISSN-0924-3755 ..... p 3517 N92-29705 #
ISSN-0924-3755 ..... p 3519 N92-29815 #
ISSN-0924-3755 ..... p 3519 N92-29816 #
ISSN-0924-3755 ..... p 3520 N92-29855 #
ISSN-0924-3755 ..... p 3526 N92-29880 #
ISSN-0924-3755 ..... p 3536 N92-29956 #
ISSN-0924-3755 ..... p 3562 N92-29957 #
ISSN-0924-3755 ..... p 3526 N92-29958 #
ISSN-0924-3755 ..... p 3437 N92-29959 #
ISSN-0924-3755 ..... p 3426 N92-29960 #
ISSN-0924-3755 ..... p 3521 N92-29961 #
ISSN-0924-3755 ..... p 3530 N92-29969 #
ISSN-0924-3755 ..... p 3521 N92-29970 #
ISSN-0924-3755 ..... p 3522 N92-29981 #
ISSN-0924-3755 ..... p 3514 N92-29982 #
ISSN-0924-3755 ..... p 3530 N92-29983 #
ISSN-0924-3755 ..... p 3437 N92-29984 #
ISSN-0924-3755 ..... p 3526 N92-29985 #
ISSN-0924-3755 ..... p 3536 N92-29995 #
ISSN-0924-3755 ..... p 3562 N92-30000 #
ISSN-0924-3755 ..... p 3522 N92-30073 #
ISSN-0924-3755 ..... p 3537 N92-30075 #
ISSN-0924-3755 ..... p 3527 N92-30142 #
ISSN-0924-3755 ..... p 3531 N92-30143 #
ISSN-0924-3755 ..... p 3523 N92-30144 #
ISSN-0924-3755 ..... p 3514 N92-30145 #
ISSN-0924-3755 ..... p 3438 N92-30170 #
ISSN-0924-3755 ..... p 3523 N92-30181 #
ISSN-0924-3755 ..... p 3527 N92-30183 #
ISSN-0924-3755 ..... p 3531 N92-30184 #
ISSN-0924-3755 ..... p 3527 N92-30189 #
ISSN-0924-3755 ..... p 3523 N92-30191 #
ISSN-0926-4493 ..... p 3540 N92-29821 #
ISSN-0926-4493 ..... p 3561 N92-29822 #
ISSN-0926-4493 ..... p 3561 N92-29823 #
ISSN-0926-4493 ..... p 3436 N92-29824 #
ISSN-0926-4493 ..... p 3525 N92-29825 #
ISSN-0926-4493 ..... p 3533 N92-29826 #
ISSN-0926-4493 ..... p 3540 N92-29827 #
ISSN-0926-4493 ..... p 3540 N92-29828 #

ISSN-0926-4493 ..... p 3535 N92-29898 #
ISSN-0939-2963 ..... p 3404 N92-29870 #
ISSN-0939-2963 ..... p 3544 N92-29997 #
ISSN-0939-2963 ..... p 3447 N92-29998 #
ISSN-0939-298X ..... p 3436 N92-29877 #

ISVR-TR-204 ..... p 3544 N92-29814 #

ITLI-LP-91-02 ..... p 3532 N92-29685 #
ITLI-LP-91-03 ..... p 3532 N92-29687 #

ITN-92-85126 ..... p 3410 N92-29480 #

ITP-91-6 ..... p 3544 N92-29415 #

IYAF-91-40 ..... p 3560 N92-30212 #

JHU/APL-TG-1382 ..... p 3552 N92-29726 #

JPL-PUBL-90-2 ..... p 3551 N92-29679 * #
JPL-PUBL-90-45 ..... p 3434 N92-29463 * #

JPL-TDA-PR-42-109 ..... p 3429 N92-29364 * #

JPL-9950-1369 ..... p 3570 N92-29360 * #
JPL-9950-1381 ..... p 3564 N92-29359 * #

JSR-90-310 ..... p 3452 N92-30140 #
JSR-91-330A ..... p 3490 N92-30088 #

KCP-613-4035 ..... p 3441 N92-29796 #

KFK-4890 ..... p 3500 N92-29690 #
KFK-4909 ..... p 3422 N92-29651 #
KFK-4941 ..... p 3515 N92-29418 #

L-17094 ..... p 3484 N92-30106 * #
L-17126-PT-1 ..... p 3456 N92-29228 * #

LA-UR-91-3097 ..... p 3425 N92-29643 #
LA-UR-92-1043 ..... p 3555 N92-29917 #
LA-UR-92-1230 ..... p 3545 N92-29515 #
LA-UR-92-1330 ..... p 3500 N92-29513 #
LA-UR-92-1343 ..... p 3427 N92-29512 #
LA-UR-92-1370 ..... p 3415 N92-29795 #
LA-UR-92-1426 ..... p 3424 N92-29479 #
LA-UR-92-1442 ..... p 3500 N92-29536 #
LA-UR-92-748 ..... p 3545 N92-29634 #
LA-UR-92-792 ..... p 3555 N92-29789 #
LA-UR-92-805 ..... p 3562 N92-29794 #
LA-UR-92-826 ..... p 3556 N92-30203 #
LA-UR-92-887 ..... p 3421 N92-29633 #

LA-12197-MS ..... p 3541 N92-30138 #
LA-12298-MS ..... p 3542 N92-30139 #

LAAS-91393 ..... p 3422 N92-29674 #
LAAS-91394 ..... p 3529 N92-29675 #
LAAS-91395 ..... p 3529 N92-29678 #
LAAS-91412 ..... p 3526 N92-29888 #
LAAS-91433 ..... p 3441 N92-29729 #
LAAS-91466 ..... p 3436 N92-29730 #

LC-91-22753 ..... p 3563 N92-30040 #

LMI-PL019R1 ..... p 3562 N92-29934 #

LMSC/P009805 ..... p 3570 N92-30204 * #

LR-669 ..... p 3482 N92-29700 #
LR-670 ..... p 3415 N92-29702 #

M-691 ..... p 3429 N92-29677 * #

MBB-FE-2-S-PUB-472 ..... p 3404 N92-29650 #
MBB-FE-202-S-PUB-0462-A ..... p 3409 N92-29680 #
MBB-FE-202-S-PUB-0463-A ..... p 3408 N92-29629 #
MBB-FE-202-S-PUB-0464-A ..... p 3400 N92-29648 #
MBB-FE-202-S-PUB-0468-A ..... p 3401 N92-29713 #
MBB-FE-202-S-PUB-0469-A ..... p 3400 N92-29649 #

MBB-UD-0603-91-PUB ..... p 3480 N92-29873 #
MBB-UD-0606-91-PUB ..... p 3399 N92-29874 #
MBB-UD-0610-91-PUB ..... p 3407 N92-30076 #

MBB-Z-0380-91-PUB ..... p 3416 N92-29875 #
MBB-Z-0395-91-PUB ..... p 3416 N92-29876 #

MBB/FE202/S/PUB/461 ..... p 3399 N92-30232 #

MCAT-92-011-PT-3 ..... p 3406 N92-29655 * #

MEMO-COSOR-91-26 ..... p 3532 N92-29742 #
MEMO-COSOR-91-28 ..... p 3539 N92-29606 #
MEMO-COSOR-91-29 ..... p 3532 N92-29607 #
MEMO-COSOR-91-30 ..... p 3516 N92-29608 #
MEMO-COSOR-91-31 ..... p 3539 N92-29609 #
MEMO-COSOR-91-32 ..... p 3539 N92-29817 #
MEMO-COSOR-91-33 ..... p 3520 N92-29818 #
MEMO-COSOR-91-34 ..... p 3520 N92-29819 #
MEMO-COSOR-91-35 ..... p 3520 N92-29820 #
MEMO-COSOR-91-36 ..... p 3540 N92-29897 #
MEMO-COSOR-91-37 ..... p 3535 N92-29898 #
MEMO-COSOR-91-38 ..... p 3540 N92-29821 #
MEMO-COSOR-91-39 ..... p 3561 N92-29822 #
MEMO-COSOR-91-40 ..... p 3561 N92-29823 #
MEMO-COSOR-91-41 ..... p 3436 N92-29824 #
MEMO-COSOR-91-42 ..... p 3525 N92-29825 #
MEMO-COSOR-92-01 ..... p 3533 N92-29826 #
MEMO-COSOR-92-02 ..... p 3540 N92-29827 #
MEMO-COSOR-92-03 ..... p 3540 N92-29828 #

MEMO-INF-91-32 ..... p 3517 N92-29705 #
MEMO-INF-91-34 ..... p 3527 N92-30142 #
MEMO-INF-91-62 ..... p 3522 N92-30073 #
MEMO-INF-91-63 ..... p 3526 N92-30074 #
MEMO-INF-91-66 ..... p 3531 N92-30143 #
MEMO-INF-91-67 ..... p 3523 N92-30181 #
MEMO-INF-91-69 ..... p 3527 N92-30183 #
MEMO-INF-91-70 ..... p 3537 N92-30075 #
MEMO-INF-91-71 ..... p 3523 N92-30144 #
MEMO-INF-91-73 ..... p 3536 N92-29995 #
MEMO-INF-91-74 ..... p 3514 N92-30145 #
MEMO-INF-91-76 ..... p 3531 N92-30184 #
MEMO-INF-91-77 ..... p 3536 N92-29956 #
MEMO-INF-91-78 ..... p 3527 N92-30189 #
MEMO-INF-91-79 ..... p 3562 N92-30000 #
MEMO-INF-91-80 ..... p 3562 N92-29957 #
MEMO-INF-91-81 ..... p 3526 N92-29958 #
MEMO-INF-91-82 ..... p 3523 N92-30191 #
MEMO-INF-91-83 ..... p 3438 N92-30170 #
MEMO-INF-91-84 ..... p 3437 N92-29959 #
MEMO-INF-91-85 ..... p 3426 N92-29960 #
MEMO-INF-91-87 ..... p 3522 N92-29981 #
MEMO-INF-91-88 ..... p 3530 N92-29969 #
MEMO-INF-91-89 ..... p 3521 N92-29970 #
MEMO-INF-91-90 ..... p 3521 N92-29961 #
MEMO-INF-91-91 ..... p 3519 N92-29815 #
MEMO-INF-91-92 ..... p 3514 N92-29982 #
MEMO-INF-91-93 ..... p 3519 N92-29816 #
MEMO-INF-91-94 ..... p 3520 N92-29855 #
MEMO-INF-92-02 ..... p 3526 N92-29880 #
MEMO-INF-92-03 ..... p 3530 N92-29983 #
MEMO-INF-92-05 ..... p 3437 N92-29984 #
MEMO-INF-92-06 ..... p 3526 N92-29985 #

MEMO-1001 ..... p 3537 N92-30077 #
MEMO-1002 ..... p 3537 N92-30078 #
MEMO-1003 ..... p 3541 N92-30079 #
MEMO-1004 ..... p 3537 N92-30080 #
MEMO-1005 ..... p 3537 N92-30081 #
MEMO-1006 ..... p 3538 N92-30185 #
MEMO-1007 ..... p 3536 N92-29999 #
MEMO-1008 ..... p 3530 N92-29971 #
MEMO-1009 ..... p 3446 N92-29972 #
MEMO-1010 ..... p 3541 N92-29973 #
MEMO-1011 ..... p 3540 N92-29974 #
MEMO-1012 ..... p 3540 N92-29975 #
MEMO-1013 ..... p 3541 N92-29976 #
MEMO-1015 ..... p 3446 N92-29977 #
MEMO-1016-PT-2 ..... p 3437 N92-29978 #
MEMO-1017 ..... p 3536 N92-29979 #
MEMO-1019 ..... p 3541 N92-29980 #
MEMO-1020 ..... p 3537 N92-30147 #
MEMO-1021 ..... p 3560 N92-30148 #
MEMO-1022 ..... p 3523 N92-30186 #
MEMO-1023 ..... p 3541 N92-30188 #
MEMO-983 ..... p 3540 N92-29856 #
MEMO-987 ..... p 3445 N92-29857 #
MEMO-988 ..... p 3533 N92-29858 #
MEMO-993 ..... p 3534 N92-29872 #

MHD-ITC-91-021 ..... p 3554 N92-29640 #

MIT-TR-36 ..... p 3419 N92-29941 #

MML-TR-91-10C ..... p 3421 N92-29587 #
MML-TR-92-13C ..... p 3421 N92-29587 #

MPE-227 ..... p 3565 N92-29833 #

MTI-R89-006-28-VOL-1 ..... p 3525 N92-29555 #

M91-113 ..... p 3436 N92-29902 #

NAS 1.15:103560 ..... p 3408 N92-30215 * #
NAS 1.15:103853 ..... p 3506 N92-29397 * #
NAS 1.15:103858 ..... p 3443 N92-29394 * #
NAS 1.15:103929 ..... p 3404 N92-29417 * #
NAS 1.15:104220 ..... p 3423 N92-30205 * #
NAS 1.15:104240 ..... p 3405 N92-29659 * #
NAS 1.15:104247 ..... p 3405 N92-29425 * #
NAS 1.15:104565 ..... p 3502 N92-29653 * #
NAS 1.15:104566-VOL-1 ..... p 3505 N92-29686 * #
NAS 1.15:104566 ..... p 3506 N92-30193 * #
NAS 1.15:104568 ..... p 3491 N92-30210 * #
NAS 1.15:104751 ..... p 3513 N92-29403 * #
NAS 1.15:105359 ..... p 3478 N92-29697 * #
NAS 1.15:105675 ..... p 3402 N92-30182 * #
NAS 1.15:105676 ..... p 3478 N92-29351 * #
NAS 1.15:105680 ..... p 3405 N92-29661 * #
NAS 1.15:105691 ..... p 3413 N92-29667 * #
NAS 1.15:105700 ..... p 3414 N92-30187 * #
NAS 1.15:105731 ..... p 3412 N92-29343 * #
NAS 1.15:105737 ..... p 3492 N92-29662 * #
NAS 1.15:105746 ..... p 3427 N92-29669 * #
NAS 1.15:105754 ..... p 3415 N92-29660 * #
NAS 1.15:107548 ..... p 3492 N92-29430 * #
NAS 1.15:107623 ..... p 3481 N92-29393 * #
NAS 1.15:107632 ..... p 3488 N92-30214 * #
NAS 1.15:107635 ..... p 3400 N92-29445 * #
NAS 1.15:107807 ..... p 3571 N92-30197 * #
NAS 1.15:107918 ..... p 3410 N92-29811 * #
NAS 1.15:107919 ..... p 3410 N92-29810 * #
NAS 1.15:107920 ..... p 3410 N92-29812 * #
NAS 1.15:107922 ..... p 3488 N92-29442 * #
NAS 1.15:107953 ..... p 3571 N92-29689 * #
NAS 1.15:107956 ..... p 3408 N92-30016 * #
NAS 1.26:177593 ..... p 3512 N92-29413 * #
NAS 1.26:184339 ..... p 3570 N92-30204 * #
NAS 1.26:184343 ..... p 3407 N92-29664 * #
NAS 1.26:186021 ..... p 3405 N92-29427 * #
NAS 1.26:189024 ..... p 3452 N92-30149 * #
NAS 1.26:189171 ..... p 3524 N92-30207 * #
NAS 1.26:189200 ..... p 3413 N92-29448 * #
NAS 1.26:189207 ..... p 3399 N92-29402 * #
NAS 1.26:189595 ..... p 3406 N92-29352 * #
NAS 1.26:189656-VOL-1 ..... p 3410 N92-30217 * #
NAS 1.26:189656-VOL-2 ..... p 3411 N92-30218 * #
NAS 1.26:189656-VOL-3 ..... p 3411 N92-30219 * #
NAS 1.26:189656-VOL-4 ..... p 3411 N92-30220 * #
NAS 1.26:189656-VOL-5 ..... p 3411 N92-30221 * #
NAS 1.26:189656-VOL-6 ..... p 3411 N92-30222 * #
NAS 1.26:189656-VOL-7 ..... p 3412 N92-30223 * #
NAS 1.26:189656-VOL-8 ..... p 3412 N92-30224 * #
NAS 1.26:189656-VOL-9 ..... p 3412 N92-30225 * #
NAS 1.26:189661 ..... p 3444 N92-29692 * #
NAS 1.26:189666 ..... p 3455 N92-30192 * #
NAS 1.26:189667 ..... p 3455 N92-30190 * #
NAS 1.26:189867 ..... p 3528 N92-29656 * #
NAS 1.26:189868 ..... p 3403 N92-29440 * #
NAS 1.26:189967 ..... p 3447 N92-30041 * #
NAS 1.26:190262 ..... p 3569 N92-30199 * #
NAS 1.26:190264 ..... p 3399 N92-29329 * #
NAS 1.26:190282 ..... p 3561 N92-29553 * #
NAS 1.26:190311 ..... p 3557 N92-29676 * #
NAS 1.26:190446 ..... p 3434 N92-29568 * #
NAS 1.26:190453 ..... p 3434 N92-29463 * #
NAS 1.26:190454 ..... p 3551 N92-29679 * #
NAS 1.26:190460 ..... p 3429 N92-29364 * #
NAS 1.26:190480 ..... p 3399 N92-29361 * #
NAS 1.26:190482 ..... p 3570 N92-29360 * #
NAS 1.26:190483 ..... p 3564 N92-29359 * #
NAS 1.26:190491 ..... p 3552 N92-29681 * #
NAS 1.26:190494 ..... p 3551 N92-29652 * #
NAS 1.26:190496 ..... p 3550 N92-29331 * #
NAS 1.26:190497 ..... p 3478 N92-29392 * #
NAS 1.26:190499 ..... p 3514 N92-29363 * #
NAS 1.26:190500 ..... p 3514 N92-29362 * #
NAS 1.26:190502 ..... p 3514 N92-29391 * #
NAS 1.26:190504 ..... p 3525 N92-29390 * #
NAS 1.26:190517 ..... p 3409 N92-29422 * #
NAS 1.26:190520 ..... p 3528 N92-29673 * #
NAS 1.26:190528 ..... p 3517 N92-29630 * #
NAS 1.26:190533 ..... p 3547 N92-30001 * #
NAS 1.26:190535 ..... p 3406 N92-29654 * #
NAS 1.26:190537 ..... p 3416 N92-30208 * #
NAS 1.26:190538 ..... p 3423 N92-30206 * #
NAS 1.26:190541 ..... p 3406 N92-29655 * #
NAS 1.26:190543 ..... p 3568 N92-29401 * #
NAS 1.26:190545 ..... p 3515 N92-29400 * #
NAS 1.26:190555 ..... p 3517 N92-29694 * #
NAS 1.26:190561 ..... p 3435 N92-29658 * #
NAS 1.26:190565 ..... p 3404 N92-30209 * #
NAS 1.26:190567 ..... p 3569 N92-29631 * #
NAS 1.26:190570 ..... p 3401 N92-29657 * #
NAS 1.26:190571 ..... p 3517 N92-29695 * #
NAS 1.26:190576 ..... p 3401 N92-29691 * #
NAS 1.26:190579 ..... p 3568 N92-29432 * #
NAS 1.26:190586 ..... p 3568 N92-29451 * #
NAS 1.26:190588 ..... p 3481 N92-29342 * #
NAS 1.26:190588 ..... p 3517 N92-29665 * #
NAS 1.26:4455 ..... p 3509 N92-29341 * #
NAS 1.55:10092 ..... p 3400 N92-29625 * #
NAS 1.55:3158-PT-1 ..... p 3456 N92-29228 * #
NAS 1.55:3160 ..... p 3484 N92-30106 * #
NAS 1.60:3249 ..... p 3429 N92-29677 * #
NAS 1.71:LAR-13805-1 ..... p 3480 N92-30097 * #

NAS 1.71:LAR-14033-2 ..... p 3447 N92-30024 * #
NAS 1.71:LAR-14219-1 ..... p 3406 N92-30025 * #
NAS 1.71:LAR-14398-1 ..... p 3419 N92-30098 * #
NAS 1.71:LAR-14559-1 ..... p 3480 N92-29829 * #
NAS 1.71:LAR-14607-1SB ..... p 3553 N92-30029 * #
NAS 1.71:LAR-14612-1 ..... p 3446 N92-29954 * #
NAS 1.71:LAR-14643-1 ..... p 3426 N92-29953 * #
NAS 1.71:LAR-14698-1 ..... p 3483 N92-30028 * #
NAS 1.71:LAR-14724-1 ..... p 3474 N92-30030 * #
NAS 1.71:LAR-14775-1 ..... p 3483 N92-30099 * #
NAS 1.71:LAR-14779-1 ..... p 3552 N92-29951 * #
NAS 1.71:LAR-14815-1-CU ..... p 3445 N92-29830 * #
NAS 1.71:MFS-28682-1 ..... p 3426 N92-29831 * #
NAS 1.71:MSC-21529-1 ..... p 3427 N92-30100 * #
NAS 1.71:MSC-21881-1 ..... p 3479 N92-30082 * #
NAS 1.71:MSC-21903-1 ..... p 3480 N92-30101 * #
NAS 1.71:MSC-21915-1 ..... p 3552 N92-30027 * #
NAS 1.71:MSC-21935-1 ..... p 3479 N92-29762 * #
NAS 1.71:MSC-21961-1 ..... p 3474 N92-29952 * #
NAS 1.71:MSC-21967-1 ..... p 3479 N92-30026 * #
NAS 1.71:NPO-17794-1-CU ..... p 3553 N92-30104 * #
NAS 1.71:NPO-17807-2-CU ..... p 3529 N92-29955 * #
NAS 1.71:NPO-18410-1-CU ..... p 3552 N92-29832 * #
NAS 1.71:NPO-18448-1-CU ..... p 3428 N92-30083 * #
NAS 1.71:NPO-18478-1-CU ..... p 3553 N92-30084 * #
NAS 1.71:NPO-18553-1-CU ..... p 3530 N92-30085 * #
NAS 1.71:NPO-18578-1-CU ..... p 3442 N92-30086 * #
NAS 1.71:NPO-18625-1-CU ..... p 3559 N92-30102 * #
NAS 1.71:NPO-18668-1-CU ..... p 3479 N92-29765 * #
NAS 1.71:NPO-18713-1-CU ..... p 3437 N92-30103 * #

NASA-CASE-LAR-13805-1 ..... p 3480 N92-30097 * #
NASA-CASE-LAR-14033-2 ..... p 3447 N92-30024 * #
NASA-CASE-LAR-14219-1 ..... p 3406 N92-30025 * #
NASA-CASE-LAR-14398-1 ..... p 3419 N92-30098 * #
NASA-CASE-LAR-14559-1 ..... p 3480 N92-29829 * #
NASA-CASE-LAR-14607-1SB ..... p 3553 N92-30029 * #
NASA-CASE-LAR-14612-1 ..... p 3446 N92-29954 * #
NASA-CASE-LAR-14643-1 ..... p 3426 N92-29953 * #
NASA-CASE-LAR-14698-1 ..... p 3483 N92-30028 * #
NASA-CASE-LAR-14724-1 ..... p 3474 N92-30030 * #
NASA-CASE-LAR-14775-1 ..... p 3483 N92-30099 * #
NASA-CASE-LAR-14779-1 ..... p 3552 N92-29951 * #
NASA-CASE-LAR-14815-1-CU ..... p 3445 N92-29830 * #

NASA-CASE-MFS-28682-1 ..... p 3426 N92-29831 * #

NASA-CASE-MSC-21529-1 ..... p 3427 N92-30100 * #
NASA-CASE-MSC-21881-1 ..... p 3479 N92-30082 * #
NASA-CASE-MSC-21903-1 ..... p 3480 N92-30101 * #
NASA-CASE-MSC-21915-1 ..... p 3552 N92-30027 * #
NASA-CASE-MSC-21935-1 ..... p 3479 N92-29762 * #
NASA-CASE-MSC-21961-1 ..... p 3474 N92-29952 * #
NASA-CASE-MSC-21967-1 ..... p 3479 N92-30026 * #

NASA-CASE-NPO-17794-1-CU ..... p 3553 N92-30104 * #
NASA-CASE-NPO-17807-2-CU ..... p 3529 N92-29955 * #
NASA-CASE-NPO-18410-1-CU ..... p 3552 N92-29832 * #
NASA-CASE-NPO-18448-1-CU ..... p 3428 N92-30083 * #
NASA-CASE-NPO-18478-1-CU ..... p 3553 N92-30084 * #
NASA-CASE-NPO-18553-1-CU ..... p 3530 N92-30085 * #
NASA-CASE-NPO-18578-1-CU ..... p 3442 N92-30086 * #
NASA-CASE-NPO-18625-1-CU ..... p 3559 N92-30102 * #
NASA-CASE-NPO-18668-1-CU ..... p 3479 N92-29765 * #
NASA-CASE-NPO-18713-1-CU ..... p 3437 N92-30103 * #

NASA-CP-10092 ..... p 3400 N92-29625 * #
NASA-CP-3158-PT-1 ..... p 3456 N92-29228 * #
NASA-CP-3160 ..... p 3484 N92-30106 * #

NASA-CR-177593 ..... p 3512 N92-29413 * #
NASA-CR-184339 ..... p 3570 N92-30204 * #
NASA-CR-184343 ..... p 3407 N92-29664 * #
NASA-CR-186021 ..... p 3405 N92-29427 * #
NASA-CR-189024 ..... p 3452 N92-30149 * #
NASA-CR-189171 ..... p 3524 N92-30207 * #
NASA-CR-189200 ..... p 3413 N92-29448 * #
NASA-CR-189207 ..... p 3399 N92-29402 * #
NASA-CR-189595 ..... p 3406 N92-29352 * #
NASA-CR-189656-VOL-1 ..... p 3410 N92-30217 * #
NASA-CR-189656-VOL-2 ..... p 3411 N92-30218 * #
NASA-CR-189656-VOL-3 ..... p 3411 N92-30219 * #
NASA-CR-189656-VOL-4 ..... p 3411 N92-30220 * #
NASA-CR-189656-VOL-5 ..... p 3411 N92-30221 * #
NASA-CR-189656-VOL-6 ..... p 3411 N92-30222 * #
NASA-CR-189656-VOL-7 ..... p 3412 N92-30223 * #
NASA-CR-189656-VOL-8 ..... p 3412 N92-30224 * #
NASA-CR-189656-VOL-9 ..... p 3412 N92-30225 * #
NASA-CR-189661 ..... p 3444 N92-29692 * #
NASA-CR-189666 ..... p 3455 N92-30192 * #
NASA-CR-189667 ..... p 3455 N92-30190 * #
NASA-CR-189867 ..... p 3528 N92-29656 * #
NASA-CR-189868 ..... p 3403 N92-29440 * #
NASA-CR-189967 ..... p 3447 N92-30041 * #
NASA-CR-190262 ..... p 3569 N92-30199 * #
NASA-CR-190264 ..... p 3399 N92-29329 * #
NASA-CR-190282 ..... p 3561 N92-29553 * #
NASA-CR-190311 ..... p 3557 N92-29676 * #
NASA-CR-190446 ..... p 3434 N92-29568 * #
NASA-CR-190453 ..... p 3434 N92-29463 * #
NASA-CR-190454 ..... p 3551 N92-29679 * #
NASA-CR-190460 ..... p 3429 N92-29364 * #
NASA-CR-190480 ..... p 3399 N92-29361 * #
NASA-CR-190482 ..... p 3570 N92-29360 * #
NASA-CR-190483 ..... p 3564 N92-29359 * #
NASA-CR-190491 ..... p 3552 N92-29681 * #
NASA-CR-190494 ..... p 3551 N92-29652 * #
NASA-CR-190496 ..... p 3550 N92-29331 * #
NASA-CR-190497 ..... p 3478 N92-29392 * #
NASA-CR-190499 ..... p 3514 N92-29363 * #
NASA-CR-190500 ..... p 3514 N92-29362 * #
NASA-CR-190502 ..... p 3514 N92-29391 * #
NASA-CR-190504 ..... p 3525 N92-29390 * #
NASA-CR-190517 ..... p 3409 N92-29422 * #
NASA-CR-190520 ..... p 3528 N92-29673 * #
NASA-CR-190528 ..... p 3517 N92-29630 * #
NASA-CR-190533 ..... p 3547 N92-30001 * #
NASA-CR-190535 ..... p 3406 N92-29654 * #
NASA-CR-190537 ..... p 3416 N92-30208 * #
NASA-CR-190538 ..... p 3423 N92-30206 * #
NASA-CR-190541 ..... p 3406 N92-29655 * #
NASA-CR-190543 ..... p 3568 N92-29401 * #
NASA-CR-190545 ..... p 3515 N92-29400 * #
NASA-CR-190555 ..... p 3517 N92-29694 * #
NASA-CR-190561 ..... p 3435 N92-29658 * #
NASA-CR-190565 ..... p 3404 N92-30209 * #
NASA-CR-190567 ..... p 3569 N92-29631 * #
NASA-CR-190570 ..... p 3401 N92-29657 * #
NASA-CR-190571 ..... p 3517 N92-29695 * #
NASA-CR-190576 ..... p 3401 N92-29691 * #
NASA-CR-190579 ..... p 3568 N92-29432 * #
NASA-CR-190586 ..... p 3568 N92-29451 * #
NASA-CR-190588 ..... p 3481 N92-29342 * #
NASA-CR-190588 ..... p 3517 N92-29665 * #
NASA-CR-4455 ..... p 3509 N92-29341 * #

NASA-HHR-55 ..... p 3571 N92-29689 * #

NASA-TM-103560 ..... p 3408 N92-30215 * #
NASA-TM-103853 ..... p 3506 N92-29397 * #
NASA-TM-103858 ..... p 3443 N92-29394 * #
NASA-TM-103929 ..... p 3404 N92-29417 * #
NASA-TM-104220 ..... p 3423 N92-30205 * #
NASA-TM-104240 ..... p 3405 N92-29659 * #
NASA-TM-104247 ..... p 3405 N92-29425 * #
NASA-TM-104565 ..... p 3502 N92-29653 * #
NASA-TM-104566-VOL-1 ..... p 3505 N92-29686 * #
NASA-TM-104566 ..... p 3506 N92-30193 * #
NASA-TM-104568 ..... p 3491 N92-30210 * #
NASA-TM-104751 ..... p 3513 N92-29403 * #
NASA-TM-105359 ..... p 3478 N92-29697 * #
NASA-TM-105675 ..... p 3402 N92-30182 * #
NASA-TM-105676 ..... p 3478 N92-29351 * #
NASA-TM-105680 ..... p 3405 N92-29661 * #
NASA-TM-105691 ..... p 3413 N92-29667 * #
NASA-TM-105700 ..... p 3414 N92-30187 * #
NASA-TM-105731 ..... p 3412 N92-29343 * #
NASA-TM-105737 ..... p 3492 N92-29662 * #
NASA-TM-105746 ..... p 3427 N92-29669 * #
NASA-TM-105754 ..... p 3415 N92-29660 * #
NASA-TM-107548 ..... p 3492 N92-29430 * #
NASA-TM-107623 ..... p 3481 N92-29393 * #
NASA-TM-107632 ..... p 3488 N92-30214 * #
NASA-TM-107635 ..... p 3400 N92-29445 * #
NASA-TM-107807 ..... p 3571 N92-30197 * #
NASA-TM-107918 ..... p 3410 N92-29811 * #
NASA-TM-107919 ..... p 3410 N92-29810 * #
NASA-TM-107920 ..... p 3410 N92-29812 * #
NASA-TM-107922 ..... p 3488 N92-29442 * #
NASA-TM-107953 ..... p 3571 N92-29689 * #
NASA-TM-107956 ..... p 3408 N92-30016 * #

NASA-TP-3249 ..... p 3429 N92-29677 * #

NAVSWC-TR-90-683 ..... p 3400 N92-29539 #

NAVY-CASE-72831 ..... p 3475 N92-30202 #
NAVY-CASE-73128 ..... p 3441 N92-29900 #

NCAR/TN-370+STR ..... p 3491 N92-30105 #

NCCOSC/RDT/E-TR-1483 ..... p 3501 N92-30087 #

NCEER-91/0026 ..... p 3501 N92-29950 #

NHRC-91-31 ..... p 3510 N92-30216 #

NIFS-132 ..... p 3555 N92-30091 #
NIFS-136 ..... p 3555 N92-30172 #

NIIYAF-MGU-91-2-206 ..... p 3560 N92-29533 #

NIKHEF-H/91-18 ..... p 3518 N92-29747 #
NIKHEF-H/91-19 ..... p 3546 N92-29750 #
NIKHEF-H/91-25 ..... p 3546 N92-29751 #

NIST/TN-1351 ..... p 3438 N92-30198 #

NISTIR-3986 ..... p 3422 N92-29803 #
NISTIR-3987 ..... p 3447 N92-30036 #
NISTIR-3988 ..... p 3437 N92-30093 #
NISTIR-4655 ..... p 3518 N92-29745 #
NISTIR-4726 ..... p 3442 N92-30032 #
NISTIR-4741 ..... p 3542 N92-30035 #
NISTIR-4757 ..... p 3542 N92-29802 #
NISTIR-4760 ..... p 3483 N92-29813 #
NISTIR-4768 ..... p 3418 N92-29744 #
NISTIR-4800 ..... p 3563 N92-30039 #
NISTIR-4810 ..... p 3522 N92-30020 #

NLR-MP-88040-U ..... p 3403 N92-29615 #
NLR-MP-88044-U ..... p 3404 N92-29616 #

NLR-TP-89103-U ..... p 3490 N92-29707 #
NLR-TP-89311-U ..... p 3512 N92-29871 #
NLR-TP-90107-U ..... p 3483 N92-29708 #
NLR-TP-90196-U ..... p 3402 N92-29703 #
NLR-TP-90267-U ..... p 3478 N92-29602 #
NLR-TP-90336-U ..... p 3482 N92-29603 #
NLR-TP-91061-U ..... p 3532 N92-29604 #
NLR-TP-91062-U-PT-1 ..... p 3403 N92-29605 #

NLR-TR-86006-U ..... p 3402 N92-29916 #
NLR-TR-88072-U ..... p 3401 N92-29884 #
NLR-TR-88086-U ..... p 3479 N92-29885 #

NOAA-TM-ERL-ARL-193 ..... p 3503 N92-30034 #

NOAA-TM-ERL-WPL-218 ..... p 3477 N92-29948 #
NOAA-TM-ERL-WPL-219 ..... p 3503 N92-29800 #

NOAA-TM-ERL-1 ..... p 3502 N92-29799 #

NOAA-TM-NWSTM-PR-37 ..... p 3502 N92-29743 #

NOARL-CR-026-91 ..... p 3505 N92-29562 #

NOSC/TR-1456 ..... p 3433 N92-29395 #

NREL/TP-214-4488 ..... p 3425 N92-29598 #
NREL/TP-411-4752 ..... p 3557 N92-29584 #

NSWCCR/RDTR-92/0003 ..... p 3427 N92-29786 #

NUWC-NL-TR-10017 ..... p 3483 N92-29915 #

NYSERDA-91-5 ..... p 3564 N92-30037 #

OCS/MMS-91/0061 ..... p 3505 N92-29704 #
OCS/MMS-91/0069 ..... p 3490 N92-30022 #

OEFZS-4570 ..... p 3561 N92-29886 #
OEFZS-4612 ..... p 3538 N92-29419 #
OEFZS-4615 ..... p 3473 N92-29469 #
OEFZS-4616 ..... p 3428 N92-29470 #

ORNL/TM-11882 ..... p 3547 N92-29910 #
ORNL/TM-12050 ..... p 3519 N92-29797 #

OTA-BP-TCT-76 ..... p 3435 N92-29696 #

OTA-F-515 ..... p 3492 N92-29416 #

OTA-TCT-512 ..... p 3563 N92-29671 #

PASC006.01.00 ..... p 3562 N92-29720 #

PB92-139393 ..... p 3495 N92-30031 #
PB92-147115 ..... p 3410 N92-29810 * #
PB92-147123 ..... p 3410 N92-29811 * #
PB92-147131 ..... p 3410 N92-29812 * #
PB92-147180 ..... p 3561 N92-29663 #
PB92-154954 ..... p 3494 N92-29698 #
PB92-157601 ..... p 3435 N92-29696 #
PB92-161363 ..... p 3489 N92-29701 #
PB92-161371 ..... p 3494 N92-29746 #
PB92-163294 ..... p 3422 N92-29807 #
PB92-163575 ..... p 3502 N92-29799 #
PB92-163807 ..... p 3501 N92-29950 #
PB92-163856 ..... p 3562 N92-29699 #
PB92-164425 ..... p 3426 N92-29804 #
PB92-164524 ..... p 3503 N92-29800 #
PB92-164656 ..... p 3513 N92-29949 #
PB92-164672 ..... p 3442 N92-30032 #
PB92-164680 ..... p 3542 N92-29802 #
PB92-164987 ..... p 3505 N92-29704 #
PB92-166404 ..... p 3477 N92-29948 #
PB92-167006 ..... p 3564 N92-29808 #

PB92-167014 ..... p 3564 N92-29809 #
PB92-167345 ..... p 3502 N92-29743 #
PB92-167352 ..... p 3563 N92-29671 #
PB92-167378 ..... p 3503 N92-29801 #
PB92-169119 ..... p 3483 N92-29813 #
PB92-170281 ..... p 3506 N92-29805 #
PB92-170299 ..... p 3506 N92-29806 #
PB92-172006 ..... p 3418 N92-29744 #
PB92-172360 ..... p 3492 N92-29519 #
PB92-172477 ..... p 3422 N92-29803 #
PB92-172493 ..... p 3518 N92-29745 #
PB92-172824 ..... p 3542 N92-30035 #
PB92-172832 ..... p 3447 N92-30036 #
PB92-172857 ..... p 3562 N92-30033 #
PB92-173251 ..... p 3542 N92-30095 #
PB92-174119 ..... p 3564 N92-30037 #
PB92-174564 ..... p 3503 N92-30034 #
PB92-176361 ..... p 3493 N92-29520 #
PB92-176379 ..... p 3493 N92-29521 #
PB92-176387 ..... p 3493 N92-29522 #
PB92-177872 ..... p 3443 N92-30094 #
PB92-178292 ..... p 3537 N92-30096 #
PB92-178631 ..... p 3563 N92-30038 #
PB92-180207 ..... p 3443 N92-30092 #
PB92-180249 ..... p 3495 N92-30173 #
PB92-180256 ..... p 3494 N92-30018 #
PB92-180678 ..... p 3447 N92-30023 #
PB92-181098 ..... p 3522 N92-30020 #
PB92-181122 ..... p 3563 N92-30039 #
PB92-181320 ..... p 3563 N92-30040 #
PB92-183672 ..... p 3437 N92-30093 #
PB92-184761 ..... p 3419 N92-30196 #
PB92-184985 ..... p 3495 N92-30021 #
PB92-185016 ..... p 3490 N92-30022 #
PB92-185073 ..... p 3494 N92-30019 #
PB92-185305 ..... p 3563 N92-30194 #
PB92-186113 ..... p 3491 N92-30105 #
PB92-186246 ..... p 3495 N92-30200 #
PB92-187020 ..... p 3438 N92-30198 #
PB92-187350 ..... p 3524 N92-30201 #
PB92-187418 ..... p 3524 N92-30195 #

PCS-TR91-156 ..... p 3517 N92-29630 * #

PNL-SA-19820 ..... p 3415 N92-29645 #
PNL-SA-20350 ..... p 3420 N92-29411 #
PNL-SA-20408 ..... p 3420 N92-29436 #
PNL-SA-20771 ..... p 3492 N92-29646 #

PNL-8053 ..... p 3569 N92-29600 #

PSU-TURBO-9201 ..... p 3445 N92-29933 #

PUBL-445 ..... p 3490 N92-29728 #

PW/GESP-FR2198-05 ..... p 3420 N92-29408 #

R/D-6750-MS-01 ..... p 3422 N92-29647 #

RAL-91-070 ..... p 3544 N92-29488 #
RAL-92-004 ..... p 3560 N92-29996 #

REF-JTN-816005 ..... p 3423 N92-29940 #

REPT-001 ..... p 3510 N92-29420 #
REPT-18-1991 ..... p 3505 N92-29684 #
REPT-1992/5 ..... p 3443 N92-30094 #
REPT-255-6491-1 ..... p 3512 N92-29930 #
REPT-32 ..... p 3490 N92-29717 #
REPT-43 ..... p 3489 N92-29495 #
REPT-68 ..... p 3447 N92-30023 #
REPT-91-36 ..... p 3544 N92-29918 #
REPT-91-37 ..... p 3535 N92-29919 #
REPT-91-38 ..... p 3535 N92-29920 #
REPT-91-39 ..... p 3535 N92-29921 #
REPT-91-40 ..... p 3535 N92-29922 #
REPT-91-41 ..... p 3535 N92-29923 #
REPT-91-42 ..... p 3536 N92-29924 #
REPT-91-46 ..... p 3521 N92-29887 #
REPT-91-48 ..... p 3518 N92-29711 #
REPT-91-49 ..... p 3518 N92-29712 #
REPT-91-50 ..... p 3519 N92-29779 #
REPT-91-51 ..... p 3444 N92-29763 #
REPT-91-52 ..... p 3529 N92-29764 #
REPT-91-53 ..... p 3539 N92-29626 #
REPT-91-57 ..... p 3517 N92-29627 #
REPT-91-60 ..... p 3543 N92-29628 #
REPT-91-62 ..... p 3543 N92-29748 #
REPT-91-63 ..... p 3518 N92-29749 #
REPT-91-64 ..... p 3525 N92-29716 #
REPT-91-81 ..... p 3495 N92-30226 #
REPT-91-82 ..... p 3524 N92-30227 #
REPT-91-84 ..... p 3524 N92-30228 #
REPT-91-85 ..... p 3527 N92-30229 #
REPT-92-005 ..... p 3517 N92-29665 * #
REPT-92B00088 ..... p 3502 N92-29653 * #
REPT-92B00089 ..... p 3505 N92-29686 * #
REPT-92B00092 ..... p 3491 N92-30210 * #
REPT-92B00097-VOL-5 ..... p 3506 N92-30193 * #

RIACS-TR-92-04 ..... p 3517 N92-29694 * #

RL-TR-91-353 ..... p 3442 N92-29914 #
RL-TR-91-378 ..... p 3417 N92-29423 #

RR-847-I-IMAG-120-LIFIA ..... p 3532 N92-29573 #
RR-858-I-IMAG-121-LIFIA ..... p 3532 N92-29574 #

RSRE-MEMO-4564 ..... p 3475 N92-29396 #

S-HRG-102-647 ..... p 3490 N92-30017 #

S-680 ..... p 3513 N92-29403 * #

SAND-91-1691C ..... p 3408 N92-29986 #
SAND-91-2346C ..... p 3440 N92-29518 #
SAND-91-2727C ..... p 3426 N92-29908 #
SAND-91-2790C ..... p 3561 N92-29552 #
SAND-91-2808C ..... p 3527 N92-29456 #
SAND-91-8230 ..... p 3517 N92-29641 #
SAND-91-8706 ..... p 3417 N92-29459 #
SAND-91-8714 ..... p 3417 N92-29431 #
SAND-91-8720 ..... p 3419 N92-29943 #
SAND-91-8743 ..... p 3417 N92-29433 #
SAND-92-0357C ..... p 3439 N92-29455 #
SAND-92-0446C ..... p 3477 N92-30135 #
SAND-92-0594C ..... p 3421 N92-29623 #
SAND-92-8464C ..... p 3475 N92-29434 #
SAND-92-8509C ..... p 3476 N92-29516 #

SKBS-A1/91-21 ..... p 3531 N92-30143 #

SLCET-TR-88-0849-F ..... p 3491 N92-29476 #
SLCET-TR-92-1 ..... p 3439 N92-29498 #

SSC-352 ..... p 3422 N92-29807 #

SSCL-PREPRINT-86 ..... p 3545 N92-29507 #

SU-E450-1 ..... p 3434 N92-29542 #

SU-SLAC-PUB-5780 ..... p 3437 N92-29988 #
SU-SLAC-PUB-5784 ..... p 3550 N92-29788 #

TAMRF-5802-92-02 ..... p 3401 N92-29657 * #

TGAL-92-13 ..... p 3505 N92-29618 #

TIOS-91/010 ..... p 3517 N92-29705 #
TIOS-91/025 ..... p 3526 N92-30074 #
TIOS-91/026 ..... p 3523 N92-30144 #
TIOS-91/028 ..... p 3531 N92-30184 #
TIOS-91/029 ..... p 3562 N92-30000 #
TIOS-91/030 ..... p 3526 N92-29958 #
TIOS-91/031 ..... p 3523 N92-30191 #
TIOS-91/032 ..... p 3514 N92-30145 #
TIOS-91/033 ..... p 3438 N92-30170 #
TIOS-91/034 ..... p 3437 N92-29959 #
TIOS-91/035 ..... p 3522 N92-29981 #
TIOS-91/036 ..... p 3514 N92-29982 #
TIOS-92/01 ..... p 3526 N92-29880 #
TIOS-92/03 ..... p 3437 N92-29984 #
TIOS-92/04 ..... p 3526 N92-29985 #

TKK-F-A669 ..... p 3492 N92-29636 #

TKK-KO/LTK-66 ..... p 3442 N92-30089 #
TKK-KO/LTK-67 ..... p 3441 N92-29912 #

TKK-V-C110 ..... p 3421 N92-29637 #

TR-16 ..... p 3418 N92-29619 #
TR-25 ..... p 3417 N92-29514 #
TR-32 ..... p 3556 N92-29429 #
TR-34 ..... p 3424 N92-29496 #
TR-3 ..... p 3418 N92-29595 #
TR-451 ..... p 3538 N92-29501 #
TR-57 ..... p 3423 N92-29349 #
TR-58 ..... p 3425 N92-29566 #
TR-60 ..... p 3425 N92-29567 #
TR-61 ..... p 3425 N92-29569 #
TR-64 ..... p 3427 N92-30136 #
TR-72 ..... p 3538 N92-29500 #
TR-8 ..... p 3556 N92-29558 #

TRW-SN-57661 ..... p 3564 N92-29359 * #

TW-91-09 ..... p 3524 N92-30201 #

UCB/R/91/N1076 ..... p 3414 N92-29556 #

UCRL-CR-104380-REV-1 ..... p 3477 N92-29937 #
UCRL-CR-110256 ..... p 3480 N92-29478 #

UCRL-ID-109373 ..... p 3551 N92-29578 #
UCRL-ID-110241 ..... p 3516 N92-29537 #
UCRL-ID-110284 ..... p 3555 N92-29798 #
UCRL-ID-110314 ..... p 3554 N92-29531 #

UCRL-JC-106149 ..... p 3556 N92-29473 #
UCRL-JC-107696 ..... p 3559 N92-29911 #
UCRL-JC-107745 ..... p 3477 N92-29987 #
UCRL-JC-107865 ..... p 3533 N92-29792 #
UCRL-JC-107866 ..... p 3481 N92-29338 #
UCRL-JC-108127 ..... p 3476 N92-29472 #
UCRL-JC-108728 ..... p 3421 N92-29639 #
UCRL-JC-108819 ..... p 3495 N92-30211 #
UCRL-JC-108973 ..... p 3524 N92-29353 #
UCRL-JC-109001 ..... p 3436 N92-29909 #
UCRL-JC-109226 ..... p 3531 N92-29481 #
UCRL-JC-109501 ..... p 3494 N92-29790 #
UCRL-JC-109672 ..... p 3438 N92-29339 #
UCRL-JC-109754 ..... p 3550 N92-29337 #
UCRL-JC-109918-REV-1 ..... p 3477 N92-29787 #
UCRL-JC-110134 ..... p 3551 N92-29484 #
UCRL-JC-110158 ..... p 3475 N92-29358 #
UCRL-JC-110159 ..... p 3475 N92-29340 #
UCRL-JC-110302 ..... p 3476 N92-29509 #

UCRL-MA-108721 ..... p 3533 N92-29791 #

UDR-TR-91-64 ..... p 3414 N92-29453 #

UILU-ENG-92-2214 ..... p 3517 N92-29695 * #

UILUENG-91-0511 ..... p 3413 N92-29913 #

US-PATENT-APPL-SN-736985 ..... p 3419 N92-30098 * #
US-PATENT-APPL-SN-770509 ..... p 3480 N92-30097 * #
US-PATENT-APPL-SN-771928 ..... p 3441 N92-29900 #
US-PATENT-APPL-SN-772999 ..... p 3435 N92-29572 #
US-PATENT-APPL-SN-783660 ..... p 3475 N92-30202 #
US-PATENT-APPL-SN-785637 ..... p 3479 N92-30082 * #
US-PATENT-APPL-SN-786612 ..... p 3428 N92-30083 * #
US-PATENT-APPL-SN-788908 ..... p 3406 N92-30025 * #
US-PATENT-APPL-SN-789567 ..... p 3529 N92-29955 * #
US-PATENT-APPL-SN-790730 ..... p 3426 N92-29953 * #
US-PATENT-APPL-SN-802078 ..... p 3437 N92-30103 * #
US-PATENT-APPL-SN-820431 ..... p 3446 N92-29954 * #
US-PATENT-APPL-SN-820432 ..... p 3445 N92-29830 * #
US-PATENT-APPL-SN-839627 ..... p 3474 N92-29571 #
US-PATENT-APPL-SN-843653 ..... p 3447 N92-30024 * #
US-PATENT-APPL-SN-855363 ..... p 3553 N92-30029 * #
US-PATENT-APPL-SN-857901 ..... p 3427 N92-30100 * #
US-PATENT-APPL-SN-863883 ..... p 3552 N92-30027 * #
US-PATENT-APPL-SN-866769 ..... p 3483 N92-30028 * #
US-PATENT-APPL-SN-876592 ..... p 3474 N92-30030 * #
US-PATENT-APPL-SN-878631 ..... p 3480 N92-29829 * #
US-PATENT-APPL-SN-881912 ..... p 3483 N92-30099 * #
US-PATENT-APPL-SN-882408 ..... p 3479 N92-29762 * #
US-PATENT-APPL-SN-883957 ..... p 3553 N92-30084 * #
US-PATENT-APPL-SN-885714 ..... p 3552 N92-29951 * #
US-PATENT-APPL-SN-892053 ..... p 3479 N92-30026 * #
US-PATENT-APPL-SN-901626 ..... p 3474 N92-29952 * #
US-PATENT-APPL-SN-902266 ..... p 3480 N92-30101 * #
US-PATENT-APPL-SN-904550 ..... p 3553 N92-30104 * #
US-PATENT-APPL-SN-908677 ..... p 3530 N92-30085 * #
US-PATENT-APPL-SN-912401 ..... p 3426 N92-29831 * #
US-PATENT-APPL-SN-912955 ..... p 3479 N92-29765 * #
US-PATENT-APPL-SN-912956 ..... p 3442 N92-30086 * #
US-PATENT-APPL-SN-912981 ..... p 3559 N92-30102 * #

USAARL-92-18 ..... p 3404 N92-29506 #
USAARL-92-5 ..... p 3510 N92-29347 #
USAARL-92-9 ..... p 3512 N92-29348 #

USCG-D-03-92 ..... p 3512 N92-29538 #

USDA/CRIS/AG-91/11 ..... p 3562 N92-30033 #

USGS-BULL-1565 ..... p 3563 N92-30040 #

USGS/G-1637 ..... p 3494 N92-29746 #
USGS/G-1645 ..... p 3489 N92-29701 #

USIP-90-09 ..... p 3518 N92-29714 #
USIP-91-02 ..... p 3546 N92-29715 #
USIP-91-04 ..... p 3519 N92-29780 #
USIP-91-05 ..... p 3560 N92-29781 #

UT-KBS-91-21 ..... p 3426 N92-29960 #
UT-KBS-91-33 ..... p 3531 N92-30143 #

UTD-23351-961-VOL-1 ..... p 3410 N92-30217 * #

UVA/528266/MS93/111 ..... p 3423 N92-30206 * #

UWA/DME/TR-92/68 ..... p 3404 N92-29511 #

WHC-SA-1258 ..... p 3550 N92-29938 #

WHOI-91-10 ..... p 3543 N92-29346 #
WHOI-91-33 ..... p 3506 N92-29806 #
WHOI-91-39 ..... p 3506 N92-29805 #

WL-TR-91-2094 ..... p 3443 N92-30176 #
WL-TR-91-3016 ..... p 3415 N92-29594 #
WL-TR-91-3021 ..... p 3415 N92-29593 #
WL-TR-91-4026 ..... p 3476 N92-29581 #
WL-TR-91-4119 ..... p 3414 N92-29453 #
WL-TR-92-8018 ..... p 3562 N92-29720 #

WRRI-262 ..... p 3489 N92-29701 #

WSRC-IM-90-83-6 ..... p 3514 N92-29907 #

WSU/DC/92-TR-80 ..... p 3544 N92-29350 #
WSU/DC/92/TR-79 ..... p 3414 N92-29460 #

YALEU/DCS/RR-888 ..... p 3531 N92-29548 #

Typical Accession Number Index Listing

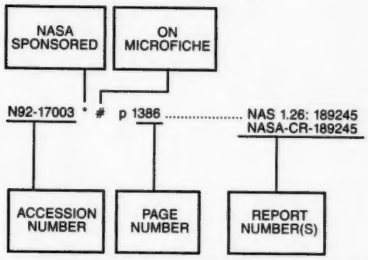

Listings in this index are arranged alphanumerically by accession number. The page number helps to locate the citation in the abstract section. An asterisk (*) indicates that the item is a NASA report. A pound sign (#) indicates that the item is available on microfiche.

N92-29228* # p 3456 ..... L-17126-PT-1
N92-29228* # p 3456 ..... NAS 1.55:3158-PT-1
NASA-CP-3158-PT-1
N92-29229* # p 3456 ..... NO REPORT NUMBER
N92-29230* # p 3456 ..... NO REPORT NUMBER
N92-29231* # p 3456 ..... NO REPORT NUMBER
N92-29232* # p 3457 ..... NO REPORT NUMBER
N92-29233* # p 3457 ..... NO REPORT NUMBER
N92-29234* # p 3457 ..... NO REPORT NUMBER
N92-29235* # p 3457 ..... NO REPORT NUMBER
N92-29236* # p 3457 ..... NO REPORT NUMBER
N92-29237* # p 3458 ..... NO REPORT NUMBER
N92-29238* # p 3458 ..... NO REPORT NUMBER
N92-29239* # p 3458 ..... NO REPORT NUMBER
N92-29240* # p 3458 ..... NO REPORT NUMBER
N92-29241* # p 3458 ..... NO REPORT NUMBER
N92-29242* # p 3459 ..... NO REPORT NUMBER
N92-29243* # p 3459 ..... NO REPORT NUMBER
N92-29244* # p 3459 ..... NO REPORT NUMBER
N92-29245* # p 3459 ..... NO REPORT NUMBER
N92-29246* # p 3459 ..... NO REPORT NUMBER
N92-29247* # p 3460 ..... NO REPORT NUMBER
N92-29248* # p 3460 ..... NO REPORT NUMBER
N92-29249* # p 3460 ..... NO REPORT NUMBER
N92-29250* # p 3460 ..... NO REPORT NUMBER
N92-29251* # p 3460 ..... NO REPORT NUMBER
N92-29252* # p 3460 ..... NO REPORT NUMBER
N92-29253* # p 3461 ..... NO REPORT NUMBER
N92-29254* # p 3461 ..... NO REPORT NUMBER
N92-29255* # p 3461 ..... NO REPORT NUMBER
N92-29256* # p 3461 ..... NO REPORT NUMBER
N92-29257* # p 3461 ..... NO REPORT NUMBER
N92-29258* # p 3462 ..... NO REPORT NUMBER
N92-29259* # p 3462 ..... NO REPORT NUMBER
N92-29260* # p 3462 ..... NO REPORT NUMBER
N92-29261* # p 3462 ..... NO REPORT NUMBER
N92-29262* # p 3462 ..... NO REPORT NUMBER
N92-29263* # p 3462 ..... NO REPORT NUMBER
N92-29264* # p 3462 ..... NO REPORT NUMBER
N92-29265* # p 3463 ..... NO REPORT NUMBER
N92-29266* # p 3463 ..... NO REPORT NUMBER
N92-29267* # p 3463 ..... NO REPORT NUMBER
N92-29268* # p 3463 ..... NO REPORT NUMBER
N92-29269* # p 3463 ..... NO REPORT NUMBER
N92-29270* # p 3463 ..... NO REPORT NUMBER
N92-29271* # p 3464 ..... NO REPORT NUMBER
N92-29272* # p 3464 ..... NO REPORT NUMBER
N92-29273* # p 3464 ..... NO REPORT NUMBER
N92-29274* # p 3464 ..... NO REPORT NUMBER
N92-29275* # p 3464 ..... NO REPORT NUMBER
N92-29276* # p 3464 ..... NO REPORT NUMBER
N92-29277* # p 3465 ..... NO REPORT NUMBER
N92-29278* # p 3465 ..... NO REPORT NUMBER
N92-29279* # p 3465 ..... NO REPORT NUMBER
N92-29280* # p 3465 ..... NO REPORT NUMBER
N92-29281* # p 3465 ..... NO REPORT NUMBER
N92-29282* # p 3465 ..... NO REPORT NUMBER
N92-29283* # p 3407 ..... NO REPORT NUMBER
N92-29284* # p 3466 ..... NO REPORT NUMBER
N92-29285* # p 3466 ..... NO REPORT NUMBER
N92-29286* # p 3466 ..... NO REPORT NUMBER
N92-29287* # p 3466 ..... NO REPORT NUMBER
N92-29288* # p 3467 ..... NO REPORT NUMBER
N92-29289* # p 3467 ..... NO REPORT NUMBER
N92-29290* # p 3467 ..... NO REPORT NUMBER
N92-29291* # p 3467 ..... NO REPORT NUMBER
N92-29292* # p 3467 ..... NO REPORT NUMBER
N92-29293* # p 3467 ..... NO REPORT NUMBER
N92-29294* # p 3468 ..... NO REPORT NUMBER
N92-29295* # p 3468 ..... NO REPORT NUMBER
N92-29296* # p 3468 ..... NO REPORT NUMBER
N92-29297* # p 3468 ..... NO REPORT NUMBER
N92-29298* # p 3468 ..... NO REPORT NUMBER
N92-29299* # p 3407 ..... NO REPORT NUMBER
N92-29300* # p 3469 ..... NO REPORT NUMBER
N92-29301* # p 3469 ..... NO REPORT NUMBER
N92-29302* # p 3469 ..... NO REPORT NUMBER
N92-29303* # p 3469 ..... NO REPORT NUMBER
N92-29304* # p 3469 ..... NO REPORT NUMBER
N92-29305* # p 3469 ..... NO REPORT NUMBER
N92-29306* # p 3469 ..... NO REPORT NUMBER
N92-29307* # p 3470 ..... NO REPORT NUMBER
N92-29308* # p 3470 ..... NO REPORT NUMBER
N92-29309* # p 3470 ..... NO REPORT NUMBER
N92-29310* # p 3470 ..... NO REPORT NUMBER
N92-29311* # p 3470 ..... NO REPORT NUMBER
N92-29312* # p 3470 ..... NO REPORT NUMBER
N92-29313* # p 3471 ..... NO REPORT NUMBER
N92-29314* # p 3471 ..... NO REPORT NUMBER
N92-29315* # p 3471 ..... NO REPORT NUMBER
N92-29316* # p 3471 ..... NO REPORT NUMBER
N92-29317* # p 3471 ..... NO REPORT NUMBER
N92-29318* # p 3471 ..... NO REPORT NUMBER
N92-29319* # p 3472 ..... NO REPORT NUMBER
N92-29320* # p 3472 ..... NO REPORT NUMBER
N92-29321* # p 3472 ..... NO REPORT NUMBER
N92-29322* # p 3472 ..... NO REPORT NUMBER
N92-29323* # p 3472 ..... NO REPORT NUMBER
N92-29324* # p 3472 ..... NO REPORT NUMBER
N92-29325* # p 3473 ..... NO REPORT NUMBER
N92-29326* # p 3473 ..... NO REPORT NUMBER
N92-29327* # p 3473 ..... NO REPORT NUMBER
N92-29328* # p 3473 ..... NO REPORT NUMBER
N92-29329* # p 3399 ..... NAS 1.26:190264
NASA-CR-190264
N92-29330 # p 3427 ..... AD-A248146
N92-29331* # p 3550 ..... NAS 1.26:190496
NASA-CR-190496
N92-29332 # p 3475 ..... AD-A250240
N92-29333 # p 3429 ..... AD-A250245
N92-29334 # p 3510 ..... AD-A250246
AFOSR-92-0363TR
N92-29335 # p 3428 ..... AD-A250252
N92-29336 # p 3553 ..... DE92-013587
DOE/ER-54109/2
N92-29337 # p 3550 ..... CONF-920124-22
DE92-011287
UCRL-JC-109754
N92-29338 # p 3481 ..... CONF-911213-25
DE92-011467
UCRL-JC-107866
N92-29339 # p 3438 ..... CONF-9204102-7
DE92-012678
UCRL-JC-109672
N92-29340 # p 3475 ..... CONF-920462-1
DE92-012698
UCRL-JC-110159
N92-29341* # p 3509 ..... NAS 1.26:4455
NASA-CR-4455
N92-29342* # p 3481 ..... NAS 1.26:190588
NASA-CR-190588
N92-29343* # p 3412 ..... AIAA PAPER 92-3338
E-7135
NAS 1.15:105731
NASA-TM-105731
N92-29344 # p 3429 ..... AD-A245970
N92-29345 # p 3504 ..... AD-A248272
N92-29346 # p 3543 ..... AD-A248281
WHOI-91-10
N92-29347 # p 3510 ..... AD-A248283
USAARL-92-5
N92-29348 # p 3512 ..... AD-A248284
USAARL-92-9
N92-29349 # p 3423 ..... AD-A248285
TR-57
N92-29350 # p 3544 ..... AD-A248299
WSU/DC/92-TR-80
N92-29351* # p 3478 ..... AVSCOM-TR-91-C-041
E-7048
NAS 1.15:105676
NASA-TM-105676
N92-29352* # p 3406 ..... NAS 1.26:189595
NASA-CR-189595
N92-29353 # p 3524 ..... CONF-920760-2
DE92-011299
UCRL-JC-108973
N92-29354 # p 3542 ..... DE92-011633
DOE/ER-45125/9
N92-29355 # p 3416 ..... CONF-9204103-2
DE92-011756
DOE/METC-C/92/7013
N92-29356 # p 3544 ..... ANL-HEP-CP-92-17
CONF-9111141-7
DE92-011833
N92-29357 # p 3478 ..... ANL/CP-74638
CONF-920439-6
DE92-011834
N92-29358 # p 3475 ..... CONF-920573-7
DE92-011946
UCRL-JC-110158
N92-29359* # p 3564 ..... JPL-9950-1381
NAS 1.26:190483
NASA-CR-190483
TRW-SN-57661
N92-29360* # p 3570 ..... JPL-9950-1369
NAS 1.26:190482
NASA-CR-190482
N92-29361* # p 3399 ..... NAS 1.26:190480
NASA-CR-190480
N92-29362* # p 3514 ..... ADANET-FD-R/T-160-1
NAS 1.26:190500
NASA-CR-190500
N92-29363* # p 3514 ..... NAS 1.26:190499
NASA-CR-190499
N92-29364* # p 3429 ..... JPL-TDA-PR-42-109
NAS 1.26:190460
NASA-CR-190460
N92-29365* # p 3409 ..... NO REPORT NUMBER
N92-29366* # p 3429 ..... NO REPORT NUMBER
N92-29367* # p 3430 ..... NO REPORT NUMBER
N92-29368* # p 3409 ..... NO REPORT NUMBER
N92-29369* # p 3409 ..... NO REPORT NUMBER
N92-29370* # p 3409 ..... NO REPORT NUMBER
N92-29371* # p 3430 ..... NO REPORT NUMBER
N92-29372* # p 3431 ..... NO REPORT NUMBER
N92-29373* # p 3431 ..... NO REPORT NUMBER
N92-29374* # p 3431 ..... NO REPORT NUMBER
N92-29375* # p 3431 ..... NO REPORT NUMBER
N92-29376* # p 3431 ..... NO REPORT NUMBER
N92-29377* # p 3431 ..... NO REPORT NUMBER
N92-29378* # p 3432 ..... NO REPORT NUMBER
N92-29379* # p 3432 ..... NO REPORT NUMBER
N92-29380* # p 3432 ..... NO REPORT NUMBER
N92-29381* # p 3432 ..... NO REPORT NUMBER
N92-29382* # p 3432 ..... NO REPORT NUMBER
N92-29383* # p 3409 ..... NO REPORT NUMBER
N92-29384* # p 3433 ..... NO REPORT NUMBER
N92-29385* # p 3433 ..... NO REPORT NUMBER
N92-29386* # p 3433 ..... NO REPORT NUMBER
N92-29387* # p 3433 ..... NO REPORT NUMBER
N92-29388* # p 3433 ..... NO REPORT NUMBER
N92-29389* # p 3433 ..... NO REPORT NUMBER
N92-29390* # p 3525 ..... NAS 1.26:190504
NASA-CR-190504
N92-29391* # p 3514 ..... NAS 1.26:190502
NASA-CR-190502
N92-29392* # p 3478 ..... ICMA-92-175
NAS 1.26:190497
NASA-CR-190497
N92-29393* # p 3481 ..... AVSCOM-TR-92-B-008
NAS 1.15:107623

NASA-TM-107623
N92-29394*# p 3443 ..... A-91119
NAS 1.15:103858
NASA-TM-103858
N92-29395 # p 3433 ..... AD-A248112
NOSC/TR-1456
N92-29396 # p 3475 ..... AD-A248123
DRIC-BR-309213
RSRE-MEMO-4564
N92-29397*# p 3506 ..... A-91108
NAS 1.15:103853
NASA-TM-103853
N92-29398 # p 3510 ..... AD-A248128
N92-29399 # p 3515 ..... AD-A248175
N92-29400*# p 3515 ..... CU-TR-92-1293
NAS 1.26:190545
NASA-CR-190545
N92-29401*# p 3568 ..... NAS 1.26:190543
NASA-CR-190543
N92-29402*# p 3399 ..... AIAA PAPER 92-3069
E-7175
NAS 1.26:189207
NASA-CR-189207
N92-29403*# p 3513 ..... NAS 1.15:104751
NASA-TM-104751
S-680
N92-29404 # p 3438 ..... AD-A248176
N92-29405 # p 3439 ..... AD-A248182
AFIT/GE/ENG/92M-07
N92-29406 # p 3434 ..... AD-A248183
AFIT/GOR/ENS/92M-13
N92-29407 # p 3482 ..... AD-A248187
AFOSR-92-0200TR
N92-29408 # p 3420 ..... AD-A248190
PW/GESP-FR2198-05
N92-29409 # p 3515 ..... AD-A248193
N92-29410 # p 3507 ..... AD-A248199
N92-29411 # p 3420 ..... CONF-920458-8
DE92-013504
PNL-SA-20350
N92-29412 # p 3554 ..... CONF-920362-27
DE92-013507
GA-A-20872
N92-29413*# p 3512 ..... A-92049
NAS 1.26:177593
NASA-CR-177593
N92-29414 # p 3439 ..... CONF-920669-5
DE92-013508
GEPP-CP-1297
N92-29415 # p 3544 ..... DE92-625013
ITP-91-6
N92-29416 # p 3492 ..... OTA-F-515
N92-29417*# p 3404 ..... A-92081
NAS 1.15:103929
NASA-TM-103929
N92-29418 # p 3515 ..... ETN-92-91503
ISSN-0303-4003
KFK-4941
N92-29419 # p 3538 ..... ETN-92-91504
OEFZS-4612
N92-29420 # p 3510 ..... AD-A248338
AFOSR-92-0206TR
REPT-001
N92-29421 # p 3569 ..... AD-A248340
N92-29422*# p 3409 ..... NAS 1.26:190517
NASA-CR-190517
N92-29423 # p 3417 ..... AD-A248342
RL-TR-91-378
N92-29424 # p 3502 ..... AD-A248347
N92-29425*# p 3405 ..... AIAA PAPER 92-3092
H-1806
NAS 1.15:104247
NASA-TM-104247
N92-29426 # p 3420 ..... AD-A250570
AFOSR-92-0281TR
N92-29427*# p 3405 ..... H-1775
NAS 1.26:186021
NASA-CR-186021
N92-29428 # p 3428 ..... AD-A250624
AFOSR-92-0424TR
N92-29429 # p 3556 ..... AD-A250632
TR-32
N92-29430*# p 3492 ..... NAS 1.15:107548
NASA-TM-107548
N92-29431 # p 3417 ..... CONF-920707-1
DE92-005328
SAND-91-8714
N92-29432*# p 3568 ..... NAS 1.26:190579
NASA-CR-190579
N92-29433 # p 3417 ..... CONF-920707-11
DE92-006699
SAND-91-8743
N92-29434 # p 3475 ..... CONF-9201103-1
DE92-012254
SAND-92-8464C
N92-29435 # p 3423 ..... DE92-012264
DOE/PC-90038/T1
N92-29436 # p 3420 ..... CONF-920430-85
DE92-012338
PNL-SA-20408
N92-29437 # p 3556 ..... BNL-47382
CONF-911202-78
DE92-012518
N92-29438 # p 3554 ..... DE92-013463
GTFR-100
N92-29439 # p 3504 ..... DE92-013500
DOE/ER-60818/3
N92-29440*# p 3403 ..... CSDL-T-1126
NAS 1.26:189868
NASA-CR-189868
N92-29441 # p 3543 ..... AD-A247688
N92-29442*# p 3488 ..... NAS 1.15:107922
NASA-TM-107922
N92-29443 # p 3439 ..... AD-A248154
AFIT/GNE/ENP/92M-9
N92-29444 # p 3412 ..... AD-A248157
AFIT/GNE/ENP/92M-03
N92-29445*# p 3400 ..... NAS 1.15:107635
NASA-TM-107635
N92-29446 # p 3531 ..... AD-A248160
N92-29447 # p 3434 ..... AD-A248452
N92-29448*# p 3413 ..... E-7167
NAS 1.26:189200
NASA-CR-189200
N92-29449 # p 3406 ..... AD-A250021
BRL-TR-3338
N92-29450 # p 3554 ..... AD-A250581
AFOSR-92-0277TR
N92-29451*# p 3568 ..... NAS 1.26:190586
NASA-CR-190586
N92-29452 # p 3439 ..... AD-A250584
N92-29453 # p 3414 ..... AD-A250612
UDR-TR-91-64
WL-TR-91-4119
N92-29454 # p 3491 ..... DE91-002110
DOE/CH-10093/90
N92-29455 # p 3439 ..... CONF-920716-1
DE92-003148
SAND-92-0357C
N92-29456 # p 3527 ..... CONF-920740-1
DE92-004360
SAND-91-2808C
N92-29457 # p 3549 ..... DE92-011173
EGG-10617-1199
N92-29458 # p 3443 ..... AD-A246110
N92-29459 # p 3417 ..... CONF-920707-2
DE92-005330
SAND-91-8706
N92-29460 # p 3414 ..... AD-A247777
WSU/DC/92/TR-79
N92-29461 # p 3413 ..... CONF-920747-1-EXTD-ABST
DE92-006608
N92-29462 # p 3414 ..... AD-A250080
N92-29463*# p 3434 ..... JPL-PUBL-90-45
NAS 1.26:190453
NASA-CR-190453
N92-29464 # p 3570 ..... AD-A247865
AFOSR-92-0217TR
N92-29465 # p 3424 ..... AD-A248072
N92-29466 # p 3424 ..... AD-A248074
N92-29467 # p 3488 ..... B-248072
GAO/IMTEC-92-44
N92-29468 # p 3564 ..... ETN-92-91494
N92-29469 # p 3473 ..... ETN-92-91505
OEFZS-4615
N92-29470 # p 3428 ..... ETN-92-91506
OEFZS-4616
N92-29471 # p 3571 ..... NO REPORT NUMBER
N92-29472 # p 3476 ..... CONF-920124-24
DE92-012695
UCRL-JC-108127
N92-29473 # p 3556 ..... CONF-910406-40
DE92-013006
UCRL-JC-106149
N92-29474 # p 3476 ..... CONF-920362-21
DE92-011393
GA-A-20849
N92-29475 # p 3550 ..... BNL-46683
CONF-920315-30
DE92-013031
N92-29476 # p 3491 ..... AD-A250027
SLCET-TR-88-0849-F
N92-29477 # p 3549 ..... BNL-47378
CONF-920315-28
DE92-013035
N92-29478 # p 3480 ..... DE92-013517
UCRL-CR-110256
N92-29479 # p 3424 ..... CONF-920402-2
DE92-013385
LA-UR-92-1426
N92-29480 # p 3410 ..... ITN-92-85126
N92-29481 # p 3531 ..... CONF-920760-4
DE92-011966
UCRL-JC-109226
N92-29482 # p 3424 ..... DE92-012548
IS-T-1603
N92-29483 # p 3420 ..... CONF-911003-25
DE92-011646
N92-29484 # p 3551 ..... CONF-9204120-1
DE92-011762
UCRL-JC-110134
N92-29485 # p 3556 ..... DE92-011811
DOE/ER-45394/3
N92-29486 # p 3531 ..... AD-A248075
N92-29487 # p 3515 ..... AD-A248077
ARCCB-TR-92006
N92-29488 # p 3544 ..... ETN-92-91718
RAL-91-070
N92-29489 # p 3545 ..... NO REPORT NUMBER
N92-29490 # p 3545 ..... NO REPORT NUMBER
N92-29491 # p 3538 ..... ETN-92-91741
N92-29492 # p 3538 ..... NO REPORT NUMBER
N92-29493 # p 3489 ..... BCRS-90-31
ETN-92-91605
ISBN-90-54-11007-4
N92-29494 # p 3489 ..... BCRS-90-38
ETN-92-91606
ISBN-90-54-11005-8
N92-29495 # p 3489 ..... BCRS-91-01
ETN-92-91607
ISBN-90-54-11004-X
ISSN-0924-3062
REPT-43
N92-29496 # p 3424 ..... AD-A248500
TR-34
N92-29497 # p 3493 ..... BCRS-91-17
ETN-92-91609
ISBN-90-54-11002-3
N92-29498 # p 3439 ..... AD-A248503
SLCET-TR-92-1
N92-29499 # p 3493 ..... BCRS-91-25
ETN-92-91610
ISBN-90-54-11001-5
N92-29500 # p 3538 ..... AD-A248507
TR-72
N92-29501 # p 3538 ..... AD-A248512
TR-451
N92-29502 # p 3549 ..... CONF-911106-94
DE92-013356
EGG-10617-2135
N92-29503 # p 3511 ..... AD-A248518
AL-TR-1992-0003
N92-29504 # p 3527 ..... CONF-9205152-1
DE92-013422
N92-29505 # p 3406 ..... AD-A248519
AL-TP-1992-0009
N92-29506 # p 3404 ..... AD-A248538
USAARL-92-18
N92-29507 # p 3545 ..... CONF-9204137-1
DE92-013464
SSCL-PREPRINT-86
N92-29508 # p 3424 ..... AD-A248540
N92-29509 # p 3476 ..... CONF-9107115-75
DE92-013515
UCRL-JC-110302
N92-29510 # p 3554 ..... AD-A248541
BRL-TR-3324
N92-29511 # p 3404 ..... AD-A248543
UWA/DME/TR-92/68
N92-29512 # p 3427 ... CONF-9203147-1-VUGRAPHS
DE92-013528
LA-UR-92-1343
N92-29513 # p 3500 ..... CONF-9203149-1
DE92-013530
LA-UR-92-1330
N92-29514 # p 3417 ..... AD-A250191
TR-25
N92-29515 # p 3545 ..... CONF-9203152-1
DE92-013546
LA-UR-92-1230
N92-29516 # p 3476 ..... CONF-920496-2
DE92-013564
SAND-92-8509C
N92-29517 # p 3560 ..... CONF-9111165-13
DE92-013665
DOE/ER-40561/038
N92-29518 # p 3440 ..... CONF-9205102-2
DE92-013669
SAND-91-2346C
N92-29519 # p 3492 ..... GRI-92/0074
PB92-172360
N92-29520 # p 3493 ..... ECAO-R-0082-VOL-1
EPA/600/8-91/049AA-VOL-1
PB92-176361
N92-29521 # p 3493 ..... ECAO-R-0082-VOL-2
EPA/600/8-91/049AB-VOL-2
PB92-176379
N92-29522 # p 3493 ..... ECAO-R-0082-VOL-3

EPA/600/8-91/049CA-VOL-3
PB92-176387
N92-29523 # p 3440 ... AD-A248080
N92-29524 # p 3444 ... AD-A248083
N92-29525 # p 3410 ... AD-A248084
AFIT/GOR/ENS/92M-03
N92-29526 # p 3440 ... AD-A248085
AFIT/GE/ENG/92M-05
N92-29527 # p 3515 ... AD-A248092
AFIT/GCS/ENG/92M-02
N92-29528 # p 3554 ... AD-A248093
AFIT/GEP/ENP/92M-01
N92-29529 # p 3440 ... AD-A248094
AFIT/GST/ENS/92M-7
N92-29530 # p 3551 ... CONF-920678-2
DE92-011437
DOE/ER-61072/4
N92-29531 # p 3554 ... DE92-014093
UCRL-ID-110314
N92-29532 # p 3550 ... DE92-014309
DOE/ER-40224/185
N92-29533 # p 3560 ... DE92-624511
INP-MSU-91-2-206
NIIYAF-MGU-91-2-206
N92-29534 # p 3478 ... ANL/CP-73256
CONF-9206161-1
DE92-013044
N92-29535 # p 3482 ... ANL/CP-75372
CONF-9206166-1
DE92-013053
N92-29536 # p 3500 ... CONF-920792-1
DE92-013240
LA-UR-92-1442
N92-29537 # p 3516 ... DE92-013752
UCRL-ID-110241
N92-29538 # p 3512 ... AD-A247182
CGR/DC-19/91
USCG-D-03-92
N92-29539 # p 3400 ... AD-A247191
NAVSWC-TR-90-683
N92-29540 # p 3516 ... AD-A248153
CMU/SEI-91-CDRL-106
N92-29541 # p 3527 ... AD-A248258
N92-29542 # p 3434 ... AD-A248260
SU-E450-1
N92-29543 # p 3543 ... AD-A250227
N92-29544 # p 3516 ... AD-A250241
N92-29545 # p 3428 ... AD-A250251
N92-29546 # p 3551 ... AD-A250261
ARO-25464.11-PH
N92-29547 # p 3421 ... AD-A250282
AFOSR-92-0387TR
N92-29548 # p 3531 ... AD-A250388
YALEU/DCS/RR-888
N92-29549 # p 3424 ... DE92-011940
DOE/ER-12119/1
N92-29550 # p 3528 ... CONF-920724-1
DE92-000424
N92-29551 # p 3417 ... CONF-920761-5
DE92-010542
N92-29552 # p 3561 ... CONF-9205138-2
DE92-012632
SAND-91-2790C
N92-29553* # p 3561 ... NAS 1.26:190282
NASA-CR-190282
N92-29554 # p 3505 ... AD-A246293
APL-UW-TR-9005
N92-29555 # p 3525 ... AD-A247836
MTI-R89-006-28-VOL-1
N92-29556 # p 3414 ... AD-A248067
UCB/R/91/N1076
N92-29557 # p 3418 ... AD-A248335
N92-29558 # p 3556 ... AD-A248098
TR-8
N92-29559 # p 3476 ... AD-A248103
N92-29560 # p 3511 ... AD-A248104
N92-29561 # p 3528 ... AD-A248110
AFIT/DS/ENG/92-02
N92-29562 # p 3505 ... AD-A248345
NOARL-CR-026-91
N92-29563 # p 3434 ... AD-A248597
CSS-TM-596-92
N92-29564 # p 3440 ... AD-A248135
N92-29565 # p 3502 ... AD-A248696
ASL-TR-0308
N92-29566 # p 3425 ... AD-A248286
TR-58
N92-29567 # p 3425 ... AD-A248287
TR-60
N92-29568* # p 3434 ... NAS 1.26:190446
NASA-CR-190446
N92-29569 # p 3425 ... AD-A248306
TR-61
N92-29570 # p 3516 ... ETN-92-91468
IMAG-RR-844-I
N92-29571 # p 3474 ... AD-D015256
US-PATENT-APPL-SN-839627
N92-29572 # p 3435 ... AD-D015257
US-PATENT-APPL-SN-772999
N92-29573 # p 3532 ... ETN-92-91469
RR-847-I-IMAG-120-LIFIA
N92-29574 # p 3532 ... ETN-92-91470
RR-858-I-IMAG-121-LIFIA
N92-29575 # p 3440 ... AD-A248545
N92-29576 # p 3435 ... AD-A248552
N92-29577 # p 3510 ... AD-A248556
AFOSR-92-0261TR
N92-29578 # p 3551 ... DE92-011588
UCRL-ID-109373
N92-29579 # p 3435 ... AD-A248557
AFOSR-92-0237TR
N92-29580 # p 3418 ... AD-A248558
AFOSR-92-0238TR
N92-29581 # p 3476 ... AD-A249233
WL-TR-91-4026
N92-29582 # p 3545 ... BNL-47420
CONF-920480-1
DE92-012208
N92-29583 # p 3557 ... AD-A245351
N92-29584 # p 3557 ... DE92-001222
NREL/TP-411-4752
N92-29585 # p 3539 ... AD-A248105
AFIT/GOR/ENS/92M-23
N92-29586 # p 3516 ... AD-A248108
AFIT/GOR/ENS/92M-14
N92-29587 # p 3421 ... AD-A248339
MML-TR-91-10C
MML-TR-92-13C
N92-29588 # p 3543 ... AD-A248341
N92-29589 # p 3532 ... AD-A250571
AFOSR-92-0270TR
N92-29590 # p 3528 ... AD-A250578
AFOSR-92-0309TR
N92-29591 # p 3511 ... AD-A250579
AFOSR-92-0267TR
N92-29592 # p 3511 ... AD-A250580
AFOSR-92-0303TR
N92-29593 # p 3415 ... AD-A250591
WL-TR-91-3021
N92-29594 # p 3415 ... AD-A250592
WL-TR-91-3016
N92-29595 # p 3418 ... AD-A250607
TR-3
N92-29596 # p 3565 ... AD-A250623
AFOSR-92-0422TR
N92-29597 # p 3493 ... DE92-013487
DOE/ER-61010/T1
N92-29598 # p 3425 ... DE92-001163
NREL/TP-214-4488
N92-29599 # p 3435 ... AD-A249121
N92-29600 # p 3569 ... DE92-011511
PNL-8053
N92-29601 # p 3482 ... DE92-011572
DOE/ER-45290/5
N92-29602 # p 3478 ... ETN-92-91443
NLR-TP-90267-U
N92-29603 # p 3482 ... ETN-92-91449
NLR-TP-90336-U
N92-29604 # p 3532 ... ETN-92-91453
NLR-TP-91061-U
N92-29605 # p 3403 ... ETN-92-91454
NLR-TP-91062-U-PT-1
N92-29606 # p 3539 ... ETN-92-91461
MEMO-COSOR-91-28
N92-29607 # p 3532 ... ETN-92-91462
MEMO-COSOR-91-29
N92-29608 # p 3516 ... ETN-92-91463
MEMO-COSOR-91-30
N92-29609 # p 3539 ... ETN-92-91464
MEMO-COSOR-91-31
N92-29610 # p 3525 ... ETN-92-91471
IMAG-RR-845-I
N92-29611 # p 3513 ... ETN-92-91474
IMAG-RR-860-I
N92-29612 # p 3441 ... ETN-92-91475
IMAG-RR-862-I
N92-29613 # p 3441 ... ETN-92-91476
IMAG-RR-863-I
N92-29614 # p 3525 ... ETN-92-91477
IMAG-RR-854-M
N92-29615 # p 3403 ... ETN-92-91513
NLR-MP-88040-U
N92-29616 # p 3404 ... ETN-92-91514
GARTEUR-TP-051
NLR-MP-88044-U
N92-29617 # p 3403 ... AD-A248252
N92-29618 # p 3505 ... AD-A248255
TGAL-92-13
N92-29619 # p 3418 ... AD-A248446
TR-16
N92-29620 # p 3511 ... AD-A248956
AL-CR-1992-001
N92-29621 # p 3516 ... ETN-92-91467
IMAG-RR-843-I
N92-29622 # p 3516 ... AD-A249381
ARO-29087.1-MA-SBI
N92-29623 # p 3421 ... CONF-9205142-1
DE92-011761
SAND-92-0594C
N92-29624 # p 3525 ... ANL/CP-75747
CONF-920538-14
DE92-011840
N92-29625* # p 3400 ... A-92072
NAS 1.55:10092
NASA-CP-10092
N92-29626 # p 3539 ... ETN-92-91422
ISSN-0922-5641
REPT-91-53
N92-29627 # p 3517 ... ETN-92-91423
ISSN-0922-5641
REPT-91-57
N92-29628 # p 3543 ... ETN-92-91424
ISSN-0922-5641
REPT-91-60
N92-29629 # p 3408 ... ETN-92-91496
MBB-FE-202-S-PUB-0463-A
N92-29630* # p 3517 ... NAS 1.26:190528
NASA-CR-190528
PCS-TR91-156
N92-29631* # p 3569 ... NAS 1.26:190567
NASA-CR-190567
N92-29632 # p 3570 ... AD-A248344
AFOSR-92-0192TR
N92-29633 # p 3421 ... CONF-920604-2
DE92-011138
LA-UR-92-887
N92-29634 # p 3545 ... CONF-920124-20
DE92-011353
LA-UR-92-748
N92-29635 # p 3557 ... AD-A250631
N92-29636 # p 3492 ... DE92-506509
TKK-F-A669
N92-29637 # p 3421 ... DE92-506510
TKK-V-C110
N92-29638 # p 3493 ... DE92-514557
IEE-SR-225
N92-29639 # p 3421 ... CONF-911195-3
DE92-012677
UCRL-JC-108728
N92-29640 # p 3554 ... DE92-012687
DOE/PC-90274/T12
MHD-ITC-91-021
N92-29641 # p 3517 ... DE92-013394
SAND-91-8230
N92-29642 # p 3546 ... DE92-013473
DOE/ER-13778/5
N92-29643 # p 3425 ... CONF-920703-1
DE92-000177
LA-UR-91-3097
N92-29644 # p 3528 ... CONF-920724-2
DE92-004464
N92-29645 # p 3415 ... CONF-911003-26
DE92-012333
PNL-SA-19820
N92-29646 # p 3492 ... CONF-9204130-1
DE92-012339
PNL-SA-20771
N92-29647 # p 3422 ... AD-A250564
R/D-6750-MS-01
N92-29648 # p 3400 ... ETN-92-91497
MBB-FE-202-S-PUB-0464-A
N92-29649 # p 3400 ... AIAA PAPER 91-5041
ETN-92-91499
MBB-FE-202-S-PUB-0469-A
N92-29650 # p 3404 ... ETN-92-91500
MBB-FE-2-S-PUB-472
N92-29651 # p 3422 ... ETN-92-91502
ISSN-0303-4003
KFK-4909
N92-29652* # p 3551 ... NAS 1.26:190494
NASA-CR-190494
N92-29653* # p 3502 ... NAS 1.15:104565
NASA-TM-104565
REPT-92B00088
N92-29654* # p 3406 ... NAS 1.26:190535
NASA-CR-190535
N92-29655* # p 3406 ... MCAT-92-011-PT-3
NAS 1.26:190541
NASA-CR-190541
N92-29656* # p 3528 ... NAS 1.26:189867
NASA-CR-189867
N92-29657* # p 3401 ... NAS 1.26:190570
NASA-CR-190570
TAMRF-5802-92-02
N92-29658* # p 3435 ... NAS 1.26:190561
NASA-CR-190561
N92-29659* # p 3405 ... H-1764
NAS 1.15:104240

NASA-TM-104240
N92-29660* # p 3415 ... E-7165
NAS 1.15:105754
NASA-TM-105754
N92-29661* # p 3405 ... AVSCOM-TR-92-C-019
E-7058
NAS 1.15:105680
NASA-TM-105680
N92-29662* # p 3492 ... E-7142
NAS 1.15:105737
NASA-TM-105737
N92-29663 # p 3561 ... PB92-147180
N92-29664* # p 3407 ... NAS 1.26:184343
NASA-CR-184343
N92-29665* # p 3517 ... NAS 1.26:190588
NASA-CR-190588
REPT-92-005
N92-29666 # p 3502 ... ISSN-0388-9653
N92-29667* # p 3413 ... E-7073
NAS 1.15:105691
NASA-TM-105691
N92-29668 p 3494 ... CSIRO-TP-25
ISBN-0-643-05249-6
N92-29669* # p 3427 ... AIAA PAPER 92-3061
E-7150
NAS 1.15:105746
NASA-TM-105746
N92-29670 p 3500 ... CSIRO-TP-23
ISBN-0-643-05248-8
N92-29671 # p 3563 ... OTA-TCT-512
PB92-167352
N92-29672 p 3482 ... AR-006-663
ARL-STRUC-R-446
N92-29673* # p 3528 ... NAS 1.26:190520
NASA-CR-190520
N92-29674 # p 3422 ... ETN-92-91478
LAAS-91393
N92-29675 # p 3529 ... ETN-92-91479
LAAS-91394
N92-29676* # p 3557 ... NAS 1.26:190311
NASA-CR-190311
N92-29677* # p 3429 ... M-691
NAS 1.60:3249
NASA-TP-3249
N92-29678 # p 3529 ... ETN-92-91480
LAAS-91395
N92-29679* # p 3551 ... JPL-PUBL-90-2
NAS 1.26:190454
NASA-CR-190454
N92-29680 # p 3409 ... ETN-92-91495
MBB-FE-202-S-PUB-0462-A
N92-29681* # p 3552 ... NAS 1.26:190491
NASA-CR-190491
N92-29682 # p 3565 ... ETN-92-91341
N92-29683 # p 3444 ... AERO-REPT-8907
ETN-92-91342
N92-29684 # p 3505 ... ETN-92-91343
REPT-18-1991
N92-29685 # p 3532 ... ETN-92-91350
ISSN-0924-2082
ITLI-LP-91-02
N92-29686* # p 3505 ... NAS 1.15:104566-VOL-1
NASA-TM-104566-VOL-1
REPT-92B00089
N92-29687 # p 3532 ... ETN-92-91351
ISSN-0924-2082
ITLI-LP-91-03
N92-29688 # p 3489 ... ETN-92-91352
N92-29689* # p 3571 ... NAS 1.15:107953
NASA-HHR-55
NASA-TM-107953
N92-29690 # p 3500 ... ETN-92-91501
ISSN-0303-4003
KFK-4890
N92-29691* # p 3401 ... NAS 1.26:190576
NASA-CR-190576
N92-29692* # p 3444 ... ICASE-92-23
NAS 1.26:189661
NASA-CR-189661
N92-29693 # p 3489 ... BCRS-91-12
ETN-92-91608
ISBN-90-54-11003-1
N92-29694* # p 3517 ... NAS 1.26:190555
NASA-CR-190555
RIACS-TR-92-04
N92-29695* # p 3517 ... CRHC-92-08
NAS 1.26:190571
NASA-CR-190571
UILU-ENG-92-2214
N92-29696 # p 3435 ... ISBN-0-16-035964-3
OTA-BP-TCT-76
PB92-157601
N92-29697* # p 3478 ... AVSCOM-TR-92-C-050
E-7127
NAS 1.15:105359
NASA-TM-105359
N92-29698 # p 3494 ... PB92-154954
N92-29699 # p 3562 ... PB92-163856
N92-29700 # p 3482 ... ETN-92-91406
LR-669
N92-29701 # p 3489 ... PB92-161363
USGS/G-1645
WRRI-262
N92-29702 # p 3415 ... ETN-92-91407
LR-670
N92-29703 # p 3402 ... ETN-92-91440
NLR-TP-90196-U
N92-29704 # p 3505 ... OCS/MMS-91/0061
PB92-164987
N92-29705 # p 3517 ... ETN-92-91465
ISSN-0924-3755
MEMO-INF-91-32
TIOS-91/010
N92-29706 # p 3422 ... DE92-012550
IS-T-1612
N92-29707 # p 3490 ... ETN-92-91517
NLR-TP-89103-U
N92-29708 # p 3483 ... ETN-92-91532
NLR-TP-90107-U
N92-29709 # p 3407 ... AD-A250293
ARI-RN-92-32
N92-29710 # p 3480 ... AD-A250582
AFOSR-92-0359TR
N92-29711 # p 3518 ... ETN-92-91417
ISSN-0922-5641
REPT-91-48
N92-29712 # p 3518 ... ETN-92-91418
ISSN-0922-5641
REPT-91-49
N92-29713 # p 3401 ... AIAA PAPER 91-5031
ETN-92-91498
MBB-FE-202-S-PUB-0468-A
N92-29714 # p 3518 ... ETN-92-91507
USIP-90-09
N92-29715 # p 3546 ... ETN-92-91508
USIP-91-02
N92-29716 # p 3525 ... ETN-92-91428
ISSN-0922-5641
REPT-91-64
N92-29717 # p 3490 ... BCRS-91-22
ETN-92-91611
ISSN-0924-3062
REPT-32
N92-29718 # p 3539 ... AD-A248662
N92-29719 # p 3418 ... AD-A248666
ARO-26238.19-CH
N92-29720 # p 3562 ... AD-A248714
PASC006.01.00
WL-TR-92-8018
N92-29721 # p 3444 ... AD-A248723
N92-29722 # p 3557 ... AD-A248725
N92-29723 # p 3415 ... AD-A248737
CDNSWC-SME-92-10
N92-29724 # p 3571 ... AD-A248764
AFOSR-92-0168TR-VOL-2
N92-29725 # p 3571 ... AD-A248765
AFOSR-92-0169TR-VOL-3
N92-29726 # p 3552 ... AD-A248865
JHU/APL-TG-1382
N92-29727 # p 3552 ... AD-A248881
ARO-28415.1-GS-CF
N92-29728 # p 3490 ... ETN-92-91466
ISSN-0166-7521
PUBL-445
N92-29729 # p 3441 ... ETN-92-91482
LAAS-91433
N92-29730 # p 3436 ... ETN-92-91483
LAAS-91466
N92-29731 # p 3474 ... ETN-92-91490
N92-29732 # p 3507 ... ETN-92-91745
N92-29733 # p 3507 ... NO REPORT NUMBER
N92-29734 # p 3507 ... NO REPORT NUMBER
N92-29735 # p 3507 ... NO REPORT NUMBER
N92-29736 # p 3507 ... NO REPORT NUMBER
N92-29737 # p 3508 ... NO REPORT NUMBER
N92-29738 # p 3508 ... NO REPORT NUMBER
N92-29739 # p 3508 ... NO REPORT NUMBER
N92-29740 # p 3508 ... NO REPORT NUMBER
N92-29741 # p 3401 ... ETN-92-91491
N92-29742 # p 3532 ... ETN-92-91460
MEMO-COSOR-91-26
N92-29743 # p 3502 ... NOAA-TM-NWSTM-PR-37
PB92-167345
N92-29744 # p 3418 ... NISTIR-4768
PB92-172006
N92-29745 # p 3518 ... NISTIR-4655
PB92-172493
N92-29746 # p 3494 ... PB92-161371
USGS/G-1637
N92-29747 # p 3518 ... ETN-92-91616
NIKHEF-H/91-18
N92-29748 # p 3543 ... ETN-92-91426
ISSN-0922-5641
REPT-91-62
N92-29749 # p 3518 ... ETN-92-91427
ISSN-0922-5641
REPT-91-63
N92-29750 # p 3546 ... ETN-92-91617
NIKHEF-H/91-19
N92-29751 # p 3546 ... ETN-92-91623
NIKHEF-H/91-25
N92-29752 # p 3444 ... ETN-92-91624
N92-29753 # p 3558 ... ETN-92-91625
N92-29754 # p 3508 ... ETN-92-91744
N92-29755 # p 3508 ... NO REPORT NUMBER
N92-29756 # p 3509 ... NO REPORT NUMBER
N92-29757 # p 3509 ... NO REPORT NUMBER
N92-29758 # p 3509 ... NO REPORT NUMBER
N92-29759 # p 3509 ... NO REPORT NUMBER
N92-29760 # p 3509 ... NO REPORT NUMBER
N92-29761 # p 3555 ... ETN-92-91627
N92-29762* # p 3479 ... NAS 1.71:MSC-21935-1
NASA-CASE-MSC-21935-1
US-PATENT-APPL-SN-882408
N92-29763 # p 3444 ... ETN-92-91420
ISSN-0922-5641
REPT-91-51
N92-29764 # p 3529 ... ETN-92-91421
ISSN-0922-5641
REPT-91-52
N92-29765* # p 3479 ... NAS 1.71:NPO-18668-1-CU
NASA-CASE-NPO-18668-1-CU
US-PATENT-APPL-SN-912955
N92-29766 # p 3558 ... ETN-92-91743
N92-29767 # p 3558 ... NO REPORT NUMBER
N92-29768 # p 3558 ... NO REPORT NUMBER
N92-29769 # p 3558 ... NO REPORT NUMBER
N92-29770 # p 3558 ... NO REPORT NUMBER
N92-29771 # p 3558 ... NO REPORT NUMBER
N92-29772 # p 3559 ... NO REPORT NUMBER
N92-29773 # p 3559 ... NO REPORT NUMBER
N92-29774 # p 3539 ... ETN-92-91628
N92-29775 # p 3445 ... ETN-92-91629
N92-29776 # p 3518 ... ETN-92-91630
N92-29777 # p 3546 ... ETN-92-91631
N92-29778 # p 3546 ... ETN-92-91632
N92-29779 # p 3519 ... ETN-92-91419
ISSN-0922-5641
REPT-91-50
N92-29780 # p 3519 ... ETN-92-91510
USIP-91-04
N92-29781 # p 3560 ... ETN-92-91511
USIP-91-05
N92-29782 # p 3519 ... ETN-92-91633
ISBN-90-9003966-X
N92-29783 # p 3559 ... ETN-92-91634
ISBN-90-9004374-8
N92-29784 # p 3445 ... CONF-920631-3
DE92-004179
N92-29785 # p 3479 ... AD-A247463
N92-29786 # p 3427 ... AD-A247932
NSWCCR/RDTR-92/0003
N92-29787 # p 3477 ... CONF-911296-8-REV-1
DE92-010712
UCRL-JC-109918-REV-1
N92-29788 # p 3550 ... CONF-920315-4
DE92-010752
SU-SLAC-PUB-5784
N92-29789 # p 3555 ... CONF-920362-14
DE92-011371
LA-UR-92-792
N92-29790 # p 3494 ... CONF-9201100-1
DE92-011389
UCRL-JC-109501
N92-29791 # p 3533 ... DE92-011444
UCRL-MA-108721
N92-29792 # p 3533 ... CONF-911213-24
DE92-011466
UCRL-JC-107865
N92-29793 # p 3533 ... DE92-622378
IC-91/374
N92-29794 # p 3562 ... CONF-920730-3
DE92-011372
LA-UR-92-805
N92-29795 # p 3415 ... CONF-920402-4
DE92-013434
LA-UR-92-1370
N92-29796 # p 3441 ... DE92-013999
KCP-613-4035
N92-29797 # p 3519 ... DE92-014071
ORNL/TM-12050
N92-29798 # p 3555 ... DE92-014092
UCRL-ID-110284
N92-29799 # p 3502 ... FSL-1
NOAA-TM-ERL-1
PB92-163575
N92-29800 # p 3503 ... NOAA-TM-ERL-WPL-219
PB92-164524

N92-29801 # p 3503 ..... PB92-167378
N92-29802 # p 3542 ..... NISTIR-4757
PB92-164680
N92-29803 # p 3422 ..... NISTIR-3986
PB92-172477
N92-29804 # p 3426 ..... GRI-91/0178
PB92-164425
N92-29805 # p 3506 ..... PB92-170281
WHOI-91-39
N92-29806 # p 3506 ..... PB92-170299
WHOI-91-33
N92-29807 # p 3422 ..... PB92-163294
SSC-352
N92-29808 # p 3564 ..... DOT-VNTSC-FRA-92-1
DOT/FRA/ORD-92/01
PB92-167006
N92-29809 # p 3564 ..... DOT-VNTSC-FRA-92-3
DOT/FRA/ORD-92/3
PB92-167014
N92-29810* # p 3410 ..... NAS 1.15:107919
NASA-TM-107919
PB92-147115
N92-29811* # p 3410 ..... NAS 1.15:107918
NASA-TM-107918
PB92-147123
N92-29812* # p 3410 ..... NAS 1.15:107920
NASA-TM-107920
PB92-147131
N92-29813 # p 3483 ..... NISTIR-4760
PB92-169119
N92-29814 # p 3544 ..... ETN-92-91370
ISVR-TR-204
N92-29815 # p 3519 ..... ETN-92-91583
ISSN-0924-3755
MEMO-INF-91-91
N92-29816 # p 3519 ..... ETN-92-91584
ISSN-0924-3755
MEMO-INF-91-93
N92-29817 # p 3539 ..... ETN-92-91786
MEMO-COSOR-91-32
N92-29818 # p 3520 ..... ETN-92-91787
MEMO-COSOR-91-33
N92-29819 # p 3520 ..... ETN-92-91788
MEMO-COSOR-91-34
N92-29820 # p 3520 ..... ETN-92-91789
MEMO-COSOR-91-35
N92-29821 # p 3540 ..... ETN-92-91792
ISSN-0926-4493
MEMO-COSOR-91-38
N92-29822 # p 3561 ..... ETN-92-91793
ISSN-0926-4493
MEMO-COSOR-91-39
N92-29823 # p 3561 ..... ETN-92-91794
ISSN-0926-4493
MEMO-COSOR-91-40
N92-29824 # p 3436 ..... ETN-92-91795
ISSN-0926-4493
MEMO-COSOR-91-41
N92-29825 # p 3525 ..... ETN-92-91796
ISSN-0926-4493
MEMO-COSOR-91-42
N92-29826 # p 3533 ..... ETN-92-91797
ISSN-0926-4493
MEMO-COSOR-92-01
N92-29827 # p 3540 ..... ETN-92-91798
ISSN-0926-4493
MEMO-COSOR-92-02
N92-29828 # p 3540 ..... ETN-92-91799
ISSN-0926-4493
MEMO-COSOR-92-03
N92-29829* # p 3480 ..... NAS 1.71:LAR-14559-1
NASA-CASE-LAR-14559-1
US-PATENT-APPL-SN-878631
N92-29830* # p 3445 ..... NAS 1.71:LAR-14815-1-CU
NASA-CASE-LAR-14815-1-CU
US-PATENT-APPL-SN-820432
N92-29831* # p 3426 ..... NAS 1.71:MFS-28682-1
NASA-CASE-MFS-28682-1
US-PATENT-APPL-SN-912401
N92-29832* # p 3552 ..... NAS 1.71:NPO-18410-1-CU
NASA-CASE-NPO-18410-1-CU
N92-29833 # p 3565 ..... ETN-92-91737
ISSN-0178-0719
MPE-227
N92-29834 # p 3565 ..... NO REPORT NUMBER
N92-29835 # p 3565 ..... NO REPORT NUMBER
N92-29836 # p 3565 ..... NO REPORT NUMBER
N92-29837 # p 3566 ..... NO REPORT NUMBER
N92-29838 # p 3566 ..... NO REPORT NUMBER
N92-29839 # p 3566 ..... NO REPORT NUMBER
N92-29840 # p 3566 ..... NO REPORT NUMBER
N92-29841 # p 3566 ..... NO REPORT NUMBER
N92-29842 # p 3566 ..... NO REPORT NUMBER
N92-29843 # p 3566 ..... NO REPORT NUMBER
N92-29844* # p 3567 ..... NO REPORT NUMBER
N92-29845 # p 3567 ..... NO REPORT NUMBER
N92-29846 # p 3567 ..... NO REPORT NUMBER
N92-29847 # p 3567 ..... NO REPORT NUMBER
N92-29848 # p 3567 ..... NO REPORT NUMBER
N92-29849 # p 3567 ..... NO REPORT NUMBER
N92-29850 # p 3567 ..... NO REPORT NUMBER
N92-29851* # p 3568 ..... NO REPORT NUMBER
N92-29852* # p 3568 ..... NO REPORT NUMBER
N92-29853 # p 3568 ..... NO REPORT NUMBER
N92-29854 # p 3441 ..... ESA-PSS-01-610-ISSUE-1
ETN-92-91384
ISSN-0379-4059
N92-29855 # p 3520 ..... ETN-92-91585
ISSN-0924-3755
MEMO-INF-91-94
N92-29856 # p 3540 ..... ETN-92-91590
ISSN-0169-2690
MEMO-983
N92-29857 # p 3445 ..... ETN-92-91593
ISSN-0169-2690
MEMO-987
N92-29858 # p 3533 ..... ETN-92-91594
ISSN-0169-2690
MEMO-988
N92-29859 # p 3552 ..... ETN-92-91626
N92-29860 # p 3540 ..... CWI-BS-R9116
ETN-92-91642
N92-29861 # p 3533 ..... CWI-BS-R9118
ETN-92-91643
ISSN-0924-0659
N92-29862 # p 3533 ..... CWI-BS-R9119
ETN-92-91644
ISSN-0924-0659
N92-29863 # p 3540 ..... CWI-BS-R9120
ETN-92-91645
ISSN-0924-0659
N92-29864 # p 3533 ..... CWI-BS-R9121
ETN-92-91646
ISSN-0924-0659
N92-29865 # p 3520 ..... CWI-BS-R9123
ETN-92-91647
ISSN-0924-0659
N92-29866 # p 3534 ..... CWI-AM-R9105
ETN-92-91648
N92-29867 # p 3526 ..... CWI-NM-R9114
ETN-92-91660
ISSN-0169-0388
N92-29868 # p 3520 ..... CWI-CS-R9128
ETN-92-91785
N92-29869 # p 3521 ..... ESA-PSS-03-105-ISSUE-2
ETN-92-91386
ISSN-0379-4059
N92-29870 # p 3404 ..... DLR-FB-91-34
ETN-92-91390
ISSN-0939-2963
N92-29871 # p 3512 ..... ETN-92-91527
NLR-TP-89311-U
N92-29872 # p 3534 ..... ETN-92-91598
ISSN-0169-2690
MEMO-993
N92-29873 # p 3480 ..... ETN-92-91695
MBB-UD-0603-91-PUB
N92-29874 # p 3399 ..... ETN-92-91696
MBB-UD-0606-91-PUB
N92-29875 # p 3416 ..... ETN-92-91698
MBB-Z-0380-91-PUB
N92-29876 # p 3416 ..... ETN-92-91699
MBB-Z-0395-91-PUB
N92-29877 # p 3436 ..... DLR-MITT-91-10
ETN-92-91731
ISSN-0939-298X
N92-29878 # p 3481 ..... ESA-PSS-01-50-ISSUE-1
ETN-92-91385
ISSN-0379-4059
N92-29879 # p 3407 ..... ESA-SP-1141
ETN-92-91388
ISBN-92-9092-140-4
N92-29880 # p 3526 ..... ETN-92-91586
ISSN-0924-3755
MEMO-INF-92-02
TIOS-92/01
N92-29881 # p 3534 ..... CWI-AM-R9111
ETN-92-91653
ISSN-0924-2953
N92-29882 # p 3534 ..... CWI-AM-R9112
ETN-92-91654
ISSN-0924-2953
N92-29883 # p 3534 ..... CWI-NM-R9108
ETN-92-91655
ISSN-0169-0388
N92-29884 # p 3401 ..... ETN-92-91547
NLR-TR-88072-U
N92-29885 # p 3479 ..... ETN-92-91548
NLR-TR-88086-U
N92-29886 # p 3561 ..... ETN-92-91337
OEFZS-4570
N92-29887 # p 3521 ..... ETN-92-91416
ISSN-0922-5641
REPT-91-46
N92-29888 # p 3526 ..... ETN-92-91481
LAAS-91412
N92-29889 # p 3401 ..... ETN-92-91492
N92-29890 # p 3521 ..... CWI-CS-R9121
ETN-92-91549
N92-29891 # p 3521 ..... CWI-CS-R9122
ETN-92-91550
N92-29892 # p 3534 ..... CWI-CS-R9123
ETN-92-91551
N92-29893 # p 3534 ..... CWI-AM-R9106
ETN-92-91649
N92-29894 # p 3535 ..... CWI-AM-R9107
ETN-92-91650
N92-29895 # p 3535 ..... CWI-AM-R9108
ETN-92-91651
ISSN-0924-2953
N92-29896 # p 3535 ..... CWI-AM-R9110
ETN-92-91652
ISSN-0924-2953
N92-29897 # p 3540 ..... ETN-92-91790
MEMO-COSOR-91-36
N92-29898 # p 3535 ..... ETN-92-91791
ISSN-0926-4493
MEMO-COSOR-91-37
N92-29899 # p 3546 ..... DE92-011188
DOE/ER-13744/12
N92-29900 # p 3441 ..... AD-D015198
NAVY-CASE-73128
US-PATENT-APPL-SN-771928
N92-29901 # p 3418 ..... AD-A247050
AFOSR-92-0153TR
N92-29902 # p 3436 ..... AD-A248065
M91-113
N92-29903 # p 3413 ..... AD-A248408
N92-29904 # p 3413 ..... AD-A248409
N92-29905 # p 3426 ..... AD-A248614
AD-E501508
IDA-D-1115
IDA/HQ-92-40803
N92-29906 # p 3403 ..... AD-A248884
N92-29907 # p 3514 ..... DE92-011374
WSRC-IM-90-83-6
N92-29908 # p 3426 ..... CONF-9203124-1
DE92-011381
SAND-91-2727C
N92-29909 # p 3436 ..... CONF-911202-69
DE92-011470
UCRL-JC-109001
N92-29910 # p 3547 ..... CONF-911004
DE92-011502
ORNL/TM-11882
N92-29911 # p 3559 ..... CONF-911202-70
DE92-011528
UCRL-JC-107696
N92-29912 # p 3441 ..... DE92-506507
TKK-KO/LTK-67
N92-29913 # p 3413 ..... AAE-91-11
AD-A247296
AFOSR-92-0160TR
UILUENG-91-0511
N92-29914 # p 3442 ..... AD-A247192
RL-TR-91-353
N92-29915 # p 3483 ..... AD-A248841
NUWC-NL-TR-10017
N92-29916 # p 3402 ..... ETN-92-91546
NLR-TR-86006-U
N92-29917 # p 3555 ..... CONF-920362-16
DE92-011228
LA-UR-92-1043
N92-29918 # p 3544 ..... ETN-92-91409
ISSN-0922-5641
REPT-91-36
N92-29919 # p 3535 ..... ETN-92-91410
ISSN-0922-5641
REPT-91-37
N92-29920 # p 3535 ..... ETN-92-91411
ISSN-0922-5641
REPT-91-38
N92-29921 # p 3535 ..... ETN-92-91412
ISSN-0922-5641
REPT-91-39
N92-29922 # p 3535 ..... ETN-92-91413
ISSN-0922-5641
REPT-91-40
N92-29923 # p 3535 ..... ETN-92-91414
ISSN-0922-5641
REPT-91-41
N92-29924 # p 3536 ..... ETN-92-91415
ISSN-0922-5641
REPT-91-42
N92-29925 # p 3483 ..... ETN-92-91488
N92-29926 # p 3445 ..... ETN-92-91489
N92-29927 # p 3405 ..... ETN-92-91493
N92-29928 # p 3477 ..... DE92-013485

DOE/ER-61229/1
N92-29929 # p 3407 ..... AD-A245978
N92-29930 # p 3512 ..... AD-A248334
AFOSR-92-0189TR
REPT-255-6491-1
N92-29931 # p 3419 ..... AD-A248336
N92-29932 # p 3419 ..... AD-A248337
N92-29933 # p 3445 ..... AD-A248458
PSU-TURBO-9201
N92-29934 # p 3562 ..... AD-A248694
LMI-PL019R1
N92-29935 # p 3442 ..... AD-A248857
N92-29936 # p 3442 ..... AD-A248950
N92-29937 # p 3477 ..... DE92-011292
UCRL-CR-104380-REV-1
N92-29938 # p 3550 ..... CONF-920423-3
DE92-011302
WHC-SA-1258
N92-29939 # p 3559 ..... DE92-012587
IS-T-1580
N92-29940 # p 3423 ..... AD-A250063
CETHA-TS-CR-91054
REF-JTN-816005
N92-29941 # p 3419 ..... AD-A250235
MIT-TR-36
N92-29942 # p 3474 ..... CONF-920362-25
DE92-013008
GA-A-20855
N92-29943 # p 3419 ..... CONF-920707-15
DE92-006705
SAND-91-8720
N92-29944 # p 3446 ..... CWI-NM-R9109
ETN-92-91656
N92-29945 # p 3446 ..... CWI-NM-R9110
ETN-92-91657
N92-29946 # p 3536 ..... CWI-NM-R9111
ETN-92-91658
N92-29947 # p 3446 ..... CWI-NM-R9112
ETN-92-91659
N92-29948 # p 3477 ..... NOAA-TM-ERL-WPL-218
PB92-166404
N92-29949 # p 3513 ..... PB92-164656
N92-29950 # p 3501 ..... NCEER-91/0026
PB92-163807
N92-29951* # p 3552 ..... NAS 1.71:LAR-14779-1
NASA-CASE-LAR-14779-1
US-PATENT-APPL-SN-885714
N92-29952* # p 3474 ..... NAS 1.71:MSC-21961-1
NASA-CASE-MSC-21961-1
US-PATENT-APPL-SN-901626
N92-29953* # p 3426 ..... NAS 1.71:LAR-14643-1
NASA-CASE-LAR-14643-1
US-PATENT-APPL-SN-790730
N92-29954* # p 3446 ..... NAS 1.71:LAR-14612-1
NASA-CASE-LAR-14612-1
US-PATENT-APPL-SN-820431
N92-29955* # p 3529 ..... NAS 1.71:NPO-17807-2-CU
NASA-CASE-NPO-17807-2-CU
US-PATENT-APPL-SN-789567
N92-29956 # p 3536 ..... ETN-92-91577
ISSN-0924-3755
MEMO-INF-91-77
N92-29957 # p 3562 ..... ETN-92-91578
ISSN-0924-3755
MEMO-INF-91-80
N92-29958 # p 3526 ..... ETN-92-91579
ISSN-0924-3755
MEMO-INF-91-81
TIOS-91/030
N92-29959 # p 3437 ..... ETN-92-91580
ISSN-0924-3755
MEMO-INF-91-84
TIOS-91/034
N92-29960 # p 3426 ..... ETN-92-91581
ISSN-0924-3755
MEMO-INF-91-85
UT-KBS-91-21
N92-29961 # p 3521 ..... ETN-92-91582
ISSN-0924-3755
MEMO-INF-91-90
N92-29962 # p 3529 ..... ETN-92-91702
N92-29963 # p 3529 ..... NO REPORT NUMBER
N92-29964 # p 3530 ..... NO REPORT NUMBER
N92-29965 # p 3530 ..... NO REPORT NUMBER
N92-29966 # p 3530 ..... NO REPORT NUMBER
N92-29967 # p 3408 ..... ETN-92-91703
FFI-91/4001
ISSN-0802-2437
N92-29968 # p 3446 ..... ETN-92-91735
ISBN-3-7983-1446-2
ISSN-0170-8902
N92-29969 # p 3530 ..... ETN-92-91775
ISSN-0924-3755
MEMO-INF-91-88
N92-29970 # p 3521 ..... ETN-92-91776
ISSN-0924-3755
MEMO-INF-91-89
N92-29971 # p 3530 ..... ETN-92-91755
ISSN-0169-2690
MEMO-1008
N92-29972 # p 3446 ..... ETN-92-91756
ISSN-0169-2690
MEMO-1009
N92-29973 # p 3541 ..... ETN-92-91757
ISSN-0169-2690
MEMO-1010
N92-29974 # p 3540 ..... ETN-92-91758
ISSN-0169-2690
MEMO-1011
N92-29975 # p 3540 ..... ETN-92-91759
ISSN-0169-2690
MEMO-1012
N92-29976 # p 3541 ..... ETN-92-91760
ISSN-0169-2690
MEMO-1013
N92-29977 # p 3446 ..... ETN-92-91761
ISSN-0169-2690
MEMO-1015
N92-29978 # p 3437 ..... ETN-92-91762
ISSN-0169-2690
MEMO-1016-PT-2
N92-29979 # p 3536 ..... ETN-92-91763
ISSN-0169-2690
MEMO-1017
N92-29980 # p 3541 ..... ETN-92-91764
ISSN-0169-2690
MEMO-1019
N92-29981 # p 3522 ..... ETN-92-91774
ISSN-0924-3755
MEMO-INF-91-87
TIOS-91/035
N92-29982 # p 3514 ..... ETN-92-91777
ISSN-0924-3755
MEMO-INF-91-92
TIOS-91/036
N92-29983 # p 3530 ..... ETN-92-91778
ISSN-0924-3755
MEMO-INF-92-03
N92-29984 # p 3437 ..... ETN-92-91779
ISSN-0924-3755
MEMO-INF-92-05
TIOS-92/03
N92-29985 # p 3526 ..... ETN-92-91780
ISSN-0924-3755
MEMO-INF-92-06
TIOS-92/04
N92-29986 # p 3408 ..... CONF-920373-2
DE92-010670
SAND-91-1691C
N92-29987 # p 3477 ..... CONF-911296-5
DE92-010714
UCRL-JC-107745
N92-29988 # p 3437 ..... CONF-920315-5
DE92-010751
SU-SLAC-PUB-5780
N92-29989 # p 3522 ..... CWI-CS-R9129
ETN-92-91554
N92-29990 # p 3522 ..... CWI-CS-R9134
ETN-92-91557
N92-29991 # p 3522 ..... CWI-CS-R9135
ETN-92-91558
N92-29992 # p 3522 ..... CWI-CS-R9136
ETN-92-91559
N92-29993 # p 3536 ..... CWI-CS-R9137
ECS-LFCS-91-169
ETN-92-91560
ISSN-0169-118X
N92-29994 # p 3522 ..... CWI-CS-R9138
ETN-92-91561
ISSN-0169-118X
N92-29995 # p 3536 ..... ETN-92-91574
ISSN-0924-3755
MEMO-INF-91-73
N92-29996 # p 3560 ..... ETN-92-91720
RAL-92-004
N92-29997 # p 3544 ..... DLR-FB-91-28
ETN-92-91733
ISSN-0939-2963
N92-29998 # p 3447 ..... DLR-FB-91-31
ETN-92-91734
ISSN-0939-2963
N92-29999 # p 3536 ..... ETN-92-91754
ISSN-0169-2690
MEMO-1007
N92-30000 # p 3562 ..... ETN-92-91771
ISSN-0924-3755
MEMO-INF-91-79
TIOS-91/029
N92-30001* # p 3547 ..... NAS 1.26:190533
NASA-CR-190533
N92-30002* # p 3547 ..... NO REPORT NUMBER
N92-30003* # p 3547 ..... NO REPORT NUMBER
N92-30004* # p 3438 ..... NO REPORT NUMBER
N92-30005* # p 3547 ..... NO REPORT NUMBER
N92-30006* # p 3548 ..... NO REPORT NUMBER
N92-30007* # p 3548 ..... NO REPORT NUMBER
N92-30008* # p 3548 ..... NO REPORT NUMBER
N92-30009* # p 3548 ..... NO REPORT NUMBER
N92-30010* # p 3548 ..... NO REPORT NUMBER
N92-30011* # p 3548 ..... NO REPORT NUMBER
N92-30012* # p 3548 ..... NO REPORT NUMBER
N92-30013* # p 3549 ..... NO REPORT NUMBER
N92-30014* # p 3549 ..... BNL-52262
DOE/OSTI-4500-R75
N92-30015* # p 3438 ..... NO REPORT NUMBER
N92-30016* # p 3408 ..... NAS 1.15:107956
NASA-TM-107956
N92-30017 # p 3490 ..... GPO-55-802CC
ISBN-0-16-038754-X
S-HRG-102-647
N92-30018 # p 3494 ..... EPA/600/A-92/106
PB92-180256
N92-30019 # p 3494 ..... PB92-185073
N92-30020 # p 3522 ..... NISTIR-4810
PB92-181098
N92-30021 # p 3495 ..... EPA/600/R-92/095
PB92-184985
N92-30022 # p 3490 ..... OCS/MMS-91/0069
PB92-185016
N92-30023 # p 3447 ..... PB92-180678
REPT-68
N92-30024* # p 3447 ..... NAS 1.71:LAR-14033-2
NASA-CASE-LAR-14033-2
US-PATENT-APPL-SN-843653
N92-30025* # p 3406 ..... NAS 1.71:LAR-14219-1
NASA-CASE-LAR-14219-1
US-PATENT-APPL-SN-788908
N92-30026* # p 3479 ..... NAS 1.71:MSC-21967-1
NASA-CASE-MSC-21967-1
US-PATENT-APPL-SN-892053
N92-30027* # p 3552 ..... NAS 1.71:MSC-21915-1
NASA-CASE-MSC-21915-1
US-PATENT-APPL-SN-863883
N92-30028* # p 3483 ..... NAS 1.71:LAR-14698-1
NASA-CASE-LAR-14698-1
US-PATENT-APPL-SN-866769
N92-30029* # p 3553 ..... NAS 1.71:LAR-14607-1SB
NASA-CASE-LAR-14607-1SB
US-PATENT-APPL-SN-855363
N92-30030* # p 3474 ..... NAS 1.71:LAR-14724-1
NASA-CASE-LAR-14724-1
US-PATENT-APPL-SN-876592
N92-30031 # p 3495 ..... EPA/600/A-92/002
PB92-139393
N92-30032 # p 3442 ..... NISTIR-4726
PB92-164672
N92-30033 # p 3562 ..... PB92-172857
USDA/CRIS/AG-91/11
N92-30034 # p 3503 ..... NOAA-TM-ERL-ARL-193
PB92-174564
N92-30035 # p 3542 ..... NISTIR-4741
PB92-172824
N92-30036 # p 3447 ..... NISTIR-3987
PB92-172832
N92-30037 # p 3564 ..... NYSERDA-91-5
PB92-174119
N92-30038 # p 3563 ..... PB92-178631
N92-30039 # p 3563 ..... NISTIR-4800
PB92-181122
N92-30040 # p 3563 ..... LC-91-22753
PB92-181320
USGS-BULL-1565
N92-30041* # p 3447 ..... NAS 1.26:189967
NASA-CR-189967
N92-30042* # p 3447 ..... NO REPORT NUMBER
N92-30043* # p 3447 ..... NO REPORT NUMBER
N92-30044* # p 3448 ..... NO REPORT NUMBER
N92-30045* # p 3448 ..... NO REPORT NUMBER
N92-30046* # p 3448 ..... NO REPORT NUMBER
N92-30047* # p 3448 ..... NO REPORT NUMBER
N92-30048* # p 3448 ..... NO REPORT NUMBER
N92-30049* # p 3449 ..... NO REPORT NUMBER
N92-30050* # p 3449 ..... NO REPORT NUMBER
N92-30051* # p 3449 ..... NO REPORT NUMBER
N92-30052* # p 3449 ..... NO REPORT NUMBER
N92-30053* # p 3449 ..... NO REPORT NUMBER
N92-30054* # p 3449 ..... NO REPORT NUMBER
N92-30055* # p 3450 ..... NO REPORT NUMBER
N92-30056* # p 3450 ..... NO REPORT NUMBER
N92-30057* # p 3450 ..... NO REPORT NUMBER
N92-30058* # p 3450 ..... NO REPORT NUMBER
N92-30059* # p 3450 ..... NO REPORT NUMBER
N92-30060* # p 3450 ..... NO REPORT NUMBER
N92-30061* # p 3450 ..... NO REPORT NUMBER
N92-30062* # p 3450 ..... NO REPORT NUMBER
N92-30063* # p 3451 ..... NO REPORT NUMBER
N92-30064* # p 3451 ..... NO REPORT NUMBER
N92-30065* # p 3451 ..... NO REPORT NUMBER

N92-30066* # p 3451 ..... NO REPORT NUMBER
N92-30067* # p 3451 ..... NO REPORT NUMBER
N92-30068* # p 3451 ..... NO REPORT NUMBER
N92-30069* # p 3451 ..... NO REPORT NUMBER
N92-30070* # p 3452 ..... NO REPORT NUMBER
N92-30071* # p 3452 ..... NO REPORT NUMBER
N92-30072 # p 3555 ..... DE92-011614
DOE/DP-40200/188
N92-30073 # p 3522 ..... ETN-92-91566
ISSN-0924-3755
MEMO-INF-91-62
N92-30074 # p 3526 ..... ETN-92-91567
ISSN-0923-1714
MEMO-INF-91-63
TIOS-91/025
N92-30075 # p 3537 ..... ETN-92-91571
ISSN-0924-3755
MEMO-INF-91-70
N92-30076 # p 3407 ..... ETN-92-91697
MBB-UD-0610-91-PUB
N92-30077 # p 3537 ..... ETN-92-91748
ISSN-0169-2690
MEMO-1001
N92-30078 # p 3537 ..... ETN-92-91749
ISSN-0169-2690
MEMO-1002
N92-30079 # p 3541 ..... ETN-92-91750
ISSN-0169-2690
MEMO-1003
N92-30080 # p 3537 ..... ETN-92-91751
ISSN-0169-2690
MEMO-1004
N92-30081 # p 3537 ..... ETN-92-91752
ISSN-0169-2690
MEMO-1005
N92-30082* # p 3479 ..... NAS 1.71:MSC-21881-1
NASA-CASE-MSC-21881-1
US-PATENT-APPL-SN-785637
N92-30083* # p 3428 ..... NAS 1.71:NPO-18448-1-CU
NASA-CASE-NPO-18448-1-CU
US-PATENT-APPL-SN-786612
N92-30084* # p 3553 ..... NAS 1.71:NPO-18478-1-CU
NASA-CASE-NPO-18478-1-CU
US-PATENT-APPL-SN-883957
N92-30085* # p 3530 ..... NAS 1.71:NPO-18553-1-CU
NASA-CASE-NPO-18553-1-CU
US-PATENT-APPL-SN-908677
N92-30086* # p 3442 ..... NAS 1.71:NPO-18578-1-CU
NASA-CASE-NPO-18578-1-CU
US-PATENT-APPL-SN-912956
N92-30087 # p 3501 ..... AD-A249740
NCCOSC/RDT/E-TR-1483
N92-30088 # p 3490 ..... DE92-013602
JSR-91-330A
N92-30089 # p 3442 ..... DE92-506506
TKK-KO/LTK-66
N92-30090 # p 3475 ..... CONF-9109256-2
DE92-011787
N92-30091 # p 3555 ..... ISSN-0915-633X
NIFS-132
N92-30092 # p 3443 ..... EPA/600/A-92/101
PB92-180207
N92-30093 # p 3437 ..... B92-0123
NISTIR-3988
PB92-183672
N92-30094 # p 3443 ..... PB92-177872
REPT-1992/5
N92-30095 # p 3542 ..... IHES/M/92/12
PB92-173251
N92-30096 # p 3537 ..... IHES/M/92/14
PB92-178292
N92-30097* # p 3480 ..... NAS 1.71:LAR-13805-1
NASA-CASE-LAR-13805-1
US-PATENT-APPL-SN-770509
N92-30098* # p 3419 ..... NAS 1.71:LAR-14398-1
NASA-CASE-LAR-14398-1
US-PATENT-APPL-SN-736985
N92-30099* # p 3483 ..... NAS 1.71:LAR-14775-1
NASA-CASE-LAR-14775-1
US-PATENT-APPL-SN-881912
N92-30100* # p 3427 ..... NAS 1.71:MSC-21529-1
NASA-CASE-MSC-21529-1
US-PATENT-APPL-SN-857901
N92-30101* # p 3480 ..... NAS 1.71:MSC-21903-1
NASA-CASE-MSC-21903-1
US-PATENT-APPL-SN-902266
N92-30102* # p 3559 ..... NAS 1.71:NPO-18625-1-CU
NASA-CASE-NPO-18625-1-CU
US-PATENT-APPL-SN-912981
N92-30103* # p 3437 ..... NAS 1.71:NPO-18713-1-CU
NASA-CASE-NPO-18713-1-CU
US-PATENT-APPL-SN-802078
N92-30104* # p 3553 ..... NAS 1.71:NPO-17794-1-CU
NASA-CASE-NPO-17794-1-CU
US-PATENT-APPL-SN-904550
N92-30105 # p 3491 ..... NCAR/TN-370+STR
PB92-186113
N92-30106* # p 3484 ..... L-17094
NAS 1.55:3160
NASA-CP-3160
N92-30107* # p 3484 ..... NO REPORT NUMBER
N92-30108* # p 3402 ..... NO REPORT NUMBER
N92-30109* # p 3484 ..... NO REPORT NUMBER
N92-30110* # p 3484 ..... NO REPORT NUMBER
N92-30111* # p 3484 ..... NO REPORT NUMBER
N92-30112* # p 3485 ..... NO REPORT NUMBER
N92-30113* # p 3485 ..... NO REPORT NUMBER
N92-30114* # p 3485 ..... NO REPORT NUMBER
N92-30115* # p 3485 ..... NO REPORT NUMBER
N92-30116* # p 3481 ..... NO REPORT NUMBER
N92-30117* # p 3481 ..... NO REPORT NUMBER
N92-30118* # p 3481 ..... NO REPORT NUMBER
N92-30119* # p 3481 ..... NO REPORT NUMBER
N92-30120* # p 3481 ..... NO REPORT NUMBER
N92-30121* # p 3481 ..... NO REPORT NUMBER
N92-30122* # p 3399 ..... NO REPORT NUMBER
N92-30123* # p 3402 ..... NO REPORT NUMBER
N92-30124* # p 3402 ..... NO REPORT NUMBER
N92-30125* # p 3487 ..... NO REPORT NUMBER
N92-30126* # p 3487 ..... NO REPORT NUMBER
N92-30127* # p 3487 ..... NO REPORT NUMBER
N92-30128* # p 3402 ..... NO REPORT NUMBER
N92-30129* # p 3402 ..... NO REPORT NUMBER
N92-30130* # p 3402 ..... NO REPORT NUMBER
N92-30131* # p 3403 ..... NO REPORT NUMBER
N92-30132* # p 3488 ..... NO REPORT NUMBER
N92-30133* # p 3403 ..... NO REPORT NUMBER
N92-30134* # p 3488 ..... NO REPORT NUMBER
N92-30135 # p 3477 ..... CONF-920657-1
DE92-010800
SAND-92-0446C
N92-30136 # p 3427 ..... AD-A248996
TR-64
N92-30137 # p 3416 ..... AD-A250285
AFOSR-92-0302TR
N92-30138 # p 3541 ..... DE92-013553
LA-12197-MS
N92-30139 # p 3542 ..... DE92-013555
LA-12298-MS
N92-30140 # p 3452 ..... DE92-013601
JSR-90-310
N92-30141 # p 3523 ..... CWI-CS-R9139
ETN-92-91562
ISSN-0169-118X
N92-30142 # p 3527 ..... ETN-92-91565
ISSN-0924-3755
MEMO-INF-91-34
N92-30143 # p 3531 ..... ETN-92-91568
ISSN-0924-3755
MEMO-INF-91-66
SKBS-A1/91-21
UT-KBS-91-33
N92-30144 # p 3523 ..... ETN-92-91572
ISSN-0924-3755
MEMO-INF-91-71
TIOS-91/026
N92-30145 # p 3514 ..... ETN-92-91575
ISSN-0924-3755
MEMO-INF-91-74
TIOS-91/032
N92-30146 # p 3523 ..... CWI-CS-R9126
ETN-92-91639
N92-30147 # p 3537 ..... ETN-92-91765
ISSN-0169-2690
MEMO-1020
N92-30148 # p 3560 ..... ETN-92-91766
ISSN-0169-2690
MEMO-1021
N92-30149* # p 3452 ..... NAS 1.26:189024
NASA-CR-189024
N92-30150* # p 3452 ..... NO REPORT NUMBER
N92-30151* # p 3452 ..... NO REPORT NUMBER
N92-30152* # p 3453 ..... NO REPORT NUMBER
N92-30153* # p 3453 ..... NO REPORT NUMBER
N92-30154* # p 3453 ..... NO REPORT NUMBER
N92-30155* # p 3453 ..... NO REPORT NUMBER
N92-30156* # p 3453 ..... NO REPORT NUMBER
N92-30157* # p 3453 ..... NO REPORT NUMBER
N92-30158* # p 3453 ..... NO REPORT NUMBER
N92-30159* # p 3454 ..... NO REPORT NUMBER
N92-30160* # p 3454 ..... NO REPORT NUMBER
N92-30161* # p 3454 ..... NO REPORT NUMBER
N92-30162* # p 3454 ..... NO REPORT NUMBER
N92-30163* # p 3454 ..... NO REPORT NUMBER
N92-30164* # p 3454 ..... NO REPORT NUMBER
N92-30165* # p 3454 ..... NO REPORT NUMBER
N92-30166* # p 3455 ..... NO REPORT NUMBER
N92-30167* # p 3455 ..... NO REPORT NUMBER
N92-30168* # p 3455 ..... NO REPORT NUMBER
N92-30169* # p 3455 ..... NO REPORT NUMBER
N92-30170 # p 3438 ..... ETN-92-91773
ISSN-0924-3755
MEMO-INF-91-83
TIOS-91/033
N92-30171 # p 3503 ..... NO REPORT NUMBER
N92-30172 # p 3555 ..... ISSN-0915-633X
NIFS-136
N92-30173 # p 3495 ..... EPA/600/A-92/105
PB92-180249
N92-30174 # p 3541 ..... AD-A248988
N92-30175 # p 3560 ..... AD-A248993
N92-30176 # p 3443 ..... AD-A249010
WL-TR-91-2094
N92-30177 # p 3537 ..... CWI-CS-R9130
ETN-92-91555
N92-30178 # p 3538 ..... CWI-CW-R9131
ETN-92-91556
N92-30179 # p 3523 ..... CWI-BS-R9122
ETN-92-91563
ISSN-0924-0659
N92-30180 # p 3541 ..... CWI-BS-R9124
ETN-92-91564
ISSN-0924-0659
N92-30181 # p 3523 ..... ETN-92-91569
ISSN-0924-3755
MEMO-INF-91-67
N92-30182* # p 3402 ..... AIAA PAPER 92-2622-CP
E-7046
NAS 1.15:105675
NASA-TM-105675
N92-30183 # p 3527 ..... ETN-92-91570
ISSN-0924-3755
MEMO-INF-91-69
N92-30184 # p 3531 ..... ETN-92-91576
ISSN-0924-3755
MEMO-INF-91-76
TIOS-91/028
N92-30185 # p 3538 ..... ETN-92-91753
ISSN-0169-2690
MEMO-1006
N92-30186 # p 3523 ..... ETN-92-91767
ISSN-0169-2690
MEMO-1022
N92-30187* # p 3414 ..... E-7088
NAS 1.15:105700
NASA-TM-105700
N92-30188 # p 3541 ..... ETN-92-91768
ISSN-0169-2690
MEMO-1023
N92-30189 # p 3527 ..... ETN-92-91770
ISSN-0924-3755
MEMO-INF-91-78
N92-30190* # p 3455 ..... ICASE-92-26
NAS 1.26:189667
NASA-CR-189667
N92-30191 # p 3523 ..... ETN-92-91772
ISSN-0924-3755
MEMO-INF-91-82
TIOS-91/031
N92-30192* # p 3455 ..... ICASE-92-25
NAS 1.26:189666
NASA-CR-189666
N92-30193* # p 3506 ..... NAS 1.15:104566
NASA-TM-104566
REPT-92B00097-VOL-5
N92-30194 # p 3563 ..... PB92-185305
N92-30195 # p 3524 ..... INTERNAL-90-NICI-08
PB92-187418
N92-30196 # p 3419 ..... ISBN-90-9004659-3
PB92-184761
N92-30197* # p 3571 ..... NAS 1.15:107807
NASA-TM-107807
N92-30198 # p 3438 ..... B91-0278
NIST/TN-1351
PB92-187020
N92-30199* # p 3569 ..... NAS 1.26:190262
NASA-CR-190262
N92-30200 # p 3495 ..... EPA/450/3-91/0100
PB92-186246
N92-30201 # p 3524 ..... PB92-187350
TW-91-09
N92-30202 # p 3475 ..... AD-D015205
NAVY-CASE-72831
US-PATENT-APPL-SN-783660
N92-30203 # p 3556 ..... CONF-920362-16
DE92-011262
LA-UR-92-826
N92-30204* # p 3570 ..... LMSC/P009805
NAS 1.26:184339
NASA-CR-184339
N92-30205* # p 3423 ..... NAS 1.15:104220
NASA-TM-104220
N92-30206* # p 3423 ..... NAS 1.26:190538
NASA-CR-190538
UVA/528266/MS93/111
N92-30207* # p 3524 ..... E-7003
NAS 1.26:189171
NASA-CR-189171

N92-30208* # p 3416 ..... AM-92-02
NAS 1.26:190537
NASA-CR-190537
N92-30209* # p 3404 ..... NAS 1.26:190565
NASA-CR-190565
N92-30210* # p 3491 ..... NAS 1.15:104568
NASA-TM-104568
REPT-92B00092
N92-30211 # p 3495 ..... CONF-9206129-3
DE92-011446
UCRL-JC-108819
N92-30212 # p 3560 ..... DE92-624516
IYAF-91-40
N92-30213 # p 3549 ..... ANU-P-1092
DE92-624790
N92-30214* # p 3488 ..... NAS 1.15:107632
NASA-TM-107632
N92-30215* # p 3408 ..... NAS 1.15:103560
NASA-TM-103560
N92-30216 # p 3510 ..... AD-A250649
NHRC-91-31
N92-30217* # p 3410 ..... NAS 1.26:189656-VOL-1
NASA-CR-189656-VOL-1
UTD-23351-961-VOL-1
N92-30218* # p 3411 ..... NAS 1.26:189656-VOL-2
NASA-CR-189656-VOL-2
N92-30219* # p 3411 ..... NAS 1.26:189656-VOL-3
NASA-CR-189656-VOL-3
N92-30220* # p 3411 ..... NAS 1.26:189656-VOL-4
NASA-CR-189656-VOL-4
N92-30221* # p 3411 ..... NAS 1.26:189656-VOL-5
NASA-CR-189656-VOL-5
N92-30222* # p 3411 ..... NAS 1.26:189656-VOL-6
NASA-CR-189656-VOL-6
N92-30223* # p 3412 ..... NAS 1.26:189656-VOL-7
NASA-CR-189656-VOL-7
N92-30224* # p 3412 ..... NAS 1.26:189656-VOL-8
NASA-CR-189656-VOL-8
N92-30225* # p 3412 ..... NAS 1.26:189656-VOL-9
NASA-CR-189656-VOL-9
N92-30226 # p 3495 ..... ETN-92-91831
ISSN-0922-5641
REPT-91-81
N92-30227 # p 3524 ..... ETN-92-91832
ISSN-0922-5641
REPT-91-82
N92-30228 # p 3524 ..... ETN-92-91834
ISSN-0922-5641
REPT-91-84
N92-30229 # p 3527 ..... ETN-92-91835
ISSN-0922-5641
REPT-91-85
N92-30230 # p 3491 ..... BCRS-91-28
ETN-92-91877
ISBN-90-5411-010-4
N92-30231 # p 3491 ..... BCRS-91-30
ETN-92-91879
ISBN-90-5411-032-5
N92-30232 # p 3399 ..... ETN-92-91903
MBB/FE202/S/PUB/461

Appendix

NASA SCIENTIFIC AND TECHNICAL INFORMATION PROGRAM PRODUCTS AND SERVICES

The NASA Scientific and Technical Information (STI) Program provides for the collection and announcement of aerospace-related reports and literature obtained worldwide through agreements and exchanges. The result of the collection is the comprehensive NASA STI Database that covers aeronautics, space, and supporting disciplines.

The STI Database, documents generated or obtained by NASA, and products and services derived from or supporting the database are made available to the NASA research community and to the public. Descriptions and sources of these items are presented in the following pages.

Scientific and Technical Aerospace Reports (*STAR*) is an abstract journal, listing citations with abstracts for aerospace-related reports obtained from worldwide sources. *STAR* is issued on the 8th and 23rd of each month and announces current documents that have been entered into the NASA STI Database during the previous two weeks. The reports are of the following types:

- NASA, NASA contractor, and NASA grantee reports;
- Reports issued by other U.S. Government agencies, domestic and foreign institutions, universities, and private firms;
- Translations in report form;
- NASA-owned patents and patent applications;
- Other U.S. Government agency and foreign patents and patent applications;
- Domestic and foreign dissertations and theses.

Journal, book, and conference literature, journal translations, and certain foreign dissertations having the same subject scope as *STAR* are announced in a companion journal, *International Aerospace Abstracts* (*IAA*). *IAA* is issued on the 1st and 15th of each month and is available from the American Institute of Aeronautics and Astronautics, Technical Information Service, 555 West 57th Street, 12th Floor, New York, NY 10019.

ELIGIBILITY AND REGISTRATION FOR NASA STI PRODUCTS AND SERVICES

Organizations of the type listed below that have registered with NASA can receive products and services.

- NASA offices and installations, contractors, subcontractors, grantees, and consultants;
- Other U.S. Government agencies and their contractors;
- Libraries in the United States that have arrangements with NASA to maintain collections of NASA documents for public reference;
- Other organizations in the United States having a need for NASA documents in work related to aeronautics and space research;
- Organizations abroad that have established reciprocal documents exchange arrangements with NASA.

The central service points — central points of document acquisition and control within qualified organizations — or individuals are eligible to register for NASA STI products and services. Domestic organizations or individuals may be eligible to receive various classes of NASA publications and services and should address their requests for registration or further information to:

NASA Center for AeroSpace Information
ATTN: Registration Services
P.O. Box 8757
Baltimore, MD 21240-0757
301-621-0390

Organizations abroad should direct requests to:

National Aeronautics and Space Administration
Scientific and Technical Information Program (JTT)
International STI Program
Washington, DC 20546-0001
USA
703-271-5640

SUBJECT SCOPE

The subject scope of *STAR* and *IAA* includes all aspects of aeronautics and space research and development, supporting basic and applied research, and applications. Aerospace aspects of Earth resources, energy development, conservation, oceanography, environmental protection, urban transportation, and other topics of high national priority are also covered.

HOW TO USE *STAR* SUBJECT CATEGORIES

Abstracts in *STAR* are categorized by 10 major subject divisions that are divided further into 76 specific subject categories. The subject divisions and categories are listed in the Table of Contents together with a note for each that defines its scope and provides any cross-references. For example:

16 SPACE TRANSPORTATION
Includes passenger and cargo space transportation, e.g., shuttle operations; and space rescue techniques. For related information see also *03 Air Transportation and Safety* and *18 Spacecraft Design, Testing and Performance*. For space suits see *54 Man/System Technology and Life Support*.

CROSS-REFERENCES

Individual *STAR* abstracts are not ordinarily cross-referenced, except for certain conference reports or book translations that have had separate abstracts written for their component papers or chapters. Citations and abstracts of the components follow immediately after those of the parent document. When the subject content of a component differs sufficiently from the general content of the parent, a cross-reference citation also is printed at the end of the category to which it normally would have been assigned if it were independent.

DOCUMENTS ON MICROFICHE

Documents available on microfiche are designated by a pound sign (#) following the accession number.

LIMITED REPRODUCIBILITY

A note of limited reproducibility appears in the citation, if there are factors affecting the reproducibility of more than 20% of the document. These factors include faint or broken type, color photographs, black and white photographs, foldouts, dot matrix print, or some other factor that limits the reproducibility of the document. This notation also appears on the microfiche header.

COLOR COPIES

An increasing number of NASA scientific and technical reports are being produced with color graphs, charts, illustrations, and photographs. An indication that a document has color pages follows the source and pricing (SAP) information in the *STAR* citation.

Registered users of the NASA Scientific and Technical Information Program will receive ordered documents with color at no additional cost, as long as stock copies of the document are available. Otherwise, an additional fee of $2.00 per color page will be charged. The NASA Center for AeroSpace Information staff will contact registered users to determine individual user's needs.

NASA PATENTS AND PATENT APPLICATIONS

Patents and patent applications owned by NASA are announced in *STAR* under appropriate subject categories and are referenced in the *STAR* indexes. In the Report/Accession Number Index, patents are indexed by the NASA Case Number, and the U.S. Patent Class. Patent applications are indexed by the NASA Case Number and the U.S. Patent Application Serial Number.

Printed copies of patents (which are not microfiched) are available for purchase from the U.S. Patent and Trademark Office.

When ordering patents, the U.S. Patent Number should be used, and payment must be remitted in advance, by money order or check payable to the Commissioner of Patents and Trademarks. Prepaid purchase coupons for ordering are also available from the U.S. Patent and Trademark Office.

NASA patent application specifications are sold in both paper copy and microfiche by the NASA Center for AeroSpace Information (CASI). The N accession number should be used in ordering either paper copy or microfiche from CASI.

The patents and patent applications announced in *STAR* are owned by NASA and are available for royalty-free licensing. Requests for licensing terms and further information should be addressed to:

National Aeronautics and Space Administration
Associate General Counsel for Intellectual Property
Code GP
Washington, DC 20546-0001

SOURCES FOR DOCUMENTS

One or more sources from which a document announced in *STAR* is available to the public is given in each citation. The most commonly indicated sources and their acronyms or abbreviations are listed on page A-6. If the publication is available from a source other than those listed, the publisher and address will be displayed on the availability line or in combination with the corporate source line.

Avail: CASI. Sold by the NASA Center for AeroSpace Information. Prices for hard copy (HC) and microfiche (MF) are indicated by a price code following the letters HC or MF in the *STAR* citation. Current values for the price codes are given in the tables on page A-7.

NOTE ON ORDERING DOCUMENTS: When ordering publications from CASI, use the N accession number or other report number. It is also advisable to cite the title and other bibliographic identification.

Avail: SOD (or GPO). Sold by the Superintendent of Documents, U.S. Government Printing Office, in hard copy.

Avail: BLL (formerly NLL): British Library Lending Division, Boston Spa, Wetherby, Yorkshire, England. Photocopies available from this organization at the price shown. (If none is given, address inquiry to the BLL.)

Avail: DOE Depository Libraries. Organizations in U.S. cities and abroad that maintain collections of Department of Energy reports, usually in microfiche form, are listed in *Energy Research Abstracts*. Services available from the DOE and its de-

positories are described in a booklet, *DOE Technical Information Center - Its Functions and Services* (TID-4660), which may be obtained without charge from the DOE Technical Information Center.

Avail: ESDU. Pricing information on specific data, computer programs, and details on Engineering Sciences Data Unit (ESDU) topic categories can be obtained from ESDU International Ltd. Requesters in North America should use the Virginia address while all other requesters should use the London address, both of which are on page A-6.

Avail: Fachinformationszentrum, Karlsruhe. Gesellschaft fur wissenschaftlich-technische Information mbH 7514 Eggenstein-Leopoldshafen 2, Germany.

Avail: HMSO. Publications of Her Majesty's Stationery Office are sold in the U.S. by Pendragon House, Inc. (PHI), Redwood City, CA. The U.S. price (including a service and mailing charge) is given, or a conversion table may be obtained from PHI.

Avail: Issuing Activity, or Corporate Author, or no indication of availability. Inquiries as to the availability of these documents should be addressed to the organization shown in the citation as the corporate author of the document.

Avail: NASA Public Document Rooms. Documents so indicated may be examined at or purchased from the National Aeronautics and Space Administration (JBD-4), Public Documents Room (Room 1H23), Washington, DC 20546-0001, or public document rooms located at NASA installations, and the NASA Pasadena Office at the Jet Propulsion Laboratory.

Avail: NTIS. Sold by the National Technical Information Service. Initially distributed microfiche under the NTIS SRIM (Selected Research Microfiche) are available. For information concerning this service, consult the NTIS Subscription Section, Springfield, VA 22161.

Avail: Univ. Microfilms. Documents so indicated are dissertations selected from *Dissertation Abstracts* and are sold by University Microfilms as xerographic copy (HC) and microfilm. All requests should cite the author and the Order Number as they appear in the citation.

Avail: US Patent and Trademark Office. Sold by Commissioner of Patents and Trademarks, U.S. Patent and Trademark Office, at the standard price of $1.50 each, postage free. (See discussion of NASA patents and patent applications below.)

Avail: (US Sales Only). These foreign documents are available to users within the United States from the National Technical Information Service (NTIS). They are available to users outside the United States through the International Nuclear Information Service (INIS) representative in their country, or by applying directly to the issuing organization.

Avail: USGS. Originals of many reports from the U.S. Geological Survey, which may contain color illustrations, or otherwise may not have the quality of illustrations preserved in the microfiche or facsimile reproduction, may be examined by the public at the libraries of the USGS field offices whose addresses are listed on page A-6. The libraries may be queried concerning the availability of specific documents and the possible utilization of local copying services, such as color reproduction.

FEDERAL DEPOSITORY LIBRARIES: To provide the general public with greater access to U.S. Government publications, Congress established the Federal Depository Library Program under the Government Printing Office (GPO), with 53 regional depositories responsible for permanent retention of material, inter-library loan, and reference services. (These libraries are not sales outlets.) At least one copy of nearly every NASA and NASA-sponsored publication, either in printed or microfiche format, is received and retained by the 53 regional depositories. A list of the regional GPO libraries, appears on page A-8. A local library can contact a regional depository library to help locate specific reports, or direct contact may be made by an individual.

PUBLIC COLLECTION OF NASA DOCUMENTS

An extensive collection of NASA and NASA-sponsored publications is maintianed by the British Library Lending Divison, Boston Spa, Wetherby, Yorkshire, England, for public access. The British Library Lending Division also has available many of the non-NASA publications cited in *STAR*.

European requesters may purchase facsimile copy or microfiche of NASA and NASA-sponsored documents, those identified by both the symbols # and * from ESA—Information Retrieval Service, European Space Agency, 8-10 rue Mario-Nikis, 75738 Paris CEDEX 15, France.

SUBMITTING DOCUMENTS

All users of this abstract service are urged to forward reports to be considered for announcement in *STAR*. This will aid NASA in its efforts to provide the fullest possible coverage of all scientific and technical publications that might support aeronautics and space research and development. If you have prepared relevant reports (other than those you will transmit to NASA, DOD, or DOE through the usual contract- or grant-reporting channels), please send them for consideration to the NASA Center for AeroSpace Information, P.O. Box 8757, Baltimore, MD 21240-0757.

Reprints of journal articles, book chapters, and conference papers are also welcome. These will be considered for announcement in *STAR*'s companion journal, *IAA*.

You may specify a particular source to be included in a report announcement if you wish; otherwise the report will be placed on a public sale at the NASA Center for AeroSpace Information. Copyrighted publications will be announced but not distributed or sold.

PURCHASE OF *STAR*

STAR is publicly available on annual subscription from the NASA Center for AeroSpace Information (CASI) at $114.00.

STAR is available to registered users on annual subscription from the NASA Center for AeroSpace Information, ATTN: Registration Services, P.O. Box 8757, Baltimore, MD 21240-0757.

Microfiche of the abstract sections of *STAR* are available, on annual subscription, from CASI. Annual subscription rates are $216.00 North America; $432.00 foreign.

ADDRESSES OF ORGANIZATIONS

American Institute of Aeronautics and Astronautics
Technical Information Service
555 West 57th Street, 12th Floor
New York, New York 10019

British Library Lending Division,
Boston Spa, Wetherby, Yorkshire,
England

Commissioner of Patents and Trademarks
U.S. Patent and Trademark Office
Washington, DC 20231

Department of Energy
Technical Information Center
P.O. Box 62
Oak Ridge, Tennessee 37830

European Space Agency-Information Retrieval Service
ESRIN
Via Galileo Galilei
00044 Frascati (Rome) Italy

Engineering Sciences Data Unit International
P.O. Box 1633
Manassas, Virginia 22110

Engineering Sciences Data Unit International, Ltd.
251-259 Regent Street
London, W1R 7AD, England

Fachinformationszentrum Karlsruhe
Gesellschaft für wissenschaftlich-technische
Information mbH
7514 Eggenstein-Leopoldshafen 2, Germany

Her Majesty's Stationery Office
P.O. Box 569, S.E. 1
London, England

NASA Center for AeroSpace Information
P.O. Box 8757
Baltimore, Maryland 21240-0757

National Aeronautics and Space Administration
Scientific and Technical Information Program (JTT)
Washington, DC 20546-0001

National Technical Information Service
5285 Port Royal Road
Springfield, Virginia 22161

Pendragon House, Inc.
899 Broadway Avenue
Redwood City, California 94063

Superintendent of Documents
U.S. Government Printing Office
Washington, DC 20402

University Microfilms
A Xerox Company
300 North Zeeb Road
Ann Arbor, Michigan 48106

University Microfilms, Ltd.
Tylers Green
London, England

U.S. Geological Survey Library National Center
MS 950
12201 Sunrise Valley Drive
Reston, Virginia 22092

U.S. Geological Survey Library
2255 North Gemini Drive
Flagstaff, Arizona 86001

U.S. Geological Survey
345 Middlefield Road
Menlo Park, California 94025

U.S. Geological Survey Library
Box 25046
Denver Federal Center, MS914
Denver, Colorado 80225

CASI PRICE TABLES

(Effective October 1, 1991)

STANDARD PRICE DOCUMENTS

PRICE CODE	NORTH AMERICAN PRICE	FOREIGN PRICE
A01	$ 9.00	$ 18.00
A02	12.50	25.00
A03	17.00	34.00
A04-A05	19.00	38.00
A06-A09	26.00	52.00
A10-A13	35.00	70.00
A14-A17	43.00	86.00
A18-A21	50.00	100.00
A22-A25	59.00	118.00
A99	69.00	138.00

MICROFICHE

PRICE CODE	NORTH AMERICAN PRICE	FOREIGN PRICE
A01	$ 9.00	$ 18.00
A02	12.50	25.00
A03	17.00	34.00
A04	19.00	38.00
A06	26.00	52.00
A10	35.00	70.00

IMPORTANT NOTICE

CASI Shipping and Handling Charges
U.S. — ADD $3.00 per TOTAL ORDER
Canada and Mexico — ADD $3.50 per TOTAL ORDER
All Other Countries — ADD $7.50 per TOTAL ORDER
Does NOT apply to orders
requesting CASI RUSH HANDLING.
Contact CASI for charge.

FEDERAL REGIONAL DEPOSITORY LIBRARIES

ALABAMA

AUBURN UNIV. AT MONTGOMERY LIBRARY
Documents Dept.
7300 University Drive
Montgomery, AL 36117-3596
(205) 244-3650 FAX: (205) 244-0678

UNIV. OF ALABAMA
Amelia Gayle Gorgas Library
Govt. Documents
Box 870266
Tuscaloosa, AL 35487-0266
(205) 348-6046 FAX: (205) 348-8833

ARIZONA

DEPT. OF LIBRARY, ARCHIVES, AND PUBLIC RECORDS
Federal Documents
Third Floor State Capitol
1700 West Washington
Phoenix, AZ 85007
(602) 542-4121 FAX: (602) 542-4400; 542-4500

ARKANSAS

ARKANSAS STATE LIBRARY
State Library Services
One Capitol Mall
Little Rock, AR 72201
(501) 682-2869

CALIFORNIA

CALIFORNIA STATE LIBRARY
Govt. Publications Section
914 Capitol Mall - P.O. Box 942837
Sacramento, CA 94237-0001
(916) 322-4572 FAX: (916) 324-8120

COLORADO

UNIV. OF COLORADO - BOULDER
Norlin Library
Govt. Publications
Campus Box 184
Boulder, CO 80309-0184
(303) 492-8834 FAX: (303) 492-2185

DENVER PUBLIC LIBRARY
Govt. Publications Dept. BS/GPD
1357 Broadway
Denver, CO 80203
(303) 571-2135

CONNECTICUT

CONNECTICUT STATE LIBRARY
231 Capitol Avenue
Hartford, CT 06106
(203) 566-4971 FAX: (203) 566-3322

FLORIDA

UNIV. OF FLORIDA LIBRARIES
Documents Dept.
Library West
Gainesville, FL 32611-2048
(904) 392-0366 FAX: (904) 392-7251

GEORGIA

UNIV. OF GEORGIA LIBRARIES
Govt. Documents Dept.
Jackson Street
Athens, GA 30602
(404) 542-8949 FAX: (404) 542-6522

HAWAII

UNIV. OF HAWAII
Hamilton Library
Govt. Documents Collection
2550 The Mall
Honolulu, HI 96822
(808) 948-8230 FAX: (808) 956-5968

IDAHO

UNIV. OF IDAHO LIBRARY
Documents Section
Moscow, ID 83843
(208) 885-6344 FAX: (208) 885-6817

ILLINOIS

ILLINOIS STATE LIBRARY
Reference Dept.
300 South Second
Springfield, IL 62701-1796
(217) 782-7596 FAX: (217) 524-0041

INDIANA

INDIANA STATE LIBRARY
Serials/Documents Section
140 North Senate Avenue
Indianapolis, IN 46204
(317) 232-3678 FAX: (317) 232-3728

IOWA

UNIV. OF IOWA LIBRARIES
Govt. Publications Dept.
Washington & Madison Streets
Iowa City, IA 52242
(319) 335-5926 FAX: (319) 335-5830

KANSAS

UNIV. OF KANSAS
Govt. Documents & Map Library
6001 Malott Hall
Lawrence, KS 66045-2800
(913) 864-4660 FAX: (913) 864-5380

KENTUCKY

UNIV. OF KENTUCKY LIBRARIES
Govt. Publications/Maps Dept.
Lexington, KY 40506-0039
(606) 257-3139 FAX: (606) 257-1563; 257-8379

LOUISIANA

LOUISIANA STATE UNIV.
Middleton Library
Govt. Documents Dept.
Baton Rouge, LA 70803
(504) 388-2570 FAX: (504) 388-6992

LOUISIANA TECHNICAL UNIV.
Prescott Memorial Library
Govt. Documents Dept.
305 Wisteria Street
Ruston, LA 71270-9985
(318) 257-4962 FAX: (318) 257-2447

MAINE

TRI-STATE DOCUMENTS DEPOSITORY
Raymond H. Fogler Library
Govt. Documents & Microforms Dept.
Univ. of Maine
Orono, ME 04469
(207) 581-1680

MARYLAND

UNIV. OF MARYLAND
Hornbake Library
Govt. Documents/Maps Unit
College Park, MD 20742
(301) 454-3034 FAX: (301) 454-4985

MASSACHUSETTS

BOSTON PUBLIC LIBRARY
Govt. Documents Dept.
666 Boylston Street
Boston, MA 02117
(617) 536-5400 ext. 226
FAX: (617) 267-8273; 267-8248

MICHIGAN

DETROIT PUBLIC LIBRARY
5201 Woodward Avenue
Detroit, MI 48202-4093
(313) 833-1440; 833-1409
FAX: (313) 833-5039

LIBRARY OF MICHIGAN
Govt. Documents Unit
P.O. Box 30007
Lansing, MI 48909
(517) 373-0640 FAX: (517) 373-3381

MINNESOTA

UNIV. OF MINNESOTA
Wilson Library
Govt. Publications Library
309 19th Avenue South
Minneapolis, MN 55455
(612) 624-5073 FAX: (612) 626-9353

MISSISSIPPI

UNIV. OF MISSISSIPPI
J.D. Williams Library
Federal Documents Dept.
106 Old Gym Bldg.
University, MS 38677
(601) 232-5857 FAX: (601) 232-5453

MISSOURI

UNIV. OF MISSOURI - COLUMBIA
Ellis Library
Govt. Documents
Columbia, MO 65201
(314) 882-6733 FAX: (314) 882-8044

MONTANA

UNIV. OF MONTANA
Maureen & Mike Mansfield Library
Documents Div.
Missoula, MT 59812-1195
(406) 243-6700 FAX: (406) 243-2060

NEBRASKA

UNIV. OF NEBRASKA - LINCOLN
D.L. Love Memorial Library
Documents Dept.
Lincoln, NE 68588
(402) 472-2562

NEVADA

UNIV. OF NEVADA
Reno Library
Govt. Publications Dept.
Reno, NV 89557
(702) 784-6579 FAX: (702) 784-1751

NEW JERSEY

NEWARK PUBLIC LIBRARY
U.S. Documents Div.
5 Washington Street - P.O. Box 630
Newark, NJ 07101-0630
(201) 733-7812 FAX: (201) 733-5648

NEW MEXICO

UNIV. OF NEW MEXICO
General Library
Govt. Publications Dept.
Albuquerque, NM 87131-1466
(505) 277-5441 FAX: (505) 277-6019

NEW MEXICO STATE LIBRARY
325 Don Gaspar Avenue
Santa Fe, NM 87503
(505) 827-3826 FAX: (505) 827-3820

NEW YORK

NEW YORK STATE LIBRARY
Documents/Gift & Exchange Section
Federal Depository Program
Cultural Education Center
Albany, NY 12230
(518) 474-5563 FAX: (518) 474-5786

NORTH CAROLINA

UNIV. OF NORTH CAROLINA - CHAPEL HILL
CB#3912, Davis Library
BA/SS Dept.—Documents
Chapel Hill, NC 27599
(919) 962-1151 FAX: (919) 962-0484

NORTH DAKOTA

NORTH DAKOTA STATE UNIV. LIBRARY
Documents Office
Fargo, ND 58105
(701) 237-8886 FAX: (701) 237-7138
In cooperation with Univ. of North Dakota, Chester Fritz Library
Grand Forks

OHIO

STATE LIBRARY OF OHIO
Documents Dept.
65 South Front Street
Columbus, OH 43266
(614) 644-7051 FAX: (614) 752-9178

OKLAHOMA

OKLAHOMA DEPT. OF LIBRARIES
U.S. Govt. Information Div.
200 NE 18th Street
Oklahoma City, OK 73105-3298
(405) 521-2502, ext. 252, 253
FAX: (405) 525-7804

OKLAHOMA STATE UNIV.
Edmon Low Library
Documents Dept.
Stillwater, OK 74078
(405) 744-6546 FAX: (405) 744-5183

OREGON

PORTLAND STATE UNIV.
Millar Library
934 SW Harrison - P.O. Box 1151
Portland, OR 97207
(503) 725-3673 FAX: (503) 725-4527

PENNSYLVANIA

STATE LIBRARY OF PENN.
Govt. Publications Section
Walnut St. & Commonwealth Ave. - P.O. Box 1601
Harrisburg, PA 17105
(717) 787-3752

SOUTH CAROLINA

CLEMSON UNIV.
Cooper Library
Public Documents Unit
Clemson, SC 29634-3001
(803) 656-5174 FAX: (803) 656-3025
In cooperation with Univ. of South Carolina, Thomas Cooper Library, Columbia

TENNESSEE

MEMPHIS STATE UNIV. LIBRARIES
Govt. Documents
Memphis, TN 38152
(901) 678-2586 FAX: (901) 678-2511

TEXAS

TEXAS STATE LIBRARY
United States Documents
P.O. Box 12927 - 1201 Brazos
Austin, TX 78711
(512) 463-5455 FAX: (512) 463-5436

TEXAS TECH. UNIV. LIBRARY
Documents Dept.
Lubbock, TX 79409
(806) 742-2268 FAX: (806) 742-1920

UTAH

UTAH STATE UNIV.
Merrill Library & Learning Resources Center, UMC-3000
Documents Dept.
Logan, UT 84322-3000
(801) 750-2684 FAX: (801) 750-2677

VIRGINIA

UNIV. OF VIRGINIA
Alderman Library
Govt. Documents
Charlottesville, VA 22903-2498
(804) 924-3133 FAX: (804) 924-4337

WASHINGTON

WASHINGTON STATE LIBRARY
Document Section
MS AJ-11
Olympia, WA 98504-0111
(206) 753-4027 FAX: (206) 753-3546

WEST VIRGINIA

WEST VIRGINIA UNIV. LIBRARY
Govt. Documents Section
P.O. Box 6069
Morgantown, WV 26506
(304) 293-3640

WISCONSIN

ST. HIST. SOC. OF WISCONSIN LIBRARY
Govt. Publications Section
816 State Street
Madison, WI 53706
(608) 262-2781 FAX: (608) 262-4711
In cooperation with Univ. of Wisconsin-Madison, Memorial Library

MILWAUKEE PUBLIC LIBRARY
Documents Div.
814 West Wisconsin Avenue
Milwaukee, WI 53233
(414) 278-2167 FAX: (414) 278-2137

*U.S. G.P.O.:1992-313-125:60020

National Aeronautics and
Space Administration
Code JTT
Washington, D.C.
20546-0001

Official Business
Penalty for Private Use, $300

SPECIAL FOURTH-CLASS RATE
POSTAGE & FEES PAID
NASA
PERMIT No. G27

POSTMASTER: If Undeliverable (Section 158
Postal Manual) Do Not Return